Technische Universität Dortmund

Max-Planck Institut für Molekulare Physiologie

Stereoselective Synthesis of Glycosides through Novel Catalytic Method Development

Dissertation

For the achievement of the academic degree of the

Doctor in Natural Science

(Dr. rer. nat.)

Submitted to

The Department of Chemistry and Chemical Biology

Technical University of Dortmund

By

M.Sc. Caiming Wang

From Ganzhou, China

Dortmund 2024

First examiner: Prof. Dr. Dr. h.c. Herbert Waldmann

Second examiner: Prof. Dr. Carsten Strohmann

PhD supervisor: Dr. Chuanjie Loh (Charles)

The work presented in this thesis was performed from March 2021 to June 2024 under the supervision and guidance of Dr. Chuanjie Loh (Charles) at the Max-Planck-Institute of Molecular Physiology in Dortmund and the Faculty of Chemistry and Chemical Biology at the Technical University of Dortmund.

The results presented in this thesis contributed to the following publications:

[1] **Caiming Wang**, Anna Krupp, Carsten Strohmann, Bastian Grabe and Charles C. J. Loh *. Harnessing multi-step chalcogen bonding activation in the α-stereoselective synthesis of iminoglycosides. *J. Am. Chem. Soc.* **2024**, *146*, 10608-10620.

[2] V. U. Bhaskara Rao,† **Caiming Wang**,† Daniel P. Demarque, Corentin Grassin, Felix Otte, Christian Merten, Carsten Strohmann & Charles C. J. Loh* A synergistic Rh(I)/organoboron-catalysed site-selective carbohydrate functionalization that involves multiple stereocontrol. *Nat. Chem.* **2023**, *15*, 424-435. (†co-first author)

Table of Contents

Abstract

Carbohydrates are one of the most prevalent natural product class with a wide range of structural and functional properties. Further, glycoside bond formation is one of the most important process in carbohydrate chemistry, particularly the production of *O*(*S*)-glycosides, which are abundant in bioactive compounds. To achieve this, glycosyl donors are synthesized and converted into reactive glycosylating species using catalysis. In this thesis, various activation strategies have been established to activate different glycosyl donors to synthesize a range of *O*(*S*)-glycosides, some of which are bioactive compounds.

A phosphonochalcogenide (PCH) catalyzed strategy was developed to catalyze a stereoselective α-iminoglycosylation of iminoglycals with a wide range of glycosyl acceptors with remarkable protecting group tolerance in chapter 3. Mechanistic research revealed the catalyst's unexpected role in serially activating both the glycosyl donor and acceptor in the upstream and downstream stages of the reaction via chalcogen bonding (ChB). The dynamic interaction of chalcogens with substrates brings up new mechanistic possibilities based on repetitive ChB catalyst engagements and disengagements in multiple elementary steps. This research addressed the overall shortage of robust catalytic iminoglycosylations and provided a feasible approach for biologically relevant sp^2-iminoglycosidic scaffolds. This methodology will demonstrate the enormously underexploited potential of sigma hole-based activation in broadening the frontiers of stereoselective carbohydrate and glycomimetic synthesis in the future.

A synergistic chiral Rh(I) and organoboron-catalyzed protocol was introduced to catalyze site selective carbohydrate functionalization to synthesize biologically relevant anomeric aryl naphthalene glycosides with excellent enantioselectivity, diastereoselectivity and regioselectivity in chapter 4. The proper choice of an organoboron catalyst and ligands are critical to the success of this protocol. Following further investigation of this approach, my study revealed that structurally related allylic carbonate substrates were also well tolerated to furnish functionalized carbohydratesl with outstanding regio- and diastereoselectivity. This successful methodology would stimulate more effort in the development of chiral transition catalytic systems for demanding site-selective functionalizations of carbohydrates with prochiral electrophiles.

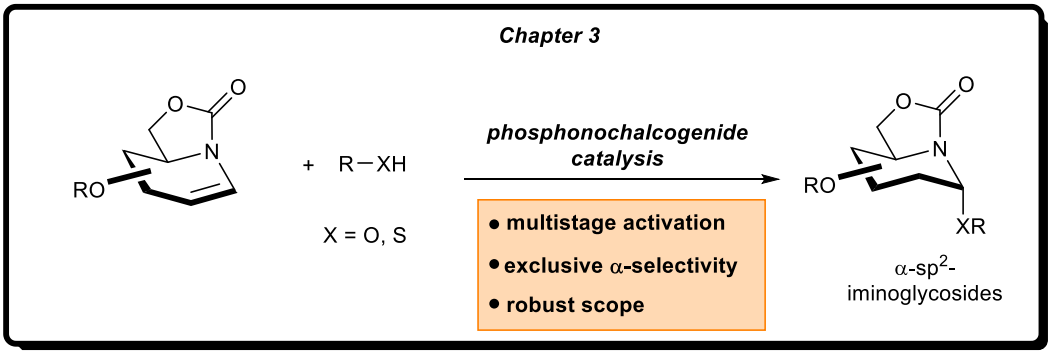
Chapter 3
RO
+ R—XH
X = O, S
phosphonochalcogenide catalysis
• multistage activation
• exclusive α-selectivity
• robust scope
RO
XR
α-sp2-iminoglycosides

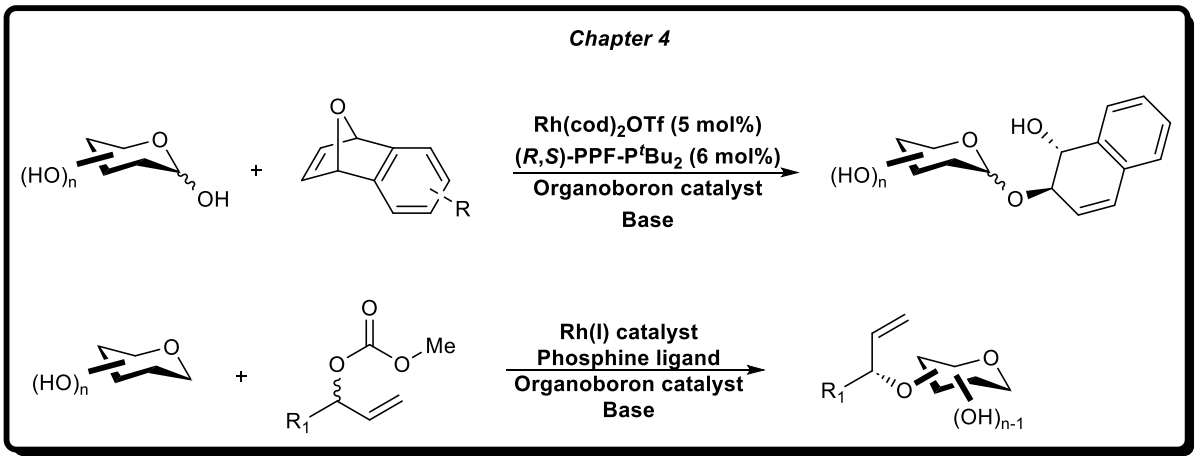
Chapter 4
(HO)n
OH
+
R
Rh(cod)2OTf (5 mol%)
(R,S)-PPF-PtBu2 (6 mol%)
Organoboron catalyst
Base
(HO)n
HO
O
(HO)n
+
Me
R1
Rh(I) catalyst
Phosphine ligand
Organoboron catalyst
Base
R1
(OH)n-1

Zusammenfassung

Kohlenhydrate sind eine der häufigsten natürlichen Produktklassen mit einem breiten Spektrum an strukturellen und funktionellen Eigenschaften. Darüber hinaus ist die Bildung von Glykosidbindungen einer der wichtigsten Prozesse in der Kohlenhydratchemie, insbesondere die Produktion von *O*(*S*)-Glykosiden, die in bioaktiven Verbindungen reichlich vorhanden sind. Um dies zu erreichen, werden Glykosyl-Spender mit Hilfe der Katalyse synthetisiert und in reaktive Glycosylationsarten umgewandelt. In dieser These wurden verschiedene Aktivierungsstrategien festgelegt, um verschiedene Glycosyl-Spender zu aktivieren, um eine Reihe von *O*(*S*)-Glycosiden zu synthetisieren, von denen einige bioaktive Verbindungen sind.

Eine phosphonochalcogenide (PCH) katalysierte Strategie wurde entwickelt, um eine stereoselektive α-Iminoglykosylierung von Iminoglykalen mit einem breiten Spektrum von Glykosylakzeptoren mit bemerkenswerter Schutzgruppe-Toleranz in kapitel 3 zu katalysieren. Mechanistische Untersuchungen zeigten die unerwartete Rolle des Katalysators bei der seriellen Aktivierung sowohl des Glycosylspenders als auch des Acceptors in den Auf- und Abwärtsstufen der Reaktion über die Chalcogenbindung (ChB). Die dynamische Wechselwirkung von Chalcogenen mit Substraten eröffnet neue mechanistische Möglichkeiten, basierend auf wiederholten ChB-Katalysatoren und Entbindungen in mehreren Elementarstufen. Diese Forschung beantwortete den allgemeinen Mangel an robusten katalytischen Iminoglykosylierungen und lieferte einen umsetzbaren Ansatz für biologisch relevante Sp^2-Iminoglycosid-Stafolds. Diese Methodik wird das enorm untergenutzte Potenzial der sigma-hole-basierten Aktivierung bei der Erweiterung der Grenzen der stereoselektiven Kohlenhydrate und der glycomimetischen Synthese in der Zukunft demonstrieren.

In kapitel 4 wurde ein synergistisches chiral Rh(I) und organoboron-katalysiertes Protokoll eingeführt, um die Site-selektive Kohlenhydratfunktionalisierung zu katalysieren, um biologisch relevante anomere Arylnaphthalenglykoside mit ausgezeichneter Enantioselektivität, Diastereoselektivität und Regio-Selektivität zu synthetisieren. Für den Erfolg dieses Protokolls sind die richtige Wahl eines Organoboron-Katalysators und Ligands von entscheidender Bedeutung. Nach weiterer Untersuchung dieses Ansatzes ergab meine Studie, dass strukturell verwandte Allylcarbonat-Substrate auch gut toleriert wurden, um funktionalisierte Carbohydratesl mit hervorragender Region- und Diastereoselektivität zu liefern. Diese erfolgreiche Methodik würde mehr Anstrengungen bei der Entwicklung von Chiral-Übergangskatalysat-Systemen für anspruchsvolle Standort-selektive Funktionalisierungen von Kohlenhydraten mit Prochiral-Elektrophilen anregen.

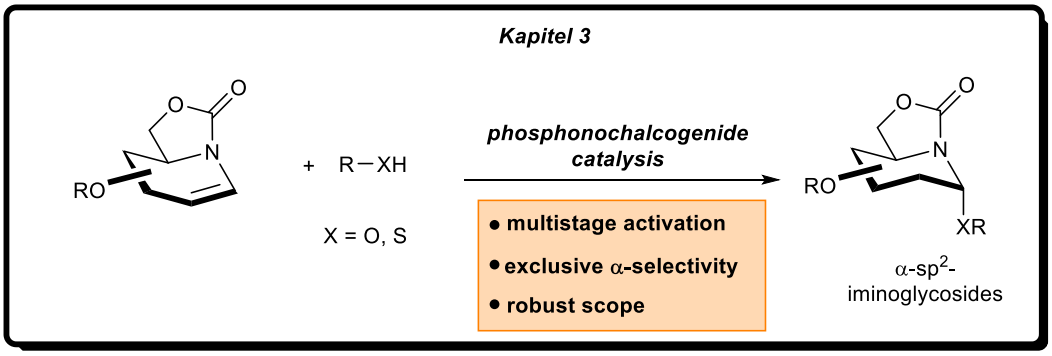
Kapitel 3
RO
+ R—XH
X = O, S
phosphonochalcogenide catalysis
• multistage activation
• exclusive α-selectivity
• robust scope
RO
XR
α-sp2-iminoglycosides

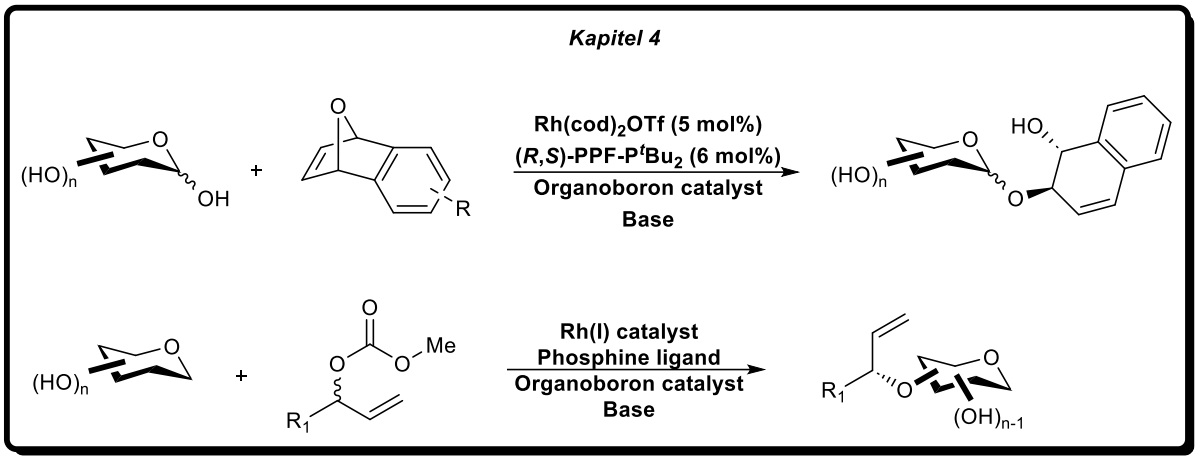
Kapitel 4
(HO)n
OH
R
Rh(cod)2OTf (5 mol%)
(R,S)-PPF-PtBu2 (6 mol%)
Organoboron catalyst
Base
HO
Me
R1
Rh(I) catalyst
Phosphine ligand
Organoboron catalyst
Base
(OH)n-1

1. Introduction

Carbohydrates are most common molecules in natural products, which have a variety of structural and functional characteristics. Most of them are found as polysaccharides, glycoconjugates, or glycosides, in which sugar units are attached to one another or to aglycones by *O*-glycosidic bonds (**Fig. 1.1**).[1] Therefore, the stereoselective synthesis of *O*-glycosidic linkages is the crucial step in the majority of glycoside synthesis. The first glycoside syntheses were introduced by Michael[2] and Fischer,[3] followed by the seminal studies of Koenigs and Knorr,[4] a large number of glycosidation methods have been developed.

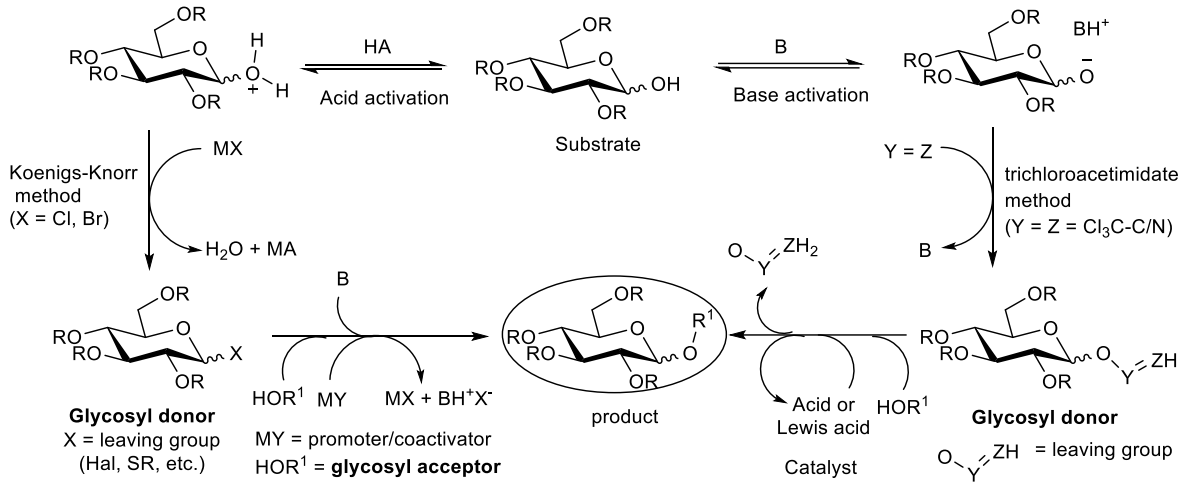

Figure 1.1 Generation of glycosidic bond

Aside from these reported methods, non-covalent interactions (NCIs) are becoming more and more popular ways to catalyze the process of glycoside synthesis,[5] especially in the area of stereoselective carbohydrate synthesis,[6] because of their functions which access to elusive glycosidic chemical space.[7] Recently, the NCIs operated by sigma hole activation has entered the stereoselective glycosylation field because they have some unique characteristics that they have distinct non-protic manifold and increased directionality.[8] These properties could allow the glycosylation process to undergo successfully under milder conditions. The most studied kind of NCIs is halogen bonding (XB) catalysis, which is very successful in different kinds of glycosylation manifolds.[9] However, other types of sigma hole-based NCIs are attracting more and more attention, because they can solve difficult reactions that halogen bonding (XB) cannot afford. Take chalcogen bonding (ChB) catalysis as an example, this kind of catalysis has been investigated frequently in recent years, especially phosphonochalcogenides (PCH) which was first reported by Wang and coworkers (**Fig. 1.2**).[10] Owing to PCH catalysts' various propeties, they have a variety of activation modes, which are ranging from bi-dentate, bi-functional, chalcogen-π, bifurcation and even synergistic ChB, π-π and CH-π. Since PCH catalysts have such lots of activation modes, they have solved many problems in carbodydrate synthesis which other kinds of catalysts cannot afford. Although PCH catalysts had made a lot progress in organic

synthesis, there are only few reports in stereoselective glycoside synthesis, not to mention the application in stereoselective iminoglycosides synthesis. As a result, developing a method for employing PCH catalysts to catalyze the stereoselective iminoglycoside synthesis process has enormous potential in this field.

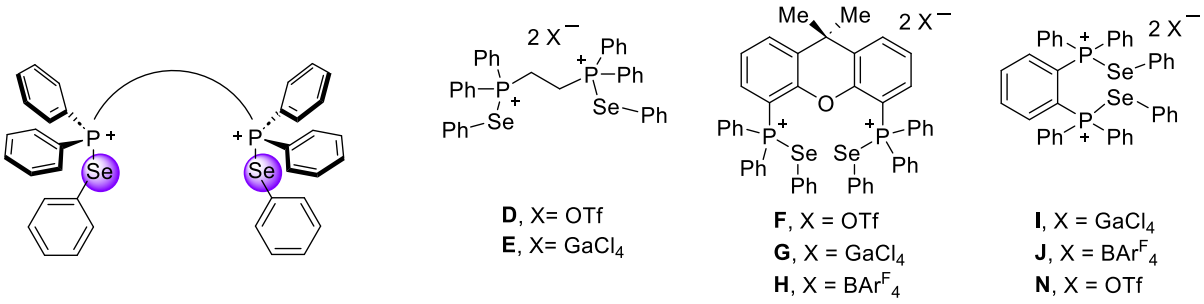

Figure 1.2 PCH catalyst mode and some representative catalysts

Apart from the NCIs involved reaction to synthesize stereoselective glycosides, site selective functionalization has becoming a potential strategy in the process of glycoside synthesis, since this method has some merits that it's able to distinguish the chemically similar functionalities in the similar stereochemical environments.[11] Site or regioselective methods that control regioselectivity are totally different from addressing challenge of enantioselectivity by using chiral catalyst to form new stereocenters in prochiral substrates, due to the involved substrates have several reaction site which has similar properties. Besides, these reactions are more relevant to biological synthesis. Therefore, developing a method to solve both the enantioselectivity and regioselectivity at the same time in carbodhydrate chemistry especially in glycoside synthesis still has potential prospects.

1.1 Stereoselectivity in carbohydrate synthesis

Stereoselectivity is an important issue in the carbohydrate synthesis, which still exists as a huge challenge in the process of selective glycoside synthesis.[12] Stereoselectivity in carbohydrate synthesis is totally different from the enantioselectivity which has been addressed by enantioselective catalysis development for a long time, it additionally includes diastereoselectivity and regioselectivity issues since carbohydrates are homochiral biomolecules with multiple proximal and contiguous stereogenic centres. Therefore, it's necessary to consider carefully the complexities of the creation of a new stereocenter in view of the stereogenic environment that existed in the substrate. Besides, the formation of a glycosidic linkage between two monosaccharide units face dual issues of the selective intermolecular bond formation between the anomeric carbon on the glycosyl donor (electrophile) and a hydroxyl group on the glycosyl acceptor (nucleophile), as well as a selection between multiple chemically equivalent but spatially distinctive hydroxyl groups on the polyol acceptor. These two issues are commonly known as the anomeric selectivity and regioselectivity/site-selectivity challenges in carbohydrate synthesis respectively (**Fig. 1.3**). These two stereoselectivity issues cannot be avoided when scientists develop synthetic method to synthesize biological carbohydrate scaffolds. Therefore,

it's obvious that these two directions need to be paid attention to when developing novel synthetic methods to realize stereoselective synthesis: The control of anomeric selectivity in glycosylations and site-selectivity or regioselectivity in glycofunctionalizations. In past decades, non-covalent interactions (NCIs) were often utilized in some methods to solve these two challenges in carbohydrate synthesis.

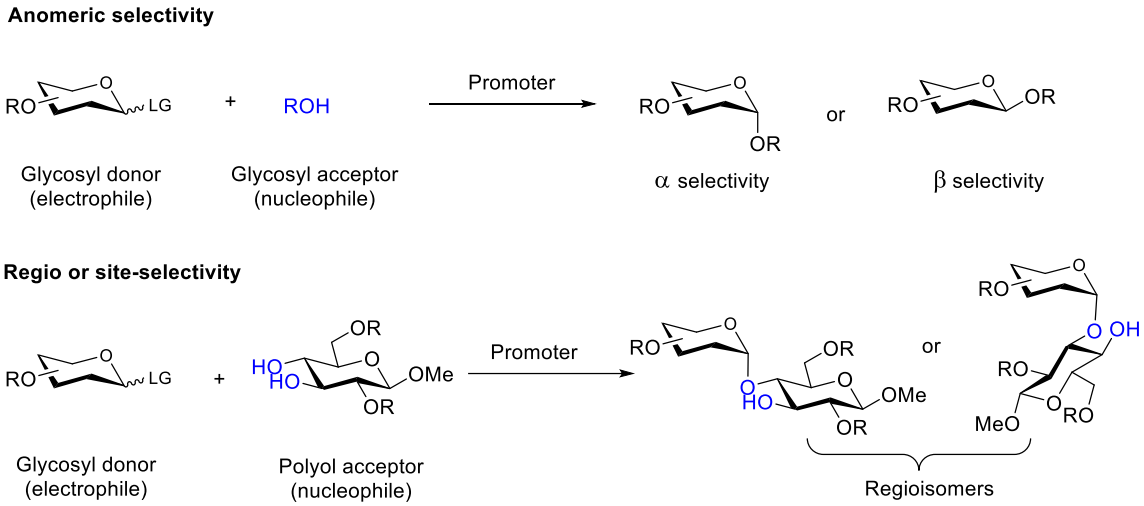

Figure 1.3 Two main stereoselectivity in carbodydrate synthesis

1.1.1 The importance of anomeric effect in carbohydrate chemistry

Anomeric effect was first discovered in 1955 by J. T. Edward in studies of carbohydrate chemistry. Originally called the ''Edward–Lemieux effect'', the phenomenon was later named as the ''anomeric effect'' by Lemieux in 1958,[13] which was in order to explain unusual conformational preferences in carbohydrates (**Fig. 1.4a**). Additionally, it was discovered that when the acceptor nature of the anomeric substituent increases, the axial preference becomes more noticeable. Besides, by comparing the anomeric stabilization of two anomers according to the free energy, the axial conformer is more preferable than the equatorial in the absence of additional substituents (**Fig. 1.4b**).

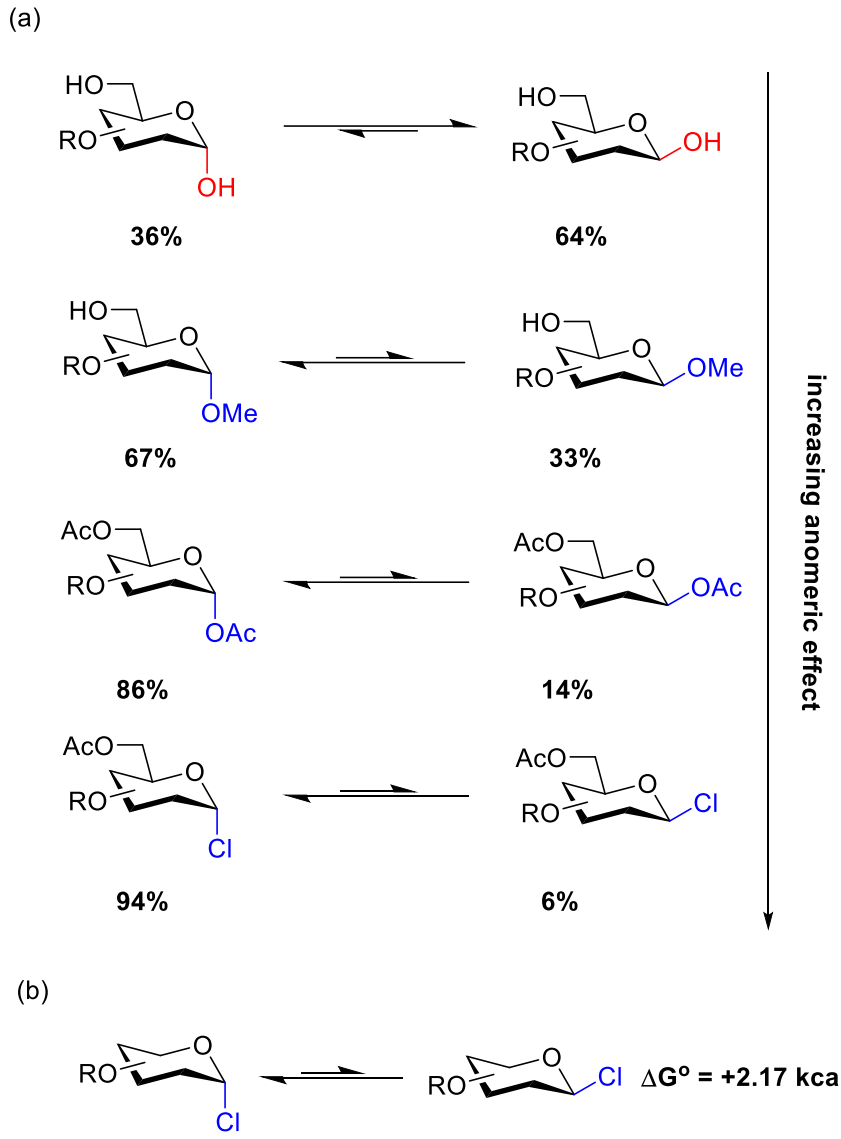

Figure 1.4 (a) Anomeric effect leads to the ‘‘abnormal’’ conformational preference. (b) The equatorial preference is switched to axial when the anomeric effect is present

The anomeric effect is a type of stereoelectronic effect, which is often confused with the stereoelectronic interactions that give rise to them. Anomeric effect, on the other hand, is what we observe-it is the reactivity and selectivity consequence that result from stabilization by anomeric interactions in ground or transition states.[14] Anomeric interaction causes anomeric effect, in other words, anomeric selectivity is controlled by the anomeric interactions including hyperconjugation and electrostatics.[15]

1.1.2 Application of non-covalent catalysis in carbohydrate synthesis

Non-covalent catalytic methods are applied more and more frequently in carbohydrate chemistry, owing to their advantages to control stereoselectivity and led to new, unexpected reactivity and broader substrate scope.[16] There are several kinds of non-covalent catalytic methods, including hydrogen bonding (HB), halogen bonding (XB), CH–π, cation–π and so on. Among these methods, HB-catalysed

glycosylation, particularly by means of thiourea catalysis, is currently most demonstrated in the field. All of these non-covalent catalytic methods have become an important strategy for glycosides synthesis and stereoselective functionalization.

Thiourea catalysis has been investigated in a variety of reactions for a long time.[17] The first example of using thiourea catalyst to process glycosylation was reported by Jacobsen and co-workers in 2008.[18] They found that the reaction of *O*-glycosylation of 2-deoxyglycosylacetates could be accelerated by using the chiral thiourea catalyst with catalytic amounts of BCl_3. Besides, according to the reaction rate on the different glycosyl acetate donor site, they concluded that the stereoselectivity could be controlled by the chiral catalyst. To get a further study of the thiourea catalyst controlling the stereoselectivity and anomeric selectivity, in 2017, Jacobsen group reported Koenigs–Knorr glycosylations of glycosyl halides catalyzed by using macrocyclic *bis*(thiourea) catalyst **1** (**Fig. 1.5**).[19] The authors found that the product was dependent on the initial anomeric configuration of the glycosyl donor and they proposed that the reaction underwent a S_N2 pathway through the combination of HB and halide recognition activation modes **2**. This activation mode was also supported by density functional theory (DFT) calculations and kinetic isotopic effect studies.

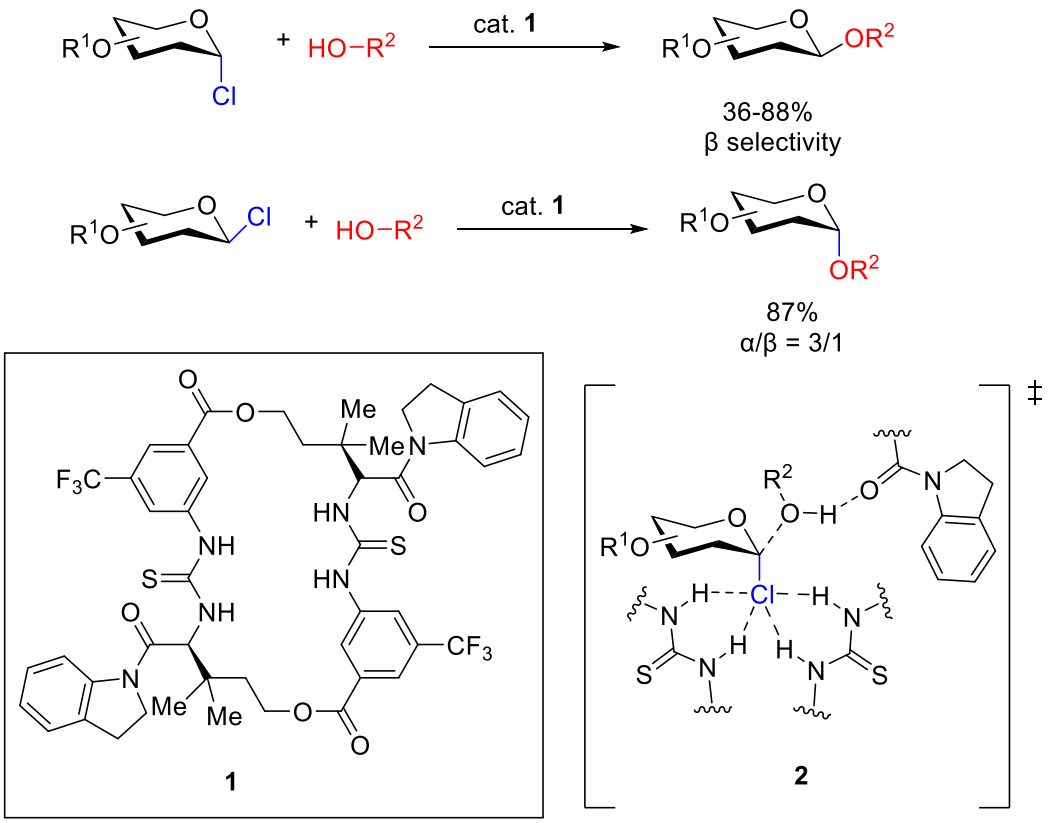

Figure 1.5 Macrocyclic bis(thiourea) catalyzed Koenigs–Knorr glycosylations

In 2019, Jacobsen and co-workers demonstrated the activation of biologically relevant pyranosyl phosphate donors by using non-cyclic *bis*(thiourea) **3** to synthesize β-selective *O*-glycosylation product

(**Fig. 1.6a**).[20] They found that the reaction rates of glycosyl phosphates were faster than those of the previously reported chloride substituent according to the kinetic experiment results. Besides, they found that the phosphate oxyanion had a better binding ability with the thiourea catalyst, which would accelerate the leaving of the phosphate group. This result is consistent with the Michaelis–Menten kinetic analysis. One year later, in 2020, they reported another example that using *bis*(thiourea) **6** activated the furanosyl donor **5** bearing a cyclic phosphate leaving group to form β-selective *O*-glycosylation product (**Fig. 1.6b**).[21] The authors postulated the formation of a resting state catalyst–donor complex which contributed to the following stereospecific S_N2-type glycosylation by the ^{31}P NMR mechanistic studies. Comparatively, the achiral Lewis acid catalyst trimethylsilyl trifluoromethanesulfonate (TMSOTf) activated this reaction to form the α -selective products. These results showed that the anomeric selectivity could be controled by catalyst.

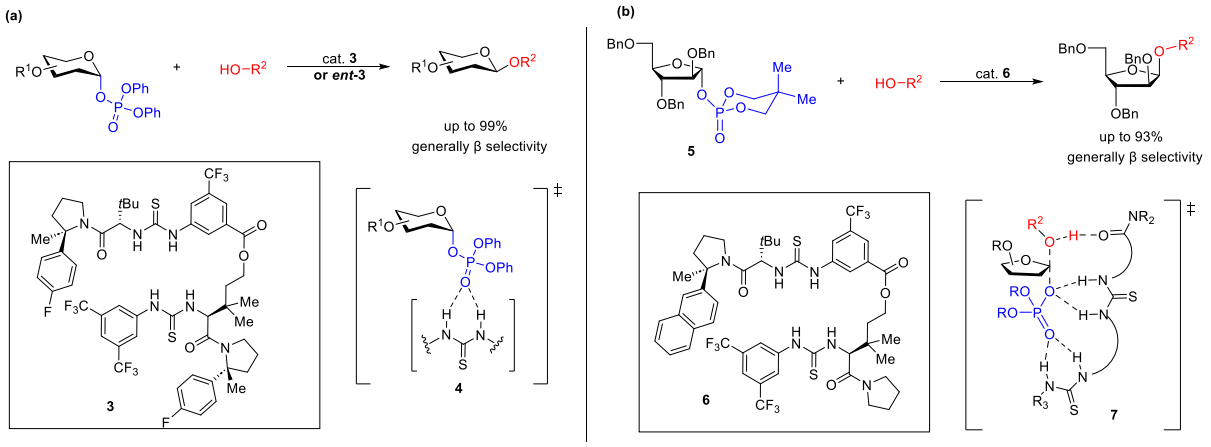

Figure 1.6 (a) Non-cyclic bis(thiourea)-catalysed pyranosylations. (b) Non-cyclic bis(thiourea)-catalysed furanosylations

Unlike HB catalysis and thiourea catalysis which had been well investigated in glycosylations, XB catalysis is emerging as new approach in chemical glycosylations.[22] Though halogen bonds are well studied in other fields including biology,[23] medicinal chemistry[24] and catalysis,[25] they are underdeveloped in carbohydrate chemistry until very recently. Compared with HB, XB has greater directionality owing to the existence of electropositive region known as a *σ*-hole on a halogen, which can function as a Lewis acid site.[26] XB has another advantage than HB, since the strength of the catalyst could been changed by replacing different halogen atoms. The first example of XB catalysis applied in glycosylation was reported by Huber and coworkers in 2014.[27] They used the stoichiometric bidentate XB promoter **11** to activate oleandrosyl chloride **8** through a Koenigs–Knorr glycosylation (**Fig. 1.7**). They proposed that the reaction underwent through a halide recognition mode via **12**, where bidentate XB interactions were pivotal in the halide abstraction step. After that, the 2-propanol acceptor **9** attacked the resulting oxacarbenium ion to produce equimolar amounts of both anomers as products **10**. Although the results presented in this reaction were not satisfied since the amount of the XB catalyst

was too high and the anomeric selectivity was bad, it provided a promising view for the later researchers that XB catalyst could be acted as a promoter or activator in carbohydrate reactions.

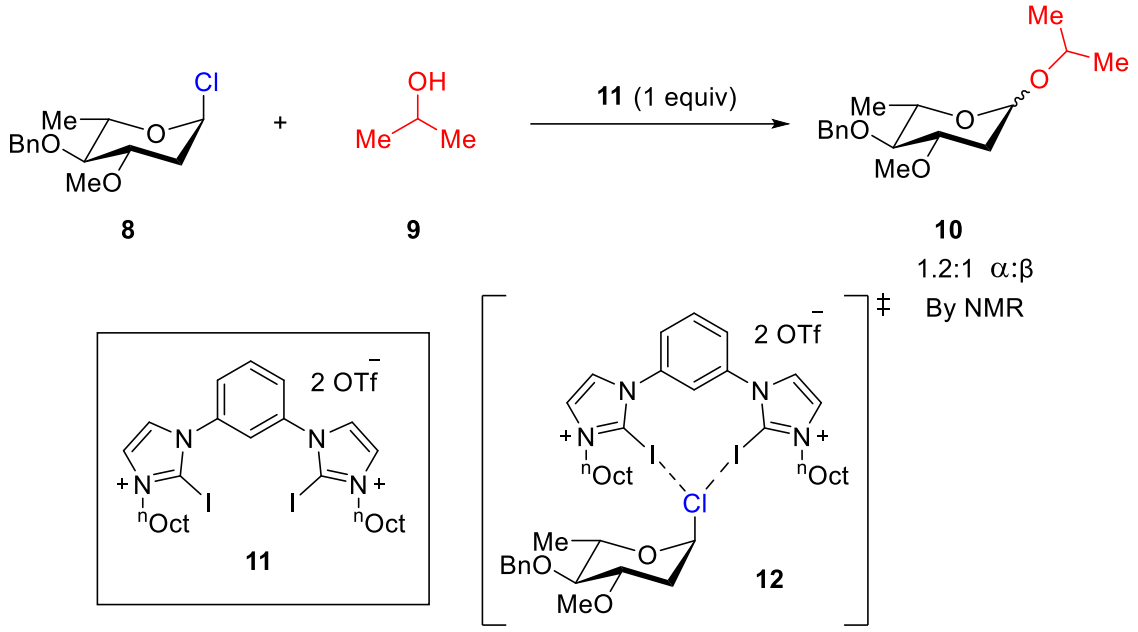

Figure 1.7 Halogen bonding (XB)-promoted Koenigs–Knorr glycosylation

In 2019, our group (by Xu and Loh) demonstrated the first exclusively XB-catalysed multi-stage strain-release glycosylation using a cyclopropanated carbohydrate donor to produce a wide range of glycosides stereoselectively and stereospecifically (**Fig. 1.8a**).[28] This protocol had a better anomeric selectivity than the method our group presented before by using the thiourea as the catalyst.[29] Through the *in situ* NMR monitoring and sequential control experiments, the authors thought that the reaction processed by a multi-stage XB activation mechanism involving activation complexes **14a**–**14c** in upstream and downstream mechanistic steps. One year later, in 2020 our group (by Xu and Loh) reported a robust XB-catalysed 2-deoxyglycosylation of hexose-based and pentose-based glycals by using XB catalyst **16** to form a broader scope of 2-deoxyglycosides (**Fig. 1.8b**).[30] It seemed that the XB catalysis was superior to thiourea catalysis when activating the glycals through a series of benchmark experiments. According to the mechanistic investigations including NMR titrations and kinetic experiments, the author found that the glycosylation proceeded through dynamic XB activation by the catalyst on multiple reaction species **17a–17c** through an intricate reaction network.

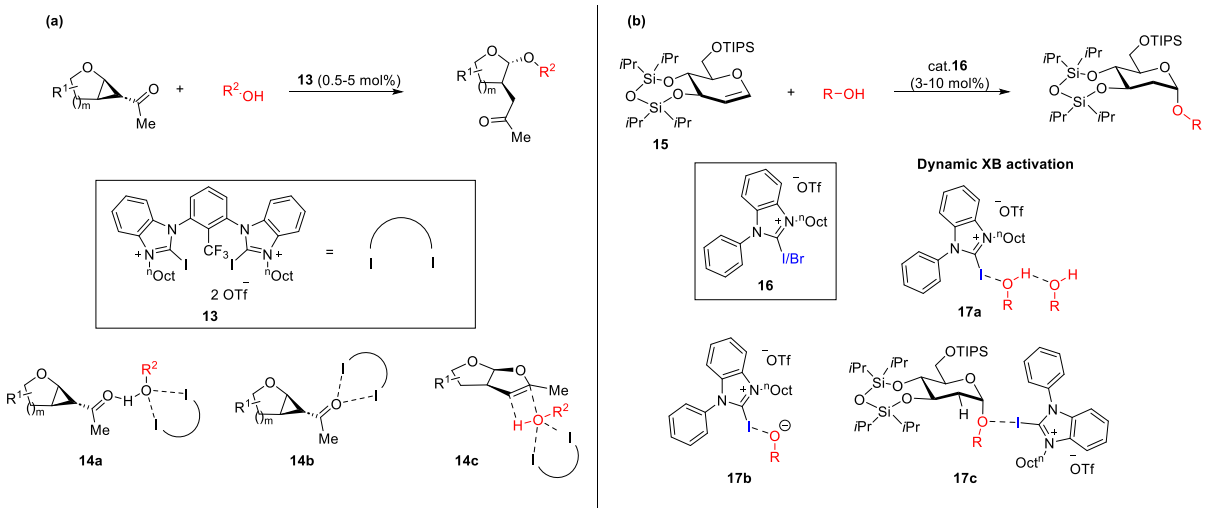

Figure 1.8 (a) XB-catalysed multi-stage strain-release glycosylation. (b) XB-catalysed 2-deoxyglycosylation.

1.2 Definition of Chalcogen Bonding and its properties

While NCIs such as HB and XB have been studied in the glycosciences, other NCIs like chalcogen bonding interaction had never been used in this field and is becoming increasingly interesting to the scientific community. Chalcogen bonding (ChB) is described as the contact between a positively polarized chalcogen atom and a Lewis base (LB) (**Fig. 1.9**).[31] Chalcogen bonds, when compared to hydrogen bonds (HB) and halogen bonds (XB), are more similar to the latter. Chalcogen bonds differ from ordinary hydrogen bonds in that they have stronger directionality, and Lewis bases typically follow divalent chalcogen molecules. The far end of the bond is 180° closer to the chalcogen atom. On the other hand, hydrogen bond donors are limited to hydrogen atoms, limiting the ability to adjust hydrogen bond strength to some extent. Whereas chalcogen bond donors can be sulfur, selenium or tellurium atoms, allowing for the adjustment of chalcogen bond strength. Chalcogen bonds are a relatively soft non-covalent bond force when compared to hydrogen bonds and they have been observed in several protein single crystal structures. Chalcogen bonds vary from halogen bonds in that their action sites are often buried on both sides of the divalent chalcogen atoms. Although chalcogen bonds have been identified for decades, study into them remains mostly untapped when compared to hydrogen bonds.

Electrostatic interactions, charge transfer and dispersion forces all have an effect on chalcogen bonds. The anisotropy in electron density of the chalcogen atoms causes the electrostatic attraction between the chalcogen bond donor and the Lewis base. This will lead the chalcogen atoms to have a positive potential area in the direction of the covalent link. This positive potential region is known as a sigma-hole.[32] Charge transfer is the ability of the Lewis base's lone pair electrons to delocalize to the sigma of the chalcogen atom. Generally speaking, the elements that influence the strength of chalcogen bonds are: 1) The strength of the Lewis base. The stronger the Lewis base, the more powerful the chalcogen

connection created. 2) The key properties of the chalcogen atoms, where the strength of the chalcogen bond is Te> Se>S; 3) The polarization ability of the substituent attached to the chalcogen atom. The interaction angle between the Lewis base and the chalcogen atom increases with the substituent's electronegativity. Chalcogen bonds should have an interaction angle of around 180°.

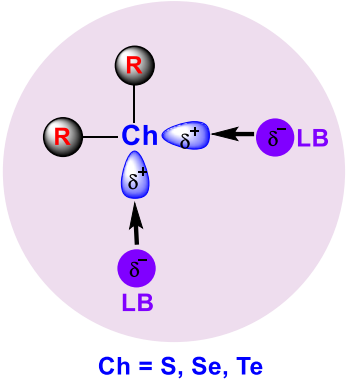

Figure 1.9 Schematic representation of a chalcogen bond

1.3 Activation modes of phosphonochalcogenide

Studies on the role of ChB catalysts are increasing in number as scientists become more and more interested in them. Unlike covalent interactions, chalcogen bonding is the non-covalent interaction between Lewis acidic chalcogen substituents and Lewis bases, so studying its mode of activation (mainly the mode of phosphonochalcogenide) in the reaction is crucial to our understanding of how the reaction proceeds. There are a variety of activating modes applied in organic synthesis according to the literature,[33] including bi-dentate, bi-functional, chalcogen-π and bifurcation activation modes. These different activating ways of the catalysis give researchers a broad understanding on the mechanism of the reaction.

1.3.1 Bi-dentate activation mode with phosphonochalcogenide

In 2019, Wang and co-workers[34] reported that a class of extraordinary chalcogen-bonding catalysts enables assembly of discrete small molecules including three β-ketoaldehydes and one indole, leading to the construction of *N*-heterocycles in a highly efficient manner (**Fig. 1.10a**). To gain insights into the chalcogen−chalcogen bonding interaction, the author carried out a series of control experiments, including competitive anion binding experiment, steric hindrance experiment, addition of base and NMR tracing experiments. All of these experiments provide a strong indication that Se···O interaction plays a crucial role in this cyclization proces. Most importantly, the author conducted ^{13}C NMR experiments reveal that the addition of catalyst **E** to the β-ketoaldehyde **19** can result in ketone group shifted downfield 0.36 ppm while the carbon signal of aldehyde group shifted downfield 0.18 ppm. Based on these significant observations, it can be concluded that these chalcogen-bonding catalysts developed herein have an exceptional ability to activate carbonyl groups, thus potentially capable of promoting previously elusive transformations. Based on the experimental results and the observation of

intermolecular noncovalent Se···O interactions. The author proposed a plausible reaction pathway for the process (**Fig. 1.10b**). Initially, upon activation of β-ketoaldehyde via Se···O interaction in the presence of a chalcogen catalyst, the condensation of indole with ketoaldehyde occured to give an isolable intermediate **21**. This intermediate then undergoes a Michael-addition process with chalcogen catalyst-activated ketoaldehyde to generate intermediate **22**. Following that, an aldol condensation reaction occured, which was catalyzed by a chalcogen catalyst, yielding intermediate **23** with appropriately placed functional groups. Finally, an intramolecular cyclization was performed, followed by a dehydration step, to provide the cyclization product **20**.

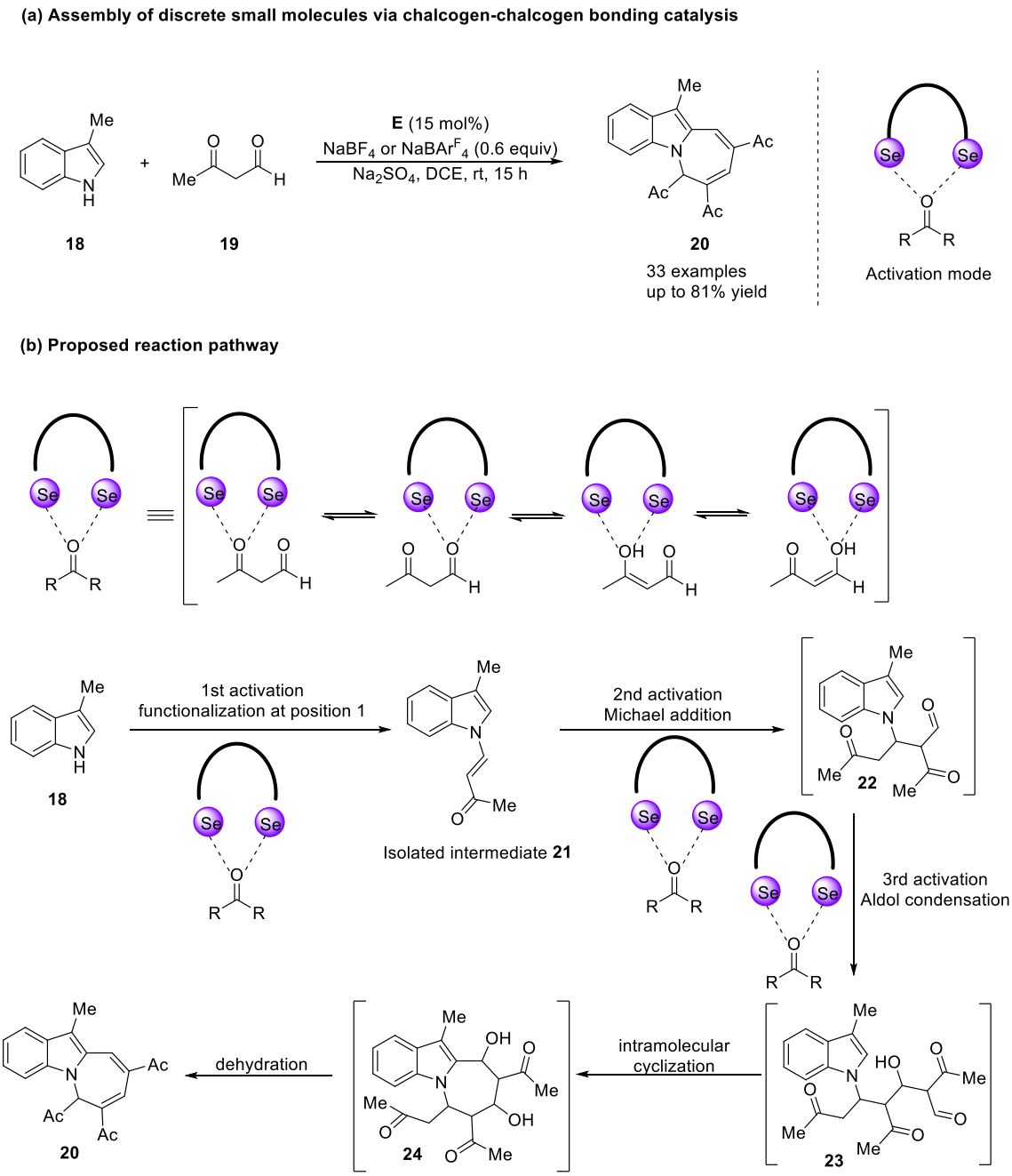

Figure 1.10 (a) Assembly of discrete small molecules via chalcogen−chalcogen bonding catalysis. (b) Proposed reaction pathway.

1.3.2 Bi-functional activation mode with phosphonochalcogenide

One year later, in 2020, Wang and co-workers reported a dual chalcogen-chalcogen bonding catalysis strategy that involves unique chalcogen atoms interacting with two chalcogen-based electron donors, resulting in catalytic activity and enabling chemical processes.[35] Conventional approaches to Rauhut-Currier reactions rely on strongly nucleophilic Lewis bases as promoters. This dual chalcogen-chalcogen bonding catalysis strategy enables simultaneous Se···O bonding interactions between chalcogen-bonded donors, an enone and an alcohol, enabling the realization of Rauhut-Currier-type reactions in a different way (**Fig. 1.11a**). By using comparative control experiment and NMR studies, the author found that "substrate as inhibitor" phenomenon was observed in this reaction, indicating a dual chalcogen-chalcogen bonding interaction approach is operative. Based on these observations, a plausible chemical route was proposed: simultaneous activation of methanol and allows for the efficient addition of methanol to enone. Then, an intramolecular proton-transfer initiates an aldol reaction, followed by MeOH elimination and dehydration to give a cyclization product (**Fig. 1.11b**). This work indicates that the nearly linear chalcogen-bonding interaction can discriminate comparable alkyl groups to give birth to regioselectivity. Using a dual Se···O bonding catalysis method allows for an initial Rauhut-Currier-type reaction to produce an enone product, followed by an alcohol-addition-induced cyclization reaction. Furthermore, the new strategy demonstrates its advantage in that it not only allows less reactive substrates to function well, but it also tolerates inaccessible substrates when utilizing conventional methods.

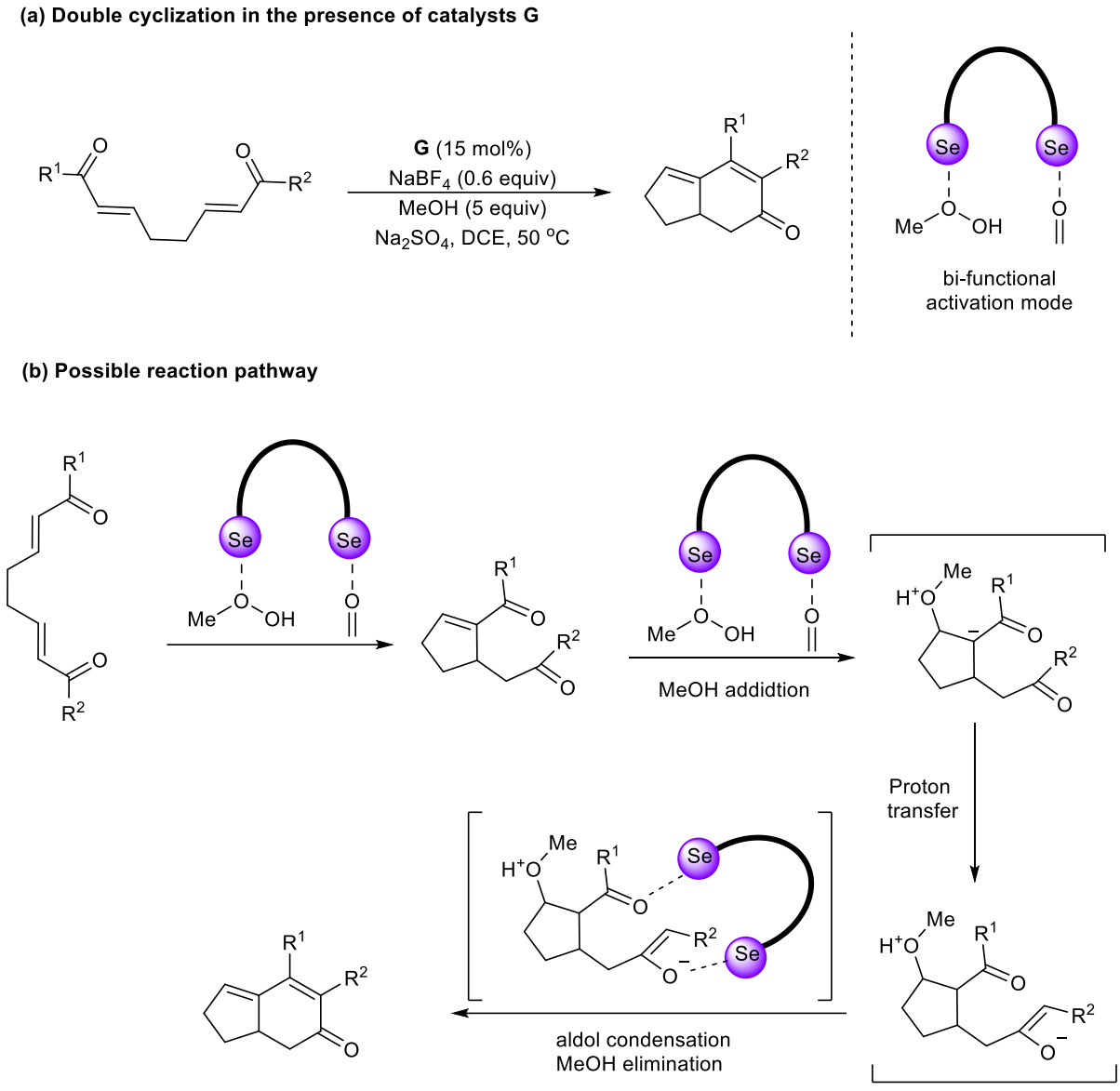

Figure 1.11 (a) Rauhut-Currier-type reactions with catalyst **G.** (b) Possible reaction pathway.

1.3.3 Chalcogen-π activation mode with phosphonochalcogenide

While the occurrence of sulfur- π bonding interaction is a ubiquitous feature in biological systems, utilization of this noncovalent force in a chemical process is still understudied. Herein, Wang's group introduce the notion of chalcogen-π bonding catalysis, which activates molecules in π systems by interacting with the chalcogen and π-electron clouds.[36] Proof-of-concept experiments employing a vinylindole-based Diels-Alder benchmark process show that S···π and Se···π bonding interactions efficiently drive the cycloaddition reaction. Based on the experimental results including steric effect, distance and π-π interaction, the author proposed the Se···π bonding catalysis mode that a Se···π bonded "electron-deficient" indole ring donates electrons to an "undisturbed" phenyl ring. The cycloaddition process fovors under this mode with good stereoselectivity (**Fig. 1.12**).

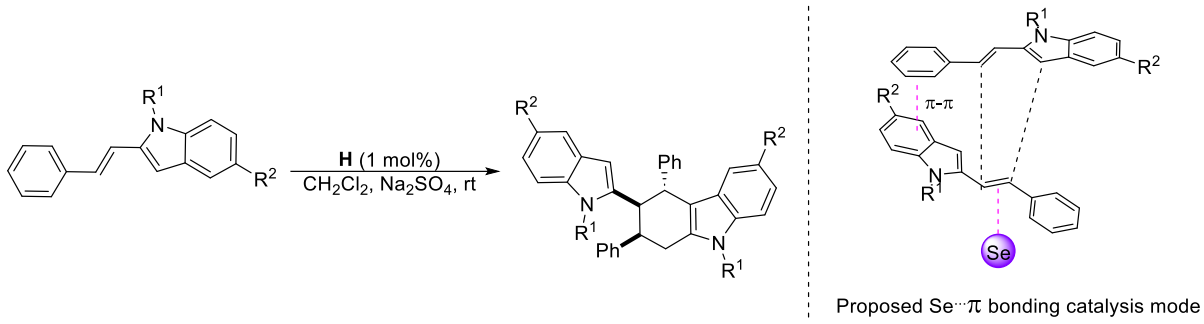

Figure 1.12 H catalysed vinylindole-based Diels-Alder benchmark reaction

As it is well-known in literature, transition metals are primarily responsible for activating alkyne triple bonds, making organocatalysts ineffective in this area. Apart from the alkene activated by PCH catalysis through Se···π bonding interactions to process cycloaddition, triple bonds of alkynes also play a key role in organic processes. In 2023, Wang and co-workers established the first example of the activation of alkynes by chalcogen bonding catalyst, and the weak Se···π bonding interaction can catalyze the intramolecular cyclization of 1,6-diynes, adding a new type of reaction in supramolecular catalysis (**Fig. 1.13**).[37] It is expected that this Se···π bonding catalysis approach would provide a new platform to solve synthetic problems with regard to alkenes, alkynes and the other π-systems.

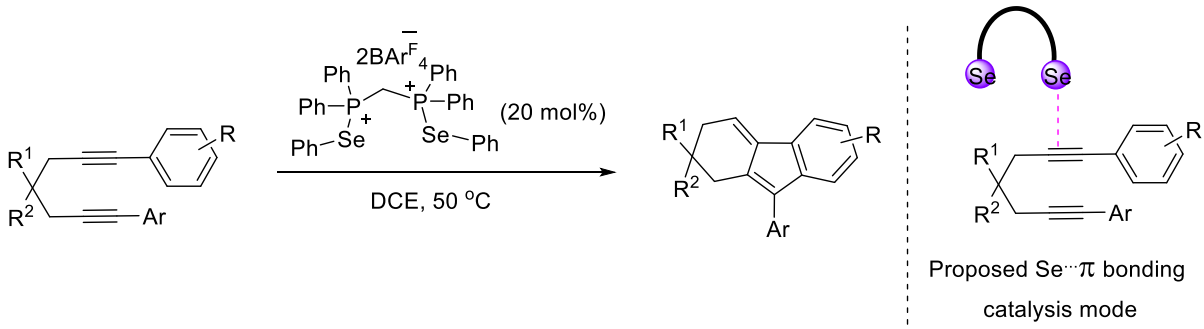

Figure 1.13 Se···π bonding catalyzed cycloaddition of 1,6-diynes

1.3.4 Bifurcation activation mode with phosphonochalcogenide

Recently, our group (By Ma and Loh) developed a catalytic method to synthesize biologically relevant seven-membered ring sugars by using an uncommon bifurcated chalcogen bonding and hydrogen bonding (HB) network (**Fig. 1.14**).[38] According to the density functional theory (DFT) modeling, NMR titration experiments, and *in situ* ^{13}C nuclear magnetic resonance (NMR) monitoring, the authors proposed a contemporaneous activation of multiple functional groups, including a bifurcated chalcogen bonding activation of the carbonyl group on the donor and HB activation of the acceptor between ester group and the catalyst. It should be pointed out that the ester moiety attached to the glycosyl donor is necessary for the formation of the proposed ternary complex for stereocontrol. Further ^{13}C kinetic isotopic effect and kinetic studies proved that the reaction underwent a dissociative S_Ni-type mechanism to get the excellent α-selectivity.

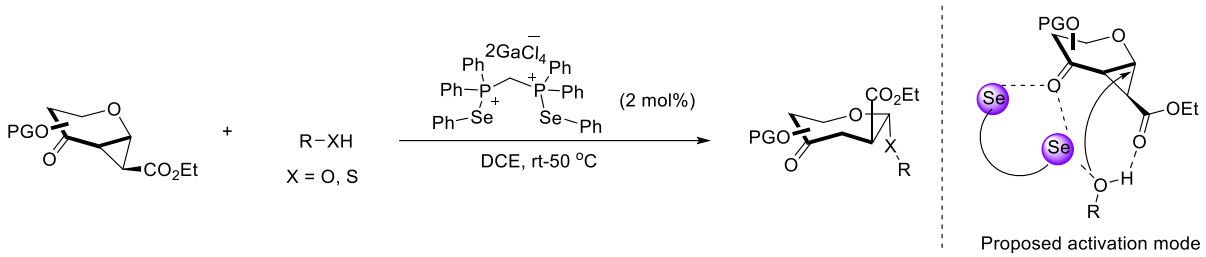

Figure 1.14 PCH catalysed ring expansion to synthesize septanosides through bifurcated chalcogen bonding interaction

1.4 Application of iminosugars in medicine and biological activity

Carbohydrate structures offer potential for new chemotherapeutic targets and therapies due to their various structures and recognition processes. The iminosugars are a diverse set of plant and microbial molecules that have sparked interest due to their propensity to interact with human glycosidases, other proteins and sugar receptors. In their simplest form, they resemble furanose and pyranose monosaccharides, but with nitrogen replacing the oxygen in the ring (**Fig. 1.15a**).[39] This substitution allows for the creation of both monocyclic and bicyclic templates, wherein the nitrogen can be added at a location that is shared by both rings. Usually, hydroxyls are used to substitute the template, but other functional groups, such amides and carboxylic acids are also present in nature and can be substituted in many different ways in synthetic equivalents. This classification includes the four most prevalent ring structures found in nature: pyrrolidine, piperidine, pyrrolizidine and indolizidine (**Fig.1.15b**).[40] These compounds have been given a variety of names in the literature, including aza-sugars, glycosidase inhibitors, and sugar analogues, and the diversity and distribution of natural molecules have been examined.[41] There are now approximately 200 reported as natural products. However, very few have been widely available for drug discovery. Until now, only few iminosugars have been accessible for investigation in medicinal applications. The early compounds were found and studied because they inhibited glycosidase, which is now acknowledged to be unnecessary for pharmacological activity and may have off-target effects. The first two iminosugar medicines are Glyset® and Zavesca®, which are developed from the naturally occurring glucosidase inhibitor 1-deoxynojirimycin. Since the discovery of this first generation, many novel natural compounds with diverse biological activity have been identified, but few are widely available. These compounds' biological features include strong oral bioavailability and particularly selective immune modulatory and chaperoning activities. Although natural products derived from plants and microorganisms are quite effective in some fields, alterations to natural product templates have recently proven quite successful in developing bioactive molecules with good profiles. The topic of iminosugars continues to open up intriguing new potential for therapeutic agent discovery and provides several new tools for precisely changing carbohydrate structures and controlling glycosidase activity *in vivo*.

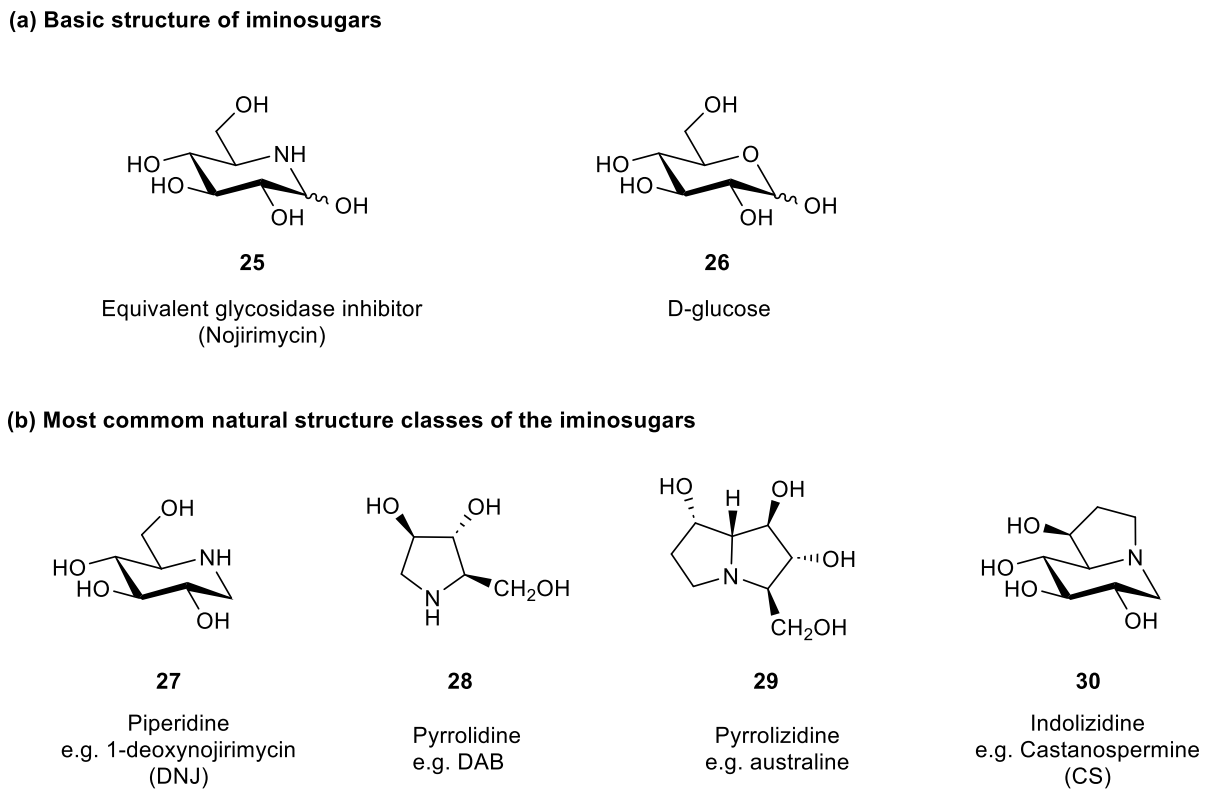

Figure 1.15 (a) Basic structure of iminosugars. (b) Most common natural structure classes of iminosugars.

1.4.1 Iminosugars as clinical and marketed compounds

Specific isolated iminosugars' biological effects have traditionally been limited to the parent natural chemicals or their simple derivatives or prodrugs. As a result, the range of first-generation chemicals investigated has been quite limited. The first-generation iminosugars have been founded on three natural products: swainsonine **31**; deoxynojirimycin (DNJ, **27**) and castanospermine **37** (**Fig. 1.16**). D-Swainsonine (GD0039, 3**1**), a main toxin found in locoweed, is believed to cause neurological problems in livestock.[42] It has numerous pharmacological actions in humans, including inhibiting *N*-linked glycosylation. It is a strong inhibitor of Golgi alphamannosidase II, an immunomodulator and a potential chemotherapeutic. Despite its complex character, it has undergone multiple studies as an anti-cancer medication. Glyset **32** and Zavesca **33**, two marketed first-generation iminosugar medicines, share similarities with the naturally occurring iminosugar DNJ **27**. Glyset **32** has been licensed for treating type II diabetes since 1996. While the *N*-alkylated DNJ derivative Zavesca **33** (Miglustat) is licensed to treat type I Gaucher's disease and Niemann-Pick type C (NPC) illness. Recent clinical trials of two first-generation iminosugars for treating LSDs support the idea that second-generation molecules will be more effective. isoFagomine (AT2101, Plicera, **34**) provides an alternative to substrate reduction therapy for the treatment of Type I Gaucher and Migalastat **35** has recently reported successful results in phase II clinical trials for Fabry's disease. In addition to uses in oncology and LSDs, first-generation

iminosugars have demonstrated antiviral activity. Celgosivir **36**, an ester prodrug of castanospermine **37**, is the most advanced clinical-stage antiviral iminosugar for Hepatitis C virus (HCV) infection.[43]

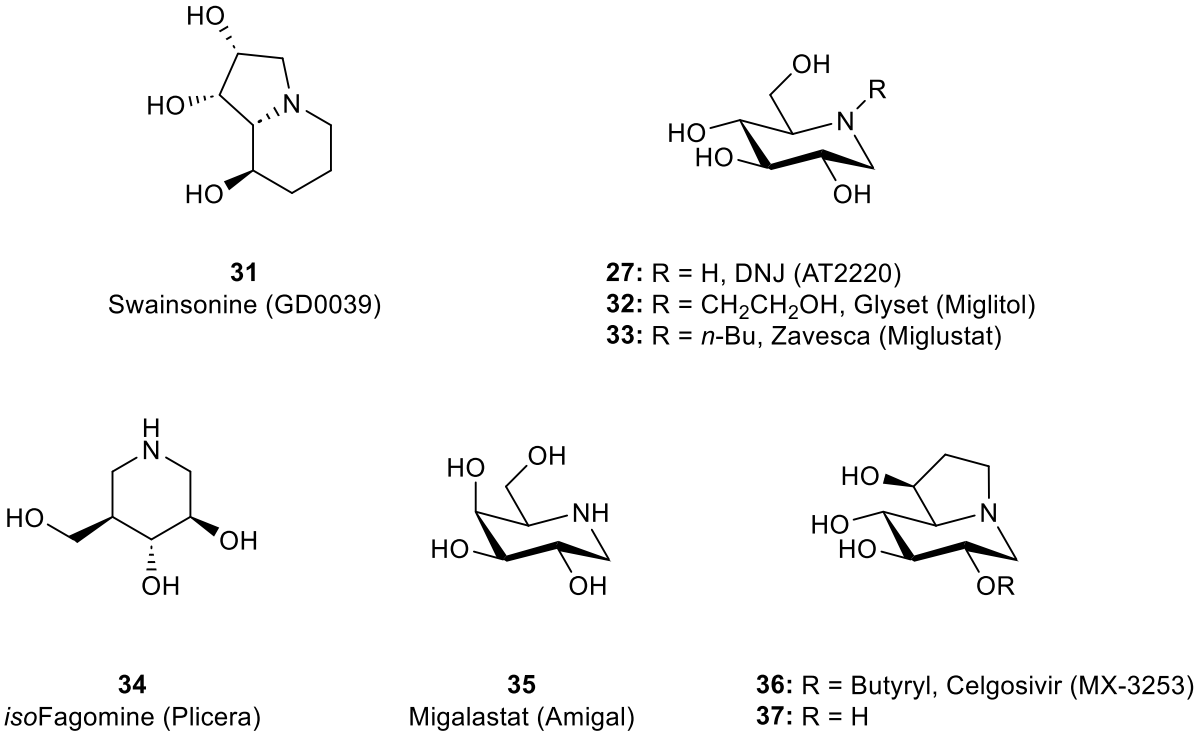

31
Swainsonine (GD0039)

27: R = H, DNJ (AT2220)
32: R = CH_2CH_2OH, Glyset (Miglitol)
33: R = *n*-Bu, Zavesca (Miglustat)

34
*iso*Fagomine (Plicera)

35
Migalastat (Amigal)

36: R = Butyryl, Celgosivir (MX-3253)
37: R = H

Figure 1.16 Selected first-generation iminosugar clinical candidates and marketed drugs.

1.4.2 Future perspective

With enhanced analytical and biological equipment and increased knowledge of carbohydrate biochemistry, this sector of drug development is proceeding quickly nowadays. Despite restricted access to them, iminosugars have demonstrated considerable potential in their capacity to interact with different mammalian biochemical processes involving carbohydrates, without demonstrating harmful effects and with high oral availability. With the availability of more natural products and synthesized compounds, it is clear that exciting new applications will emerge as a result of their diverse biological features. Iminosugars can exhibit high stereoselectivity in biological activity. This selectivity is related to the chemical and biological variability in the structural information of tiny sugars. The incredible biological diversity in such small molecules demonstrates a remarkable economy in structural information in nature, much exceeding what amino acids can achieve in terms of molecular weight. The problems with broad glycosidase activity of early molecules such as DNJ are largely due to the screening and isolation methods used for their discovery, and with the realization that glycosidase activity is not required, the field of iminosugars is no longer limited by attempting to reduce off-target glycosidase effects.

1.5 Site-selective transformation of carbohydrates

Carbohydrates perform crucial roles in biology and are closely linked to all physiological and pathological processes.[44] They are the structural foundation of genetic information (deoxyribose in DNA), an energy source (like starch) and a major component of the cell walls seen in bacteria and plants when they are in their polymer form, or polysaccharides.[45] Their oligomer form, also known as oligosaccharides, serves a variety of purposes in cell adhesion and intercellular communication. Glycans are normally attached to lipids or proteins through an *O*- or *N*-glycosidic linkage.[46] In addition to being the building block of all poly- and oligosaccharides, their monomer form, or monosaccharide, is also a coenzyme (ribose in acetyl-CoA) and an essential metabolite (ribose in adenosine triphosphate: ATP) involved in a variety of in-cell biochemistry.[47] Due to their diverse and important roles in biology, they themselves and their natural/non-natural derivatives have been attracting significant attention from diverse research fields as biomolecules of interest, medicines and biomaterials.

Therefore, creating a method for modifying, synthesizing, and functionalizing carbohydrates is crucial. However, because of the inherent molecular complexity of carbohydrates, developing such a system is not simple. First of all, because carbohydrates include several hydroxy groups with comparable reactivities, it is challenging to selectively functionalize one over the others. Second, by quenching the reactivity (e.g., protonolysis), the many hydroxy groups frequently make it difficult to use polar reactive species (e.g., carbanions). Third, because unprotected carbohydrates are very polar, they are frequently insoluble in standard organic solvents. To achieve the necessary transformation, a polar coordinating solvent such as water, DMSO, or DMF must be used, which would also deactivate reactive species. Carbohydrate chemistry relies on protecting group chemistry to conceal nontarget hydroxy groups and disclose only the desired hydroxy group, reducing synthetic challenges.[48] The recurrent protection/deprotection sequence reduces the synthesis efficiency of carbohydrate chemistry.

Since these issues with carbohydrate chemistry have long been known, experiments have been carried out to allow for the selective transformation of carbohydrate polyols without a significant need on protective groups. The usage of diol structures, which are frequently found in carbohydrate substrates, is one of the representative methods toward achieving the goal. Using an external catalyst or reagent to regulate the reactivity of the carbohydrate substrates is another practical strategy. Enhancement of one of the hydroxy group's intrinsic reactivity or even reversal of the intrinsic reactivity order should be achievable if the reagent/catalyst is sufficiently reactive and selective.

1.5.1 Specific reactivity of carbohydrates

The reactivity of carbohydrate is influenced by several factors. Steric barrier around a hydroxy group in reaction, acidity of a hydroxy group, hydrogen bonding networks in the hydroxy groups and protecting groups on the nonreacting hydroxy groups are all factors that needed to be considered. Carbohydrates' primary hydroxy groups are often more reactive than secondary ones due to their greater

steric accessibility. The difference in steric hindrance has been used to selectively functionalize primary hydroxy groups, particularly with sterically bulky electrophiles. For instance, the methyl α-D-glucopyranoside 6-OH **38** group was shown to be preferentially protected in 75% yield as its tert-butyldiphenylsilyl (TBDPS) ether **39** (**Fig. 1.17a**). [49] Other sterically bulky groups were installed preferentially at the 6-OH group, including pivaloyl ester, *p*-toluenesulfonyl ester and triphenylmethyl ether. Because of steric factors, the secondary hydroxy groups in carbohydrates interact with one another differently. If inductive and other electronic effects on the hydroxy groups are similar, an equatorial hydroxy group is frequently more reactive than its axial counterpart (**Fig. 1.17b, left**). A secondary hydroxy group that is equatorially orientated and has an axial neighbor is more reactive (**Fig. 1.17b, right**). As an example, 9.1% of the 3,6-bispivaloylated product **41** was produced when pivaloyl chloride was added to methyl α-D-mannoside **40** (**Fig. 1.17c**).[50] The most reactive hydroxy group is the primary hydroxy group at the 6-position. The second most reactive hydroxy group is at the 3-position, where it is surrounded by one axial (2-OH) and one equatorial (4-OH) hydroxy group. Due to its hemiacetal structure, the anomeric hydroxy group of a reducing sugar has a significantly lower pKa than other hydroxy groups, making selective deprotonation and functionalization of the anomeric hydroxy group conceivable. After 6-*O*-TBDPS D-glucopyranose **42** was treated with 1.1 equiv of sodium hydroxide and 1.0 equiv of decyl triflate, 1-*O*-alkylated product **43** was produced in a 58% yield (**Fig. 1.17d**).[51]

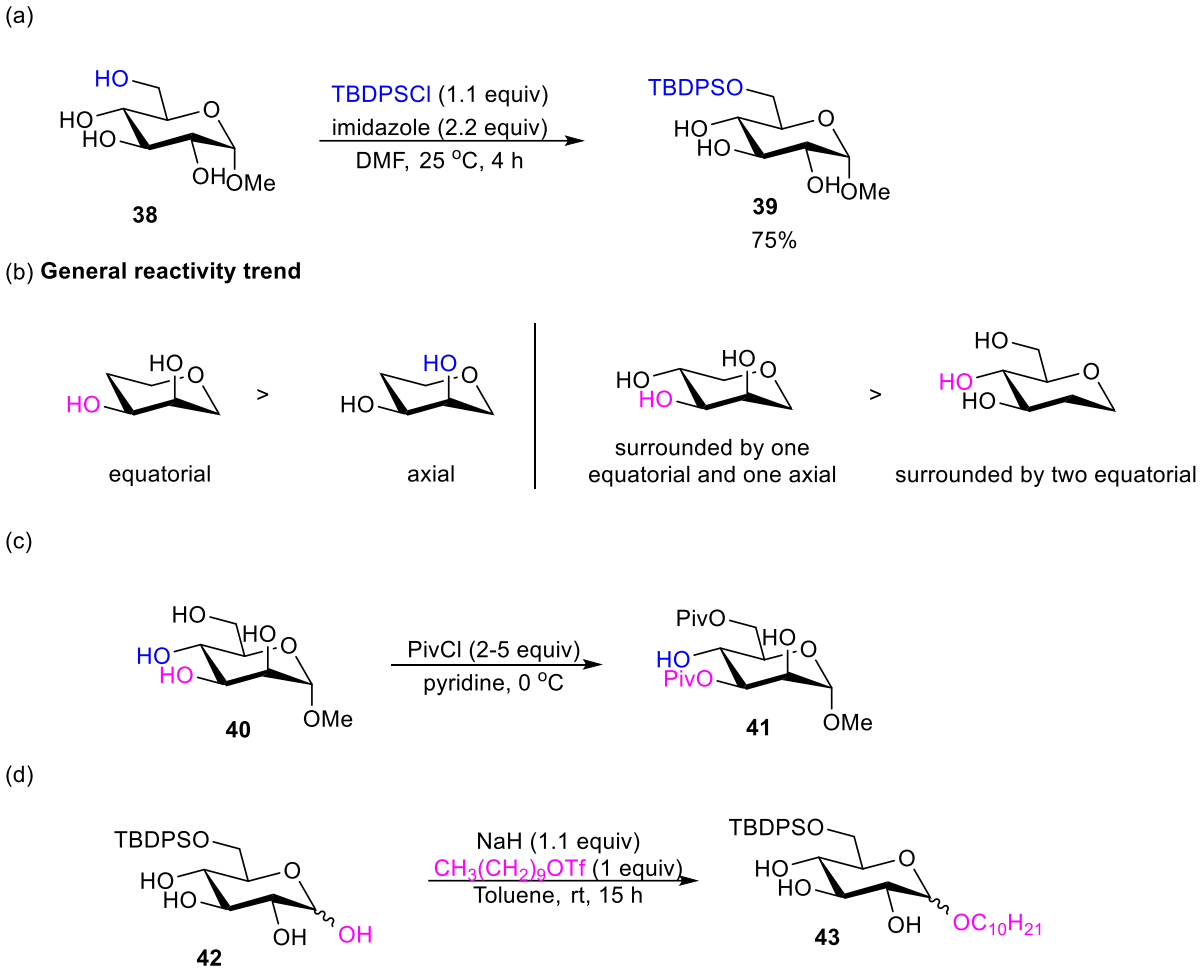

Figure 1.17 Effects on innate reactivity of carbohydrates. (a) Selective functionalization of a sterically less hindered primary hydroxy group. (b) General reactivity trend of secondary hydroxy groups of carbohydrates. (c) Difference of steric environments among secondary hydroxy groups in a pyranose. (d) Selective deprotonation of anomeric hydroxy group.

Intramolecular hydrogen bonding between hydroxy groups in a carbohydrate can affect the reactivity of the hydroxy groups. Since the negative charge on the oxygen atom increases in a hydrogen bond donor but decreases in an acceptor, hydroxy groups acting as donors of hydrogen bonds are more nucleophilic than acceptors of hydrogen bonds. The transition state stabilizes as a result of the hydrogen bonding interaction's tendency to grow along the reaction coordinate. Yoshida and co-workers observed that the acetylation reaction of nonprotected octyl β-D-glucopyranoside **44** with 0.7 equiv of acetic anhydride and 5 mol% of 4-dimehylaminopyridine (DMAP) in the presence of 9.7 equiv of potassium carbonate produced a greater proportion of 3-*O*- **45** and 4-*O*-acetylated products **46** than the sterically less hindered and consequently more reactive 6-*O*-acetylated product **47** (**45**:**46**:**47** = 42:37:19, **Fig. 1.18**).[52]

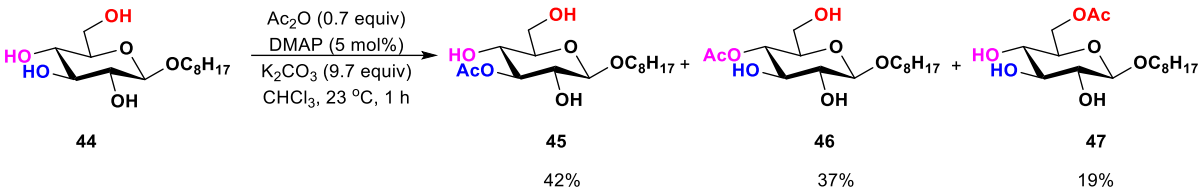

Figure 1.18 Hydrogen bonding networks in a pyranose affect regioselectivity. (a) Acetylation of octyl β-D-glucopyranoside with acetic anhydride and DMAP.

Protecting groups on hydroxy groups in a carbohydrate substrate not only mask them for avoiding undesired reactions but also modulate the reactivity and stereochemical outcomes. A typical example is seen in the effect of the 4,6-*O*-benzylidene acetal group on the stereoselectivity of a glycosylation reaction. According to Crich and colleagues, the 4,6-*O*-benzylidene acetal group is essential for the β-mannosylation processes that take place between glycosyl acceptors and glycocosyl triflates. They used triflic anhydride and a sterically bulky base, 2,6-di-tert-butyl-4-methylpyridine (DTBMP), to treat glycosyl sulfoxide **48** at -78 °C. Then, they treated the *in-situ* generated glycosyl triflate **49** with glycosyl acceptor to obtain β-mannoside product **50** in 90% yield, while leaving α-mannoside product **51** undetectable (**Fig. 1.19**).[53]

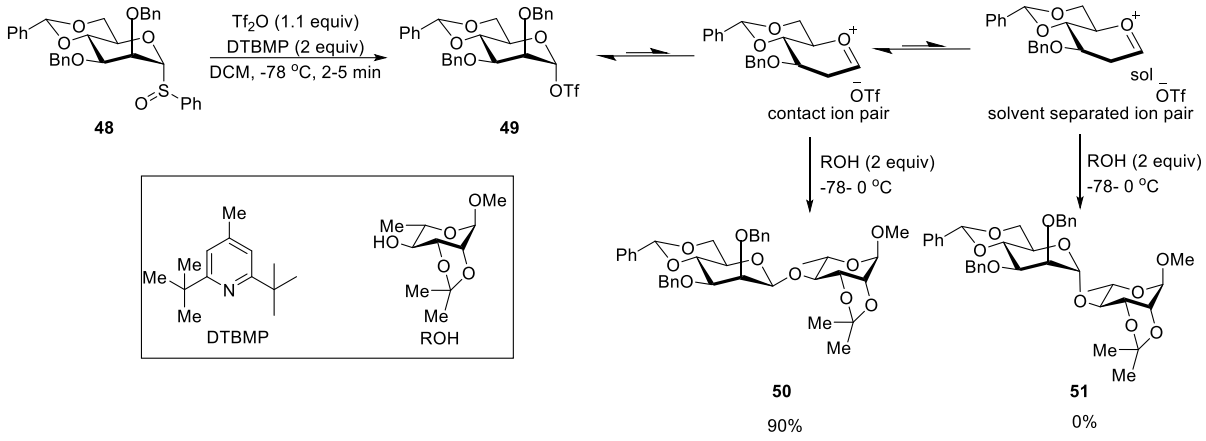

Figure 1.19 Protecting group effects on the innate reactivity of carbohydrates. A 4,6-*O*-benzylidene acetal group is a critical determinant of the stereochemistry in a β-mannosylation reaction.

1.5.2 Catalytic methods for site-selective functionalization of carbohydrates

As carbohydrates play a vital role in all the biological process, it's essential to develop methods for synthesizing, functionalizing and manipulating carbohydrates for further understanding of their functions. There are several ways for the transformation of carbohydrates, including covalent bond-forming catalysis, achiral metal catalysis, acid-base catalysis, asymmetric catalyst, borinate metal hybrid catalysis and radical catalysis.

In 2011, Taylor and co-workers reported diarylborinic acid-catalyzed regioselective acylation of carbohydrates (**Fig. 1.20**).[54] They found that the efficient and universal approach of dialylborinic acid catalysis may be used to monotosylate pyranoside derivatives **53** with three secondary hydroxyl groups **52**. Furthermore, the range of selective acylation, sulfonylation and alkylation is expanded to include

1,2- and 1,3-diols that are not derived from carbohydrates; the method's efficiency, generality and ease of use are comparable to those of cutting-edge protocols, such as the widely used organotin-catalyzed or -mediated reactions. Competition experiments, kinetics and catalyst structure-activity relationships are used to investigate the mechanistic aspects of the organoboron-catalyzed processes. These results are in line with a mechanism wherein the electrophilic species is reacted with by a tetracoordinate borinate complex **54** during the turnover-limiting step of the catalytic cycle.

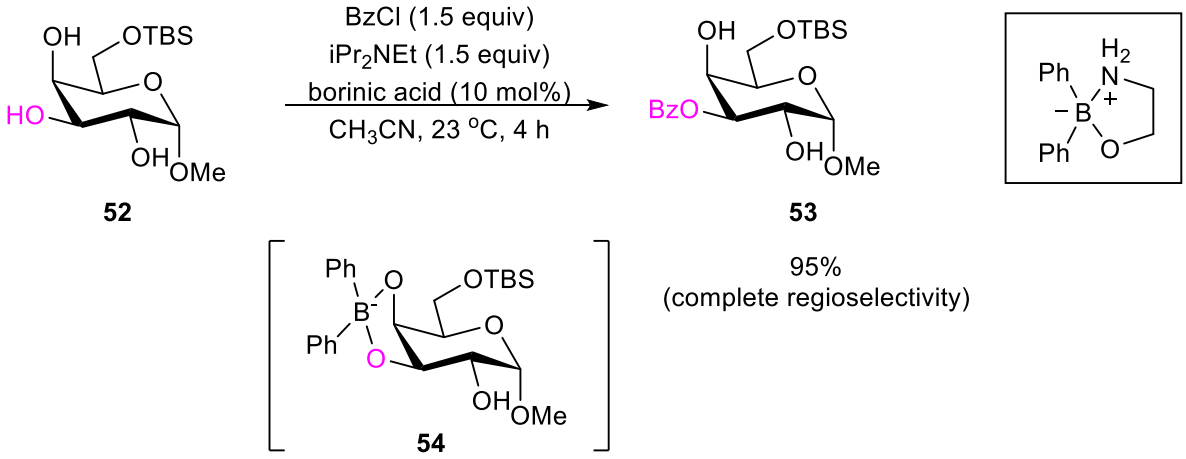

Figure 1.20 Regioselective acylation of carbohydrates through a catalytic generation of borinate esters

In 2016, Dong and co-workers reported an iron(III)-catalyzed regioselective alkylation of minimally protected carbohydrates with broad substrate scope including those possessing 1,2-*cis*- or 1,2-*trans*-diol motifs (**Fig. 1.21**).[55] Initially, they discovered that basic iron(III) salts, including $FeCl_3$ and $FeBr_3$, could alkylate 4,6-protected methyl α-D-mannopyranoside in a selective manner. However, the regioselectivity of these simple salts was low for other *cis*-diols. Following ligand screening, they discovered that [Fe-$(dibm)_3$] (dibm: diisobutyrylmethane) offered strong regioselectivity for a variety of substrates. After treating nonprotected methyl β-D-galactopyranoside **55** with 1.5 equiv of benzyl bromide and 1.5 equiv of potassium carbonate in the presence of 10 mol% of [$Fe(dibm)_3$] at 80 °C for 24 hours, a 90% yield of 3-*O*-benzylated product **56** was obtained. The mechanism is proposed to proceed via acyclic dioxolane-type intermediate **57a-57b**, formed between the iron(III) species and two adjacent hydroxyl groups.

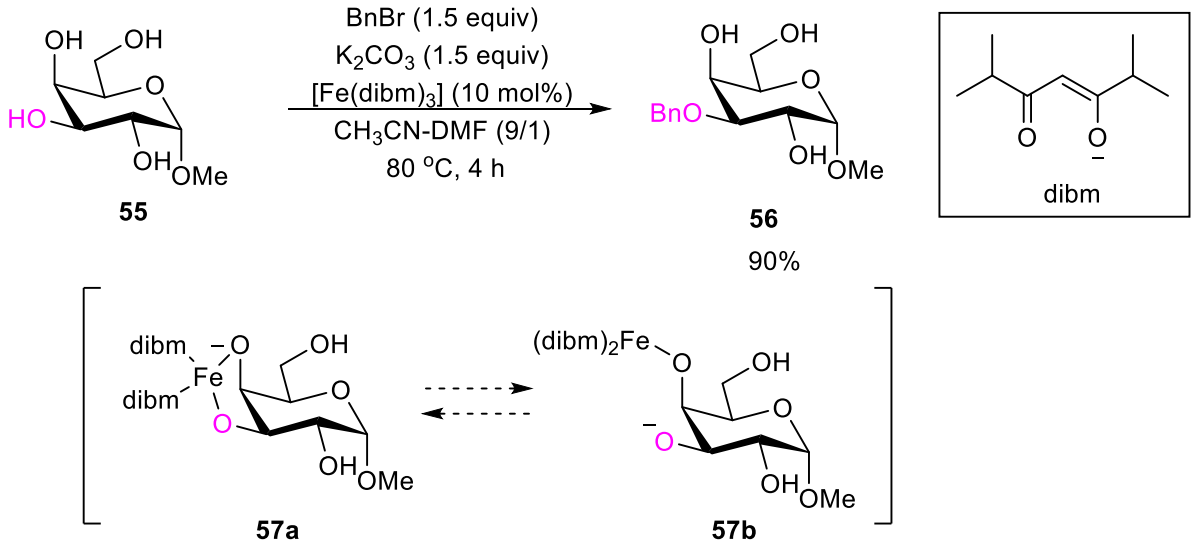

Figure 1.21 Iron-catalyzed regioselective transformation of 1,2-*cis*- and 1,2-*trans*-diols.

In 2013, Schmidt and co-workers reported that bis(4-nitrophenyl) phosphate and Schreiner's thiourea cooperatively catalyzed glycosylation reactions between a glycosyl trichloroacetimidate **58** and a glycosyl acceptor **59** with moderate stereoselectivity (**Fig. 1.22**).[56] ^{1}H NMR studies revealed that thiourea and phosphate, a glycosyl acceptor, formed a rapid combination quickly. The development of stereoselective glycosidic bonds is subsequently encouraged by this ternary complex's interaction with a glycosyl donor **61**. Although the mechanism is interesting, its substrate scope and stereoselectivity were not as broad and high as other reported examples.

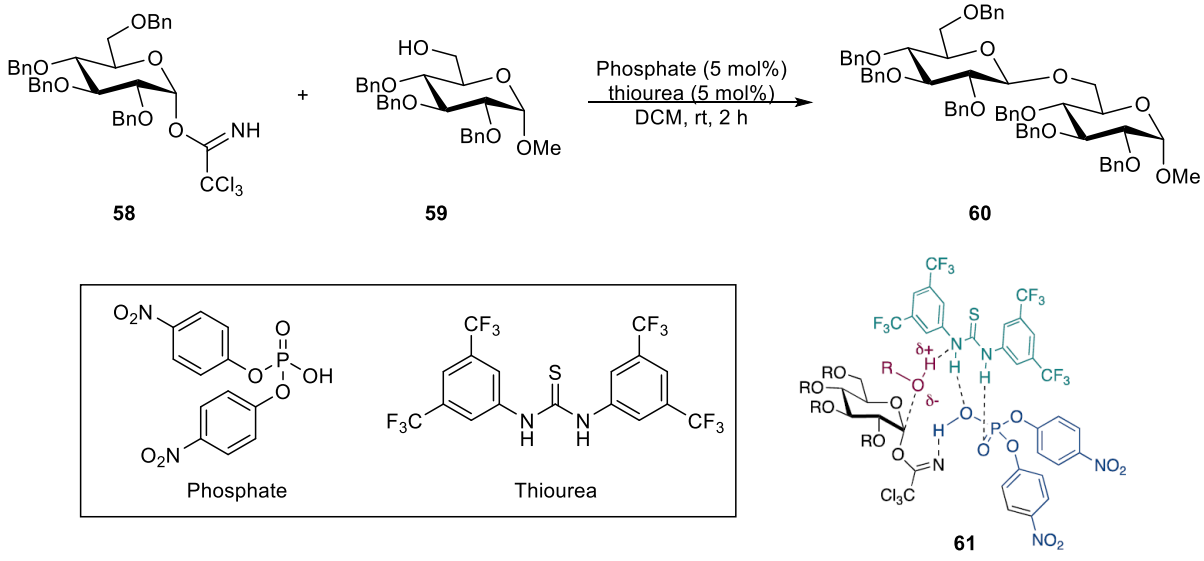

Figure 1.22 An example of two-component acid−base catalyzed β-selective glycosylation

In 2007, Kawabata and co-workers reported an organocatalytic method for the chemo- and regioselective acylation of monosaccharides using *C*2-symmetric chiral 4-pyrrolidinopyridine (PPY) catalyst **63** (**Fig. 1.23**).[57] They postulated that the main hydroxy group at the 6-position of

carbohydrates would preferentially establish a hydrogen bond with a catalyst due to its high reactivity. The conformation of the carbohydrate would be fixed by additional interactions between the catalyst and other hydroxy groups (e.g., 2-OH and 3-OH) to place a particular hydroxy group (e.g, 4-OH) of the substrate in close proximity to reactive acylpyridinium species. Anticipating that amide carbonyl groups would establish a hydrogen bond with the 6-OH and that the amino acid's varied side chains would establish further contacts with the carbohydrates, they selected an amino acid as the interacting motif in the catalyst. Tryptophan was discovered to provide the most selective catalyst **63**, which is in line with the observation that two tryptophan moieties are substantially conserved in the β-glucosidases' substate recognition sites. After octyl β-glucopyranoside **61** was treated with 1.1 equiv of isobutyric anhydride and 1.5 equiv of 2,4,6-collidine in chloroform containing 1.0 mol% of **63** for 24 hours at -20 °C, 4-acylated product **62** was produced in 98% yield and 99% regioselectivity.

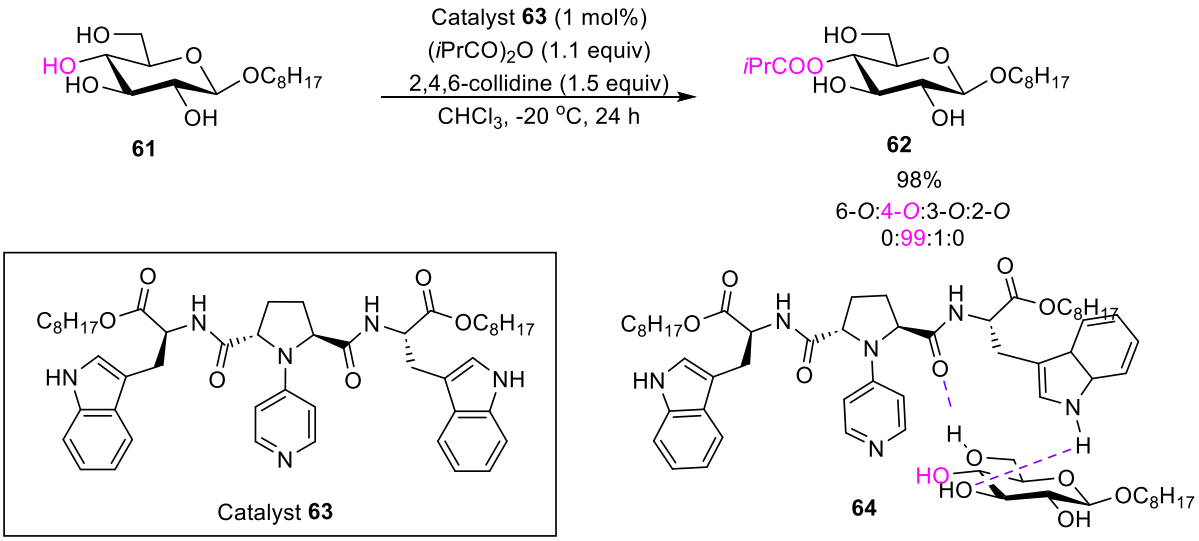

Figure 1.23 Regioselective isobutyrylation of the 4-OH group by the chiral 4-pyrrolidinopyridine catalyst

In 2017, Taylor and co-workers revealed a combination of two distinct activation mechanisms in the regioselective *O*-arylation of carbohydrates (**Fig. 1.24**).[58] They experimented with Chan-Lam coupling mediated by copper(II) between a hydroxy group of poorly protected carbohydrates **65** and phenylboronic acid. 4-*O*-arylated product **66** was obtained in 72% yield by treating methyl α-L-rhamnopyranoside with 5.0 equiv of phenylboronic acid and 2.0 equiv of copper(II) acetate in the presence of 4.0 equiv of diisopropylethylamine and 4A molecular sieves. This 4-*O*-selectivity was exceptional in light of numerous instances of boronate-assisted regioselective transformations, in which a reaction occured between an equatorially oriented hydroxy group (3-OH group in this instance) in a boronate derived from 1,2-cis-diol. When the reaction mixture was analyzed using ^{1}H NMR without the presence of copper(II) acetate, boronate was formed, forming bonds with the cis-hydroxy groups at positions 2 and 3. This suggested that boronate acted as a temporary protective group for the *cis*-hydroxy

groups. DFT calculations proposed two possible transition states (TSs) to explain the 4-*O*-selectivity. In TS **68**, the 4-OH group is deprotonated from a phenyl copper species connected to the boronate ester, whereas in TS **67** transmetalation between a monosolvated copper alkoxide generated from the 4-OH group and acetate-activated boronate occured intramolecularly. The 4-*O*-selective arylation reaction was accelerated in both structures by a Lewis acid/base interaction between the acetate ligand and the boronate group, which stabilized the transition states. Phenylboronic acid plays a unique role in preserving nonreacting hydroxy groups and speeding the arylation of nearby hydroxy groups, revealing a new aspect of boronic acids' interactions with carbohydrates.

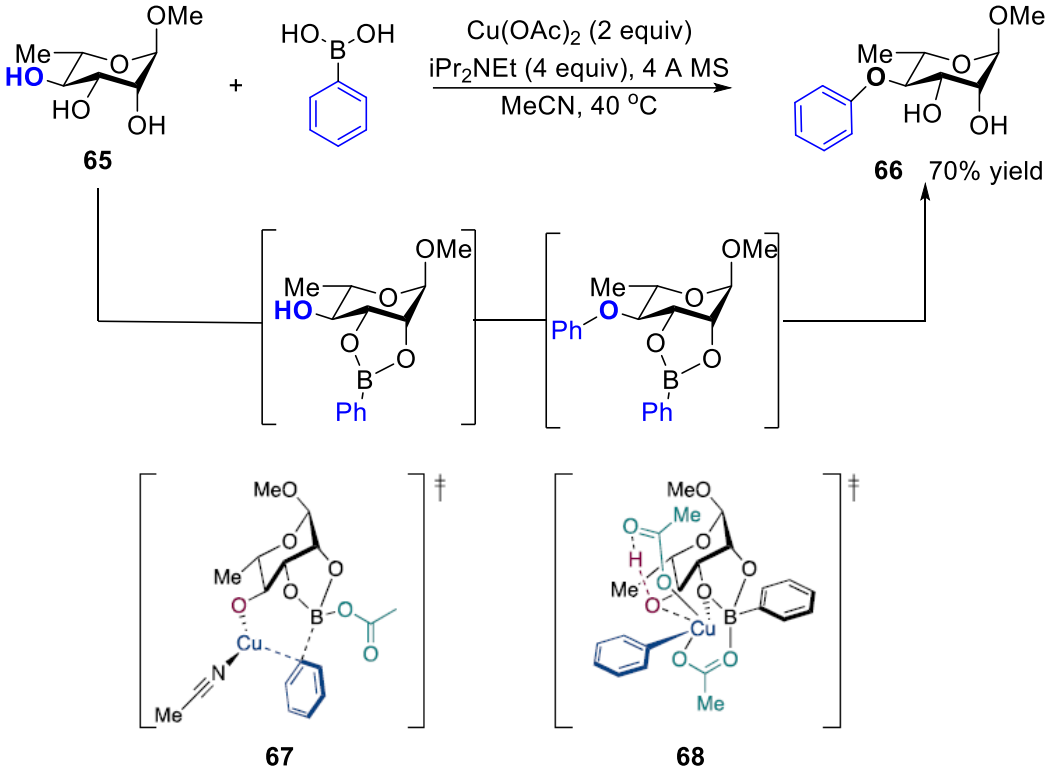

Figure 1.24 Regioselective Chan−Lam *O*-arylation of carbohydrates and two postulated transition states

Minnaard, Witte and co-workers reported C3- selective carbon−carbon bond formation in unprotected monosaccharides using photoredox catalysis in 2017 (**Fig. 1.25a**).[59] Drawing from MacMillan's groundbreaking research, photocatalyzed hydrogen atom transfer (HAT) could be specifically carried out at the α-carbon of an unprotected hydroxy group when dihydrogen phosphate was present as a hydrogen bond acceptor. They applied the reaction conditions to non-protected methyl glycosides **69**. Due to the limited solubility of nonprotected glycosides, MacMillan's catalyst system ([Ir(dF(CF$_3$)ppy)$_2$(dtbpy)]) required DMSO as a solvent. PF$_6$(IrF, dF(CF$_3$)ppy: 3,5-difluoro-2-[5-(trifluoromethyl)-2-pyridinyl]phenyl, dtbpy: 4,4'-di-tert-butyl-2,2'-dipyridyl) as a photoredox catalyst, quinuclidine as a reagent and tetrabutylammonium dihydrogen phosphate as an acceptor resulted in modest yields of C3-alkylated compounds **71** (**Fig. 1.25b**).[60] The mechanism of C3-selectivity was

unclear. Vinyl sulfone, vinyl phosphate and cyclopentenone were effective somophiles. Several methyl α-glycosides including glucoside, xyloside and alloside, showed C3-equatorial alkylation selectivity. However, β-glycosides and mannosides had poorer stereoselectivity. Methyl galactosides did not react.

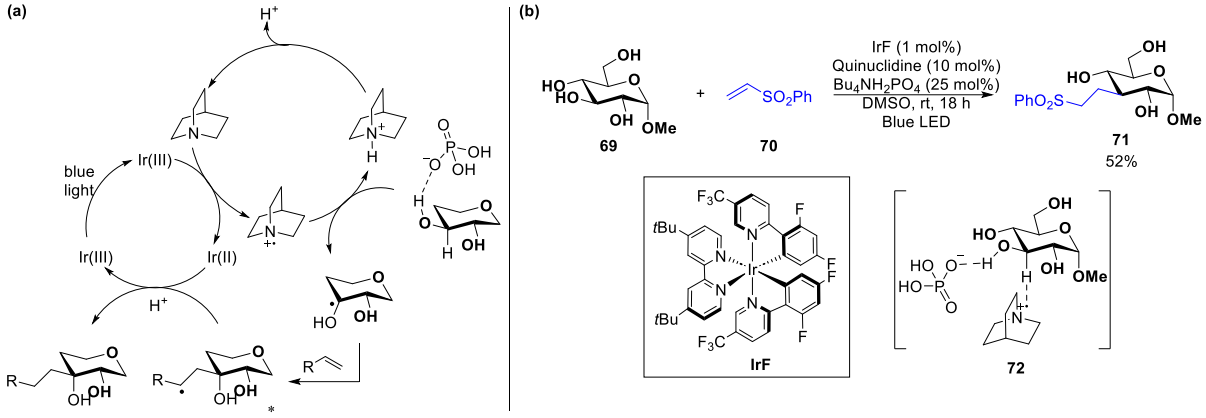

Figure 1.25 Radical-mediated *C*-alkylation of carbohydrates. (a) A postulated mechanism of radical-mediated *C*-alkylation of carbohydrates promoted by a photoredox catalyst−hydrogen atom transfer catalyst−hydrogen bond acceptor catalyst ternary system. (b) A representative example of a radical-mediated *C*-alkylation reaction of a carbohydrate.

2. Design and aim of the thesis

Carbohydrates play pivotal roles in biology, and as a result, they are closely linked to almost every physiological and pathological event. Therefore, it's of great importance to develop a method of synthesizing, functionalizing and manipulating carbohydrates. However, there are still limited synthetic methods for some kinds of carbohydrates, and iminosugars are one of them. Iminosugars are polyhydroxylated secondary and tertiary amines in which the molecules resemble monosaccharide sugars in which the ring oxygen is replaced by the nitrogen. A class of widely distributed plant and microbial molecules known as iminosugars has gathered attention because of their capacity to interact with human glycosidases, other proteins and sugar receptors. Despite the widespread use of iminosugars, synthetic production of stereoselective iminoglycosylations is quite limited.

In chapter 3, an efficient method to synthesize stereoselective iminosugar 2-deoxy(thio)glycosides from bicyclic iminoglycal carbamates catalyzed by PCH catalyst was developed. The method worked with both glucal and galactal donors, as well as a variety of *O*- and *S*-glycosyl acceptors. It was also compatible with common protection (acetyl, benzyl ether, etc.) at the glycal donor's 3 and 4 positions. Detailed mechanistic studies were carried out to reveal the catalyst's surprising function of sequentially activating the glycosyl acceptor and donor in both the upstream and downstream phases of the reaction. All in all, this work provided a good strategy for building iminosugar scaffold.

In chapter 4, in light of our group's prior results (done by Bhaskara Rao and Loh) regarding asymmetric ring opening reaction using oxanorbornadiene with carbohydrate polyols, which is catalyzed by a Rh(I) and boronic acid synergistic system. An approach using chiral Rh(I) catalysis combined with boronic acid catalysis is presented in site-selective functionalization of the anomeric oxygen of anomeric unprotected saccharides to form α-selective arylhydronapthalene glycosides which were more commonly found bioactive molecules. Furthermore, apart from the oxanorbornadiene donor, the methodology could be used for a variety of allylic carbonates donors with sterically and electronically differing substituent ranging from aliphatic, cyclic to aromatic substituents. Interestingly, position 2 functionalized product were formed in this method, which was totally different from the position 3 product reported in the literature. Obviously, according to the comparative experiments with the enantiomer ligand of the matched ligand, chiral catalyst control was determined to be responsible for the site-selective functionalization.

3. Harnessing multi-step chalcogen bonding activation in the α-stereoselective synthesis of iminoglycosides

3.1 Background

3.1.1 Chalcogen bonding catalysis with phosphonochalcogenide

Recently, chalcogen bonding catalysis has emerged as a novel approach to organic synthesis. It has proven to be a valuable synthetic tool that can effectively tackle challenging reactivity and selectivity problems. For a chalcogenide catalyst, the replacements and the chalcogen atom are changeable. Because of the polarization effect, the chalcogen bonding strength is arranged in the following order: O < S < Se < Te. Among these kinds of chalcogen bonding catalysts, phosphonium chalcogenide or phosphonochalcogenide (PCH) catalysts which were discovered by Wang and co-workers[61] were investigated and applied to organic synthesis mostly. PCH catalysts are highly active which a phosphonium substituent is attached to the chalcogen atom (**Fig. 3.1a**), they can be easily and modularly synthesized while there is plenty of room for structural modification from either the phosphonium part or the chalcogen part. Based on the properties of the PCH catalysts and the relationship between structure and catalysis, a variety of catalysis strategies were established, including Se···O bonding catalysis, Se···π bonding catalysis, dual chalcogen bonding catalysis and chalcogen-chalcogen bonding catalysis (**Fig. 3.1b**). These catalysis modes showed wide potential in organic synthesis, enabling achievement of a diverse array of transformations while addressing reactivity and selectivity issues (**Fig. 3.1c**). Despite the significant advancements in PCH catalysis's ability to solve complex synthetic problems, there are still some areas that these catalysts haven't tackled. Take the chemistry of carbohydrates as an example, despite recent scientific advancements, no reports on PCH-catalyzed glycosylation reaction have been published, with the exception of our groups'. Therefore, there is still a lot of room for PCH catalysis in carbohydrate chemistry.

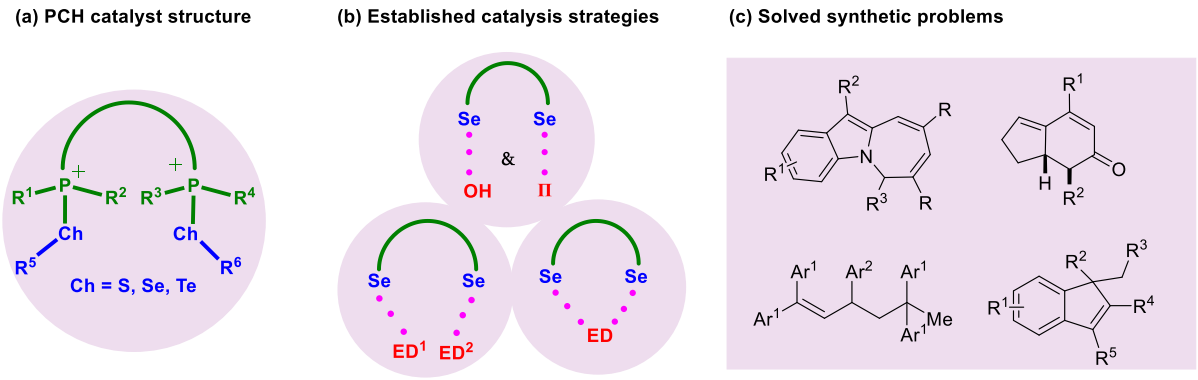

Figure 3.1. (a) PCH catalyst structure. (b) Some established catalysis strategies. (c) Solved some synthetic problems

3.1.2 Reported method for synthesis of iminosugar 2-deoxy(thio)glycosides

A first synthesis of iminosugar-type 2-deoxy(thio)glycoside mimics was described in 2020 by Carmen Ortiz Mellet and colleagues (**Fig. 3.2**).[62] Full α-stereoselectivity was demonstrated by cerium(IV) ammonium nitrate, which efficiently promoted the synthesis of 2-deoxy *S*-glycosides in the presence of thiols, most likely by catalytic HNO_3 produced *in-situ*. Besides, the production of 2-deoxy *O*-glycosides were shown to be more successful using cooperative phosphoric acid/Schreiner's thiourea organocatalysis, thus broadening the approach's use. They believe that the key step is activating a bicyclic iminoglycal carbamate to yield a very reactive acyliminium cation. The authors, to some extent, had provided a useful method to access to the formation of the 2-deoxyiminoglycosides. However, there were a wide range of drawbacks that existed in this methodology. First of all, the Lewis acid loading of cerium(IV) ammonium nitrate (CAN, 50 mol%) was too high, which was not effective. Secondly, the only catalyst of strong Bronsted acid such as phosphoric acid was not sufficient for this reaction. Finally, the substrate tolerance was limited under the reported acidic conditions with Schreiner's thiourea as the cocatalyst. For example, when sterically more hindered secondary alcohols on saccharide substrates were used under such conditions, migration of the isopropylidene protecting group was detected, and the yield became much lower.

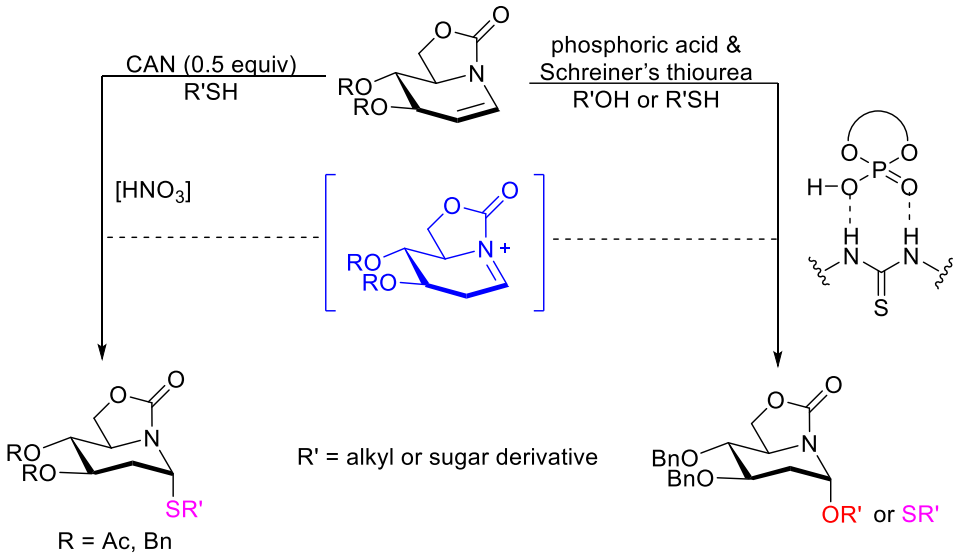

Figure 3.2. Reported synthesis of 2-deoxyiminosugar glycosides

3.2 Project design

Iminoglycosides are a kind of glycomimetic containing a well-recognized privileged piperidine core scaffold which is relevant in a wide range of diseases (**Fig. 3.3**).[63,64] These include influenza infection,[65] cystic fibrosis,[66] lysosomal storage disorders (Gaucher disease)[67] and, more recently, the replication of the coronavirus SARS-CoV-2.[68] Additionally, natural chemicals like nojirimycin (NJ) **73** and deoxynojirimycin **27**,[69] an inhibitor of β-glucosidase, have the iminoglycoside scaffold. There are also reports of antihyperglycemic benefits from the naturally occurring 2-deoxy derivative

fabomine.[70] It is also known that drug development is interested in the iminoglycoside scaffold. In particular, iminosugar frameworks based on the glucose mimic, like Miglustat (Zavesca) **33** and Miglitol **32** (Glyset), had been licensed for the treatment of diabetes and for the treatment of Gaucher and Niemann-Pick C diseases (**Fig. 3.3a**).[69] In chaperone-based therapy for Fabry disease,[69] galactose mimics like Lucerastat **75** and Migalastat **35** (Galafold) have also shown promise (**Fig. 3.3b**). Recently, The discovery of α-sp^2-iminosugars as a useful glycomimetic with potential anti-inflammatory **77** and anti-cancer characteristics **76** has attracted a lot of interest (**Fig. 3.3c**).[69] Past research has shown that the sp^2-iminoglycosyl donors are also chemical mimics that mirror the glycosyl profile of typical donors of monosaccharides.[71]

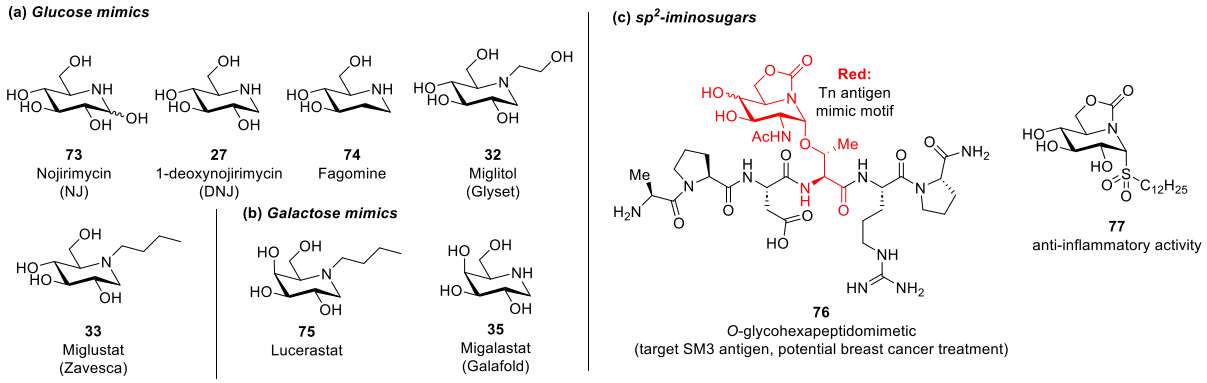

Figure 3.3. Biologically relevant iminoglycosides.

Although iminosugars are widely used, very little has been done to synthesize stereoselective iminosugar-based conjugates. Compared to traditional pyrano- and furanosylations, catalytic iminoglycosylation is definitely rare. When compared to the iminoglycal congener, this is especially noticeable in the numerous instances in the *O*-2-deoxyglycosylations.[72] The known challenges in iminoglycal donor activation from previous literature are of significant synthetic interest.[63] Since there are a lot of the difficulties existed in 2-deoxyiminoglycosides synthesis (see **3.1.2**) and limited synthesized method for access to the biological iminoglycosides, it was necessary to develop a novel strategy to solve these problems. Besides, exploring the possiblity of harnessing PCH catalysis in the glycosylation fiels is good for diversification of glycosylation modes. Therefore, a strategy of PCH catalysts activated iminoglycals to react with a wide range of acceptors to form exclusive α-selective iminoglycosylated products was designed as follows (**Fig. 3.4**).

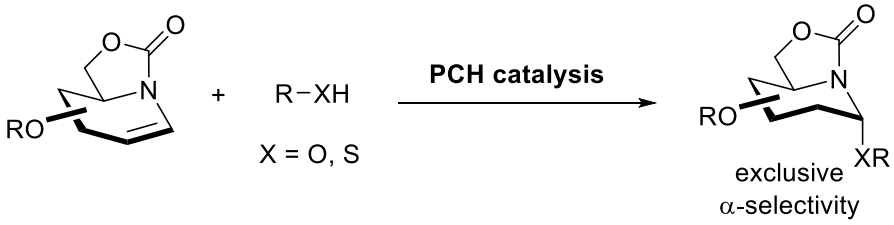

Figure 3.4. PCH catalysis of iminoglycals to synthesize α-selective iminoglycosides (this work)

3.3 Optimization of conditions

The initial study involved examining a panel of frequently used noncovalent catalysts in a model reaction involving 3,4-disiloxoiminoglycal **78a** and *n*-octanol **79a** as a typical glycosyl donor and acceptor respectively. The reaction was carried out at 50 ℃ with 1,2-dichloroethane as the solvent in order to increase the success rate. Initially, a wide range of noncovalent catalysts were tested on this reaction, it was unexpected that the well-known, versatile halogen bonding-based catalysts **A**[73] and **B**[74], which our group had previously successfully used to catalyze glycosylations,[75] were likewise unable to activate the more difficult iminaglycals (Table 3.1, entry 1 and 2). It was likewise unsuccessful in my attempts with the Schreiner's hydrogen bonding thiourea catalyst **C**[76], a finding that was supported by earlier research (Table 3.1, entry 3).[63] Next, The latest iterations of ChB-based phosphonochalcogenide (PCH) catalysts[61] were then examined. To our delight, PCH catalysts resulted in an obvious improvement in catalytic robustness (Table 3.1, entries 4-12, 14). Using the 1,2-bis-(diphenylphosphino)ethane (dppe) derived PCH catalyst **D**, 88% of the iminoglycoside **80a** could be produced with exclusive α-selectivity (Table 3.1, entry 4), similar good results were also obtained with a tetrachlorogalate congener of the dppe scaffold **E** (Table 3.1, entry 5), it indicated that fine-tuning of the central diphosphino core was possible. When PCH derivatives **F**-**H** generated from Xantphos were screened, the target product **80a** was produced with excellent yield and selectivity as well (Table 3.1, entry 6-8). Overall, it was obvious that the PCH catalysts remained efficient even when the counteranion was changed from triflate to non-coordinating, sterically hindered ones such as tetrachlorogallate or tetrakis(3,5-bis(trifluoromethyl)phenyl)borate (BAr^F). This PCH-based catalytic manifold was unlikely to be influenced by triflate interference, based on the same reactivity profiles towards variants of counteranions. By deepening the chalcogens' sigma-holes through the utility of derivatives **I-J** and **N** which were developed by Wang group[77] lately, it was easy to find that all these dication-conjugated planar backbone catalysts could obtain excellent yield of **80a** with absolute α-selectivity (Table 3.1, entry 9-10, 14). Furthermore, using triphenylphosphine derived PCH catalyst **K** (Table 3.1, entry 11) and other chalcogen atom like Te catalyst **L** (Table 3.1, entry 12) could form product **80a** with good yield and excellent α-selectivity. Besides, decreasing the catalyst loading of **N** to 2% would reduce the yield and increase the time but without any change on selectivity (Table 3.1, entry 15). It's interesting to note that at room temperature, 2% trifluoroacetate (Table 3.1, entry 16) could quickly enhance the reaction while trace phosphoric acid **M** (Table 3.1, entry 13) was unable to catalyze it even at 50 ℃. Further screening of solvents including toluene and tetrahydrofuran couldn't improve the results, which resulted in a product **80a** yield of 45% (Table 3.1, entry 17) and 83% (Table 3.1, entry 18) respectively. The yield of **80a** might be increased to 87% by reducing the catalyst loading to 0.5% (Table 3.1, entry 19), however this would need a three-fold increase in reaction time, up to 72 hours. Based on the screening results of these catalysts and solvents, the ideal conditions were easy to figure out: methylene

chloride as the solvent, catalyst **J** at 2 mol% catalyst loading, and room temperature for 24 hours to provide the final product **80a** with exclusive α-selectivity and 93% yield (Table 3.1, entry 10).

Table 3.1. Condition screening of ChB catalyzed iminoglycosylation.

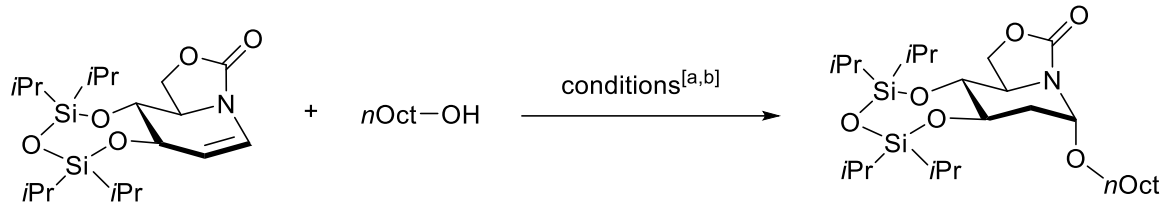

78a **79a** **80a**

Entry	Cat (mol%)	Solvent	Additive (mol%)	Time (h)	Yield (**80a**)	α : β
1	**A** (5 %)	DCE	-	48	n.d.	-
2[c]	**B** (3 %)	DCM	-	40	n.d.	-
3	**C** (2 %)	DCM	-	48	n.d.	-
4	**D** (5 %)	DCE	-	3	88%	>20/1
5	**E** (5 %)	DCE	-	20	88%	>20/1
6	**F** (5 %)	DCE	-	5	89%	>20/1
7	**G** (5 %)	DCE	-	20	86%	>20/1
8	**H** (5 %)	DCE	-	21	78%	>20/1
9	**I** (5 %)	DCE	-	2	91%	>20/1
10[c]	**J** (2 %)	DCM	-	24	93%	>20/1
11	**K** (5 %)	DCE	-	45	89%	>20/1
12	**L** (5 %)	DCE	-	45	83%	>20/1
13	**M** (0.5 %)	DCE	-	3	6%	>20/1
14	**N** (5 %)	DCE	-	2	91%	>20/1
15[c]	**N** (2 %)	DCM	-	36	84%	>20/1
16[c]	TfOH (2 %)	DCM	-	8	75%	>20/1
17[c]	**J** (2 %)	Toluene	-	24	45%	>20/1
18[c]	**J** (2 %)	THF	-	24	83%	>20/1
19[c]	**J** (0.5 %)	DCM	-	72	87%	>20/1
20[c]	**J** (2 %)	DCM	K_2CO_3 (20%)	24	n.d.	-
21[c]	**J** (2 %)	DCM	(*R*)-BINAP (20%)	24	n.d.	-
22[c]	**J** (2 %)	DCM	TBAC (20%)	24	15%	>20/1
23[c, d]	**J** (2 %)	DCM	3Å molecular sieves (15 mg)	24	n.d.	-

Conditions: [a] **78a** (0.05 mmol), **79a** (0.075 mmol), catalyst, 50 °C, solvent (0.2 mL), time, argon. [b] Yield and α:β selectivity of **80a** were determined by crude ^{1}H NMR spectra analysis using 1,3,5-trimethoxybenzene as an internal standard. n.d.: not detected. [c] Conducted at rt. TBAC = tetrabutylammonium chloride. TfOH = trifluoromethanesulfonic acid.

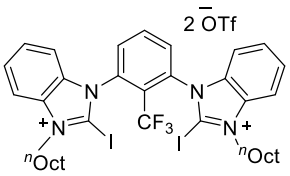

A

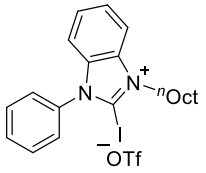

B

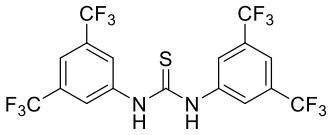

C

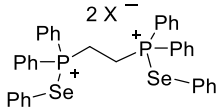

D, X= OTf
E, X= $GaCl_4$

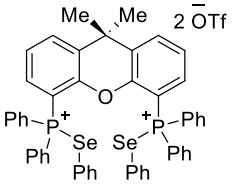

F

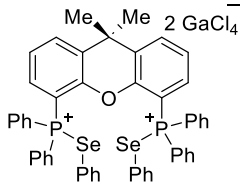

G

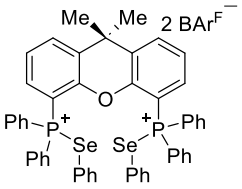

H

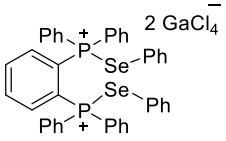

I

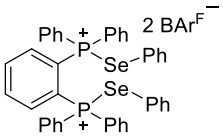

J

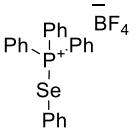

K

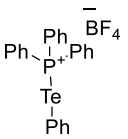

L

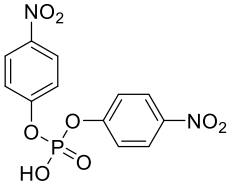

M

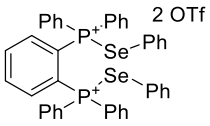

N

Additionally, it was necessary to carry out the required verification controls using well-known ChB catalytic poisons from the literature[78] which had a very high affinity for binding to chalcogens, in order to make sure that ChB activation catalysts was essential to the process.[79] First, the catalyst was terminated and found no product **80a** formed by introducing 20 mol% (*R*)-BINAP as a phosphine poison at the optimal condition (Table 3.1, entry 21). Second, the addition of halide poison, which was achieved at the optimal condition by employing 20 mol% tetrabutyl ammonium chloride (TBAC), significantly inhibited the catalysis of ChB and produced a 15% NMR yield of **80a** (Table 3.1, entry 22). These diagnostic poisoning tests confirmed that manifolds based on sigma holes were involved in the catalytic mode of action.

3.4 Substrate scope study

Once the optimal condition was achieved, the substrate scope was tested in order to increase the synthetic utility of this approach (**Figure 3.4** and **Figure 3.5**). Overall, the methodology was compatible with a wide variety of *O*- and *S*-glycosyl acceptors with different stereochemical environments as well as a broad range of iminoglycal scaffolds, including glucosyl (**Figure 3.4**) and galactosyl (**Figure 3.5**). Additionally, the exclusive α-selectivity was obtained across the whole substrate range.

Firstly, the application of saccharide acceptors in the 2-iminoglycosylation process was examined, and it was shown that different naturally occurring sugar structures with different protective groups installed could be readily assimilated using this methodology. These included D-glucopyranoses (**80b, 80d, 80e, 80i and 80j**), D-galactopyranoses (**80c, 80k**), D-fructopyranoses **80f**, D-ribofuranoses **80g** and L-

rhamnopyranose **80h**. Additionally, this protocol accommodated a wide range of primary and secondary hydroxyl groups that were located at various places within the pyrano/furanoside rings.

Next, some easily available aliphatic alcohols were investigated as possible nucleophiles. To our delight, this approach also included steric robustness in the form of a wide range of primary alcohols (**80a-80o**) from straight chain, propargyl, to benzylic alcohols; Even sterically difficult tertiary alcohol acceptors **80s**, such as 1-adamantanol, could be effectively used in conjunction with secondary alcohols (**80p–80r**), which ranged from isopropanol to the sterically bigger 2-adamantanol. Furthermore, lipidic chiral alcohols with biological significance, such as testosterone **80t** and menthol **80u**, could likewise be utilized as glycosyl acceptors. Additionally, the biologically significant Tn antigen mimetic scaffold would be easier to enter into 2-deoxyiminoglycoside derivatives if amino-acid acceptors were added. It was delightful to find that this approach could tolerate *N*-terminus Fmoc and *C*-terminus Boc (tert-butyloxycarbonyl) protected L-serine **80v** and L-threonine **80w** derivatives. This permited compatibility with protective group techniques that were orthogonal and frequently used in solid phase peptide synthesis. Moreover, this method could also accommodate phenolic acceptors (**80x, 80y**) and thiol-based acceptors (**80z, 80za**) without any depletion of the anomeric selectivity.

Considering the importance of protecting group tolerance in chemical glycosylations, iminoglycosylation's adaptability was investigated in protecting group permutations. In this strategy, "arming" protective groups like benzyl **80zb** and TBS groups (**80zc, 80zd**) were well-suited. Crucially, this ChB-catalyzed approach could also be used with more difficult iminoglucal substrates with electron withdrawing “disarming” protecting groups,[80] like acetyl, to create fully protected schemes in (**80ze-80zi)** or hybrid schemes in **80zd** with a TBS group that had good yields and didn’t negatively impact the exclusive α-selectivity. Additionally, it was observed that the acetyl protected iminoglucal donor could withstand a wide variety of glycosyl acceptors, including saccharide, simple alcohols, phenolic and thiol-based ones.

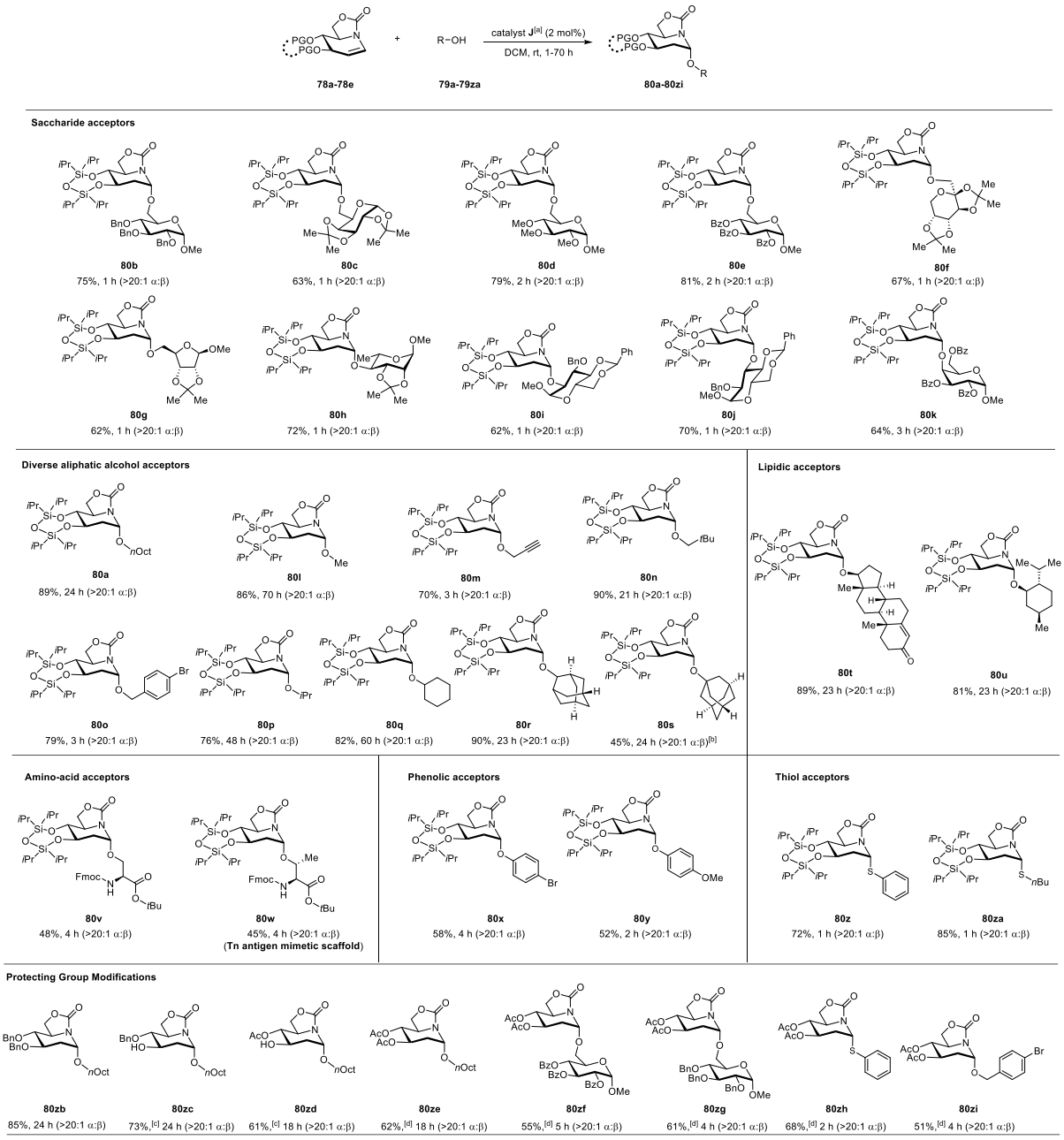

Conditions: [a] **78a** (0.2 mmol), **79a** (0.3 mmol), rt, CH_2Cl_2 (0.8 mL), time, argon. Isolated yields after silica gel chromatography, α:β ratios are shown in parenthesis respectively. α:β ratios were determined by crude ^{1}H-NMR spectra analysis. [b] 40 °C. [c] The TBS protecting group at the 3-OH position was cleaved under the catalytic conditions. [d] Catalyst **D** (2 mol%) was used instead, 40 °C. Me = methyl. Et = ethyl. *i*Pr = isopropyl. TBS = *tert*-butyldimethylsilyl. rt = room temperature. For X-ray structure, thermal ellipsoids shown at 50% probability and the monomeric component of the tetrameric unit cell for **80a** is displayed.

Figure 3.4. Substrate scope of glucosyl iminoglycal donors

After the successful preparation of a wide range of iminoglucosides, it was necessary to expand the substrate scope to iminogalactal donors (**Figure 3.5**). Luckily, galactosyl iminosugars could also be accessed with robustness preservation using the ChB catalyzed approach. A wide range of nucleophiles, such as saccharide-based acceptors (**82a, 82b, 82h, 82i, 82j, 82k, 82l**), lipidic acceptors **82c**, sterically hindered 2-adamantanol **82d**, thiol-based acceptor **82e**, benzyl alcohol acceptor **82f** and linear aliphatic

alcohol **82h**, could be utilized to produce the desired iminogalactosides with reliable exclusive α-selectivity and good to excellent yields. Crucially, access into the 2-deoxy variant of the SM3 antigen core scaffold **82g** could also be easily obtained by using protected L-threonine. An examination of protecting groups was also beneficial, as this ChB-catalyzed approach allowed for the tolerance of arming groups like benzyl and TBS, disarming acetyl groups and even donors with hybrid protecting schemes. It was likewise crucial to highlight that this approach was more generally feasible in synthetic handling because it did not utilize Schlenk or strict water exclusion strategies over the whole scope.

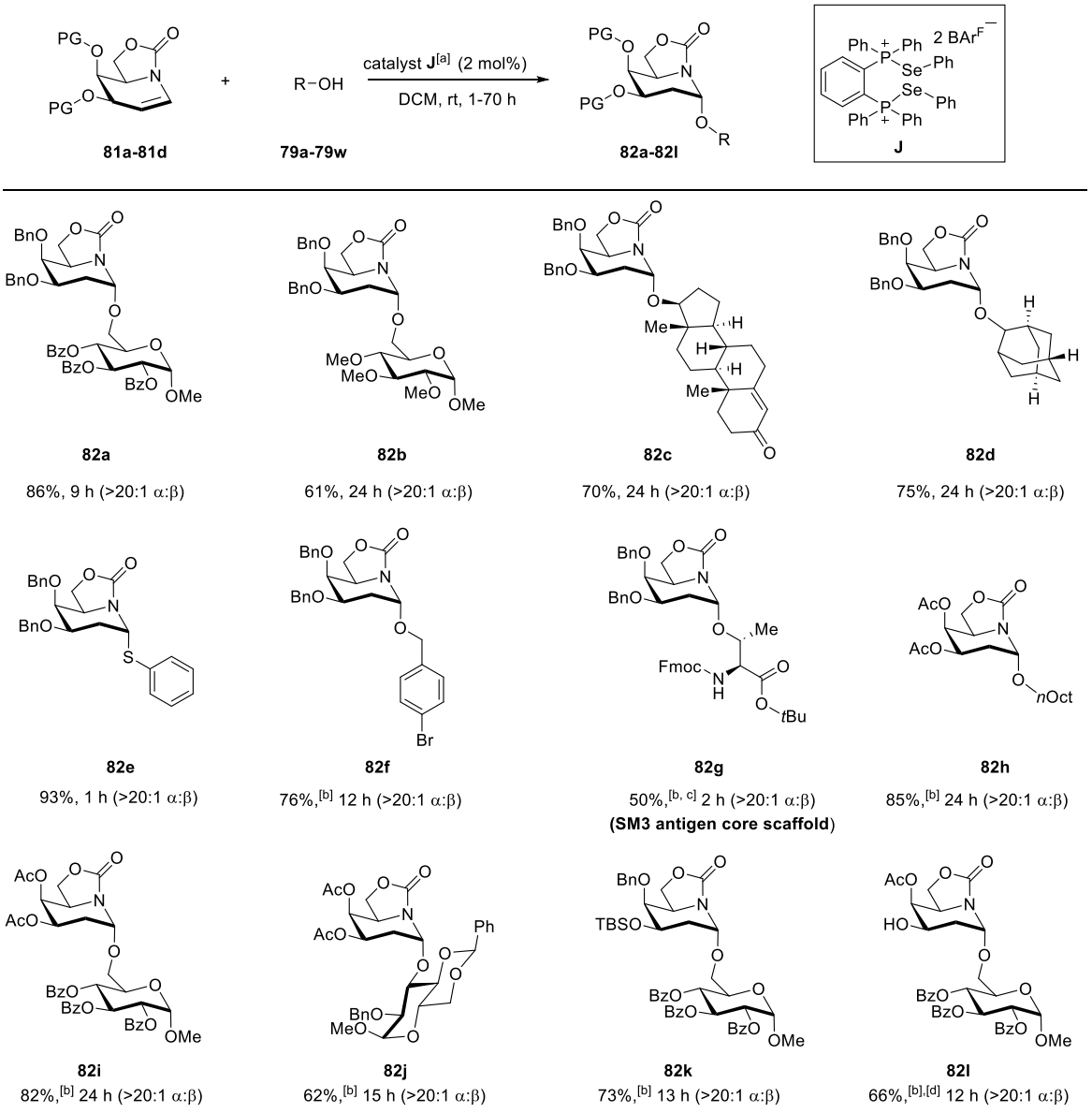

Conditions: [a] **81a** (0.2 mmol), **79a** (0.3 mmol), rt, CH_2Cl_2 (0.8 mL), time, argon. Isolated yields after silica gel chromatography, α:β ratios are shown in parenthesis respectively. α:β ratios were determined by crude ^{1}H-NMR spectra analysis. [b] 40 °C instead. [c] **81a** (0.1 mmol), **79w** (0.15 mmol), CH_2Cl_2 (0.4 mL) instead. [d] The TBS protecting group at the 3-OH position was cleaved under the catalytic conditions. Me = methyl. Et = ethyl. *i*Pr = isopropyl. TBS = *tert*-butyldimethylsilyl. Fmoc = fluorenylmethyloxycarbonyl. rt = room temperature.

Figure 3.5. Substrate scope of galactosyl iminoglycal donors

3.5 Mechanistic investigation

3.5.1 Observation of intermediate 83 between donor 78a and catalyst J

The appearance of a novel product peak was unexpectedly noticed in the NMR tube during the performance of NMR titrations of the PCH catalyst **J** against the iminoglucal donor **78a** in order to comprehend participating NCIs that might contribute to catalysis (**Figure 3.6**). Through thorough isolation and comprehensive characterization of the unexpected result, the molecule was definitively identified as a water addition product **83** onto the glycal. The existence of trace water in ambient conditions—when water was not purposefully removed from the reaction flask—was most likely the cause of this water source. This came as a little surprise because the majority of 2-deoxyglycosylations that had been documented were suggested to mechanistically involve the direct addition of alcohols across the C1-C2 olefin,[81] frequently by means of an initial C2 protonation.

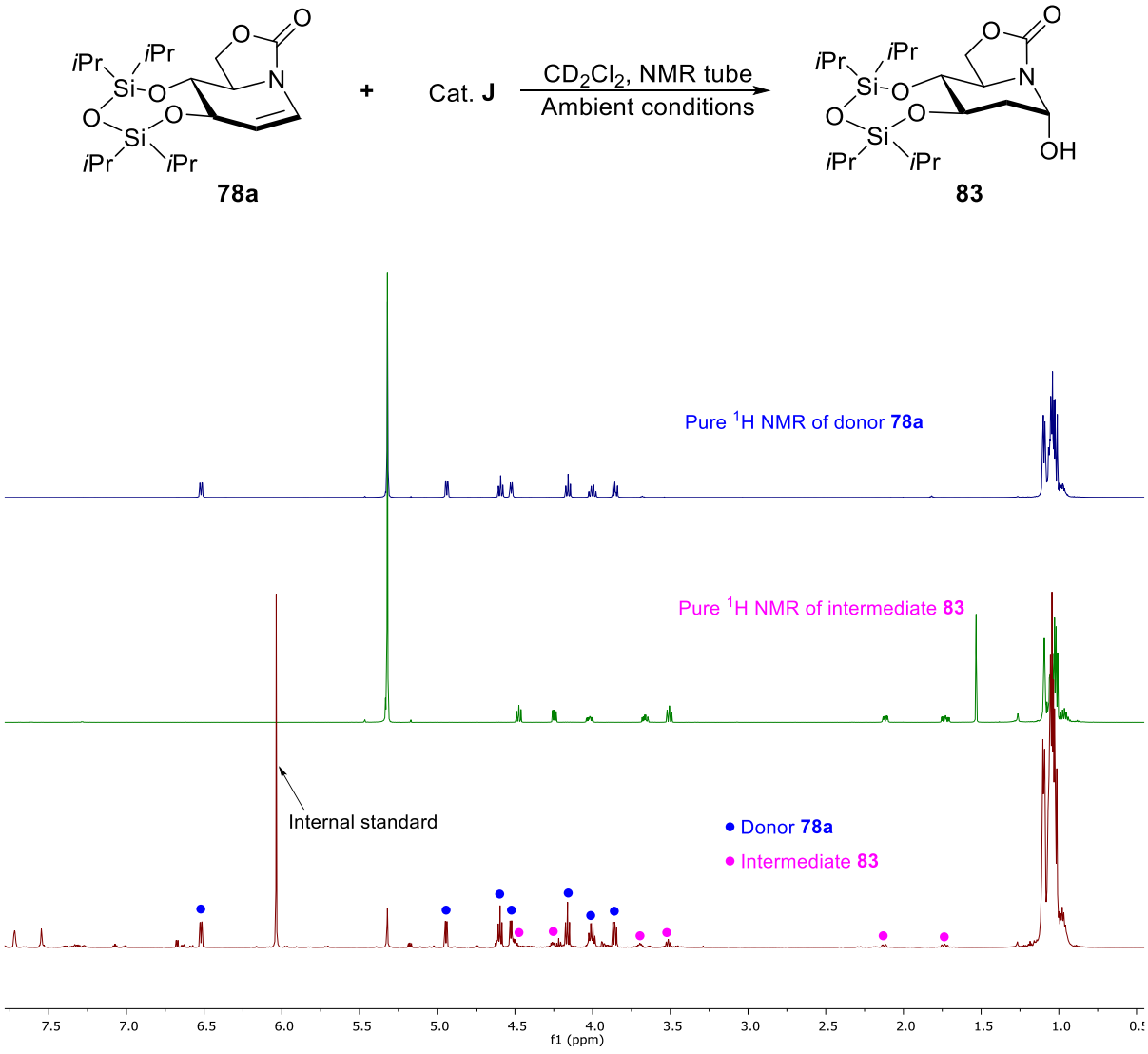

Figure 3.6. Crude ^{1}H NMR spectra for observation of intermediate **83**

3.5.2 Several experiments measured to investigate possible intermediate 83

In order to investigate whether or not **83** could be an important intermediate within the reaction's mechanistic manifold under standard conditions. First of all, an *in-situ* ^{1}H NMR monitoring experiment was performed (**Figure 3.7**) and the kinetic NMR data was transferred to temporal kinetic profile (**Figure 3.8**). From the first NMR detection data point, it was easy to detect **83** as a gradually declining species, which was consistent with the temporal kinetic profile of intermediate **83** participating in the mechanism.

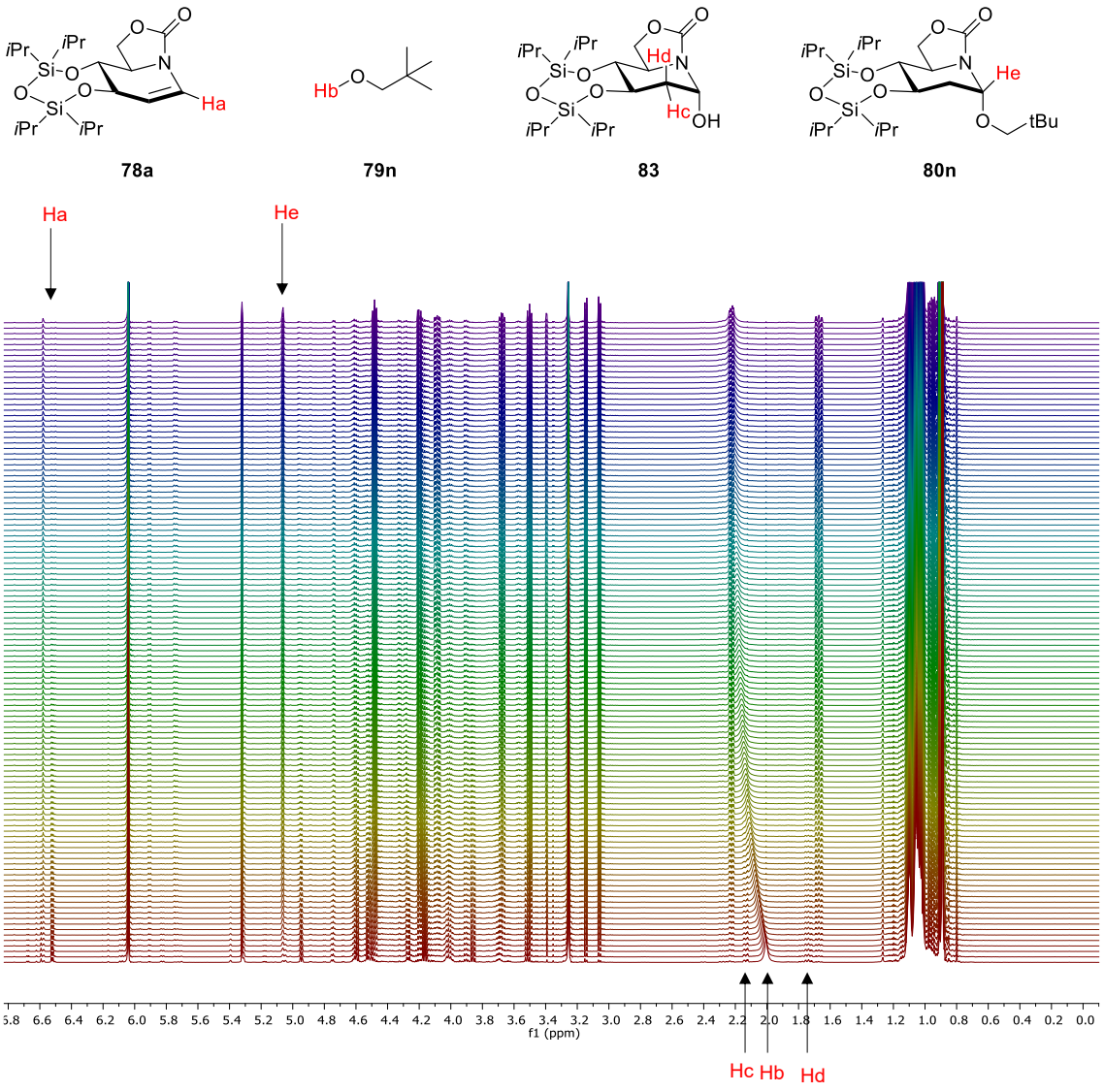

Figure 3.7. Stacked ^{1}H NMR spectra for the monitoring under standard conditions

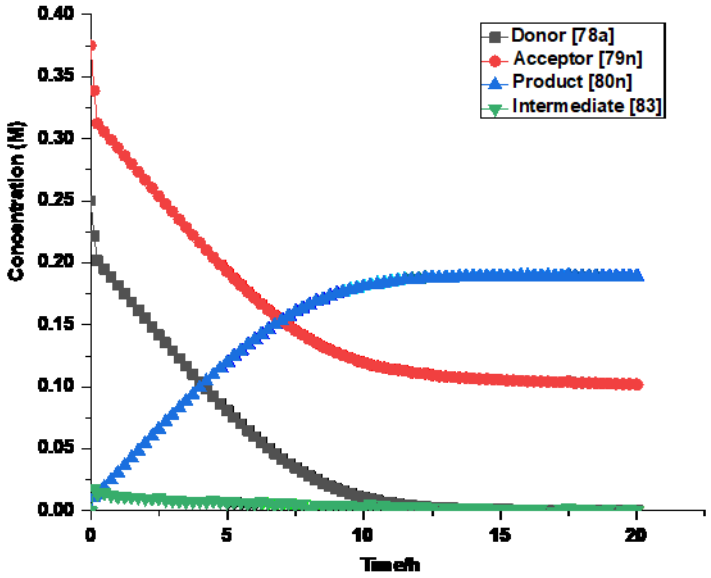

Figure 3.8. Temporal kinetic profile of the standard reaction in NMR tube

Next, to further investigate whether **83** could be a meaningful intermediate *en-route* to the iminoglycoside product, pure **83** was submitted to the typical catalytic conditions utilizing catalyst **J** in the presence of *n*-octanol as a glycosyl acceptor (**Figure 3.9**). Luckily, the target α-glycoside was produced with 90% yield and anomeric selectivity as a result of the successful glycosylation process. This confirmed further that the intermediacy of **83** in two sequential elementary phases was probably a part of the reaction mechanism.

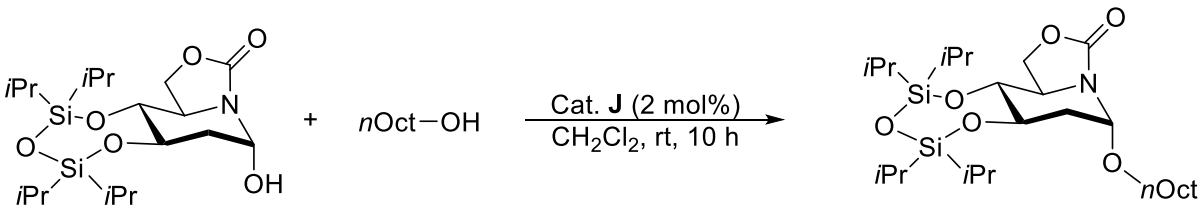

83 **79a** **80a**

90% (>20:1 α:β)

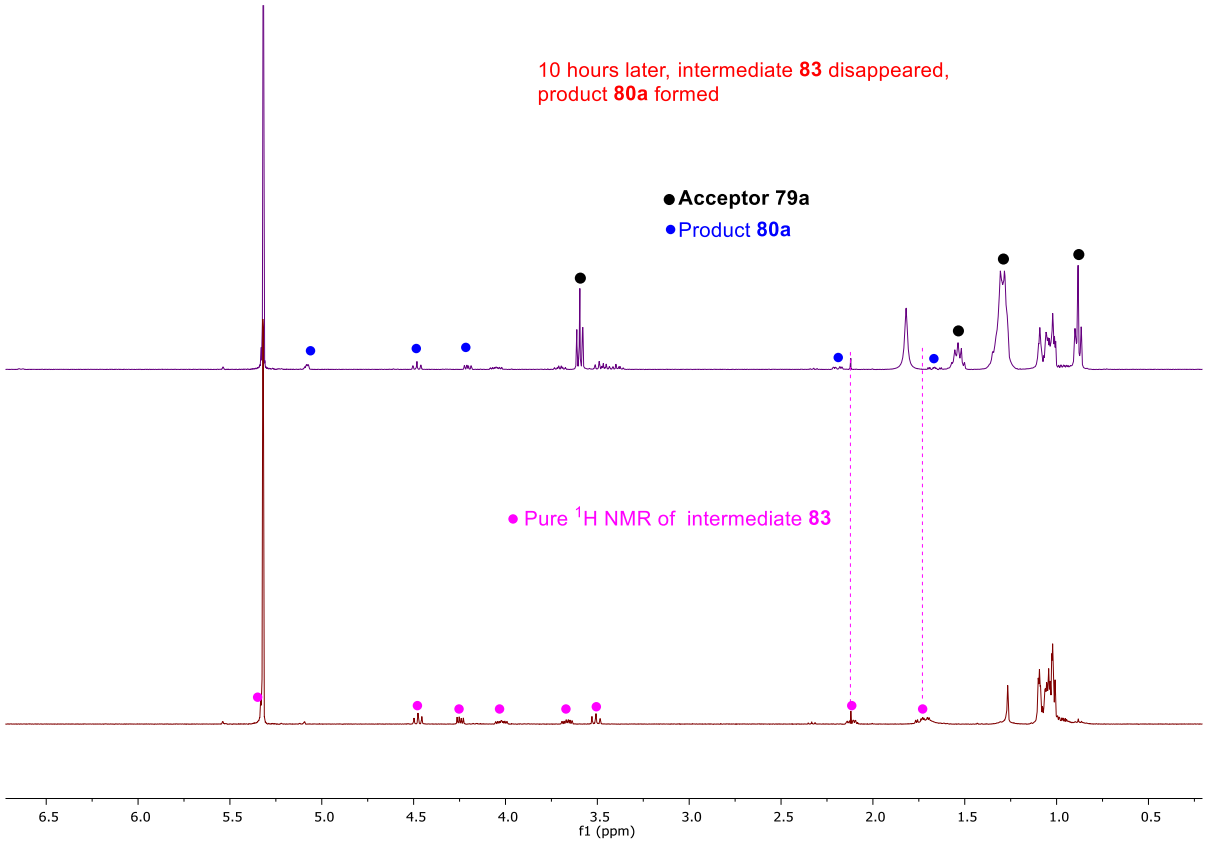

Figure 3.9. ^{1}H NMR Spectra of intermediate **83** react with **79a** under standard condition

Furthermore, to get a deeper understanding of the mechanism, a sequential *in-situ* ^{1}H NMR monitoring experiment was conducted (**Figure 3.10, 3.11** and **3.12**). First of all, catalyst **J** was added to the donor **78a** in the NMR tube to monitor for 0.5 hours. Secondly, acceptor **79n** was added and continued to monitor the reaction until it finished. According to the NMR spectra, **83** was formed and the amount of **78a** decreased at the same time in the first step. Interestingly, **83** almost kept the same level during this time, which indicated that the first step might be reversible and reached dynamic equilibrium. In the second step, an obvious drop of **83** and the subsequent appearance of product **80n** were observed during the rest of the reaction time, which was approximately 7 h. This experiment proved that **83** was most likely an intermediate in the next step to form the iminoglycoside product.

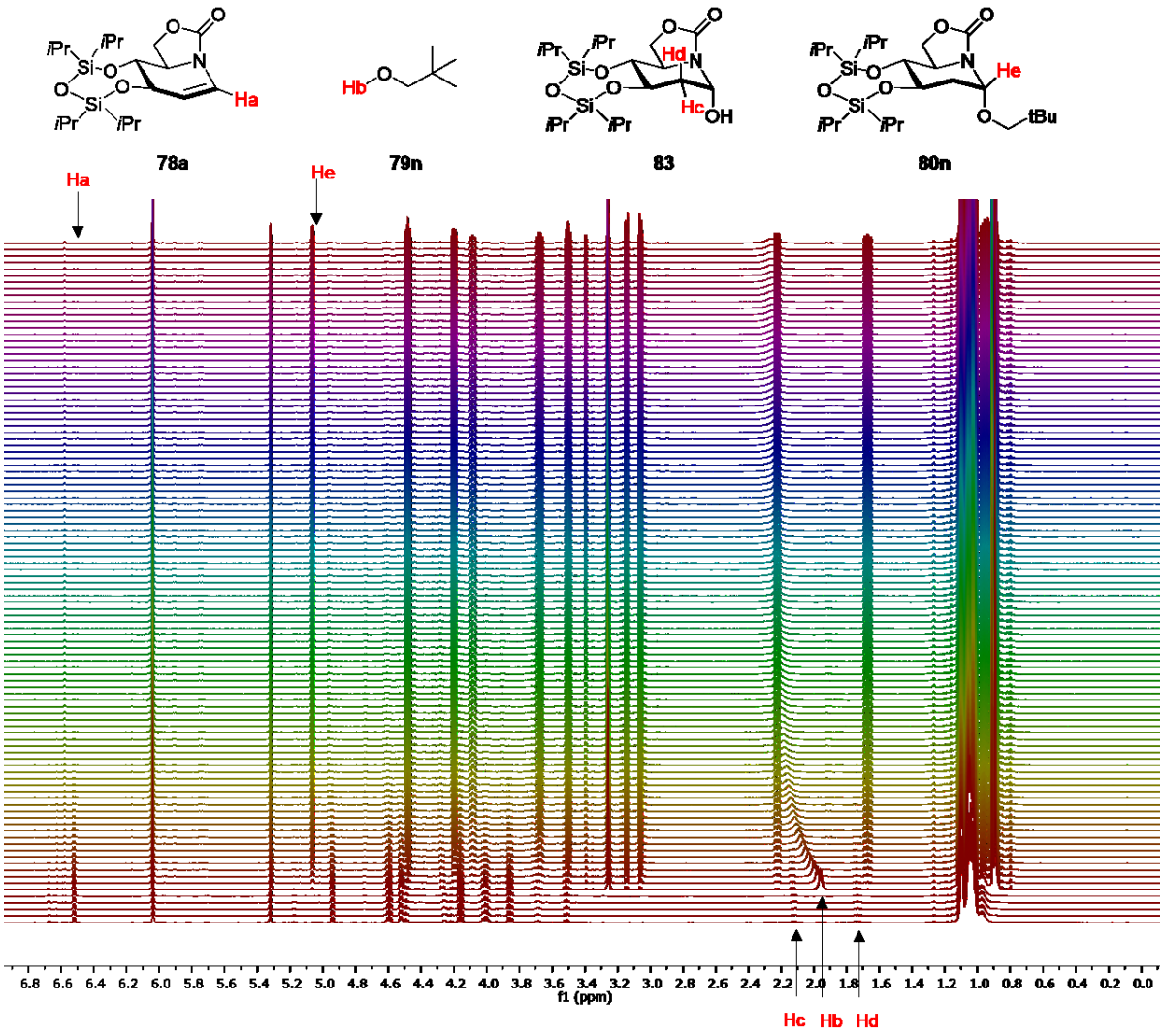

Figure 3.10. Stacked ^{1}H NMR spectra for *sequential in-situ* reaction monitoring

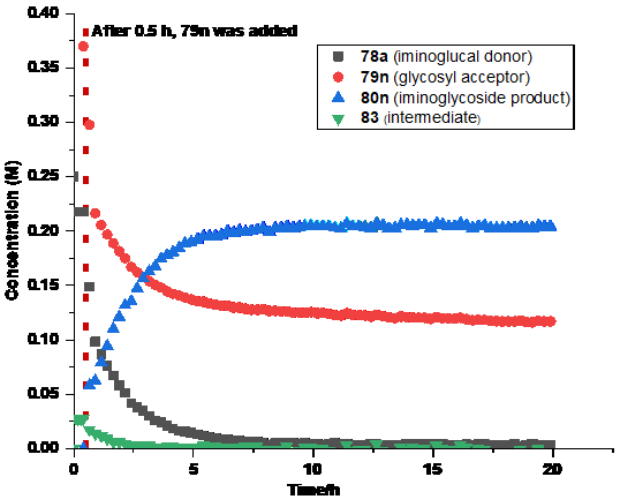

Figure 3.11. Temporal kinetic profile of *sequential in-situ* reaction monitoring

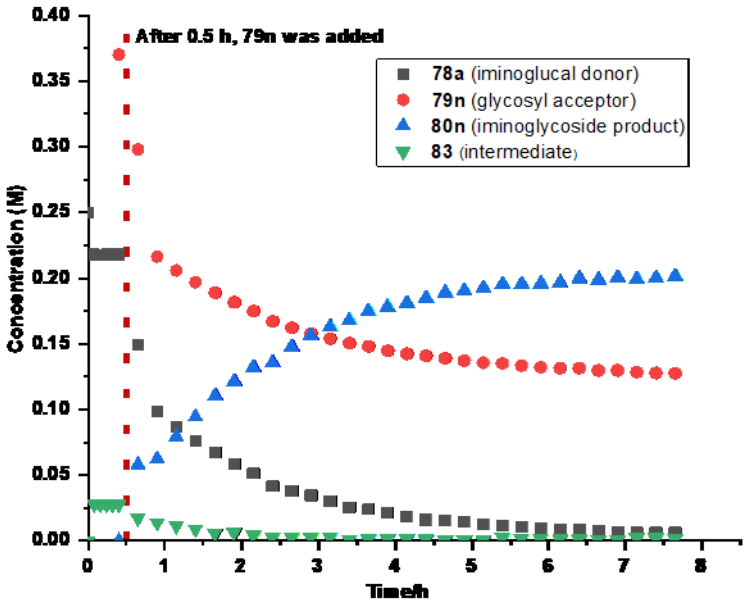

Figure 3.12. Zoomed-in temporal kinetic profile of **figure 3.11** for clarity

3.5.3 Control experiments on intermediate

It was necessary to conduct more control experiments to ascertain the catalytic influence during the conversion from intermediate **83** to **80a**. Firstly, a negative control was established by not adding any catalyst under the usual reaction conditions, as a result, the substrate was left unreacted and no product **80a** was produced (**Figure 3.13**). Second, *rac*-BINAP was added to the reaction as an additive in a phosphine poisoning experiment and the reaction was carried out under standard conditions to determine if sigma bond activation was involved in the downstream elementary step. In a similar manner, the substrates remained unreacted when this poisoning control stopped the process (**Figure 3.14**).

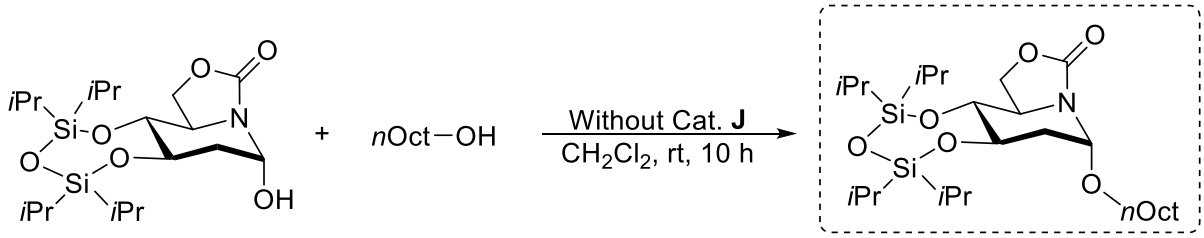

83 **79a** **80a**

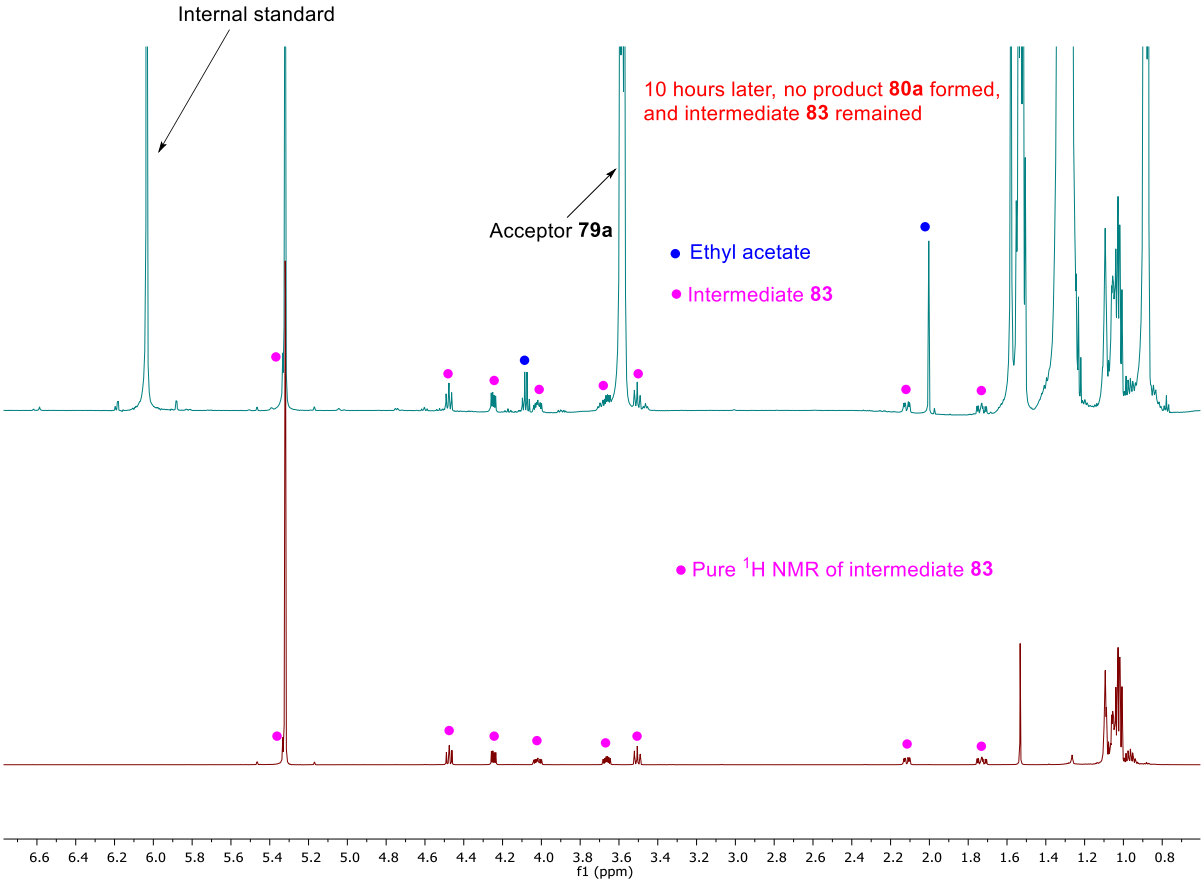

Figure 3.13. Crude ^{1}H NMR spectra of intermediate **83** react with **79a** without catalyst **J**

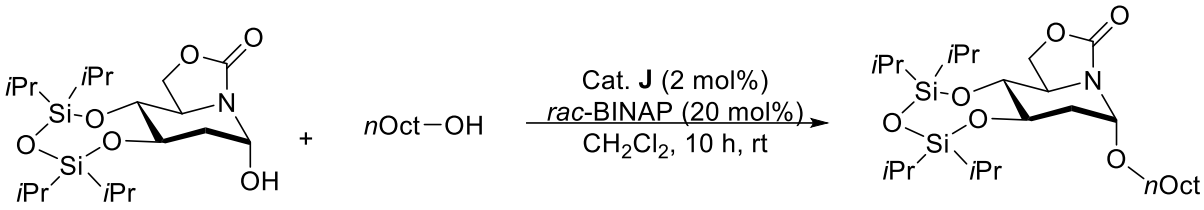

83 **79a** **80a**

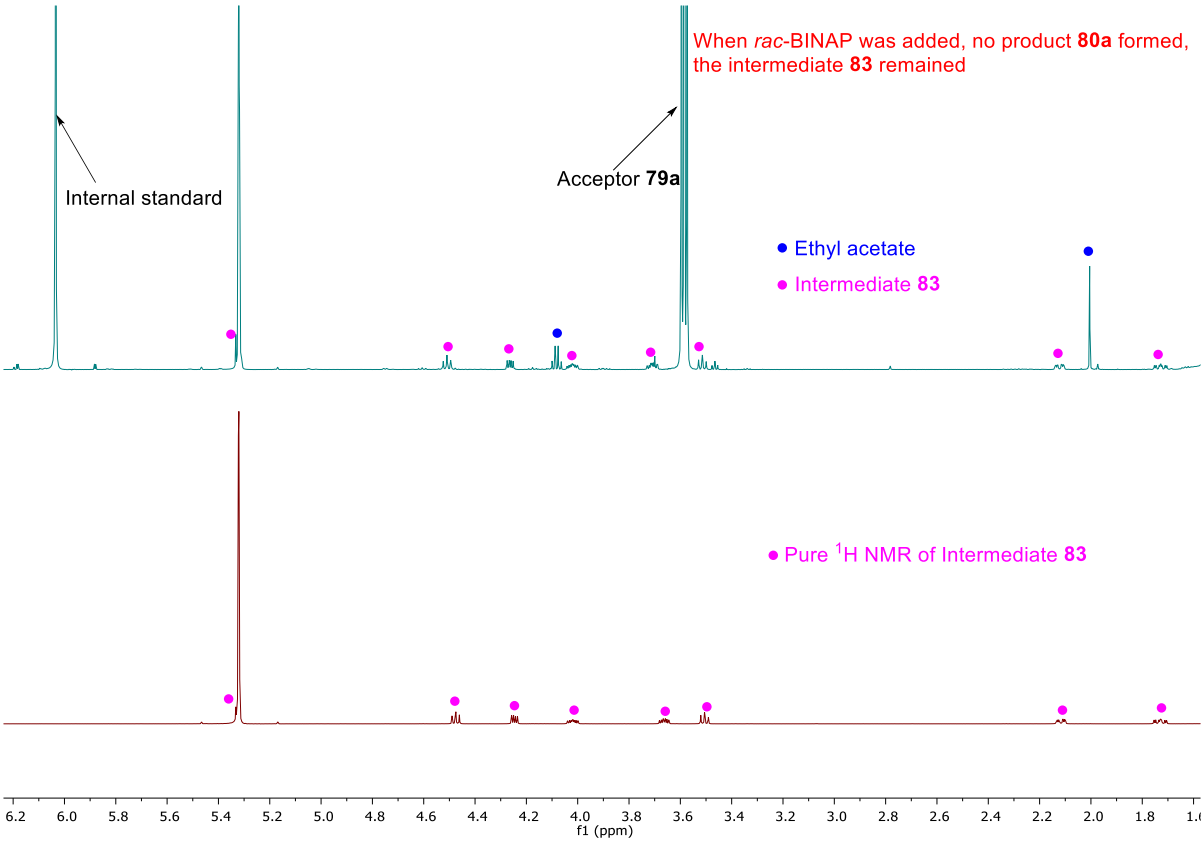

Figure 3.14. Crude ^{1}H NMR spectra of poisoning experiment with *rac*-BINAP

3.5.4 Experiments on upstream step

Since the intermediate **83** was formed through the reaction between glycal and H_2O in the first step, it was important to make sure whether ChB catalyst was responsible for it. Therefore, more experiment should be done to support it. Initially, one drop of water was added to the reaction under the standard conditions but without acceptor added to the solution, 10% of **83** was formed in 0.5 h (**Figure 3.15**). After that, 20 mol% of *rac*-BINAP as the ChB poison reagent was added to the solution which had the same conditions with the first step (**Figure 3.16**), surprisingly, no intermediate **83** was formed and the reaction remained the same without any consumption of glycal. These phenomenons suggested that the first step of water addition to the glycal to produce the intermediate **83** was catalyzed by the catalyst **J**.

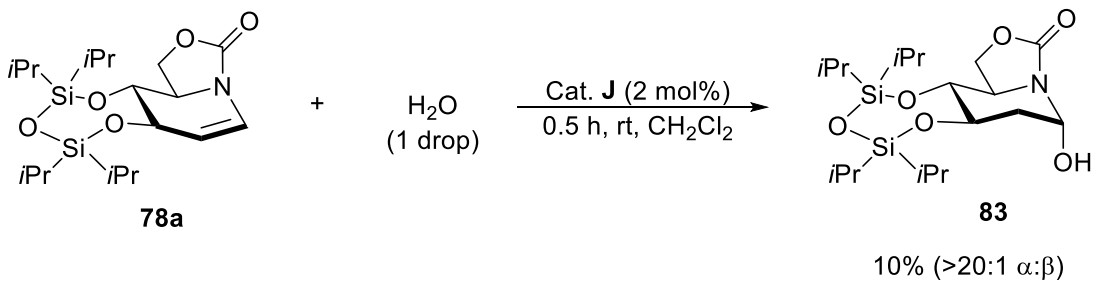

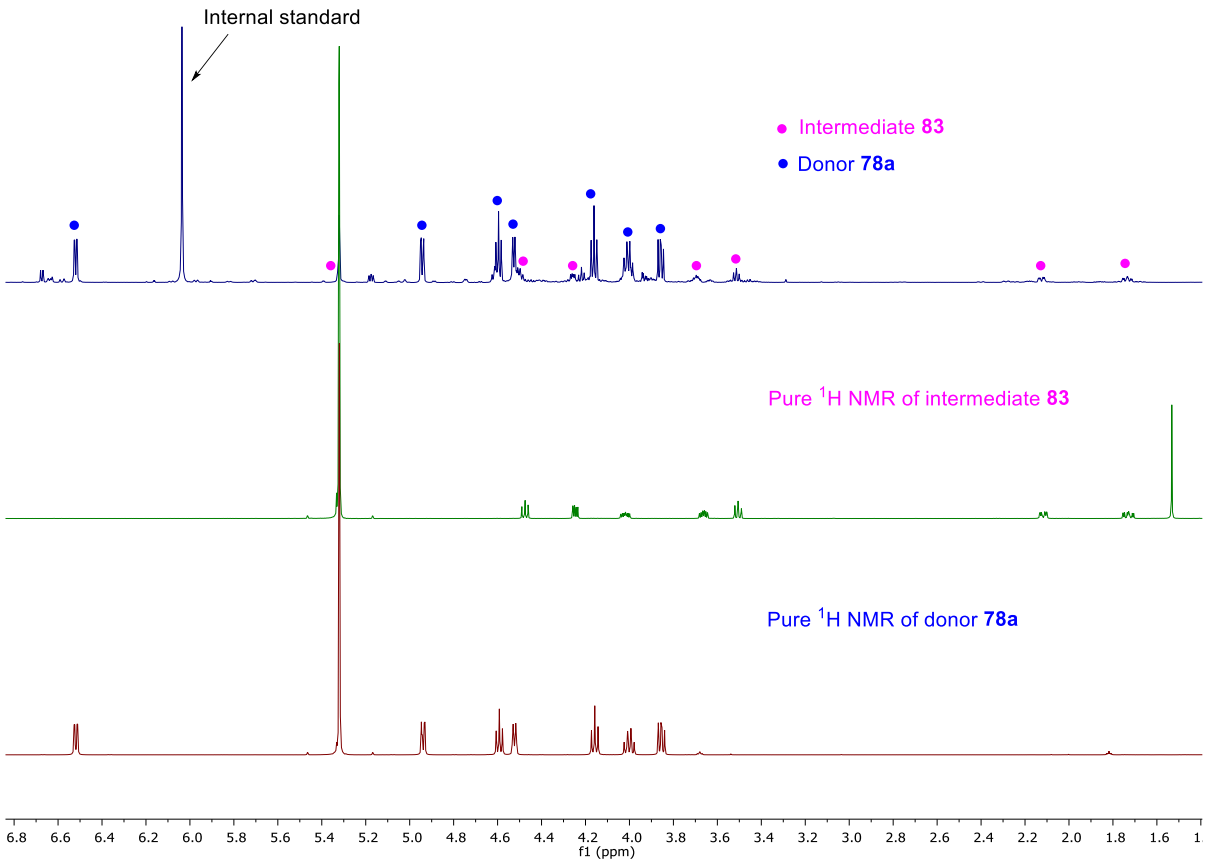

Figure 3.15. Crude ^{1}H NMR spectra of H_2O addition to the upstream step

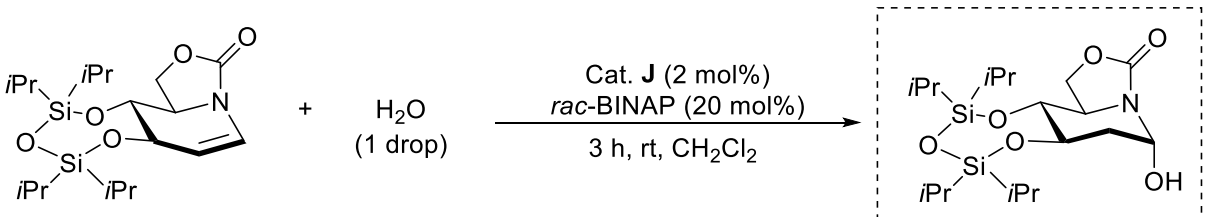

78a **83**

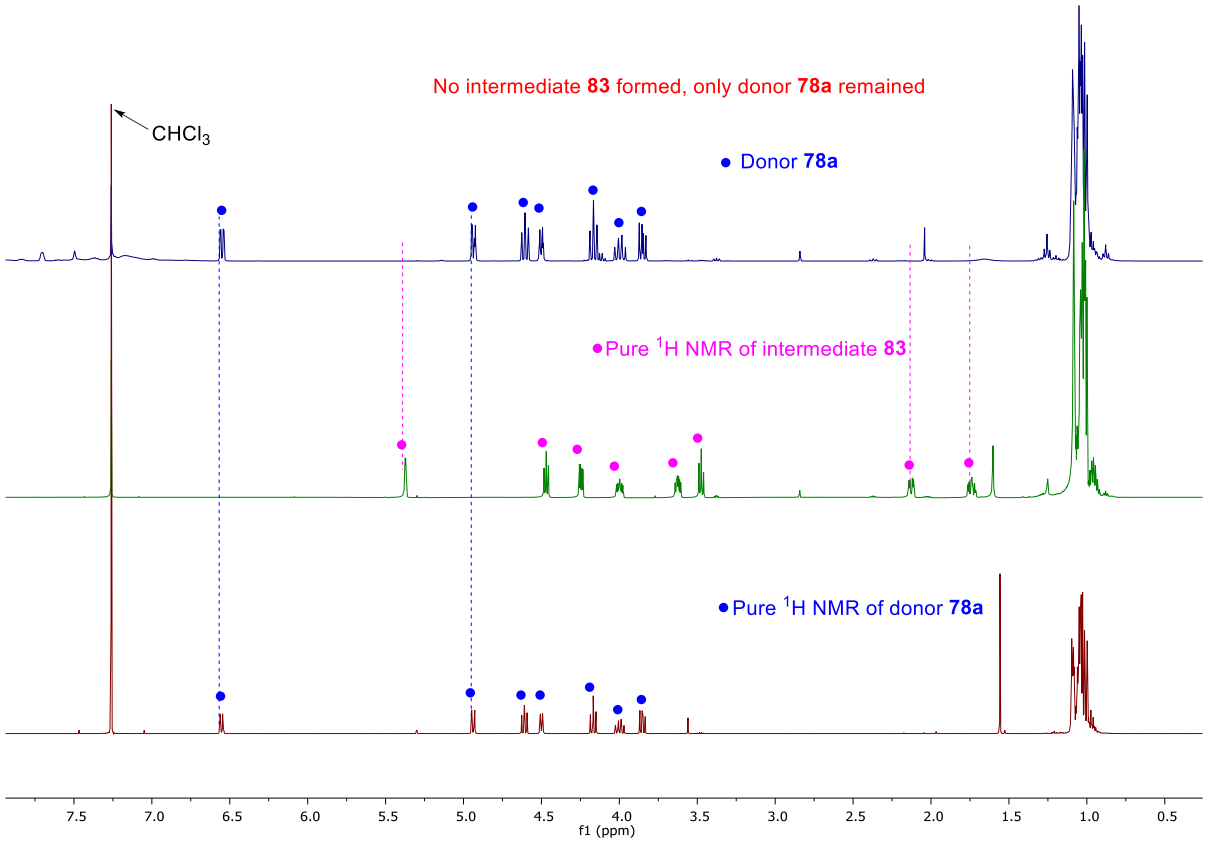

Figure 3.16. Crude ^{1}H NMR spectra of poisoning experiment by *rac*-BINAP on the upstream step

3.5.5 NMR titration experiments between each component

In order to investigate the interaction between catalyst **J** and the iminoglycal, a series of NMR titrations with activated powdered 3Å molecular sieves in the NMR tube to suppress the water addition step were conducted. First of all, an approximate 0.232 ppm downfield shift was seen on the ^{77}Se NMR resonance during the NMR titration between donor **78a** and catalyst **J** (**Figure 3.17**), while the ^{31}P NMR resonance kept almost the same (**Figure 3.18**). Then, 0.155 ppm downfield shifts in the carbonyl carbon in comparison to pure **78a** were detected during the ^{13}C NMR measurements of titrations (**Figure 3.19**). These changes were consistent with the hypothesis that the carbamate's carbonyl oxygen was likely being activated by the selenium's sigma holes. Therefore, bidentate ChB's participation was probably operational.

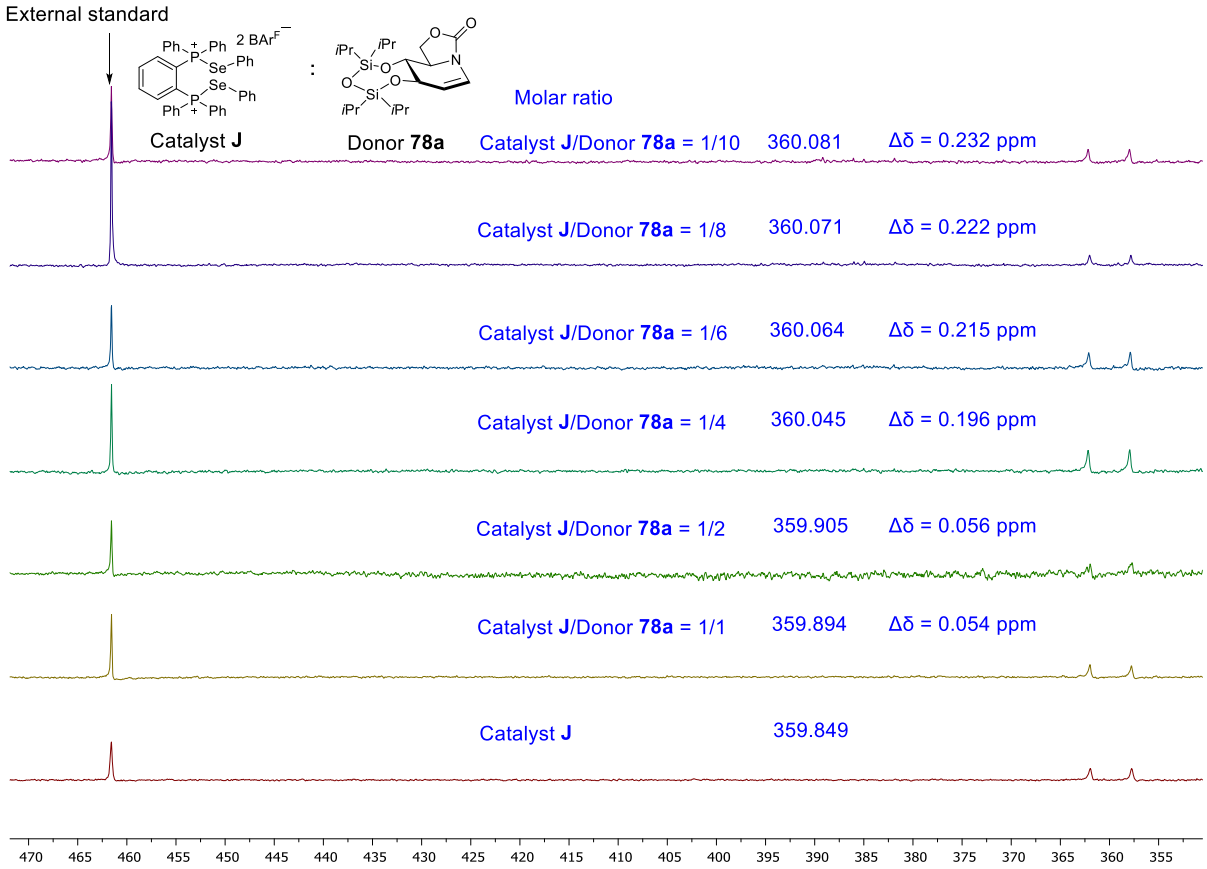

Figure 3.17. ^{77}Se titration for catalyst **J** and donor **78a**

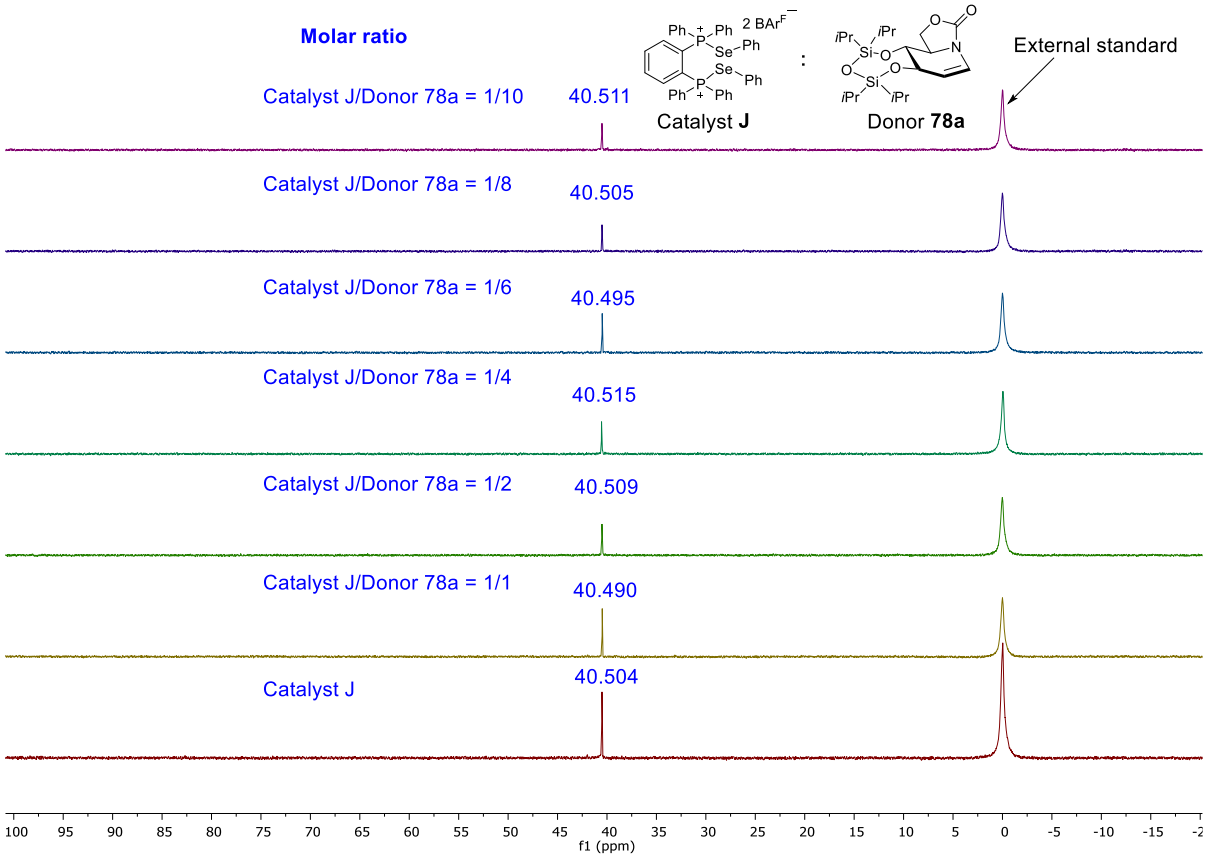

Figure 3.18. ^{31}P titration for catalyst **J** and donor **78a**

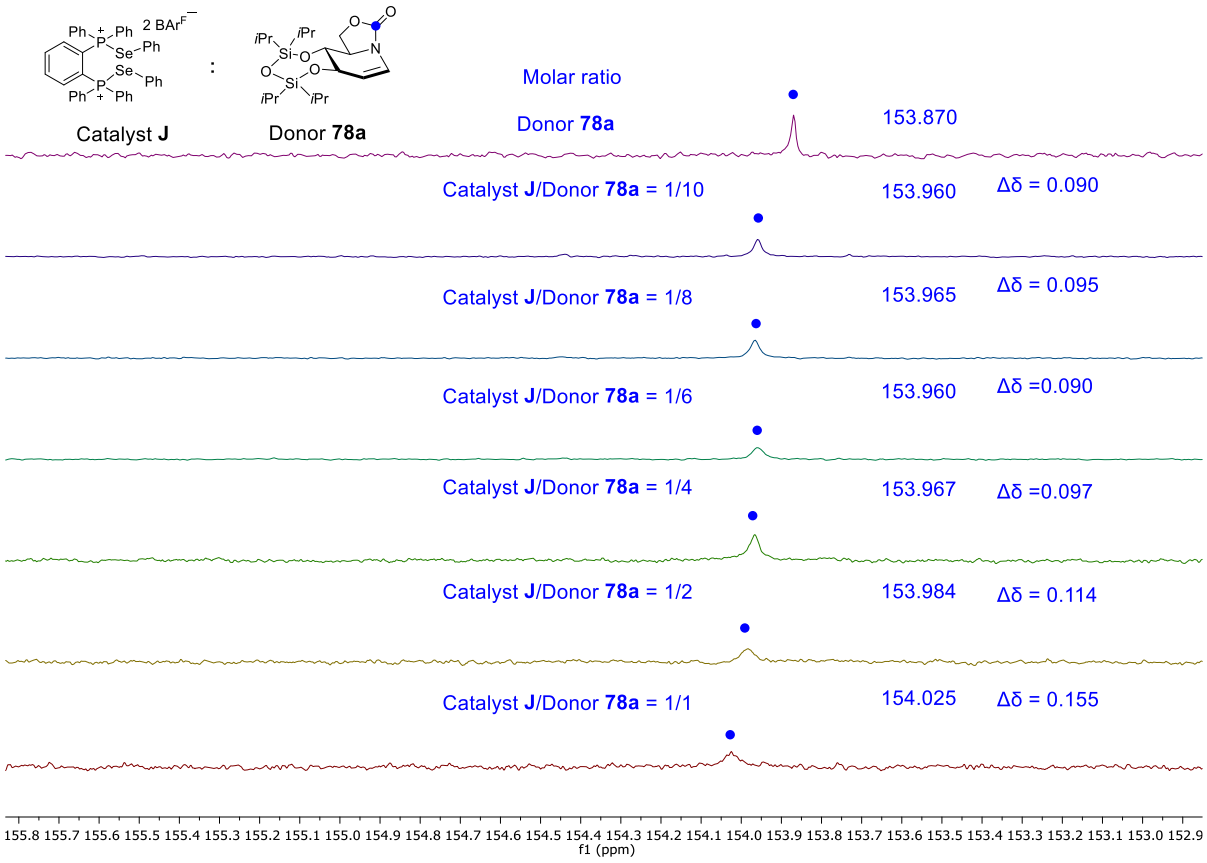

Figure 3.19. ^{13}C titration of carbonyl group for catalyst **J** and donor **78a**

After finishing the titration between catalyst **J** and donor **78a**, the titration between catalyst **J** and acceptor was carried out subsequently. Initially, a typical glycosyl acceptor **79n** was chosed to titrate with catalyst **J** to perform ^{77}Se NMR titration. After a series of titration experiments, a around 0.187 ppm downfield shift of the ^{77}Se resonance of the catalyst compared to pure **J** was detected as the acceptor concentration increased (**Figure 3.20**), which supported the hypothesis that ChB activation between the catalyst and the glycosyl acceptor was operative during the catalytic cycle. Besides, a downfield shifting of the hydroxyl proton was found in a contemporaneous ^{1}H NMR titration when the catalyst concentration increased (**Figure 3.21**). These results indicated that the catalyst was likely resposible for the activation of the hydroxyl group of the acceptor.[7],[8]

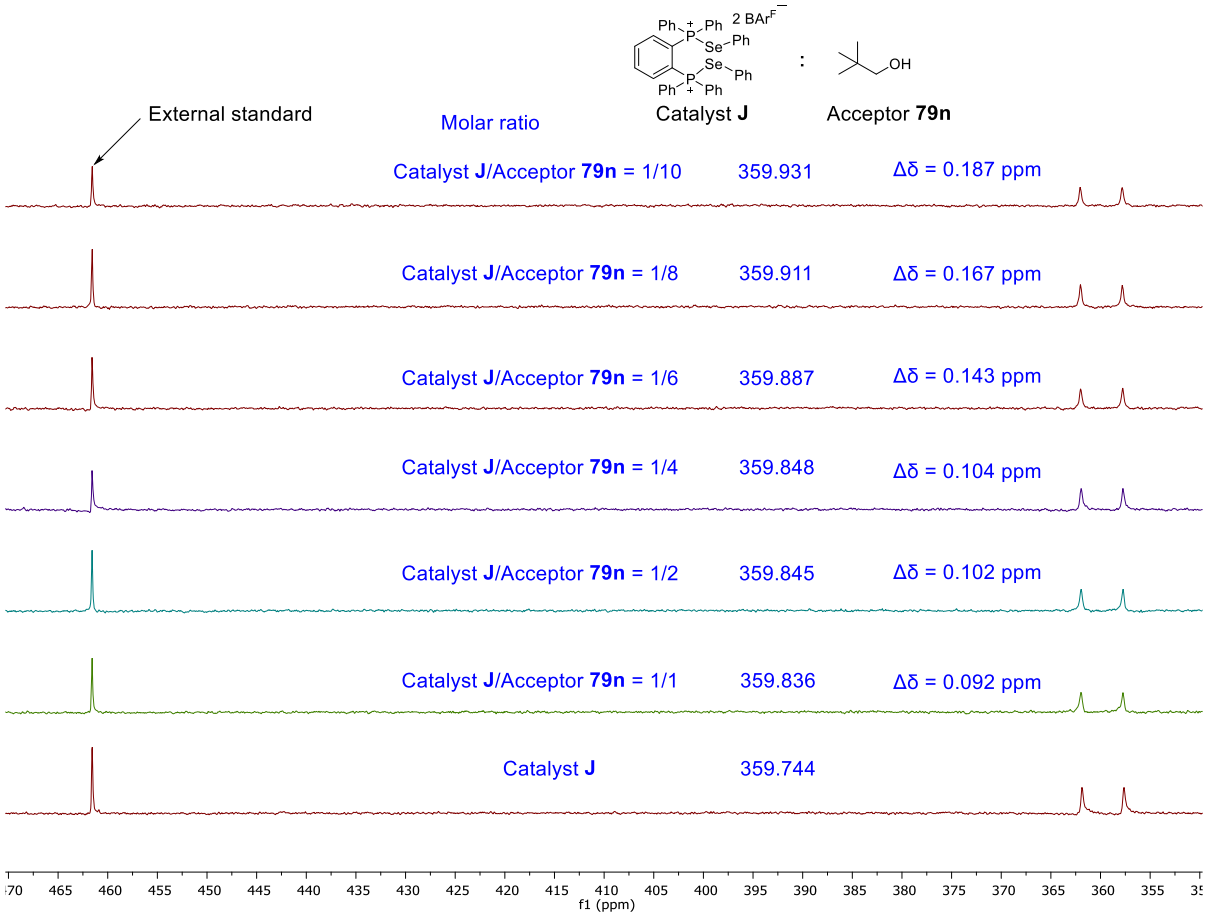

Figure 3.20. ^{77}Se titration for catalyst **J** and acceptor **79n**

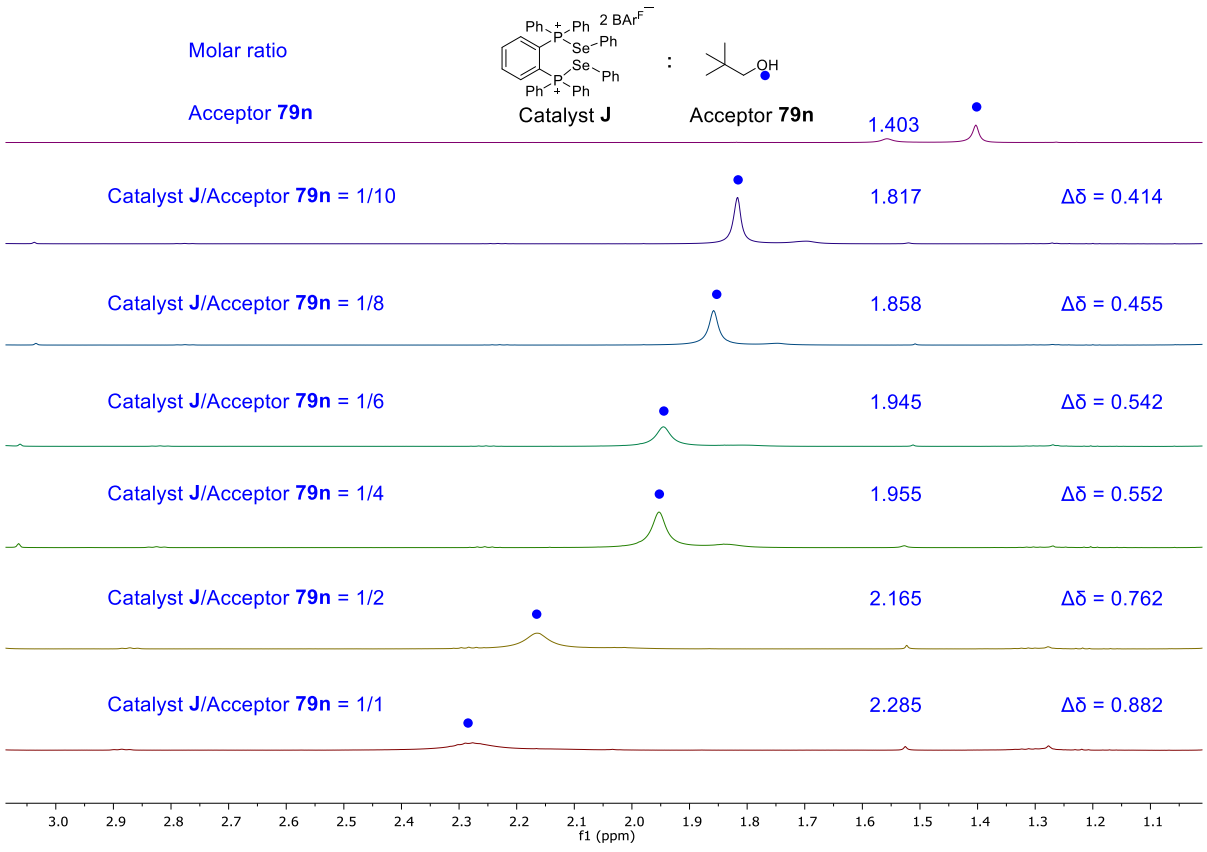

Figure 3.21. ^{1}H NMR shift of the hydroxyl proton on acceptor **79n**

Subsequently, a series of ^{77}Se and ^{13}C NMR titrations between catalyst **J** and intermediate **83** were conducted. As the concentration of **83** rose, there was a ^{77}Se NMR downfield shift (0.028 ppm downfield compared to pure **J**) (**Figure 3.22**), but no noticeable ^{31}P NMR shift on the catalyst **J** (**Figure 3.23**). Besides, there was a simultaneous downfield shift of the carbonyl ^{13}C resonance of the carbamate (1.70 ppm downfield with reference to pure 5) (**Figure 3.24**) when the concentration of **83** was increased. These studies revealed that in the downstream mechanistic step, catalyst **J** might be bi-functionally activating both intermediate **83** and the hydroxyl oxygen of the acceptor.

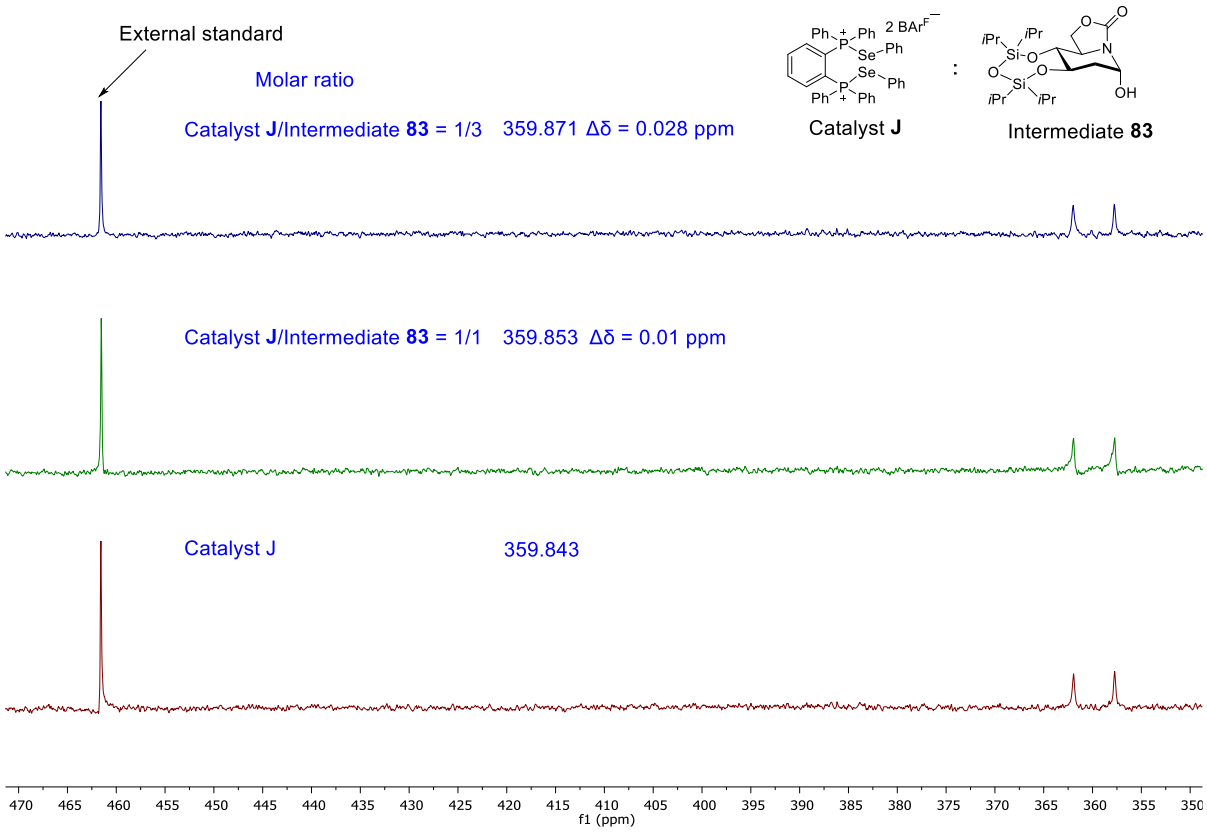

Figure 3.22. ^{77}Se NMR titration for catalyst **J** and intermediate **83**

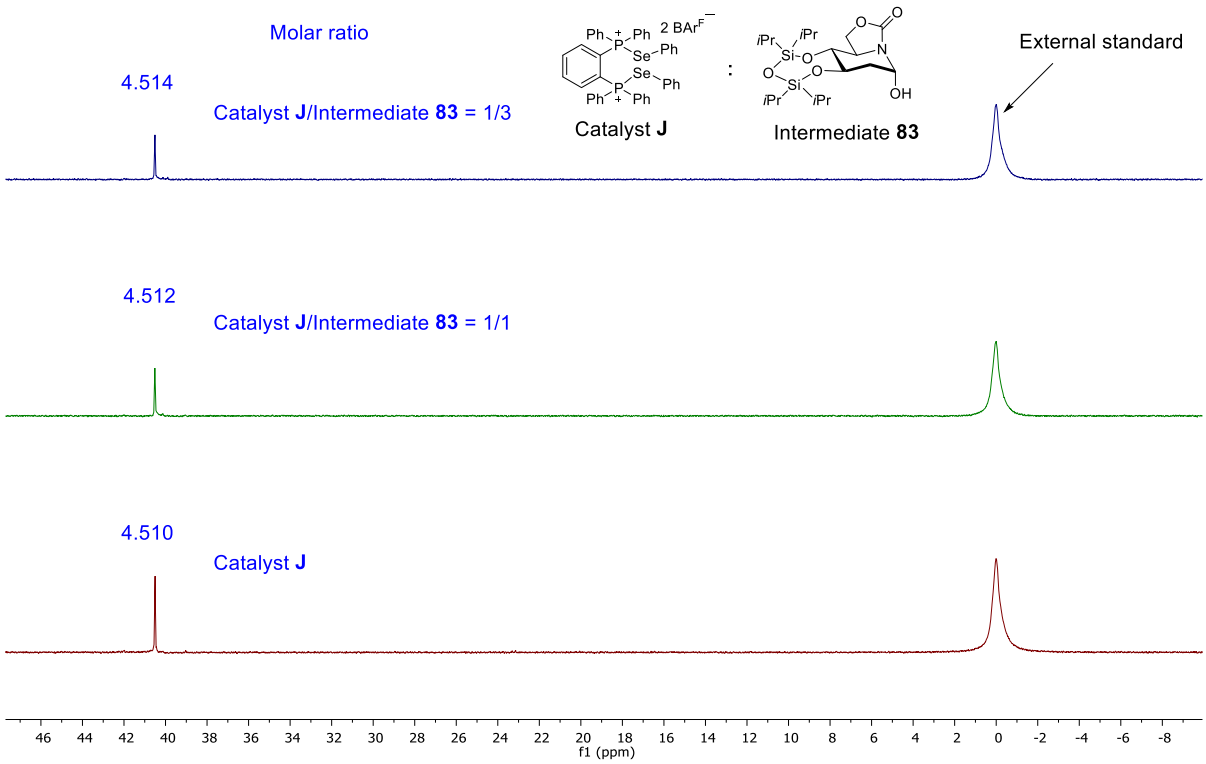

Figure 3.23. ^{31}P NMR titration for catalyst **J** and intermediate **83**

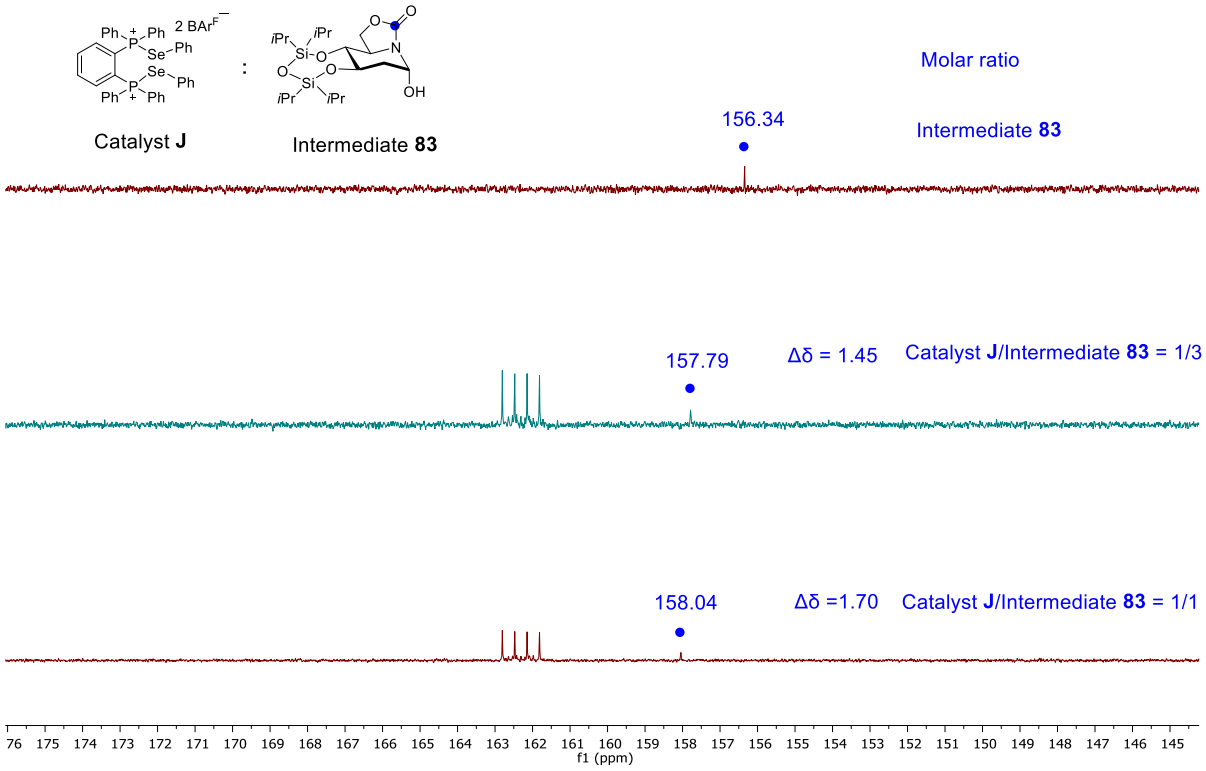

Figure 3.24. ^{13}C NMR titration for catalyst **J** and intermediate **83**

Besides, according to the result of conditions screening (**Table 3.1**, entry 20), the reaction was terminated when 20 mol% K_2CO_3 was added to the solution, which pointed out that proton transfer was essential in the catalytic mechanism's elementary steps, since base could disrupt the proton shuttling process.

3.5.6 Competitive experiment between different phenols

In order to investigate the influence of the acceptor's acidity on the rate limiting step, a competitive experiment was subsequently established, equal equivalent of *p*-bromophenol acceptor **79x** (pK_a ~ 9.37) and *p*-methoxyphenol acceptor **79y** (pK_a ~ 10.4) which had distinctly difference in their pK_a were permitted to react parallel in the same pot with the same glycosyl donor **78a** (**Figure 3.25** and **Figure 3.26**). This experiment could shed light on whether the acidity of the acceptor effects the rate limiting step mechanistically because the ratio of both iminoglycosides (**80x:80y**) generated in this experiment could be used to determine the rate constants of both competing processes. Interestingly, an approximate decrease of 1 in the pK_a could lead to a two-fold increase in the reaction rate. This competitive experiment supported the idea that proton transfer from the glycosyl acceptor was embedded in the rate-limiting step due to the correlation between acceptor pK_a and the OH bond breaking mechanism.

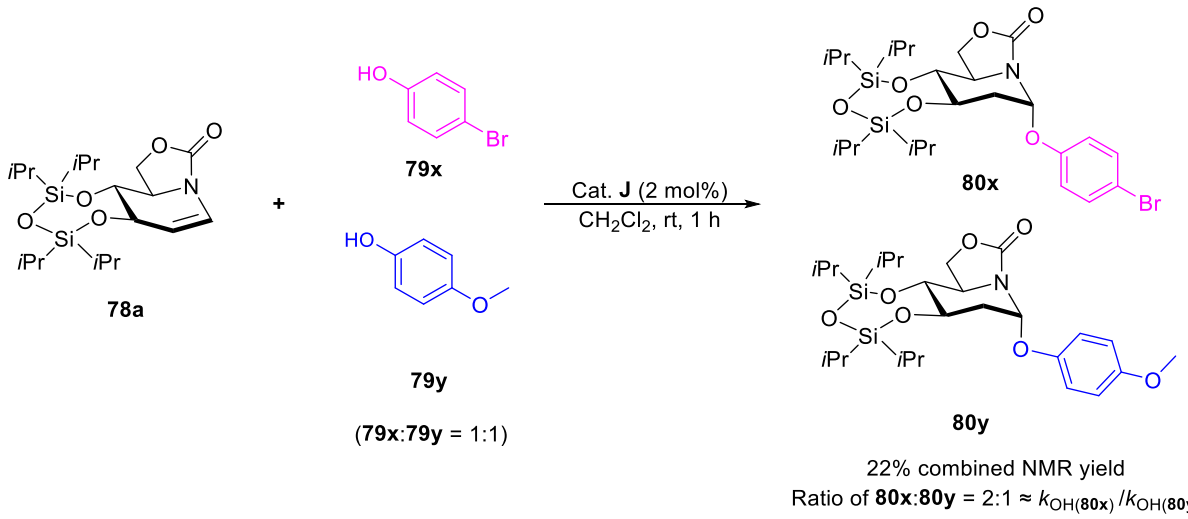

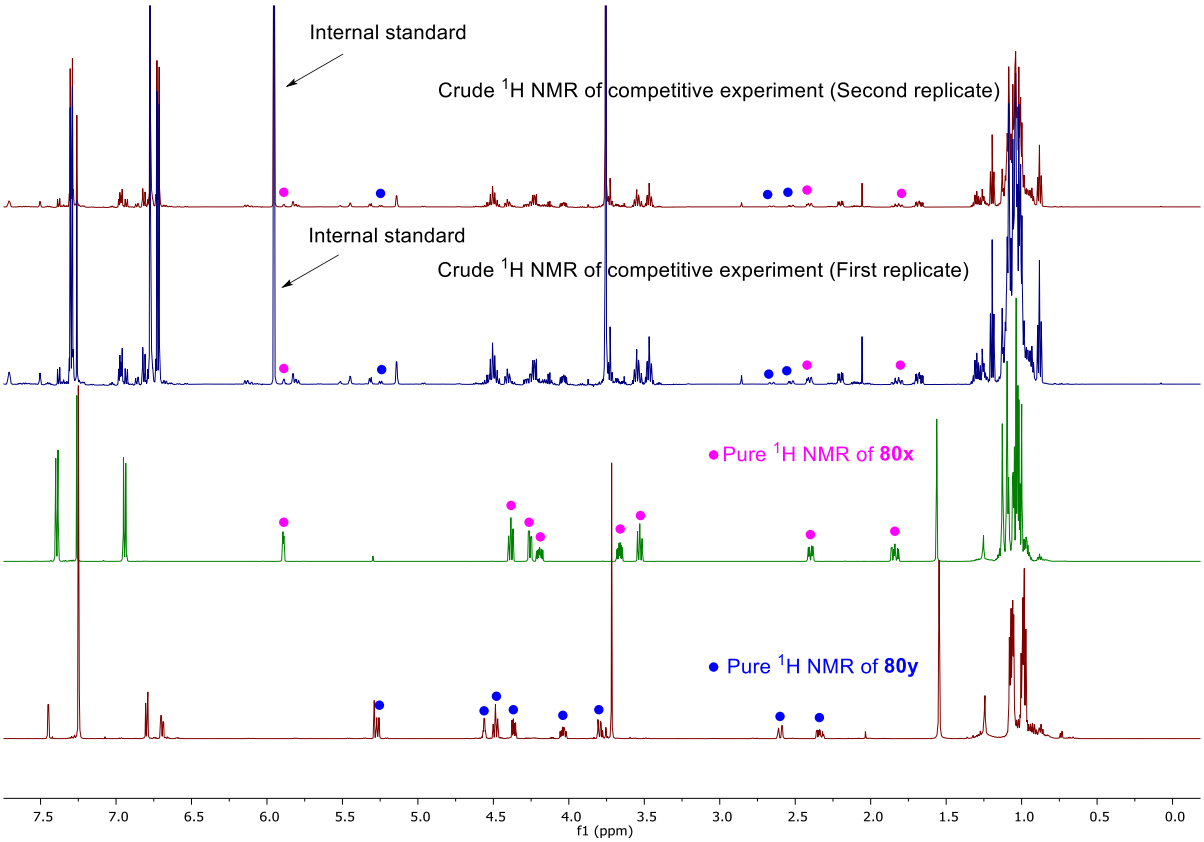

Figure 3.25. Crude ^{1}H NMR spectra of competitive experiment

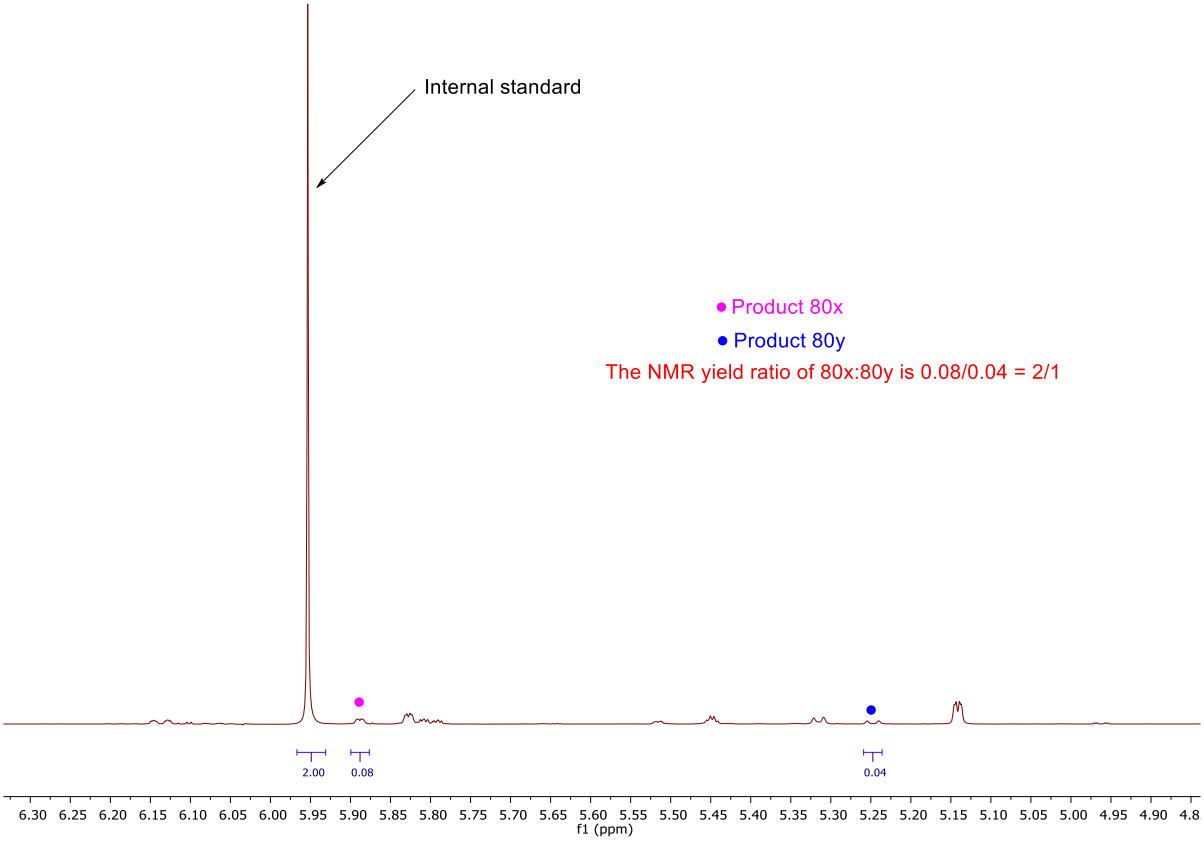

Figure 3.26. Zoomed in spectra between 4.800-6.300 ppm field of **Figure 3.25**

3.5.7 Kinetic experiments

Since all these three experiments including the control experiments, titration results and identification of the intermediate **83** pointed to multiple stage mechanism which the catalyst might involve the two elementary steps. It was necessary to carry out more experiments like kinetic studies including the whole reaction and the downstream step to determine the rate limiting step (rls) of this reaction mechanism.

3.5.7.1 Kinetic experiments on the overall reaction

Firstly, the concentrations of the glycosyl donor **78a**, acceptor **79n** and catalyst **J** were changed to examine the kinetic behavior of the overall iminoglycosylation. A general rise in reaction rate was seen in the kinetic profile when the concentration of glycosyl donor **78a** was adjusted, as seen by the kinetic curve shifting to the left (**Figure 3.27**). In reference to **78a**, this demonstrated that the reaction had a positive order.

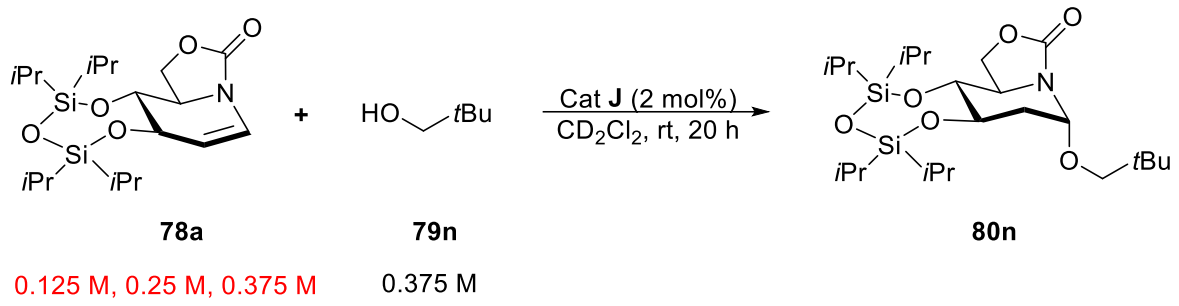

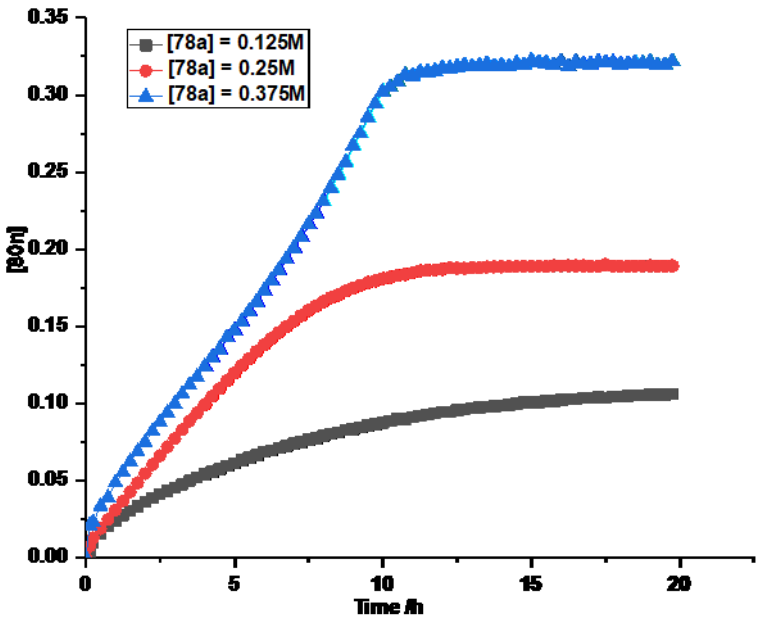

Figure 3.27 Overlapped profile for the donor **78a** concentration dependence experiments

Secondly, the concentration of acceptor **79n** was then adjusted, and an inverse relationship between rising concentration and falling reaction rates were observed (**Figure 3.28**). Since this kind of negative order profile in our groups' work had been presented when saccharides containing free alcohols were used,[82] which might be related to the development of hydrogen bonding aggregates.[83] This supramolecular clusters would be stabilized by the formation of aggregates with high concentration of the acceptor, which would reduce the ChB-hydroxyl interactions and ultimately decreased the reaction rate.

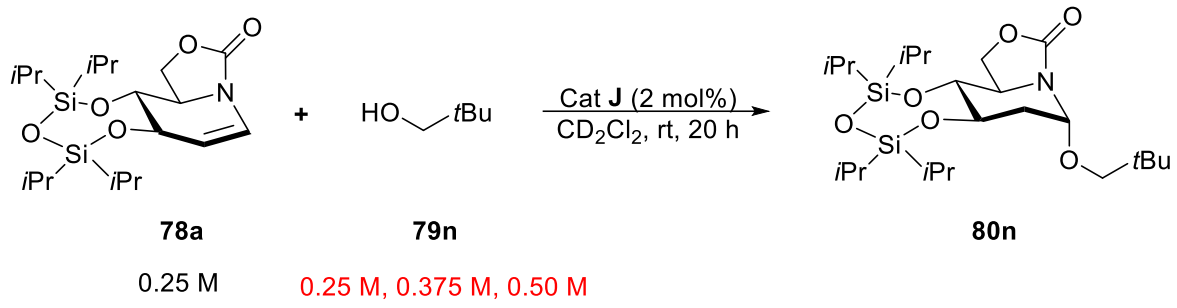

78a **79n** **80n**

0.25 M 0.25 M, 0.375 M, 0.50 M

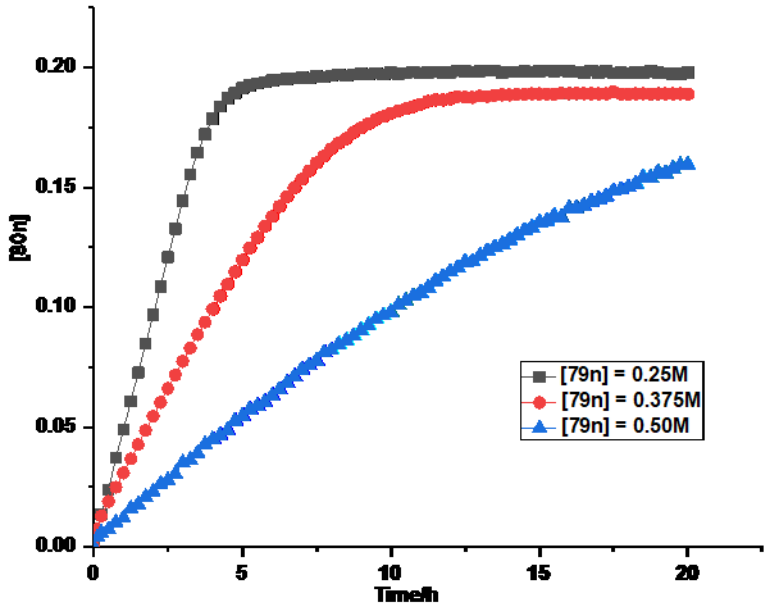

Figure 3.28 Overlapped profile for the acceptor **79n** concentration dependence experiments

Finally, a positive order with respect to the catalyst was obtained when catalyst **J**'s concentration was permuted (**Figure 3.29**). This was in line with the hypothesis that the catalyst is directly involved in the rls.

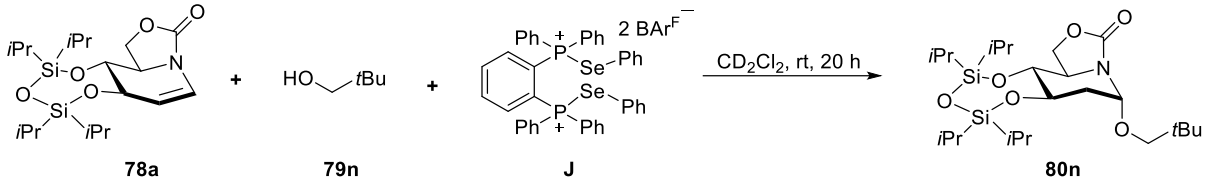

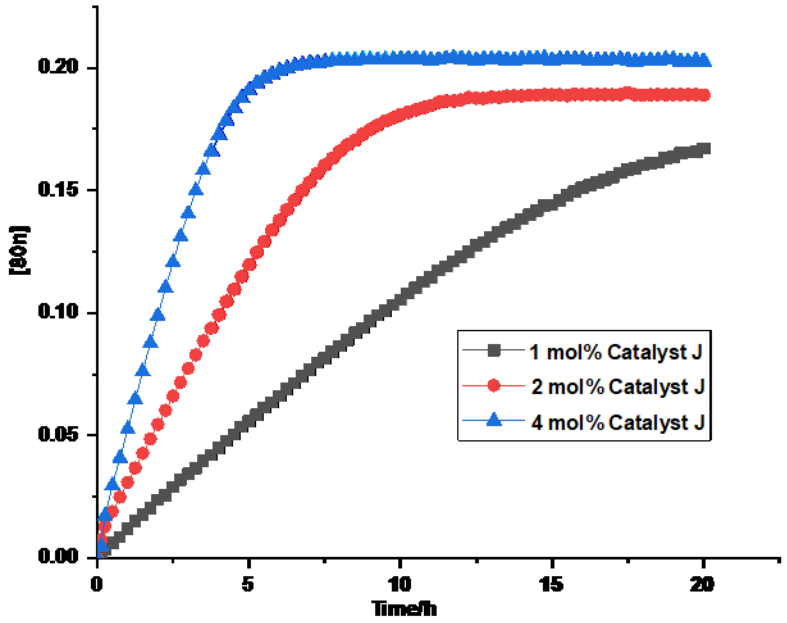

Figure 3.29 Overlapped profile for the catalyst **J** concentration dependence experiments

3.5.7.2 Kinetic experiments on the downstream step

Since the intermediate **83** could be synthesized and isolated, it was necessary to conduct a similar NMR kinetic investigation with the overall reaction by replacing the glycosyl donor with **83**. Through this experiment, it was easy to compare the kinetic profile of the proposed downstream elementary step with the kinetic profile of the entire multi-step reaction, giving us a "zoomed-in" understanding of the kinetic profile. Intriguingly, the kinetic behavior of the downstream step was closely related to that of the overall reaction, with generally positive orders for both **83** (**Figure 3.30**) and the catalyst **J** (**Figure 3.31**) and negative orders for the glycosyl acceptor **79n** (**Figure 3.32**).

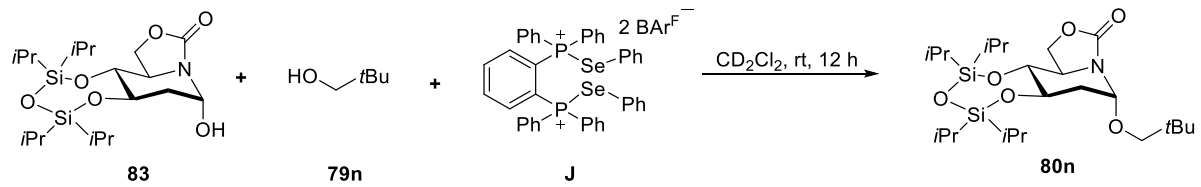

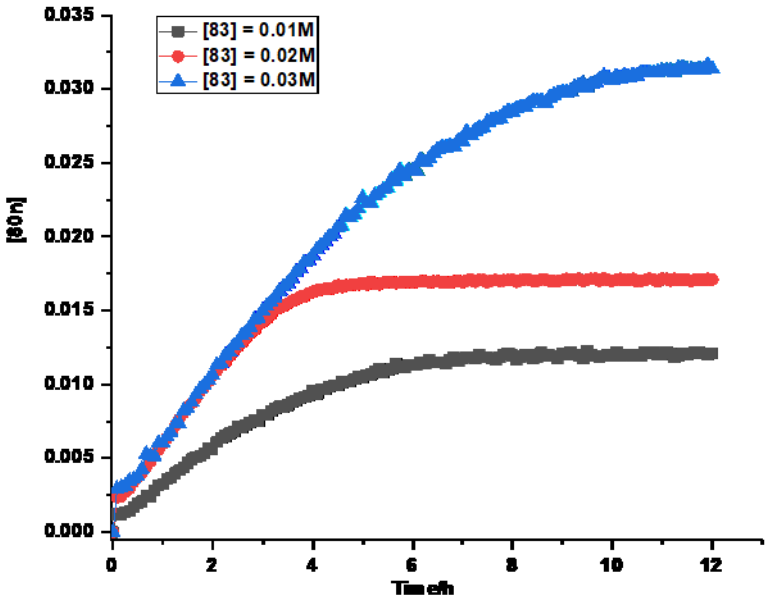

Figure 3.30 Overlapped profile for the intermediate **83** concentration dependence experiments

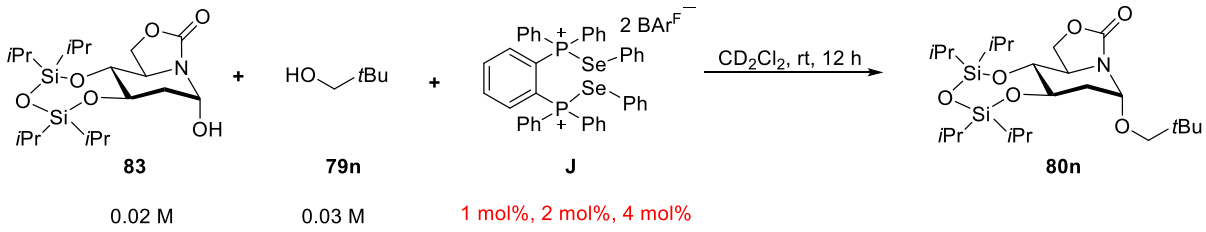

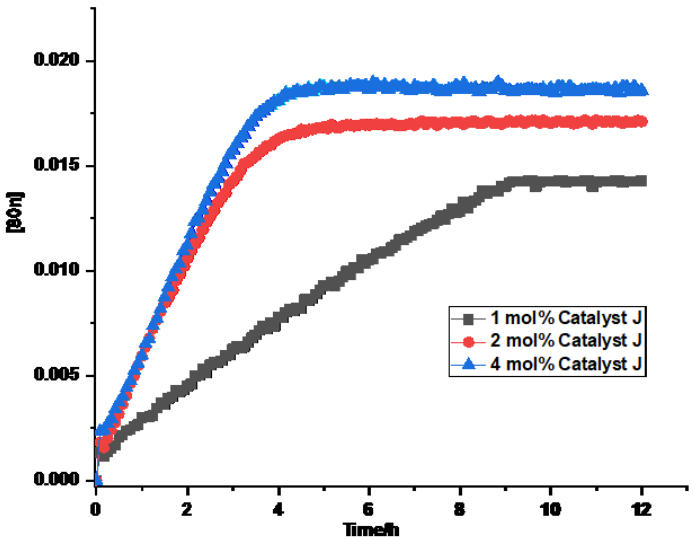

Figure 3.31 Overlapped profile for the catalyst **J** concentration dependence experiments

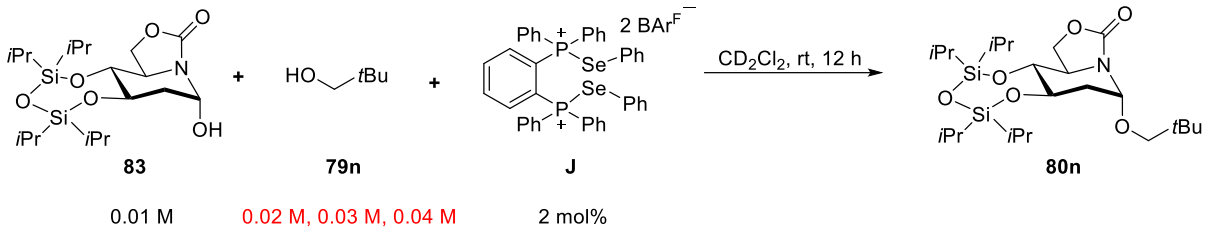

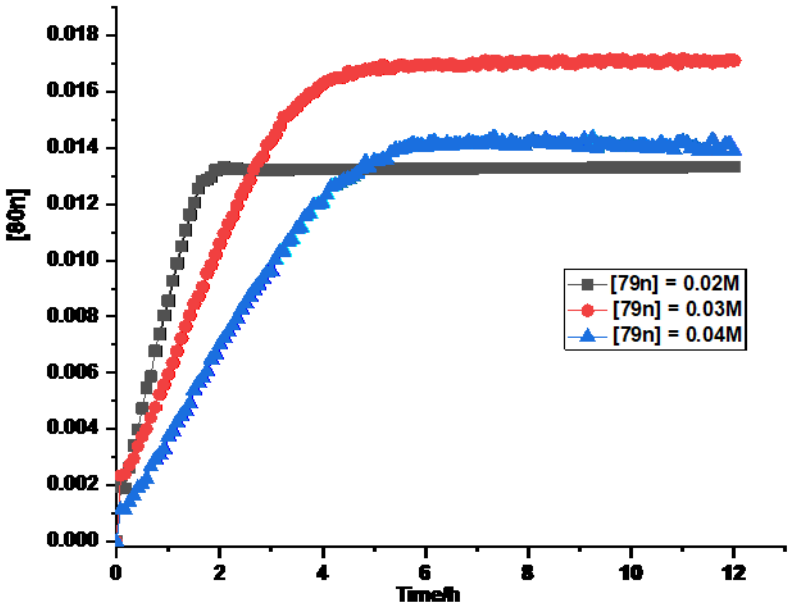

Figure 3.32 Overlapped profile for the acceptor **79n** concentration dependence experiments

Based on the similar kinetic profile, the rate limiting step in the process appeared to be the iminoglycosylation of intermediate **83** with the glycosyl acceptor. Furthermore, the sequential ^{1}H NMR monitoring experiment in the absence of glycosyl acceptor yielded rather low yield (~10%) of **83** without advancing to completion (**Figure 3.11 and Figure 3.12**), which showed that the upstream elementary step between iminoglycal **78a** and water was a reversible reaction.

3.5.8 Proposed mechanism

Based on the suite of NMR titration and kinetic investigations, a proposed hypothesis was presented as following, which served as the foundation for the multi-step ChB activation mechanism (**Figure 3.33**). The reaction started by activating the iminoglycal donor with the phosphonochalcogenide catalyst **J** to generate a donor-catalyst complex **84**. Based on ^{77}Se and ^{13}C NMR titration, the noncovalent activation might involve in a bidentate activation of the carbonyl oxygen in the upstream step. Next, one molecule of water existed in the solution attacked **84** to generate the water addition intermediate **83**, which was isolated and characterized. And this process was reversible. It is important to point out that this molecule of water functioned catalytically in the reaction. This is because it was re-expelled from the catalytic

cycle in the further downstream step, so it was no need to add extra water to the solution and exclude it during the reaction. On the other hand, the importance of catalytic water should be emphasized since the reaction was terminated totally when the 3Å molecular sieves was added to the solution at standard condition. Besides, the catalyst **J** would liberate from the substrate at the same time in this step. Then, catalyst **J** would interact with the glycosyl acceptor molecule on the oxygen atom of the hydroxyl or on the sulfur atom of the thiol again, which might decrease the strength of X-H bond in the process. According to the results of the NMR titration between intermediate **83** and the catalyst **J**, this step might involve a bifunctional mode **85**, in which one of the catalyst seleniums binded to the carbonyl oxygen of the carbamate while the other selenium activated the hydroxyl group of the acceptor simultaneously. Next, the anomeric hydroxyl's oxygen on the intermediate **83** received the acidic hydrogen on the X-H bond, and this step's activation complex was regared as **85**.

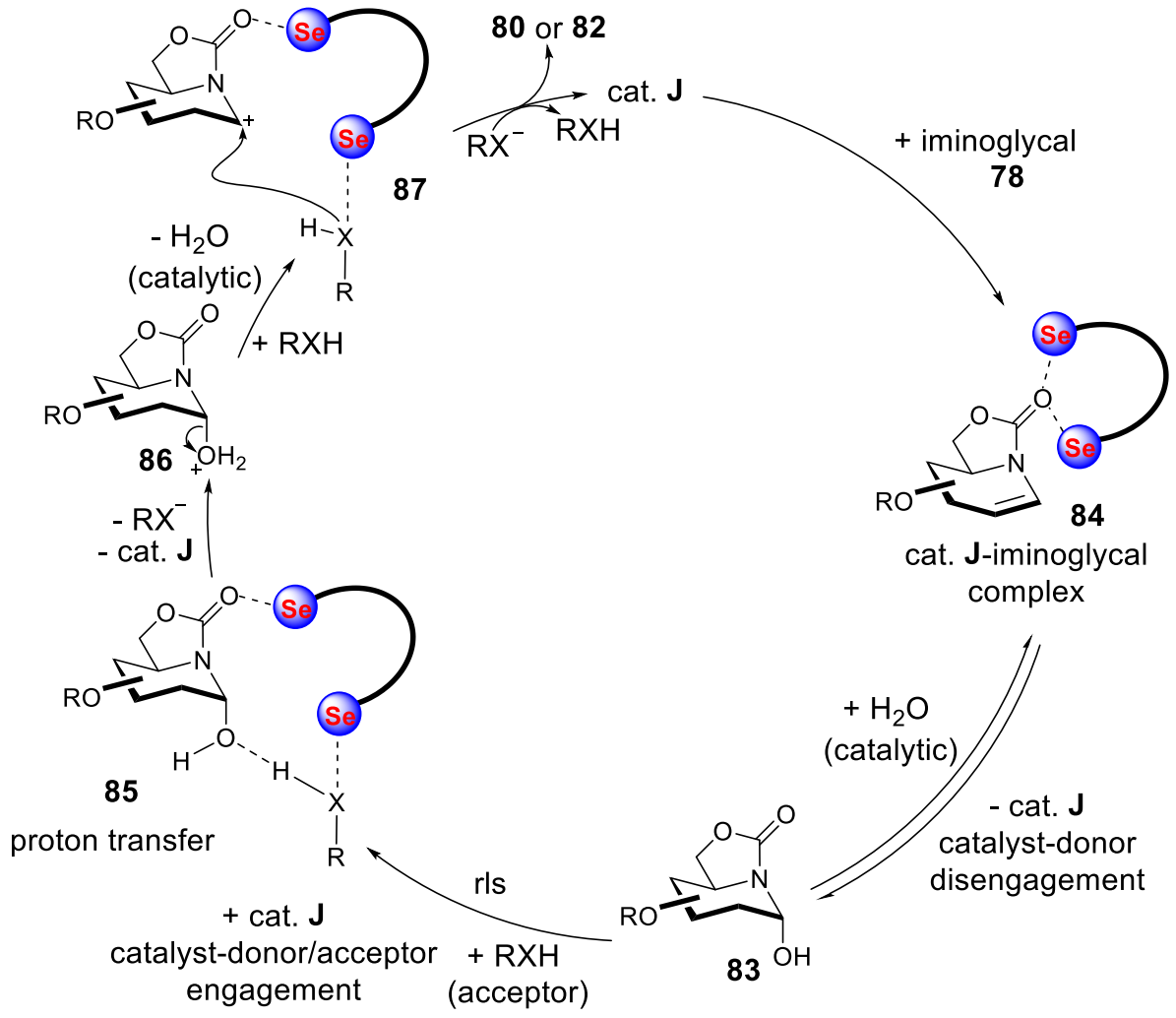

Figure 3.33 Proposed hypothesis of the multi-staged ChB catalyzed mechanism.

It was worth noting that this elementary step was most likely the mechanism's rate limiting step (rls), as the competitive experiment (**Figure 3.25**) showed that the decrease of the pK_a of the acceptor could increase the reaction rate, which was consistent with the protic nature of this elementary step.

Additionally, the kinetic profile of the whole reaction was correlated with the downstream step's kinetic profile, and it was reversible between **84** and **83**. These results indicated that the rls would involve intermediate **83**, the glycosyl acceptor and the catalyst in the elementary step. After that, **86** would be formed with the proton transfering to the hydroxyl group which would act as a good water leaving group to process the final glycosylation. Then, catalyst **J** would disconnect to allow the oxyanion/thiolate intermediate to exit the catalytic cycle temporarily. Further downstream, as catalytic water leaves **86** to produce the iminoglycosyl carbocation in **87**, the catalyst would reestablish a bifunctional activation mode similar to **85** to activate a new glycosyl acceptor molecule. This would therefore make the O/S nucleophile attack on the anomeric center more effective. Finally, proton transfer from oxygen which constructed the glycosidic bond would neutralize the previous formed oxyanion/thiolate species to form α-iminoglycosides **80**-**82** and recycle catalyst **J** into a new catalytic round.

3.5.9 DFT computed geometries and relevant ChB modes (By Dr. Charles Loh)

In order to obtain a more comprehensive understanding of the theoretical viability of the hypothesized ChB catalytic modes throughout several phases of the suggested mechanism, in collaboration with my supervisor Dr. Charles Loh, he used ORCA[84] to model the suggested species **84**, **85**, **86**, and **87** at the M06-2X-D3(0)/def2-SVP/CPCM(CH_2Cl_2) theoretical level,[85] as it was established that the Minnesota functionals were appropriate for characterizing chalcogen bonding interactions (**Figure 3.34**).[86] After acquiring the DFT optimized geometries, he used the wavefunction analyzer Multiwfn[87] to perform NCI analysis[88] on **84**, **85** and **87** (putative ChB modes) in order to identify important portions of NCIs through colored isosurfaces. Fortunately, for these conjectured species, his DFT studies produced well-converged geometric minima. Additionally, NCI study also backed up the following: 1) A bidentate interaction between the catalyst and the carbonyl oxygen of the carbamate in **84** (**Figure 3.34a**). 2) A hydrogen bond between the glycosyl acceptor and the intermediate **83** was present in a bifunctional activation mode in **85** where the catalyst's seleniums were participating in two ChBs with the oxygen of the glycosyl acceptor and the oxygen of the carbamate (**Figure 3.34b**). 3) On the iminoglycosyl cation, there was a comparable bidentate downstream activation mode in **87** (**Figure 3.34c**).

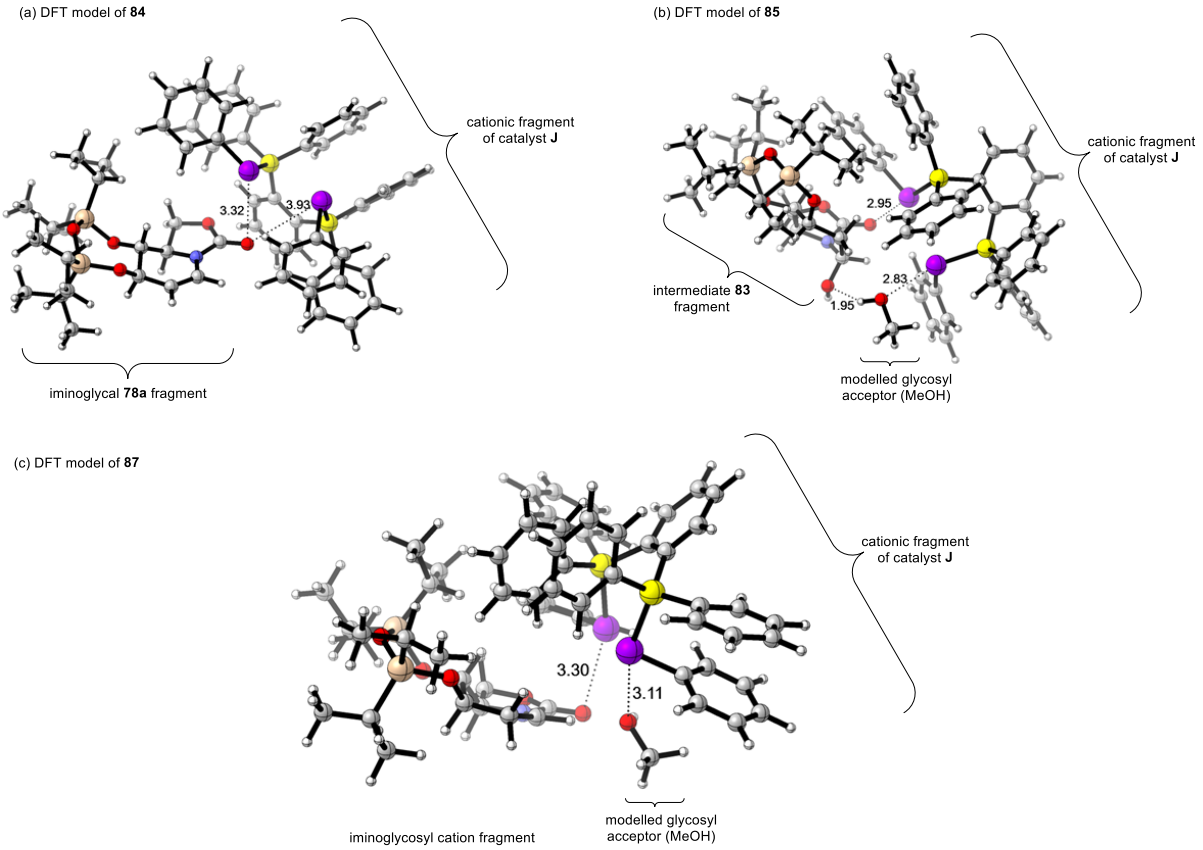

Figure 3.34 DFT computed geometries and relevant ChB modes of participating catalytic species in the postulated mechanism. (a) DFT model of upstream complex **84** in a bidentate carbonyl activation mode. (b) DFT model of downstream complex **85**. in a bifunctional ChB mode and a hydrogen bond established between the glycosyl acceptor and intermediate **83**. (c) DFT model of downstream bidentate ChB activation activation mode **87**. (Red atoms = oxygen, grey atoms = carbon, yellow atoms = phosphorus, purple atoms = selenium, light orange atoms = silicon, white atoms = hydrogen). The relevant NCIs were displayed using dotted lines, and the relevant distances (in in Å) were shown alongside. (Done by Dr. Charles Loh)

3.6 Summary and outlook

In this project, a method of α-selective iminoglycosylation catalyzed by phosphonochalcogenides which involved multiple ChB activation in both upstream and downstream mechanistic stages was developed (**Figure 3.35**). The mechanism of this manifold was different from previous ChB catalytic modes, which were mostly based on manifolds of mono-elementary step activation. Additionally, using PCH catalyst improved the overall usability of the reaction under mild conditions by eliminating the need for moisture exclusion and even using trace water catalytically inside the mechanistic manifold. Significantly, this demonstration provided a workable approach towards sp^2-iminoglycosidic scaffolds that were biologically relevant and addressed the overall lack of robust catalytic iminoglycosylations. Finally, a multi-elementary step mechanism with a proton transfer process as the rate limiting step through comprehensive NMR titrations and kinetic experiment was proposed. With this approach, the frontier of glycomimetic synthesis and stereoselective carbohydrate synthesis was advanced, by utilizing the largely untapped potential of sigma hole based activation.

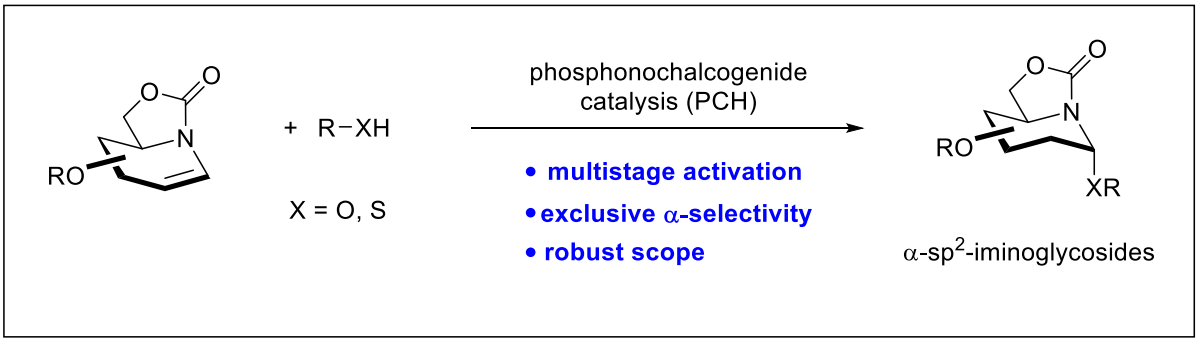

Figure 3.35 Summary of phosphonochalcogenide catalyzed α-selective iminoglycosylation

4. A Synergistic Rh(I)/Organoboron Catalyzed Site Selective Carbohydrate Functionalization that involves Multiple Stereocontrol

4.1 Background

4.1.1 Multiple stereoselective functionalization of carbohydrates

Carbohydrates are a significant natural class of biomolecules and perform essential roles in living organisms. Therefore, synthesizing and modifying carbohydrates are essential for the understanding of their functions and for the development of effective therapeutic reagents. Chiral catalytic strategies for site-selective functionalizations of carbohydrates could offer a very promising way to obtain glycosidic scaffolds that were previously unattainable. Despite the fact that chiral catalytic methods for site-selective functionalization of carbohydrates had witnessed some progress, however, according to the literature, only two examples had attempted to address the dual stereoselectivity difficulties of chirality formation on the external prochiral electrophile while also performing site-selective carbohydrate functionalization. In 2017, Niu and co-workers presented a method that enabled the delivery of terminal propargyls to different monosaccharides, the building blocks of carbohydrates, in a site-selective and site-divergent manner (**Fig. 4.1**).[89] This strategy relied on a combination of copper and borinic acid catalysis, which were known as synergistic catalysis. This method could be adjusted to propargylate the axial or equatorial hydroxyl with high selectivity using a pair of antipodal ligands. The direct propargylation of complex, unprotected glycosylated natural compounds demonstrated the broad scope of this reaction. This process produced compounds containing terminal alkyne groups, allowing for additional manipulations such as copper-catalyzed azide-alkyne coupling.

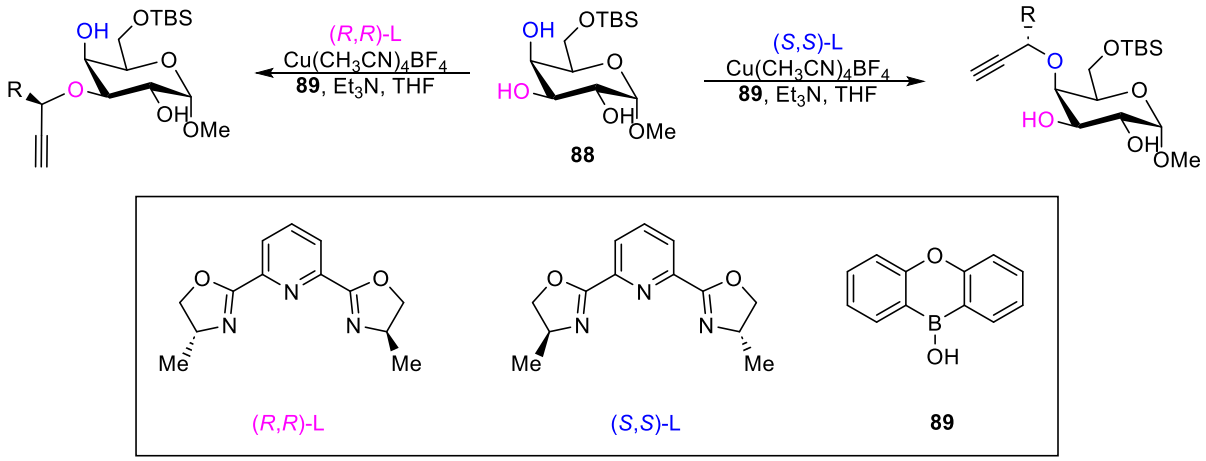

Figure 4.1 Site-divergent propargylation of monosaccharides by Cu/borinic acid dual catalysis.

In 2019, Tang group presented a viable and reliable approach for the site- and stereoselective alkylation of carbohydrate hydroxyl groups using Rh(II)-catalyzed insertion of metal carbenoid intermediates (**Fig. 4.2**).[90] It was one of the mildest approaches for the systematic alteration of carbohydrates. Density functional theory (DFT) studies indicated that site selectivity was established during the Rh(II)-carbenoid insertion step, which favored insertion into hydroxyl groups with an adjacent axial substituent.

The following intramolecular enolate protonation was responsible for the unexpectedly high stereoselectivity. The most common *trans*-1,2-diols in various pyranoses could be separated systematically and consistently using a model built from DFT calculations. They also showed that the selective *O*-alkylation approach might considerably increase the efficiency and stereoselectivity of glycosylation processes. The alkyl groups incorporated into carbohydrates by the OH insertion reaction could operate as functional, protective and directing groups.

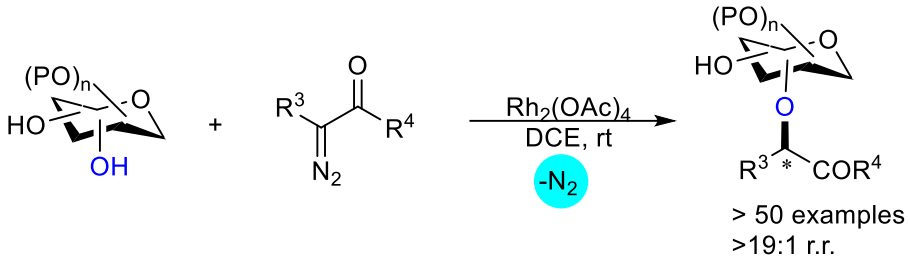

Figure 4.2 Selective *O*-alkylation of glycosides by Rh (II) catalysis.

4.1.2 Established transmetalating role of boronic acids in Rh(I) catalysis

Transmetalation between organo/main group metal reagents and transition metal compounds was crucial for organic synthesis since it created new carbon-carbon bonds between organometallic units and electrophilic chemicals. Organoboron compounds, such as boronic acids, were frequently used in Rh(I) catalysis. Miyaura and Hayashi had done great pioneering work in this aspect.[91] However, the currently only known catalytic action before the publication of this work was that of transmetallating agents for *cis*-carborhodation (**Fig. 4.3**).[92] Recently, there has been an increasing interest in the alternative use of organoboron reagents as glycofunctionalization catalysts.[93] Thus, the integration of organoboron catalysis with chiral Rh(I) catalysis would open up a new direct pathway into hydronapthalene glycoside motifs. However, this was not a simple task because it involved coordinating a difficult molecular maneuver that avoided the transmetallation pathway from boron to Rh(I).

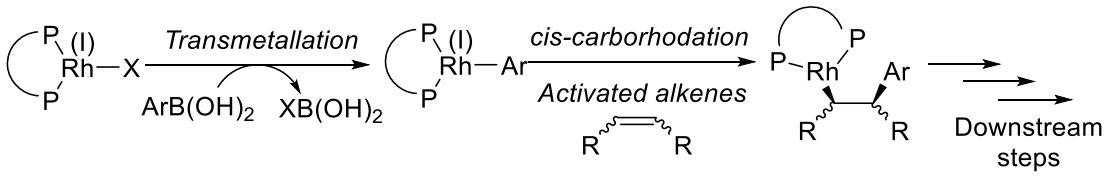

Figure 4.3 Transmetalating role of boronic acids in Rh(I) catalysis

4.1.3 Biologically active arylnapthalene glycosides

Arylnaphthalene compounds have been widely investigated and recorded for their biological activities, particularly podophyllotoxin and its derivatives.[94] Among them, arylnaphthalene glycosides have gained increasing interests due to their pharmacological effect in cancer chemotherapy and other bioactivities, such as their anti-inflammatory, antitumor and antiviral activities. For example, some

arylnaphthalene glucopyranoside derivatives have been developed to three clinically used anticancer drugs: etoposide **90**, teniposide **91** and etoposide phosphate **92**,[95] while analogue **93** displays important antitumor activity[96] (**Fig. 4.4**). Therefore, it's essential to develop new strategies for these arylnaphthalene glucopyranoside derivatives synthesis.

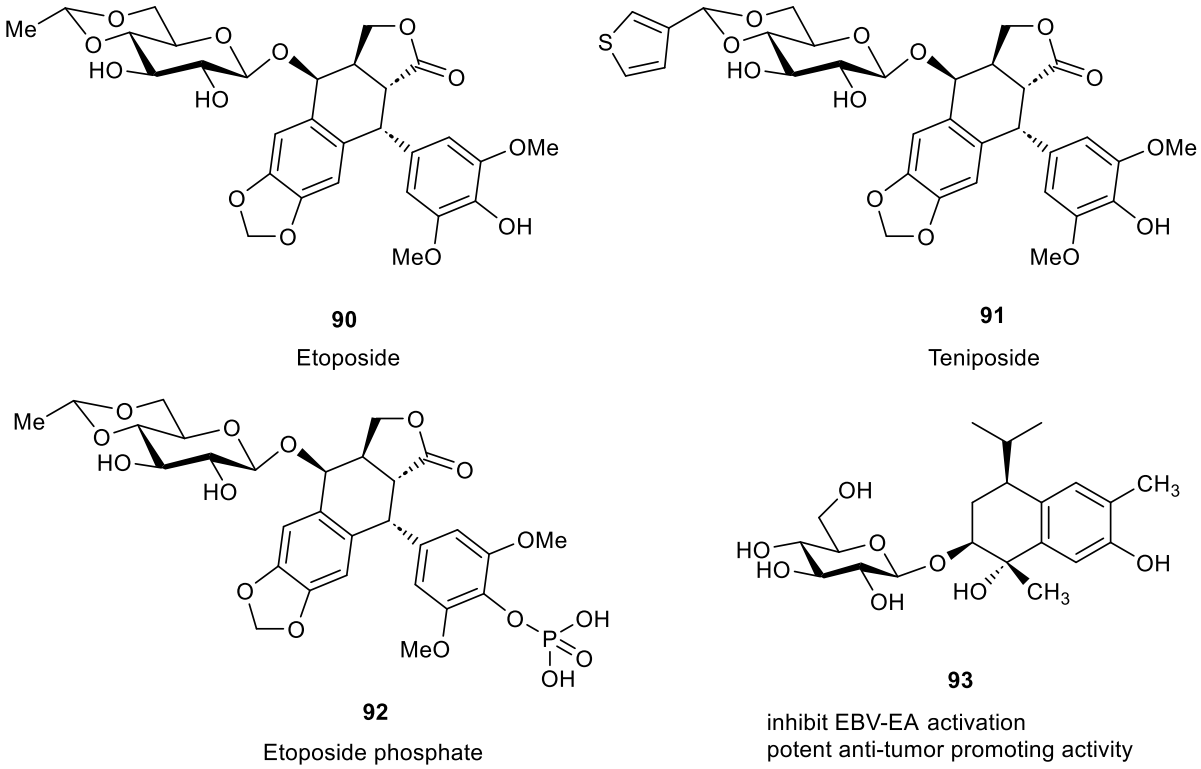

Figure 4.4 Anticancer drugs and biological activity of arylnapthalene glycosides

4.2 Project design

Site selective functionalization is a fundamental synthetic strategy with wide-ranging applications in organic synthesis. Specifically, using chiral catalysis to modulate site selectivity in complicated carbohydrate functionalizations has emerged as a major approach for discovering novel pathways into biologically relevant glycosides. However, there are few examples in the literature that use site-selective carbohydrate functionalization to address the various stereoselectivity challenges of creating chirality on an external prochiral electrophile (see **Fig. 4.1** and **Fig. 4.2**). In order to overcome numerous aspects of stereoselectivity challenges, my colleague Dr. Uday Vippilli Bhaskara Rao, who was a post-doc in Dr. Charles Loh research group between 2018-2021, developed a site-selective access of biologically interesting aryl hydronapthalene glycosides by harnessing the power of synergistic chiral Rh(I) and organoboron catalysis, This effort resulted in the concurrent formation of two external stereogenic centers on a prochiral meso-oxanorbornadiene with diastereo- and enantiocontrol (**Fig. 4.5a**). To the best of our knowledge, his method was the first one to use chiral Rh(I) catalysis for site-selective carbohydrate functionalization. Significantly, his procedure introduced a novel co-catalytic role for boronic acids in the domain of Rh(I) catalysis, which took precedence over the usual transmetallation

pathway. Furthermore, the *trans*-diastereoselectivity reported in his method differed significantly from the *cis*-selectivity observed in asymmetric ring opening (ARO) reactions using boronic acid nucleophiles. In collaboration with Bhaskara Rao, I contemplated employing his approach to accomplish the functionalization of unprotected saccharides' anomeric oxygen, which was generally present in bioactive aryl naphthalene glycosides (see **Fig. 4.4**). Besides, I extended the electrophiles beyond *meso*-oxanorbornadiene to allylic carbonates, which played a significant role in Rh-catalyzed functionalization processes (**Fig. 4.5b**).

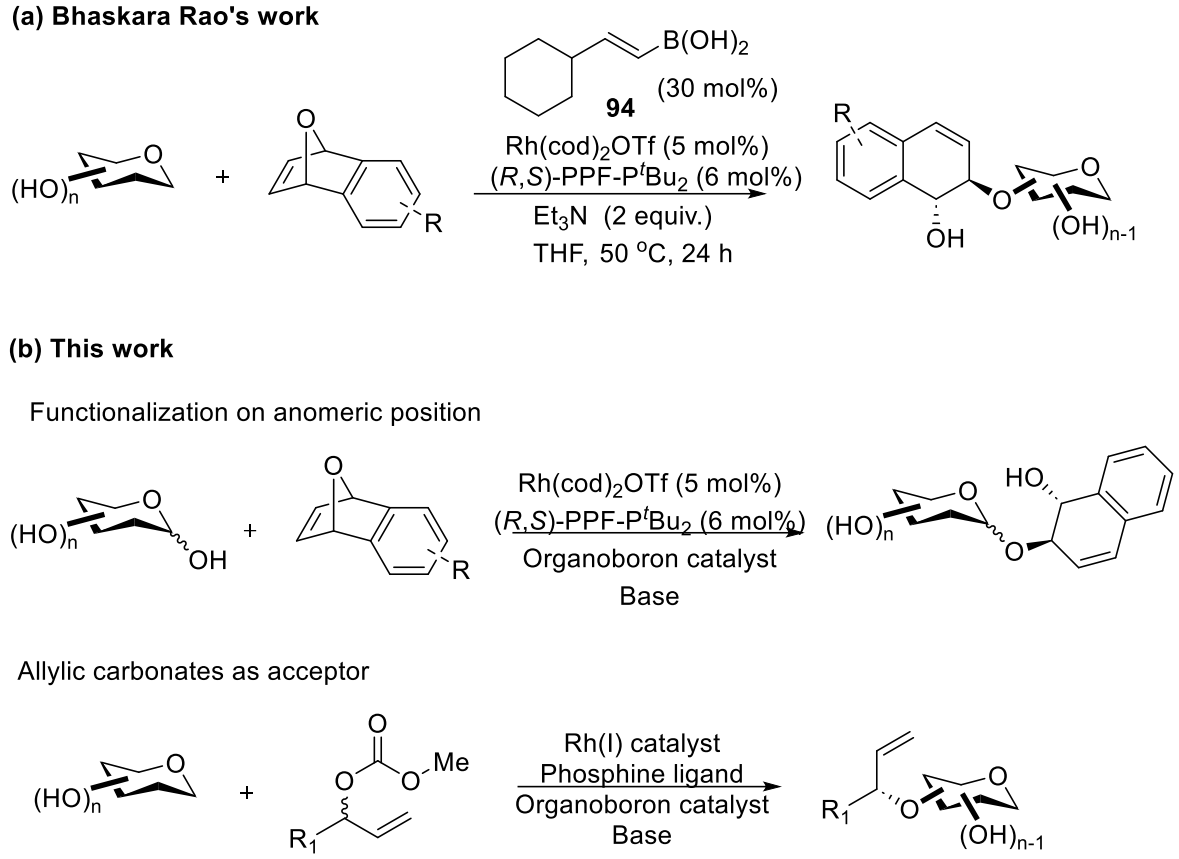

Figure 4.5 (a) Bhaskara Rao's work. (b) This work

4.3 Results and discussion

4.3.1 Research on the anomeric site-selective functionalization

Initially, the anomeric substrate **95a** was used to react with oxanorbornadiene **96** under the optimal reaction conditions which were optimized by Rao in his previous research. Unfortunately, there was no site selective functionalization product formed. The challenge was not trivial considering that anomeric substrates were the only ones with a hemiacetal moiety that allowed for quick equilibration between the α- and β-anomers, thus increasing the difficulty of stereoselectivity. A brief condition screening was conducted. Gratifyingly, by replacing the organoboron catalyst **94** to **89** and the base triethylamine to diisopropylethylamine respectively,[97],[98] 75% yield of 1,2-*cis* product **97a** was obtained in 2 hours with excellent enantio-, diastereo-, site- and anomeric selectivity. Next, the use of 4,6- siloxane

protected anomeric substrate **95b** was employed, and a yield of 65% was achieved for the 1,2-*cis* product **97b**, which also exhibited high enantio-, diastereo-, site-, and anomeric selectivity. In addition to the glucose anomeric substrate, the lyxose substrate was also tolerated with strong enantio-, diastereo-, site- and anomeric selectivity, yielding 61% 1,2-*cis* product **97c** (**Fig. 4.6**).

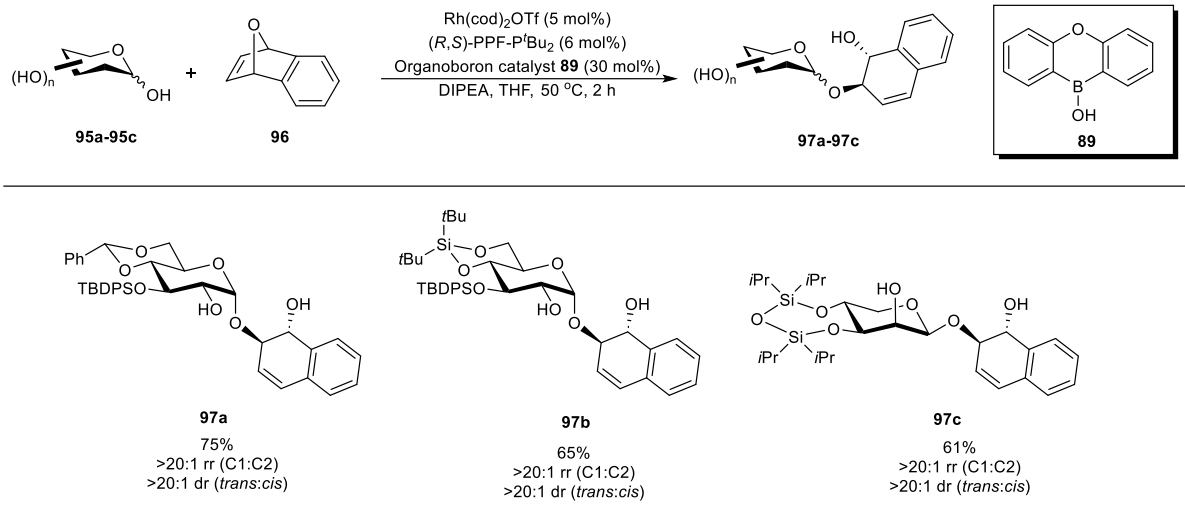

Figure 4.6 Examples for anomeric site selective functionalization of carbohydrate

4.3.2 Site-selective functionalization using allylic carbonate as the electrophile

4.3.2.1 Conditions screening

In the beginning, in order to determine the ideal reaction conditions, the allylic carbonates with α-branched methyl **99a** as the donor and the mannosyl triol derivative **98a**, which has been previously reported, were selected as the model substrate acceptor. There was no site-selective product generated when the prior ideal conditions were applied to this reaction (Table 4.1, entry 1). Changing the chiral ligand to the opposite enantiomeric ligand did not improve the reaction result and there was no detectable product (Table 4.1, entry 2). The Rhodium catalyst and ligand types appeared to be essential to the reaction, as the reaction progressed smoothly to generate 65% of the corresponding functionalized product **100a** with concurrent regio- and diastereoselectivity (Ratio of **100a**/**101**: > 20/1) when catalyst $Rh(cod)_2BF_4$ and ligand (*S*)-NPN were utilized (Table 4.1, entry 4).[99] However, when the opposite enantiomeric ligand (*R*)-NPN was utilized instead of the (*S*)-NPN, the total yield of the product was 53%, but the regeoselectivity was too low at only 2:1 (**101**/**102**) (Table 4.1, entry 5). The solvent was critical to the reaction; replacing acetonitrile (ACN) with tetrahydrofuran (THF) resulted in no functionalized product (Table 4.1, entry 3). Other Rhodium catalysts including $Rh(NBD)_2OTf$ and $Rh(NBD)_2BF_4$ could not catalyze the process (Table 4.1, entry 6 and 7). Interestingly, 55% of the product was generated when ligand (*R*)-NPN was combined with catalyst $Rh(NBD)_2BF_4$, but regeoselectivity was only 2:1 (Table 4.1, entry 8). These findings suggested that any of these components had a significant impact on the result. Fortunately, after screening a variety of conditions,

I arrived at the optimal reaction condition with high yield and excellent regeoselectivity and diastereoselectivity (Table 4.1, entry 4).

Table 4.1 Conditions screening for allylic carbonate reaction

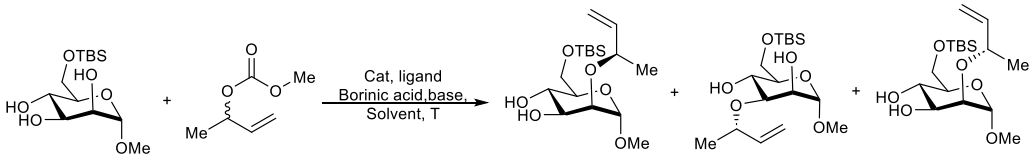

98a **99a** **100a** **101** **102**

Entry	Metal catalyst	Ligand	Boronic acid (30 mol%)	Base 2 equiv.	Solvent	Temp °C	Time	Yield (%)	**Ratio 100a/101/102**
1	$Rh(cod)_2OTf$ (5 mol%)	(*R*,*S*)-PPF-P*t*Bu_2	**94**	Et_3N	THF 1 mL	50	24 h	n.d.	-
2	$Rh(cod)_2OTf$ (5 mol%)	(*S*,*R*)-PPF-P*t*Bu_2	**94**	Et_3N	THF 1 mL	50	24 h	n.d.	-
3	$Rh(cod)_2BF_4$ (5 mol%)	(*S*)-NPN	**89**	DIPEA	THF 1 mL	50	24 h	n.d.	-
4	$Rh(cod)_2BF_4$ (5 mol%)	(*S*)-NPN	**89**	DIPEA	ACN 1 mL	50	18 h	65%(63%[b])	20/1/0
5	$Rh(cod)_2BF_4$ (5 mol%)	(*R*)-NPN	**89**	DIPEA	ACN 1 mL	50	18 h	53%	0/2/1
6	$Rh(NBD)_2OTf$ (5 mol%)	(*S*)-NPN	**89**	DIPEA	ACN 1 mL	50	18 h	n.d.	-
7	$Rh(NBD)_2BF_4$ (5 mol%)	(*S*)-NPN	**89**	DIPEA	ACN 1 mL	50	18 h	n.d.	-
8	$Rh(NBD)_2BF_4$ (5 mol%)	(*R*)-NPN	**89**	DIPEA	ACN 1 mL	50	18 h	55%	0/2/1

Conditions: [a]Polyol **98a** (0.1 mmol), **99a** (0.15 mmol), cat.(5 mol%), ligand(6 mol%), organoboron catalyst(30 mol%), argon, 50 °C, 18-24 h.[b]Isolated yield, n.d.: not detected.

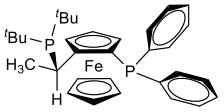

(*S*,*R*)-PPF-P^tBu_2 Josiphos

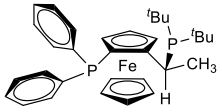

(*R*,*S*)-PPF-P^tBu_2 Josiphos

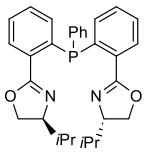

(*S*)-NPN

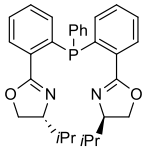

(*R*)-NPN

4.3.2.2 Substrate scope study

With all these five optimized conditions in hand, a number of allylic substituted products were employed (**Fig. 4.7**). The majority of these substrates were compatible with the reaction conditions. I discovered that allylic substitution could be extended to allylic carbonates with sterically and electrically distinct substituents ranging from aliphatic, cyclic, to aromatic substituents (**100a-100d**). All of these substituents resulted in C-2 functionalized products with good diastereoselectivity and regeoselectivity (>20/1) and a moderate to good yield. Besides, apart from the mannosyl triol derivative substrate, lyxose substrate was also well tolerated, resulting the C-2 functionalized product with moderate yield and excellent regeoselectivity and diastereoselectivity (**100f**). The absolute configuration of **100a** was further determined by using VCD analysis (By Christian Merten Group in Ruhr University of Bochum) and the other derivatives were assigned by analogy. Furthermore, the relative configurations of all allylic substitution products were double checked with 2-dimensional Hetereonuclear Multiple Bond Correlation (HMBC) NMR spectroscopy.

A Synergistic Rh(I)/Organoboron Catalyzed Site Selective Carbohydrate Functionalization that involves Multiple Stereocontrol

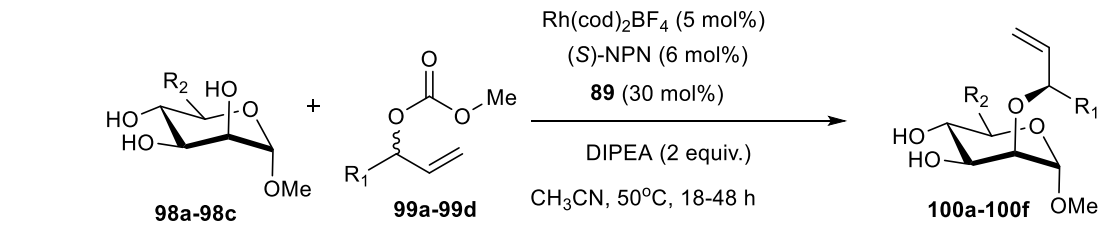

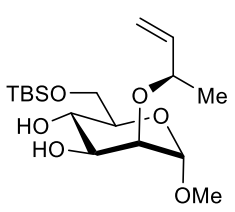

100a
63%
>20:1 rr (C2:C3)
>20:1 dr

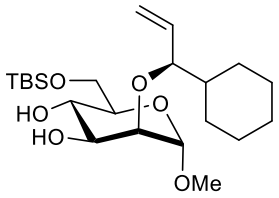

100b
70%
>20:1 rr (C2:C3)
>20:1 dr

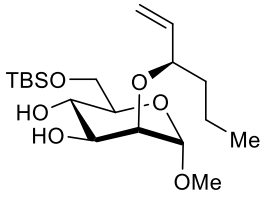

100c
81%
>20:1 rr (C2:C3)
>20:1 dr

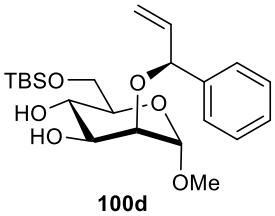

100d
63%[a]
>20:1 rr (C2:C3)
>20:1 dr

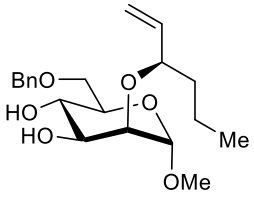

100e
60%
>20:1 rr (C2:C3)
>20:1 dr

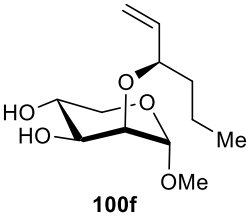

100f
61%
>20:1 rr (C2:C3)
>20:1 dr

Polyol **98a** (0.2 mmol), **99a** (0.24 mmol), $Rh(cod)_2BF_4$ (5 mol%), (*S*)-NPN (6 mol%), organoboron catalyst **89** (30 mol%), in CH_3CN (1 mL), argon, 50 °C, 18-48 h. rr and dr were determined by crude ^1H NMR spectra analysis. [a] 10 mol% $Rh(cod)_2BF_4$, 12 mol% (*S*)-NPN, 70 °C.

Figure 4.7 Substrate scope for the allylic carbonate reaction

4.4 Summary and outlook

In this project, in the collaboration with my colleague Dr. Uday Vippilli Bhaskara Rao, the first example of chiral Rh(I) catalysis in conjunction with boronic acid catalysis in solving the problem of functionalizing the anomeric oxygen of anomeric unprotected saccharides was demonstrated. This method possessed the advantages of overcoming the challenge of multiple regio-, diastereo-, enantio- and anomeric control within a single bond formation step (**Fig. 4.8a**). Therefore, this approach provided a practical way to synthesize biologically stereoselective arylnapthalene glycosides. It was worth noting that this strategy could also be applied to the structurally related allylic carbonate substrates to synthesize the corresponding functionalized products with excellent regio- and diastereoselectivity (**Fig. 4.8b**). Furthermore, the protocol presented a novel insight of the co-catalytic role for organoboron reagents in Rh(I) catalysis. This strategy thus offered carbohydrate chemists a new approach to access complex functionalized carbohydrates. Finally, this protocol would inspire scientists develop novel chiral transition catalytic systems for difficult site selective functionalizations of carbohydrates with prochiral electrophiles.

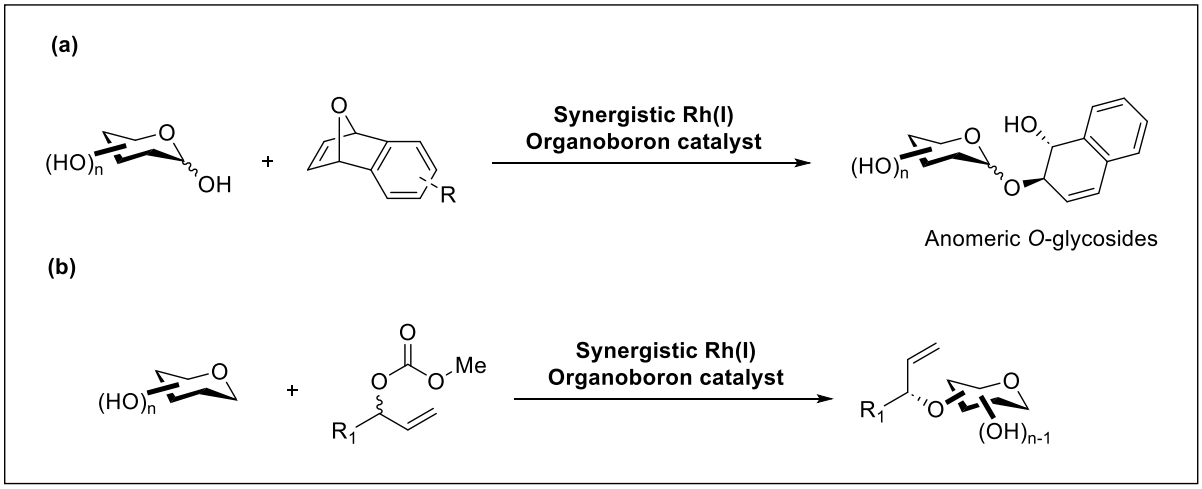

Figure 4.8 Synergistic Rh(I) and boronic acid catalyzed functionalization of unprotected saccharides

5. Experimental section

5.1 General information

Unless otherwise stated, all reactions were setted up under inert atmosphere (argon) utilizing glassware that were oven dried and cooled under argon purging. Silica Gel Flash Column Chromatography was performed on *Silica gel Merck 60* (*particle size 40-63 µm*). Starting materials were purchased directly from commercial suppliers (Sigma Aldrich, Acros, Alfa Aesar, VWR, TCI) and used without further purifications unless otherwise stated. All solvents were dried according to standard procedures or brought from commercial suppliers. Reactions were monitored using thin-layer chromatography (TLC) on *Merck silica gel aluminium plates with F254 indicator*. Visualization of the developed plates was performed under UV light (254 nm) or $KMnO_4$ stain.

NMR characterization data (^{1}H NMR, ^{13}C NMR and 2D spectra) were collected at 300 K on a *Bruker DRX400 (400 MHz)*, *Bruker DRX500 (500 MHz)*, *INOVA500 (500 MHz), DRX600 (600 MHz)* and *Bruker DRX700 (700 MHz)* using $CDCl_3$, CD_2Cl_2 and CD_3OD as solvent. Data for ^{1}H NMR were reported as follows: chemical shift (δ ppm), multiplicity (s = singlet, d = doublet, t = triplet, q = quartet, m = multiplet, br = broad), coupling constant (*J*) were given in Hertz (Hz). Referenced to the solvent resonance as internal standard ($CDCl_3$: δ = 7.26 ppm for ^{1}H, δ = 77.16 ppm for ^{13}C; CD_2Cl_2: δ = 5.32 ppm for ^{1}H, δ = 54.00 ppm for ^{13}C; CD_3OD: δ = 3.31 ppm for ^{1}H, δ = 49.00 ppm for ^{13}C).

High resolution mass spectra were recorded on an *LTQ Orbitrap* mass spectrometer coupled to an *Accela HPLC*-System (HPLC column: *Hypersyl GOLD*, 50 mm x 1 mm, particle size 1.9 µm, ionization method: electron spray ionization) and Bruker ultrafleXtreme MALDI-TOF-TOF (3 decimal accuracy). Optical rotations were measured in a *Schmidt + Haensch Polartronic HH8* polarimeter equipped with a sodium lamp source (589 nm) and were reported as follows: $[\alpha]_D^{T\,°C}$ (*c* = g/100 mL, solvent).

The anomeric selectivity was determined by ^{1}H-NMR of the crude reaction mixture *via* integration of characteristic signals in the ^{1}H NMR spectra, Chemical yields referred to isolated substances after flash column chromatography. NMR yields were determined using 1,3,5-trimethoxybenzene or 1,1,2,2-tetrachloroethane as internal standard.

5.2 Experimental part for synthesis of iminoglycosides

5.2.1 Preparation of catalysts

Catalysts **A** and **B** were prepared according to the literature procedure.[100] **C** and **M** were commercially available, **D-J** and **N** were prepared according to the literature procedure.[101], [102] **K** and **L** were prepared using the following procedure (**Fig. 5.1**).

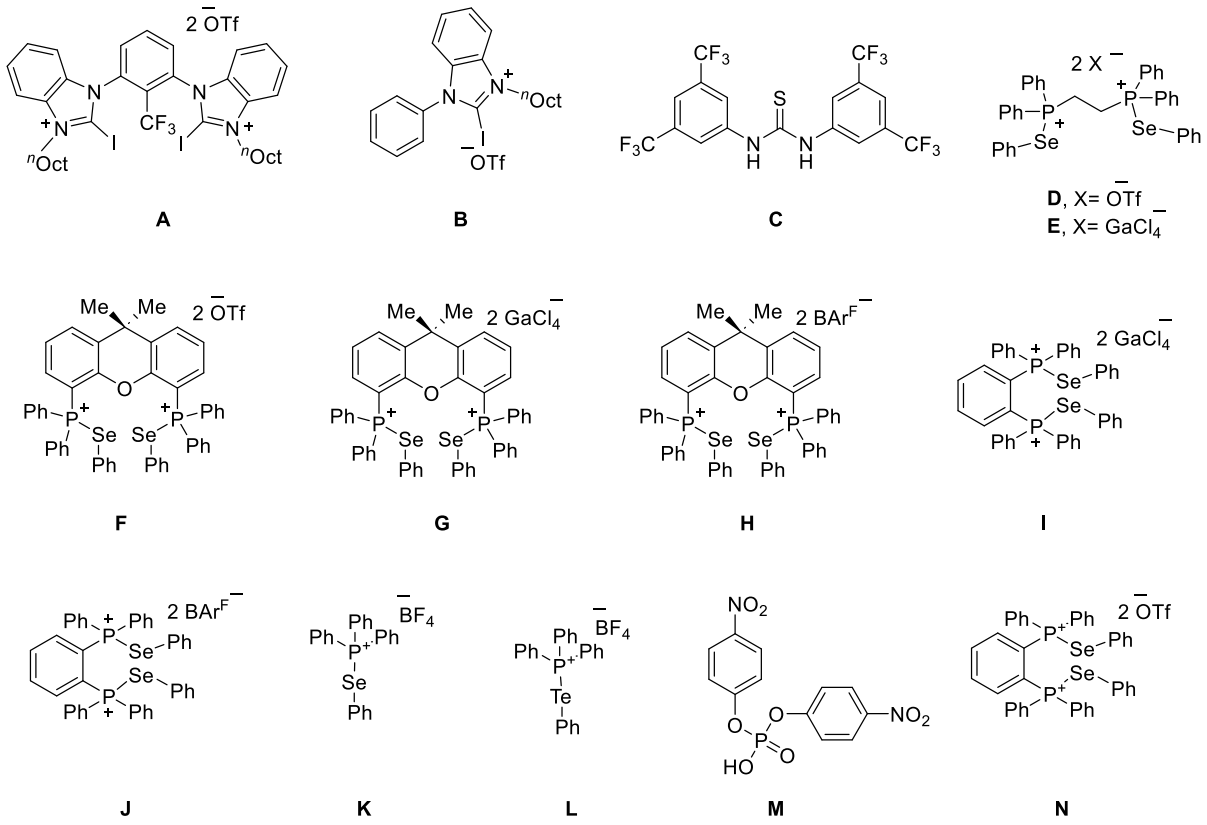

Figure 5.1 Structure of some catalysts

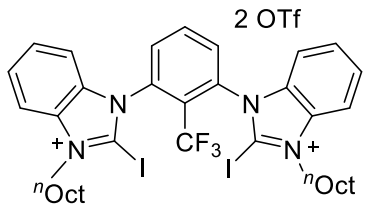

^{1}H NMR (600 MHz, CD_2Cl_2) δ 8.33 (t, *J* = 8.4 Hz, 1H), 8.21 – 8.17 (m, 2H), 7.98 – 7.93 (m, 2H), 7.82 – 7.78 (m, 2H), 7.75 – 7.68 (m, 4H), 4.66 – 4.50 (m, 4H), 2.01 (p, *J* = 7.8 Hz, 4H), 1.50 – 1.35 (m, 8H), 1.33 – 1.23 (m, 12H), 0.87 (t, *J* = 7.2 Hz, 6H). **^{13}C NMR** (150 MHz, CD_2Cl_2) δ 138.49, 136.52, 136.05, 135.08, 133.13, 129.34, 128.46, 127.81 (d, *J* = 31.1 Hz), 121.57 (d, *J* = 275.6 Hz), 120.86 (d, *J* = 318.3 Hz), 116.25, 115.19, 113.16, 51.85, 32.17, 29.58, 29.54, 29.50, 27.08, 23.11, 14.35. **^{19}F NMR** (565 MHz, CD_2Cl_2) δ -55.85, -78.76. The analytical data are in accordance with the reported literature. [100]

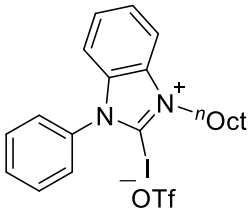

B

^{1}H NMR (600 MHz, CD_2Cl_2) δ 7.85 – 7.73 (m, 4H), 7.70 – 7.66 (m, 1H), 7.61 – 7.57 (m, 1H), 7.55 – 7.50 (m, 2H), 7.42 – 7.36 (m, 1H), 4.61 (t, *J* = 7.8 Hz, 2H), 2.06 – 1.99 (m, 2H), 1.56 – 1.50 (m, 2H), 1.42 (dq, *J* = 9.2, 6.7 Hz, 2H), 1.37 – 1.26 (m, 6H), 0.89 (t, *J* = 7.2 Hz, 3H). **^{13}C NMR** (150 MHz, CD_2Cl_2) δ 135.64, 134.64, 133.70, 132.61, 131.46, 128.38, 128.13, 128.08, 113.77 (d, *J* = 113.77 Hz), 112.85, 51.64, 32.24, 29.73, 29.62, 29.59, 27.28, 23.15, 14.38. **^{19}F NMR** (565 MHz, CD_2Cl_2) δ -78.80. The analytical data are in accordance with the reported literature. [100]

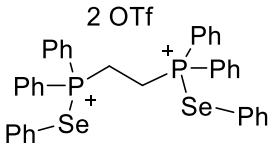

D

TMSOTf (2.0 mmol, 444.52 mg, 0.362 mL) was added to a red solution of PhSeCl (2.0 mmol) in dry CH_2Cl_2 (5.0 mL) at 0 °C. The reaction mixture was allowed to warm to room temperature and stirred for 40 minutes to give a dark orange solution. Then 1,2-bis(diphenylphosphanyl)ethane (1.0 mmol, 398.43 mg) in anhydrous CH_2Cl_2 (5.0 mL) was added over 10 minutes at 0 °C. The reaction mixture was allowed to warm to room temperature and stand for 1 h to generate suspended solid. The suspension was filtered and washed by anhydrous diethyl ether to obtain a white solid (800 mg, 80 %). The analytical data are in accordance with the reported literature. [101]

^{1}H NMR (600 MHz, CD_2Cl_2) δ 7.83 – 7.79 (m, 4H), 7.76 – 7.71 (m, 6H), 7.68 – 7.60 (m, 10H), 7.36 – 7.31 (m, 2H), 7.09 – 7.03 (m, 8H), 3.30 (d, *J* = 3.7 Hz, 4H). **^{13}C NMR** (150 MHz, CD_2Cl_2) δ 137.99, 136.47, 134.41, 134.37, 134.34, 132.04, 132.01, 131.18, 131.14, 131.09, 129.76, 128.33, 121.29 (q, *J* = 318.8 Hz), 118.66. **^{31}P NMR** (243 MHz, CD_2Cl_2) δ 42.91.

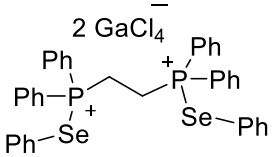

E

^{1}H NMR (600 MHz, CD_2Cl_2) δ 7.93 – 7.85 (m, 4H), 7.76 – 7.69 (m, 8H), 7.65 – 7.56 (m, 8H), 7.43 – 7.37 (m, 2H), 7.15 – 7.07 (m, 4H), 7.05 – 6.98 (m, 4H), 3.09 (d, *J* = 3.6 Hz, 4H). **^{13}C NMR** (150 MHz, CD_2Cl_2) δ 137.89, 137.24, 134.11, 134.07, 134.03, 132.57, 131.75, 131.71, 131.66, 131.53, 117.81,

116.46 (td, *J* = 70.5, 70.6 Hz), 20.65(t, *J* = 20.9 Hz). **^{31}P NMR** (243 MHz, CD_2Cl_2) δ 41.37. The analytical data are in accordance with the reported literature. [101]

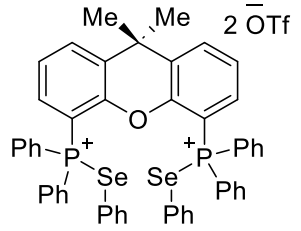

F

^{1}H NMR (400 MHz, CD_2Cl_2) δ 8.24 – 8.09 (m, 2H), 7.63 – 7.36 (m, 26H), 7.22 – 7.16 (m, 8H), 1.96 (s, 6H). **^{13}C NMR** (100 MHz, CD_2Cl_2) δ 153.01, 138.25 (d, *J* = 3.7 Hz), 137.13, 136.90, 136.87, 136.46 (d, *J* = 3.5 Hz), 134.86 (d, *J* = 10.7 Hz), 133.84, 132.38 (d, *J* = 3.5 Hz), 131.30, 131.24, 131.21, 131.16, 126.59, 126.46, 121.32, 121.23, 120.36, 119.58, 35.43, 34.24. The analytical data are in accordance with the reported literature. [101]

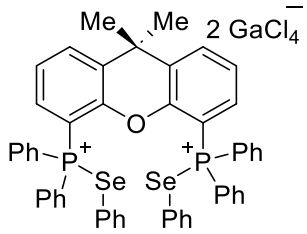

G

^{1}H NMR (400 MHz, CD_2Cl_2) δ 8.17 (d, *J* = 7.9, 2H), 7.65 – 7.59 (m, 4H), 7.57 – 7.51 (m, 8H), 7.50 – 7.38 (m, 13H), 7.22 (t, *J* = 7.6 Hz, 4H), 7.16 – 7.09 (m, 5H), 1.98 (s, 6H). **^{13}C NMR** (100 MHz, CD_2Cl_2) δ 153.09 (d, *J* = 2.3 Hz), 138.15 (d, *J* = 3.8 Hz), 137.21(d, *J* = 8.5 Hz), 137.03(d, *J* = 2.6 Hz), 136.54 (d, *J* = 3.3 Hz), 134.79 (d, *J* = 10.2 Hz), 133.83 (d, *J* = 6.7 Hz), 132.52 (d, *J* = 3.3 Hz), 131.25 (d, *J* = 3.5 Hz), 126.65 (d, *J* = 13.2 Hz), 120.34, 119.56, 34.39. The analytical data are in accordance with the reported literature. [102]

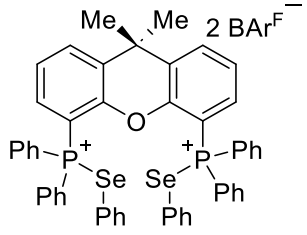

H

^{1}H NMR (600 MHz, CD_2Cl_2) δ 8.12 – 8.07 (m, 2H), 7.75 – 7.69 (m, 16H), 7.62 – 7.58 (m, 4H), 7.56 – 7.52 (m, 8H), 7.49 – 7.43 (m, 8H), 7.41 – 7.38 (m, 4H), 7.35 – 7.28 (m, 8H), 7.19 – 7.13 (m, 4H), 7.13 – 7.06 (m, 2H), 7.01 – 6.96 (m, 4H), 1.87 (s, 6H). **^{13}C NMR** (150 MHz, CD_2Cl_2) δ 162.79, 162.46, 162.13, 161.80, 152.98, 152.96, 137.70, 137.68, 137.30, 137.25, 136.98, 136.97, 136.88, 136.85, 135.35,

134.53, 134.46, 133.86, 133.81, 132.94, 132.91, 131.45, 131.43, 131.25, 131.16, 129.75, 129.71, 129.56, 129.54, 129.52, 129.50, 129.35, 129.33, 129.31, 129.29, 129.11, 127.84, 126.84, 126.75, 126.03, 124.23, 122.42, 120.79, 120.73, 119.93, 119.41, 118.10, 118.07, 118.04, 118.01, 117.99, 35.39, 33.96. **^{19}F NMR** (565 MHz, CD_2Cl_2) δ -62.80. The analytical data are in accordance with the reported literature. [102]

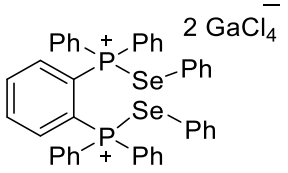

I

^{1}H NMR (400 MHz, CD_2Cl_2) δ 8.23 – 8.15 (m, 4H), 7.83 – 7.77 (m, 4H), 7.65 – 7.59 (m, 8H), 7.50 – 7.44 (m, 8H), 7.41 – 7.36 (m, 2H), 7.13 – 7.08 (m, 4H), 6.74 – 6.66 (m, 4H). **^{13}C NMR** (100 MHz, CD_2Cl_2) δ 143.08, 142.98, 137.92, 137.90, 137.88, 137.40, 137.32, 136.95, 134.77, 134.71, 134.66, 132.94, 131.99, 131.54, 131.48, 131.40, 119.68, 118.91.

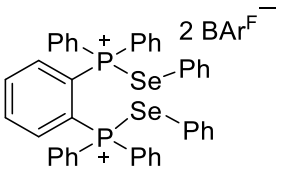

J

The sodium tetrakis[3,5-bis(trifluoromethyl) phenyl]borate (1.0 mmol, 886.2 mg) was added to a solution of catalyst **N** (0.5 mmol, 528.0 mg) in dry CH_2Cl_2 (6.0 mL) under argon and the reaction mixture was stirred at room temperature for 4 h. Then the reaction mixture was filtered and the filtrate was concentrated to give a saturated solution (~4 mL CH_2Cl_2) under reduced pressure and then 10.0 mL *n*-hexane was slowly added. The two-phase solution was then placed for 12 h at 0 °C under argon and the desirable product precipitated out as a white solid. Then the precipitated white solid was collected by filtration and recrystallized from dichloromethane and n-hexane to give pure catalyst **J** as a white solid in 62% yield.

^{1}H NMR (600 MHz, CD_2Cl_2) δ 8.09 – 7.98 (m, 4H), 7.80 – 7.76 (m, 4H), 7.73 – 7.71 (m, 16H), 7.57 – 7.52 (m, 16H), 7.41 – 7.37 (m, 2H), 7.34 – 7.28 (m, 8H), 7.07 (t, *J* = 7.8 Hz, 4H), 6.68 – 6.59 (m, 4H). **^{13}C NMR** (150 MHz, CD_2Cl_2) δ 162.81, 162.48, 162.15, 161.82, 142.68, 142.62, 142.55, 137.58, 137.55, 137.52, 136.84, 136.81, 136.78, 136.75, 136.72, 135.36, 134.40, 134.37, 134.34, 134.31, 134.28, 133.52, 133.50, 131.69, 131.68, 131.64, 131.62, 131.57, 131.53, 131.51, 129.79, 129.77, 129.75, 129.73, 129.58, 129.56, 129.54, 129.52, 129.37, 129.35, 129.33, 129.31, 129.16, 129.14, 129.12, 129.11, 127.85, 126.09, 126.05, 125.61, 125.56, 124.24, 122.44, 121.75, 121.72, 121.70, 119.16, 118.65, 118.12, 118.09,

118.06, 118.04, 118.01. **^{31}P NMR** (243 MHz, CD_2Cl_2) δ 40.23. **^{77}Se NMR** (115 MHz, CD_2Cl_2) δ 363.50 (d, $J_{se\text{-}p}$ = 425.96 Hz). The analytical data are in accordance with the reported literature. [32]

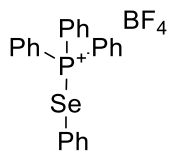

K

$[Ph_3C][BF_4]$(1.0 mmol, 330.15 mg) was added to a solution of 1,2-diphenyldiselane (1.0 mmol, 312.13 mg) in dry CH_2Cl_2 (10.0 mL) and the reaction mixture was stirred for 10 minutes to give a dark green solution. Then Ph_3P (1.0 mmol, 262.29 mg) was added to the above reaction mixture and the reaction was run for 24 hours to generate an pale yellow solution. The solution was reduced to 2.0 mL under vacuum, and 5.0 mL of n-hexane was added with rigorous stirring to give a white precipitate. The precipitate was filtered off and washed by anhydrous diethyl ether to afford pure catalyst as an light yellow solid in 91% yield (460 mg).

^{1}H NMR (600 MHz, CD_2Cl_2) δ 7.89 – 7.84 (m, 3H), 7.71 – 7.66 (m, 6H), 7.58 (ddd, J = 14.1, 8.3, 1.3 Hz, 6H), 7.52 – 7.47 (m, 1H), 7.31 – 7.24 (m, 4H). **^{13}C NMR** (150 MHz, CD_2Cl_2) δ 138.31, 136.50, 136.48, 134.45, 134.38, 132.50, 131.32, 131.12, 131.03, 119.51, 119.08, 118.56. **^{19}F NMR** (565 MHz, CD_2Cl_2) δ -153.00. **^{31}P NMR** (243 MHz, CD_2Cl_2) δ 37.68.

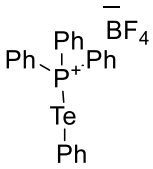

L

$[Ph_3C][BF_4]$ (0.5 mmol, 165.06 mg) was added to a solution of 1,2-diphenylditellurid (0.5 mmol, 204.7 mg) in dry CH_2Cl_2 (5.0 mL) and the reaction mixture was stirred for 10 minutes to give a dark green solution. Then Ph_3P (0.5 mmol, 131.1 mg) was added to the above reaction mixture and the reaction was run for 24 hours to generate an pale yellow solution. The solution was reduced to 2.0 mL under vacuum, and 5.0 mL of n-pantene was added with rigorous stirring to give a yellow precipitate (twice). The precipitate was filtered off and washed by n-pantene to afford pure catalyst **L** as a yellow solid in 54% yield (150 mg).

^{1}H NMR (600 MHz, $CDCl_3$) δ 7.76 – 7.72 (m, 3H), 7.64 – 7.60 (m, 6H), 7.56 – 7.48 (m, 8H), 7.44 – 7.39 (m, 1H), 7.18 – 7.13 (m, 2H). **^{13}C NMR** (150 MHz, $CDCl_3$) δ 142.18, 135.44, 135.42, 134.10,

134.03, 133.22, 133.14, 131.71, 130.86, 130.71, 130.62, 129.44, 129.35, 120.10, 119.65. **^{31}P NMR** (243 MHz, $CDCl_3$) δ 10.06.

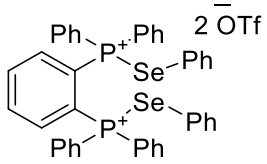

N

TMSOTf (3.0 mmol, 666.7 mg, 2.0 equiv) was added to a red solution of Phenylselenylchlorid (3.0 mmol, 574.5 mg, 2.0 equiv) in dry Et_2O (7.0 mL) at 0 °C under argon. The reaction mixture was allowed to warm to room temperature and stirred for 1 h to give a dark orange solution. Then 1,2-Bis(diphenylphosphino)benzene (1.5 mmol, 669.7 mg, 1.0 equiv) in anhydrous CH_2Cl_2 (4.0 mL) was added over 30 minutes at 0 °C. The reaction mixture was allowed to warm to room temperature and stand for 1 h. After the reaction, a small amount of ether was added to the system, and the white solid suspension was filtered, then dissolve the white solid with 3 ml DCM, add diether until white solid Precipitate，then filtered to get the white solid, washed by ether to get the final product as white solid in 47% yield (750 mg).

^{1}H NMR (500 MHz, CD_2Cl_2) δ 8.23 – 8.11 (m, 4H), 7.79 – 7.73 (m, 4H), 7.62 – 7.51 (m, 16H), 7.39 – 7.35 (m, 2H), 7.12 – 7.07 (m, 4H), 6.85 – 6.73 (m, 4H). **^{13}C NMR** (150 MHz, CD_2Cl_2) δ 143.13, 143.06, 143.00, 138.05, 137.00, 136.70, 135.45, 134.99, 134.95, 134.92, 132.94, 132.90, 132.86, 132.68, 132.01, 131.41, 131.25, 131.17, 130.26, 130.22, 130.17, 129.76, 128.33, 122.61, 119.83, 119.32.**^{19}F NMR** (565 MHz, CD_2Cl_2) δ -78.81.

5.2.2 Synthesis of glycosyl iminoglycal donors

5.2.2.1 Glucosyl iminoglycal donors synthesis

General steps to synthesize glucosyl iminoglycal donors 78a (Method 1)

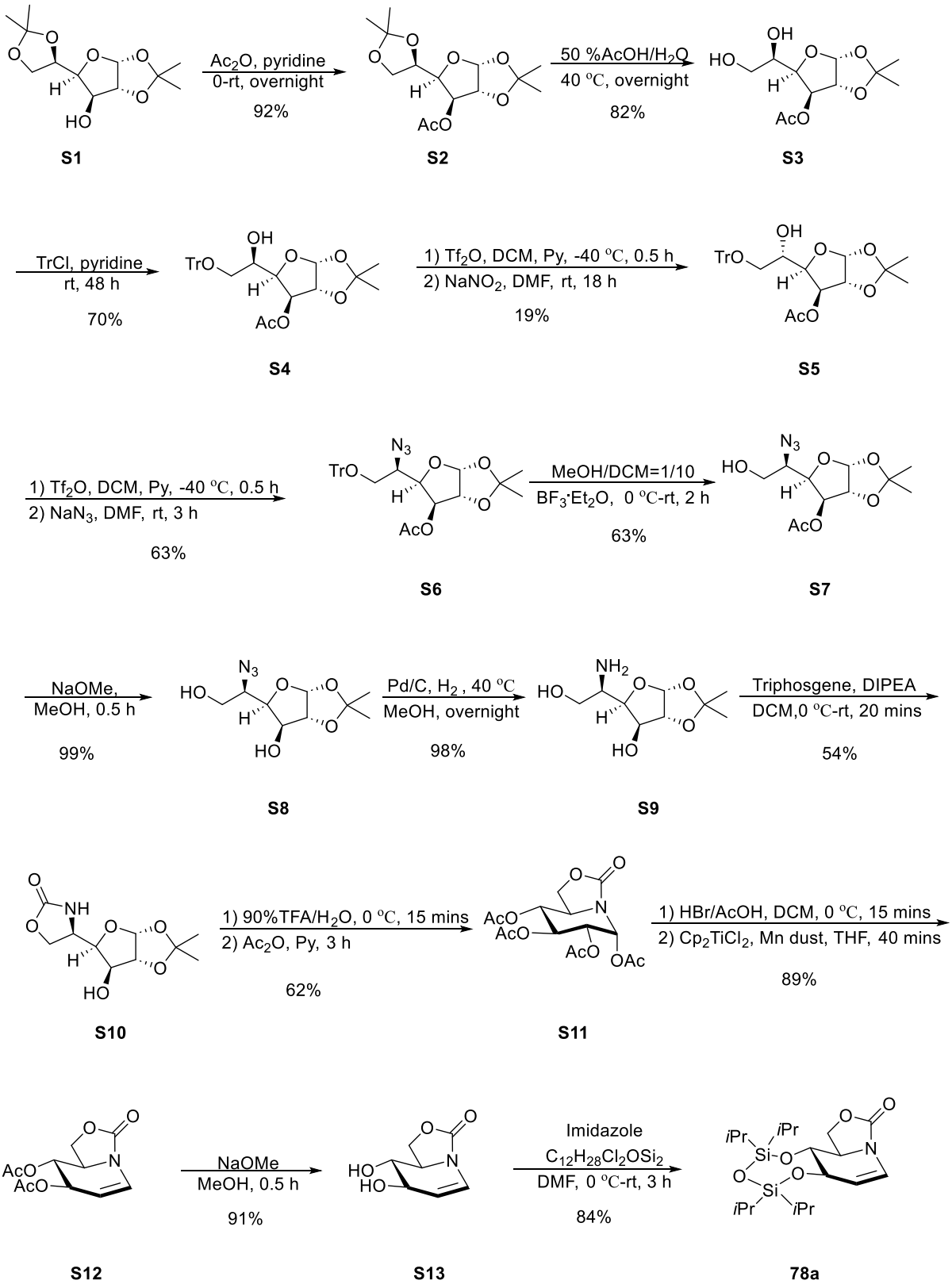

Figure 5.2 Steps to synthesize **78a** (Method 1)

General steps to synthesize glucosyl iminoglycal donors 78a (Method 2)

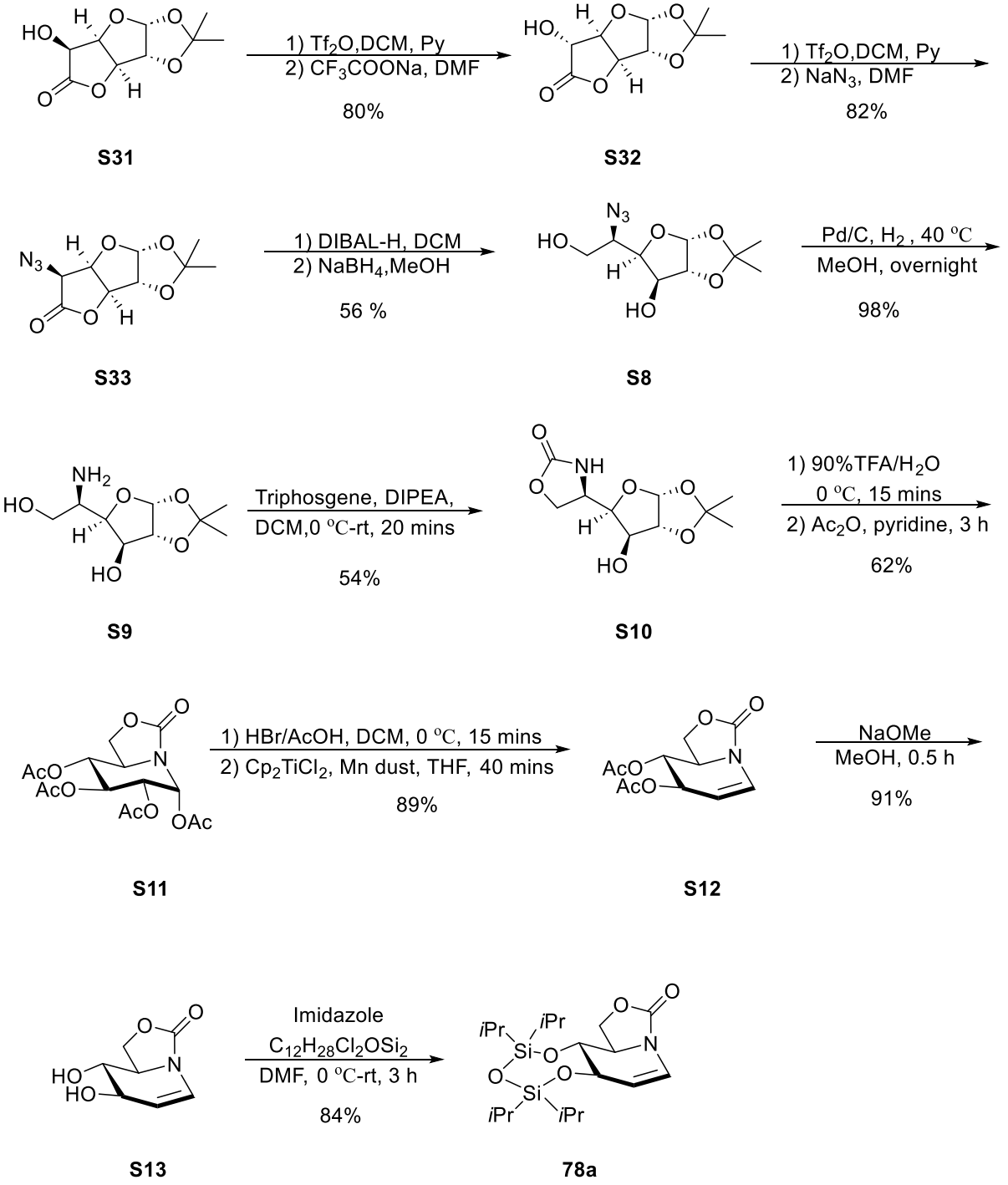

Figure 5.3 Steps to synthesize **78a** (Method 2)

General steps to synthesize glucosyl iminoglycal donors bearing different protecting groups

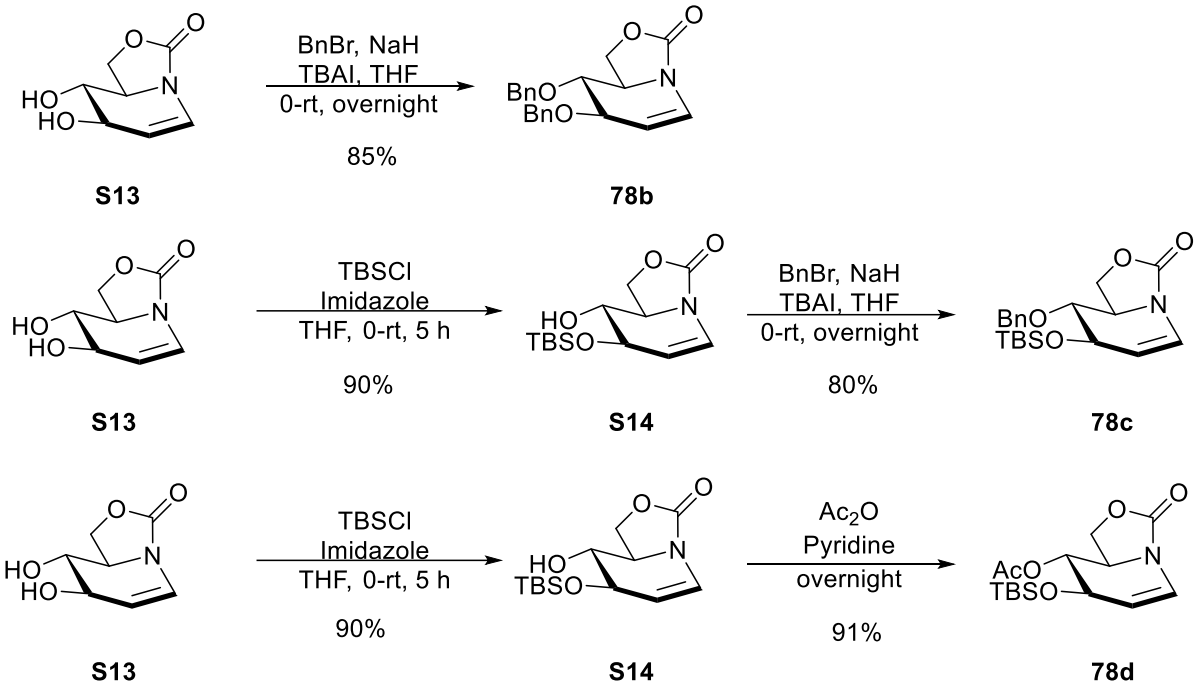

Figure 5.4 Steps to synthesize different protecting groups glucosyl iminoglycal donors

5.2.2.2 Galactosyl iminoglycal donors synthesis

General steps to synthesize galactosyl iminoglycal donors 81

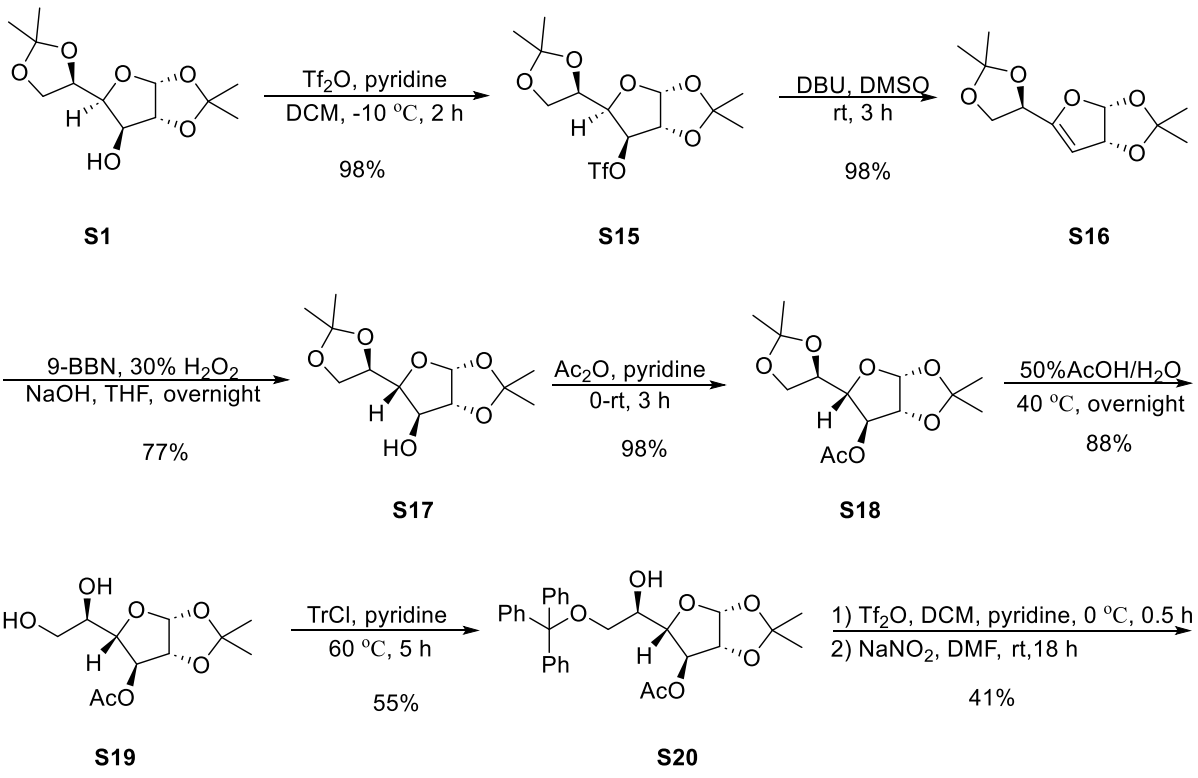

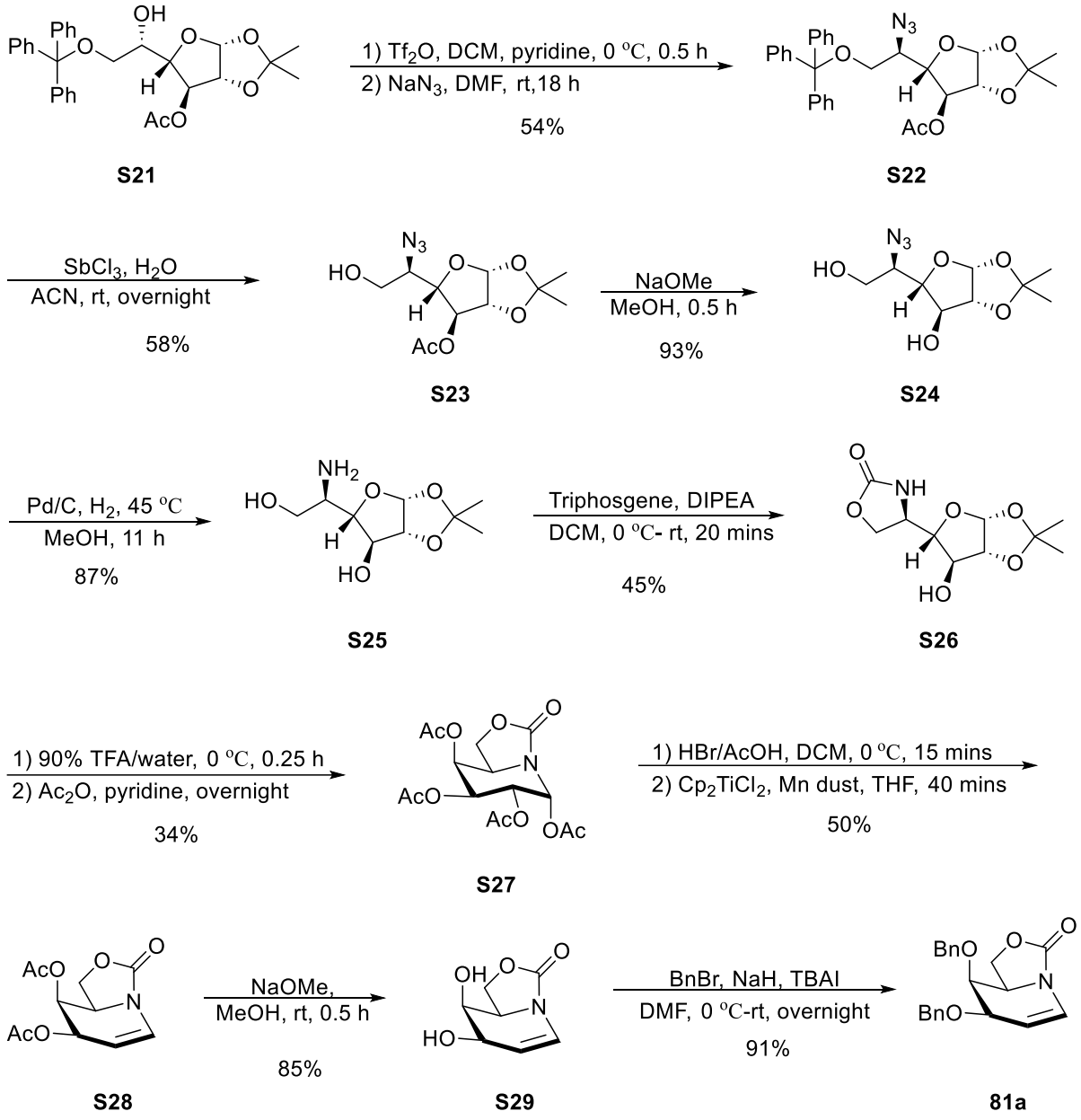

Figure 5.5 Steps to synthesize **81a**

General steps to synthesize galactosyl iminoglycal donors bearing different protecting groups

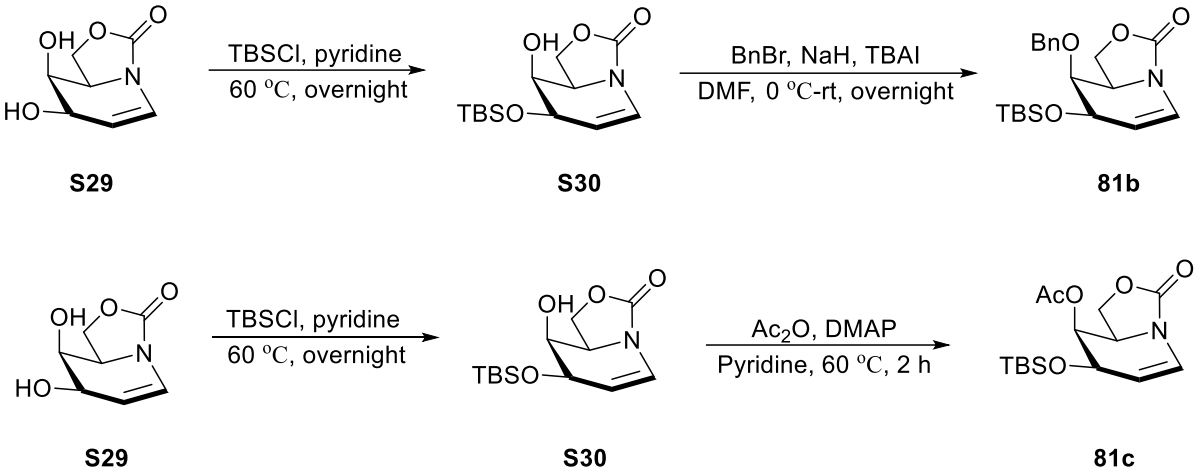

Figure 5.6 Steps to synthesize different protecting groups galactosyl iminoglycal donors

5.2.3 Procedure and data of synthesizing iminoglycal donors

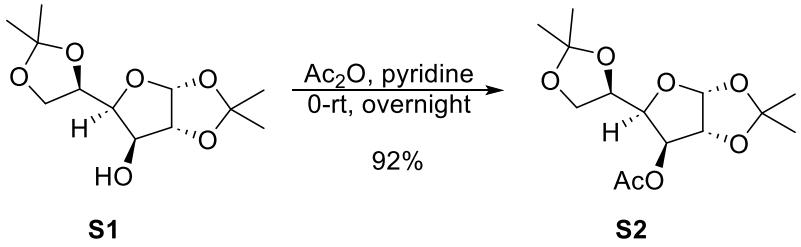

Compound **S2** was prepared according to the literature procedure.[103] Dissolve **S1** (150 g, 0.577 mol, 1 equiv) in 800 mL of absolute pyridine at room temperature, add Ac_2O (65.5 mL, 0.692 mol, 1.2 equiv) dropwise to the mixture at 0 ℃, then the reaction stirred at room temperature for overnight. After it finished through TLC, add 500 mL water to the mixture at 0 ℃, evaporate the pyridine, extract the mixture 3 times with 150 mL of petroleum ether, wash the extract twice with 200 mL of 5% aqueous sodium hydroxide solution and three times with 100 mL of water, dry the extract over anhydrous sodium sulfate, remove the solvent in vacuo. Purify the crude product by flash silica gel chromatography with ethyl acetate: petroleum ether (1:4) as eluent, get the product **S2** 160.0 g (92% yield) as white solid.
^{1}H NMR (600 MHz, $CDCl_3$) δ 5.86 (d, *J* = 4.2 Hz, 1H), 5.24 (d, *J* = 2.4 Hz, 1H), 4.49 (d, *J* = 3.6 Hz, 1H), 4.25 – 4.17 (m, 2H), 4.06 (dd, *J* = 8.4, 5.4 Hz, 1H), 4.02 – 3.99 (m, 1H), 2.09 (s, 3H), 1.50 (s, 3H), 1.40 (s, 3H), 1.30 (d, *J* = 10.2 Hz, 6H). **^{13}C NMR** (150 MHz, $CDCl_3$) δ 169.72, 112.39, 109.45, 105.15, 83.45, 79.80, 76.25, 72.55, 67.29, 26.97, 26.83, 26.31, 25.39, 21.00. **ESI-HRMS**: Calculated for $C_{14}H_{22}O_7Na$ $(M+Na)^+$: 325.1258, Found: 325.1254. $[\alpha]_D^{20}$ = +23.5 (c = 1.0, $CHCl_3$).

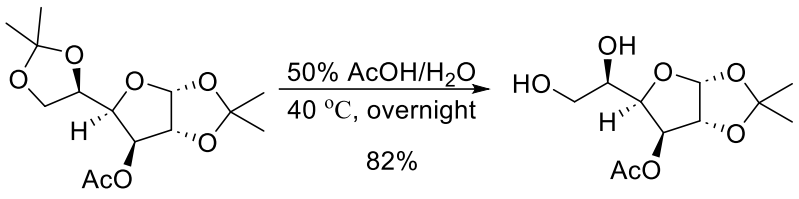

S2 **S3**

Compound **S3** was prepared according to the literature procedure.[79] The protected carbohydrate derivative **S2** (160 g, 0.530 mol, 1.0 equiv) was dissolved in 50% AcOH/H_2O (300 mL) and stirred overnight at 40 °C. Upon the completion of the reaction, the solvent was removed under pressure and the obtained product was dried under high vacuum. This result in white solid product **S3** 120.0 g (82% yield).

^{1}H NMR (600 MHz, $CDCl_3$) δ 5.96 (d, *J* = 3.6 Hz, 1H), 4.54 (d, *J* = 3.6 Hz, 1H), 4.43 (d, *J* = 9.0 Hz, 1H), 4.37 (t, *J* = 3.0 Hz, 1H), 4.26 – 4.22 (m, 2H), 4.08 (dd, *J* = 6.0, 3.0 Hz, 1H), 3.10 (d, *J* = 3.6 Hz, 1H), 2.96 (d, *J* = 4.2 Hz, 1H), 2.12 (s, 3H), 1.49 (s, 3H), 1.32 (s, 3H). **^{13}C NMR** (150 MHz, $CDCl_3$) δ 171.75, 112.02, 105.11, 85.32, 79.37, 75.84, 69.56, 66.24, 26.96, 26.32, 20.97. **ESI-HRMS**: Calculated for $C_{11}H_{18}O_7Na$ $(M+Na)^+$: 285.0945, Found: 285.0939. $[\alpha]_D^{20}$ = +21.2 (c = 1.0, $CHCl_3$).

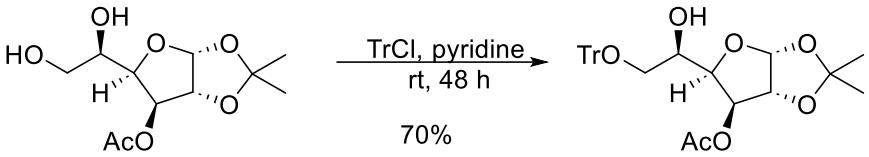

S3 **S4**

Compound **S4** was prepared according to the literature procedure.[103] Trityl chloride (165 g, 594 mmol, 1.3 equiv.) was added to a solution of **S3** (120 g, 458 mmol, 1.0 equiv) in pyridine (400 mL) and the solution was stirred at room temperature for 48 h. The solution was filtered through diatomaceous earth to collect the filtrate. After evaporation to eliminate the pyridne by adding cyclohexane. Then the resulting solution was dissolved in EA and washed with saturated copper sulfate solution twice to eliminate the pyridine, then dried in anhydrous Na_2SO_4, and the solvents evaporated under reduced pressure. The residue was purified by column chromatography eluting with ethyl acetate/petroleum ether (1:5) to get the product **S4** 160 g (70% yield) as colorless oil.

^{1}H NMR (600 MHz, $CDCl_3$) δ 7.47 – 7.43 (m, 5H), 7.32 – 7.28 (m, 5H), 7.26 – 7.22 (m, 5H), 5.86 (d, *J* = 3.6 Hz, 1H), 5.34 (d, *J* = 3.0 Hz, 1H), 4.51 (d, *J* = 3.6 Hz, 1H), 4.37 (dd, *J* = 9.0, 2.4 Hz, 1H), 3.86 – 3.78 (m, 1H), 3.43 – 3.35 (m, 2H), 2.51 (d, *J* = 5.4 Hz, 1H), 2.09 (s, 3H), 1.51 (s, 3H), 1.31 (s, 3H). **^{13}C NMR** (150 MHz, $CDCl_3$) δ 170.25, 143.90, 128.81, 128.05, 127.25, 112.35, 105.06, 86.91, 83.30, 78.76, 76.42, 67.89, 64.94, 26.80, 26.44, 21.02. **ESI-HRMS**: Calculated for $C_{30}H_{32}O_7Na$ $(M+Na)^+$: 527.2040, Found: 527.2045. $[\alpha]_D^{20}$ = -24.6 (c = 2.0, $CHCl_3$).

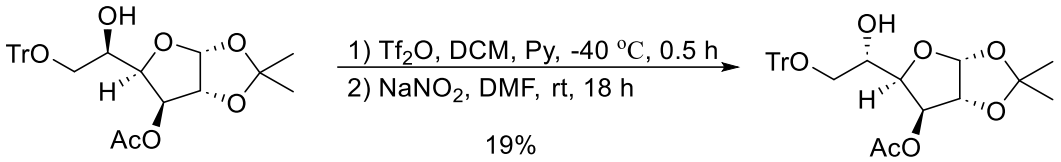

S4 **S5**

Compound **S5** was prepared according to the literature procedure.[103] Pyridine (88.7 mL,1.10 mol, 1.5 equiv) and trifluoromethanesulfonic anhydride (135.8 mL, 807.4 mmol, 1.1 equiv) were added under nitrogen to a solution of **S4** (370 g, 734 mmol, 1.0 equiv) in CH_2Cl_2 (800 mL) at -40 °C. The reaction mixture was allowed to reach room temperature and after stirring for 30 mins, the mixture was diluted with CH_2Cl_2 (400 mL), washed with iced saturated aqueous $NaHCO_3$ (400 mL), dried (anhydrous Na_2SO_4) and concentrated. The resulting triflate ester was dissolved in DMF (400 mL), $NaNO_2$ (505.7 g, 7.34 mol, 10.0 equiv) was added and the reaction mixture was stirred at room temperature for 18 h. The resulting residue was dissolved in CH_2Cl_2 (500 mL) and washed with water (2×300 mL). The organic extract was dried (anhydrous Na_2SO_4) and concentrated. The resulting residue was purified by column chromatography using 1:8-1:5 PE/EA as eluent to give **S5** 70 g (19% yield) as colorless oil.

^{1}H NMR (500 MHz, $CDCl_3$) δ 7.46 – 7.40 (m, 6H), 7.34 – 7.27 (m, 6H), 7.25 – 7.21 (m, 3H), 5.93 (d, *J* = 4.0 Hz, 1H), 5.02 (d, *J* = 3.0 Hz, 1H), 4.50 (d, *J* = 3.5 Hz, 1H), 4.46 (dd, *J* = 6.0, 3.0 Hz, 1H), 4.10 – 4.01 (m, 1H), 3.26 (dd, *J* = 9.5, 4.5 Hz, 1H), 3.06 (dd, *J* = 9.5, 5.5 Hz, 1H), 2.39 (d, *J* = 5.0 Hz, 1H), 1.93 (s, 3H), 1.52 (s, 3H), 1.31 (s, 3H). **^{13}C NMR** (125 MHz, $CDCl_3$) δ 169.82, 143.75, 128.72, 128.05, 127.26, 112.35, 104.49, 86.83, 83.85, 79.18, 76.85, 69.35, 64.53, 26.79, 26.47, 20.90. **ESI-HRMS**: Calculated for $C_{30}H_{32}O_7Na$ $(M+Na)^+$: 527.2040, Found: 527.2044. $[\alpha]_D^{20}$ = -19.0 (c = 1.0, $CHCl_3$).

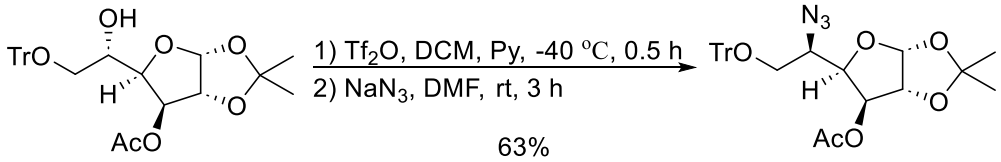

S5 **S6**

Compound **S6** was prepared according to the literature procedure.[103] Pyridine (16.7 mL, 208.3 mmol, 1.5 equiv) and trifluoromethanesulfonic anhydride (25.7 mL, 152.8 mmol, 1.1 equiv) were added under nitrogen to a solution of **S5** (70.0 g, 138.9 mmol, 1.0 equiv) in CH_2Cl_2 (150 mL) at -40 °C. The reaction mixture was allowed to reach room temperature, after the reaction finished (detected through TLC), saturated aqueous $NaHCO_3$ (80 mL) was added until no bulbs formed, the solution was extracted with CH_2Cl_2, washed with saturated sodium chloride solution, and dried (anhydrous Na_2SO_4) and concentrated. The resulting triflate ester was dissolved in DMF (100 mL), NaN_3 (90.3 g, 1.39 mol, 10.0 equiv) was added and the reaction mixture was stirred at room temperature for 3 h. The resulting residue was dissolved in ethyl acetate (100 mL) and washed with saturated sodium chloride solution (2×80 mL). The organic extract was dried (anhydrous Na_2SO_4) and concentrated. The resulting residue was purified by column chromatography (PE/EA=10/1) to give **S6** 46.0 g (63% yield) as colorless oil.

^{1}H NMR (500 MHz, $CDCl_3$) δ 7.50 – 7.45 (m, 6H), 7.34 – 7.29 (m, 6H), 7.26 – 7.22 (m, 3H), 5.82 (d, *J* = 3.5 Hz, 1H), 5.24 (d, *J* = 3.0 Hz, 1H), 4.48 (d, *J* = 4.0 Hz, 1H), 4.19 (dd, *J* = 9.5, 3.0 Hz, 1H), 3.66 (ddd, *J* = 9.5, 7.5, 2.5 Hz, 1H), 3.54 (dd, *J* = 10.0, 2.5 Hz, 1H), 3.37 (dd, *J* = 10.0, 7.5 Hz, 1H), 2.12 (s, 3H), 1.46 (s, 3H), 1.28 (s, 3H). **^{13}C NMR** (125 MHz, $CDCl_3$) δ 169.72, 143.72, 128.84, 128.02, 127.24, 112.47, 105.11, 87.29, 83.03, 77.22, 76.34, 64.36, 60.02, 26.74, 26.32, 21.03. **ESI-HRMS**: Calculated for $C_{30}H_{31}N_3O_6Na$ $(M+Na)^+$: 552.2105, Found:552.2110. $[\alpha]_D^{20}$ = -19.8 (c = 1.1, $CHCl_3$).

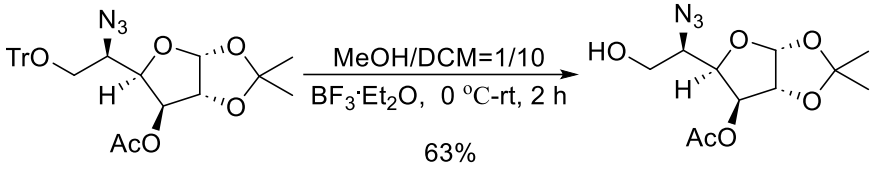

S6 **S7**

Compound **S7** was prepared according to the literature procedure.[103] $BF_3 \cdot Et_2O$ complex (25.0 mL) and MeOH (10 mL) were added to a solution of the tritylated azido derivative **S6** (46 g, 91.2 mmol, 1.0 equiv) in CH_2Cl_2 (100 mL) at 0 °C under argon. The reaction mixture was allowed to reach room temperature and stirred for 2 h, diluted with CH_2Cl_2 (100 mL), then washed with saturated aqueous $NaHCO_3$ (2×50 mL), dried (anhydrous Na_2SO_4) and concentrated. The resulting residue was purified by column chromatography (1:5 - 1:2 EtOAc/petroleum ether) to give **S7** 14.0 g (63% yield) as an amorphous white solid.

^{1}H NMR (500 MHz, $CDCl_3$) δ 5.89 (d, *J* = 3.5 Hz, 1H), 5.26 (d, *J* = 3.0 Hz, 1H), 4.53 (d, *J* = 4.0 Hz, 1H), 4.21 (dd, *J* = 9.5, 3.0 Hz, 1H), 3.99 (ddd, *J* = 11.0, 5.5, 3.5 Hz, 1H), 3.82 – 3.71 (m, 2H), 2.20 – 3.15 (m, 1H), 2.13 (s, 3H), 1.50 (s, 3H), 1.30 (s, 3H). **^{13}C NMR** (125 MHz, $CDCl_3$) δ 169.72, 112.66, 105.08, 83.10, 77.78, 76.39, 63.56, 61.26, 26.77, 26.27, 21.03. **ESI-HRMS**: Calculated for $C_{11}H_{17}N_3O_6Na$ $(M+Na)^+$: 310.1010, Found: 310.1005. $[\alpha]_D^{20}$ = -29.7 (c = 1.5, $CHCl_3$).

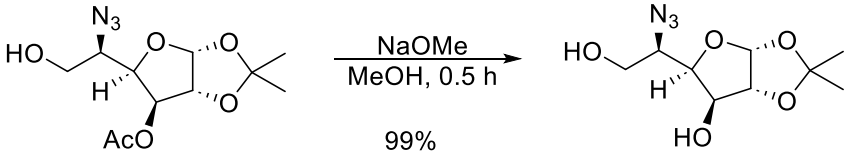

S7 **S8**

Compound **S8** was prepared according to the literature procedure.[103] NaOMe (2.89 g, 53.6 mmol, 1.1 equiv) was added to a solution of **S7** (14 g, 48.7 mmol, 1.0 equiv) in MeOH (50 mL) at room temperature, and stirred for 30 mins. Filter to remove solids, evaporate the solvent in vacuo, Purify the residue by flash column chromatography (PE/EA, 2:1) to obtain **S8** 12.0 g (99% yield) as yellow oil.

^{1}H NMR (500 MHz, $CDCl_3$) δ 5.93 (d, *J* = 4.0 Hz, 1H), 4.53 (d, *J* = 4.0 Hz, 1H), 4.34 – 4.30 (m, 1H), 4.14 – 4.10 (m, 1H), 3.97 (dd, *J* = 11.5, 3.5 Hz, 1H), 3.89 – 3.84 (m, 1H), 3.83 – 3.77 (m, 1H), 2.86 (s, 1H), 2.64 (s, 1H), 1.49 (s, 3H), 1.31 (s, 3H). **^{13}C NMR** (125 MHz, $CDCl_3$) δ 112.23, 104.96, 85.09, 79.29, 74.94, 63.09, 60.91, 26.80, 26.24. **ESI-HRMS**: Calculated for $C_9H_{15}N_3O_5Na$ $(M+Na)^+$: 268.0904, Found: 268.0897. $[\alpha]_D^{20}$ = -13.1 (c = 2.2, $CHCl_3$).

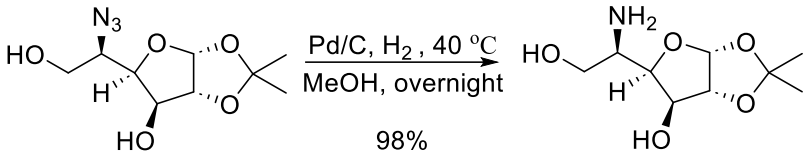

S8 **S9**

Compound **S9** was prepared according to the literature procedure.[103] A solution of azido sugar **S8** (12.0 g, 48.9 mmol, 1.0 equiv) and 10% Pd/C (2.64 g) in MeOH (80 mL) was hydrogenated under an atmospheric pressure of hydrogen using a balloon. The mixture was stirred at 40 °C overnight, filtered through diatomite and concentrated to give **S9** 10.5 g (98% yield) as a hygroscopic solid that was used in the next step without further purification.

^{1}H NMR (600 MHz, CD_3OD) δ 5.88 (d, *J* = 3.7 Hz, 1H), 4.48 (d, *J* = 3.7 Hz, 1H), 4.19 (d, *J* = 2.8 Hz, 1H), 3.98 (dd, *J* = 8.3, 2.8 Hz, 1H), 3.78 (dd, *J* = 11.0, 3.6 Hz, 1H), 3.57 (dd, *J* = 11.0, 6.8 Hz, 1H), 3.18 (ddd, *J* = 8.2, 6.8, 3.6 Hz, 1H), 1.44 (s, 3H), 1.29 (s, 3H). **^{13}C NMR** (150 MHz, CD_3OD) δ 112.63, 106.27, 86.74, 81.65, 75.81, 64.42, 52.73, 27.00, 26.38. **ESI-HRMS**: Calculated for $C_9H_{18}NO_5$ $(M+H)^+$: 220.1180, Found: 220.1172. $[\alpha]_D^{20}$ = -17.2 (c = 1.3, $CHCl_3$).

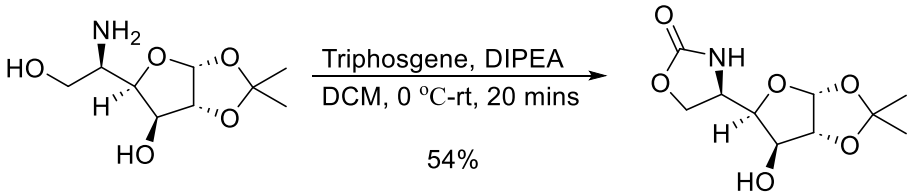

S9 **S10**

Compound **S10** was prepared according to the literature procedure.[104] Diisopropylethylamine (60.3 mL, 478.9 mmol, 10.0 equiv) was added to a stirred solution of **S9** (10.5 g, 47.89 mmol, 1.0 equiv) in CH_2Cl_2 (90 mL) at 0 °C. Then triphosgene (21.3 g, 54.74 mmol, 1.5 equiv) was dissolved in CH_2Cl_2 (20 mL) and added to the solution in dropwise. The reaction mixture was allowed to reach room temperature and stirred for 15 mins. The solvent was removed under reduced pressure and the residue was purified by column chromatography EtOAc/MeOH (40:1) to give **S10** 6.3 g (53% yield) as yellow solid.

^{1}H NMR (600 MHz, CD_3OD) δ 5.96 – 5.88 (m, 1H), 4.53 – 4.43 (m, 3H), 4.20 – 4.10 (m, 3H), 1.46 (s, 3H), 1.30 (s, 3H). **^{13}C NMR** (150 MHz, CD_3OD) δ 162.22, 112.98, 106.65, 86.91, 82.96, 75.51, 68.58, 52.72, 27.14, 26.41. **ESI-HRMS**: Calculated for $C_{10}H_{16}NO_6$ $(M+H)^+$: 246.0972, Found: 246.0965. $[\alpha]_D^{20}$ = -26.5 (c = 1.2, MeOH).

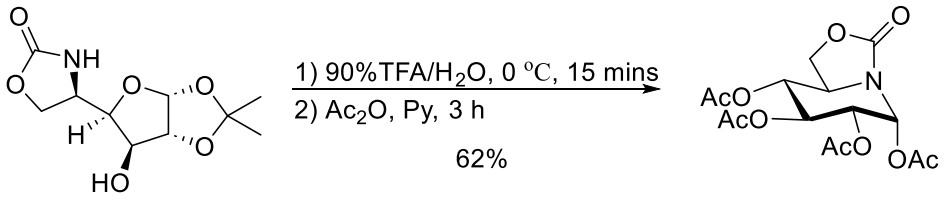

S10 **S11**

Compound **S11** was prepared according to the literature procedure.[104] Compound **S10** (6.3 g, 25.69 mmol, 1.0 equiv) was deacetylated by treatment with 90% TFA/water (60 mL). The reaction mixture was concentrated and the residue was evaporated several times with water to eliminate traces of acid. The resulting residue was subjected to conventional acetylation with Ac_2O/pyridine (1:1, 20 mL), after the reaction finished, quenched with water and wash the solution with saturated copper sulfate solution to eliminate the pyridine. Then the peracetylated mixture was purified by column chromatography using 1:1 EA/PE as eluent. This result in **S11** 5.9 g (62% yield) as white solid.

^{1}H NMR (500 MHz, $CDCl_3$) δ 6.72 (d, *J* = 4.0 Hz, 1H), 5.50 (t, *J* = 10.0 Hz, 1H), 5.09 (dd, *J* = 10.5, 4.0 Hz, 1H), 4.96 (t, *J* = 10.0 Hz, 1H), 4.45 (dd, *J* = 9.5, 8.0 Hz, 1H), 4.28 (t, *J* = 9.0 Hz, 1H), 4.05 (dt, *J* = 9.5, 8.0 Hz, 1H), 2.14 (s, 3H), 2.08 (s, 3H), 2.05 (s, 3H), 2.01 (s, 3H). **^{13}C NMR** (125 MHz, $CDCl_3$) δ 170.12, 169.97, 169.47, 168.73, 154.31, 77.36, 72.39, 69.16, 69.01, 67.05, 52.84, 20.78, 20.72, 20.66, 20.49. **ESI-HRMS**: Calculated for $C_{15}H_{20}NO_{10}$ $(M+H)^+$: 396.0901, Found: 396.0899. $[\alpha]_D^{20}$ = +52.6 (c = 1.0, $CHCl_3$).

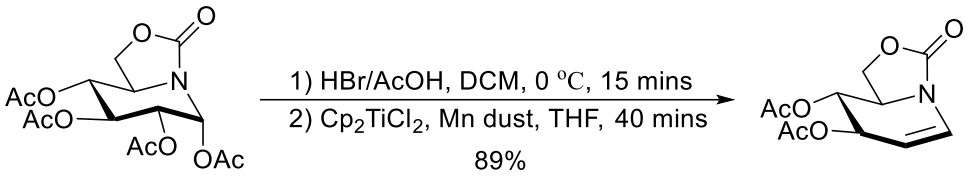

S11 **S12**

Compound **S12** was prepared according to the literature procedure.[104] To a solution of **S11** (5.7 g, 15.27 mmol, 1.0 equiv) in anhydrous DCM (50 mL), HBr/AcOH (33%, 9.56 mL) were dropwise added at 0 °C and the reaction mixture was stirred for 15 mins, detected by TLC(PE/EA=1/1), diluted with DCM (30 mL) and washed with saturated aqueous $NaHCO_3$ (20 mL). The organic layer was dried (anhydrous Na_2SO_4) and concentrated under reduced pressure to yield the corresponding 1-bromo derivative as a white solid. This product was used without further purification in the next step. A mixture of Cp_2TiCl_2 (3.74g, 18.4 mmol, 1.2 equiv) and Mn dust (2.227g, 40.35 mmol, 2.6 equiv) in deoxygenated THF (40 mL) was stirred at rt until the red solution turned green. Then the glycosyl bromo derivative in deoxygenated THF (20 mL) was added and the reaction mixture was stirred for 40 mins. Diluted with EtOAc (80 mL), quenched with 1 M HCl (2 x 10 mL), washed with brine, and dried (anhydrous Na_2SO_4). The resulting crude was purified by column chromatography (PE/EA=1/1) to yield the corresponding product **S12** 3.5 g (89% yield) as red oil.

^{1}H NMR (500 MHz, $CDCl_3$) δ 6.64 (dd, *J* = 8.0, 2.0 Hz, 1H), 5.60 (dt, *J* = 8.0, 2.0 Hz, 1H), 5.15 (dd, *J* = 10.5, 8.0 Hz, 1H), 4.91 (dd, *J* = 8.0, 2.5 Hz, 1H), 4.47 (t, *J* = 9.0 Hz, 1H), 4.23 (t, *J* = 9.0 Hz, 1H), 4.14 (dd, *J* = 10.5, 8.0 Hz, 1H), 2.05 (s, 3H), 2.03 (s, 3H). **^{13}C NMR** (125 MHz, $CDCl_3$) δ 170.62, 170.19, 153.03, 123.47, 105.80, 71.03, 70.11, 67.03, 53.97, 20.97, 20.73. **ESI-HRMS**: Calculated for $C_{19}H_{32}NO_7$ $(M+H)^+$: 386.2173, Found: 386.2181. $[\alpha]_D^{20}$ = -1.6 (c = 3.5, $CHCl_3$).

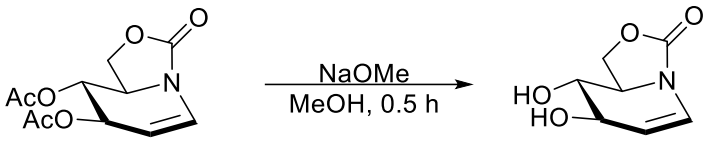

S12 **S13**

Compound **S13** was prepared according to the literature procedure.[105] NaOMe (1.3 g, 24.29 mmol, 2.0 equiv) was added to a solution of **S12** (3.1g, 12.15 mmol, 1.0 equiv) in MeOH (20 ml) at room temperature and stirred for 30 mins. Filter out the solid with MeOH to wash solid, collected the liquid and evaporate the solvent in vacuo, purify the residue by flash column chromatography (DCM/MeOH: 10:1) to obtain **S13** 1.9 g (91% yield) as yellow oil.

^{1}H NMR (500 MHz, CD_3OD) δ 6.50 (dd, *J* = 7.9, 1.9 Hz, 1H), 4.99 (dd, *J* = 7.9, 2.1 Hz, 1H), 4.65 (t, *J* = 8.5 Hz, 1H), 4.29 – 4.19 (m, 2H), 4.07 – 3.94 (m, 1H), 3.55 (dd, *J* = 10.4, 7.8 Hz, 1H). **^{13}C NMR** (125 MHz, CD_3OD) δ 155.95, 122.03, 112.83, 74.47, 72.06, 69.12, 56.86. **ESI-HRMS**: Calculated for $C_7H_{10}NO_4$ $(M+H)^+$: 172.0604, Found:172.0604. $[\alpha]_D^{20}$ = +138.3 (c = 0.3, MeOH).

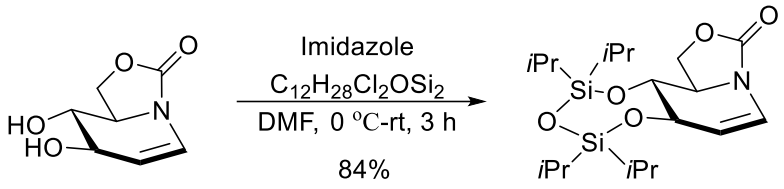

S13 **78a**

Compound **78a** was prepared according to the literature procedure.[100] **S13** (1.5 g, 8.76 mmol, 1.0 equiv) and imidazole (1.193 g, 17.53 mmol, 2.0 equiv) were dissolved in anhydrous DMF (30 mL) under an argon atmosphere and the solution was cooled to 0℃, and 1,3-dichloro-1,1,3,3-tetraisopropyldisiloxane (4.2 ml, 13.15 mmol, 1.5 equiv) was added dropwise at this temperature, then increase the solution to room temperature and stirred for 3 h. Afterwards, the solution was poured into ice water, and extracted with EA (20 mL) twice, the organic layer was washed with brine (15 mL), dried over anhydrous Na_2SO_4, filtered and concentrated in vacuo. Following by column chromatography (20:1 n-pentane/EA), the title compound **78a** was obtained 3.05 g (84% yield) as white solid.

^{1}H NMR (500 MHz, $CDCl_3$) δ 6.55 (dd, *J* = 8.0, 2.0 Hz, 1H), 4.94 (dd, *J* = 8.0, 2.0 Hz, 1H), 4.61 (t, *J* = 9.0 Hz, 1H), 4.50 (dt, *J* = 7.0, 2.0 Hz, 1H), 4.17 (t, *J* = 9.0 Hz, 1H), 4.05 – 3.93 (m, 1H), 3.85 (dd, *J* = 10.0, 7.0 Hz, 1H), 1.12 – 0.96 (m, 28H). **^{13}C NMR** (125 MHz, $CDCl_3$) δ 153.64, 121.52, 111.04, 77.36, 76.34, 73.65, 67.51, 55.65, 17.69, 17.47, 17.37, 17.35, 17.30, 17.25, 17.24, 13.08, 12.90, 12.46, 12.27. **ESI-HRMS**: Calculated for $C_{19}H_{36}NO_5Si_2$ $(M+H)^+$: 414.2127, Found:414.2124. $[\alpha]_D^{20}$ = +46.9 (c = 0.9, $CHCl_3$).

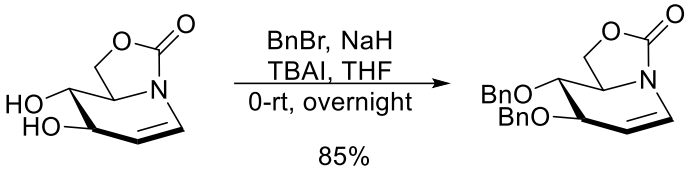

S13 **78b**

Compound **78b** was prepared according to the literature procedure. [105] Substrate **S13** (171.15 mg, 1 mmol, 1.0 equiv) was dissolved in anhydrous THF (10 ml), cooled to 0℃, NaH (60%, 159.98 mg, 4 mmol, 4.0 equiv) was added, stirred for 1 h at rt, then added BnBr (0.475 ml, 4 mmol, 4.0 equiv) and TBAI (184.684 mg, 0.5 mmol, 0.5 equiv) to the solution, stirred for overnight, the residue dissolved in DCM, washed with water, extracted with DCM, dry over anhydrous Na_2SO_4, concentrated in vacuo, then purified through flash chromatography (PE/EA=3/1) to obtain **78b** 300 mg (85% yield) as white solid.

^{1}H NMR (600 MHz, $CDCl_3$) δ 7.26 – 7.19 (m, 7H), 7.17 – 7.14 (m, 3H), 6.46 (dd, *J* = 7.8, 1.8 Hz, 1H), 4.98 (dd, *J* = 7.8, 1.8 Hz, 1H), 4.80 (d, *J* = 12.0 Hz, 1H), 4.64 – 4.48 (m, 3H), 4.38 – 4.33 (m, 1H), 4.28 (dt, *J* = 7.2, 1.8 Hz, 1H), 3.88 – 3.81 (m, 1H), 3.66 (t, *J* = 9.0 Hz, 1H), 3.54 (dd, *J* = 10.2, 7.2 Hz, 1H). **^{13}C NMR** (150 MHz, $CDCl_3$) δ 153.49, 137.85, 137.80, 128.77, 128.70, 128.43, 128.38, 128.11, 128.02, 122.32, 107.37, 79.11, 77.64, 74.09, 71.53, 67.76, 54.56. **ESI-HRMS**: Calculated for $C_{21}H_{22}NO_4$ $(M+H)^+$: 352.1543, Found:352.1542. $[\alpha]_D^{20}$ = +65.2 (c = 1.0, $CHCl_3$).

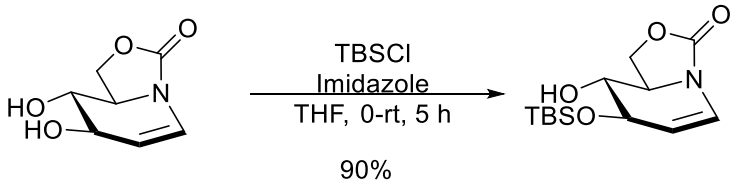

S13 **S14**

Compound **S14** was prepared under the following procedure. **S13** (100 mg, 0.58 mmol, 1.0 equiv) and imidazole (87.5 mg, 1.29 mmol, 2.2 equiv) were dissolved in anhydrous THF (10 mL) under an argon atmosphere and the solution was cooled to 0℃, then added TBSCl (193 mg, 1.29 mmol, 2.2 equiv) to the solution at this temperature and stirred for 5 h. Afterwards, the solution was quenched with water, and extracted with EA (20 mL) twice, the organic layer was washed with brine (15 mL), dried over anhydrous Na_2SO_4, filtered and concentrated in vacuo. then purified through flash chromatography (3:1 PE/EA), the title compound **S14** (150 mg, 90% yield) was obtained as white solid.

^{1}H NMR (700 MHz, $CDCl_3$) δ 6.51 (dd, *J* = 8.4, 2.1 Hz, 1H), 4.86 (dd, *J* = 8.4, 2.1 Hz, 1H), 4.63 (t, *J* = 8.4 Hz, 1H), 4.36 (dt, *J* = 7.0, 2.1 Hz, 1H), 4.21 (t, *J* = 9.1 Hz, 1H), 4.06 – 3.97 (m, 1H), 3.67 (ddd, *J* = 10.5, 7.7, 2.8 Hz, 1H), 0.92 (s, 9H), 0.14 (d, *J* = 3.5 Hz, 6H). **^{13}C NMR** (175 MHz, $CDCl_3$) δ 153.79, 121.69, 110.44, 74.01, 72.54, 67.59, 54.74, 25.88, 18.16, -4.17, -4.38. **ESI-HRMS**: Calculated for $C_{13}H_{24}NO_4Si$ $(M+H)^+$: 286.1469, Found: 286.1464. $[\alpha]_D^{20}$ = +28.1 (c = 0.2, $CHCl_3$).

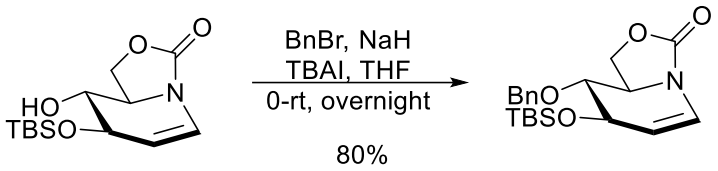

S14 **78c**

Compound **78c** was prepared under the following procedure. Substrate **S14** (85.6 mg, 0.3 mmol, 1.0 equiv) dissolved in anhydrous THF (5 ml), cooled to 0℃, NaH (60%, 23.98 mg, 0.6 mmol, 2.0 equiv) was added, stirred for 1 h at rt, then added BnBr (102.62 mg, 0.6 mmol, 2.0 equiv) and TBAI (55.4 mg, 0.15 mmol, 0.5 equiv) to the solution, the solution were stirred overnight. The residue dissolved in DCM, washed with water, extracted with DCM, dried over anhydrous Na_2SO_4, concentrated in vacuo, and purified through flash chromatography (PE/EA=5/1) to obtain **78c** 90.6 mg (80%, yield) as white solid.

^{1}H NMR (600 MHz, $CDCl_3$) δ 7.40 – 7.32 (m, 3H), 7.31 – 7.28 (m, 2H), 6.49 (dd, *J* = 7.8, 1.8 Hz, 1H), 4.92 (d, *J* = 12.0 Hz, 1H), 4.85 (dd, *J* = 7.8, 1.8 Hz, 1H), 4.62 (d, *J* = 12.0 Hz, 1H), 4.56 (dt, *J* = 7.2, 1.8 Hz, 1H), 4.36 (t, *J* = 9.0 Hz, 1H), 3.93 (td, *J* = 10.2, 8.4 Hz, 1H), 3.58 (t, *J* = 9.0 Hz, 1H), 3.53 (dd, *J* = 10.2, 7.2 Hz, 1H), 0.96 (s, 9H), 0.17 (d, *J* = 5.4 Hz, 6H). **^{13}C NMR** (150 MHz, $CDCl_3$) δ 153.55, 137.90, 128.84, 128.55, 128.47, 121.22, 111.31, 79.56, 74.67, 72.66, 67.63, 54.59, 25.96, 18.12, -4.24, -4.43. **ESI-HRMS**: Calculated for $C_{20}H_{30}NO_4Si$ $(M+H)^+$: 376.1939, Found: 376.1938. $[\alpha]_D^{20}$ = +76.1 (c = 1.1, $CHCl_3$).

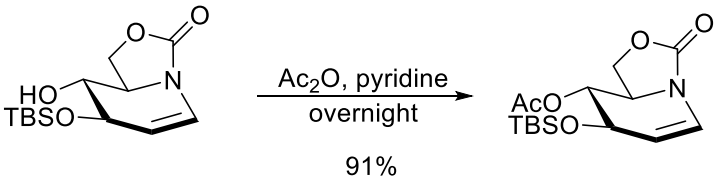

S14 **78d**

Compound **78d** was prepared under the following procedure. Dissolve (85.6 mg, 0.3 mmol, 1.0 equiv) in 5.0 mL of absolute pyridine at room temperature, then add Ac_2O (0.56 mL, 0.6 mmol, 2.0 equiv) dropwise to the mixture at 0 ℃, then the reaction stirred at room temperature overnight. After it finished through TLC, add 10 mL water to the mixture, evaporate the pyridine, extract the mixture with 20 mL of EA, wash the extract twice with 20 mL of saturated copper(II) sulphate solution and three times with 10 mL of water, dry the extract over anhydrous sodium sulfate, remove the solvent in vacuo, the product was purified through flash chromatography (n-pentane/EA=3/1) to get the title compound **78d** 88.3 mg (91%, yield) as white solid.

^{1}H NMR (600 MHz, $CDCl_3$) δ 6.57 (dd, *J* = 7.8, 1.8 Hz, 1H), 5.01 (dd, *J* = 10.8, 7.8 Hz, 1H), 4.88 (dd, *J* = 7.8, 1.8 Hz, 1H), 4.53 (dt, *J* = 7.2, 2.4 Hz, 1H), 4.43 (dd, *J* = 9.0, 7.8 Hz, 1H), 4.29 (t, *J* = 9.0 Hz, 1H), 4.03 (td, *J* = 10.2, 7.8 Hz, 1H), 2.11 (s, 3H), 0.88 (s, 9H), 0.09 (d, *J* = 21.0 Hz, 6H). **^{13}C NMR** (150 MHz, $CDCl_3$) δ 170.29, 153.42, 121.43, 110.48, 74.28, 69.16, 67.32, 54.51, 25.66, 20.99, 18.04, -

4.43, -4.69. **ESI-HRMS**: Calculated for $C_{15}H_{26}NO_5Si$ $(M+H)^+$: 328.1575, Found: 328.1573. $[\alpha]_D^{20}$ = -46.0 (c = 0.5, $CHCl_3$).

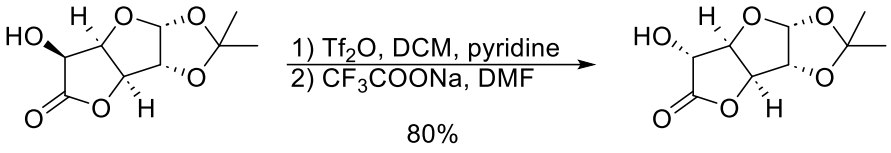

S31 **S32**

Compound **S32** was prepared according to the literature procedure.[106] Triflic anhydride (46.6 mL, 277.54 mmol, 1.2 equiv) was added to a solution of the acetonide **S31** (50.0 g, 231.3 mmol, 1.0 equiv) in DCM (300 mL) and pyridine (37.26 mL, 462.6 mmol, 2.0 equiv) at -30 °Cand stirred for 1 h at room temperature (the solution turned to dark red). The reaction mixture was washed with 2 M HCl (3 x 250 mL) and the organic fraction was dried over anhydrous sodium sulfate, filtered and concentrated. The crude triflate was dissolved in DMF (250 mL) and sodium trifluoroacetate (62.9 g, 462.6 mmol, 2.0 equiv) was added dropwise. The reaction mixture was stirred for overnight at RT and diluted with saturated aqueous $NaHCO_3$ (125 mL), extracted with EA (3 x 250 mL), and the organic phase was dried over anhydrous sodium sulfate, filtered and concentrated. The crude product was purified by recrystallization using EA/PE = 1/3 as solvent to get the compound **S32** 40.0 g (80% yield, over two steps) as white solid.

^{1}H NMR (600 MHz, $CDCl_3$) δ 5.93 (d, *J* = 3.6 Hz, 1H), 5.05 (d, *J* = 3.6 Hz, 1H), 4.83 (d, *J* = 3.6 Hz, 1H), 4.79 (d, *J* = 3.0 Hz, 1H), 4.35 – 4.30 (m, 1H), 3.04 – 2.92 (m, 1H), 1.52 (s, 3H), 1.35 (s, 3H). **^{13}C NMR** (150 MHz, $CDCl_3$) δ 174.75, 113.33, 106.27, 85.20, 82.51, 82.15, 71.84, 27.15, 26.70. **ESI-HRMS**: Calculated for $C_9H_{13}O_6(M+H)^+$: 217.0707, Found: 217.0706. $[\alpha]_D^{20}$ = +110.2 (c = 1.0, $CHCl_3$).

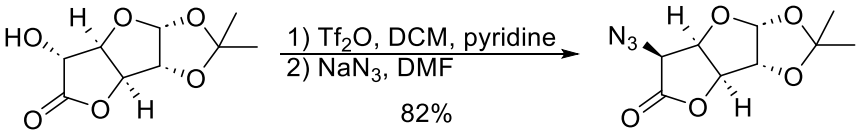

S32 **S33**

Compound **S33** was prepared according to the literature procedure.[106] Triflic anhydride (37.4 mL, 222.03 mmol, 1.2 equiv) was added to a solution of **S32** (40 g, 185.02 mmol, 1.0 equiv) in DCM (300 mL) and pyridine (17.95 mL, 222.03 mmol, 1.2 equiv) at -30 °C and the reaction mixture was then stirred at that temperature for a further 1 h. The reaction mixture was diluted with DCM (200 mL) and washed with 2 M HCl (3 x 100 mL), dried over anhydrous sodium sulfate, filtered and concentrated. The crude triflate was dissolved in DMF (200 mL), cooled to -20 °C, and sodium azide (42.1 g, 647.6 mmol, 3.5 equiv) was added. The reaction mixture was stirred at that temperature for 1 h. The reaction mixture was diluted with 5% aq. NaCl (50 mL) and extracted with EtOAc (3 x 20 mL). The combined organic fractions were dried, filtered and concentrated. The crude product was purified by column

chromatography using 1:5 EA-PE as eluent to get the product **S33** 37.0 g (82%, over two steps) as white solid.

^{1}H NMR (600 MHz, $CDCl_3$) δ 6.02 (d, *J* = 3.6 Hz, 1H), 5.02 (dd, *J* = 4.2, 3.0 Hz, 1H), 4.87 – 4.83 (m, 2H), 4.08 (d, *J* = 4.2 Hz, 1H), 1.53 (s, 3H), 1.36 (d, *J* = 0.8 Hz, 3H). **^{13}C NMR** (150 MHz, $CDCl_3$) δ 169.81, 113.80, 106.93, 82.64, 82.58, 79.22, 60.64, 27.05, 26.63. **ESI-HRMS**: Calculated for $C_9H_{12}N_3O_5(M+H)^+$: 242.0771, Found: 242.0776. $[\alpha]_D^{20}$ = +21.6 (c = 1.0, $CHCl_3$).

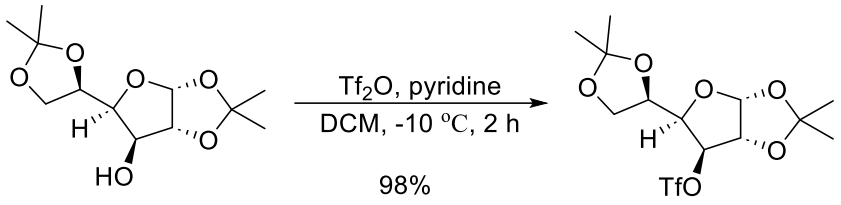

S1 **S15**

Compound **S15** was prepared according to the literature procedure.[107] Add anhydrous pyridine (92.8 mL, 1.155 mol, 1.5 equiv) to a cooled and stirred solution (-10 °C) of 1,2:5,6-di-O-isopropylidene-D-glucofuranose **S1** (200.0 g, 0.77 mol) in dry CH_2Cl_2 (1000 mL) kept under argon atmosphere. Add Tf_2O (142.0 mL, 0.085 mol, 1.1 equiv) dropwise to the mixture. Stir the mixture at -10 °C for 2 hours. Pour the crude mixture into ice and saturated aqueous solution of $NaHCO_3$ (500 mL). Extract the aqueous layer with dichloromethane (500 mL). Dry the combined organic layers over anhydrous sodium sulfate and concentrate under reduced pressure to afford crude product, which was purified through flash chromatography with PE/EA=20/1 to get product **S15** 290.0 g (98% yield) as white solid.

^{1}H NMR (600 MHz, $CDCl_3$) δ 5.98 (d, *J* = 3.6 Hz, 1H), 5.25 (d, *J* = 2.4 Hz, 1H), 4.76 (d, *J* = 3.6 Hz, 1H), 4.23 – 4.17 (m, 2H), 4.15 (dd, *J* = 8.4, 6.0 Hz, 1H), 3.97 (dd, *J* = 8.4, 4.2 Hz, 1H), 1.51 (s, 3H), 1.42 (s, 3H), 1.33 (d, *J* = 5.4 Hz, 6H). **^{13}C NMR** (150 MHz, $CDCl_3$) δ 121.71, 119.59, 117.47, 115.35, 113.25, 109.99, 105.14, 88.30, 83.37, 80.02, 71.83, 67.73, 26.92, 26.68, 26.35, 24.97. **ESI-HRMS**: Calculated for $C_{13}H_{20}F_3O_8S$ $(M+H)^+$: 393.0825, Found: 393.0833. $[\alpha]_D^{20}$ = -33.3 (c = 2.0, $CHCl_3$).

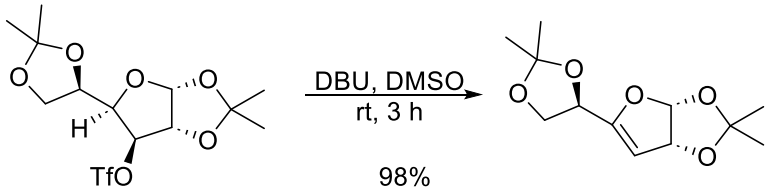

S15 **S16**

Compound **S16** was prepared according to the literature procedure.[108] Add DBU (220 ml, 1.478 mol, 2.0 equiv) to **S15** (290.0 g, 739.0 mmol, 1.0 equiv) in 1000 ml DMSO, the reaction stirred for 3 hours at room temperature. The solution was extracted with EA, and washed with water several times to eliminate DMSO to get the crude product. The residue was purified by flash chromatography eluting with EtOAc/petroleum ether (1:20) to obtain the product **S16** 190.0 g (98 yield) as white solid.

^{1}H NMR (600 MHz, $CDCl_3$) δ 6.08 (d, *J* = 5.4 Hz, 1H), 5.32 – 5.28 (m, 1H), 5.24 (dd, *J* = 2.4, 1.2 Hz, 1H), 4.61 – 4.56 (m, 1H), 4.14 (dd, *J* = 8.4, 6.6 Hz, 1H), 3.97 (dd, *J* = 8.4, 5.4 Hz, 1H), 1.47 (s, 6H), 1.44 (s, 3H), 1.39 (s, 3H). **^{13}C NMR** (150 MHz, $CDCl_3$) δ 160.19, 112.47, 110.49, 106.74, 99.11, 83.55, 71.44, 67.13, 28.40, 28.07, 26.38, 25.67. **ESI-HRMS**: Calculated for $C_{12}H_{19}O_5$ $(M+H)^+$: 243.1227, Found: 243.1220. $[\alpha]_D^{20}$ = +24.8 (c = 2.6, $CHCl_3$).

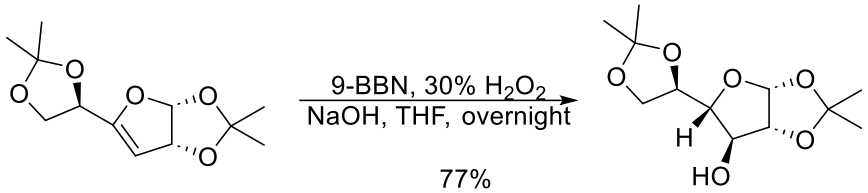

Compound **S17** was prepared according to the literature procedure. [109] A solution of the acetal **S16** (190 g, 785 mmol, 1.0 equiv) in 1000 mL of dry THF at 0 °C was treated with 9-BBN (1.884 L, 0.5 M in THF, 1.2 equiv) dropwise. The solution was stirred at rt for 2 hours under argon until the acetal consumed, then decease the solution to 0 °C with ice bar and treated sequentially with 30% H_2O_2 solution (250 mL), add 6 N NaOH (190 mL) to the solution dropwise (give off a lot of heat) and stirred overnight prior to dilution with EA and washing with water and brine. The organic phase was dried, filtered and concentrated. The crude oil was purified by flash chromatography on silica gel with the fluent PE/EA=1/1 to get the compound **S17** 158.0 g (77% yield) as white solid.

^{1}H NMR (600 MHz, $CDCl_3$) δ 5.86 (d, *J* = 4.2 Hz, 1H), 4.54 (dd, *J* = 3.6, 1.2 Hz, 1H), 4.38 – 4.33 (m, 1H), 4.14 – 4.09 (m, 1H), 4.08 – 4.04 (m, 1H), 3.88 – 3.82 (m, 2H), 2.44 – 2.30 (m, 1H), 1.54 (s, 3H), 1.44 (s, 3H), 1.36 (d, *J* = 15.0 Hz, 6H). **^{13}C NMR** (150 MHz, $CDCl_3$) δ 113.77, 110.04, 105.08, 87.75, 86.07, 76.30, 75.51, 65.80, 27.55, 26.86, 26.68, 25.41. **ESI-HRMS**: Calculated for $C_{12}H_{20}O_6Na$ $(M+Na)^+$: 283.1152, Found: 283.1147. $[\alpha]_D^{20}$ = -24.7 (c = 3.4, $CHCl_3$).

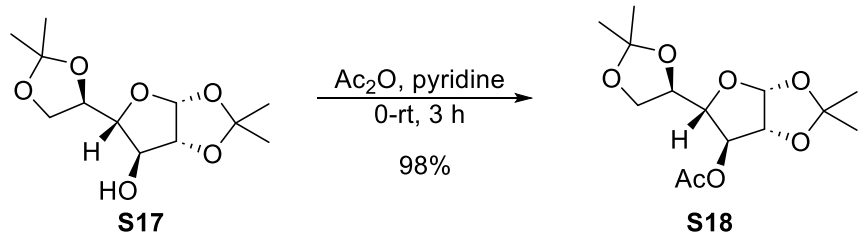

Compound **S18** was prepared according to the literature procedure.[109] Dissolve the sugar **S17** (158.0 g, 608.0 mmol, 1.0 equiv) in 350 mL of absolute pyridine at room temperature, add Ac_2O (68.9 mL, 729.6 mmol, 1.2 eq) dropwise to the mixture at 0 °C, then the reaction stirred at rt for 3 hours. After it finished through TLC, add 400 mL water to the mixture, evaporate the pyridine, extract the mixture with 200 mL of EA, wash the extract twice with 300 mL of saturated copper (II) sulphate solution and three times with 100 mL of water, dry the extract over anhydrous sodium sulfate, remove the solvent in vacuo. Purify the crude product by flash silica gel chromatography with ethyl acetate/ petroleum ether (1/8) as eluent to get the product **S18** 180.0 g (98% yield) as white solid.

^{1}H NMR (600 MHz, $CDCl_3$) δ 5.89 (d, *J* = 3.6 Hz, 1H), 4.87 (d, *J* = 2.4 Hz, 1H), 4.53 (d, *J* = 3.6 Hz, 1H), 4.39 – 4.31 (m, 1H), 4.04 (dd, *J* = 8.4, 6.6 Hz, 1H), 3.96 (dd, *J* = 8.4, 2.4 Hz, 1H), 3.81 (dd, *J* = 8.4, 6.6 Hz, 1H), 2.05 (s, 3H), 1.53 (s, 3H), 1.39 (s, 3H), 1.32 (s, 3H), 1.28 (s, 3H). **^{13}C NMR** (150 MHz, $CDCl_3$) δ 169.83, 113.31, 109.95, 105.68, 86.28, 84.60, 75.58, 65.92, 26.93, 26.71, 26.20, 25.37, 20.82. **ESI-**HRMS: Calculated for $C_{14}H_{22}O_7Na$ $(M+Na)^+$: 325.1258, Found: 325.1254. $[\alpha]_D^{20}$ = -16.5 (c = 4.0, CHCl3).

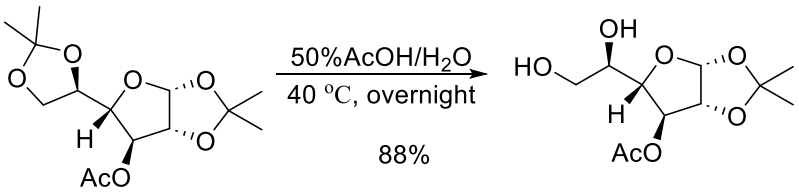

Compound **S19** was prepared according to the literature procedure.[103] The protected carbohydrate derivative **S18** (180.0 g, 596.0 mmol, 1.0 equiv) was dissolved in 50% AcOH (300 mL) and stirred overnight at 40 °C. Upon the completion of the reaction, add DCM to extract the product, then purified the residue by flash silica gel chromatography with the eluent PE/EA=1/1 to get the compound **S19** 137.0 g (88% yield) as colorless oil.

^{1}H NMR (600 MHz, $CDCl_3$) δ 5.91 (d, *J* = 4.2 Hz, 1H), 5.04 (d, *J* = 1.8 Hz, 1H), 4.61 (d, *J* = 3.6 Hz, 1H), 4.05 (dd, *J* = 7.8, 1.2 Hz, 1H), 3.90 – 3.84 (m, 1H), 3.73 (d, *J* = 11.4 Hz, 1H), 3.64 (d, *J* = 11.4 Hz, 1H), 3.13 (s, 1H), 2.82 (s, 1H), 2.05 (s, 3H), 1.50 (s, 3H), 1.27 (s, 3H). **^{13}C NMR** (150 MHz, $CDCl_3$) δ 170.35, 112.93, 105.60, 86.43, 84.66, 77.88, 70.63, 63.36, 26.52, 25.85, 20.82. **ESI-HRMS**: Calculated for $C_{11}H_{18}O_7Na$ $(M+Na)^+$: 285.0945, Found: 285.0939. $[\alpha]_D^{20}$ = +27.0 (c = 1.5, $CHCl_3$).

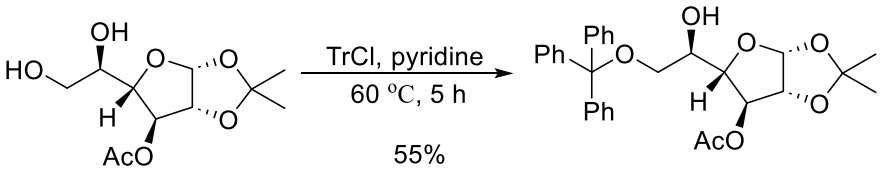

Compound **S20** was prepared according to the literature procedure.[110] **S19** (137.0 g, 522.9 mmol, 1.0 equiv), trityl chloride (174.4 g, 627.5 mmol, 1.2 equiv), and DMAP (1.405 g, 11.5 mmol, 2.2 %) were dissolved under argon in pyridine (200 mL) at rt. The reaction mixture was stirred at 60 °C for 5 h and concentrated. The crude product was purified by flash silica gel chromatography with the eluent PE/EA=5/1 to get the compound **S20** 175.0 g (55% yield) as white solid.

^{1}H NMR (600 MHz, $CDCl_3$) δ 7.50 – 7.44 (m, 6H), 7.35 – 7.30 (m, 6H), 7.29 – 7.24 (m, 3H), 5.94 (d, *J* = 4.2 Hz, 1H), 5.16 (d, *J* = 2.4 Hz, 1H), 4.63 (d, *J* = 3.6 Hz, 1H), 4.27 (dd, *J* = 6.6, 2.4 Hz, 1H), 4.07 – 3.99 (m, 1H), 3.36 – 3.25 (m, 2H), 2.72 (s, 1H), 2.07 (s, 3H), 1.57 (s, 3H), 1.34 (s, 3H). **^{13}C NMR** (150 MHz, $CDCl_3$) δ 169.87, 143.92, 128.77, 127.92, 127.13, 113.04, 105.54, 87.00, 86.34, 85.14, 78.20,

69.88, 65.06, 26.74, 26.11, 20.89. **ESI-HRMS**: Calculated for $C_{30}H_{32}O_7Na$ $(M+Na)^+$: 527.2040, Found: 527.2045. $[\alpha]_D^{20}$ = -7.4 (c = 2.8, $CHCl_3$).

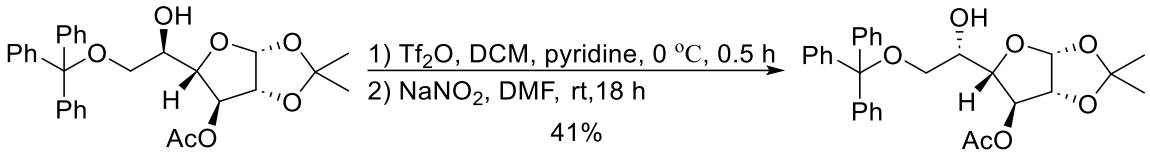

S20 **S21**

Compound **S21** was prepared according to the literature procedure.[103] Pyridine (55.9 mL, 694.4 mmol, 2.0 equiv) and trifluoromethanesulfonic anhydride (87.6 mL, 520.8 mmol, 1.5 equiv) were added under nitrogen to a solution of sugar **S20** (175 g, 347.2 mmol, 1.0 equiv) in CH_2Cl_2 (400 mL) under 0 °C(ice bath). The reaction mixture was allowed to reach room temperature and after stirring for 30 mins, the mixture was diluted with CH_2Cl_2 (200 mL), washed with iced saturated aqueous $NaHCO_3$ (100 mL), dried (anhydrous Na_2SO_4) and concentrated. The resulting triflate ester was dissolved in DMF (200 mL), $NaNO_2$ (119.6 g, 1.736 mol, 5.0 equiv) was added in three times and the reaction mixture was stirred at room temperature for 18 h. The resulting residue was dissolved in CH_2Cl_2 (200 mL) and washed with water (2×80 mL). The organic extract was dried (anhydrous Na_2SO_4) and concentrated. The resulting residue was purified by column chromatography using 1:8-1:5 PE/EA as eluent to give **S21** 72.0 g (41% yield) as yellow solid.

^{1}H NMR (500 MHz, $CDCl_3$) δ 7.48 – 7.44 (m, 6H), 7.35 – 7.30 (m, 9H), 7.29 – 7.24 (m, 3H), 5.91 (d, *J* = 4.0 Hz, 1H), 5.42 (d, *J* = 1.0 Hz, 1H), 4.59 (d, *J* = 3.5 Hz, 1H), 4.22 – 4.18 (m, 1H), 4.10 – 4.03 (m, 1H), 3.46 – 3.31 (m, 2H), 2.10 (s, 3H), 1.51 (s, 3H), 1.31 (s, 3H). **^{13}C NMR** (125 MHz, $CDCl_3$) δ 170.08, 143.87, 128.77, 128.01, 127.24, 112.65, 106.03, 86.92, 85.89, 84.87, 77.94, 70.41, 64.16, 26.80, 25.88, 21.09. **ESI-HRMS**: Calculated for $C_{30}H_{32}O_7Na$ $(M+Na)^+$: 527.2040, Found:527.2044, Found: 527.2045. $[\alpha]_D^{20}$ = -11.5 (c = 1.0, $CHCl_3$).

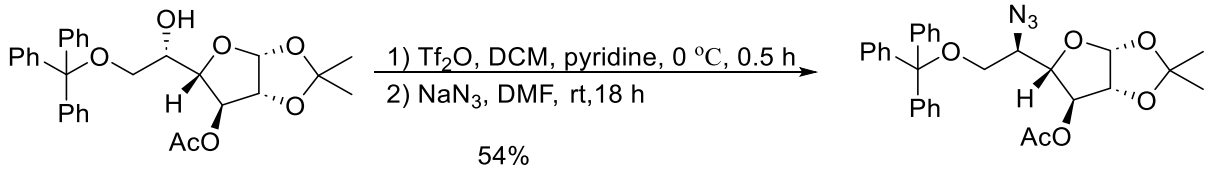

S21 **S22**

Compound **S22** was prepared according to the literature procedure.[103] Pyridine (22.9 mL, 285.2 mmol, 2.0 equiv) and trifluoromethanesulfonic anhydride (36.0 mL, 213.9 mmol, 1.5 equiv) were added under nitrogen to a solution of sugar **S21** (72.0 g, 142.6 mmol, 1.0 equiv) in CH_2Cl_2 (150 mL) under 0 °C. The reaction mixture was allowed to reach room temperature and after stirring for 30 mins, the mixture was diluted with CH_2Cl_2 (100 mL), washed with iced saturated aqueous $NaHCO_3$ (40 mL), dried (anhydrous Na_2SO_4) and concentrated. The resulting triflate ester was dissolved in DMF (150 mL), NaN_3 (46.3 g, 713.0 mmol, 5.0 equiv) was added and the reaction mixture was stirred at room temperature for 18 h. The resulting residue was dissolved in CH_2Cl_2 (200 mL) and washed with water

(2×100 mL). The organic extract was dried (anhydrous Na_2SO_4) and concentrated. The resulting residue was purified by column chromatography using 1:10-1:5 PE/EA as eluent to give **S22** 41.0 g (54% yield) as colorless oil.

^{1}H NMR (600 MHz, $CDCl_3$) δ 7.49 – 7.44 (m, 6H), 7.35 – 7.30 (m, 6H), 7.29 – 7.24 (m, 3H), 5.88 (d, *J* = 4.2 Hz, 1H), 5.00 (d, *J* = 2.4 Hz, 1H), 4.56 (d, *J* = 4.2 Hz, 1H), 4.09 (dd, *J* = 7.8, 3.0 Hz, 1H), 3.86 – 3.78 (m, 1H), 3.40 (dd, *J* = 10.2, 3.6 Hz, 1H), 3.30 (dd, *J* = 10.2, 6.6 Hz, 1H), 2.03 (s, 3H), 1.58 (s, 3H), 1.34 (s, 3H). **^{13}C NMR** (150 MHz, $CDCl_3$) δ 169.71, 143.61, 128.71, 128.04, 128.03, 127.30, 113.59, 105.43, 87.44, 84.89, 84.20, 77.37, 63.97, 62.56, 27.04, 26.27, 20.82. **ESI-HRMS**: Calculated for $C_{30}H_{31}N_3O_6Na$ $(M+Na)^+$: 552.2105, Found:552.2110. $[\alpha]_D^{20}$ = -17.1 (c = 1.1, $CHCl_3$).

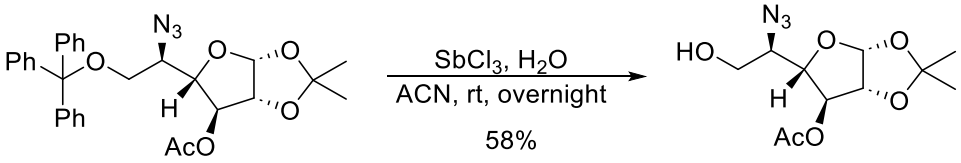

S22 **S23**

Compound **S23** was prepared under the following procedure. Antimony trichloride (1.76 g, 7.74 mmol, 10%) was added to a stirred solution of substrates **S22** (41.0 g, 77.4 mmol, 1.0 equiv) in acetonitrile (150 mL), followed by the addition of water (2.8 mL, 154.8 mmol, 2.0 equiv) at room temperature. After complete conversion, a saturated solution of sodium bicarbonate (80 mL) was added, and the reaction mixture was concentrated under reduced pressure. The residue was extracted with DCM (60 mL). The organic layer was dried (anhydrous Na_2SO_4) and concentrated under reduced pressure to give a crude product, which was isolated through column chromatography (PE/EA = 1/1) to get the compound **S23** 12.8 g (58% yield) as colorless oil.

^{1}H NMR (600 MHz, $CDCl_3$) δ 5.95 (d, *J* = 4.2 Hz, 1H), 5.09 (d, *J* = 1.2 Hz, 1H), 4.65 (d, *J* = 3.6 Hz, 1H), 4.10 (d, *J* = 9.0 Hz, 1H), 3.82 – 3.75 (m, 2H), 3.71 (dd, *J* = 12.0, 4.8 Hz, 1H), 2.75 (s, 1H), 2.07 (s, 3H), 1.55 (s, 3H), 1.29 (s, 3H). **^{13}C NMR** (150 MHz, $CDCl_3$) δ 170.69, 113.12, 105.74, 86.03, 84.29, 77.63, 63.50, 62.51, 26.63, 25.73, 20.80. **ESI-HRMS**: Calculated for $C_{11}H_{17}N_3O_6Na$ $(M+Na)^+$: 310.1010, Found: 310.1005. $[\alpha]_D^{20}$ = -20.1 (c = 2.8, $CHCl_3$).

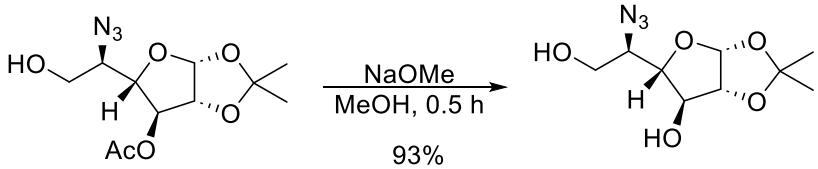

S23 **S24**

Compound **S24** was prepared according to the literature procedure.[103] NaOMe (2.648g, 49.0 mmol, 1.1 equiv) was added to a solution of **S23** (12.8g, 44.56 mmol, 1.0 equiv) in MeOH (50 mL) at room temperature and stirred for 30 mins. Filter to remove solids, evaporate the solvent in vacuo, purify the residue by flash column chromatography (PE/EA = 2:1) to obtain **S24** 10.2g (93% yield) as yellow solid.

^{1}H NMR (600 MHz, $CDCl_3$) δ 5.91 (d, *J* = 3.6 Hz, 1H), 4.59 (dd, *J* = 4.2, 1.2 Hz, 1H), 4.28 (d, *J* = 3.6 Hz, 1H), 4.01 (dd, *J* = 7.8, 3.6 Hz, 1H), 3.84 – 3.73 (m, 3H), 3.11 (s, 1H), 2.62 (s, 1H), 1.56 (s, 3H), 1.35 (s, 3H). **^{13}C NMR** (150 MHz, $CDCl_3$) δ 113.64, 105.30, 87.32, 86.58, 76.44, 63.57, 62.71, 27.27, 26.46. **ESI-HRMS**: Calculated for $C_9H_{15}N_3O_5Na$ $(M+Na)^+$: 268.0904, Found:268.0897. $[\alpha]_D^{20}$ = -62.6 (c = 1.4, $CHCl_3$).

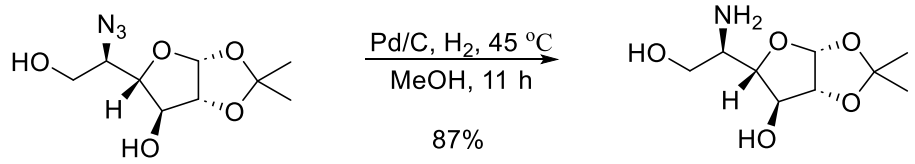

S24 **S25**

Compound **S25** was prepared according to the literature procedure.[103] A solution of azido sugar **S24** (10.2 g, 41.59 mmol, 1.0 equiv) and 10% Pd/C (1.02 g) in MeOH (15 mL) was hydrogenated under an atmospheric pressure of hydrogen using a balloon. The mixture was stirred at 45 °C for 11 h, filtered through celite and concentrated to give **S25** 7.9 g (87% yield) as oil which was used in the next step without further purification.

^{1}H NMR (600 MHz, $CDCl_3$) δ 5.88 (d, *J* = 3.6 Hz, 1H), 4.55 (d, *J* = 4.2 Hz, 1H), 4.20 (d, *J* = 3.0 Hz, 1H), 3.83 (dd, *J* = 8.4, 3.0 Hz, 1H), 3.67 (dd, *J* = 11.4, 4.2 Hz, 1H), 3.60 (dd, *J* = 11.4, 4.8 Hz, 1H), 3.10 (dt, *J* = 9.0, 4.8 Hz, 1H), 1.49 (s, 3H), 1.31 (s, 3H). **^{13}C NMR** (150 MHz, $CDCl_3$) δ 112.82, 105.31, 88.40, 87.48, 76.06, 63.49, 53.75, 27.21, 26.32. **ESI-HRMS**: Calculated for $C_9H_{18}NO_5$ $(M+H)^+$: 220.1180, Found:220.1172. $[\alpha]_D^{20}$ = -8.0 (c = 0.7, $CHCl_3$).

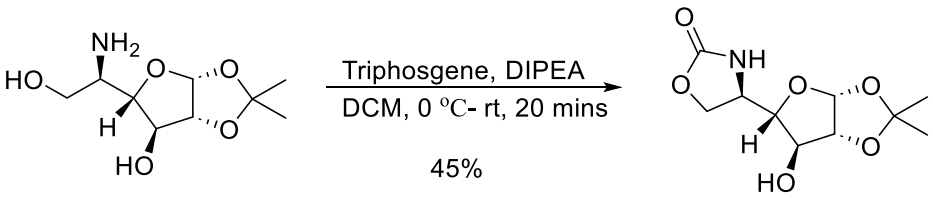

S25 **S26**

Compound **S26** was prepared according to the literature procedure.[104] Diisopropylethylamine (62.8ml, 360.3 mmol, 10.0 equiv) and triphosgene (16.0g, 54.05 mmol, 1.5 equiv) were added to a stirred solution of **S25** (7.9 g, 36.03 mmol, 1.0 equiv) in CH_2Cl_2 (50 mL) at 0 °C. The reaction mixture was allowed to reach room temperature and stirred for 20 mins. The solvent was removed under reduced pressure and the residue was purified by column chromatography (60:1 EtOAc/MeOH) to give **S26** 4.0 g (45% yield) as yellow solid.

^{1}H NMR (600 MHz, $CDCl_3$) δ 6.24 (d, *J* = 25.8 Hz, 1H), 5.94 (d, *J* = 3.6 Hz, 1H), 4.57 (d, *J* = 4.2 Hz, 1H), 4.47 (t, *J* = 9.0 Hz, 1H), 4.26 (dd, *J* = 9.0, 5.4 Hz, 1H), 4.17 – 4.09 (m, 2H), 4.06 (s, 1H), 4.00 (dd, *J* = 9.0, 1.8 Hz, 1H), 1.51 (s, 3H), 1.31 (s, 3H). **^{13}C NMR** (150 MHz, $CDCl_3$) δ 159.80, 113.06, 105.80, 89.14, 86.83, 77.37, 77.16, 76.95, 75.11, 66.69, 53.89, 27.00, 25.95. **ESI-HRMS**: Calculated for $C_{10}H_{16}NO_6$ $(M+H)^+$: 246.0972, Found:246.0965. $[\alpha]_D^{20}$ = -27.5 (c = 0.2, MeOH).

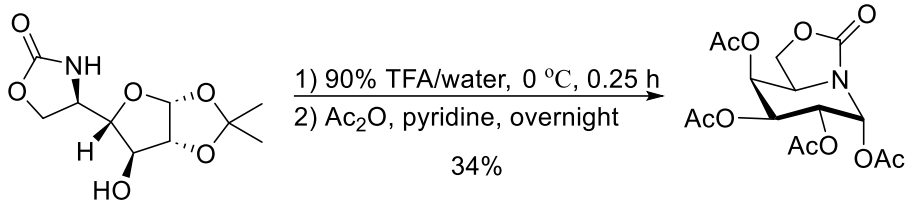

S26 **S27**

Compound **S27** was prepared according to the literature procedure.[104] Compound **S26** (4.0 g, 16.31 mmol, 1.0 equiv) was deacetylated by treatment with 90% TFA/water (20 mL). The reaction mixture was concentrated and the residue evaporated several times with water to eliminate trace of acid. The resulting residue was subjected to conventional acetylation with Ac_2O/pyridine (1:1, 60 mL) and the peracetylated mixture was purified by column chromatography using 1:1 EtOAc/petroleum ether as eluent to get **S27** 2.05 g (34% yield) as white solid.

^{1}H NMR (600 MHz, $CDCl_3$) δ 6.73 (d, *J* = 7.8 Hz, 1H), 5.46 (s, 1H), 5.34 – 5.21 (m, 2H), 4.39 (t, *J* = 9.0 Hz, 1H), 4.34 – 4.29 (m, 1H), 4.03 – 3.98 (m, 1H), 2.18 – 2.13 (m, 3H), 2.12 – 2.09 (m, 3H), 2.00 – 1.96 (m, 6H). **^{13}C NMR** (150 MHz, $CDCl_3$) δ 170.29, 170.07, 169.48, 168.72, 154.39, 72.99, 68.08, 67.51, 65.80, 63.03, 51.46, 20.68, 20.63, 20.62, 20.47. **ESI-HRMS**: Calculated for $C_{15}H_{20}NO_{10}$ $(M+H)^+$: 396.0901, Found:396.0899. $[\alpha]_D^{20}$ = +75.6 (c = 1.3, $CHCl_3$).

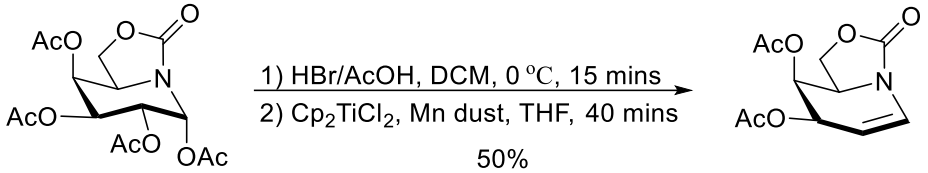

S27 **S28**

Compound **S28** was prepared according to the literature procedure.[104] To a solution of **S27** (2.05 g, 5.49 mmol, 1.0 equiv) in anhydrous DCM (20 mL), HBr/AcOH (33%, 0.7 mL) were added dropwise at 0 °C and the reaction mixture was stirred for 15 mins, detected by TLC, diluted with DCM (30 mL) and washed with saturated aqueous $NaHCO_3$ (20 mL). The organic layer was dried (anhydrous Na_2SO_4) and concentrated under reduced pressure to yield the corresponding 1-bromo derivative as a white solid. This product was used without further purification in the next step. A mixture of Cp_2TiCl_2 (1.639 g, 6.588 mmol, 1.2 equiv) and Mn dust (0.8 g, 14.5 mmol, 2.6 equiv) in deoxygenated THF (20 mL) was stirred at rt until the red solution turned green. Then the 1-bromo derivative (2.0 g) in deoxygenated THF (10 mL) was added and the reaction mixture was stirred for 40 mins. The solvent was removed under reduced pressure, diluted with EtOAc (30 mL), quenched with 1 M HCl (2 x 10 mL), washed with brine, and dried (anhydrous Na_2SO_4). The resulting crude was purified by column chromatography (PE/EA=1/1) to yield the corresponding product **S28** 0.7 g (50% yield) as yellow solid.

^{1}H NMR (600 MHz, $CDCl_3$) δ 6.73 (d, *J* = 7.8 Hz, 1H), 5.65 (d, *J* = 1.2 Hz, 1H), 5.46 (t, *J* = 1.8 Hz, 1H), 4.85 (dt, *J* = 7.8, 1.8 Hz, 1H), 4.49 (t, *J* = 9.0 Hz, 1H), 4.41 (t, *J* = 8.7 Hz, 2H), 4.04 (t, *J* = 8.4 Hz, 1H), 2.15 (s, 3H), 2.04 (s, 3H). **^{13}C NMR** (150 MHz, $CDCl_3$) δ 170.63, 170.39, 153.67, 124.06, 104.99,

66.76, 63.42, 61.49, 53.70, 20.85, 20.79. **ESI-HRMS**: Calculated for $C_{11}H_{14}NO_6$ $(M+H)^+$: 256.0816, Found:256.0809. $[\alpha]_D^{20}$ = +60.8 (c = 1.1, $CHCl_3$).

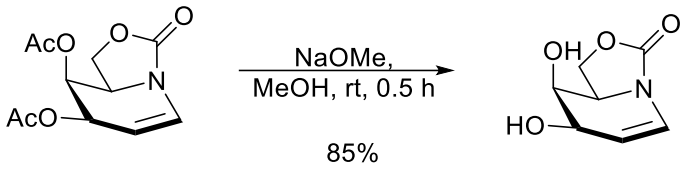

S28 **S29**

Compound **S29** was prepared according to the literature procedure.[105] NaOMe (254 mg, 4.7 mmol, 2.0 equiv) was added to a solution of **S28** (0.6g, 2.35 mmol, 1.0 equiv) in MeOH (20 mL) at room temperature and stirred for 30 mins. Filter out the solid with MeOH to wash solid, collected the liquid and evaporate the solvent in vacuo, purify the residue by flash column chromatography (DCM/MeOH, 10:1) to obtain **S29** 0.34 g (85% yield) as colorless oil.

^{1}H NMR (500 MHz, CD_3OD) δ 6.50 (dd, *J* = 8.0, 2.0 Hz, 1H), 4.89 (dt, *J* = 8.1, 1.8 Hz, 1H), 4.53 – 4.48 (m, 1H), 4.47 – 4.45 (m, 1H), 4.40 – 4.34 (m, 1H), 4.29 (t, *J* = 9.0 Hz, 1H), 3.84 – 3.80 (m, 1H). **^{13}C NMR** (125 MHz, CD_3OD) δ 156.76, 122.57, 111.44, 67.49, 65.49, 64.60, 56.82. **ESI-HRMS**: Calculated for $C_7H_{10}NO_4$ $(M+H)^+$: 172.0604, Found:172.0604. $[\alpha]_D^{20}$ = +31.8 (c = 0.8, MeOH).

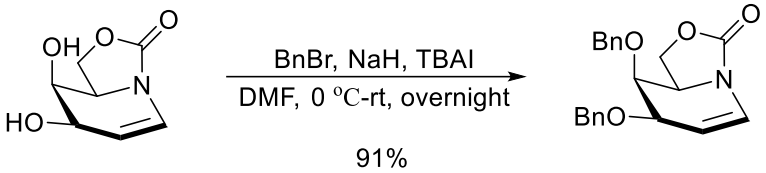

S29 **81a**

Compound **81a** was prepared according to the literature procedure.[105] To a solution of compound **S29** (0.34 g, 2.0 mmol, 1.0 equiv) in anhydrous DMF (10 mL) stirred at 0 °C was added sodium hydride (320 mg in 60% mineral oil, 8.0 mmol, 4.0 equiv) over a 15 min period. The reaction mixture was stirred for 30 mins and warmed up to room temperature. Then, benzyl bromide (0.95 mL, 8.0 mmol, 4.0 equiv) and tetra-n-butylammonium iodide (TBAI, 147.7 mg, 1.0 mmol, 0.5 equiv) were sequentially added in dropwise. The mixture was stirred at room temperature overnight under a nitrogen atmosphere. After completion of the reaction as monitored by TLC, the resultant was diluted with EtOAc and washed twice with brine. The combined organic layer was dried over anhydrous Na_2SO_4. The filtrate was condensed under reduced pressure and purified by silica gel flash chromatography (EtOAc:PE = 1:1) to get the desired product **81a** 525 mg (91% yield) as an amorphous white solid.

^{1}H NMR (600 MHz, $CDCl_3$) δ 7.40 – 7.36 (m, 4H), 7.35 – 7.29 (m, 6H), 6.63 (dd, *J* = 8.4, 2.4 Hz, 1H), 5.10 – 5.05 (m, 2H), 4.73 (dd, *J* = 24.4, 12.0 Hz, 2H), 4.65 (d, *J* = 12.0 Hz, 1H), 4.38 (s, 1H), 4.23 (t, *J* = 7.8 Hz, 1H), 4.16 – 4.07 (m, 2H), 3.84 – 3.80 (m, 1H). **^{13}C NMR** (150 MHz, $CDCl_3$) δ 154.19, 137.99, 137.90, 128.73, 128.66, 128.35, 128.11, 128.08, 127.63, 122.80, 106.36, 75.30, 74.38, 71.45, 67.59,

63.69, 55.34. **ESI-HRMS**: Calculated for $C_{21}H_{22}NO_4$ $(M+H)^+$: 352.1543, Found: 352.1542. $[\alpha]_D^{20}$ = +25.4 (c = 0.7, $CHCl_3$).

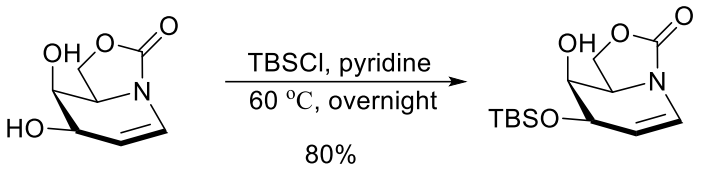

S29 **S30**

Compound **S30** was prepared under the following procedure. D-galactcal **S29** (8.558 mg, 0.05 mmol, 1.0 equiv) was dissolved in anhydrous pyridine (2.0 mL) under an argon atmosphere and TBSCl (30.144 mg, 0.1 mmol, 2.0 equiv) was added at this temperature. Afterwards, the solution was poured into ice water, and extracted with EA (5 mL) twice, the organic layer was washed with brine (5 mL), dried over anhydrous Na_2SO_4, filtered and concentrated in vacuo and purified by flash chromatography (20:1 n-pentane/EA), the title compound **S30** 11.4 g (80% yield) was obtained as a white solid.

^{1}H NMR (600 MHz, $CDCl_3$) δ 6.61 (dd, *J* = 8.4, 1.8 Hz, 1H), 4.71 (dt, *J* = 7.8, 1.8 Hz, 1H), 4.58 – 4.55 (m, 1H), 4.51 (dd, *J* = 9.6, 8.4 Hz, 1H), 4.44 (t, *J* = 8.4 Hz, 1H), 4.14 (t, *J* = 9.0 Hz, 1H), 3.81 – 3.77 (m, 1H), 2.76 (d, *J* = 1.2 Hz, 1H), 0.92 (s, 9H), 0.14 (d, *J* = 9.0 Hz, 6H). **^{13}C NMR** (150 MHz, $CDCl_3$) δ 154.27, 122.58, 108.06, 67.00, 63.76, 63.52, 54.78, 25.84, 25.84, 18.23, -4.54, -4.77. **ESI-HRMS**: Calculated for $C_{13}H_{24}NO_4Si$ $(M+H)^+$: 285.1396, Found: 285.1394. $[\alpha]_D^{20}$ = +18.5 (c = 1.0, $CHCl_3$).

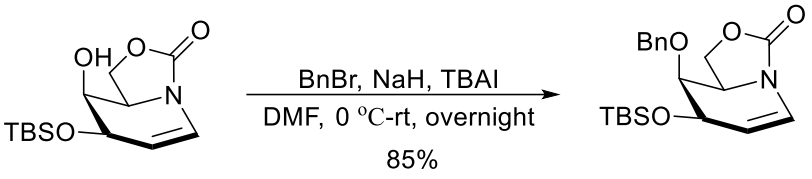

S30 **81b**

Compound **81b** was prepared under the following procedure. To a solution of compound **S30** (14.271 mg, 0.05 mmol, 1.0 equiv) in anhydrous DMF (2.0 mL) stirred at 0 °C was added sodium hydride (3.0 mg in 60% mineral oil, 0.08 mmol, 1.5 equiv) over a 15 min period. The reaction mixture was stirred for 30 mins and warmed up to room temperature. Then, benzyl bromide (10.26 mg, 0.06 mmol, 1.2 equiv) and tetra-n-butylammonium iodide (TBAI, 1.847 mg, 0.01 mmol, 20%) were sequentially added in dropwise. The mixture was stirred at room temperature overnight under a nitrogen atmosphere. After completion of the reaction as monitored by TLC, the resultant was diluted with EtOAc and washed twice with brine. The combined organic layer was dried over anhydrous Na_2SO_4. The filtrate was condensed under reduced pressure and purified by silica gel flash column chromatography (EA:PE = 1:3, v/v). The desired products **81b** 15.69 mg (85% yield) as an amorphous white solid.

^{1}H NMR (600 MHz, $CDCl_3$) δ 7.37 – 7.28 (m, 5H), 6.57 (dd, *J* = 8.4, 2.4 Hz, 1H), 5.12 (d, *J* = 12.0 Hz, 1H), 4.84 (dt, *J* = 7.8, 1.8 Hz, 1H), 4.74 – 4.62 (m, 2H), 4.24 – 4.20 (m, 1H), 4.17 – 4.12 (m, 1H), 4.11 – 4.08 (m, 1H), 3.66 – 3.63 (m, 1H), 0.96 (s, 9H), 0.16 (d, *J* = 1.8 Hz, 6H). **^{13}C NMR** (150 MHz, $CDCl_3$) δ 154.22, 138.21, 128.66, 128.22, 128.07, 122.00, 109.83, 74.83, 70.24, 69.60, 63.70, 55.29, 26.00,

18.31, -4.52, -4.60. **ESI-HRMS**: Calculated for $C_{20}H_{30}NO_4Si$ $(M+H)^+$: 376.1939, Found: 376.1938. $[\alpha]_D^{20}$ = +4.0 (c = 0.3, $CHCl_3$).

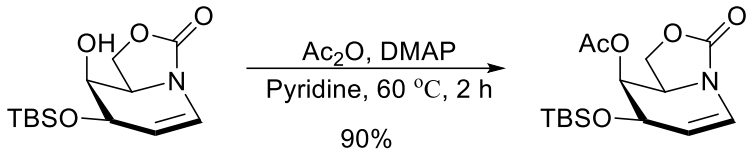

S30 **81c**

Compound **81c** was prepared under the following procedure. To a solution of compound **S30** (14.271 mg, 0.05 mmol, 1.0 equiv) in pyridine (2.0 mL) stirred at rt, was added DMAP (1.22 mg, 0.01 mmol, 20%), Ac_2O (5.6 ul, 0.06 mmol, 1.2 equiv) was added to the solution dropwise, the mixture was stirred at 60 °C for 2 hours. After it finished through TLC detection, add 5 mL water to the mixture, evaporate the pyridine, extract the mixture with 5 mL of EA, wash the extract twice with 5 mL of saturated copper(II) sulphate solution and three times with 5 mL of water, dry the extract over anhydrous sodium sulfate, remove the solvent in vacuo, the product was purified through flash chromatography (n-pentane/EA=3/1) to get the title compound **81c** 14.7 mg (90% yield) as white solid.

^{1}H NMR (600 MHz, $CDCl_3$) δ 6.60 (dd, *J* = 8.4, 1.8 Hz, 1H), 5.29 (d, *J* = 4.2 Hz, 1H), 4.83 (d, *J* = 7.8 Hz, 1H), 4.66 – 4.62 (m, 1H), 4.45 (t, *J* = 9.0 Hz, 1H), 4.34 (d, *J* = 9.0 Hz, 1H), 4.00 (t, *J* = 9.0 Hz, 1H), 2.14 (s, 3H), 0.87 (s, 9H), 0.09 (d, *J* = 24.6 Hz, 6H). **^{13}C NMR** (150 MHz, $CDCl_3$) δ 170.97, 153.80, 122.00, 110.05, 65.94, 64.26, 63.57, 54.02, 25.76, 20.96, 18.20, -4.93, -4.97. **ESI-HRMS**: Calculated for $C_{15}H_{26}NO_5Si$ $(M+H)^+$: 328.1575, Found: 328.1573. $[\alpha]_D^{20}$ = +10.5 (c = 0.4, $CHCl_3$).

5.2.4 Characterization data for iminoglycal products

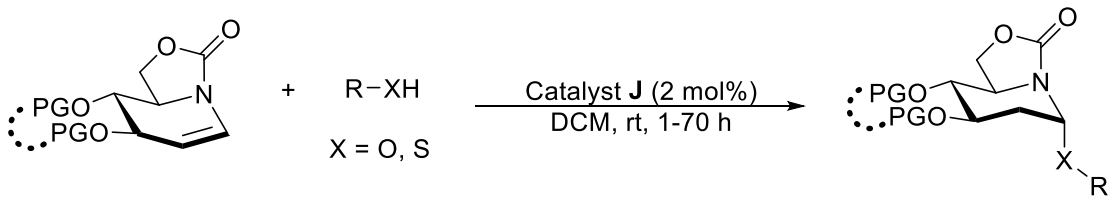

78a-78e **79** **80a-82l**

General procedure A1: To an oven dried vial was charged donor iminoglycal **78** or **81** (0.2 mmol, 1.0 equiv), catalyst **J** (0.004 mmol, 2 mol%), dry CH_2Cl_2 (0.8 mL) and then acceptor alcohol **79** (0.3 mmol, 1.5 equiv). The vial was sealed and the mixture was stirred at room temperature for 1-70 h. The reaction mixture was filtered over a short silica plug and flushed with 20 mL of ethyl acetate twice. The filtrate was then evaporated and the determination of the anomeric selectivity (α/β) and yield were by ^{1}H-NMR analysis of this concentrated crude mixture with 1,3,5-trimethoxybenzene as the internal standard. The crude mixture is subsequently dry loaded onto silica gel and subjected to flash column chromatography for purification.

General procedure B1: To an oven dried vial was charged donor iminoglycal **78** (0.2 mmol, 1.0 equiv), catalyst **D** (0.004 mmol, 2 mol%), dry CH_2Cl_2 (0.8 mL) and then acceptor alcohol **79** (0.3 mmol, 1.5

equiv). The vial was sealed and the mixture was stirred at 40 ºC for 1-24 h. The reaction mixture was filtered over a short silica plug and flushed with 20 mL of ethyl acetate twice. The filtrate was then evaporated and the determination of the anomeric selectivity (α/β) and yield were by ^{1}H-NMR analysis of this concentrated crude mixture with 1,3,5-trimethoxybenzene as the internal standard. The crude mixture is subsequently dry loaded onto silica gel and subjected to flash column chromatography for purification.

(5a*R*,7*R*,178a*R*,11b*R*)-7-hydroxy-2,2,4,4-tetraisopropylhexahydro-9*H*-oxazolo[3,4-*a*][1,3,5,2,4]trioxadisilepino[6,7-*c*]pyridin-9-one (83)

The title product compound is prepared according to the following procedure: To an oven dried vial was charged iminoglycal **78a** (0.2 mmol, 1.0 equiv), 2 mol% catalyst **J**, dry CH_2Cl_2 (0.8 mL), the vial was sealed and the mixture was stirred at room temperature for 0.5 h. The reaction mixture was filtered over a short silica plug and flushed with 20 mL of ethyl acetate twice, the filtrate was then evaporated and isolated by flash column chromatography (3:1 Pentane: Ethyl Acetate) giving **83** as a white solid (8.6 mg, 10% yield, α/β ratio > 20:1).

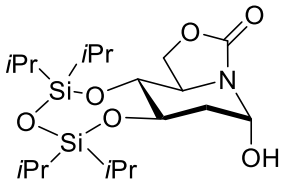

83

^{1}H NMR (600 MHz, $CDCl_3$) δ 5.37 (dd, *J* = 3.9, 1.6 Hz, 1H), 4.47 (t, *J* = 8.5 Hz, 1H), 4.25 (dd, *J* = 9.0, 4.3 Hz, 1H), 4.00 (dd, *J* = 5.7, 2.8 Hz, 1H), 3.62 (ddd, *J* = 9.4, 8.0, 4.3 Hz, 1H), 3.47 (t, *J* = 8.9 Hz, 1H), 2.13 (ddd, *J* = 13.8, 4.6, 1.7 Hz, 1H), 1.74 (ddd, *J* = 13.8, 11.4, 3.9 Hz, 1H), 1.10 – 0.98 (m, 28H).**^{13}C NMR** (150 MHz, $CDCl_3$) δ 155.98, 77.88, 77.23, 71.26, 66.17, 54.98, 37.80, 17.69, 17.59, 17.48, 17.41, 17.35, 17.31, 13.07, 12.96, 12.39, 12.23. **ESI-HRMS**: $C_{19}H_{38}NO_6Si_2$ $(M+H)^+$: 432.2232, Found: 432.2233. $[\alpha]_D^{20}$ = +36.1 (c = 1.0, $CHCl_3$).

(5a*R*,7*R*,178a*R*,11b*R*)-2,2,4,4-tetraisopropyl-7-(octyloxy)hexahydro-9*H*-oxazolo[3,4-*a*][1,3,5,2,4]trioxadisilepino[6,7-*c*]pyridin-9-one (80a)

The title product compound is prepared according to general procedure **A1** with iminoglycal **78a** (0.2 mmol, 1.0 equiv), 2 mol% catalyst **J**, dry CH_2Cl_2 (0.8 mL) and acceptor at room temperature for 24 h and isolated by flash column chromatography (25:1 Pentane: Ethyl Acetate) giving **80a** as a white solid (97 mg, 89% yield, α/β ratio > 20:1).

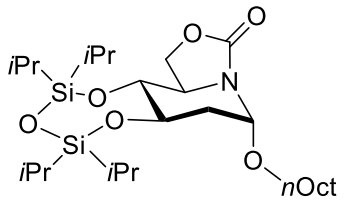

80a

^{1}H NMR (700 MHz, $CDCl_3$) δ 5.12 (d, *J* = 2.8 Hz, 1H), 4.48 (t, *J* = 9.1 Hz, 1H), 4.20 (dd, *J* = 9.1, 5.6 Hz, 1H), 4.03 (ddd, *J* = 11.2, 8.4, 4.9 Hz, 1H), 3.71 – 3.65 (m, 1H), 3.49 – 3.44 (m, 2H), 3.43 – 3.38 (m, 1H), 2.19 (ddd, *J* = 13.3, 4.9, 1.4 Hz, 1H), 1.67 (ddd, *J* = 14.0, 11.2, 4.2 Hz, 1H), 1.59 – 1.52 (m, 2H), 1.35 – 1.23 (m, 10H), 1.12 – 0.93 (m, 28H), 0.88 (t, *J* = 7.0 Hz, 3H). **^{13}C NMR** (175 MHz, $CDCl_3$) δ 156.54, 79.63, 78.95, 71.47, 68.13, 66.69, 54.45, 38.12, 31.94, 29.48, 29.46, 29.41, 26.28, 22.81, 17.73, 17.63, 17.53, 17.44, 17.37, 17.33, 14.23, 13.09, 12.96, 12.41, 12.33. **ESI-HRMS**: Calculated for $C_{27}H_{54}NO_6Si_2$ $(M+H)^+$: 544.3484, Found: 544.3488. $[\alpha]_D^{20}$ = +54.8 (c = 1.0, $CHCl_3$).

(5a*R*,7*R*,178a*R*,11b*R*)-2,2,4,4-tetraisopropyl-7-(((2*R*,3*R*,4*S*,5*R*,6*S*)-3,4,5-tris(benzyloxy)-6-methoxytetrahydro-2*H*-pyran-2-yl)methoxy)hexahydro-9*H*-oxazolo[3,4-*a*][1,3,5,2,4]trioxadisilepino[6,7-*c*]pyridin-9-one (80b)

The title product compound is prepared according to general procedure **A1** with iminoglycal **78a** (0.2 mmol, 1.0 equiv), 2 mol% catalyst **J**, dry CH_2Cl_2 (0.8 mL) and acceptor at room temperature for 1 h and isolated by flash column chromatography (5:1 Pentane: Ethyl Acetate) giving **80b** as a colorless oil (132 mg, 75% yield, α/β ratio > 20:1).

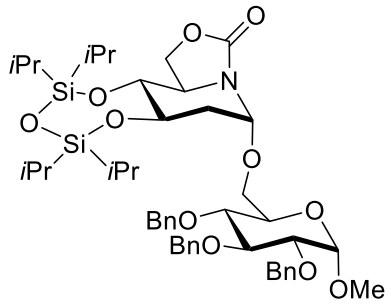

80b

^{1}H NMR (700 MHz, $CDCl_3$) δ 7.39 – 7.25 (m, 15H), 5.18 (d, *J* = 2.8 Hz, 1H), 4.98 (dd, *J* = 27.3, 11.2 Hz, 2H), 4.79 (dd, *J* = 12.6, 7.0 Hz, 2H), 4.68 (d, *J* = 11.9 Hz, 1H), 4.60 (d, *J* = 3.5 Hz, 1H), 4.56 (d, *J* = 11.2 Hz, 1H), 4.19 (t, *J* = 8.4 Hz, 1H), 4.09 (dd, *J* = 8.4, 5.6 Hz, 1H), 4.03 – 3.95 (m, 2H), 3.79– 3.75 (m, 1H), 3.69 – 3.63 (m, 2H), 3.60 – 3.56 (m, 1H), 3.52 (dd, *J* = 9.1, 3.5 Hz, 1H), 3.47 – 3.40 (m, 2H), 3.36 (s, 3H), 2.24 (dd, *J* = 11.9, 4.2 Hz, 1H), 1.70 – 1.60 (m, 1H), 1.11 – 0.93 (m, 28H). **^{13}C NMR** (175 MHz, $CDCl_3$) δ 156.50, 138.79, 138.43, 138.26, 128.62, 128.57, 128.24, 128.10, 128.09, 127.81, 127.80, 127.32, 98.10, 82.27, 80.20, 78.76, 78.15, 75.87, 75.01, 73.51, 71.50, 69.87, 66.69, 66.65,

55.12, 54.31, 37.89, 17.70, 17.68, 17.49, 17.39, 17.37, 17.36, 17.34, 17.30, 13.04, 12.96, 12.39, 12.23. **ESI-HRMS**: Calculated for $C_{47}H_{67}NO_{11}Si_2Na$ $(M+Na)^+$: 900.4145, Found: 900.4158. $[\alpha]_D^{20}$ = +40.4 (c = 1.4, $CHCl_3$).

(5a*R*,7*R*,178a*R*,11b*R*)-2,2,4,4-tetraisopropyl-7-(((80a*R*,5*R*,5a*S*,8a*S*,8b*R*)-2,2,7,7-tetramethyltetrahydro-5*H*-bis([1,3]dioxolo)[4,5-b:4',5'-d]pyran-5-yl)methoxy)hexahydro-9*H*-oxazolo[3,4-*a*][1,3,5,2,4]trioxadisilepino[6,7-*c*]pyridin-9-one (80c)

The title product compound is prepared according to general procedure **A1** with iminoglycal **78a** (0.2 mmol, 1.0 equiv), 2 mol% catalyst **J**, dry CH_2Cl_2 (0.8 mL) and acceptor at room temperature for 1 h and isolated by flash column chromatography (5:1 Pentane: Ethyl Acetate) giving **80c** as a white solid (85 mg, 63% yield, α/β ratio > 20:1).

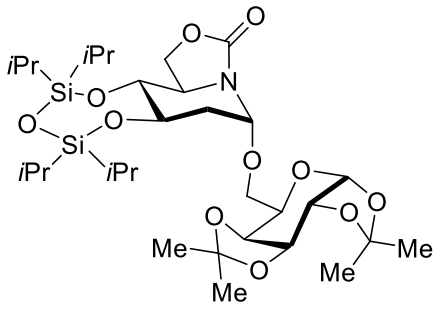

80c

^{1}H NMR (500 MHz, $CDCl_3$) δ 5.51 (d, *J* = 5.0 Hz, 1H), 5.18 (d, *J* = 2.5 Hz, 1H), 4.59 (dd, *J* = 8.0, 2.5 Hz, 1H), 4.49 (t, *J* = 8.5 Hz, 1H), 4.30 (dd, *J* = 5.0, 2.5 Hz, 1H), 4.22 – 4.15 (m, 2H), 4.07 – 4.00 (m, 1H), 3.99 – 3.93 (m, 1H), 3.92 – 3.82 (m, 1H), 3.72 – 3.66 (m, 2H), 3.46 (t, *J* = 9.0 Hz, 1H), 2.22 (ddd, *J* = 13.5, 4.5, 1.5 Hz, 1H), 1.73 – 1.61 (m, 1H), 1.53 (s, 3H), 1.43 (s, 3H), 1.31 (d, *J* = 4.5 Hz, 6H), 1.10 – 0.98 (m, 28H). **^{13}C NMR** (125 MHz, $CDCl_3$) δ 156.65, 109.70, 108.79, 96.48, 79.42, 78.96, 71.58, 71.49, 70.88, 70.65, 67.39, 67.02, 66.80, 54.04, 38.04, 26.11, 26.08, 25.15, 24.66, 17.72, 17.68, 17.52, 17.43, 17.40, 17.35, 17.34, 17.32, 13.08, 12.89, 12.38, 12.27. **ESI-HRMS**: Calculated for $C_{31}H_{56}NO_{11}Si_2$ $(M+H)^+$: 674.3386, Found: 674.3396. $[\alpha]_D^{20}$ = +9.3 (c = 1.3, $CHCl_3$).

(5a*R*,7*R*,178a*R*,11b*R*)-2,2,4,4-tetraisopropyl-7-(((2*R*,3*R*,4*S*,5*R*,6*S*)-3,4,5,6-tetramethoxytetrahydro-2*H*-pyran-2-yl)methoxy)hexahydro-9*H*-oxazolo[3,4-*a*][1,3,5,2,4]trioxadisilepino[6,7-*c*]pyridin-9-one (80d)

The title product compound is prepared according to general procedure **A1** with iminoglycal **78a** (0.2 mmol, 1.0 equiv), 2 mol% catalyst **J**, dry CH_2Cl_2 (0.8 mL) and acceptor at room temperature for 2 h and isolated by flash column chromatography (5:1 Pentane: Ethyl Acetate) giving **80d** as a colorless oil (102 mg, 79% yield, α/β ratio > 20:1).

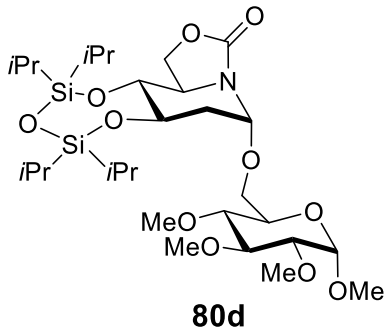

80d

^{1}H NMR (500 MHz, $CDCl_3$) δ 5.22 (d, *J* = 2.5 Hz, 1H), 4.79 (d, *J* = 3.5 Hz, 1H), 4.50 (t, *J* = 9.0 Hz, 1H), 4.20 (dd, *J* = 9.0, 6.0 Hz, 1H), 4.08 – 3.99 (m, 1H), 3.76 (td, *J* = 8.5, 6.0 Hz, 1H), 3.70 – 3.65 (m, 1H), 3.64 – 3.58 (m, 5H), 3.54 – 3.45 (m, 8H), 3.37 (s, 3H), 3.17 (dd, *J* = 9.5, 3.5 Hz, 1H), 3.02 (t, *J* = 9.5 Hz, 1H), 2.25 (ddd, *J* = 13.0, 5.0, 1.5 Hz, 1H), 1.68 (ddd, *J* = 14.0, 11.5, 4.0 Hz, 1H), 1.11 – 0.94 (m, 28H). **^{13}C NMR** (125 MHz, $CDCl_3$) δ 156.54, 97.34, 83.78, 81.99, 80.07, 79.75, 78.82, 71.44, 69.81, 66.85, 66.72, 61.04, 60.60, 59.13, 55.01, 54.36, 37.90, 17.70, 17.60, 17.48, 17.39, 17.33, 17.32, 17.31, 17.29, 13.05, 12.94, 12.35, 12.16. **ESI-HRMS**: Calculated for $C_{29}H_{56}NO_{11}Si_2$ $(M+H)^+$: 650.3386, Found: 674.3399. $[\alpha]_D^{20}$ = +90.8 (c = 1.0, $CHCl_3$).

(2*S*,3*R*,4*S*,5*R*,6*R*)-2-methoxy-6-((((5a*R*,7*R*,178a*R*,11b*R*)-2,2,4,4-tetraisopropyl-9-oxohexahydro-9*H*-oxazolo[3,4-*a*][1,3,5,2,4]trioxadisilepino[6,7-*c*]pyridin-7-yl)oxy)methyl)tetrahydro-2*H*-pyran-3,4,5-triyl tribenzoate (80e)

The title product compound is prepared according to general procedure **A1** with iminoglycal **78a** (0.2 mmol, 1.0 equiv), 2 mol% catalyst **J**, dry CH_2Cl_2 (0.8 mL) and acceptor at room temperature for 2 h and isolated by flash column chromatography (3:1 Pentane: Ethyl Acetate) giving **80e** as a white solid (149 mg, 81% yield, α/β ratio > 20:1).

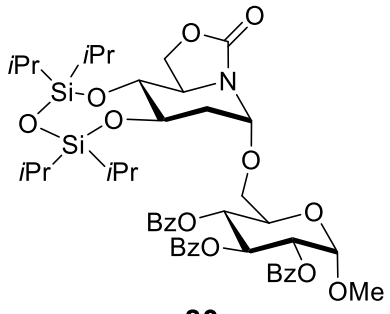

80e

^{1}H NMR (500 MHz, $CDCl_3$) δ 7.98 (dd, *J* = 8.5, 1.5 Hz, 2H), 7.94 (dd, *J* = 8.5, 1.0 Hz, 2H), 7.87 (dd, *J* = 8.5, 1.0 Hz, 2H), 7.55 – 7.48 (m, 2H), 7.46 – 7.35 (m, 5H), 7.30 (t, *J* = 7.5 Hz, 2H), 6.11 (t, *J* = 9.5 Hz, 1H), 5.63 (t, *J* = 10.0 Hz, 1H), 5.26 – 5.21 (m, 2H), 5.18 (d, *J* = 2.5 Hz, 1H), 4.25 – 4.04 (m, 4H), 3.66 (d, *J* = 3.5 Hz, 2H), 3.62 (td, *J* = 8.0, 5.5 Hz, 1H), 3.46 (s, 3H), 3.42 (t, *J* = 9.0 Hz, 1H), 2.31 – 2.25 (m, 1H), 1.68 (ddd, *J* = 14.5, 11.5, 4.0 Hz, 1H), 1.22 – 0.93 (m, 28H). **^{13}C NMR** (125 MHz, $CDCl_3$)

δ 166.04, 165.91, 165.04, 156.57, 133.58, 133.54, 133.21, 130.09, 129.93, 129.85, 129.43, 129.17, 129.11, 128.65, 128.57, 128.38, 97.15, 80.03, 78.72, 72.32, 71.09, 70.75, 68.94, 68.31, 66.58, 65.79, 55.60, 54.15, 37.84, 17.75, 17.70, 17.52, 17.44, 17.42, 17.41, 17.36, 13.06, 12.92, 12.39, 12.28. **ESI-HRMS**: Calculated for $C_{47}H_{62}NO_{14}Si_2$ $(M+H)^+$: 920.3703, Found: 920.3724. $[\alpha]_D^{20}$ = +55.3 (c = 2.0, $CHCl_3$).

(5a*R*,7*R*,178a*R*,11b*R*)-2,2,4,4-tetraisopropyl-7-(((80a*S*,5a*R*,8a*R*,8b*S*)-2,2,7,7-tetramethyltetrahydro-80a*H*-bis([1,3]dioxolo)[4,5-b:4',5'-d]pyran-80a-yl)methoxy)hexahydro-9*H*-oxazolo[3,4-*a*][1,3,5,2,4]trioxadisilepino[6,7-*c*]pyridin-9-one (80f)

The title product compound is prepared according to general procedure **A1** with iminoglycal **78a** (0.2 mmol, 1.0 equiv), 2 mol% catalyst **J**, dry CH_2Cl_2 (0.8 mL) and acceptor at room temperature for 1 h and isolated by flash column chromatography (3:1 Pentane: Ethyl Acetate) giving **80f** as a colorless oil (90 mg, 67% yield, α/β ratio > 20:1).

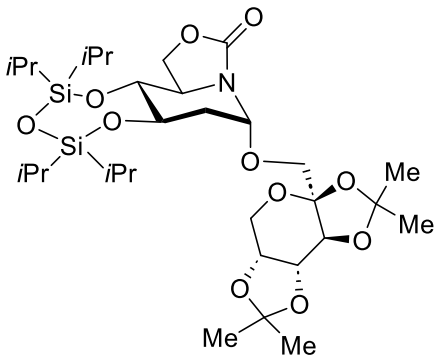

80f

^{1}H NMR (500 MHz, $CDCl_3$) δ 5.19 (d, *J* = 2.5 Hz, 1H), 4.62 (dd, *J* = 8.0, 3.0 Hz, 1H), 4.48 (t, *J* = 8.5 Hz, 1H), 4.41 (d, *J* = 2.5 Hz, 1H), 4.27 – 4.17 (m, 2H), 4.02 (ddd, *J* = 11.5, 8.0, 4.5 Hz, 1H), 3.90 (dd, *J* = 12.5, 1.5 Hz, 1H), 3.79 – 3.70 (m, 2H), 3.67 (d, *J* = 10.5 Hz, 1H), 3.55 – 3.41 (m, 1H), 2.25 (ddd, *J* = 13.5, 5.0, 1.5 Hz, 1H), 1.76 – 1.67 (m, 1H), 1.54 (s, 3H), 1.48 (s, 3H), 1.40 (s, 3H), 1.35 (s, 3H), 1.09 – 0.94 (m, 28H). **^{13}C NMR** (125 MHz, $CDCl_3$) δ 156.33, 109.35, 108.63, 102.13, 80.04, 78.58, 71.42, 71.11, 70.20, 69.91, 68.42, 66.59, 61.23, 54.07, 37.71, 26.67, 26.06, 25.81, 24.23, 17.72, 17.56, 17.52, 17.45, 17.34, 17.29, 17.27, 13.02, 12.93, 12.24, 12.10. **ESI-HRMS**: Calculated for $C_{31}H_{56}NO_{11}Si_2$ $(M+H)^+$: 674.3386, Found: 674.3396. $[\alpha]_D^{20}$ = +23.1 (c = 1.8, $CHCl_3$).

(5a*R*,7*R*,178a*R*,11b*R*)-2,2,4,4-tetraisopropyl-7-(((80a*R*,4*R*,6*R*,6a*R*)-6-methoxy-2,2-dimethyltetrahydrofuro[3,4-*d*][1,3]dioxol-4-yl)methoxy)hexahydro-9*H*-oxazolo[3,4-*a*][1,3,5,2,4]trioxadisilepino[6,7-*c*]pyridin-9-one (80g)

The title product compound is prepared according to general procedure **A1** with iminoglycal **78a** (0.2 mmol, 1.0 equiv), 2 mol% catalyst **J**, dry CH_2Cl_2 (0.8 mL) and acceptor at room temperature for 1 h

and isolated by flash column chromatography (3:1 Pentane: Ethyl Acetate) giving **80g** as a colorless oil (77 mg, 62% yield, α/β ratio > 20:1).

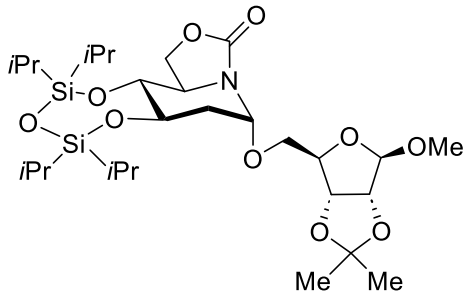

80g

^{1}H NMR (600 MHz, $CDCl_3$) δ 5.15 (d, *J* = 2.4Hz, 1H), 4.95 (s, 1H), 4.69 – 4.61 (m, 1H), 4.57 (d, *J* = 6.0 Hz, 1H), 4.48 (t, *J* = 8.4 Hz, 1H), 4.31 (ddd, *J* = 7.2, 6.0, 1.2 Hz, 1H), 4.22 (dd, *J* = 9.0, 5.6 Hz, 1H), 4.07 – 4.01 (m, 1H), 3.75 – 3.68 (m, 1H), 3.55 (dd, *J* = 10.2, 6.6 Hz, 1H), 3.46 (ddd, *J* = 9.6, 7.2, 6.6 Hz, 2H), 3.31 (s, 3H), 2.25 (ddd, *J* = 13.8, 4.8, 1.8 Hz, 1H), 1.68 (ddd, *J* = 13.8, 10.8, 3.6 Hz, 1H), 1.49 (s, 3H), 1.32(s, 3H), 1.11 – 0.98 (m, 28H). **^{13}C NMR** (150 MHz, $CDCl_3$) δ 156.43, 112.55, 109.63, 85.33, 85.01, 82.20, 80.30, 78.74, 71.34, 69.19, 66.70, 55.05, 54.39, 37.88, 26.60, 25.10, 17.73, 17.63, 17.53, 17.42, 17.37, 17.36, 17.35, 17.33, 13.07, 12.94, 12.40, 12.29. **ESI-HRMS**: Calculated for $C_{28}H_{52}NO_{10}Si_2$ $(M+H)^+$: 618.3124, Found: 618.3132. $[\alpha]_D^{20}$ = +12.1 (c = 0.7, $CHCl_3$).

(5a*R*,7*R*,178a*R*,11b*R*)-2,2,4,4-tetraisopropyl-7-(((80a*R*,4*R*,6*S*,7*S*,7a*R*)-4-methoxy-2,2,6-trimethyltetrahydro-4*H*-[1,3]dioxolo[4,5-*c*]pyran-7-yl)oxy)hexahydro-9*H*-oxazolo[3,4-*a*][1,3,5,2,4]trioxadisilepino[6,7-*c*]pyridin-9-one (80h)

The title product compound is prepared according to general procedure **A1** with iminoglycal **78a** (0.2 mmol, 1.0 equiv), 2 mol% catalyst **J**, dry CH_2Cl_2 (0.8 mL) and acceptor at room temperature for 1 h and isolated by flash column chromatography (10:1 Pentane: Ethyl Acetate) giving **80h** as a white solid (88 mg, 72% yield, α/β ratio > 20:1).

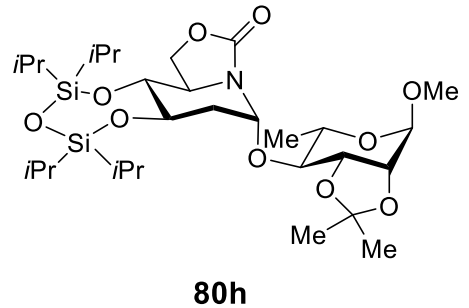

80h

^{1}H NMR (600 MHz, $CDCl_3$) δ 5.22 (dd, *J* = 4.2, 1.8 Hz, 1H), 4.84 (s, 1H), 4.43 (t, *J* = 8.4 Hz, 1H), 4.22 (dd, *J* = 9.0, 5.4 Hz, 1H), 4.10 (d, *J* = 5.4 Hz, 1H), 4.04 – 3.98 (m, 2H), 3.94 – 3.87 (m, 1H), 3.66 – 3.59 (m, 1H), 3.46 (t, *J* = 9.0 Hz, 1H), 3.36 (s, 3H), 3.23 (dd, *J* = 10.2, 7.2 Hz, 1H), 2.19 (ddd, *J* =

13.8, 5.4, 1.8 Hz, 1H), 1.67 (ddd, *J* = 13.8, 11.4, 4.2 Hz, 1H), 1.48 (s, 3H), 1.37 – 1.29 (m, 6H), 1.13 – 0.89 (m, 28H). **^{13}C NMR** (150 MHz, $CDCl_3$) δ 156.25, 109.44, 98.06, 80.49, 80.34, 78.97, 77.32, 75.99, 71.60, 66.53, 64.74, 54.99, 53.89, 38.11, 27.74, 26.48, 17.76, 17.69, 17.58, 17.47, 17.43, 17.40, 17.33, 13.03, 12.96, 12.44, 12.41. **ESI-HRMS**: Calculated for $C_{29}H_{54}NO_{10}Si_2$ $(M+H)^+$: 632.3281, Found: 632.3288. $[\alpha]_D^{20}$ = +27.8 (c = 1.3, $CHCl_3$).

(5a*R*,7*R*,178a*R*,11b*R*)-7-(((2*S*,6*S*,7*R*,8*S*)-8-(benzyloxy)-6-methoxy-2-phenylhexahydropyrano[3,2-*d*][1,3]dioxin-7-yl)oxy)-2,2,4,4-tetraisopropylhexahydro-9*H*-oxazolo[3,4-*a*][1,3,5,2,4]trioxadisilepino[6,7-c]pyridin-9-one (80i)

The title product compound is prepared according to general procedure **A1** with iminoglycal **78a** (0.2 mmol, 1.0 equiv), 2 mol% catalyst **J**, dry CH_2Cl_2 (0.8 mL) and acceptor at room temperature for 1 h and isolated by flash column chromatography (5:1 Pentane: Ethyl Acetate) giving **80i** as a white solid (97 mg, 62% yield, α/β ratio > 20:1).

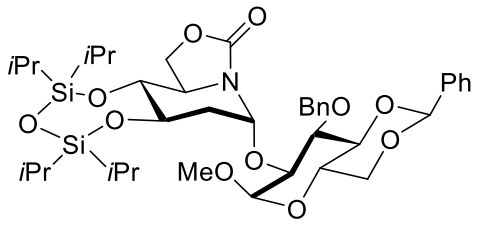

80i

^{1}H NMR (500 MHz, $CDCl_3$) δ 7.49 – 7.44 (m, 2H), 7.40 – 7.30 (m, 5H), 7.28 – 7.24 (m, 3H), 5.57 (s, 1H), 5.26 (d, *J* = 2.5 Hz, 1H), 5.02 (d, *J* = 3.5 Hz, 1H), 4.89 (d, *J* = 11.0 Hz, 1H), 4.70 (d, *J* = 10.5 Hz, 1H), 4.29 (dd, *J* = 10.0, 4.5 Hz, 1H), 4.15 – 4.07 (m, 1H), 4.06 – 4.01 (m, 2H), 3.92 (t, *J* = 9.5 Hz, 1H), 3.85 – 3.79 (m, 1H), 3.78 – 3.70 (m, 2H), 3.67 – 3.59 (m, 2H), 3.46 (s, 3H), 3.44 – 3.38 (m, 1H), 2.34 (ddd, *J* = 14.0, 5.0, 1.5 Hz, 1H), 1.72 (ddd, *J* = 13.5, 11.5, 4.0 Hz, 1H), 1.11 – 0.98 (m, 28H). **^{13}C NMR** (125 MHz, $CDCl_3$) δ 156.80, 138.43, 137.46, 129.07, 128.50, 128.37, 128.16, 127.88, 126.14, 101.42, 97.48, 82.24, 78.65, 77.36, 77.07, 75.63, 75.40, 71.58, 69.15, 66.56, 62.38, 55.47, 53.88, 37.86, 17.71, 17.70, 17.54, 17.46, 17.42, 17.38, 17.31, 13.00, 12.94, 12.34, 12.32. **ESI-HRMS**: Calculated for $C_{40}H_{60}NO_{11}Si_2$ $(M+H)^+$: 786.3699, Found: 786.3714. $[\alpha]_D^{20}$ = +46.7 (c = 1.1, $CHCl_3$).

(5a*R*,7*R*,178a*R*,11b*R*)-7-(((2*S*,6*S*,7*R*,8*S*)-7-(benzyloxy)-6-methoxy-2-phenylhexahydropyrano[3,2-*d*][1,3]dioxin-8-yl)oxy)-2,2,4,4-tetraisopropylhexahydro-9*H*-oxazolo[3,4-*a*][1,3,5,2,4]trioxadisilepino[6,7-*c*]pyridin-9-one (80j)

The title product compound is prepared according to general procedure **A1** with iminoglycal **78a** (0.2 mmol, 1.0 equiv), 2 mol% catalyst **J**, dry CH_2Cl_2 (0.8 mL) and acceptor at room temperature for 1 h

and isolated by flash column chromatography (3:1 Pentane: Ethyl Acetate) giving **80j** as a white solid (110 mg, 70% yield, α/β ratio > 20:1).

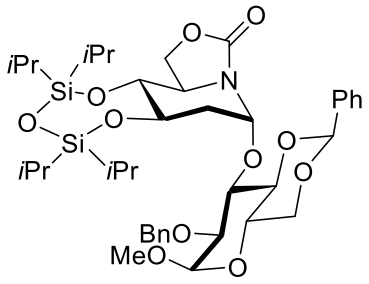

80j

^{1}H NMR (600 MHz, $CDCl_3$) δ 7.54 (d, *J* = 6.6 Hz, 1H), 7.41 – 7.30 (m, 8H), 5.60 (dd, *J* = 4.2, 1.8 Hz, 1H), 5.53 (s, 1H), 4.71 (d, *J* = 12.0 Hz, 1H), 4.64 – 4.57 (m, 2H), 4.23 (dd, *J* = 10.2, 4.8 Hz, 1H), 4.14 – 4.06 (m, 2H), 4.04 – 4.01 (m, 2H), 3.84 – 3.78 (m, 2H), 3.69 (t, *J* = 10.2 Hz, 1H), 3.57 (t, *J* = 9.6 Hz, 1H), 3.44 (dd, *J* = 9.6, 3.6 Hz, 1H), 3.41 – 3.37 (m, 4H), 2.22 (ddd, *J* = 13.8, 4.8, 1.8 Hz, 1H), 1.62 (ddd, *J* = 14.4, 12.0, 4.2 Hz, 1H), 1.15 – 0.95 (m, 28H). **^{13}C NMR** (150 MHz, $CDCl_3$) δ 156.39, 137.83, 137.33, 129.14, 128.74, 128.74, 128.44, 128.42, 128.34, 126.38, 101.68, 98.83, 82.53, 80.68, 78.49, 77.83, 74.06, 73.46, 71.63, 69.18, 66.16, 62.11, 55.38, 54.21, 38.05, 17.84, 17.69, 17.51, 17.49, 17.42, 17.38, 17.37, 17.32, 13.08, 13.02, 12.40, 12.23. **ESI-HRMS**: Calculated for $C_{40}H_{60}NO_{11}Si_2$ $(M+H)^+$: 786.3699, Found: 786.3716. $[\alpha]_D^{20}$ = +44.1 (c = 1.2, $CHCl_3$).

(2*S*,3*R*,4*S*,5*S*,6*R*)-6-((benzoyloxy)methyl)-2-methoxy-5-(((5a*R*,7*R*,178a*R*,11b*R*)-2,2,4,4-tetraisopropyl-9-oxohexahydro-9*H*-oxazolo[3,4-*a*][1,3,5,2,4]trioxadisilepino[6,7-c]pyridin-7-yl)oxy)tetrahydro-2*H*-pyran-3,4-diyl dibenzoate (80k)

The title product compound is prepared according to general procedure **A1** with iminoglycal **78a** (0.2 mmol, 1.0 equiv), 2 mol% catalyst **J**, dry CH_2Cl_2 (0.8 mL) and acceptor at room temperature for 3 h and isolated by flash column chromatography (3:1 Pentane: Ethyl Acetate) giving **80k** as a white solid (118 mg, 64% yield, α/β ratio > 20:1).

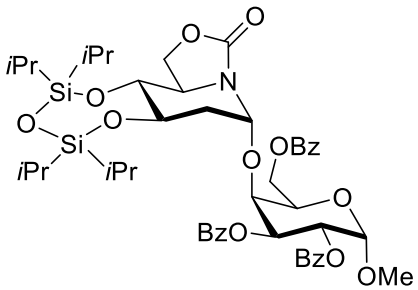

80k

^{1}H NMR (600 MHz, $CDCl_3$) δ 8.19 – 8.14 (m, 2H), 8.01 – 7.96 (m, 4H), 7.60 – 7.45 (m, 5H), 7.40 – 7.32 (m, 4H), 5.71 – 5.58 (m, 2H). 5.27 (dd, *J* = 4.8, 1.5 Hz, 1H), 5.19 (d, *J* = 3.6 Hz, 1H), 4.81 – 4.73

(m, 1H), 4.61 (d, *J* = 3.6 Hz, 1H), 4.41 – 4.34 (m, 2H), 4.19 – 4.09 (m, 1H), 3.69 – 3.58 (m, 2H), 3.44 (s, 3H), 3.27 (t, *J* = 9.0 Hz, 1H), 2.80 (t, *J* = 7.8 Hz,1H), 2.38 (ddd, *J* = 13.8, 4.8, 1.2 Hz, 1H), 1.68 (ddd, *J* = 13.2, 11.4, 4.2 Hz, 1H), 1.18 – 0.93 (m, 28H). **^{13}C NMR** (150 MHz, $CDCl_3$) δ 166.30, 166.14, 165.72, 156.31, 133.58, 133.51, 133.44, 130.11, 129.91, 129.54, 129.53, 129.45, 128.71, 128.68, 128.57, 97.64, 81.14, 78.96, 74.61, 71.09, 70.14, 68.78, 67.88, 66.40, 62.24, 55.71, 54.35, 37.90, 17.72, 17.63, 17.46, 17.44, 17.43, 17.41, 17.40, 17.32, 13.02, 12.95, 12.45, 12.42. **ESI-HRMS**: Calculated for $C_{47}H_{62}NO_{14}Si_2$ $(M+H)^+$: 920.3703, Found: 920.3724. $[\alpha]_D^{20}$ = +102.5 (c = 1.4, $CHCl_3$).

(5a*R*,7*R*,178a*R*,11b*R*)-2,2,4,4-tetraisopropyl-7-methoxyhexahydro-9*H*-oxazolo[3,4-*a*][1,3,5,2,4]trioxadisilepino[6,7-*c*]pyridin-9-one (80l)

The title product compound is prepared according to general procedure **A1** with iminoglycal **78a** (0.2 mmol, 1.0 equiv), 2 mol% catalyst **J**, dry CH_2Cl_2 (0.8 mL) and acceptor at room temperature for 70 h and isolated by flash column chromatography (20:1 Pentane: Ethyl Acetate) giving **80l** as a white solid (76 mg, 86% yield, α/β ratio > 20:1).

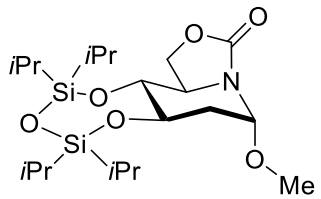

80l

^{1}H NMR (700 MHz, $CDCl_3$) δ 5.04 (dd, *J* = 4.2, 1.4 Hz, 1H), 4.50 (t, *J* = 8.4 Hz, 1H), 4.22 (dd, *J* = 9.1, 5.6 Hz, 1H), 4.01 (ddd, *J* = 11.2, 8.4, 4.9 Hz, 1H), 3.70 (ddd, *J* = 9.1, 8.4, 5.6 Hz, 1H), 3.50 – 3.44 (m, 1H), 3.31 (s, 3H), 2.20 (ddd, *J* = 14.0, 4.9, 1.4 Hz, 1H), 1.68 (ddd, *J* = 14.0, 11.2, 4.2 Hz, 1H), 1.11 – 0.94 (m, 28H). **^{13}C NMR** (175 MHz, $CDCl_3$) δ 156.65, 81.16, 78.89, 71.35, 66.72, 55.59, 54.25, 37.92, 17.73, 17.64, 17.53, 17.44, 17.35, 17.33, 13.08, 12.92, 12.35, 12.26. **ESI-HRMS**: Calculated for $C_{20}H_{40}NO_6Si_2$ $(M+H)^+$: 446.2389, Found: 446.2395. $[\alpha]_D^{20}$ = +47.9 (c = 1.0, $CHCl_3$).

(5a*R*,7*R*,178a*R*,11b*R*)-2,2,4,4-tetraisopropyl-7-(prop-2-yn-1-yloxy)hexahydro-9*H*-oxazolo[3,4-*a*][1,3,5,2,4]trioxadisilepino[6,7-c]pyridin-9-one (80m)

The title product compound is prepared according to general procedure **A1** with iminoglycal **78a** (0.2 mmol, 1.0 equiv), 2 mol% catalyst **J**, dry CH_2Cl_2 (0.8 mL) and acceptor at room temperature for 3 h and isolated by flash column chromatography (20:1 Pentane: Ethyl Acetate) giving **80m** as a white solid (66 mg, 70% yield, α/β ratio > 20:1).

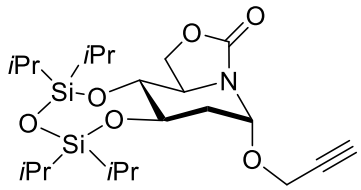

80m

^{1}H NMR (600 MHz, $CDCl_3$) δ 5.31 (dd, *J* = 4.2, 1.8 Hz, 1H), 4.48 (t, *J* = 8.4 Hz, 1H), 4.25 – 4.13 (m, 3H), 4.03 (ddd, *J* = 10.8, 8.4, 4.8 Hz, 1H), 3.77 (ddd, *J* = 9.0, 8.4, 5.4 Hz, 1H), 3.48 (t, *J* = 9.0 Hz, 1H), 2.45 (t, *J* = 2.4 Hz, 1H), 2.24 (ddd, *J* = 13.8, 4.8, 1.8 Hz, 1H), 1.72 (ddd, *J* = 13.8, 11.4, 4.2 Hz, 1H), 1.11 – 0.94 (m, 28H). **^{13}C NMR** (150 MHz, $CDCl_3$) δ 156.44, 79.76, 79.45, 78.80, 74.52, 71.29, 66.70, 55.81, 54.40, 37.90, 17.73, 17.64, 17.53, 17.43, 17.35, 17.33, 13.05, 12.92, 12.34, 12.27. **ESI-HRMS**: Calculated for $C_{22}H_{40}NO_6Si_2$ $(M+H)^+$: 470.2389, Found: 470.2388. $[\alpha]_D^{20}$ = +71.3 (c = 1.0, $CHCl_3$).

(5a*R*,7*R*,178a*R*,11b*R*)-2,2,4,4-tetraisopropyl-7-(neopentyloxy)hexahydro-9*H*-oxazolo[3,4-*a*][1,3,5,2,4]trioxadisilepino[6,7-*c*]pyridin-9-one (80n)

The title product compound is prepared according to general procedure **A1** with iminoglycal **78a** (0.2 mmol, 1.0 equiv), 2 mol% catalyst **J**, dry CH_2Cl_2 (0.8 mL) and acceptor at room temperature for 21 h and isolated by flash column chromatography (20:1 Pentane: Ethyl Acetate) giving **80n** as a white solid (90 mg, 90% yield, α/β ratio > 20:1).

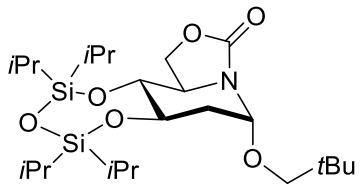

80n

^{1}H NMR (600 MHz, $CDCl_3$) δ 5.09 (dd, *J* = 3.6, 1.8 Hz, 1H), 4.48 (t, *J* = 9.0 Hz, 1H), 4.20 (dd, *J* = 9.0, 6.0 Hz, 1H), 4.06 (ddd, *J* = 11.4, 8.4, 4.8 Hz, 1H), 3.66 (td, *J* = 9.0, 5.4 Hz, 1H), 3.47 (t, *J* = 9.0 Hz, 1H), 3.17 – 3.03 (m, 2H), 2.22 (ddd, *J* = 13.8, 4.8, 1.8 Hz, 1H), 1.67 (ddd, *J* = 13.8, 11.4, 3.6 Hz, 1H), 1.13 – 0.95 (m, 28H), 0.90 (s, 9H). **^{13}C NMR** (150 MHz, $CDCl_3$) δ 156.55, 80.06, 78.93, 78.13, 71.44, 66.74, 54.65, 38.06, 31.89, 26.73, 17.71, 17.52, 17.50, 17.41, 17.37, 17.31, 17.29, 13.11, 12.94, 12.46, 12.38. **ESI-HRMS**: Calculated for $C_{24}H_{48}NO_6Si_2$ $(M+H)^+$: 502.3015, Found:502.3028. $[\alpha]_D^{20}$ = +46.5 (c = 1.0, $CHCl_3$).

(5a*R*,7*R*,178a*R*,11b*R*)-7-((4-bromobenzyl)oxy)-2,2,4,4-tetraisopropylhexahydro-9*H*-oxazolo[3,4-*a*][1,3,5,2,4]trioxadisilepino[6,7-*c*]pyridin-9-one (80o)

The title product compound is prepared according to general procedure **A1** with iminoglycal **78a** (0.2 mmol, 1.0 equiv), 2 mol% catalyst **J**, dry CH_2Cl_2 (0.8 mL) and acceptor at room temperature for 3 h

and isolated by flash column chromatography (3:1 Pentane: Ethyl Acetate) giving **80o** as a colorless oil (95 mg, 79% yield, α/β ratio > 20:1).

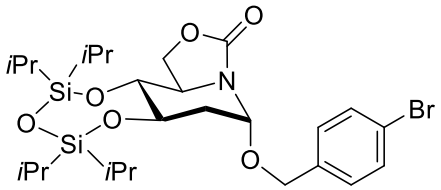

80o

^{1}H NMR (600 MHz, $CDCl_3$) δ 7.48 (d, *J* = 8.4 Hz, 1H), 7.22 (d, *J* = 8.4 Hz, 2H), 5.22 (dd, *J* = 4.2, 1.8 Hz, 1H), 4.56 – 4.36 (m, 3H), 4.20 (dd, *J* = 9.0, 5.4 Hz, 1H), 4.11 – 4.00 (m, 1H), 3.70 – 3.62 (m, 1H), 3.47 (t, *J* = 9.0 Hz, 1H), 2.23 (ddd, *J* = 13.8, 4.8, 1.8 Hz, 1H), 1.70 (ddd, *J* = 13.8, 10.8, 3.6 Hz, 1H), 1.12 – 0.93 (m, 28H). **^{13}C NMR** (150 MHz, $CDCl_3$) δ 156.48, 136.63, 131.72, 131.71, 129.50, 121.91, 79.36, 78.86, 71.39, 69.15, 66.73, 54.41, 38.04, 17.72, 17.65, 17.52, 17.42, 17.36, 17.32, 13.06, 12.94, 12.38, 12.30. **ESI-HRMS**: Calculated for $C_{26}H_{43}BrNO_6Si_2$ $(M+H)^+$: 600.1807, Found: 600.1813. $[\alpha]_D^{20}$ = +33.2 (c = 1.1, $CHCl_3$).

(5a*R*,7*R*,178a*R*,11b*R*)-7-isopropoxy-2,2,4,4-tetraisopropylhexahydro-9*H*-oxazolo[3,4-*a*][1,3,5,2,4]trioxadisilepino[6,7-*c*]pyridin-9-one (80p)

The title product compound is prepared according to general procedure **A1** with iminoglycal **78a** (0.2 mmol, 1.0 equiv), 2 mol% catalyst **J**, dry CH_2Cl_2 (0.8 mL) and acceptor at room temperature for 48 h and isolated by flash column chromatography (20:1 Pentane: Ethyl Acetate) giving **80p** as a white solid (72 mg, 76% yield, α/β ratio > 20:1).

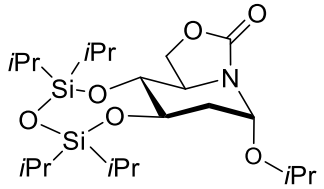

80p

^{1}H NMR (700 MHz, $CDCl_3$) δ 5.23 (dd, *J* = 4.2, 1.4 Hz, 1H), 4.46 (t, *J* = 8.4 Hz, 1H), 4.21 (dd, *J* = 9.1, 5.6 Hz, 1H), 4.04 (ddd, *J* = 11.2, 8.4, 4.9 Hz, 1H), 3.74 (p, *J* = 6.3 Hz, 1H), 3.69 (ddd, *J* = 9.8, 8.4, 5.6 Hz, 1H), 3.46 (t, *J* = 9.1 Hz, 1H), 2.13 (ddd, *J* = 13.3, 4.9, 1.4 Hz, 1H), 1.67 (ddd, *J* = 15.4, 11.2, 4.2 Hz, 1H), 1.18 (d, *J* = 6.3 Hz, 3H), 1.15 (d, *J* = 6.3 Hz, 3H), 1.10 – 0.95 (m, 28H). **^{13}C NMR** (175 MHz, $CDCl_3$) δ 156.44, 78.95, 71.48, 69.00, 66.59, 54.45, 38.53, 23.39, 21.37, 17.74, 17.63, 17.55, 17.44, 17.38, 17.34, 13.08, 12.96, 12.43, 12.36. **ESI-HRMS**: Calculated for $C_{22}H_{44}NO_6Si_2$ $(M+H)^+$: 474.2701, Found:474.2708. $[\alpha]_D^{20}$ = +56.9 (c = 1.3, $CHCl_3$).

(5a*R*,7*R*,178a*R*,11b*R*)-7-(cyclohexyloxy)-2,2,4,4-tetraisopropylhexahydro-9*H*-oxazolo[3,4-*a*][1,3,5,2,4]trioxadisilepino[6,7-*c*]pyridin-9-one (80q)

The title product compound is prepared according to general procedure **A1** with iminoglycal **78a** (0.2 mmol, 1.0 equiv), 2 mol% catalyst **J**, dry CH_2Cl_2 (0.8 mL) and acceptor at room temperature for 60 h and isolated by flash column chromatography (20:1 Pentane: Ethyl Acetate) giving **80q** as a white solid (84 mg, 82% yield, α/β ratio > 20:1).

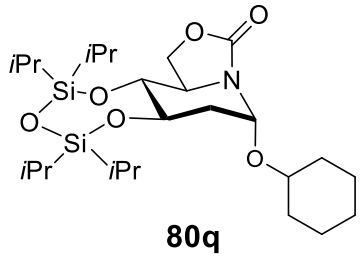

80q

^{1}H NMR (600 MHz, $CDCl_3$) δ 5.27 (d, *J* = 2.4 Hz, 1H), 4.46 (t, *J* = 8.4 Hz, 1H), 4.20 (dd, *J* = 9.0, 5.4 Hz, 1H), 4.06 (ddd, *J* = 11.4, 8.4, 4.8 Hz, 1H), 3.70 (td, *J* = 9.0, 5.4 Hz, 1H), 3.49 – 3.37 (m, 2H), 2.14 (ddd, *J* = 13.2, 4.8, 1.2 Hz, 1H), 1.93 (d, *J* = 10.2 Hz, 1H), 1.77 – 1.63 (m, 4H), 1.56 – 1.44 (m, 1H), 1.39 – 1.19 (m, 5H), 1.12 – 0.91 (m, 28H). **^{13}C NMR** (150 MHz, $CDCl_3$) δ 156.39, 78.91, 77.18, 71.47, 66.57, 54.53, 38.58, 33.44, 31.33, 25.79, 24.16, 23.89, 22.48, 17.72, 17.61, 17.53, 17.43, 17.38, 17.36, 17.33, 13.07, 12.96, 12.42, 12.34. **ESI-HRMS**: Calculated for $C_{25}H_{48}NO_6Si_2$ $(M+H)^+$: 514.3015, Found: 514.3017. $[\alpha]_D^{20}$ = +55.9 (c = 1.4, $CHCl_3$).

(5a*R*,7*R*,178a*R*,11b*R*)-7-(((1*R*,3*S*,5*R*,7*S*)-adamantan-2-yl)oxy)-2,2,4,4-tetraisopropylhexahydro-9*H*-oxazolo[3,4-*a*][1,3,5,2,4]trioxadisilepino[6,7-*c*]pyridin-9-one (80r)

The title product compound is prepared according to general procedure **A1** with iminoglycal **78a** (0.2 mmol, 1.0 equiv), 2 mol% catalyst **J**, dry CH_2Cl_2 (0.8 mL) and acceptor at room temperature for 23 h and isolated by flash column chromatography (20:1 Pentane: Ethyl Acetate) giving **80r** as a colorless oil (102 mg, 90% yield, α/β ratio > 20:1).

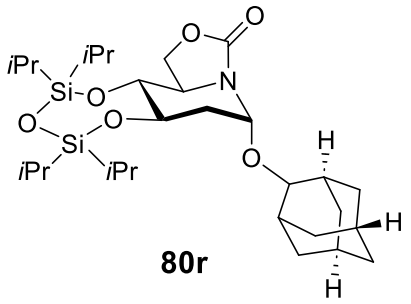

80r

^{1}H NMR (600 MHz, $CDCl_3$) δ 5.28 (dd, *J* = 3.6, 1.8 Hz, 1H), 4.46 (t, *J* = 8.4 Hz, 1H), 4.20 (dd, *J* = 9.0, 5.4 Hz, 1H), 4.16 – 4.08 (m, 1H), 3.71 (ddd, *J* = 9.0, 8.4, 5.4 Hz, 1H), 3.60 (t, *J* = 3.6 Hz, 1H), 3.47 (t, *J* = 9.0 Hz, 1H), 2.19 (ddd, *J* = 13.8, 4.8, 1.8 Hz, 1H), 2.10 (d, *J* = 3.6 Hz, 1H), 2.03 – 1.94 (m, 2H),

1.86 – 1.75 (m, 5H), 1.72 – 1.61 (m, 5H), 1.52 – 1.46 (m, 2H), 1.12 – 0.91 (m, 28H). **^{13}C NMR** (150 MHz, $CDCl_3$) δ 156.39, 79.07, 78.91, 77.22, 71.49, 66.61, 54.76, 38.72, 37.62, 36.75, 36.32, 33.64, 31.91, 31.58, 30.86, 27.56, 27.32, 17.71, 17.53, 17.51, 17.43, 17.39, 17.33, 17.30, 13.10, 12.97, 12.45, 12.36. **ESI-HRMS**: Calculated for $C_{29}H_{52}NO_6Si_2$ $(M+H)^+$: 566.3328, Found:566.3333. $[\alpha]_D^{20}$ = +44.9 (c = 3.8, $CHCl_3$).

(5a*R*,7*R*,178a*R*,11b*R*)-7-(((3*S*,5*S*,7*S*)-adamantan-1-yl)oxy)-2,2,4,4-tetraisopropylhexahydro-9*H*-oxazolo[3,4-*a*][1,3,5,2,4]trioxadisilepino[6,7-*c*]pyridin-9-one (80s)

The title product compound is prepared according to general procedure **A1** with iminoglycal **78a** (0.2 mmol, 1.0 equiv), 2 mol% catalyst **J**, dry CH_2Cl_2 (0.8 mL) and acceptor at room temperature for 24 h and isolated by flash column chromatography (3:1 Pentane: Ethyl Acetate) giving **80s** as a white solid (51 mg, 45% yield, α/β ratio > 20:1).

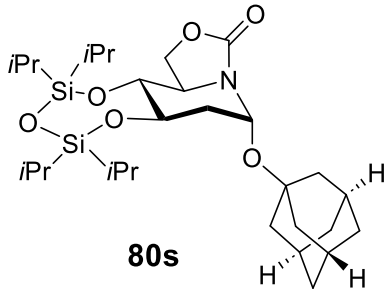

80s

^{1}H NMR (600 MHz, $CDCl_3$) δ 5.47 (dd, *J* = 3.6, 1.8 Hz, 1H), 4.40 (t, *J* = 8.4 Hz, 1H), 4.21 (dd, *J* = 9.0, 4.8 Hz, 1H), 4.10 (ddd, *J* = 10.8, 8.4, 4.2 Hz, 1H), 3.78 (td, *J* = 8.4, 4.2 Hz, 1H), 3.43 (t, *J* = 9.0 Hz, 1H), 2.13 (s, 3H), 2.00 (ddd, *J* = 13.8, 4.8, 1.8 Hz, 1H), 1.77 (q, *J* = 11.4 Hz, 6H), 1.67 – 1.57 (m, 7H), 1.12 – 0.94 (m, 28H). **^{13}C NMR** (150 MHz, $CDCl_3$) δ 155.13, 78.76, 74.40, 72.65, 71.46, 66.20, 54.64, 42.22, 40.18, 36.36, 30.69, 17.74, 17.58, 17.56, 17.45, 17.41, 17.36, 13.09, 12.99, 12.46, 12.34. **ESI-HRMS**: Calculated for $C_{29}H_{51}NO_6Si_2Na$ $(M+Na)^+$: 588.3147, Found: 588.3144. $[\alpha]_D^{20}$ = +21.5 (c = 1.0, $CHCl_3$).

(5a*R*,7*R*,178a*R*,11b*R*)-7-(((8*R*,9*S*,10*R*,13*S*,14*S*,17*S*)-10,13-dimethyl-3-oxo-2,3,6,7,8,9,10,11,12,13,14,15,16,17-tetradecahydro-1*H*-cyclopenta[a]phenanthren-17-yl)oxy)-2,2,4,4-tetraisopropylhexahydro-9*H*-oxazolo[3,4-*a*][1,3,5,2,4]trioxadisilepino[6,7-*c*]pyridin-9-one (80t)

The title product compound is prepared according to general procedure **A1** with iminoglycal **78a** (0.2 mmol, 1.0 equiv), 2 mol% catalyst **J**, dry CH_2Cl_2 (0.8 mL) and acceptor at room temperature for 23 h and isolated by flash column chromatography (3:1 Pentane: Ethyl Acetate) giving **80t** as a white solid (125 mg, 89% yield, α/β ratio > 20:1).

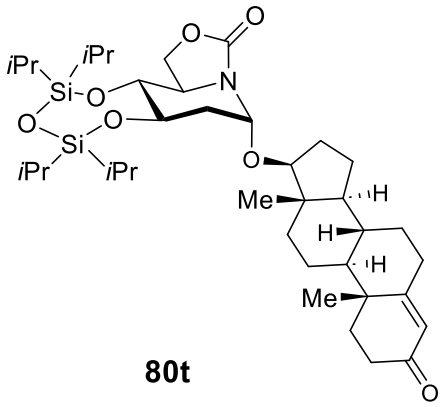

80t

^{1}H NMR (600 MHz, CD_2Cl_2) δ 5.67 – 5.62 (m, 1H), 5.10 (dd, *J* = 3.6, 1.8 Hz, 1H), 4.44 (t, *J* = 8.4 Hz, 1H), 4.17 (dd, *J* = 9.0, 6.0 Hz, 1H), 4.09 – 4.02 (m, 1H), 3.79 (d, *J* = 10.2 Hz, 1H), 3.64 (td, *J* = 9.0, 6.0 Hz, 1H), 3.47 (t, *J* = 9.0 Hz, 1H), 3.38 (t, *J* = 7.8 Hz, 1H), 2.42 – 2.33 (m, 2H), 2.28 – 2.20 (m, 2H), 2.17 – 2.07 (m, 2H), 2.03 – 1.97 (m, 1H), 1.85 – 1.79 (m, 1H), 1.78 – 1.72 (m, 1H), 1.70 – 1.60 (m, 3H), 1.59 – 1.55 (m, 2H), 1.52 – 1.39 (m, 2H), 1.38 – 1.28 (m, 1H), 1.17 (s, 3H), 1.12 – 0.98 (m, 30H), 0.78 (s, 3H). **^{13}C NMR** (150 MHz, CD_2Cl_2) δ 199.41, 171.59, 156.72, 124.20, 84.94, 79.38, 78.41, 71.90, 67.12, 54.94, 54.56, 54.40, 50.91, 42.87, 39.18, 38.70, 37.36, 36.34, 35.90, 34.51, 33.29, 32.11, 27.48, 23.92, 21.18, 17.91, 17.77, 17.71, 17.60, 17.57, 17.57, 17.54, 17.50, 13.54, 13.40, 12.90, 12.86, 11.91. **ESI-HRMS**: Calculated for $C_{38}H_{64}NO_7Si_2$ $(M+H)^+$: 702.4216, Found: 702.4228. $[\alpha]_D^{20}$ = +90.3 (c = 1.8, $CHCl_3$).

(5a*R*,7*R*,178a*R*,11b*R*)-2,2,4,4-tetraisopropyl-7-(((1*R*,2*S*,5*R*)-2-isopropyl-5-methylcyclohexyl)oxy)hexahydro-9*H*-oxazolo[3,4-*a*][1,3,5,2,4]trioxadisilepino[6,7-*c*]pyridin-9-one (80u)

The title product compound is prepared according to general procedure **A1** with iminoglycal **78a** (0.2 mmol, 1.0 equiv), 2 mol% catalyst **J**, dry CH_2Cl_2 (0.8 mL) and acceptor at room temperature for 23 h and isolated by flash column chromatography (3:1 Pentane: Ethyl Acetate) giving **80u** as a colorless oil (92 mg, 81% yield, α/β ratio > 20:1).

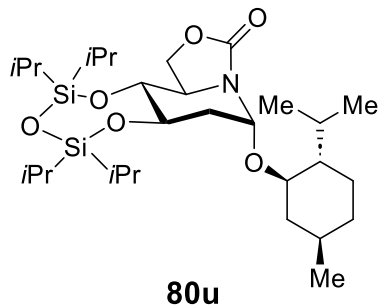

80u

^{1}H NMR (600 MHz, $CDCl_3$) δ 5.17 (dd, *J* = 4.2, 1.8 Hz, 1H), 4.46 (t, *J* = 8.4 Hz, 1H), 4.19 (dd, *J* = 9.0, 6.0 Hz, 1H), 4.04 (ddd, *J* = 10.8, 8.4, 4.2 Hz, 1H), 3.77 (ddd, *J* = 9.6, 8.4, 5.4 Hz, 1H), 3.45 (t, *J* = 9.0

Hz, 1H), 3.32 (td, *J* = 10.8, 4.2 Hz, 1H), 2.19 (ddd, *J* = 13.2, 4.8, 1.8 Hz, 1H), 2.08 (td, *J* = 7.2, 3.0 Hz, 1H), 1.93 – 1.86 (m, 1H), 1.67 – 1.56 (m, 3H), 1.41 – 1.34 (m, 1H), 1.22 – 1.16 (m, 1H), 1.12 – 0.92 (m, 31H), 0.90 (dd, *J* = 13.8, 7.2 Hz, 6H), 0.82 (d, *J* = 6.6 Hz, 3H). **^{13}C NMR** (150 MHz, $CDCl_3$) δ 155.95, 80.64, 80.12, 78.91, 71.50, 66.52, 54.68, 48.88, 42.64, 38.56, 34.45, 31.64, 26.03, 23.38, 22.46, 21.25, 17.71, 17.52, 17.44, 17.36, 17.33, 17.31, 16.55, 13.04, 12.93, 12.39, 12.30. **ESI-HRMS**: Calculated for $C_{29}H_{56}NO_6Si_2$ $(M+H)^+$: 570.3641, Found: 570.3644. $[\alpha]_D^{20}$ = +10.1 (c = 1.2, $CHCl_3$).

***tert*-butyl *N*-(((9*H*-fluoren-9-yl)methoxy)carbonyl)-*O*-((5a*R*,7*R*,178a*R*,11b*R*)-2,2,4,4-tetraisopropyl-9-oxohexahydro-9*H*-oxazolo[3,4-*a*][1,3,5,2,4]trioxadisilepino[6,7-*c*]pyridin-7-yl)-*L*-serinate (80v)**

The title product compound is prepared according to general procedure **A1** with iminoglycal **78a** (0.2 mmol, 1.0 equiv), 2 mol% catalyst **J**, dry CH_2Cl_2 (0.8 mL) and acceptor at room temperature for 4 h and isolated by flash column chromatography (3:1 Pentane: Ethyl Acetate) giving **80v** as a colorless oil (77.2 mg, 48% yield, α/β ratio > 20:1).

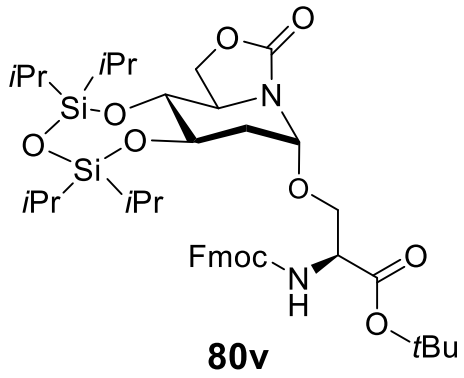

80v

^{1}H NMR (600 MHz, $CDCl_3$) δ 7.83 – 7.73 (m, 2H), 7.65 – 7.54 (m, 2H), 7.43 – 7.38 (m, 2H), 7.34 – 7.29 (m, 2H), 5.55 (d, J = 8.0 Hz, 1H), 5.18 – 5.11 (m, 1H), 4.51 – 4.39 (m, 3H), 4.34 (dd, J = 10.7, 7.3 Hz, 1H), 4.26 – 4.17 (m, 2H), 3.99 (ddd, J = 12.3, 8.3, 4.7 Hz, 1H), 3.88 (dd, J = 10.0, 3.5 Hz, 1H), 3.80 (dd, J = 10.0, 3.3 Hz, 1H), 3.67 (td, J = 8.8, 5.5 Hz, 1H), 3.45 (t, J = 8.9 Hz, 1H), 2.19 – 2.10 (m, 1H), 1.68 (ddd, J = 13.9, 11.3, 4.1 Hz, 1H), 1.49 (s, 9H), 1.12 – 0.95 (m, 28H). **^{13}C NMR** (150 MHz, $CDCl_3$) δ 169.09, 156.40, 155.92, 144.04, 143.87, 141.45, 127.89, 127.24, 127.20, 125.24, 125.19, 120.17, 120.15, 82.83, 80.62, 78.61, 71.22, 68.91, 67.36, 66.69, 54.85, 54.43, 47.27, 37.82, 28.14, 17.72, 17.59, 17.52, 17.42, 17.37, 17.31, 13.05, 12.93, 12.36, 12.32. **ESI-HRMS**: Calculated for $C_{41}H_{60}N_2O_{10}Si_2Na$ $(M+H)^+$: 819.3679, Found: 819.3679. $[\alpha]_D^{20}$ = +25.3 (c = 1.0, $CHCl_3$).

***tert*-butyl *N*-(((9*H*-fluoren-9-yl)methoxy)carbonyl)-*O*-((5a*R*,7*R*,178a*R*,11b*R*)-2,2,4,4-tetraisopropyl-9-oxohexahydro-9*H*-oxazolo[3,4-*a*][1,3,5,2,4]trioxadisilepino[6,7-*c*]pyridin-7-yl)-*L*-threoninate (80w)**

The title product compound is prepared according to general procedure **A1** with iminoglycal **78a** (0.2 mmol, 1.0 equiv), 2 mol% catalyst **J**, dry CH_2Cl_2 (0.8 mL) and acceptor at room temperature for 4 h and isolated by flash column chromatography (3:1 Pentane: Ethyl Acetate) giving **80w** as a colorless oil (73 mg, 45% yield, α/β ratio > 20:1).

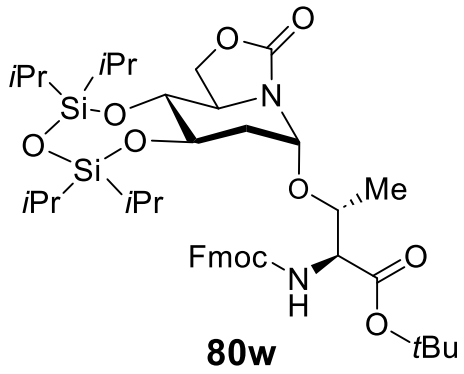

80w

^{1}H NMR (600 MHz, $CDCl_3$) δ 7.77 (dd, J = 7.6, 2.3 Hz, 2H), 7.62 (t, J = 7.0 Hz, 2H), 7.43 – 7.38 (m, 2H), 7.36 – 7.29 (m, 2H), 5.36 (d, J = 9.7 Hz, 1H), 5.21 (dd, J = 4.3, 1.6 Hz, 1H), 4.51 – 4.36 (m, 3H), 4.35 – 4.30 (m, 1H), 4.29 – 4.19 (m, 3H), 4.01 (ddd, J = 11.3, 8.4, 4.7 Hz, 1H), 3.70 (td, J = 8.8, 5.5 Hz, 1H), 3.46 (t, J = 8.9 Hz, 1H), 2.14 (ddd, J = 13.9, 4.8, 1.6 Hz, 1H), 1.63 (ddd, J = 13.8, 11.3, 4.2 Hz, 1H), 1.52 (s, 9H), 1.21 (d, J = 6.4 Hz, 3H), 1.13 – 0.98 (m, 28H). **^{13}C NMR** (150 MHz, $CDCl_3$) δ 169.57, 156.73, 156.12, 144.12, 143.89, 141.46, 127.88, 127.22, 127.18, 125.27, 120.15, 120.13, 82.88, 81.08, 78.67, 75.86, 71.27, 67.37, 66.65, 59.24, 54.56, 47.36, 38.17, 28.16, 18.87, 17.72, 17.66, 17.53, 17.40, 17.38, 17.32, 13.04, 13.01, 12.38, 12.33. **ESI-HRMS**: Calculated for $C_{41}H_{62}N_2O_{10}Si_2Na$ $(M+H)^+$: 833.3835, Found: 833.3835. $[\alpha]_D^{20}$ = +35.6 (c = 1.0, $CHCl_3$).

(5a*R*,7*R*,178a*R*,11b*R*)-7-(4-bromophenoxy)-2,2,4,4-tetraisopropylhexahydro-9*H*-oxazolo[3,4-*a*][1,3,5,2,4]trioxadisilepino[6,7-*c*]pyridin-9-one (80x)

The title product compound is prepared according to general procedure **A1** with iminoglycal **78a** (0.2 mmol, 1.0 equiv), 2 mol% catalyst **J**, dry CH_2Cl_2 (0.8 mL) and acceptor at room temperature for 4 h and isolated by flash column chromatography (3:1 Pentane: Ethyl Acetate) giving **80x** as a colorless oil (68 mg, 58% yield, α/β ratio > 20:1).

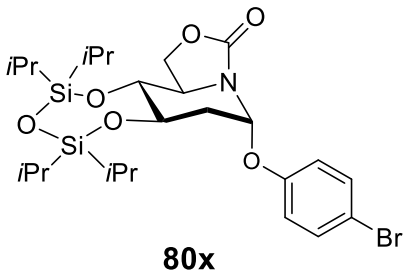

80x

^{1}H NMR (600 MHz, $CDCl_3$) δ 7.39 (d, *J* = 9.0 Hz, 2H), 6.94 (d, *J* = 9.0 Hz, 2H), 5.89 (dd, *J* = 4.2, 1.8 Hz, 1H), 4.38 (dd, *J* = 9.0, 8.4 Hz, 1H), 4.26 (dd, *J* = 9.0, 4.2 Hz, 1H), 4.19 (ddd, *J* = 11.4, 8.4, 4.8 Hz, 1H), 3.66 (ddd, *J* = 9.6, 8.4, 4.2 Hz, 1H), 3.53 (t, *J* = 9.0 Hz, 1H), 2.40 (ddd, *J* = 14.4, 4.8, 1.8 Hz, 1H), 1.84 (ddd, *J* = 14.4, 11.4, 4.2 Hz, 1H), 1.16 – 0.95 (m, 28H). **^{13}C NMR** (150 MHz, $CDCl_3$) δ 155.79, 154.68, 132.71, 117.91, 114.86, 78.18, 78.03, 71.13, 66.31, 54.53, 37.65, 17.74, 17.66, 17.54, 17.42, 17.37, 17.35, 17.32, 13.07, 12.98, 12.37, 12.27. **ESI-HRMS**: Calculated for $C_{25}H_{41}BrNO_6Si_2$ $(M+H)^+$: 586.1650, Found: 586.1655. $[\alpha]_D^{20}$ = +73.2 (c = 1.1, $CHCl_3$).

(5a*R*,7*R*,178a*R*,11b*R*)-2,2,4,4-tetraisopropyl-7-(4-methoxyphenoxy)hexahydro-9*H*-oxazolo[3,4-*a*][1,3,5,2,4]trioxadisilepino[6,7-*c*]pyridin-9-one (80y)

The title product compound is prepared according to general procedure **A1** with iminoglycal **78a** (0.2 mmol, 1.0 equiv), 2 mol% catalyst **J**, dry CH_2Cl_2 (0.8 mL) and acceptor at room temperature for 2 h and isolated by flash column chromatography (20:1 Pentane: Ethyl Acetate) giving **80y** as a colorless oil (56 mg, 52% yield, α/β ratio > 20:1).

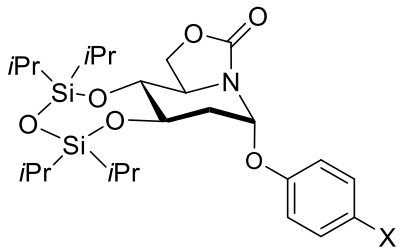

80y

^{1}H NMR (600 MHz, $CDCl_3$) δ 7.46 (d, *J* = 3.0 Hz, 1H), 7.25 (d, *J* = 4.2 Hz, 1H), 6.81 (d, *J* = 9.0 Hz, 1H), 6.70 (dd, *J* = 9.0, 3.0 Hz, 1H), 5.28 (d, *J* = 9.0 Hz, 1H), 4.57 (d, *J* = 3.0 Hz, 1H), 4.50 (t, *J* = 9.0 Hz, 1H), 4.37 (dd, *J* = 9.0, 4.8 Hz, 1H), 4.05 (ddd, *J* = 10.2, 9.0, 5.4 Hz, 1H), 3.83 – 3.78 (m, 1H), 3.73 (s, 3H), 2.61 (ddd, *J* = 15.6, 3.6, 1.2 Hz, 1H), 2.35 (ddd, *J* = 15.6, 9.0, 3.6 Hz, 1H), 1.10 – 1.05 (m, 14H), 1.02 – 0.97 (m, 14H). **^{13}C NMR** (150 MHz, $CDCl_3$) δ 159.08, 153.63, 148.58, 128.06, 117.93, 116.45, 113.09, 75.89, 68.79, 66.97, 56.09, 50.72, 46.32, 33.38, 17.76, 17.65, 17.47, 17.38, 17.28, 17.02, 14.50, 13.43, 13.07, 12.81. **ESI-HRMS**: Calculated for $C_{26}H_{44}NO_7Si_2$ $(M+H)^+$: 538.2651, Found: 538.2656. $[\alpha]_D^{20}$ = +21.4 (c = 0.2, $CHCl_3$).

(5a*R*,7*R*,178a*R*,11b*R*)-2,2,4,4-tetraisopropyl-7-(phenylthio)hexahydro-9*H*-oxazolo[3,4-*a*][1,3,5,2,4]trioxadisilepino[6,7-*c*]pyridin-9-one (80z)

The title product compound is prepared according to general procedure **A1** with iminoglycal **78a** (0.2 mmol, 1.0 equiv), 2 mol% catalyst **J**, dry CH_2Cl_2 (0.8 mL) and acceptor at room temperature for 1 h and isolated by flash column chromatography (20:1 Pentane: Ethyl Acetate) giving **80z** as a colorless oil (75 mg, 72% yield, α/β ratio > 20:1).

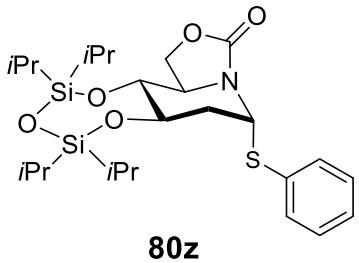

80z

^{1}H NMR (600 MHz, $CDCl_3$) δ 7.49 – 7.44 (m, 2H), 7.35 – 7.27 (m, 3H), 5.58 (dd, *J* = 6.0, 1.2 Hz, 1H), 4.39 (t, *J* = 9.0 Hz, 1H), 4.20 (dd, *J* = 9.0, 4.8 Hz, 1H), 4.13 (ddd, *J* = 11.4, 8.4, 4.2 Hz, 1H), 3.93 (td, *J* = 9.0, 4.8 Hz, 1H), 3.47 (t, *J* = 9.0 Hz, 1H), 2.25 (ddd, *J* = 14.4, 4.8, 1.2 Hz, 1H), 2.00 (ddd, *J* = 13.8, 10.8, 5.4 Hz, 1H), 1.16 – 0.94 (m, 28H). **^{13}C NMR** (150 MHz, $CDCl_3$) δ 155.59, 132.62, 132.36, 129.40, 128.31, 78.78, 72.01, 66.13, 57.98, 54.28, 37.49, 17.71, 17.67, 17.51, 17.41, 17.37, 17.36, 17.30, 13.06, 12.96, 12.35, 12.30. **ESI-HRMS**: Calculated for $C_{25}H_{42}NO_5SSi_2$ $(M+H)^+$: 524.2317, Found:524.2318. $[\alpha]_D^{20}$ = +120.1 (c = 1.0, $CHCl_3$).

(5a*R*,7*R*,178a*R*,11b*R*)-7-(butylthio)-2,2,4,4-tetraisopropylhexahydro-9*H*-oxazolo[3,4-*a*][1,3,5,2,4]trioxadisilepino[6,7-*c*]pyridin-9-one (80za)

The title product compound is prepared according to general procedure **A1** with iminoglycal **78a** (0.2 mmol, 1.0 equiv), 2 mol% catalyst **J**, dry CH_2Cl_2 (0.8 mL) and acceptor at room temperature for 1 h and isolated by flash column chromatography (20:1 Pentane: Ethyl Acetate) giving **80za** as a colorless oil (85 mg, 85% yield, α/β ratio > 20:1).

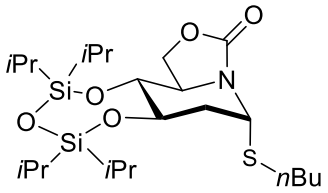

80za

^{1}H NMR (600 MHz, $CDCl_3$) δ 5.33 – 5.23 (m, 1H), 4.49 (t, *J* = 8.4 Hz, 1H), 4.23 (dd, *J* = 9.0, 5.4 Hz, 1H), 4.00 (ddd, *J* = 11.4, 8.4, 4.8 Hz, 1H), 3.92 (td, *J* = 9.0, 5.4 Hz, 1H), 3.44 (t, *J* = 9.0 Hz, 1H), 2.63 (ddd, *J* = 12.6, 8.4, 6.0 Hz, 1H), 2.49 (ddd, *J* = 13.2, 8.4, 6.6 Hz, 1H), 2.13 (ddd, *J* = 13.8, 4.8, 1.2 Hz, 1H), 1.96 (ddd, *J* = 14.4, 11.4, 6.0 Hz, 1H), 1.65 – 1.54 (m, 2H), 1.44 – 1.35 (m, 2H), 1.12 – 0.93 (m, 28H), 0.91 (t, *J* = 7.2 Hz, 3H). **^{13}C NMR** (150 MHz, $CDCl_3$) δ 156.22, 79.15, 72.12, 66.48, 55.01, 53.92, 38.03, 31.62, 31.06, 22.09, 17.72, 17.61, 17.51, 17.40, 17.36, 17.33, 17.30, 13.75, 13.06, 12.93, 12.35, 12.28. **ESI-HRMS**: Calculated for $C_{23}H_{46}NO_5SSi_2$ $(M+H)^+$: 504.2630, Found: 504.2631. $[\alpha]_D^{20}$ = +81.8 (c = 1.4, $CHCl_3$).

(5*R*,7*R*,8*R*,8a*R*)-7,8-bis(benzyloxy)-5-(octyloxy)hexahydro-3*H*-oxazolo[3,4-*a*]pyridin-3-one (80zb)

The title product compound is prepared according to general procedure **A1** with iminoglycal **78b** (0.2 mmol, 1.0 equiv), 2 mol% catalyst **J**, dry CH_2Cl_2 (0.8 mL) and acceptor at room temperature for 24 h and isolated by flash column chromatography (3:1 Pentane: Ethyl Acetate) giving **80zb** as a white solid (82 mg, 85% yield, α/β ratio > 20:1).

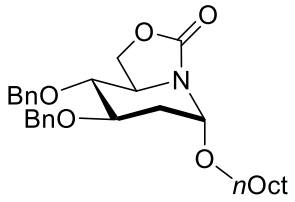

80zb

^{1}H NMR (700 MHz, $CDCl_3$) δ 7.37 – 7.34 (m, 6H), 7.33 – 7.30 (m, 2H), 7.29 – 7.27 (m, 2H), 5.13 (dd, *J* = 4.2, 2.1 Hz, 1H), 4.97 (d, *J* = 11.9 Hz, 1H), 4.71 (d, *J* = 11.9 Hz, 1H), 4.65 (dd, *J* = 11.9, 7.7 Hz, 2H), 4.36 (t, *J* = 8.4 Hz, 1H), 3.98 (ddd, *J* = 11.9, 9.1, 4.9 Hz, 1H), 3.82 (dd, *J* = 9.1, 6.3 Hz, 1H), 3.75 (ddd, *J* = 9.8, 8.4, 6.3 Hz, 1H), 3.46 – 3.37 (m, 2H), 3.32 (t, *J* = 9.1 Hz, 1H), 2.38 (ddd, *J* = 13.3, 4.9, 2.1 Hz, 1H), 1.62 (ddd, *J* = 13.3, 11.2, 3.5 Hz, 1H), 1.56 – 1.51 (m, 2H), 1.33 – 1.24 (m, 10H), 0.89 (t, *J* = 7.0 Hz, 3H). **^{13}C NMR** (175 MHz, $CDCl_3$) δ 156.47, 138.31, 138.11, 128.72, 128.60, 128.33, 128.29, 127.91, 127.84, 81.60, 79.51, 77.75, 74.92, 72.20, 68.13, 66.94, 53.20, 35.13, 31.96, 29.51, 29.49, 29.36, 26.28, 22.79, 14.24. **ESI-HRMS**: Calculated for $C_{29}H_{40}NO_5$ $(M+H)^+$: 504.2720, Found: 504.2724. $[\alpha]_D^{20}$ = +64.5 (c = 2.7, $CHCl_3$).

(5*R*,7*R*,8*R*,8a*R*)-8-(benzyloxy)-7-hydroxy-5-(octyloxy)hexahydro-3*H*-oxazolo[3,4-*a*]pyridin-3-one (80zc)

The title product compound is prepared according to general procedure **A1** with iminoglycal **78c** (0.2 mmol, 1.0 equiv), 2 mol% catalyst **J**, dry CH_2Cl_2 (0.8 mL) and acceptor at room temperature for 24 h and isolated by flash column chromatography (2:1 Pentane: Ethyl Acetate) giving **80zc** as a white solid (57 mg, 73% yield, α/β ratio > 20:1).

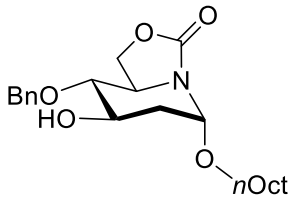

80zc

^{1}H NMR (600 MHz, $CDCl_3$) δ 7.40 – 7.36 (m, 2H), 7.36 – 7.31 (m, 3H), 5.13 (dd, *J* = 3.6, 1.8 Hz, 1H), 4.83 (d, *J* = 11.4 Hz, 1H), 4.69 (d, *J* = 12.0 Hz, 1H), 4.38 (t, *J* = 8.4 Hz, 1H), 4.17 – 4.08 (m, 1H), 3.91

(dd, *J* = 9.0, 6.6 Hz, 1H), 3.76 (ddd, *J* = 9.0, 8.4, 6.6 Hz, 1H), 3.48 – 3.36 (m, 2H), 3.21 (t, *J* = 9.0 Hz, 1H), 2.26 – 2.17 (m, 2H), 1.67 (ddd, *J* = 13.2, 12.0, 3.6 Hz, 1H), 1.55 – 1.46 (m, 2H), 1.33 – 1.19 (m, 10H), 0.88 (t, *J* = 7.2 Hz, 3H). **^{13}C NMR** (150 MHz, $CDCl_3$) δ 156.43, 137.79, 128.94, 128.57, 128.13, 83.87, 79.41, 74.76, 69.36, 68.24, 66.95, 53.32, 37.38, 31.96, 29.55, 29.49, 29.37, 26.28, 22.79, 14.24. **ESI-HRMS**: Calculated for $C_{22}H_{34}NO_5$ $(M+H)^+$: 392.2431, Found: 392.2436. $[\alpha]_D^{20}$ = +60.9 (c = 1.1, $CHCl_3$).

(5*R*,7*R*,8*R*,8a*R*)-7-hydroxy-5-(octyloxy)-3-oxohexahydro-3*H*-oxazolo[3,4-*a*]pyridin-8-yl acetate (80zd)

The title product compound is prepared according to general procedure **A1** with iminoglycal **78d** (0.2 mmol, 1.0 equiv), 2 mol% catalyst **J**, dry CH_2Cl_2 (0.8 mL) and acceptor at room temperature for 18 h and isolated by flash column chromatography (2:1 Pentane: Ethyl Acetate) giving **80zd** as a colorless oil (42 mg, 61% yield, α/β ratio > 20:1).

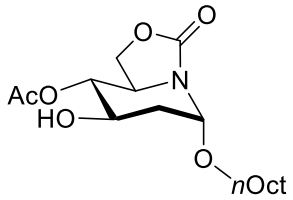

80zd

^{1}H NMR (600 MHz, $CDCl_3$) δ 5.18 (dd, *J* = 3.6, 1.8 Hz, 1H), 4.65 (t, *J* = 9.6 Hz, 1H), 4.41 (t, *J* = 9.0 Hz, 1H), 4.24 (dd, *J* = 9.0, 7.2 Hz, 1H), 4.17 – 4.08 (m, 1H), 3.85 (ddd, *J* = 9.6, 7.8, 6.6 Hz, 1H), 3.50 – 3.40 (m, 2H), 2.31 (ddd, *J* = 13.2, 4.8, 1.8 Hz, 1H), 2.15 (s, 3H), 2.13 – 2.09 (m, 1H), 1.73 (ddd, *J* = 13.2, 11.4, 3.6 Hz, 1H), 1.57 – 1.51 (m, 2H), 1.34 – 1.23 (m, 10H), 0.88 (t, *J* = 7.2 Hz, 3H). **^{13}C NMR** (150 MHz, $CDCl_3$) δ 171.33, 156.31, 79.36, 77.32, 68.44, 67.30, 66.71, 52.67, 37.64, 31.95, 29.53, 29.48, 29.37, 26.26, 22.79, 21.03, 14.24. **ESI-HRMS**: Calculated for $C_{17}H_{30}NO_6$ $(M+H)^+$: 344.2068, Found:344.2066. $[\alpha]_D^{20}$ = +14.0 (c = 0.7, $CHCl_3$).

(5*R*,7*R*,8*R*,8a*R*)-5-(octyloxy)-3-oxohexahydro-3*H*-oxazolo[3,4-*a*]pyridine-7,8-diyl diacetate (80ze)

The title product compound is prepared according to general procedure **B1** with iminoglycal **S12** (0.2 mmol, 1.0 equiv), 2 mol% catalyst **D**, dry CH_2Cl_2 (0.8 mL) and acceptor at 40 ºC for 18 h and isolated by flash column chromatography (3:1 Pentane: Ethyl Acetate) giving **80ze** as a white solid (48 mg, 62% yield, α/β ratio > 20:1).

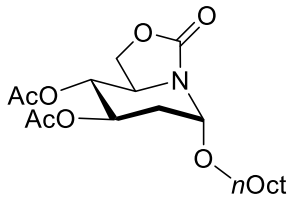

80ze

^{1}H NMR (700 MHz, $CDCl_3$) δ 5.40 – 5.32 (m, 1H), 5.18 (dd, *J* = 4.2, 2.1 Hz, 1H), 4.86 (t, *J* = 9.8 Hz, 1H), 4.41 (t, *J* = 8.4 Hz, 1H), 4.23 (dd, *J* = 9.1, 6.3 Hz, 1H), 3.92 (ddd, *J* = 9.8, 8.4, 6.3 Hz, 1H), 3.52 – 3.38 (m, 2H), 2.31 (ddd, *J* = 13.3, 4.9, 2.1 Hz, 1H), 2.07 (s, 3H), 2.03 (s, 3H), 1.77 (ddd, *J* = 13.3, 11.9, 4.2 Hz, 1H), 1.58 – 1.52 (m, 2H), 1.34 – 1.22 (m, 10H), 0.88 (t, *J* = 7.0 Hz, 3H). **^{13}C NMR** (175 MHz, $CDCl_3$) δ 170.43, 170.04, 156.14, 79.06, 73.67, 68.53, 68.50, 66.52, 52.54, 34.87, 31.95, 29.47, 29.35, 26.24, 22.78, 21.03, 20.81, 14.23. **ESI-HRMS**: Calculated for $C_{19}H_{32}NO_7$ $(M+H)^+$: 386.2173, Found: 386.2181. $[\alpha]_D^{20}$ = +28.3 (c = 1.1, $CHCl_3$).

(2*R*,3*R*,4*S*,5*R*,6*S*)-2-((((5*R*,7*R*,8*R*,8a*R*)-7,8-diacetoxy-3-oxohexahydro-3*H*-oxazolo[3,4-*a*]pyridin-5-yl)oxy)methyl)-6-methoxytetrahydro-2*H*-pyran-3,4,5-triyl tribenzoate (80zf)

The title product compound is prepared according to general procedure **B1** with iminoglycal **S12** (0.2 mmol, 1.0 equiv), 2 mol% catalyst **D**, dry CH_2Cl_2 (0.8 mL) and acceptor at 40 °C for 5 h and isolated by flash column chromatography (3:1 Pentane: Ethyl Acetate) giving **80zf** as a white solid (83 mg, 55% yield, α/β ratio > 20:1).

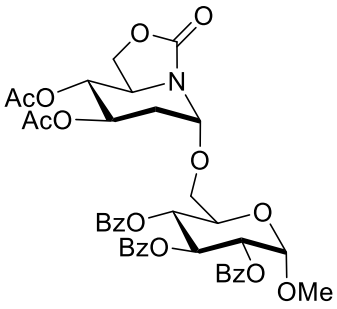

80zf

^{1}H NMR (600 MHz, $CDCl_3$) δ 7.99 – 7.86 (m, 6H), 7.55 – 7.48 (m, 2H), 7.45 – 7.35 (m, 5H), 7.32 – 7.28 (m, 2H), 6.14 (t, *J* = 9.6 Hz, 1H), 5.63 (t, *J* = 9.6 Hz, 1H), 5.39 (ddd, *J* = 11.4, 9.0, 4.8 Hz, 1H), 5.31 – 5.25 (m, 2H), 5.22 (dd, *J* = 3.6, 1.8 Hz, 2H), 4.83 (t, *J* = 9.6 Hz, 1H), 4.22 – 4.10 (m, 3H), 4.03 – 3.97 (m, 1H), 3.76 – 3.68 (m, 2H), 3.48 (s, 3H), 2.37 (ddd, *J* = 13.8, 4.8, 2.4 Hz, 1H), 2.10 (s, 3H), 2.03 (s, 3H), 1.83 (ddd, *J* = 13.2, 11.4, 4.2 Hz, 1H). **^{13}C NMR** (150 MHz, $CDCl_3$) δ 170.50, 169.88, 165.94, 165.42, 156.28, 133.68, 133.49, 133.22, 130.08, 129.90, 129.87, 129.37, 129.20, 129.00, 128.68, 128.55, 128.42, 97.19, 79.46, 73.51, 72.20, 70.66, 69.18, 68.33, 68.27, 66.55, 66.35, 55.81, 52.30, 34.44,

21.03, 20.87. **ESI-HRMS**: Calculated for $C_{39}H_{39}NO_{15}Na$ (M+Na)+: 784.2212, Found: 784.2223. $[\alpha]_D^{20}$ = +56.9 (c = 1.1, $CHCl_3$).

(5*R*,7*R*,8*R*,8a*R*)-3-oxo-5-(((2*R*,3*R*,4*S*,5*R*,6*S*)-3,4,5-tris(benzyloxy)-6-methoxytetrahydro-2*H*-pyran-2-yl)methoxy)hexahydro-3*H*-oxazolo[3,4-*a*]pyridine-7,8-diyl diacetate (80zg)

The title product compound is prepared according to general procedure **B1** with iminoglycal **S12** (0.2 mmol, 1.0 equiv), 2 mol% catalyst **D**, dry CH_2Cl_2 (0.8 mL) and acceptor at 40 °C for 4 h and isolated by flash column chromatography (3:1 Pentane: Ethyl Acetate) giving **80zg** as a colorless oil (88 mg, 61% yield, α/β ratio > 20:1).

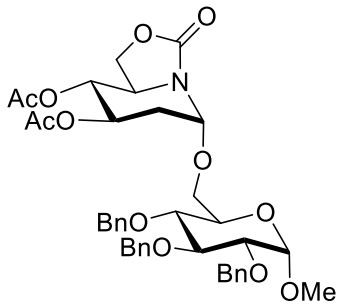

80zg

^{1}H NMR (600 MHz, $CDCl_3$) δ 7.39 – 7.36 (m, 2H), 7.36 – 7.30 (m, 9H), 7.30 – 7.26 (m, 4H), 5.29 – 5.25 (m, 1H), 5.24 (dd, *J* = 3.6, 1.8 Hz, 1H), 5.00 (dd, *J* = 11.4, 2.4 Hz, 2H), 4.82 – 4.77 (m, 3H), 4.67 (d, *J* = 12.6 Hz, 1H), 4.60 (d, *J* = 3.6 Hz, 1H), 4.13 – 3.97 (m, 3H), 3.81 – 3.75 (m, 1H), 3.74 – 3.63 (m, 3H), 3.58 – 3.46 (m, 2H), 3.39 (s, 3H), 3.34 (d, *J* = 18.0 Hz, 1H), 2.35 (ddd, *J* = 13.2, 4.8, 1.8 Hz, 1H), 2.04 (s, 3H), 2.02 (s, 3H), 1.75 (ddd, *J* = 13.2, 12.0, 4.2 Hz, 1H). **^{13}C NMR** (150 MHz, $CDCl_3$) δ 170.33, 169.88, 156.08, 138.75, 138.58, 138.27, 128.62, 128.59, 128.55, 128.25, 128.13, 128.06, 127.77, 127.74, 127.23, 98.20, 82.24, 80.25, 79.63, 77.86, 75.88, 74.87, 73.58, 73.44, 69.66, 68.27, 66.97, 66.47, 55.35, 52.35, 34.59, 21.00, 20.77. **ESI-HRMS**: Calculated for $C_{39}H_{45}NO_{12}Na$ $(M+Na)^+$: 742.2834, Found: 742.2844. $[\alpha]_D^{20}$ = +47.5 (c = 1.0, $CHCl_3$).

(5*R*,7*R*,8*R*,8a*R*)-3-oxo-5-(phenylthio)hexahydro-3*H*-oxazolo[3,4-*a*]pyridine-7,8-diyl diacetate (80zh)

The title product compound is prepared according to general procedure **B1** with iminoglycal **S12** (0.2 mmol, 1.0 equiv), 2 mol% catalyst **D**, dry CH_2Cl_2 (0.8 mL) and acceptor at 40 °C for 2 h and isolated by flash column chromatography (3:1 Pentane: Ethyl Acetate) giving **80zh** as a colorless oil (50 mg, 68% yield, α/β ratio > 20:1).

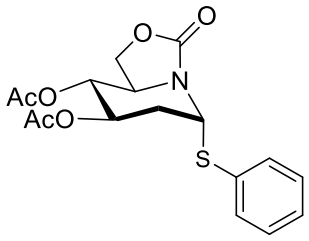

80zh

^{1}H NMR (700 MHz, $CDCl_3$) δ 7.52 – 7.46 (m, 2H), 7.38 – 7.29 (m, 3H), 5.64 – 5.56 (m, 1H), 5.44 (ddd, *J* = 11.9, 9.8, 4.9 Hz, 1H), 4.89 (t, *J* = 9.8 Hz, 1H), 4.33 (t, *J* = 8.4 Hz, 1H), 4.20 (dd, *J* = 9.1, 5.6 Hz, 1H), 4.15 (ddd, *J* = 9.8, 8.4, 5.6 Hz, 1H), 2.36 (ddd, *J* = 13.3, 4.9, 1.4 Hz, 1H), 2.09 (s, 3H), 2.08 – 2.02 (m, 4H). **^{13}C NMR** (175 MHz, $CDCl_3$) δ 170.38, 169.99, 155.16, 133.35, 131.49, 129.50, 128.79, 73.38, 68.91, 66.02, 57.45, 52.48, 34.12, 21.00, 20.83. **ESI-HRMS**: Calculated for $C_{17}H_{19}NO_6SNa$ $(M+Na)^+$: 388.0825, Found: 388.0826. $[\alpha]_D^{20}$ = +91.2 (c = 0.6, $CHCl_3$).

(5*R*,7*R*,8*R*,8a*R*)-5-((4-bromobenzyl)oxy)-3-oxohexahydro-3*H*-oxazolo[3,4-*a*]pyridine-7,8-diyl diacetate (80zi)

The title product compound is prepared according to the procedure **B1** with iminoglycal **S12** (0.2 mmol, 1.0 equiv), 2 mol% catalyst **D**, dry CH_2Cl_2 (0.8 mL) and acceptor at 40 °C for 4 h and isolated by flash column chromatography (3:1 Pentane: Ethyl Acetate) giving **80zi** as a colorless oil (45 mg, 51% yield, α/β ratio > 20:1).

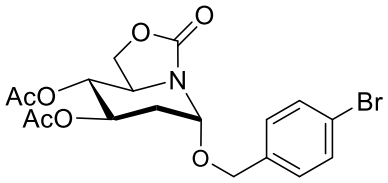

80zi

^{1}H NMR (700 MHz, $CDCl_3$) δ 7.51 – 7.45 (m, 2H), 7.23 (d, *J* = 8.4 Hz, 2H), 5.36 (ddd, *J* = 11.9, 9.8, 4.9 Hz, 1H), 5.32 – 5.27 (m, 1H), 4.87 (t, *J* = 9.8 Hz, 1H), 4.51 (s, 2H), 4.32(t, *J* = 8.4 Hz, 1H), 4.21 (dd, *J* = 9.1, 6.3 Hz, 1H), 3.83 (ddd, *J* = 9.8, 8.4, 6.3 Hz, 1H), 2.35 (ddd, *J* = 13.3, 4.9, 2.1 Hz, 1H), 2.07 (s, 3H), 2.03 (s, 3H), 1.80 (ddd, *J* = 13.3, 11.9, 4.2 Hz, 1H). **^{13}C NMR** (175 MHz, $CDCl_3$) δ 170.40, 170.03, 156.05, 136.24, 131.78, 129.63, 122.11, 78.78, 73.48, 69.55, 68.33, 66.58, 52.59, 34.79, 21.02, 20.81. **ESI-HRMS**: Calculated for $C_{18}H_{21}BrNO_7$ $(M+H)^+$: 442.0496, Found: 442.0501. $[\alpha]_D^{20}$ = +29.1 (c = 1.3, $CHCl_3$).

(2*R*,3*R*,4*S*,5*R*,6*S*)-2-((((5*R*,7*R*,8*S*,8a*R*)-7,8-bis(benzyloxy)-3-oxohexahydro-3*H*-oxazolo[3,4-*a*]pyridin-5-yl)oxy)methyl)-6-methoxytetrahydro-2*H*-pyran-3,4,5-triyl tribenzoate (82a)

The title product compound is prepared according to general procedure A with iminoglycal **81a** (0.2 mmol, 1.0 equiv), 2 mol% catalyst **J**, dry CH_2Cl_2 (0.8 mL) and acceptor at room temperature for 9 h and isolated by flash column chromatography (2:1 Pentane: Ethyl Acetate) giving **82a** as a white solid (147 mg, 86% yield, α/β ratio > 20:1).

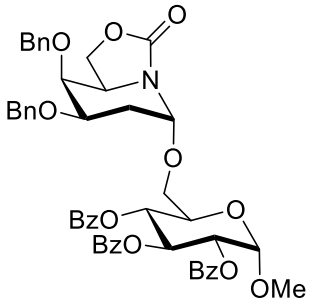

82a

^{1}H NMR (600 MHz, $CDCl_3$) δ 8.01 – 7.97 (m, 2H), 7.91 – 7.86 (m, 4H), 7.56 – 7.49 (m, 2H), 7.46 – 7.36 (m, 9H), 7.35 – 7.26 (m, 8H), 6.10 (t, *J* = 10.2 Hz, 1H), 5.66 (t, *J* = 10.2 Hz, 1H), 5.32 (dd, *J* = 10.2, 3.6 Hz, 1H), 5.27 – 5.23 (m, 2H), 5.01 (d, *J* = 12.0 Hz, 1H), 4.76 – 4.66 (m, 2H), 4.62 (d, *J* = 12.0 Hz, 1H), 4.21 – 4.16 (m, 1H), 4.07 – 3.99 (m, 2H), 3.86 – 3.81 (m, 1H), 3.75 – 3.65 (m, 4H), 3.45 (s, 3H), 2.30 – 2.18 (m, 2H). **^{13}C NMR** (150 MHz, $CDCl_3$) δ 166.03, 165.91, 165.52, 157.23, 138.33, 133.80, 133.54, 133.21, 130.09, 129.80, 129.71, 129.46, 129.18, 129.02, 128.82, 128.64, 128.57, 128.54, 128.42, 127.91, 127.86, 127.81, 127.71, 97.37, 80.62, 75.19, 73.83, 72.84, 72.01, 71.25, 70.93, 68.87, 68.19, 65.36, 63.63, 55.79, 53.38, 29.76. **ESI-HRMS**: Calculated for $C_{49}H_{48}NO_{13}$ $(M+H)^+$: 858.3120, Found: 858.3138. $[\alpha]_D^{20}$ = +37.9 (c = 1.2, $CHCl_3$).

(5R,7R,8S,8aR)-7,8-bis(benzyloxy)-5-(((2R,3R,4S,5R,6S)-3,4,5,6-tetramethoxytetrahydro-2H-pyran-2-yl)methoxy)hexahydro-3H-oxazolo[3,4-a]pyridin-3-one (82b)

The title product compound is prepared according to general procedure **A1** with iminoglycal **81a** (0.2 mmol, 1.0 equiv), 2 mol% catalyst **J**, dry CH_2Cl_2 (0.8 mL) and acceptor at room temperature for 24 h and isolated by flash column chromatography (1:3 Pentane: Ethyl Acetate) giving **82b** as a white solid (71 mg, 61% yield, α/β ratio > 20:1).

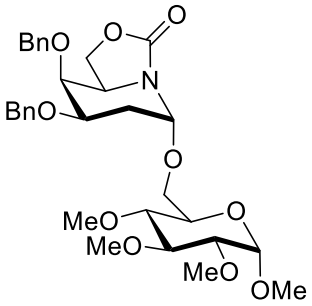

82b

^{1}H NMR (600 MHz, $CDCl_3$) δ 7.40 – 7.28 (m, 10H), 5.30 (d, *J* = 2.4 Hz, 1H), 5.03 (d, *J* = 12.0 Hz, 1H), 4.77 (d, *J* = 3.6 Hz, 1H), 4.66 (dd, *J* = 12.0, 3.6 Hz, 2H), 4.58 (d, *J* = 12.0 Hz, 1H), 4.26 – 4.16 (m, 2H), 3.95 – 3.85 (m, 2H), 3.72 (s, 1H), 3.64 – 3.61 (m, 5H), 3.53 – 3.50 (m, 4H), 3.45 (s, 3H), 3.41 (s, 1H), 3.33 (s, 3H), 3.20 – 3.15 (m, 1H), 3.05 (t, *J* = 9.0 Hz, 1H), 2.28 – 2.12 (m, 2H). **^{13}C NMR** (150 MHz, $CDCl_3$) δ 157.11, 138.23, 138.10, 128.68, 128.60, 127.98, 127.96, 127.90, 127.58, 97.41, 83.43, 82.06, 80.61, 79.44, 74.96, 73.92, 72.72, 70.90, 69.55, 66.57, 63.61, 61.01, 60.11, 59.11, 55.15, 53.64, 29.78. **ESI-HRMS**: Calculated for $C_{31}H_{42}NO_{10}$ $(M+H)^+$: 588.2803, Found: 588.2815. $[\alpha]_D^{20}$ = +104.3 (c = 0.4, $CHCl_3$).

(5*R*,7*R*,8S,8a*R*)-7,8-bis(benzyloxy)-5-(((8*R*,9*S*,10*R*,13*S*,14*S*,17*S*)-10,13-dimethyl-3-oxo-2,3,6,7,8,9,10,11,12,13,14,15,16,17-tetradecahydro-1*H*-cyclopenta[*a*]phenanthren-17-yl)oxy)hexahydro-3*H*-oxazolo[3,4-*a*]pyridin-3-one (82c)

The title product compound is prepared according to general procedure **A1** with iminoglycal **81a** (0.2 mmol, 1.0 equiv), 2 mol% catalyst **J**, dry CH_2Cl_2 (0.8 mL) and acceptor at room temperature for 24 h and isolated by flash column chromatography (3:1 Pentane: Ethyl Acetate) giving **82c** as a white solid (89 mg, 70% yield, α/β ratio > 20:1).

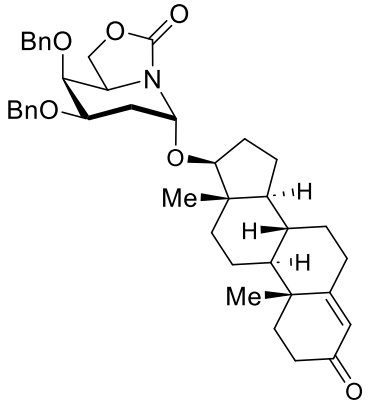

82c

^{1}H NMR (600 MHz, $CDCl_3$) δ 7.39 – 7.27 (m, 10H), 5.76 (s, 1H), 5.27 – 5.19 (m, 1H), 5.03 (d, *J* = 12.0 Hz, 1H), 4.71 – 4.57 (m, 3H), 4.25 – 4.17 (m, 2H), 3.94 – 3.83 (m, 2H), 3.72 (s, 1H), 3.37 (t, *J* = 8.4 Hz, 1H), 2.48 – 2.34 (m, 3H), 2.32 – 1.97 (m, 5H), 1.89 – 1.79 (m, 1H), 1.75 – 1.27 (m, 7H), 1.19 (d, *J* = 9.6 Hz, 3H), 1.10 – 0.88 (m, 4H), 0.78 (d, *J* = 24.0 Hz, 3H). **^{13}C NMR** (150 MHz, $CDCl_3$) δ 200.58, 172.63, 157.29, 138.25, 128.65, 128.60, 127.95, 127.94, 127.90, 127.69, 127.53, 123.88, 84.64, 78.58, 75.13, 73.90, 72.88, 70.98, 63.66, 53.98, 53.68, 50.40, 42.41, 38.84, 36.81, 35.71, 35.50, 33.88, 33.00, 31.55, 30.15, 27.17, 23.49, 20.69, 17.55, 11.85. **ESI-HRMS**: Calculated for $C_{40}H_{50}NO_6$ $(M+H)^+$: 640.3633, Found: 640.3647. $[\alpha]_D^{20}$ = +2.0 (c = 0.1, $CHCl_3$).

(5*R*,7*R*,8*S*,8a*R*)-5-(((1*R*,3*S*,5*R*,7*S*)-adamantan-2-yl)oxy)-7,8-bis(benzyloxy)hexahydro-3*H*-oxazolo[3,4-*a*]pyridin-3-one (82d)

The title product compound is prepared according to general procedure **A1** with iminoglycal **81a** (0.2 mmol, 1.0 equiv), 2 mol% catalyst **J**, dry CH_2Cl_2 (0.8 mL) and acceptor at room temperature for 24 h and isolated by flash column chromatography (1:1 Pentane: Ethyl Acetate) giving **82d** as a white solid (75 mg, 75% yield, α/β ratio > 20:1).

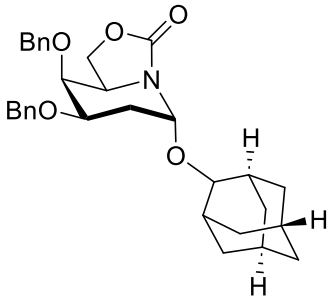

82d

^{1}H NMR (600 MHz, $CDCl_3$) δ 7.39 – 7.36 (m, 4H), 7.34 – 7.28 (m, 6H), 5.37 (d, *J* = 2.4 Hz, 1H), 5.04 (d, *J* = 12.0 Hz, 1H), 4.71 – 4.59 (m, 3H), 4.27 – 4.15 (m, 2H), 4.01 (ddd, *J* = 12.0, 4.2, 1.8 Hz, 1H), 3.97 – 3.88 (m, 1H), 3.73 (s, 1H), 3.58 (s, 1H), 2.22 (td, *J* = 12.0, 3.6 Hz, 1H), 2.13 – 2.06 (m, 2H), 2.01 – 1.94 (m, 2H), 1.85 – 1.61 (m, 9H), 1.52 – 1.42 (m, 2H). **^{13}C NMR** (150 MHz, $CDCl_3$) δ 156.92, 138.41, 138.27, 128.63, 128.57, 127.90, 127.82, 127.70, 78.83, 77.71, 75.32, 73.90, 73.24, 70.96, 63.56, 53.83, 37.64, 36.76, 36.34, 33.72, 31.96, 31.65, 30.95, 30.54, 27.59, 27.33. **ESI-HRMS**: Calculated for $C_{31}H_{37}NO_5Na$ $(M+Na)^+$: 526.2564, Found: 526.2569. $[\alpha]_D^{20}$ = +32.7 (c = 0.6, $CHCl_3$).

(5R,7R,8S,8aR)-7,8-bis(benzyloxy)-5-(phenylthio)hexahydro-3H-oxazolo[3,4-a]pyridin-3-one (82e)

The title product compound is prepared according to general procedure **A1** with iminoglycal **81a** (0.2 mmol, 1.0 equiv), 2 mol% catalyst **J**, dry CH_2Cl_2 (0.8 mL) and acceptor at room temperature for 1 h and isolated by flash column chromatography (1:1 Pentane: Ethyl Acetate) giving **82e** as a white solid (86 mg, 93% yield, α/β ratio > 20:1).

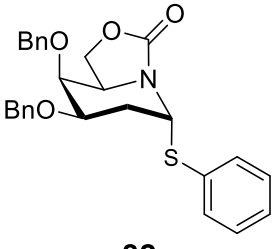

82e

^{1}H NMR (600 MHz, $CDCl_3$) δ 7.44 – 7.36 (m, 6H), 7.35 – 7.27 (m, 9H), 5.73 (d, *J* = 5.4 Hz, 1H), 5.02 (d, *J* = 12.0 Hz, 1H), 4.67 (dd, *J* = 12.0, 8.4 Hz, 2H), 4.61 (d, *J* = 12.0 Hz, 1H), 4.15 – 4.06 (m, 3H), 4.02 (ddd, *J* = 12.0, 4.2, 1.8 Hz, 1H), 3.76 (s, 1H), 2.50 (td, *J* = 12.6, 5.4 Hz, 1H), 2.10 (dd, *J* = 13.2,

4.2 Hz, 1H). **^{13}C NMR** (150 MHz, $CDCl_3$) δ 156.17, 138.16, 138.02, 132.55, 132.48, 129.33, 128.73, 128.61, 128.13, 128.05, 128.02, 127.93, 127.61, 75.90, 74.00, 73.16, 71.17, 63.38, 58.14, 53.43, 29.28. **ESI-HRMS**: Calculated for $C_{27}H_{27}NO_4SNa$ $(M+Na)^+$: 484.1553, Found: 484.1557. $[\alpha]_D^{20}$ = +93.3 (c = 1.0, $CHCl_3$).

(5*R*,7*R*,8*S*,8a*R*)-7,8-bis(benzyloxy)-5-((4-bromobenzyl)oxy)hexahydro-3*H*-oxazolo[3,4-*a*]pyridin-3-one (82f)

The title product compound is prepared according to general procedure **A1** with iminoglycal **81a** (0.2 mmol, 1.0 equiv), 2 mol% catalyst **J**, dry CH_2Cl_2 (0.8 mL) and acceptor at 40 °C for 12 h and isolated by flash column chromatography (3:1 Pentane: Ethyl Acetate) giving **82f** as a white solid (82 mg, 76% yield, α/β ratio > 20:1).

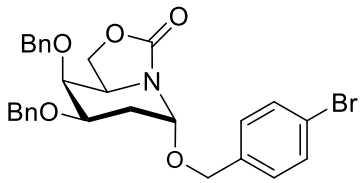

82f

^{1}H NMR (600 MHz, $CDCl_3$) δ 7.48 – 7.45 (m, 2H), 7.39 – 7.27 (m, 10H), 7.20 – 7.17 (m, 2H), 5.34 (d, *J* = 2.4 Hz, 1H), 5.02 (d, *J* = 12.0 Hz, 1H), 4.69 – 4.57 (m, 3H), 4.51 – 4.44 (m, 2H), 4.16 (dd, *J* = 8.4, 5.4 Hz, 1H), 4.11 (t, *J* = 8.4 Hz, 1H), 3.94 (ddd, *J* = 12.0, 4.2, 1.8 Hz, 1H), 3.79 (ddd, *J* = 9.0, 5.4, 2.4 Hz, 1H), 3.73 (s, 1H), 2.24 (td, *J* = 16.2, 12.0, 4.2 Hz, 1H), 2.14 (dd, *J* = 12.6, 4.2 Hz, 1H). **^{13}C NMR** (150 MHz, $CDCl_3$) δ 157.06, 138.20, 138.18, 137.01, 131.68, 129.50, 128.67, 128.60, 127.97, 127.96, 127.92, 127.54, 121.81, 80.15, 75.31, 73.91, 72.69, 71.11, 69.16, 63.61, 53.67, 29.91. **ESI-HRMS**: Calculated for $C_{28}H_{28}BrNO_5Na$ $(M+Na)^+$: 560.1043, Found: 560.1050. $[\alpha]_D^{20}$ = +4.9 (c = 1.7, $CHCl_3$).

***tert*-butyl *N*-(((9*H*-fluoren-9-yl)methoxy)carbonyl)-*O*-((5*R*,7*R*,8*S*,8a*R*)-7,8-bis(benzyloxy)-3-oxohexahydro-3*H*-oxazolo[3,4-*a*]pyridin-5-yl)-*L*-threoninate (82g)**

The title product compound is prepared according to general procedure **A1** with iminoglycal **81a** (0.1 mmol, 1.0 equiv), 2 mol% catalyst **J**, dry CH_2Cl_2 (0.4 mL) and acceptor at 40 °C for 4 h and isolated by flash column chromatography (1:1 Pentane: Ethyl Acetate) giving **82g** as a white solid (37.4 mg, 50% yield, α/β ratio > 20:1).

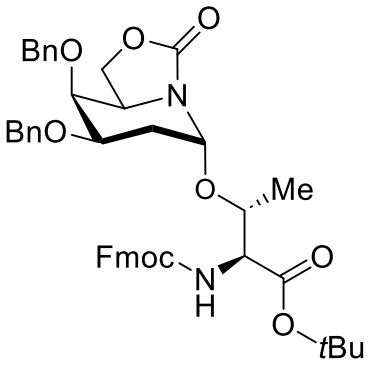

82g

^{1}H NMR (600 MHz, $CDCl_3$) δ 7.81 – 7.73 (m, 2H), 7.68 – 7.62 (m, 2H), 7.41 – 7.37 (m, 5H), 7.34 – 7.28 (m, 9H), 5.37 (d, J = 9.7 Hz, 1H), 5.33 – 5.28 (m, 1H), 5.02 (d, J = 11.9 Hz, 1H), 4.65 (dt, J = 22.6, 11.5 Hz, 3H), 4.50 – 4.40 (m, 2H), 4.32 – 4.19 (m, 5H), 3.93 – 3.86 (m, 2H), 3.75 (d, J = 2.1 Hz, 1H), 2.15 (td, J = 12.5, 4.3 Hz, 1H), 2.07 – 2.00 (m, 1H), 1.53 (s, 9H), 1.15 (d, J = 6.4 Hz, 3H). **^{13}C NMR** (150 MHz, $CDCl_3$) δ 169.62, 156.79, 156.70, 144.10, 143.92, 141.46, 138.17, 138.05, 128.68, 128.60, 128.03, 127.92, 127.90, 127.88, 127.86, 127.63, 127.22, 127.21, 125.26, 125.24, 120.15, 120.13, 82.90, 81.59, 75.44, 74.99, 73.98, 72.74, 71.06, 67.26, 63.64, 59.43, 53.71, 47.40, 29.93, 28.17, 18.86. **ESI-HRMS**: Calculated for $C_{44}H_{48}N_2O_9Na$ $(M+Na)^+$: 771.3252, Found: 771.3260. $[\alpha]_D^{20}$ = +21.6 (c = 1.0, $CHCl_3$).

(5*R*,7*R*,8*S*,8a*R*)-5-(octyloxy)-3-oxohexahydro-3*H*-oxazolo[3,4-*a*]pyridine-7,8-diyl diacetate (82h)

The title product compound is prepared according to general procedure **A1** with iminoglycal **S28** (0.2 mmol, 1.0 equiv), 2 mol% catalyst **J**, dry CH_2Cl_2 (0.8 mL) and acceptor at 40 ºC for 24 h and isolated by flash column chromatography (2:1 Pentane: Ethyl Acetate) giving **82h** as a white solid (65 mg, 85% yield, α/β ratio > 20:1).

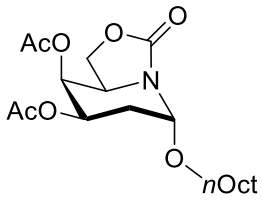

82h

^{1}H NMR (600 MHz, $CDCl_3$) δ 5.35 (s, 1H), 5.29 – 5.23 (m, 2H), 4.38 (t, *J* = 9.0 Hz, 1H), 4.17 (ddd, *J* = 9.0, 5.4, 1.8 Hz, 1H), 4.03 (dd, *J* = 9.0, 5.4 Hz, 1H), 3.49 (dt, *J* = 9.6, 7.2 Hz, 1H), 3.43 (dt, *J* = 9.6, 6.6 Hz, 1H), 2.15 (s, 3H), 2.08 (td, *J* = 13.2, 4.2 Hz, 1H), 2.01 – 1.95 (m, 4H), 1.58 – 1.51 (m, 2H), 1.34 – 1.22 (m, 10H), 0.88 (t, *J* = 7.2 Hz, 3H). **^{13}C NMR** (150 MHz, $CDCl_3$) δ 170.59, 170.20, 156.53, 79.68, 68.36, 67.10, 66.94, 63.19, 51.66, 31.96, 29.71, 29.49, 29.37, 26.29, 22.78, 20.97, 20.85, 14.23. **ESI-**

HRMS: Calculated for $C_{19}H_{32}NO_7$ $(M+H)^+$: 386.2173, Found: 386.2174. $[\alpha]_D^{20}$ = +39.8 (c = 2.2, $CHCl_3$).

(2*R*,3*R*,4*S*,5*R*,6*S*)-2-((((5*R*,7*R*,8*S*,8a*R*)-7,8-diacetoxy-3-oxohexahydro-3*H*-oxazolo[3,4-*a*]pyridin-5-yl)oxy)methyl)-6-methoxytetrahydro-2*H*-pyran-3,4,5-triyl tribenzoate (82i)

The title product compound is prepared according to general procedure **A1** with iminoglycal **S28** (0.2 mmol, 1.0 equiv), 2 mol% catalyst **J**, dry CH_2Cl_2 (0.8 mL) and acceptor at 40 °C for 24 h and isolated by flash column chromatography (1:1 Pentane: Ethyl Acetate) giving **82i** as a white solid (125 mg, 82% yield, α/β ratio > 20:1).

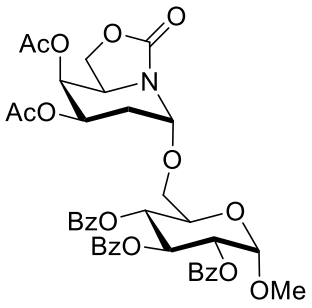

82i

^{1}H NMR (600 MHz, $CDCl_3$) δ 8.01 – 7.86 (m, 6H), 7.56 – 7.48 (m, 2H), 7.46 – 7.36 (m, 5H), 7.33 – 7.28 (m, 2H), 6.13 (t, *J* = 9.6 Hz, 1H), 5.66 (t, *J* = 9.6 Hz, 1H), 5.39 – 5.37 (m, 1H), 5.33 (ddd, *J* = 10.8, 6.0, 2.4 Hz, 1H), 5.30 – 5.24 (m, 3H), 4.27 (ddd, *J* = 9.0, 4.8, 1.8 Hz, 1H), 4.18 (dt, *J* = 10.2, 3.0 Hz, 1H), 4.09 (t, *J* = 9.6 Hz, 1H), 3.92 (dd, *J* = 9.0, 4.8 Hz, 1H), 3.76 – 3.68 (m, 2H), 3.48 (s, 3H), 2.13 (s, 3H), 2.12 – 2.07 (m, 2H), 2.02 (s, 3H). **^{13}C NMR** (150 MHz, $CDCl_3$) δ 170.56, 170.07, 165.95, 165.93, 165.49, 156.70, 133.76, 133.50, 133.25, 130.09, 129.88, 129.86, 129.34, 129.20, 128.95, 128.79, 128.55, 128.44, 97.32, 80.17, 72.14, 70.62, 69.08, 68.24, 67.12, 66.83, 66.02, 63.39, 55.89, 51.51, 29.37, 20.99, 20.83. **ESI-HRMS**: Calculated for $C_{39}H_{39}NO_{15}Na$ $(M+Na)^+$: 784.2212, Found: 784.2223. $[\alpha]_D^{20}$ = +79.0 (c = 0.7, $CHCl_3$).

(5*R*,7*R*,8*S*,8a*R*)-5-(((2*S*,6*S*,7*R*,8*S*)-7-(benzyloxy)-6-methoxy-2-phenylhexahydropyrano[3,2-*d*][1,3]dioxin-8-yl)oxy)-3-oxohexahydro-3*H*-oxazolo[3,4-*a*]pyridine-7,8-diyl diacetate (82j)

The title product compound is prepared according to general procedure **A1** with iminoglycal **S28** (0.2 mmol, 1.0 equiv), 2 mol% catalyst **J**, dry CH_2Cl_2 (0.8 mL) and acceptor at 40 °C for 15 h and isolated by flash column chromatography (2:1 Pentane: Ethyl Acetate) giving **82j** as a white solid (78 mg, 62% yield, α/β ratio > 20:1).

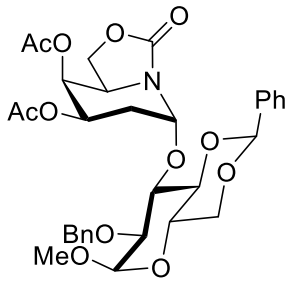

82j

^{1}H NMR (600 MHz, $CDCl_3$) δ 7.53 – 7.48 (m, 2H), 7.42 – 7.31 (m, 8H), 5.63 (t, *J* = 3.0 Hz, 1H), 5.52 (s, 1H), 5.26 (td, *J* = 9.0, 2.4 Hz, 1H), 5.08 (t, *J* = 2.4 Hz, 1H), 4.78 (d, *J* = 3.6 Hz, 1H), 4.66 (d, *J* = 10.8 Hz, 1H), 4.55 (d, *J* = 10.8 Hz, 1H), 4.25 (dd, *J* = 10.2, 4.8 Hz, 1H), 4.08 – 4.00 (m, 2H), 3.82 (td, *J* = 10.2, 4.8 Hz, 1H), 3.76 – 3.65 (m, 3H), 3.56 (t, *J* = 9.0 Hz, 1H), 3.50 (dd, *J* = 9.0, 3.6 Hz, 1H), 3.41 (s, 3H), 2.07 (s, 3H), 2.01 – 1.96 (m, 4H). **^{13}C NMR** (150 MHz, $CDCl_3$) δ 170.64, 170.20, 156.37, 137.75, 137.34, 129.19, 128.86, 128.64, 128.51, 128.45, 126.37, 101.77, 98.30, 82.27, 80.69, 78.66, 74.01, 72.93, 69.17, 67.43, 66.84, 62.92, 62.13, 55.38, 51.35, 29.70, 21.01, 20.82. **ESI-HRMS**: Calculated for $C_{32}H_{38}NO_{12}$ $(M+H)^+$: 628.2389, Found: 628.2399. $[\alpha]_D^{20}$ = +100.9 (c = 1.1, $CHCl_3$).

(2*R*,3*R*,4*S*,5*R*,6*S*)-2-((((5*R*,7*R*,8*S*,8a*R*)-8-(benzyloxy)-7-((tert-butyldimethylsilyl)oxy)-3-oxohexahydro-3*H*-oxazolo[3,4-*a*]pyridin-5-yl)oxy)methyl)-6-methoxytetrahydro-2*H*-pyran-3,4,5-triyl tribenzoate (82k)

The title product compound is prepared according to general procedure **A1** with iminoglycal **81b** (0.2 mmol, 1.0 equiv), 2 mol% catalyst **J**, dry CH_2Cl_2 (0.8 mL) and acceptor at 40 °C for 13 h and isolated by flash column chromatography (3:1 Pentane: Ethyl Acetate) giving **82k** as a white solid (128 mg, 73% yield, α/β ratio > 20:1).

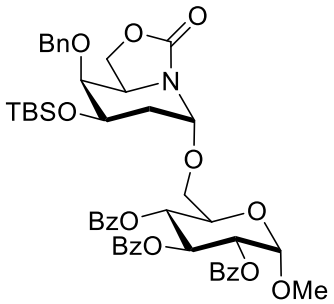

82k

^{1}H NMR (600 MHz, $CDCl_3$) δ 8.01 – 7.95 (m, 2H), 7.93 – 7.84 (m, 4H), 7.52 (q, *J* = 7.2 Hz, 2H), 7.47 – 7.36 (m, 5H), 7.35 – 7.27 (m, 7H), 6.10 (t, *J* = 9.6 Hz, 1H), 5.67 (t, *J* = 9.6 Hz, 1H), 5.30 – 5.18 (m, 3H), 5.07 (d, *J* = 12.0 Hz, 1H), 4.60 (d, *J* = 12.0 Hz, 1H), 4.35 (dd, *J* = 12.0, 2.4 Hz, 1H), 4.20 (d, *J* = 10.2 Hz, 1H), 4.04 (dd, *J* = 7.2, 4.8 Hz, 1H), 3.84 – 3.75 (m, 2H), 3.70 – 3.60 (m, 2H), 3.51 (s, 1H),

3.47 (s, 3H), 2.24 (td, *J* = 13.2, 4.2 Hz, 1H), 1.97 (dd, *J* = 13.2, 4.2 Hz, 1H), 0.99 (s, 9H), 0.22 (d, *J* = 1.2 Hz, 6H). **^{13}C NMR** (150 MHz, $CDCl_3$) δ 166.03, 165.87, 165.33, 157.17, 138.60, 133.73, 133.53, 133.19, 130.09, 129.83, 129.75, 129.48, 129.21, 129.10, 128.78, 128.57, 128.54, 128.39, 127.75, 127.67, 97.24, 80.62, 75.75, 74.29, 72.26, 70.92, 68.86, 68.31, 65.23, 63.55, 55.70, 53.35, 32.99, 26.05, 18.34, -4.55. **ESI-HRMS**: Calculated for $C_{48}H_{56}NO_{13}Si$ $(M+H)^+$: 882.3515, Found: 882.3531. $[\alpha]_D^{20}$ = +42.3 (c = 1.0, $CHCl_3$).

(2*R*,3*R*,4*S*,5*R*,6*S*)-2-((((5*R*,7*R*,8*S*,8a*R*)-8-acetoxy-7-hydroxy-3-oxohexahydro-3*H*-oxazolo[3,4-*a*]pyridin-5-yl)oxy)methyl)-6-methoxytetrahydro-2*H*-pyran-3,4,5-triyl tribenzoate (82l)

The title product compound is prepared according to general procedure **A1** with iminoglycal **81c** (0.2 mmol, 1.0 equiv), 2 mol% catalyst **J**, dry CH_2Cl_2 (0.8 mL) and acceptor at 40 °C for 12 h and isolated by flash column chromatography (1:1 Pentane: Ethyl Acetate) giving **82l** as a white solid (95 mg, 66% yield, α/β ratio > 20:1).

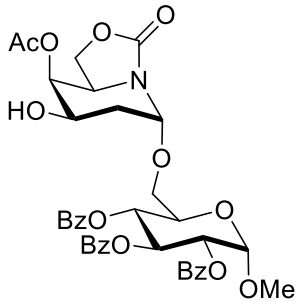

82l

^{1}H NMR (600 MHz, $CDCl_3$) δ 7.99 – 7.85 (m, 6H), 7.56 – 7.49 (m, 2H), 7.45 – 7.35 (m, 5H), 7.30 (t, *J* = 7.8 Hz, 2H), 6.12 (t, *J* = 9.6 Hz, 1H), 5.66 (t, *J* = 9.6 Hz, 1H), 5.31 – 5.22 (m, 3H), 4.33 (dd, *J* = 7.8, 4.8 Hz, 1H), 4.19 (dt, *J* = 10.2, 3.0 Hz, 1H), 4.10 – 4.01 (m, 2H), 3.96 (s, 1H), 3.71 (d, *J* = 3.0 Hz, 2H), 3.47 (s, 3H), 2.18 – 2.09 (m, 4H), 2.08 – 2.00 (m, 2H). **^{13}C NMR** (150 MHz, $CDCl_3$) δ 169.81, 165.95, 165.47, 157.10, 133.72, 133.48, 133.21, 130.09, 129.87, 129.84, 129.40, 129.23, 129.04, 128.76, 128.55, 128.42, 97.28, 80.01, 72.18, 70.78, 69.29, 69.06, 68.24, 65.95, 65.86, 63.28, 55.83, 52.33, 28.50, 21.28. **ESI-HRMS**: $C_{37}H_{38}NO_{14}$ $(M+H)^+$: 720.2287, Found: 720.2301. $[\alpha]_D^{20}$ = +26.1 (c = 1.0, $CHCl_3$).

5.2.5 X-ray crystallographic data of 80a (By Anna Krupp and Prof. Dr. Carsten Strohmann)

The crystal structure of compounds **80a** was determined using the *Bruker D8 Venture four-circle diffractometer* equipped with a *PHOTON II* CPAD detector by *Bruker AXS GmbH*. The X-ray radiation was generated by the *IμS* microfocus source Mo (□ = 0.71073 Å) from *Incoatec GmbH* equipped with HELIOS mirror optics and a single-hole collimator by *Bruker AXS GmbH*. The selected single crystal of **80a** was covered with an inert oil (perfluoropolyalkyl ether) and mounted on the *MicroMount* from

MiTeGen. The APEX 4 Suite (v.2021.10-0) software integrated with SAINT (integration) and SADABS (adsorption correction) programs by *Bruker AXS GmbH* was used for data collection. The processing and finalization of the crystal structure were performed using the Olex2 program.[111] The crystal structures were solved by the ShelXT[112] structure solution program using the Intrinsic Phasing option, which were further refined by the ShelXL[113] refinement package using Least Squares minimization. The non-hydrogen atoms were anisotropically refined. The C-bound H atoms were placed in geometrically calculated positions, and a fixed isotropic displacement parameter was assigned to each atom according to the riding-model: C–H = 0.95–1.00 Å with U_{iso}(H) = 1.5U_{eq}(CH_3) and 1.2U_{eq}(CH_2, CH) for other hydrogen atoms. The crystallographic data for the structures of **80a** has been deposited under the CCDC number 2215612 (B2720) in the Cambridge Crystallographic Data Centre. A copy of these data can be obtained for free by applying to CCDC, 12 Union Road, Cambridge CB2 IEZ, UK, fax: 144-(0)1223-336033 or e-mail: deposit@ccdc.cam.ac.uk.

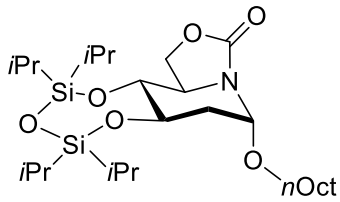

80a

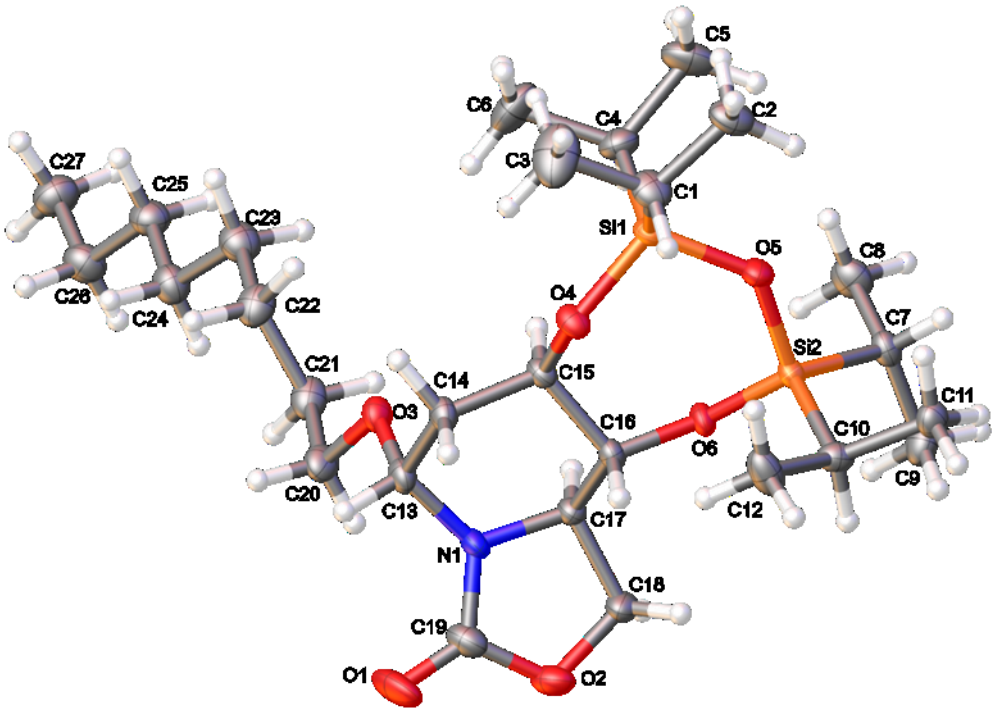

Figure 5.7. Molecular structure in the crystal of compound **80a**. The displacement ellipsoids are drawn at the 50% probability level. The asymmetric unit contains four of the shown molecules, which has been omitted for clarity. In addition, for reason of clarity, the disorder of an *n*-octyl and an *i*-propyl group was not shown.

Table 5.1. Crystallographic data of compound **80a**.

Compound	**80a**
Empirical formula	$C_{27}H_{53}NO_6Si_2$
Formula weight	543.88
Temperature/K	100.00
Crystal system	monoclinic
Space group	$P2_1$
a/Å	23.3220(12)
b/Å	7.6496(4)
c/Å	36.0472(18)
α/°	90
β/°	98.683(2)
γ/°	90
Volume/Å^3	6357.3(6)
Z	8
ρ_{calc}g/cm^3	1.137
μ/mm^{-1}	0.148
F(000)	2384.0
Crystal size/mm^3	0.605 × 0.252 × 0.115
Radiation	MoKα (λ = 0.71073)
2Θ range for data collection/°	3.612 to 61.108
Index ranges	–33 ≤ h ≤ 33, –10 ≤ k ≤ 10, –48 ≤ l ≤ 51
Reflections collected	157288
Independent reflections	38800 [R_{int} = 0.0417, R_{sigma} = 0.0413]
Data/restraints/parameters	38800/1/1372
Goodness-of-fit on F^2	1.088
Final *R* indexes [I>=2σ (I)]	R_1 = 0.0545, wR_2 = 0.1361
Final *R* indexes [all data]	R_1 = 0.0649, wR_2 = 0.1432
Largest diff. peak/hole / e Å^{-3}	0.92/–0.39
Flack parameter	–0.040(19)

5.2.6 *In-situ* and Sequential *In-situ* ^{1}H NMR monitoring experiment

5.2.6.1 *In-situ* ^{1}H NMR monitoring experiment

Procedure: To a dry NMR tube was added donor **78a** (51.7 mg, 0.125 mmol), catalyst **J** (6.2 mg, 2.0 mol%) and 0.5 mL CD_2Cl_2, then acceptor **79n** (16.5 mg, 0.1875 mmol, 1.5 equiv.), 1,1,2,2-tetrachloroethane (10.0 μL) as the internal standard were added. Afterwards, the tube was sealed with cap and measured on the NMR spectrometer at room temperature by recording ^{1}H spectra at different time.

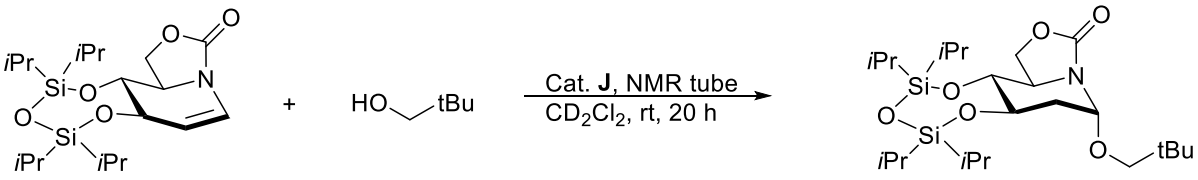

78a **79n** **80n**

Table 5.2. Temporal concentrations for **78a**, **79n**, **80n** and **83** as calculated by ^{1}H NMR integrals

Time (h)	[J]/M	[79n]/M	[80n]/M	[83]/M
0	0.25	0.375	0	0
0.13	0.222003	0.33871	0.011121	0.018225
0.25	0.201743	0.312202	0.012875	0.013566
0.5	0.195025	0.305612	0.018942	0.014359
0.75	0.188439	0.299252	0.024892	0.012705
1	0.181781	0.292816	0.030892	0.011468
1.25	0.174923	0.286254	0.036825	0.011573
1.5	0.16826	0.279745	0.042749	0.011197
1.75	0.16158	0.273433	0.048561	0.011216
2	0.155092	0.266863	0.054576	0.010097
2.25	0.148544	0.260557	0.060291	0.00993
2.5	0.142001	0.253918	0.066079	0.010142
2.75	0.135475	0.247576	0.071769	0.009096
3	0.129035	0.241245	0.077389	0.008281
3.25	0.122794	0.234904	0.082971	0.008134
3.5	0.116527	0.228676	0.088598	0.007787
3.75	0.110217	0.222442	0.09379	0.007781
4	0.104011	0.216317	0.099255	0.007864
4.25	0.098161	0.210344	0.10464	0.007852
4.5	0.092167	0.204374	0.109637	0.008394
4.75	0.086513	0.198518	0.114855	0.007624
5	0.080751	0.192818	0.119694	0.007083
5.25	0.075391	0.18731	0.124814	0.007521
5.5	0.070037	0.182007	0.12914	0.006983
5.75	0.064845	0.176571	0.13375	0.006068
6	0.059798	0.171489	0.137932	0.005794
6.25	0.055087	0.166573	0.142136	0.00715
6.5	0.050518	0.161839	0.146085	0.006971
6.75	0.046152	0.157486	0.149931	0.004558
7	0.041989	0.153182	0.153426	0.006157
7.25	0.038119	0.14922	0.156957	0.006456
7.5	0.034677	0.145306	0.160326	0.004559
7.75	0.031198	0.141929	0.163198	0.005859
8	0.027948	0.138614	0.166096	0.001736
8.25	0.025185	0.1355	0.168638	0.004832
8.5	0.022087	0.132224	0.170427	0.004682

8.75	0.019942	0.129888	0.172975	0.003571
9	0.017678	0.127506	0.174874	0.004853
9.25	0.015767	0.125269	0.17669	0.003054
9.5	0.01405	0.123287	0.178417	0.004541
9.75	0.012108	0.121173	0.179601	0.003247
10	0.010769	0.119509	0.180936	0.002015
10.25	0.00943	0.117814	0.181977	0.005072
10.5	0.008343	0.116452	0.182906	0.002811
10.75	0.007139	0.115394	0.183753	0.004406
11	0.006429	0.114352	0.184671	0.002785
11.25	0.005789	0.113732	0.185886	0.003197
11.5	0.00485	0.112988	0.186534	0.0035
11.75	0.004237	0.111411	0.186469	0.003964
12	0.003866	0.110924	0.186937	0.002821
12.25	0.003275	0.11084	0.187909	0.003351
12.5	0.003063	0.109398	0.187676	0.002768
12.75	0.002351	0.108781	0.187554	-0.00065
13	0.00236	0.108275	0.188111	0.0023
13.25	0.001998	0.107847	0.187949	0.001043
13.5	0.00182	0.107397	0.188477	0.002836
13.75	0.001567	0.107162	0.188616	0.002122
14	0.001367	0.106775	0.18866	0.002122
14.25	0.001339	0.106443	0.188851	0.00051
14.5	0.001082	0.106252	0.188857	0.002323
14.75	0.001106	0.106062	0.189084	0.001697
15	0.001037	0.10571	0.188997	0.001661
15.25	0.001087	0.105268	0.188966	0.001443
15.5	0.000176	0.105108	0.188801	0.001417
15.75	0.000801	0.104939	0.189309	0.000687
16	0.000695	0.104718	0.18914	0.001828
16.25	0.000645	0.104422	0.189239	0.000876
16.5	0.000605	0.104205	0.18915	0.001832
16.75	0.000607	0.104132	0.189136	-0.00224
17	0.000391	0.103909	0.189005	-0.00103
17.25	0.000445	0.103737	0.189095	0.001354
17.5	0.000482	0.104393	0.18994	0.002241
17.75	0.000437	0.10309	0.188937	0.001126
18	-0.00018	0.103116	0.188855	0.000461
18.25	0.000459	0.103067	0.189054	0.000867
18.5	0.000384	0.102917	0.189065	-0.00017
18.75	0.000197	0.102779	0.188959	0.000845
19	0.000419	0.102653	0.189115	0.001627
19.25	0.000467	0.102474	0.189066	-0.00297
19.5	0.000366	0.102356	0.189088	0.000155
19.75	0.000457	0.102176	0.189181	0.001367

20	0.000266	0.101866	0.188975	-1.1E-05

5.2.6.2 Sequential *in-situ* ^{1}H NMR monitoring experiment

Procedure: To a dry NMR tube was added donor **78a** (51.7 mg, 0.125 mmol, 1.0 equiv.), catalyst **J** (6.2 mg, 2.0 mol%), 0.5 mL CD_2Cl_2 and 1,1,2,2-tetrachloroethane (10.0 µL) as the internal standard were added, the tube was sealed with cap and measured on the NMR spectrometer every 5 mins at room temperature for 0.5 h, which showed around 10% intermediate **83** was formed. Afterwards, acceptor **79n** (16.5 mg, 0.1875 mmol, 1.5 equiv.) was added and the tube was sealed with cap again and measured on the NMR spectrometer under the same NMR device at room temperature by recording ^{1}H spectra every 15 mins for 20 h.

Frist step: Without **79n**

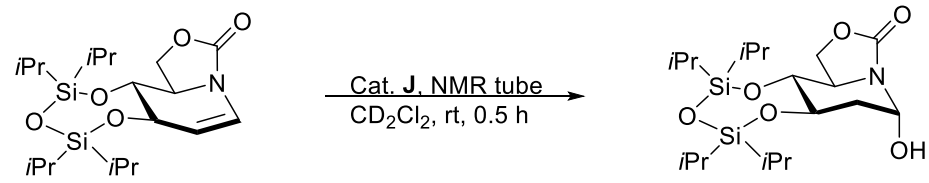

78a **83**

Second step: Add **2n** to the tube after 0.5 h

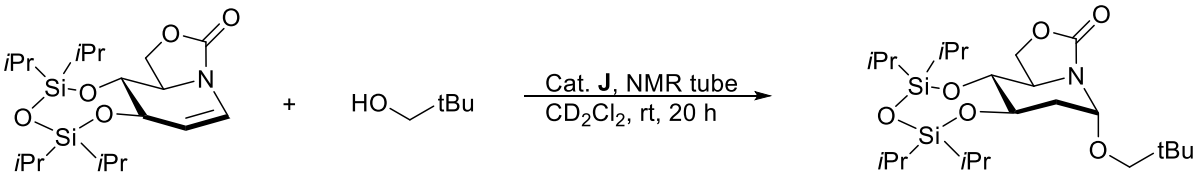

78a **79n** **80n**

Table 5.3. Temporal concentrations for **78a**, **79n**, **80n** and **83** as calculated by ^{1}H NMR integrals

Time (h)	[78a]/M	[79n]/M	[80n]/M	[83]/M
0	0.25			0
0.08	0.21793941			0.02756311
0.16	0.21784562			0.02748213
0.24	0.21792134			0.02759416
0.32	0.21789554			0.02750912
0.4	0.21789043	0.375	0	0.02748921
0.65	0.148923126	0.297826833	0.057967913	0.017086638
0.9	0.098300944	0.216415713	0.062368266	0.013724963
1.15	0.086522622	0.205676566	0.079288123	0.011475684
1.4	0.075778986	0.196847064	0.09426899	0.008799367
1.65	0.067009185	0.188856323	0.110055443	0.005757983
1.9	0.058190484	0.181494086	0.121157546	0.006238767
2.15	0.051160494	0.174916176	0.131849906	0.004434955
2.4	0.041493283	0.167094808	0.135440004	0.002869941

2.65	0.037938683	0.162236814	0.147505963	0.00288531
2.9	0.034374891	0.15775962	0.156359187	0.002576887
3.15	0.030067931	0.153783986	0.162712077	0.002754359
3.4	0.025516287	0.150433302	0.167634674	0.000976147
3.65	0.02384046	0.148066681	0.174864599	0.00112224
3.9	0.021195616	0.144531909	0.178012036	0.001587689
4.15	0.018167636	0.142261906	0.18068297	0.001336932
4.4	0.015968486	0.140772809	0.18451465	0.001128069
4.65	0.01561672	0.138867946	0.188628852	0.000579535
4.9	0.014260012	0.137152004	0.1901031	0.000699625
5.15	0.012831807	0.135518154	0.192086487	0.000428046
5.4	0.011912299	0.135023074	0.195102853	0.002760796
5.65	0.010214109	0.133401732	0.195154462	0.00156636
5.9	0.009262432	0.132176394	0.195504445	0.001485242
6.15	0.008063544	0.131418809	0.196250319	0.001296382
6.4	0.00825642	0.131438964	0.199610305	0.001111458
6.65	0.007814833	0.129650021	0.198350946	0.000935575
6.9	0.006940447	0.129711492	0.200183058	0.000345838
7.15	0.006167675	0.1284195	0.198990353	0.002301824
7.4	0.006348001	0.127677089	0.19979283	0.002239964
7.65	0.00609651	0.127533893	0.201135196	0.001763944
7.9	0.005690105	0.127970956	0.202729921	-0.00136187
8.15	0.002987097	0.126285514	0.198969478	-0.007653191
8.4	0.004708935	0.126657776	0.202474965	-0.001827931
8.65	0.004747147	0.126064947	0.202805467	-0.00113438
8.9	0.005542133	0.126015908	0.204049898	0.001576733
9.15	0.005510536	0.124936719	0.202568387	-0.004269308
9.4	0.004157725	0.125139666	0.203717253	-0.001872328
9.65	0.004826394	0.124873718	0.204245275	0.001287336
9.9	0.003934003	0.125515797	0.204930919	0.000394994
10.15	0.003971232	0.124336808	0.204103895	-0.000917184
10.4	0.003459763	0.124680354	0.204478955	-0.000629985
10.65	0.003852789	0.123649045	0.204420465	-0.002102571
10.9	0.004937404	0.122571308	0.20316993	-0.006412447
11.15	0.003844444	0.122290635	0.202215425	-0.006265259
11.4	0.003842534	0.124272807	0.206810046	0.003229138
11.65	0.003334411	0.122806231	0.204262551	-0.001924104
11.9	0.003362805	0.12256627	0.204360483	-0.001428547
12.15	0.002636117	0.122331476	0.203792182	-0.001140523
12.4	0.003844524	0.121404211	0.202956863	-0.005878159
12.65	0.003767973	0.123076023	0.206986133	0.003675357
12.9	0.0033704	0.121779711	0.204976074	-0.002769621
13.15	0.003308693	0.120505297	0.202344798	-0.006711405
13.4	0.003451952	0.119973395	0.202430591	-0.007874925
13.65	0.003485348	0.121391461	0.205177133	0.001046663

13.9	0.00433966	0.120920672	0.205448685	-0.00132465
14.15	0.00433019	0.120597074	0.204999003	0.000717506
14.4	0.004059033	0.120438163	0.205171533	-3.16399E-06
14.65	0.003951339	0.120333903	0.20538759	-0.000198203
14.9	0.003986308	0.119130416	0.202536696	-0.007330043
15.15	0.003864652	0.120807819	0.20665867	0.002855246
15.4	0.004050217	0.119701578	0.20553205	0.000201384
15.65	0.002648577	0.119694537	0.204304978	-0.002453941
15.9	0.003017574	0.119417823	0.204309325	-0.00176387
16.15	0.003279986	0.120219352	0.206690676	0.002948263
16.4	0.003826818	0.118970581	0.204720913	0.000859752
16.65	0.003252355	0.117830213	0.202501372	-0.007536952
16.9	0.003993285	0.118357075	0.204430541	-0.000614619
17.15	0.003722753	0.118281044	0.204542304	-0.001041846
17.4	0.003376266	0.117271928	0.202303405	-0.006756772
17.65	0.003150583	0.117106472	0.202107536	-0.006177869
17.9	0.002930166	0.116811393	0.202164854	-0.007392409
18.15	0.002974256	0.116859272	0.202525626	-0.00642389
18.4	0.004256673	0.116835285	0.202794394	-0.006113652
18.65	0.002284137	0.117584093	0.204087082	-0.001239555
18.9	0.003399968	0.116262791	0.202235378	-0.006901611
19.15	0.004081245	0.116177632	0.202899442	-0.006800301
19.4	0.002580039	0.117249181	0.204766303	-0.000741548
19.65	0.00293384	0.116815056	0.203938771	-0.002980937
19.9	0.00293384	0.116815056	0.203938771	-0.002980937

5.2.7 Kinetic experiments study

5.2.7.1 Kinetic experiment on the overall reaction

Donor 78a concentration dependence

Procedure: To a dry NMR tube, donor **78a** (25.9 mg, 0.0625 mmol), catalyst **J** (6.2 mg, 0.00125 mmol), acceptor **79n** (16.5 mg, 0.1875 mmol) and 1,1,2,2-tetrachloroethane (10 µL) as the internal standard, CD_2Cl_2 was added in order to reach a total volume of 500 µL. Afterwards, the tube was sealed with cap and measured on the NMR spectrometer at room temperature by recording ^1H spectra at different time.

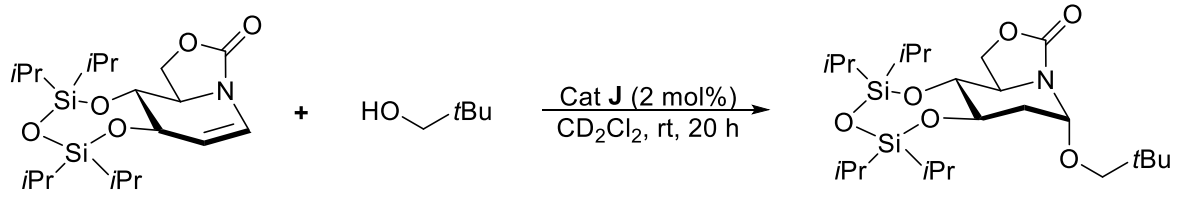

78a 0.125 M | **79n** 0.375 M | **80n**

Experimental section

Procedure: To a dry NMR tube, donor **78a** (77.5 mg, 0.1875 mmol), catalyst **J** (6.2 mg, 0.00125 mmol), acceptor **79n** (16.5 mg, 0.1875 mmol) and 1,1,2,2-tetrachloroethane (10 μL) as the internal standard, CD_2Cl_2 was added in order to reach a total volume of 500 μL. Afterwards, the tube was sealed with cap and measured on the NMR spectrometer at room temperature by recording ^1H spectra at different time.

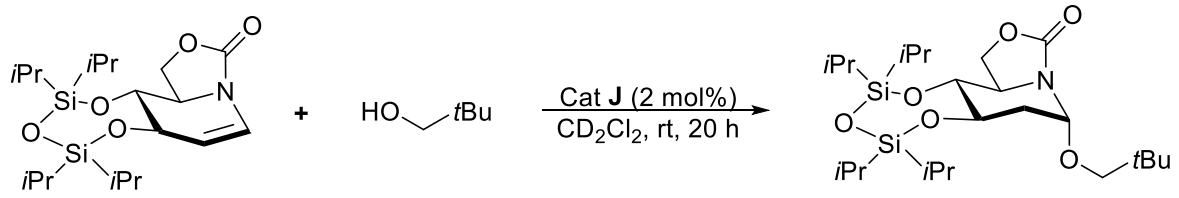

78a **79n** **80n**

0.375 M 0.375 M

Table 5.4. Concentration for **80n** calculated by ^1H NMR analysis for varying the donor concentration experiment

Time/h	**80n** (**78a** =0.125M)	**80n** (**78a** =0.25M)	**80n** (**78a** =0.375M)
0	0	0	0
0.13	0.002909406	0.007454567	0.021069363
0.25	0.010149164	0.012875205	0.023171831
0.5	0.015840583	0.018941507	0.031556055
0.75	0.02029985	0.024891528	0.040501979
1	0.023920862	0.030891828	0.048623108
1.25	0.027601678	0.036824752	0.055538261
1.5	0.030641474	0.04274904	0.062253341
1.75	0.033412465	0.04856081	0.068730045
2	0.036386294	0.054575775	0.074867064
2.25	0.038634339	0.060291205	0.082091297
2.5	0.041179689	0.06607881	0.087961816
2.75	0.043345663	0.071768692	0.093951009
3	0.045479268	0.077389176	0.099824111
3.25	0.047627703	0.08297125	0.106143558
3.5	0.049816148	0.088598229	0.111976006
3.75	0.051988124	0.093789873	0.117294418
4	0.054054629	0.099255414	0.123817375
4.25	0.055660776	0.104640102	0.129764048
4.5	0.05741323	0.109636738	0.134888006
4.75	0.059748392	0.114854794	0.14268528
5	0.061174263	0.119694249	0.147148419
5.25	0.063073216	0.124814048	0.152772039
5.5	0.064853511	0.129140135	0.15964661
5.75	0.066464179	0.1337502	0.165788557
6	0.068603803	0.137931833	0.172981086
6.25	0.069312719	0.142135686	0.179800528
6.5	0.071066116	0.146085487	0.186410551
6.75	0.072498647	0.149931012	0.193456481
7	0.074011273	0.153426106	0.200676159
7.25	0.075048858	0.156956915	0.207869907
7.5	0.076739577	0.160325716	0.216066931
7.75	0.077458949	0.163198368	0.223172909
8	0.079079808	0.166095627	0.231104333
8.25	0.080196384	0.168638359	0.239988395

8.5	0.081276736	0.170427213	0.24830506
8.75	0.082905335	0.172975252	0.256278386
9	0.083344163	0.174874224	0.267109313
9.25	0.084389511	0.176689624	0.274997077
9.5	0.085762503	0.1784175	0.285504423
9.75	0.086691244	0.179601269	0.294362329
10	0.087521961	0.180935598	0.302128248
10.25	0.088852446	0.181977271	0.304937343
10.5	0.089898659	0.182906249	0.308476897
10.75	0.090041837	0.183753131	0.312776785
11	0.090982948	0.184671471	0.312387867
11.25	0.091992109	0.185885674	0.314704127
11.5	0.092929891	0.186534338	0.3146613
11.75	0.0937166	0.186468876	0.315246297
12	0.094358651	0.186936721	0.317360276
12.25	0.094401619	0.187909208	0.317000495
12.5	0.095712394	0.187675959	0.318080497
12.75	0.0963055	0.187554157	0.318963169
13	0.096868714	0.18811096	0.318335054
13.25	0.097487619	0.187949172	0.318935312
13.5	0.097869935	0.188477014	0.319895678
13.75	0.09806173	0.188615654	0.318464586
14	0.098733714	0.188659756	0.318938582
14.25	0.099076599	0.188851015	0.318162767
14.5	0.099855852	0.18885694	0.320235391
14.75	0.100565198	0.189084114	0.319283425
15	0.100799603	0.188997165	0.321993449
15.25	0.100702247	0.188966027	0.320785123
15.5	0.101427559	0.188801099	0.320611816
15.75	0.10159461	0.189308751	0.319232094
16	0.102240913	0.189140431	0.321529059
16.25	0.102759792	0.189239049	0.31835022
16.5	0.10281612	0.189150414	0.321256931
16.75	0.103405369	0.189135781	0.320007646
17	0.103347228	0.189005221	0.319754898
17.25	0.103925784	0.189095341	0.321222753
17.5	0.103599912	0.189939579	0.320832556
17.75	0.10434133	0.188936583	0.320906597
18	0.104631937	0.188854589	0.319833848
18.25	0.104920119	0.189053772	0.32014916
18.5	0.105471876	0.189065235	0.320768351
18.75	0.105140451	0.188958698	0.320242553
19	0.105555277	0.189115007	0.321511159
19.25	0.105595836	0.189066007	0.319209773
19.5	0.10569332	0.189087778	0.319415482
19.75	0.106008594	0.189181266	0.321717576
20	0.106223531	0.188974569	0.321536953

Acceptor 79n concentration dependence

Procedure: To a dry NMR tube, donor **78a** (51.7 mg, 0.125 mmol), catalyst **J** (6.2 mg, 0.00125 mmol), acceptor **79n** (11.0 mg, 0.125 mmol) and 1,1,2,2-tetrachloroethane (10 μL) as the internal standard, CD_2Cl_2 was added in order to reach a total volume of 500 μL. Afterwards, the tube was sealed with cap and measured on the NMR spectrometer at room temperature by recording ^1H spectra at different time.

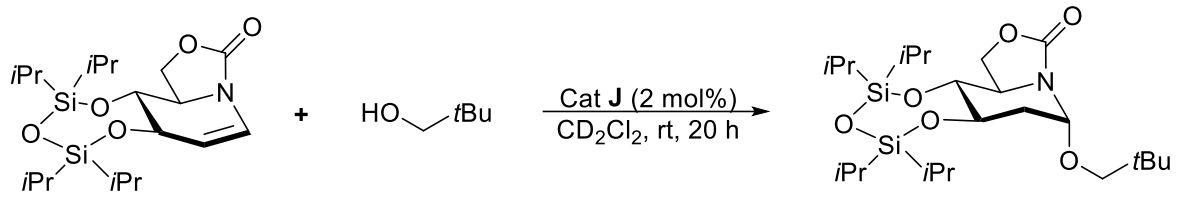

Procedure: To a dry NMR tube, donor **78a** (51.7 mg, 0.125 mmol), catalyst **J** (6.2 mg, 0.00125 mmol), acceptor **79n** (22.0 mg, 0.25 mmol) and 1,1,2,2-tetrachloroethane (10 µL) as the internal standard, CD_2Cl_2 was added in order to reach a total volume of 500 µL. Afterwards, the tube was sealed with cap and measured on the NMR spectrometer at room temperature by recording ^1H spectra at different time.

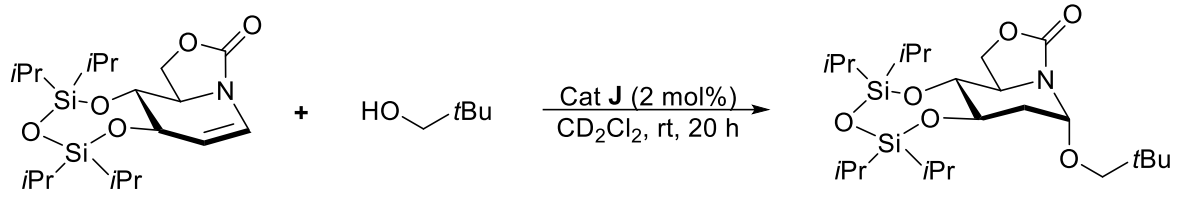

Table 5.5. Concentration for **80n** calculated by ^1H NMR analysis for varying the acceptor concentration experiment

Time/h	**80n** (**79n** =0.25M)	**80n** (**79n** =0.375M)	**80n** (**79n** =0.50M)
0	0	0	0
0.13	0.005749023	0.007454567	0.004107864
0.25	0.013756622	0.012875205	0.006133061
0.5	0.023950153	0.018941507	0.007316883
0.75	0.037261336	0.024891528	0.010403472
1	0.048885162	0.030891828	0.0121223
1.25	0.060822387	0.036824752	0.016148672
1.5	0.0727052	0.04274904	0.017753084
1.75	0.084813301	0.04856081	0.020909103
2	0.096764955	0.054575775	0.023128446
2.25	0.108679639	0.060291205	0.0263176
2.5	0.120916211	0.06607881	0.028025495
2.75	0.132746872	0.071768692	0.030489716
3	0.144457506	0.077389176	0.035353177
3.25	0.155368204	0.08297125	0.036310594
3.5	0.164510968	0.088598229	0.039233068
3.75	0.172174031	0.093789873	0.043004064
4	0.178699763	0.099255414	0.044997943
4.25	0.183727507	0.104640102	0.046718465
4.5	0.187243815	0.109636738	0.048537204
4.75	0.189452204	0.114854794	0.052598284
5	0.191492694	0.119694249	0.05459226
5.25	0.192544174	0.124814048	0.057402283
5.5	0.193417758	0.129140135	0.058689874

5.75	0.194079167	0.1337502	0.060261377
6	0.194625756	0.137931833	0.063017693
6.25	0.195004949	0.142135686	0.065601027
6.5	0.195353815	0.146085487	0.068404087
6.75	0.19565584	0.149931012	0.071000051
7	0.195856431	0.153426106	0.073957817
7.25	0.195581889	0.156956915	0.07572264
7.5	0.196388325	0.160325716	0.077656844
7.75	0.196080617	0.163198368	0.081070126
8	0.196654282	0.166095627	0.082148708
8.25	0.197035766	0.168638359	0.084564412
8.5	0.196602763	0.170427213	0.086112044
8.75	0.196974505	0.172975252	0.087998261
9	0.197374978	0.174874224	0.090426046
9.25	0.196986087	0.176689624	0.092396405
9.5	0.19763486	0.1784175	0.094992156
9.75	0.197201119	0.179601269	0.096600848
10	0.197824025	0.180935598	0.097975877
10.25	0.197440178	0.181977271	0.100932306
10.5	0.197643504	0.182906249	0.102681365
10.75	0.198106576	0.183753131	0.104699998
11	0.197608331	0.184671471	0.106026743
11.25	0.19780252	0.185885674	0.108074997
11.5	0.198280025	0.186534338	0.110931065
11.75	0.197906504	0.186468876	0.112569155
12	0.198033926	0.186936721	0.114734488
12.25	0.198734858	0.187909208	0.116516069
12.5	0.19845967	0.187675959	0.118853891
12.75	0.198157874	0.187554157	0.119085183
13	0.198596049	0.18811096	0.121370422
13.25	0.198841561	0.187949172	0.123485322
13.5	0.198703314	0.188477014	0.124954614
13.75	0.197990117	0.188615654	0.126217879
14	0.198118625	0.188659756	0.128034756
14.25	0.198264322	0.188851015	0.130121711
14.5	0.198382441	0.18885694	0.131987875
14.75	0.198246138	0.189084114	0.133180929
15	0.198430025	0.188997165	0.135233985
15.25	0.198694931	0.188966027	0.135987536
15.5	0.198494132	0.188801099	0.137955054
15.75	0.198680711	0.189308751	0.137420182
16	0.198550232	0.189140431	0.141092221
16.25	0.198304022	0.189239049	0.141418303
16.5	0.197838906	0.189150414	0.142375074
16.75	0.198650007	0.189135781	0.14401866
17	0.197997498	0.189005221	0.145062668
17.25	0.198502158	0.189095341	0.146258126
17.5	0.19776042	0.189939579	0.148446043
17.75	0.197889345	0.188936583	0.148986314
18	0.197718042	0.188854589	0.150146694
18.25	0.197979413	0.189053772	0.15153835
18.5	0.19799414	0.189065235	0.154194279
18.75	0.198402507	0.188958698	0.153979241
19	0.197877727	0.189115007	0.156303399
19.25	0.19759592	0.189066007	0.155785131
19.5	0.19748061	0.189087778	0.157629864
19.75	0.197485605	0.189181266	0.159091825
20	0.197824891	0.188974569	0.159314205

Catalyst J concentration dependence

Procedure: To a dry NMR tube, donor **78a** (51.7 mg, 0.125 mmol), catalyst **J** (3.1 mg, 1.0 mol%), acceptor **79n** (16.5 mg, 0.1875 mmol) and 1,1,2,2-tetrachloroethane (10 μL) as the internal standard, CD_2Cl_2 was added in order to reach a total volume of 500 μL. Afterwards, the tube was sealed with cap and measured on the NMR spectrometer at room temperature by recording ^1H spectra at different time.

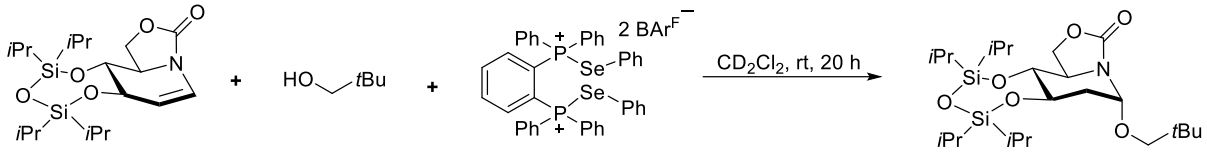

78a **79n** **J** **80n**

0.25 M 0.375 M 1 mol%

Procedure: To a dry NMR tube, donor **78a** (51.7 mg, 0.125 mmol), catalyst **J** (12.4 mg, 4.0 mol%), acceptor **79n** (16.5 mg, 0.1875 mmol) and 1,1,2,2-tetrachloroethane (10 μL) as the internal standard, CD_2Cl_2 was added in order to reach a total volume of 500 μL. Afterwards, the tube was sealed with cap and measured on the NMR spectrometer at room temperature by recording ^1H spectra at different time.

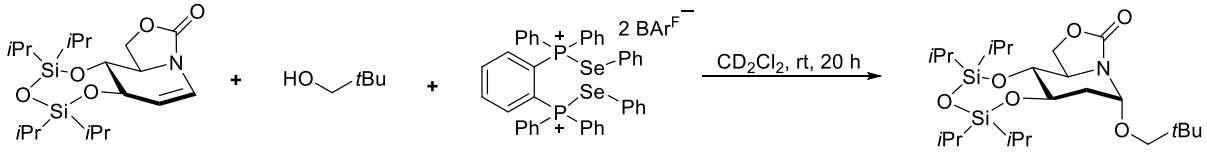

78a **79n** **J** **80n**

0.25 M 0.375 M 4 mol%

Table 5.6. Concentration for **80n** calculated by ^1H NMR analysis for varying the catalyst concentration experiment

Time/h	**80n** (**J** = 1.0 mol%)	**80n** (**J** = 2.0 mol%)	**80n** (**J** = 4.0 mol%)
0	0	0	0
0.13	3.04E-04	0.00745	0.00484
0.25	0.00328	0.01288	0.01734
0.5	0.0061	0.01894	0.02969
0.75	0.00861	0.02489	0.04093
1	0.01184	0.03089	0.05256
1.25	0.01495	0.03682	0.06478
1.5	0.01771	0.04275	0.07613
1.75	0.02045	0.04856	0.08771
2	0.02376	0.05458	0.09891
2.25	0.02574	0.06029	0.11031
2.5	0.029	0.06608	0.12062
2.75	0.03198	0.07177	0.13113
3	0.0344	0.07739	0.1405
3.25	0.03659	0.08297	0.14999
3.5	0.03967	0.0886	0.15838
3.75	0.04212	0.09379	0.16598
4	0.04506	0.09926	0.17261
4.25	0.04778	0.10464	0.17852
4.5	0.0505	0.10964	0.18353

4.75	0.05352	0.11485	0.18768
5	0.05582	0.11969	0.19078
5.25	0.0584	0.12481	0.19373
5.5	0.06135	0.12914	0.19577
5.75	0.06362	0.13375	0.19739
6	0.06616	0.13793	0.19872
6.25	0.06896	0.14214	0.19969
6.5	0.07142	0.14609	0.20068
6.75	0.07414	0.14993	0.20131
7	0.07675	0.15343	0.20204
7.25	0.07966	0.15696	0.20186
7.5	0.08145	0.16033	0.20232
7.75	0.08427	0.1632	0.20287
8	0.08652	0.1661	0.20307
8.25	0.08898	0.16864	0.20319
8.5	0.09195	0.17043	0.20304
8.75	0.09384	0.17298	0.20346
9	0.09667	0.17487	0.20339
9.25	0.09905	0.17669	0.20321
9.5	0.10077	0.17842	0.20343
9.75	0.10321	0.1796	0.20323
10	0.10541	0.18094	0.20333
10.25	0.1079	0.18198	0.20359
10.5	0.11029	0.18291	0.20355
10.75	0.11276	0.18375	0.20341
11	0.11452	0.18467	0.20314
11.25	0.1174	0.18589	0.20328
11.5	0.11904	0.18653	0.20374
11.75	0.12119	0.18647	0.20398
12	0.12281	0.18694	0.20367
12.25	0.12503	0.18791	0.20334
12.5	0.1277	0.18768	0.20313
12.75	0.12901	0.18755	0.20348
13	0.131	0.18811	0.20338
13.25	0.13312	0.18795	0.20352
13.5	0.13498	0.18848	0.20317
13.75	0.13625	0.18862	0.20312
14	0.13826	0.18866	0.2035
14.25	0.14001	0.18885	0.20356
14.5	0.14184	0.18886	0.20357
14.75	0.14371	0.18908	0.20382
15	0.14417	0.189	0.20303
15.25	0.14592	0.18897	0.20331
15.5	0.14791	0.1888	0.20349
15.75	0.14958	0.18931	0.20351
16	0.15103	0.18914	0.20336
16.25	0.15214	0.18924	0.20284
16.5	0.15323	0.18915	0.20305
16.75	0.15443	0.18914	0.20315
17	0.15545	0.18901	0.20325
17.25	0.15714	0.1891	0.20342
17.5	0.15854	0.18994	0.20309
17.75	0.15893	0.18894	0.20246
18	0.16027	0.18885	0.20294
18.25	0.16114	0.18905	0.20285
18.5	0.16131	0.18907	0.20299
18.75	0.16332	0.18896	0.20347
19	0.1637	0.18912	0.20332

19.25	0.16516	0.18907	0.20257
19.5	0.16551	0.18909	0.20232
19.75	0.16565	0.18918	0.20288
20	0.16718	0.18897	0.20268

5.2.7.2 Kinetic experiment on the downstream reaction

NMR monitoring of the downstream step under standard conditions

Procedure: To a dry NMR tube, intermediate **83** (4.31 mg, 0.01 mmol), 100 uL catalyst **J** (0.5 mg, 2.0 mol%, 5 mg in 1 mL CD_2Cl_2 solution), 150 uL acceptor **79n** (1.32 mg, 0.015 mmol, 8.8 mg in 1 mL CD_2Cl_2 solution) and 1,1,2,2-tetrachloroethane (5 µL) as the internal standard, CD_2Cl_2 was added in order to reach a total volume of 500 µL. Afterwards, the tube was sealed with cap and measured on the NMR spectrometer at room temperature by recording ^1H spectra at different time.

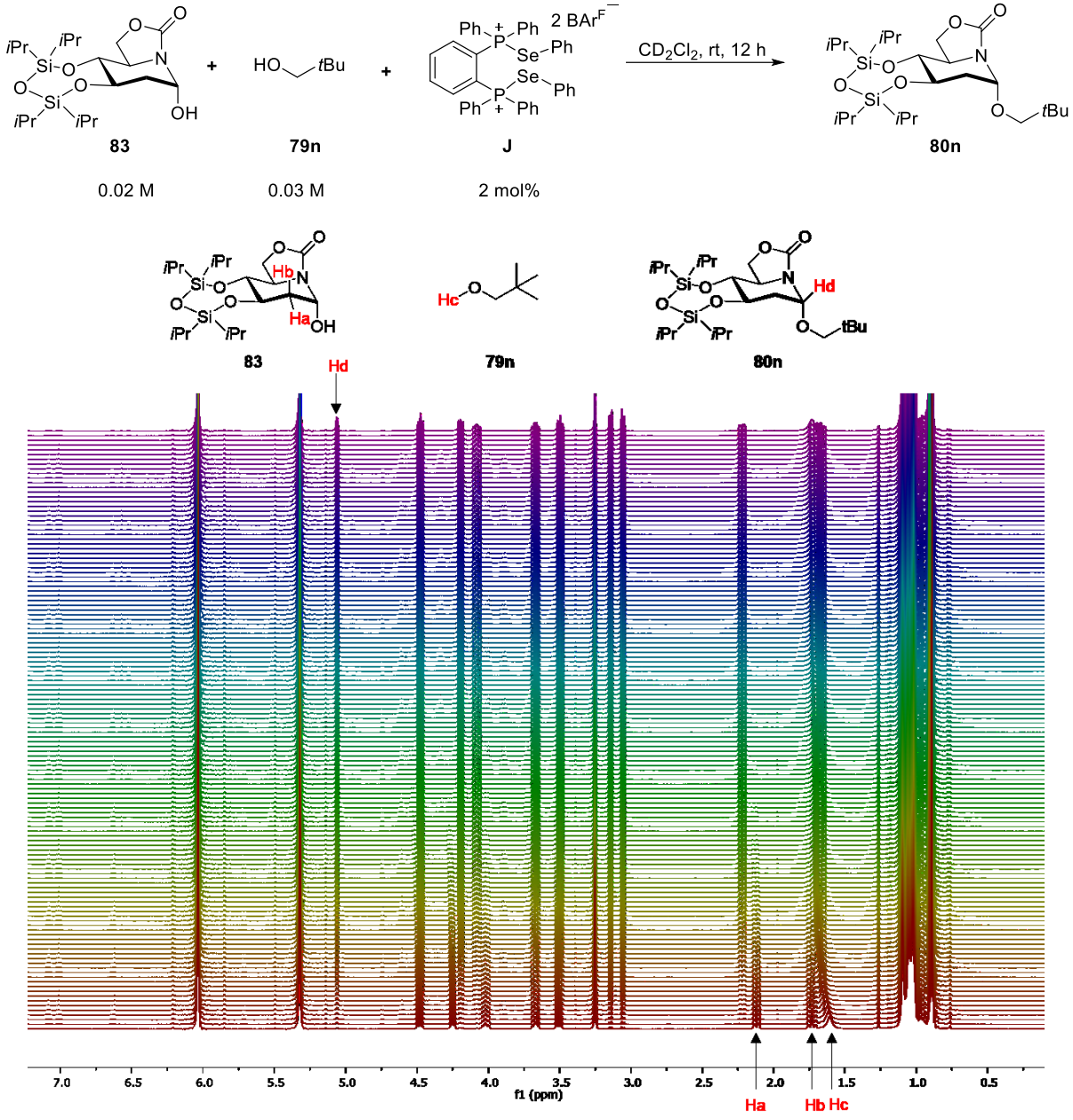

Figure 5.8. Stacked ^{1}H NMR spectra for the monitoring of the downstream step under standard conditions

Table 5.7. Concentration for **83**, **79n**, **80n** calculated by ^{1}H NMR analysis for the monitoring of the downstream step under standard conditions

Time/h	[**INT 83**]/M	[**Acceptor 79n**]/M	[**Product 80n**]/M
0	0.02	0.03	0
0.083333333	0.015862224	0.029009081	0.002250139
0.166666667	0.014955739	0.027614601	0.002400277
0.25	0.01456833	0.027238127	0.002707422
0.333333333	0.014187169	0.02686771	0.002943161
0.416666667	0.013827234	0.026414959	0.003087869
0.5	0.013478372	0.026101064	0.003532359
0.583333333	0.013076045	0.025710892	0.003797842
0.666666667	0.012687608	0.025230099	0.004009203
0.75	0.012287516	0.024925469	0.004366604
0.833333333	0.011929391	0.024493276	0.004733963
0.916666667	0.011588844	0.024069273	0.005171606
1	0.011165766	0.02360739	0.005659506
1.083333333	0.0107915	0.023240958	0.006053219
1.166666667	0.010404049	0.02278384	0.006572896
1.25	0.009984903	0.022475337	0.007026405
1.333333333	0.009617776	0.022041338	0.007649822
1.416666667	0.009211646	0.021635386	0.008045616
1.5	0.008819664	0.021303233	0.008446858
1.583333333	0.008428917	0.020896904	0.008725427
1.666666667	0.008130727	0.02057929	0.00905207
1.75	0.007749846	0.020123626	0.009543294
1.833333333	0.007393915	0.019744202	0.009828941
1.916666667	0.006966747	0.019410224	0.01020221
2	0.006564496	0.019099871	0.010587932
2.083333333	0.006273556	0.018722255	0.010946142
2.166666667	0.005949303	0.018365086	0.011286493
2.25	0.005599022	0.018033197	0.011562825
2.333333333	0.005265048	0.017685753	0.011943869
2.416666667	0.004940979	0.017375764	0.012313545
2.5	0.004651463	0.017082706	0.012589046
2.583333333	0.004356195	0.016768146	0.012859592
2.666666667	0.004093988	0.01653627	0.013224876
2.75	0.003775204	0.016219104	0.013483244
2.833333333	0.003557167	0.015951085	0.013693776
2.916666667	0.003257125	0.015768235	0.01409764
3	0.003112064	0.015466554	0.014252346
3.083333333	0.002809253	0.015238754	0.014481878
3.166666667	0.00254104	0.015064256	0.014773471
3.25	0.002300924	0.014881976	0.015099843
3.333333333	0.002137092	0.014719233	0.015176988
3.416666667	0.00199633	0.014488888	0.015310585
3.5	0.001827223	0.014307828	0.015468782
3.583333333	0.001729546	0.014109967	0.015642104
3.666666667	0.001542235	0.014019388	0.015765478
3.75	0.001339949	0.013957942	0.01594802
3.833333333	0.001317069	0.013733235	0.015971532
3.916666667	0.001121937	0.01373961	0.016156747
4	0.001081826	0.01359148	0.016265489

4.083333333	0.00105261	0.013535881	0.01636509
4.166666667	0.000891104	0.01348045	0.016428835
4.25	0.000843232	0.013420744	0.016483845
4.333333333	0.000719627	0.013315145	0.016499361
4.416666667	0.000831423	0.013224839	0.016522247
4.5	0.000666556	0.013224202	0.016701461
4.583333333	0.00067634	0.013173734	0.016605256
4.666666667	0.000582588	0.01314629	0.016710188
4.75	0.00058099	0.013131461	0.01671996
4.833333333	0.000576095	0.013111487	0.016780776
4.916666667	0.000527876	0.013042435	0.016792551
5	0.000457018	0.013092588	0.016849661
5.083333333	0.000508152	0.013032857	0.016772025
5.166666667	0.00036375	0.013067867	0.016944123
5.25	0.000426755	0.012997477	0.016820912
5.333333333	0.000497881	0.012969715	0.016797036
5.416666667	0.000448498	0.012985164	0.016884001
5.5	0.000503055	0.012925893	0.016941149
5.583333333	0.000410776	0.012942769	0.016925489
5.666666667	0.000507977	0.012904532	0.016879239
5.75	0.000447727	0.0129025	0.016901507
5.833333333	0.000385356	0.012968686	0.016952203
5.916666667	0.000352712	0.012952106	0.016947636
6	0.000405115	0.012915115	0.016928687
6.083333333	0.000404054	0.012865953	0.016948507
6.166666667	0.000409406	0.012905554	0.016978312
6.25	0.000427426	0.012943477	0.016971856
6.333333333	0.00038356	0.012871981	0.016925596
6.416666667	0.000347691	0.012885307	0.016947605
6.5	0.00039409	0.012906388	0.016993448
6.583333333	0.000425765	0.012877401	0.016907982
6.666666667	0.000448047	0.012837197	0.016899595
6.75	0.000460081	0.012832714	0.016890986
6.833333333	0.000392467	0.01290488	0.016959148
6.916666667	0.000410327	0.012906327	0.017018772
7	0.000398738	0.012873648	0.016923385
7.083333333	0.000350843	0.012898636	0.017023565
7.166666667	0.000368851	0.012923961	0.017111199
7.25	0.000410812	0.012867528	0.016956393
7.333333333	0.000359758	0.012898173	0.017081688
7.416666667	0.000353538	0.012958742	0.017072405
7.5	0.000442703	0.012819123	0.016917833
7.583333333	0.000325928	0.012888361	0.017030209
7.666666667	0.000392471	0.012879068	0.017069772
7.75	0.000408782	0.01284818	0.016991674
7.833333333	0.000323276	0.012920192	0.017048957
7.916666667	0.000373586	0.012848049	0.017074615
8	0.000374383	0.012847972	0.017074235
8.083333333	0.000448286	0.01281947	0.016967664
8.166666667	0.000392311	0.012874306	0.01704508
8.25	0.000343517	0.012835142	0.017094348
8.333333333	0.000398458	0.012878518	0.017095463
8.416666667	0.000417225	0.012837281	0.017017191
8.5	0.000394627	0.012836365	0.017004782
8.583333333	0.000393759	0.012852429	0.01710298
8.666666667	0.000356449	0.012833897	0.017101542
8.75	0.000382477	0.012801053	0.017001028
8.833333333	0.000511008	0.012788177	0.017008351

8.916666667	0.00045202	0.012768629	0.016979521
9	0.00041714	0.012785574	0.017046574
9.083333333	0.000398307	0.012854197	0.017138496
9.166666667	0.000371416	0.012833064	0.017070213
9.25	0.000383132	0.012815436	0.017096934
9.333333333	0.000319452	0.012899006	0.01713887
9.416666667	0.000440834	0.012816366	0.017019152
9.5	0.000425976	0.012788179	0.017096596
9.583333333	0.000380322	0.012838361	0.017140241
9.666666667	0.000383848	0.012801671	0.017139515
9.75	0.000467918	0.012725303	0.017028461
9.833333333	0.000478706	0.012781864	0.017154886
9.916666667	0.000456937	0.012835755	0.017076474
10	0.000516862	0.012756219	0.01701293
10.08333333	0.00043213	0.012753488	0.017069941
10.16666667	0.000433299	0.012805942	0.017130085
10.25	0.00038867	0.01277923	0.017072181
10.33333333	0.000494985	0.012773793	0.017060047
10.41666667	0.000450861	0.012811034	0.017133211
10.5	0.000519756	0.012707637	0.016993155
10.58333333	0.000473437	0.012740034	0.017026993
10.66666667	0.00041339	0.012804079	0.017084216
10.75	0.000398532	0.012818823	0.017164315
10.83333333	0.000428231	0.012742331	0.017088407
10.91666667	0.000511813	0.012698786	0.016979483
11	0.000449442	0.012771063	0.017162896
11.08333333	0.000479662	0.012710537	0.017126893
11.16666667	0.000456659	0.012753382	0.017055771
11.25	0.000427337	0.01273881	0.017121147
11.33333333	0.000525872	0.012679869	0.017073888
11.41666667	0.000544664	0.012694752	0.017113296
11.5	0.000450426	0.012714099	0.017083011
11.58333333	0.000594133	0.012638384	0.017023204
11.66666667	0.00055349	0.012677041	0.017090576
11.75	0.000466769	0.01273823	0.017076713
11.83333333	0.00054984	0.012651918	0.017073141
11.91666667	0.000432884	0.012756517	0.017142872
12	0.000458227	0.012734061	0.017101449

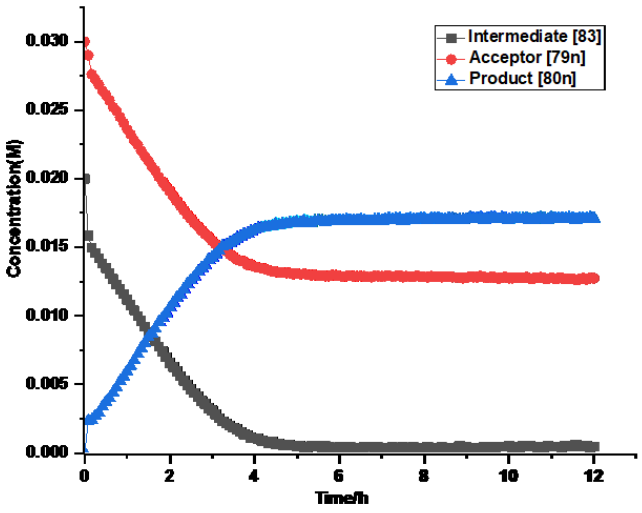

Figure 5.9. Temporal kinetics profile for the monitoring under standard conditions

Intermediate 83 concentration dependence

Procedure: To a dry NMR tube, intermediate **83** (2.15 mg, 0.005 mmol), 100 uL catalyst **J** (0.5 mg, 2.0 mol%, 5 mg in 1 mL CD_2Cl_2 solution), 150 uL acceptor **79n** (1.32 mg, 0.015 mmol, 8.8 mg in 1 mL CD_2Cl_2 solution) and 1,1,2,2-tetrachloroethane (5 μL) as the internal standard, CD_2Cl_2 was added in order to reach a total volume of 500 μL. Afterwards, the tube was sealed with cap and measured on the NMR spectrometer at room temperature by recording ^1H spectra at different time.

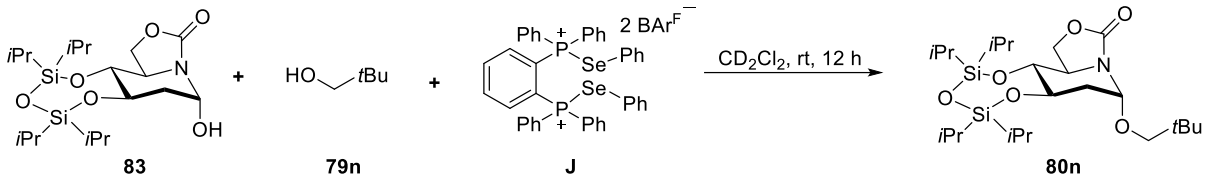

Procedure: To a dry NMR tube, intermediate **83** (6.45 mg, 0.015 mmol), 100 uL catalyst **J** (0.5 mg, 2.0 mol%, 5 mg in 1 mL CD_2Cl_2 solution), 150 uL acceptor **79n** (1.32 mg, 0.015 mmol, 8.8 mg in 1 mL CD_2Cl_2 solution) and 1,1,2,2-tetrachloroethane (5 μL) as the internal standard, CD_2Cl_2 was added in order to reach a total volume of 500 μL. Afterwards, the tube was sealed with cap and measured on the NMR spectrometer at room temperature by recording ^1H spectra at different time.

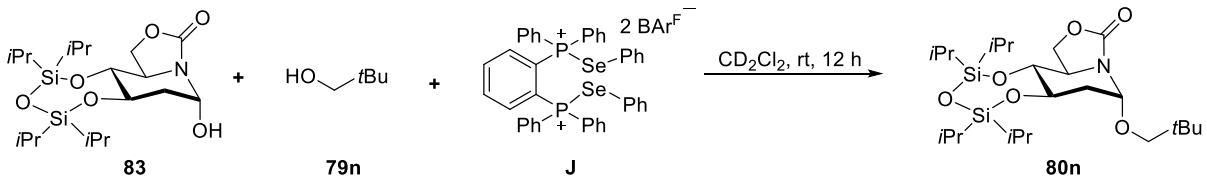

Table 5.8. Concentration for **80n** calculated by ^1H NMR analysis for varying the intermediate concentration experiment

Time/h	**80n** (**83** =0.01M)	**80n** (**83** =0.02M)	**80n** (**83** =0.03M)
0	0	0	0
0.083333333	0.001018559	0.002250139	0.002445645
0.166666667	0.001133386	0.002400277	0.002744085
0.25	0.001361327	0.002707422	0.003140676
0.333333333	0.001409775	0.002943161	0.003489459
0.416666667	0.001657371	0.003087869	0.00378169
0.5	0.001959813	0.003532359	0.004161465
0.583333333	0.00208164	0.003797842	0.004566873
0.666666667	0.002438764	0.004009203	0.005001738
0.75	0.002657091	0.004366604	0.00536088
0.833333333	0.002841954	0.004733963	0.005637585
0.916666667	0.003154602	0.005171606	0.006061223
1	0.003334886	0.005659506	0.006342497
1.083333333	0.00356497	0.006053219	0.00650596
1.166666667	0.003707335	0.006572896	0.006760321

1.25	0.003980393	0.007026405	0.007314329
1.333333333	0.004176297	0.007649822	0.007327426
1.416666667	0.004403842	0.008045616	0.008235678
1.5	0.004679201	0.008446858	0.008373619
1.583333333	0.004945057	0.008725427	0.008793195
1.666666667	0.005079132	0.00905207	0.009318178
1.75	0.005156259	0.009543294	0.009679479
1.833333333	0.005306414	0.009828941	0.009965638
1.916666667	0.005633547	0.01020221	0.010306031
2	0.005630087	0.010587932	0.010657663
2.083333333	0.00607986	0.010946142	0.011320146
2.166666667	0.006393092	0.011286493	0.01146261
2.25	0.006499689	0.011562825	0.011976189
2.333333333	0.006668549	0.011943869	0.012214081
2.416666667	0.006791376	0.012313545	0.012608538
2.5	0.007101646	0.012589046	0.012839328
2.583333333	0.0070823	0.012859592	0.013330337
2.666666667	0.007269776	0.013224876	0.013528915
2.75	0.00744119	0.013483244	0.013884715
2.833333333	0.007575864	0.013693776	0.014376452
2.916666667	0.007514969	0.01409764	0.014492244
3	0.007913145	0.014252346	0.015023635
3.083333333	0.007904412	0.014481878	0.015315648
3.166666667	0.008175984	0.014773471	0.015561329
3.25	0.008353083	0.015099843	0.015879669
3.333333333	0.008486643	0.015176988	0.016321477
3.416666667	0.008474968	0.015310585	0.016602394
3.5	0.008592387	0.015468782	0.016824406
3.583333333	0.008774907	0.015642104	0.017148017
3.666666667	0.008896362	0.015765478	0.017617755
3.75	0.009076068	0.01594802	0.017840733
3.833333333	0.009151265	0.015971532	0.018279496
3.916666667	0.009240418	0.016156747	0.018346837
4	0.009591067	0.016265489	0.018701253
4.083333333	0.009347275	0.01636509	0.019123373
4.166666667	0.009640756	0.016428835	0.019398097
4.25	0.009642731	0.016483845	0.019661915
4.333333333	0.009834102	0.016499361	0.020012031
4.416666667	0.009902493	0.016522247	0.02018868
4.5	0.009934223	0.016701461	0.020635083
4.583333333	0.010147939	0.016605256	0.020697931
4.666666667	0.010162595	0.016710188	0.021479005
4.75	0.010167936	0.01671996	0.021335593
4.833333333	0.010353252	0.016780776	0.021514997
4.916666667	0.010498472	0.016792551	0.021894241
5	0.010448015	0.016849661	0.022620648
5.083333333	0.010596611	0.016772025	0.022244551
5.166666667	0.010658522	0.016944123	0.022316994
5.25	0.010870589	0.016820912	0.022823789
5.333333333	0.011028524	0.016797036	0.022923397
5.416666667	0.010818901	0.016884001	0.023189071
5.5	0.010976796	0.016941149	0.023320765
5.583333333	0.011052014	0.016925489	0.023892454
5.666666667	0.011348478	0.016879239	0.023781154
5.75	0.011247966	0.016901507	0.024538334
5.833333333	0.011121543	0.016952203	0.024128036
5.916666667	0.011316798	0.016947636	0.024493104
6	0.011342117	0.016928687	0.024461672

6.083333333	0.011298645	0.016948507	0.024457297
6.166666667	0.011495984	0.016978312	0.025237001
6.25	0.01139904	0.016971856	0.025042724
6.333333333	0.011622144	0.016925596	0.025280289
6.416666667	0.011469009	0.016947605	0.025661833
6.5	0.011493719	0.016993448	0.025898342
6.583333333	0.011498159	0.016907982	0.026017106
6.666666667	0.01143441	0.016899595	0.026009848
6.75	0.011626853	0.016890986	0.026172538
6.833333333	0.011842182	0.016959148	0.026048654
6.916666667	0.01157513	0.017018772	0.026475339
7	0.011738831	0.016923385	0.026431259
7.083333333	0.011826146	0.017023565	0.027097473
7.166666667	0.011864818	0.017111199	0.02688298
7.25	0.011771961	0.016956393	0.027169938
7.333333333	0.011982375	0.017081688	0.027314479
7.416666667	0.01185099	0.017072405	0.027367546
7.5	0.011831618	0.016917833	0.027765677
7.583333333	0.011775928	0.017030209	0.027911888
7.666666667	0.011659911	0.017069772	0.027915447
7.75	0.011801988	0.016991674	0.028010596
7.833333333	0.012023037	0.017048957	0.028311109
7.916666667	0.012088133	0.017074615	0.028489496
8	0.011974474	0.017074235	0.028467533
8.083333333	0.011694862	0.016967664	0.028675805
8.166666667	0.011803103	0.01704508	0.028781851
8.25	0.011966565	0.017094348	0.028789231
8.333333333	0.012007049	0.017095463	0.029010563
8.416666667	0.011786647	0.017017191	0.029185961
8.5	0.011888207	0.017004782	0.029198392
8.583333333	0.012157391	0.01710298	0.029200782
8.666666667	0.011942335	0.017101542	0.029071177
8.75	0.011963694	0.017001028	0.029410964
8.833333333	0.011927236	0.017008351	0.029588149
8.916666667	0.011765289	0.016979521	0.029701601
9	0.012076118	0.017046574	0.029788813
9.083333333	0.012042156	0.017138496	0.029781257
9.166666667	0.012188771	0.017070213	0.029826892
9.25	0.012033696	0.017096934	0.030111449
9.333333333	0.011946008	0.01713887	0.030252192
9.416666667	0.011786108	0.017019152	0.030359856
9.5	0.012257706	0.017096596	0.030105505
9.583333333	0.012021887	0.017140241	0.03035585
9.666666667	0.011948006	0.017139515	0.030440851
9.75	0.011890653	0.017028461	0.030669549
9.833333333	0.011892945	0.017154886	0.03086399
9.916666667	0.011971231	0.017076474	0.030752184
10	0.011960579	0.01701293	0.030608835
10.08333333	0.012159815	0.017069941	0.030854518
10.16666667	0.011926703	0.017130085	0.030711155
10.25	0.011988333	0.017072181	0.030917265
10.33333333	0.012016388	0.017060047	0.030807634
10.41666667	0.01191057	0.017133211	0.030964283
10.5	0.011965636	0.016993155	0.03087043
10.58333333	0.011952381	0.017026993	0.031134726
10.66666667	0.012200789	0.017084216	0.031103032
10.75	0.012172803	0.017164315	0.031122198
10.83333333	0.01214108	0.017088407	0.03108192

10.91666667	0.011998613	0.016979483	0.031157413
11	0.012037202	0.017162896	0.031244993
11.08333333	0.0121947	0.017126893	0.031248122
11.16666667	0.012129116	0.017055771	0.031260859
11.25	0.011844561	0.017121147	0.03115943
11.33333333	0.011976774	0.017073888	0.031414742
11.41666667	0.012066533	0.017113296	0.031470563
11.5	0.012032365	0.017083011	0.031327453
11.58333333	0.01210186	0.017023204	0.031301431
11.66666667	0.012178324	0.017090576	0.031295062
11.75	0.012135605	0.017076713	0.031334671
11.83333333	0.012125048	0.017073141	0.031333468
11.91666667	0.012046384	0.017142872	0.031620944
12	0.012078365	0.017101449	0.031380164

Acceptor 79n concentration dependence

Procedure: To a dry NMR tube, intermediate **83** (4.31 mg, 0.01 mmol), 100 uL catalyst **J** (0.5 mg, 2.0 mol%, 5 mg in 1 mL CD_2Cl_2 solution), 100 uL acceptor **79n** (0.88 mg, 0.01 mmol, 8.8 mg in 1 mL CD_2Cl_2 solution) and 1,1,2,2-tetrachloroethane (5 µL) as the internal standard, CD_2Cl_2 was added in order to reach a total volume of 500 µL. Afterwards, the tube was sealed with cap and measured on the NMR spectrometer at room temperature by recording ^1H spectra at different time.

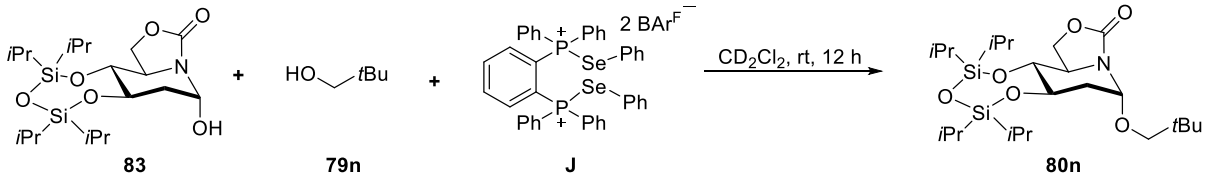

83 **79n** **J** **80n**

0.01 M 0.02 M 2 mol%

Procedure: To a dry NMR tube, intermediate **83** (4.31 mg, 0.01 mmol), 100 uL catalyst **J** (0.5 mg, 2.0 mol%, 5 mg in 1 mL CD_2Cl_2 solution), 200 uL acceptor **79n** (1.76 mg, 0.02 mmol, 8.8 mg in 1 mL CD_2Cl_2 solution) and 1,1,2,2-tetrachloroethane (5 µL) as the internal standard, CD_2Cl_2 was added in order to reach a total volume of 500 µL. Afterwards, the tube was sealed with cap and measured on the NMR spectrometer at room temperature by recording ^1H spectra at different time.

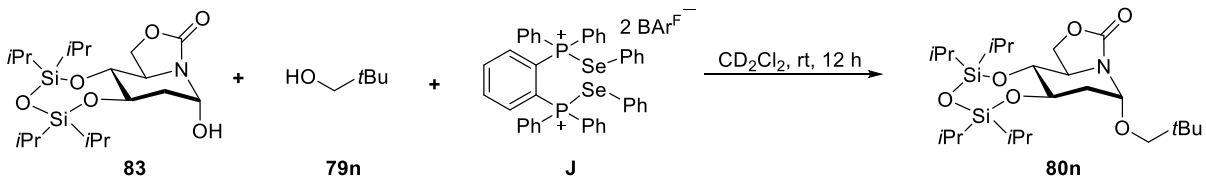

83 **79n** **J** **80n**

0.01 M 0.04 M 2 mol%

Table 5.9. Concentration for **80n** calculated by ^{1}H NMR analysis for varying the acceptor concentration experiment

Time/h	**80n** (**79n** =0.02M)	**80n** (**79n** =0.03M)	**80n** (**79n** =0.04M)
0	0	0	0
0.083333333	0.001252007	0.002250139	0.000924891
0.166666667	0.001889968	0.002400277	0.001115415
0.25	0.002627733	0.002707422	0.001411238
0.333333333	0.003405758	0.002943161	0.00163545
0.416666667	0.003994215	0.003387869	0.001905497
0.5	0.004733537	0.003732359	0.002034402
0.583333333	0.005474477	0.003997842	0.00223826
0.666666667	0.005866983	0.004409203	0.002674978
0.75	0.006775113	0.00476666	0.0029193
0.833333333	0.0073818	0.005233963	0.003082433
0.916666667	0.008029887	0.005571606	0.003275703
1	0.008564403	0.005959506	0.003716667
1.083333333	0.00927999	0.006353219	0.003921386
1.166666667	0.009897023	0.006772896	0.004224273
1.25	0.010506217	0.007226405	0.004452735
1.333333333	0.011061636	0.007649822	0.004645836
1.416666667	0.011624209	0.008045616	0.004902049
1.5	0.01205512	0.008446858	0.005380849
1.583333333	0.012539261	0.008725427	0.005630007
1.666666667	0.012817742	0.00905207	0.005809793
1.75	0.012868791	0.009543294	0.006045612
1.833333333	0.012962322	0.009828941	0.006478416
1.916666667	0.013205481	0.01020221	0.006659499
2	0.013239706	0.010587932	0.006988229
2.083333333	0.013316066	0.010946142	0.007224878
2.166666667	0.013262426	0.011286493	0.007446348
2.25	0.013270418	0.011562825	0.007683328
2.333333333	0.013254437	0.011943869	0.007920701
2.416666667	0.013228859	0.012313545	0.008234948
2.5	0.013223457	0.012589046	0.008468021
2.583333333	0.013130611	0.012859592	0.008711187
2.666666667	0.013214	0.013224876	0.008921709
2.75	0.013215	0.013483244	0.009128386
2.833333333	0.013216	0.013693776	0.00934165
2.916666667	0.013217	0.01409764	0.009560342
3	0.013218	0.014252346	0.009612058
3.083333333	0.013219	0.014481878	0.010030172
3.166666667	0.01322	0.014773471	0.010283009
3.25	0.013221	0.015099843	0.010310044
3.333333333	0.013222	0.015176988	0.010667604
3.416666667	0.013223	0.015310585	0.010730345
3.5	0.013224	0.015468782	0.011111139
3.583333333	0.013225	0.015642104	0.011172833
3.666666667	0.013226	0.015765478	0.011556114
3.75	0.013227	0.01594802	0.011668928
3.833333333	0.013228	0.015971532	0.011956653
3.916666667	0.013229	0.016156747	0.011983147
4	0.01323	0.016265489	0.012041128
4.083333333	0.013231	0.01636509	0.012335673
4.166666667	0.013232	0.016428835	0.012610592
4.25	0.013233	0.016483845	0.012679032
4.333333333	0.013234	0.016499361	0.012729532

4.416666667	0.013235	0.016522247	0.012856067
4.5	0.013236	0.016701461	0.012897096
4.583333333	0.013237	0.016605256	0.012964359
4.666666667	0.013238	0.016710188	0.013087684
4.75	0.013239	0.01671996	0.013246528
4.833333333	0.01324	0.016780776	0.013502873
4.916666667	0.013241	0.016792551	0.013312124
5	0.013242	0.016849661	0.013527481
5.083333333	0.013243	0.016772025	0.013507428
5.166666667	0.013244	0.016944123	0.01359324
5.25	0.013245	0.016820912	0.013556902
5.333333333	0.013246	0.016797036	0.01383873
5.416666667	0.013247	0.016884001	0.013926772
5.5	0.013248	0.016941149	0.013930984
5.583333333	0.013249	0.016925489	0.013985518
5.666666667	0.01325	0.016879239	0.014028965
5.75	0.013251	0.016901507	0.014155642
5.833333333	0.013252	0.016952203	0.014076838
5.916666667	0.013253	0.016947636	0.014088985
6	0.013254	0.016928687	0.0140064
6.083333333	0.013255	0.016948507	0.014176955
6.166666667	0.013256	0.016978312	0.014231766
6.25	0.013257	0.016971856	0.014073297
6.333333333	0.013258	0.016925596	0.014069419
6.416666667	0.013259	0.016947605	0.014154298
6.5	0.01326	0.016993448	0.014077799
6.583333333	0.013261	0.016907982	0.014155333
6.666666667	0.013262	0.016899595	0.014107524
6.75	0.013263	0.016890986	0.014104048
6.833333333	0.013264	0.016959148	0.014221869
6.916666667	0.013265	0.017018772	0.014172578
7	0.013266	0.016923385	0.014143029
7.083333333	0.013267	0.017023565	0.014131724
7.166666667	0.013268	0.017111199	0.014172136
7.25	0.013269	0.016956393	0.014265494
7.333333333	0.01327	0.017081688	0.014375901
7.416666667	0.013271	0.017072405	0.014097034
7.5	0.013272	0.016917833	0.014208475
7.583333333	0.013273	0.017030209	0.014054531
7.666666667	0.013274	0.017069772	0.014235771
7.75	0.013275	0.016991674	0.014131538
7.833333333	0.013276	0.017048957	0.014081997
7.916666667	0.013277	0.017074615	0.014069153
8	0.013278	0.017074235	0.014204959
8.083333333	0.013279	0.016967664	0.014263083
8.166666667	0.01328	0.01704508	0.014190256
8.25	0.013281	0.017094348	0.014154041
8.333333333	0.013282	0.017095463	0.014293545
8.416666667	0.013283	0.017017191	0.014188412
8.5	0.013284	0.017004782	0.014135319
8.583333333	0.013285	0.01710298	0.014142062
8.666666667	0.013286	0.017101542	0.014276344
8.75	0.013287	0.017001028	0.014108207
8.833333333	0.013288	0.017008351	0.014098073
8.916666667	0.013289	0.016979521	0.014099845
9	0.01329	0.017046574	0.014029405
9.083333333	0.013291	0.017138496	0.014287226
9.166666667	0.013292	0.017070213	0.014018914

9.25	0.013293	0.017096934	0.014357278
9.333333333	0.013294	0.01713887	0.014003798
9.416666667	0.013295	0.017019152	0.014129729
9.5	0.013296	0.017096596	0.014110809
9.583333333	0.013297	0.017140241	0.014124842
9.666666667	0.013298	0.017139515	0.014090041
9.75	0.013299	0.017028461	0.014018113
9.833333333	0.0133	0.017154886	0.01407576
9.916666667	0.013301	0.017076474	0.014083269
10	0.013302	0.01701293	0.014106545
10.08333333	0.013303	0.017069941	0.014008315
10.16666667	0.013304	0.017130085	0.014081751
10.25	0.013305	0.017072181	0.014111853
10.33333333	0.013306	0.017060047	0.013984845
10.41666667	0.013307	0.017133211	0.014031684
10.5	0.013308	0.016993155	0.01397883
10.58333333	0.013309	0.017026993	0.014183065
10.66666667	0.01331	0.017084216	0.01403771
10.75	0.013311	0.017164315	0.014021125
10.83333333	0.013312	0.017088407	0.013915042
10.91666667	0.013313	0.016979483	0.014201927
11	0.013314	0.017162896	0.014209898
11.08333333	0.013315	0.017126893	0.014168051
11.16666667	0.013316	0.017055771	0.013990742
11.25	0.013317	0.017121147	0.014029849
11.33333333	0.013318	0.017073888	0.01389576
11.41666667	0.013319	0.017113296	0.013910963
11.5	0.01332	0.017083011	0.013933641
11.58333333	0.013321	0.017023204	0.014277404
11.66666667	0.013322	0.017090576	0.014005184
11.75	0.013323	0.017076713	0.013903902
11.83333333	0.013324	0.017073141	0.01412044
11.91666667	0.013325	0.017142872	0.014129621
12	0.013326	0.017101449	0.013875603

Catalyst J concentration dependence

Procedure: To a dry NMR tube, intermediate **83** (4.31 mg, 0.01 mmol), 50 uL catalyst **J** (0.25 mg, 1.0 mol%, 5 mg in 1 mL CD_2Cl_2 solution), 150 uL acceptor **79n** (1.32 mg, 0.015 mmol, 8.8 mg in 1 mL CD_2Cl_2 solution) and 1,1,2,2-tetrachloroethane (5 µL) as the internal standard, CD_2Cl_2 was added in order to reach a total volume of 500 µL. Afterwards, the tube was sealed with cap and measured on the NMR spectrometer at room temperature by recording ^1H spectra at different time.

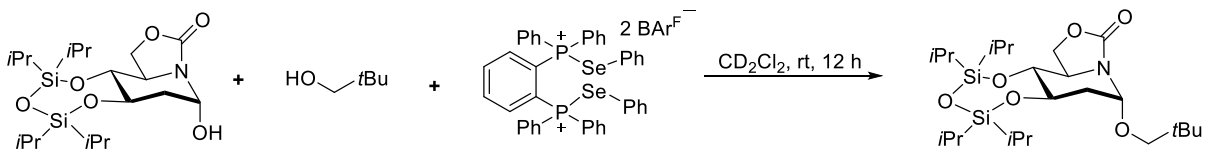

83 **79n** **J** **80n**

0.02 M 0.03 M 1 mol%

Procedure: To a dry NMR tube, intermediate **83** (4.31 mg, 0.01 mmol), 200 uL catalyst **J** (1.0 mg, 4.0 mol%, 5 mg in 1 mL CD_2Cl_2 solution), 150 uL acceptor **79n** (1.32 mg, 0.015 mmol, 8.8 mg in 1 mL

CD_2Cl_2 solution) and 1,1,2,2-tetrachloroethane (5 µL) as the internal standard, CD_2Cl_2 was added in order to reach a total volume of 500 µL. Afterwards, the tube was sealed with cap and measured on the NMR spectrometer at room temperature by recording ^1H spectra at different time.

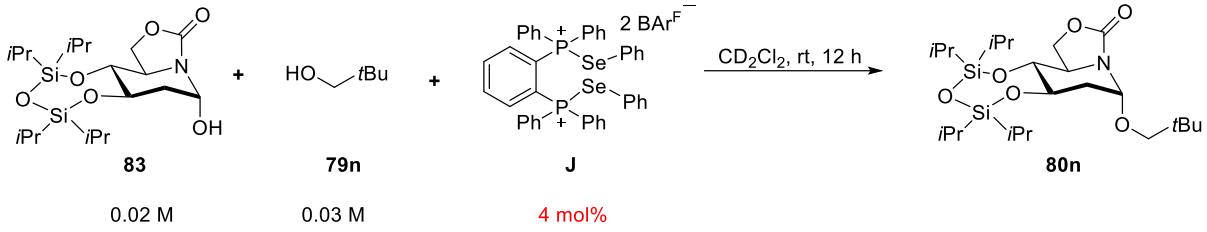

83 **79n** **J** **80n**

0.02 M 0.03 M 4 mol%

Table 5.10. Concentration for **80n** calculated by ^1H NMR analysis for varying the catalyst concentration experiment

Time/h	**80n** (**J** =1.0 mol%)	**80n** (**J** =2.0 mol%)	**80n** (**J** =4.0 mol%)
0	0	0	0
0.083333333	0.001303396	0.001807902	0.002350139
0.166666667	0.001141359	0.001555842	0.002400277
0.25	0.001356538	0.002004458	0.002707422
0.333333333	0.001501213	0.002410083	0.002943161
0.416666667	0.001674877	0.002749532	0.003387869
0.5	0.002067001	0.003160112	0.003732359
0.583333333	0.002147713	0.003622271	0.003997842
0.666666667	0.002371864	0.004038682	0.004409203
0.75	0.00242771	0.00461082	0.00476666
0.833333333	0.002585764	0.004974012	0.005233963
0.916666667	0.002653771	0.005464259	0.005571606
1	0.002999161	0.005919555	0.005959506
1.083333333	0.003017463	0.006353219	0.006520234
1.166666667	0.003035424	0.006772896	0.006726917
1.25	0.003102649	0.007226405	0.007373659
1.333333333	0.00344962	0.007649822	0.007719528
1.416666667	0.003715008	0.008045616	0.008173315
1.5	0.003612512	0.008446858	0.00871686
1.583333333	0.003909598	0.008725427	0.009203691
1.666666667	0.003991046	0.00905207	0.009675574
1.75	0.00426227	0.009543294	0.010050322
1.833333333	0.004225834	0.009828941	0.010334686
1.916666667	0.004303283	0.01020221	0.010931785
2	0.004487461	0.010587932	0.011193025
2.083333333	0.004584286	0.010946142	0.011751539
2.166666667	0.004977048	0.011286493	0.012323566
2.25	0.00500907	0.011562825	0.012497552
2.333333333	0.005303647	0.011943869	0.012894818
2.416666667	0.005136527	0.012313545	0.013298308
2.5	0.005511159	0.012589046	0.013725874
2.583333333	0.005642238	0.012859592	0.014128029
2.666666667	0.005608459	0.013224876	0.01439336
2.75	0.005709397	0.013483244	0.014697621
2.833333333	0.005930211	0.013693776	0.015072194
2.916666667	0.005973292	0.01409764	0.015480096
3	0.006270684	0.014252346	0.015739519
3.083333333	0.006391275	0.014481878	0.016038024
3.166666667	0.006291027	0.014773471	0.016311658

3.25	0.006381486	0.015099843	0.016476942
3.333333333	0.006598661	0.015176988	0.016857863
3.416666667	0.00679134	0.015310585	0.017071657
3.5	0.006935236	0.015468782	0.017317754
3.583333333	0.007159958	0.015642104	0.017483873
3.666666667	0.007342589	0.015765478	0.017604311
3.75	0.007244659	0.01594802	0.017763921
3.833333333	0.007524521	0.015971532	0.017875384
3.916666667	0.007349194	0.016156747	0.018032751
4	0.007772982	0.016265489	0.018089431
4.083333333	0.007738597	0.01636509	0.018238726
4.166666667	0.007995206	0.016428835	0.018459805
4.25	0.008129173	0.016483845	0.018343419
4.333333333	0.008051917	0.016499361	0.018461418
4.416666667	0.008217736	0.016522247	0.018592097
4.5	0.008185699	0.016701461	0.018449981
4.583333333	0.008621457	0.016605256	0.01855951
4.666666667	0.008582504	0.016710188	0.018666229
4.75	0.00864585	0.01671996	0.018513225
4.833333333	0.008865297	0.016780776	0.018650923
4.916666667	0.00908036	0.016792551	0.018789136
5	0.009258326	0.016849661	0.018763488
5.083333333	0.009284871	0.016772025	0.01856241
5.166666667	0.009427526	0.016944123	0.018740916
5.25	0.009247307	0.016820912	0.018661135
5.333333333	0.009474084	0.016797036	0.018718942
5.416666667	0.009710498	0.016884001	0.018617787
5.5	0.00995853	0.016941149	0.018724067
5.583333333	0.009806011	0.016925489	0.0188222
5.666666667	0.010168296	0.016879239	0.01873457
5.75	0.010126325	0.016901507	0.018829159
5.833333333	0.010510291	0.016952203	0.018746975
5.916666667	0.010341993	0.016947636	0.018803245
6	0.010516166	0.016928687	0.018633879
6.083333333	0.010552799	0.016948507	0.018929508
6.166666667	0.010799132	0.016978312	0.018876821
6.25	0.010825913	0.016971856	0.018715477
6.333333333	0.010900001	0.016925596	0.018829009
6.416666667	0.010915572	0.016947605	0.018621971
6.5	0.011099073	0.016993448	0.018737484
6.583333333	0.011195414	0.016907982	0.018795081
6.666666667	0.011467614	0.016899595	0.018707557
6.75	0.011471732	0.016890986	0.018787145
6.833333333	0.011566463	0.016959148	0.018629535
6.916666667	0.011670704	0.017018772	0.018551556
7	0.011874812	0.016923385	0.0187706
7.083333333	0.011902741	0.017023565	0.018670851
7.166666667	0.012019853	0.017111199	0.018623334
7.25	0.012112865	0.016956393	0.018687658
7.333333333	0.012192892	0.017081688	0.018650773
7.416666667	0.012242374	0.017072405	0.018802718
7.5	0.012377029	0.016917833	0.018591294
7.583333333	0.012598235	0.017030209	0.018527817
7.666666667	0.012430628	0.017069772	0.018501518
7.75	0.012696395	0.016991674	0.018607806
7.833333333	0.012935524	0.017048957	0.018617147
7.916666667	0.012740097	0.017074615	0.018810813
8	0.012832229	0.017074235	0.018696684

8.083333333	0.013271483	0.016967664	0.01891257
8.166666667	0.012958466	0.01704508	0.018638277
8.25	0.013248218	0.017094348	0.018608624
8.333333333	0.013325507	0.017095463	0.018678651
8.416666667	0.013500851	0.017017191	0.018518142
8.5	0.013779755	0.017004782	0.018674764
8.583333333	0.013671749	0.01710298	0.018659752
8.666666667	0.013784402	0.017101542	0.018610757
8.75	0.013796856	0.017001028	0.018706204
8.833333333	0.013788285	0.017008351	0.018944511
8.916666667	0.013991646	0.016979521	0.018774705
9	0.01400472	0.017046574	0.01856988
9.083333333	0.014189505	0.017138496	0.018597872
9.166666667	0.014238821	0.017070213	0.018495216
9.25	0.014245	0.017096934	0.01856475
9.333333333	0.014243	0.01713887	0.018586372
9.416666667	0.014257358	0.017019152	0.018591092
9.5	0.014263537	0.017096596	0.018634777
9.583333333	0.014269715	0.017140241	0.01860652
9.666666667	0.01400472	0.017139515	0.01857478
9.75	0.014189505	0.017028461	0.018566159
9.833333333	0.014238821	0.017154886	0.018650463
9.916666667	0.014245	0.017076474	0.018498935
10	0.014251179	0.01701293	0.018681397
10.08333333	0.014257358	0.017069941	0.018437202
10.16666667	0.014263537	0.017130085	0.018758952
10.25	0.014269715	0.017072181	0.018744347
10.33333333	0.014189505	0.017060047	0.01848702
10.41666667	0.014238821	0.017133211	0.018772457
10.5	0.014245	0.016993155	0.018597872
10.58333333	0.014251179	0.017026993	0.018495216
10.66666667	0.014257358	0.017084216	0.01856475
10.75	0.014263537	0.017164315	0.018586372
10.83333333	0.014269715	0.017088407	0.018591092
10.91666667	0.01400472	0.016979483	0.018634777
11	0.014189505	0.017162896	0.01860652
11.08333333	0.014238821	0.017126893	0.01857478
11.16666667	0.014245	0.017055771	0.018566159
11.25	0.014251179	0.017121147	0.018650463
11.33333333	0.014257358	0.017073888	0.018498935
11.41666667	0.014263537	0.017113296	0.018681397
11.5	0.014269715	0.017083011	0.018437202
11.58333333	0.014189505	0.017023204	0.018758952
11.66666667	0.014238821	0.017090576	0.018744347
11.75	0.014245	0.017076713	0.01848702
11.83333333	0.014251179	0.017073141	0.018772457
11.91666667	0.014257358	0.017142872	0.018495216
12	0.014263537	0.017101449	0.01856475

5.2.8 Kinetic experiments analysis to determine order

5.2.8.1 The order of catalyst J, donor 78a, acceptor 79n of the overall reaction

The order of catalyst J: catalyst **J**' s order was determined by Burés method according to the literature.[114],[115]

Table 5.11. Concentration for **80n** & Product formation over time multiplied by [catalyst] to the 1.2 power.

	1.0 mol% catalyst **J**		2.0 mol% catalyst **J**		4.0 mol% catalyst **J**	
Time/min	t[**cat**]$^{1.2}$	**[80n]**	t[**cat**]$^{1.2}$	**[80n]**	t[**cat**]$^{1.2}$	**[80n]**
0	0	0.0003	0.0000	0.00745	0.0000	0.00484
15	0.01131	0.0033	0.0259	0.01288	0.0596	0.01734
30	0.02263	0.0061	0.0519	0.01894	0.1191	0.02969
45	0.03394	0.0086	0.0778	0.02489	0.1787	0.04093
60	0.04526	0.0118	0.1037	0.03089	0.2383	0.05256
75	0.05657	0.0149	0.1297	0.03682	0.2979	0.06478
90	0.06788	0.0177	0.1556	0.04275	0.3574	0.07613
105	0.0792	0.0204	0.1815	0.04856	0.4170	0.08771
120	0.09051	0.0238	0.2074	0.05458	0.4766	0.09891
135	0.10183	0.0257	0.2334	0.06029	0.5362	0.11031
150	0.11314	0.0290	0.2593	0.06608	0.5957	0.12062
165	0.12445	0.0320	0.2852	0.07177	0.6553	0.13113
180	0.13577	0.0344	0.3112	0.07739	0.7149	0.1405
195	0.14708	0.0366	0.3371	0.08297	0.7744	0.14999
210	0.1584	0.0397	0.3630	0.0886	0.8340	0.15838
225	0.16971	0.0421	0.3890	0.09379	0.8936	0.16598
240	0.18103	0.0451	0.4149	0.09926	0.9532	0.17261
255	0.19234	0.0478	0.4408	0.10464	1.0127	0.17852
270	0.20365	0.0505	0.4668	0.10964	1.0723	0.18353
285	0.21497	0.0535	0.4927	0.11485	1.1319	0.18768
300	0.22628	0.0558	0.5186	0.11969	1.1915	0.19078
315	0.2376	0.0584	0.5445	0.12481	1.2510	0.19373
330	0.24891	0.0613	0.5705	0.12914	1.3106	0.19577
345	0.26022	0.0636	0.5964	0.13375	1.3702	0.19739
360	0.27154	0.0662	0.6223	0.13793	1.4297	0.19872
375	0.28285	0.0690	0.6483	0.14214	1.4893	0.19969
390	0.29417	0.0714	0.6742	0.14609	1.5489	0.20068
405	0.30548	0.0741	0.7001	0.14993	1.6085	0.20131
420	0.31679	0.0767	0.7261	0.15343	1.6680	0.20204
435	0.32811	0.0797	0.7520	0.15696	1.7276	0.20186
450	0.33942	0.0815	0.7779	0.16033	1.7872	0.20232
465	0.35074	0.0843	0.8038	0.1632	1.8468	0.20287
480	0.36205	0.0865	0.8298	0.1661	1.9063	0.20307
495	0.37336	0.0890	0.8557	0.16864	1.9659	0.20319
510	0.38468	0.0920	0.8816	0.17043	2.0255	0.20304
525	0.39599	0.0938	0.9076	0.17298	2.0850	0.20346
540	0.40731	0.0967	0.9335	0.17487	2.1446	0.20339
555	0.41862	0.0991	0.9594	0.17669	2.2042	0.20321
570	0.42994	0.1008	0.9854	0.17842	2.2638	0.20343
585	0.44125	0.1032	1.0113	0.1796	2.3233	0.20323
600	0.45256	0.1054	1.0372	0.18094	2.3829	0.20333
615	0.46388	0.1079	1.0632	0.18198	2.4425	0.20359
630	0.47519	0.1103	1.0891	0.18291	2.5021	0.20355
645	0.48651	0.1128	1.1150	0.18375	2.5616	0.20341
660	0.49782	0.1145	1.1409	0.18467	2.6212	0.20314
675	0.50913	0.1174	1.1669	0.18589	2.6808	0.20328
690	0.52045	0.1190	1.1928	0.18653	2.7403	0.20374
705	0.53176	0.1212	1.2187	0.18647	2.7999	0.20398
720	0.54308	0.1228	1.2447	0.18694	2.8595	0.20367
735	0.55439	0.1250	1.2706	0.18791	2.9191	0.20334
750	0.5657	0.1277	1.2965	0.18768	2.9786	0.20313
765	0.57702	0.1290	1.3225	0.18755	3.0382	0.20348

780	0.58833	0.1310	1.3484	0.18811	3.0978	0.20338
795	0.59965	0.1331	1.3743	0.18795	3.1574	0.20352
810	0.61096	0.1350	1.4003	0.18848	3.2169	0.20317
825	0.62227	0.1363	1.4262	0.18862	3.2765	0.20312
840	0.63359	0.1383	1.4521	0.18866	3.3361	0.2035
855	0.6449	0.1400	1.4780	0.18885	3.3956	0.20356
870	0.65622	0.1418	1.5040	0.18886	3.4552	0.20357
885	0.66753	0.1437	1.5299	0.18908	3.5148	0.20382
900	0.67884	0.1442	1.5558	0.189	3.5744	0.20303
915	0.69016	0.1459	1.5818	0.18897	3.6339	0.20331
930	0.70147	0.1479	1.6077	0.1888	3.6935	0.20349
945	0.71279	0.1496	1.6336	0.18931	3.7531	0.20351
960	0.7241	0.1510	1.6596	0.18914	3.8127	0.20336
975	0.73542	0.1521	1.6855	0.18924	3.8722	0.20284
990	0.74673	0.1532	1.7114	0.18915	3.9318	0.20305
1005	0.75804	0.1544	1.7373	0.18914	3.9914	0.20315
1020	0.76936	0.1555	1.7633	0.18901	4.0509	0.20325
1035	0.78067	0.1571	1.7892	0.1891	4.1105	0.20342
1050	0.79199	0.1585	1.8151	0.18994	4.1701	0.20309
1065	0.8033	0.1589	1.8411	0.18894	4.2297	0.20246
1080	0.81461	0.1603	1.8670	0.18885	4.2892	0.20294
1095	0.82593	0.1611	1.8929	0.18905	4.3488	0.20285
1110	0.83724	0.1613	1.9189	0.18907	4.4084	0.20299
1125	0.84856	0.1633	1.9448	0.18896	4.4680	0.20347
1140	0.85987	0.1637	1.9707	0.18912	4.5275	0.20332
1155	0.87118	0.1652	1.9967	0.18907	4.5871	0.20257
1170	0.8825	0.1655	2.0226	0.18909	4.6467	0.20232
1185	0.89381	0.1657	2.0485	0.18918	4.7063	0.20288
1200	0.90513	0.1672	2.0744	0.18897	4.7658	0.20268

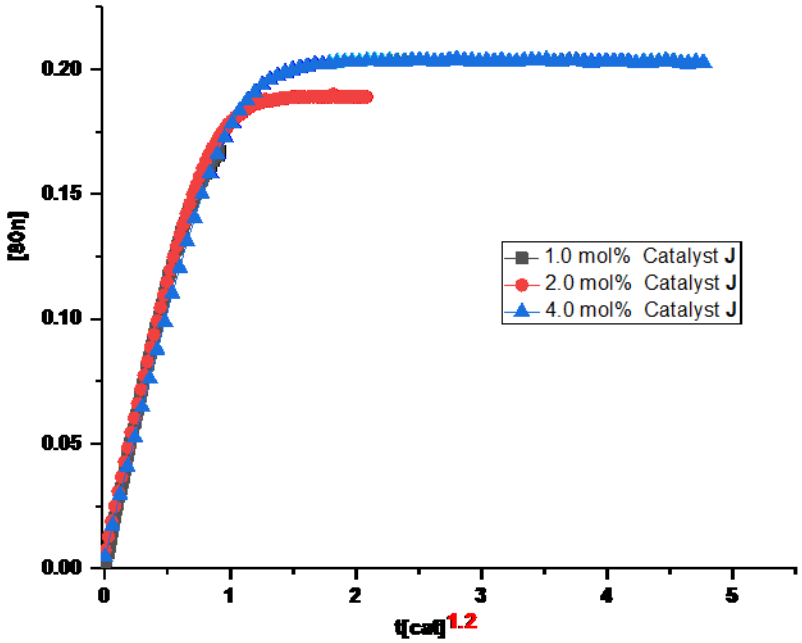

Figure 5.10. Product formation over time multiplied by [**catalyst J**] to the 1.2 power. Graphical overlay represents a 1.2 dependence.

Initial rate method to determine order with respect to donor 78a

Table 5.12. Initial rate of donor **80n** under different concentration of donor **78a**.

Time/mins	$[\mathbf{80n}]_{initial}$ (Donor **78a** = 0.125M)	$[\mathbf{80n}]_{initial}$ (Donor **78a** = 0.25M)	$[\mathbf{80n}]_{initial}$ (Donor **78a** = 0.375M)
15	0.010149164	0.012875205	0.023171831
30	0.015840583	0.018941507	0.031556055
45	0.02029985	0.024891528	0.040501979
60	0.023920862	0.030891828	0.048623108
75	0.027601678	0.036824752	0.055538261
90	0.030641474	0.04274904	0.062253341
105	0.033412465	0.04856081	0.068730045

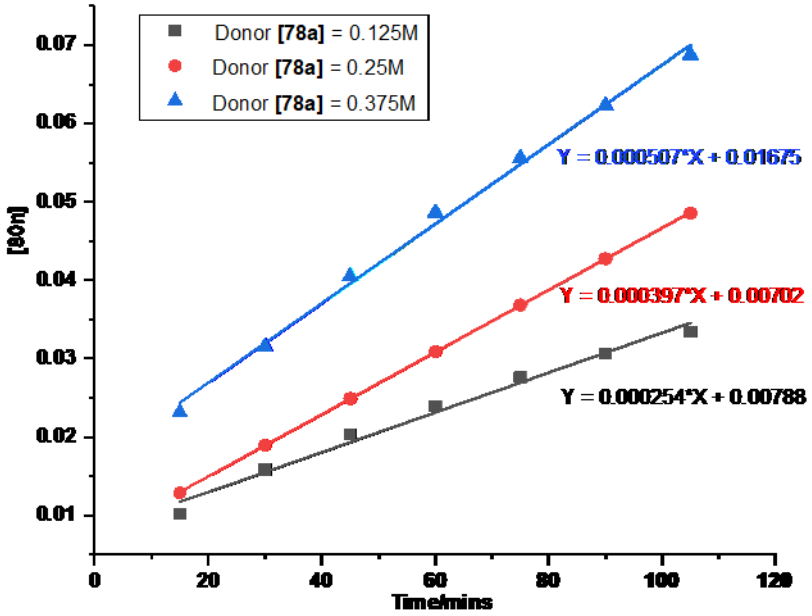

Figure 5.11. Initial rate of product **80n** under different concentration of donor.

Table 5.13. Determination of order with respect to donor **78a**.

Entry	Concentration of **78a**	$[\mathbf{78a}]^{0.5}$	Reaction rate
1	0.125M	0.353553391	0.000254 mmol/min
2	0.25M	0.5	0.000397 mmol/min
3	0.375M	0.612372436	0.000507 mmol/min

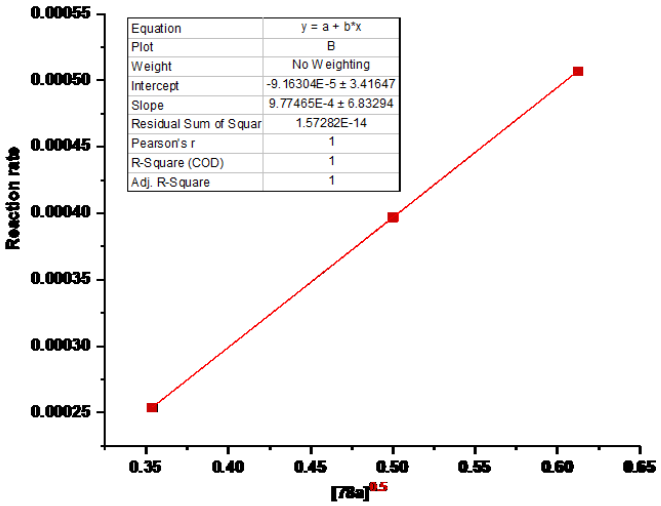

Figure 5.12. Determination of order w.r.t **78a** using initial rate method

Initial rate method to determine order with respect to acceptor 79n

Table 5.14. Initial rate of donor **80n** under different concentration of acceptor **79n**.

Time/mins	$[\mathbf{80n}]_{initial}$ (Acceptor **79n** = 0.25M)	$[\mathbf{80n}]_{initial}$ (Acceptor **79n** = 0.375M)	$[\mathbf{80n}]_{initial}$ (Acceptor **79n** = 0.50M)
15	0.01376	0.01288	0.00613
30	0.02395	0.01894	0.00732
45	0.03726	0.02489	0.0104
60	0.04889	0.03089	0.01212
75	0.06082	0.03682	0.01615
90	0.07271	0.04275	0.01775
105	0.08481	0.04856	0.02091
120	0.09676	0.05458	0.02313
135	0.10868	0.06029	0.02632
150	0.12092	0.06608	0.02803
165	0.13275	0.07177	0.03049
180	0.14446	0.07739	0.03535

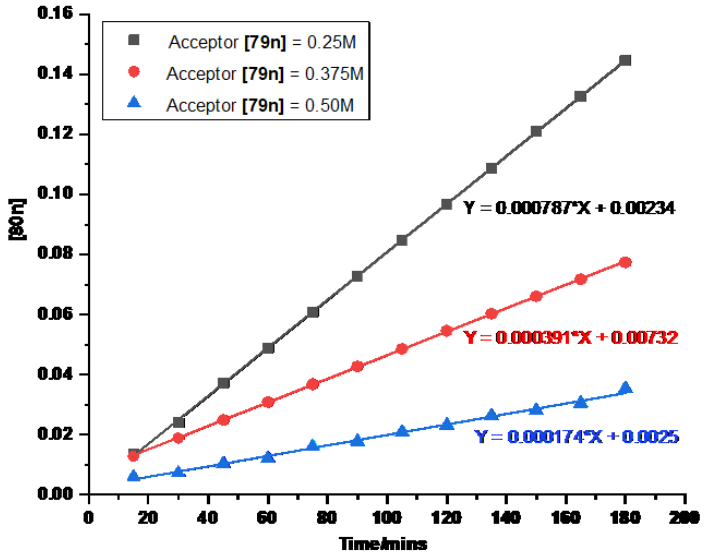

Figure 5.13. Initial rate of product **80n** under different concentration of acceptor **79n**.

Table 5.15. Determination of order with respect to acceptor **79n**.

Entry	Concentration of **79n**	[**79n**]$^{-0.7}$	Reaction rate
1	0.25M	2.639015822	0.000787 mmol/min
2	0.375M	1.98690962	0.000391 mmol/min
3	0.50M	1.624504793	0.000174 mmol/min

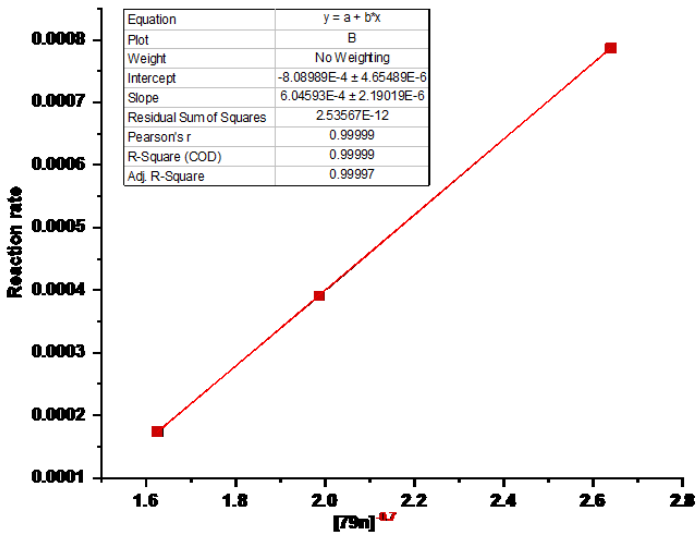

Figure 5.14. Determination of order w.r.t **79n** using initial rate method

5.2.8.2 The order of catalyst J, intermediate 83 and acceptor 79n of the downstream step

Burés method to determine order with respect to catalyst J

Table 5.16. Concentration for **80n** & Product formation over time multiplied by [catalyst] to the 1.1 power

	1.0 mol% catalyst **J**		2.0 mol% catalyst **J**		4.0 mol% catalyst **J**	
Time/min	t**[cat]**$^{1.1}$	**[80n]**	t**[cat]**$^{1.1}$	**[80n]**	t**[cat]**$^{1.1}$	**[80n]**
0	0	0	0	0	0	0
5	0.000426681	0.001303396	0.001117726	0.002250139	0.001428685	0.002350139
10	0.000853361	0.001141359	0.002235452	0.002400277	0.002857369	0.002400277
15	0.001280042	0.001356538	0.003353178	0.002707422	0.004286054	0.002707422
20	0.001706723	0.001501213	0.004470904	0.002943161	0.005714739	0.002943161
25	0.002133404	0.001674877	0.00558863	0.003387869	0.007143423	0.003387869
30	0.002560084	0.002067001	0.006706356	0.003732359	0.008572108	0.003732359
35	0.002986765	0.002147713	0.007824082	0.003997842	0.010000793	0.003997842
40	0.003413446	0.002371864	0.008941808	0.004409203	0.011429477	0.004409203
45	0.003840126	0.00242771	0.010059534	0.00476666	0.012858162	0.00476666
50	0.004266807	0.002585764	0.01117726	0.005233963	0.014286847	0.005233963
55	0.004693488	0.002653771	0.012294986	0.005571606	0.015715531	0.005571606
60	0.005120168	0.002999161	0.013412712	0.005959506	0.017144216	0.005959506
65	0.005546849	0.003017463	0.014530438	0.006353219	0.0185729	0.006520234
70	0.00597353	0.003035424	0.015648164	0.006772896	0.020001585	0.006726917
75	0.006400211	0.003102649	0.01676589	0.007226405	0.02143027	0.007373659
80	0.006826891	0.00344962	0.017883616	0.007649822	0.022858954	0.007719528
85	0.007253572	0.003715008	0.019001343	0.008045616	0.024287639	0.008173315
90	0.007680253	0.003612512	0.020119069	0.008446858	0.025716324	0.00871686
95	0.008106933	0.003909598	0.021236795	0.008725427	0.027145008	0.009203691
100	0.008533614	0.003991046	0.022354521	0.00905207	0.028573693	0.009675574
105	0.008960295	0.00426227	0.023472247	0.009543294	0.030002378	0.010050322
110	0.009386975	0.004225834	0.024589973	0.009828941	0.031431062	0.010334686
115	0.009813656	0.004303283	0.025707699	0.01020221	0.032859747	0.010931785
120	0.010240337	0.004487461	0.026825425	0.010587932	0.034288432	0.011193025
125	0.010667018	0.004584286	0.027943151	0.010946142	0.035717116	0.011751539
130	0.011093698	0.004977048	0.029060877	0.011286493	0.037145801	0.012323566
135	0.011520379	0.00500907	0.030178603	0.011562825	0.038574486	0.012497552
140	0.01194706	0.005303647	0.031296329	0.011943869	0.04000317	0.012894818
145	0.01237374	0.005136527	0.032414055	0.012313545	0.041431855	0.013298308
150	0.012800421	0.005511159	0.033531781	0.012589046	0.04286054	0.013725874
155	0.013227102	0.005642238	0.034649507	0.012859592	0.044289224	0.014128029
160	0.013653782	0.005608459	0.035767233	0.013224876	0.045717909	0.01439336
165	0.014080463	0.005709397	0.036884959	0.013483244	0.047146594	0.014697621
170	0.014507144	0.005930211	0.038002685	0.013693776	0.048575278	0.015072194
175	0.014933825	0.005973292	0.039120411	0.01409764	0.050003963	0.015480096
180	0.015360505	0.006270684	0.040238137	0.014252346	0.051432648	0.015739519
185	0.015787186	0.006391275	0.041355863	0.014481878	0.052861332	0.016038024
190	0.016213867	0.006291027	0.042473589	0.014773471	0.054290017	0.016311658
195	0.016640547	0.006381486	0.043591315	0.015099843	0.055718701	0.016476942
200	0.017067228	0.006598661	0.044709041	0.015176988	0.057147386	0.016857863
205	0.017493909	0.00679134	0.045826767	0.015310585	0.058576071	0.017071657
210	0.017920589	0.006935236	0.046944493	0.015468782	0.060004755	0.017317754
215	0.01834727	0.007159958	0.048062219	0.015642104	0.06143344	0.017483873
220	0.018773951	0.007342589	0.049179945	0.015765478	0.062862125	0.017604311
225	0.019200632	0.007244659	0.050297671	0.01594802	0.064290809	0.017763921
230	0.019627312	0.007524521	0.051415397	0.015971532	0.065719494	0.017875384
235	0.020053993	0.007349194	0.052533123	0.016156747	0.067148179	0.018032751

240	0.020480674	0.007772982	0.053650849	0.016265489	0.068576863	0.018089431
245	0.020907354	0.007738597	0.054768576	0.01636509	0.070005548	0.018238726
250	0.021334035	0.007995206	0.055886302	0.016428835	0.071434233	0.018459805
255	0.021760716	0.008129173	0.057004028	0.016483845	0.072862917	0.018343419
260	0.022187396	0.008051917	0.058121754	0.016499361	0.074291602	0.018461418
265	0.022614077	0.008217736	0.05923948	0.016522247	0.075720287	0.018592097
270	0.023040758	0.008185699	0.060357206	0.016701461	0.077148971	0.018449981
275	0.023467439	0.008621457	0.061474932	0.016605256	0.078577656	0.01855951
280	0.023894119	0.008582504	0.062592658	0.016710188	0.080006341	0.018666229
285	0.0243208	0.00864585	0.063710384	0.01671996	0.081435025	0.018513225
290	0.024747481	0.008865297	0.06482811	0.016780776	0.08286371	0.018650923
295	0.025174161	0.00908036	0.065945836	0.016792551	0.084292395	0.018789136
300	0.025600842	0.009258326	0.067063562	0.016849661	0.085721079	0.018763488
305	0.026027523	0.009284871	0.068181288	0.016772025	0.087149764	0.01856241
310	0.026454203	0.009427526	0.069299014	0.016944123	0.088578449	0.018740916
315	0.026880884	0.009247307	0.07041674	0.016820912	0.090007133	0.018661135
320	0.027307565	0.009474084	0.071534466	0.016797036	0.091435818	0.018718942
325	0.027734246	0.009710498	0.072652192	0.016884001	0.092864502	0.018617787
330	0.028160926	0.00995853	0.073769918	0.016941149	0.094293187	0.018724067
335	0.028587607	0.009806011	0.074887644	0.016925489	0.095721872	0.0188222
340	0.029014288	0.010168296	0.07600537	0.016879239	0.097150556	0.01873457
345	0.029440968	0.010126325	0.077123096	0.016901507	0.098579241	0.018829159
350	0.029867649	0.010510291	0.078240822	0.016952203	0.100007926	0.018746975
355	0.03029433	0.010341993	0.079358548	0.016947636	0.10143661	0.018803245
360	0.03072101	0.010516166	0.080476274	0.016928687	0.102865295	0.018633879
365	0.031147691	0.010552799	0.081594	0.016948507	0.10429398	0.018929508
370	0.031574372	0.010799132	0.082711726	0.016978312	0.105722664	0.018876821
375	0.032001053	0.010825913	0.083829452	0.016971856	0.107151349	0.018715477
380	0.032427733	0.010900001	0.084947178	0.016925596	0.108580034	0.018829009
385	0.032854414	0.010915572	0.086064904	0.016947605	0.110008718	0.018621971
390	0.033281095	0.011099073	0.08718263	0.016993448	0.111437403	0.018737484
395	0.033707775	0.011195414	0.088300356	0.016907982	0.112866088	0.018795081
400	0.034134456	0.011467614	0.089418082	0.016899595	0.114294772	0.018707557
405	0.034561137	0.011471732	0.090535809	0.016890986	0.115723457	0.018787145
410	0.034987817	0.011566463	0.091653535	0.016959148	0.117152142	0.018629535
415	0.035414498	0.011670704	0.092771261	0.017018772	0.118580826	0.018551556
420	0.035841179	0.011874812	0.093888987	0.016923385	0.120009511	0.0187706
425	0.03626786	0.011902741	0.095006713	0.017023565	0.121438196	0.018670851
430	0.03669454	0.012019853	0.096124439	0.017111199	0.12286688	0.018623334
435	0.037121221	0.012112865	0.097242165	0.016956393	0.124295565	0.018687658
440	0.037547902	0.012192892	0.098359891	0.017081688	0.12572425	0.018650773
445	0.037974582	0.012242374	0.099477617	0.017072405	0.127152934	0.018802718
450	0.038401263	0.012377029	0.100595343	0.016917833	0.128581619	0.018591294
455	0.038827944	0.012598235	0.101713069	0.017030209	0.130010303	0.018527817
460	0.039254624	0.012430628	0.102830795	0.017069772	0.131438988	0.018501518
465	0.039681305	0.012696395	0.103948521	0.016991674	0.132867673	0.018607806
470	0.040107986	0.012935524	0.105066247	0.017048957	0.134296357	0.018617147
475	0.040534667	0.012740097	0.106183973	0.017074615	0.135725042	0.018810813
480	0.040961347	0.012832229	0.107301699	0.017074235	0.137153727	0.018696684
485	0.041388028	0.013271483	0.108419425	0.016967664	0.138582411	0.01891257
490	0.041814709	0.012958466	0.109537151	0.01704508	0.140011096	0.018638277
495	0.042241389	0.013248218	0.110654877	0.017094348	0.141439781	0.018608624
500	0.04266807	0.013325507	0.111772603	0.017095463	0.142868465	0.018678651
505	0.043094751	0.013500851	0.112890329	0.017017191	0.14429715	0.018518142
510	0.043521431	0.013779755	0.114008055	0.017004782	0.145725835	0.018674764
515	0.043948112	0.013671749	0.115125781	0.01710298	0.147154519	0.018659752
520	0.044374793	0.013784402	0.116243507	0.017101542	0.148583204	0.018610757
525	0.044801474	0.013796856	0.117361233	0.017001028	0.150011889	0.018706204
530	0.045228154	0.013788285	0.118478959	0.017008351	0.151440573	0.018944511
535	0.045654835	0.013991646	0.119596685	0.016979521	0.152869258	0.018774705
540	0.046081516	0.01400472	0.120714411	0.017046574	0.154297943	0.01856988
545	0.046508196	0.014189505	0.121832137	0.017138496	0.155726627	0.018597872
550	0.046934877	0.014238821	0.122949863	0.017070213	0.157155312	0.018495216
555	0.047361558	0.014245	0.124067589	0.017096934	0.158583997	0.01856475

560	0.047788238	0.014243	0.125185315	0.01713887	0.160012681	0.018586372
565	0.048214919	0.014257358	0.126303042	0.017019152	0.161441366	0.018591092
570	0.0486416	0.014263537	0.127420768	0.017096596	0.162870051	0.018634777
575	0.049068281	0.014269715	0.128538494	0.017140241	0.164298735	0.01860652
580	0.049494961	0.01400472	0.12965622	0.017139515	0.16572742	0.01857478
585	0.049921642	0.014189505	0.130773946	0.017028461	0.167156104	0.018566159
590	0.050348323	0.014238821	0.131891672	0.017154886	0.168584789	0.018650463
595	0.050775003	0.014245	0.133009398	0.017076474	0.170013474	0.018498935
600	0.051201684	0.014251179	0.134127124	0.01701293	0.171442158	0.018681397
605	0.051628365	0.014257358	0.13524485	0.017069941	0.172870843	0.018437202
610	0.052055045	0.014263537	0.136362576	0.017130085	0.174299528	0.018758952
615	0.052481726	0.014269715	0.137480302	0.017072181	0.175728212	0.018744347
620	0.052908407	0.014189505	0.138598028	0.017060047	0.177156897	0.01848702
625	0.053335088	0.014238821	0.139715754	0.017133211	0.178585582	0.018772457
630	0.053761768	0.014245	0.14083348	0.016993155	0.180014266	0.018597872
635	0.054188449	0.014251179	0.141951206	0.017026993	0.181442951	0.018495216
640	0.05461513	0.014257358	0.143068932	0.017084216	0.182871636	0.01856475
645	0.05504181	0.014263537	0.144186658	0.017164315	0.18430032	0.018586372
650	0.055468491	0.014269715	0.145304384	0.017088407	0.185729005	0.018591092
655	0.055895172	0.01400472	0.14642211	0.016979483	0.18715769	0.018634777
660	0.056321852	0.014189505	0.147539836	0.017162896	0.188586374	0.01860652
665	0.056748533	0.014238821	0.148657562	0.017126893	0.190015059	0.01857478
670	0.057175214	0.014245	0.149775288	0.017055771	0.191443744	0.018566159
675	0.057601895	0.014251179	0.150893014	0.017121147	0.192872428	0.018650463
680	0.058028575	0.014257358	0.15201074	0.017073888	0.194301113	0.018498935
685	0.058455256	0.014263537	0.153128466	0.017113296	0.195729798	0.018681397
690	0.058881937	0.014269715	0.154246192	0.017083011	0.197158482	0.018437202
695	0.059308617	0.014189505	0.155363918	0.017023204	0.198587167	0.018758952
700	0.059735298	0.014238821	0.156481644	0.017090576	0.200015852	0.018744347
705	0.060161979	0.014245	0.15759937	0.017076713	0.201444536	0.01848702
710	0.060588659	0.014251179	0.158717096	0.017073141	0.202873221	0.018772457
715	0.06101534	0.014257358	0.159834822	0.017142872	0.204301905	0.018495216
720	0.061442021	0.014263537	0.160952548	0.017101449	0.20573059	0.01856475

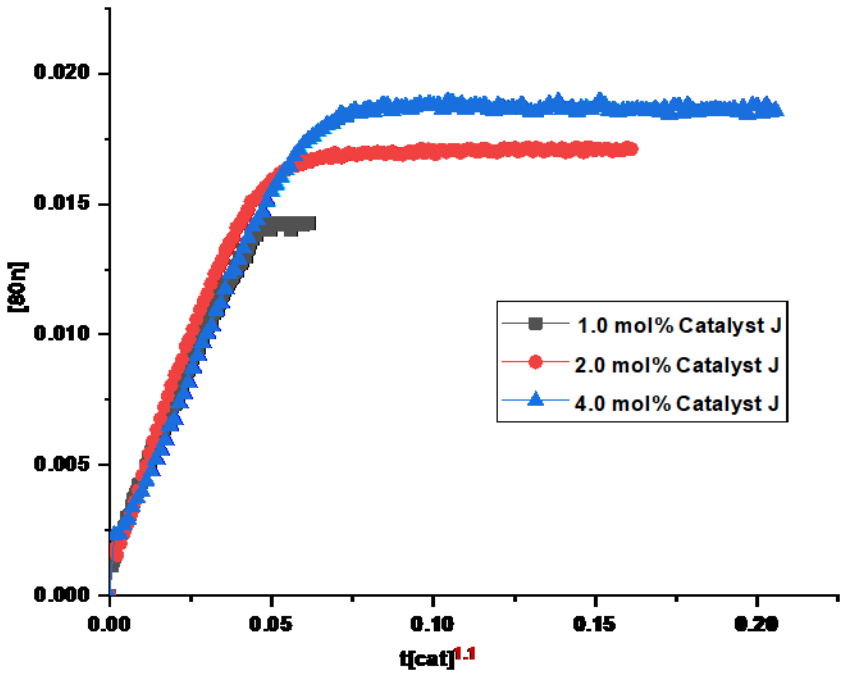

Figure 5.15. Product formation over time multiplied by [**catalyst J**] to the 1.1 power.

Graphical overlay represents a 1.1 dependence.

Initial rate method to determine order with respect to intermediate 83

Table 5.17. Initial rate of donor **80n** under different concentration of intermediate **83**.

Time/mins	$[\mathbf{80n}]_{initial}$ (Intermediate **83** = 0.01M)	$[\mathbf{80n}]_{initial}$ (Intermediate **83** = 0.02M)	$[\mathbf{80n}]_{initial}$ (Intermediate **83** = 0.03M)
5	0.001018559	0.002250139	0.002445645
10	0.001133386	0.002400277	0.002744085
15	0.001361327	0.002707422	0.003140676
20	0.001409775	0.002943161	0.003489459
25	0.001657371	0.003387869	0.00378169
30	0.001959813	0.003732359	0.004161465
35	0.00208164	0.003997842	0.004566873
40	0.002438764	0.004409203	0.005001738
45	0.002657091	0.00476666	0.00536088
50	0.002841954	0.005233963	0.005637585
55	0.003154602	0.005571606	0.006061223
60	0.003334886	0.005959506	0.006342497

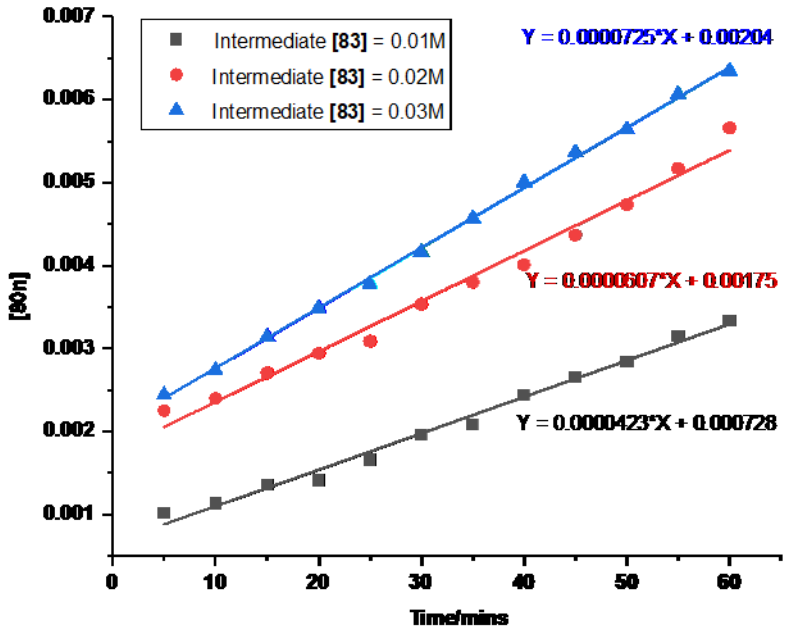

Figure 5.16. Initial rate of product **80n** under different concentration of intermediate **83**.

Table 5.18. Determination of order with respect to intermediate **83**.

Entry	Concentration of **83**	$[\mathbf{83}]^{0.2}$	Reaction rate
1	0.01M	0.398107171	0.0000423 mmol/min
2	0.02M	0.457305052	0.0000607 mmol/min
3	0.03M	0.49593442	0.0000725 mmol/min

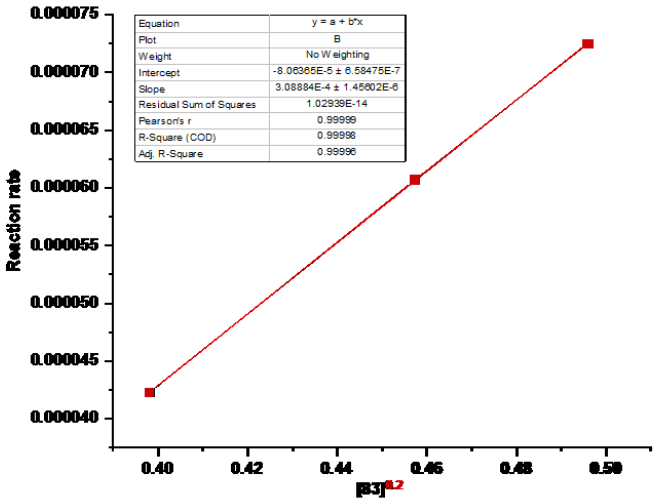

Figure 5.17. Determination of order w.r.t **83** using initial rate method

Initial rate method to determine order with respect to acceptor 79n of the downstream step

Table 5.19. Initial rate of donor **80n** under different concentration of acceptor **79n**.

Time/mins	$[\mathbf{80n}]_{initial}$ (Acceptor **[79n]** = 0.02M)	$[\mathbf{80n}]_{initial}$ (Acceptor **[79n]** = 0.03M)	$[\mathbf{80n}]_{initial}$ (Acceptor **[79n]** = 0.04M)
5	0.001252007	0.002250139	0.000924891
10	0.001889968	0.002400277	0.001115415
15	0.002627733	0.002707422	0.001411238
20	0.003405758	0.002943161	0.00163545
25	0.003994215	0.003387869	0.001905497
30	0.004733537	0.003732359	0.002034402
35	0.005474477	0.003997842	0.00223826
40	0.005866983	0.004409203	0.002674978
45	0.006775113	0.00476666	0.0029193
50	0.0073818	0.005233963	0.003082433
55	0.008029887	0.005571606	0.003275703
60	0.008564403	0.005959506	0.003716667

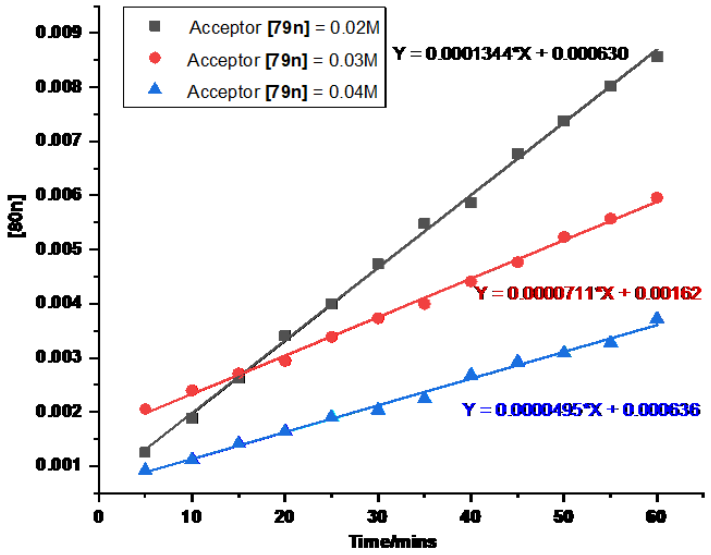

Figure 5.18. Initial rate of product **80n** under different concentration of acceptor **[79n]**.

Table 5.20. Determination of order with respect to acceptor **79n**.

Entry	Concentration of **[79n]**	**[79n]**$^{-2.0}$	Reaction rate
1	0.02M	2500	0.000134 mmol/min
2	0.03M	1111.111111	0.0000711 mmol/min
3	0.04M	625	0.0000495 mmol/min

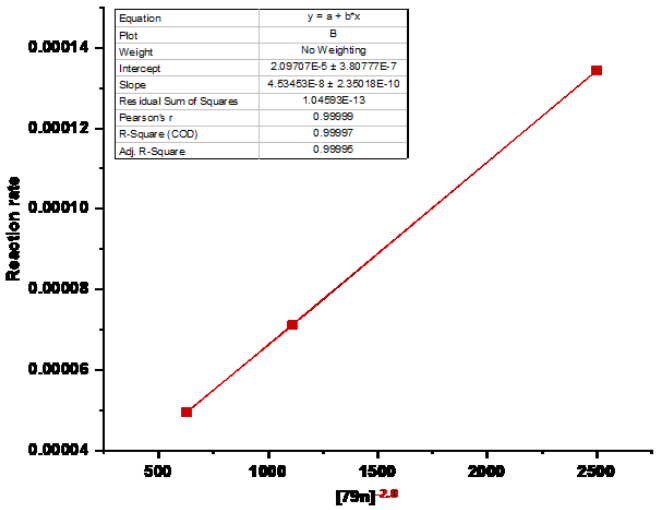

Figure 5.19. Determination of order w.r.t **79n** using initial rate method

5.2.9 Experiments to test the stability of catalyst J with deprotonated alcohol

To a dry NMR tube, glycosyl acceptor **79n** (0.88 mg, 0.01 mmol), base K_2CO_3 (1.38 mg, 0.01 mmol) and 0.5 ml CD_2Cl_2 were added sequently, then catalyst **J** (24.85 mg, 0.00125 mmol) was added later. At the same time, to another dry NMR tube, the same amount of acceptor **79n**, catalyst **J** and CD_2Cl_2 were added. Afterwards, the two tubes were sealed with cap and measured on the NMR spectrometer at room temperature by recording ^1H, ^{13}C and ^{77}Se spectra at 1 hour and 24 hours respectively. As a result, we found that the ^1H, ^{13}C and ^{77}Se NMR were almost the same with the pure catalyst **J**'s spectra (**Fig. 5.20, 5.21** and **5.22**). These phenomena demonstrated that the catalyst **J** remained stable and did not breakdown during the reaction.

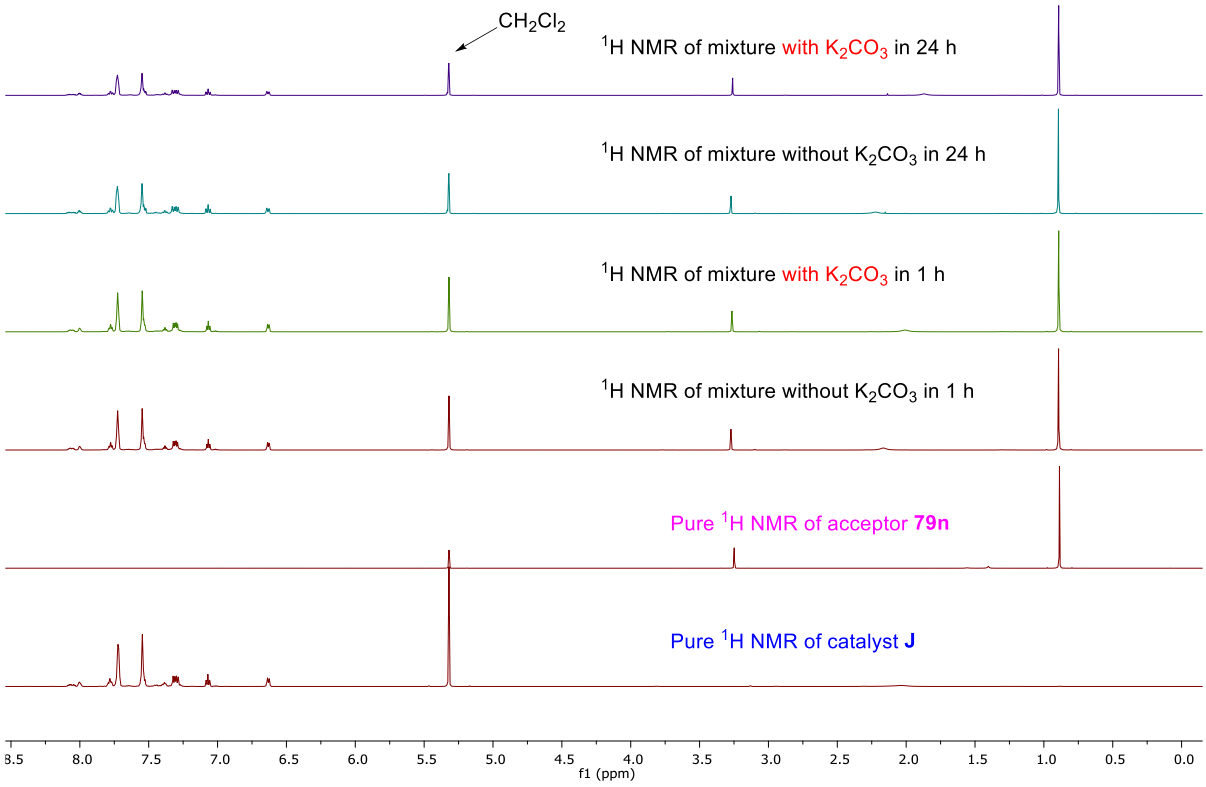

Figure 5.20. ^1H NMR of the experiment to test stability of catalyst **J**

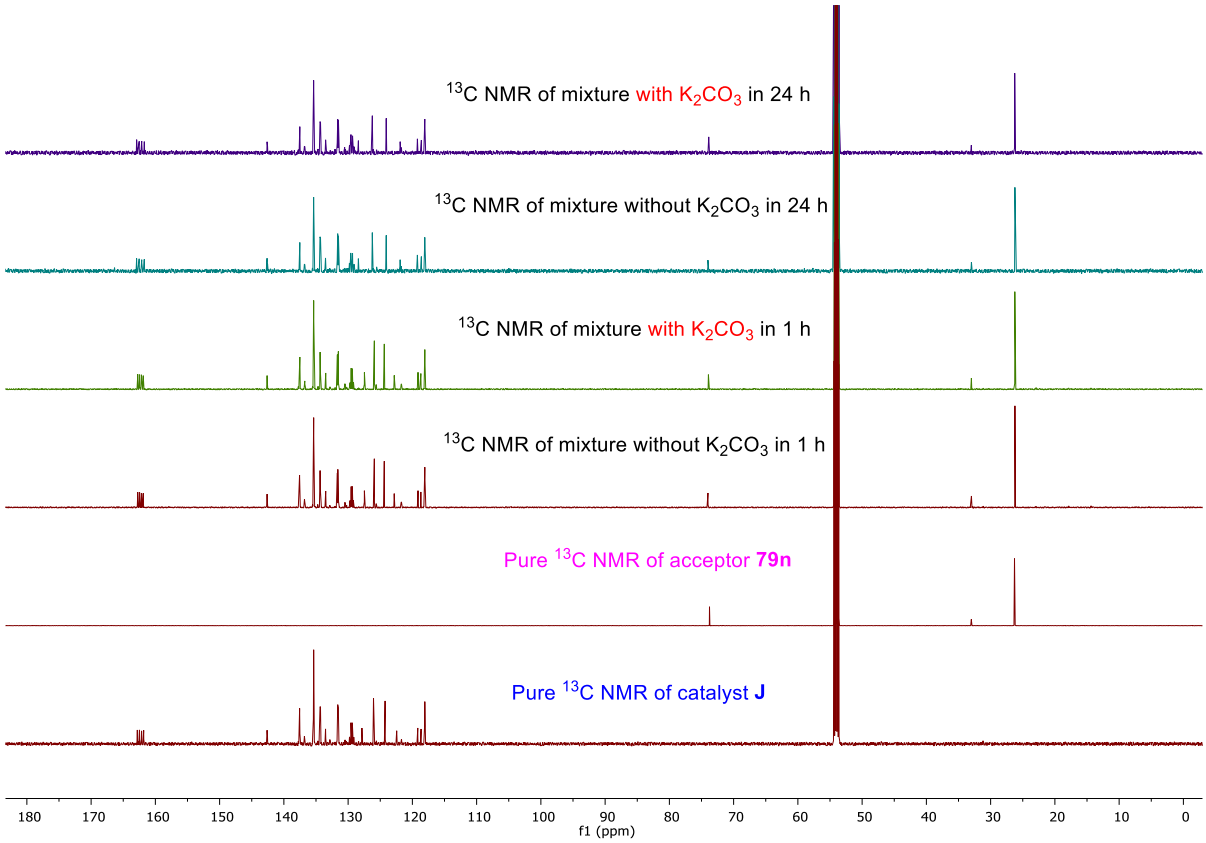

Figure 5.21. ^{13}C NMR of the experiment to test stability of catalyst **J**

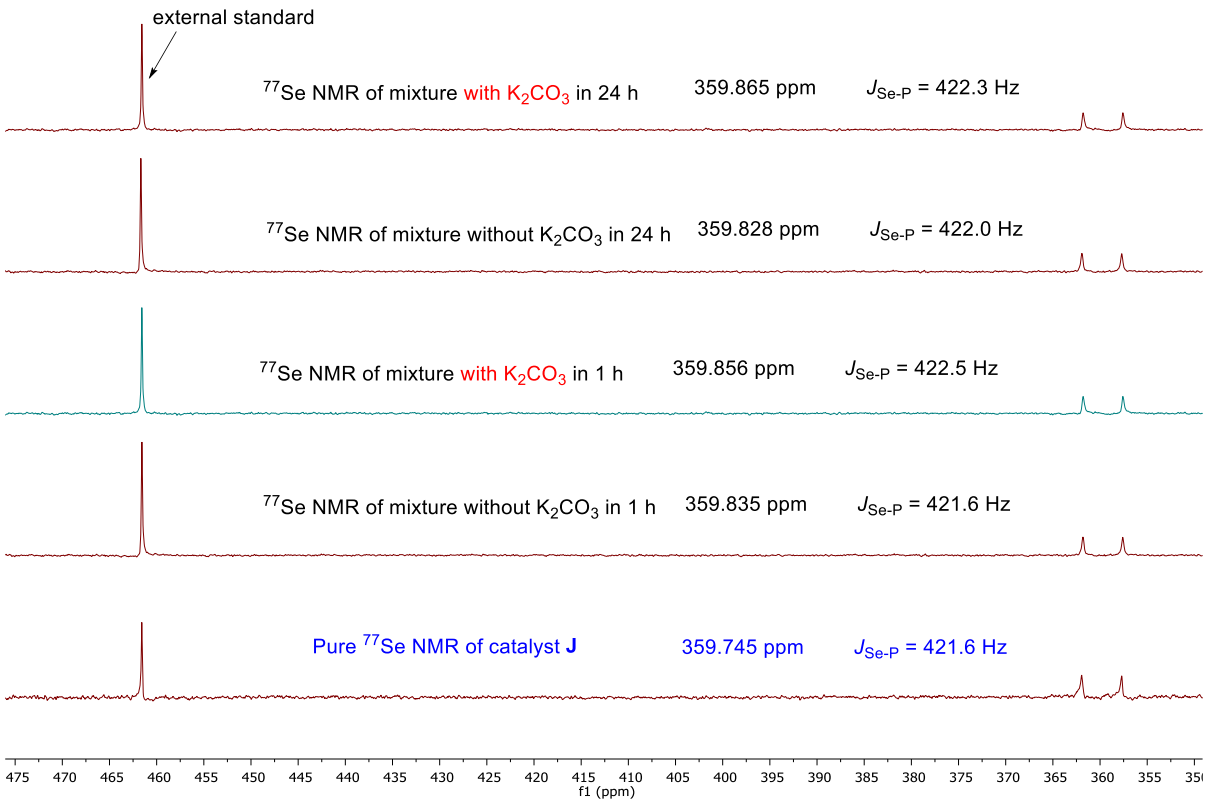

Figure 5.22. ^{77}Se NMR of the experiment to test stability of catalyst **J**

5.3 Experimental part for site selective carbohydrate functionalization

5.3.1 Experiment part for anomeric functionalization

5.3.1.1 Synthesis of starting materials

Synthesis of starting materials: Diols (**95a and 95b)** were prepared according to the previous published protocols.[116] **95c'** and **95c** were prepared using procedure **I** and procedure **II** respectively.

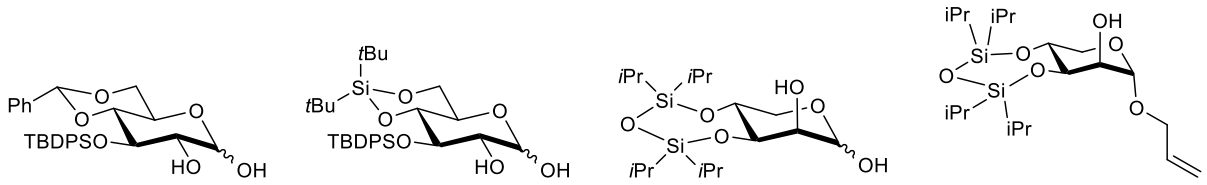

95a **95b** **95c** **95c'**

Procedure I: A mixture of lyxose (380.388 mg, 2 mmol) and imidazole (299.54 mg, 4.4 mmol) were dissolved in anhydrous DMF (15 mL) under an argon atmosphere and the solution was cooled to 0 ºC. and 1,3-dichloro-1,1,3,3-tetraisopropyldisiloxane (946.28 mg, 3 mmol) was added dropwise at this temperature. Afterwards, the solution was quenched with water, and extracted with DCM (20 mL) twice, the organic layer was washed with brine (20 mL), dried over Na_2SO_4, filtered and concentrated in vacuo. Following by column chromatography (PE/EA=20/1), the title compound was obtained **95c'** (677 mg, 78%) as a colorless oil.

Procedure II: A mixture of **95c'** (216.35 mg, 0.5 mmol), $PdCl_2$ (177.325 mg, 1 mmol), and NaOAc (328.135 mg, 4 mmol) in AcOH-H_2O (9:1, v/v, 5 mL) was stirred 2 h at 30 °C. Then, the insoluble material was filtered off. The filtrate was concentrated in vacuo to give a residue which was extracted with EtOAc (20 mL × 2). The combined organic extracts were washed with water (10 mL × 2), saturated aqueous $NaHCO_3$ (15 mL × 2), and brine (15 mL), dried over anhydrous Na_2SO_4, and concentrated. The resulting residue was purified by column chromatography (5:1, petroleum ether-EtOAc) to afford the desired lactol **95c** (98 mg, 50%) as a colorless oil.

5.3.1.2 Characterization data for substrates and anomeric products

Procedure C1: To an oven dried dram vial purged with an argon balloon was charged with (*R,S*)-PPF-P ^{t}Bu$_2$ Josiphos ligand (6.51 mg, 0.012 mmol, 6 mol%), Taylor's boronic acid **89** (11.76 mg, 0.06 mmol, 30 mol%), oxabicycle **96** (0.4 mmol, 2 equiv.), carbohydrate polyol **95** (0.2 mmol, 1 equiv.), $Rh(cod)_2OTf$ (4.68 mg, 0.01 mmol, 5 mol%) and then dry THF (2 mL), DIPEA base (0.4 mmol, 2 equiv.) were added. The dram vial was sealed and the mixture was immersed in a 50 °C oil bath stirred for 2-6 h. Upon completion of the reaction, the reaction mixture was filtered over a short silica plug and flushed with 30-50 mL of ethyl acetate. The filtrate was then evaporated and the determination of the regiomeric ratio (rr) is by ^{1}H-NMR analysis of this concentrated crude mixture with 1,3,5-

trimethoxybenzene as the internal standard. The crude mixture is subsequently dry loaded onto silica gel and subjected to flash column chromatography for purification.

Procedure D1: To an oven dried dram vial purged with an argon balloon was charged with (*S,R*)-PPF-P $^{t}Bu_2$ Josiphos ligand (6.51 mg, 0.012 mmol, 6 mol%), Taylor's boronic acid **89** (11.76 mg, 0.06 mmol, 30 mol%), oxabicycle **96** (0.4 mmol, 2 equiv.), carbohydrate polyol **95** (0.2 mmol, 1 equiv.), $Rh(cod)_2OTf$ (4.68 mg, 0.01 mmol, 5 mol%) and then dry THF (2 mL), DIPEA base (0.4 mmol, 2 equiv.) were added. The dram vial was sealed and the mixture was immersed in a 50 °C oil bath stirred for 16 h. Upon completion of the reaction, the reaction mixture was filtered over a short silica plug and flushed with 30-50 mL of ethyl acetate. The filtrate was then evaporated and the determination of the regiomeric ratio (rr) is by ^{1}H-NMR analysis of this concentrated crude mixture with 1,3,5-trimethoxybenzene as the internal standard. The crude mixture is subsequently dry loaded onto silica gel and subjected to flash column chromatography for purification.

(*5aR,8S,9S,9aR*)-8-(allyloxy)-2,2,4,4-tetraisopropyltetrahydro-6*H*-pyrano[3,4-f][1,3,5,2,4]trioxadisilepin-9-ol(95c')

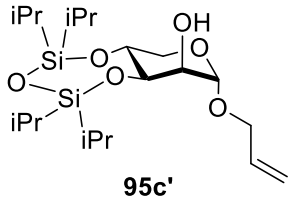

95c'

The title product compound is prepared according to the general procedure **I**. **^{1}H NMR** (600 MHz, $CDCl_3$) δ 5.97 – 5.86 (m, 1H), 5.30 (dd, J = 17.4, 3.6 Hz, 1H), 5.21 (dd, J = 10.8, 3.0 Hz, 1H), 4.88 (s, 1H), 4.26 – 4.16 (m, 1H), 4.08 – 3.96 (m, 2H), 3.92 – 3.86 (m, 2H), 3.67 (dd, J = 10.8, 5. Hz, 1H), 3.49 (t, J = 10.8 Hz, 1H), 2.68 (s, 1H), 1.09 – 1.00 (m, 28H). **^{13}C NMR** (151 MHz, $CDCl_3$) δ 134.00, 117.55, 98.16, 74.86, 71.31, 69.87, 68.05, 62.15, 17.66, 17.64, 17.52, 17.42, 17.35, 17.34, 17.32, 13.08, 13.06, 12.36, 12.20. **ESI-HRMS**: Calculated for $C_{20}H_{40}O_6NaSi_2$ $(M+Na)^+$: 455.22556, Found: 455.22514, $[a]_D^{20}$ =+40.2 (c =0.73, $CHCl_3$).

(*5aR,9S,9aR*)-2,2,4,4-tetraisopropyltetrahydro-6*H*-pyrano[3,4-f][1,3,5,2,4]trioxadisilepine-8,9-diol(95c)

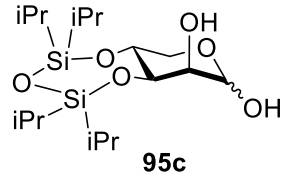

95c

The title product compound is prepared according to the general procedure **II**. **^{1}H NMR** (600 MHz, $CDCl_3$) δ 5.28 (d, J = 3.0 Hz, 1H), 4.71 (d, J = 12.0 Hz, 1H), 4.08 – 4.01 (m, 1H), 4.01 – 3.95 (m, 1H), 3.97 – 3.90 (m, 3.5H), 3.86 (d, J = 11.4 Hz, 1H), 3.74 – 3.67 (m, 3H), 3.21 – 3.14 (m, 1H), 2.69 (d, J = 12.6 Hz, 2H), 2.48 (d, J = 3.0z Hz, 1H), 2.06 (d, J = 3.0 Hz, 0.5H), 1.12 – 0.98 (m, 55H). **^{13}C NMR** (151 MHz, $CDCl_3$) δ 94.67, 93.98, 77.08, 74.41, 71.40, 71.33, 69.82, 69.58, 65.84, 62.19, 17.64, 17.61, 17.53, 17.49, 17.40, 17.33, 17.31, 17.29, 13.07, 13.03, 12.31, 12.20. **ESI-HRMS**: Calculated for $C_{17}H_{36}O_6NaSi_2$ $(M+Na)^+$: 415.19426, Found: 415.19413. $[a]_D^{20}$ =+19.1 (c =0.59, $CHCl_3$).

(*2R,4aR,6S,7R,8R,8aR*)-8-((tert-butyldiphenylsilyl)oxy)-6-(((*1R,2R*)-1-hydroxy-1,2-dihydronaphthalen-2-yl)oxy)-2-phenylhexahydropyrano[3,2-d][1,3]dioxin-7-ol(97a)

The title product compound is prepared according to the general procedure **C1** with 5 mol% $Rh(cod)_2OTf$ catalyst, 30 mol% Taylor's boronic acid **89**, oxabicycle **96** (0.4 mmol, 2 equiv.), and 0.2 mmol carbohydrate polyol **95a** at 50 °C for 2 h and isolated by flash column chromatography (10:1-5:1 Pentane: Ethyl Acetate) giving **97a** as a yellow solid (98.0 mg, 75% yield, rr >20:1 (C1:C2), dr > 20:1(trans:cis)).

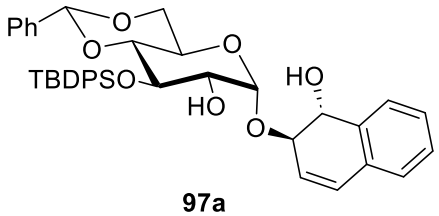

97a

^{1}H NMR (600 MHz, $CDCl_3$) δ 7.68 – 7.61 (m, 4H), 7.56 (d, J = 7.8 Hz, 1H), 7.45 – 7.34 (m, 2H), 7.34 – 7.29 (m, 3H), 7.29 – 7.26 (m, 3H), 7.26 – 7.20 (m, 3H), 7.15 – 7.12 (m, 2H), 7.05 (d, J = 7.2 Hz, 1H), 6.35 (dd, J = 10.2, 2.4 Hz, 1H), 5.85 (dd, J = 9.6, 1.8 Hz, 1H), 5.25 (s, 1H), 5.12 (d, J = 4.2 Hz, 1H), 4.86 (d, J = 11.4 Hz, 1H), 4.38 (d, J = 10.8 Hz, 1H), 4.23 (dd, J = 10.2, 4.8 Hz, 1H), 4.18 (t, J = 9.0 Hz, 1H), 4.00 – 3.91 (m, 1H), 3.86 – 3.78 (m, 2H), 3.67 (t, J = 10.2 Hz, 1H), 3.55 (t, J = 9.6 Hz, 1H), 2.31 (d, J = 5.4 Hz, 1H), 1.03 (s, 9H). **^{13}C NMR** (151 MHz, $CDCl_3$) δ 137.16, 136.09, 136.03, 136.03, 136.02, 133.79, 133.78, 132.14, 129.96, 129.79, 129.38, 128.92, 128.07, 128.05, 127.89, 127.75, 127.61, 126.40, 126.32, 124.48, 101.80, 101.72, 85.57, 81.45, 74.56, 74.05, 73.55, 69.04, 63.49, 27.12, 19.69. **ESI-HRMS**: Calculated for $C_{39}H_{42}ONaSi$ $(M+Na)^+$: 673.25920, Found: 673.25810. $[\alpha]_D^{20}$ = -13.9 (c =0.18, $CHCl_3$).

(*2R,4aR,6S,7R,8R,8aR*)-8-((tert-butyldiphenylsilyl)oxy)-6-(((*1S,2S*)-1-hydroxy-1,2-dihydronaphthalen-2-yl)oxy)-2-phenylhexahydropyrano[3,2-d][1,3]dioxin-7-ol(97a')

(*2R,4aR,7R,8S,8aR*)-8-((tert-butyldiphenylsilyl)oxy)-7-(((*1S,2S*)-1-hydroxy-1,2-dihydronaphthalen-2-yl)oxy)-2-phenylhexahydropyrano[3,2-d][1,3]dioxin-6-ol (97a'')

The title product compound is prepared according to the general procedure **D1** with 5 mol% $Rh(cod)_2OTf$ catalyst, 30 mol% Taylor's boronic acid **89**, oxabicycle **96** (0.4 mmol, 2 equiv.), and 0.2 mmol carbohydrate polyol **95a** at 50 ºC for 16 h and isolated by flash column chromatography (10:1-5:1 Pentane: Ethyl Acetate) giving C1 regioisomer **97a'** (33.0 mg, dr > 20:1(trans:cis)) as a yellow solid and C2 regioisomer **97a''** (34.0 mg, dr > 20:1(trans:cis)) as a yellow solid (67 mg combined total mass of **97a'** and **97a''**, 51% combined yield of **97a'** and **97a''**, rr 1:1(C1:C2)).

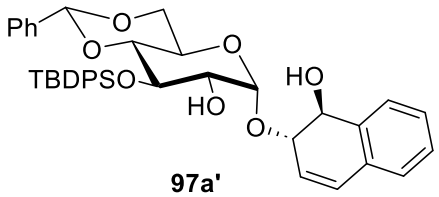

97a'

^{1}H NMR (700 MHz, $CDCl_3$) δ 7.68 – 7.61 (m, 4H), 7.56 (d, J = 7.7 Hz, 1H), 7.42 – 7.37 (m, 1H), 7.37 – 7.34 (m, 1H), 7.33 – 7.28 (m, 3H), 7.28 – 7.26 (m, 2H), 7.25 – 7.21 (m, 4H), 7.16 – 7.12 (m, 2H), 7.05 (d, J = 7.0 Hz, 1H), 6.42 (dd, J = 10.5, 2.1 Hz, 1H), 5.78 (dd, J = 9.1, 2.1 Hz, 1H), 5.30 (s, 1H), 5.13 (d, J = 4.2 Hz, 1H), 4.97 – 4.84 (m, 1H), 4.47 (dt, J = 10.5, 2.1 Hz, 1H), 4.25 (dd, J = 9.8, 4.9 Hz, 1H), 4.03 (t, J = 9.1 Hz, 1H), 3.93 (td, J = 9.8, 4.9 Hz, 1H), 3.77 (td, J = 8.4, 4.2 Hz, 1H), 3.70 (t, J = 10.5 Hz, 1H), 3.59 (t, J = 9.1 Hz, 1H), 3.39 (d, J = 3.5 Hz, 1H), 1.76 (d, J = 8.4 Hz, 1H), 1.03 (s, 9H). **^{13}C NMR** (176 MHz, $CDCl_3$) δ 137.08, 136.28, 136.07, 135.51, 134.19, 133.73, 131.87, 129.79, 129.62, 129.21, 128.94, 128.37, 128.07, 128.04, 127.64, 127.48, 126.90, 126.47, 126.44, 125.34, 101.75, 98.68, 82.83, 81.38, 73.71, 73.57, 72.72, 68.81, 63.73, 27.13, 19.76. **ESI-HRMS**: Calculated for $C_{39}H_{42}ONaSi$ $(M+Na)^+$: 673.25920, Found: 673.25823. $[\alpha]_D^{20}$ = +175.0 (c =0.22, $CHCl_3$).

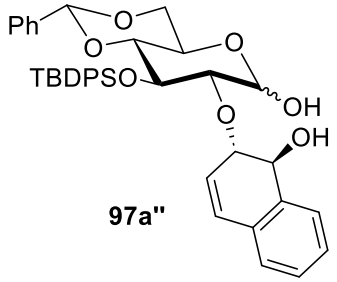

97a''

^{1}H NMR (700 MHz, $CDCl_3$) δ 7.67 – 7.55 (m, 4H), 7.48 (d, J = 7.7 Hz, 2H), 7.41 – 7.30 (m, 2H), 7.28 – 7.26 (m, 3H), 7.25 – 7.20 (m, 3H), 7.20 – 7.15 (m, 2H), 7.15 – 7.10 (m, 2H), 7.08 – 7.00 (m, 2H), 6.65 (d, J = 7.7 Hz, 2H), 6.42 – 6.32 (m, 2H), 6.26 (d, J = 9.8 Hz, 1H), 5.97 (d, J = 10.5 Hz, 1H), 5.11 (d, J = 11.9 Hz, 1H), 4.99 (d, J = 11.9 Hz, 2H), 4.82 (d, J = 7.0 Hz, 1H), 4.72 (s, 1H), 4.57 (d, J = 10.5 Hz, 1H), 4.19 – 4.11 (m, 2H), 4.03 (t, J = 9.1 Hz, 1H), 3.90 (t, J = 7.7 Hz, 1H), 3.70 (s, 1H), 3.57 (t, J = 9.8 Hz, 1H), 3.51 (t, J = 9.1 Hz, 1H),), 3.22 – 3.13 (m, 1H), 0.93 (s, 7H). **^{13}C NMR** (176 MHz, $CDCl_3$) δ 136.60, 136.37, 136.21, 135.94, 135.40, 135.32, 132.63, 132.59, 132.26, 129.81, 129.56, 129.44, 129.18, 128.79, 128.26, 128.02, 127.88, 127.85, 127.83, 127.77, 127.40, 127.26, 126.60, 126.26, 126.16, 124.95, 124.49, 105.09, 101.76, 84.55, 82.70, 80.96, 80.81, 75.58, 74.52, 73.17, 68.59, 66.07,

26.98, 19.84. **ESI-HRMS**: Calculated for $C_{39}H_{42}ONaSi$ $(M+Na)^+$: 673.25920, Found: 673.25888. $[\alpha]_D^{20}$ = +84.2 (c =0.19, $CHCl_3$).

(*4aR,6S,7R,8R,8aR*)-2,2-di-tert-butyl-8-((tert-butyldiphenylsilyl)oxy)hexahydropyrano[3,2-d][1,3,2]dioxasiline-6,7-diol (97b)

The title product compound is prepared according to the general procedure **C1** with 5 mol% $Rh(cod)_2OTf$ catalyst, 30 mol% Taylor's boronic acid **89**, oxabicycle **96** (0.4 mmol, 2 equiv.), and 0.2 mmol carbohydrate polyol **95b** at 50 °C for 2 h and isolated by flash column chromatography (10:1-5:1 Pentane: Ethyl Acetate) giving **97b** as a yellow solid (91.0 mg, 65% yield, rr >20:1 (C1:C2), dr > 20:1(trans:cis)).

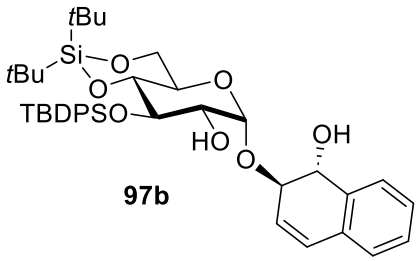

97b

^{1}H NMR (600 MHz, $CDCl_3$) δ 7.83 – 7.80 (m, 2H), 7.75 – 7.70 (m, 2H), 7.50 (d, J = 7.2 Hz, 1H), 7.46 – 7.34 (m, 6H), 7.25 – 7.18 (m, 2H), 7.07 – 6.97 (m, 1H), 6.32 (dd, J = 10.2, 2.4 Hz, 1H), 5.79 (dd, J = 9.6, 1.8 Hz, 1H), 4.95 (d, J = 3.6 Hz, 1H), 4.73 (d, J = 11.4 Hz, 1H), 4.28 (td, J = 11.4 Hz, J = 2.4 Hz 1H), 4.12 – 4.06 (m, 1H), 3.98 – 3.93 (m, 1H), 3.91 – 3.84 (m, 3H), 3.79 (d, J = 2.4 Hz, 1H), 3.68 – 3.62 (m, 1H), 1.90 (d, J = 5.4 Hz, 1H), 1.12 (s, 9H), 1.10 (s, 9H), 0.98 (s, 9H). **^{13}C NMR** (151 MHz, $CDCl_3$) δ 136.51, 136.12, 135.51, 135.20, 132.74, 132.08, 130.12, 130.01, 129.44, 128.14, 128.00, 127.95, 127.68, 126.26, 124.52, 101.51, 85.39, 77.82, 76.25, 73.98, 73.86, 67.41, 66.87, 27.74, 27.20, 27.15, 22.92, 20.08, 19.88. **ESI-HRMS**: Calculated for $C_{40}H_{54}O_7NaSi_2$ $(M+Na)^+$: 725.33003, Found: 725.32924. $[\alpha]_D^{20}$ = -7.7 (c =0.43, $CHCl_3$).

(*5aR,8S,9S,9aR*)-8-(((*1R,2R*)-1-hydroxy-1,2-dihydronaphthalen-2-yl)oxy)-2,2,4,4-tetraisopropyltetrahydro-6*H*-pyrano[3,4-f][1,3,5,2,4]trioxadisilepin-9-ol (97c)

The title product compound is prepared according to the general procedure **C1** with 5 mol% $Rh(cod)_2OTf$ catalyst, 30 mol% Taylor's boronic acid **89**, oxabicycle **96** (0.4 mmol, 2 equiv.), and 0.2 mmol carbohydrate polyol **95c** at 50 °C for 6 h and isolated by flash column chromatography (15:1-8:1 Pentane: Ethyl Acetate) giving **97c** as a yellow solid (66.0 mg, 61% yield, rr >20:1 (C1:C2), dr > 20:1(trans:cis)).

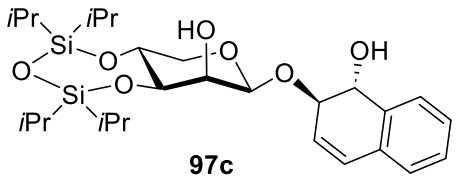

97c

^{1}H NMR (500 MHz, $CDCl_3$) δ 7.66 (d, J = 7.5 Hz, 1H), 7.29 – 7.24 (m, 1H), 7.21 (t, J = 7.5 Hz, 1H), 7.05 (d, J = 7.0 Hz, 1H), 6.39 (dd, J = 10.0, 2.5 Hz, 1H), 5.86 (dd, J = 10.0, 2.0 Hz, 1H), 5.07 (d, J = 11.0 Hz, 1H), 4.59 (s, 1H), 4.56 (t, J = 2.0 Hz, 1H), 4.46 (s, 1H), 4.16 – 4.12 (m, 1H), 4.11 (d, J = 2.5 Hz, 1H), 4.06 (dd, J = 11.5, 6.0 Hz, 1H), 3.70 (dd, J = 8.5, 3.5 Hz, 1H), 3.24 (dd, J = 11.5, 10.0 Hz, 1H), 2.66 (s, 1H), 1.12 – 0.98 (m, 28H). **^{13}C NMR** (126 MHz, $CDCl_3$) δ 135.88, 131.85, 128.50, 128.42, 128.24, 127.67, 126.20, 125.11, 101.75, 86.57, 77.05, 72.82, 71.66, 69.35, 66.22, 17.69, 17.61, 17.46, 17.45, 17.36, 17.32, 17.29, 13.09, 12.99, 12.30, 12.27. **ESI-HRMS**: Calculated for $C_{27}H_{44}O_7NaSi_2$ $(M+Na)^+$: 559.25178, Found: 559.25097. $[\alpha]_D^{20}$ = -33.2 (c =0.69, $CHCl_3$).

(*5aR,8S,9S,9aR*)-8-(((*1S,2S*)-1-hydroxy-1,2-dihydronaphthalen-2-yl)oxy)-2,2,4,4-tetraisopropyltetrahydro-6*H*-pyrano[3,4-f][1,3,5,2,4]trioxadisilepin-9-ol (97c')

(*5aR,9S,9aR*)-9-(((*1S,2S*)-1-hydroxy-1,2-dihydronaphthalen-2-yl)oxy)-2,2,4,4-tetraisopropyltetrahydro-6*H*-pyrano[3,4-f][1,3,5,2,4]trioxadisilepin-8-ol (97c'')

The title product compound is prepared according to the general procedure **D1** with 5 mol% $Rh(cod)_2OTf$ catalyst, 30 mol% Taylor's boronic acid **89**, oxabicycle **96** (0.4 mmol, 2 equiv.), and 0.2 mmol carbohydrate polyol **95c** at 50 °C for 16 h and isolated by flash column chromatography (15:1-8:1 Pentane: Ethyl Acetate) giving inseparable mixture of **97c'** and **97c''** as a white solid (59.0 mg, 55% yield, rr 2:1 (C1:C2), dr > 20:1(trans:cis)).

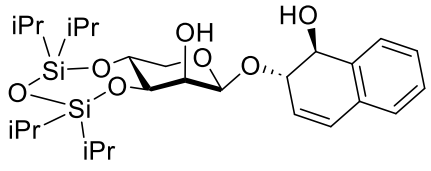

97c'

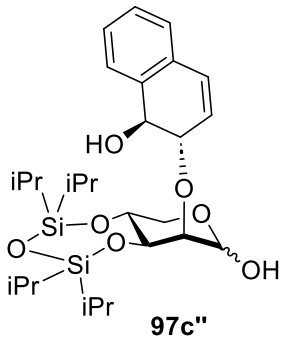

97c''

^{1}H NMR (700 MHz, $CDCl_3$) δ 7.65 – 7.57 (m, 2H), 7.25 – 7.18 (m, 3H), 7.09 – 7.01 (m, 2H), 6.45 – 6.38 (m, 1.3H), 6.35 (dd, J = 9.8, 2.8 Hz, 0.6H), 6.10 (dd, J = 9.8, 2.1 Hz, 0.3H), 6.07 (dd, J = 9.8, 2.1 Hz, 1H), 5.90 (dd, J = 9.8, 2.1 Hz, 0.6H), 5.25 – 5.20 (m, 0.5H), 5.08 (d, J = 11.2 Hz, 1H), 5.02 (d, J = 11.9 Hz, 1H), 4.76 (s, 1H), 4.71 (d, J = 10.5 Hz, 0.3H), 4.64 (dt, J = 11.2, 2.1 Hz, 1H), 4.58 (dt, J = 11.2, 2.1 Hz, 0.3H), 4.50 (d, J = 2.1 Hz, 0.6H), 4.35 (dt, J = 11.9, 2.1 Hz, 0.6H), 4.27 – 4.21 (m, 0.6H), 4.19 – 4.14 (m, 0.3H), 4.12 – 4.06 (m, 2.5H), 4.02 – 3.94 (m, 2H), 3.92 (d, J = 2.8 Hz, 0.3H), 3.79 (dd, J =

11.2, 5.6 Hz, 0.6H), 3.77 – 3.73 (m, 0.3H), 3.70 – 3.66 (m, 1.5H), 3.49 (d, J = 10.5 Hz, 0.3H), 3.19 (dd, J = 11.9, 9.8 Hz, 0.3H), 3.14 (dd, J = 11.9, 10.5 Hz, 1H), 2.95 (s, 1H), 2.69 (s, 1H), 2.52 (d, J = 2.8 Hz, 0.6H), 1.14 – 0.98 (m, 51H). **^{13}C NMR** (176 MHz, $CDCl_3$) δ 136.73, 136.54, 135.98, 132.25, 132.11, 131.94, 129.99, 129.64, 128.62, 128.60, 128.37, 128.08, 128.03, 127.96, 127.93, 127.91, 127.91, 127.65, 127.42, 126.36, 126.36, 126.22, 126.04, 125.06, 124.77, 124.49, 100.96, 94.63, 94.18, 86.26, 85.58, 82.90, 81.44, 79.98, 78.13, 77.09, 74.82, 74.52, 73.74, 72.96, 71.27, 70.00, 69.77, 69.62, 66.49, 66.24, 62.92, 17.71, 17.70, 17.65, 17.62, 17.61, 17.46, 17.46, 17.46, 17.44, 17.37, 17.37, 17.35, 17.33, 17.31, 17.30, 17.28, 17.25, 17.22, 13.11, 13.08, 13.02, 12.94, 12.88, 12.58, 12.57, 12.35, 12.32, 12.31, 12.29. **ESI-HRMS**: Calculated for $C_{27}H_{44}O_7NaSi_2$ $(M+Na)^+$: 559.25178, Found: 559.25042. $[\alpha]_D^{20}$ = +55.3 (c =0.27, $CHCl_3$).

5.3.2 Experiment part for anomeric functionalization

Synthesis of starting materials: The allylic carbonate (**99a-99d**)[117] and methyl α-D-lyxopyranoside(**98c**)[118] were prepared according to the previous published protocols.

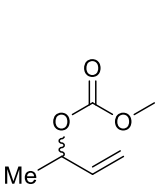

99a

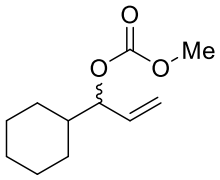

99b

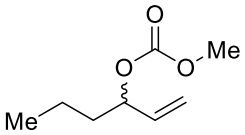

99c

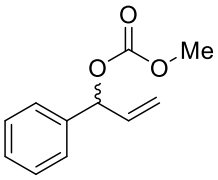

99d

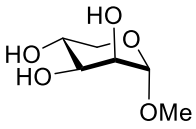

98c

5.3.2.1 Characterization data for allylic carbonate functionalization products

Procedure E1: To an oven dried dram vial purged with an argon balloon was charged with (*S*)-NPN ligand (5.82 mg, 0.012 mmol, 6 mol%), Taylor's boronic acid **89** (11.76 mg, 0.06 mmol, 30 mol%), allylic carbonate **99** (0.24 mmol, 1.2 equiv.), carbohydrate polyol **98** (0.2 mmol, 1 equiv.), $Rh(cod)_2BF_4$ (4.06 mg, 0.01 mmol, 5 mol%) and then dry acetonitrile (1 mL), DIPEA base (0.4 mmol, 2 equiv.) were added. The dram vial was sealed and the mixture was immersed in a 50 °C oil bath stirred for 18-41 h. Upon completion of the reaction, the reaction mixture was filtered over a short silica plug and flushed with 30-50 mL of ethyl acetate. The filtrate was then evaporated and the determination of the regiomeric ratio (rr) is by ^{1}H-NMR analysis of this concentrated crude mixture with 1,3,5-trimethoxybenzene as the internal standard. The crude mixture is subsequently dry loaded onto silica gel and subjected to flash column chromatography for purification.

Procedure F1: To an oven dried dram vial purged with an argon balloon was charged with (*R*)-NPN ligand (5.82 mg, 0.012 mmol, 6 mol%), Taylor's boronic acid **89** (11.76 mg, 0.06 mmol, 30 mol%), allylic carbonate **99** (0.24 mmol, 1.2 equiv.), carbohydrate polyol **98** (0.2 mmol, 1 equiv.), $Rh(cod)_2BF_4$ (4.06 mg, 0.01 mmol, 5 mol%) and then dry acetonitrile (1 mL), DIPEA base (0.4 mmol, 2 equiv.) were added. The dram vial was sealed and the mixture was immersed in a 50 °C oil bath stirred for 18-24 h. Upon completion of the reaction, the reaction mixture was filtered over a short silica plug and flushed

with 30-50 mL of ethyl acetate. The filtrate was then evaporated and the determination of the regiomeric ratio (rr) is by ^{1}H-NMR analysis of this concentrated crude mixture with 1,3,5-trimethoxybenzene as the internal standard. The crude mixture is subsequently dry loaded onto silica gel and subjected to flash column chromatography for purification.

(*2R,3S,5S,6S*)-5-(((*R*)-but-3-en-2-yl)oxy)-2-(((tert-butyldimethylsilyl)oxy)methyl)-6-methoxytetrahydro-2*H*-pyran-3,4-diol(100a)

The title product compound is prepared according to the general procedure **E1** with 5 mol% $Rh(cod)_2BF_4$ catalyst, 6% (*S*)-NPN ligand, 30 mol% Taylor's boronic acid **89**, allylic carbonate **99a** (0.24 mmol, 1.2 equiv.), and 0.2 mmol carbohydrate polyol **98a** at 50 °C for 18 h and isolated by flash column chromatography (5:1-1:1 Pentane: Ethyl Acetate) giving **100a** as a colorless oil (45.6 mg, 63% yield, rr >20:1 (C2:C1), dr > 20:1).

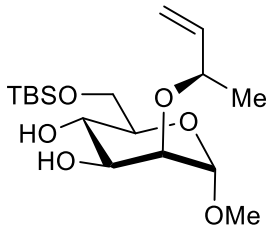

100a

^{1}H NMR (500 MHz, $CDCl_3$) δ 5.76 (ddd, J = 17.0, 10.0, 6.5 Hz, 1H), 5.22 (dt, J = 17.0, 1.5 Hz, 1H), 5.10 (dt, J = 10.5, 1.0 Hz, 1H), 4.65 (d, J = 1.5 Hz, 1H), 4.05 – 3.97 (m, 1H), 3.86 (d, J = 5.5 Hz, 2H), 3.80 – 3.73 (m, 1H), 3.70 (t, J = 9.5 Hz, 1H), 3.63 (dd, J = 4.0, 1.5 Hz, 1H), 3.54 – 3.47 (m, 1H), 3.32 (s, 3H), 3.09 (s, 1H), 2.31 (d, J = 9.0 Hz, 1H), 1.27 (d, J = 6.5 Hz, 3H), 0.90 (s, 9H), 0.09 (d, J = 3.0 Hz, 6H). **^{13}C NMR** (126 MHz, $CDCl_3$) δ 140.20, 116.09, 99.70, 78.86, 76.66, 71.50, 71.27, 70.75, 64.74, 54.83, 25.99, 21.38, 18.37, -5.30, -5.33. **ESI-HRMS**: Calculated for $C_{17}H_{34}O_6NaSi$ $(M+Na)^+$: 385.20169, Found: 385.20161. $[\alpha]_D^{20}$ = +9.6 (c =0.49, $CHCl_3$).

(*2R,3R,5S,6S*)-4-(((*S*)-but-3-en-2-yl)oxy)-2-(((tert-butyldimethylsilyl)oxy)methyl)-6-methoxytetrahydro-2*H*-pyran-3,5-diol (101)

(*2R,3S,5S,6S*)-5-(((*S*)-but-3-en-2-yl)oxy)-2-(((tert-butyldimethylsilyl)oxy)methyl)-6-methoxytetrahydro-2*H*-pyran-3,4-diol (102)

The title product compound is prepared according to the general procedure **F1** with 5 mol% $Rh(cod)_2BF_4$ catalyst, 6% (*R*)-NPN ligand, 30 mol% Taylor's boronic acid **89**, allylic carbonate **99a** (0.24 mmol, 1.2 equiv.), and 0.2 mmol carbohydrate polyol **98a** at 50 °C for 18 h and isolated by flash column chromatography (5:1-1:1 Pentane: Ethyl Acetate) giving C3 regioisomer **101** (25.0 mg, dr > 20:1) as a colorless oil and C2 regioisomer **102** (12.5 mg, dr > 20:1) as a colorless oil (37.5 mg combined total mass of **101** and **102**, 53% combined yield of **101** and **102**, rr 2:1(C3:C2)).

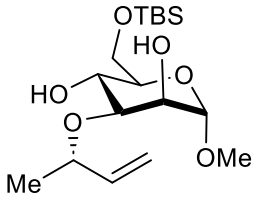

101

^{1}H NMR (600 MHz, $CDCl_3$) δ 5.78 (ddd, J = 17.4, 10.2, 7.2 Hz, 1H), 5.25 (dt, J = 17.4, 1.2 Hz, 1H), 5.21 – 5.17 (m,1H), 4.75 (d, J = 1.8 Hz, 1H), 4.12 – 4.04 (m, 1H), 3.92 (dd, J = 3.6, 1.8 Hz, 1H), 3.86 (d, J = 5.4 Hz, 2H), 3.77 (td, J = 9.6, 1.2 Hz, 1H), 3.66 (dd, J = 9.0, 3.6 Hz, 1H), 3.61 – 3.55 (m, 1H), 3.36 (s, 3H), 2.79 (s, 1H), 2.40 (s, 1H), 1.31 (d, J = 6.0 Hz, 3H), 0.89 (s, 9H), 0.08 (s, 6H). **^{13}C NMR** (151 MHz, $CDCl_3$) δ 139.71, 117.16, 100.42, 76.45, 75.02, 71.07, 68.50, 67.65, 64.77, 54.96, 26.03, 22.09, 18.44, -5.31. **ESI-HRMS**: Calculated for $C_{17}H_{34}O_6NaSi$ $(M+Na)^+$: 385.20169, Found: 385.20149. $[\alpha]_D^{20}$ = +6.0 (c =0.30, $CHCl_3$).

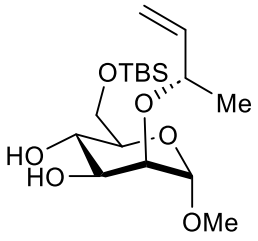

102

^{1}H NMR (600 MHz, $CDCl_3$) δ 5.69 (ddd, J = 17.4, 10.2, 7.8 Hz, 1H), 5.22 – 5.18 (m, 1H), 5.18 – 5.16 (m, 1H), 4.71 (d, J = 1.2 Hz, 1H), 4.00 – 3.93 (m, 1H), 3.90 – 3.83 (m, 2H), 3.74 – 3.69 (m, 1H), 3.69 – 3.66 (m, 1H), 3.66 – 3.63 (m, 1H), 3.53 – 3.48 (m, 1H), 3.35 (s, 3H), 2.90 (s, 1H), 2.26 (d, J = 9.0 Hz, 1H), 1.25 (d, J = 6.6 Hz, 3H), 0.90 (s, 9H), 0.09 (d, J = 2.4 Hz, 6H). **^{13}C NMR** (151 MHz, $CDCl_3$) δ 139.51, 117.45, 98.39, 76.64, 74.81, 71.29, 71.21, 70.55, 64.22, 54.83, 26.01, 21.80, 18.40, -5.22, -5.28. **ESI-HRMS**: Calculated for $C_{17}H_{34}O_6NaSi$ $(M+Na)^+$: 385.20169, Found: 385.20149. $[\alpha]_D^{20}$ = -4.1 (c =0.39, $CHCl_3$).

(*2R,3S,4S,5S,6S*)-2-(((tert-butyldimethylsilyl)oxy)methyl)-5-(((*S*)-1-cyclohexylallyl)oxy)-6-methoxytetrahydro-2*H*-pyran-3,4-diol (100b)

The title product compound is prepared according to the general procedure **E1** with 5 mol% $Rh(cod)_2BF_4$ catalyst, 6% (*S*)-NPN ligand, 30 mol% Taylor's boronic acid **89**, allylic carbonate **99b** (0.24 mmol, 1.2 equiv.), and 0.2 mmol carbohydrate polyol **98a** at 50 °C for 40 h and isolated by flash column chromatography (5:1-1:1 Pentane: Ethyl Acetate) giving **100b** as a colorless oil (60.2 mg, 70% yield, rr >20:1 (C2:C1), dr > 20:1).

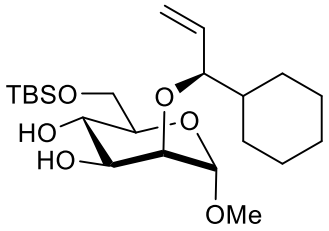

100b

^{1}H NMR (600 MHz, $CDCl_3$) δ 5.66 (ddd, J = 16.8, 10.8, 8.4 Hz, 1H), 5.22 – 5.19 (m, 1H), 5.19 – 5.16 (m,1H), 4.61 (d, J = 1.2 Hz, 1H), 3.91 – 3.82 (m, 2H), 3.77 (td, J = 9.0, 3.6 Hz, 1H), 3.73 (td, J = 9.0, 1.8 Hz, 1H), 3.59 (dd, J = 3.6, 1.2 Hz, 1H), 3.54 (t, J = 7.2 Hz, 1H), 3.50 (dt, J = 9.0, 5.4 Hz, 1H), 3.31 (s, 3H), 3.03 (d, J = 1.2 Hz, 1H), 2.17 (d, J = 8.4 Hz, 1H), 1.99– 1.91 (m,1H), 1.77 – 1.68 (m, 2H), 1.67 – 1.61 (m, 2H), 1.53 – 1.45 (m,1H), 1.27 – 1.08 (m, 3H), 1.06 – 0.96 (m, 1H), 0.90 (s, 9H), 0.09 (d, J = 3.6 Hz, 6H). **^{13}C NMR** (151 MHz, $CDCl_3$) δ 137.93, 118.54, 100.24, 88.83, 76.82, 72.16, 71.43, 70.79, 64.69, 54.82, 42.45, 29.34, 29.08, 26.63, 26.16, 26.08, 25.99, 18.37, -5.29, -5.34. **ESI-HRMS**: Calculated for $C_{22}H_{36}O_6NaSi$ $(M+Na)^+$: 453.26429, Found: 453.26379. $[\alpha]_D^{20}$ = +10.0 (c =0.30, $CHCl_3$).

(*2R,3S,5S,6S*)-2-(((tert-butyldimethylsilyl)oxy)methyl)-5-(((*R*)-hex-1-en-3-yl)oxy)-6-methoxytetrahydro-2*H*-pyran-3,4-diol (100c)

The title product compound is prepared according to the general procedure **E1** with 5 mol% $Rh(cod)_2BF_4$ catalyst, 6% (*S*)-NPN ligand, 30 mol% Taylor's boronic acid **89**, allylic carbonate **99c** (0.24 mmol, 1.2 equiv.), and 0.2 mmol carbohydrate polyol **98a** at 50 °C for 40 h and isolated by flash column chromatography (5:1-3:1 Pentane: Ethyl Acetate) giving **100c** as a colorless oil (63.5 mg, 81% yield, rr >20:1 (C2:C1), dr > 20:1).

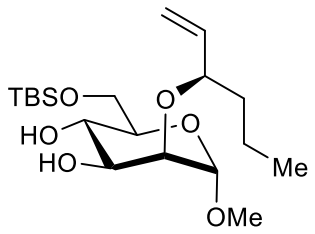

100c

^{1}H NMR (700 MHz, $CDCl_3$) δ 5.74 – 5.65 (m, 1H), 5.21 (dt, J = 17.5, 1.4 Hz, 1H), 5.16 – 5.12 (m, 1H), 4.64 (d, J = 1.4 Hz, 1H), 3.87 (dt, J = 10.5, 5.6 Hz, 2H), 3.85 – 3.81 (m, 1H), 3.77 (td, J = 9.1, 3.5 Hz, 1H), 3.71 (td, J = 9.1, 1.4 Hz, 1H), 3.62 (dd, J = 3.5, 1.4 Hz, 1H), 3.50 (dt, J = 9.8, 5.6 Hz, 1H), 3.31 (s, 3H), 3.07 (s, 1H), 2.25 (d, J = 9.1 Hz, 1H), 1.70 – 1.61 (m, 1H), 1.48 – 1.37 (m, 2H), 1.37 – 1.32 (m,1H), 0.91 (t, J = 9.1 Hz, 12H), 0.09 (d, J = 4.4 Hz, 6H). **^{13}C NMR** (176 MHz, $CDCl_3$) δ 139.33, 117.21, 100.04, 83.68, 76.87, 71.87, 71.42, 70.76, 64.79, 54.83, 37.92, 25.99, 18.84, 18.37, 14.15, -5.31, -5.34.

ESI-HRMS: Calculated for $C_{19}H_{38}O_6NaSi$ $(M+Na)^+$: 413.23299, Found: 413.23281. $[\alpha]_D^{20}$ = +11.1 (c =0.45, $CHCl_3$).

(*2R,3S,4S,5S,6S*)-2-(((tert-butyldimethylsilyl)oxy)methyl)-6-methoxy-5-(((*S*)-1-phenylallyl)oxy)tetrahydro-2*H*-pyran-3,4-diol (100d)

The title product compound is prepared according to the general procedure **E1** with 10 mol% $Rh(cod)_2BF_4$ catalyst, 12% (*S*)-NPN ligand, 30 mol% Taylor's boronic acid **89**, allylic carbonate **99d** (0.24 mmol, 1.2 equiv.), and 0.2 mmol carbohydrate polyol **98a** at 70 ºC for 41 h and isolated by flash column chromatography (5:1-3:1 Pentane: Ethyl Acetate) giving **100d** as a colorless oil (53.3 mg, 63% yield, rr >20:1 (C2:C1), dr > 20:1).

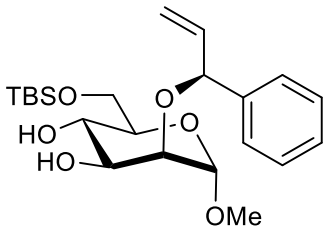

100d

^{1}H NMR (700 MHz, $CDCl_3$) δ 7.38 – 7.31 (m, 4H), 7.32 – 7.27 (m, 1H), 5.96 – 5.87 (m, 1H), 5.35 (dt, J = 16.8, 1.4 Hz, 1H), 5.21 (dt, J = 10.5, 1.4 Hz, 1H), 4.92 (d, J = 6.3 Hz, 1H), 4.80 (s, 1H), 3.93 – 3.86 (m, 2H), 3.81 – 3.77 (m, 1H), 3.76 – 3.74 (m, 1H), 3.74 – 3.73 (m, 1H), 3.53 (dt, J = 9.1, 4.9 Hz, 1H), 3.36 (s, 3H), 2.89 – 2.84 (m, 1H), 2.06 (d, J = 9.1 Hz, 1H), 0.92 (s, 9H), 0.11 (d, J = 3.5 Hz, 6H). **^{13}C NMR** (176 MHz, $CDCl_3$) δ 140.53, 138.68, 128.82, 128.19, 126.99, 116.79, 99.19, 83.83, 76.48, 71.60, 71.23, 70.86, 64.39, 54.90, 26.04, 18.43, -5.23, -5.30. **ESI-HRMS**: Calculated for $C_{22}H_{36}O_6NaSi$ $(M+Na)^+$: 447.21734, Found: 447.21688. $[\alpha]_D^{20}$ = +3.6 (c =0.28, $CHCl_3$).

(*2R,3S,5S,6S*)-2-((benzyloxy)methyl)-5-(((*R*)-hex-1-en-3-yl)oxy)-6-methoxytetrahydro-2*H*-pyran-3,4-diol (100e)

The title product compound is prepared according to the general procedure **E1** with 5 mol% $Rh(cod)_2BF_4$ catalyst, 6% (*S*)-NPN ligand, 30 mol% Taylor's boronic acid **89**, allylic carbonate **99c** (0.24 mmol, 1.2 equiv.), and 0.2 mmol carbohydrate polyol **98b** at 50 ºC for 24 h and isolated by flash column chromatography (5:1-3:1 Pentane: Ethyl Acetate) giving **100e** as a colorless oil (44.0 mg, 60% yield, rr >20:1 (C2:C1), dr > 20:1).

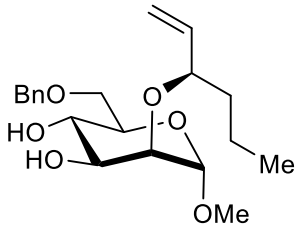

100e

^{1}H NMR (700 MHz, $CDCl_3$) δ 7.37 – 7.31 (m, 4H), 7.30 – 7.26 (m, 1H), 5.75 – 5.67 (m, 1H), 5.26 – 5.20 (m, 1H), 5.17 – 5.12 (m, 1H), 4.68 (d, J = 1.4 Hz, 1H), 4.63 (d, J = 11.9 Hz, 1H), 4.59 (d, J = 11.9 Hz, 1H), 3.87 – 3.81 (m, 1H), 3.79 – 3.73 (m, 3H), 3.72 (t, J = 9.1 Hz, 1H), 3.68 – 3.65 (m, 1H), 3.64 (dd, J = 3.5, 1.4 Hz, 1H), 3.33 (s, 3H), 2.75 (s, 1H), 2.29 (d, J = 9.1 Hz, 1H), 1.70 – 1.63 (m, 1H), 1.48 – 1.38 (m, 2H), 1.37 – 1.31 (m, 1H), 0.92 (t, J = 7.0 Hz, 3H). **^{13}C NMR** (176 MHz, $CDCl_3$) δ 139.25, 138.22, 128.51, 127.78, 127.77, 117.31, 100.07, 83.82, 76.98, 73.72, 71.92, 70.71, 70.51, 70.28, 54.94, 37.87, 18.85, 14.14. **ESI-HRMS**: Calculated for $C_{20}H_{30}O_6Na$ $(M+Na)^+$: 389.19346, Found: 389.19329. $[\alpha]_D^{20}$ = +15.6 (c =0.34, $CHCl_3$).

(*3R,5S,6S*)-5-(((*R*)-hex-1-en-3-yl)oxy)-6-methoxytetrahydro-2*H*-pyran-3,4-diol (100f)

The title product compound is prepared according to the general procedure **E1** with 5 mol% $Rh(cod)_2BF_4$ catalyst, 6% (*S*)-NPN ligand, 30 mol% Taylor's boronic acid **89**, allylic carbonate **99c** (0.24 mmol, 1.2 equiv.), and 0.2 mmol carbohydrate polyol **98c** at 50 ºC for 24 h and isolated by flash column chromatography (5:1-1:1 Pentane: Ethyl Acetate) giving **100f** as a white solid (30.0 mg, 61% yield, rr >20:1 (C2:C1), dr > 20:1).

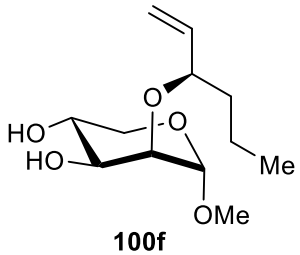

100f

^{1}H NMR (700 MHz, $CDCl_3$) δ 5.72 (ddd, J = 17.5, 10.5, 7.7 Hz, 1H), 5.22 (dt, J = 16.8, 1.4 Hz, 1H), 5.20 – 5.15 (m, 1H), 4.61 (d, J = 2.1 Hz, 1H), 3.85 – 3.81 (m, 1H), 3.83 – 3.79 (m, 1H), 3.78 – 3.73 (m, 1H), 3.75 – 3.70 (m, 1H), 3.63 – 3.60 (m, 1H), 3.47 – 3.42 (m, 1H), 3.35 (s, 3H), 2.24 – 2.16 (m, 2H), 1.70 – 1.63 (m, 1H), 1.49 – 1.43 (m, 1H), 1.43 – 1.38 (m, 1H), 1.37 – 1.33 (m, 1H), 0.93 (t, J = 7.0 Hz, 3H). **^{13}C NMR** (176 MHz, $CDCl_3$) δ 139.17, 117.44, 100.37, 83.68, 76.98, 71.90, 68.87, 62.11, 55.28, 37.85, 18.91, 14.12. **ESI-HRMS**: Calculated for $C_{12}H_{23}O_5Na$ $(M+Na)^+$: 269.13594, Found: 269.13603. $[\alpha]_D^{20}$ = +27.1 (c =0.17, $CHCl_3$).

(*3R,5S,6S*)-5-(((*S*)-hex-1-en-3-yl)oxy)-6-methoxytetrahydro-2*H*-pyran-3,4-diol (100f')

The title product compound is prepared according to the general procedure **F1** with 5 mol% $Rh(cod)_2BF_4$ catalyst, 6% (*R*)-NPN ligand, 30 mol% Taylor's boronic acid **89**, allylic carbonate **99c** (0.24 mmol, 1.2 equiv.), and 0.2 mmol carbohydrate polyol **98c** at 50 ºC for 24 h and isolated by flash column chromatography (5:1-1:1 Pentane: Ethyl Acetate) giving **100f'** as a colorless oil (35.0 mg, 73% yield, rr >20:1 (C2:C3), dr > 20:1).

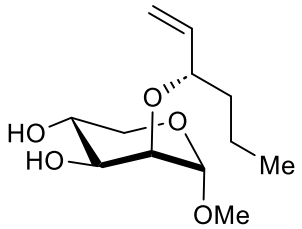

100f'

^{1}H NMR (700 MHz, $CDCl_3$) δ 5.63 (ddd, J = 17.5, 10.5, 8.4 Hz, 1H), 5.23 (dd, J = 10.5, 1.4 Hz, 1H), 5.20 (ddd, J = 17.5, 1.4, 0.7 Hz, 1H), 4.62 (d, J = 2.8 Hz, 1H), 3.85 – 3.80 (m, 1H), 3.79 (dd, J = 8.4, 4.9 Hz, 1H), 3.77 – 3.74 (m, 1H), 3.71 – 3.66 (m, 1H), 3.64 (dd, J = 4.2, 2.8 Hz, 1H), 3.48 (dd, J = 10.5, 8.4 Hz, 1H), 3.39 (s, 3H), 2.26 (d, J = 8.4 Hz, 1H), 2.23 (d, J = 3.5 Hz, 1H), 1.64 – 1.58 (m, 1H), 1.48 – 1.39 (m, 2H), 1.37 – 1.30 (m, 1H), 0.92 (t, J = 7.7 Hz, 3H). **^{13}C NMR** (176 MHz, $CDCl_3$) δ 138.49, 118.53, 99.37, 81.11, 74.43, 71.68, 68.79, 62.42, 55.44, 37.86, 18.71, 14.09. **ESI-HRMS**: Calculated for $C_{12}H_{23}O_5Na$ $(M+Na)^+$: 269.13594, Found: 269.13593. $[\alpha]_D^{20}$ = -5.7 (c =0.44, $CHCl_3$).

6. References

[1] Zhu, X., & Schmidt, R. R. (**2009**). New principles for glycoside-bond formation. *Angewandte Chemie International Edition*, *48*(11), 1900-1934.

[2] A. Michael, *Am. Chem. J.* **1879**, *1*, 305 – 312.

[3] E. Fischer, Ber. Dtsch. *Chem. Ges.* **1893**, *26*, 2400 – 2412.

[4] W. Koenigs, E. Knorr, Ber. Dtsch. *Chem. Ges.* **1901**, *34*, 957 – 981.

[5] Neel, A. J.; Hilton, M. J.; Sigman, M. S.; Toste, F. D., Exploiting non-covalent π interactions for catalyst design. *Nature.* **2017,** *543*, 637.

[6] Boltje, T. J.; Buskas, T.; Boons, G.-J., Opportunities and challenges in synthetic oligosaccharide and glycoconjugate research. *Nat. Chem.* **2009,** *1*, 611.

[7] Loh, C. C. J., Exploiting non-covalent interactions in selective carbohydrate synthesis. *Nat. Rev. Chem.* **2021,** *5*, 792-815.

[8] (a) Sutar, R. L.; Huber, S. M., Catalysis of Organic Reactions through Halogen Bonding. *ACS Catal.* **2019,** *9* (10), 9622-9639; (b) Bamberger, J.; Ostler, F.; Mancheño, O. G., Frontiers in Halogen and Chalcogen-Bond Donor Organocatalysis. *ChemCatChem* **2019,** *11* (21), 5198-5211.

[9] (a) Sutar, R. L.; Huber, S. M., Catalysis of Organic Reactions through Halogen Bonding. *ACS Catal.* **2019,** *9* (10), 9622-9639; (b) Castelli, R.; Schindler, S.; Walter, S. M.; Kniep, F.; Overkleeft, H. S.; Van der Marel, G. A.; Huber, S. M.; Codée, J. D. C., Activation of Glycosyl Halides by Halogen Bonding. *Chem. - Asian J.* **2014,** *9*, 2095-2098.

[10] Zhao, Z.; Wang, Y., Chalcogen Bonding Catalysis with Phosphonium Chalcogenide (PCH). *Acc. Chem. Res.* **2023,** *56*, 608-621.

[11] Toste, F. D., Sigman, M. S. & Miller, S. J. Pursuit of Noncovalent Interactions for Strategic Site-Selective Catalysis. *Acc. Chem. Res.* **50**, 609-615.

[12] Das, R. & Mukhopadhyay, B. Chemical*O*-glycosylations: an overview. *ChemistryOpen 5*, 401–433 (**2016**).

[13] (a) I. V. Alabugin, Stereoelectronic Effects: A Bridge Between Structure and Reactivity, Wiley, **2016**, p. 392. (b) I. V. Alabugin, G. Dos Passos Gomes and M. A. Abdo, Hyperconjugation, Wiley Interdiscip. Rev.: *Comput. Mol.Sci*., **2019**, *9*(2), e1389.

[14] Filloux, Claire M. "The Problem of Origins and Origins of the Problem: Influence of Language on Studies Concerning the Anomeric Effect." *Angewandte Chemie (International ed. in English) 54* (31) (**2015**): 8880-8894.

[15] Alabugin, I. V., Kuhn, L., Krivoshchapov, N. V., Mehaffy, P., & Medvedev, M. G. (**2021**). Anomeric effect, hyperconjugation and electrostatics: Lessons from complexity in a classic stereoelectronic phenomenon. *Chemical Society Reviews*, *50*(18), 10212-10252.

[16] (a) Peng, P. & Schmidt, R. R. Acid–base catalysis in glycosidations: a nature derived alternative to the generally employed methodology. *Acc. Chem. Res. 50*, 1171–1183 (**2017**). (b) Doyle, A. G.

& Jacobsen, E. N. Small-molecule H-bond donors in asymmetric catalysis. *Chem. Rev. 107*, 5713–5743 (**2007**).

[17] (a) Doyle, A. G. & Jacobsen, E. N. Small-molecule H-bond donors in asymmetric catalysis. *Chem. Rev*. *107*, 5713–5743 (**2007**). (b) Schreiner, P. R. Metal-free organocatalysis through explicit hydrogen bonding interactions. *Chem. Soc. Rev. 32*, 289–296 (**2003**).

[18] Reisman, S. E., Doyle, A. G. & Jacobsen, E. N. Enantioselective thiourea-catalyzed additions to oxocarbenium ions. *J. Am. Chem. Soc. 130*, 7198–7199 (**2008**).

[19] Park, Y. et al. Macrocyclic bis-thioureas catalyse stereospecific glycosylation reactions. Science *355*, 162–166 (**2017**).

[20] Levi, S. M., Li, Q., Rötheli, A. R. & Jacobsen, E. N. Catalytic activation of glycosyl phosphates for stereoselective coupling reactions. *Proc. Natl Acad. Sci. USA 116*, 35–39 (**2019**).

[21] Mayfield, A. B., Metternich, J. B., Trotta, A. H. & Jacobsen, E. N. Stereospecific furanosylations catalyzed by bis-thiourea hydrogen-bond donors. *J. Am. Chem. Soc. 142*, 4061–4069 (**2020**).

[22] Beale, T. M., Chudzinski, M. G., Sarwar, M. G. & Taylor, M. S. Halogen bonding in solution: thermodynamics and applications. *Chem. Soc. Rev.***42**, 1667–1680 (2013).

[23] Scholfield, M. R., Zanden, C. M. V., Carter, M. & Ho, P. S. Halogen bonding (X-bonding): a biological perspective. *Protein Sci.* **22**, 139–152 (2013).

[24] Persch, E., Dumele, O. & Diederich, F. Molecular recognition in chemical and biological systems. *Angew. Chem. Int. Ed.* **54**, 3290–3327 (2015).

[25] Bulfield, D. & Huber, S. M. Halogen bonding in organic synthesis and organocatalysis. *Chem. Eur. J.* **22**, 14434–14450 (2016).

[26] Cavallo, G. et al. The halogen bond. *Chem. Rev.* **116**, 2478–2601 (2016).

[27] Castelli, R. et al. Activation of glycosyl halides by halogen bonding. *Chem. Asian J.* **9**, 2095–2098 (2014).

[28] Xu, C., Rao, V. U. B., Weigen, J. & Loh, C. C. J. A robust and tunable halogen bond organocatalysed 2-deoxyglycosylation involving quantum tunneling. *Nat. Commun.* **11**, 4911 (2020).

[29] Xu, C. & Loh, C. C. J. An ultra-low thiourea catalysed strain-release glycosylation and a multicatalytic diversification strategy. *Nat. Commun.* **9**, 4057 (2018).

[30] Xu, C., Rao, V. U. B., Weigen, J. & Loh, C. C. J. A robust and tunable halogen bond organocatalysed 2-deoxyglycosylation involving quantum tunneling. *Nat. Commun.* **11**, 4911 (2020).

[31] Vogel, L. Wonner, P. Huber, S . M. Chalcogen bonding: an overview. *Angew. Chem. Int. Ed.* **2019**, *58*, 1880-1891.

[32] Alcock, N. W. Secondary bonding to nonmetallic elements. *Adv. Inorg. Chem*. **1972**, *15*, 1-58.

References

[33] Zhao, Z.; Wang, Y., Chalcogen Bonding Catalysis with Phosphonium Chalcogenide (PCH). *Acc. Chem. Res.* **2023,** *56*, 608-621.

[34] Wang, W.; Zhu, H.; Liu, S.; Zhao, Z.; Zhang, L.; Hao, J.; Wang, Y., Chalcogen–Chalcogen Bonding Catalysis Enables Assembly of Discrete Molecules. *J. Am. Chem. Soc.* **2019,** *141*, 9175-9179.

[35] Wang, W.; Zhu, H.; Feng, L.; Yu, Q.; Hao, J.; Zhu, R.; Wang, Y., Dual Chalcogen–Chalcogen Bonding Catalysis. *J. Am. Chem. Soc.* **2020,** *142*, 3117-3124.

[36] Kong, X.; Zhou, P.-P.; Wang, Y., Chalcogen···π Bonding Catalysis. *Angew. Chem. Int. Ed.* **2021,** *60*, 9395-9400.

[37] Pang, Y.; Zhao, Z.; Wang, Y., Activation of alkynes by chalcogen bonding: a Se···π interaction catalyzed intramolecular cyclization of 1,6-diynes. *Chem. Commun*. **2023**, *59*, 12278-12281.

[38] Ma, W.; Kirchhoff, J.-L.; Strohmann, C.; Grabe, B.; Loh, C. C. J., Cooperative Bifurcated Chalcogen Bonding and Hydrogen Bonding as Stereocontrolling Elements for Selective Strain-Release Septanosylation. *J. Am. Chem. Soc*. **2023**, *145*, 26611-26622.

[39] Horne, G.; Wilson, F. X.; Tinsley, J.; Williams, D. H.; Storer, R., Iminosugars past, present and future: medicines for tomorrow. *Drug Discovery Today* **2011,** *16* (3), 107-118;

[40] Nash, R. J.; Kato, A.; Yu, C.-Y.; Fleet, G. W. J., Iminosugars as therapeutic agents: recent advances and promising trends. *Future Med. Chem.* **2011**, *3*, 1513-1521.

[41] Watson, A. A., Fleet, G. W., Asano, N., Molyneux, R. J., & Nash, R. J. (**2001**). Polyhydroxylated alkaloids—natural occurrence and therapeutic applications. *Phytochemistry*, *56*(*3*), 265-295.

[42] Broquist HP, Mason PS, Hagler WM, Harris TM. Identification of swainsonine as a probable contributory mycotoxin in moldy forage mycotoxicoses. *Appl Environ Microbiol.* **1984**, *48*(*2*):386-8.

[43] Sorbera, L. A., Castaner, J., & Garcia-Capdevila, L. (**2005**). Celgosivir. *Drugs of the Future*, 30(*6*).

[44] Stern, R.; Jedrzejas, M. J. Carbohydrate Polymers at the Center of Life's Origins: The Importance of Molecular Processivity. *Chem. Rev.* **2008**, *108*, 5061−5085.

[45] Lovegrove, A.; Edwards, C. H.; De Noni, I.; Patel, H.; El, S. N.; Grassby, T.; Zielke, C.; Ulmius, M.; Nilsson, L.; Butterworth, P. J.; et al. Role of Polysaccharides in Food, Digestion, and Health. *Crit. Rev. Food Sci. Nutr*. **2017**, *57*, 237−253.

[46] Varki, A. Biological Roles of Glycans. *Glycobiology* **2017**, *27*, 3−49.

[47] Martínez-Reyes, I.; Chandel, N. S. Mitochondrial TCA Cycle Metabolites Control Physiology and Disease. *Nat. Commun.* **2020**, *11*, 102.

[48] Pétursson, S. Protecting Groups in Carbohydrate Chemistry. *J. Chem. Educ.* **1997**, *74*, 1297.

[49] Hanessian, S.; Lavallee, P. The Preparation and Synthetic Utility of tert-Butyldiphenylsilyl Ethers. *Can. J. Chem.* **1975**, *53*, 2975−2977.

[50] Jiang, L.; Chan, T.-H. Regioselective Acylation of Hexopyranosides with Pivaloyl Chloride. *J. Org. Chem.* **1998**, *63*, 6035−6038.

[51] Crich, D.; Sun, S. Are Glycosyl Triflates Intermediates in the Sulfoxide Glycosylation Method? A Chemical and 1H, 13C, and 19F NMR Spectroscopic Investigation. *J. Am. Chem. Soc.* **1997**, *119*, 11217−11223.

[52] Kurahashi, T.; Mizutani, T.; Yoshida, J.-i. Effect of Intramolecular Hydrogen-Bonding Network on the Relative Reactivities of Carbohydrate OH Groups †. *J. Chem. Soc., Perkin Trans.* **1999**, *1,* 465−474.

[53] Crich, D.; Sun, S. Are Glycosyl Triflates Intermediates in the Sulfoxide Glycosylation Method A Chemical and 1H, 13C, and 19F NMR Spectroscopic Investigation. *J. Am. Chem. Soc.* **1997**, *119*, 11217−11223.

[54] Lee, D.; Taylor, M. S. Borinic Acid-Catalyzed Regioselective Acylation of Carbohydrate Derivatives. *J. Am. Chem. Soc.* **2011**, *133*, 3724−3727.

[55] Ren, B.; Ramstrom, O.; Zhang, Q.; Ge, J.; Dong, H. An Iron(III) Catalyst with Unusually Broad Substrate Scope in Regioselective Alkylation of Diols and Polyols. *Chem.Eur. J.* **2016**, *22*, 2481−2486.

[56] Geng, Y.; Kumar, A.; Faidallah, H. M.; Albar, H. A.; Mhkalid, I. A.; Schmidt, R. R. Cooperative Catalysis in Glycosidation Reactions with O-Glycosyl Trichloroacetimidates as Glycosyl Donors. *Angew. Chem., Int. Ed.* **2013**, *52*, 10089−10092.

[57] Verdoucq, L.; Morinière, J.; Bevan, D. R.; Esen, A.; Vasella, A.; Henrissat, B.; Czjze, M. Structural Determinants of Substrate Specificity in Family 1 beta-Glucosidases: Novel Insights from the Crystal Structure of Sorghum Dhurrinase-1, a Plant beta-Glucosidase with Strict Specificity, in Complex with Its Natural Substrate. *J. Biol. Chem.* **2004**, *279*, 31796−31803.

[58] Dimakos, V.; Garrett, G. E.; Taylor, M. S. Site-Selective, Copper-Mediated O-Arylation of Carbohydrate Derivatives. *J. Am. Chem. Soc.* **2017**, *139*, 15515−15521.

[59] Jeffrey, J. L.; Terrett, J. A.; MacMillan, D. W. O-H Hydrogen Bonding Promotes H-Atom Transfer from alpha C-H Bonds for Calkylation of Alcohols. *Science* **2015**, *349*, 1532−1536.

[60] Wan, I. C. S.; Witte, M. D.; Minnaard, A. J. Site-Selective Carbon-Carbon Bond Formation in Unprotected Monosaccharides Using Photoredox Catalysis. *Chem. Commun.* **2017**, *53*, 4926−4929.

[61] Zhao, Z.; Wang, Y., Chalcogen Bonding Catalysis with Phosphonium Chalcogenide (PCH). *Acc. Chem. Res.* **2023,** *56*, 608-621.

[62] Stereoselective Synthesis of Iminosugar 2-Deoxy(thio)glycosides from Bicyclic Iminoglycal Carbamates Promoted by Cerium(IV) Ammonium Nitrate and Cooperative Brønsted Acid-Type Organocatalysis. Irene Herrera-González, Elena M. Sánchez-Fernández, Abhijit Sau, Cristina Nativi, José M. García Fernández, M. Carmen Galán, and Carmen Ortiz Mellet. . *J. Org. Chem*. **2020**, *85*, 5038−5047.

[63] Horne, G.; Wilson, F. X.; Tinsley, J.; Williams, D. H.; Storer, R., Iminosugars past, present and future: medicines for tomorrow. *Drug Discovery Today* **2011,** *16* (3), 107-118;

[64] Nash, R. J.; Kato, A.; Yu, C.-Y.; Fleet, G. W. J., Iminosugars as therapeutic agents: recent advances and promising trends. *Future Med. Chem.* **2011,** *3*, 1513-1521.

[65] Tyrrell, B. E.; Sayce, A. C.; Warfield, K. L.; Miller, J. L.; Zitzmann, N., Iminosugars: Promising therapeutics for influenza infection. *Crit. Rev. Microbiol.* **2017,** *43*, 521-545.

[66] Esposito, A.; D'Alonzo, D.; De Fenza, M.; De Gregorio, E.; Tamanini, A.; Lippi, G.; Dechecchi, M. C.; Guaragna, A., Synthesis and Therapeutic Applications of Iminosugars in Cystic Fibrosis. *Int. J. Mol. Sci.* **2020,** *21*, 3353.

[67] Sánchez-Fernández, E. M.; García Fernández, J. M.; Mellet, C. O., Glycomimetic-based pharmacological chaperones for lysosomal storage disorders: lessons from Gaucher, GM1-gangliosidosis and Fabry diseases. *Chem. Commun.* **2016,** *52*, 5497-5515.

[68] Williams, S. J.; Goddard-Borger, E. D., α-glucosidase inhibitors as host-directed antiviral agents with potential for the treatment of COVID-19. *Biochem. Soc. Trans.* **2020,** *48*, 1287-1295.

[69] Sánchez-Fernández, E. M.; García-Moreno, M. I.; García Fernández, J. M.; Mellet, C. O., sp^2-Iminosugars as chemical mimics for glycodrug design. In *Small Molecule Drug Discovery: Methods, Molecules and Applications*, **2019**; pp 197-224.

[70] Takahata, H.; Banba, Y.; Ouchi, H.; Nemoto, H.; Kato, A.; Adachi, I., Asymmetric Synthesis of the Four Possible Fagomine Isomers. *J. Org. Chem.* **2003,** *68*, 3603-3607.

[71] Díaz Pérez, P.; García-Moreno, M. I.; Ortiz Mellet, C.; García Fernández, J. M., Synthesis and Comparative Glycosidase Inhibitory Properties of Reducing Castanospermine Analogues. *Eur. J. Org. Chem.* **2005,** *2005*, 2903-2913.

[72] (a) Balmond, E. I.; Benito-Alifonso, D.; Coe, D. M.; Alder, R. W.; McGarrigle, E. M.; Galan, M. C., A 3,4-*trans*-Fused Cyclic Protecting Group Facilitates α-Selective Catalytic Synthesis of 2-Deoxyglycosides. *Angew. Chem.* **2014,** *126*, 8329-8333; (b) Balmond, E. I.; Coe, D. M.; Galan, M. C.; McGarrigle, E. M., α-Selective Organocatalytic Synthesis of 2-Deoxygalactosides. *Angew. Chem. Int. Ed.* **2012,** *51*, 9152-9155;

[73] Jungbauer, S. H.; Huber, S. M., Cationic Multidentate Halogen-Bond Donors in Halide Abstraction Organocatalysis: Catalyst Optimization by Preorganization. *J. Am. Chem. Soc.* **2015,** *137*, 12110-12120.

[74] Takeda, Y.; Hisakuni, D.; Lin, C.-H.; Minakata, S., 2-Halogenoimidazolium Salt Catalyzed Aza-Diels–Alder Reaction through Halogen-Bond Formation. *Org. Lett.* **2015,** *17*, 318-321.

[75] (a) Xu, C.; Loh, C. C. J., A Multistage Halogen Bond Catalyzed Strain-Release Glycosylation Unravels New Hedgehog Signaling Inhibitors. *J. Am. Chem. Soc.* **2019,** *141*, 5381-5391. (b) Xu, C.; Rao, V. U. B.; Weigen, J.; Loh, C. C. J., A robust and tunable halogen bond organocatalyzed 2-deoxyglycosylation involving quantum tunneling. *Nat. Commun.* **2020,** *11*, 4911.

[76] Schreiner, P. R.; Wittkopp, A., H-Bonding Additives Act Like Lewis Acid Catalysts. *Org. Lett.* **2002,** *4*, 217-220.

[77] Yuan, X.; Wang, Y., A Selenide Catalyst for the Activation of Alkenes through Se···π Bonding. *Angew. Chem. Int. Ed.* **2022,** *61*, e202203671.

[78] (a) Bao, L.; Kong, X.; Wang, Y., Noncovalent Chalcogen-Bonding Catalysis Using ppm-Level Catalyst Loading to Achieve Cyanosilylation of Ketones. *Asian J. Org. Chem.* **2020,** *9*, 757-760; (b) Dutton, J. L.; Ragogna, P. J., Donor−Acceptor Chemistry at Heavy Chalcogen Centers. *Inorg. Chem.* **2009,** *48*, 1722-1730.

[79] Wonner, P.; Vogel, L.; Kniep, F.; Huber, S. M., Catalytic Carbon–Chlorine Bond Activation by Selenium-Based Chalcogen Bond Donors. *Chem. Eur. J.* **2017,** *23*, 16972-16975.

[80] (a) Mootoo, D. R.; Konradsson, P.; Udodong, U.; Fraser-Reid, B., Armed and disarmed *n*-pentenyl glycosides in saccharide couplings leading to oligosaccharides. *J. Am. Chem. Soc.* **1988,** *110* (16), 5583-5584; (b) Zhang, Z.; Ollmann, I. R.; Ye, X.-S.; Wischnat, R.; Baasov, T.; Wong, C.-H., Programmable One-Pot Oligosaccharide Synthesis. *J. Am. Chem. Soc.* **1999,** *121*, 734-753.

[81] Liu, K.-M.; Wang, P.-Y.; Guo, Z.-Y.; Xiong, D.-C.; Qin, X.-J.; Liu, M.; Liu, M.; Xue, W.-Y.; Ye, X.-S. Iterative Synthesis of 2-Deoxyoligosaccharides Enabled by Stereoselective Visible-Light-Promoted Glycosylation. *Angew. Chem. Int. Ed.* **2022**, *61* (20), e202114726.

[82] (a) Xu, C.; Bhaskara Rao, V. U.; Weigen, J.; Loh, C. C. J. A Robust and Tunable Halogen Bond Organocatalyzed 2-Deoxyglycosylation Involving Quantum Tunneling. *Nat. Commun.* **2020**, *11*, 4911. (b) Rao, V. U. B.; Wang, C.; Demarque, D. P.; Grassin, C.; Otte, F.; Merten, C.; Strohmann, C.; Loh, C. C. J. A synergistic Rh(I)/organoboron-catalysed site-selective carbohydrate functionalization that involves multiple stereocontrol. *Nat. Chem.* **2023**, *15* (3), 424-435. DOI: 10.1038/s41557-022-01110-z.

[83] (a) Kononov, L. O.; Malysheva, N. N.; Kononova, E. G.; Orlova, A. V. Intermolecular Hydrogen-Bonding Pattern of a Glycosyl Donor: The Key to Understanding the Outcome of Sialylation. *Eur. J. Org. Chem.* **2008**, *2008* (19), 3251-3255. DOI: 10.1002/ejoc.200800324.

[84] Neese, F. Software update: The ORCA program system—Version 5.0. *WIREs Computational Molecular Science* **2022**, *12* (5), e1606. DOI: https://doi.org/10.1002/wcms.1606.

[85] Zhao, Y.; Truhlar, D. G. The M06 suite of density functionals for main group thermochemistry, thermochemical kinetics, noncovalent interactions, excited states, and transition elements: two new functionals and systematic testing of four M06-class functionals and 12 other functionals. *Theor. Chem. Acc.* **2008**, *120* (1), 215-241. DOI: 10.1007/s00214-007-0310-x.

[86] Docker, A.; Marques, I.; Kuhn, H.; Zhang, Z.; Félix, V.; Beer, P. D. Selective Potassium Chloride Recognition, Sensing, Extraction, and Transport Using a Chalcogen-Bonding Heteroditopic Receptor. *J. Am. Chem. Soc.* **2022**, *144* (32), 14778-14789. DOI: 10.1021/jacs.2c05333.

[87] Lu, T.; Chen, F. Multiwfn: A multifunctional wavefunction analyzer. *J. Comput. Chem.* **2012**, *33* (5), 580-592. DOI: https://doi.org/10.1002/jcc.22885.

References

[88] Johnson, E. R.; Keinan, S.; Mori-Sánchez, P.; Contreras-García, J.; Cohen, A. J.; Yang, W. Revealing Noncovalent Interactions. *J. Am. Chem. Soc.* **2010**, *132* (18), 6498-6506. DOI: 10.1021/ja100936w.

[89] Li, R.-Z. *et al.* Site-Divergent Delivery of Terminal Propargyls to Carbohydrates by Synergistic Catalysis. *Chem* **3**, 834-845 (2017).

[90] Wu, J. *et al.* Site-Selective and Stereoselective *O*-Alkylation of Glycosides by Rh (II)-Catalyzed Carbenoid Insertion. *J. Am. Chem. Soc.* **141**, 19902-19910 (2019).

[91] (a) Sakai, M., Hayashi, H. & Miyaura, N. Rhodium-Catalyzed Conjugate Addition of Aryl- or 1-Alkenylboronic Acids to Enones. *Organometallics* **16**, 4229-4231 (1997). (b) Sakai, M., Ueda, M. & Miyaura, N. Rhodium-Catalyzed Addition of Organoboronic Acids to Aldehydes. *Angew. Chem. Int. Ed.* **37**, 3279-3281 (1998). (c) Takaya, Y., Ogasawara, M., Hayashi, T., Sakai, M. & Miyaura, N. Rhodium-Catalyzed Asymmetric 1,4-Addition of Aryl- and Alkenylboronic Acids to Enones. *J. Am. Chem. Soc.* **120**, 5579-5580 (1998).

[92] Lautens, M., Dockendorff, C., Fagnou, K. & Malicki, A. Rhodium-Catalyzed Asymmetric Ring Opening of Oxabicyclic Alkenes with Organoboronic Acids. *Org. Lett.* **4**, 1311-1314 (2002).

[93] Dimakos, V. *et al.* Site-selective redox isomerizations of furanosides using a combined arylboronic acid/photoredox catalyst system. *Chem. Sci.* **11**, 1531-1537 (2020).

[94] Ding H, Lu W, Li H, Yang L, Zhang Q, Zhou C, Wu X, Baudoin O, Cai J, Guéritte F, Zhao Y. Synthesis and biological evaluation of novel compounds related to 1-arylnaphthalene lignans and isoquinolines. *Chem Biodivers.* **2005**, *2(9),* 1217-31.

[95] Li, S. *et al.* Update on naturally occurring novel arylnaphthalenes from plants. *Phytochem. Rev.* **19**, 337-403 (2020).

[96] Nagatsu, A. *et al.* Tyrosinase Inhibitory and Anti-Tumor Promoting Activities of Compounds Isolated from Safflower (Carthamus Tinctorius L.) and Cotton (Gossypium Hirsutum L.) Oil Cakes. *Nat. Prod. Lett.* **14**, 153-158 (2000).

[97] Izumi, S., Kobayashi, Y. & Takemoto, Y. Regio- and Stereoselective Synthesis of 1,2-*cis*-Glycosides by Anomeric *O*-Alkylation with Organoboron Catalysis. *Org. Lett.* **21**, 665-670 (2019).

[98] Izumi, S., Kobayashi, Y. & Takemoto, Y. Stereoselective Synthesis of 1,1'-Disacharides by Organoboron Catalysis. *Angew. Chem. Int. Ed.* **59**, 14054-14059 (2020).

[99] Xu, W-B., Ghorai, S., Huang, W. & Li, C. Rh(I)/Bisoxazolinephosphine-Catalyzed Regio- and Enantioselective Allylic Substitutions. *ACS Catal.* **10**, 4491-4496 (2020).

[100] C. Xu, V. U. Bhaskara Rao, J. Weigen, C. C. J. Loh*, *Nat. Commun.* **2020**, *11*, 4911.

[101] Wang, W., Zhu, H., Liu, S., Zhao, Z., Zhang, L., Hao, J., & Wang, Y. Chalcogen–chalcogen bonding catalysis enables assembly of discrete molecules. *Journal of the American Chemical Society*, **2019**(*23*), 9175-9179.

[102] Yuan, X., & Wang, Y. A Selenide Catalyst for the Activation of Alkenes through Se··· π Bonding. *Angewandte Chemie International Edition*, **2022**(*27*), e202203671.

[103] García-Moreno, M. I., Ortiz Mellet, C., & García Fernández, J. M. Synthesis of Calystegine B2, B3, and B4 Analogues: Mapping the Structure-Glycosidase Inhibitory Activity Relationships in the 1-Deoxy-6-oxacalystegine Series. *European Journal of Organic Chemistry*, **2004**(*8*), 1803-1819.

[104] Díaz Pérez, P., García-Moreno, M.I., Ortiz Mellet, C. and García Fernández, J.M., 2005. Synthesis and comparative glycosidase inhibitory properties of reducing castanospermine analogues. *Eur. J. Org. Chem*. **2005**, 2903–2913.

[105] Herrera-González, I., Sánchez-Fernández, E. M., Sau, A., Nativi, C., García Fernández, J. M., Galán, M. C., & Ortiz Mellet, C. Stereoselective synthesis of iminosugar 2-deoxy (thio) glycosides from bicyclic iminoglycal carbamates promoted by Cerium (IV) ammonium nitrate and cooperative Brønsted acid-type organocatalysis. *The Journal of Organic Chemistry*, **2020**(*85)*, 5038-5047.

[106] Raji Reddy C, Subbarao M, Kolgave DH, Ajaykumar U, Vinaya PP. Access to Diverse Seleno-spirocyclohexadienones via Ag(II)-Catalyzed Selenylative ipso-Annulation with Se and Boronic Acids. *ACS Omega*. **2022** (*42*), 38045-38052.

[107] Sato, K. I., Akai, S., Sakuma, M., Kojima, M., & Suzuki, K. J. Practical synthesis of [1-13C]- and [6-13C]-d-galactose. *Tetrahedron letters*, **2003**(*44*), 4903-4907.

[108] Hussain, N., Tatina, M. B., & Mukherjee, D. Cross dehydrogenative coupling of sugar enol ethers with terminal alkenes in the synthesis of pseudo-disaccharides, chiral oxadecalins and a conjugated triene. *Organic & Biomolecular Chemistry*, **2018** (*16*), 2666-2677.

[109] Watterson, M. P., Pickering, L., Smith, M. D., Hudson, S. J., Marsh, P. R., Mordaunt, J. E., ... & Fleet, G. W. 3-Azidotetrahydrofuran-2-carboxylates: monomers for five-ring templated β-amino acid foldamers? *Tetrahedron: Asymmetry*, **1999**(*10*), 1855-1859.

[110] Mariano, S., Roos, A. K., Mowbray, S. L., & Salmon, L. Competitive inhibitors of type B ribose 5-phosphate isomerases: design, synthesis and kinetic evaluation of new D-allose and D-allulose 6-phosphate derivatives. *Carbohydrate research*, **2009**, *344*(7), 869-880.

[111] Dolomanov, O.V., Bourhis, L.J., Gildea, R.J, Howard, J.A.K. & Puschmann, H. (**2009**), *J. Appl. Cryst.* 42, 339-341.

[112] Sheldrick, G.M. (**2015**). *Acta Cryst.* A71, 3-8.

[113] Sheldrick, G.M. (**2015**). *Acta Cryst.* C71, 3-8.

[114] Burés, J. A Simple Graphical Method to Determine the Order in Catalyst. *Angew. Chem. Int. Ed*. **2016**, *55*, 2028-2031.

[115] Nielsen, C. D.-T.; Burés, J. Visual kinetic analysis, *Chem. Sci*., **2019**, *10*, 348-353.

References

[116] Sanae Izumi, Yusuke Kobayashi, and Yoshiji Takemoto*. Regio- and Stereoselective Synthesis of 1,2-cis-Glycosides by Anomeric O-Alkylation with Organoboron Catalysis. *Org. Lett*. **2019**, *21*, 665−670.

[117] Wen-Bin Xu, Samir Ghorai, Wenyu Huang, and Changkun Li*. Rh(I)/Bisoxazolinephosphine-Catalyzed Regio- and Enantioselective Allylic Substitutions. *ACS Catal*. **2020**, *10*, 4491−4496.

[118] Narinder Mohal and Andrea Vasella*. Synthesis of Fusion-Isomeric Imidazopyridines and Their Evaluation as Inhibitors of syn- and anti-Protonating Glycosidase; Helvetica Chimica Acta- Vol. *88* (2005).

7. Appendix

7.1 Abbreviations

Ac	Acyl
ACN	Acetonitrile
Ar	Aryl
ARO	Asymmetric ring opening
BAr^F	Tetrakis(3,5-*bis*(trifluoromethyl)phenyl)borate
9-BBN	9-Borabicyclo[3.3.1]nonane
Bn	Benzyl
BINAP	(2,2′-bis(diphenylphosphino)-1,1′-binaphthyl)
Bu	Butyl
Bz	Benzoyl
cat	Catalyst
$CDCl_3$	Deuterated chloroform
ChB	Chalcogen bonding
$CHCl_3$	Chloroform
Cp	Pentamethylcyclopentadieny
CS	Castanospermine
DBU	1,8-Diazabicyclo[5.4.0]undec-7-ene
DCM	Dichloromethane
DFT	Density functional theory
DIBAL-H	Diisobutylaluminium hydride
Dibm	Diisobutyrylmethane
DIPEA	N, N-Diisopropylethylamine
DMAP	4-dimehylaminopyridine
DMF	Dimethyl formamide
DMSO	Dimethyl sulfoxide
DNJ	1-deoxynojirimycin
d.r.	Diastereomeric ratio
DTBMP	2,6-di-tert-butyl-4-methylpyridine
Dtbpy	4,4'-di-tert-butyl-2,2'-dipyridyl)
EA	Ethyl acetate
equiv.	Equivalent
ESI	Electrospray ionization
Et_2O	Diethyl ether

Appendix

Et	Ethyl
Et_3N	Triethylamine
Fmoc	Fluorenylmethoxycarbonyl
HAT	Hydrogen atom transfer
HB	Hydrogen bonds
HCV	Hepatitis C virus
HMBC	Heteronuclear Multiple Bond Correlation
HPLC	High performance liquid chromatography
HRMS	High resolution mass spectroscopy
HSQC	Heteronuclear Single Quantum Coherence
iPr	Isopropyl
J	Coupling constant
LB	Lewis base
Me	Methyl
MeOH	Methanol
MHz	Megahertz
NBD	Norbornadien
*n*Bu	*n*-butyl
NMR	Nuclear magnetic resonance
*n*Oct	*n*-Octanol
NCIs	Noncovalent interactions
NPC	Niemann-Pick type C
NPN	Bisoxazolinephosphine
n.d.	Not detected
OTf	Trifluoromethanesulfonyl
PCH	Phosphono-chalcogenides
PE	Petroleum ether
Ph	Phenyl
pKa	Logarithm of the acid dissociation constant
PPY	4-pyrrolidinopyridine
Py	Pyridine
rls	Rate limiting step
r.t.	Room temperature
r.r.	Regioselective ratio
T	Temperature
TBAC	Tetrabutyl ammonium chloride

TBAI	Tetra-n-butylammonium iodide
TBDPS	*tert*-Butyldiphenylsilyl
TBS	*tert*-Butyldimethylsilyl
TfOH	Trifluoromethanesulfonic acid
Tf_2O	Trifluoromethanesulfonic anhydride
Tr	Triphenylmethyl
TSs	Transition states
t-Bu	*tert*-Butyl
TBDPS	*tert*-butyldiphenylsilyl
TFA	Trifluoroacetic acid
THF	Tetrahydrofuran
TLC	Thin layer chromatography
VCD	Vibrational circular dichroism
XB	Halogen bonding

7.2 Acknowledgement

My three-year PhD study in German is coming to an end. Looking back on this period, I've gained a great deal of experience and knowledge in both my life and in science. I would like to offer my heartfelt gratitude to everyone who has assisted me throughout this time.

First of all, I would like to thank Dr. Charles C. J. Loh for all of his help and critical advice throughout my PhD studies and life in Dortmund. I still remember his assistances to me when I first arrived in Dortmund, which helped me get through the difficulties and adjust to life in a foreign country. I would like to thank him for his encouragement to work on such a challenging and interesting project. He always provides me excellent suggestions and teaches me some useful tips when I have challenges in scientific research. Without his guidence and supervision, the project wouldn't be achieved smoothly. Particularly, I would like to thank the Boehringer Ingelheim Foundation for supporting my PhD financially through the Plus 3 Perspectives Programme funding granted to Dr. Charles Loh in the exploration of noncovalent interactions in stereoselective carbohydrate synthesis.

I am also thankful to Prof. Herbert Waldmann for the excellent infrastructural support for the Loh research group, for my PhD work in Department IV, and for taking over the role as the first examiner for my PhD. Besides, I am also grateful to Prof. Dr. Carsten Strohmann for accepting my invitation to be the second examiner for my PhD.

I would like to express my special gratitude to fellow colleagues from the Loh research group, Dr. Hao Guo and Dr. Wenpeng Ma for their inspiring discussion and supporting assistance throughout my PhD program. Many thanks to my previous colleague Dr. Vippili Uday Bhaskara Rao for giving me a detailed introduction of the lab and other facilities in MPI when I first arrived, I also thank him for his excellent collaboration throught the Rh(I) catalysis project. Without his dedicated support, I would not be able to finish the project so successfully.

I would like to thank all the analytic teams: HRMS team (Dr. Petra Janning and Miss. Christiane Heitbrink) for their measurements for my compounds. NMR team (Mr. Bernhard Griewel and Sasikala Thavam in MPI; Dr. Bastian Grade, Benjamin Kissel and Jan Schonert in TU Dortmund) for their wonderful kinetic experiments and measurement for my project. X-ray team (Prof. Dr. Carsten Strohmann and Anna Krupp) for the confirmation of the molecular structures. HPLC team (Jens Warmers) for teaching me how to use LCMS instrument. VCD team (Prof. Dr. Christian Merten, Corentin Grassin from Ruhr University Bochum) for their effort to comfirm the absolute structure of my molecules.

I would like to thank Christa Hornemann for her warmhearted help in getting me registered smoothly in Dortmund. Thanks Brigitte Rose and Birgit Apprecht for their help in daily affairs. Thanks Lara, Sarah and Aylin for their help to let me learn more about German culture. Thank other members in

department IV and CGC including Dr. Xiufen Cheng, Dr. Gang Xue, Dr. Jianing Xie, Dr. Fubao Huang, Dr. Lin Wang, Dr. Hui Chun-ngai, Dr. Jing Chen, Dr. RuiRui Zhang, Dr. Suyuan Chen, Zhou Zhao, Yang Liu, Mao Jiang, Xiaqiu Qiu and Siyu Liu. I greatly cherish the moments we spent together having parties and celebrating Chinese festivals.

Last but not least, I appreciate my parents for allowing me to pursue a PhD overseas, and I thank my sisters for caring for our parents when I am not around. Without your understanding, I would be unable to concentrate on my PhD studies. I thank my wife, Miss Zhu, for your accompaniment which helped me overcome my loneliness, your encouragement and assistance which made me more confident and stronger.

There aren't many choices in life, so seize them and move forward bravely, never regretting anything. Choosing to pursue a PhD at Dortmund is the best decision I've ever made, and it will have a profound impact on my life. Thank you, everyone I met in Dortmund.

7.3 Eidesstattliche Versicherung (Affidavit)

Name, Vorname
(Surname, first name)

Matrikel-Nr.
(Enrolment number)

Belehrung:

Wer vorsätzlich gegen eine die Täuschung über Prüfungsleistungen betreffende Regelung einer Hochschulprüfungsordnung verstößt, handelt ordnungswidrig. Die Ordnungswidrigkeit kann mit einer Geldbuße von bis zu 50.000,00 € geahndet werden. Zuständige Verwaltungsbehörde für die Verfolgung und Ahndung von Ordnungswidrigkeiten ist der Kanzler/die Kanzlerin der Technischen Universität Dortmund. Im Falle eines mehrfachen oder sonstigen schwerwiegenden Täuschungsversuches kann der Prüfling zudem exmatrikuliert werden, § 63 Abs. 5 Hochschulgesetz NRW.

Die Abgabe einer falschen Versicherung an Eides statt ist strafbar.

Wer vorsätzlich eine falsche Versicherung an Eides statt abgibt, kann mit einer Freiheitsstrafe bis zu drei Jahren oder mit Geldstrafe bestraft werden, § 156 StGB. Die fahrlässige Abgabe einer falschen Versicherung an Eides statt kann mit einer Freiheitsstrafe bis zu einem Jahr oder Geldstrafe bestraft werden, § 161 StGB.

Die oben stehende Belehrung habe ich zur Kenntnis genommen:

Official notification:

Any person who intentionally breaches any regulation of university examination regulations relating to deception in examination performance is acting improperly. This offence can be punished with a fine of up to EUR 50,000.00. The competent administrative authority for the pursuit and prosecution of offences of this type is the chancellor of the TU Dortmund University. In the case of multiple or other serious attempts at deception, the candidate can also be unenrolled, Section 63, paragraph 5 of the Universities Act of North Rhine-Westphalia.

The submission of a false affidavit is punishable.

Any person who intentionally submits a false affidavit can be punished with a prison sentence of up to three years or a fine, Section 156 of the Criminal Code. The negligent submission of a false affidavit can be punished with a prison sentence of up to one year or a fine, Section 161 of the Criminal Code.

I have taken note of the above official notification.

Ort, Datum
(Place, date)

Unterschrift
(Signature)

Titel der Dissertation:
(Title of the thesis):

Ich versichere hiermit an Eides statt, dass ich die vorliegende Dissertation mit dem Titel selbstständig und ohne unzulässige fremde Hilfe angefertigt habe. Ich habe keine anderen als die angegebenen Quellen und Hilfsmittel benutzt sowie wörtliche und sinngemäße Zitate kenntlich gemacht.
Die Arbeit hat in gegenwärtiger oder in einer anderen Fassung weder der TU Dortmund noch einer anderen Hochschule im Zusammenhang mit einer staatlichen oder akademischen Prüfung vorgelegen.

I hereby swear that I have completed the present dissertation independently and without inadmissible external support. I have not used any sources or tools other than those indicated and have identified literal and analogous quotations.

The thesis in its current version or another version has not been presented to the TU Dortmund University or another university in connection with a state or academic examination.*

*Please be aware that solely the German version of the affidavit ("Eidesstattliche Versicherung") for the PhD thesis is the official and legally binding version.

Ort, Datum
(Place, date)

Unterschrift
(Signature)

8. NMR spectra

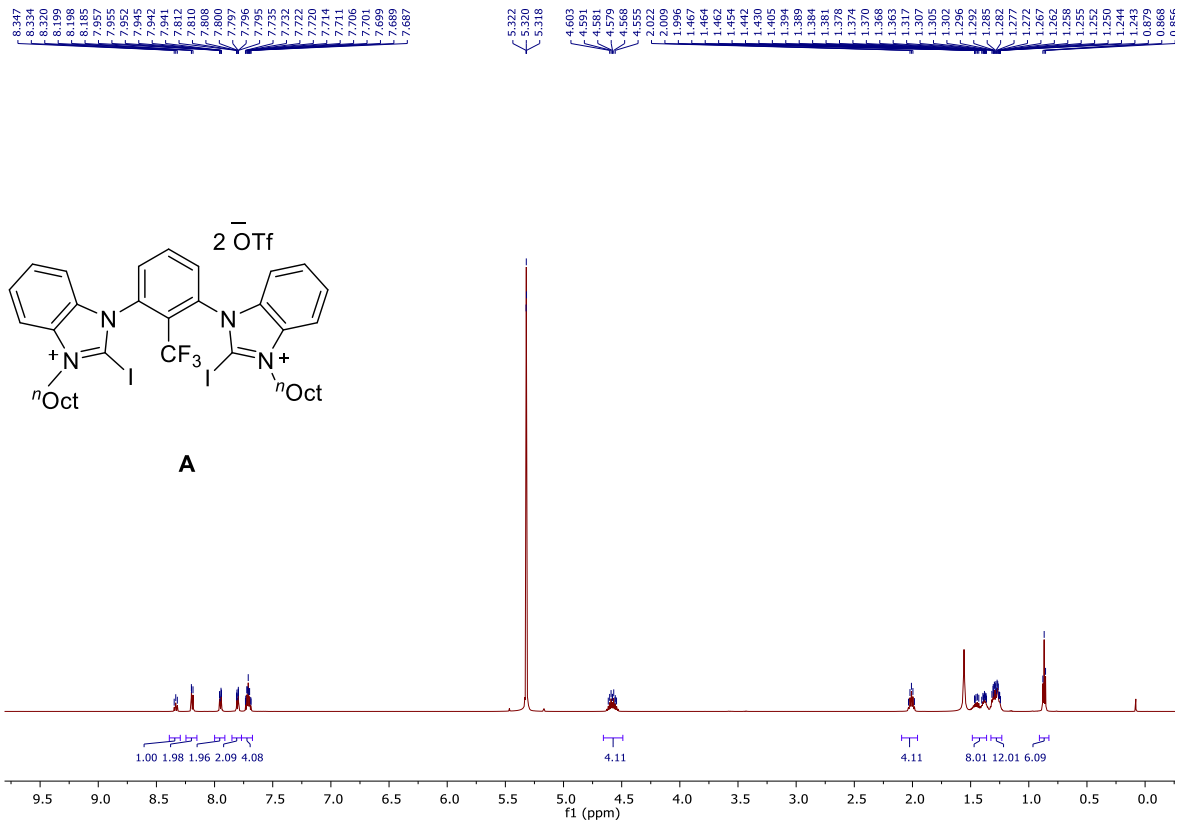

Figure 8.1. ^{1}H NMR spectra for A

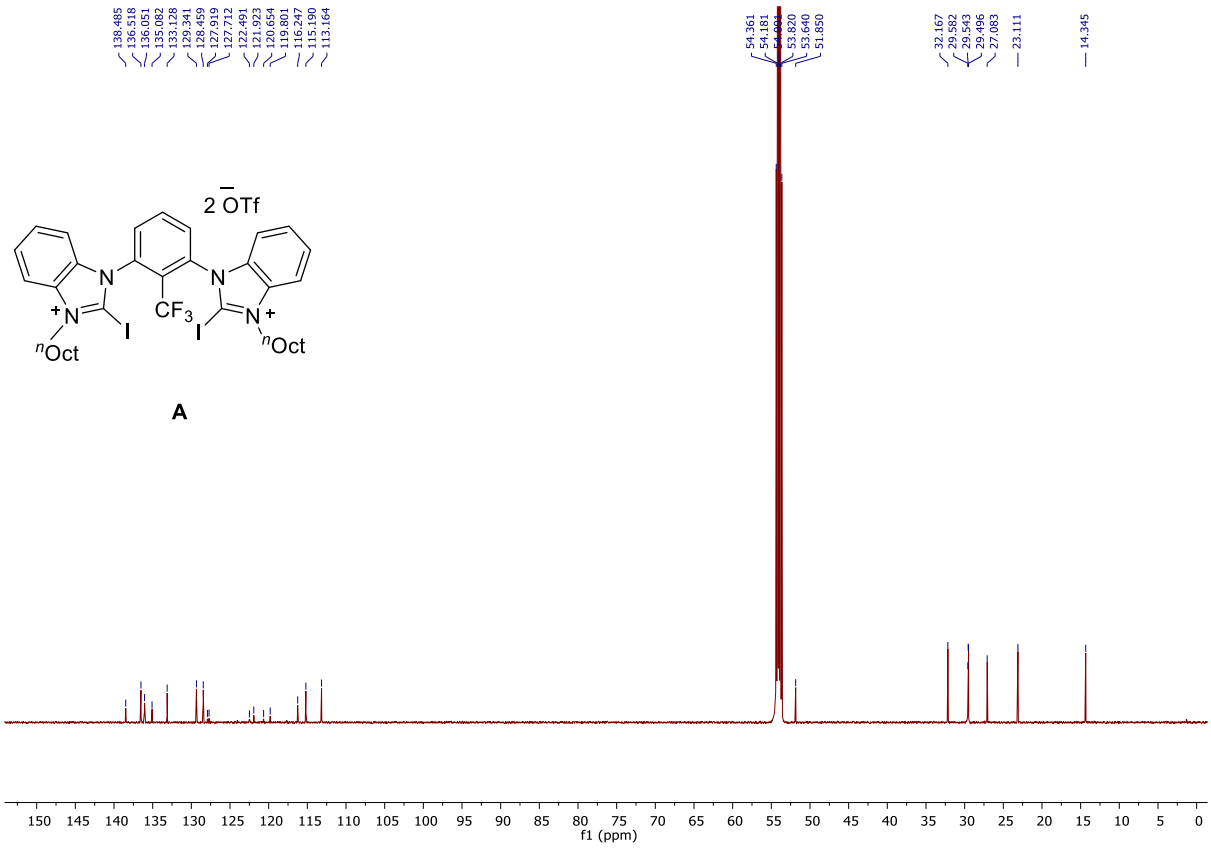

Figure 8.2. ^{13}C NMR spectra for A

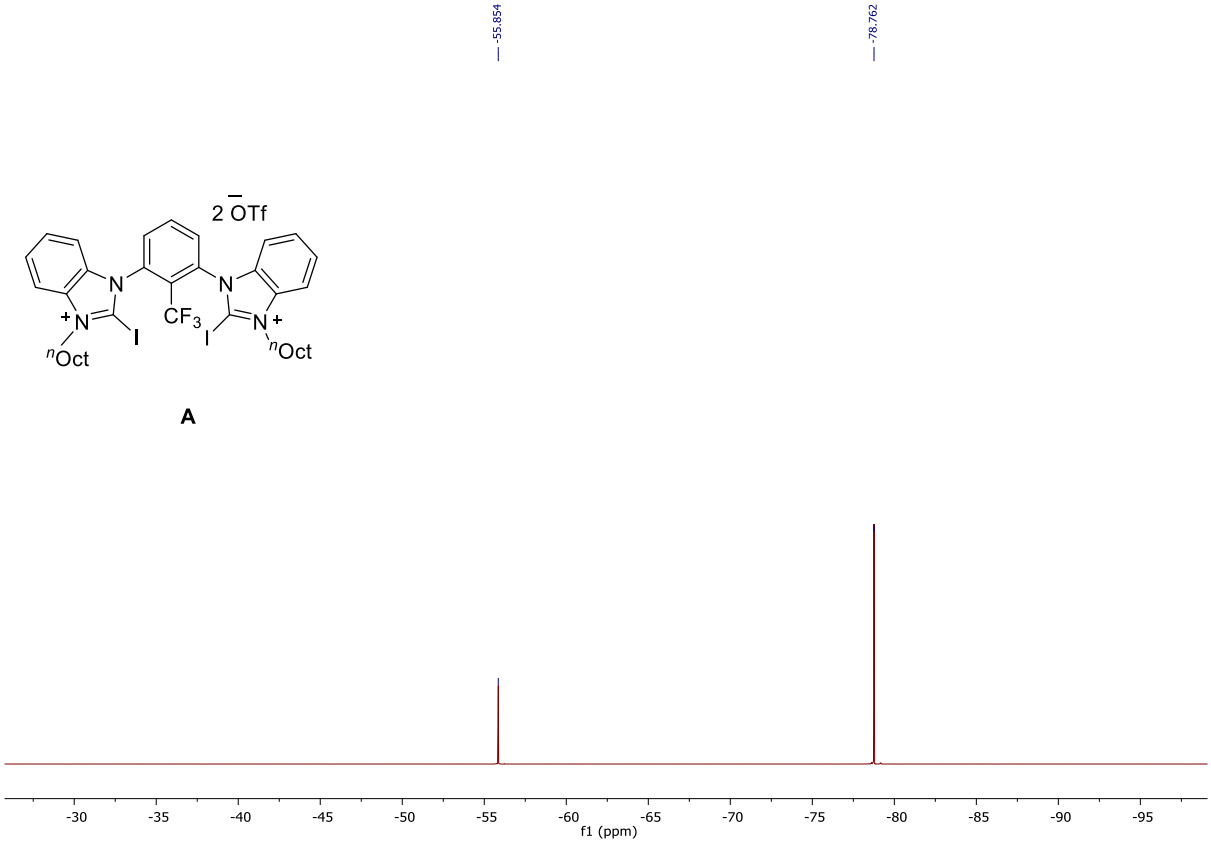

Figure 8.3. ^{19}F NMR spectra for A

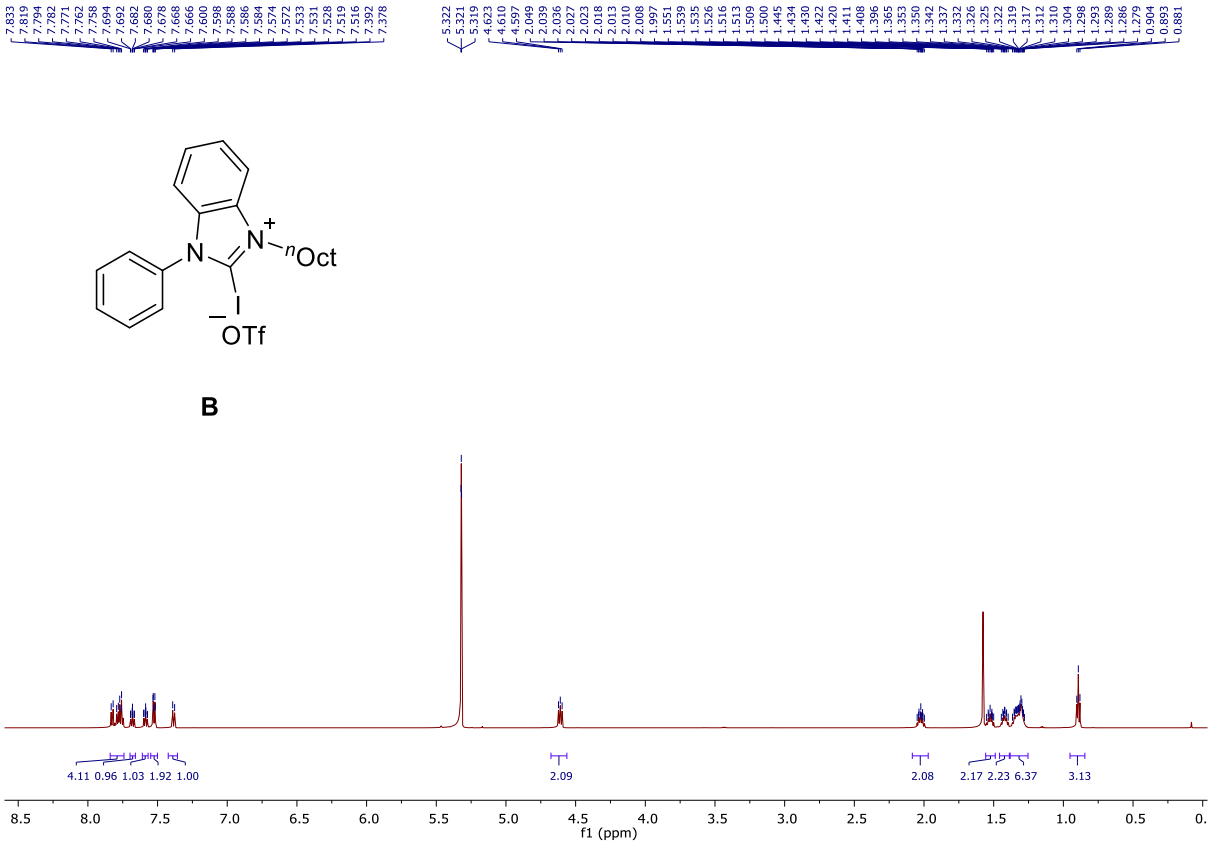

Figure 8.4. ^{1}H NMR spectra for B

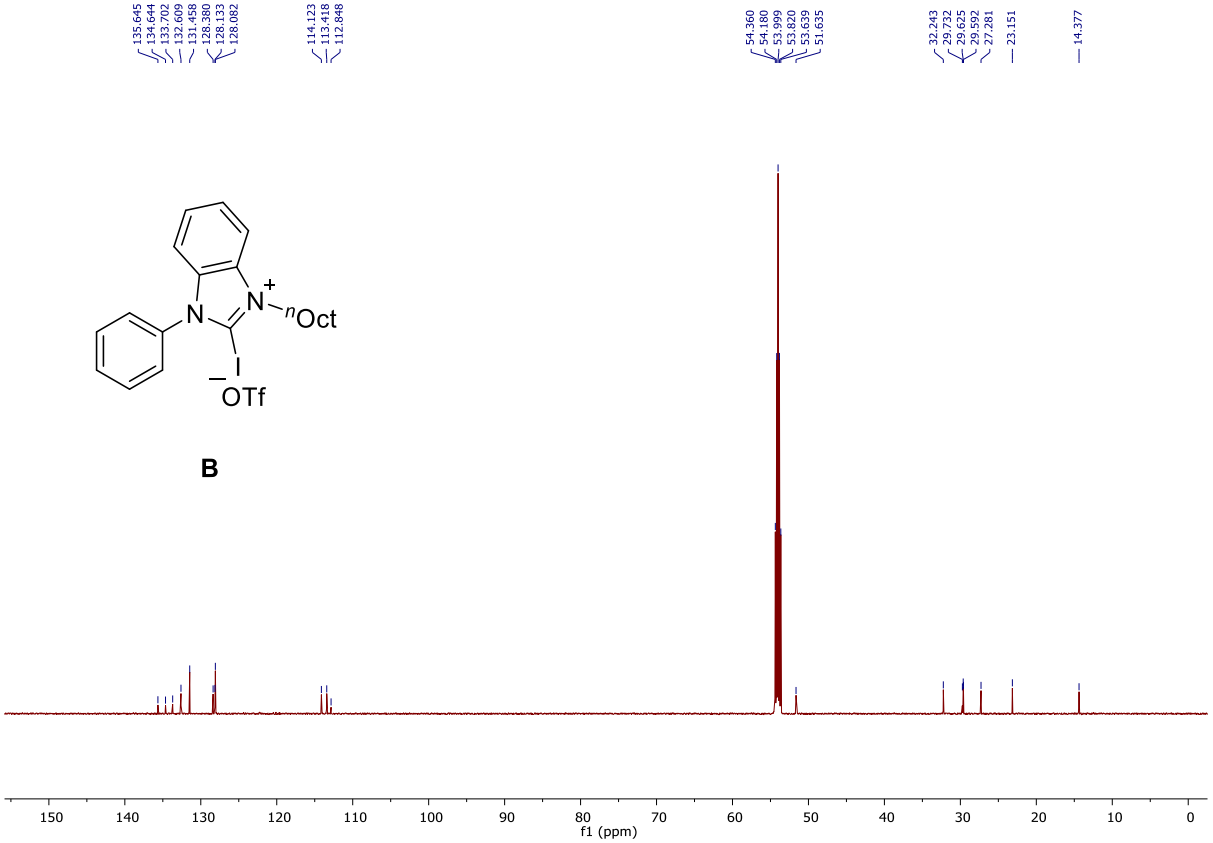

Figure 8.5. ^{13}C NMR spectra for B

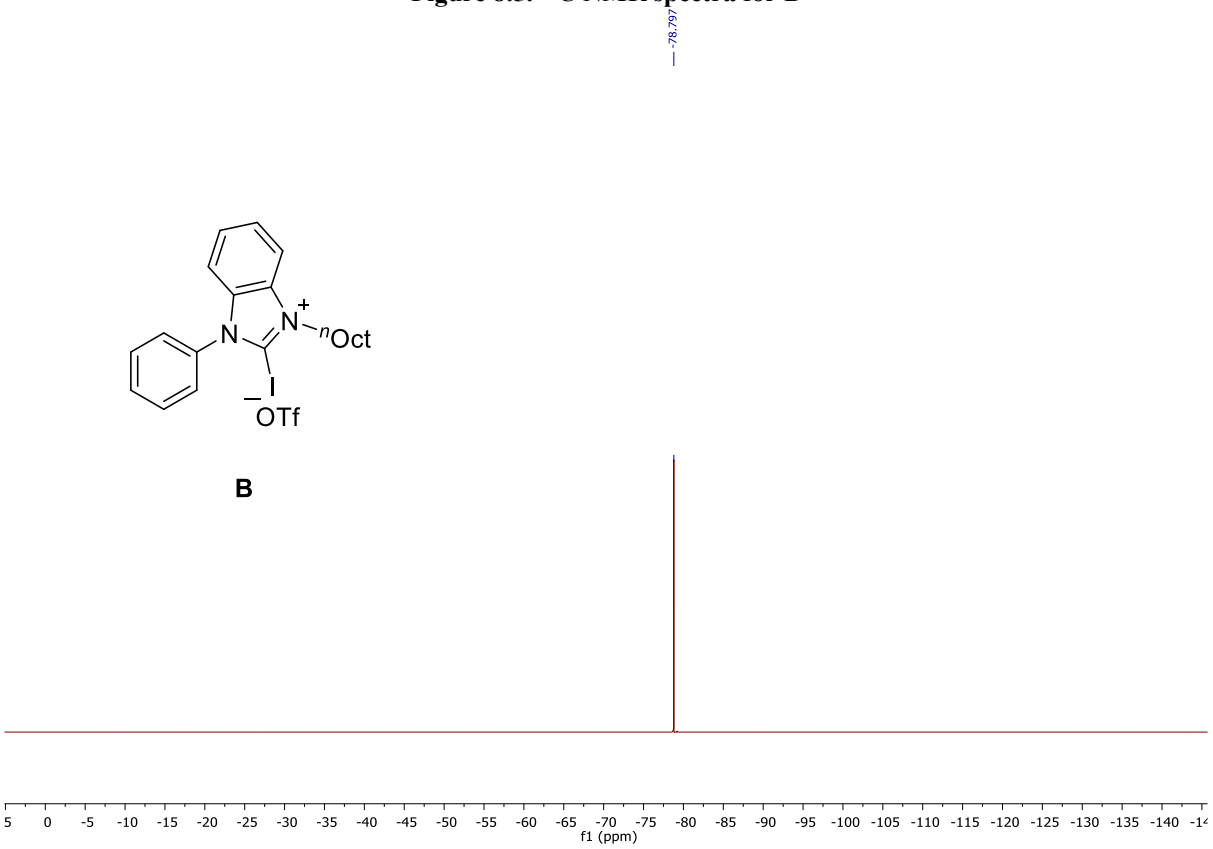

Figure 8.6. ^{19}F NMR spectra for B

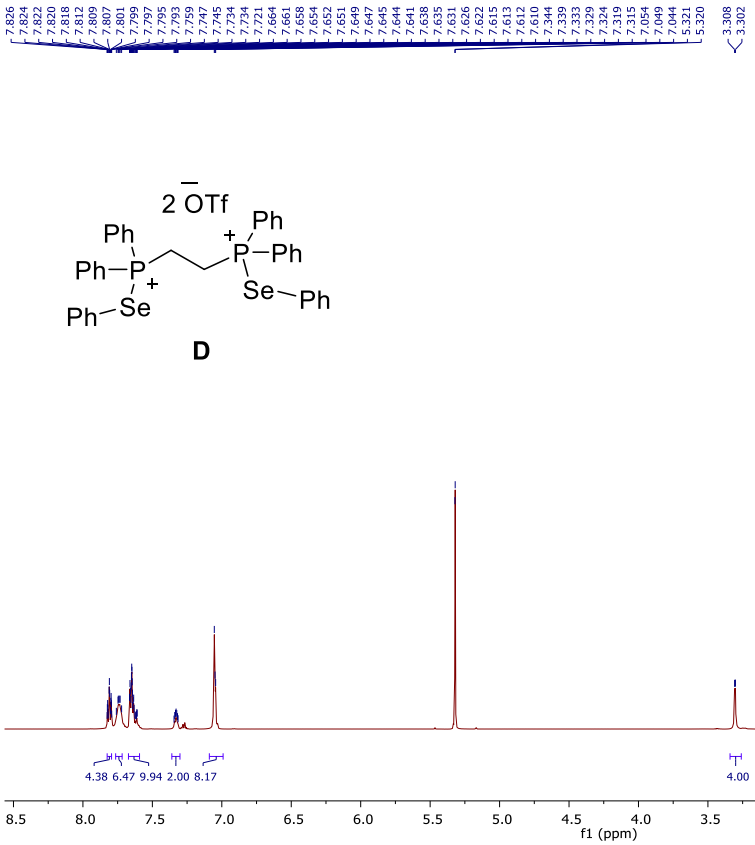

Figure 8.7. ^{1}H NMR spectra for D

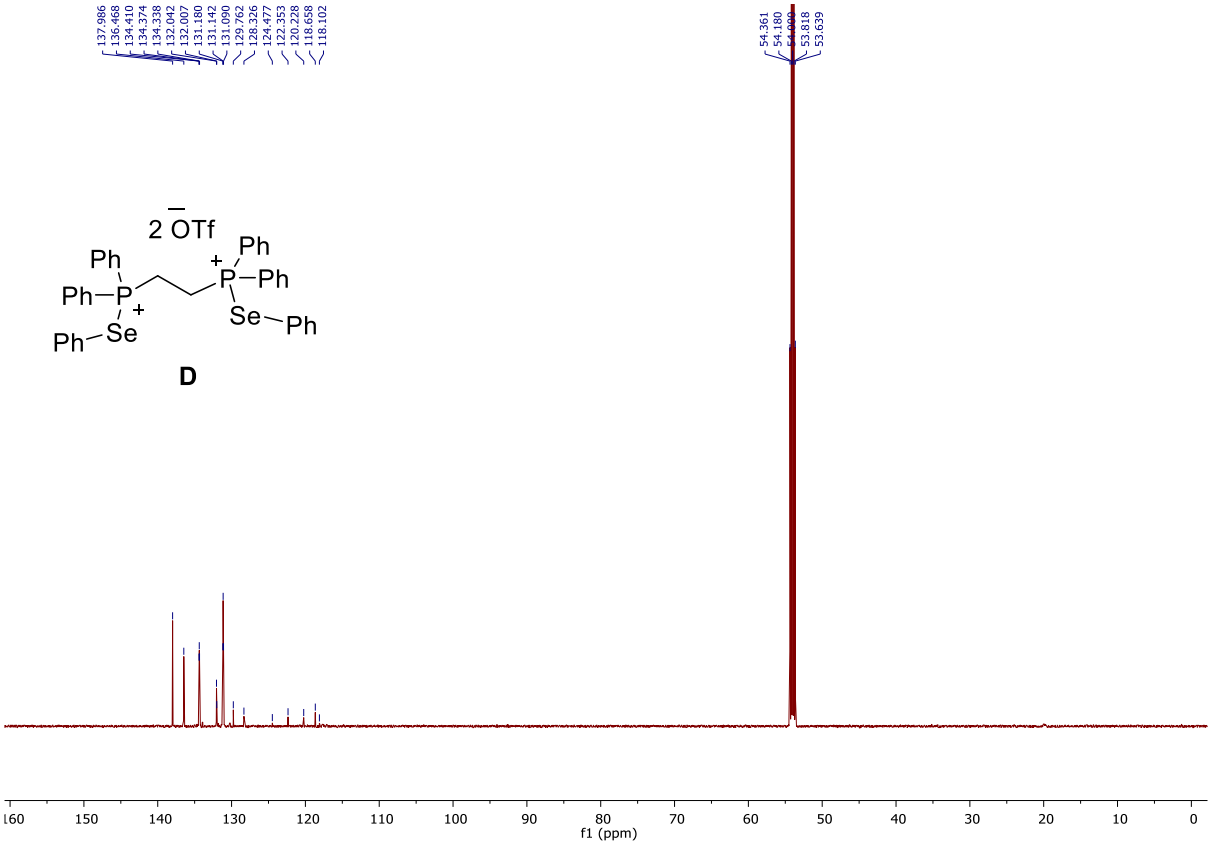

Figure 8.8. ^{13}C NMR spectra for D

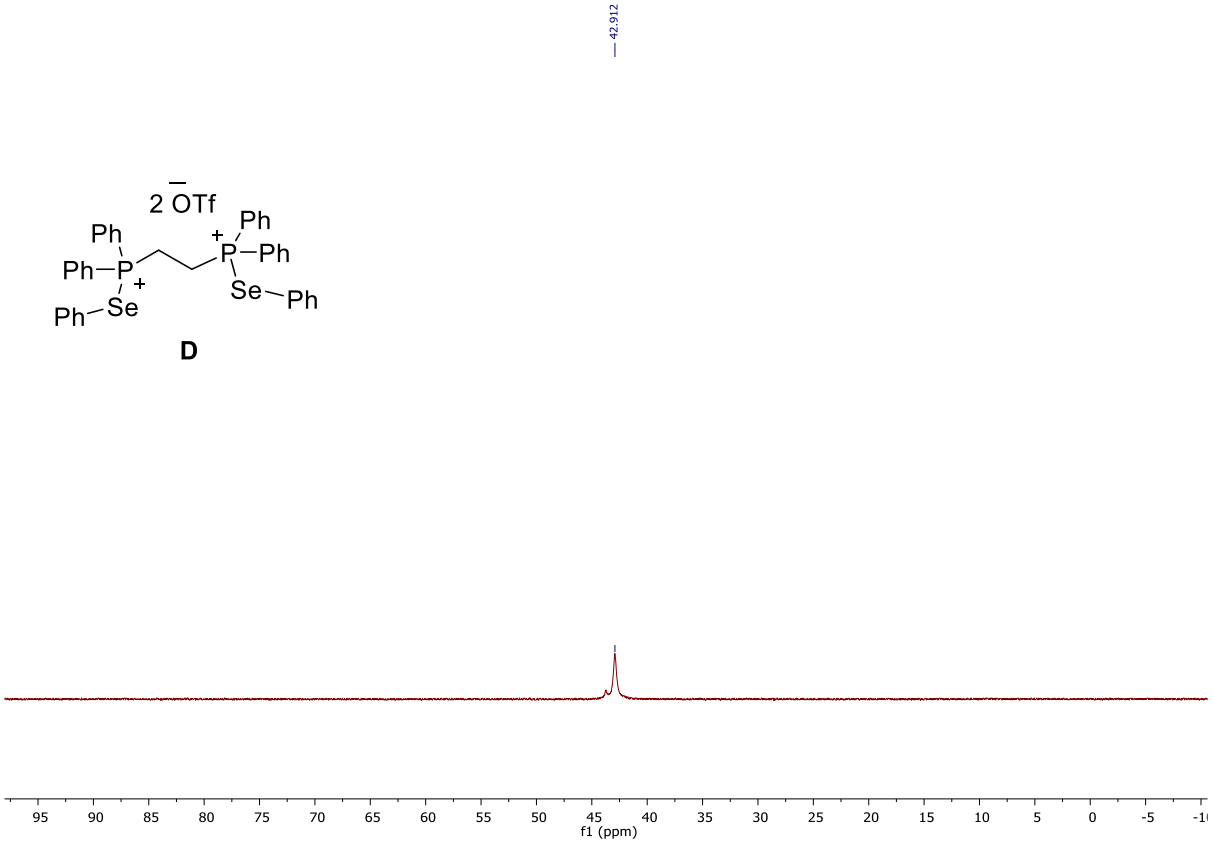

Figure 8.9. ^{31}P NMR spectra for D

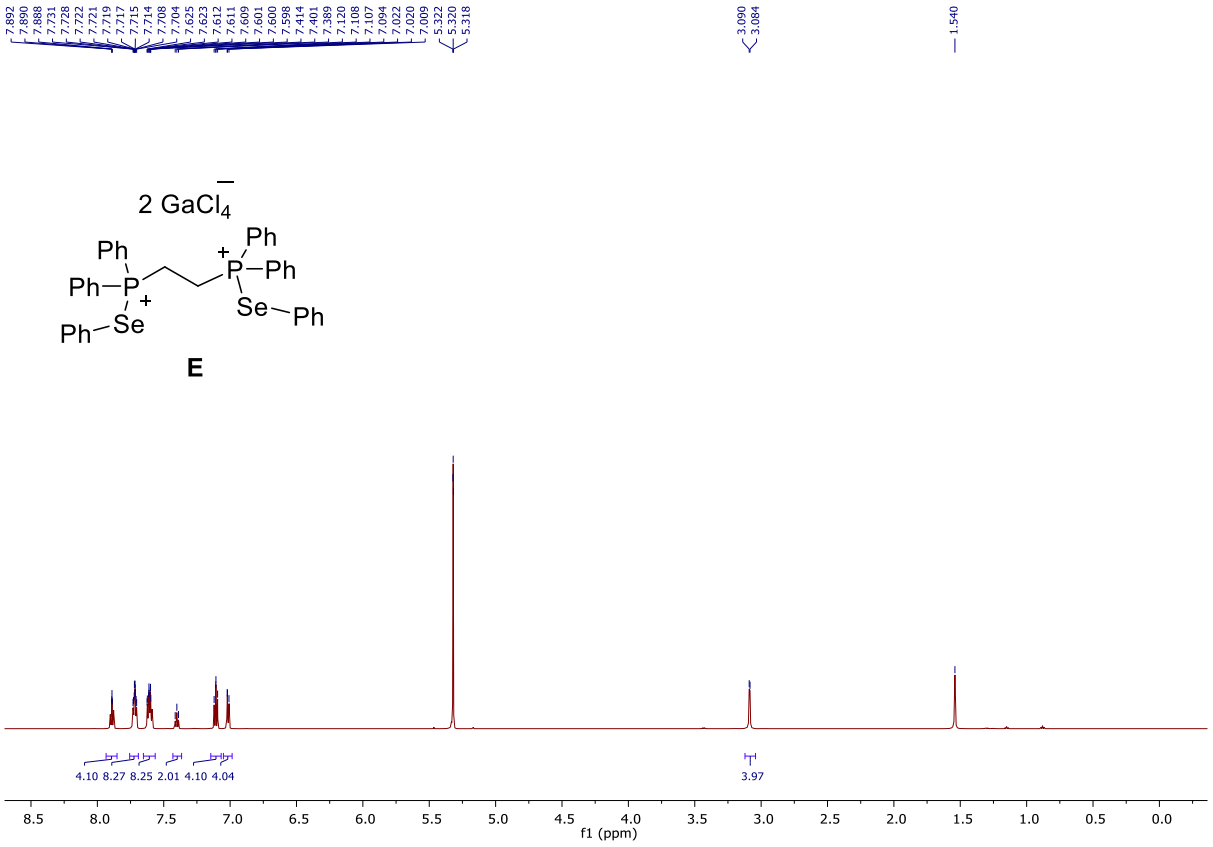

Figure 8.10. ^{1}H NMR spectra for E

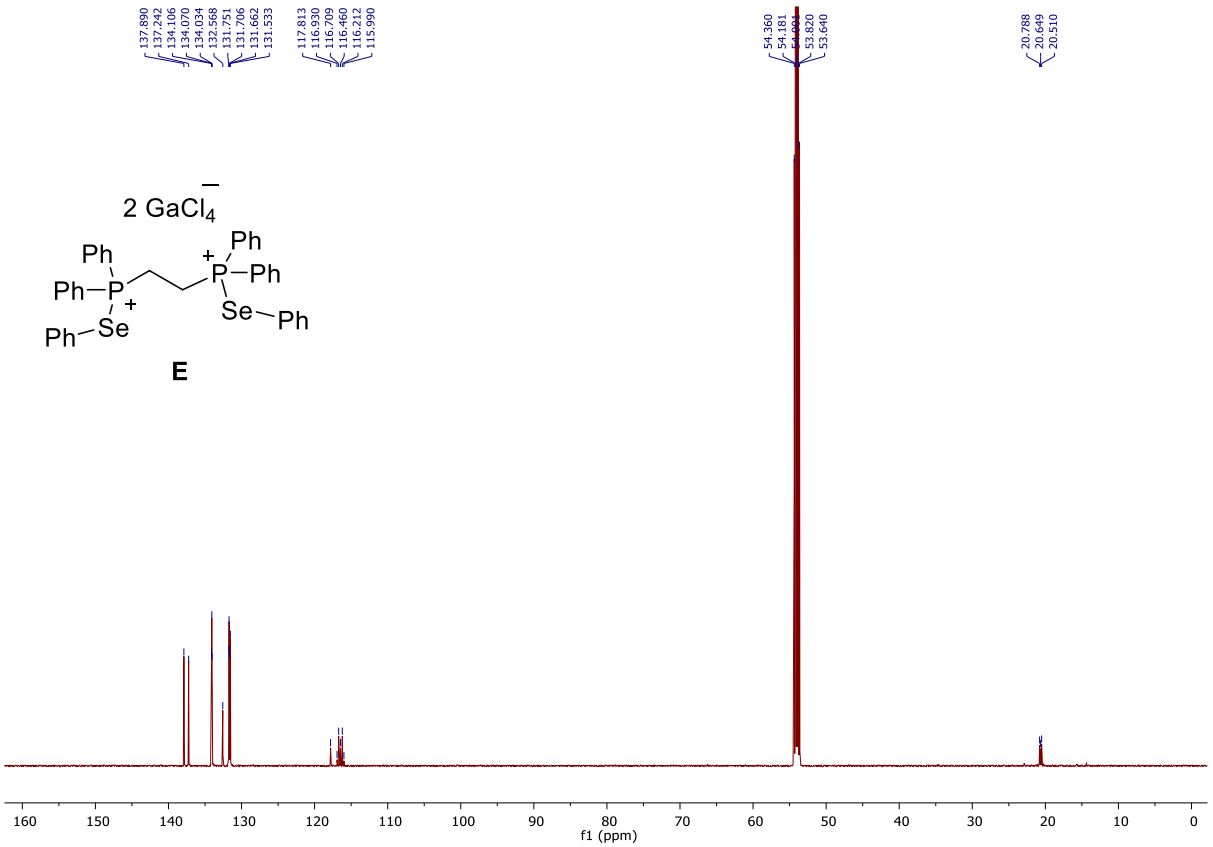

Figure 8.11. ^{13}C NMR spectra for E

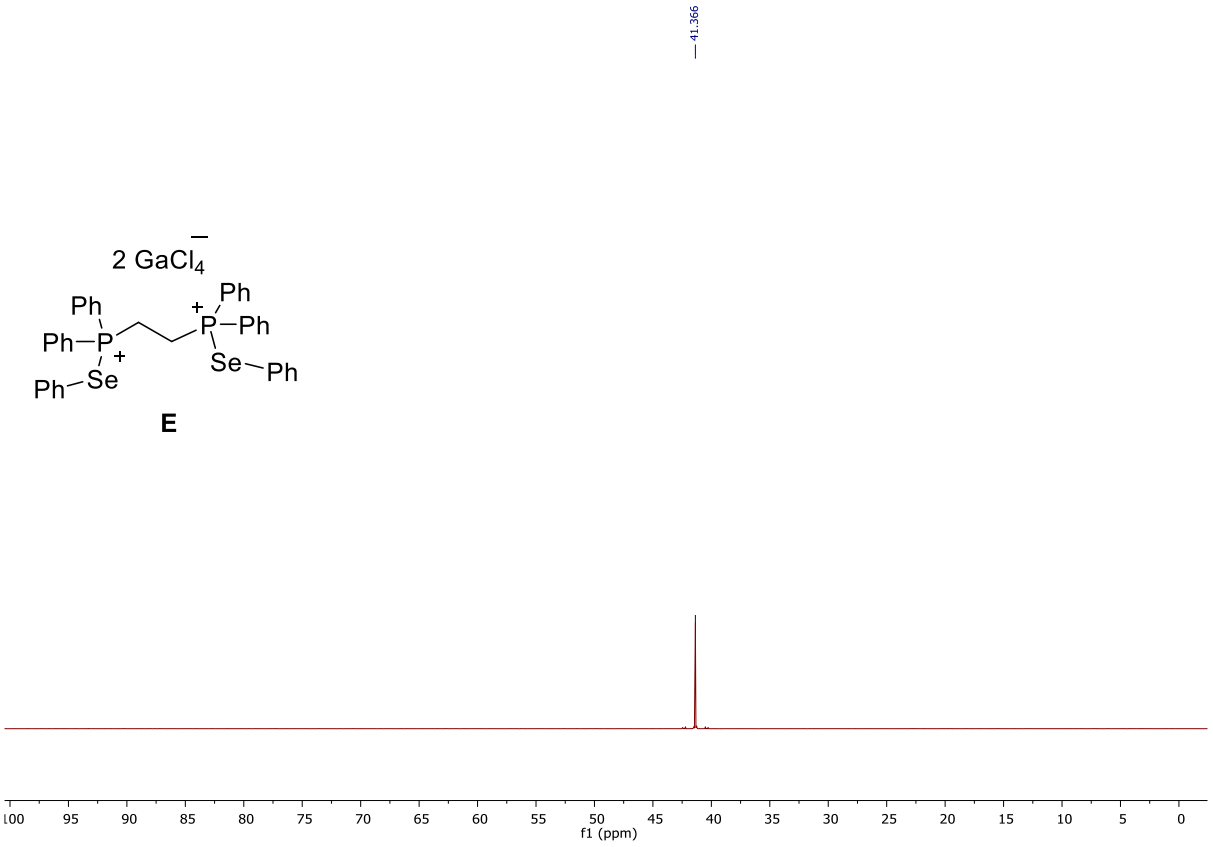

Figure 8.12. ^{31}P NMR spectra for E

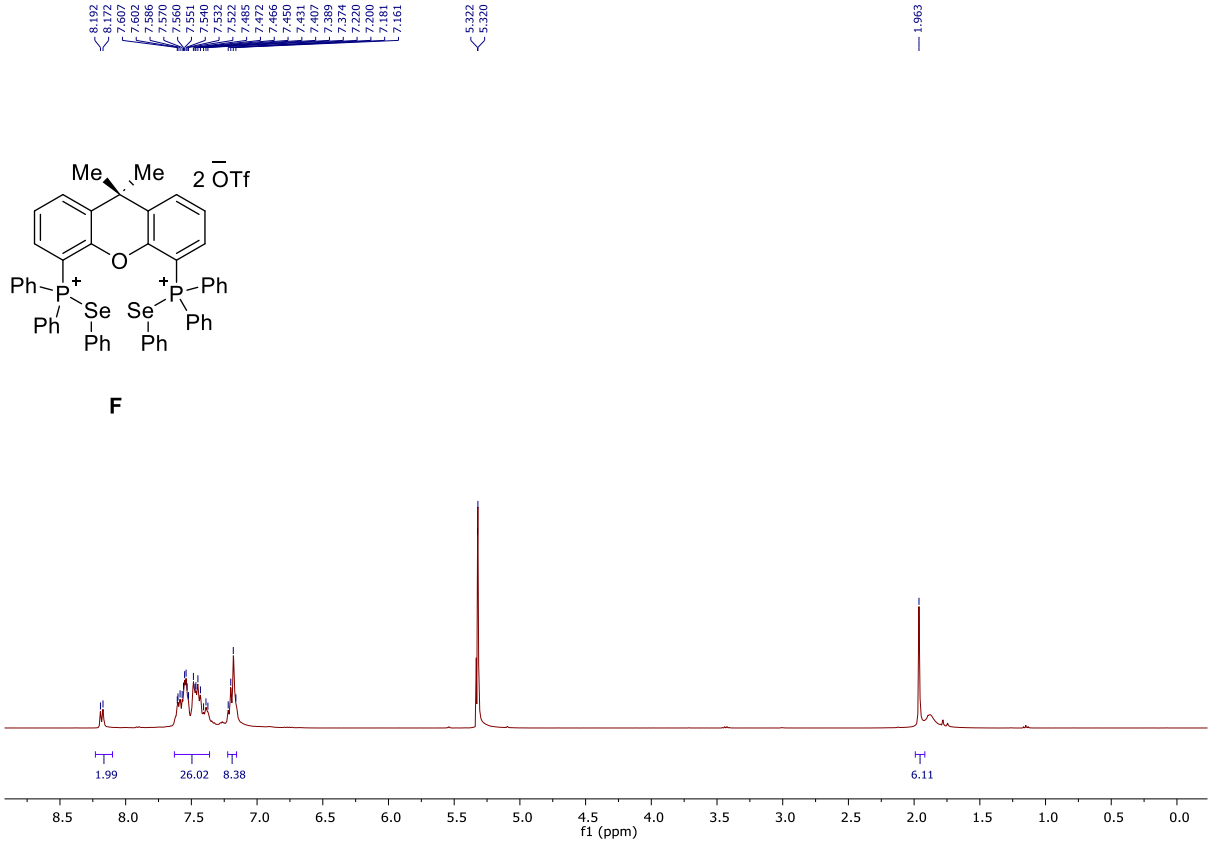

Figure 8.13. ^{1}H NMR spectra for F

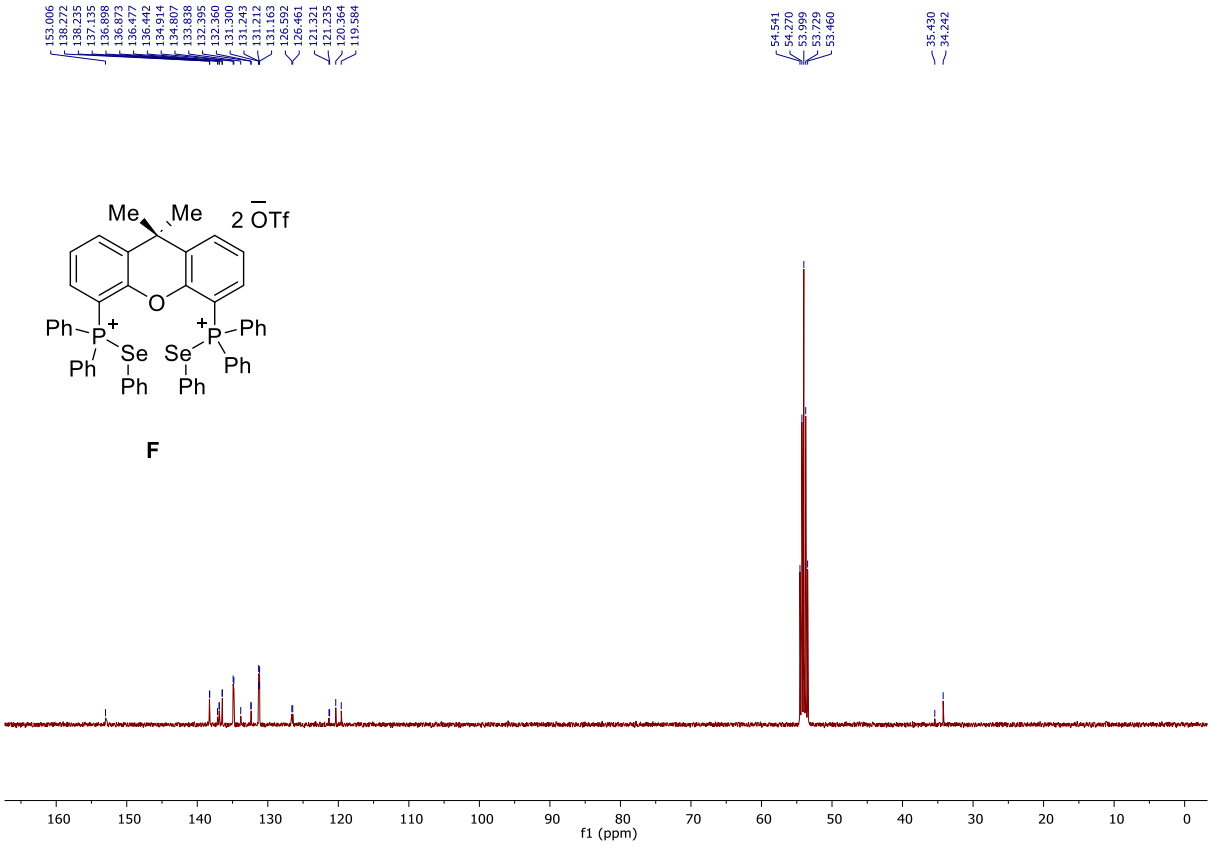

Figure 8.14. ^{13}C NMR spectra for F

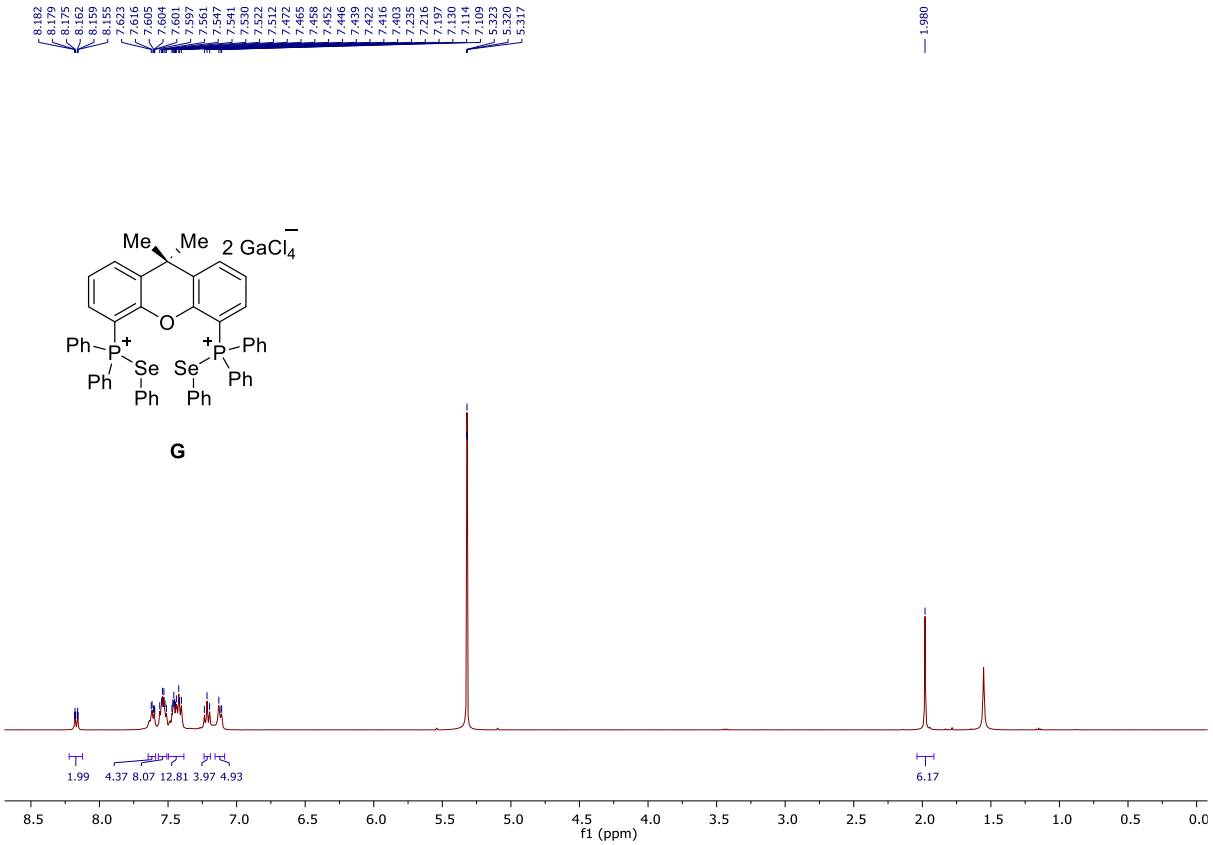

Figure 8.15. ^{1}H NMR spectra for G

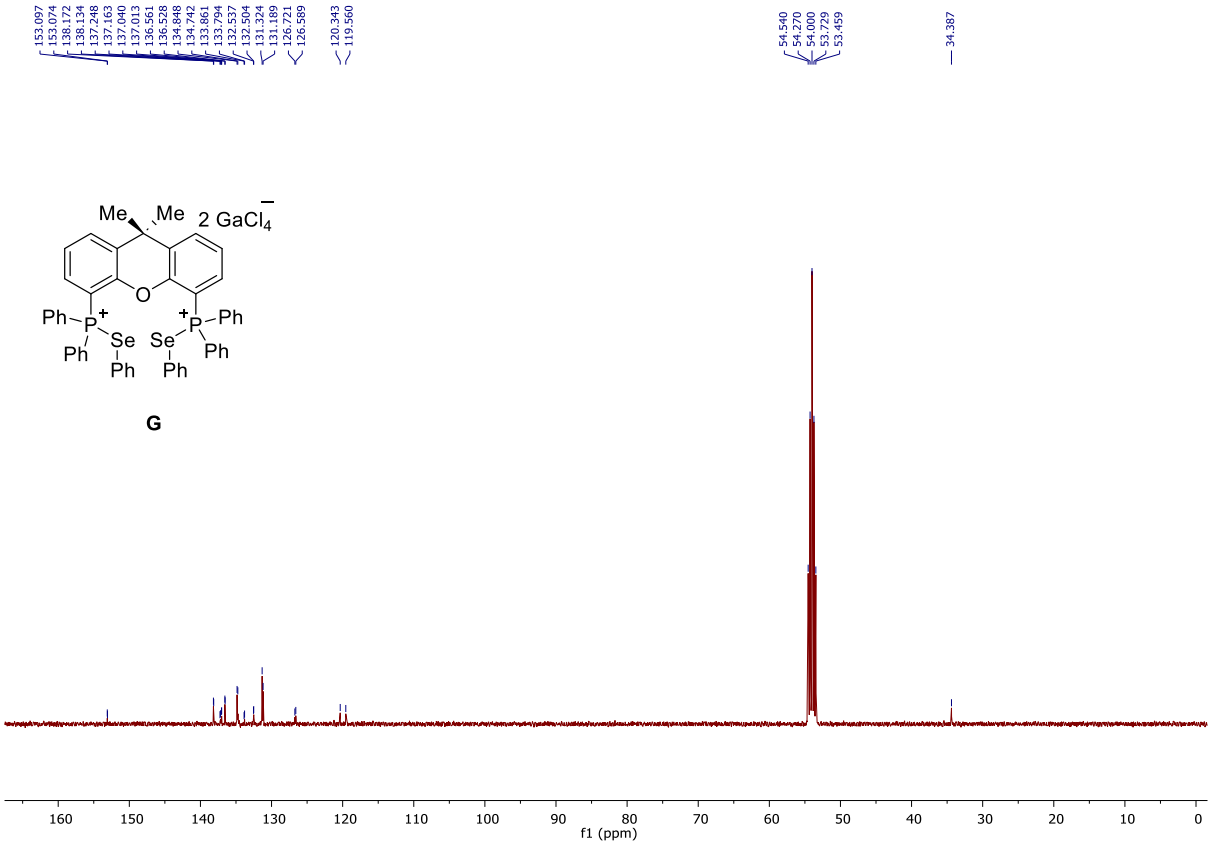

Figure 8.16. ^{13}C NMR spectra for G

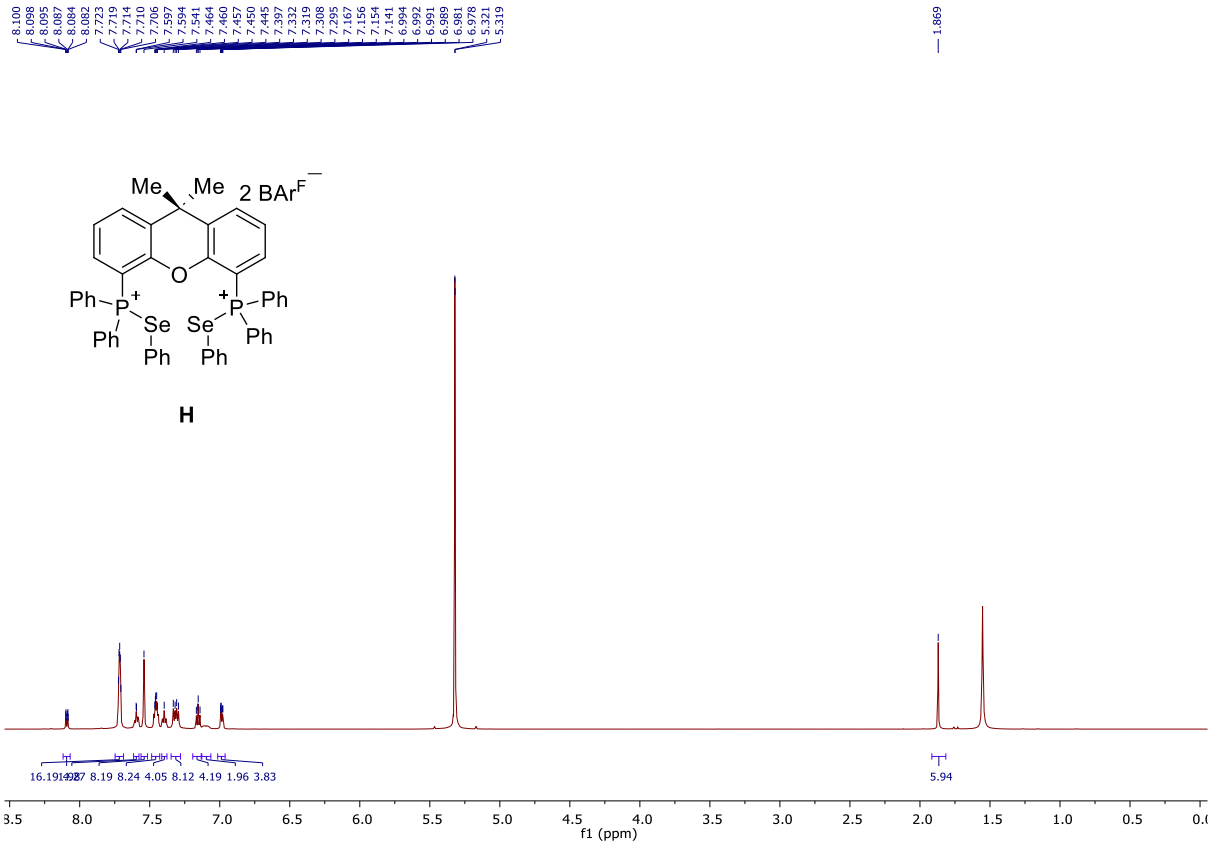

Figure 8.17. ^{1}H NMR spectra for H

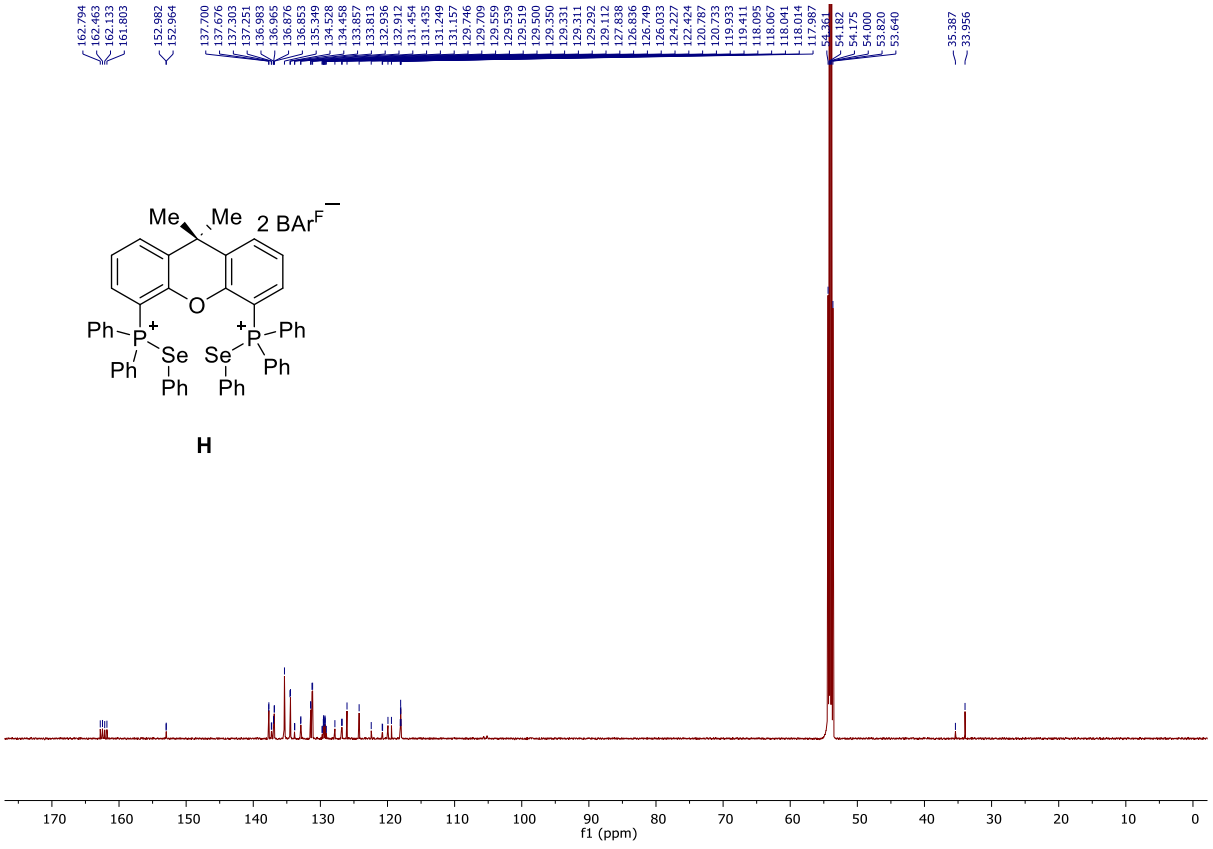

Figure 8.18. ^{13}C NMR spectra for H

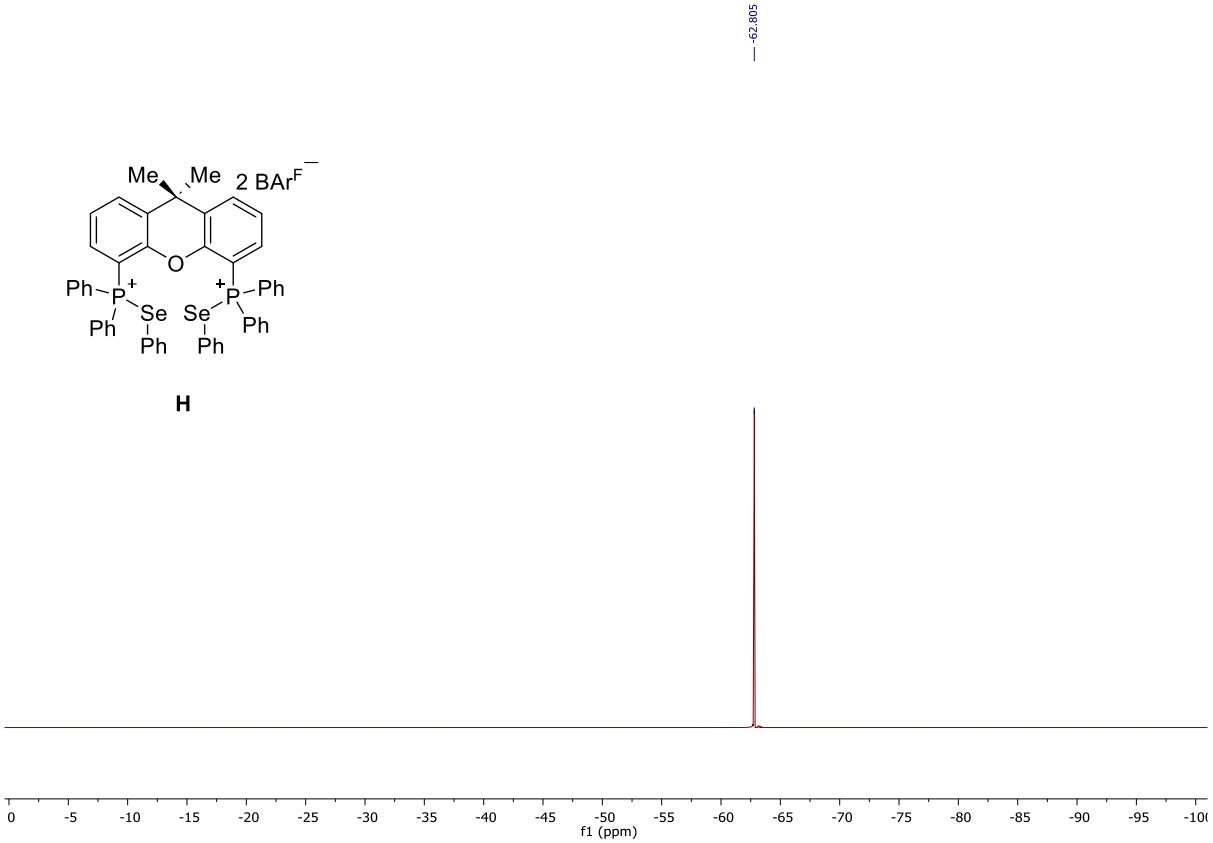

H

Figure 8.19. ^{19}F NMR spectra for H

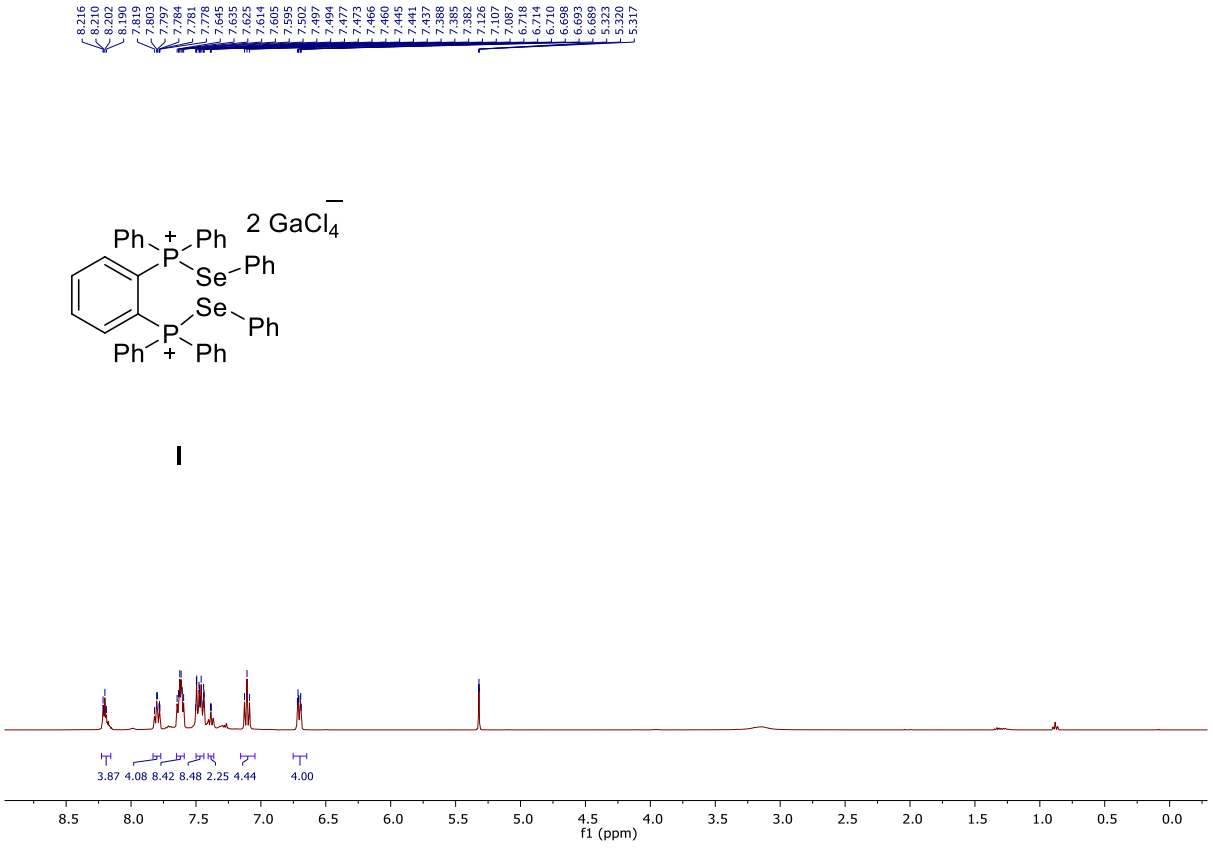

I

Figure 8.20. ^{1}H NMR spectra for I

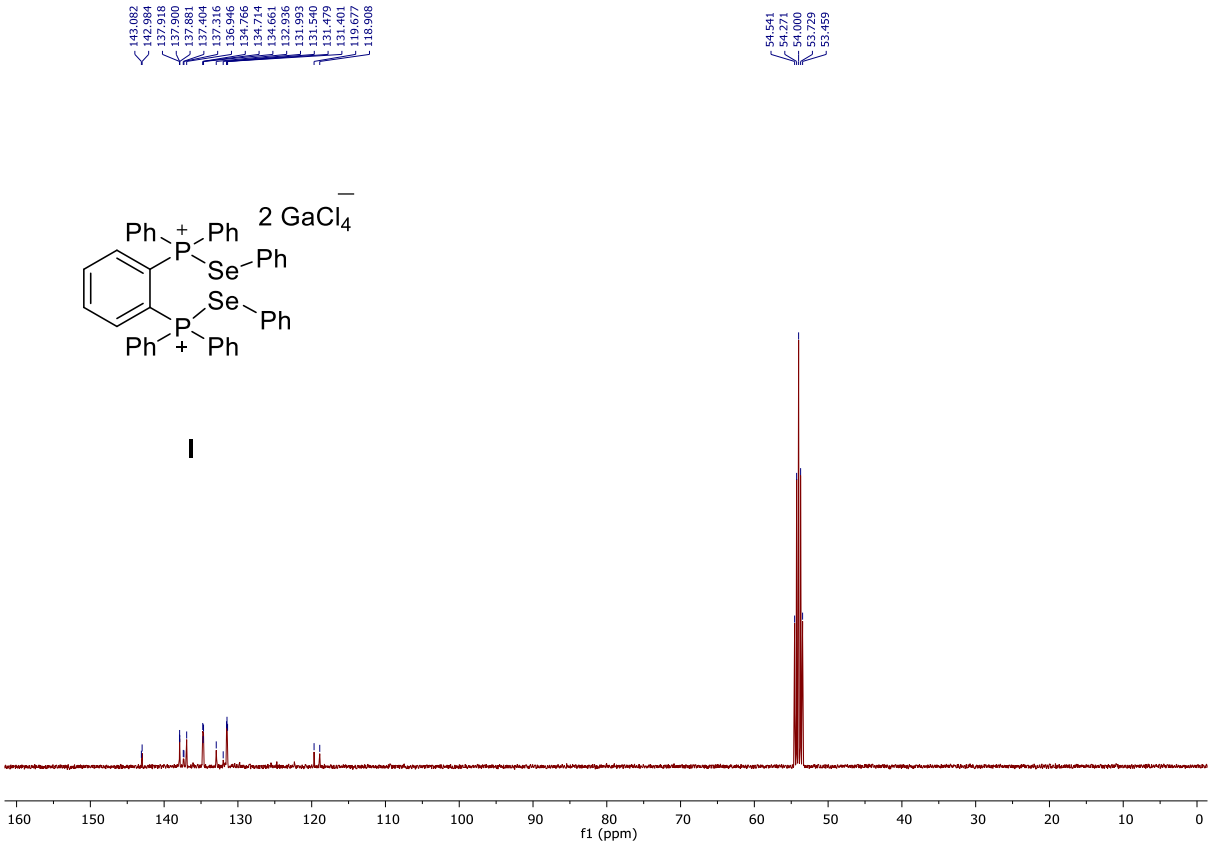

Figure 8.21. ^{13}C NMR spectra for I

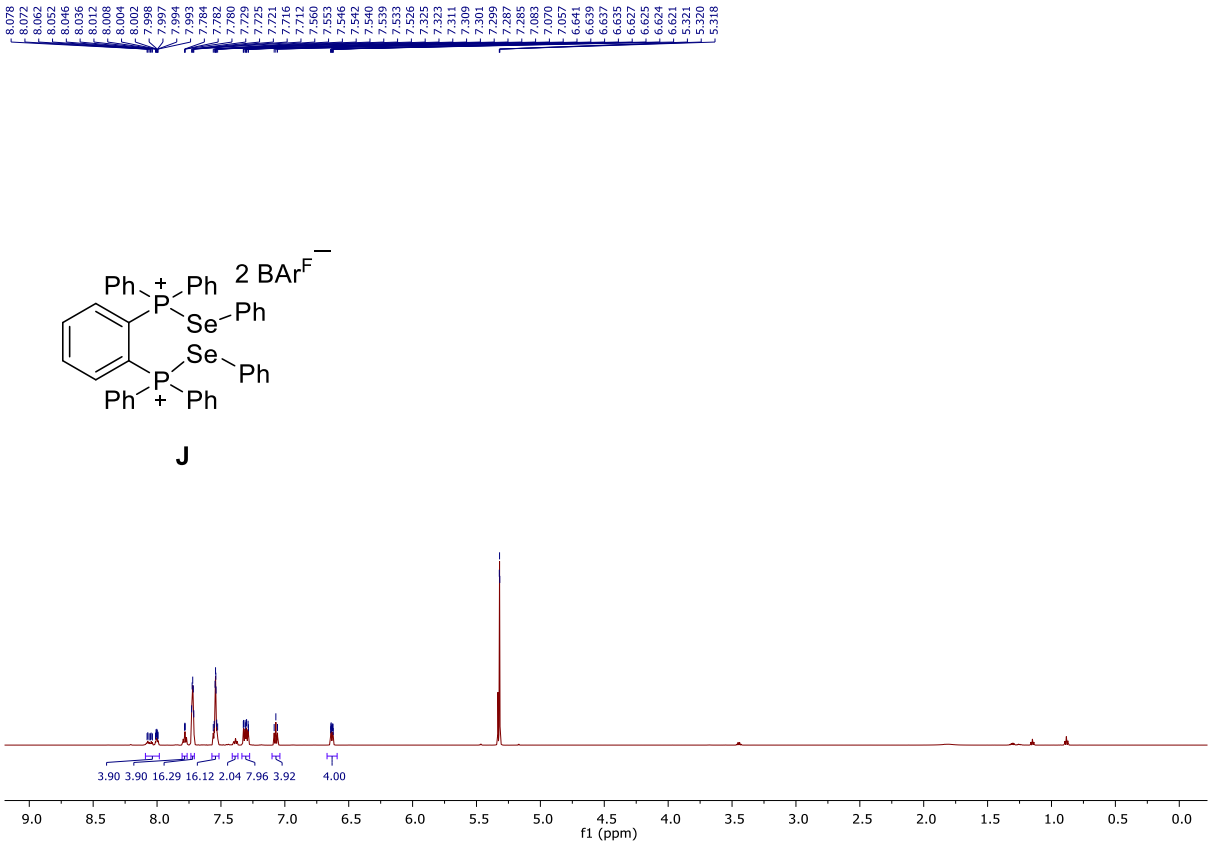

Figure 8.22. ^{1}H NMR spectra for J

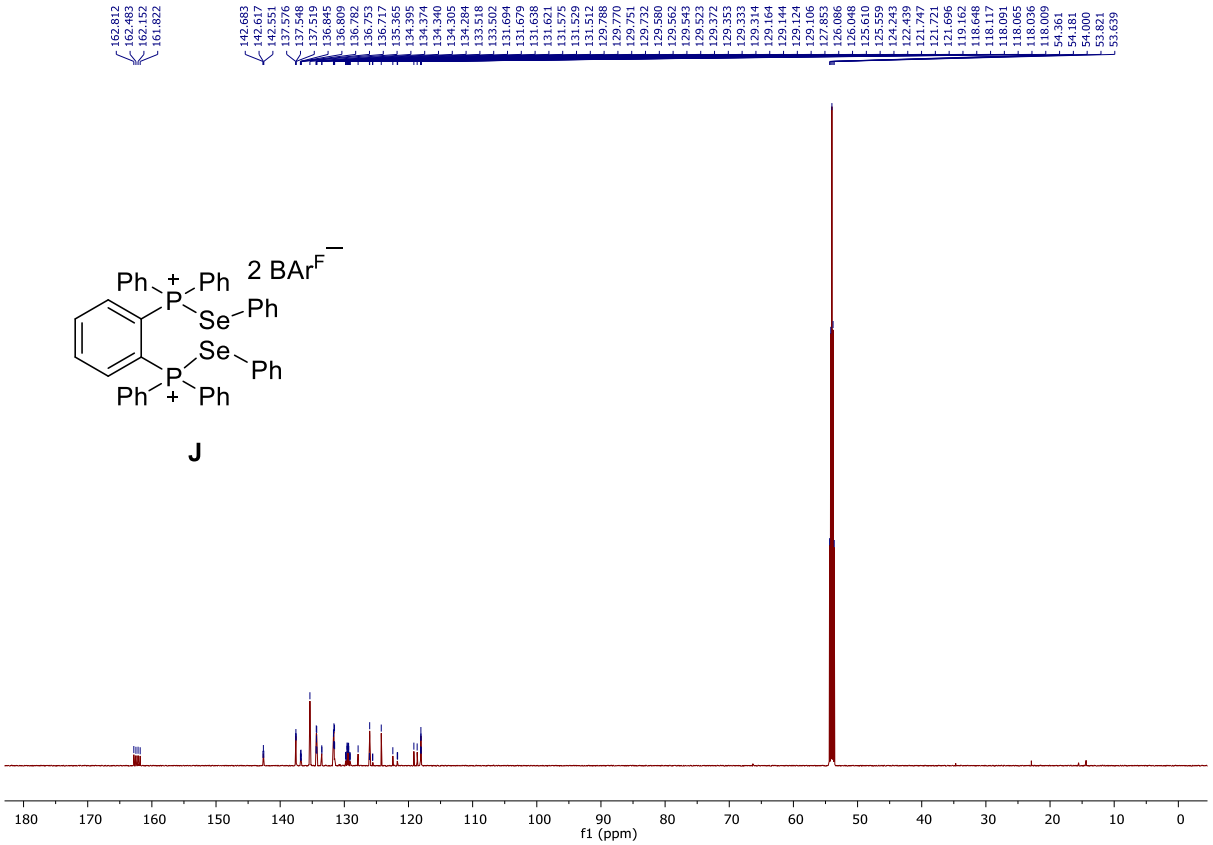

Figure 8.23. ^{13}C NMR spectra for J

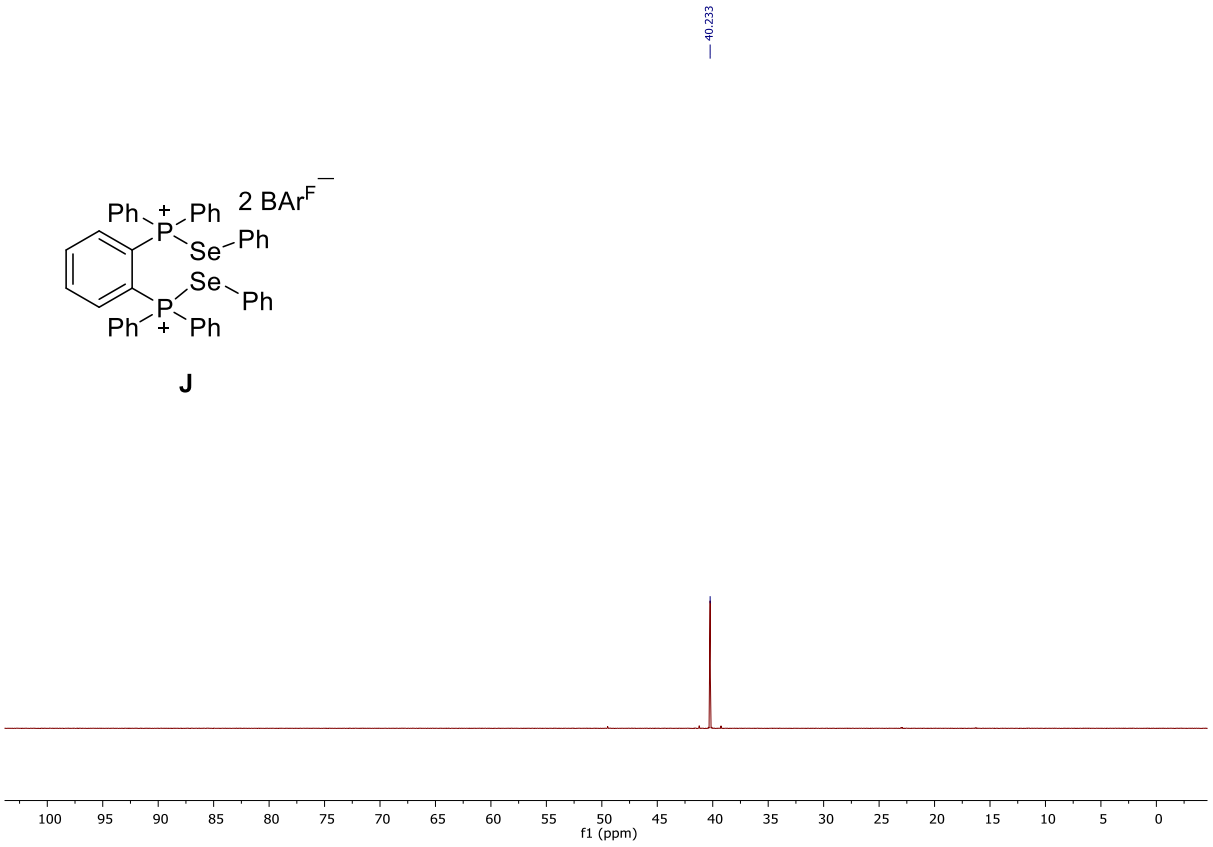

Figure 8.24. ^{31}P NMR spectra for J

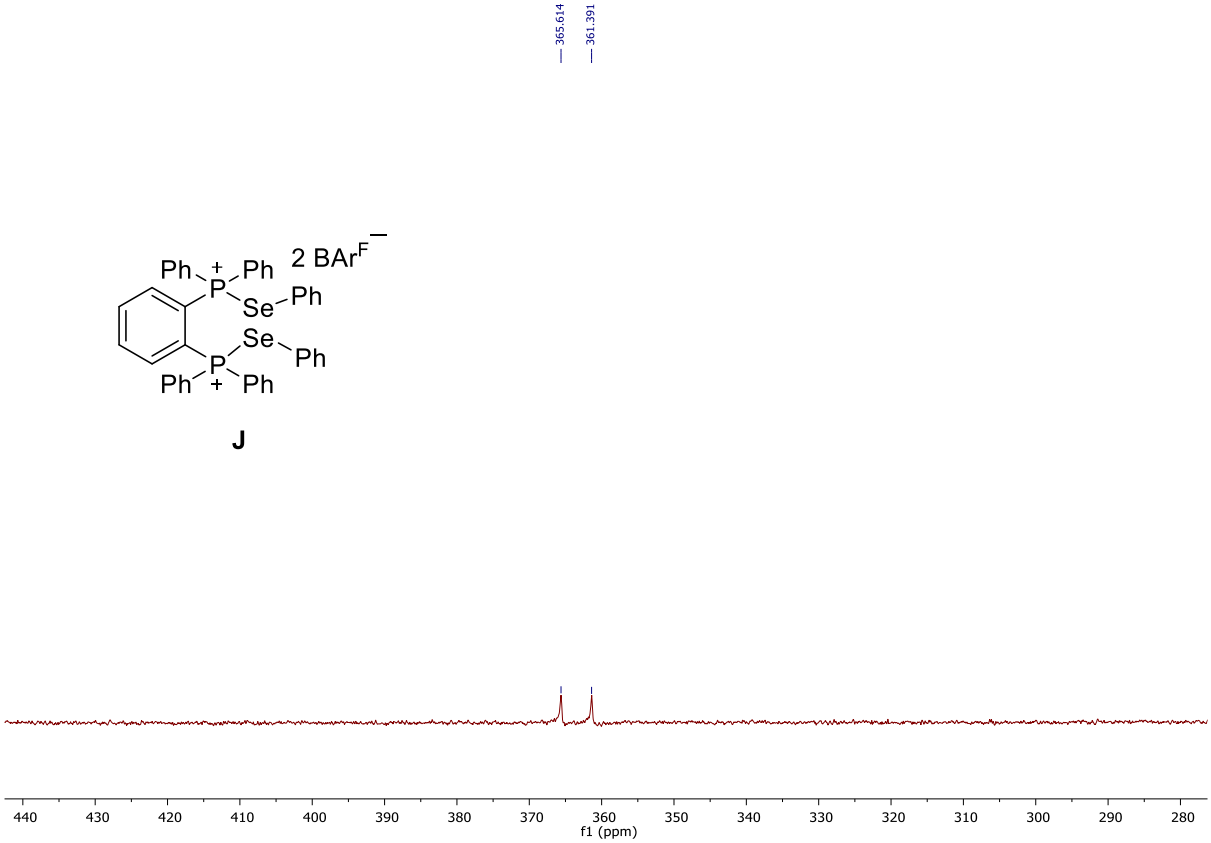

J

Figure 8.25. ^{77}Se NMR spectra for J

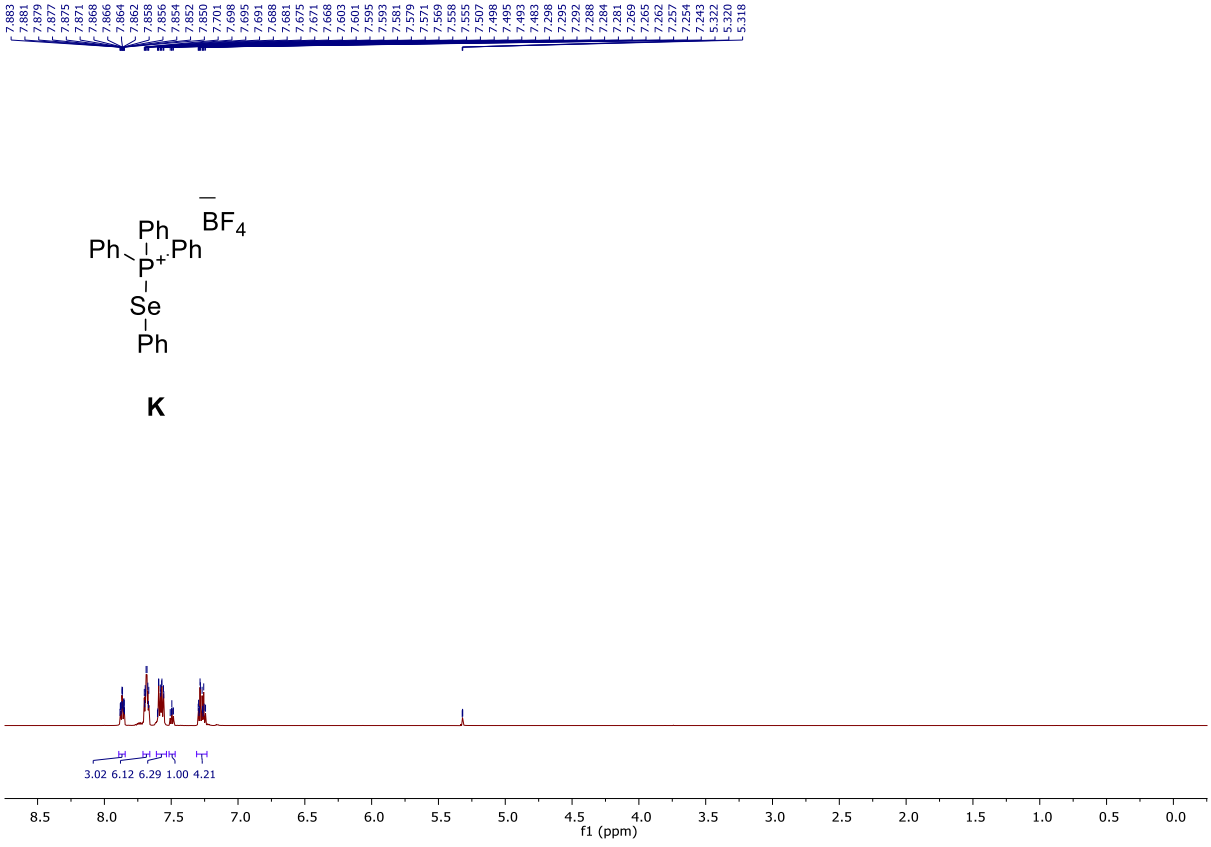

K

Figure 8.26. ^{1}H NMR spectra for K

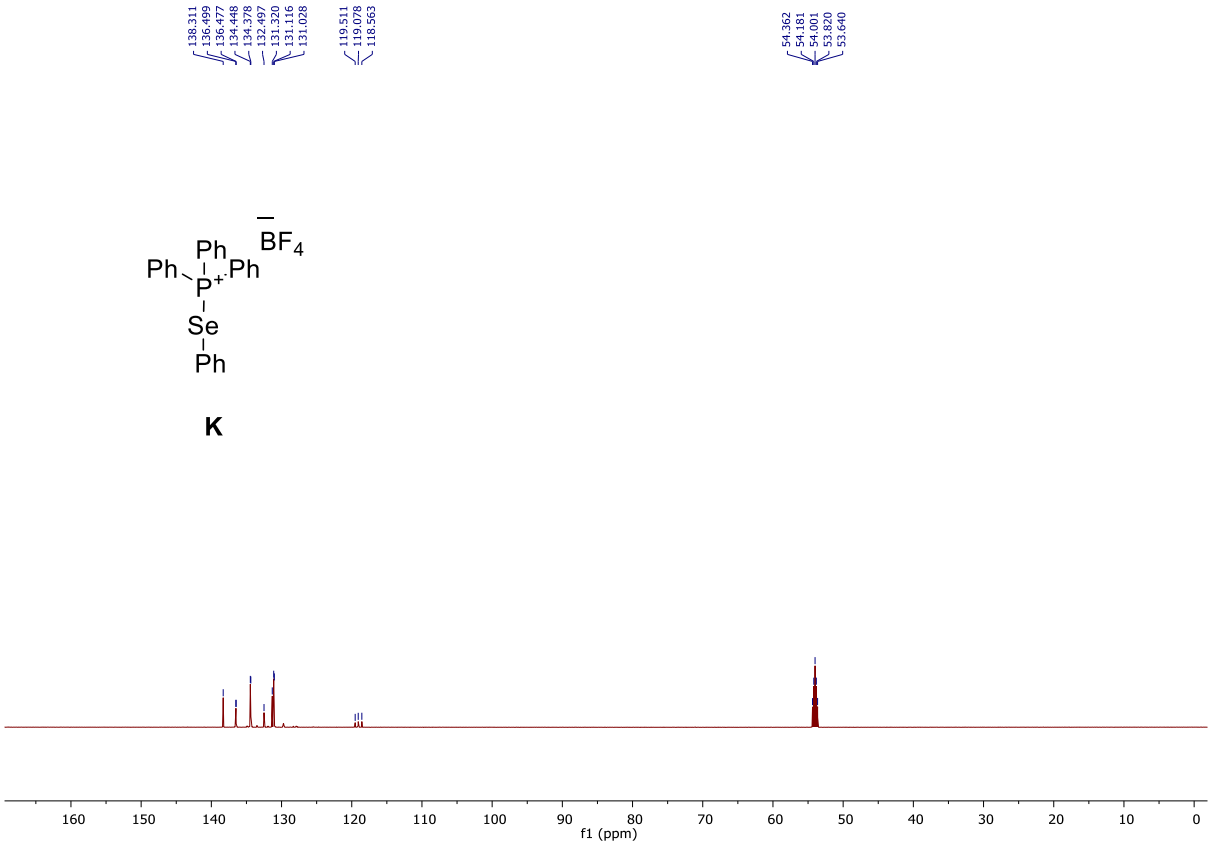

K

Figure 8.27. ^{13}C NMR spectra for K

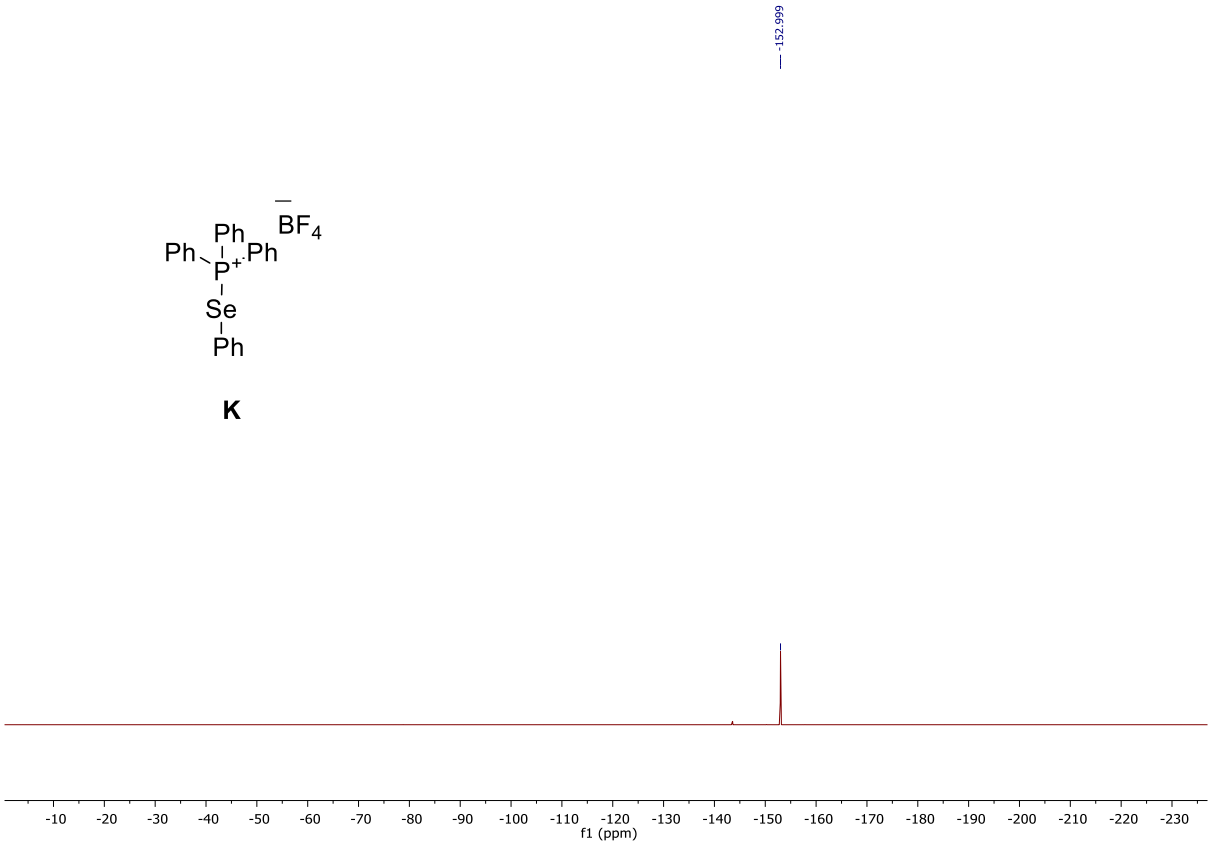

K

Figure 8.28. ^{19}F NMR spectra for K

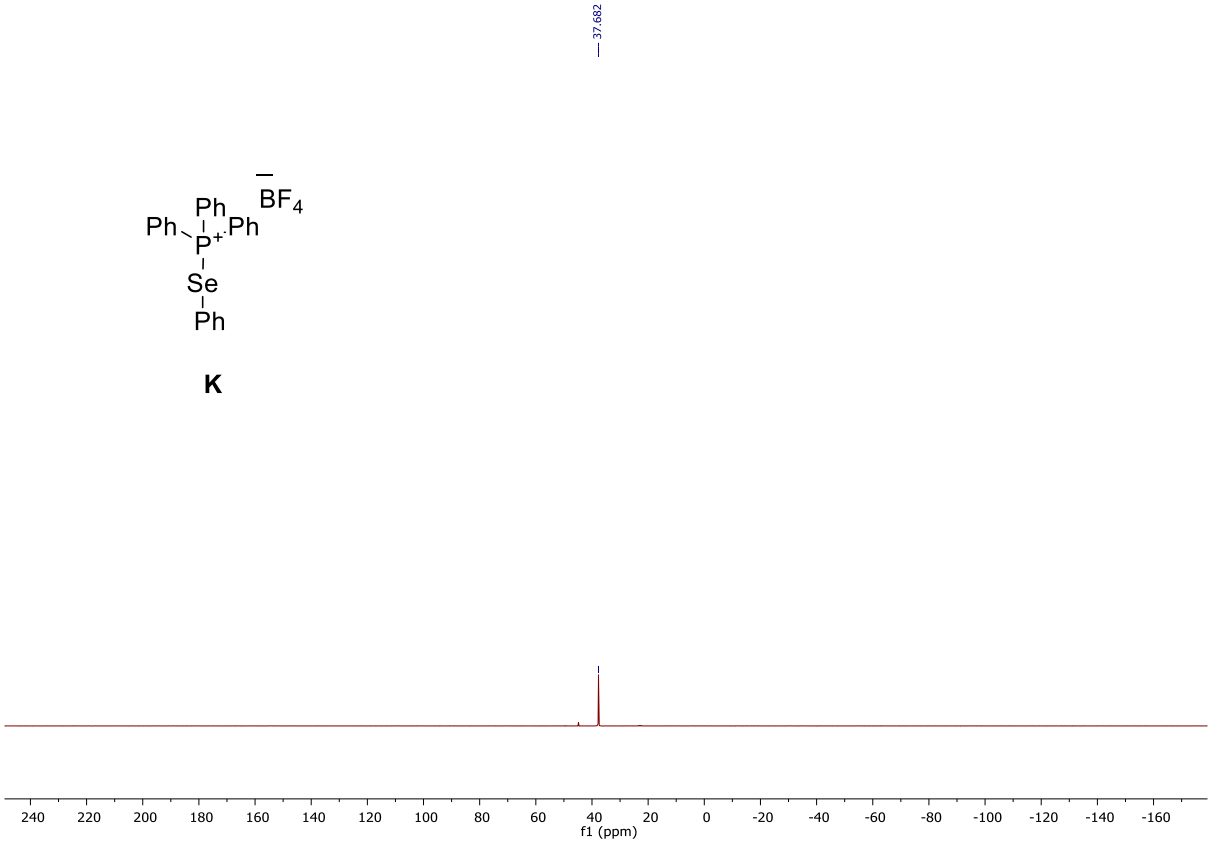

K

Figure 8.29. ^{31}P NMR spectra for K

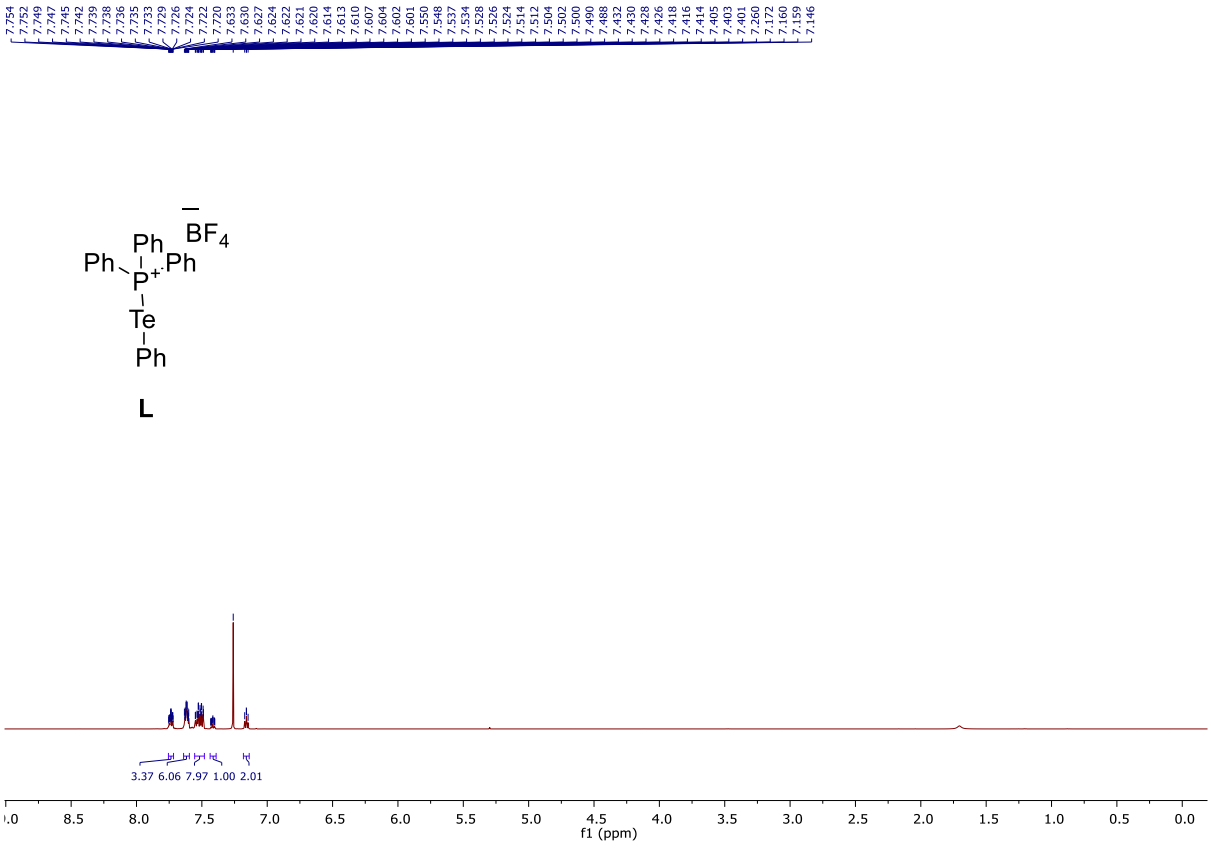

L

Figure 8.30. ^{1}H NMR spectra for L

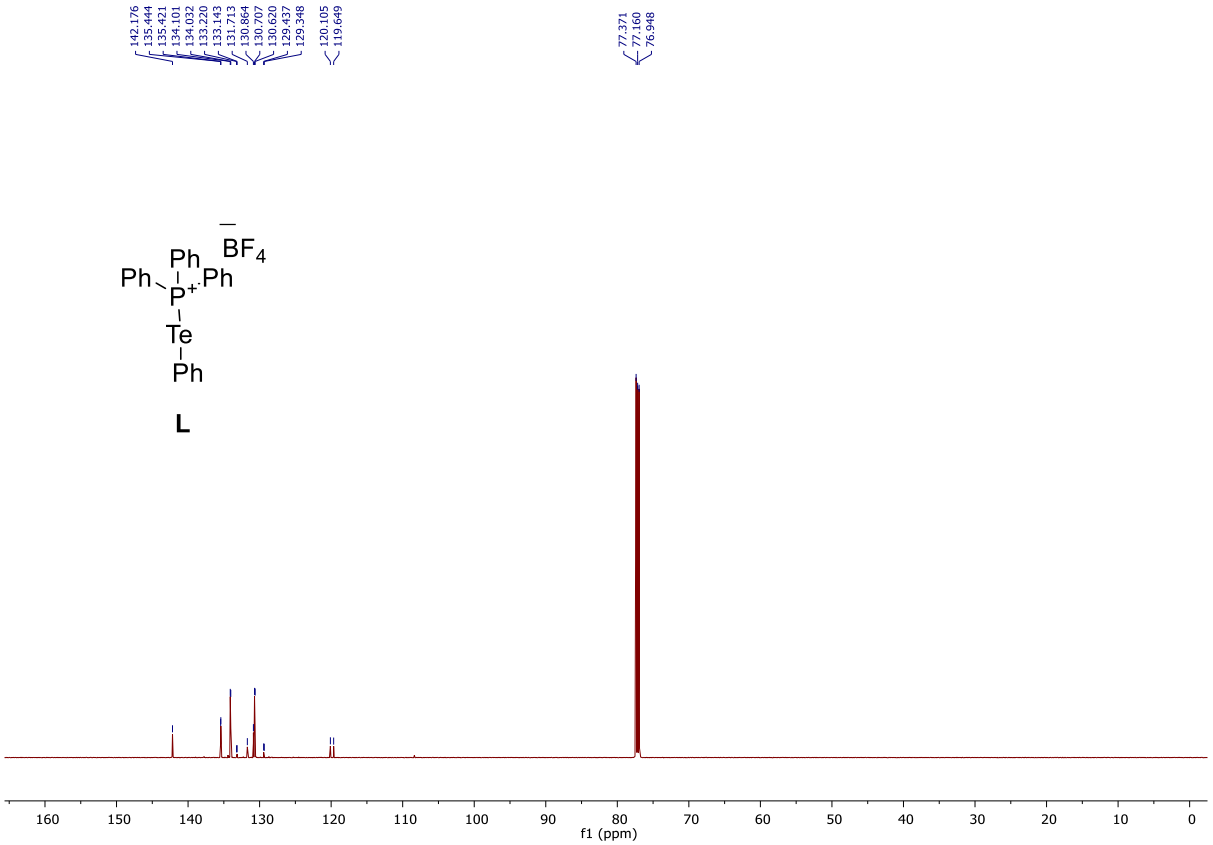

Figure 8.31. ^{13}C NMR spectra for L

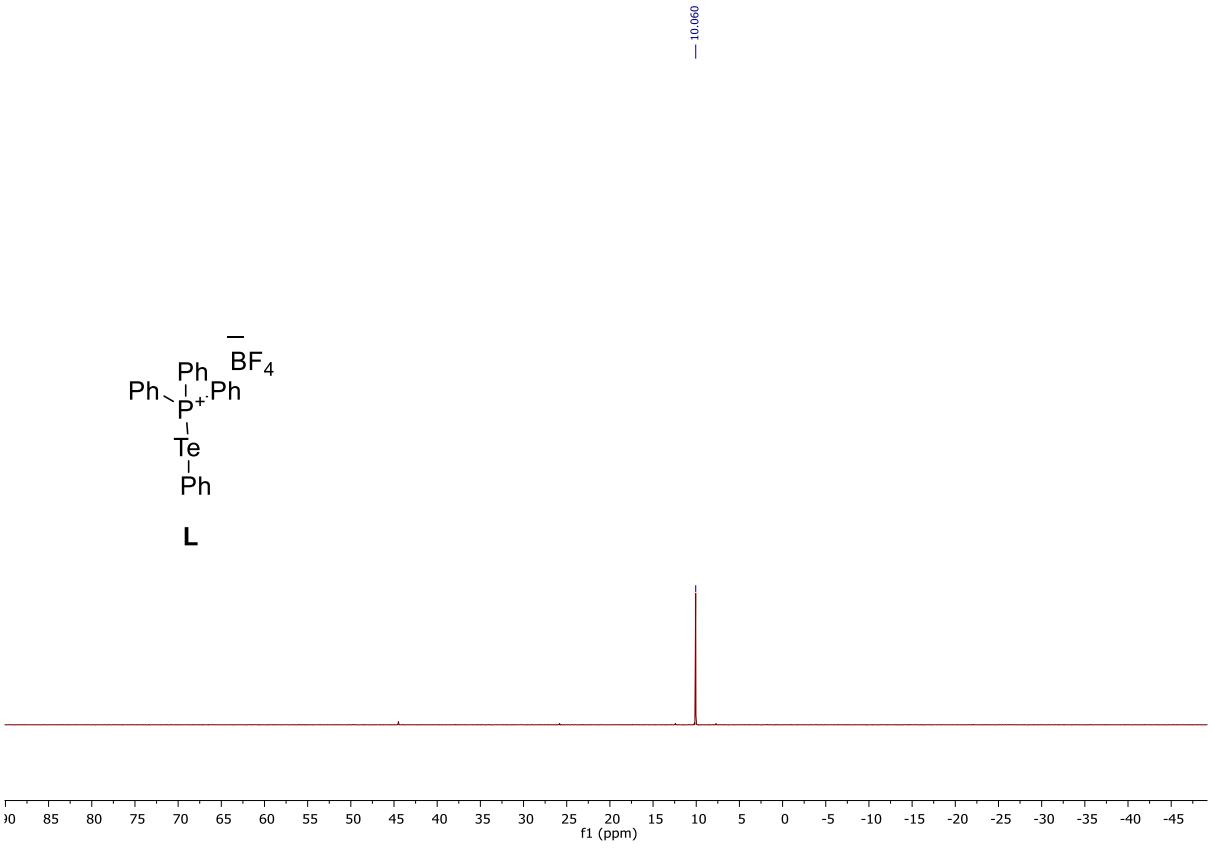

Figure 8.32. ^{31}P NMR spectra for L

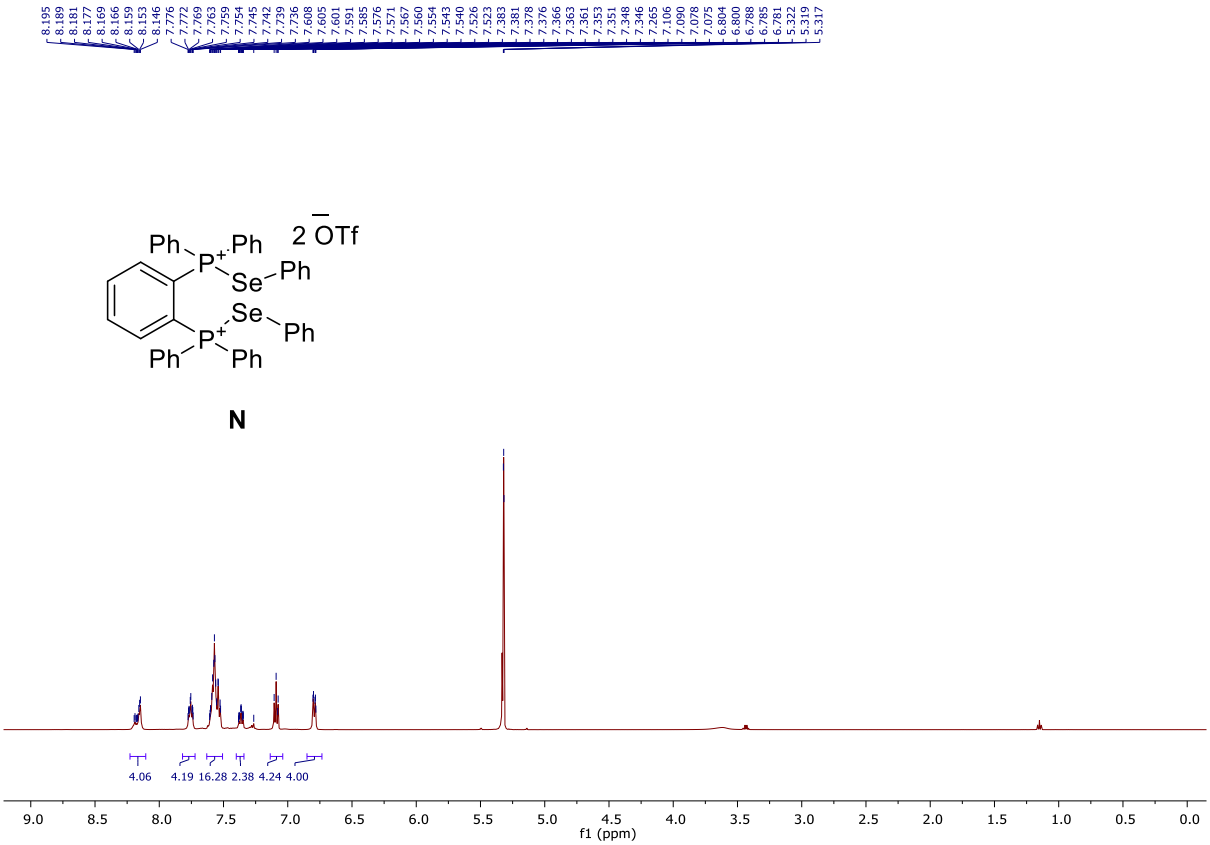

Figure 8.33. ^{1}H NMR spectra for N

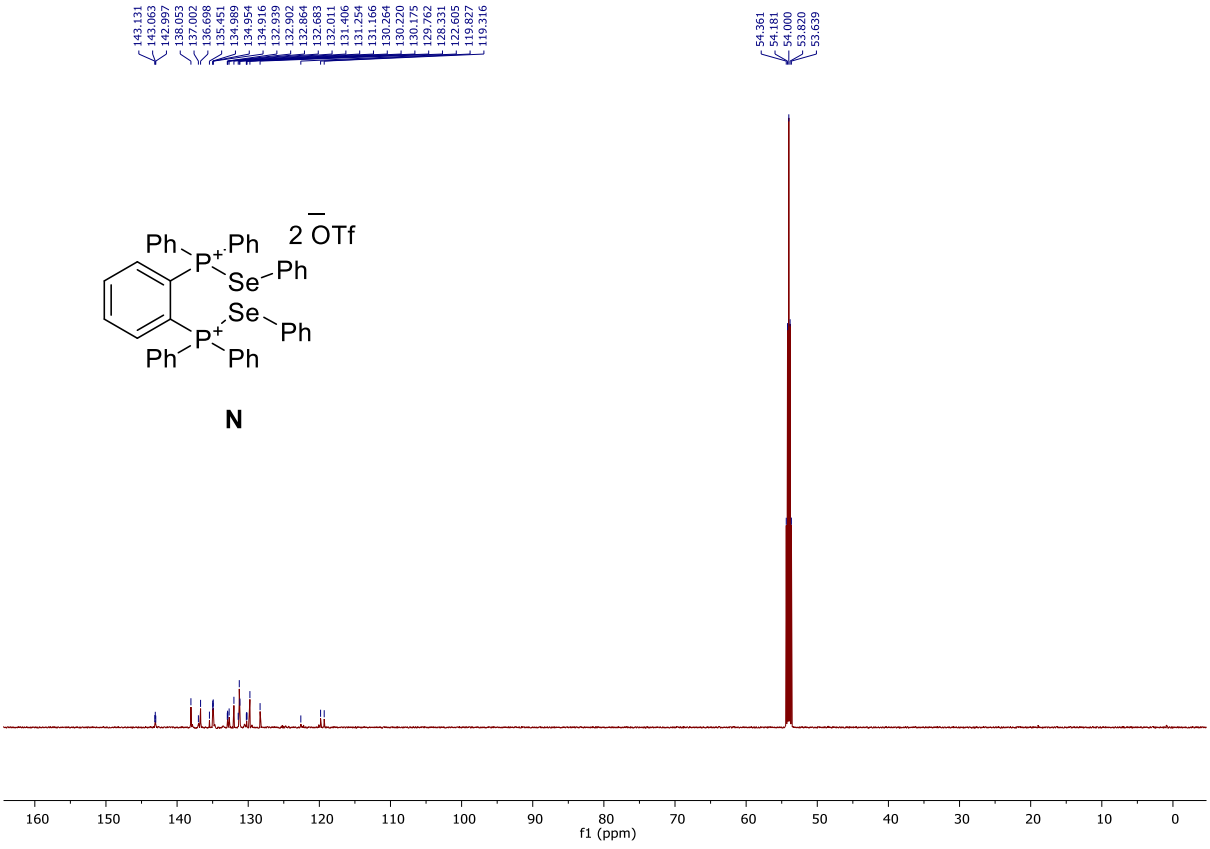

Figure 8.34. ^{13}C NMR spectra for N

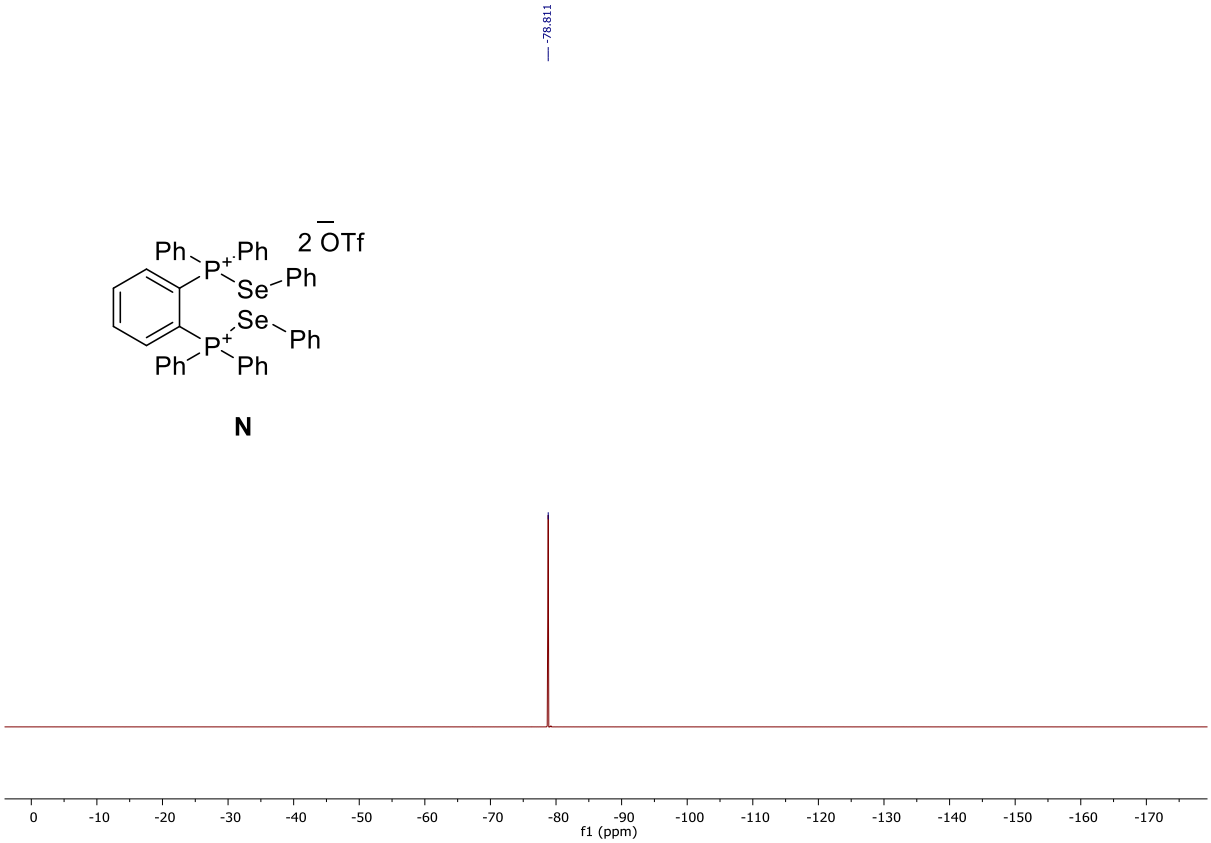

N

Figure 8.35. ^{19}F NMR spectra for N

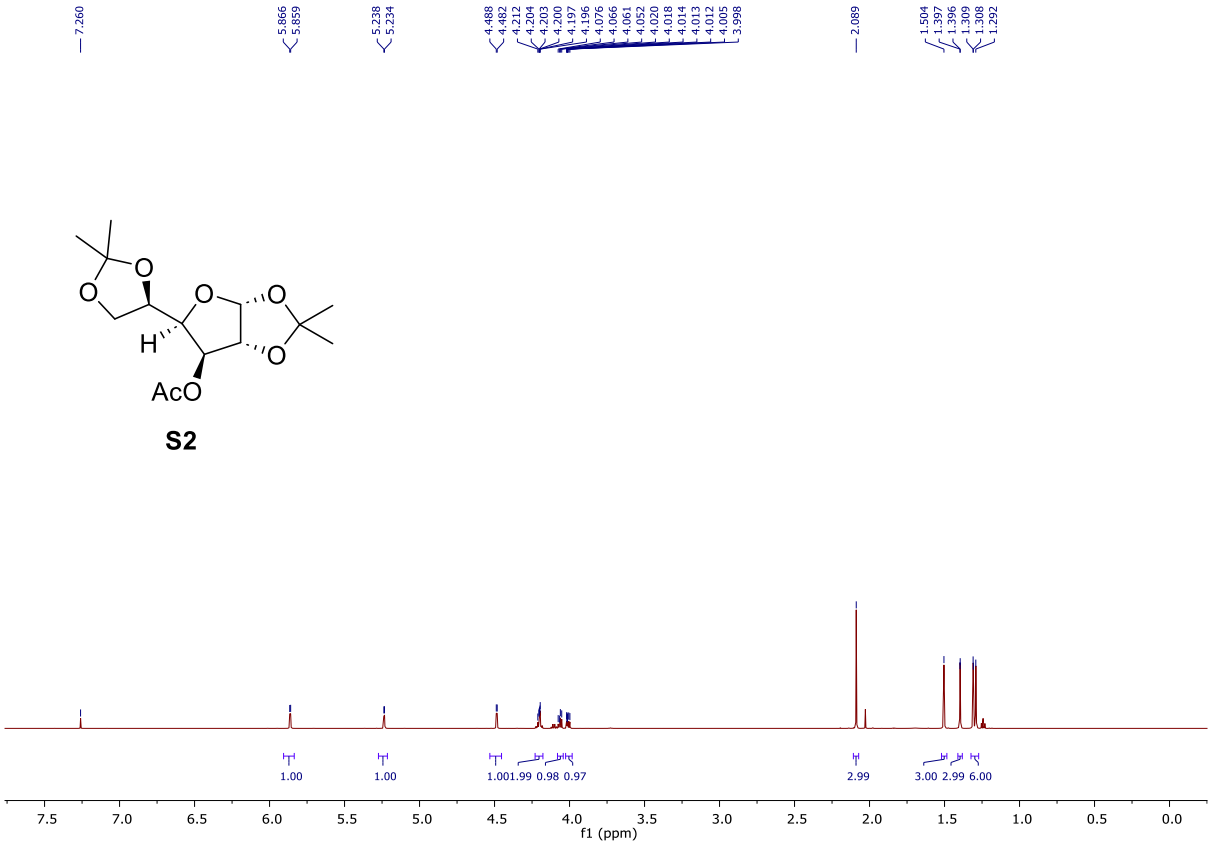

S2

Figure 8.36. ^{1}H NMR spectra for S2

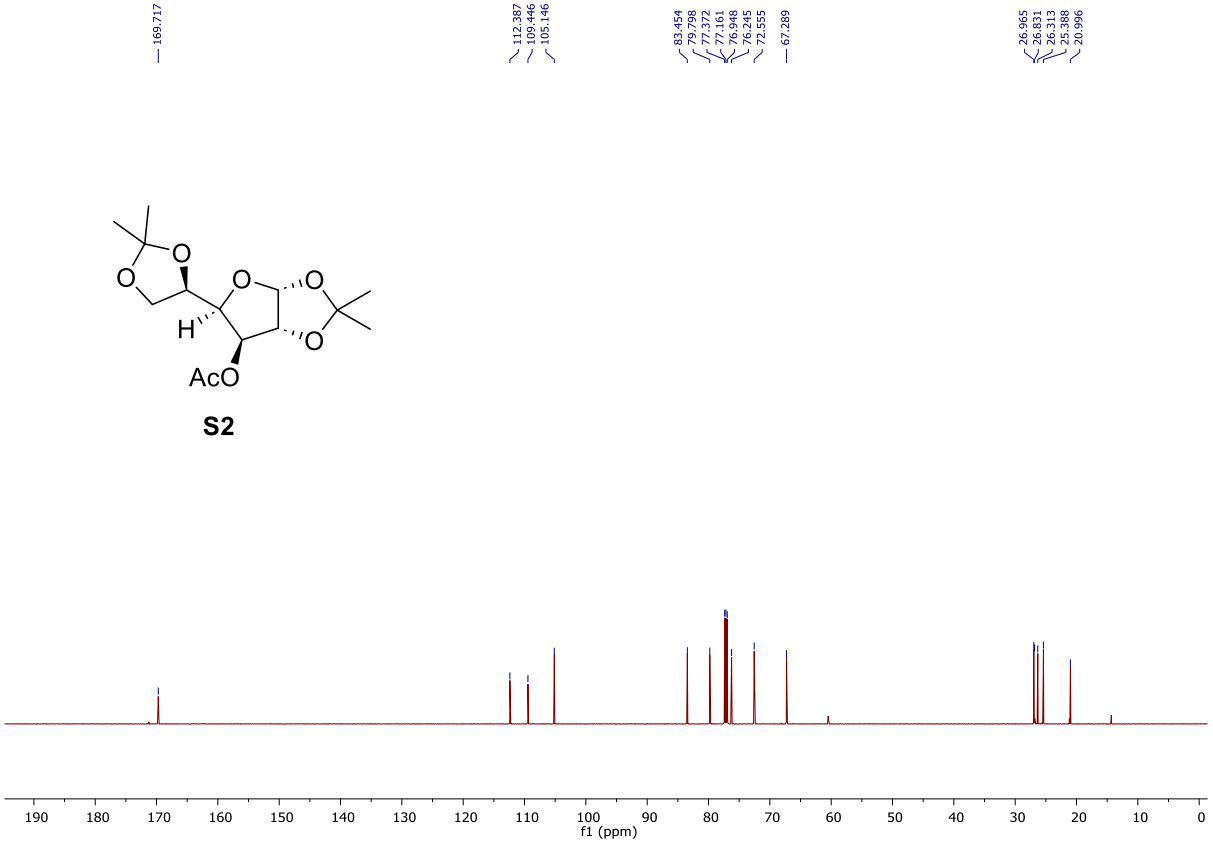

Figure 8.37. ^{13}C NMR spectra for S2

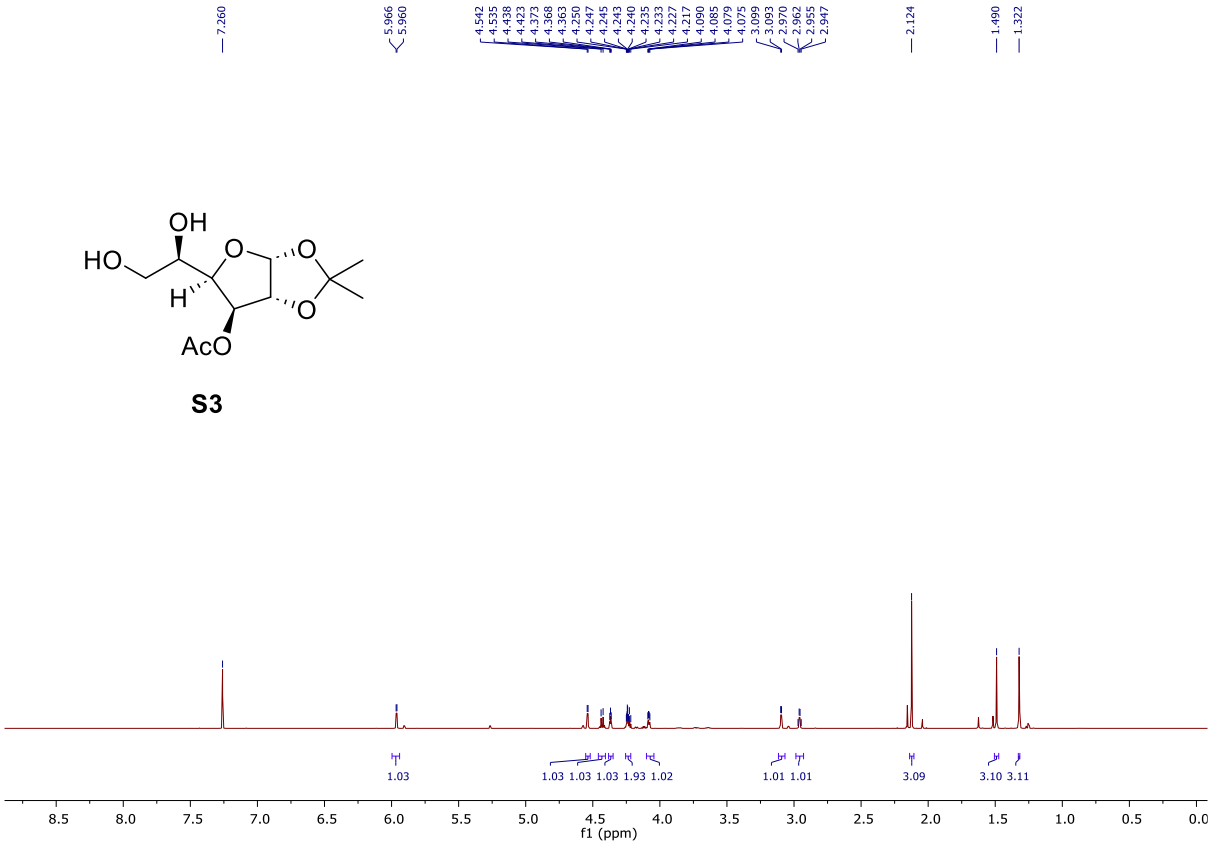

Figure 8.38. ^{1}H NMR spectra for S3

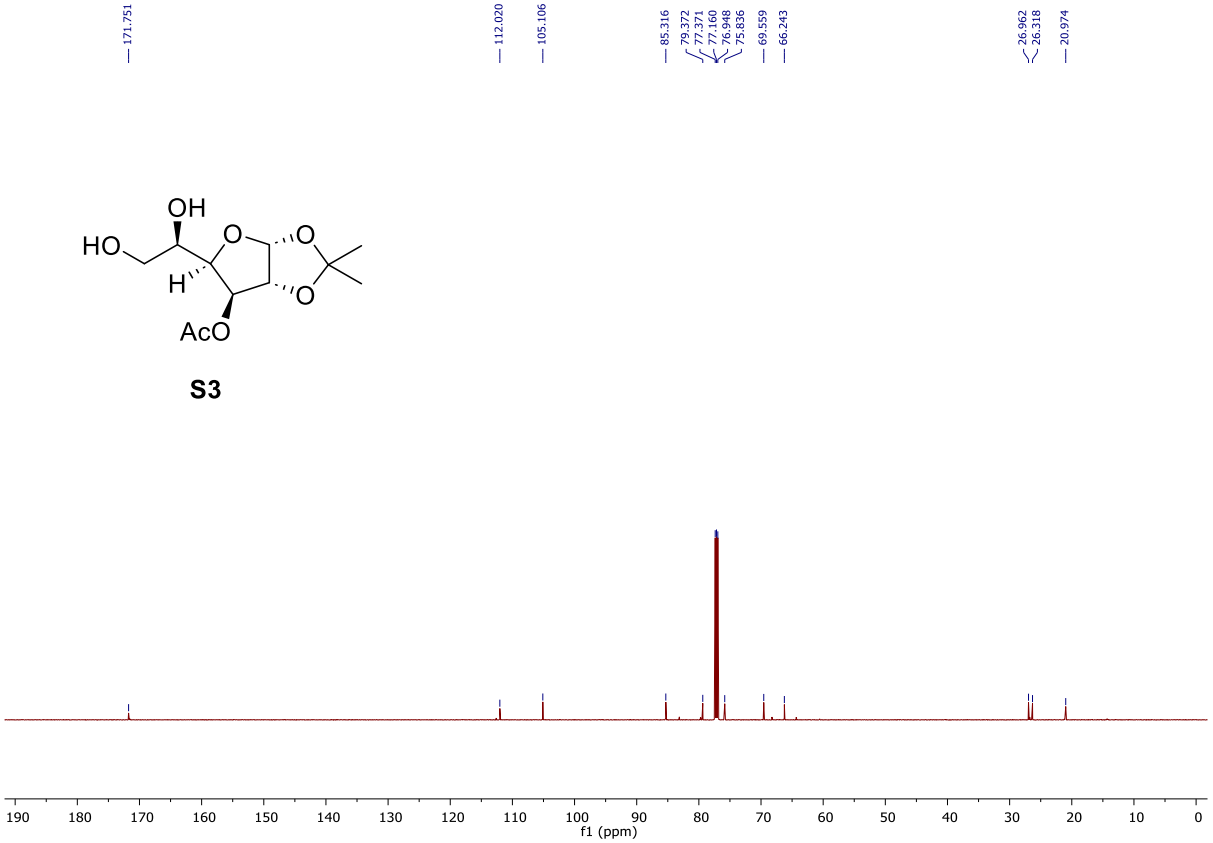

S3

Figure 8.39. ^{13}C NMR spectra for S3

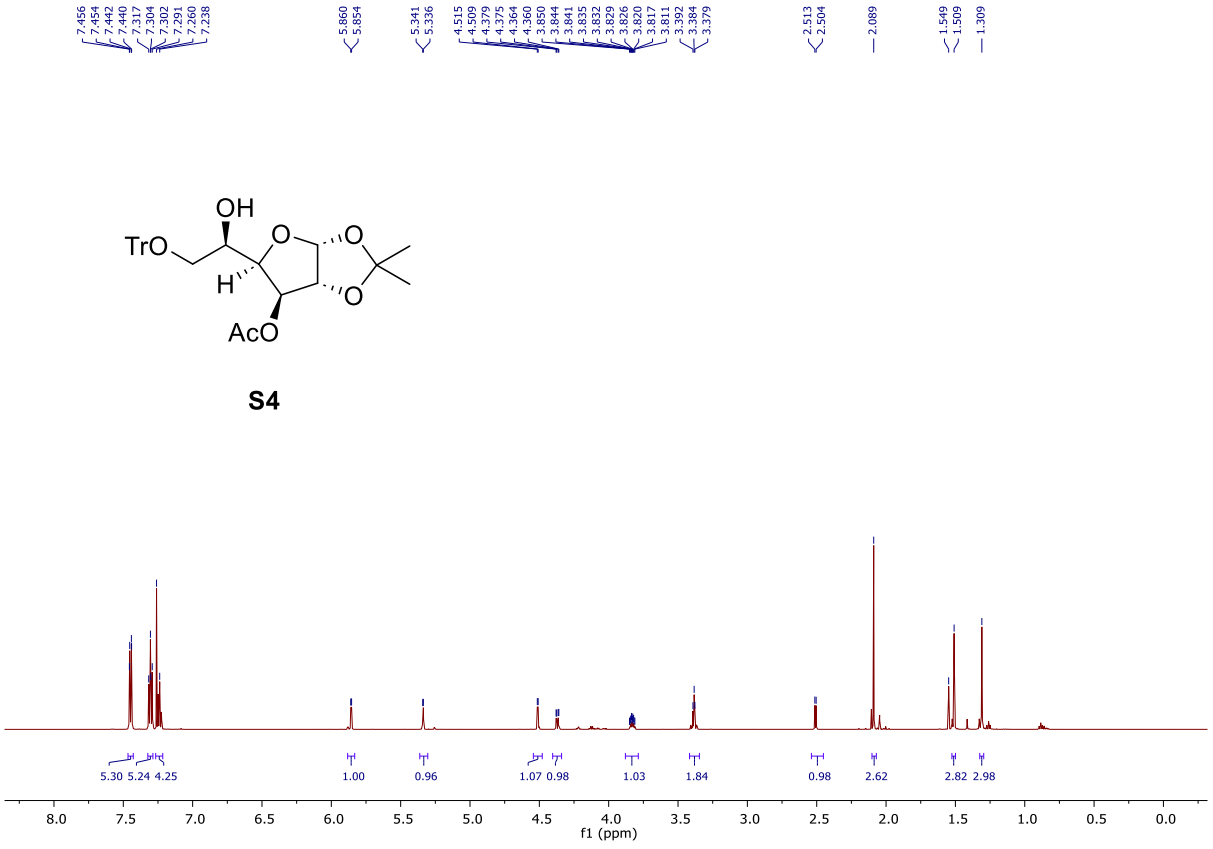

S4

Figure 8.40. ^{1}H NMR spectra for S4

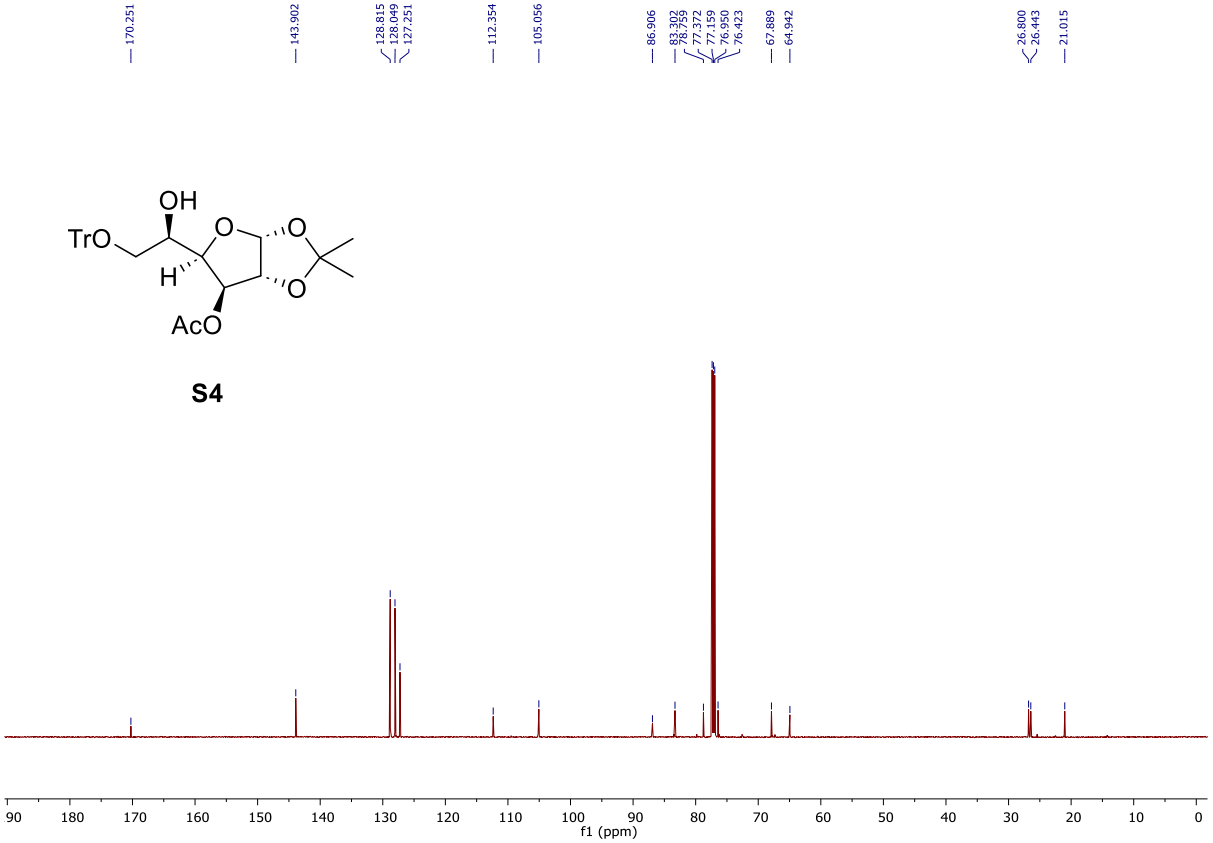

S4

Figure 8.41. ^{13}C NMR spectra for S4

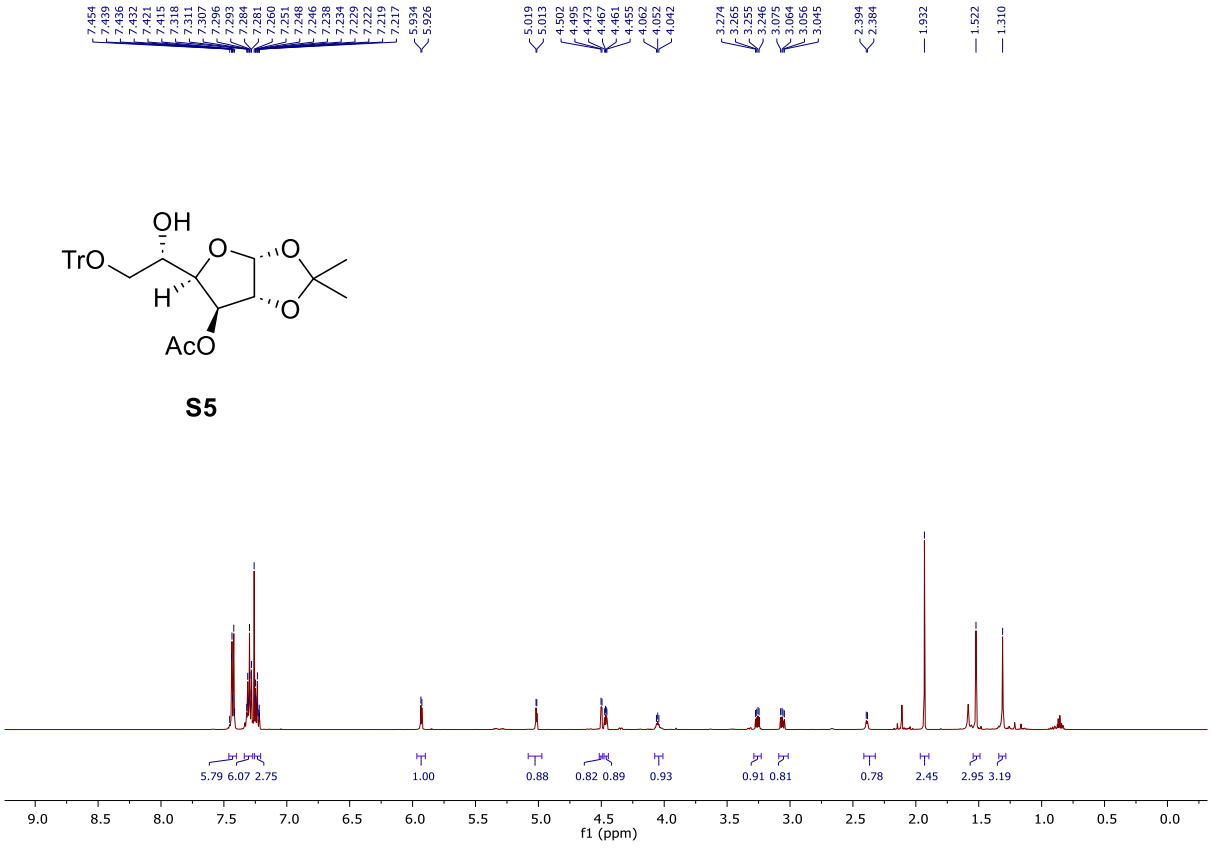

S5

Figure 8.42. ^{1}H NMR spectra for S5

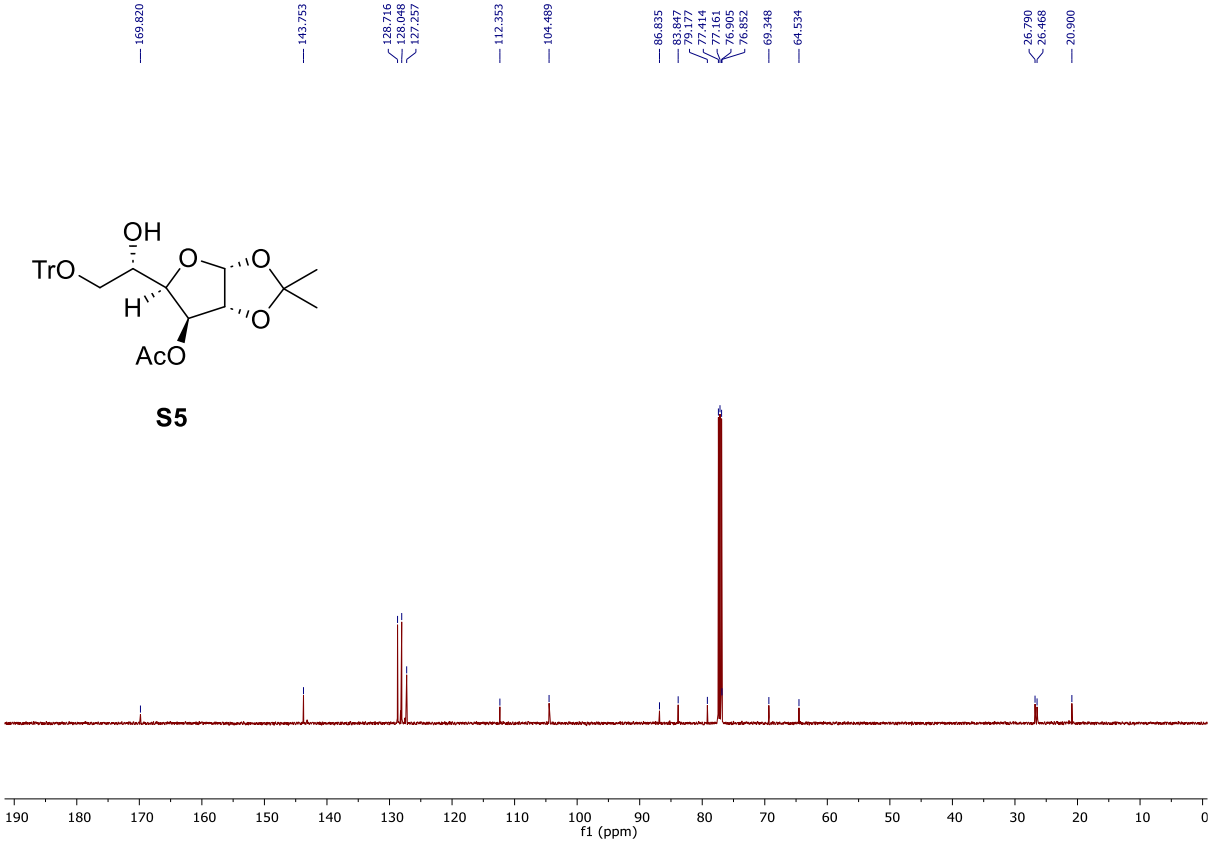

Figure 8.43. ^{13}C NMR spectra for S5

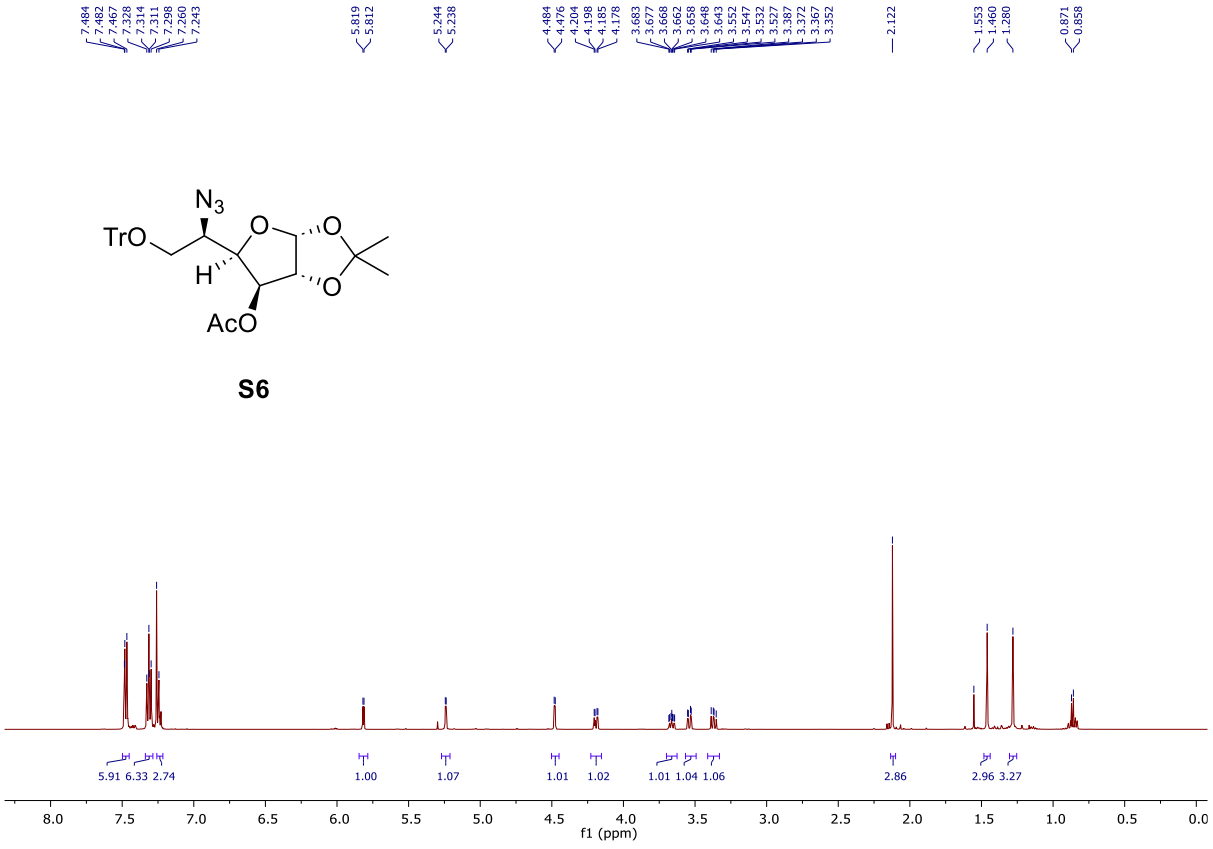

Figure 8.44. ^{1}H NMR spectra for S6

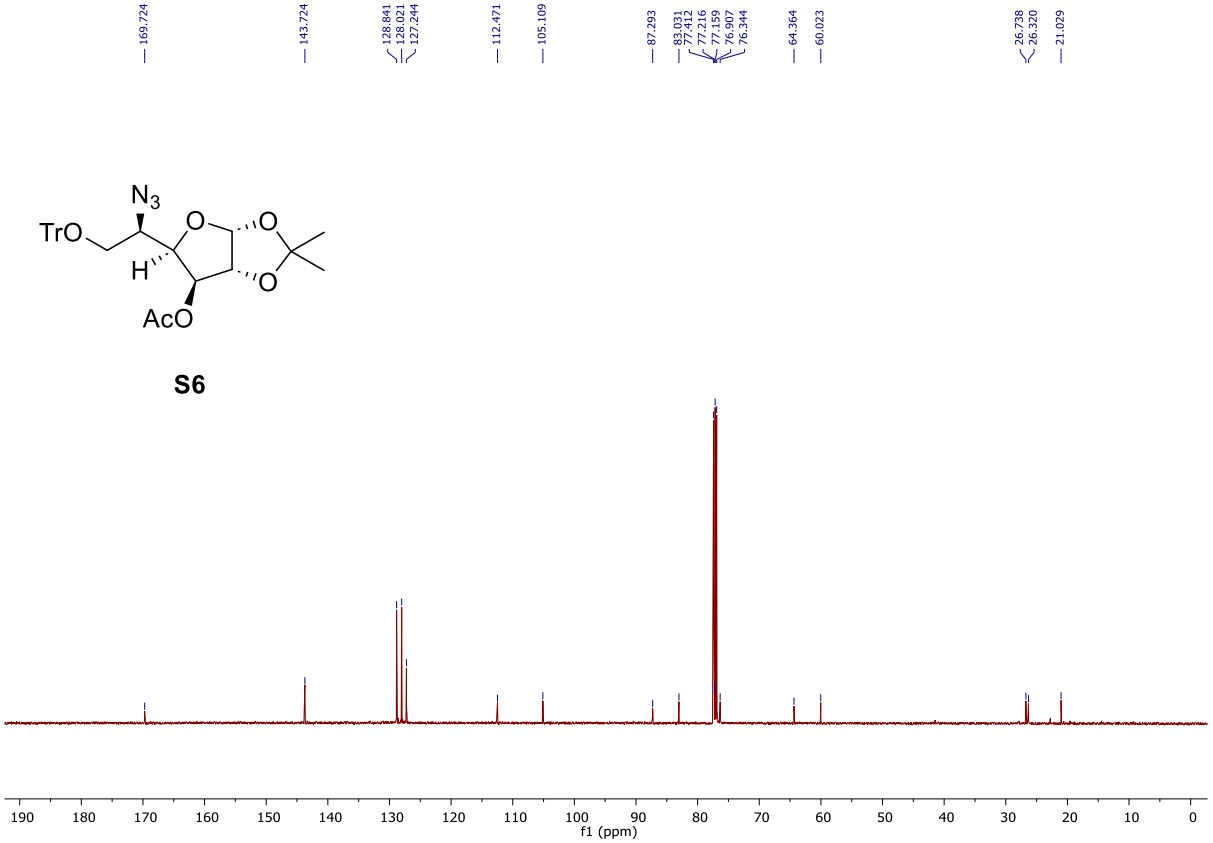

S6

Figure 8.45. ^{13}C NMR spectra for S6

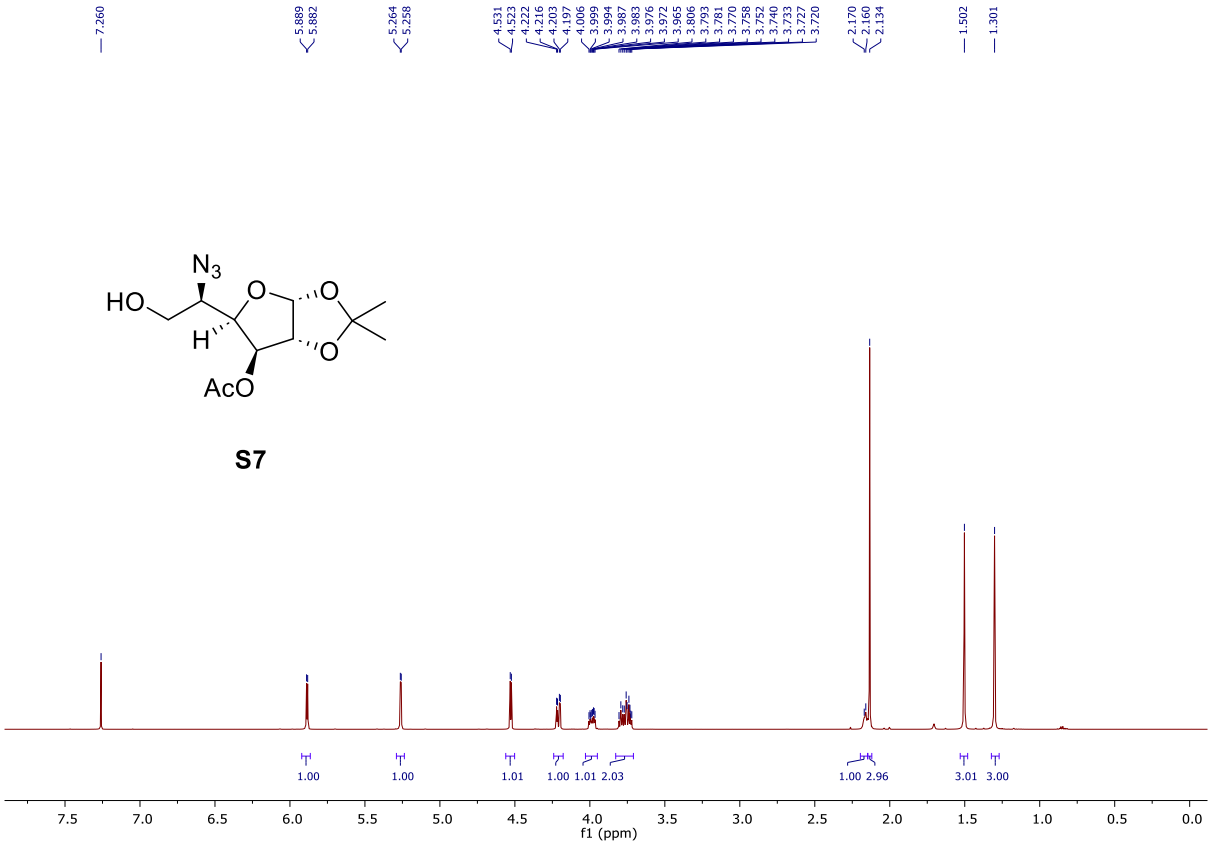

S7

Figure 8.46. ^{1}H NMR spectra for S7

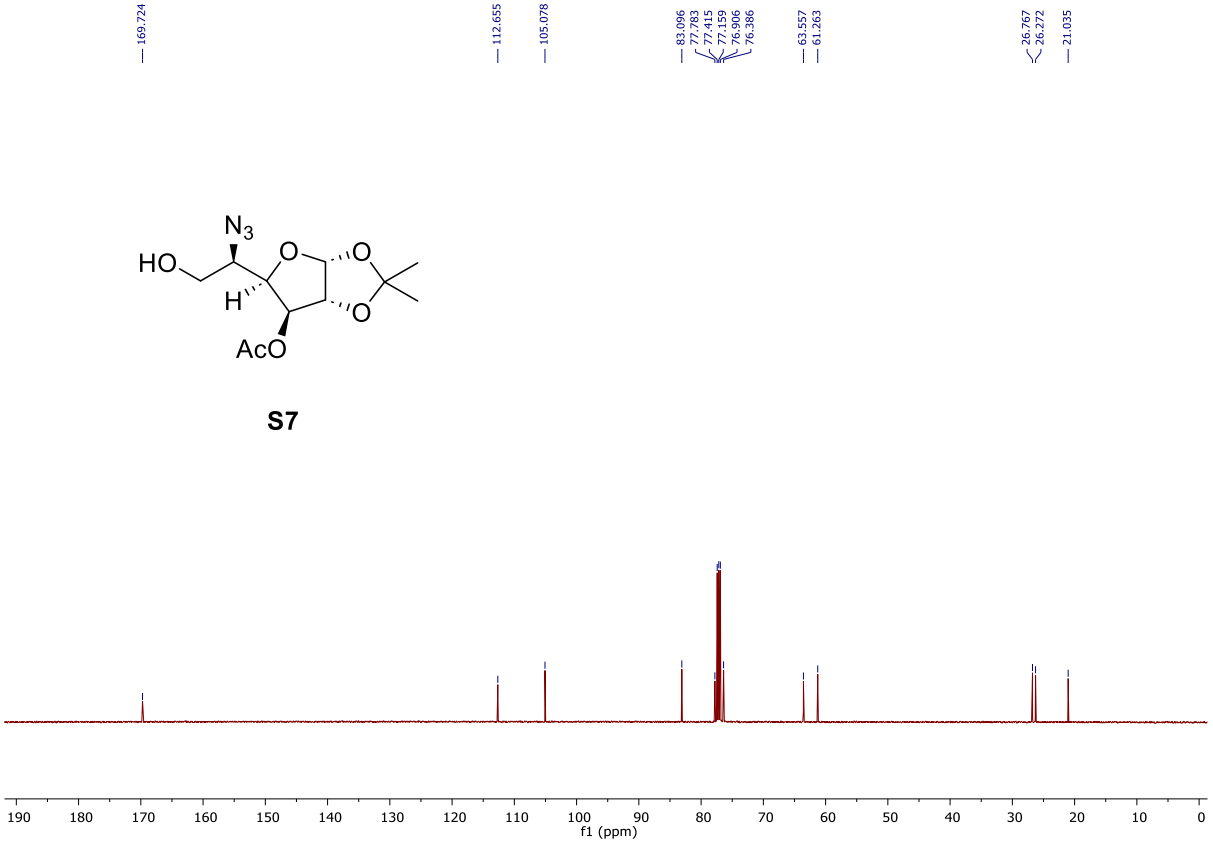

S7

Figure 8.47. ^{13}C NMR spectra for S7

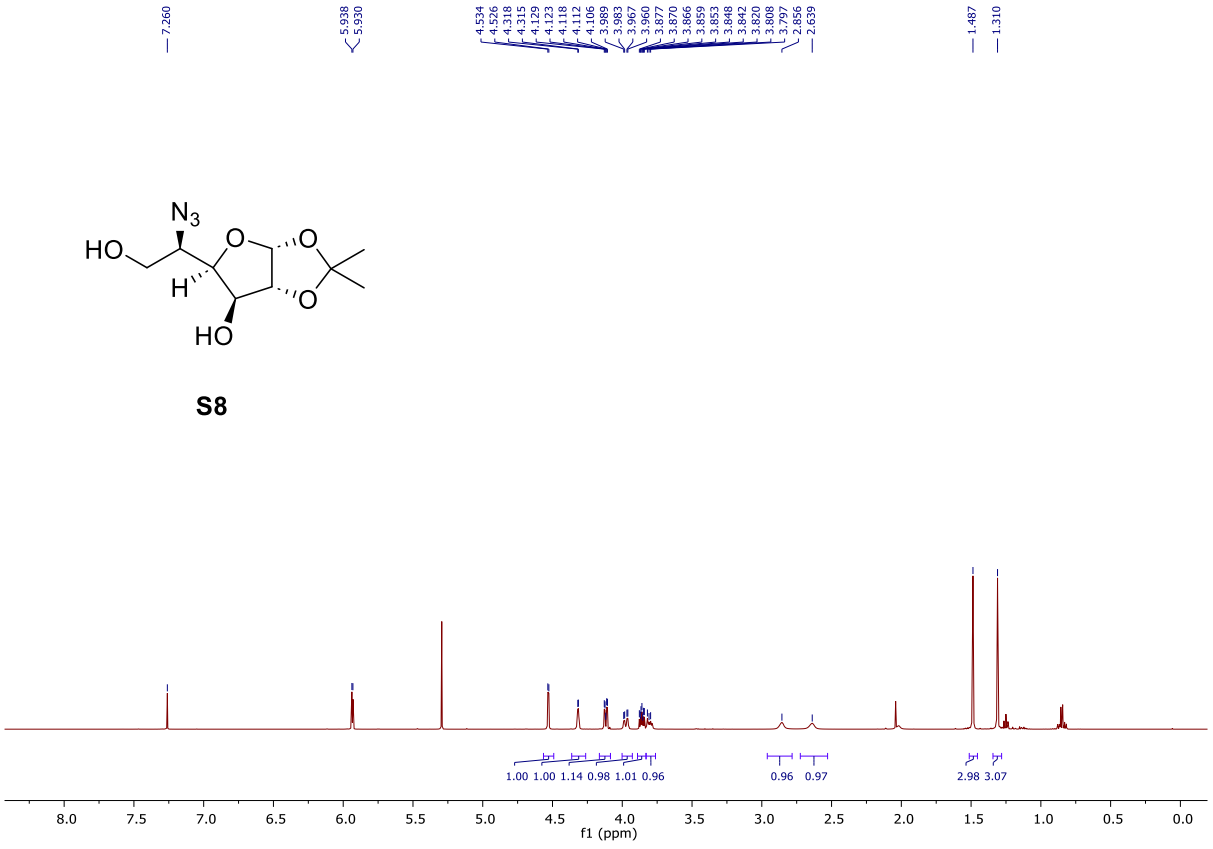

S8

Figure 8.48. ^{1}H NMR spectra for S8

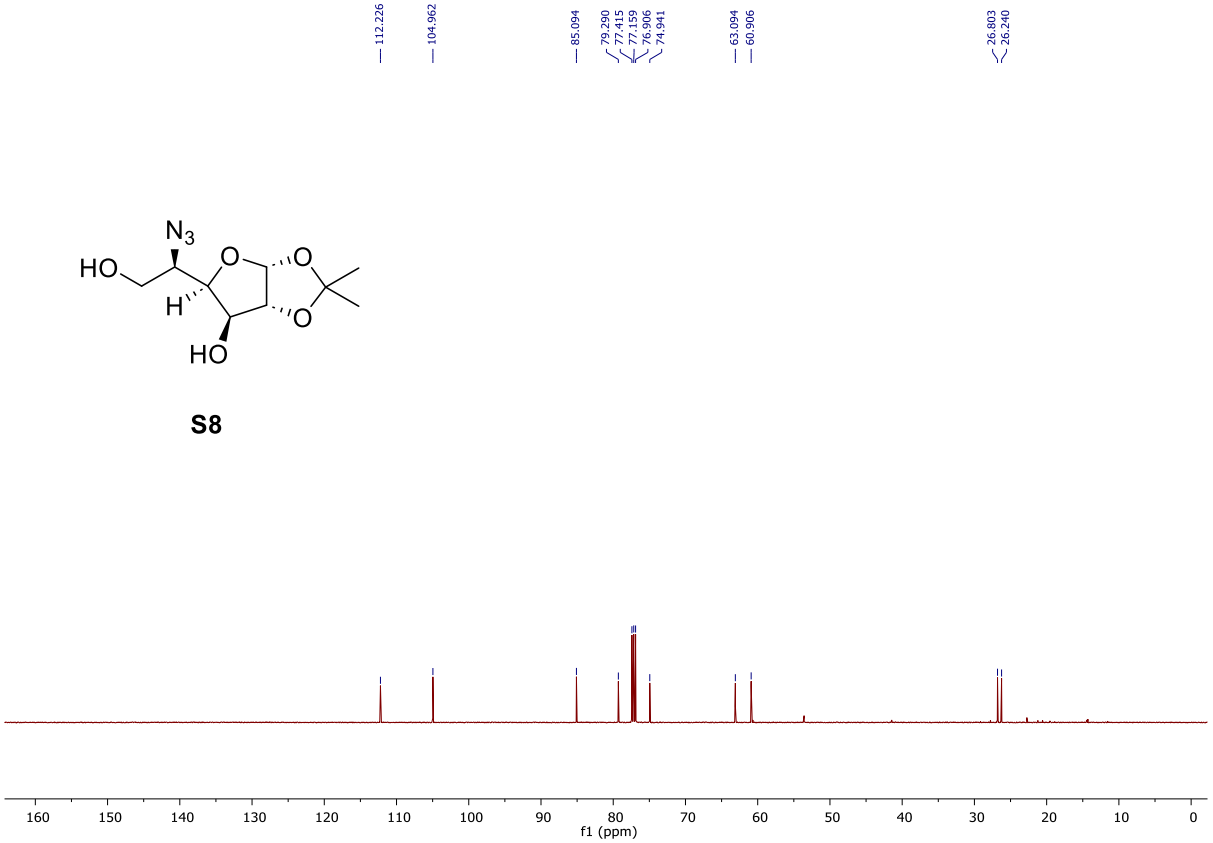

S8

Figure 8.49. ^{13}C NMR spectra for S8

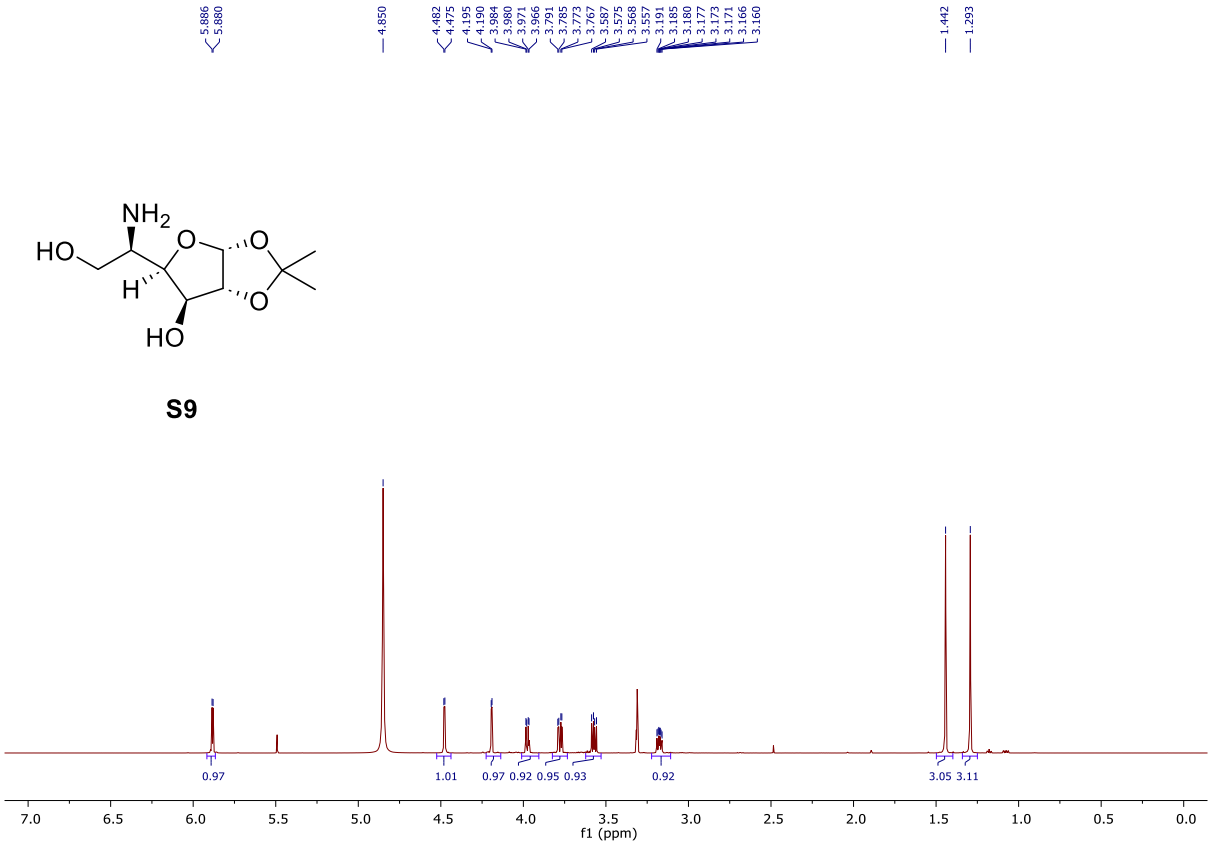

S9

Figure 8.50. ^{1}H NMR spectra for S9

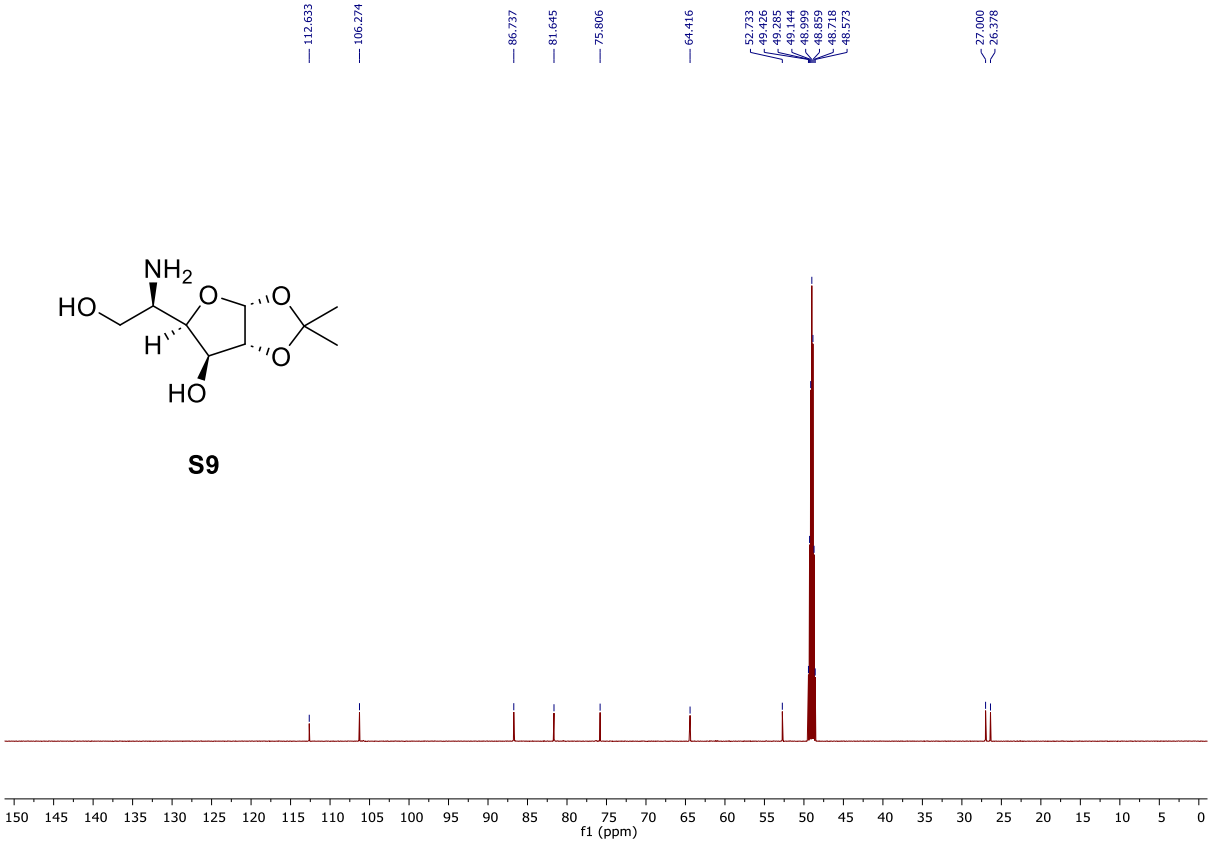

Figure 8.51. ^{13}C NMR spectra for S9

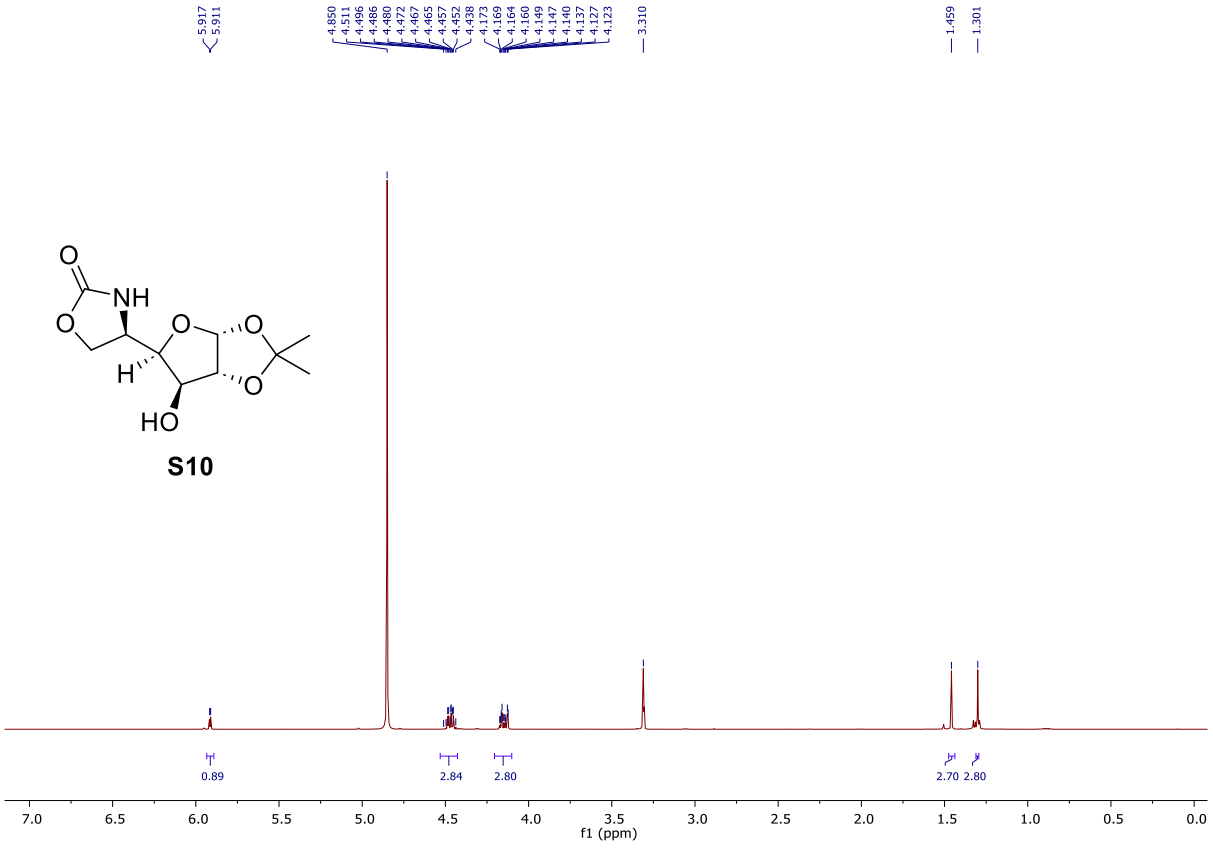

Figure 8.52. ^{1}H NMR spectra for S10

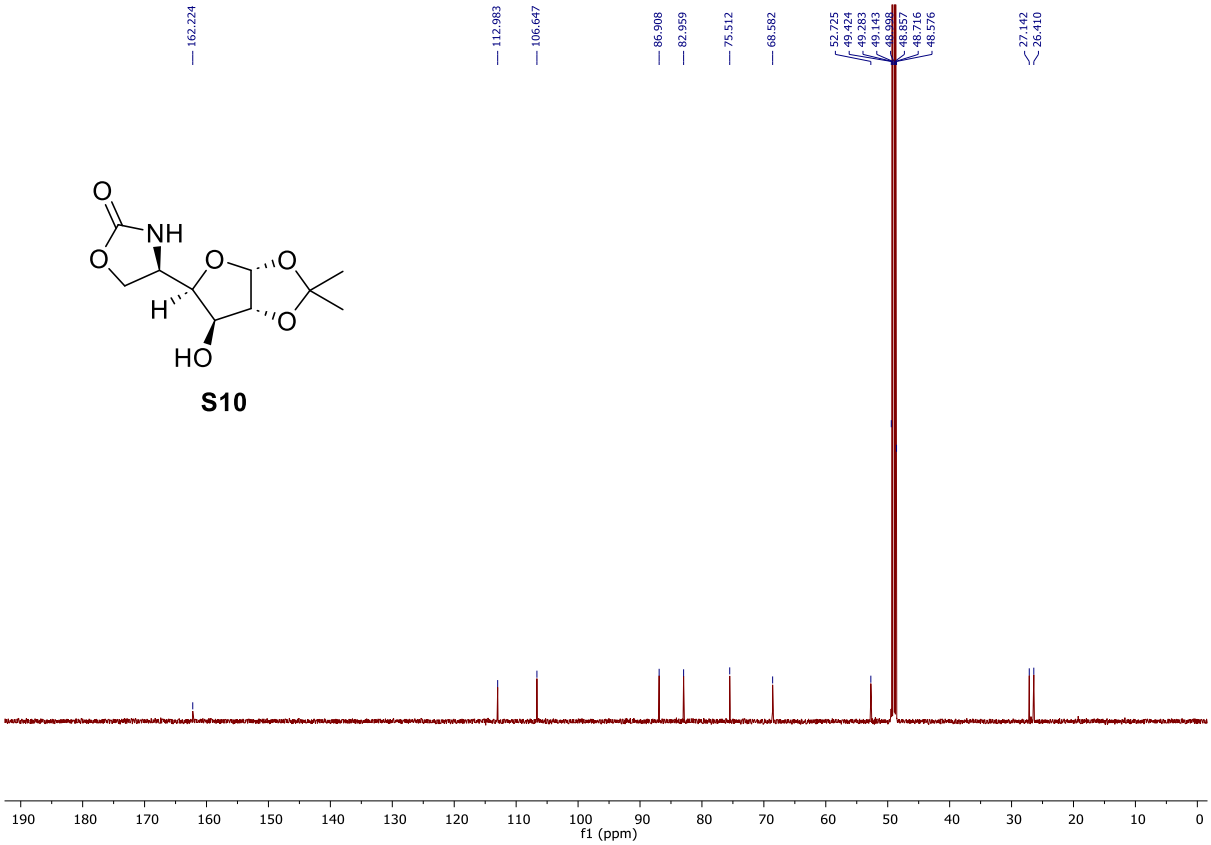

Figure 8.53. ^{13}C NMR spectra for S10

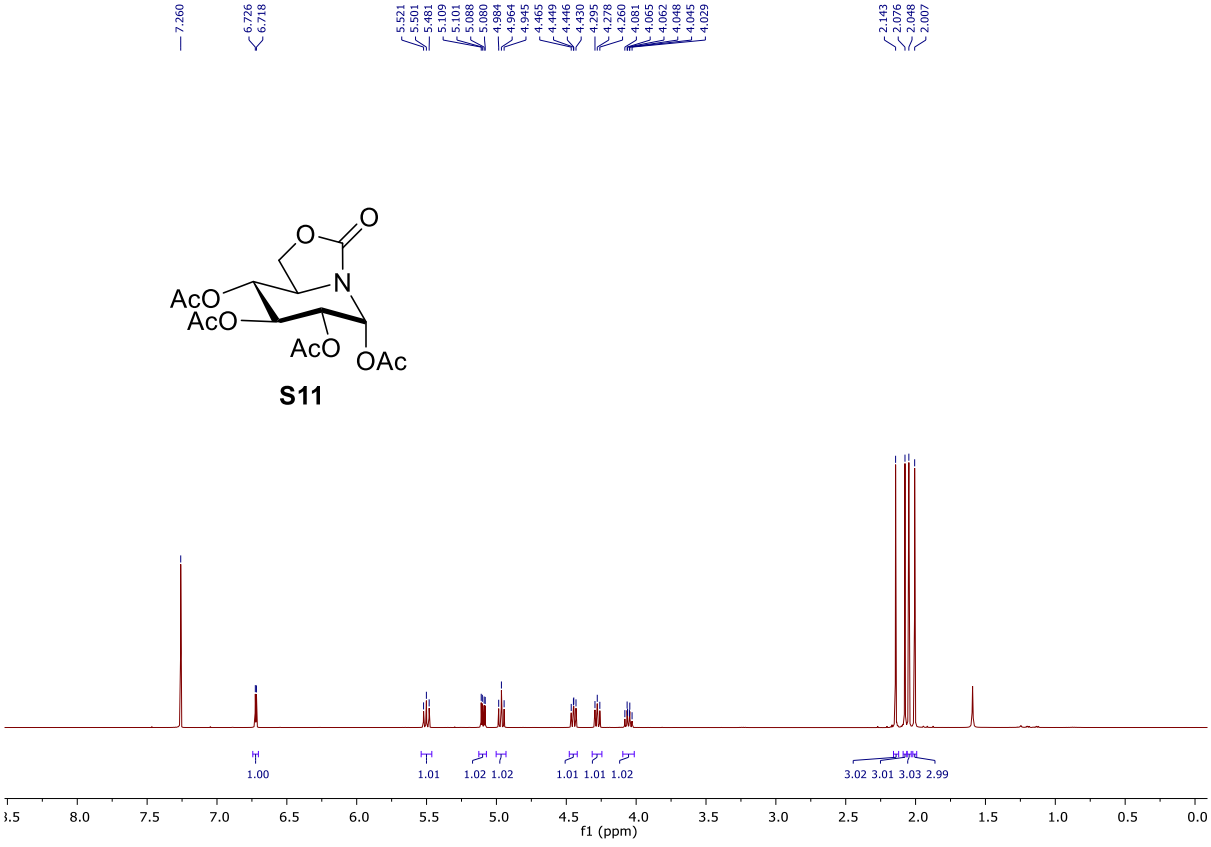

Figure 8.54. ^{1}H NMR spectra for S11

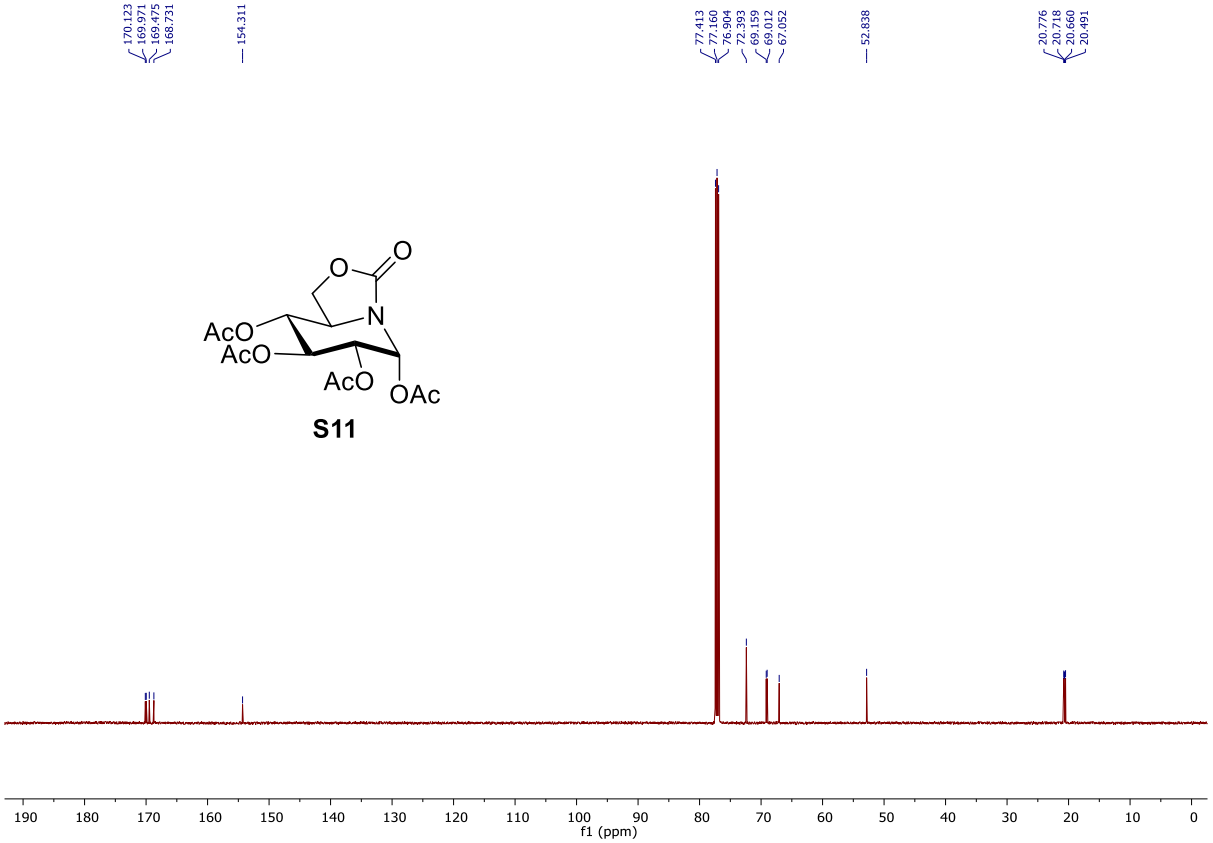

S11

Figure 8.55. ^{13}C NMR spectra for S11

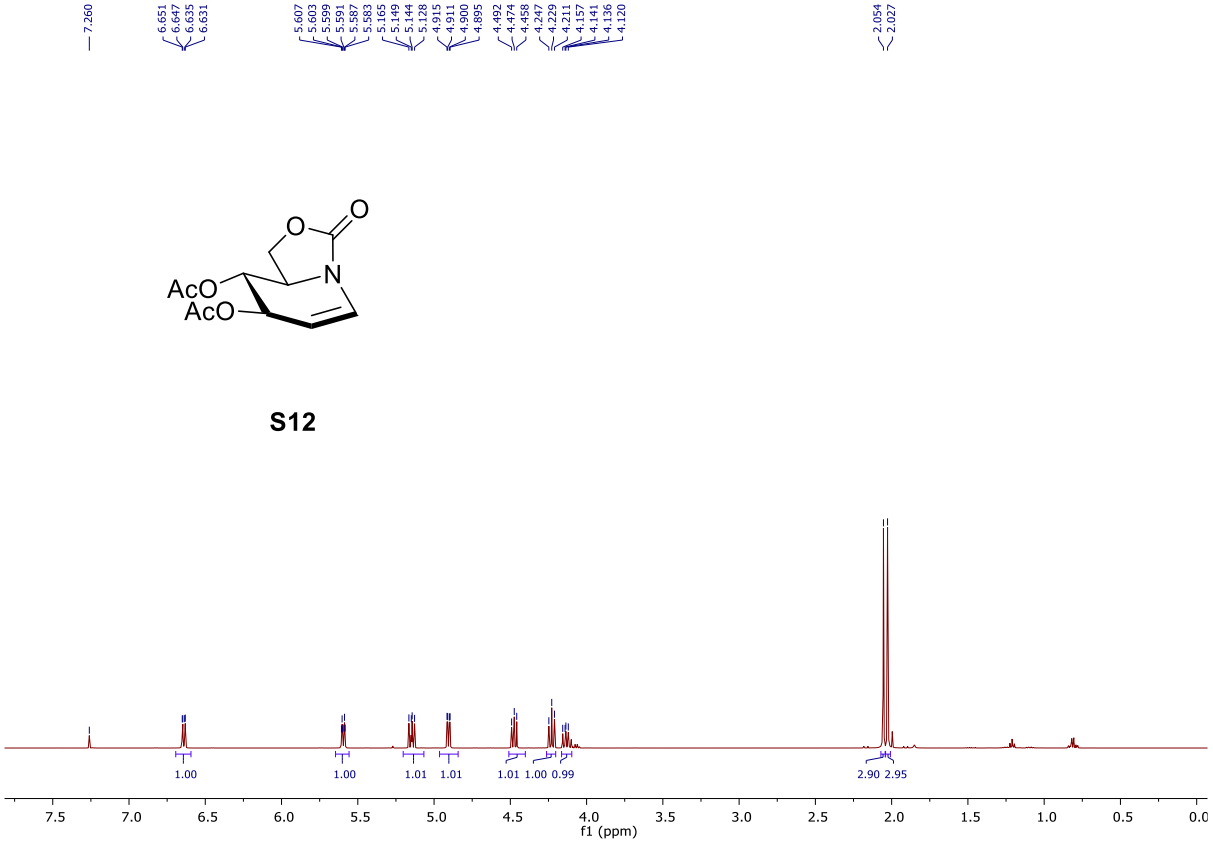

S12

Figure 8.56. ^{1}H NMR spectra for S12

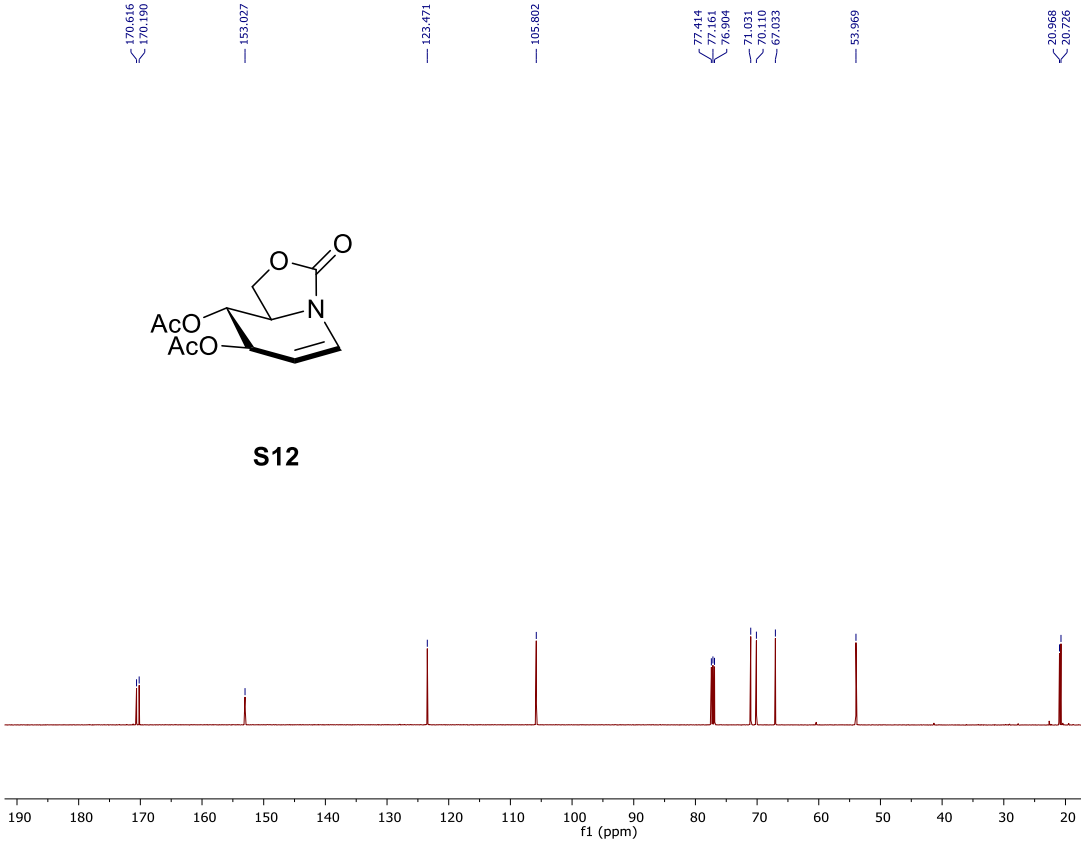

Figure 8.57. ^{13}C NMR spectra for S12

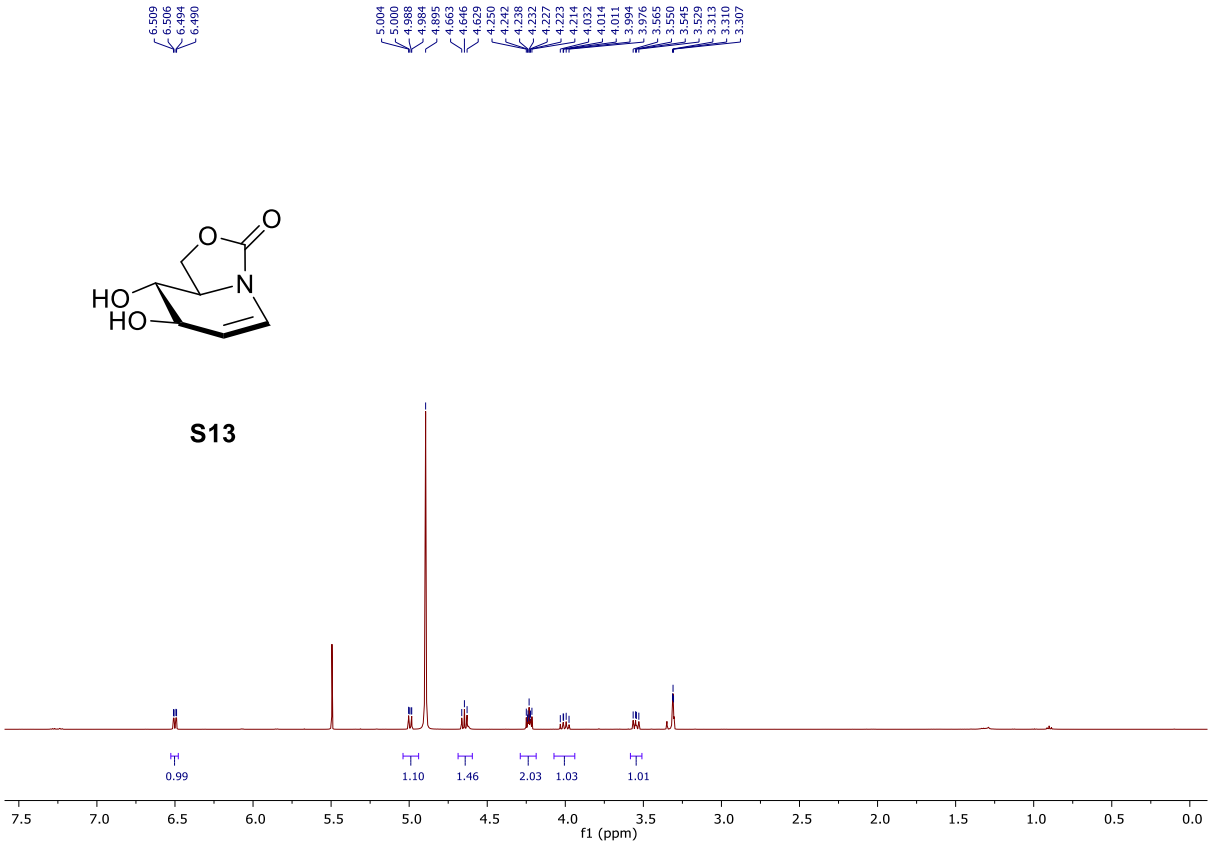

Figure 8.58. ^{1}H NMR spectra for S13

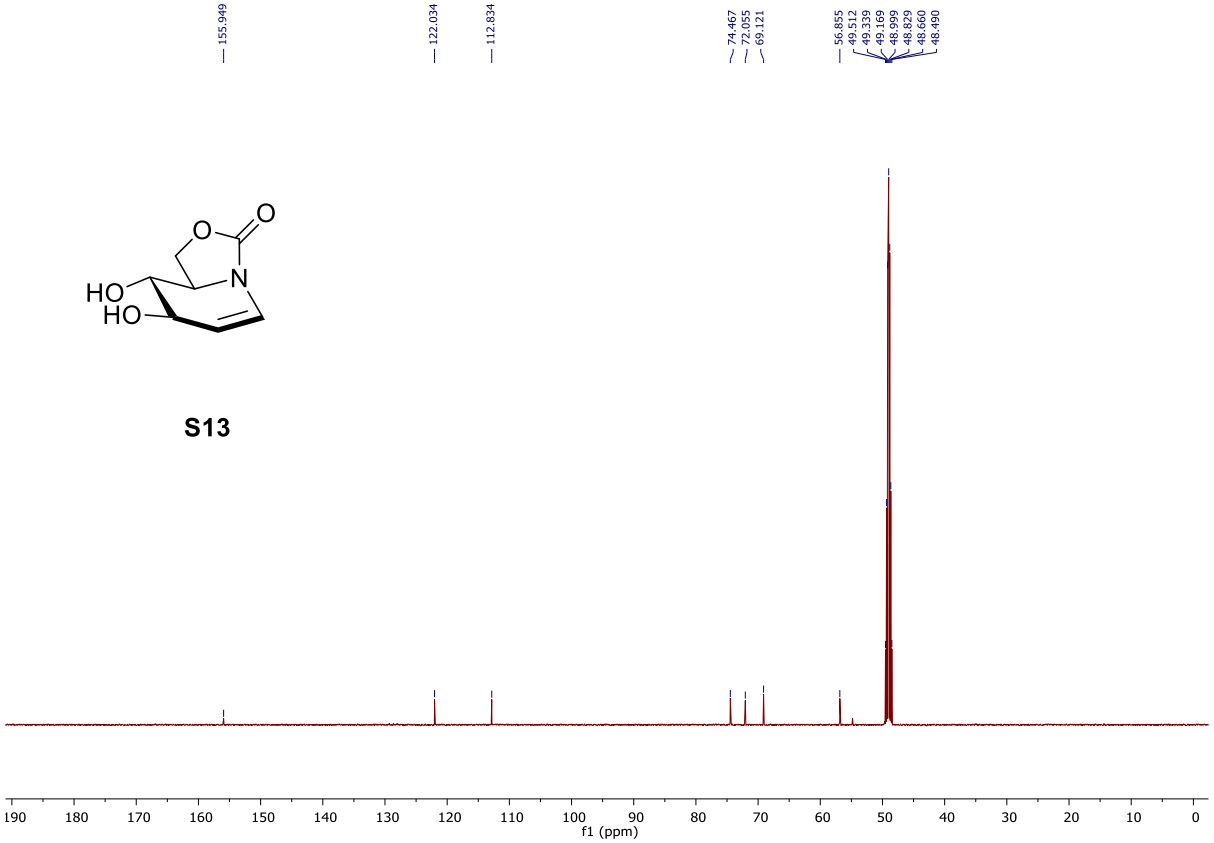

Figure 8.59. ^{13}C NMR spectra for S13

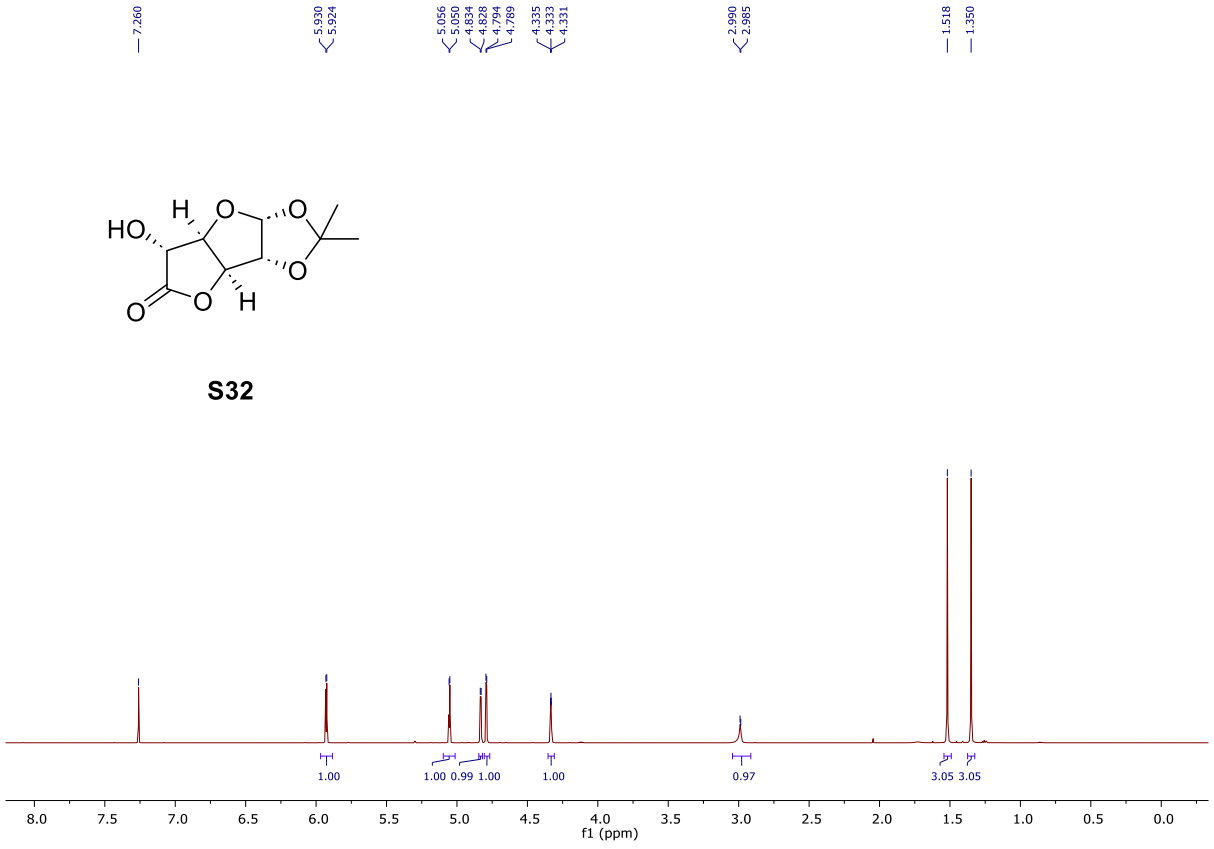

Figure 8.60. ^{1}H NMR spectra for S32

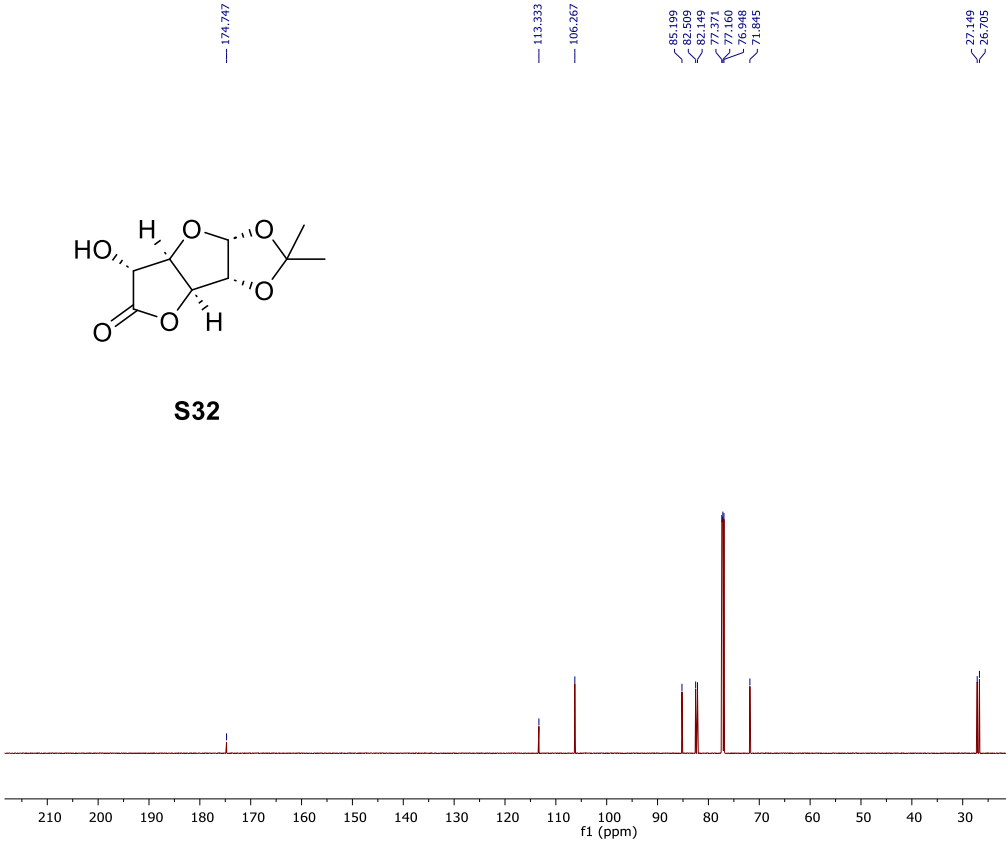

Figure 8.61. ^{13}C NMR spectra for S32

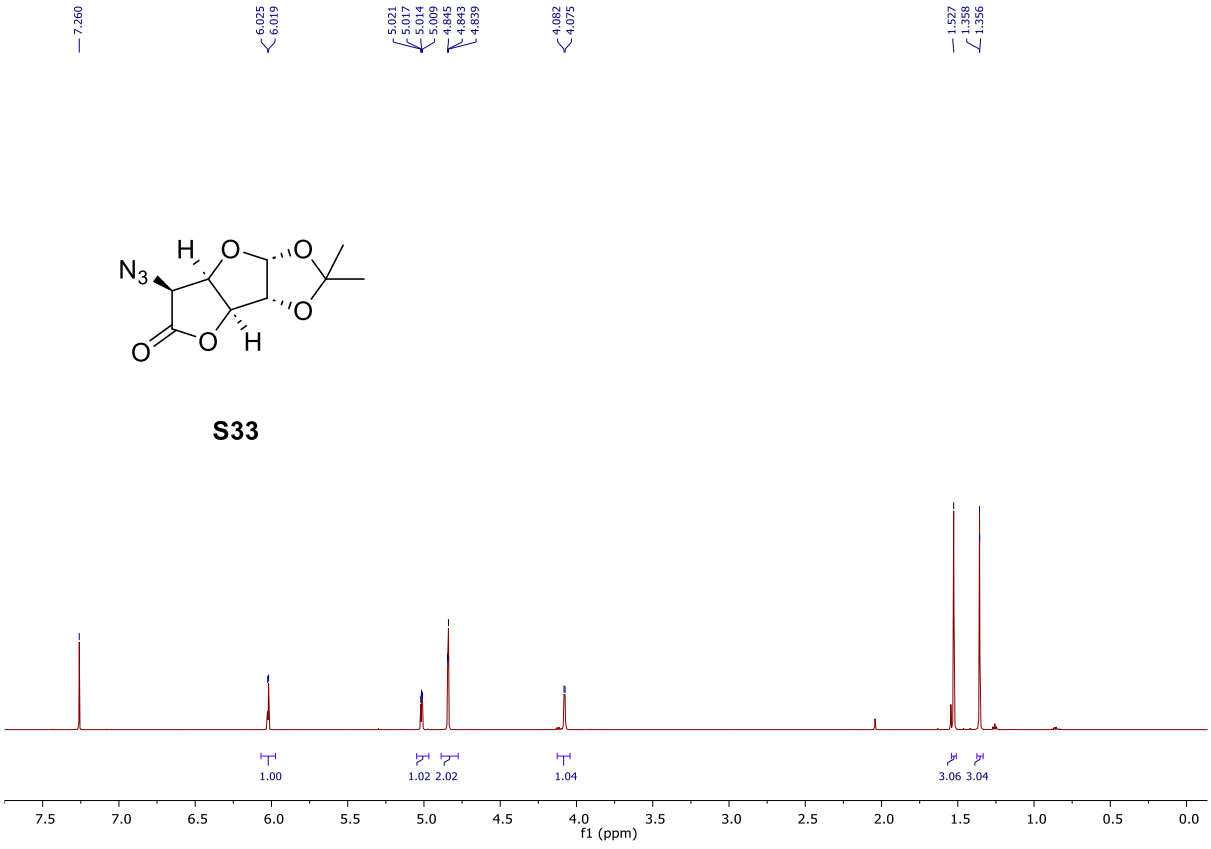

Figure 8.62. ^{1}H NMR spectra for S33

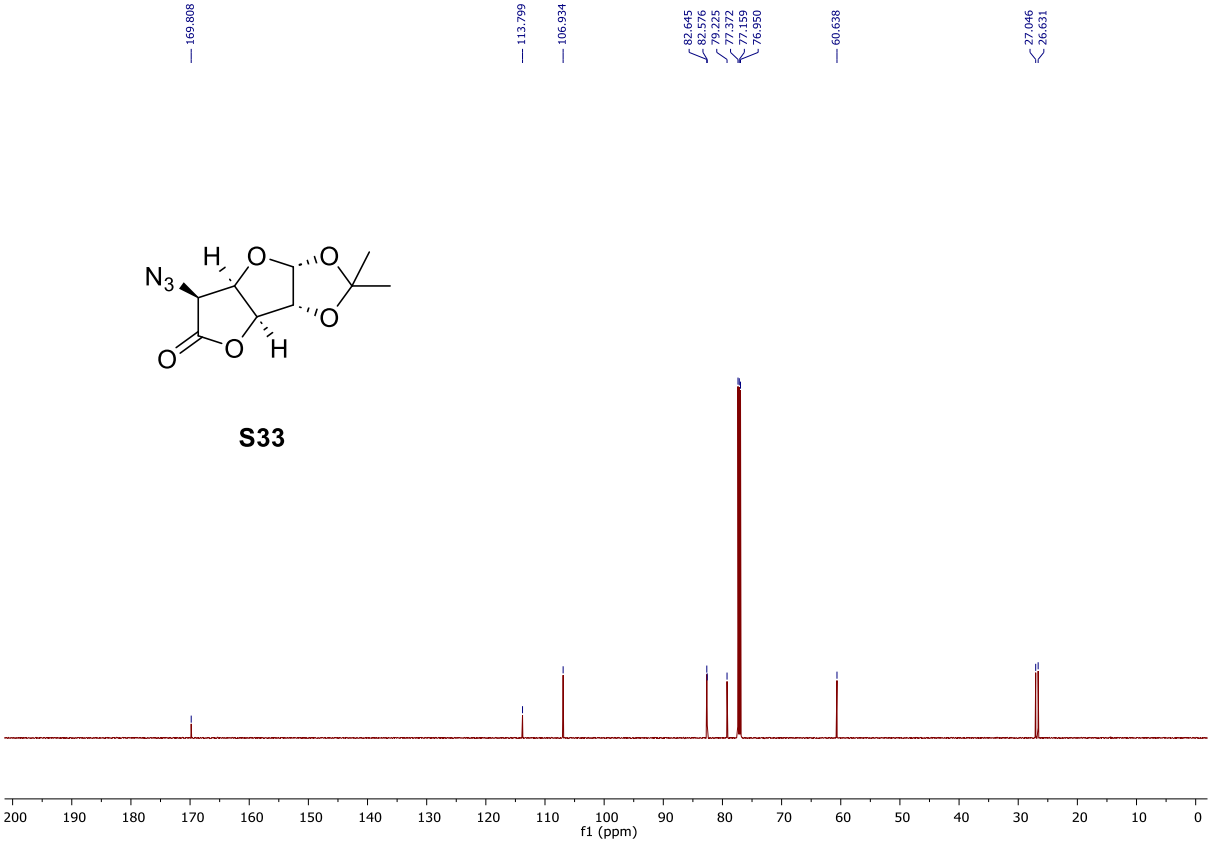

Figure 8.63. ^{13}C NMR spectra for S33

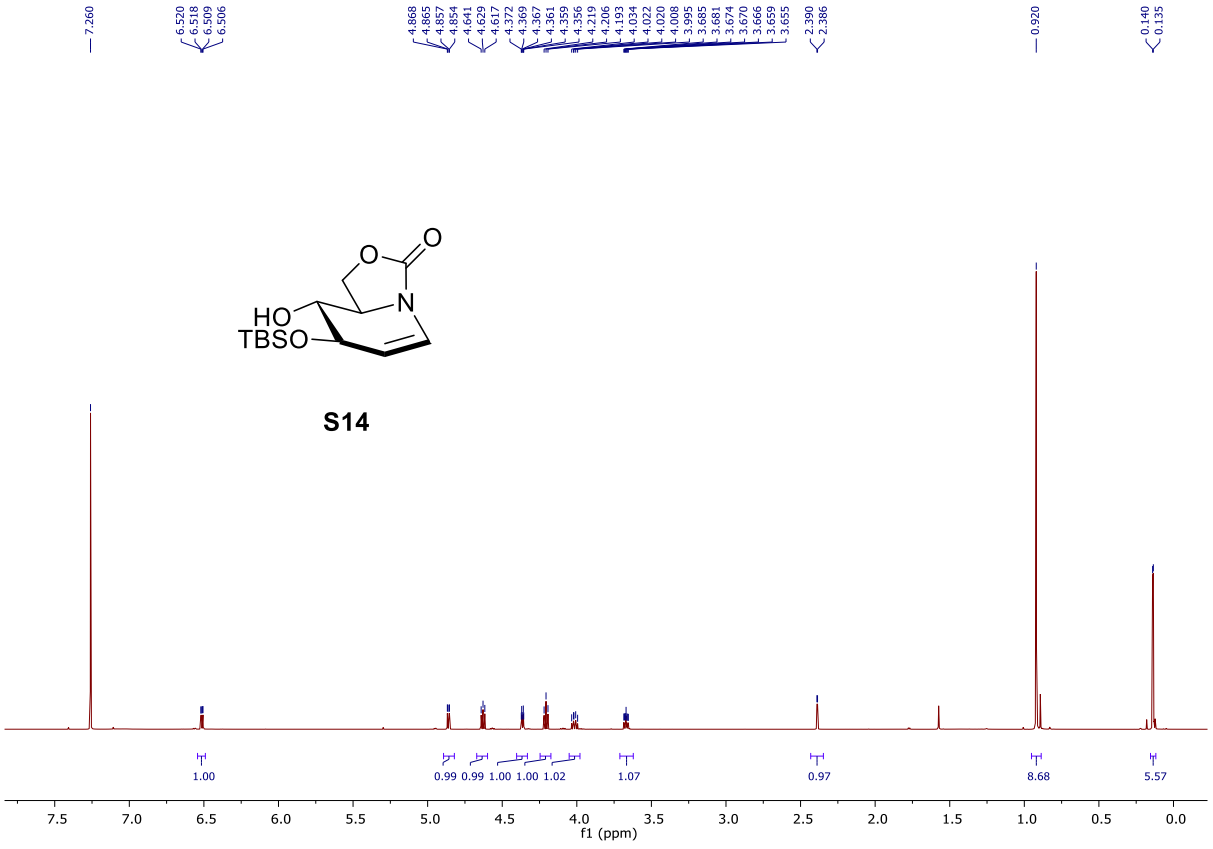

Figure 8.64. ^{1}H NMR spectra for S14

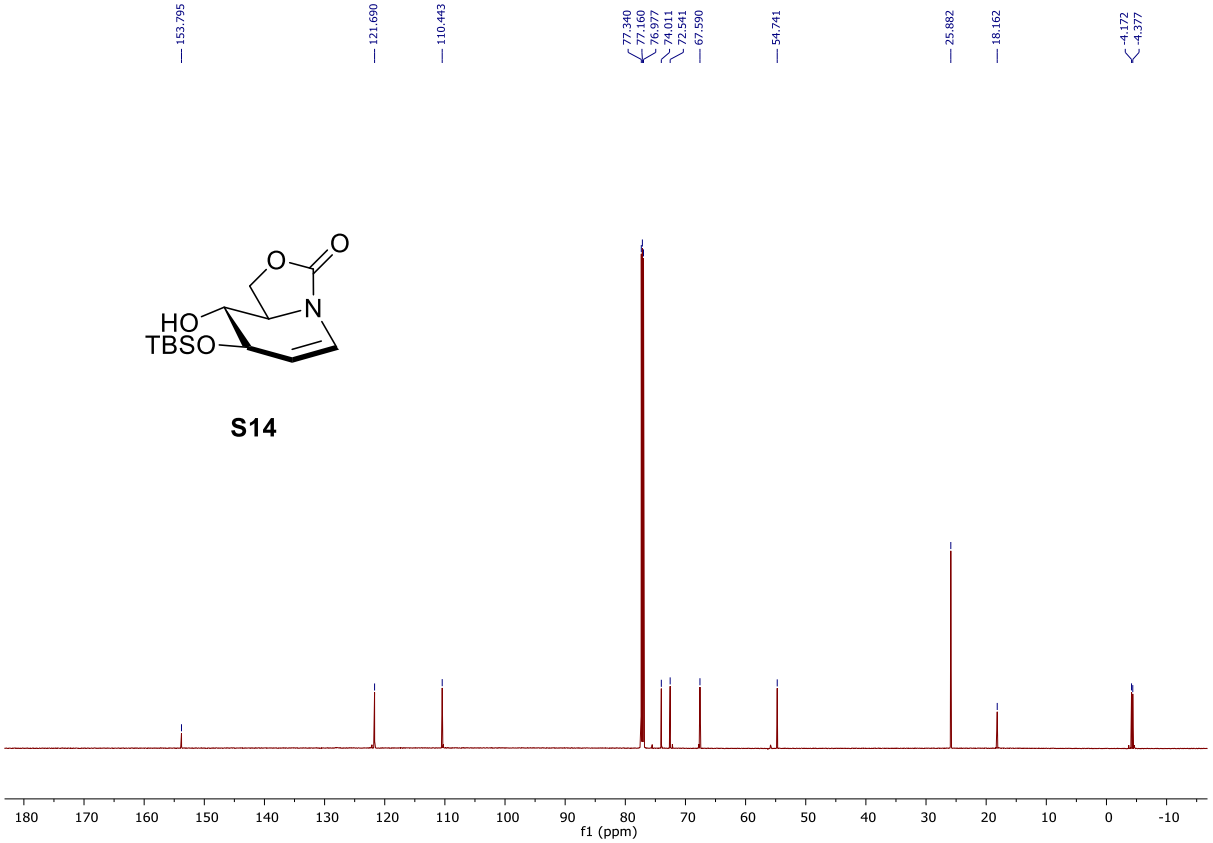

Figure 8.65. ^{13}C NMR spectra for S14

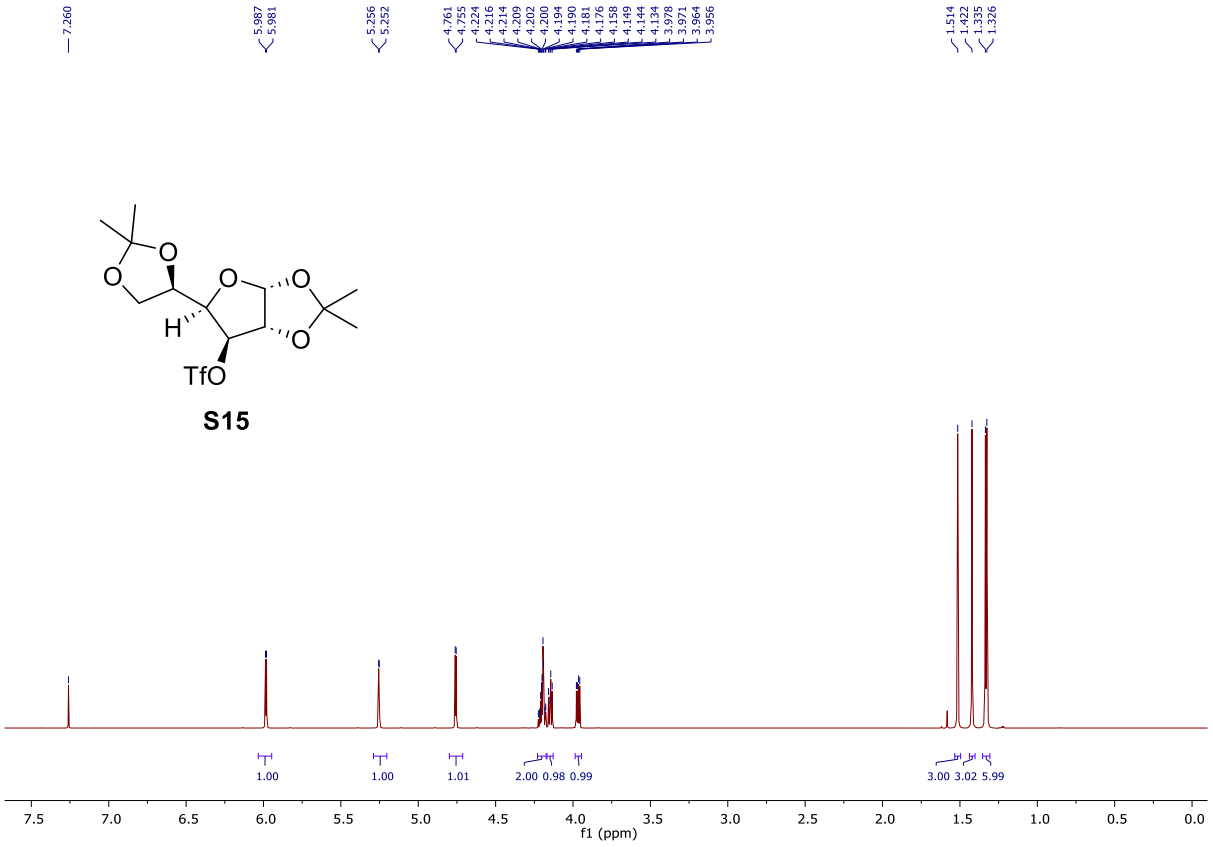

Figure 8.66. ^{1}H NMR spectra for S15

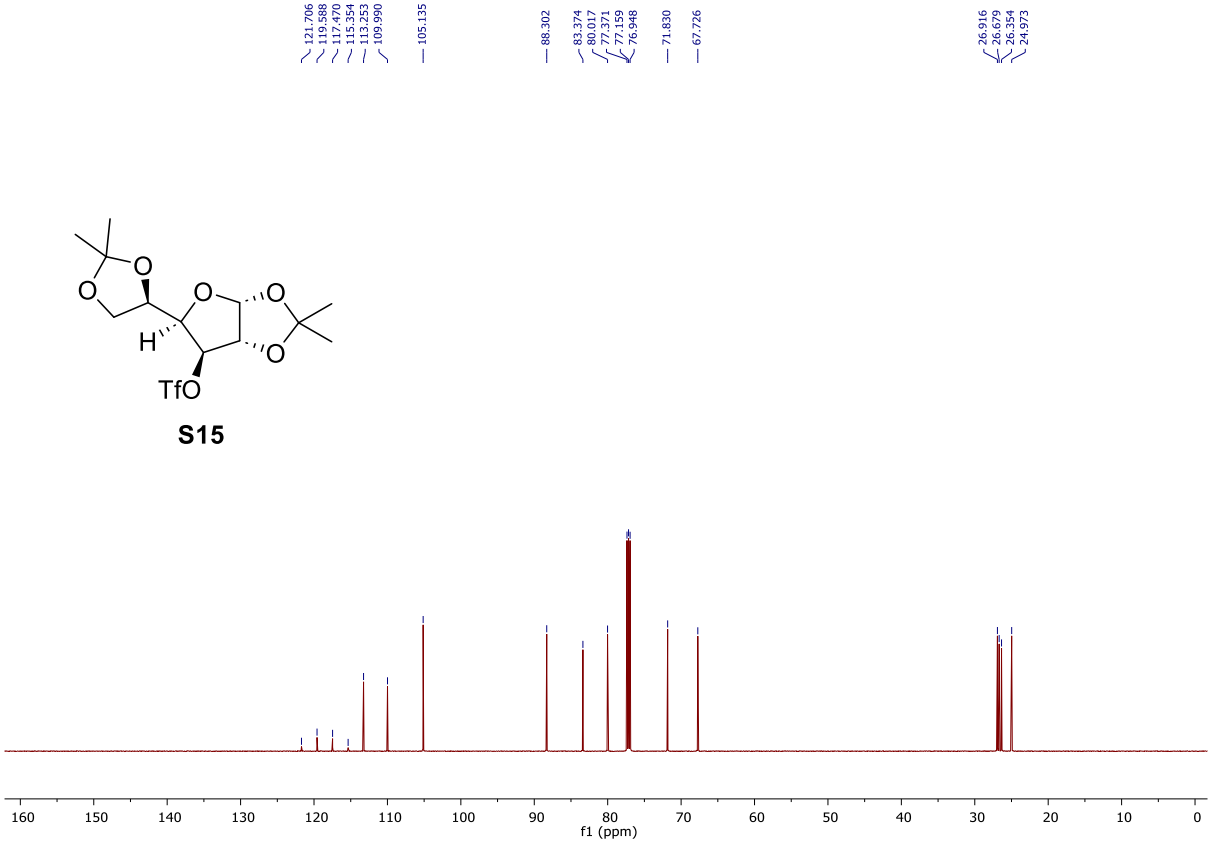

S15

Figure 8.67. ^{13}C NMR spectra for S15

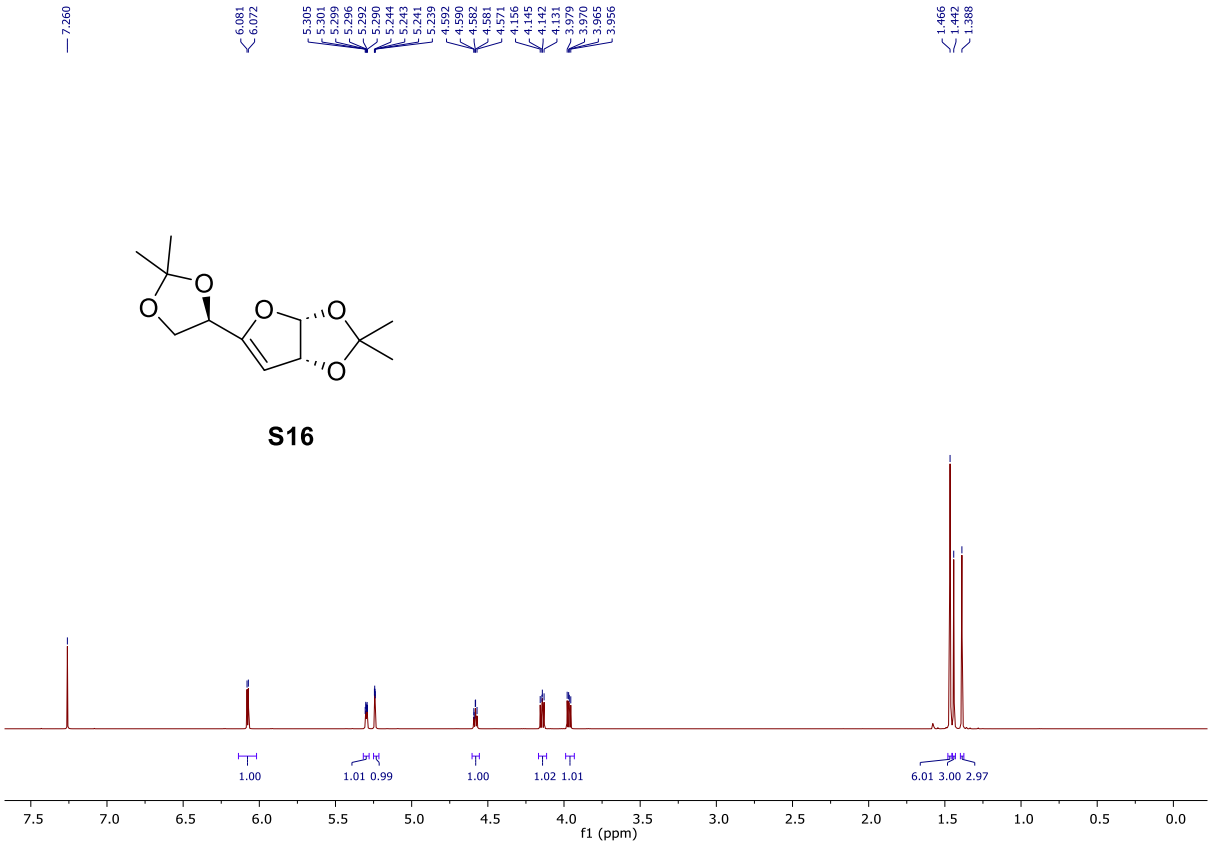

S16

Figure 8.68. ^{1}H NMR spectra for S16

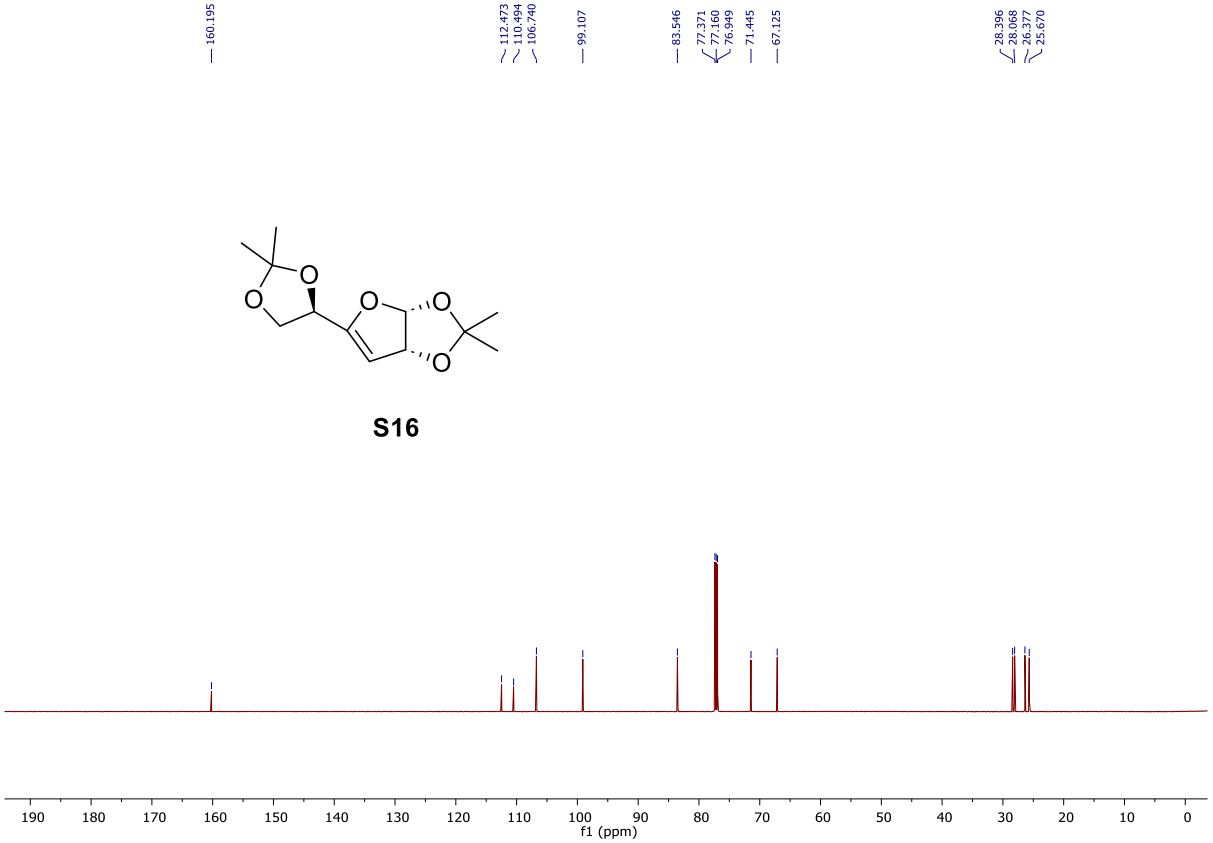

Figure 8.69. ^{13}C NMR spectra for S16

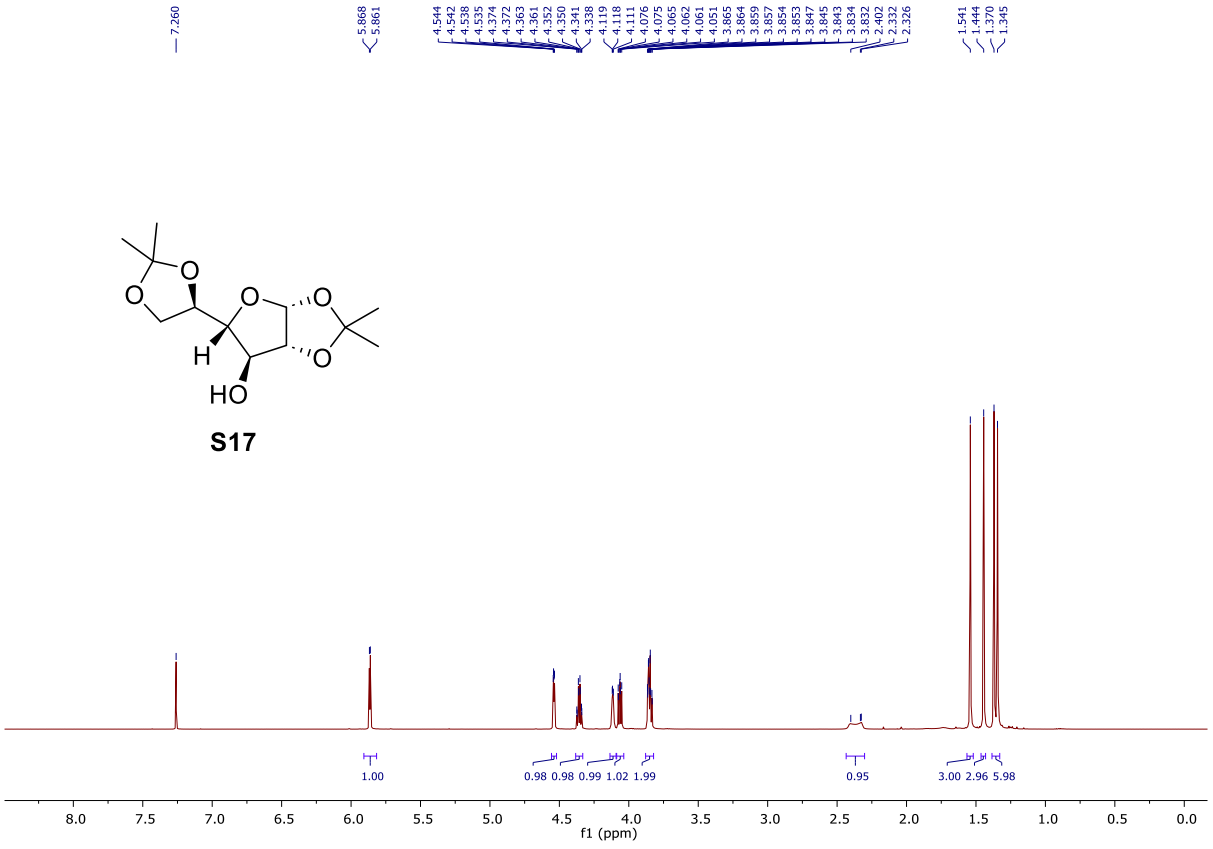

Figure 8.70. ^{1}H NMR spectra for S17

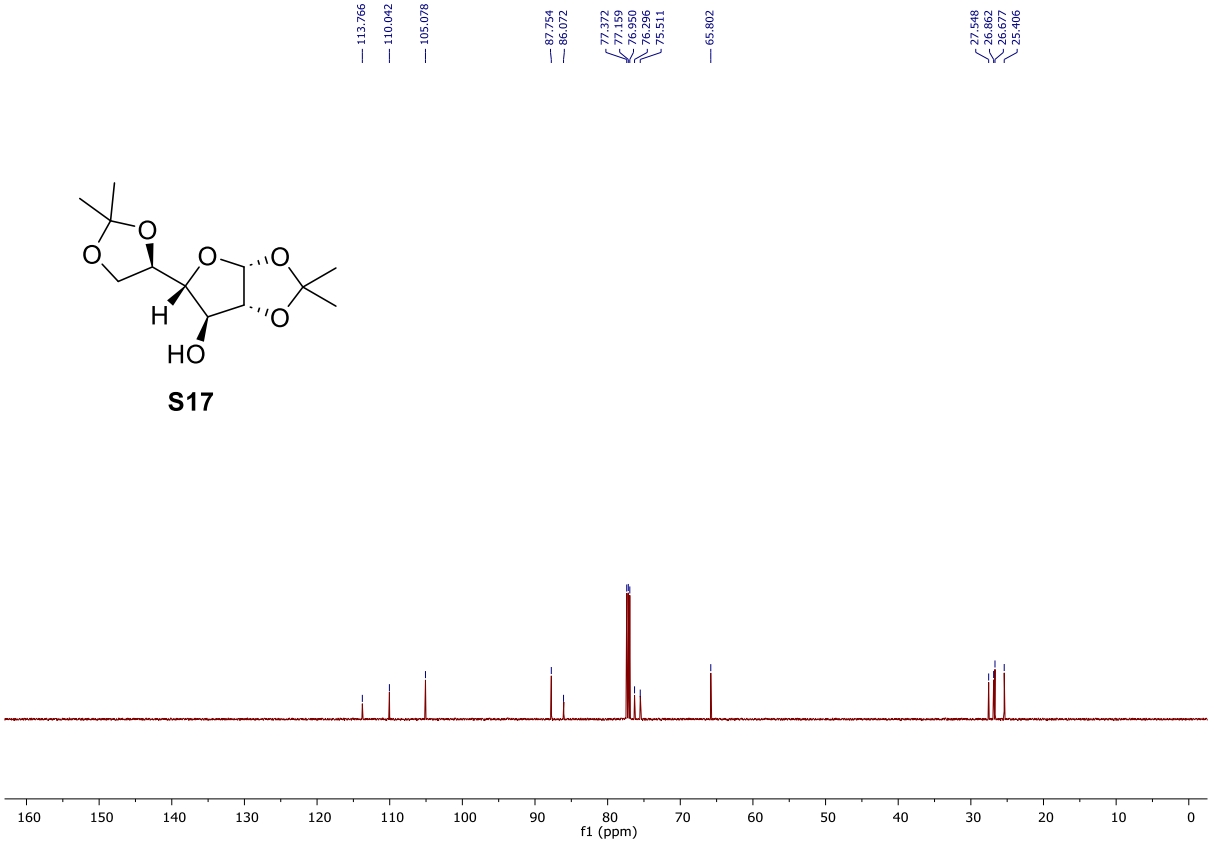

S17

Figure 8.71. ^{13}C NMR spectra for S17

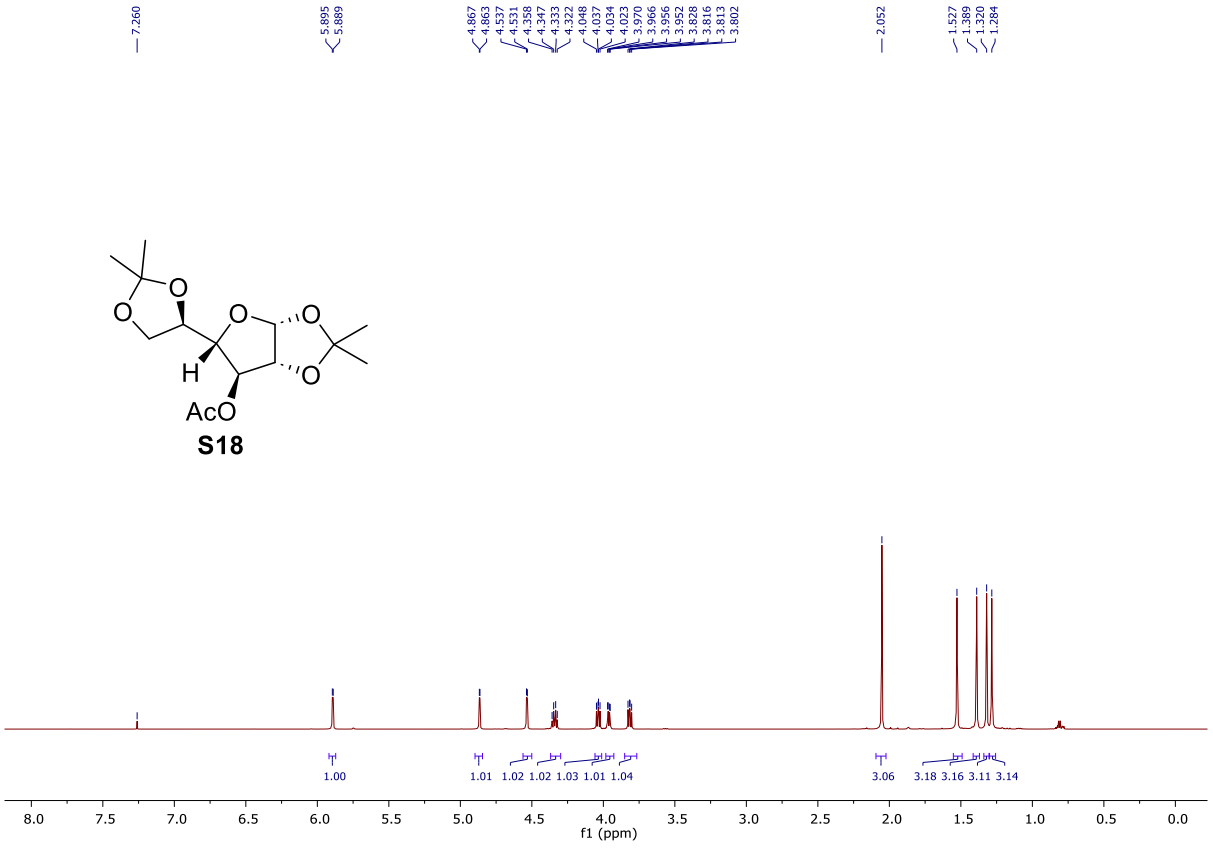

S18

Figure 8.72. ^{1}H NMR spectra for S18

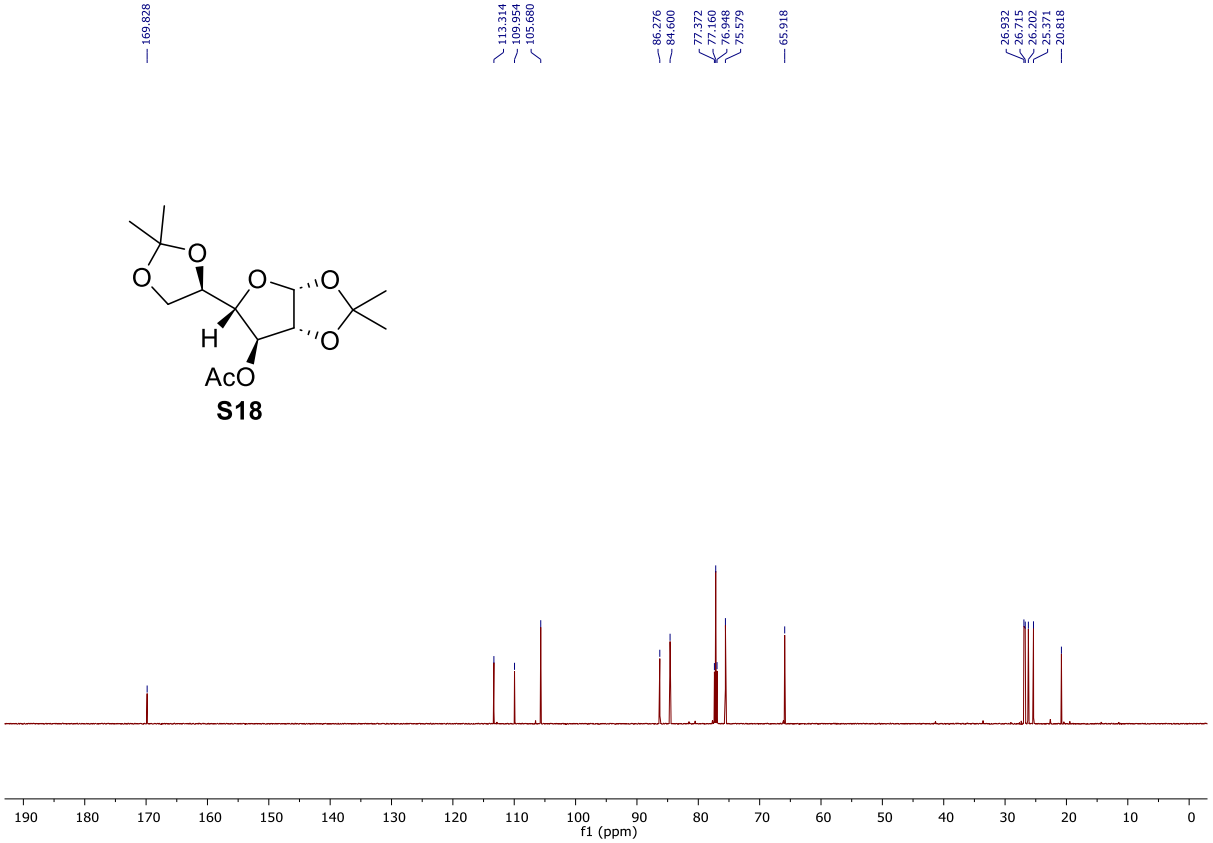

Figure 8.73. ^{13}C NMR spectra for S18

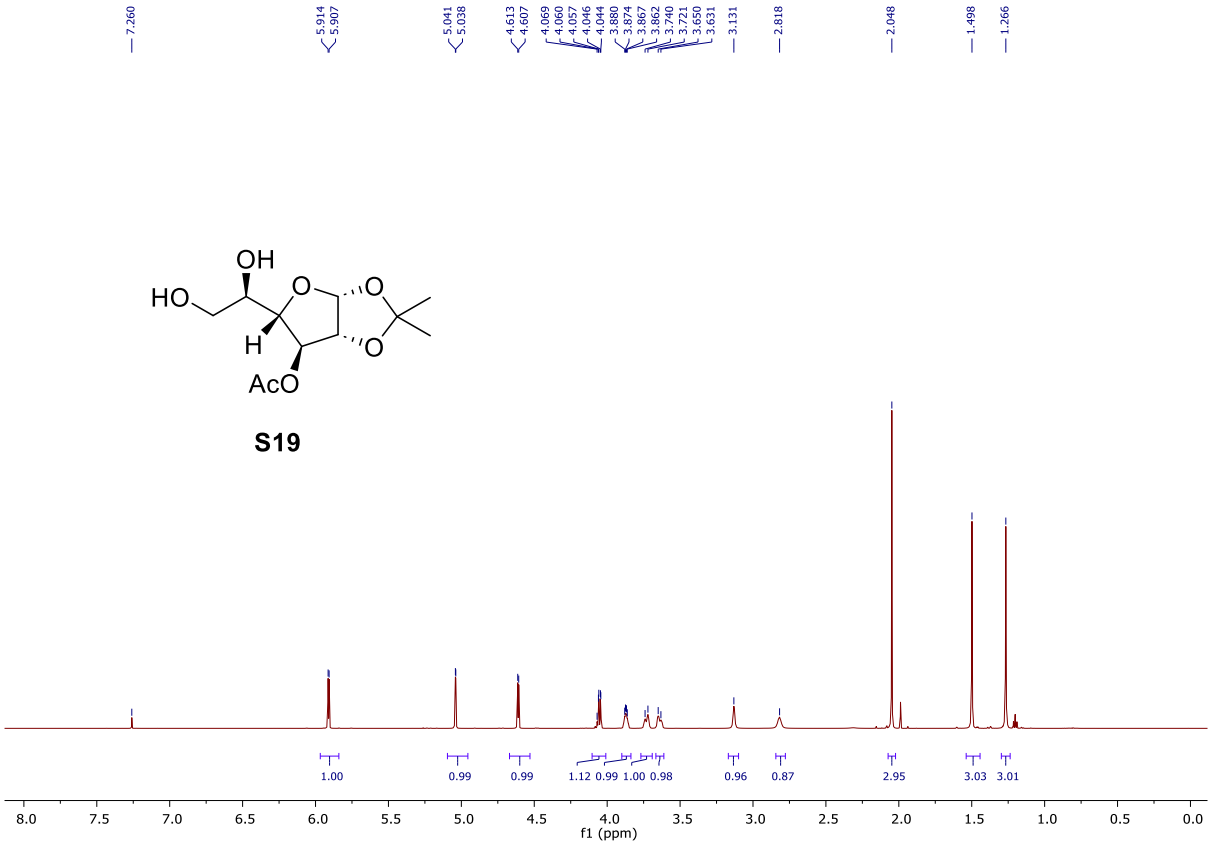

Figure 8.74. ^{1}H NMR spectra for S19

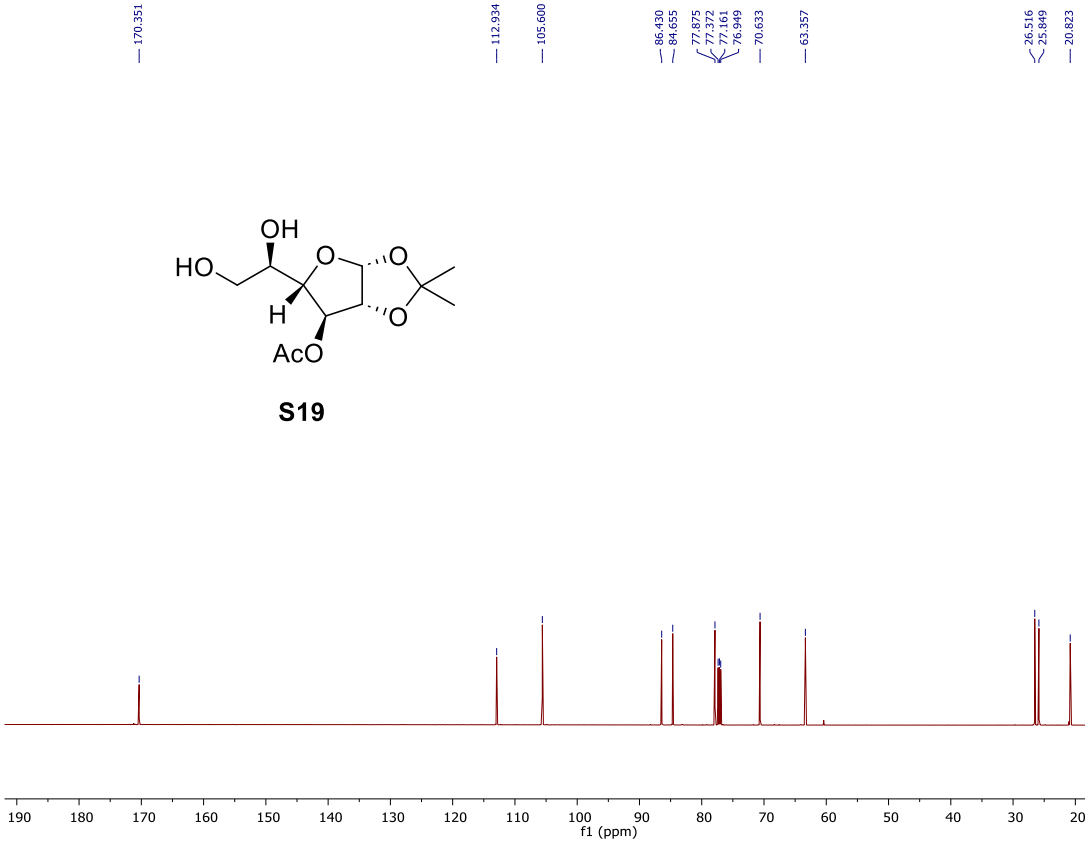

S19

Figure 8.75. ^{13}C NMR spectra for S19

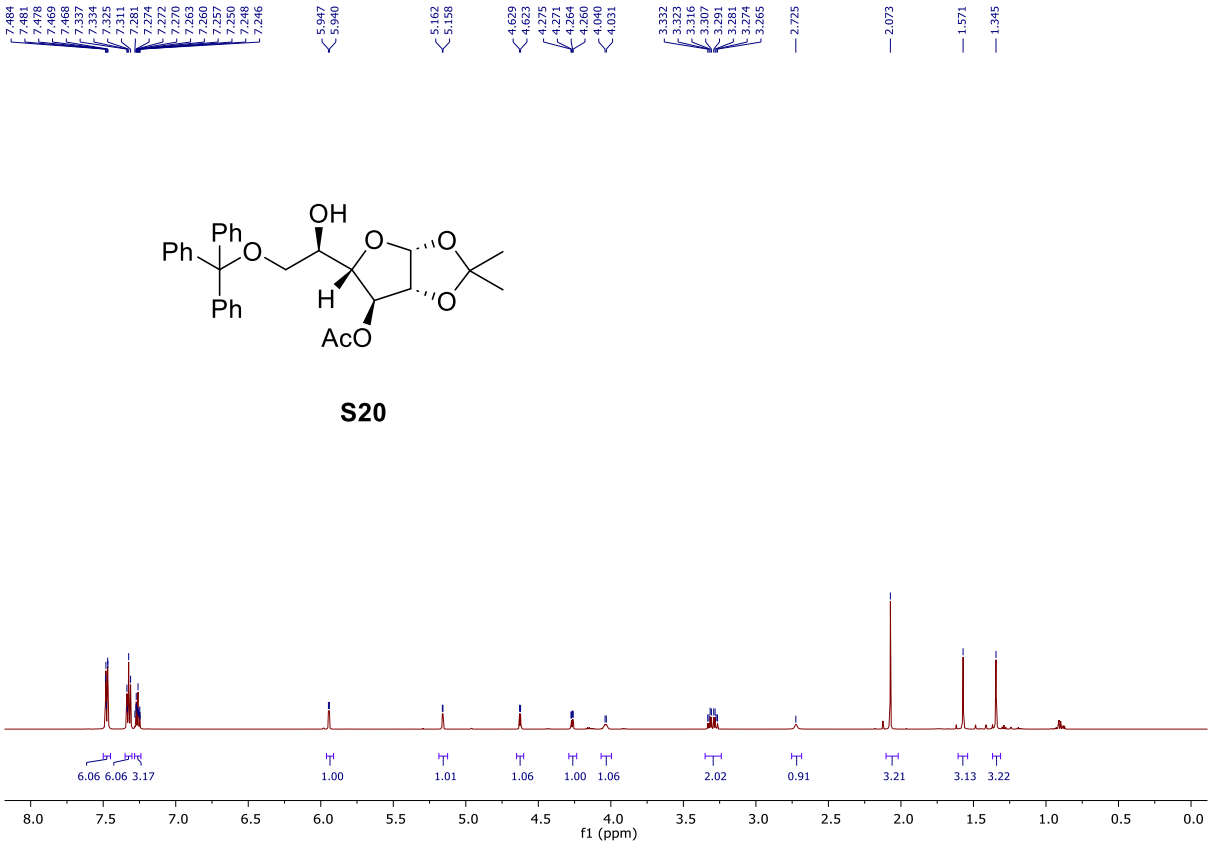

S20

Figure 8.76. ^{1}H NMR spectra for S20

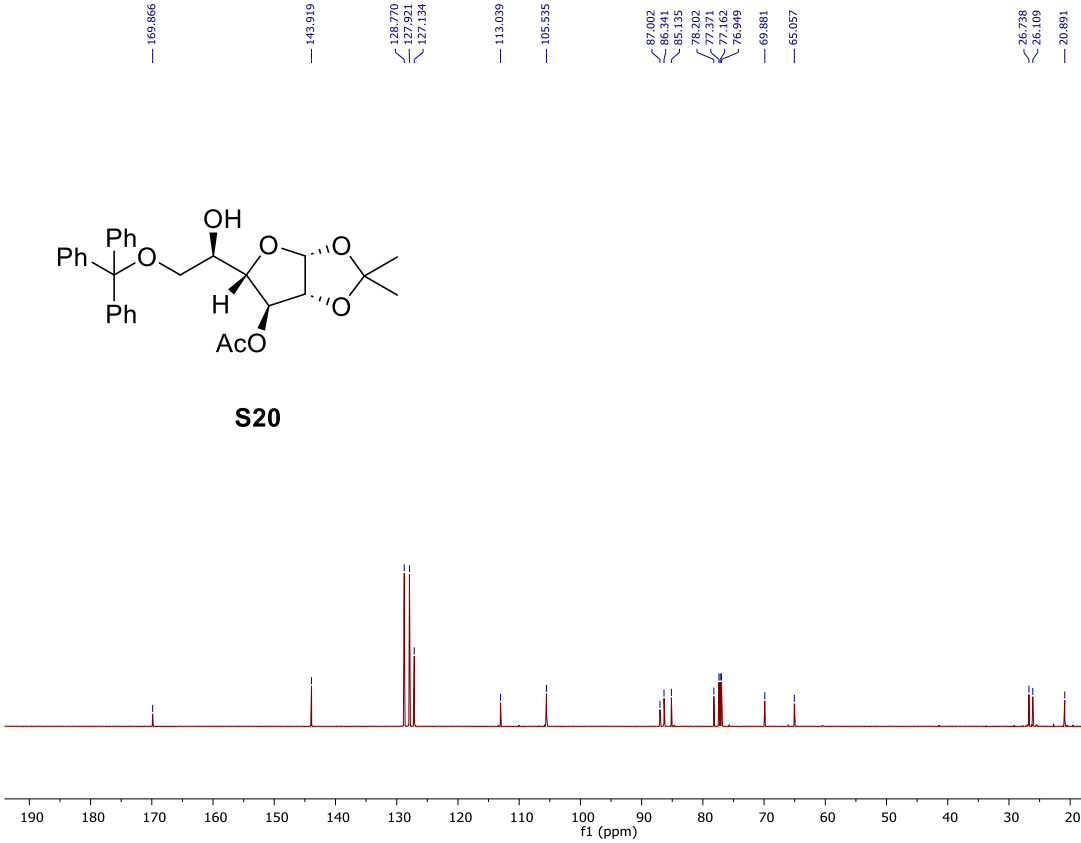

S20

Figure 8.77. ^{13}C NMR spectra for S20

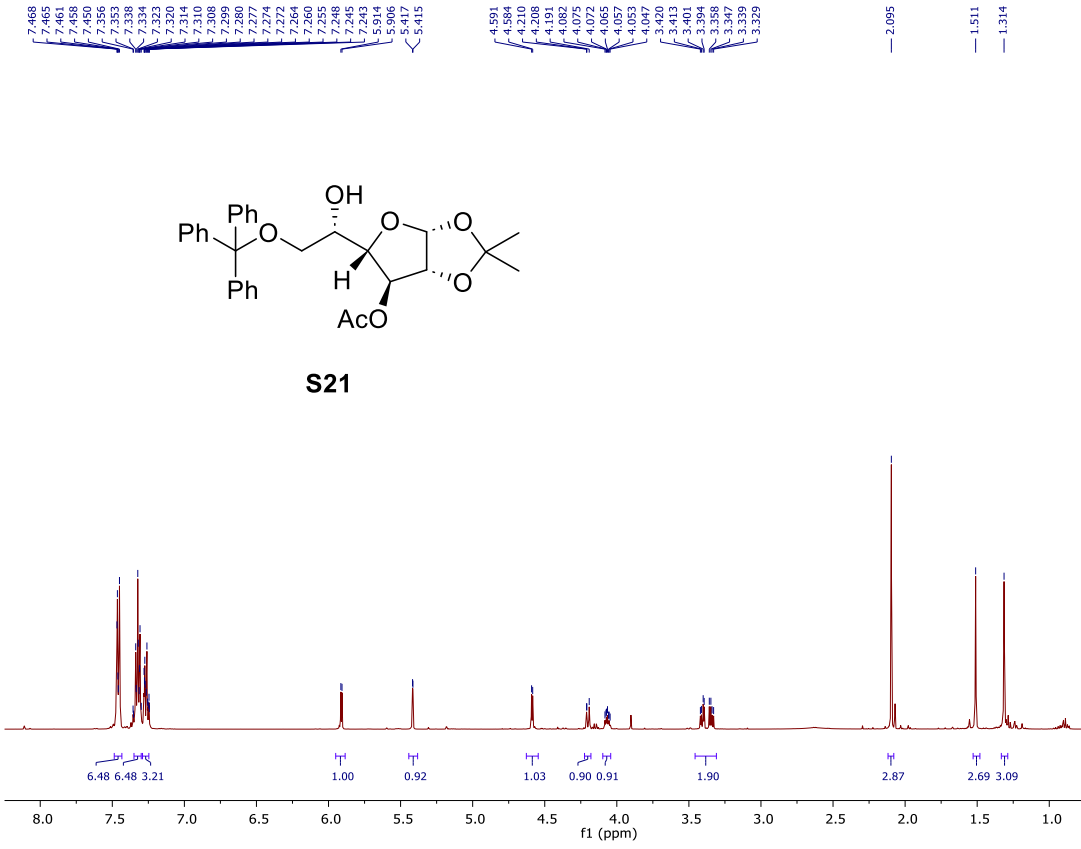

S21

Figure 8.78. ^{1}H NMR spectra for S21

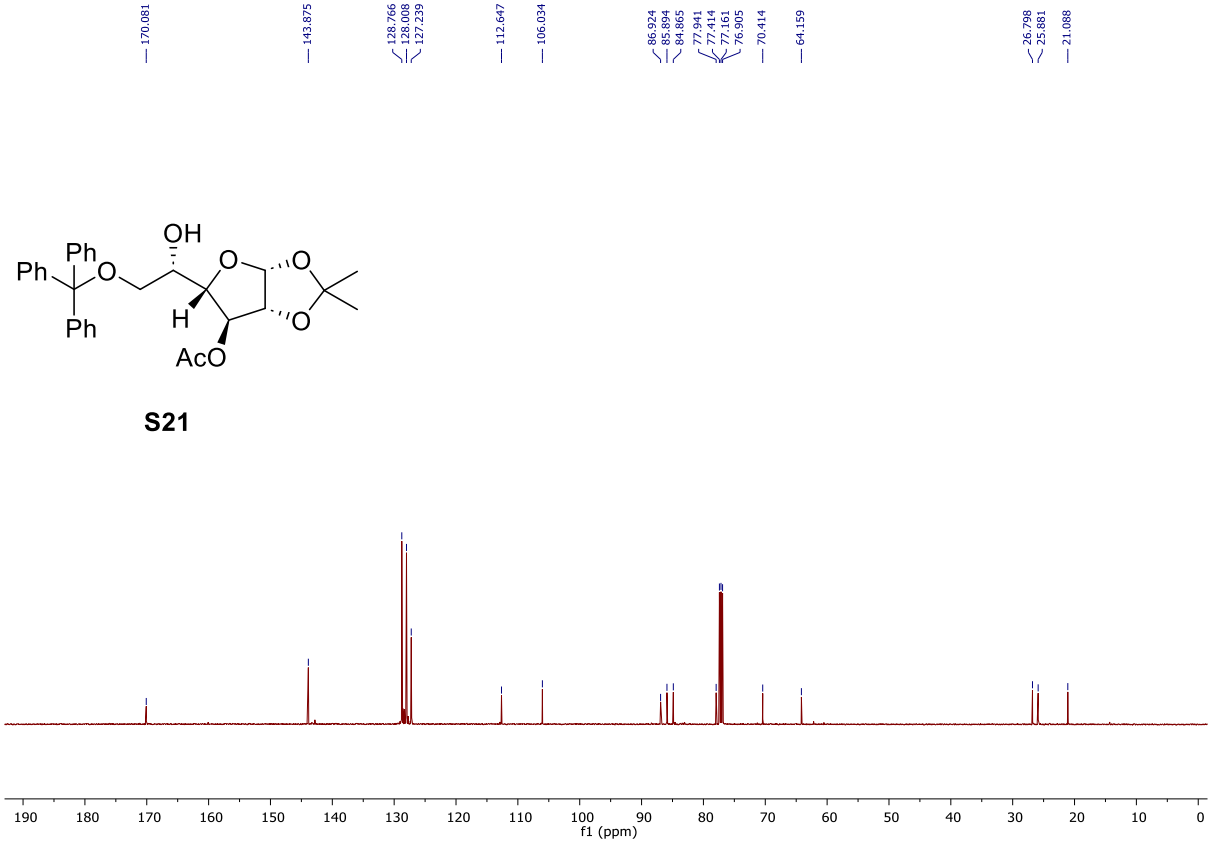

S21

Figure 8.79. ^{13}C NMR spectra for S21

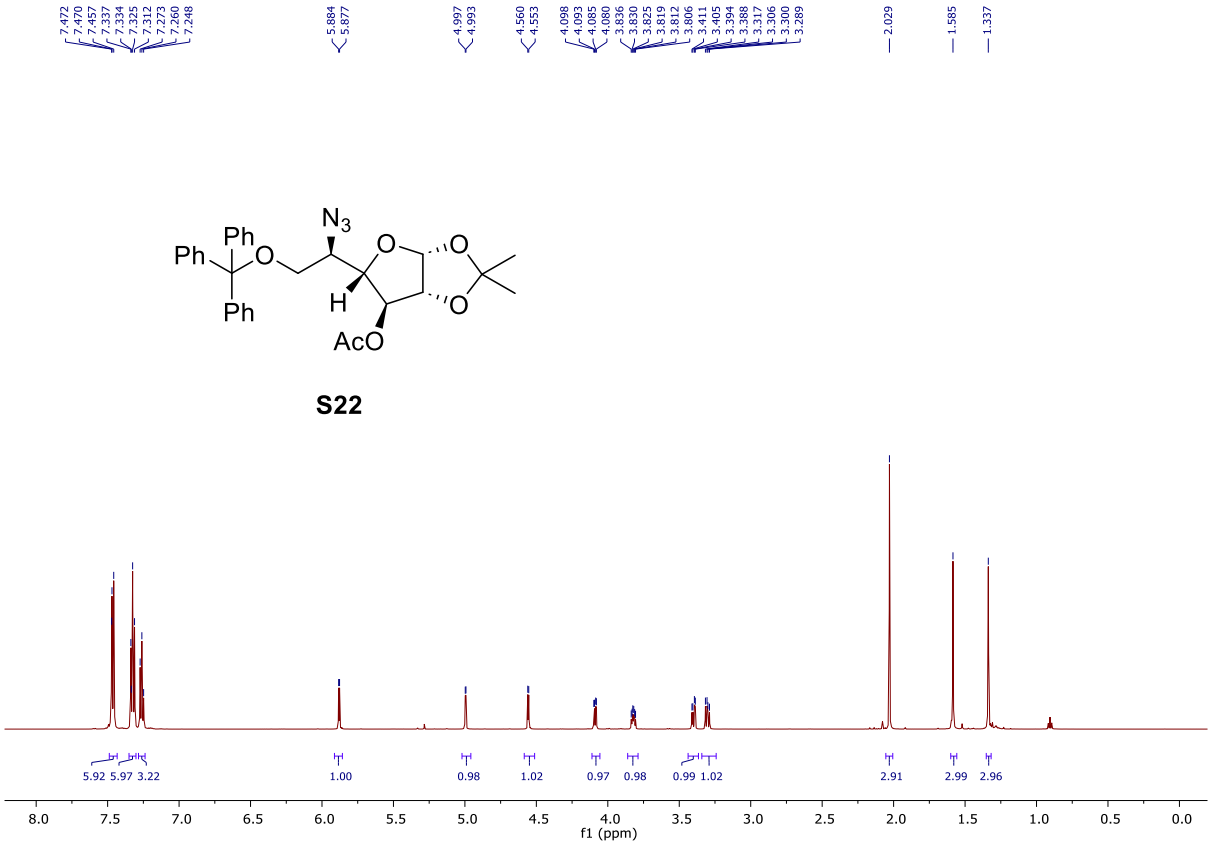

S22

Figure 8.80. ^{1}H NMR spectra for S22

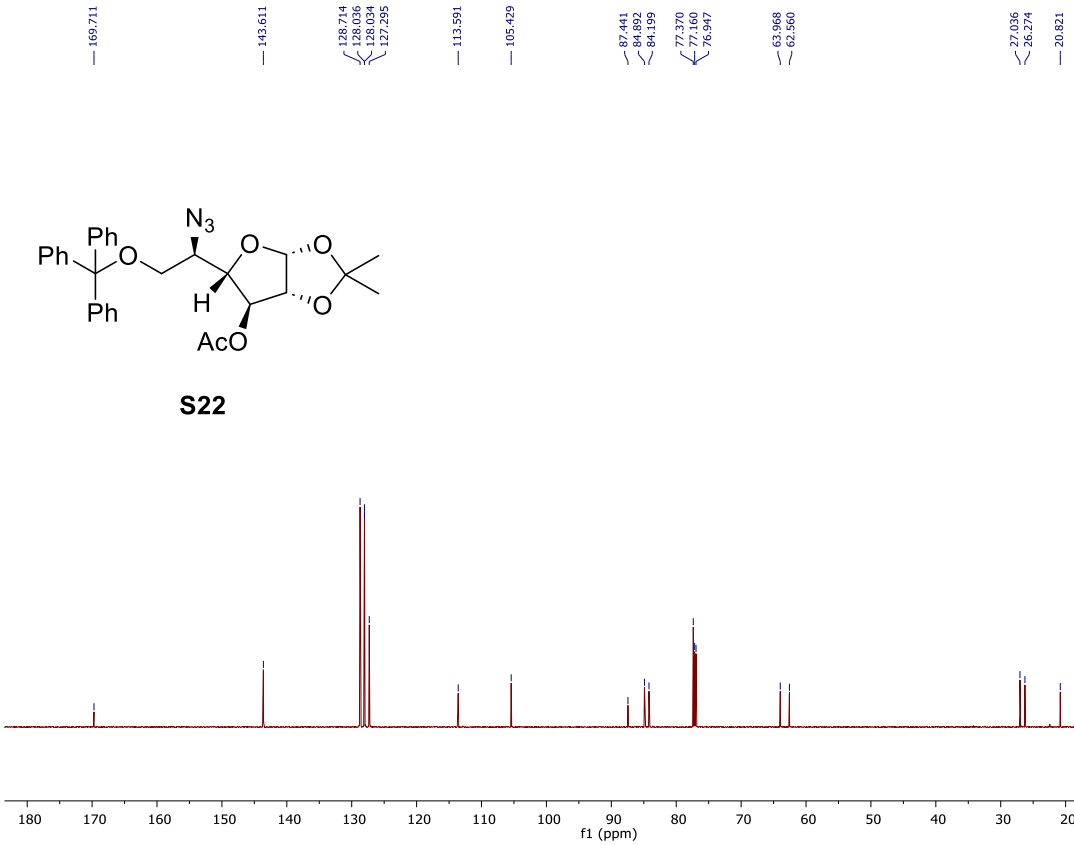

S22

Figure 8.81. ^{13}C NMR spectra for S22

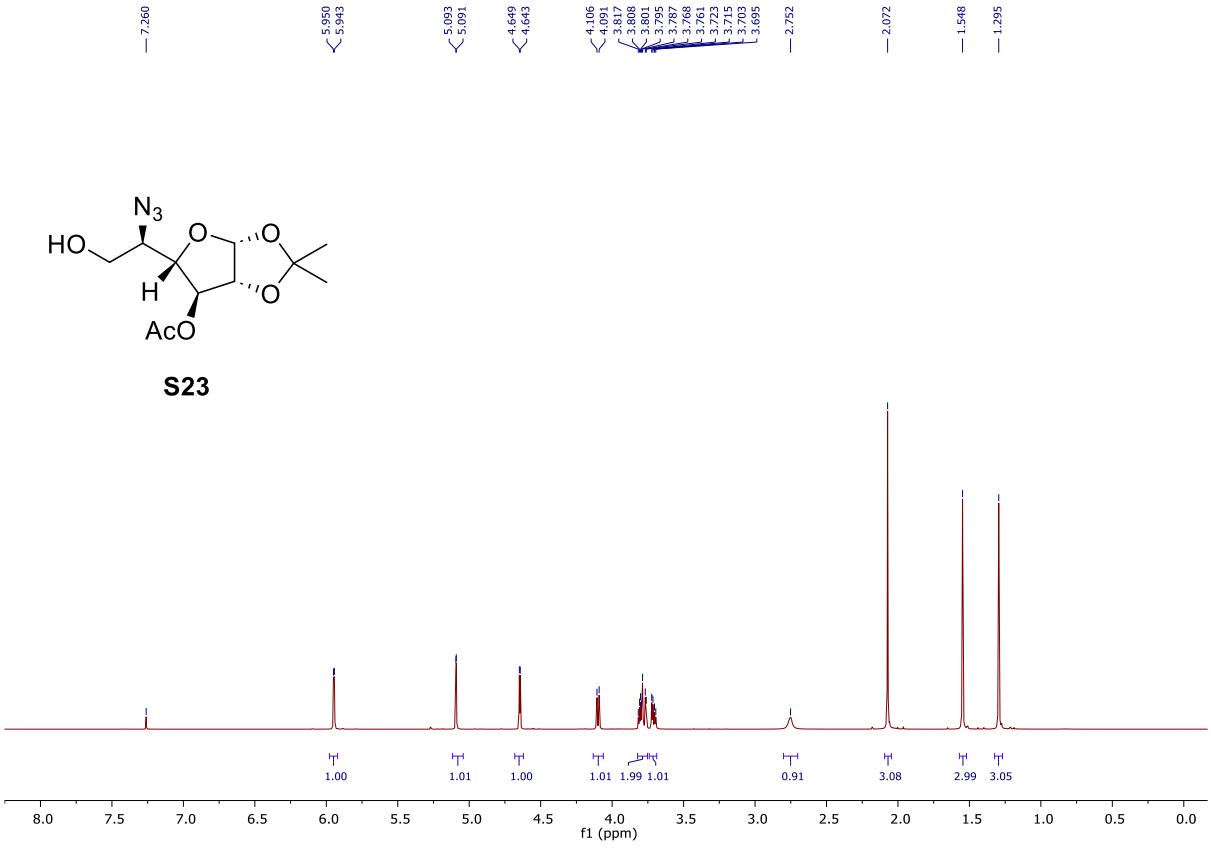

S23

Figure 8.82. ^{1}H NMR spectra for S23

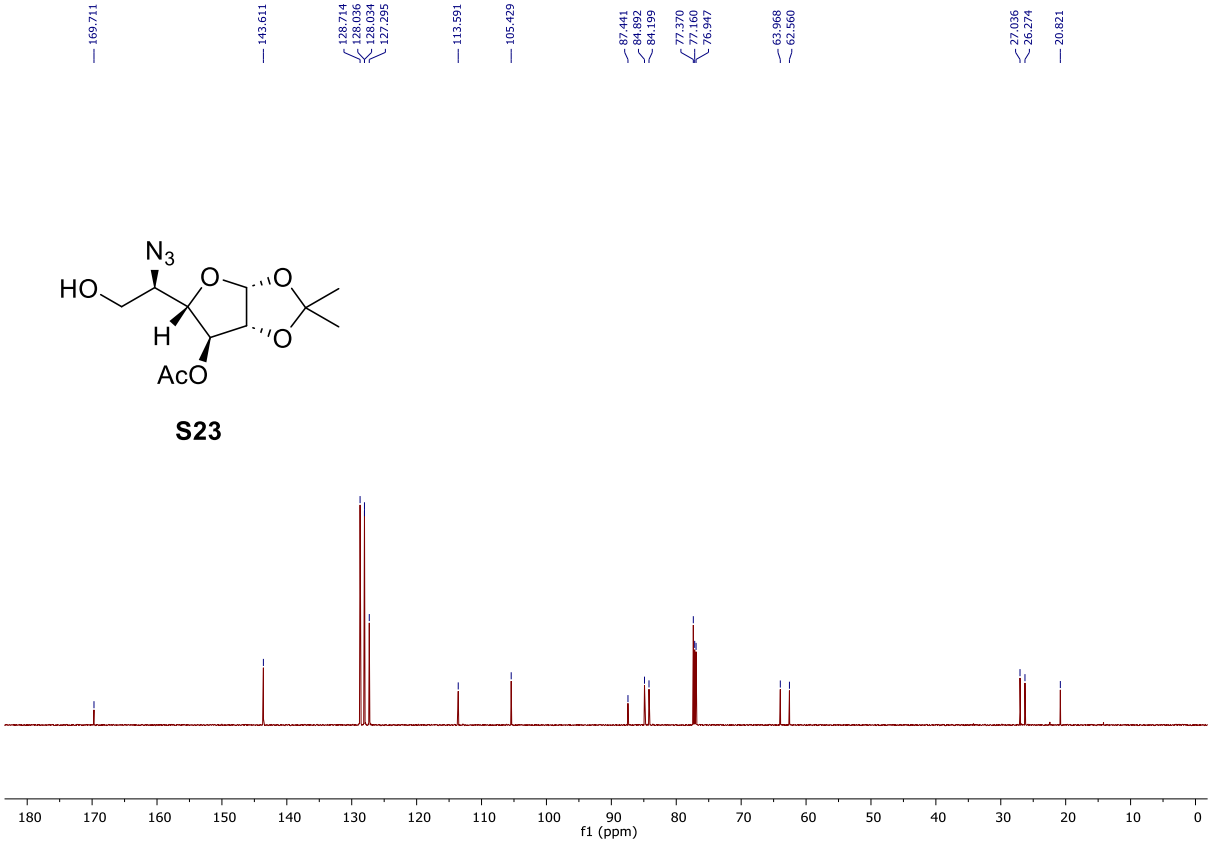

Figure 8.83. ^{13}C NMR spectra for S23

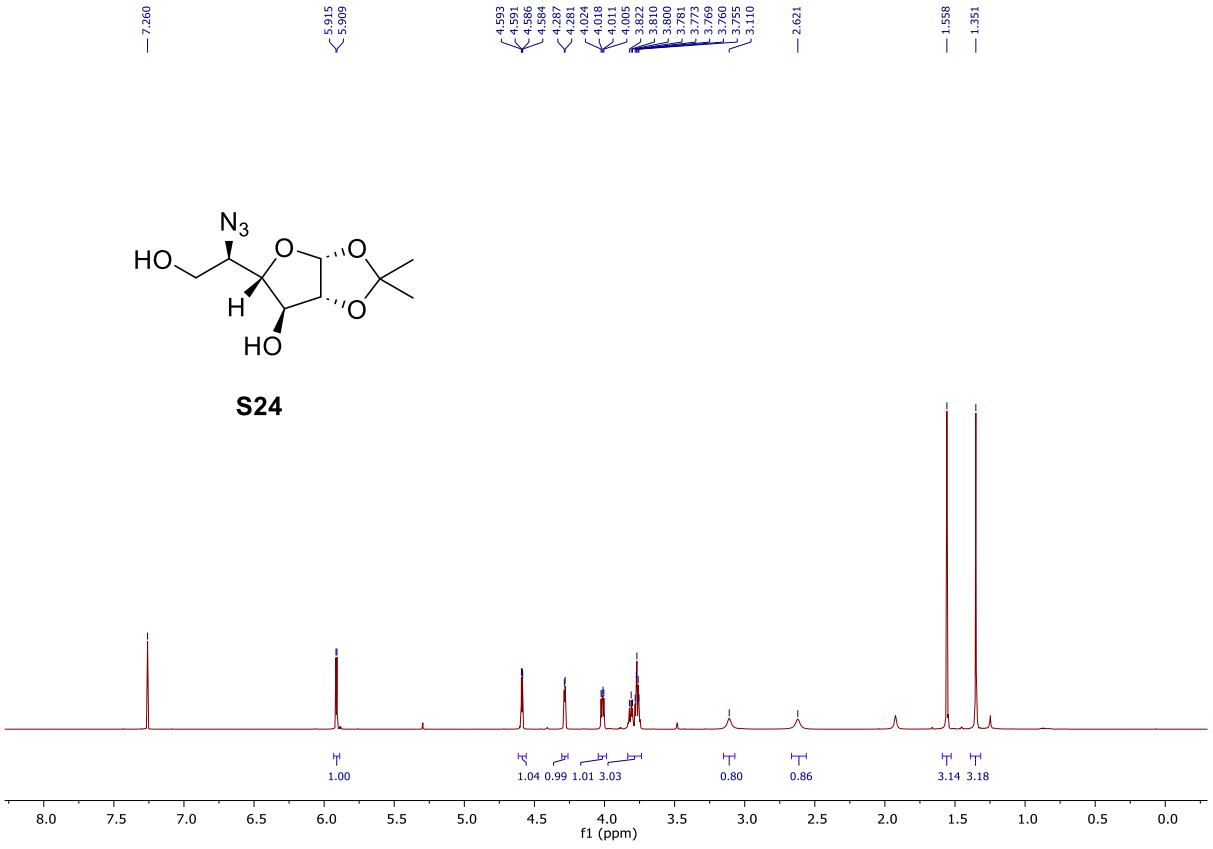

Figure 8.84. ^{1}H NMR spectra for S24

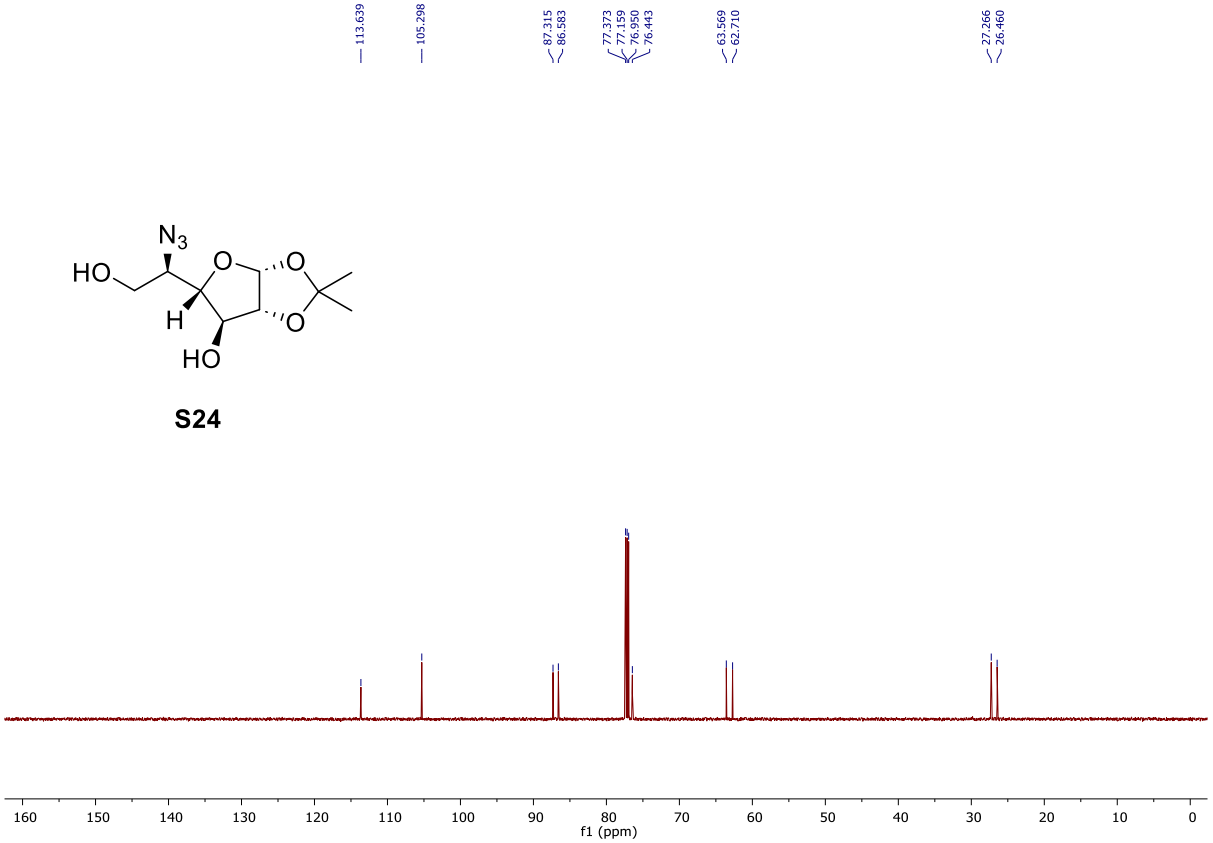

S24

Figure 8.85. ^{13}C NMR spectra for S24

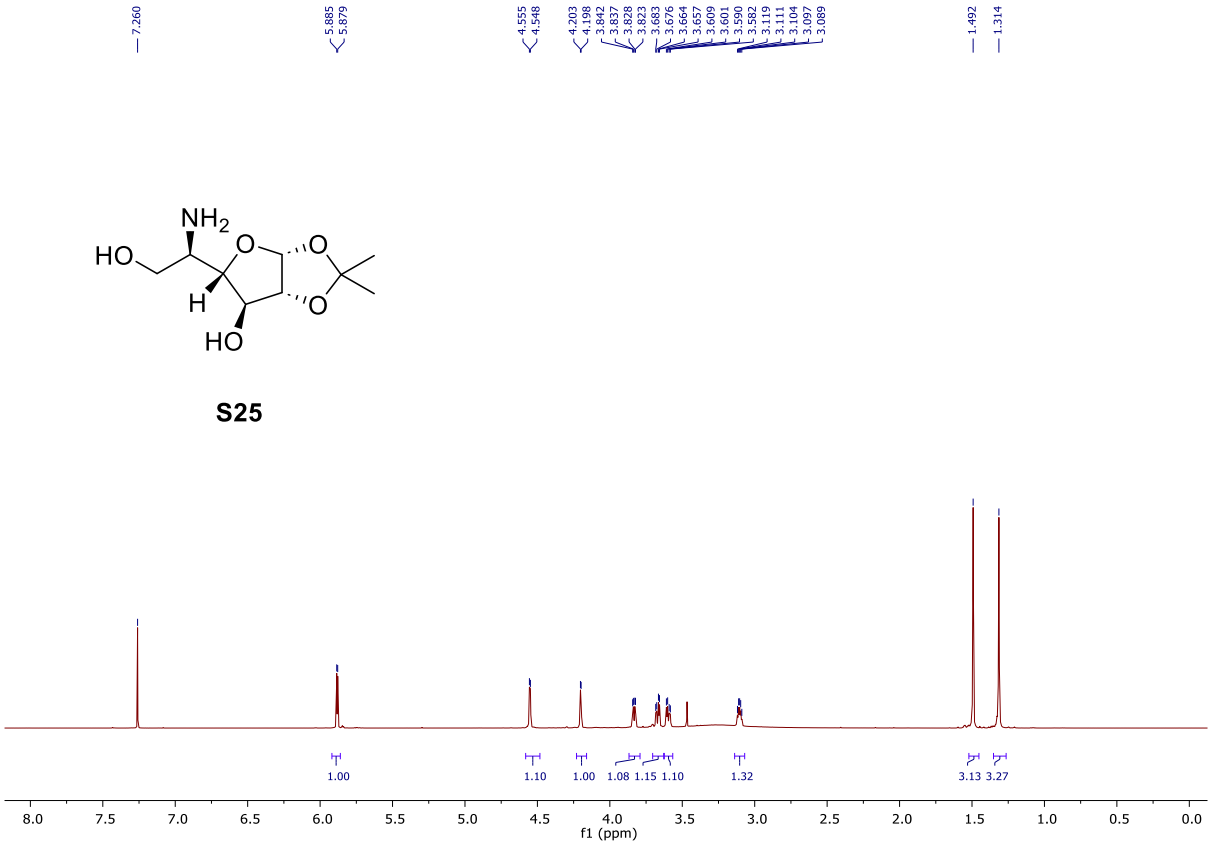

S25

Figure 8.86. ^{1}H NMR spectra for S25

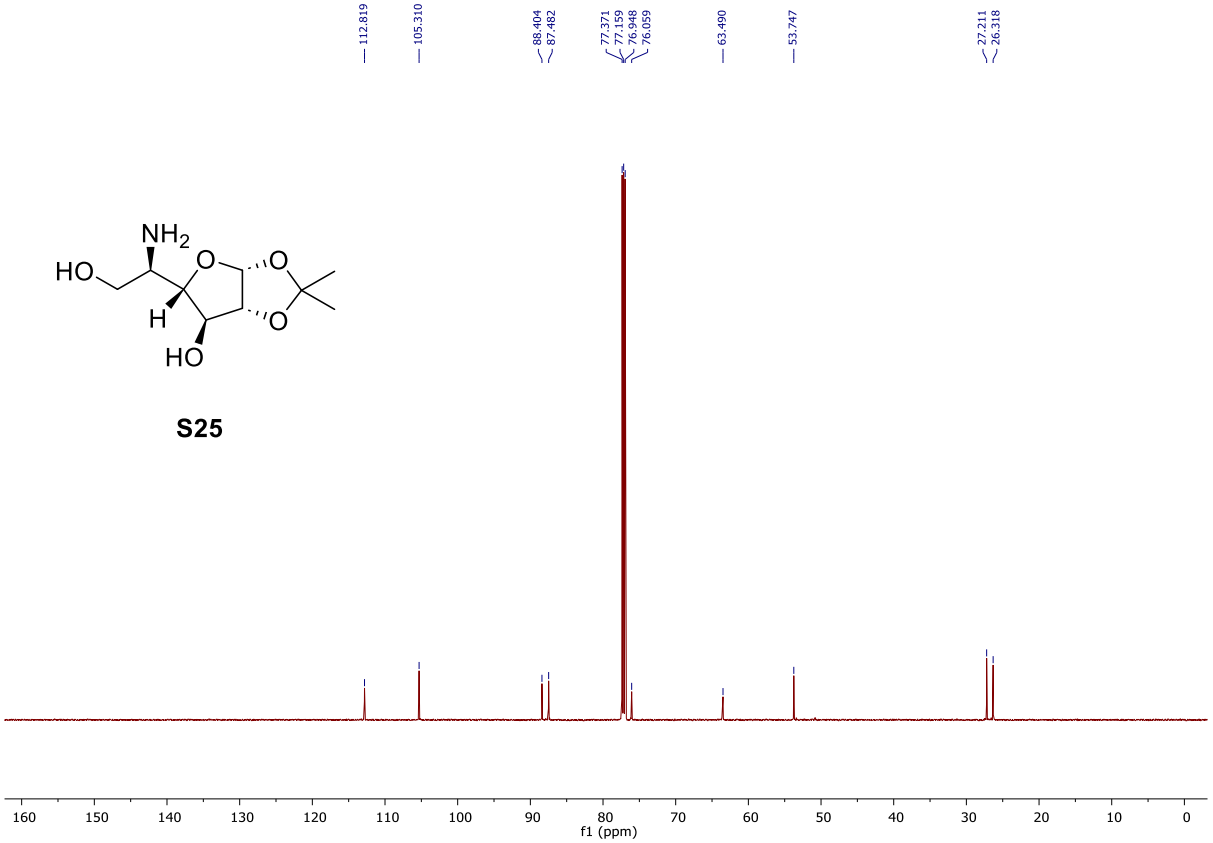

Figure 8.87. ^{13}C NMR spectra for S25

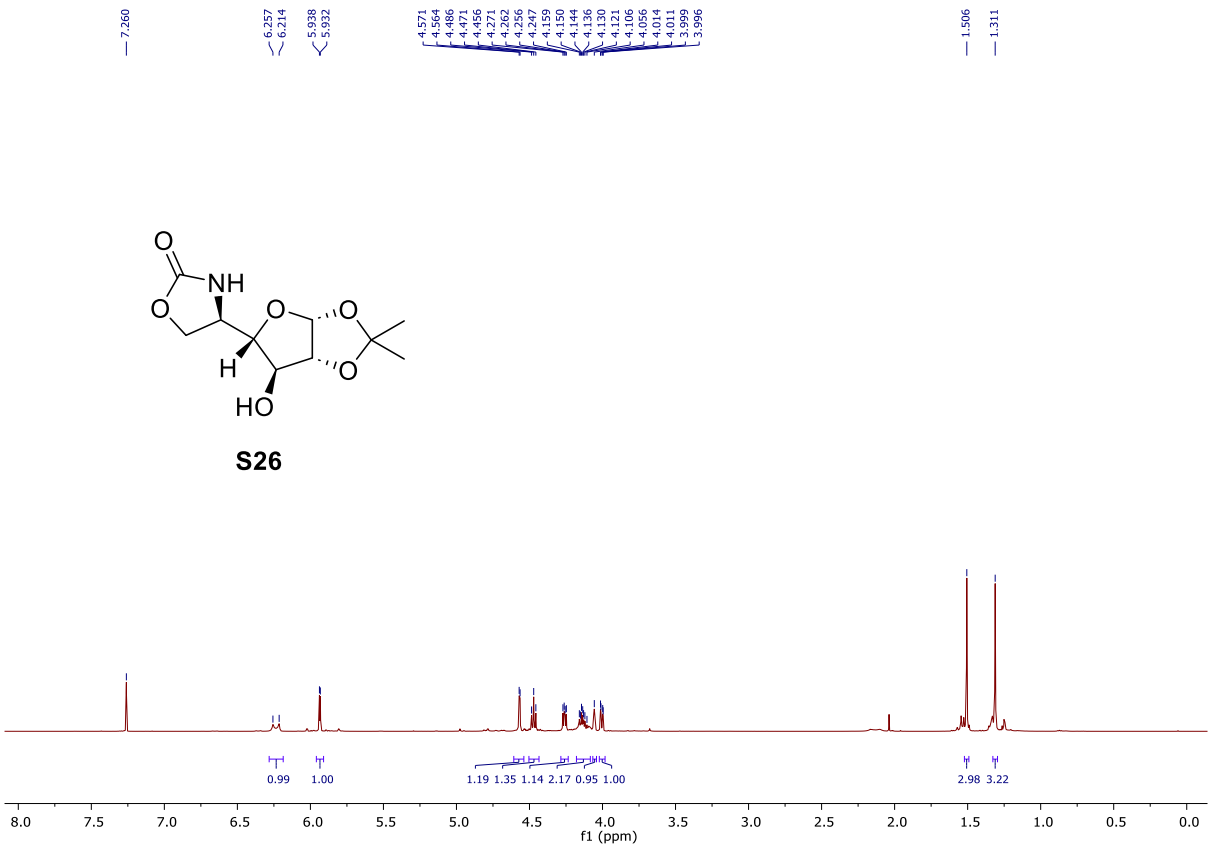

Figure 8.88. ^{1}H NMR spectra for S26

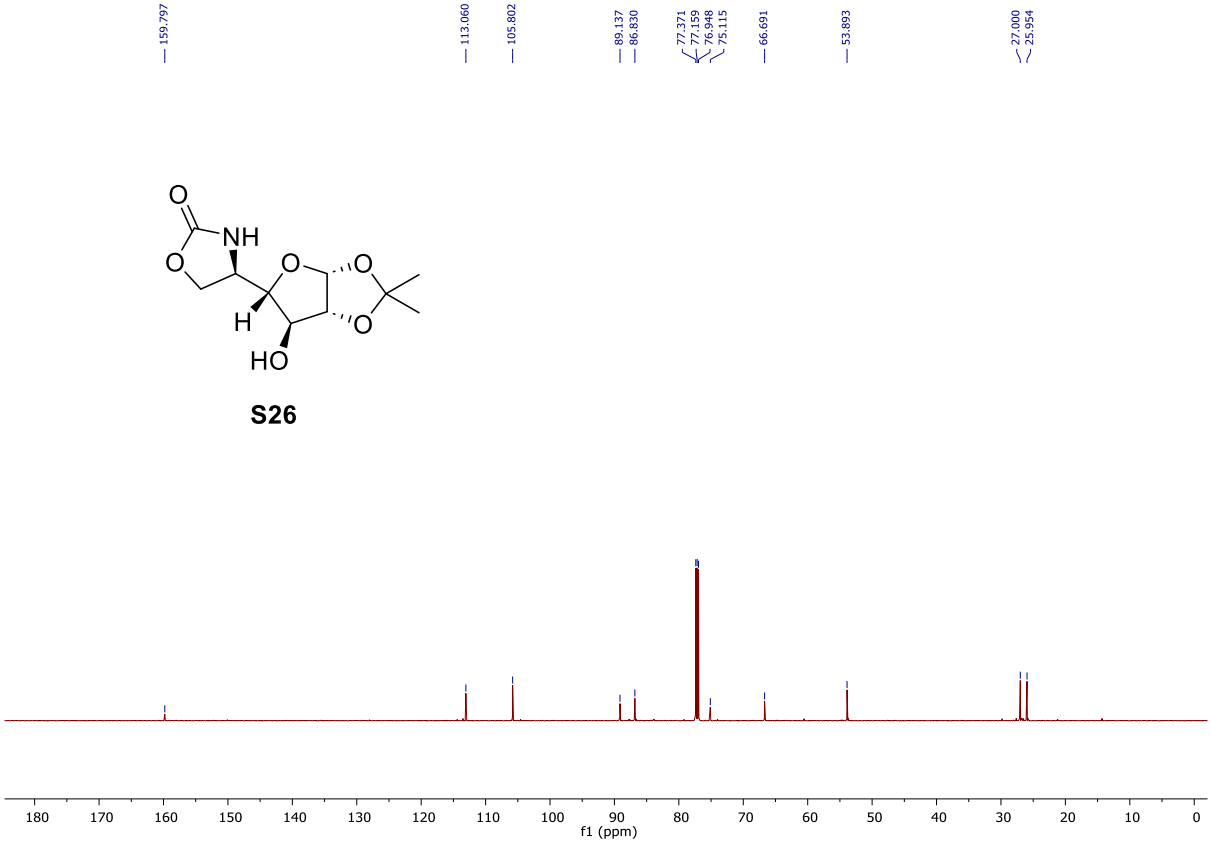

Figure 8.89. ^{13}C NMR spectra for S26

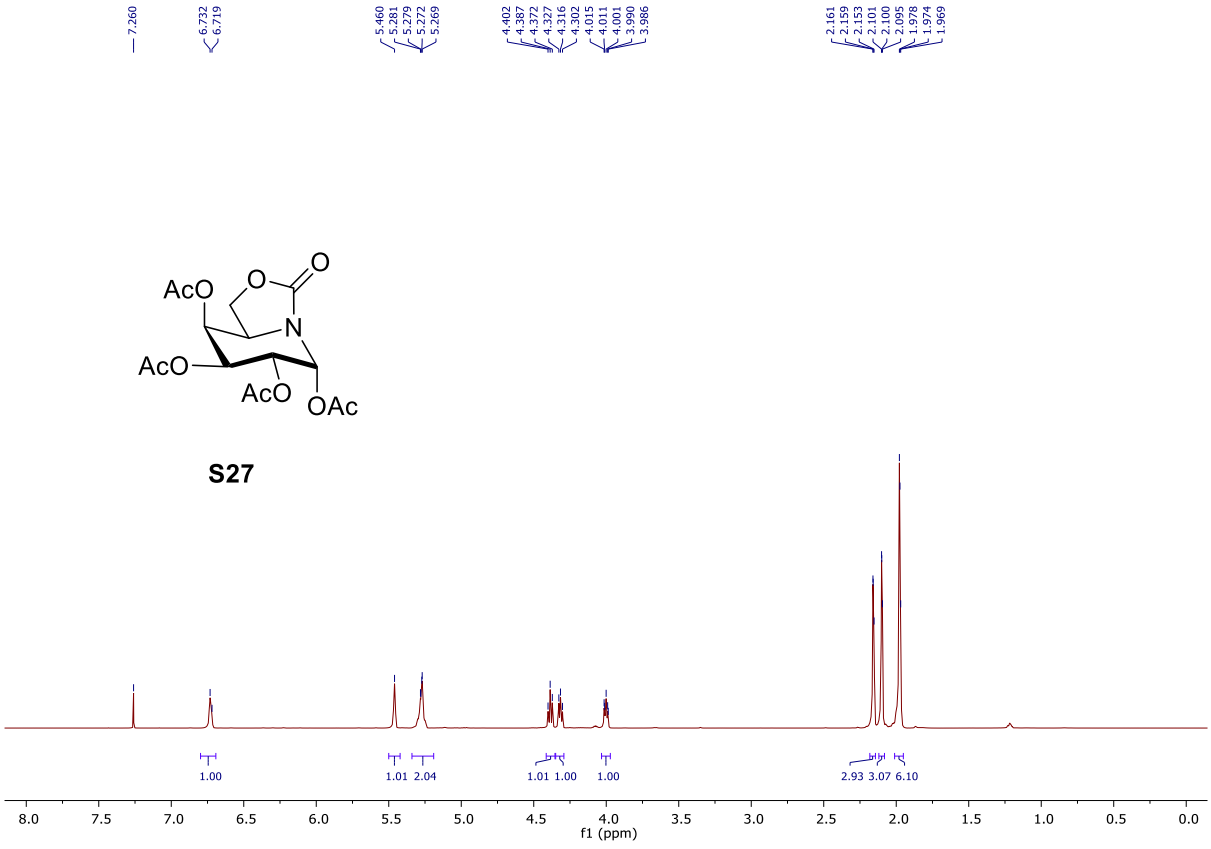

Figure 8.90. ^{1}H NMR spectra for S27

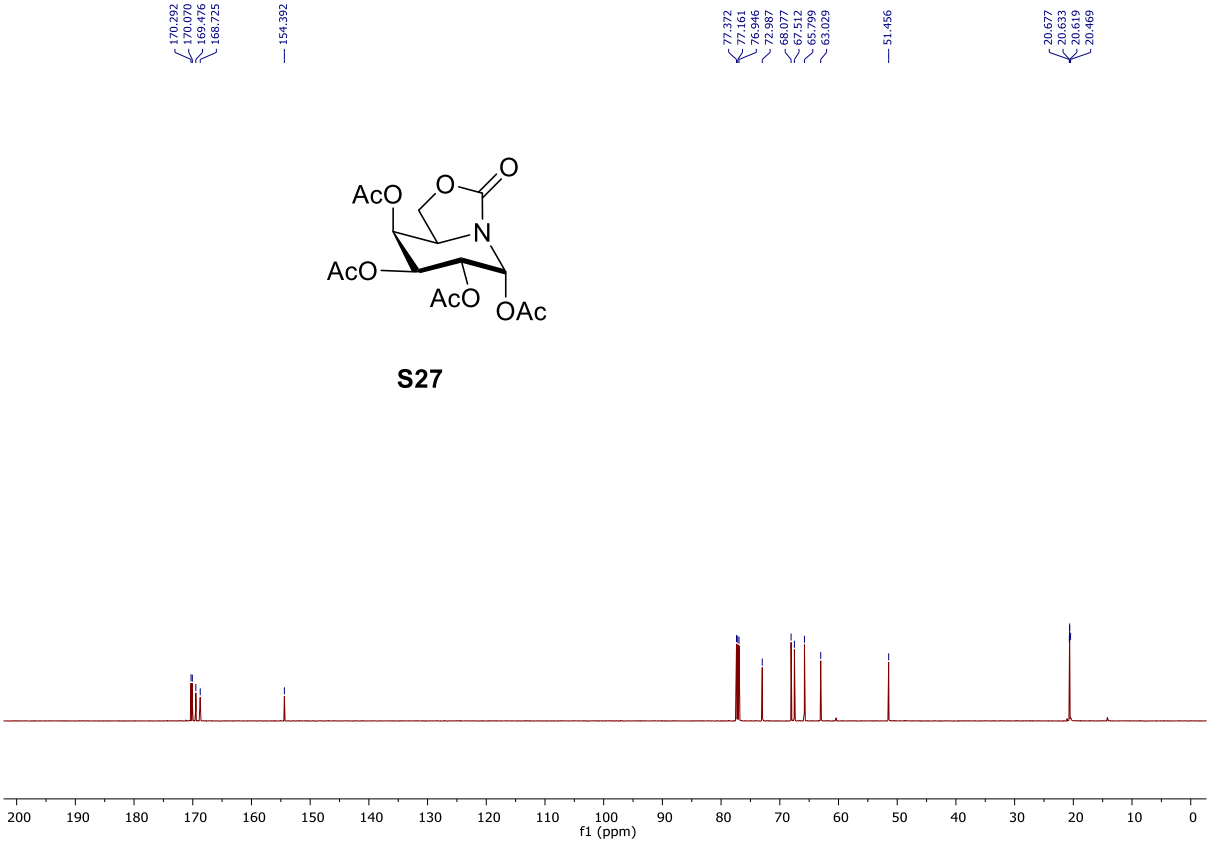

S27

Figure 8.91. ^{13}C NMR spectra for S27

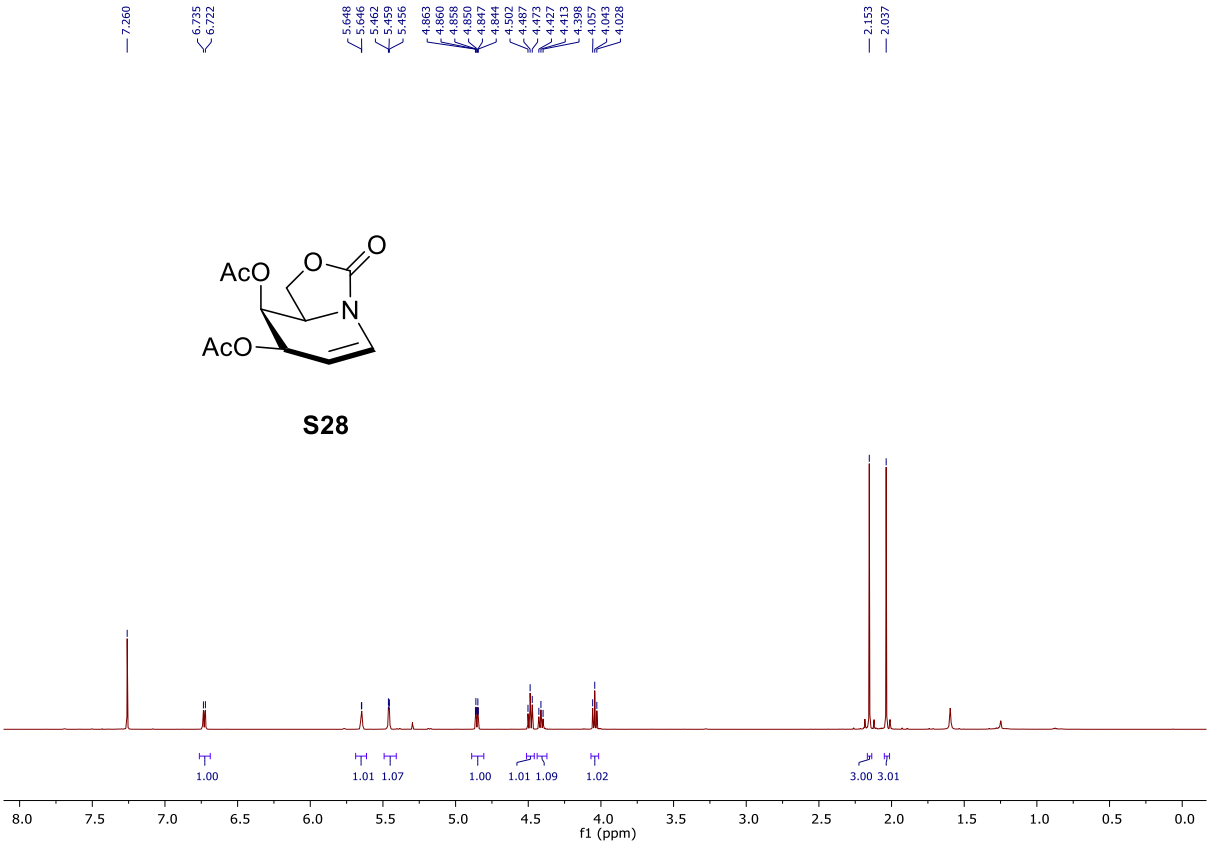

S28

Figure 8.92. ^{1}H NMR spectra for S28

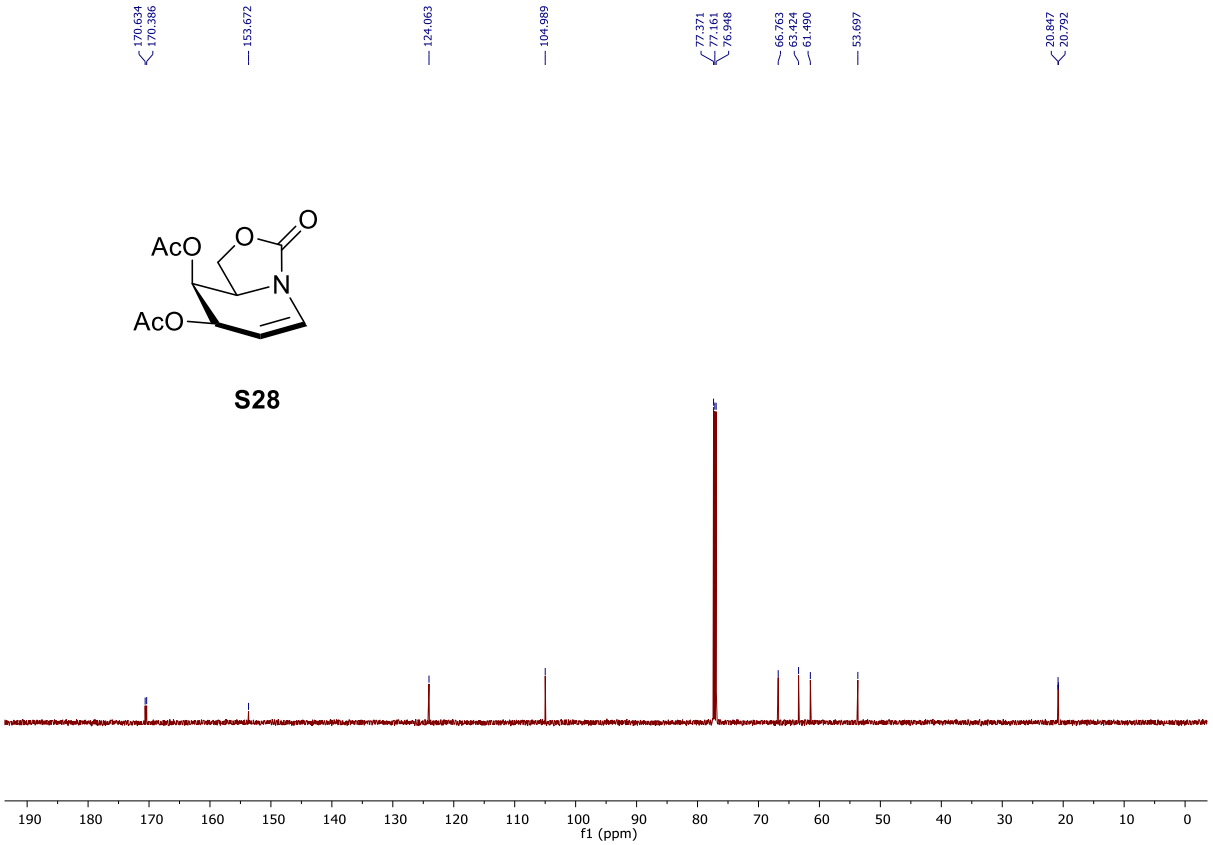

Figure 8.93. ^{13}C NMR spectra for S28

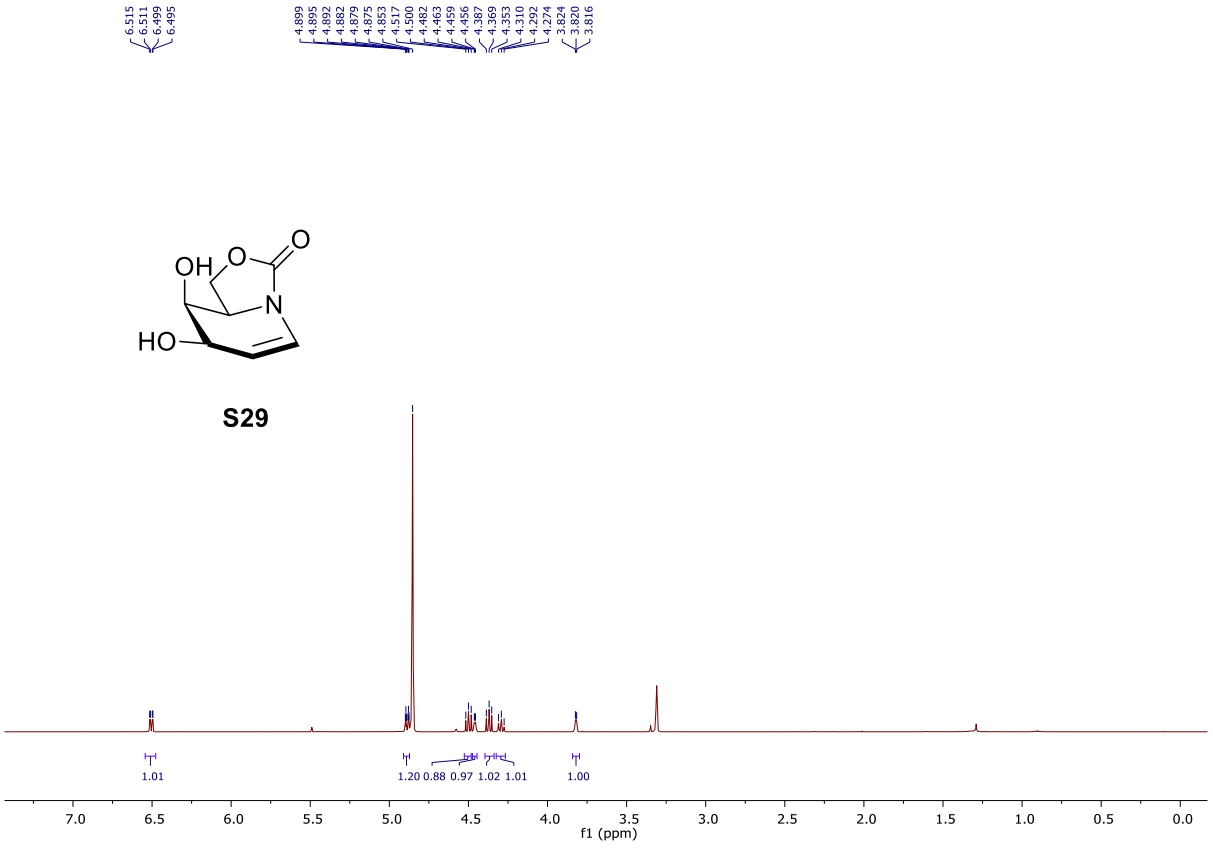

Figure 8.94. ^{1}H NMR spectra for S29

NMR spectra

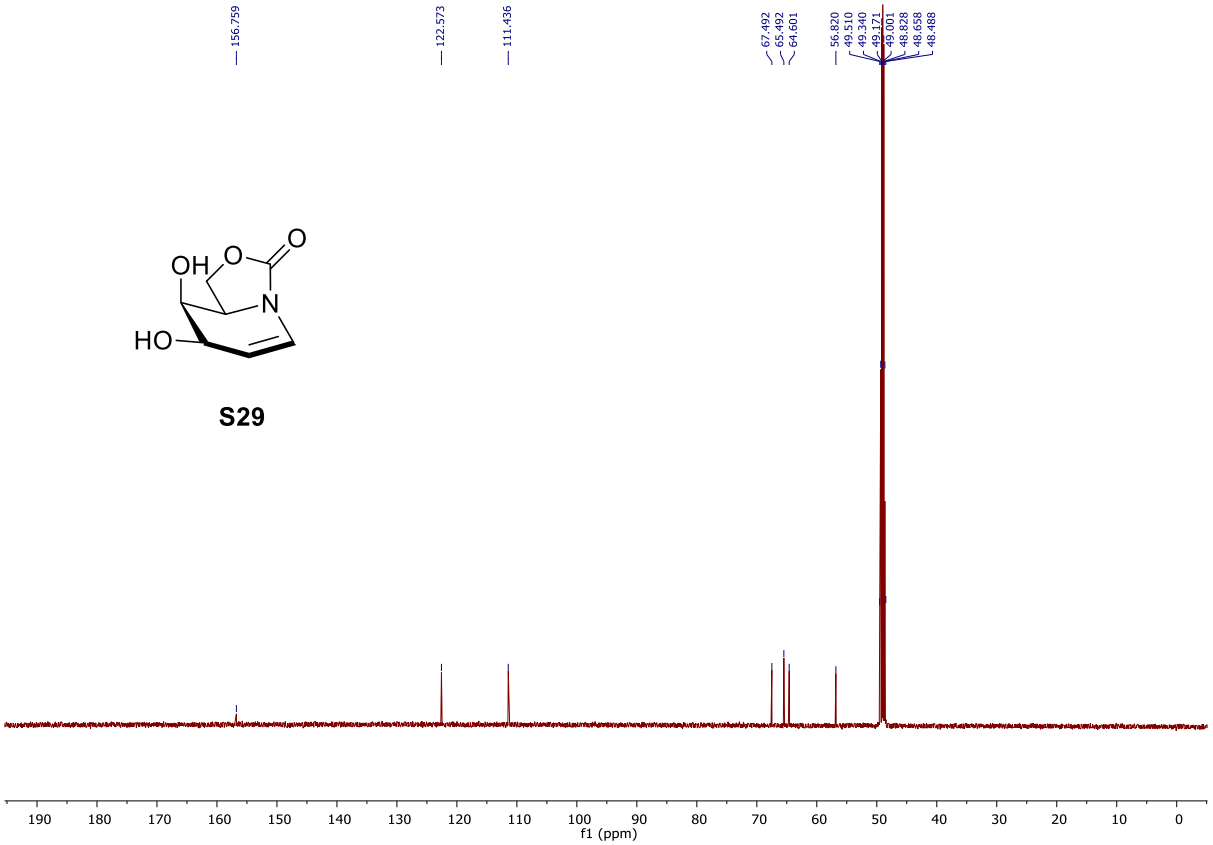

Figure 8.95. ^{13}C NMR spectra for S29

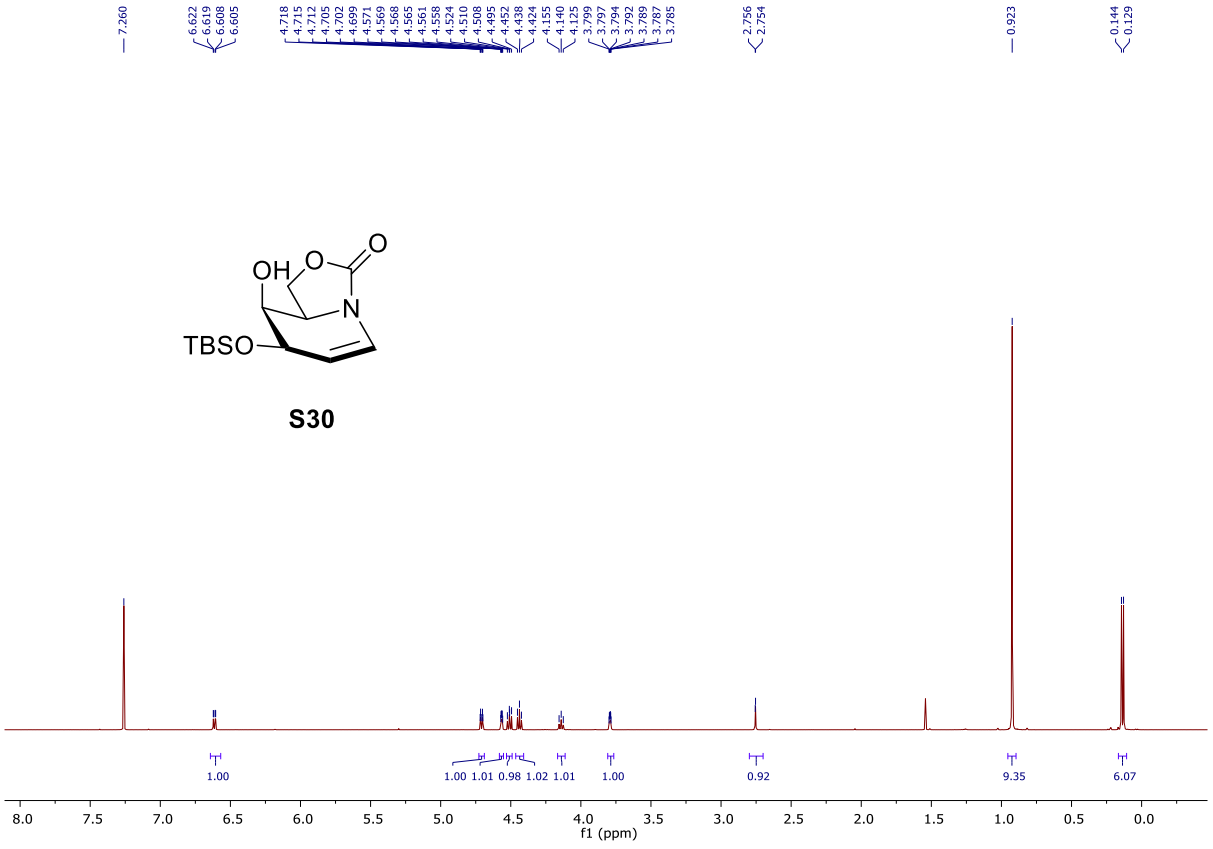

Figure 8.96. ^{1}H NMR spectra for S30

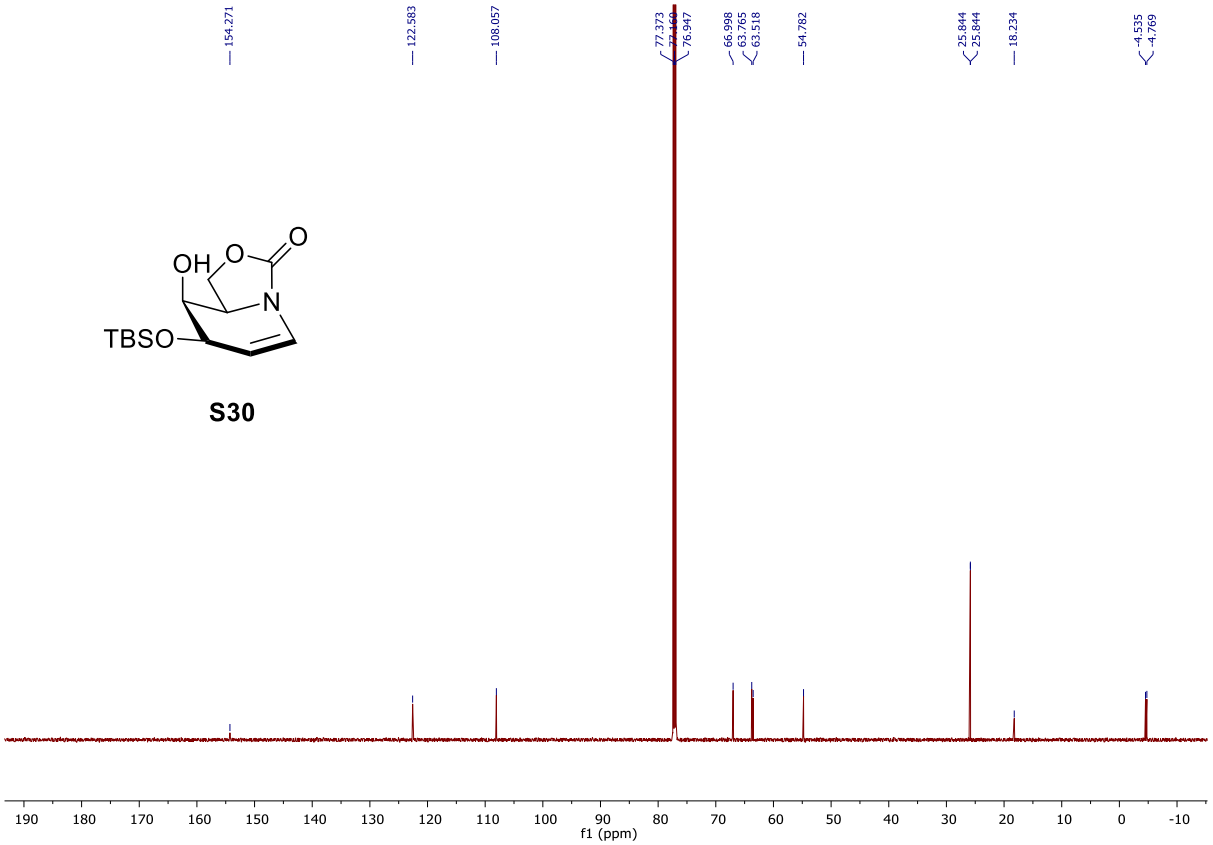

Figure 8.97. ^{13}C NMR spectra for S30

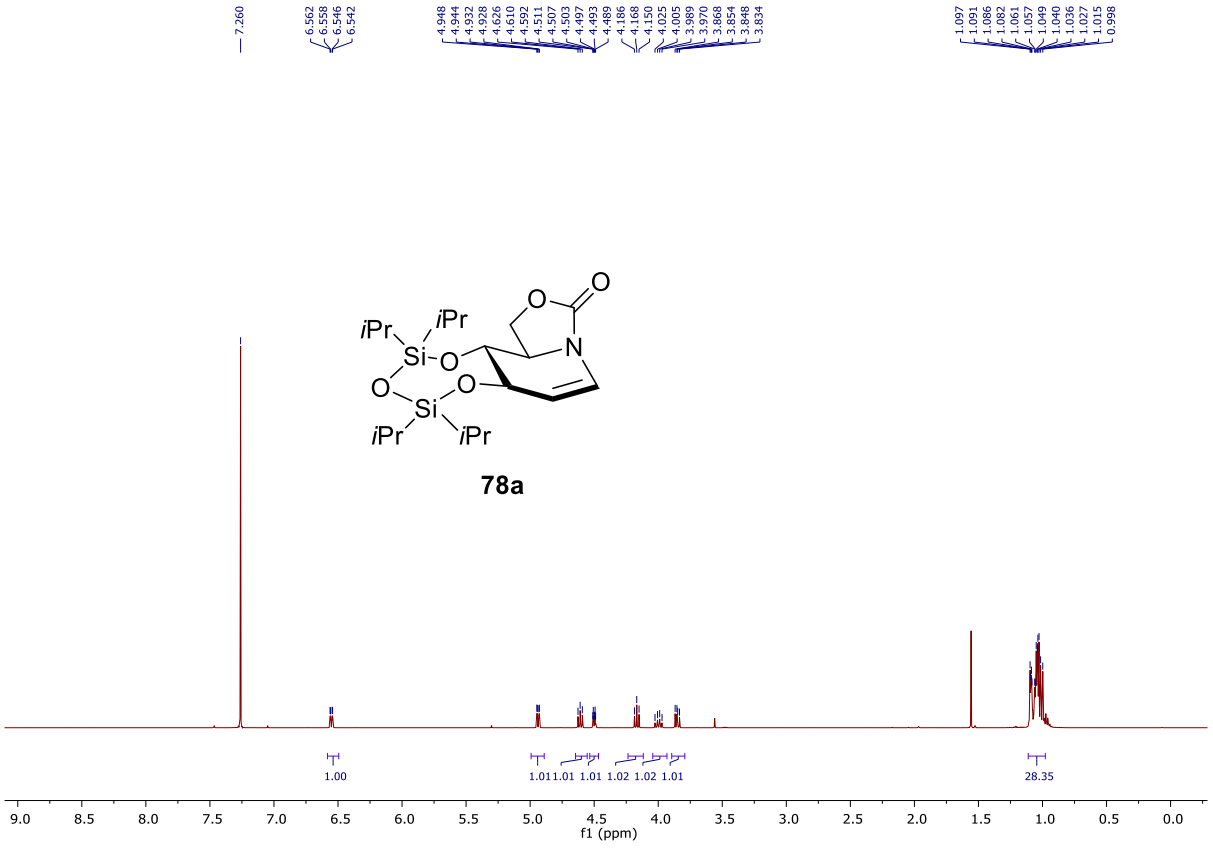

Figure 8.98. ^{1}H NMR spectra for 78a

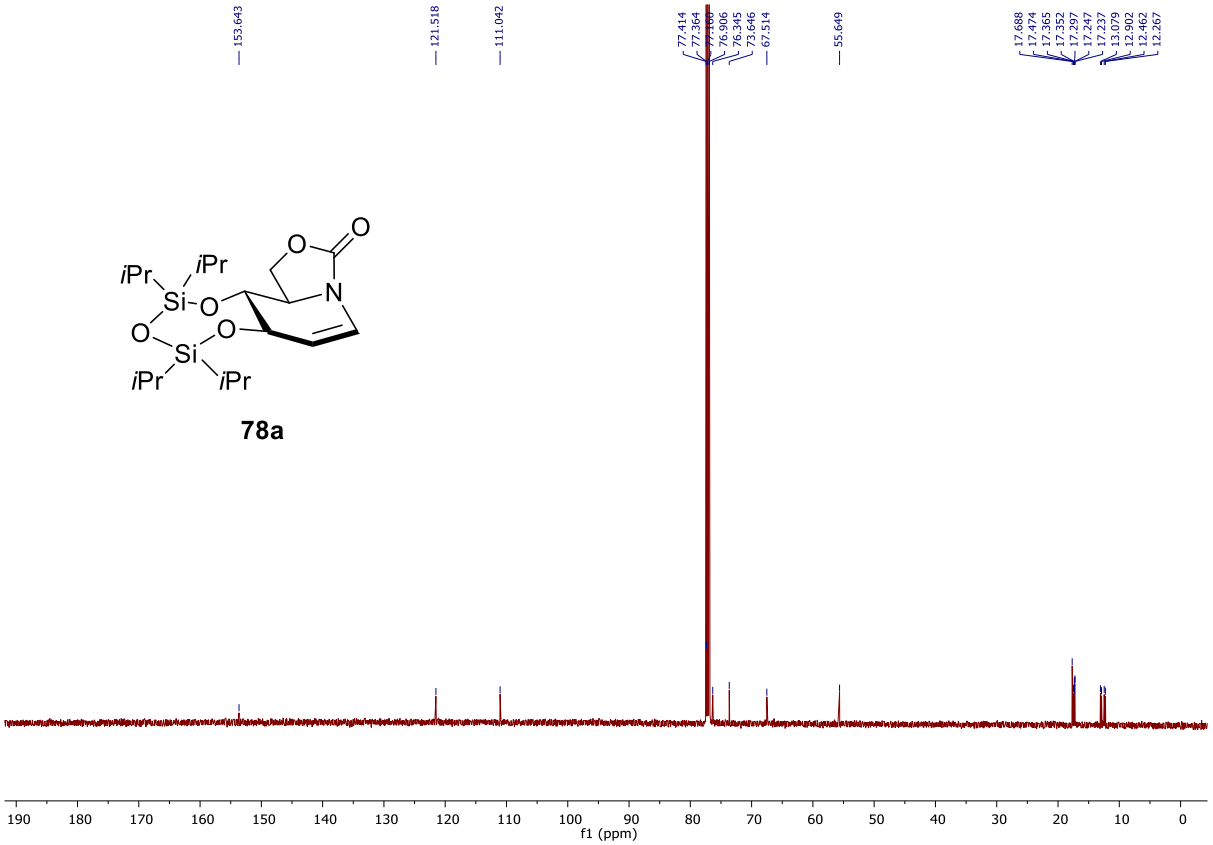

Figure 8.99. ^{13}C NMR spectra for 78a

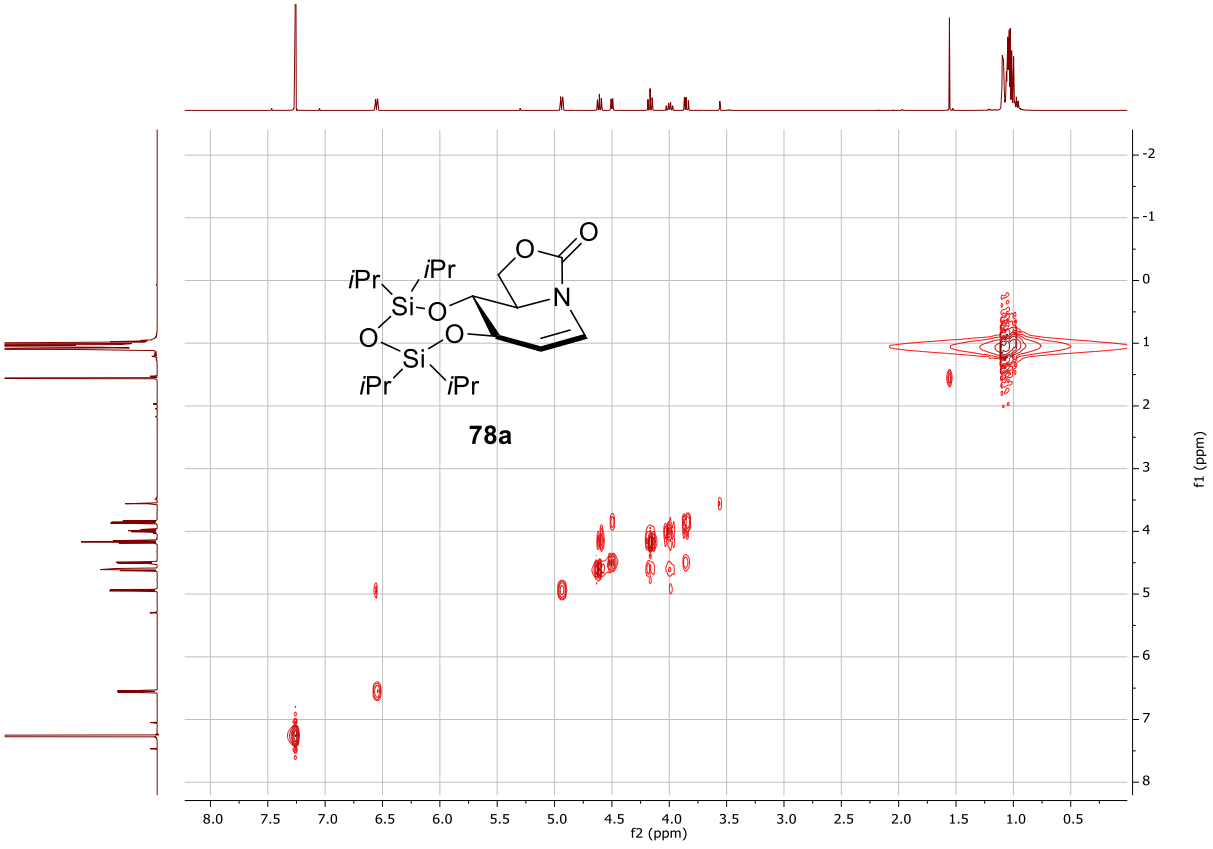

Figure 8.100. COSY spectra for 78a

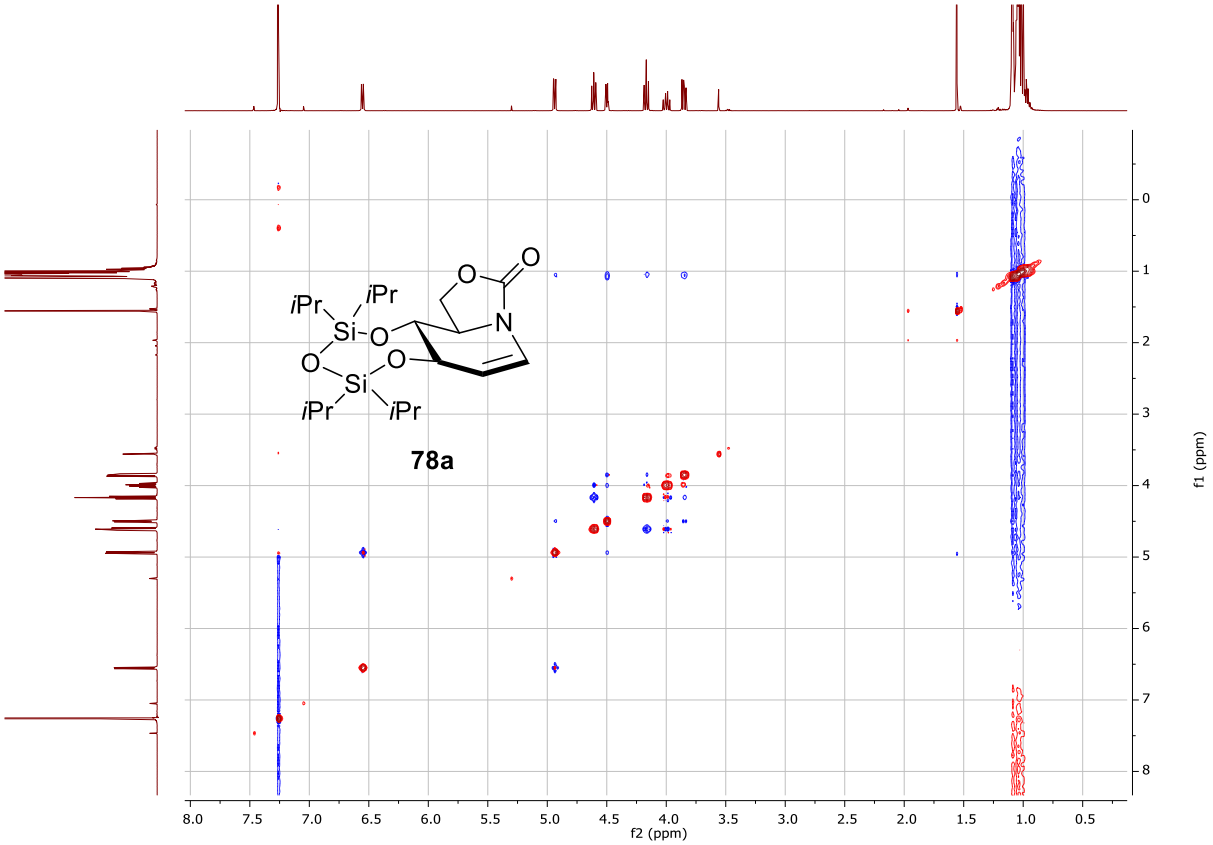

Figure 8.101. NOESY spectra for 78a

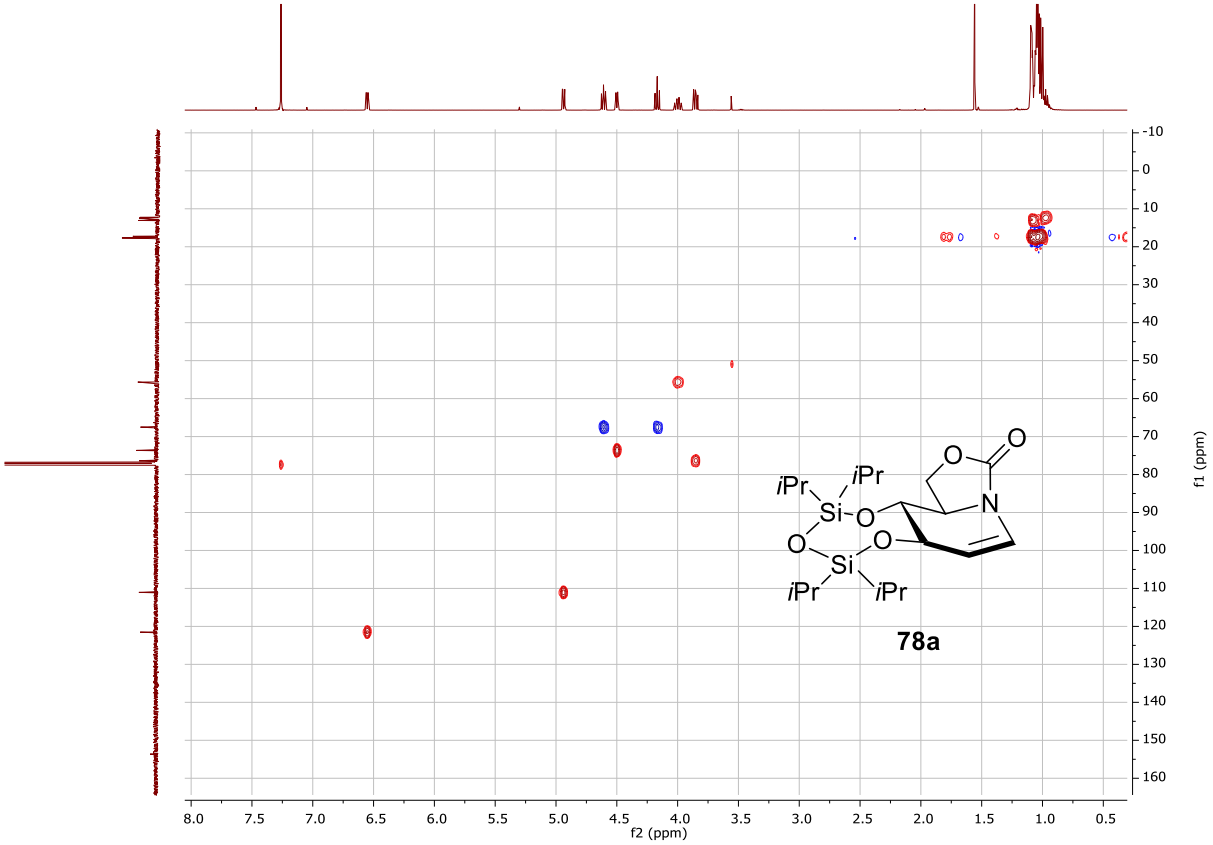

Figure 8.102. HSQC spectra for 78a

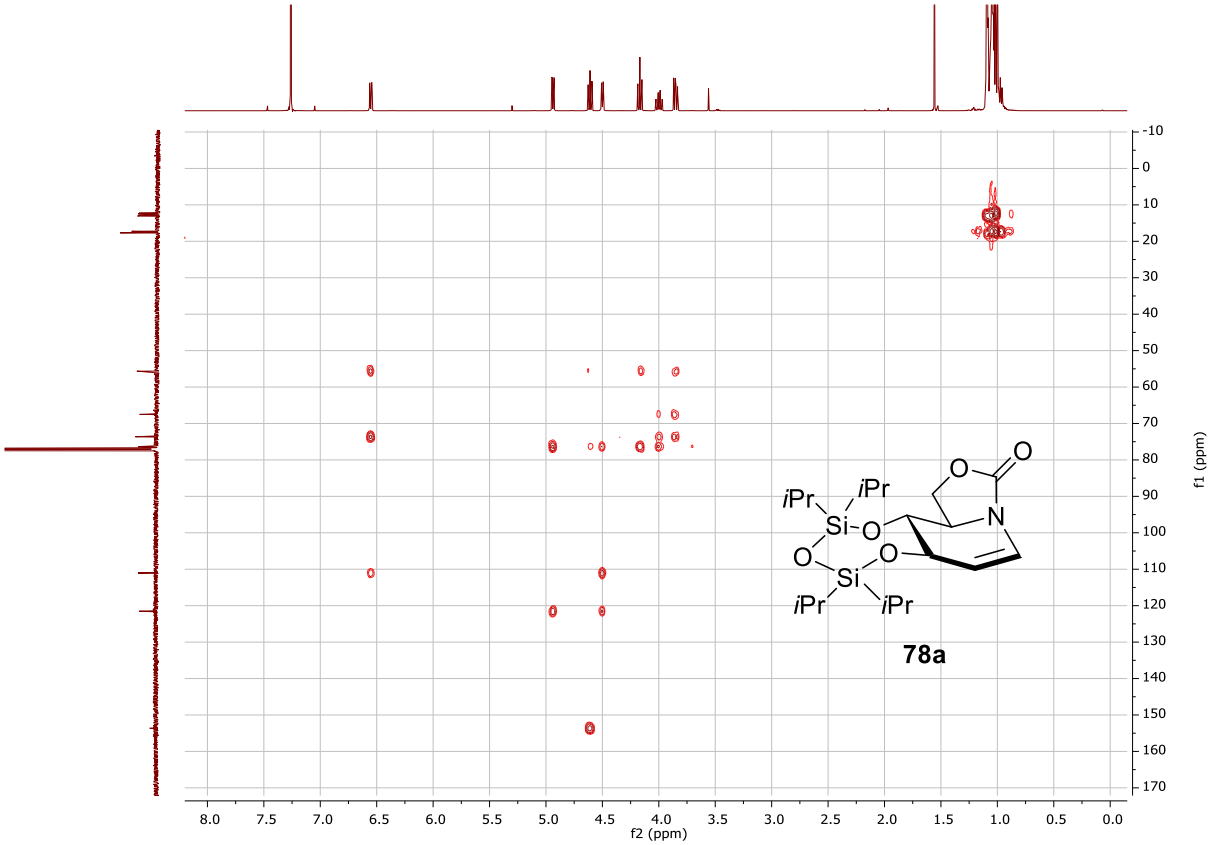

Figure 8.103. HMBC spectra for 78a

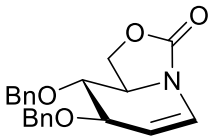

78b

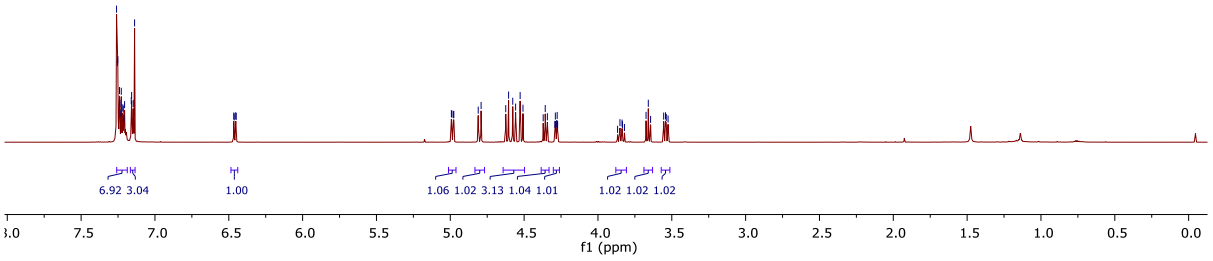

Figure 8.104. ^{1}H NMR spectra for 78b

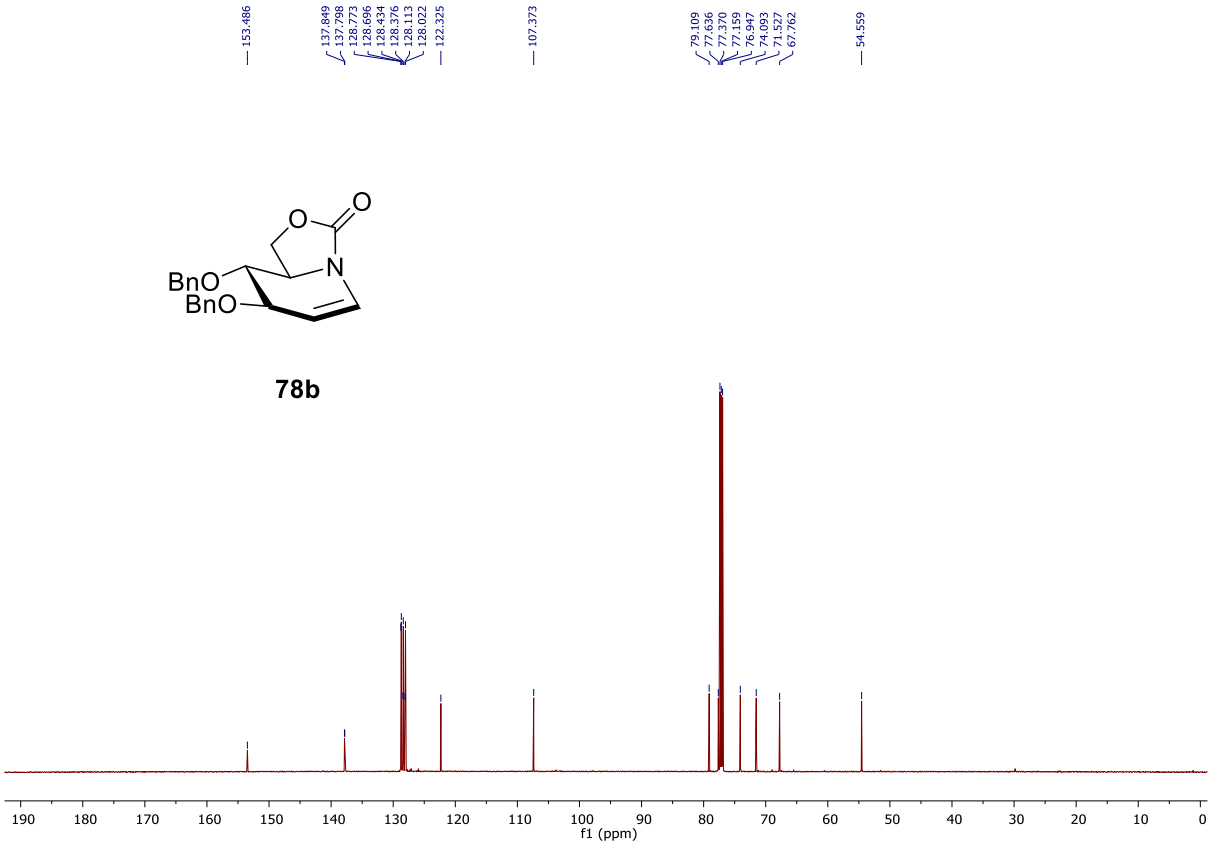

Figure 8.105. ^{13}C NMR spectra for 78b

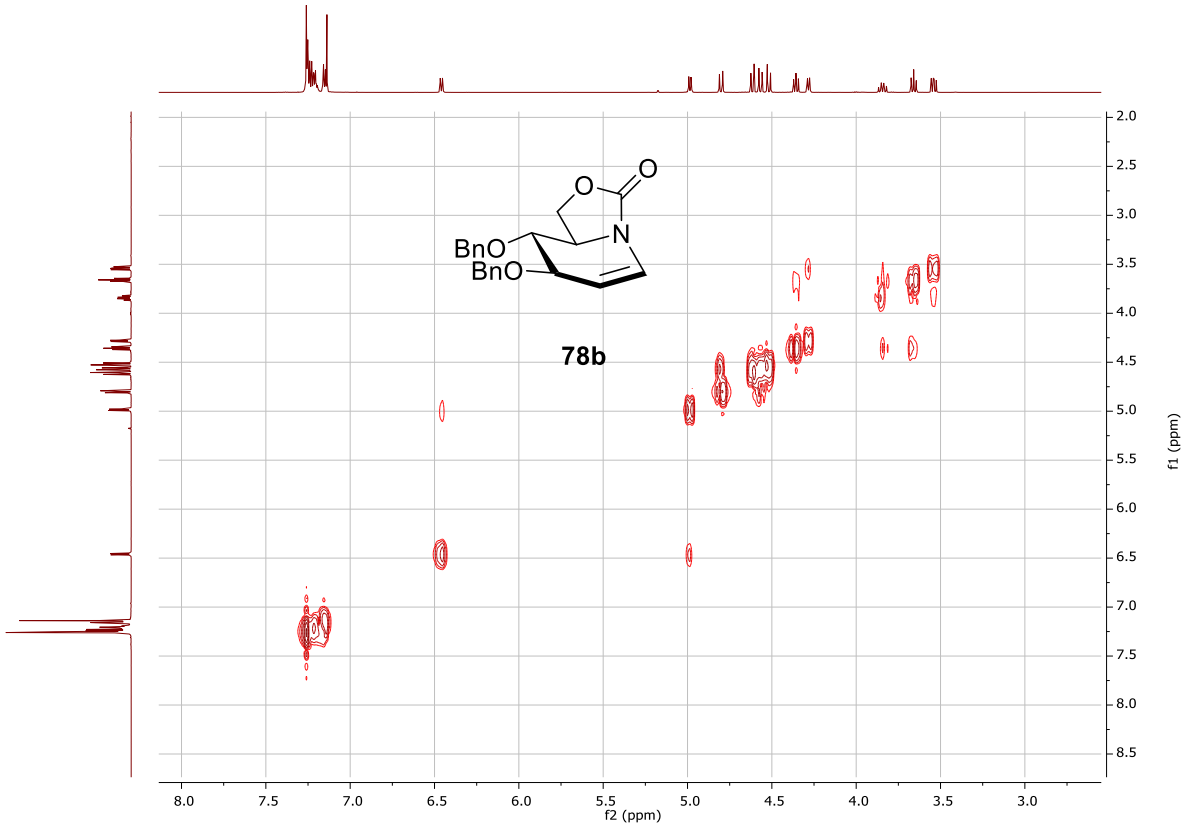

Figure 8.106. COSY spectra for 78b

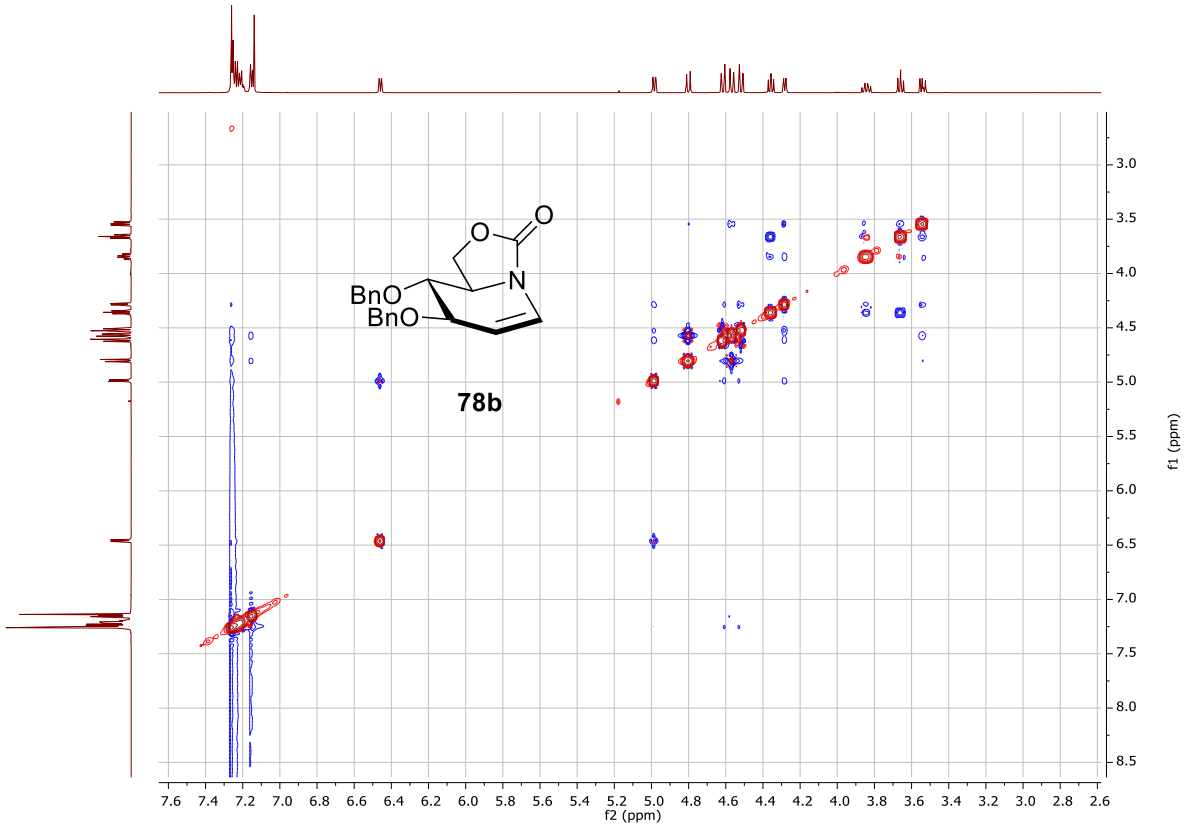

Figure 8.107. NOESY spectra for 78b

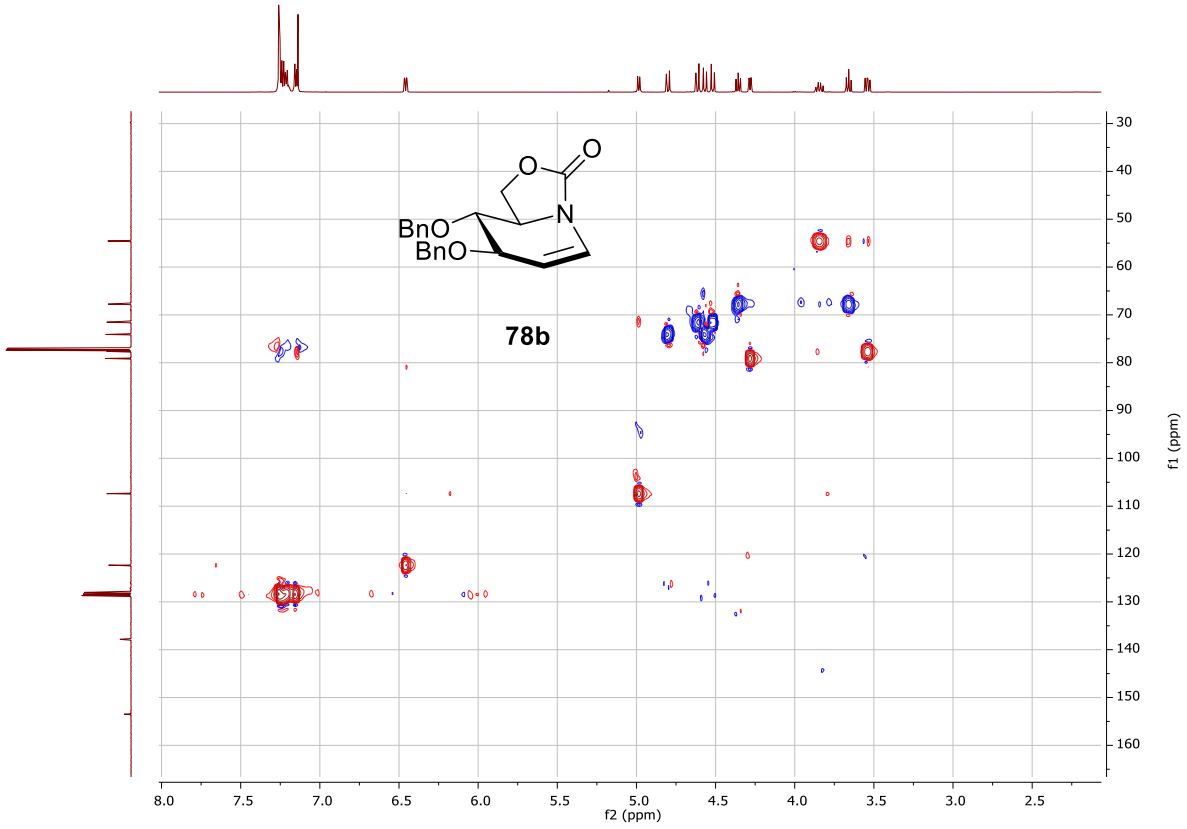

Figure 8.108. HSQC spectra for 78b

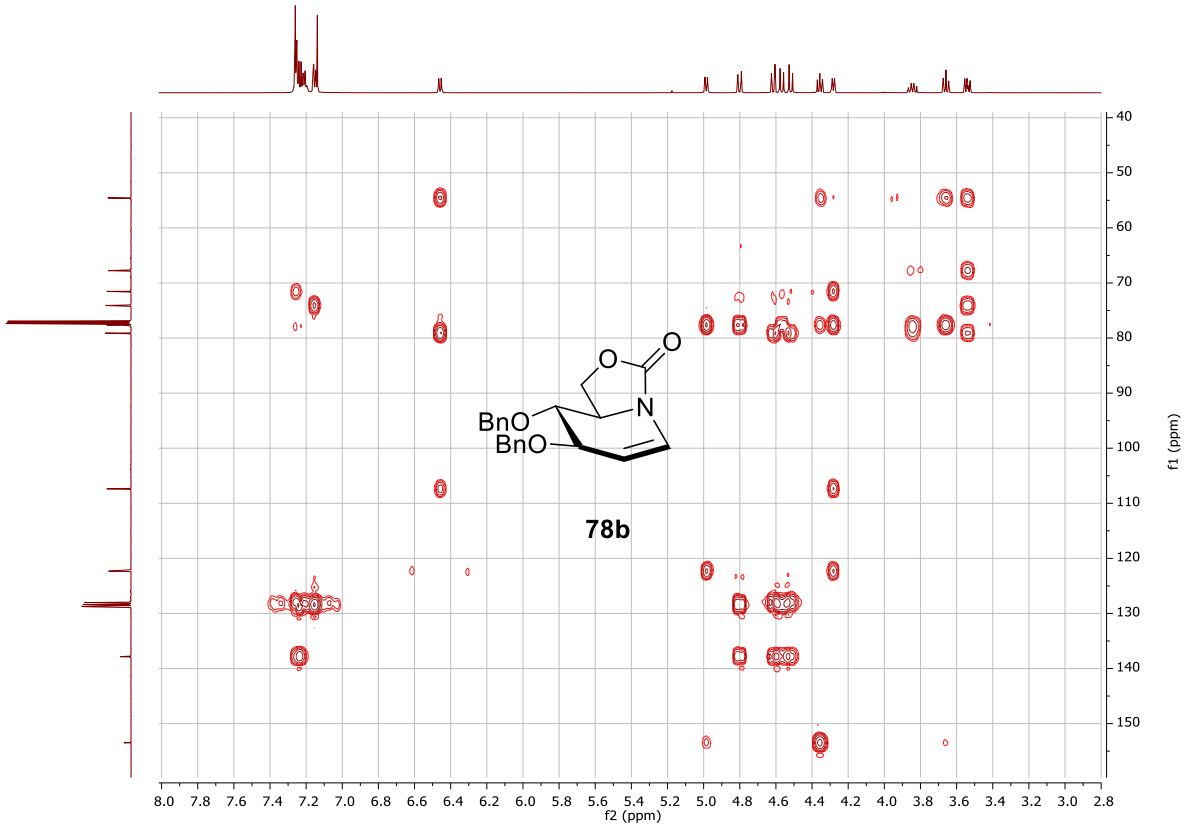

Figure 8.109. HMBC spectra for 78b

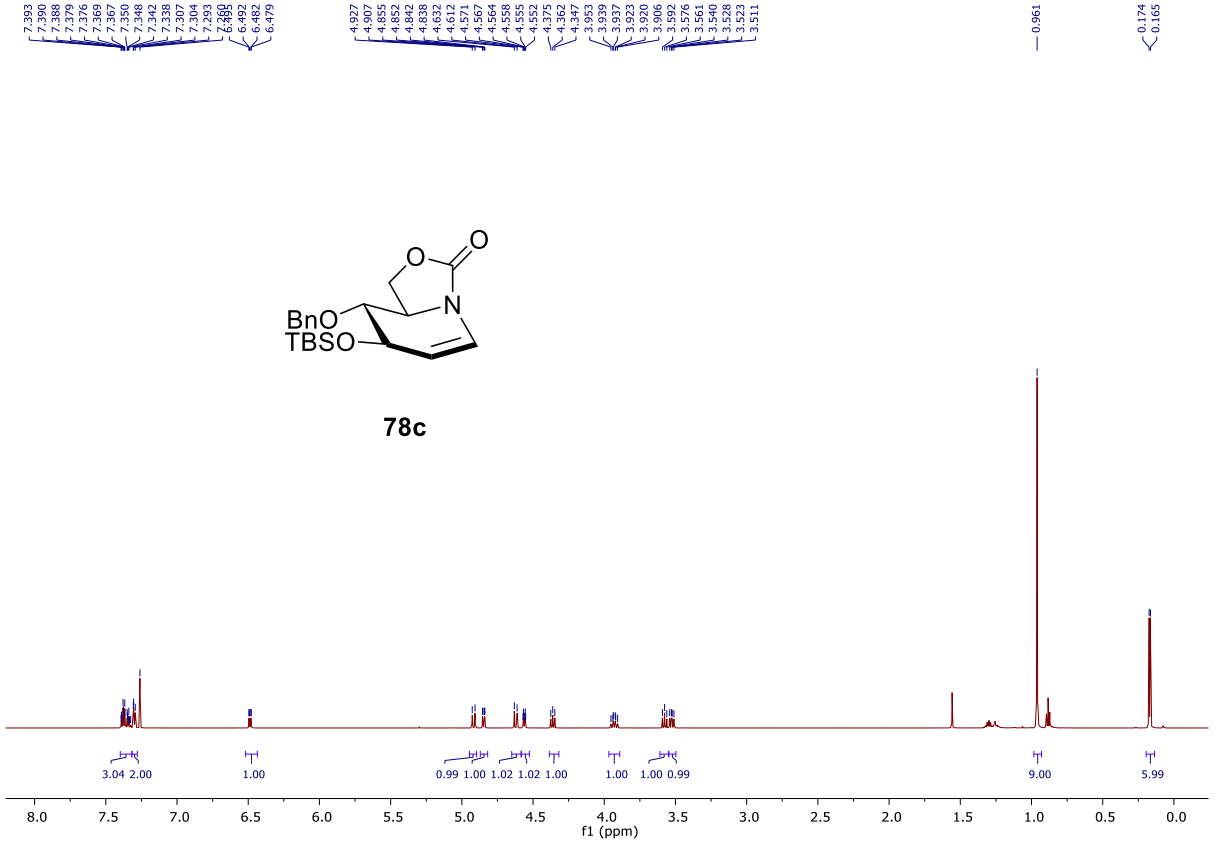

Figure 8.110. ^{1}H NMR spectra for 78c

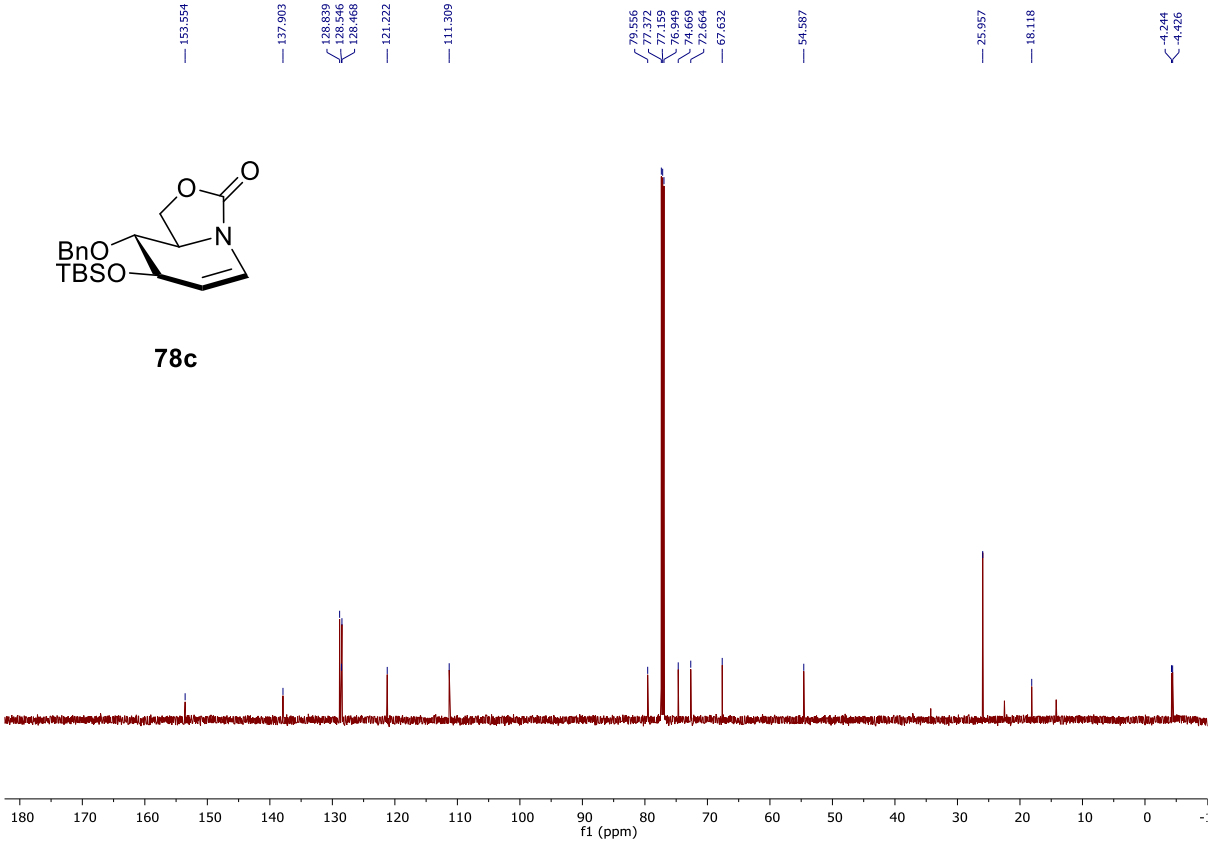

Figure 8.111. ^{13}C NMR spectra for 78c

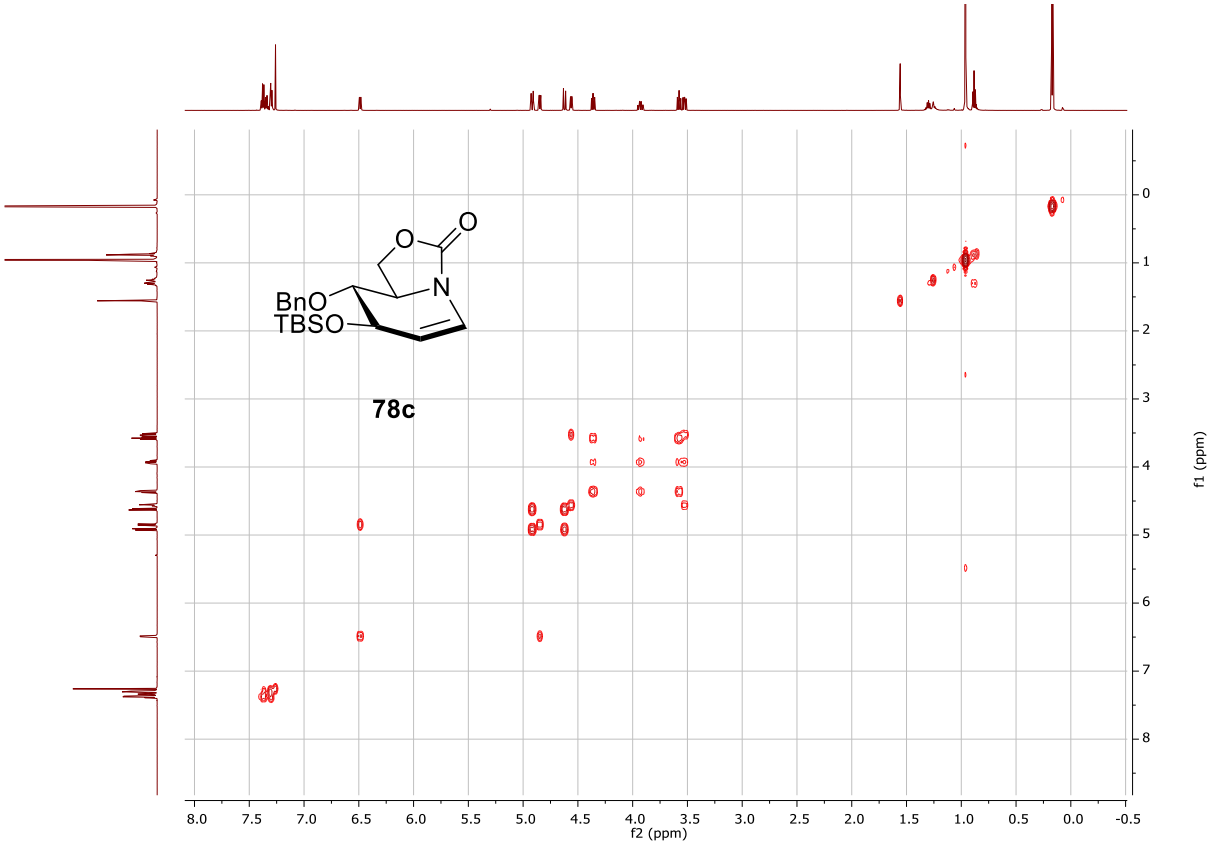

Figure 8.112. COSY spectra for 78c

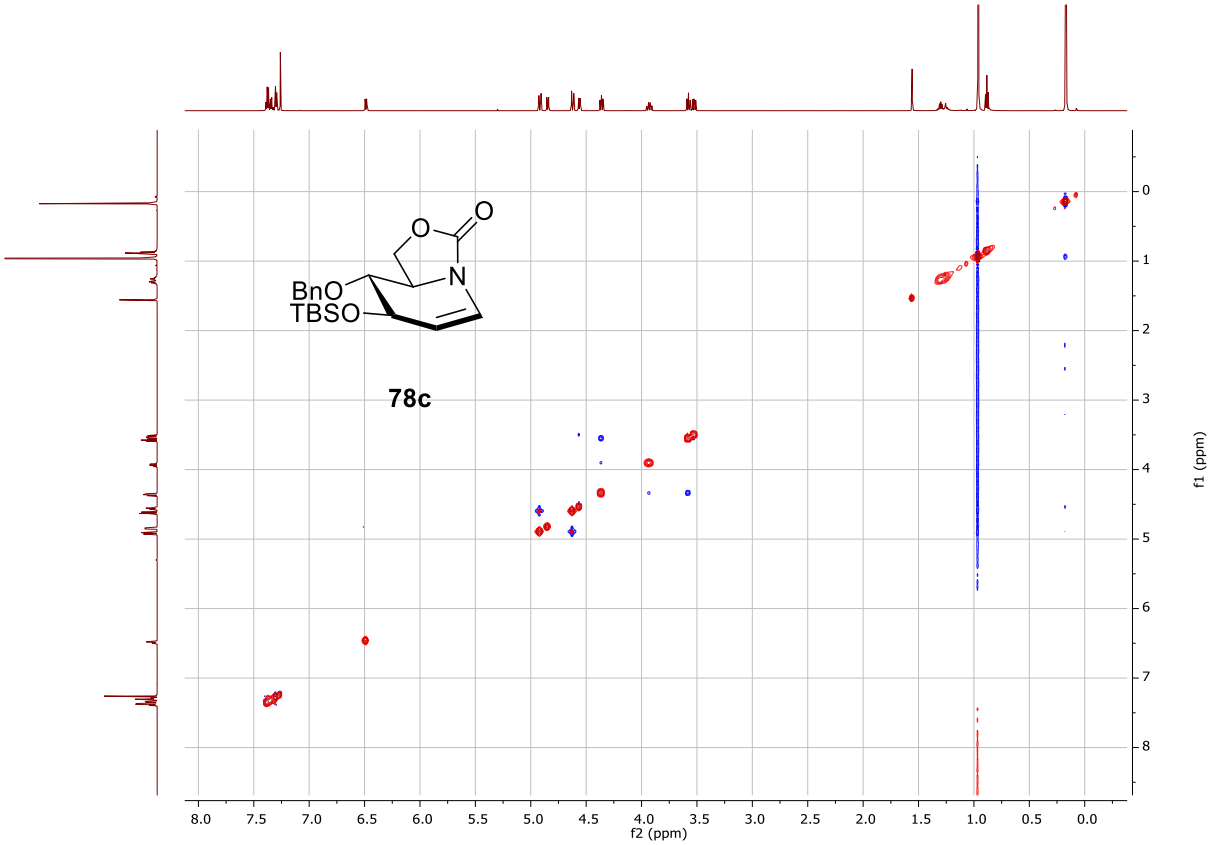

Figure 8.113. NOESY spectra for 78c

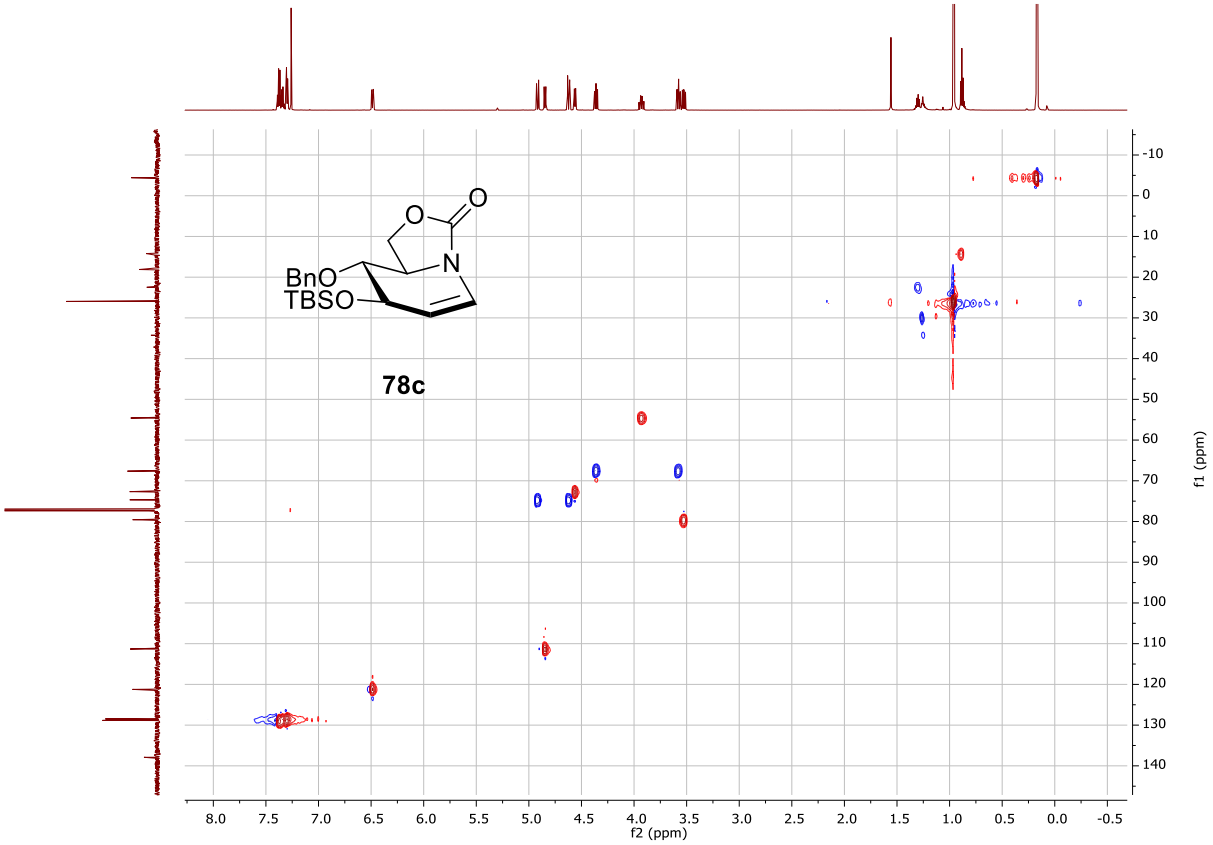

Figure 8.114. HSQC spectra for 78c

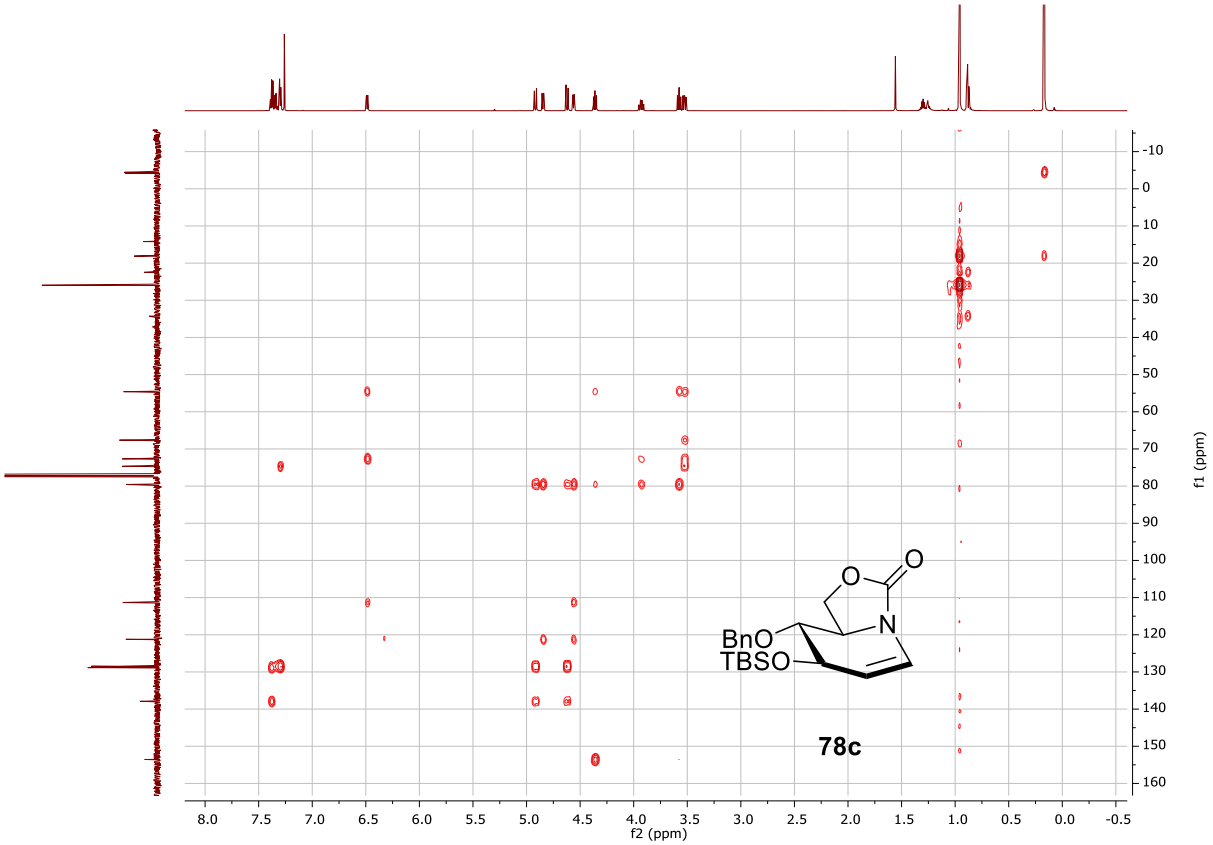

Figure 8.115. HMBC spectra for 78c

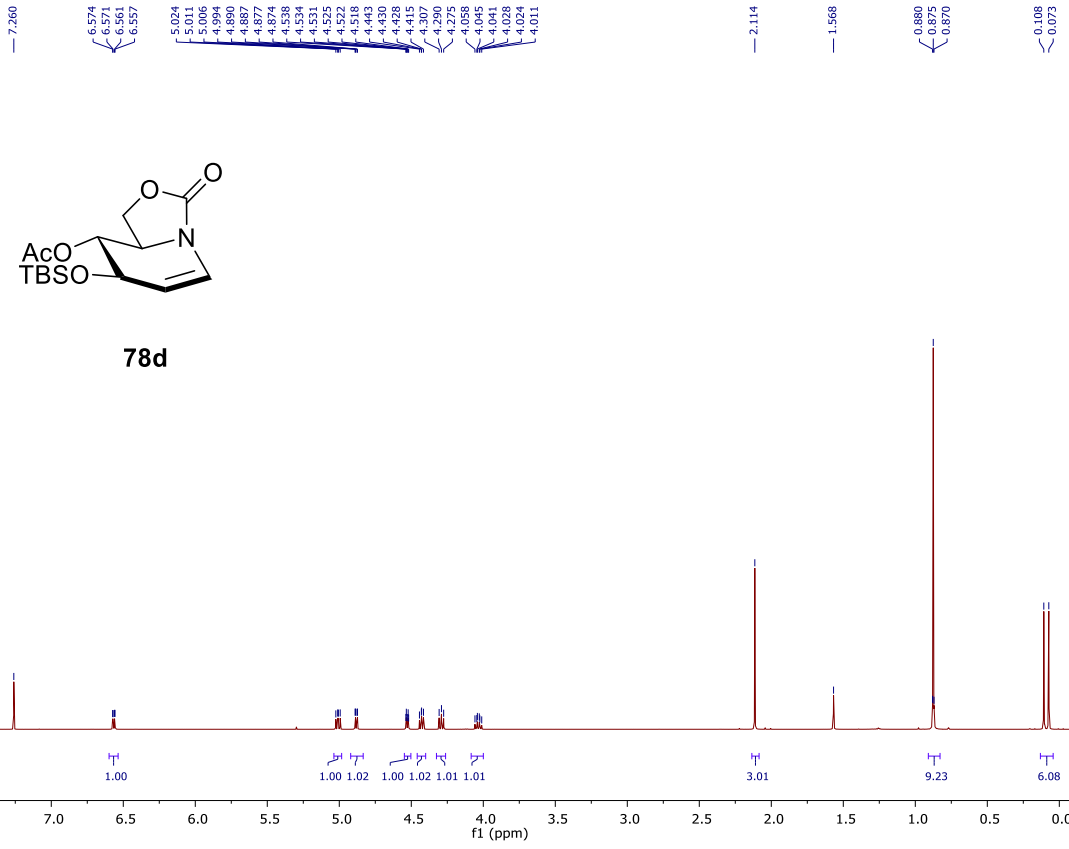

Figure 8.116. ^{1}H NMR spectra for 78d

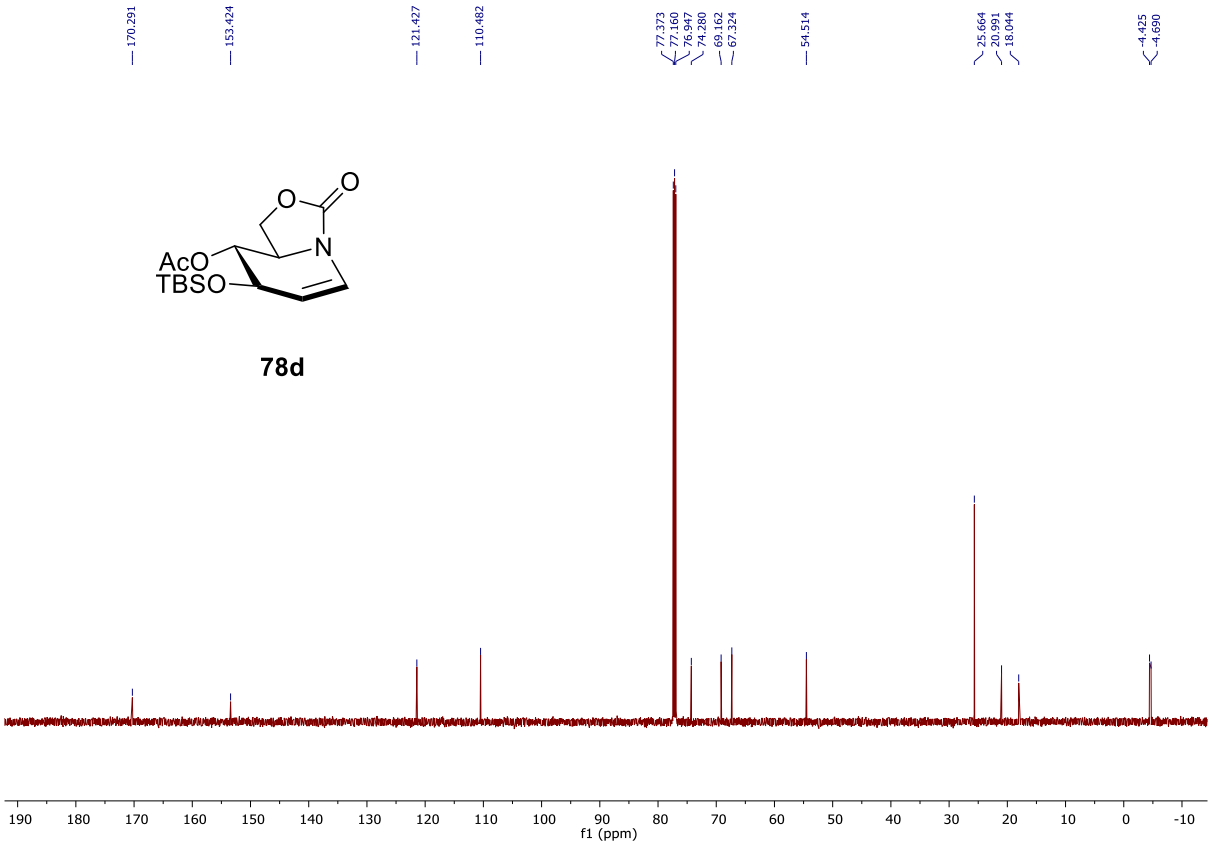

Figure 8.117. ^{13}C NMR spectra for 78d

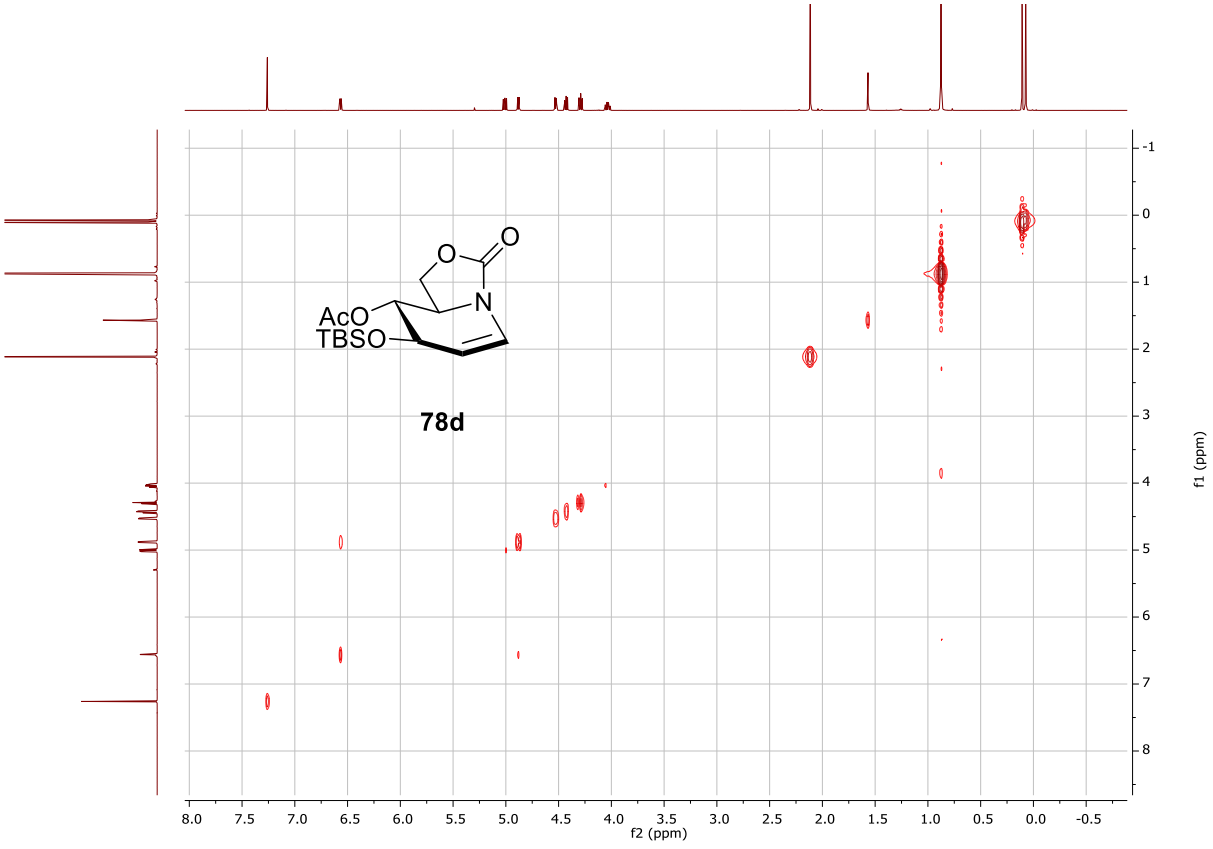

Figure 8.118. COSY spectra for 78d

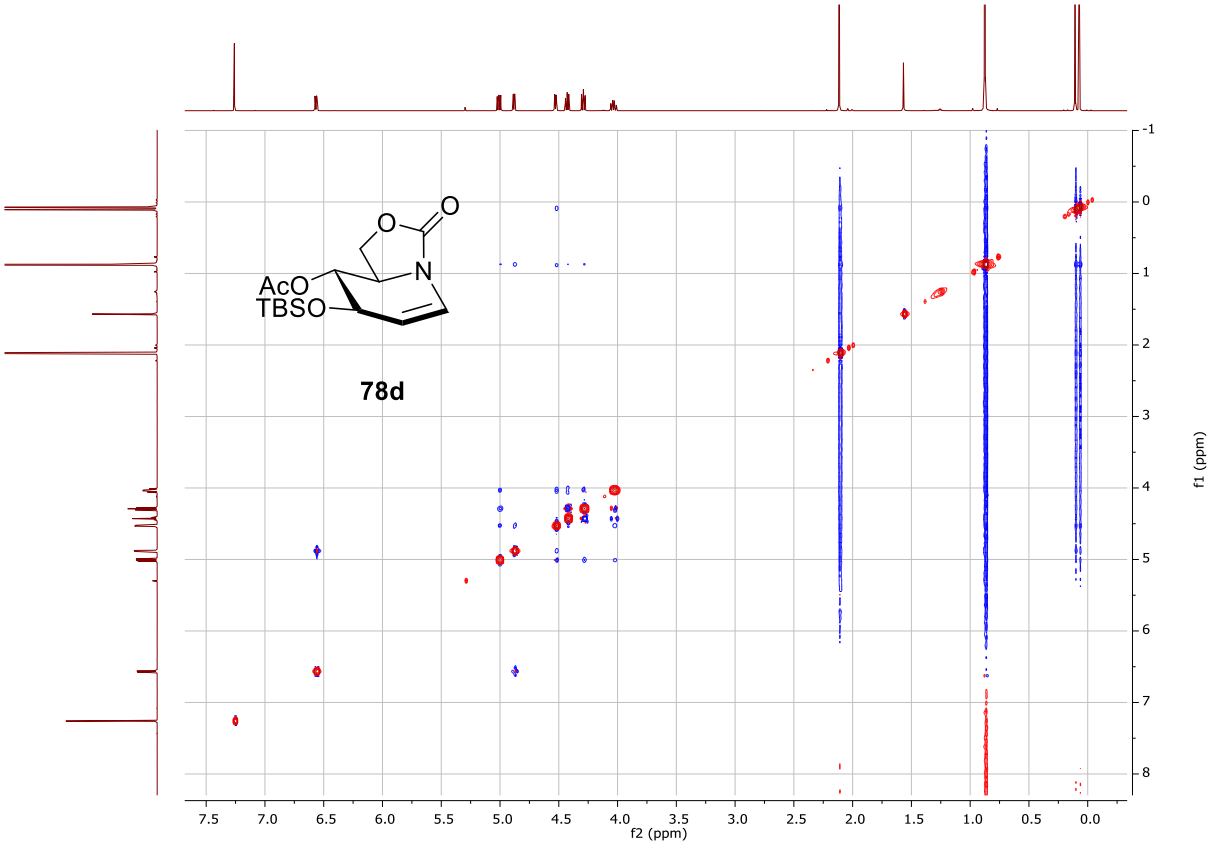

Figure 8.119. NOESY spectra for 78d

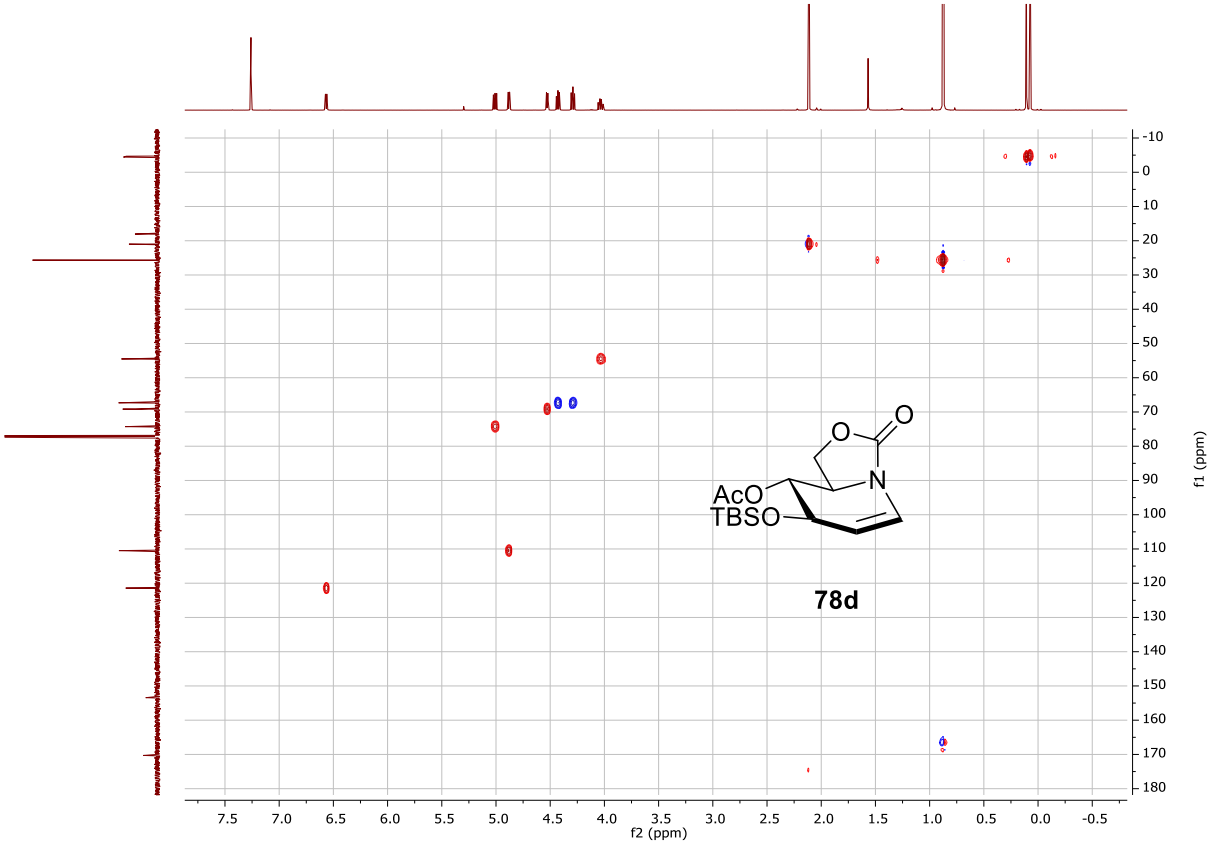

Figure 8.120. HSQC spectra for 78d

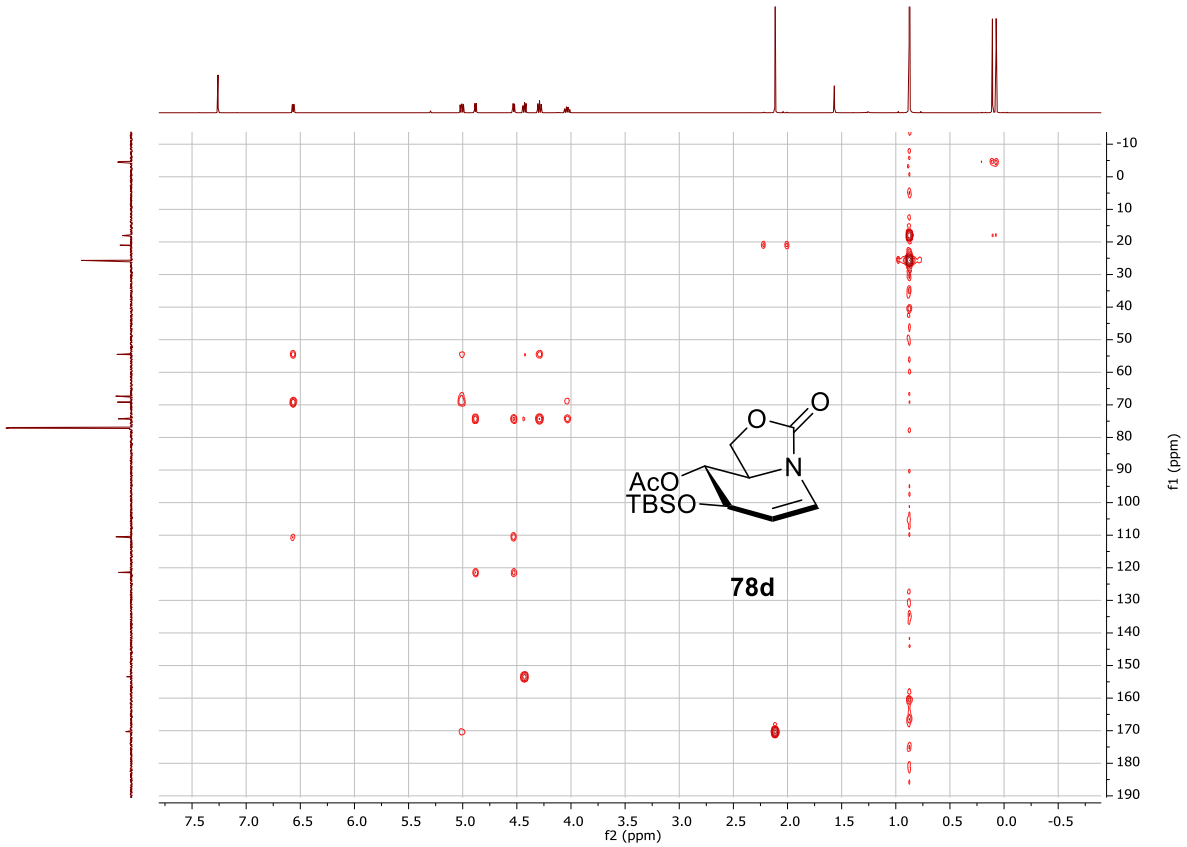

Figure 8.121. HMBC spectra for 78d

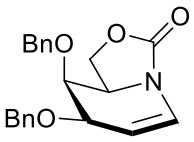

81a

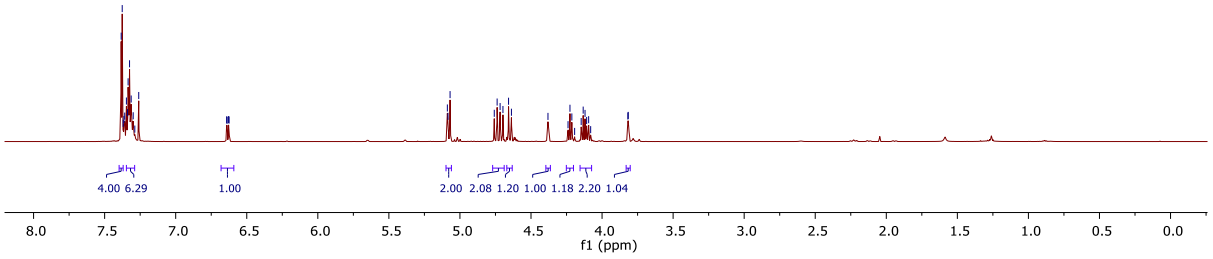

Figure 8.122. ^{1}H NMR spectra for 81a

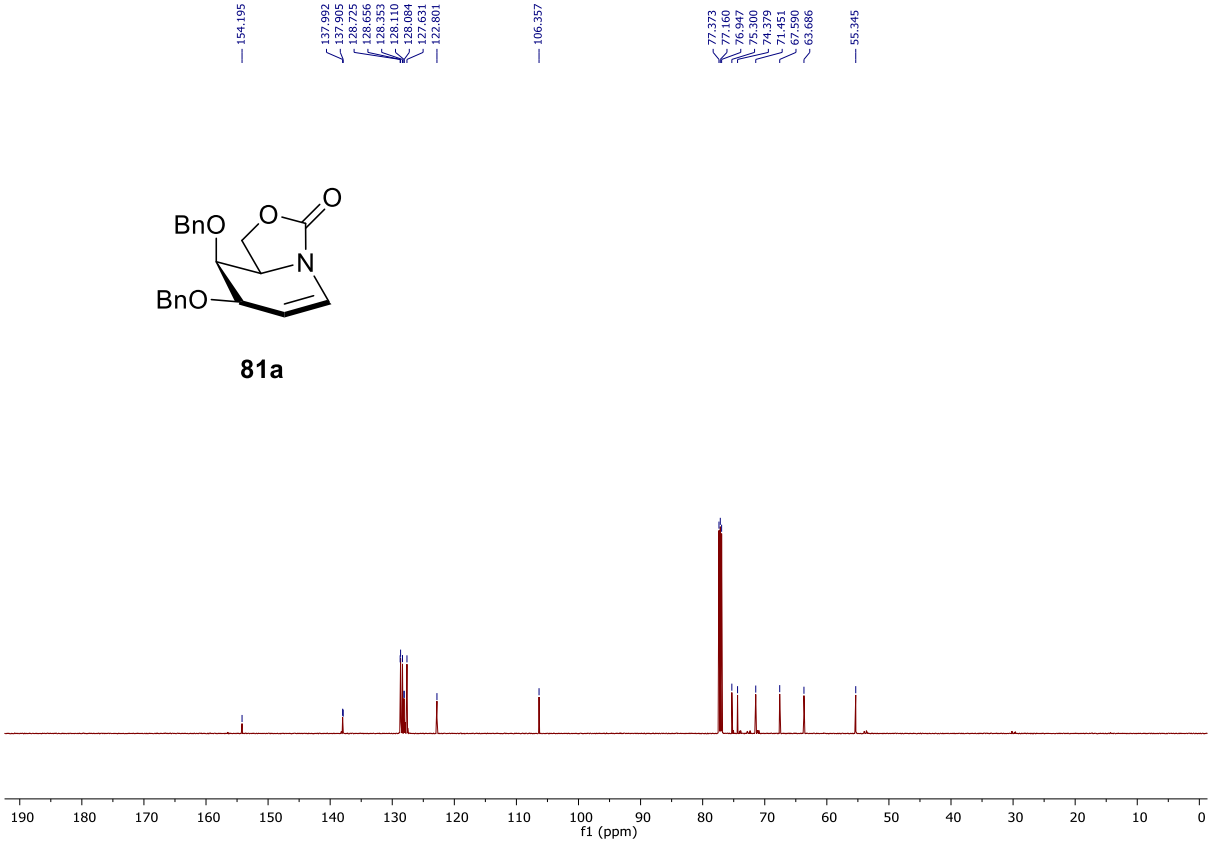

Figure 8.123. ^{13}C NMR spectra for 81a

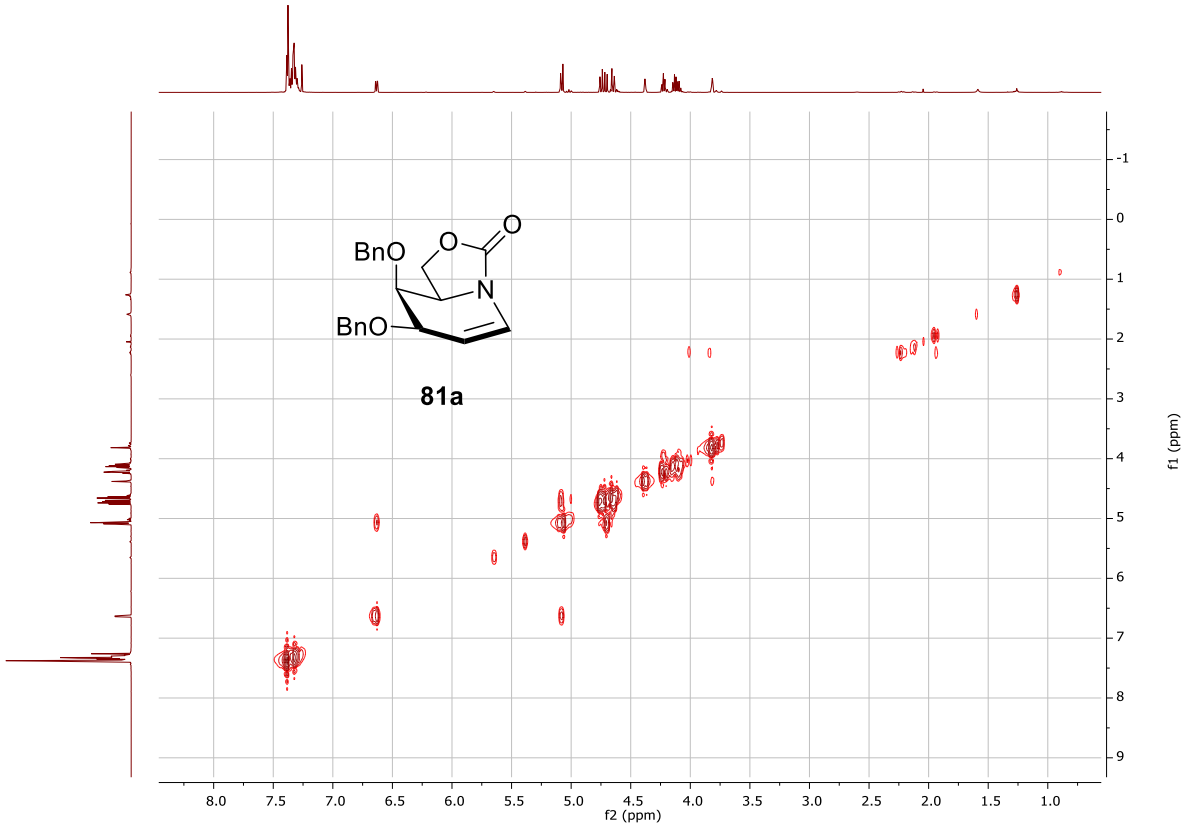

Figure 8.124. COSY spectra for 81a

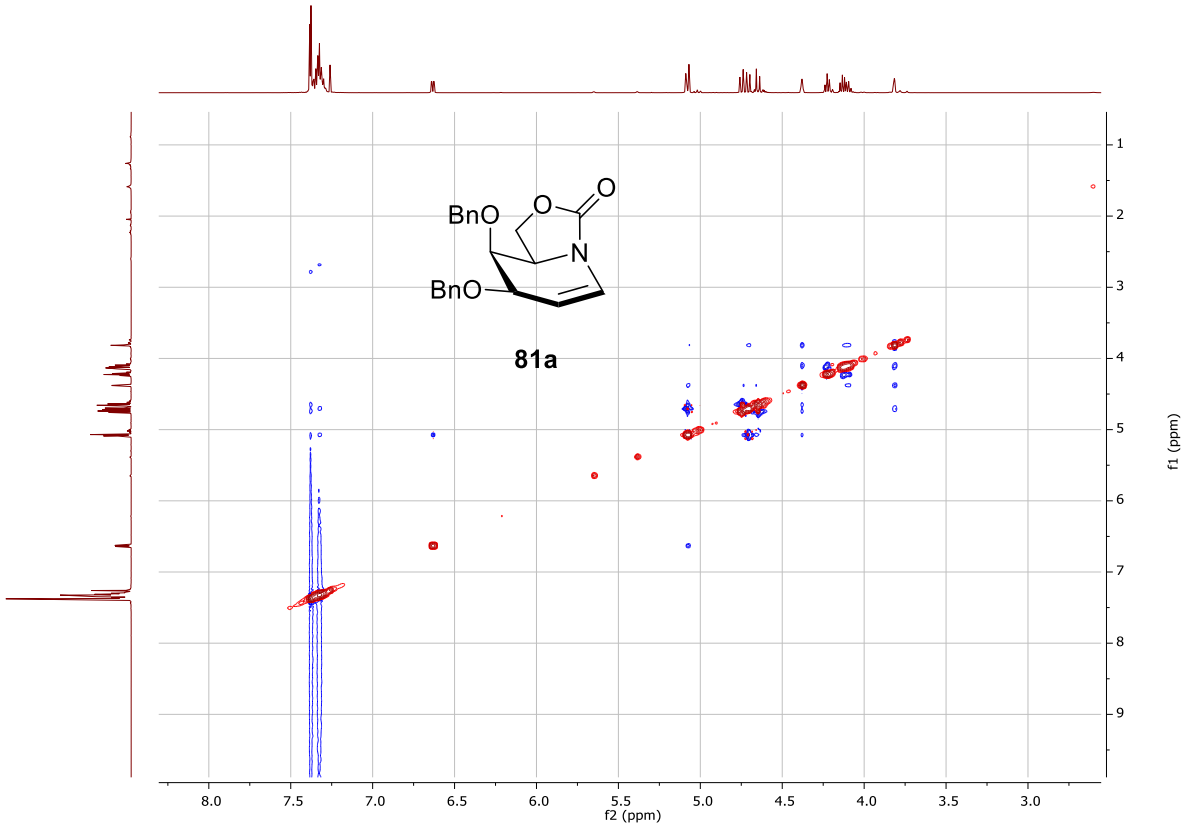

Figure 8.125. NOESY spectra for 81a

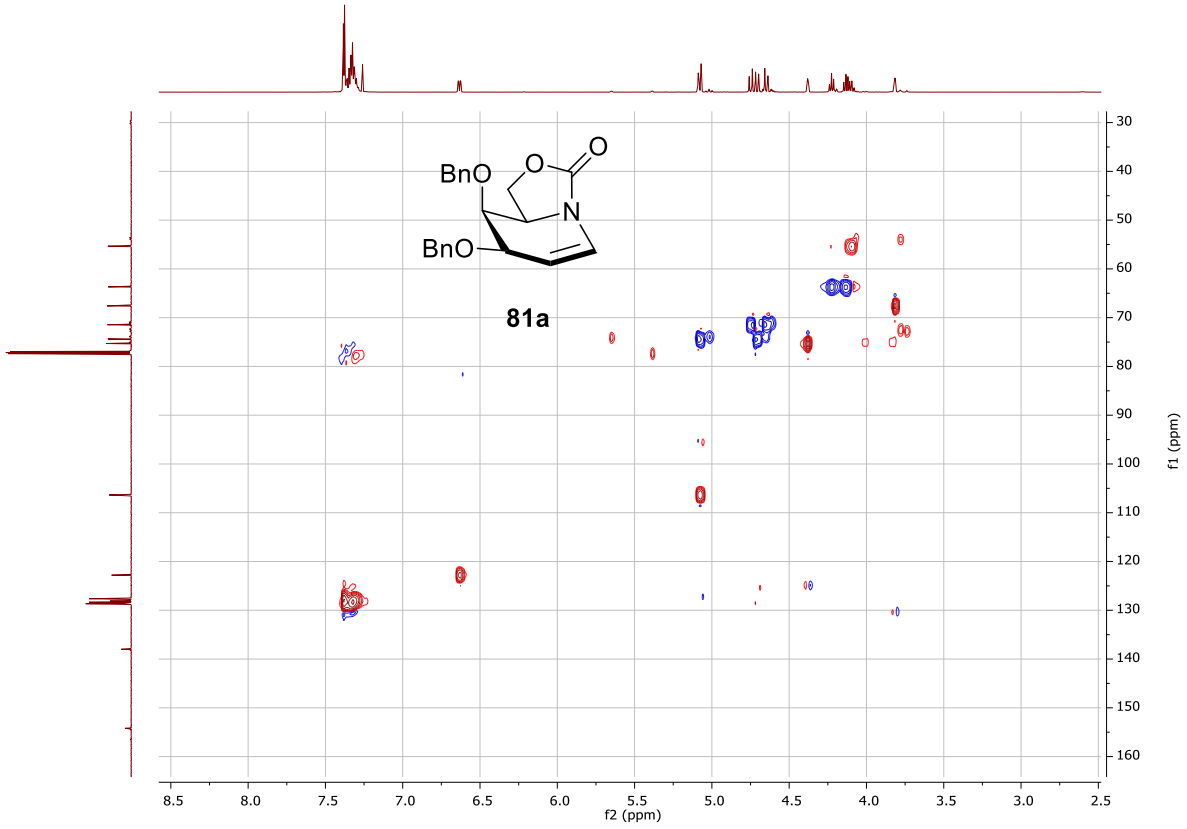

Figure 8.126. HSQC spectra for 81a

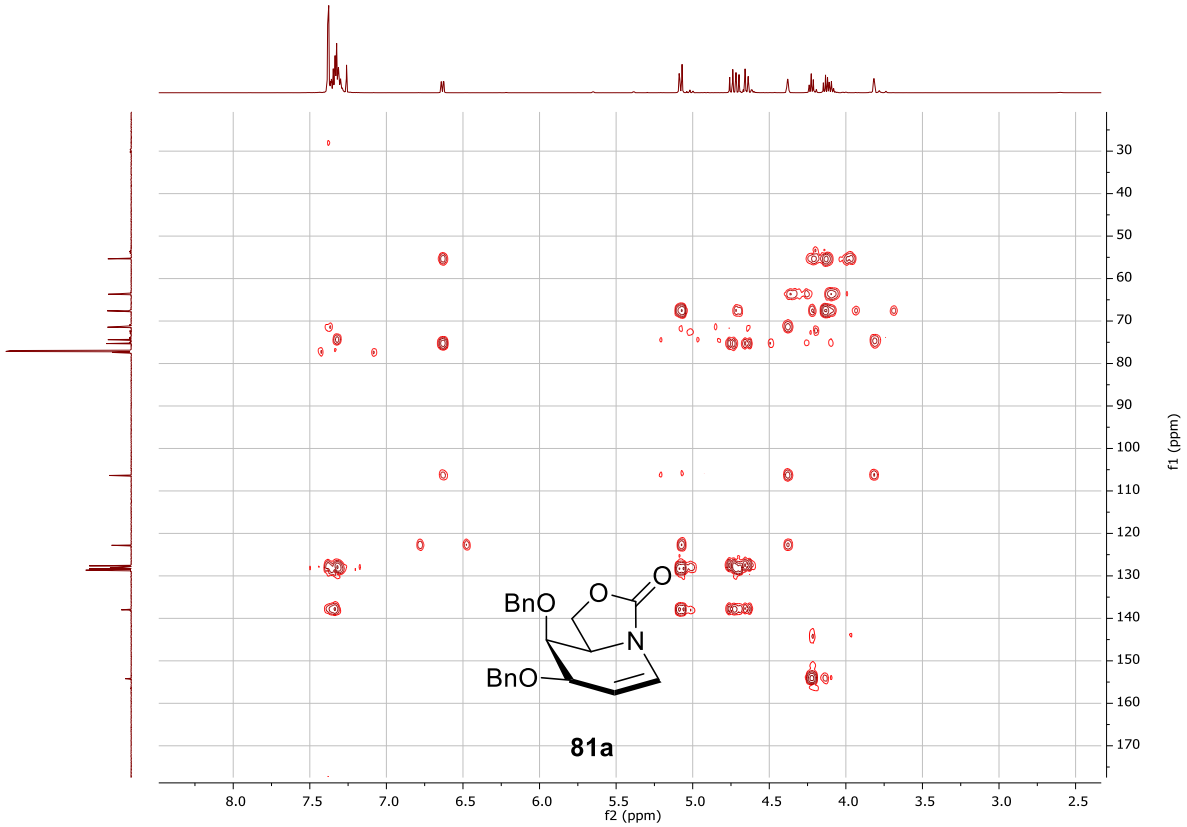

Figure 8.127. HMBC spectra for 81a

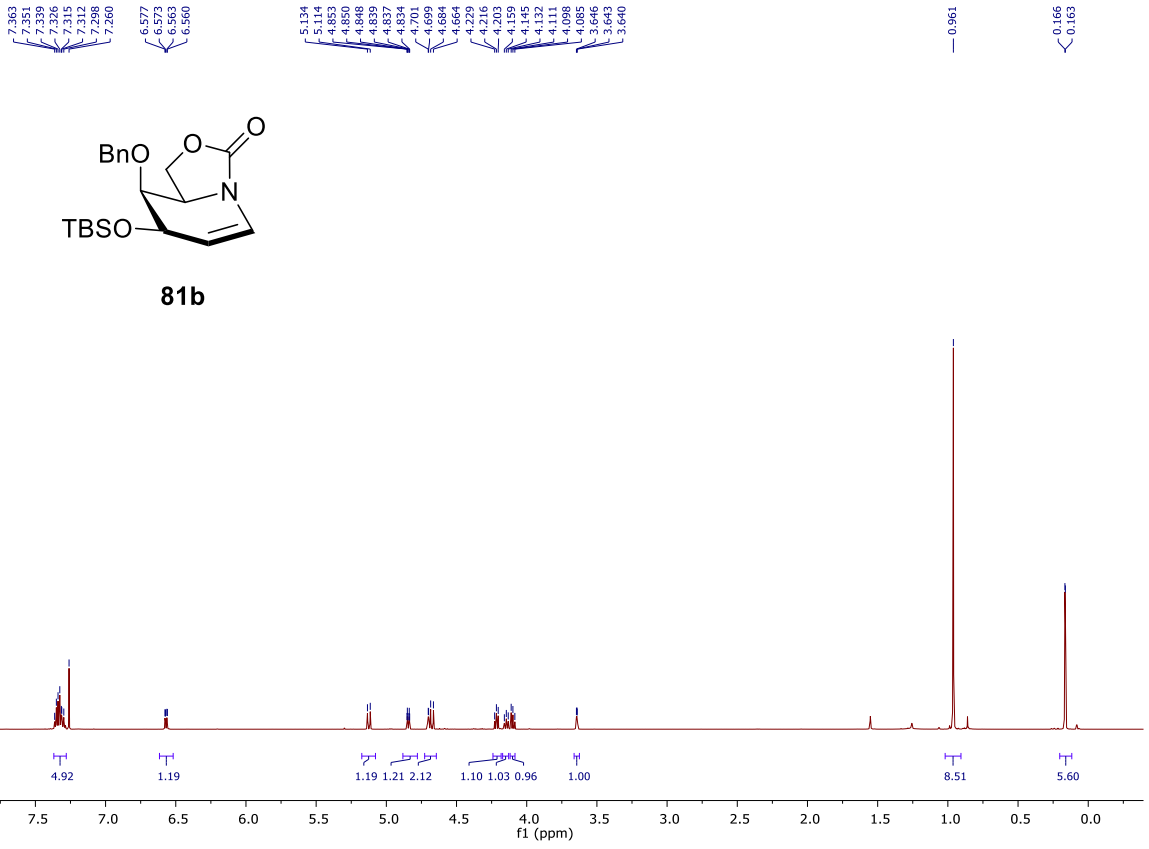

Figure 8.128. ^{1}H NMR spectra for 81b

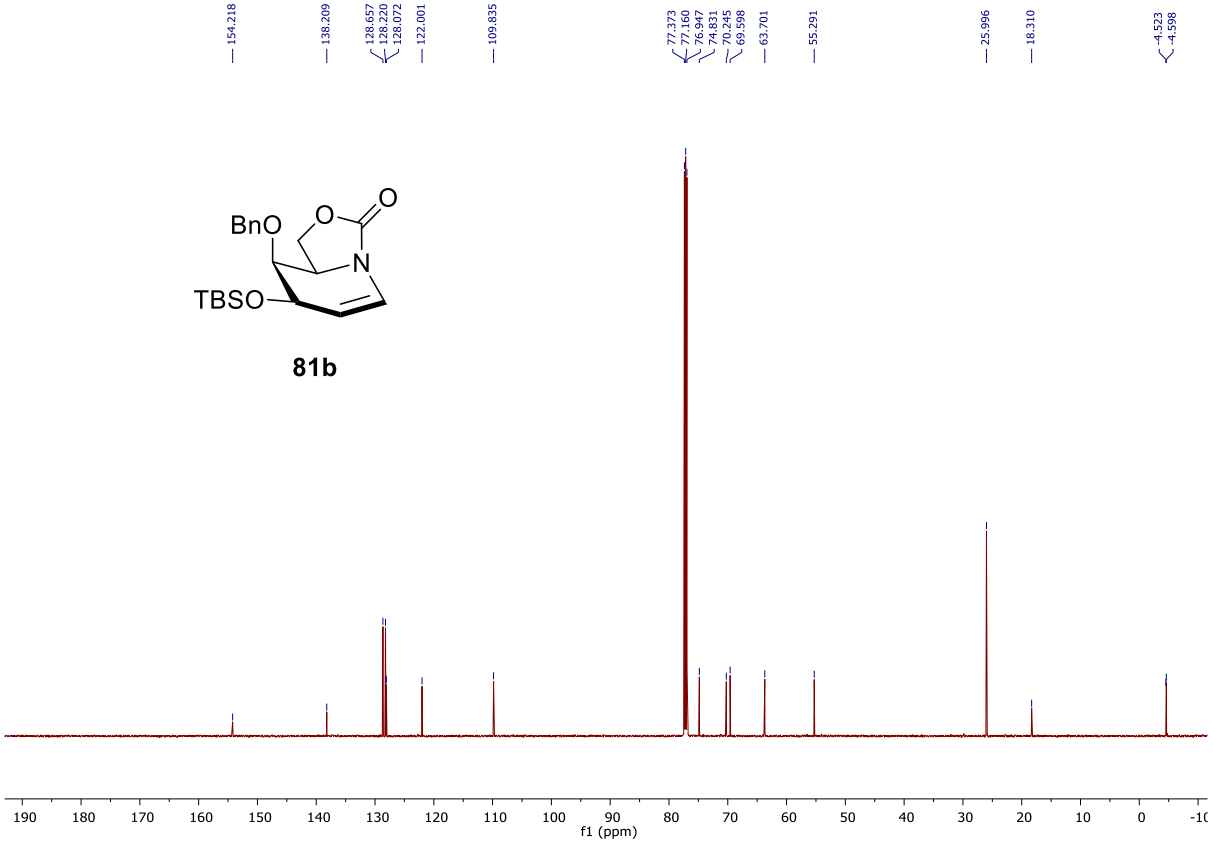

Figure 8.129. ^{13}C NMR spectra for 81b

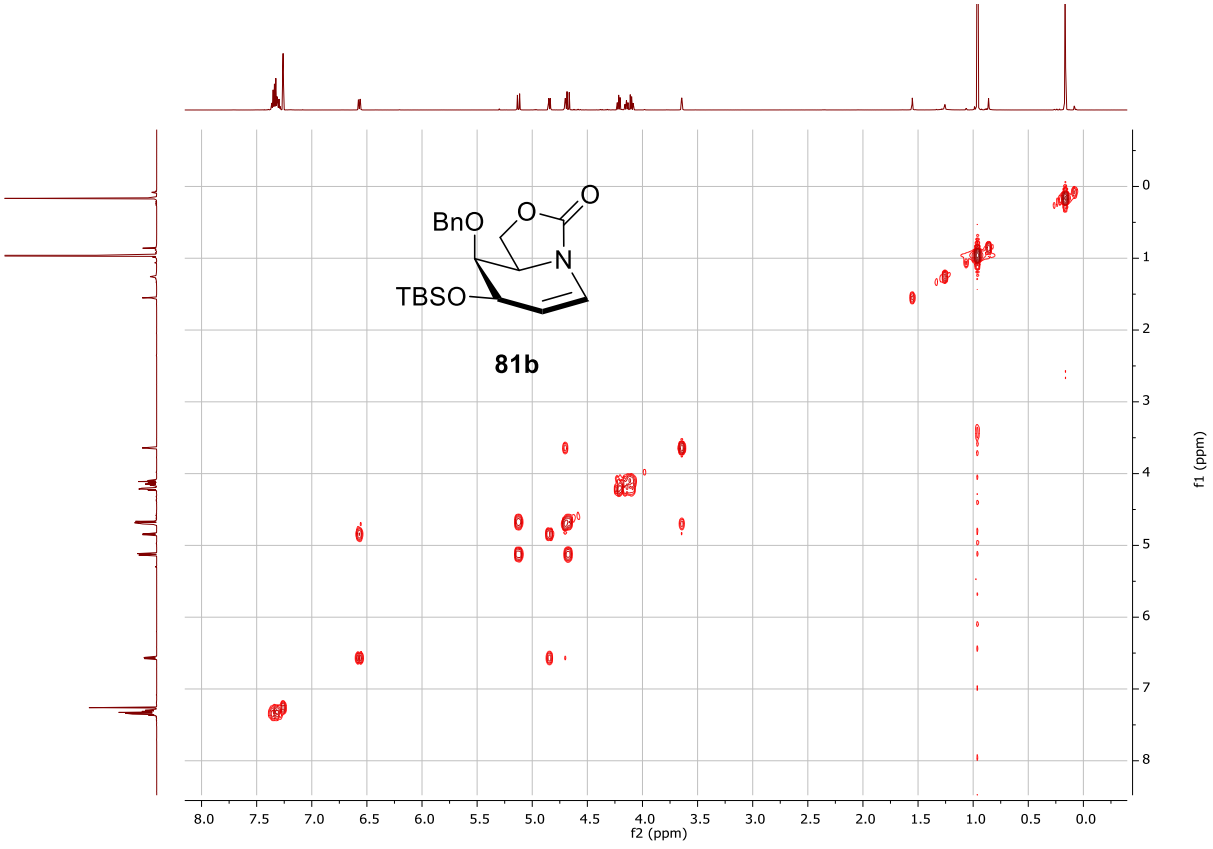

Figure 8.130. COSY spectra for 81b

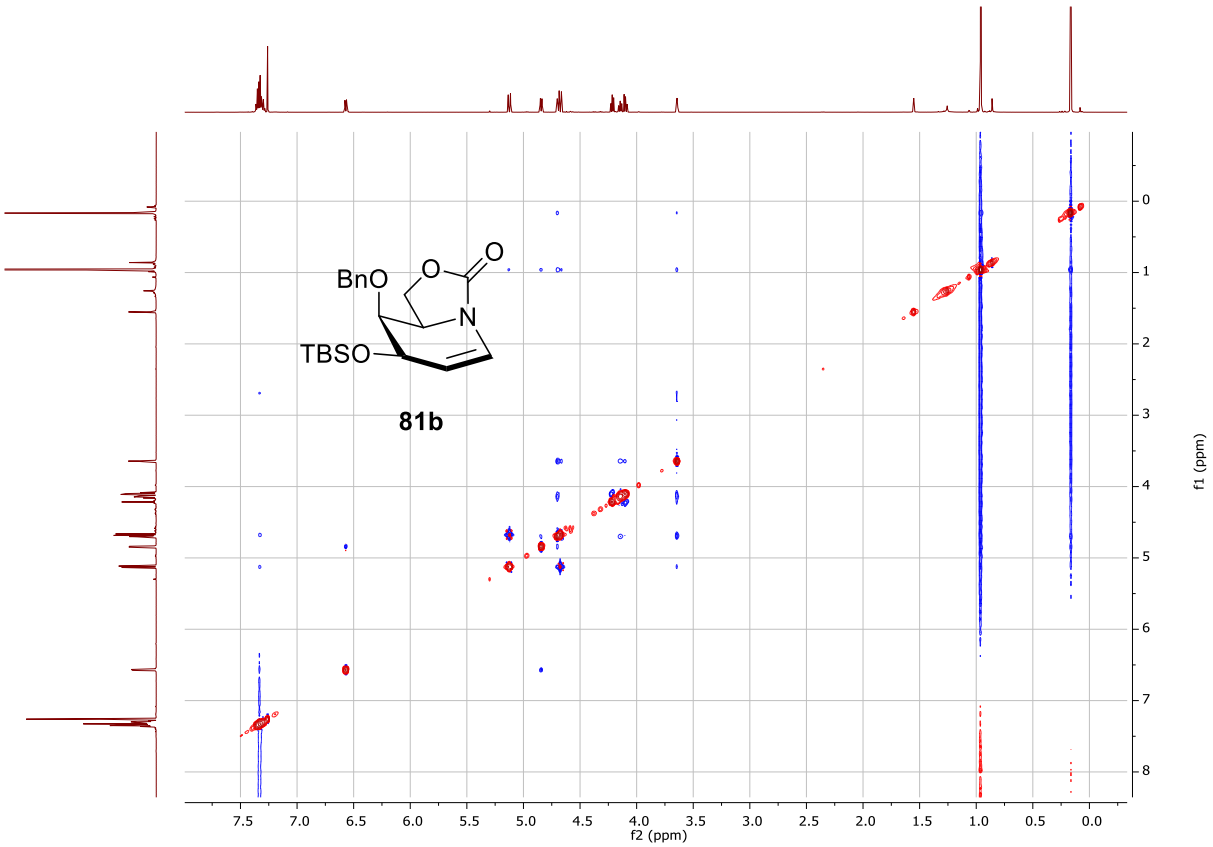

Figure 8.131. NOESY spectra for 81b

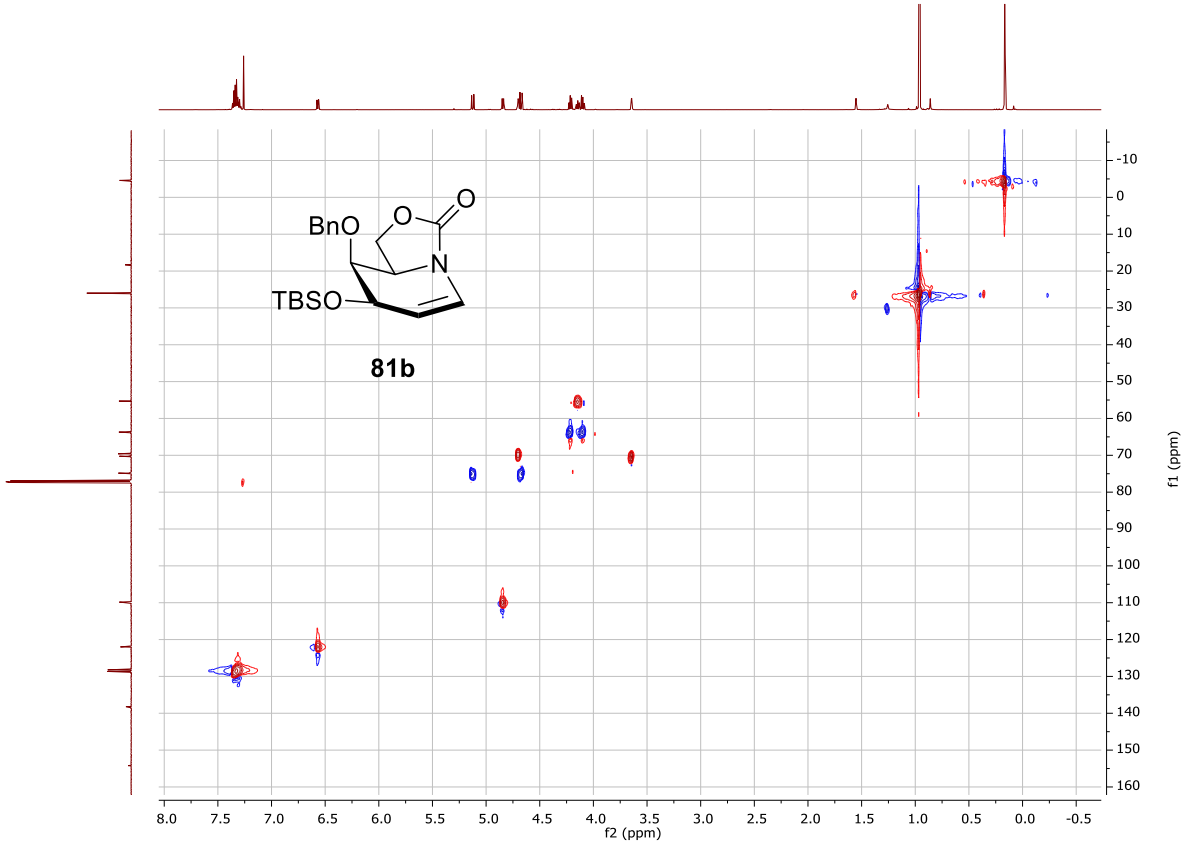

Figure 8.132. HSQC spectra for 81b

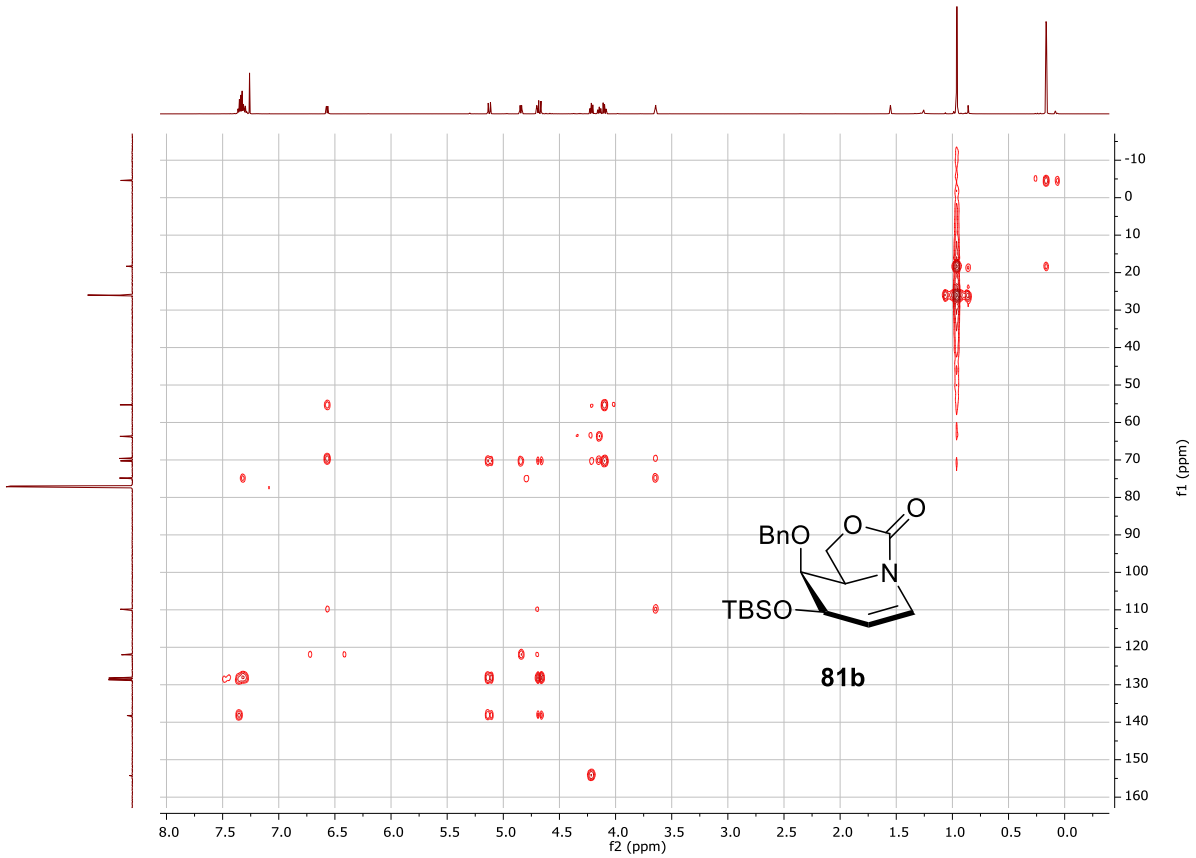

Figure 8.133. HMBC spectra for 81b

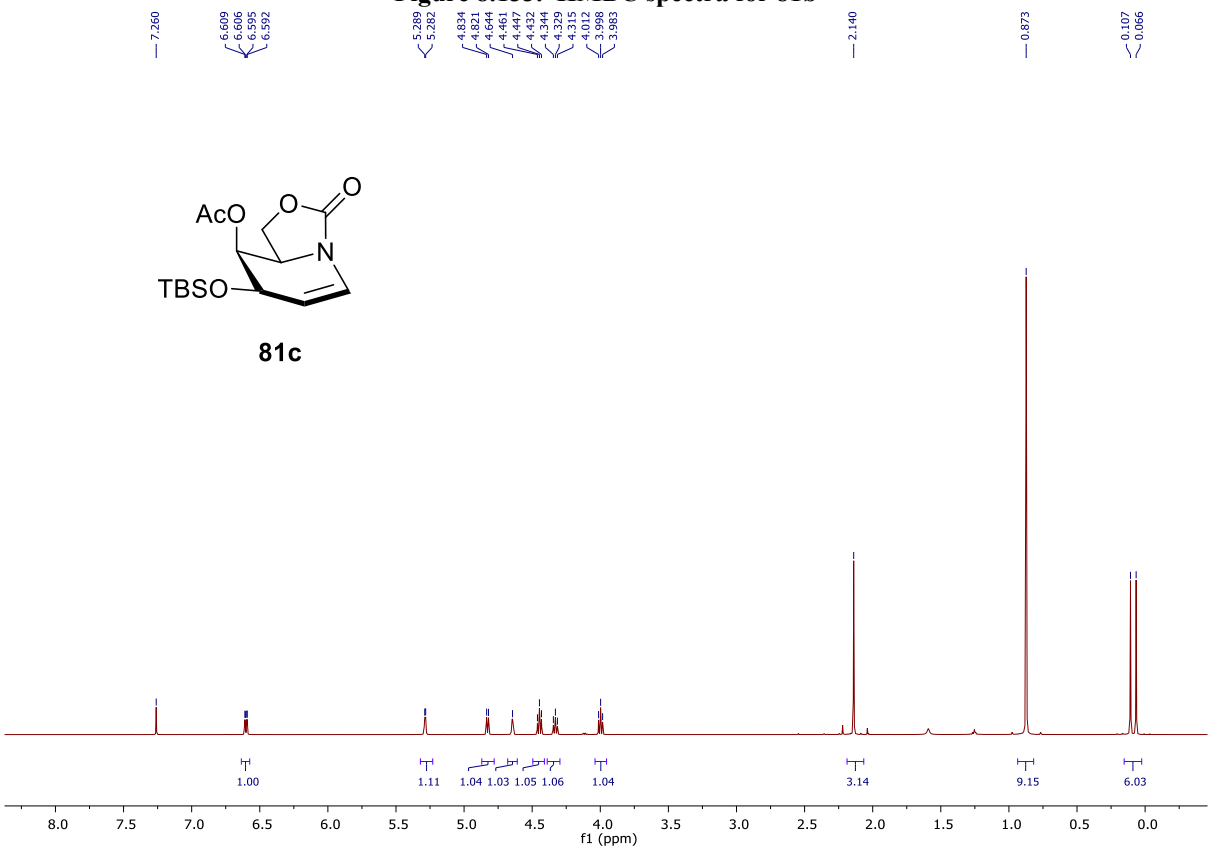

Figure 8.134. ^{1}H NMR spectra for 81c

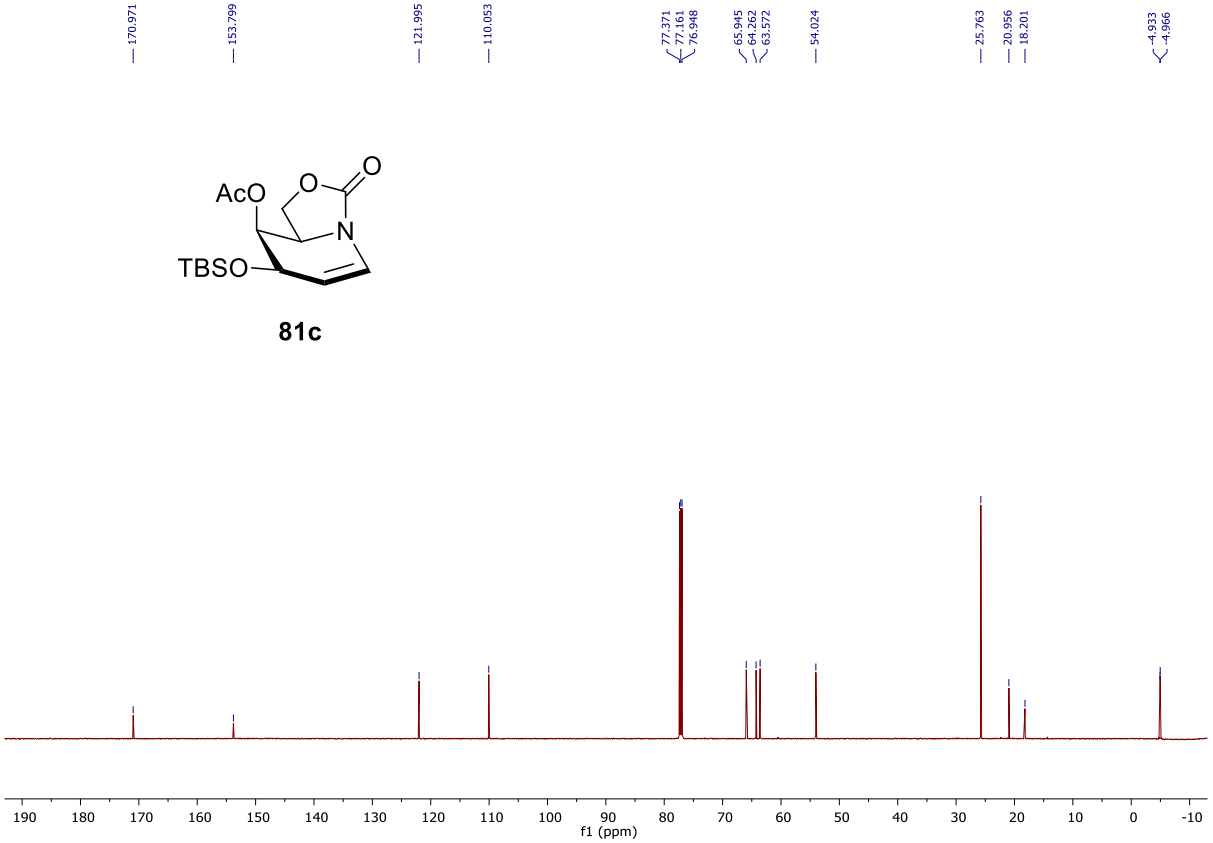

Figure 8.135. ^{13}C NMR spectra for 81c

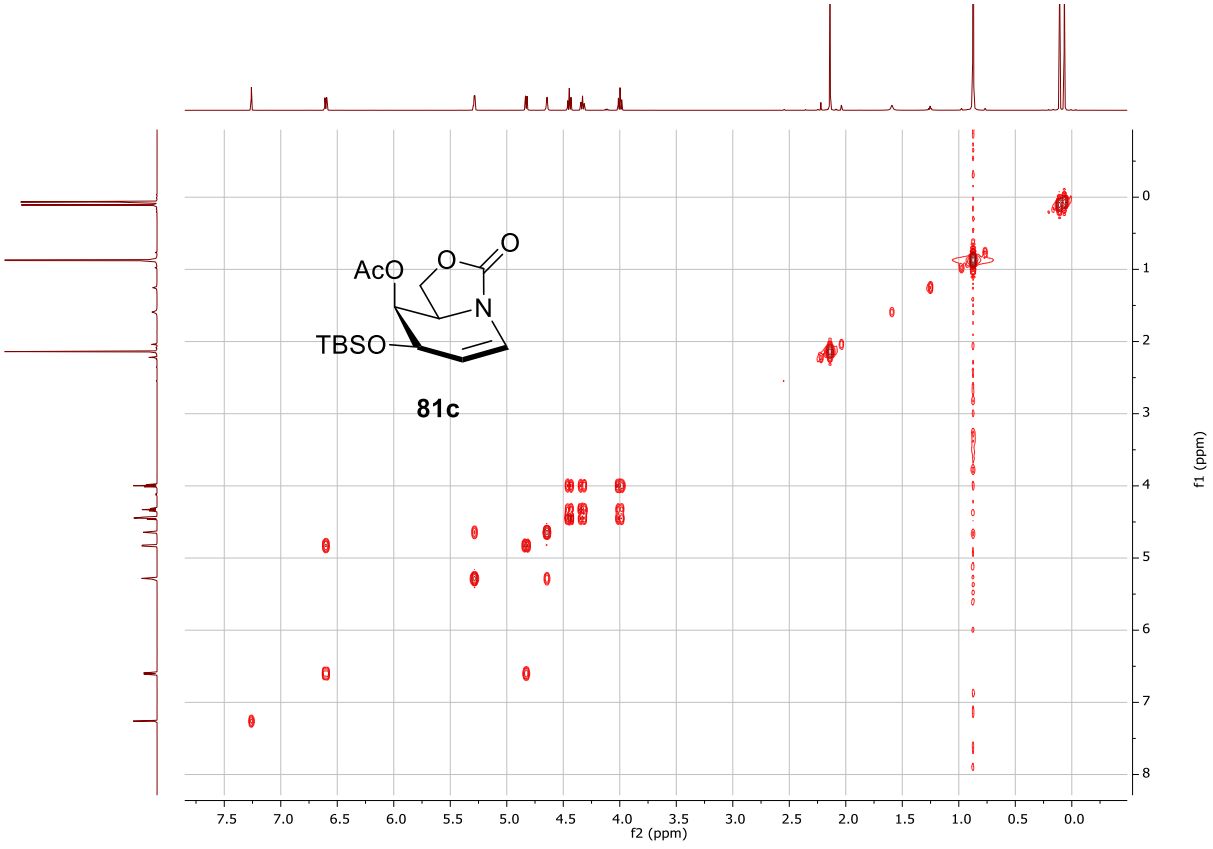

Figure 8.136. COSY spectra for 81c

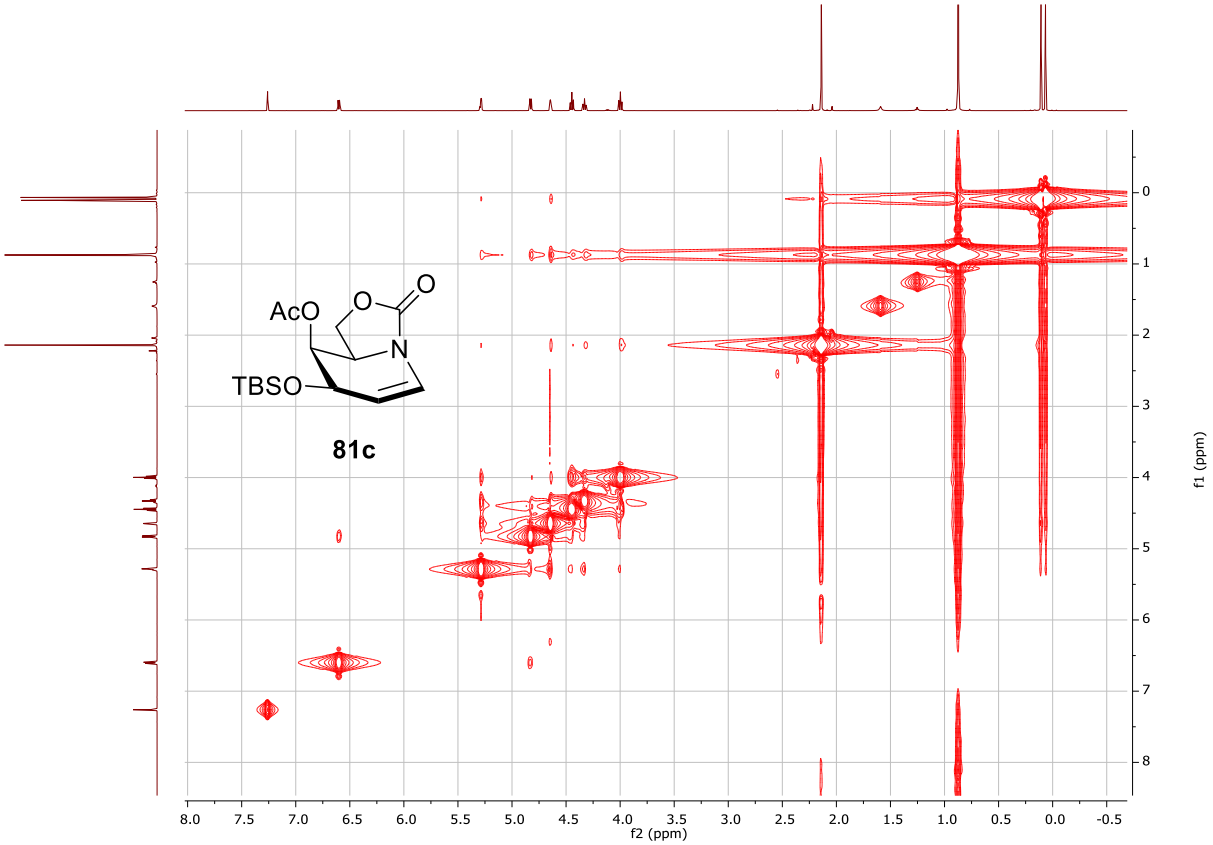

Figure 8.137. NOESY spectra for 81c

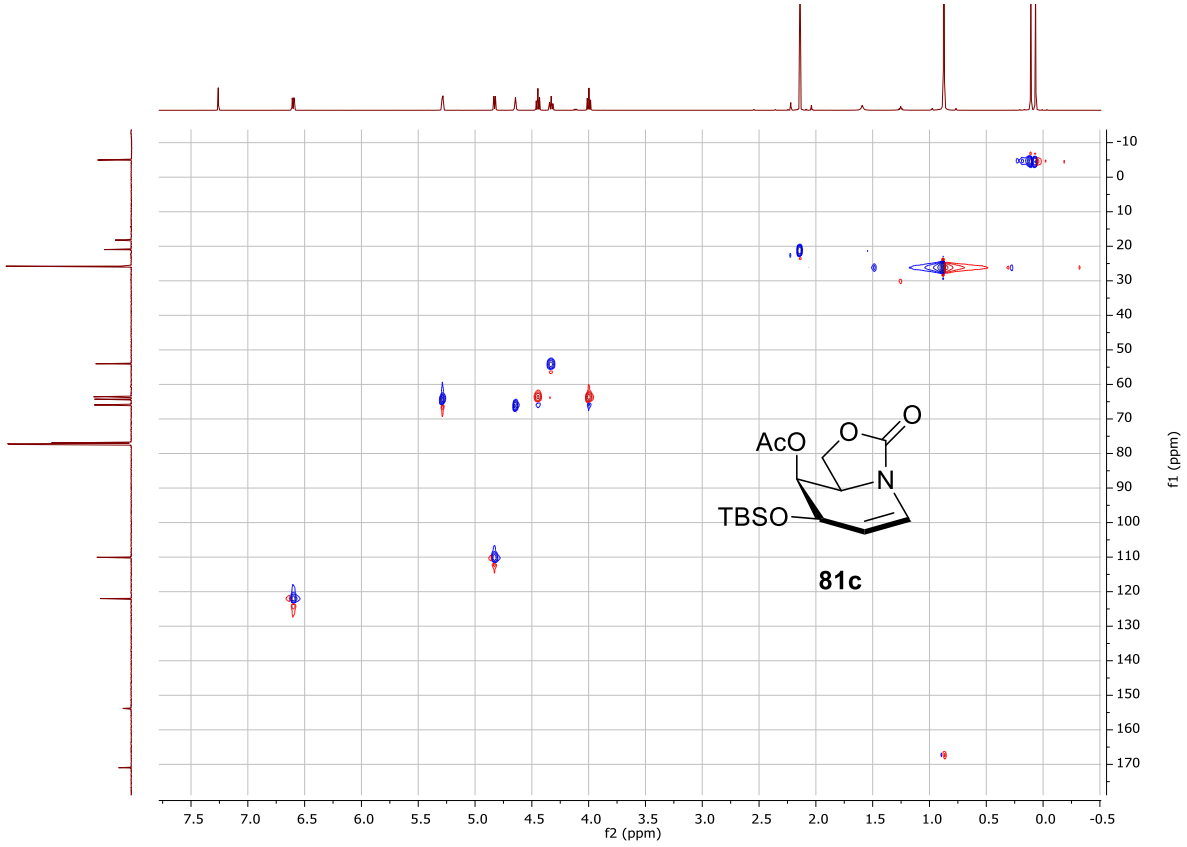

Figure 8.138. HSQC spectra for 81c

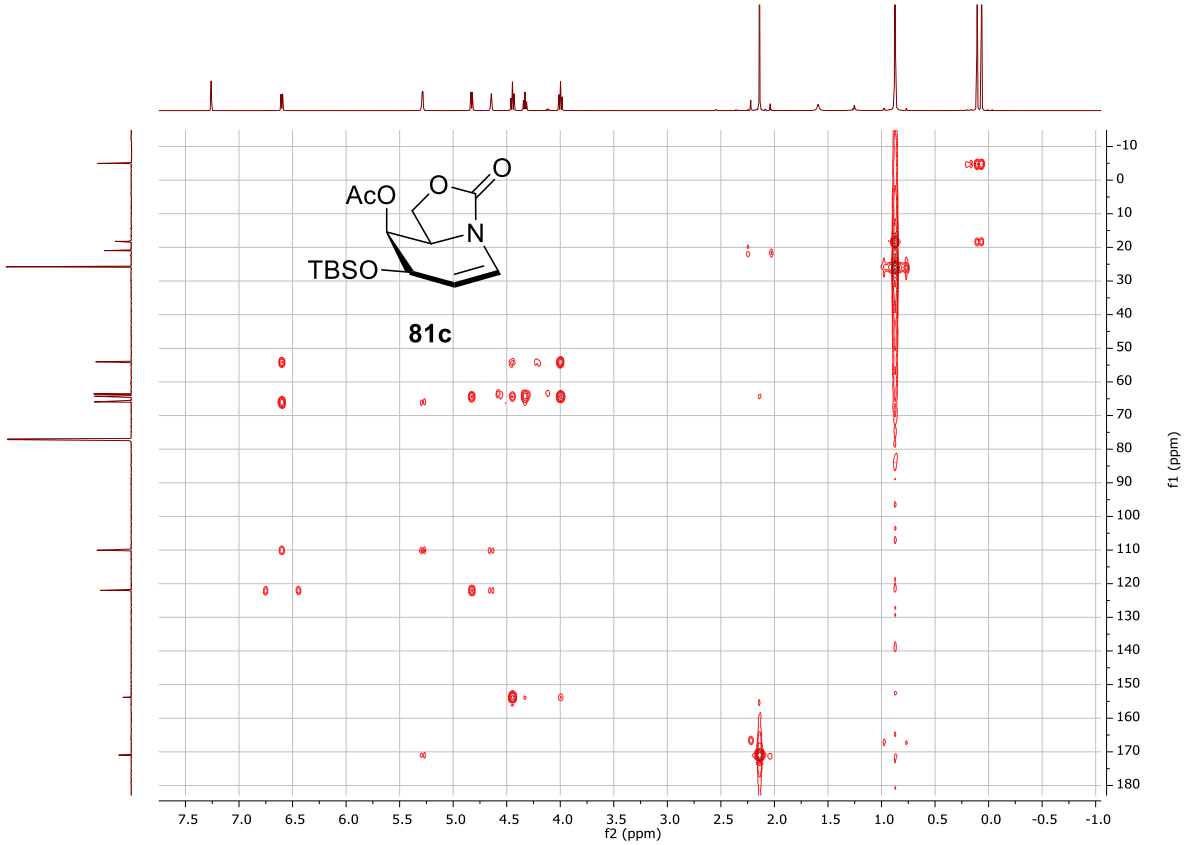

Figure 8.139. HMBC spectra for 81c

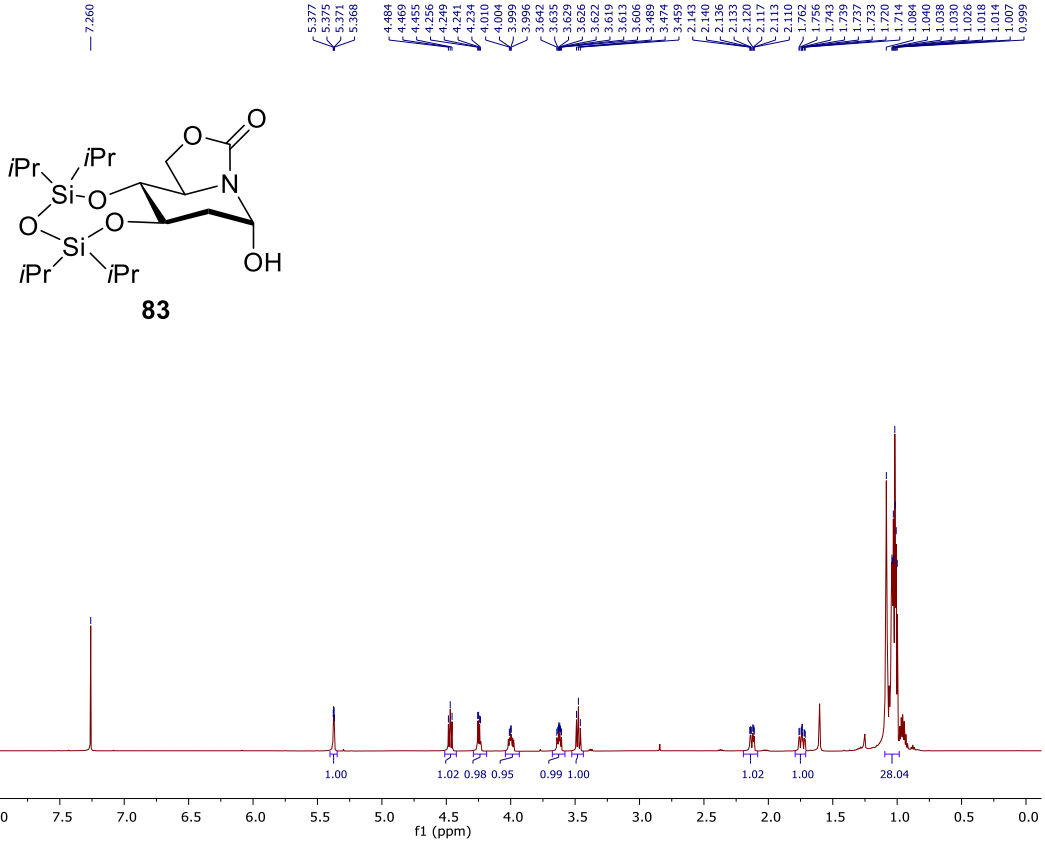

Figure 8.140. ^{1}H NMR spectra for 83

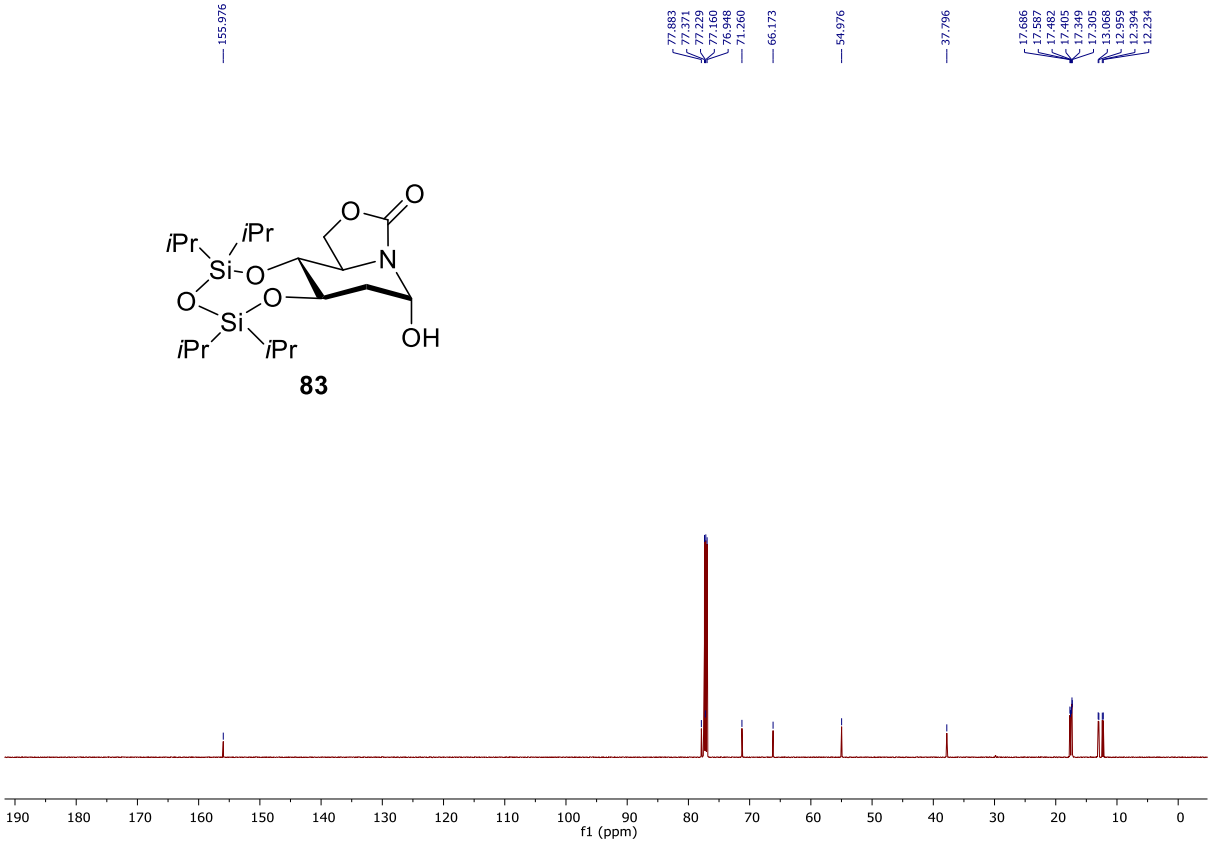

Figure 8.141. ^{13}C NMR spectra for 83

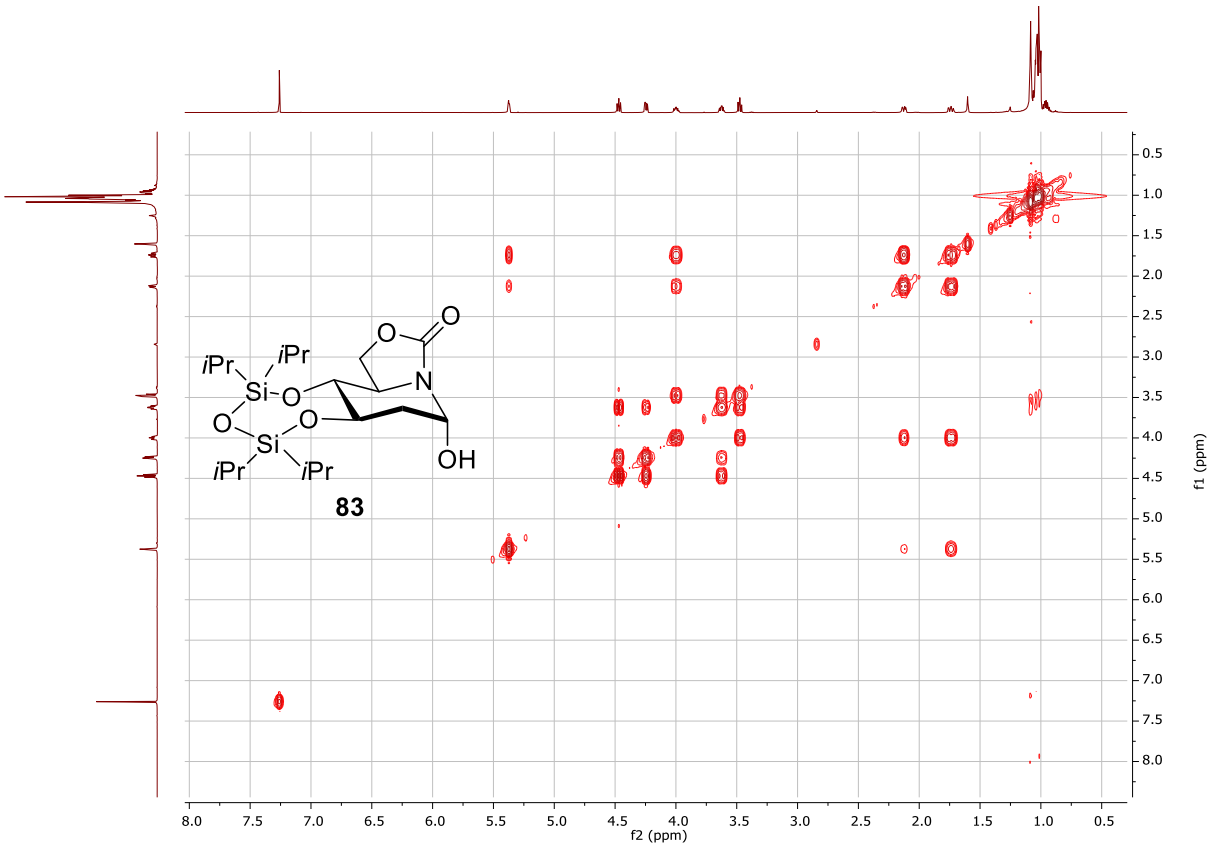

Figure 8.142. COSY spectra for 83

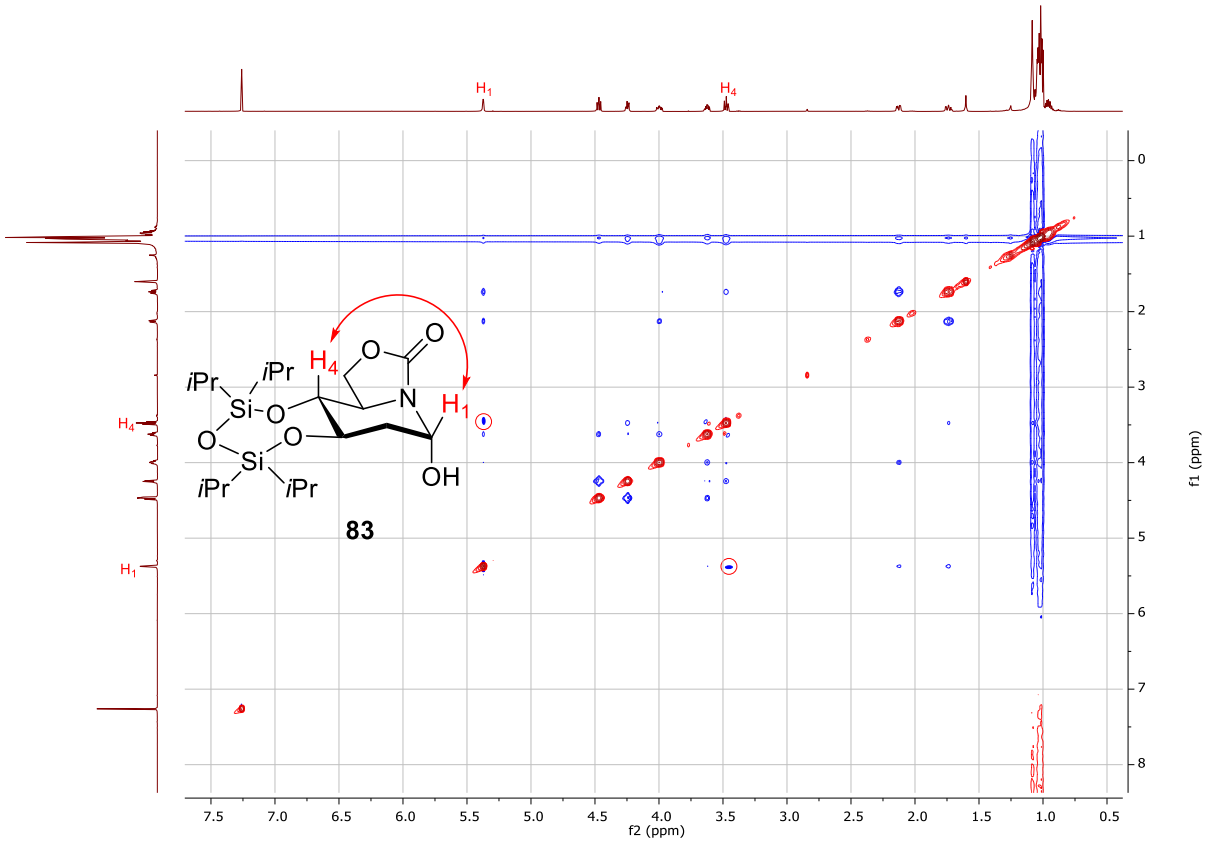

Figure 8.143. NOESY spectra for 83

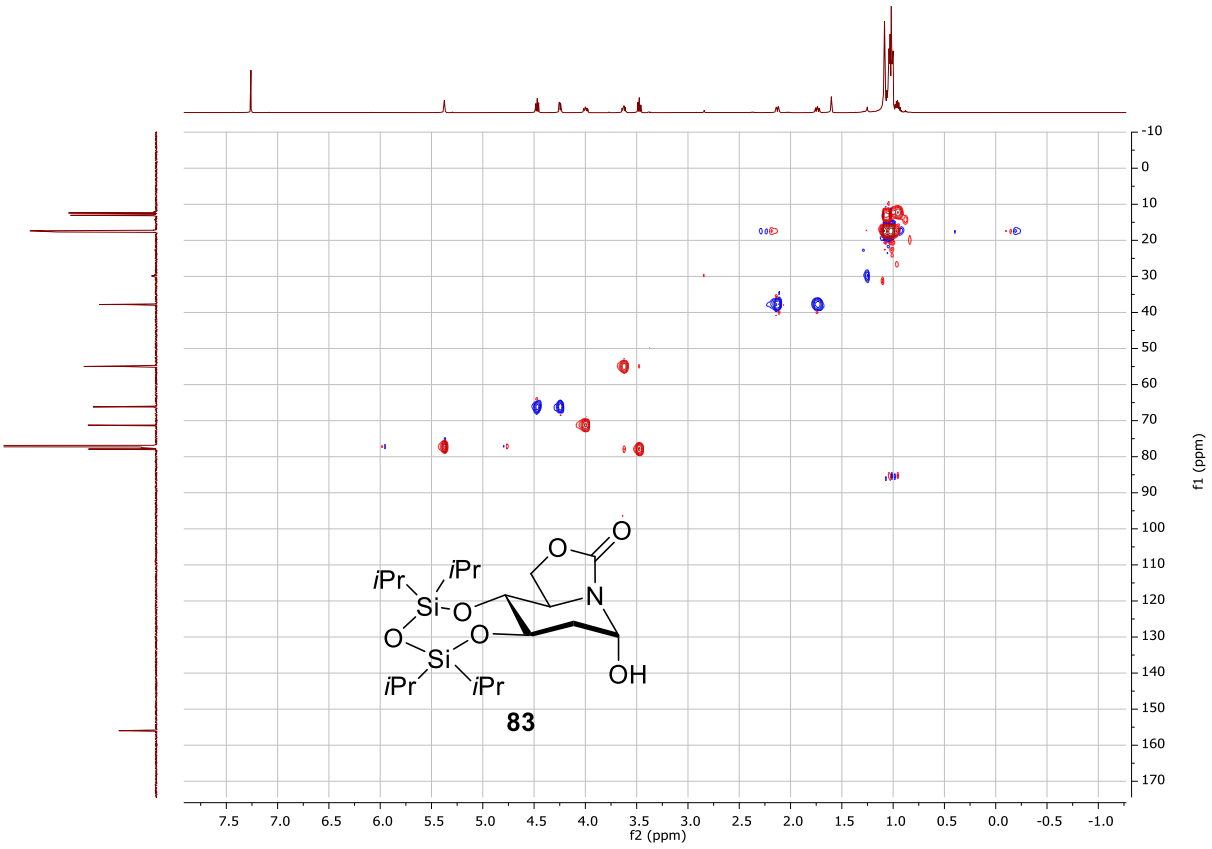

Figure 8.144. HSQC spectra for 83

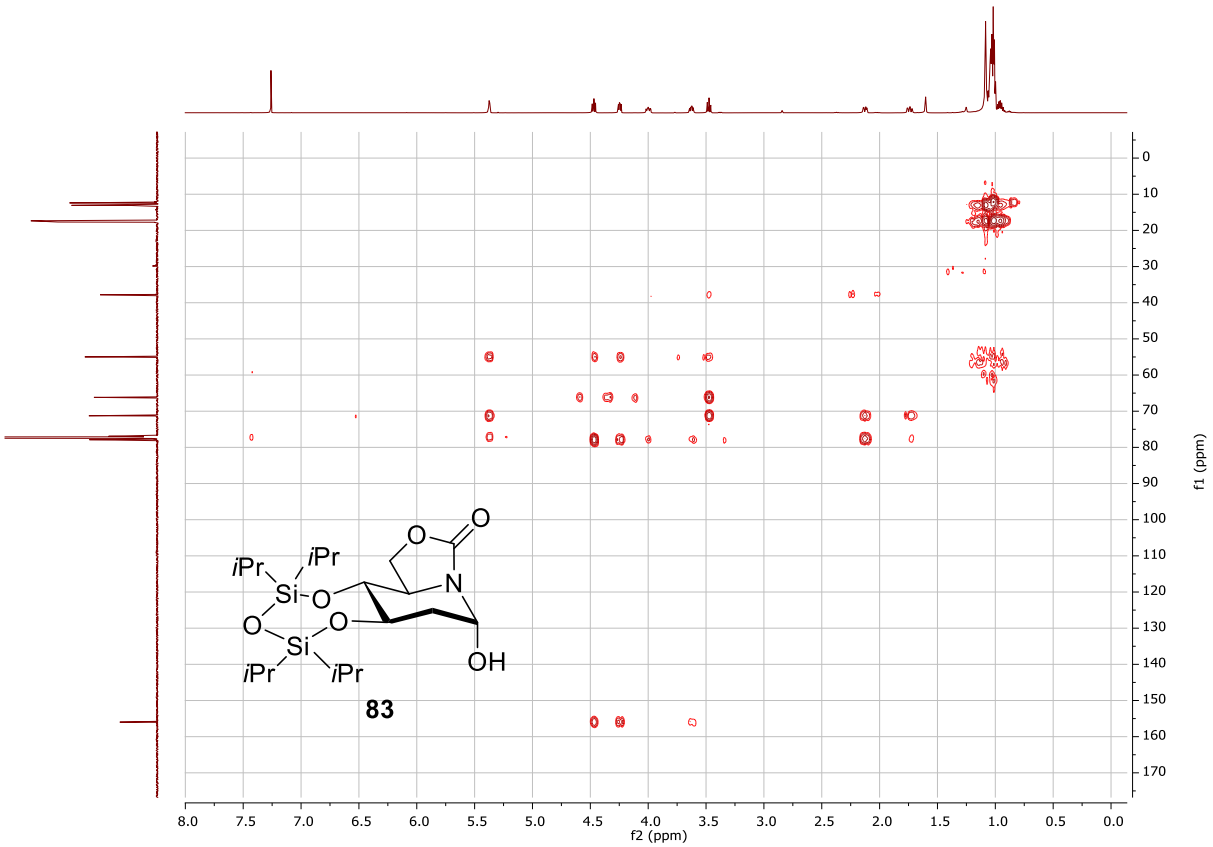

Figure 8.145. HMBC spectra for 83

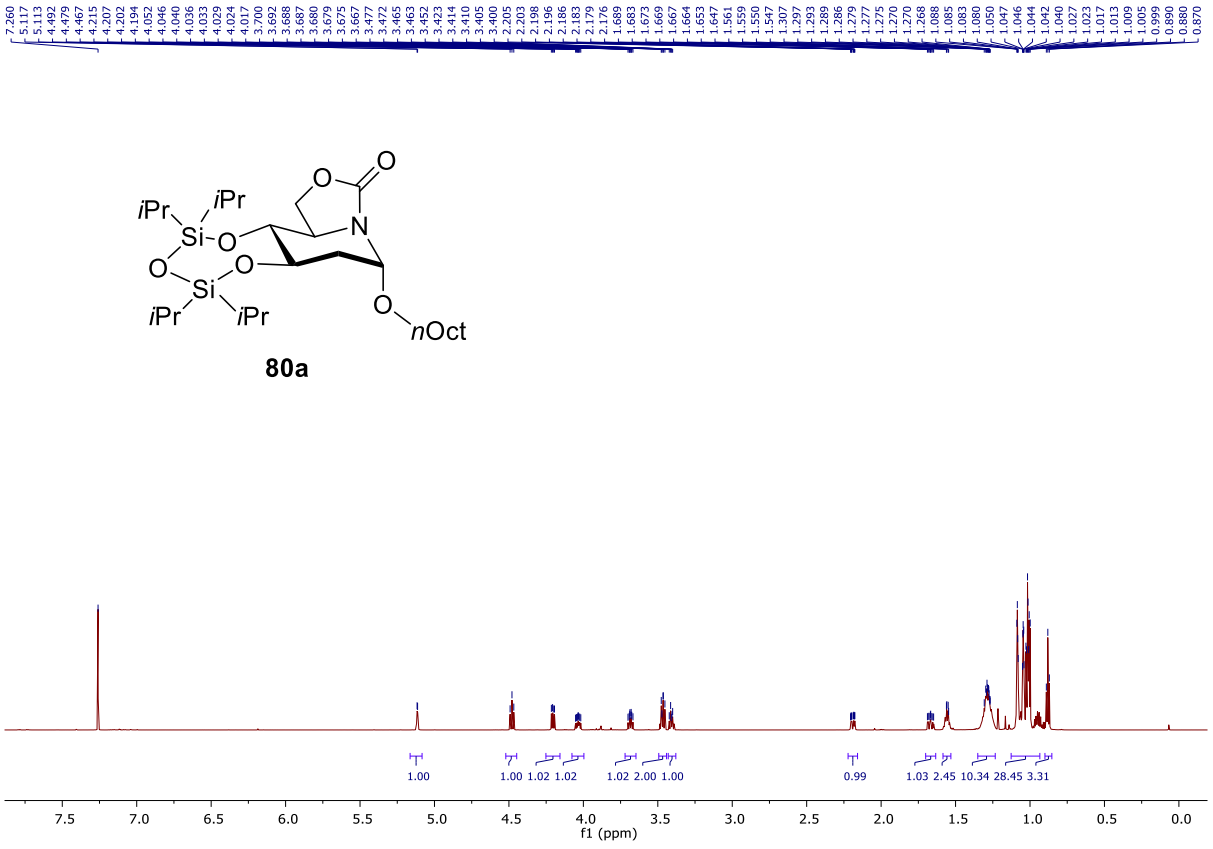

Figure 8.146. ^{1}H NMR spectra for 80a

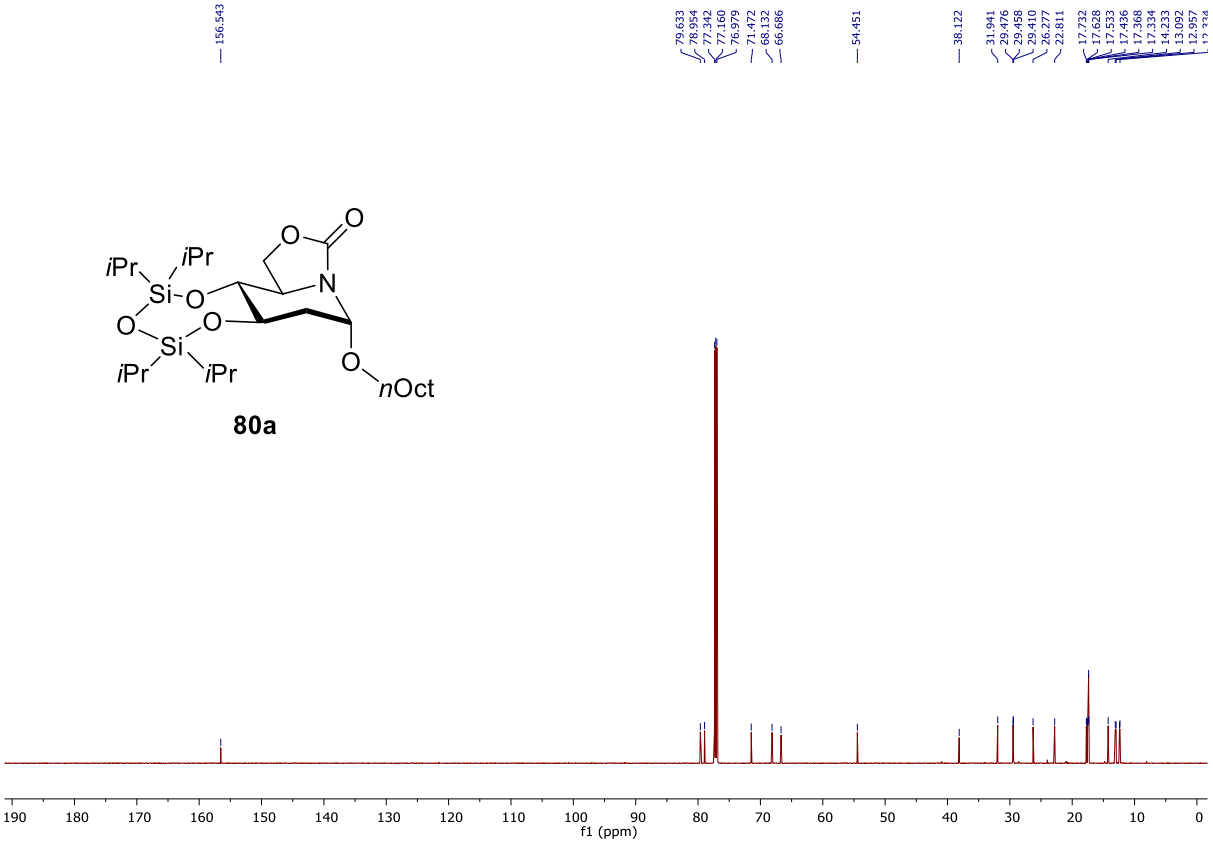

Figure 8.147. ^{13}C NMR spectra for 80a

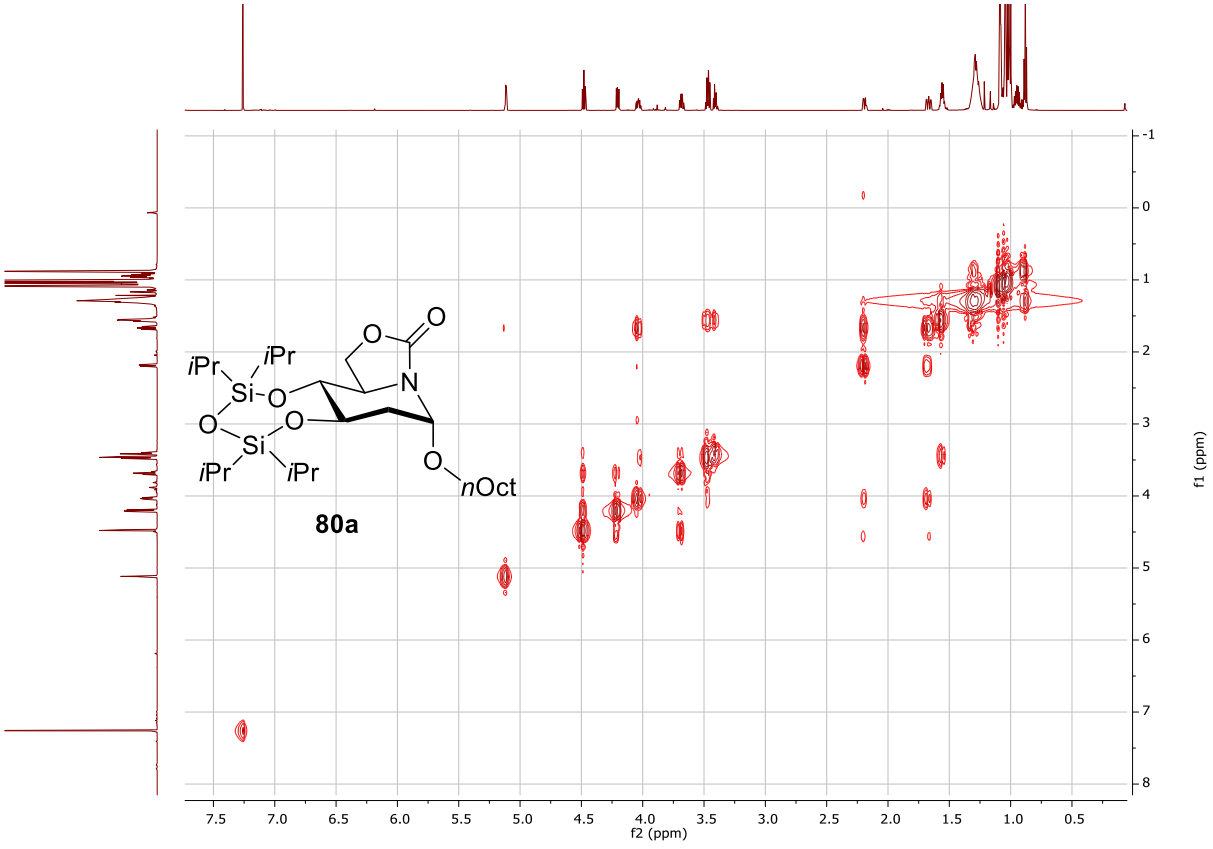

Figure 8.148. COSY spectra for 80a

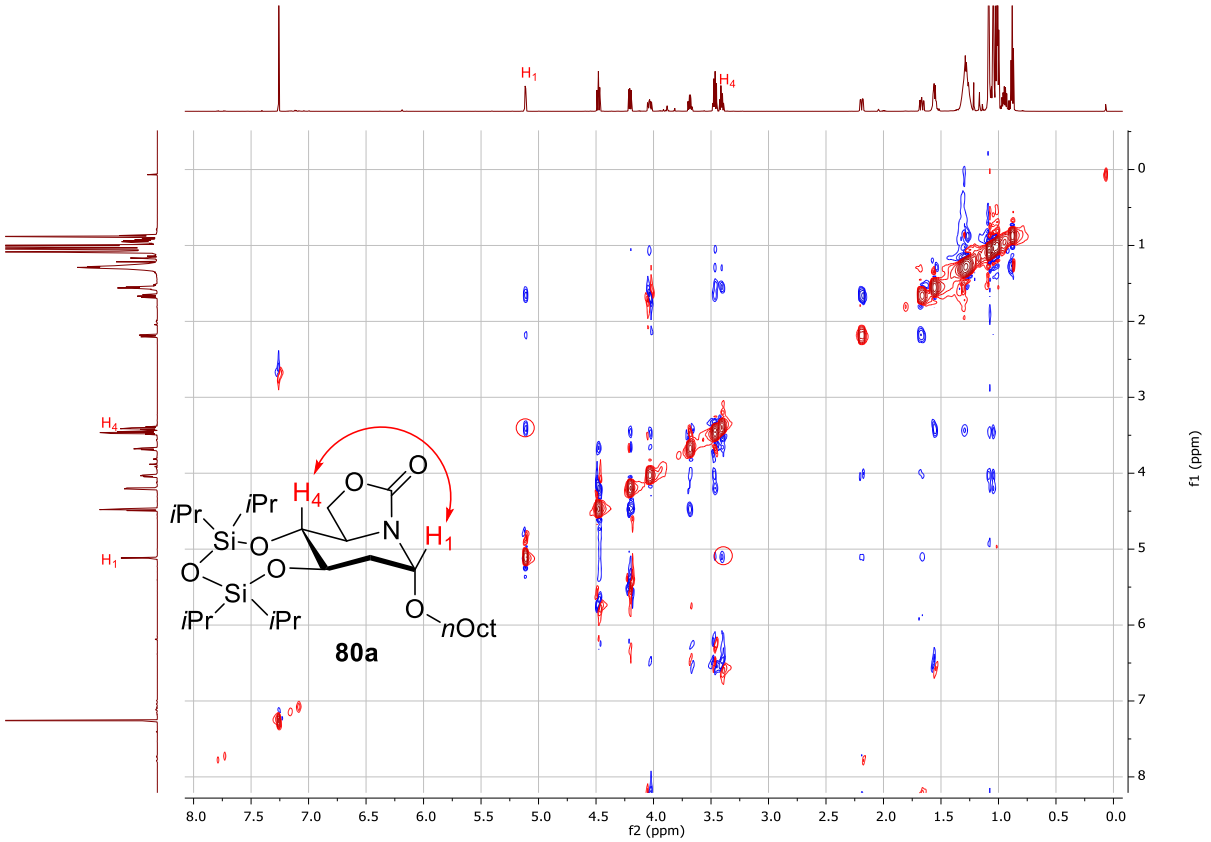

Figure 8.149. NOESY spectra for 80a

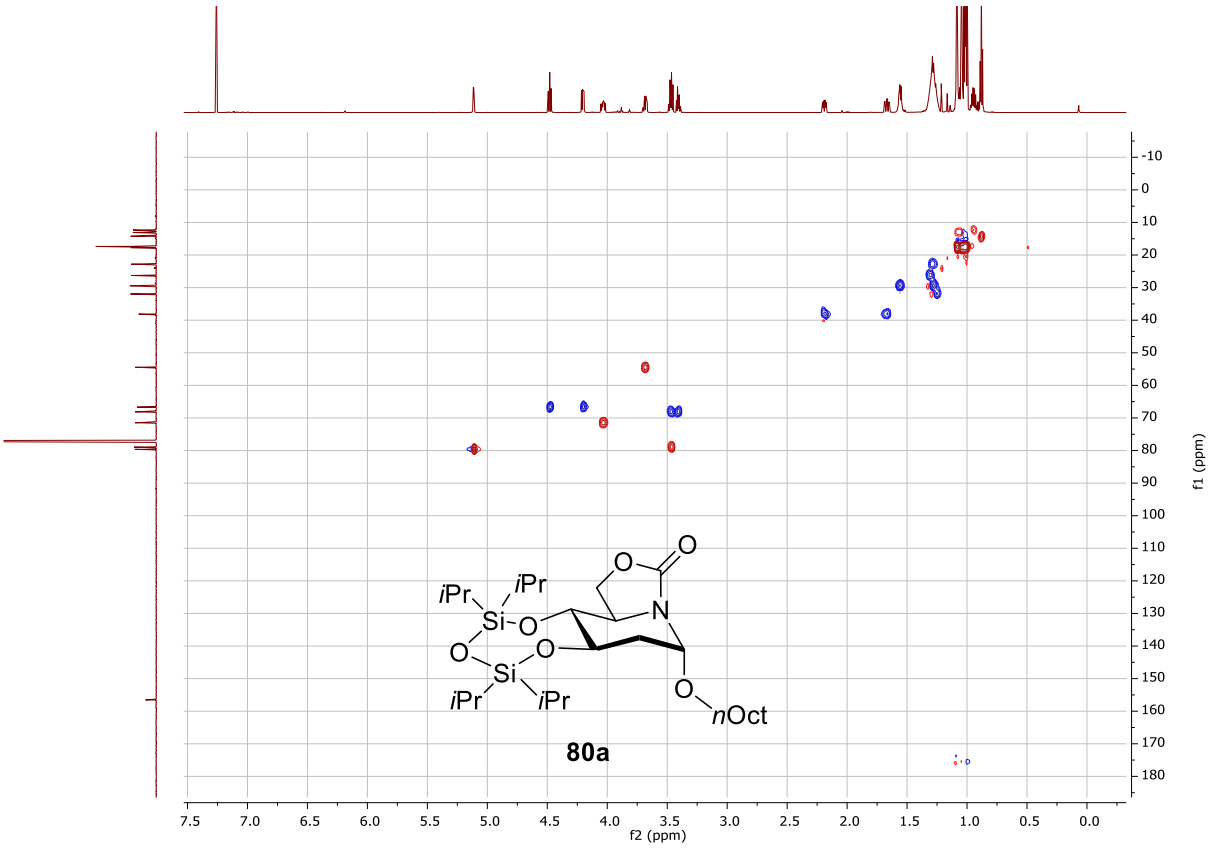

Figure 8.140. HSQC spectra for 80a

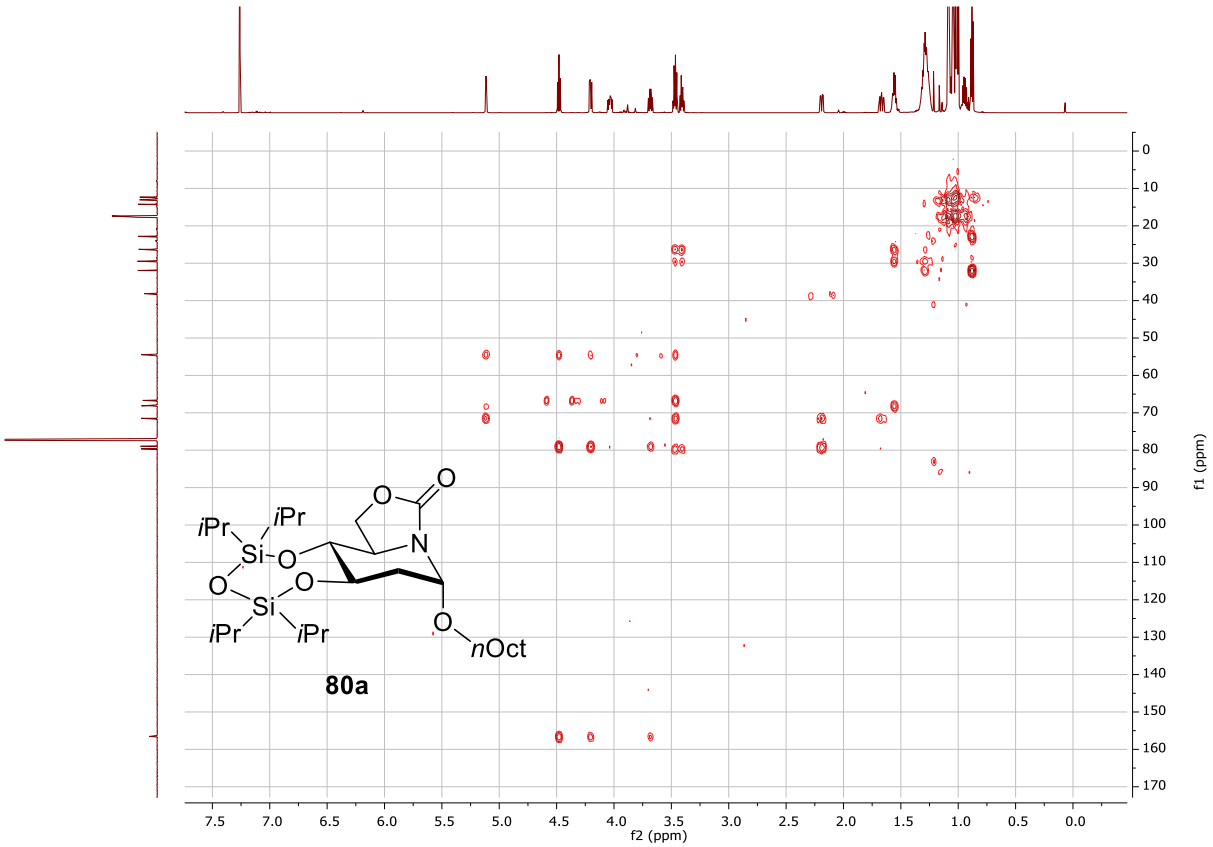

Figure 8.141. HMBC spectra for 80a

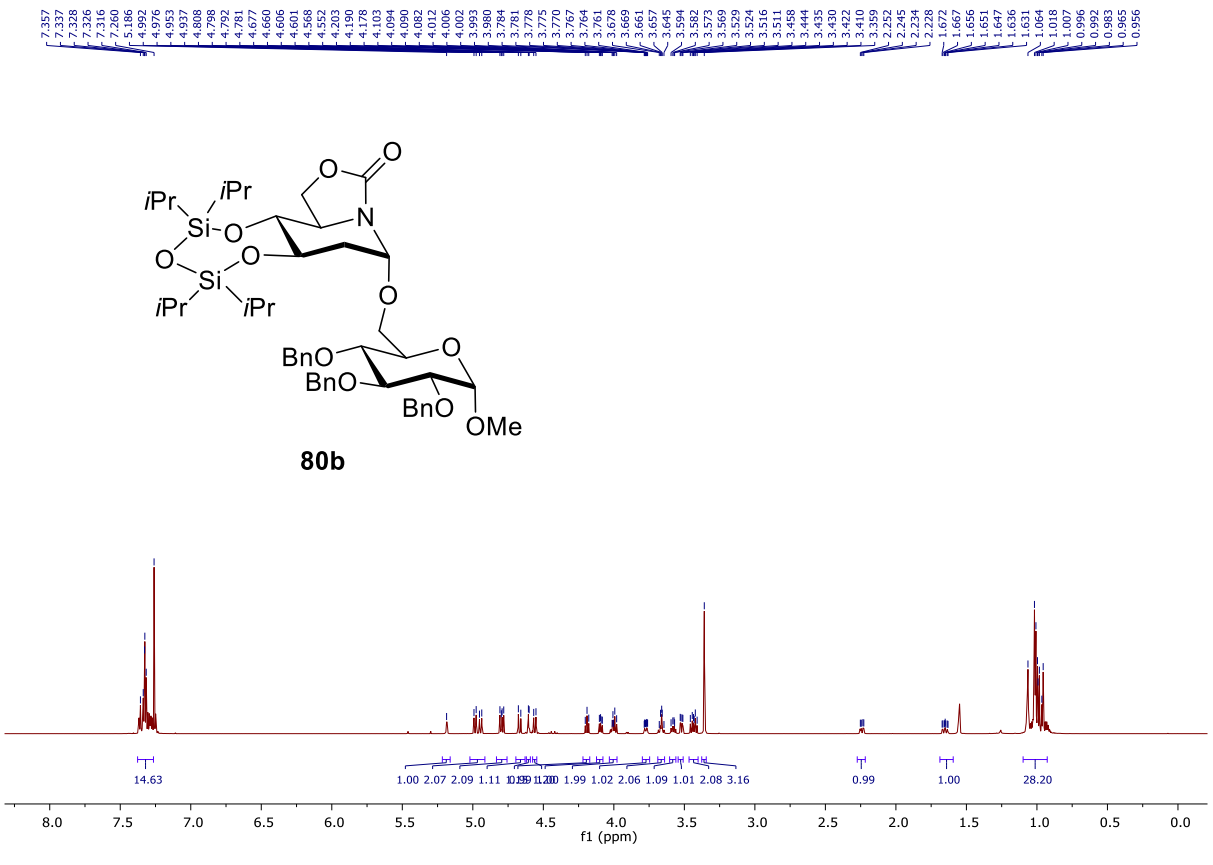

Figure 8.142. ^{1}H NMR spectra for 80b

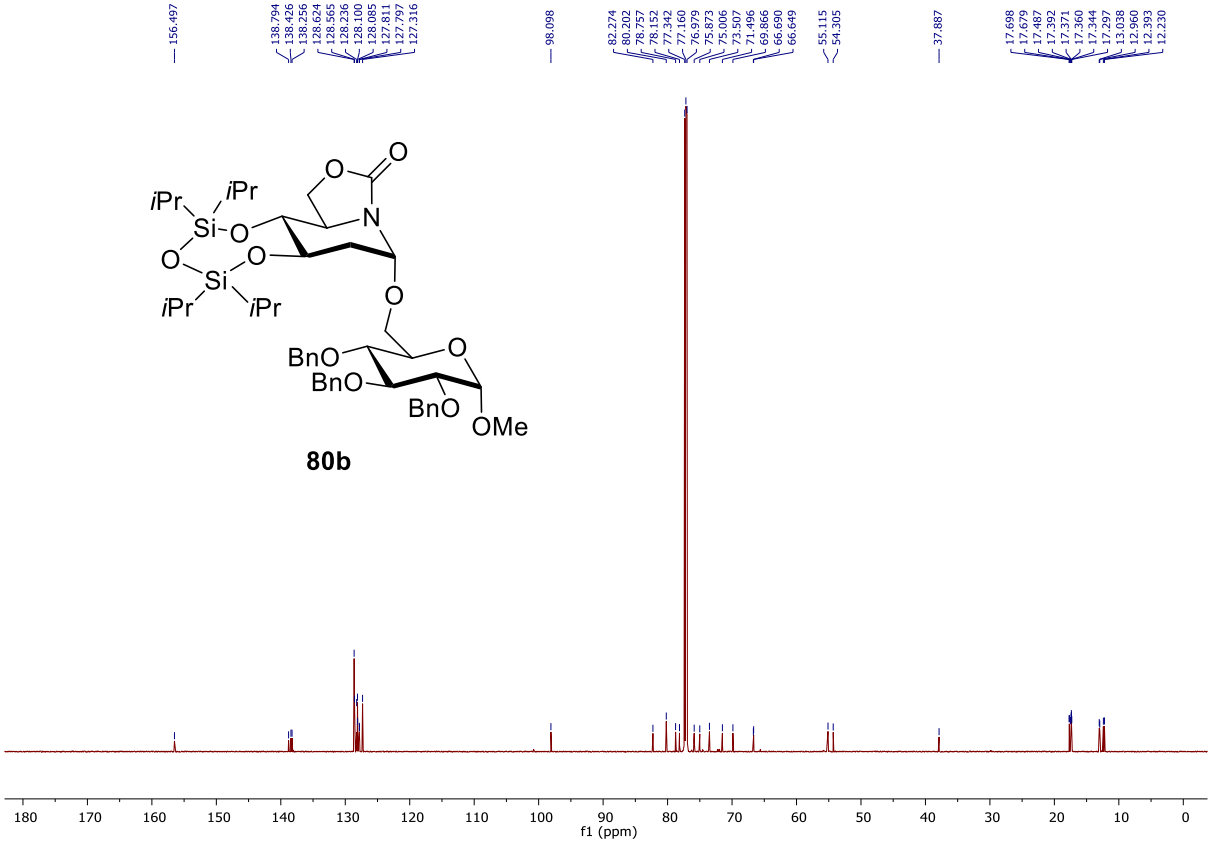

Figure 8.143. ^{13}C NMR spectra for 80b

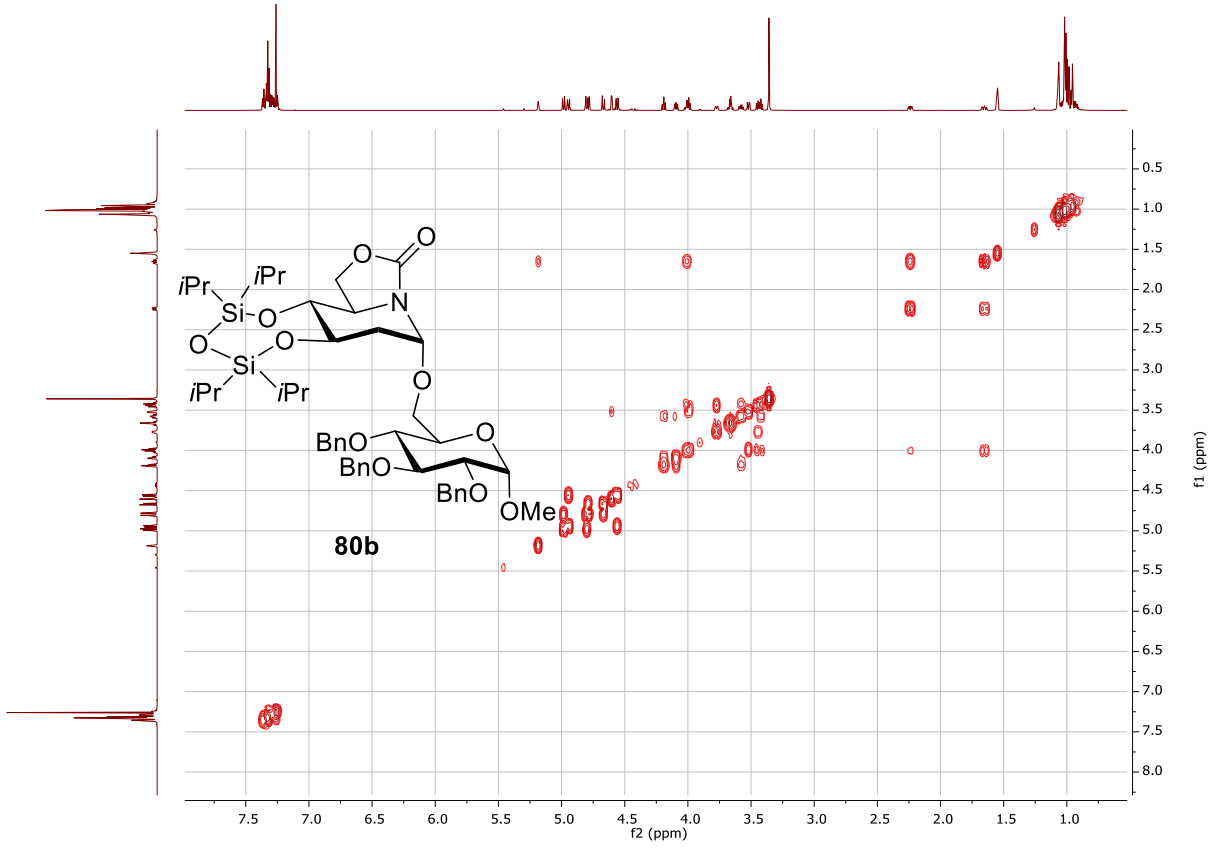

Figure 8.144. COSY spectra for 80b

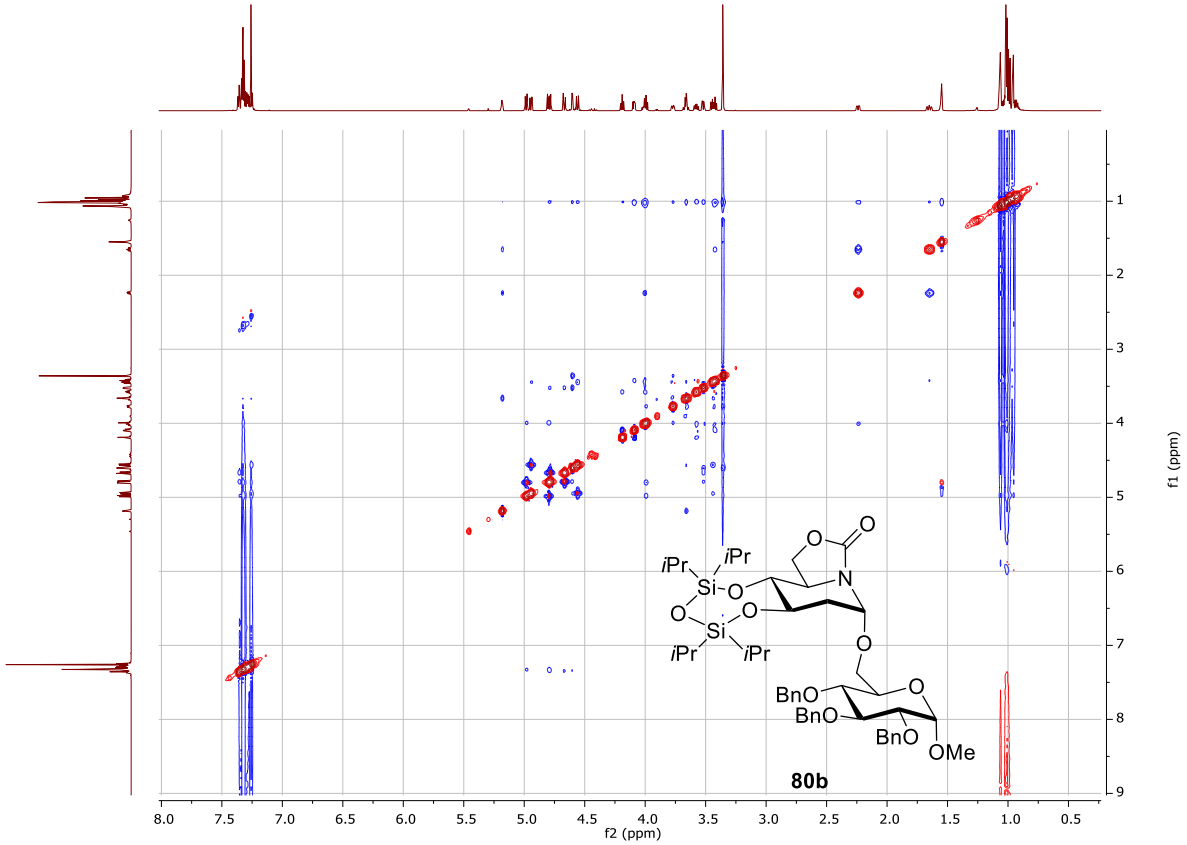

Figure 8.145. NOESY spectra for 80b

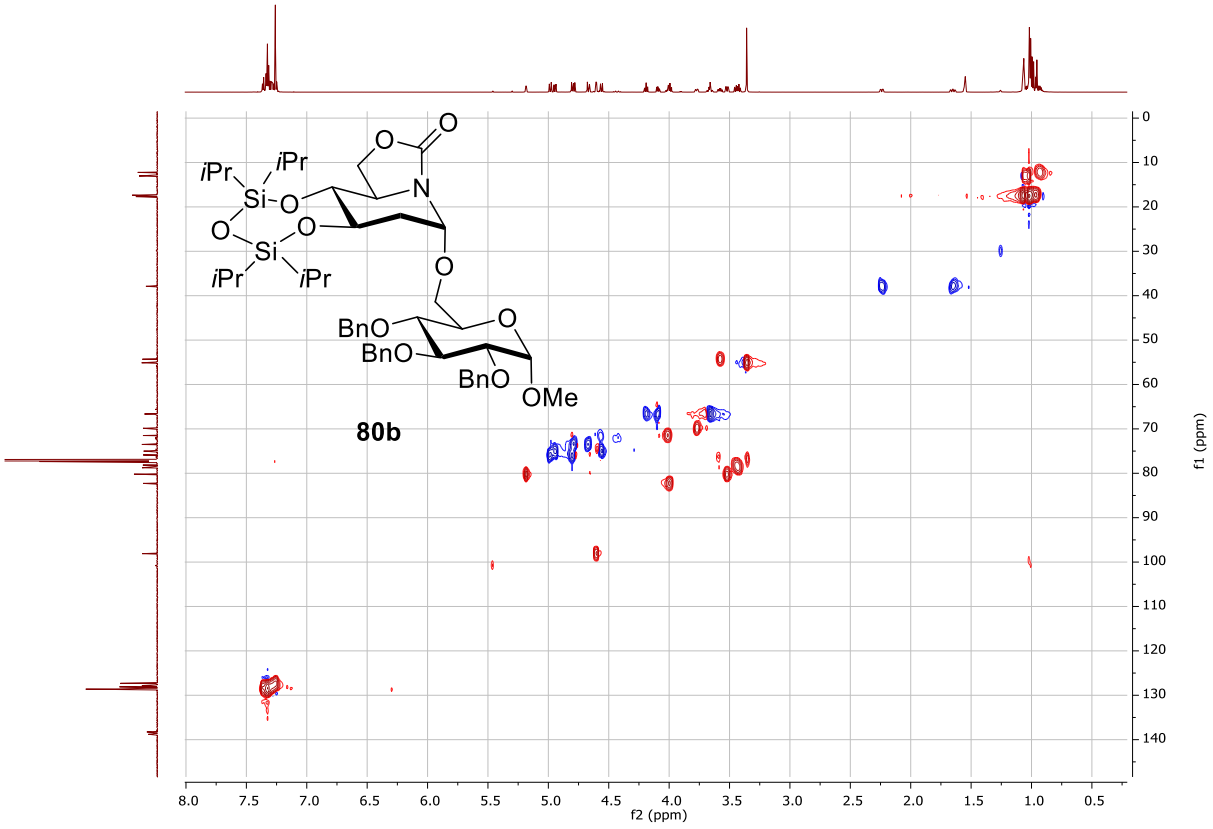

Figure 8.146. HSQC spectra for 80b

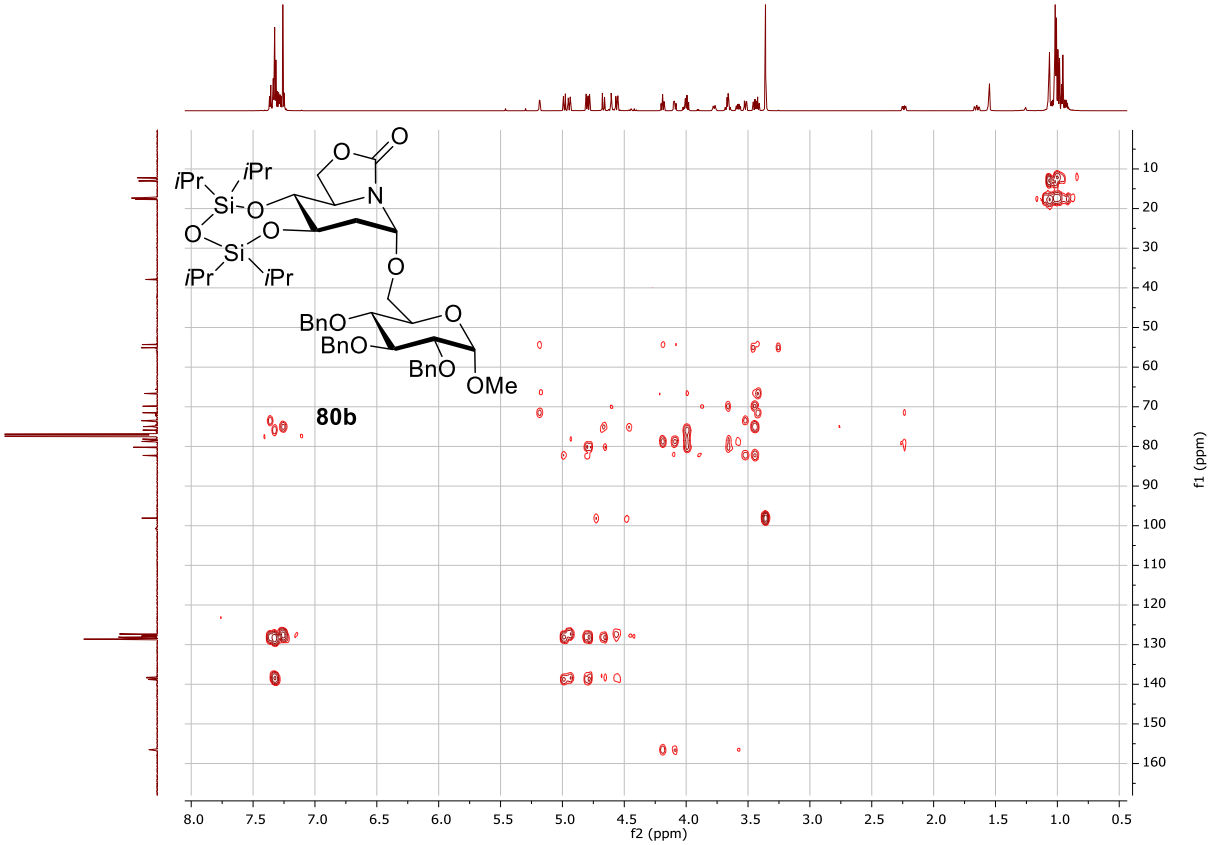

Figure 8.147. HMBC spectra for 80b

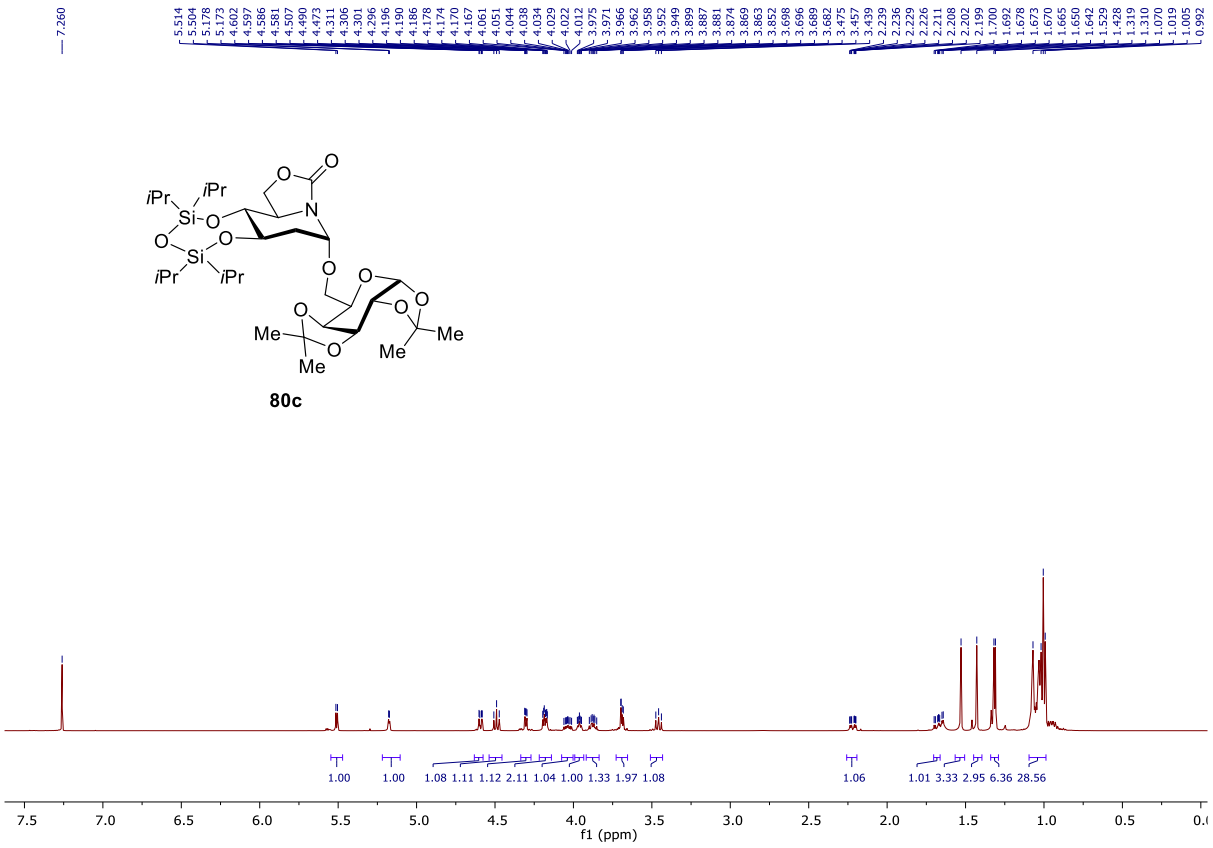

Figure 8.148. ^{1}H NMR spectra for 80c

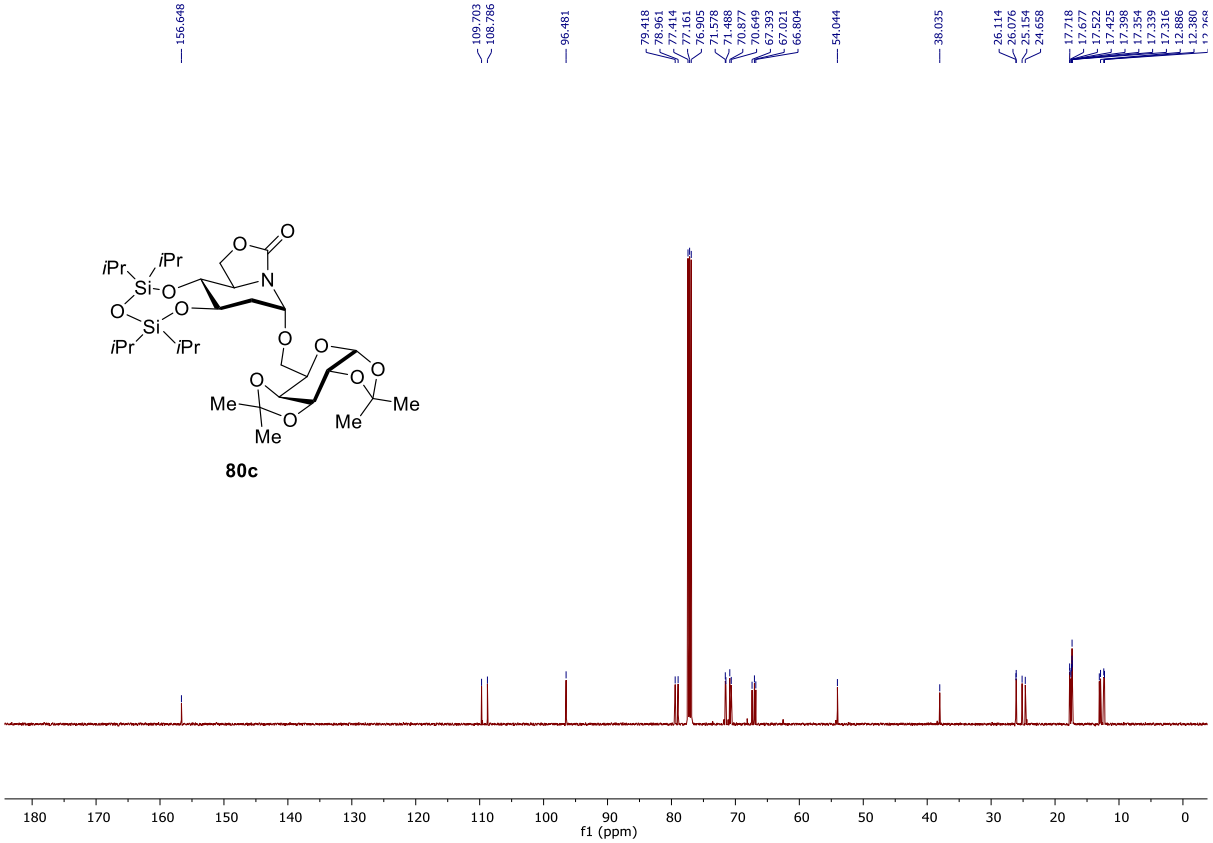

Figure 8.149. ^{13}C NMR spectra for 80c

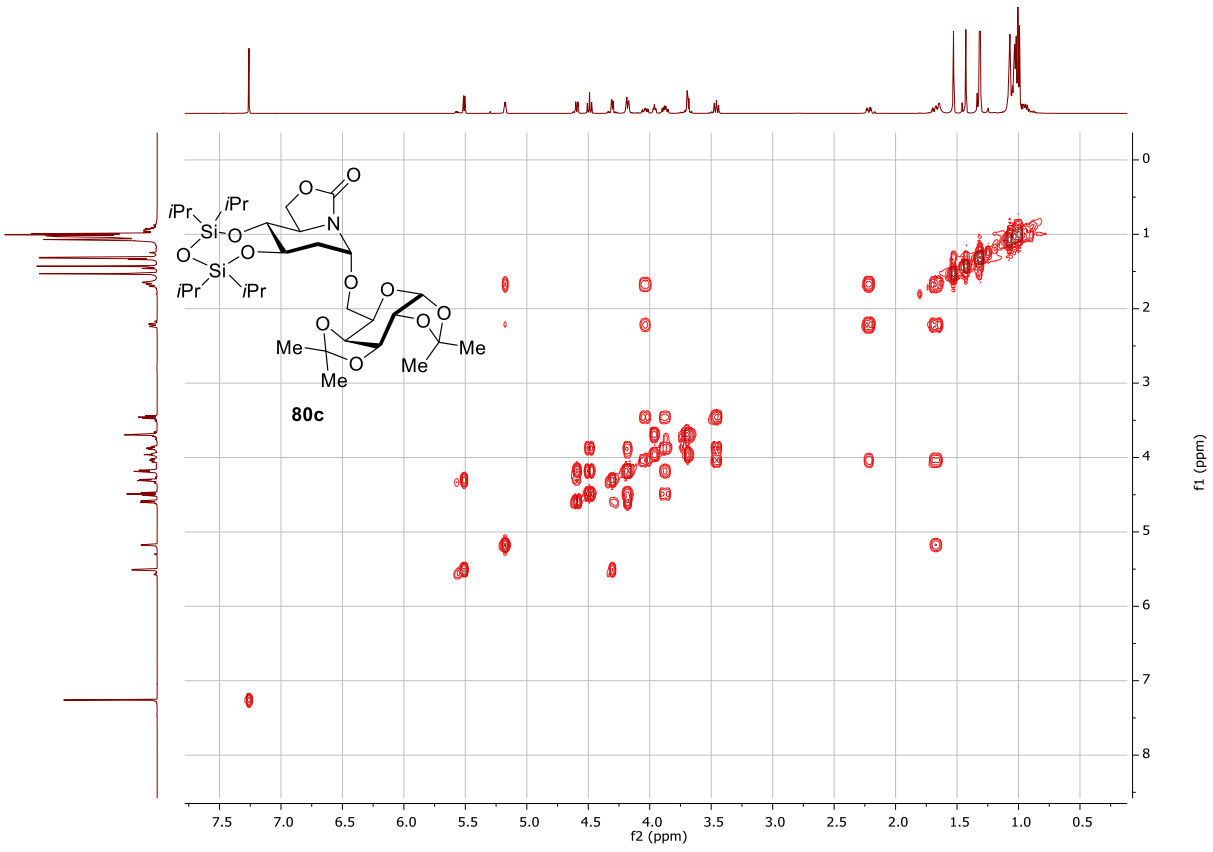

Figure 8.150. COSY spectra for 80c

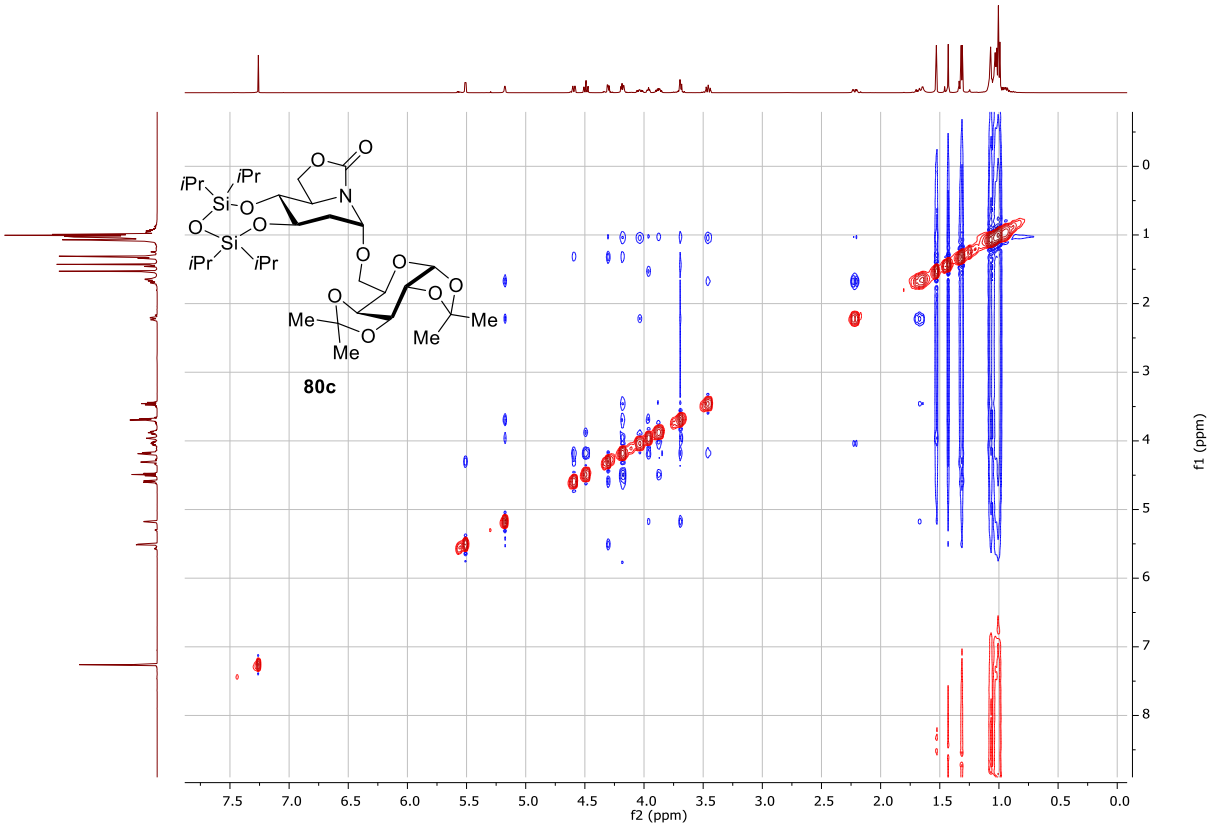

Figure 8.151. NOESY spectra for 80c

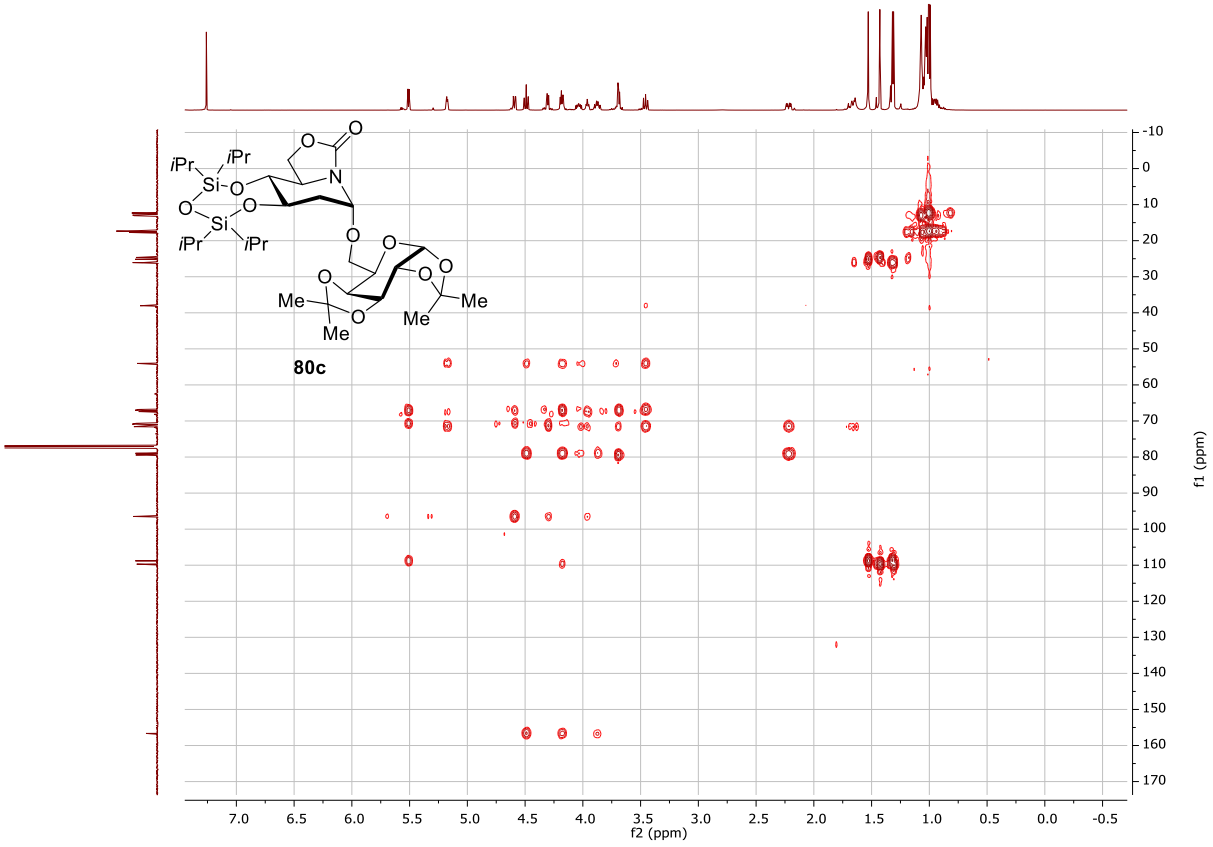

Figure 8.152. HMBC spectra for 80c

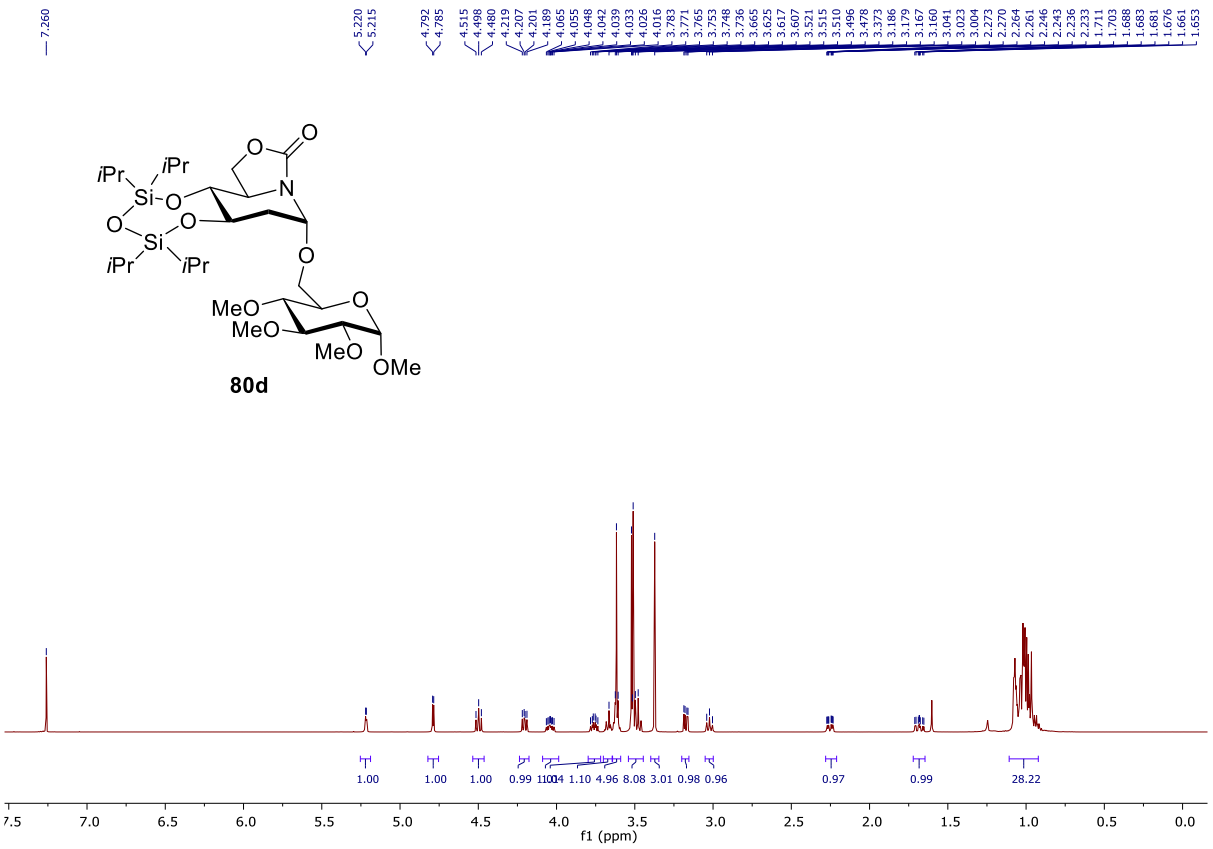

Figure 8.153. ^{1}H NMR spectra for 80d

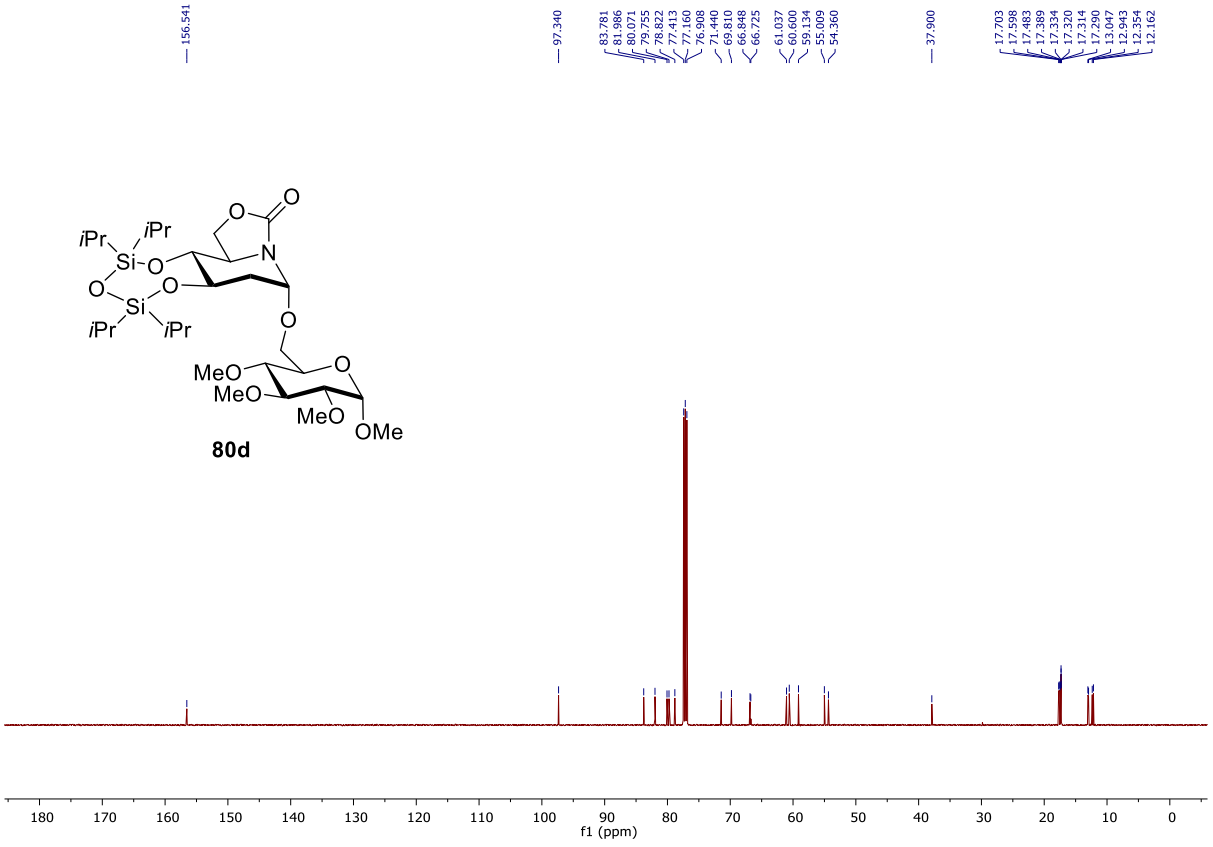

Figure 8.154. ^{13}C NMR spectra for 80d

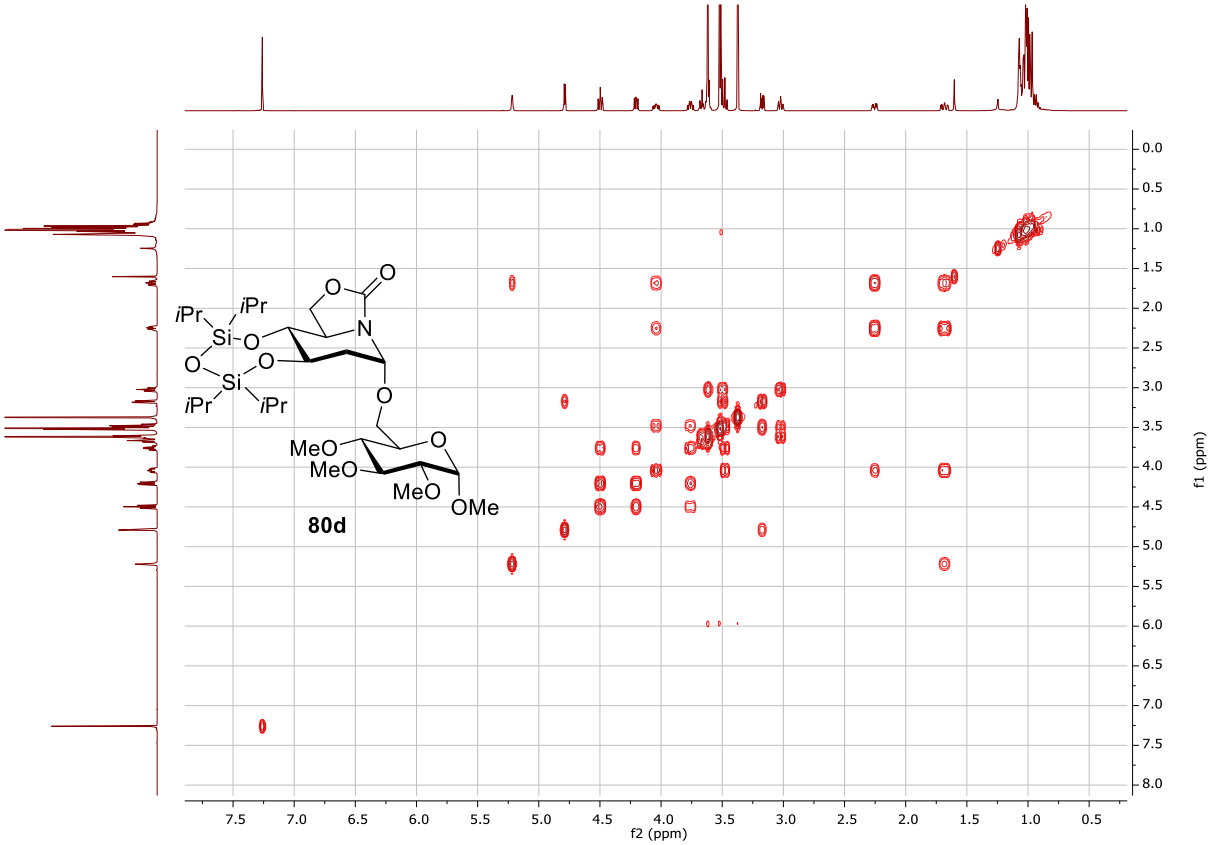

Figure 8.155. COSY spectra for 80d

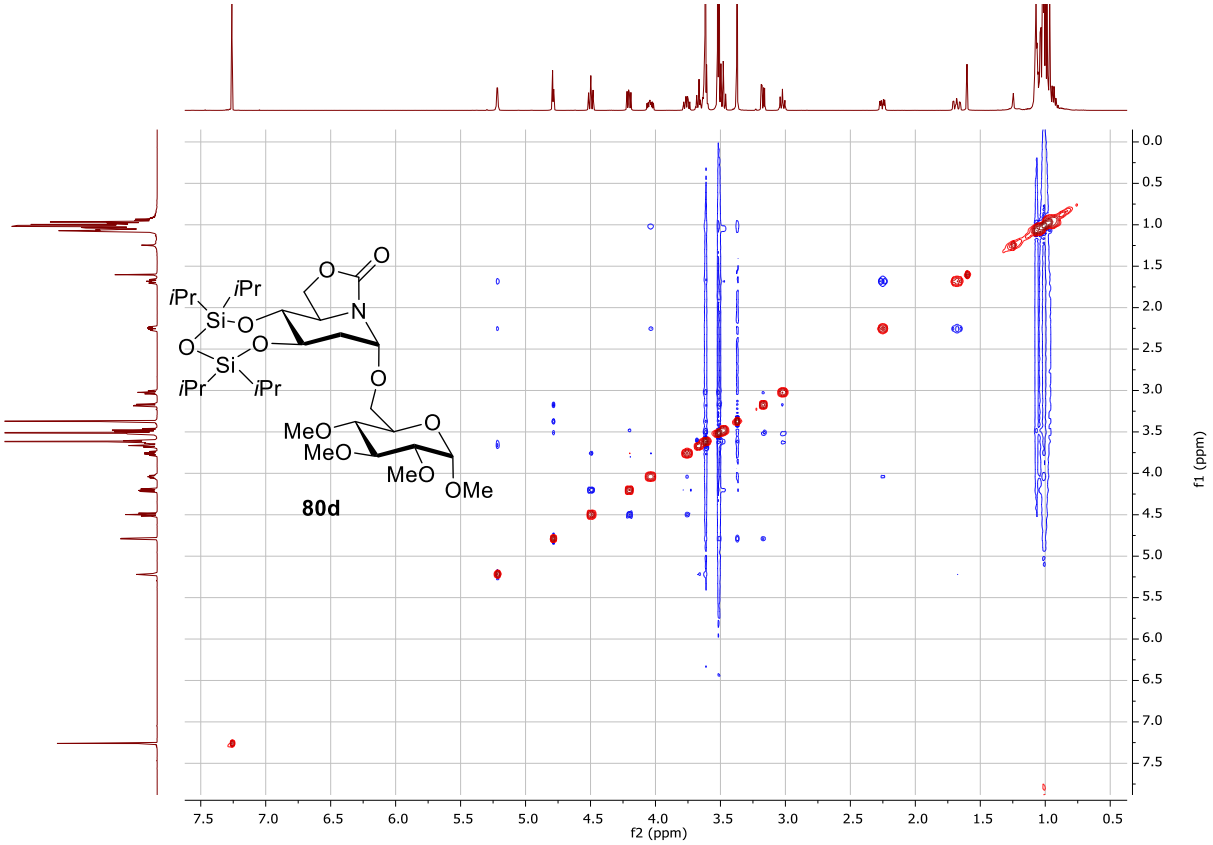

Figure 8.156. NOESY spectra for 80d

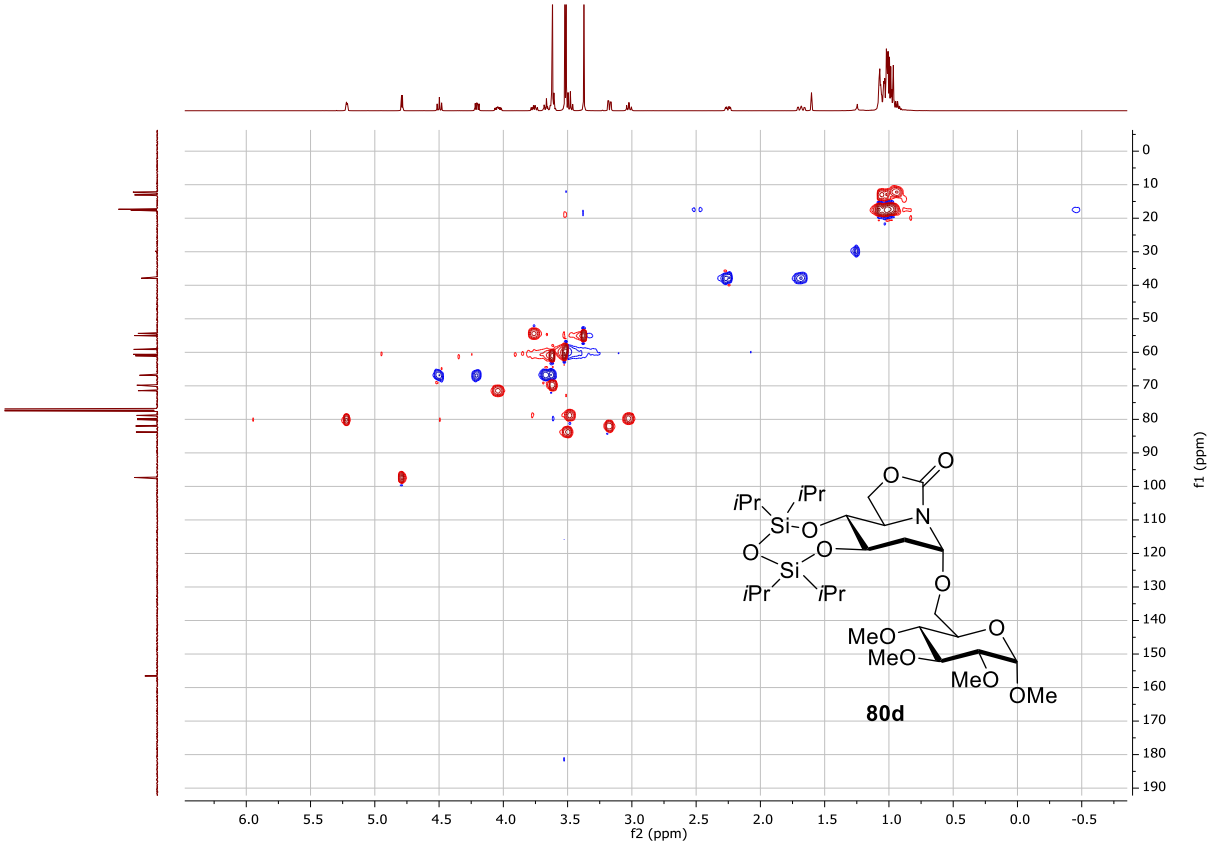

Figure 8.157. HSQC spectra for 80d

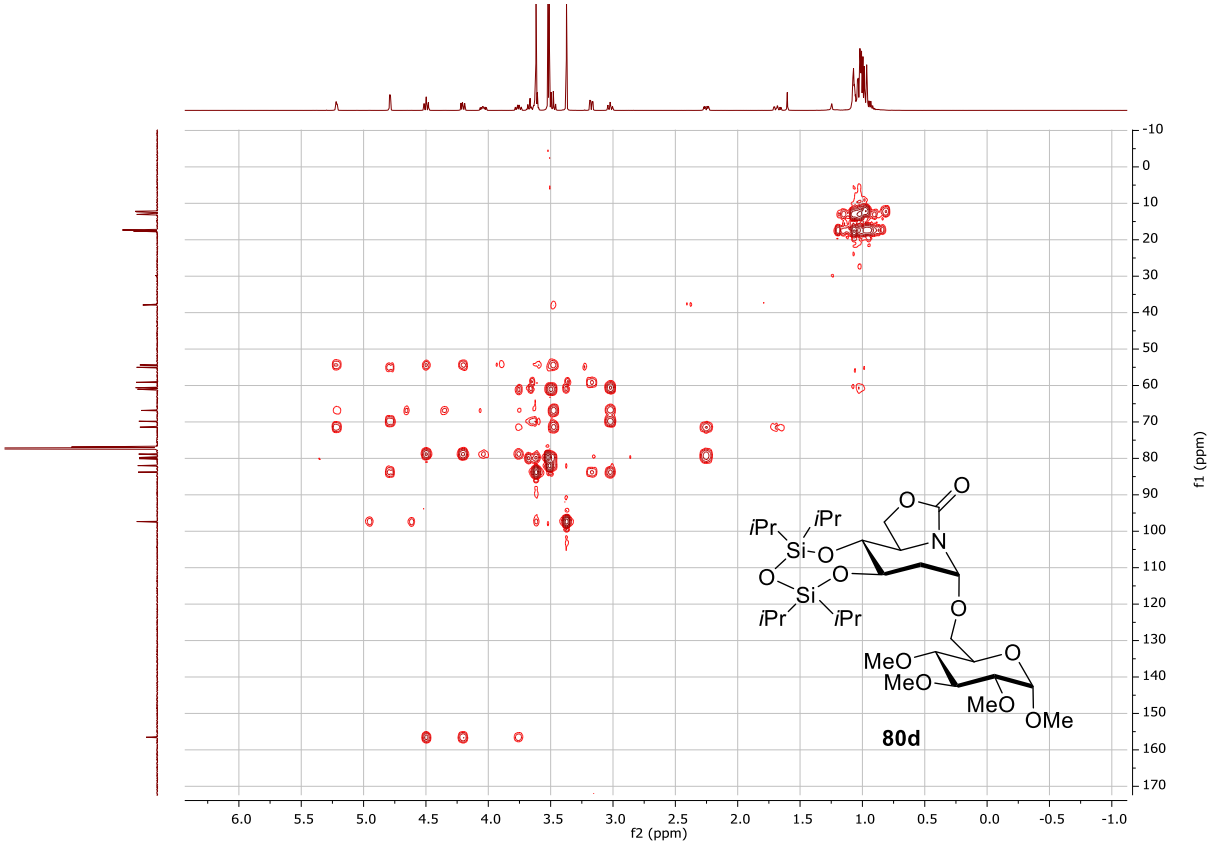

Figure 8.158. HMBC spectra for 80d

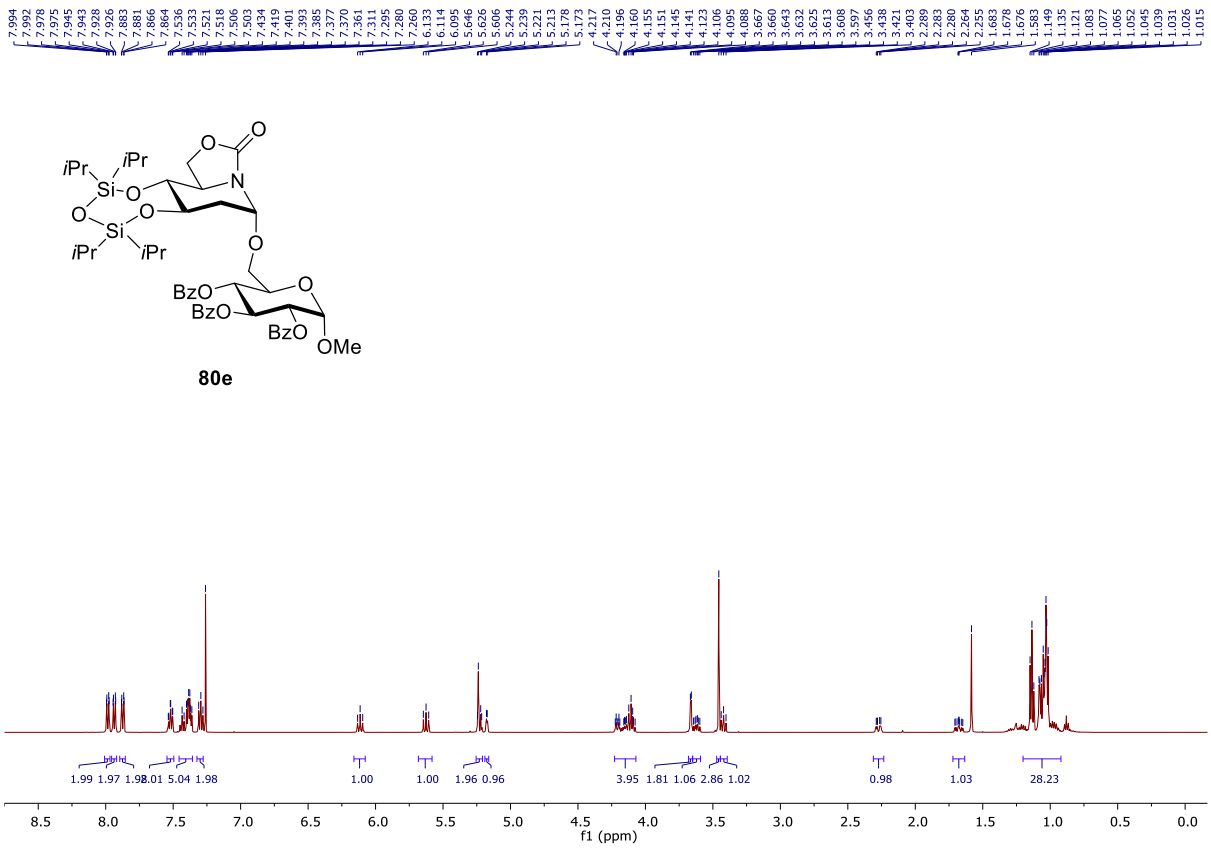

Figure 8.159. ^{1}H NMR spectra for 80e

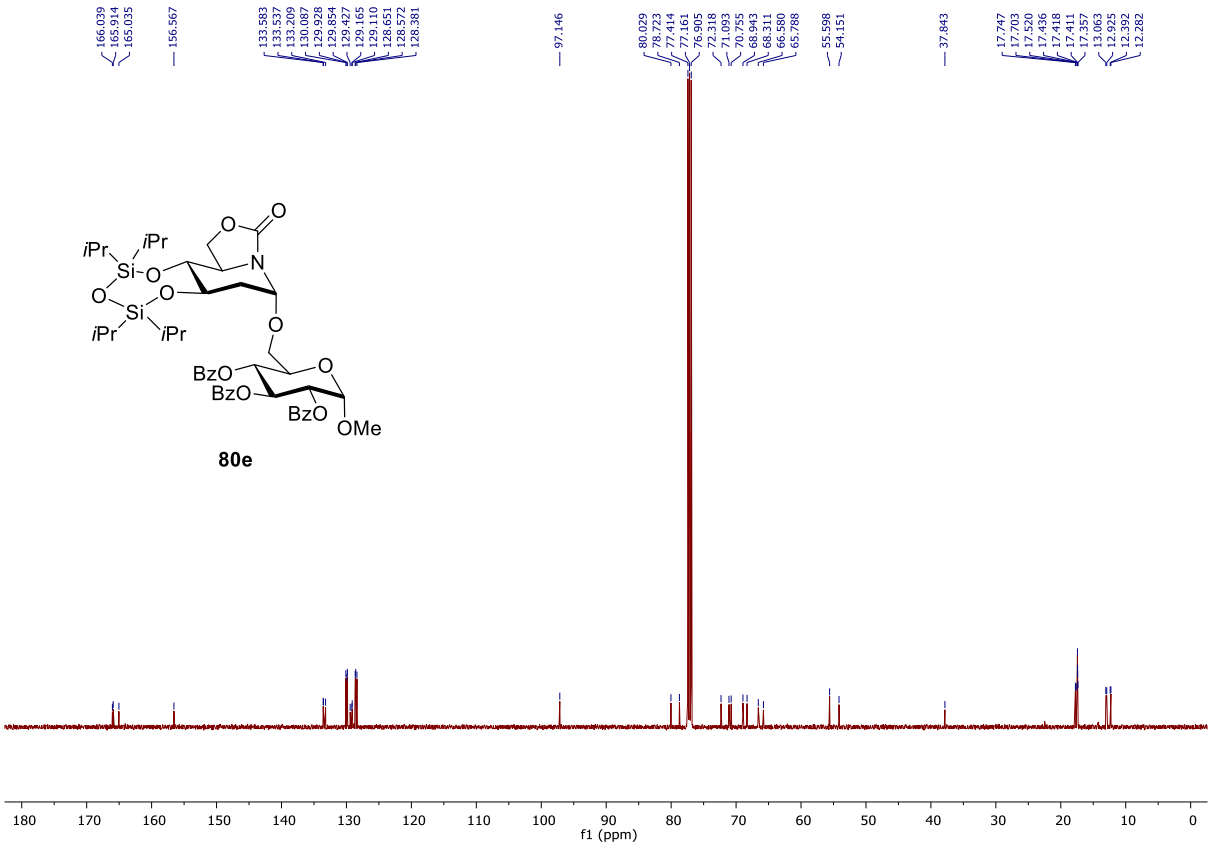

Figure 8.160. ^{13}C NMR spectra for 80e

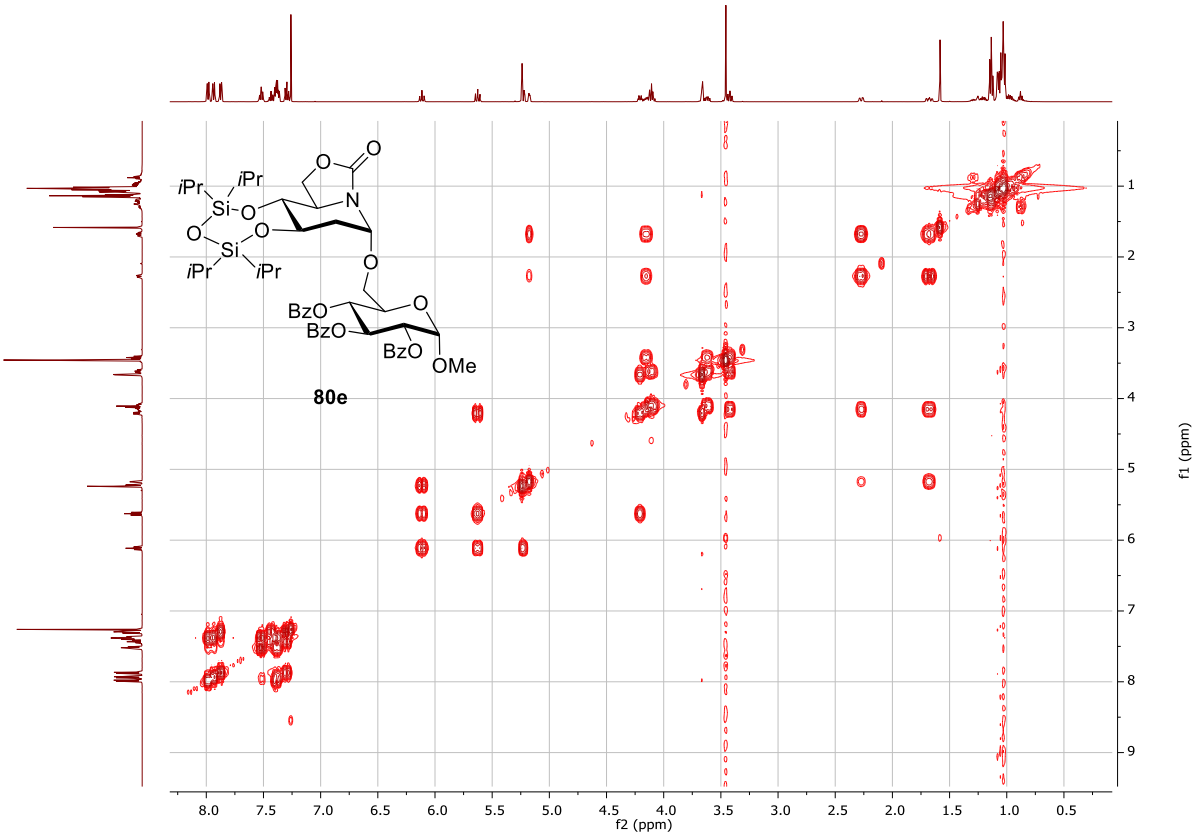

Figure 8.161. COSY spectra for 80e

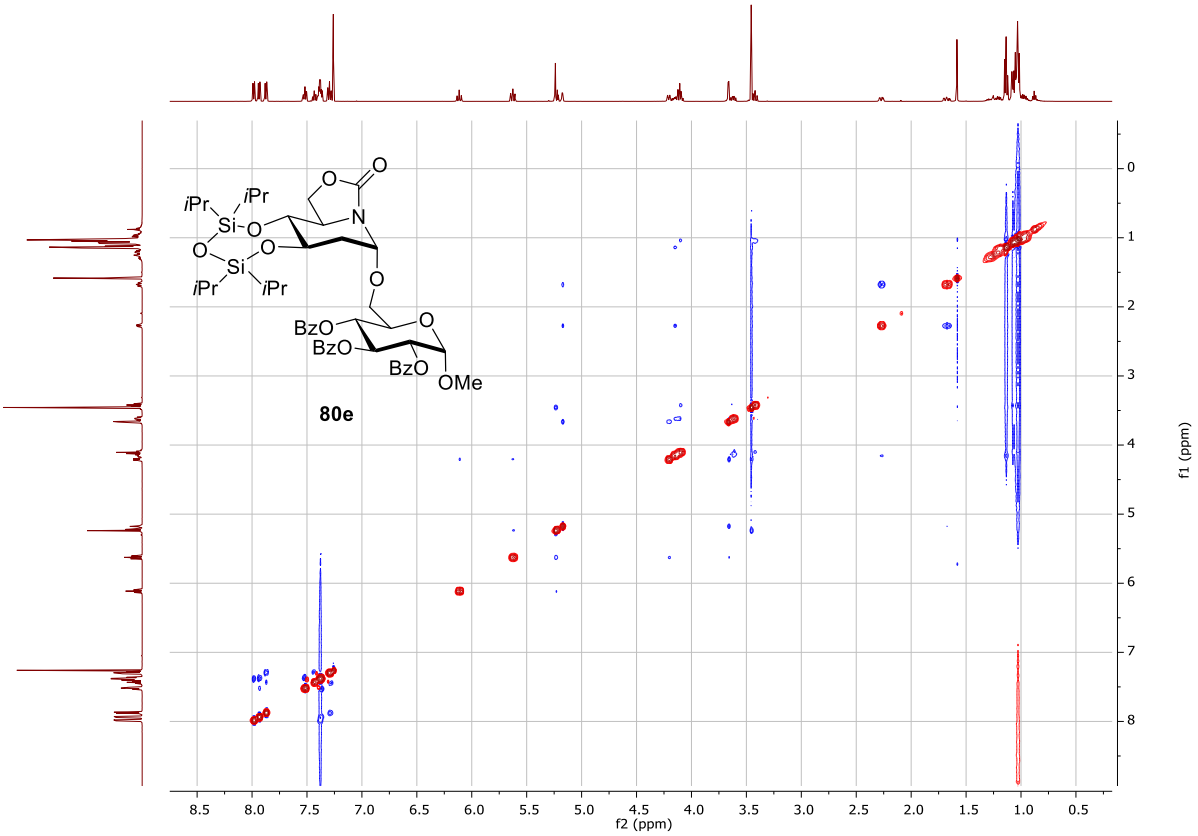

Figure 8.162. NOESY spectra for 80e

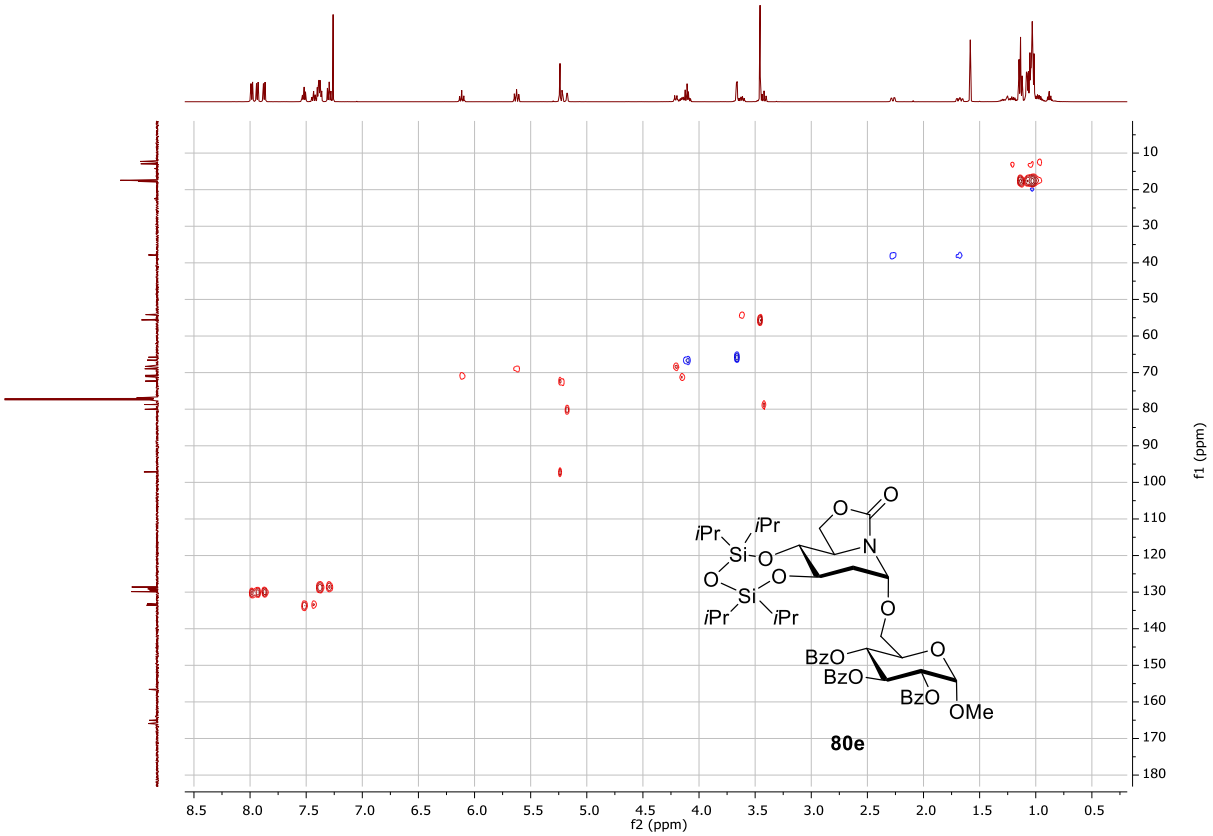

Figure 8.163. HSQC spectra for 80e

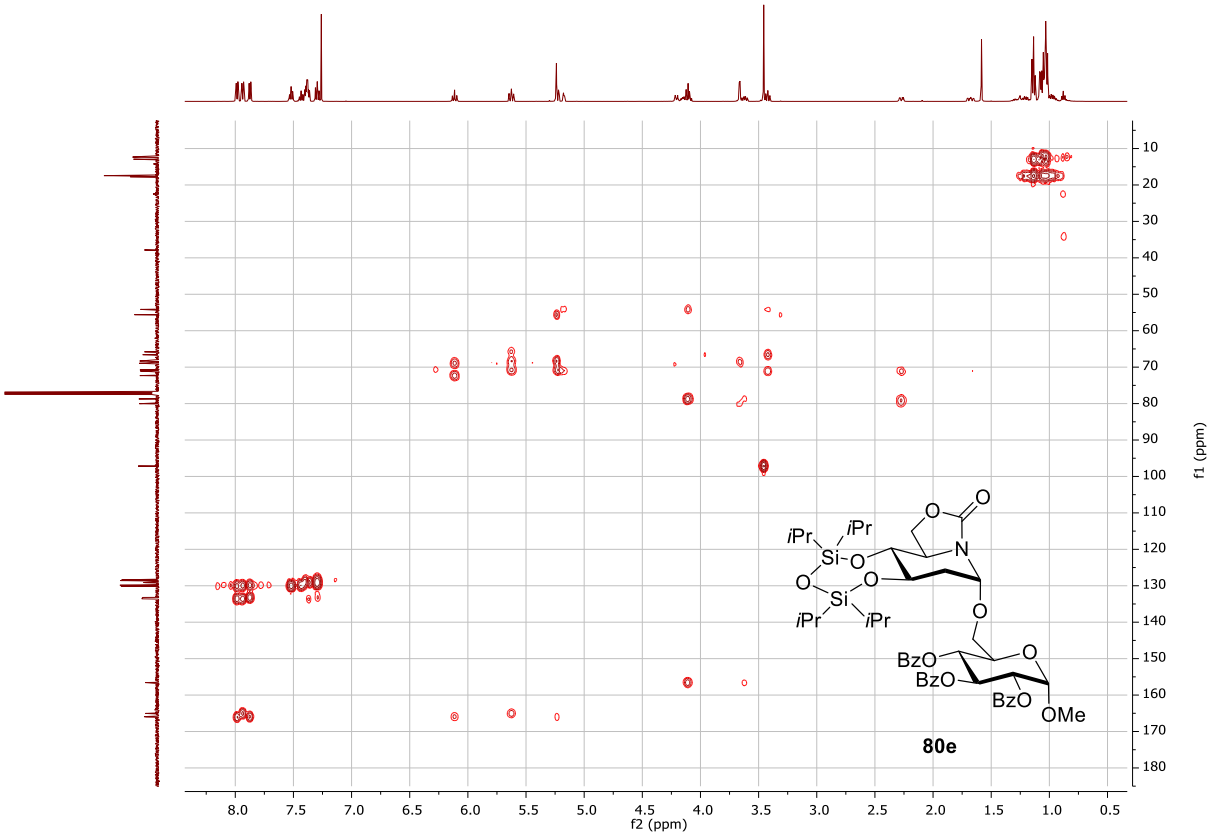

Figure 8.164. HMBC spectra for 80e

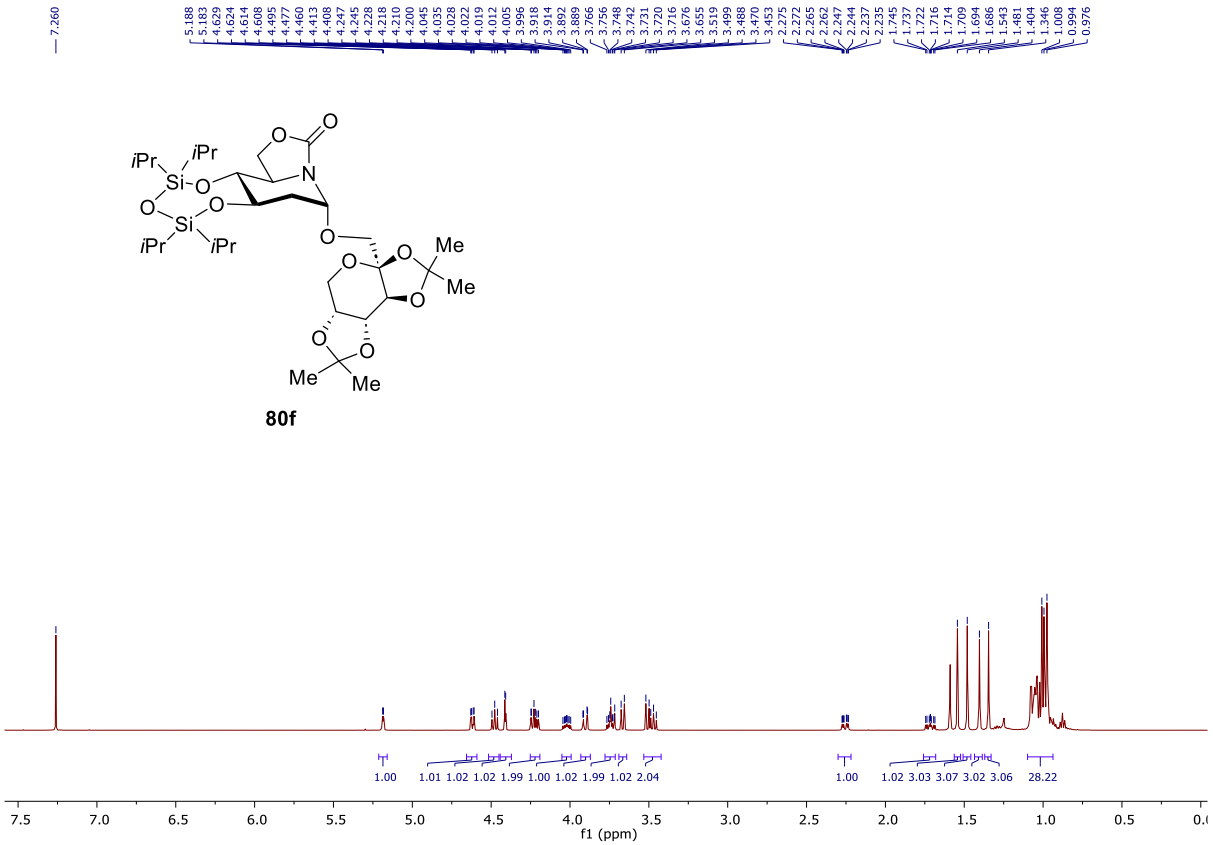

Figure 8.165. ^{1}H NMR spectra for 80f

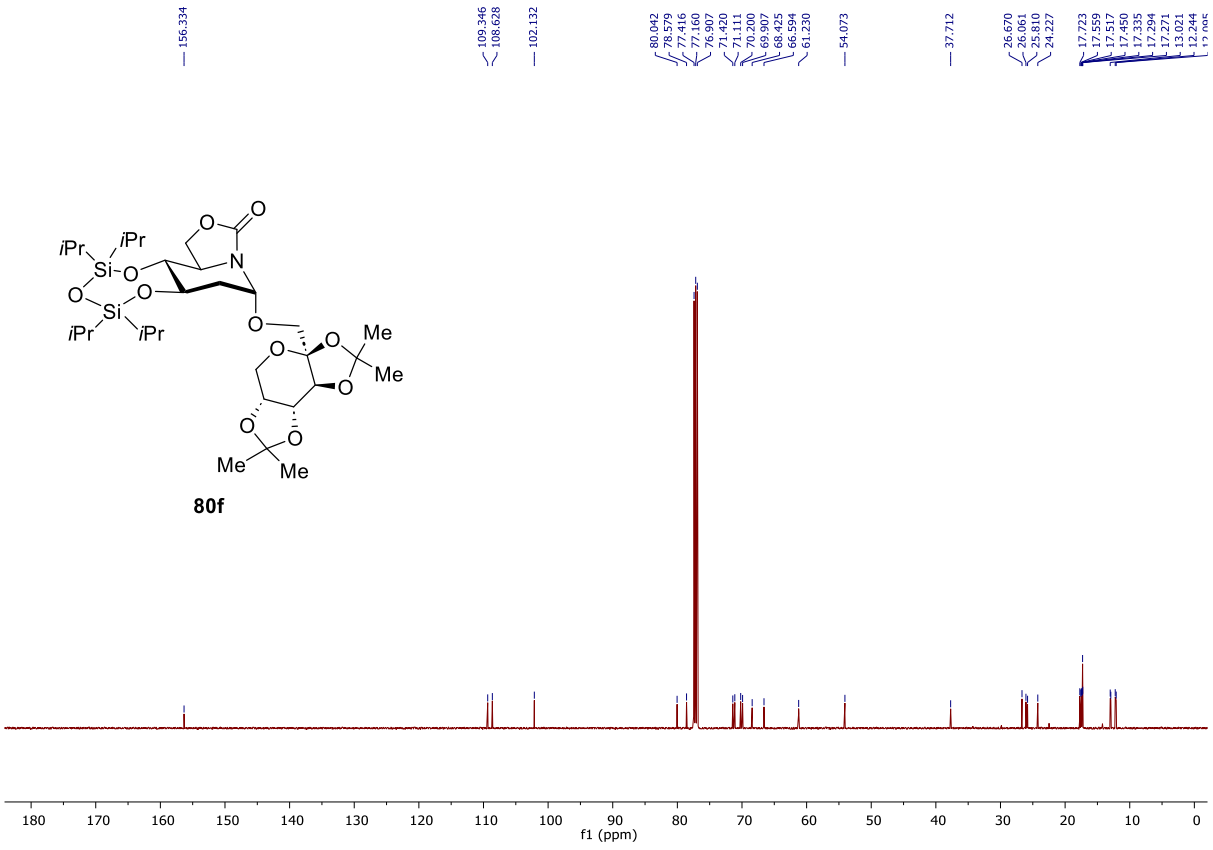

Figure 8.166. ^{13}C NMR spectra for 80f

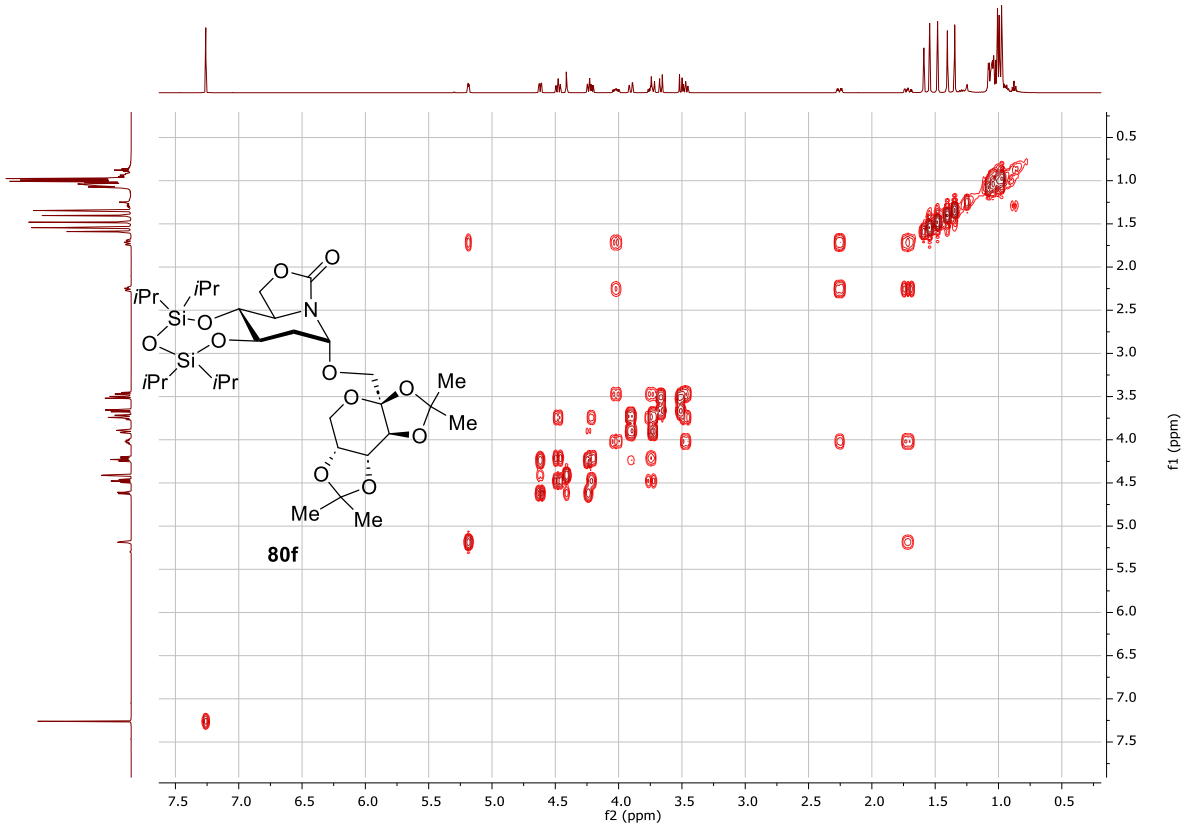

Figure 8.167. COSY spectra for 80f

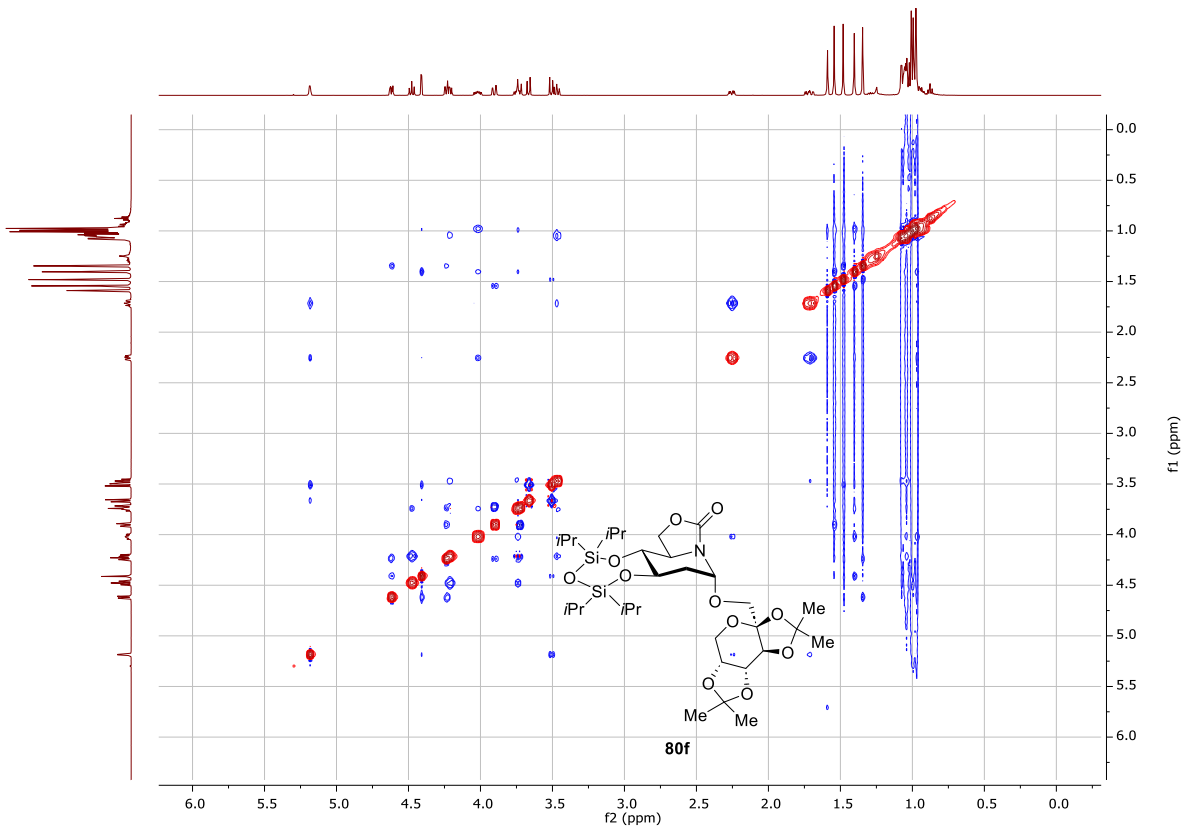

Figure 8.168. NOESY spectra for 80f

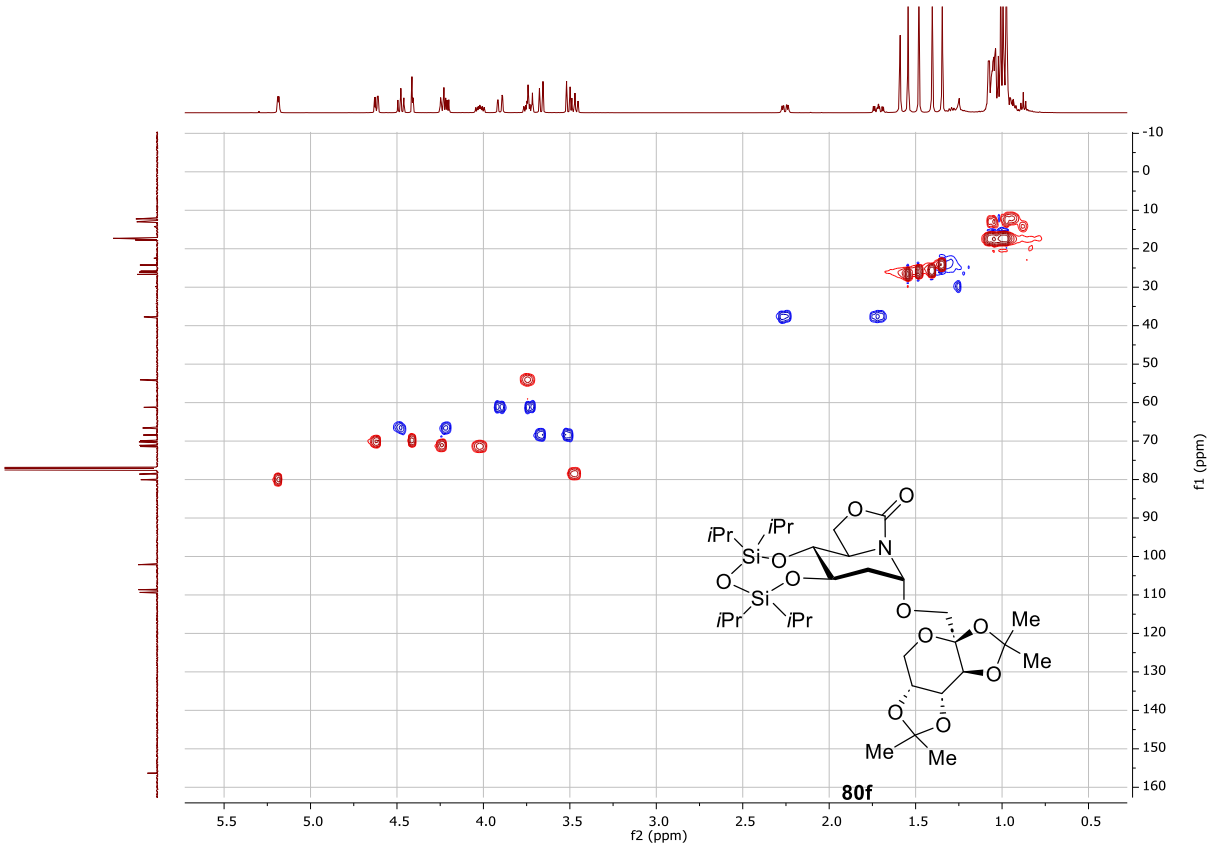

Figure 8.169. HSQC spectra for 80f

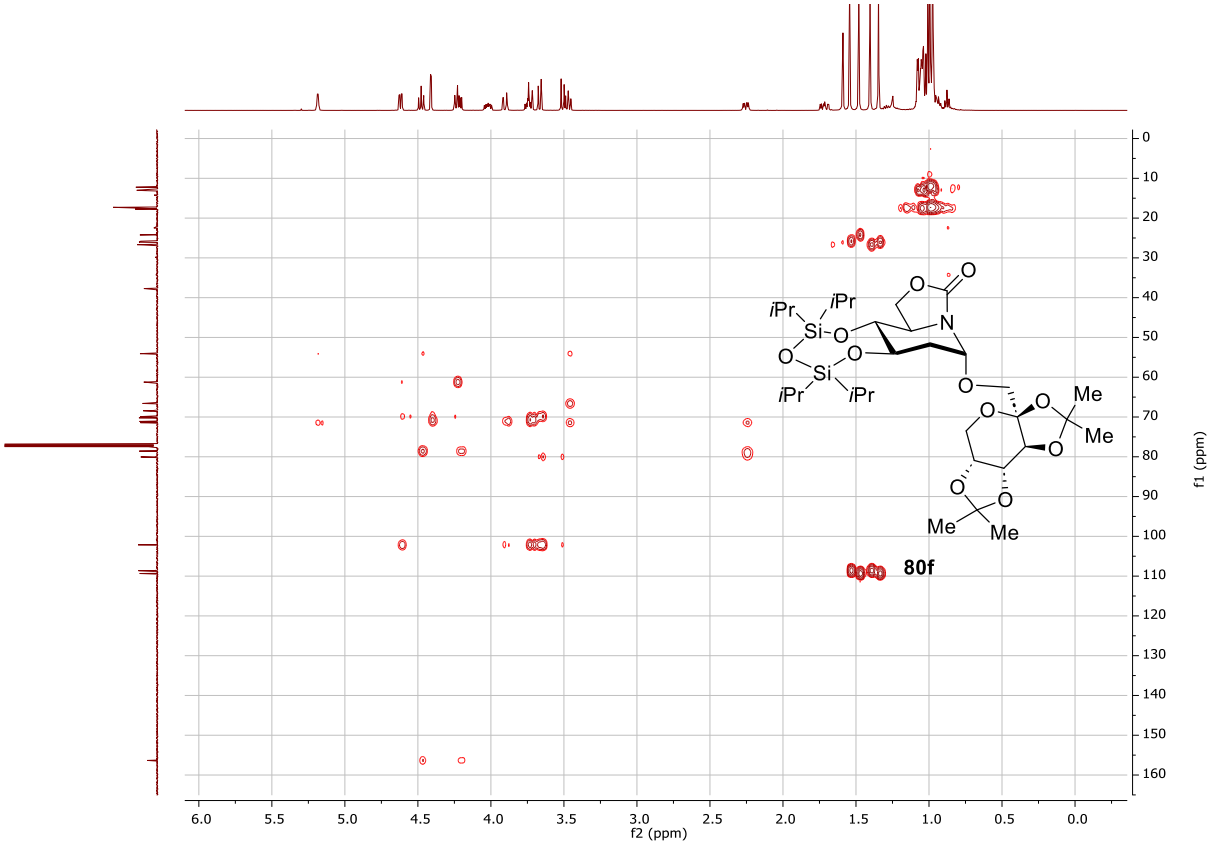

Figure 8.170. HMBC spectra for 80f

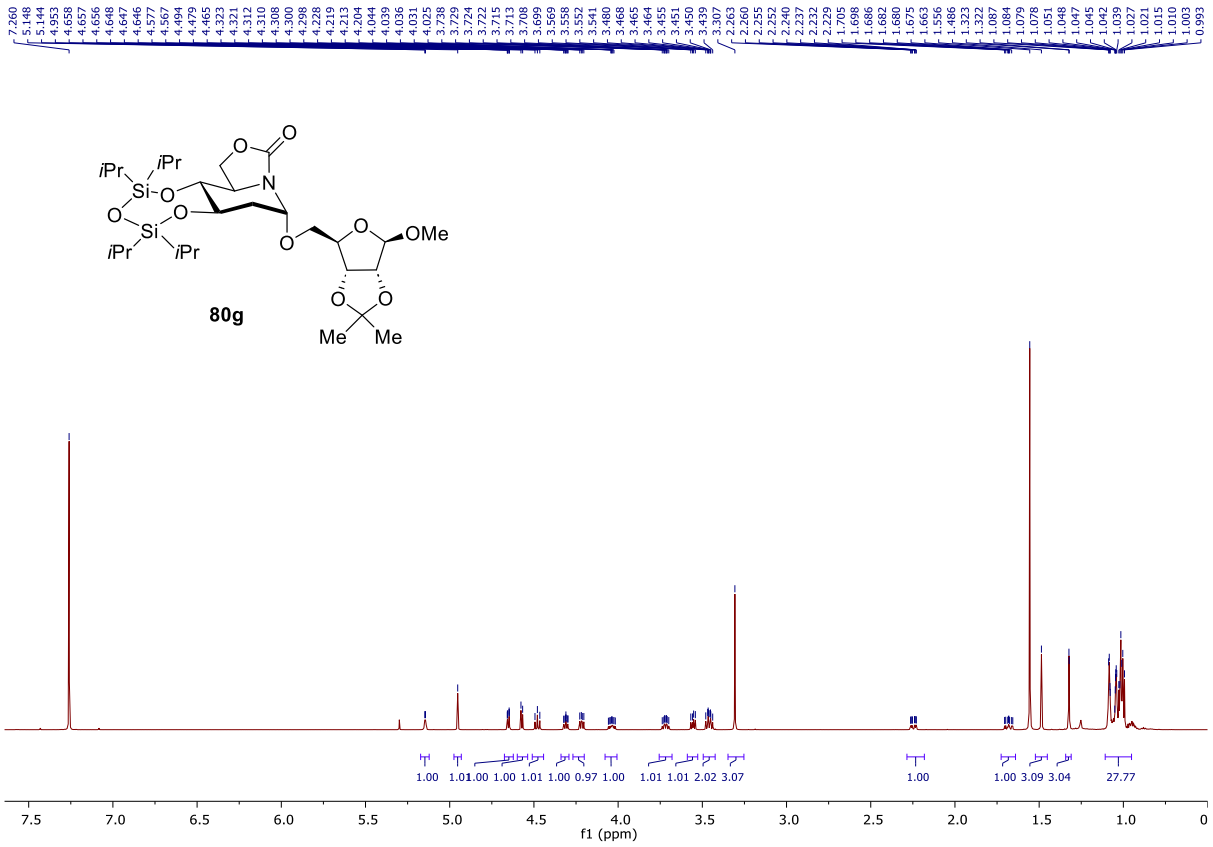

Figure 8.171. ^{1}H NMR spectra for 80g

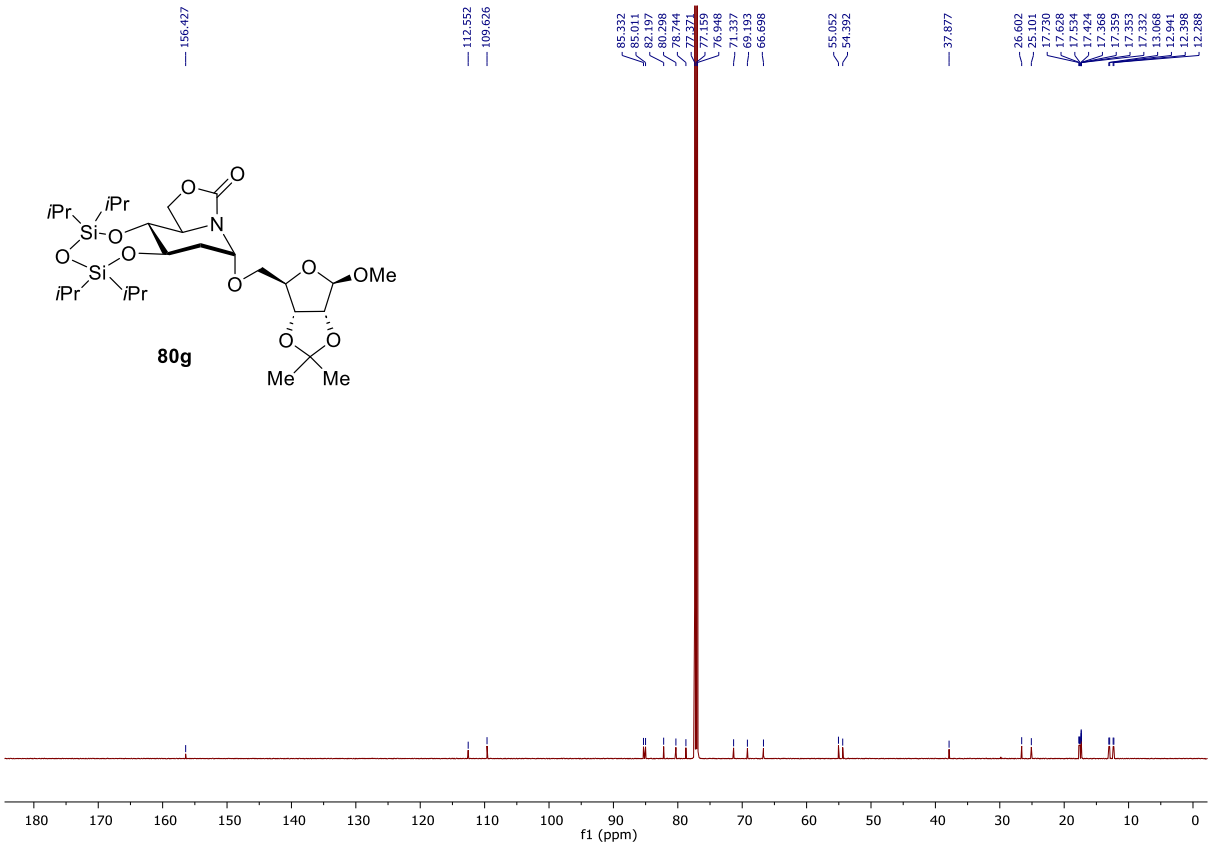

Figure 8.172. ^{13}C NMR spectra for 80g

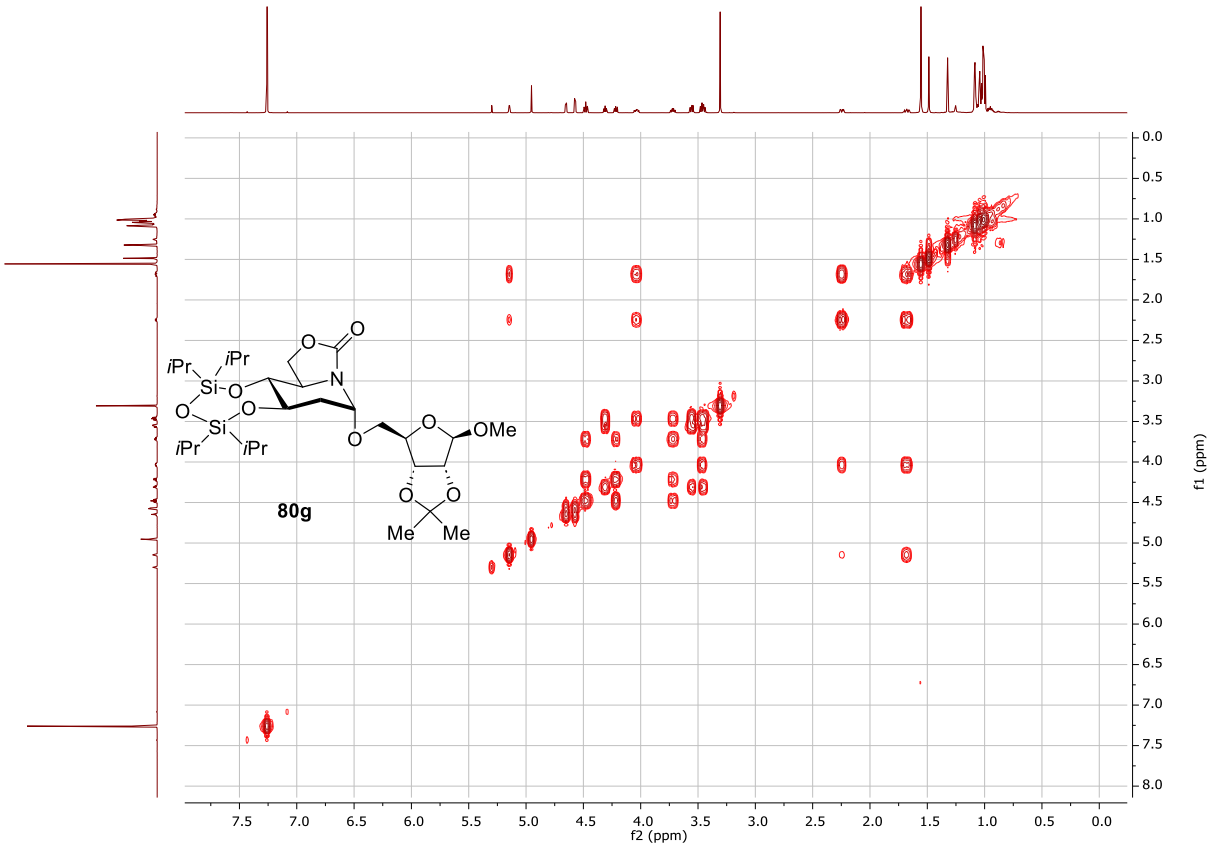

Figure 8.173. COSY spectra for 80g

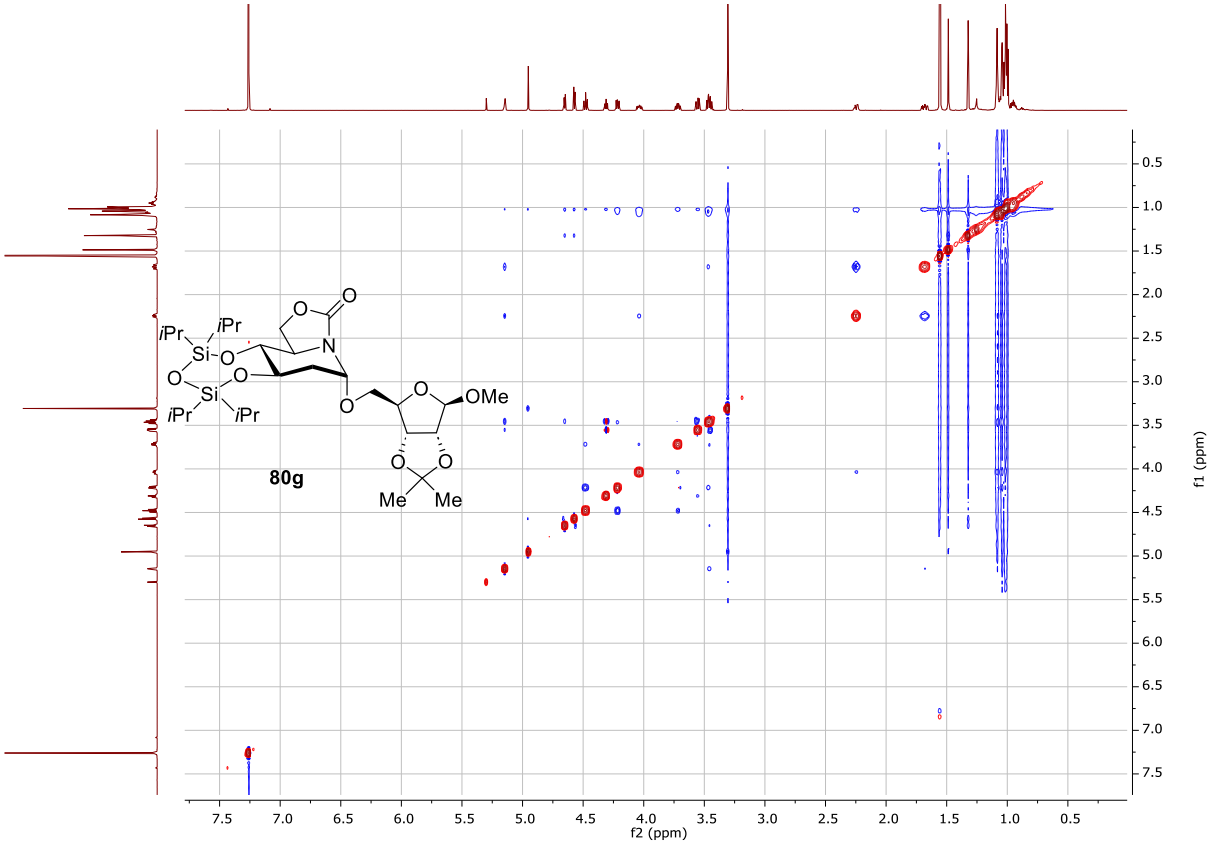

Figure 8.174. NOESY spectra for 80g

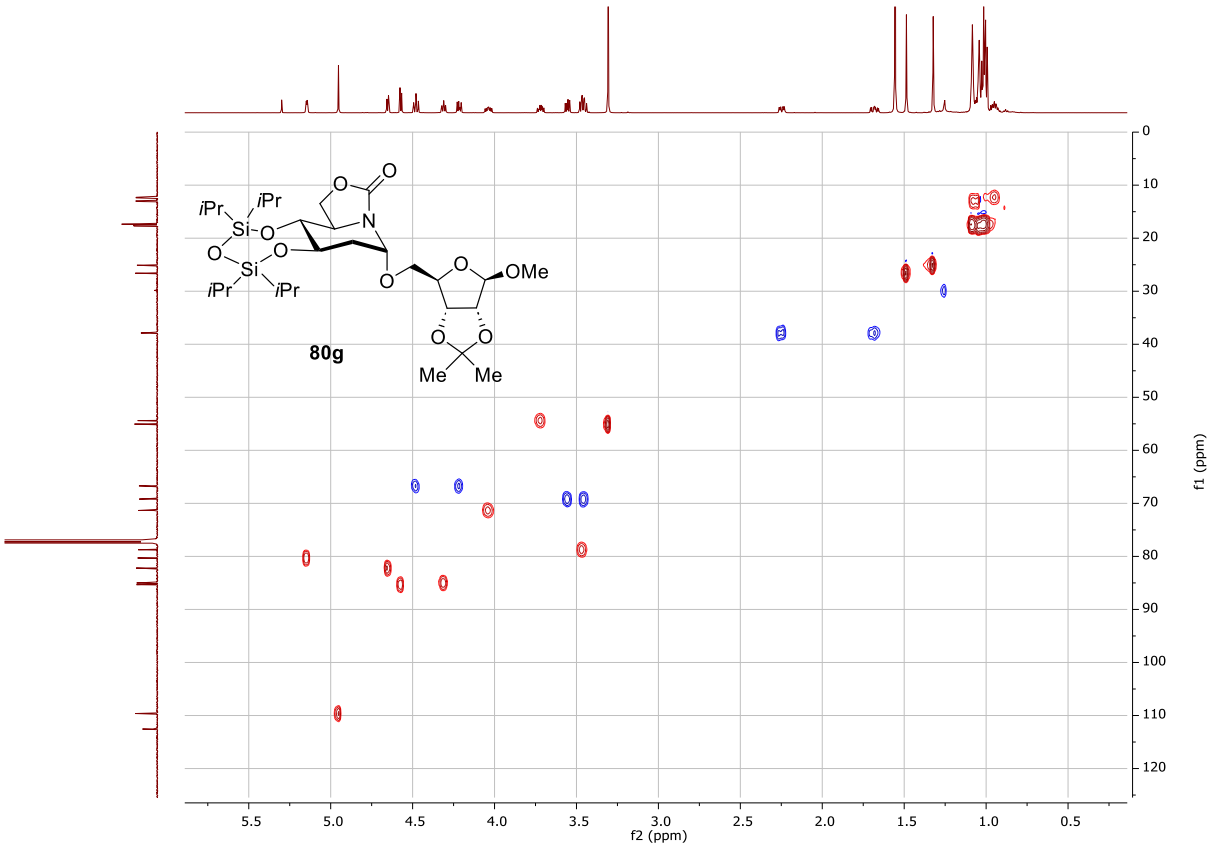

Figure 8.175. HSQC spectra for 80g

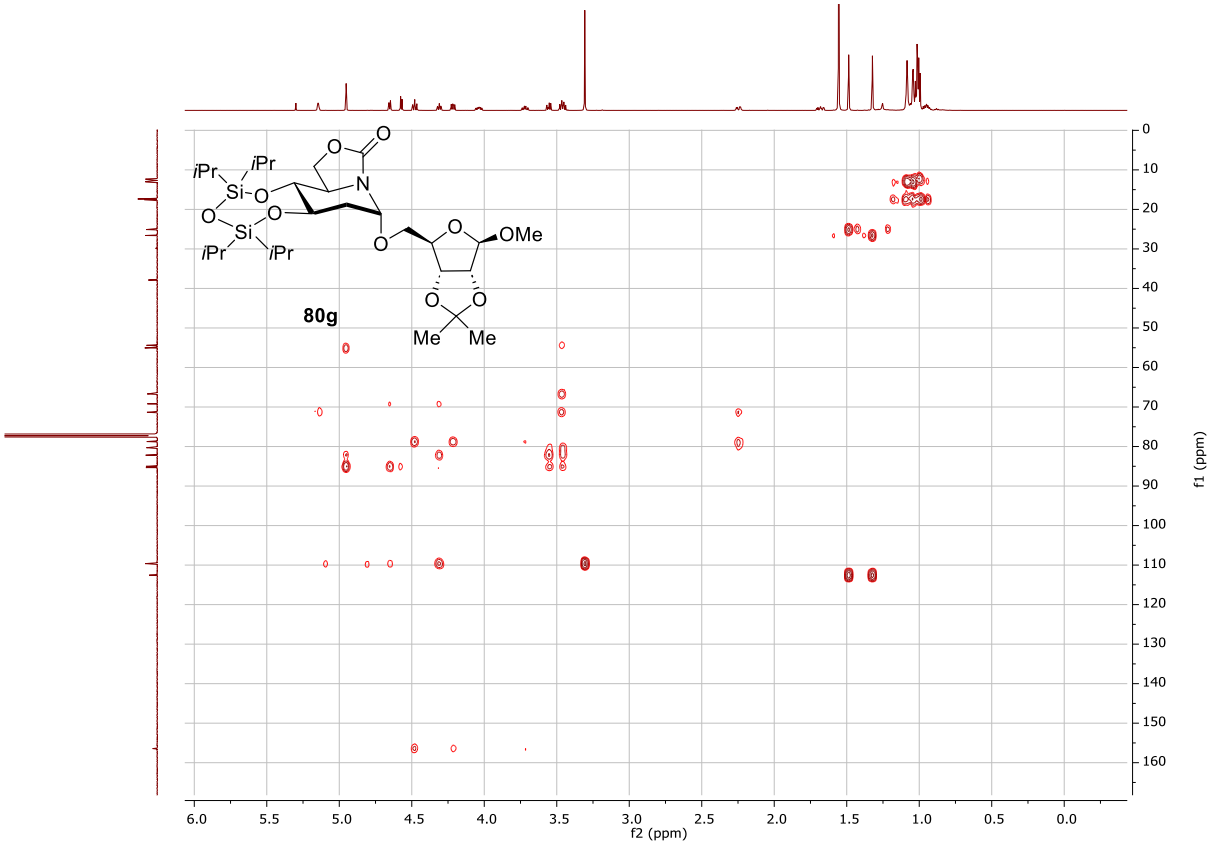

Figure 8.176. HMBC spectra for 80g

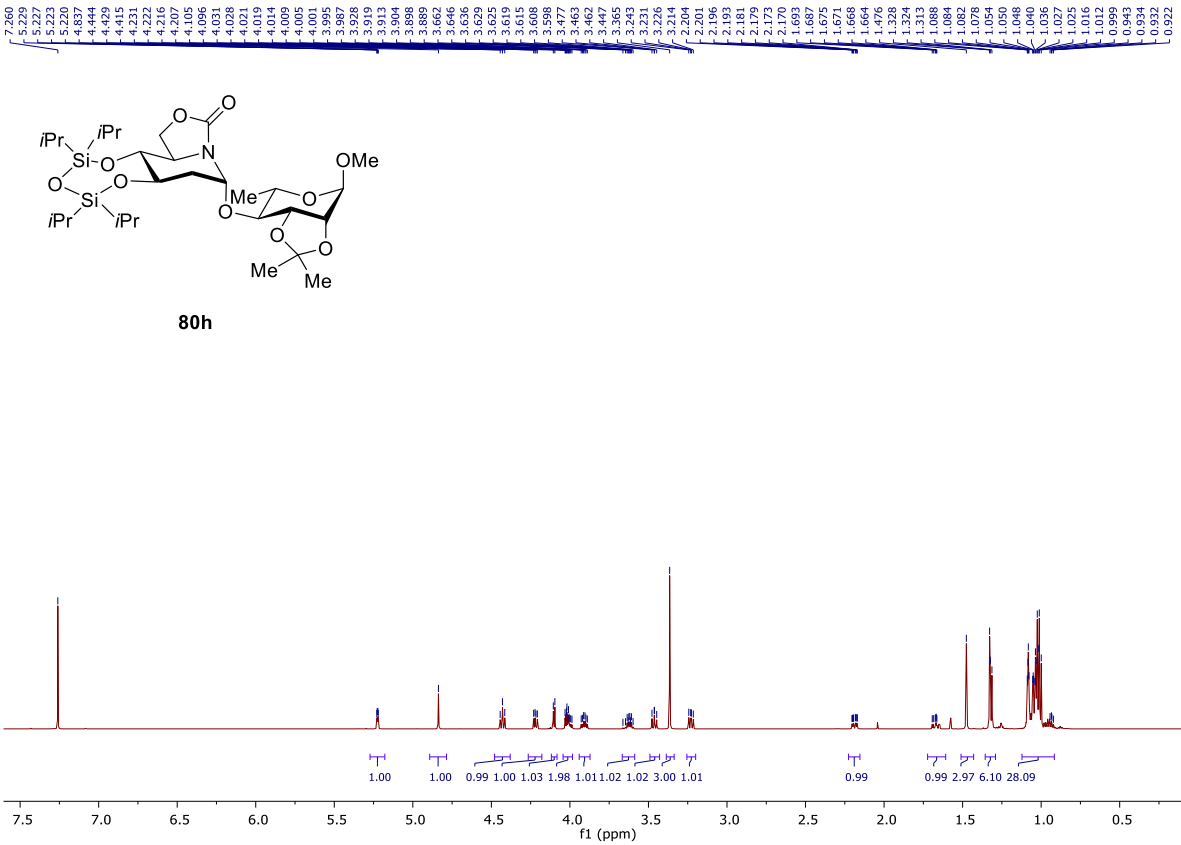

80h

Figure 8.177. ^{1}H NMR spectra for 80h

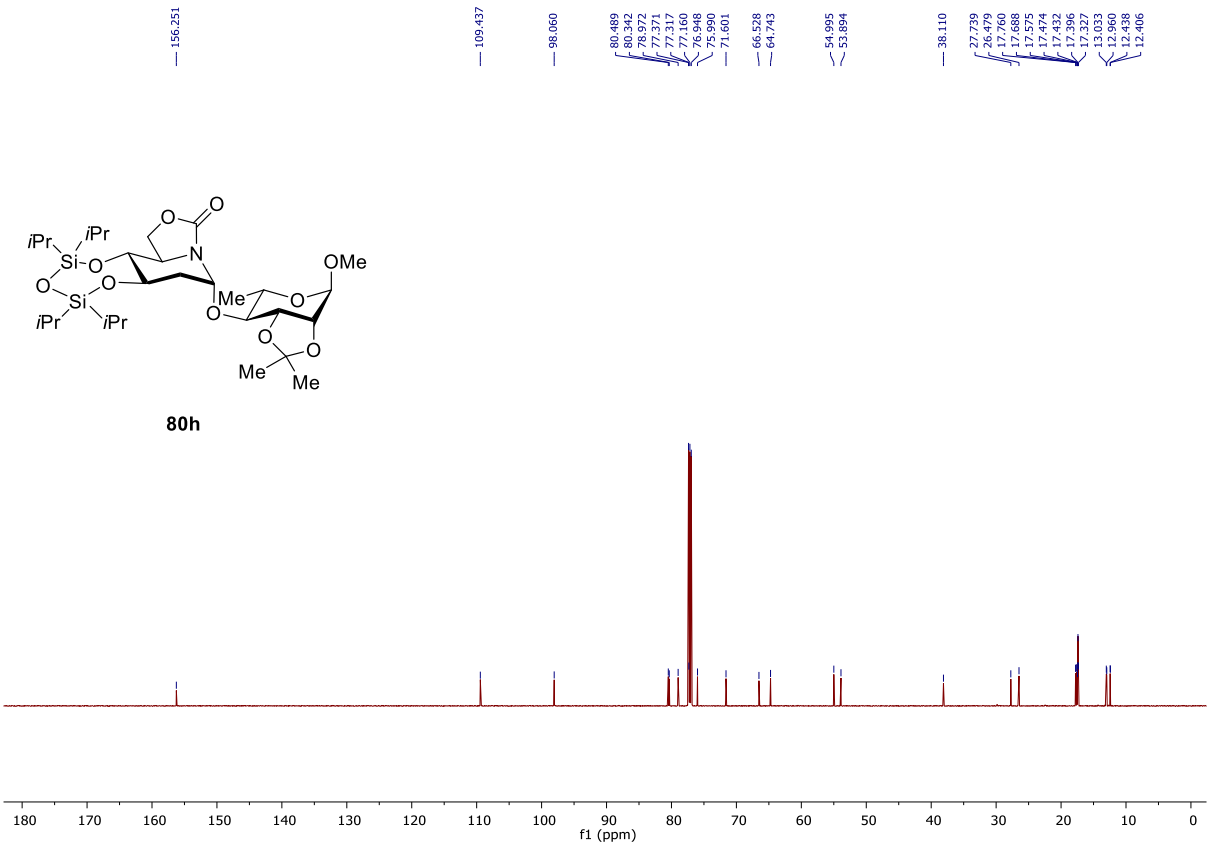

80h

Figure 8.178. ^{13}C NMR spectra for 80h

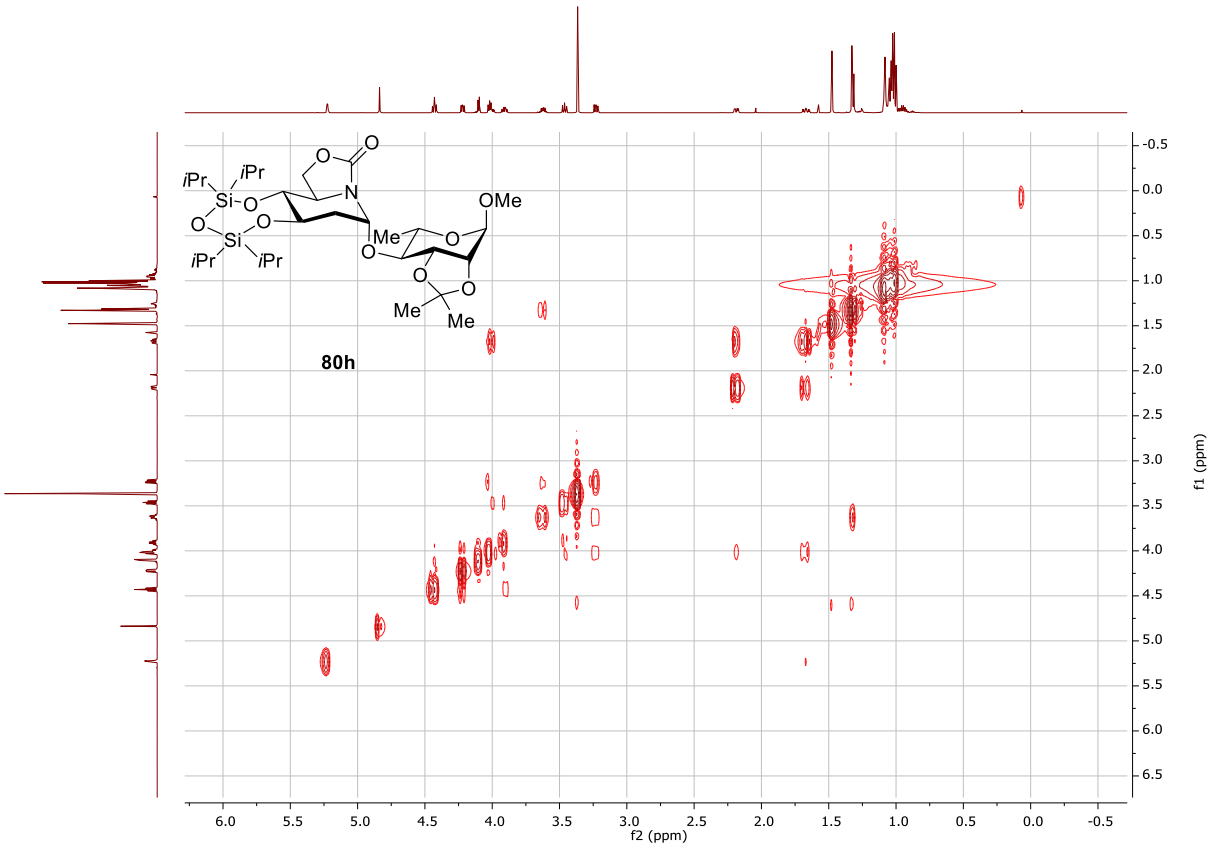

Figure 8.179. COSY spectra for 80h

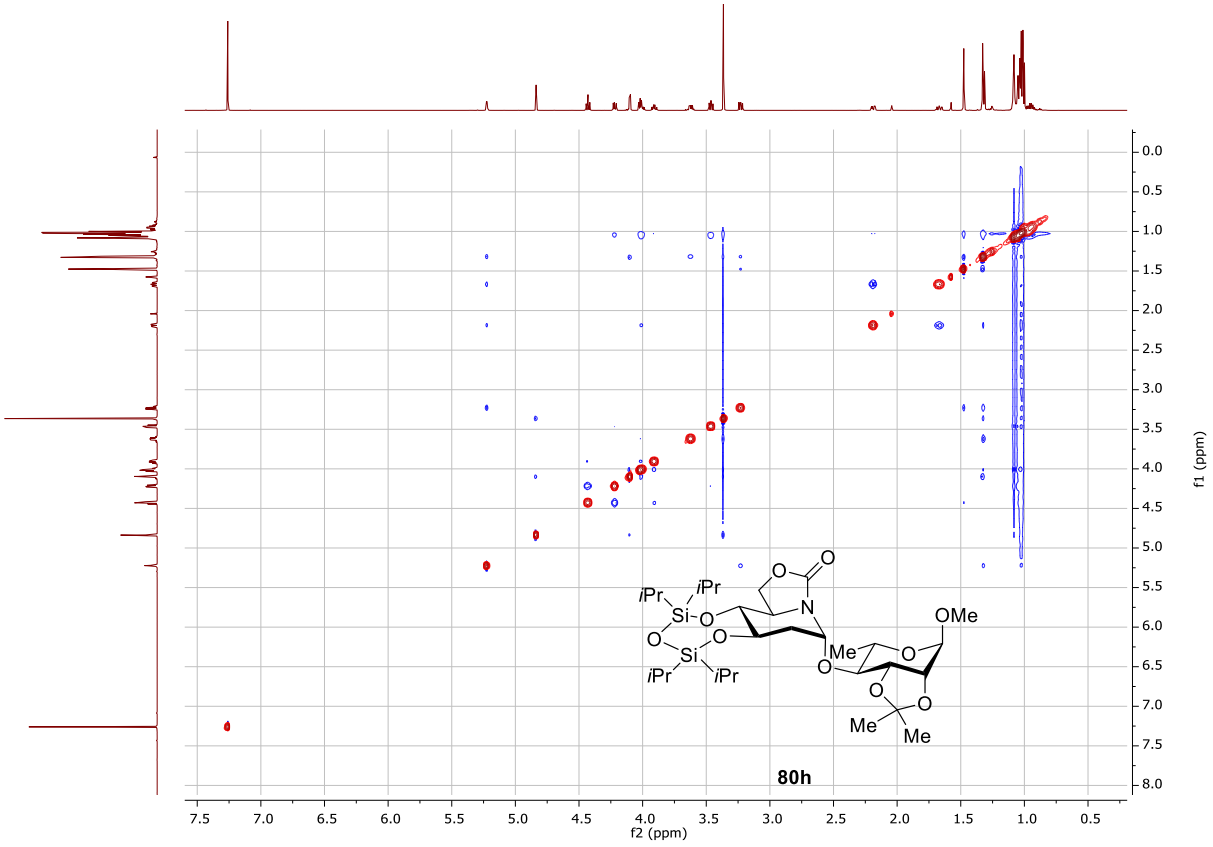

Figure 8.180. NOESY spectra for 80h

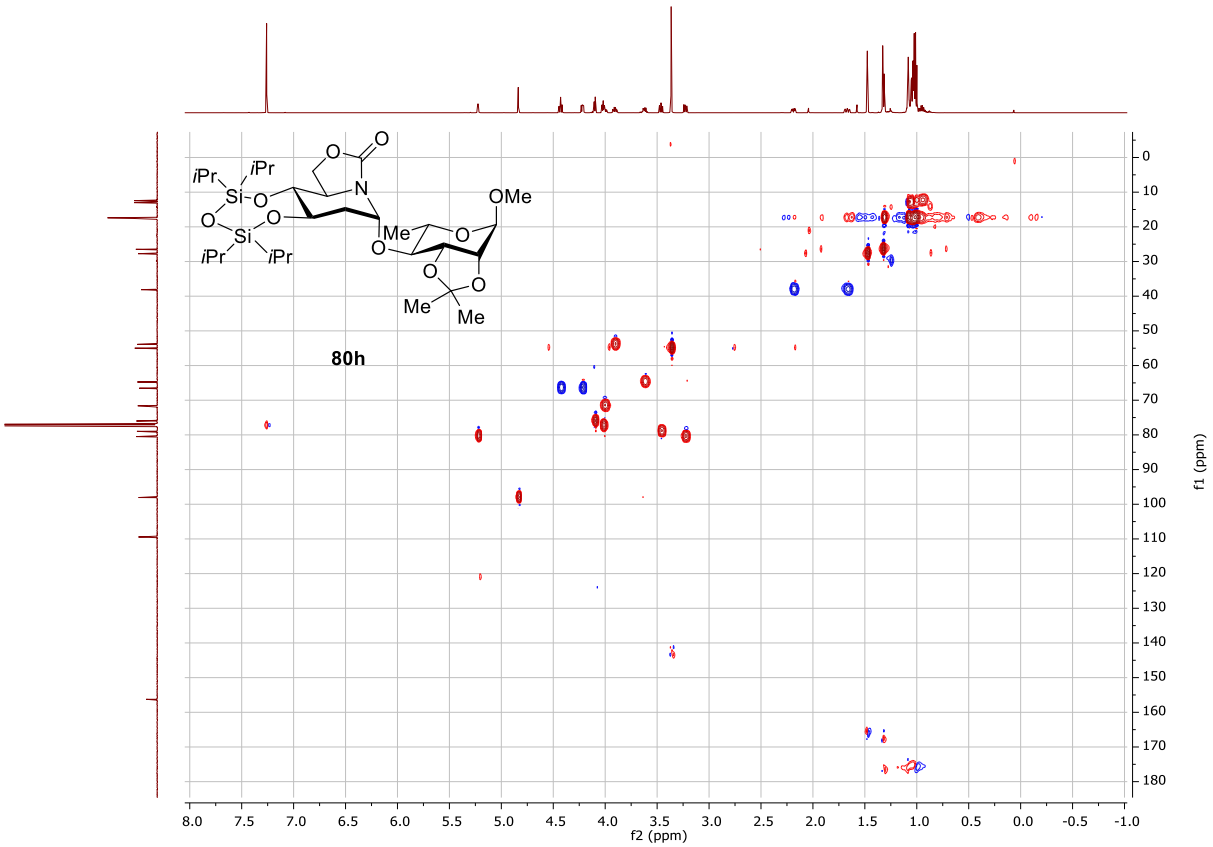

Figure 8.181. HSQC spectra for 80h

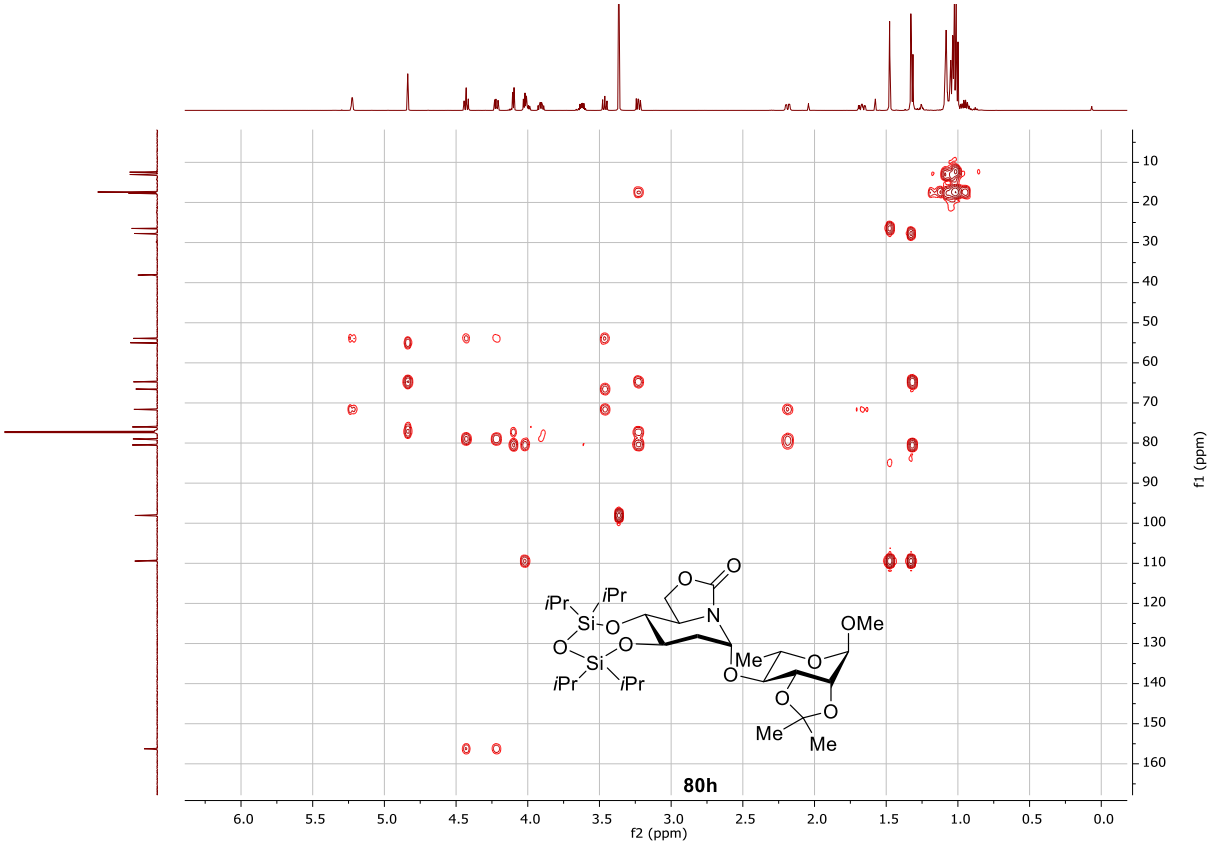

Figure 8.182. HMBC spectra for 80h

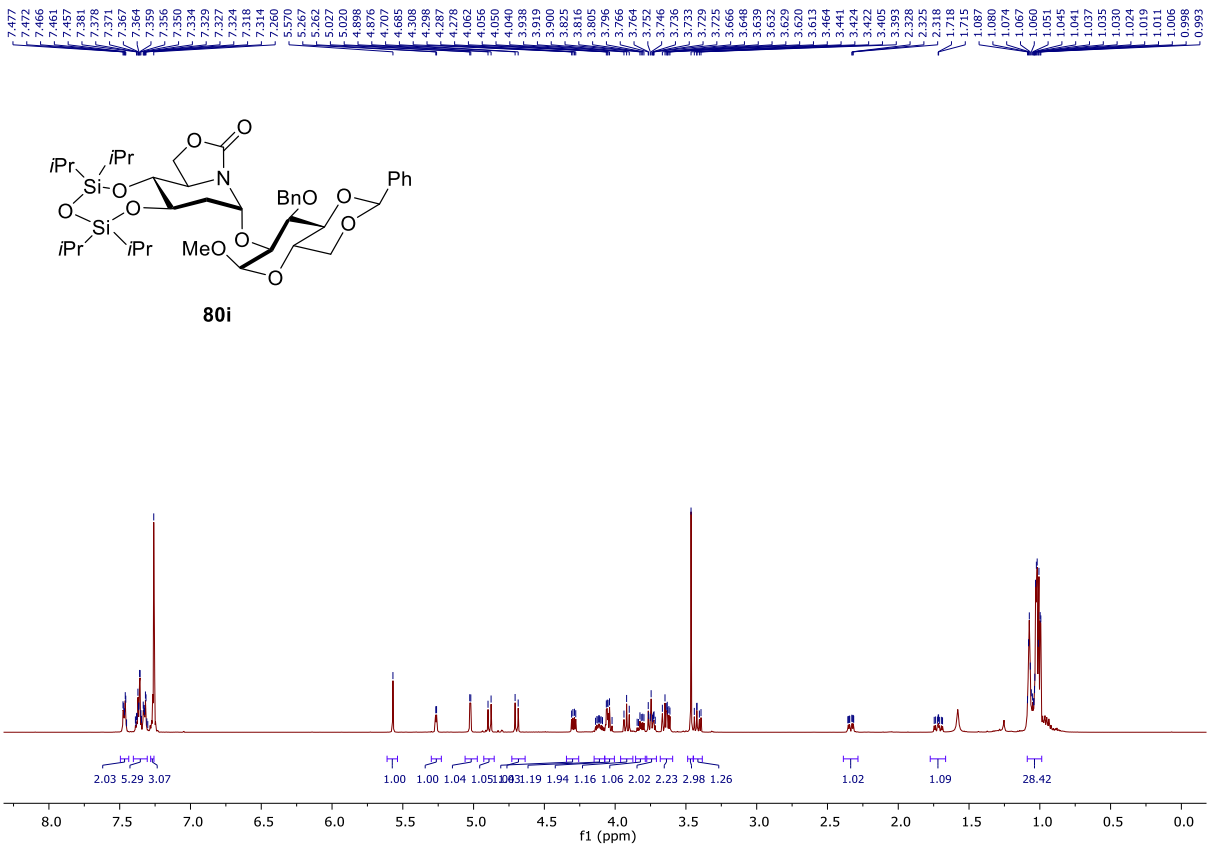

80i

Figure 8.183. ^{1}H NMR spectra for 80i

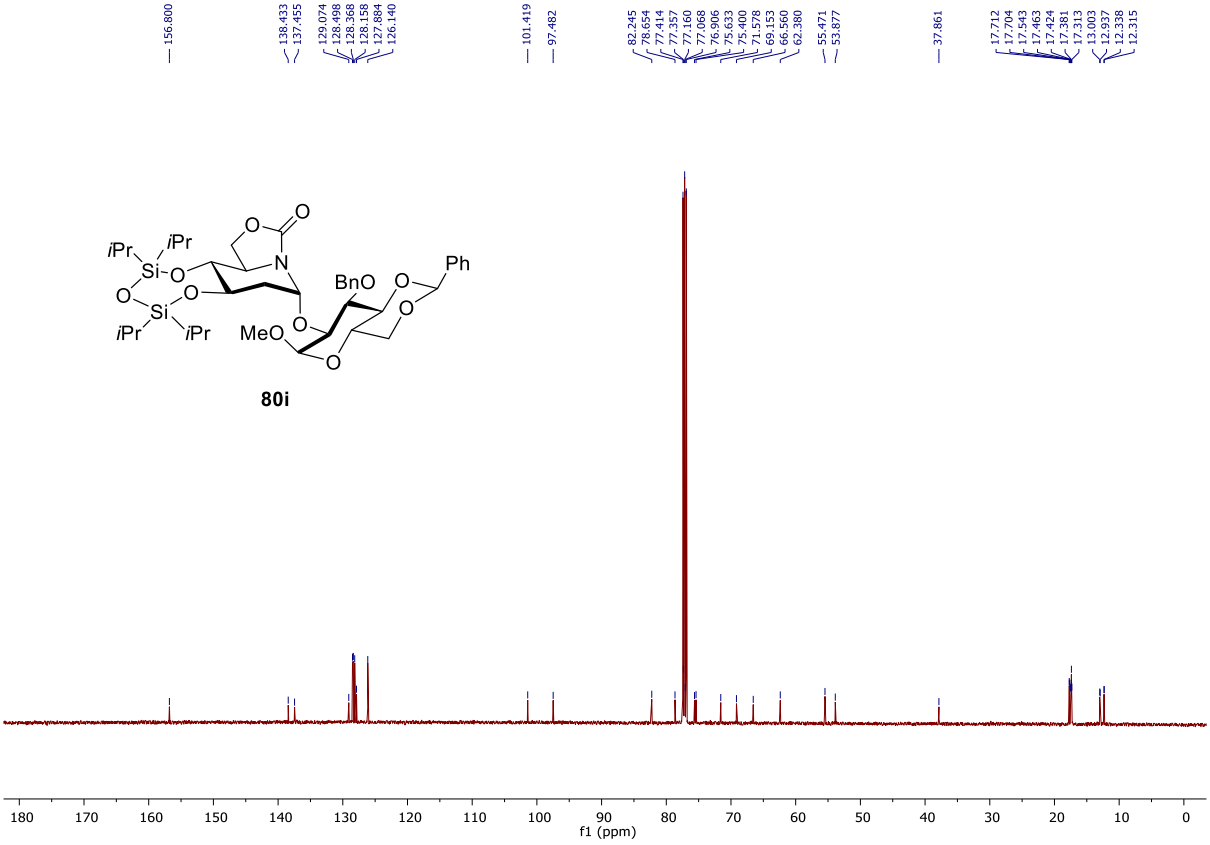

80i

Figure 8.184. ^{13}C NMR spectra for 80i

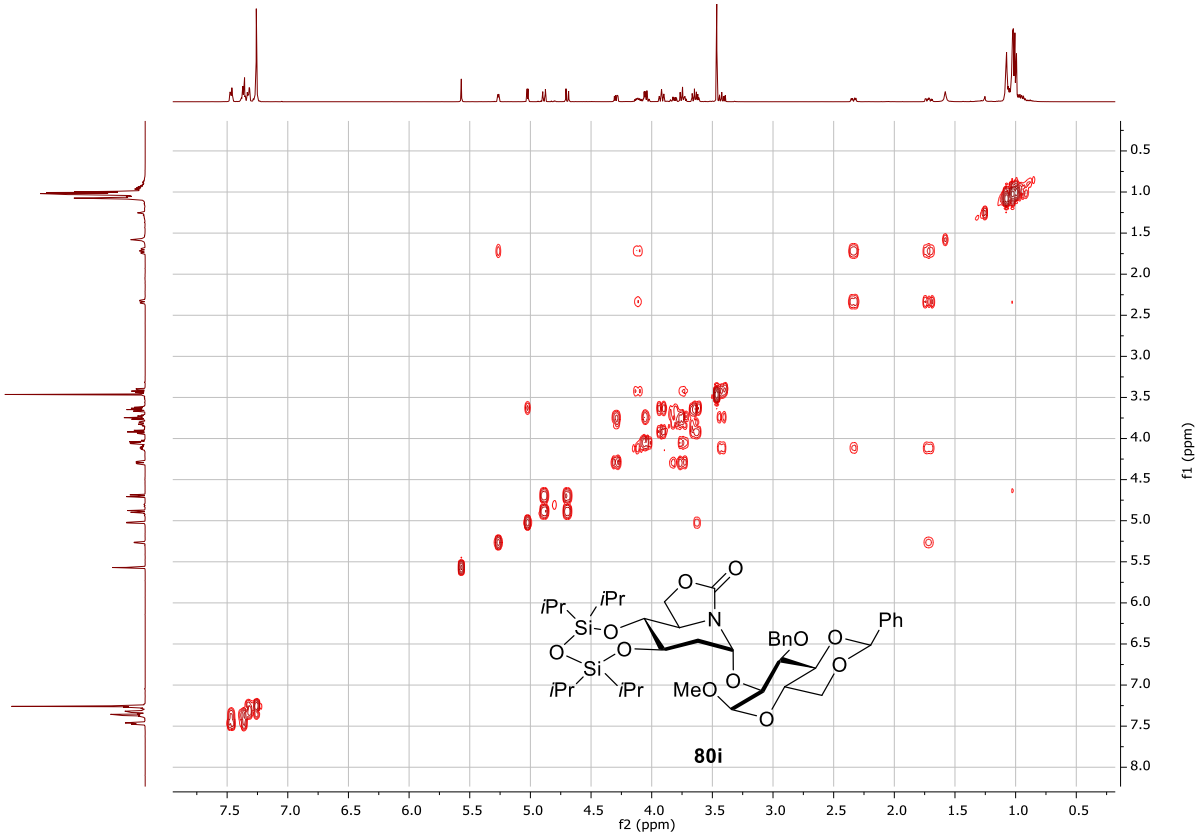

Figure 8.185. COSY spectra for 80i

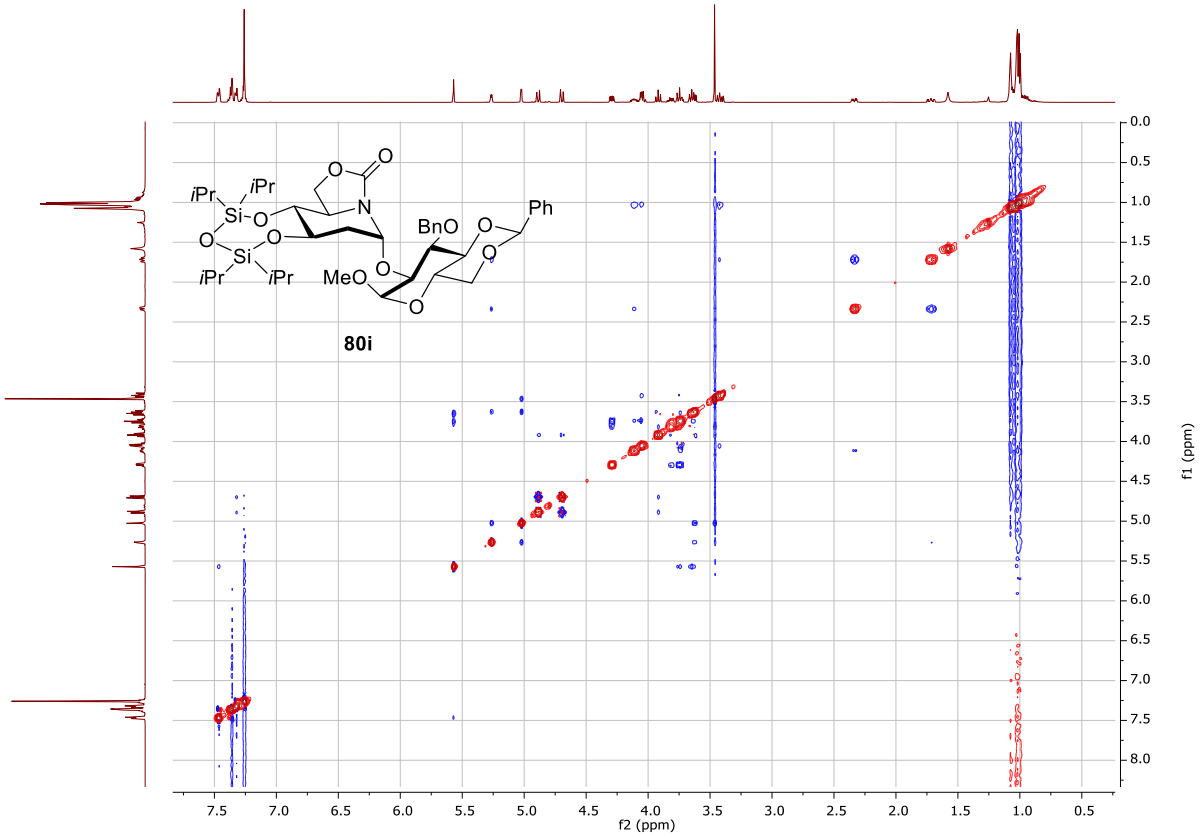

Figure 8.186. NOESY spectra for 80i

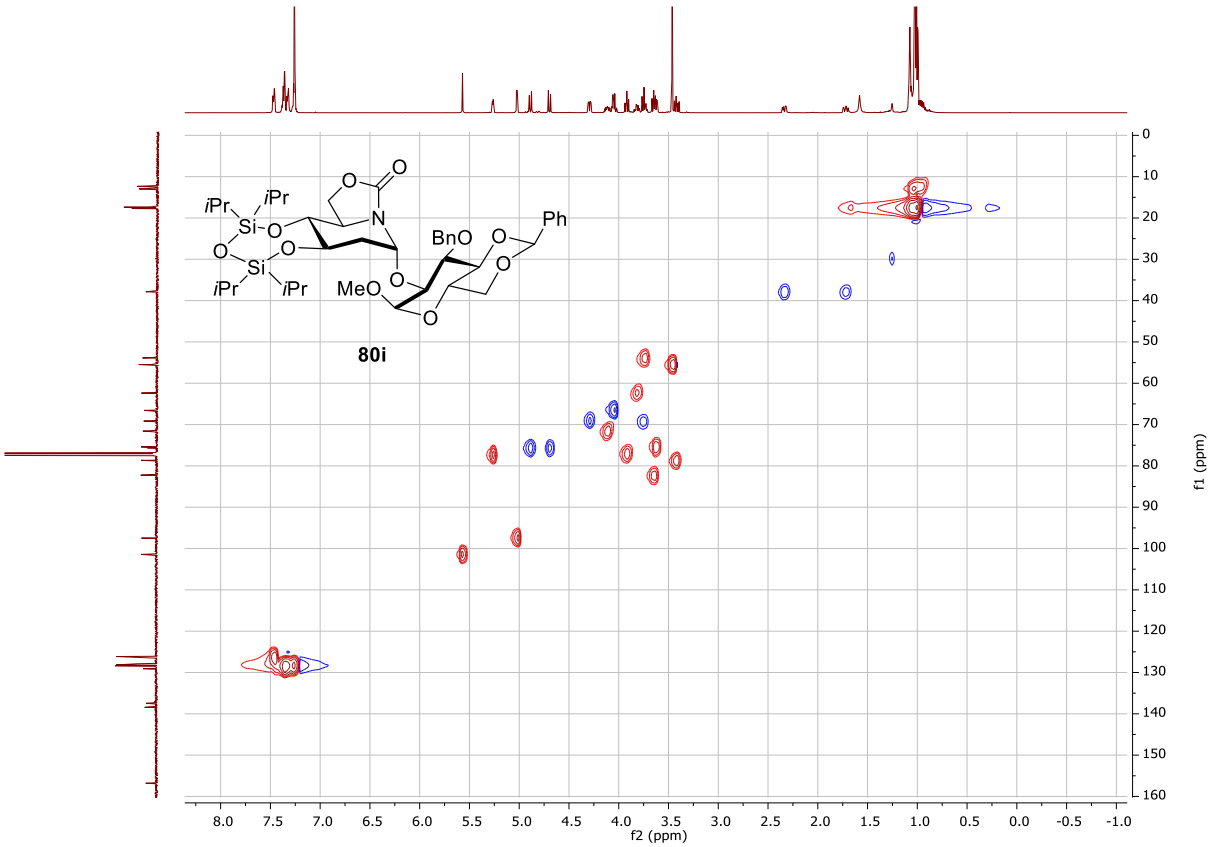

Figure 8.187. HSQC spectra for 80i

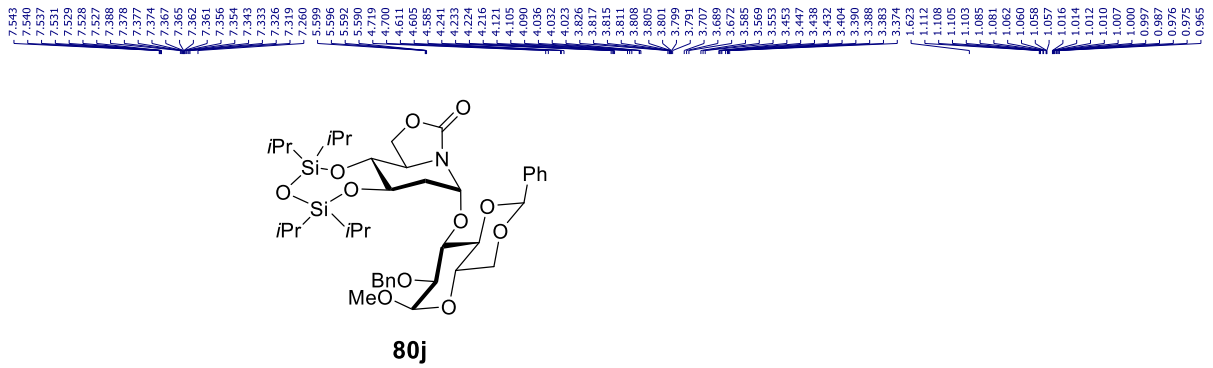

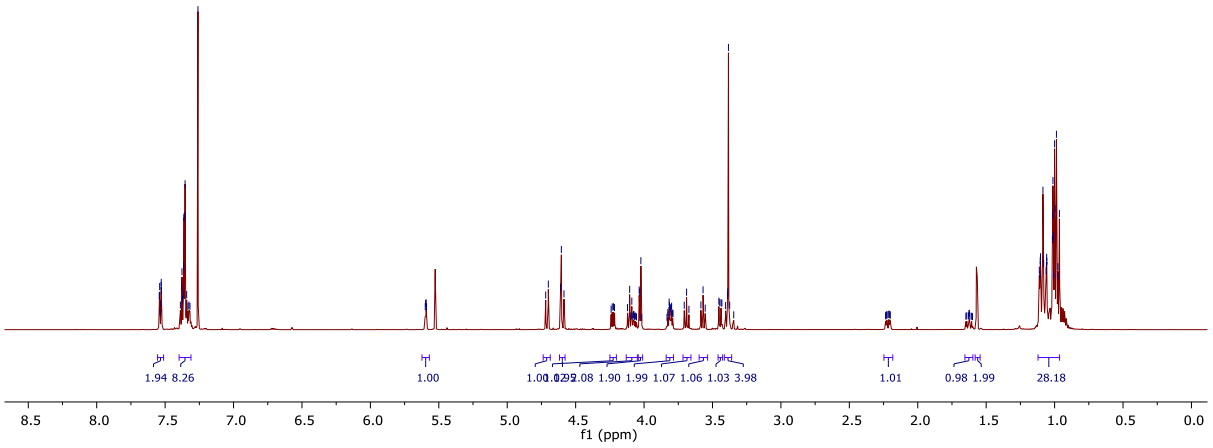

Figure 8.188. ^{1}H NMR spectra for 80j

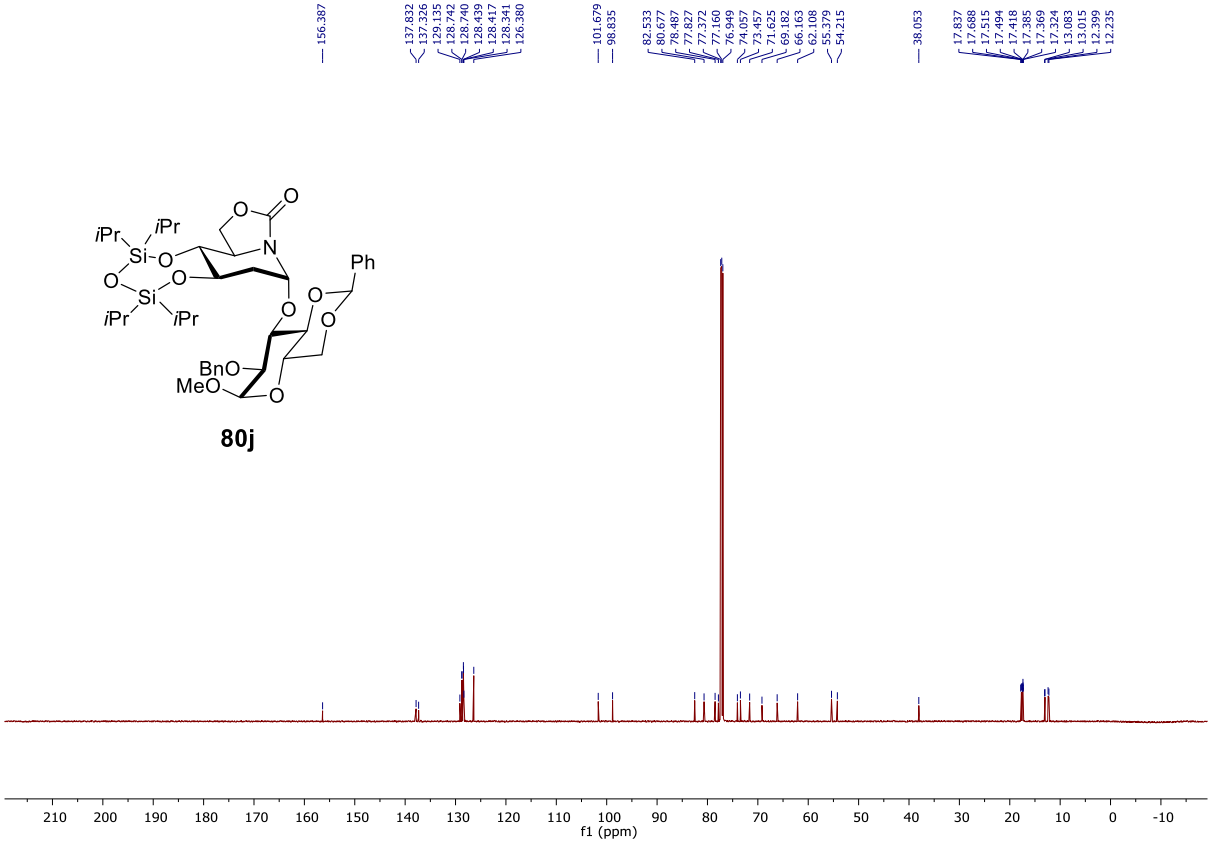

Figure 8.189. ^{13}C NMR spectra for 80j

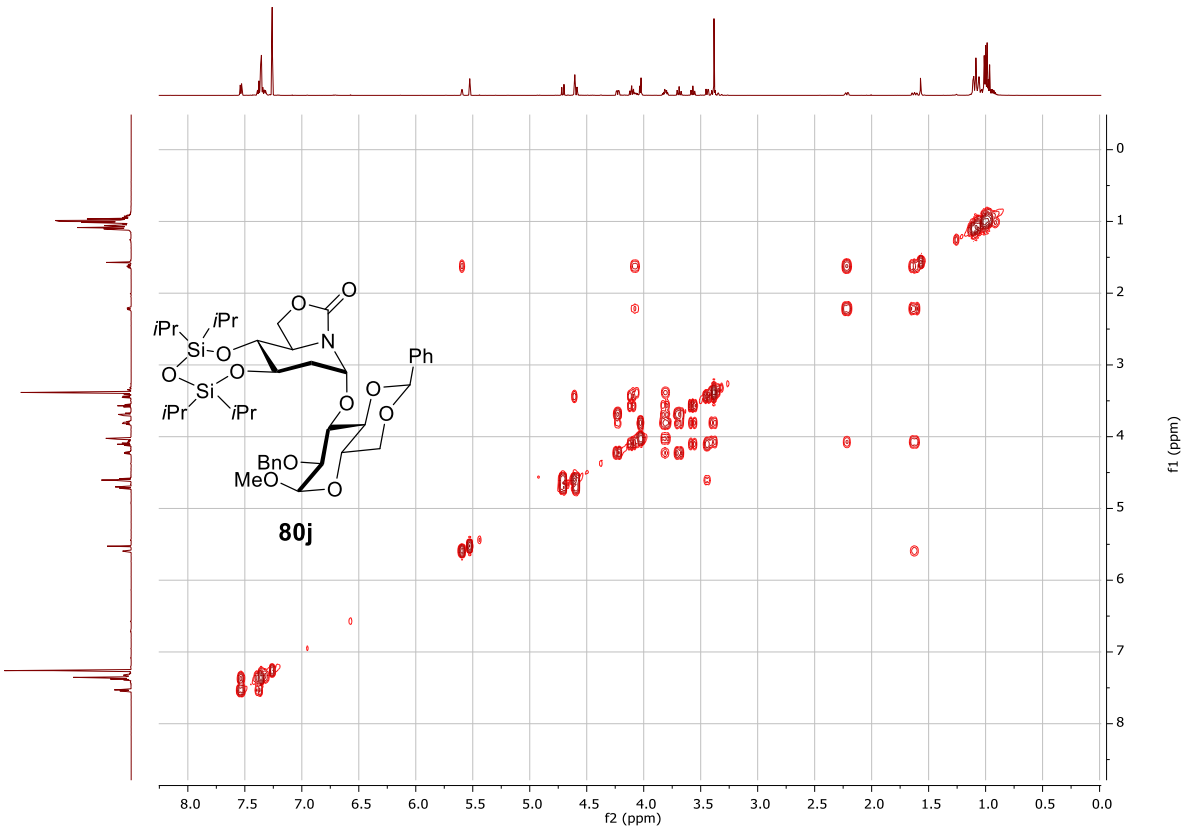

Figure 8.190. COSY spectra for 80j

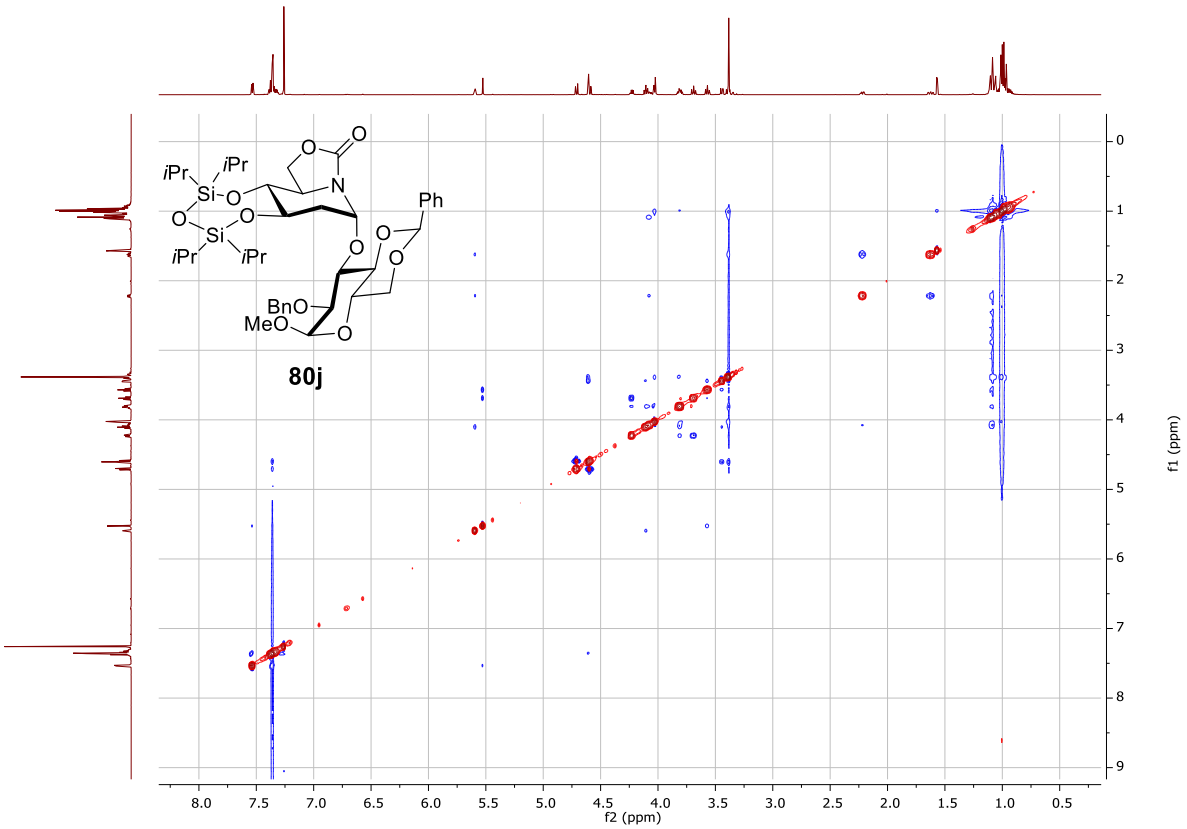

Figure 8.191. NOESY spectra for 80j

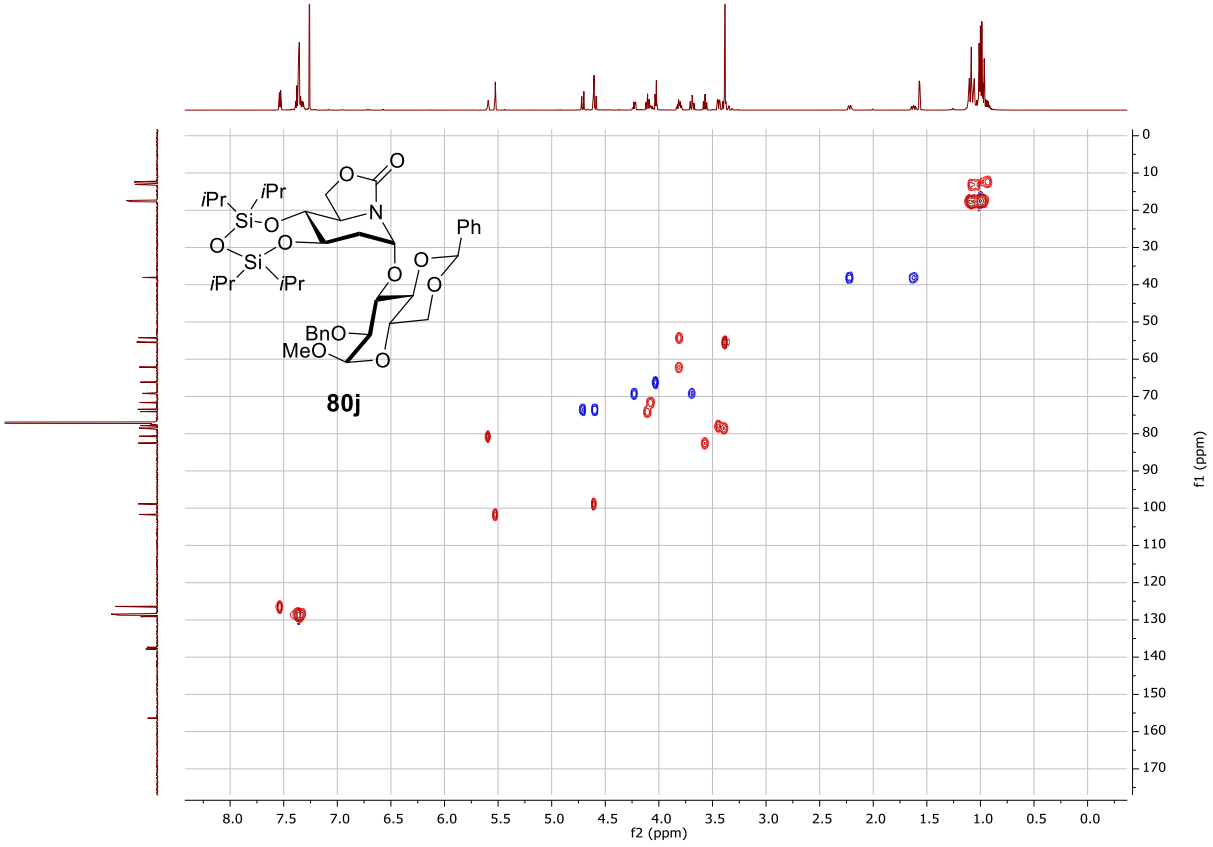

Figure 8.192. HSQC spectra for 80j

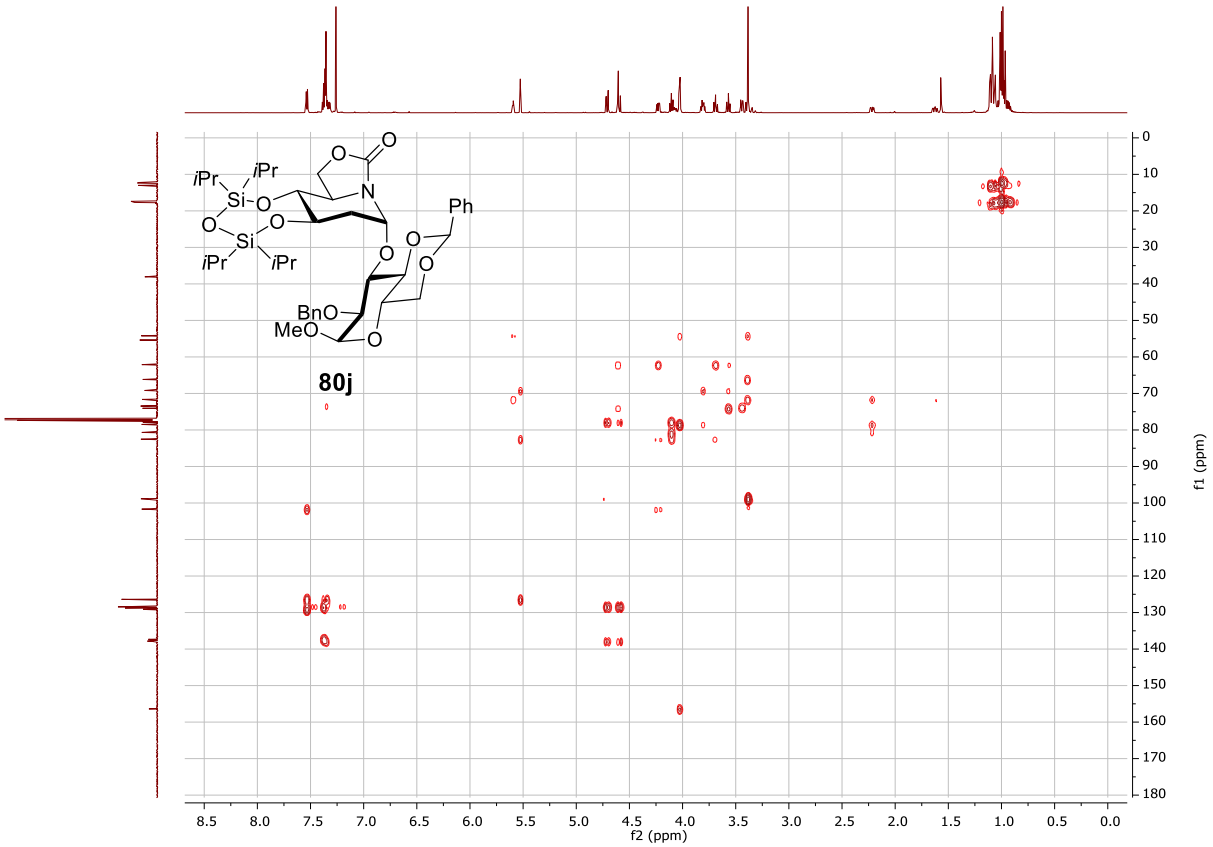

Figure 8.193. HMBC spectra for 80j

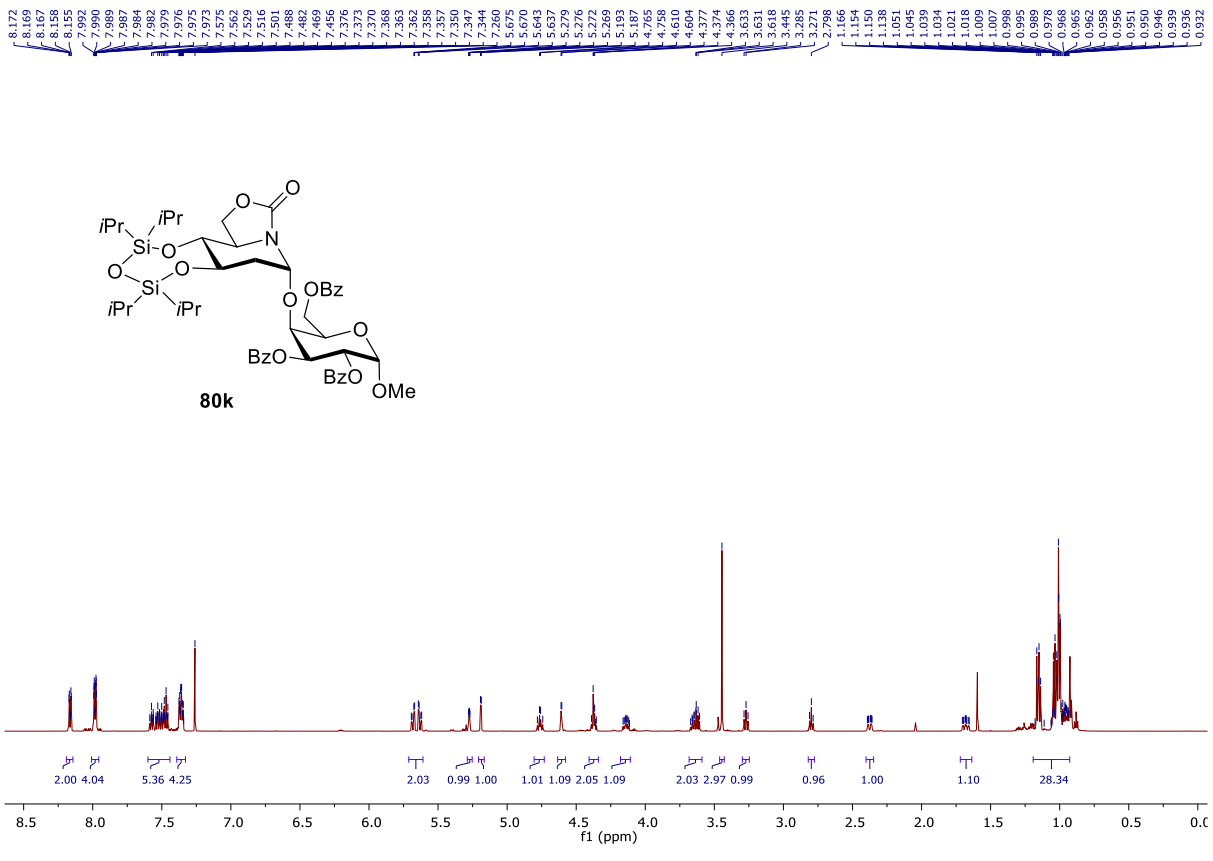

Figure 8.194. ^{1}H NMR spectra for 80k

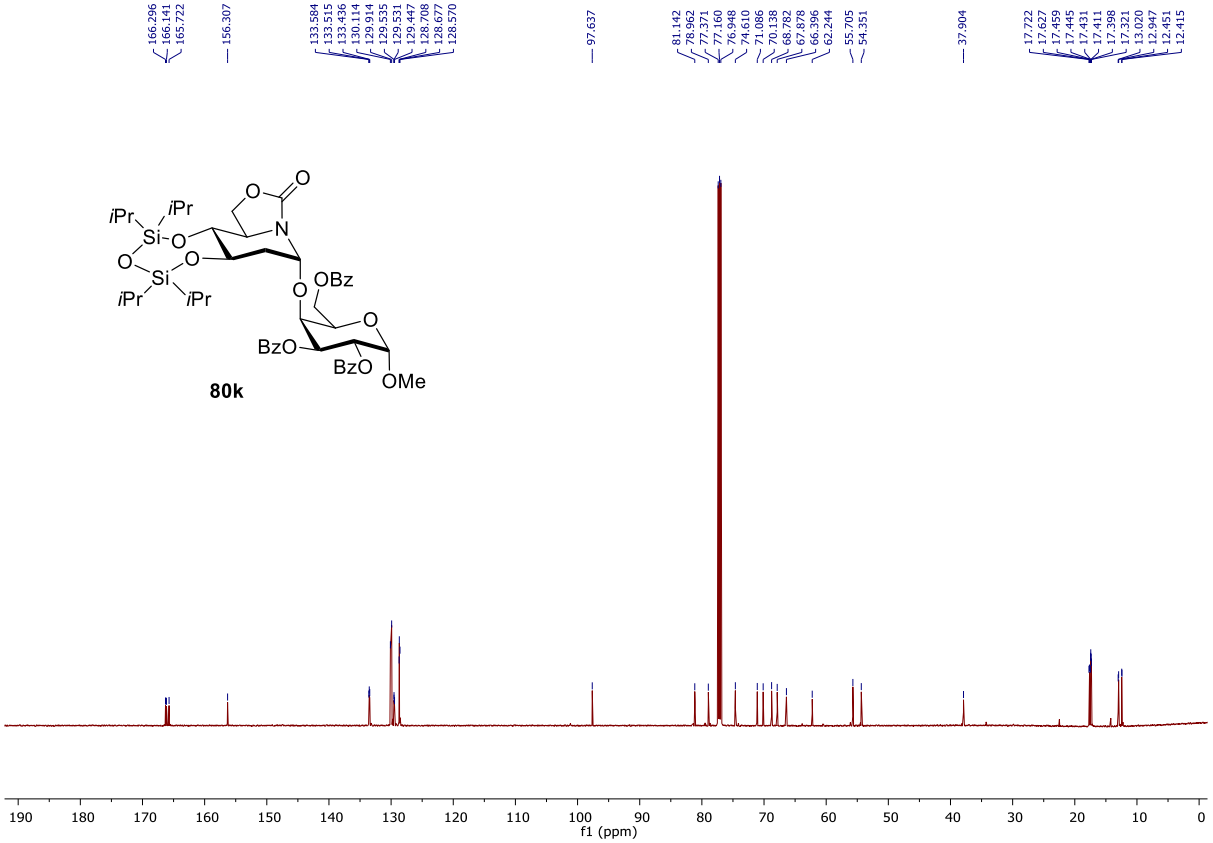

Figure 8.195. ^{13}C NMR spectra for 80k

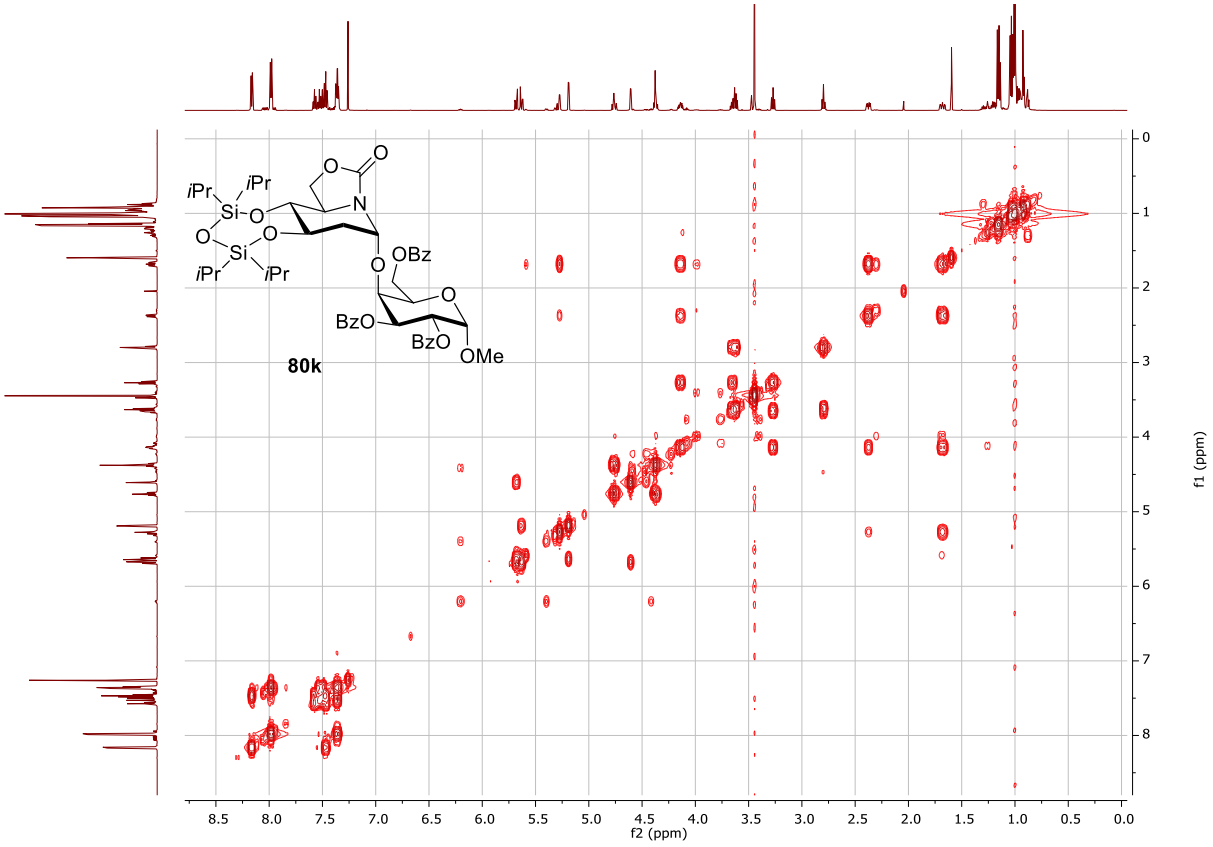

Figure 8.196. COSY spectra for 80k

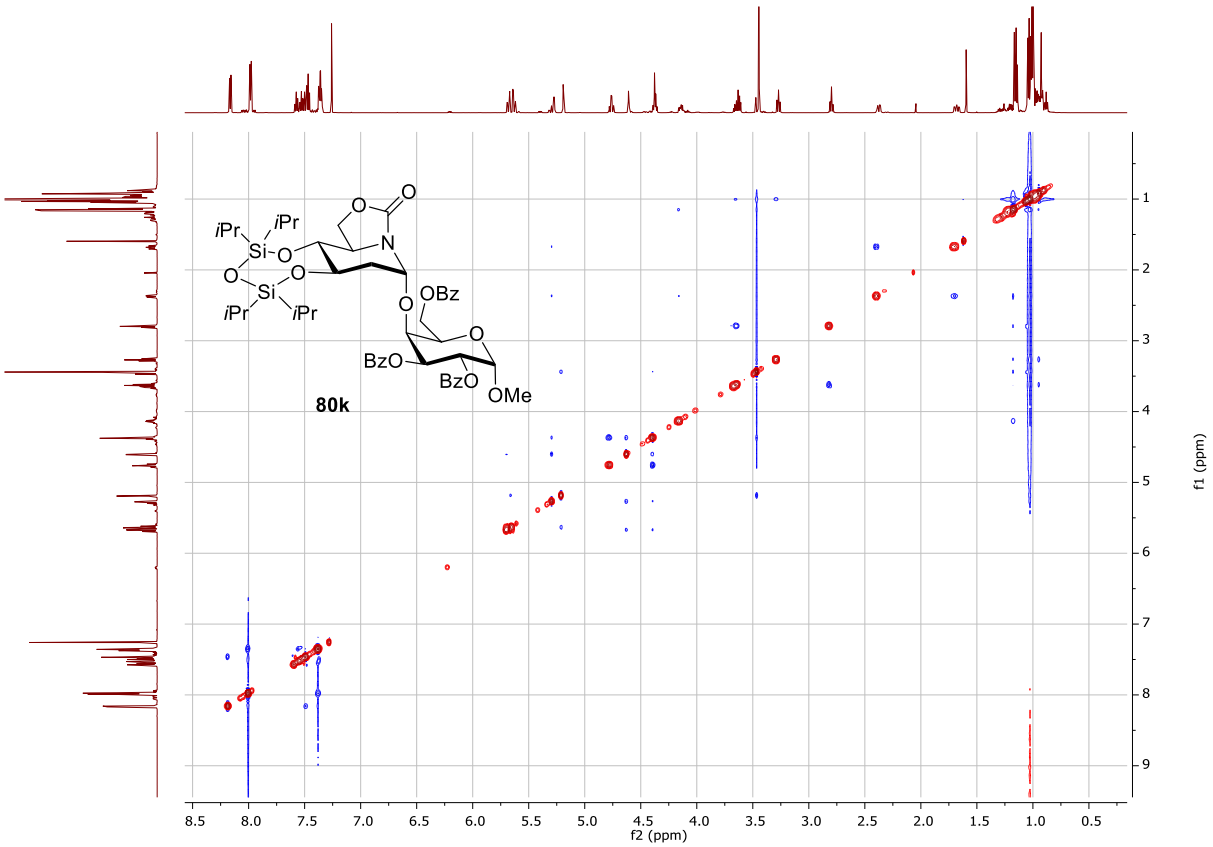

Figure 8.197. NOESY spectra for 80k

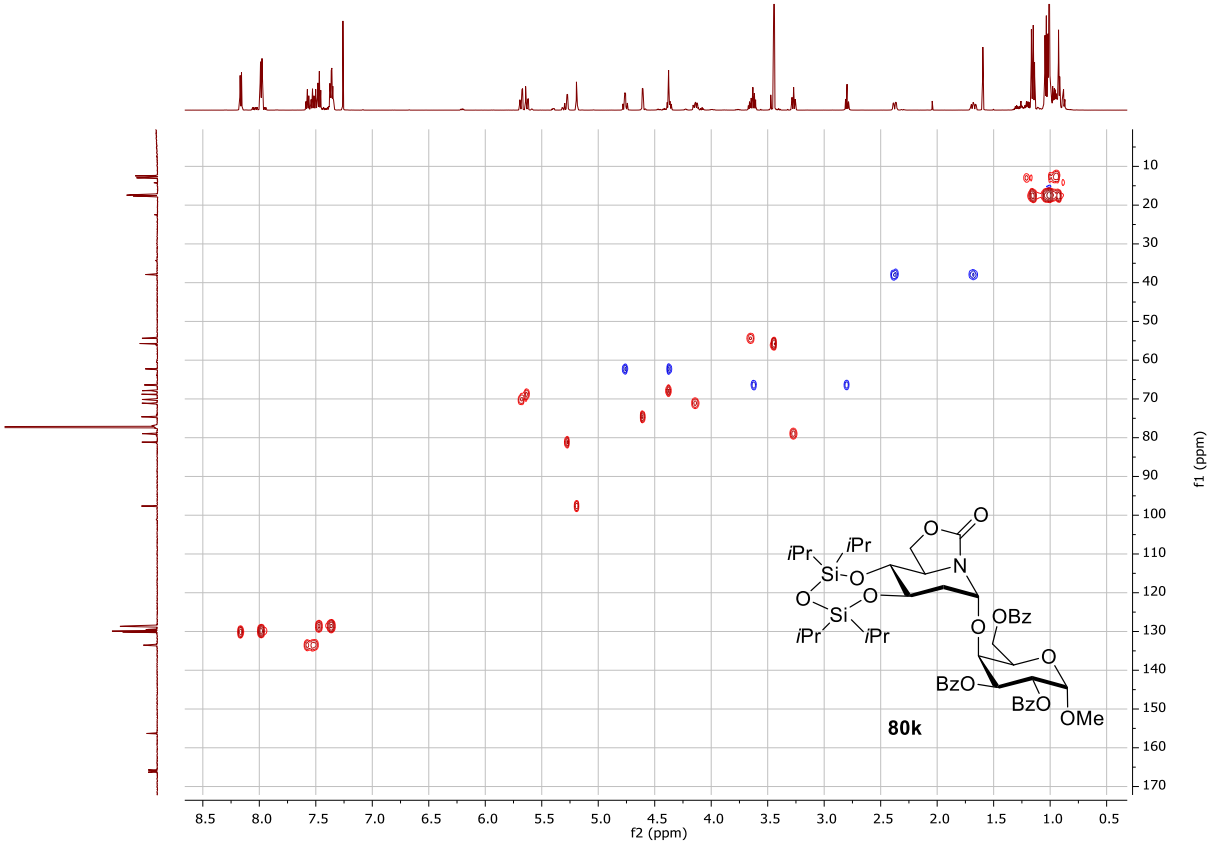

Figure 8.198. HSQC spectra for 80k

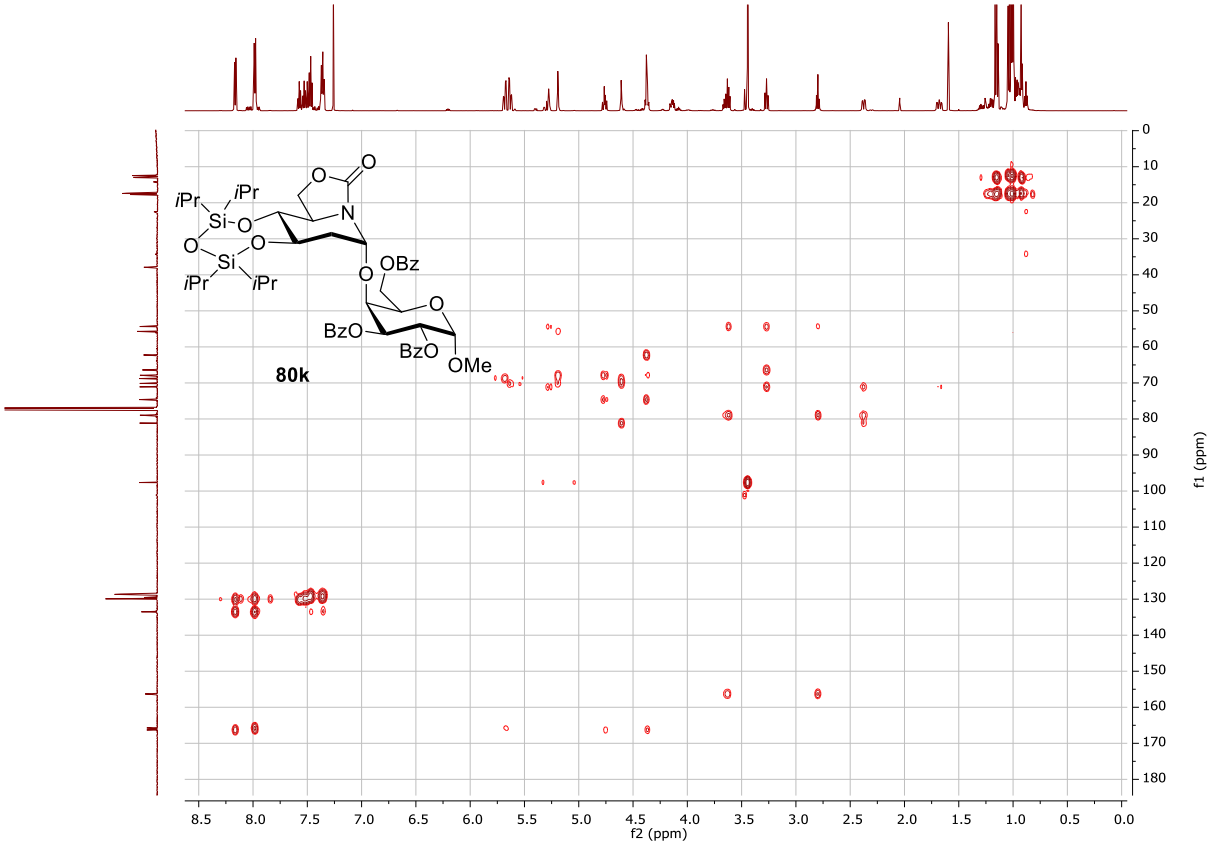

Figure 8.199. HMBC spectra for 80k

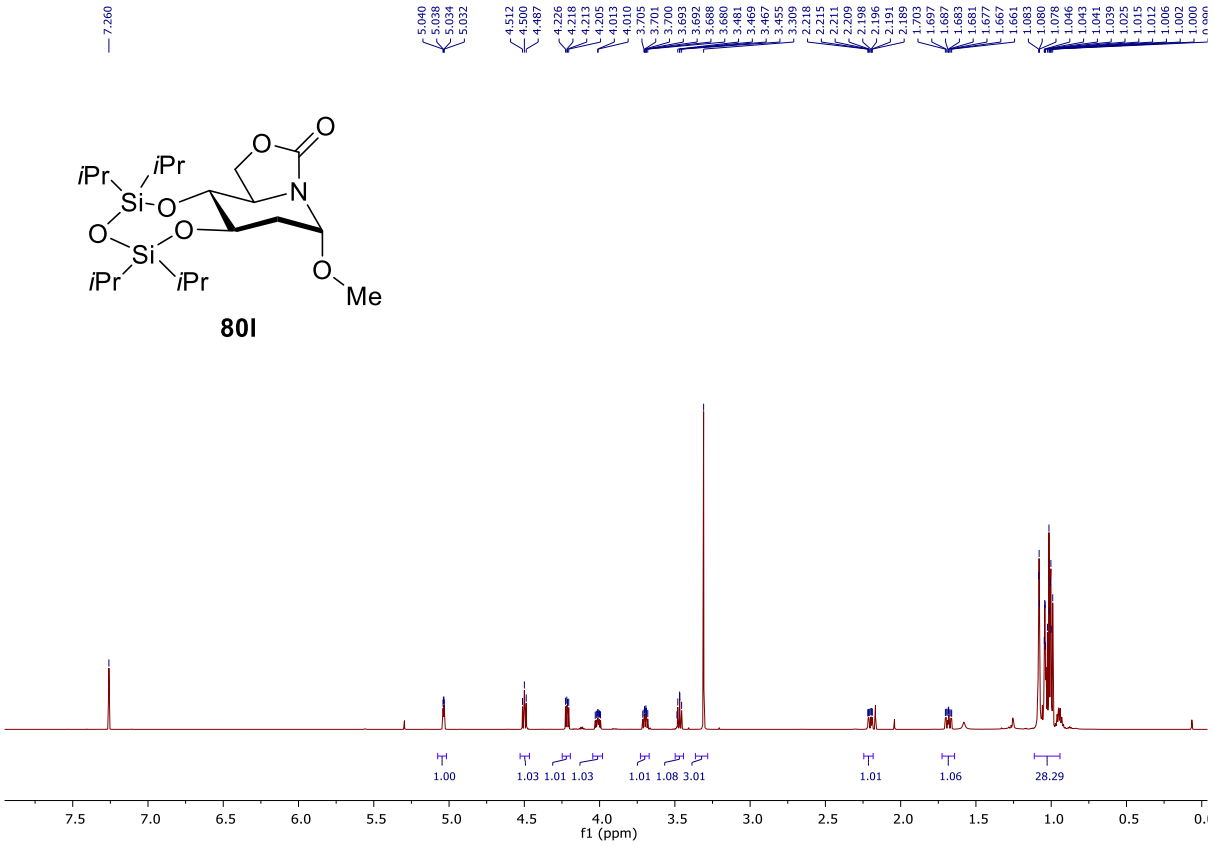

Figure 8.200. ^{1}H NMR spectra for 80l

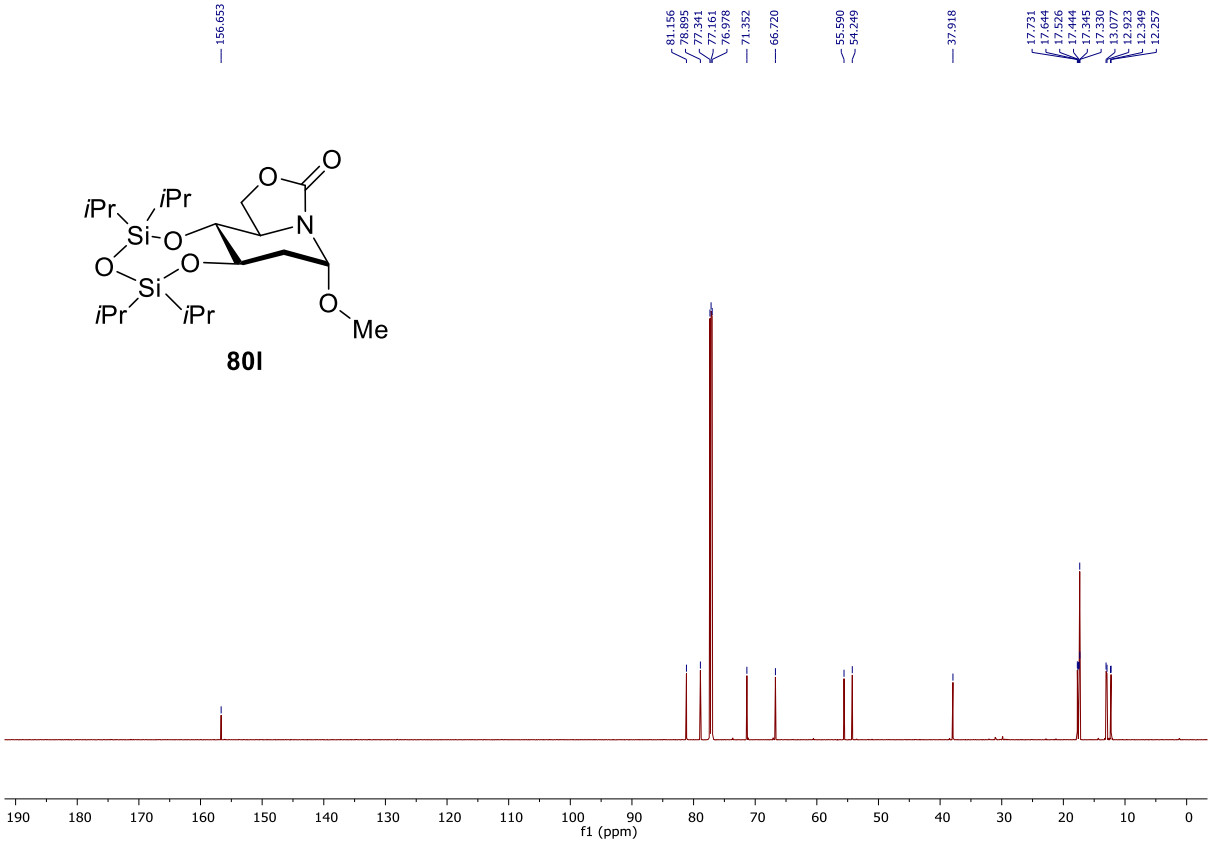

Figure 8.201. ^{13}C NMR spectra for 80l

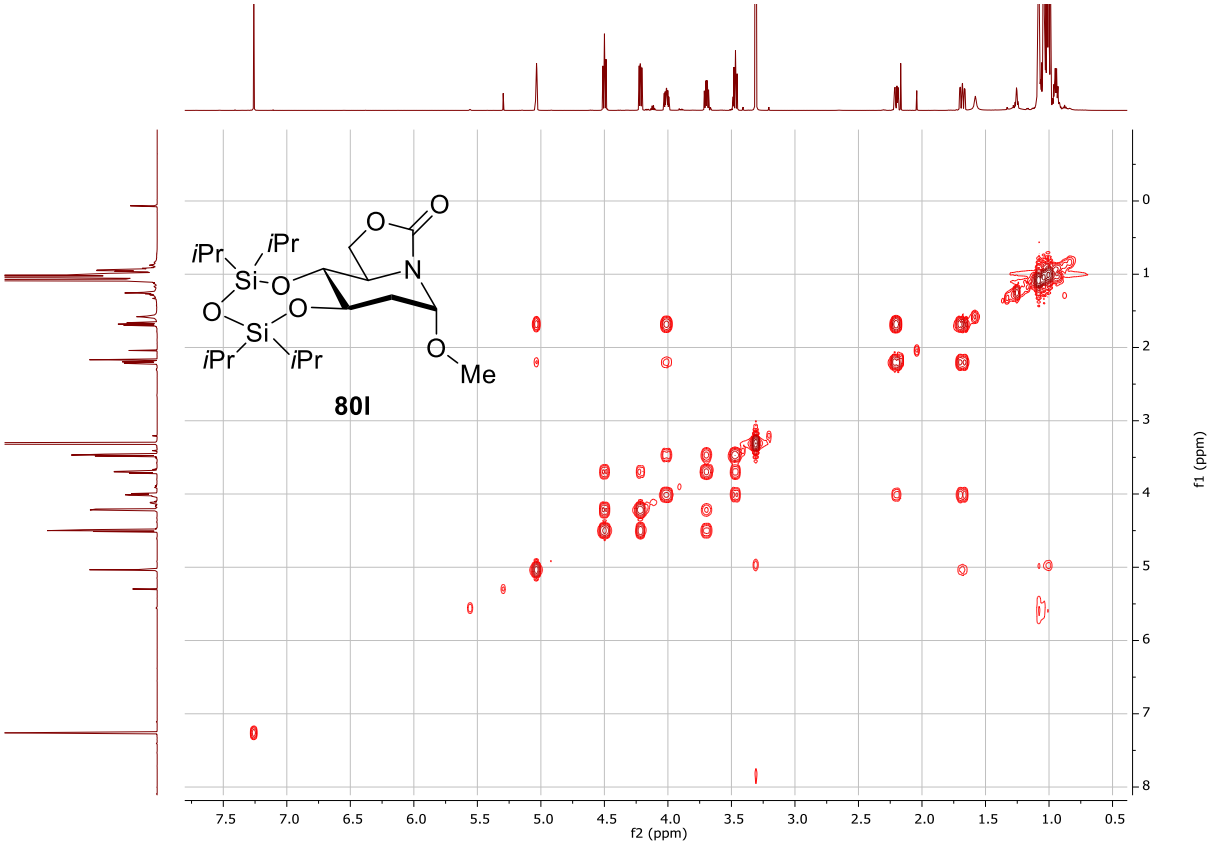

Figure 8.202. COSY spectra for 80l

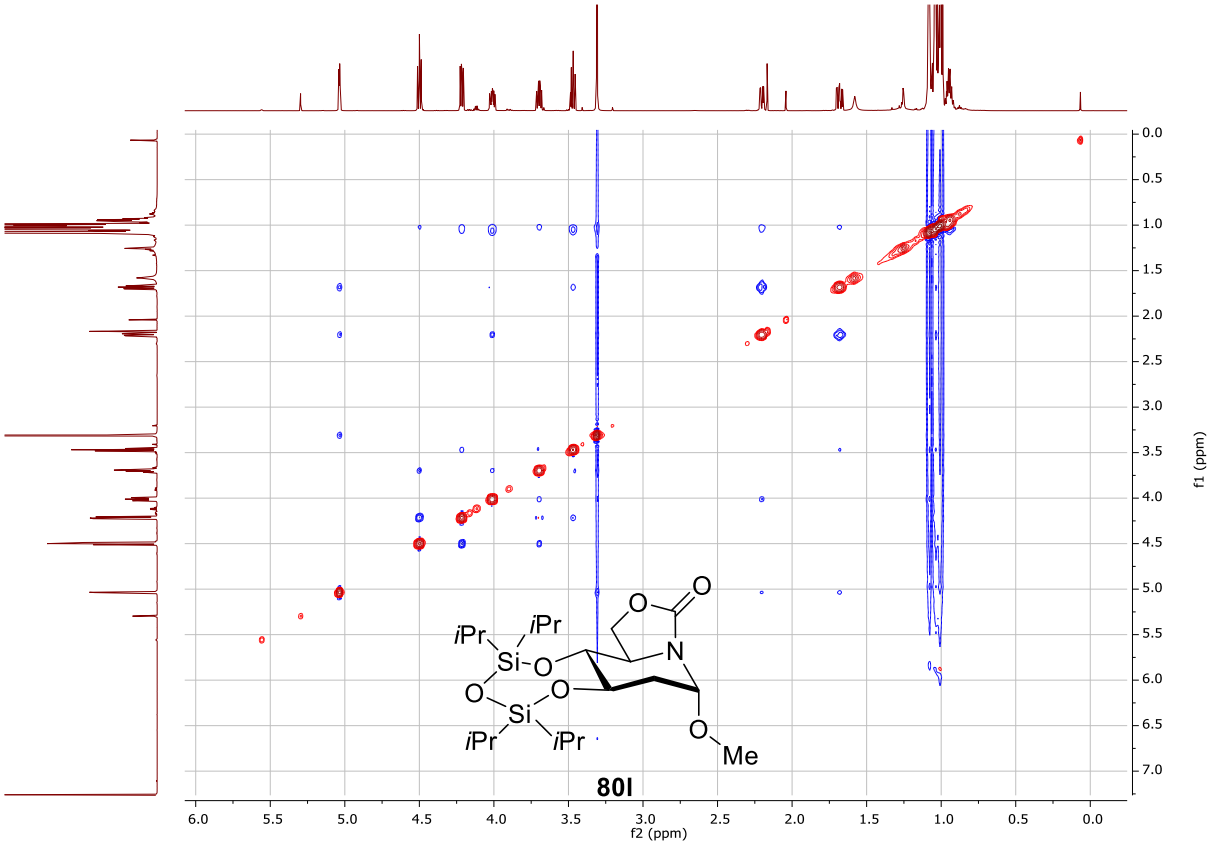

Figure 8.203. NOESY spectra for 80l

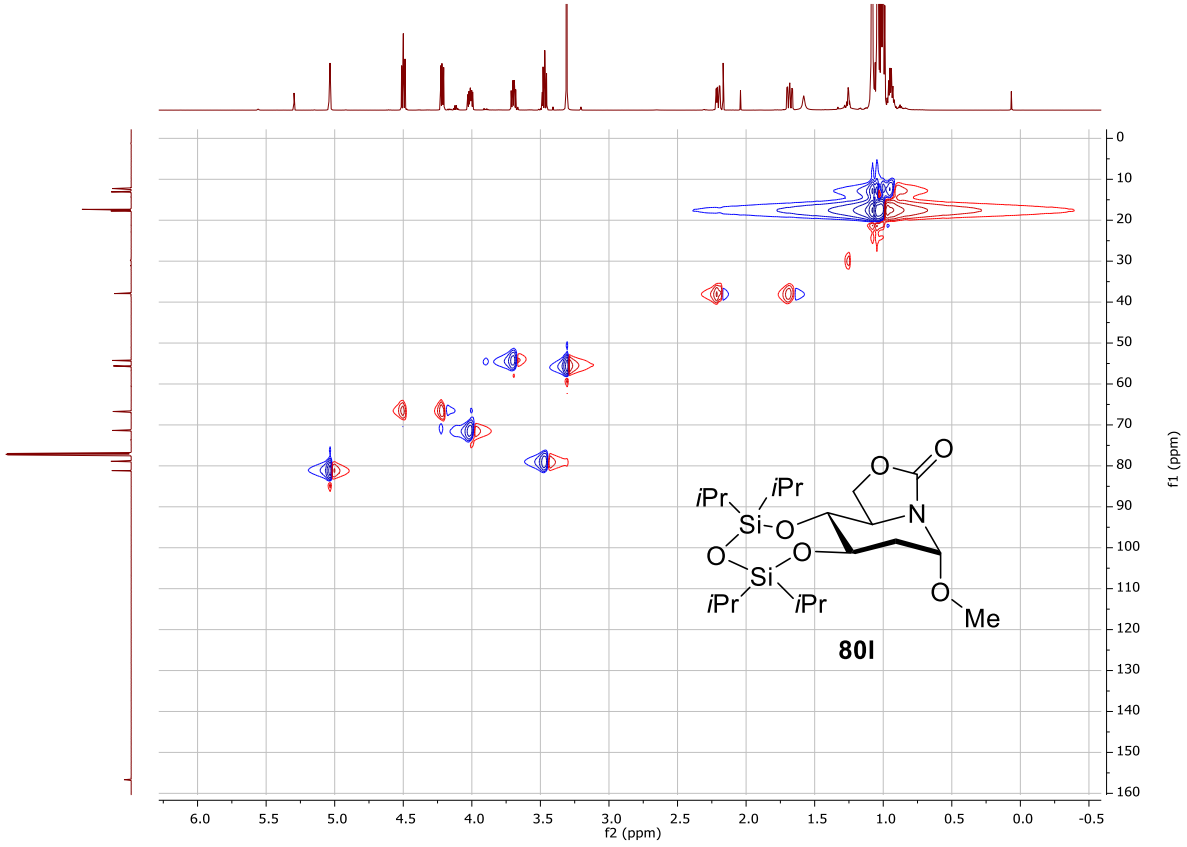

Figure 8.204. HSQC spectra for 80l

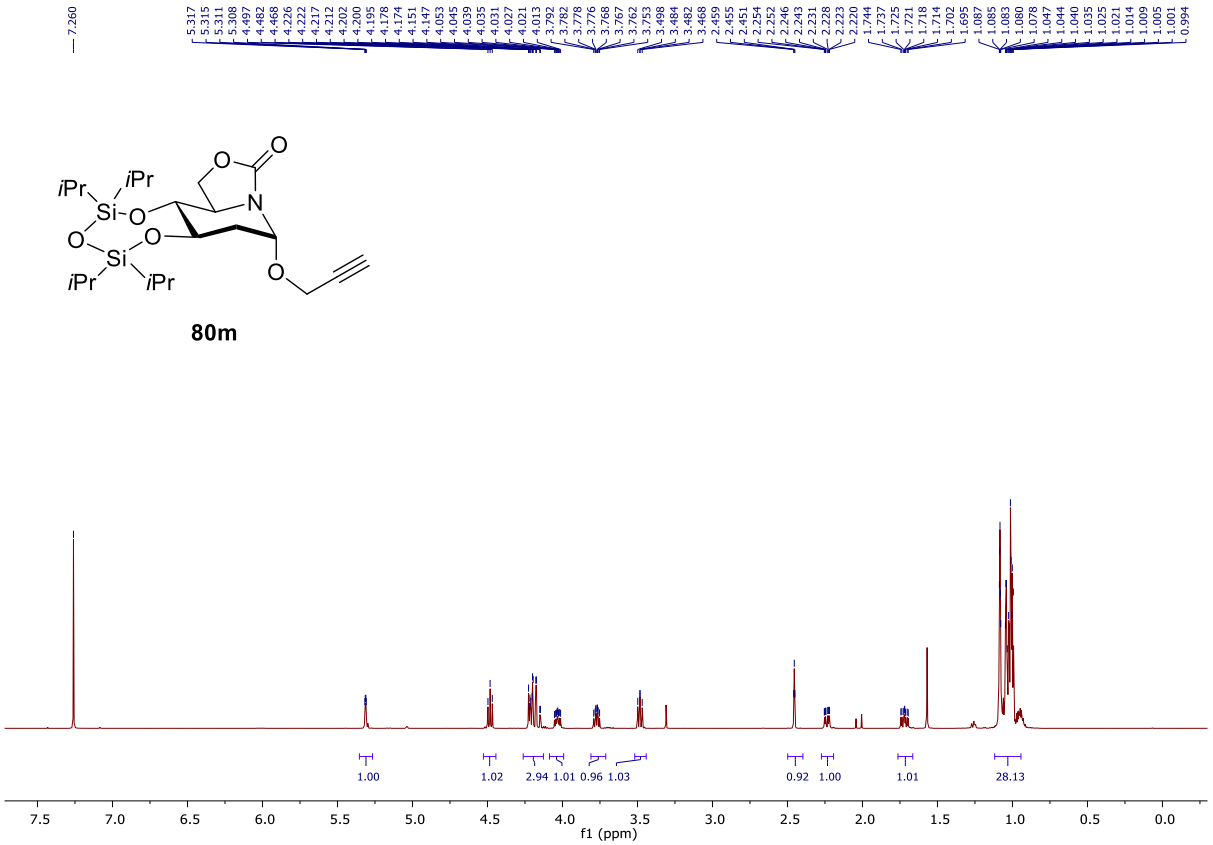

Figure 8.205. ^{1}H NMR spectra for 80m

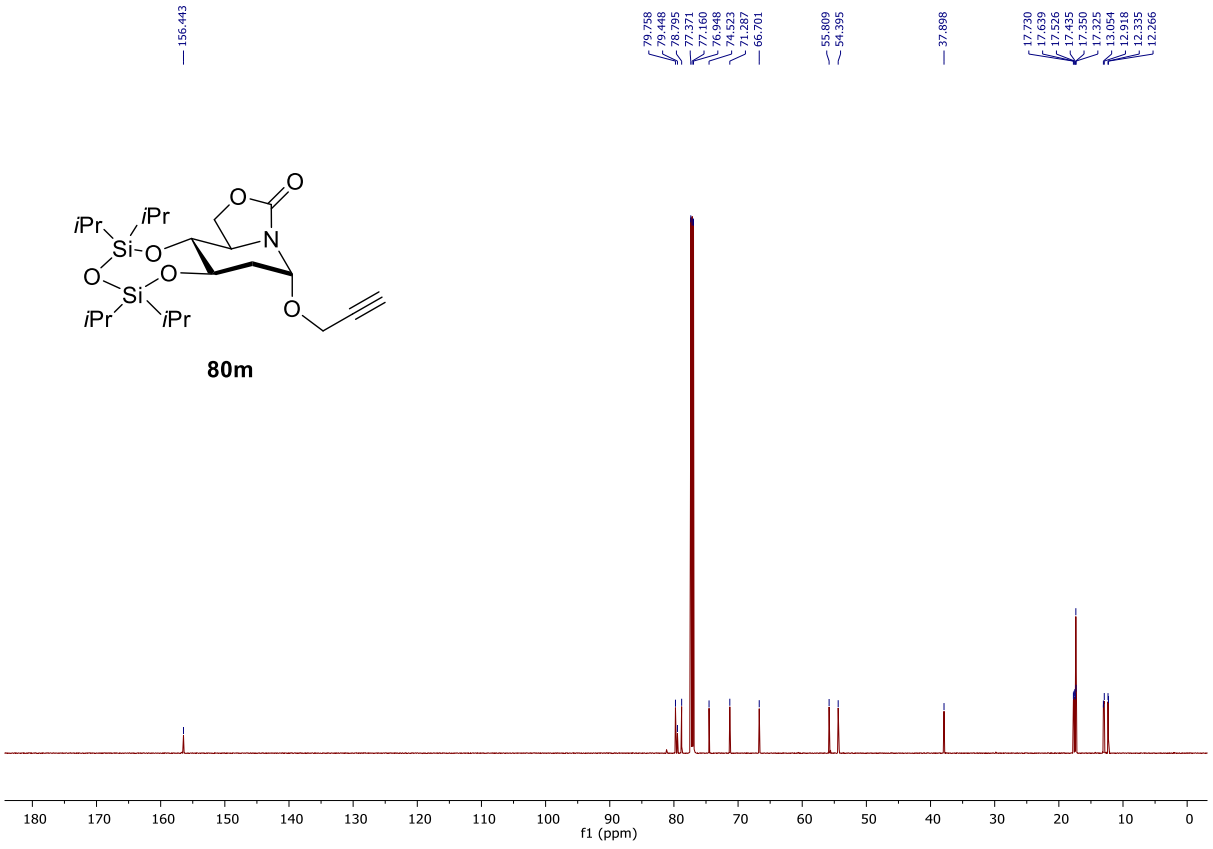

Figure 8.206. ^{13}C NMR spectra for 80m

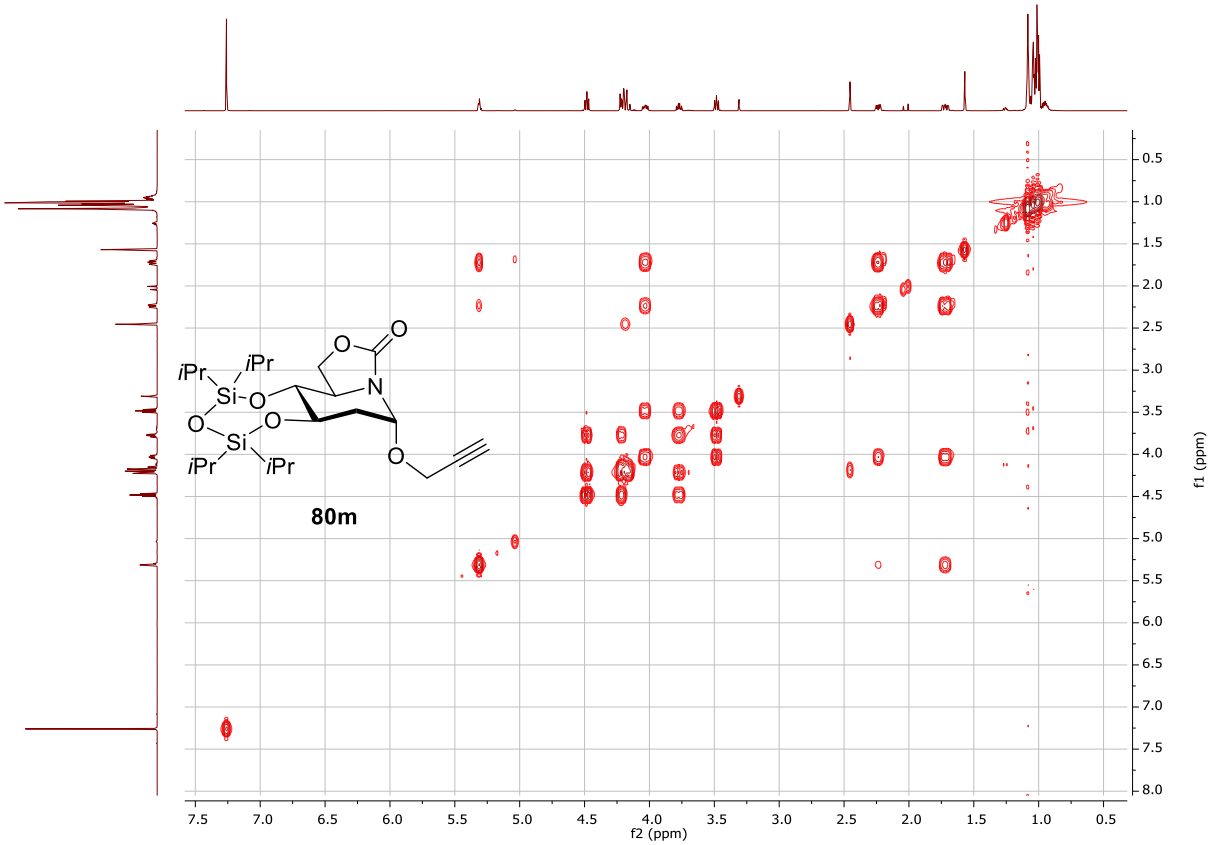

Figure 8.207. COSY spectra for 80m

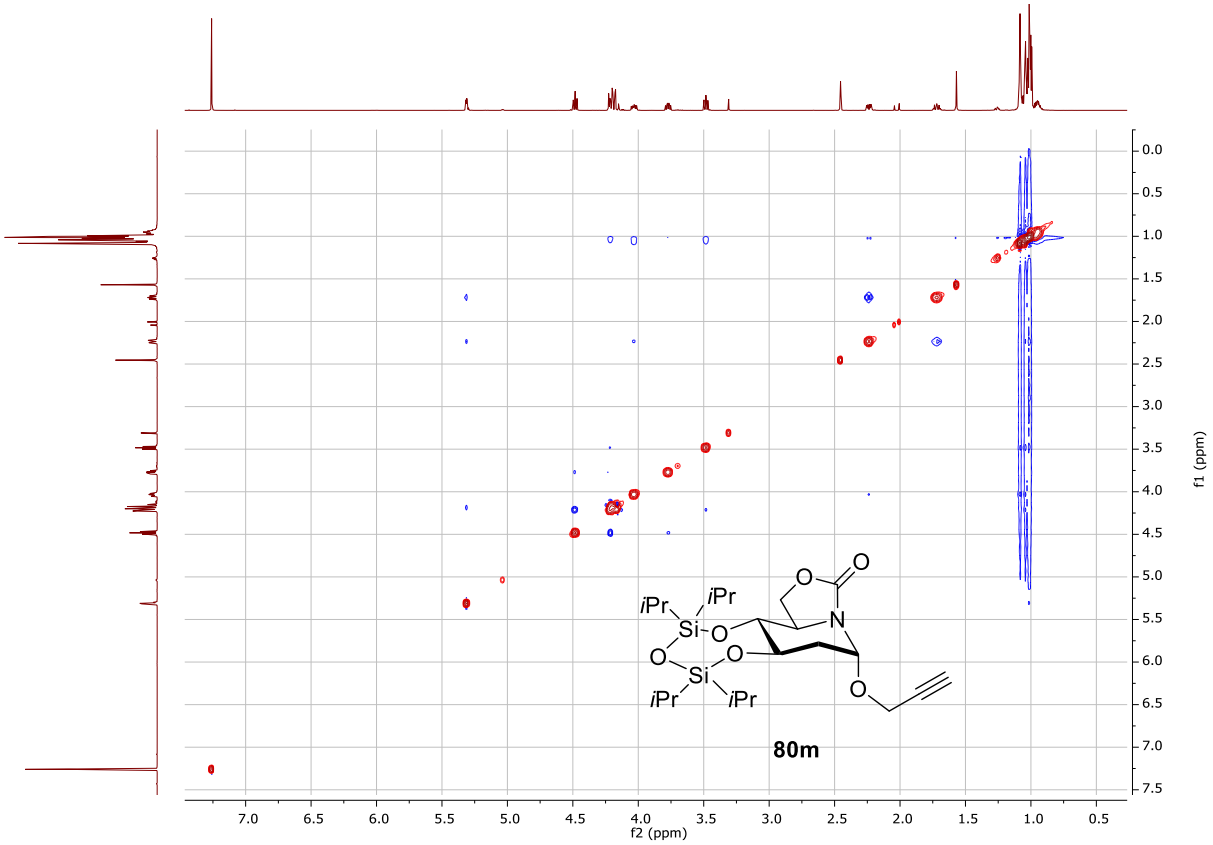

Figure 8.208. NOESY spectra for 80m

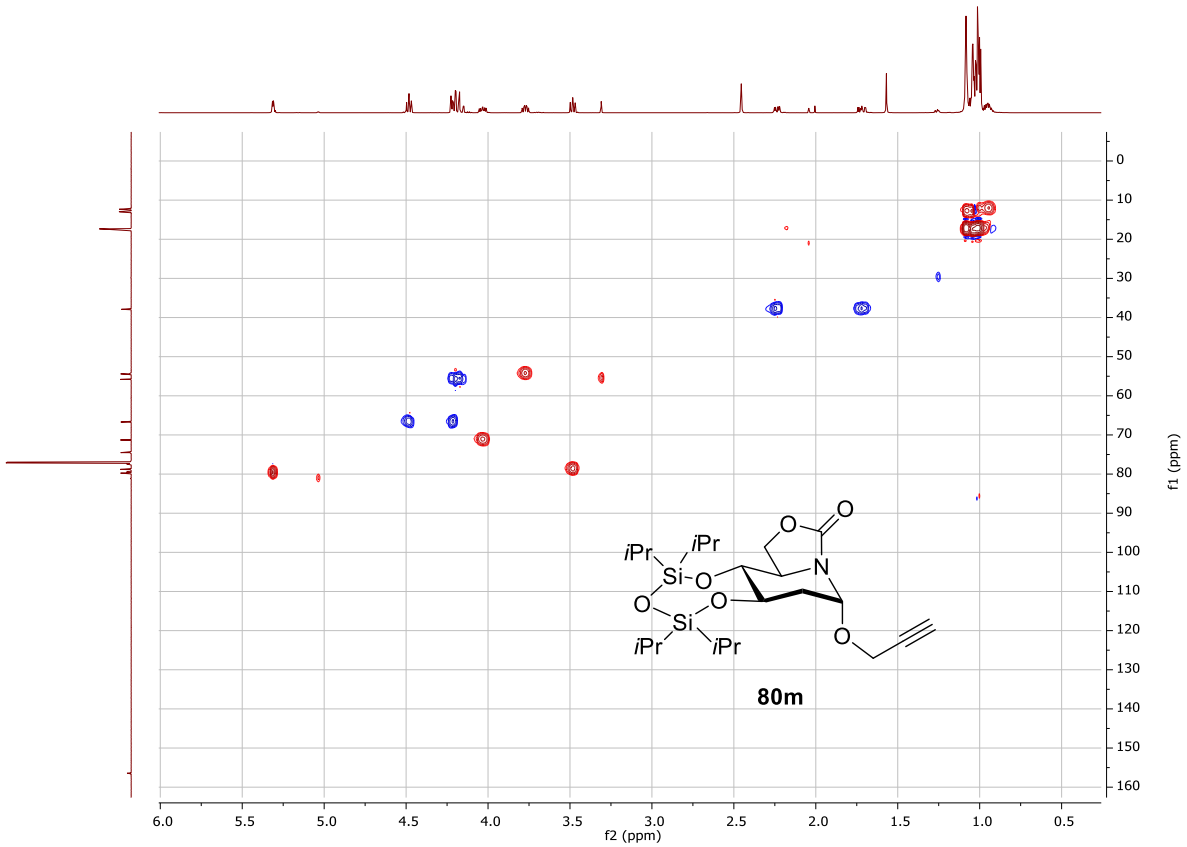

Figure 8.209. HSQC spectra for 80m

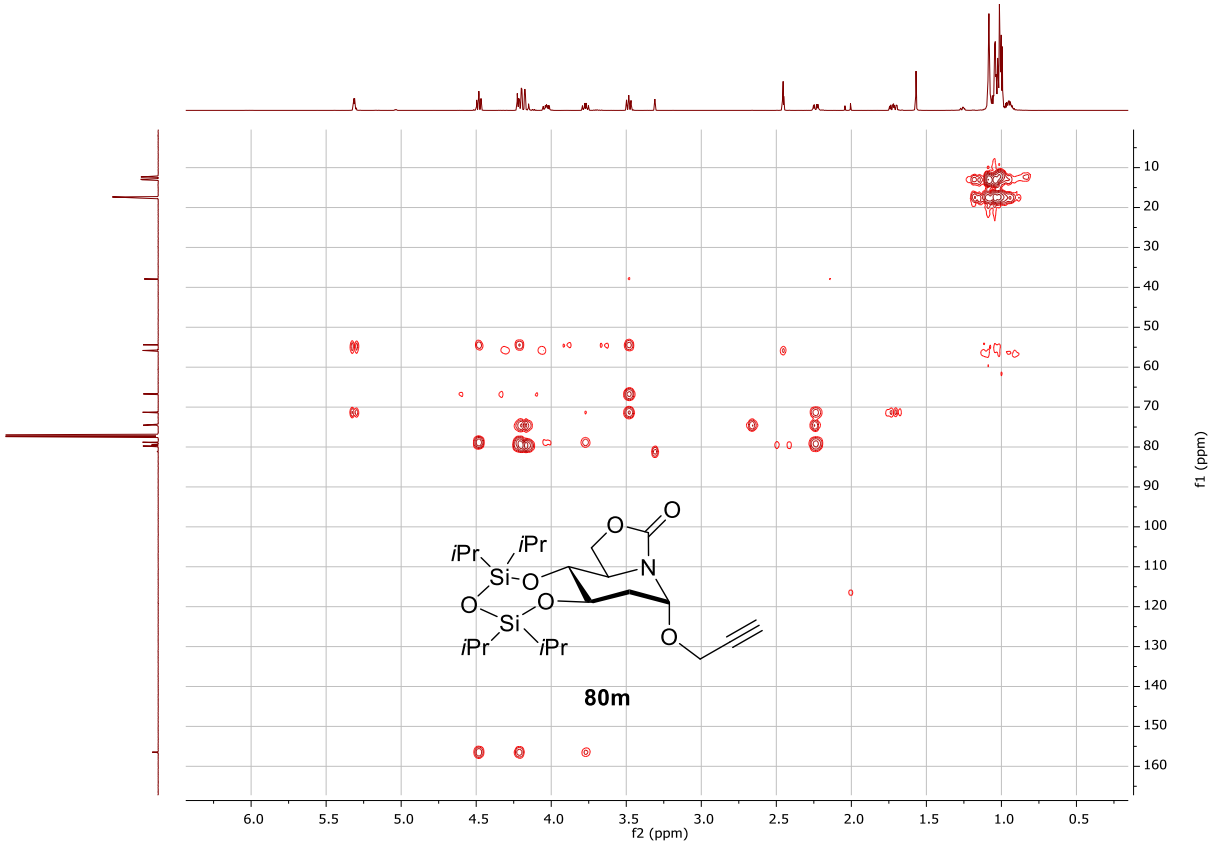

Figure 8.210. HMBC spectra for 80m

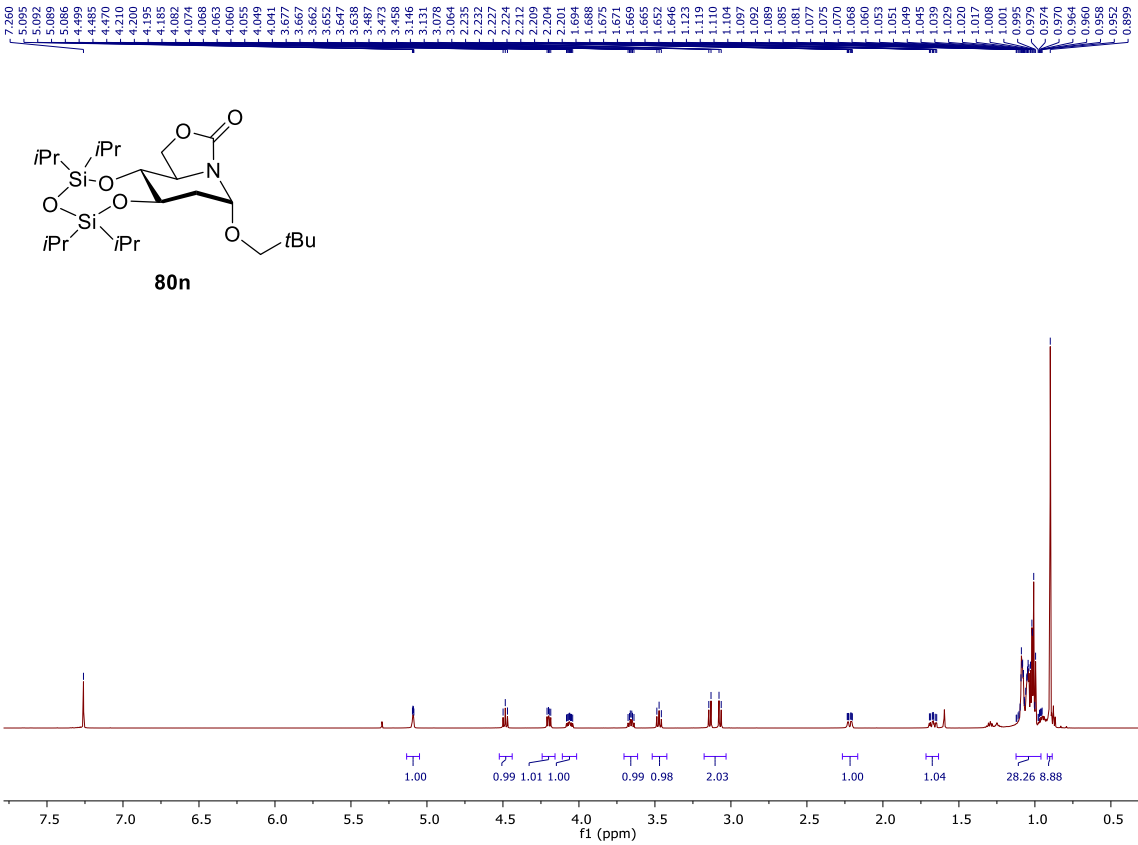

Figure 8.211. ^{1}H NMR spectra for 80n

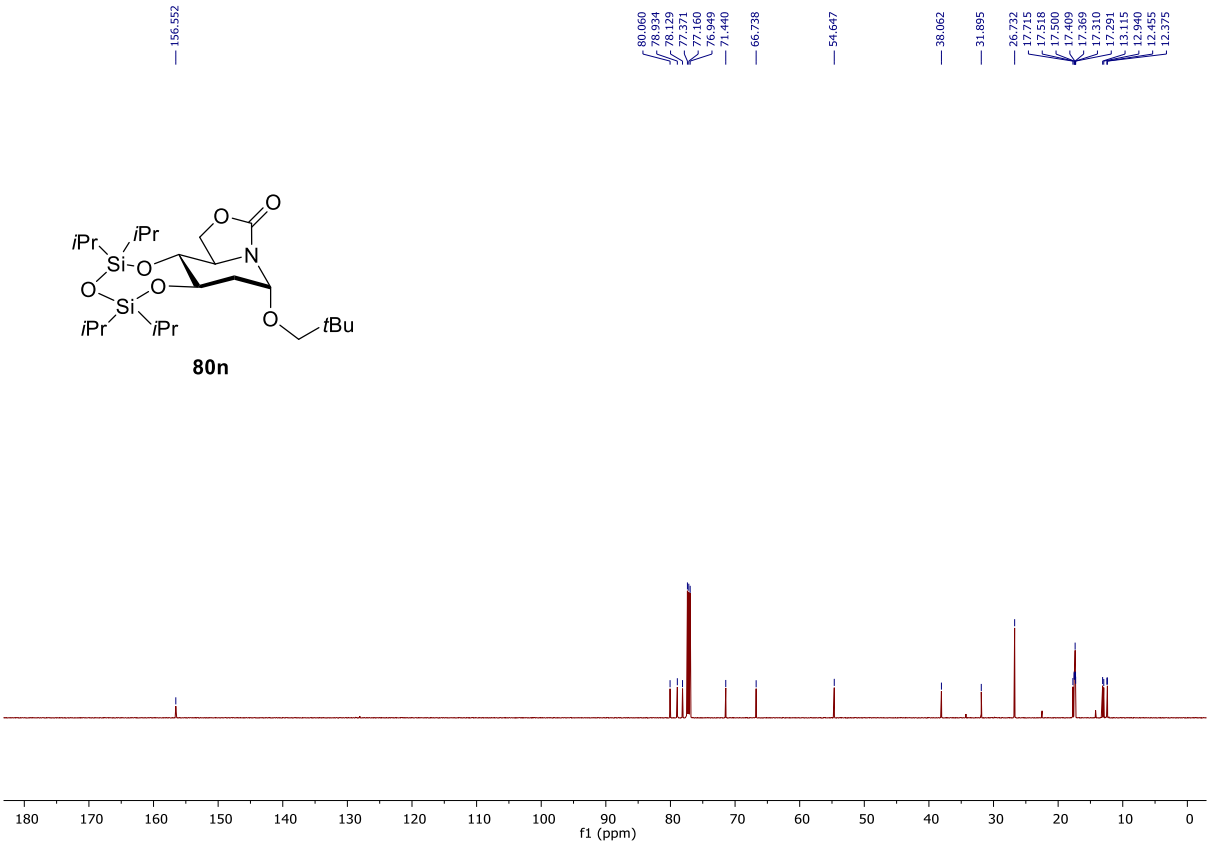

Figure 8.212. ^{13}C NMR spectra for 80n

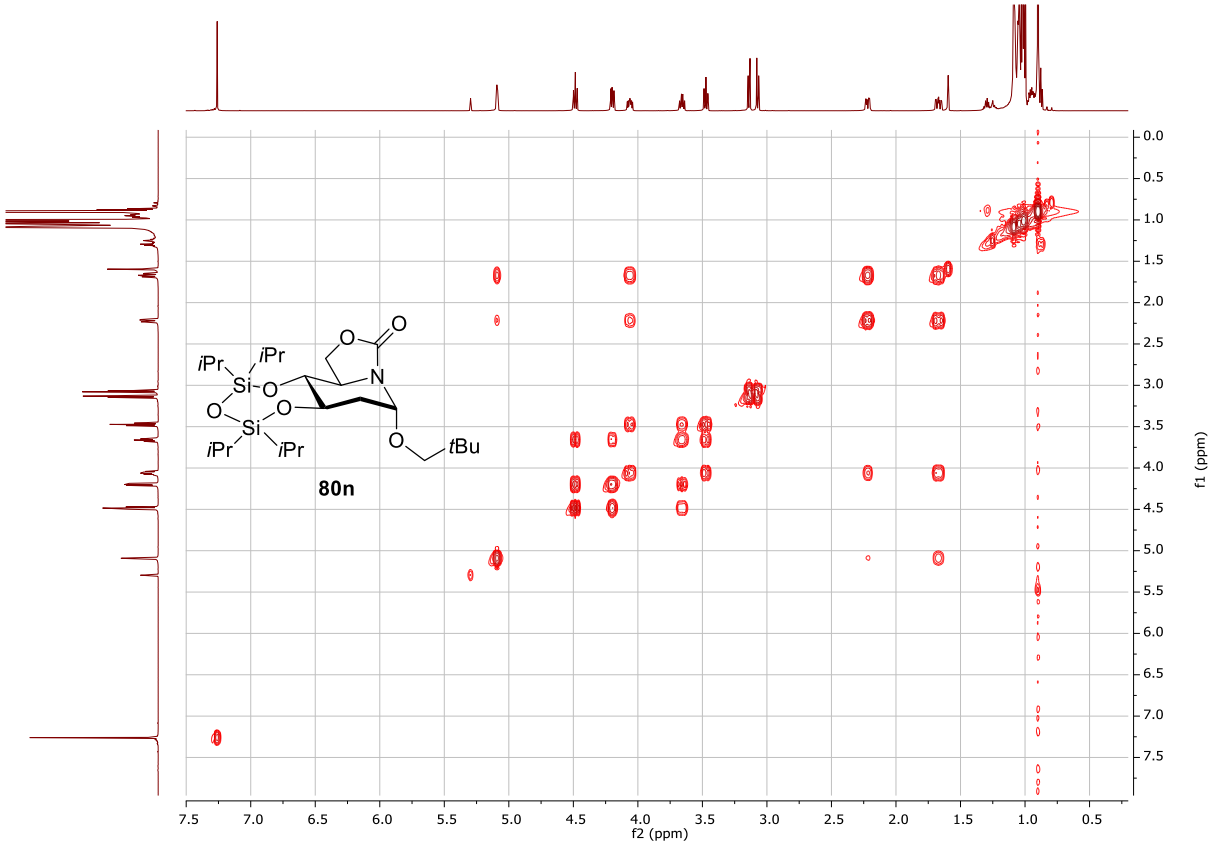

Figure 8.213. COSY spectra for 80n

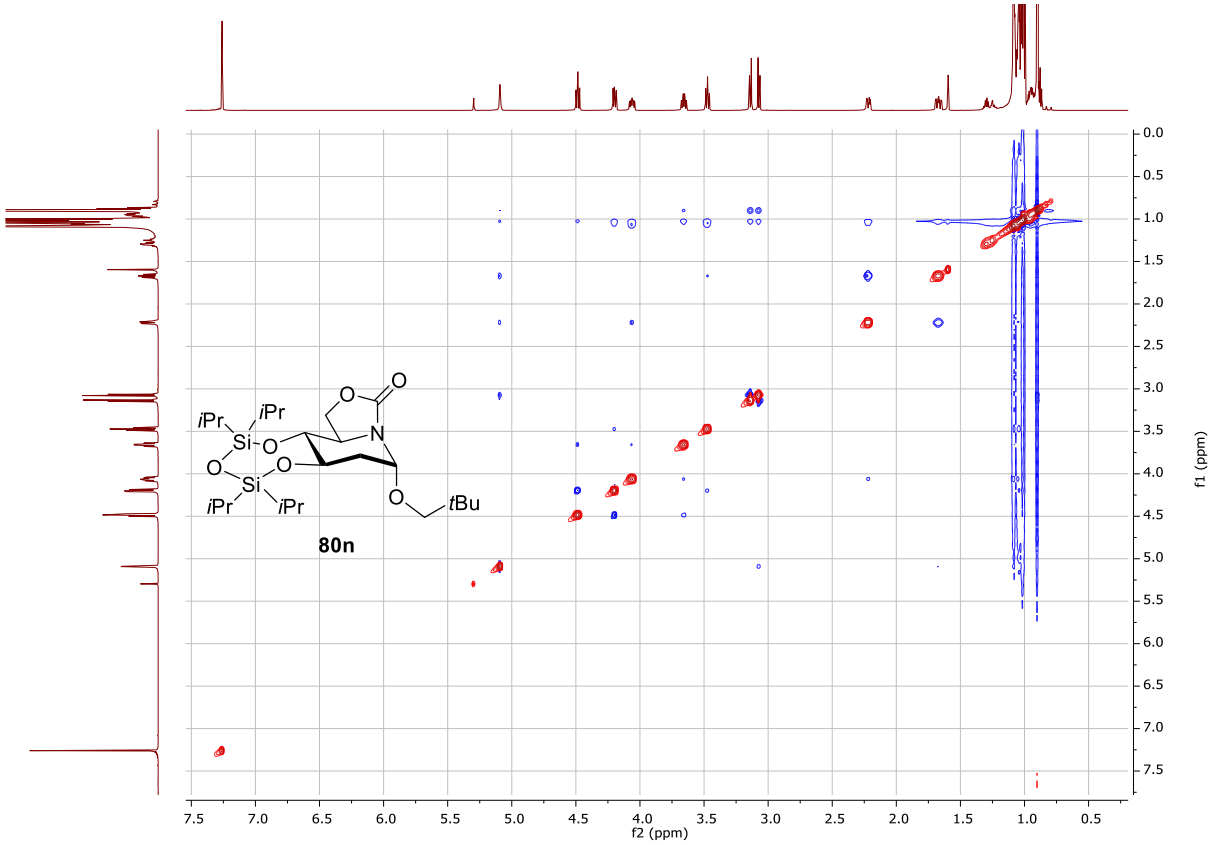

Figure 8.214. NOESY spectra for 80n

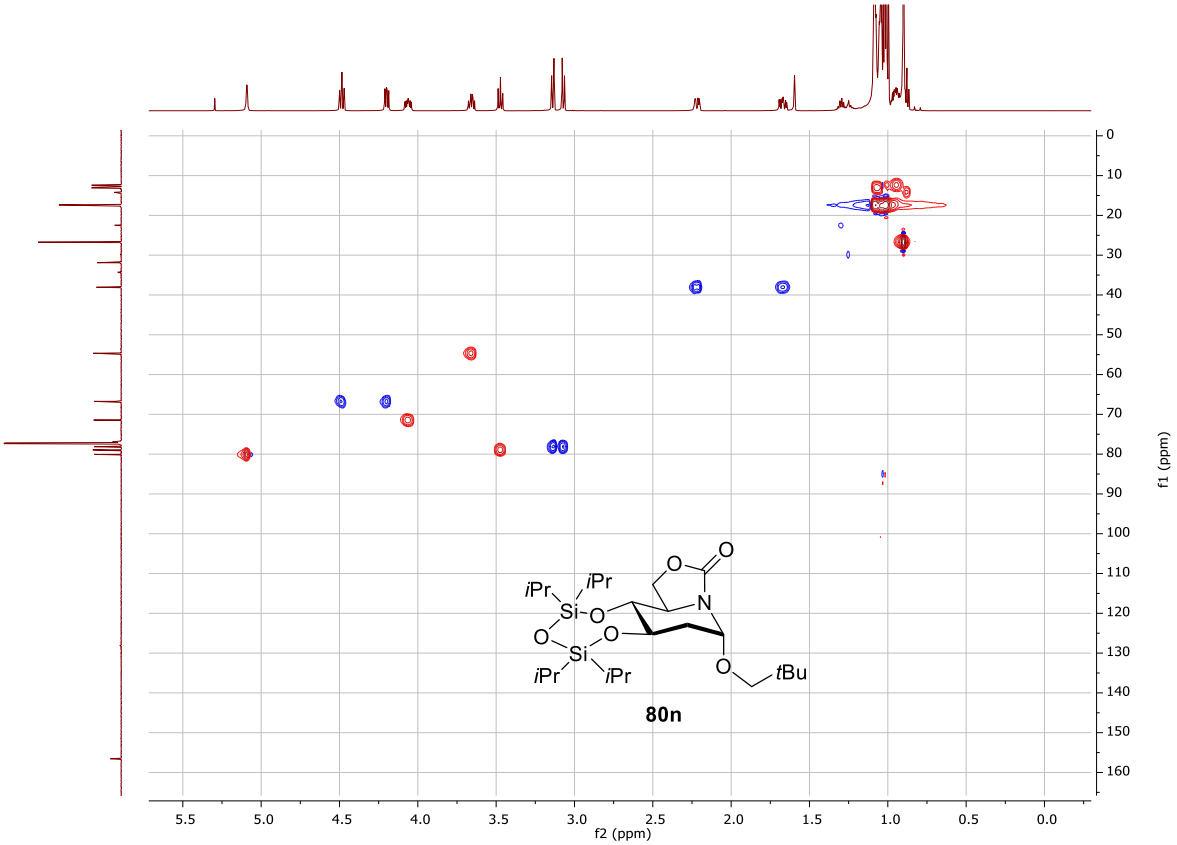

Figure 8.215. HSQC spectra for 80n

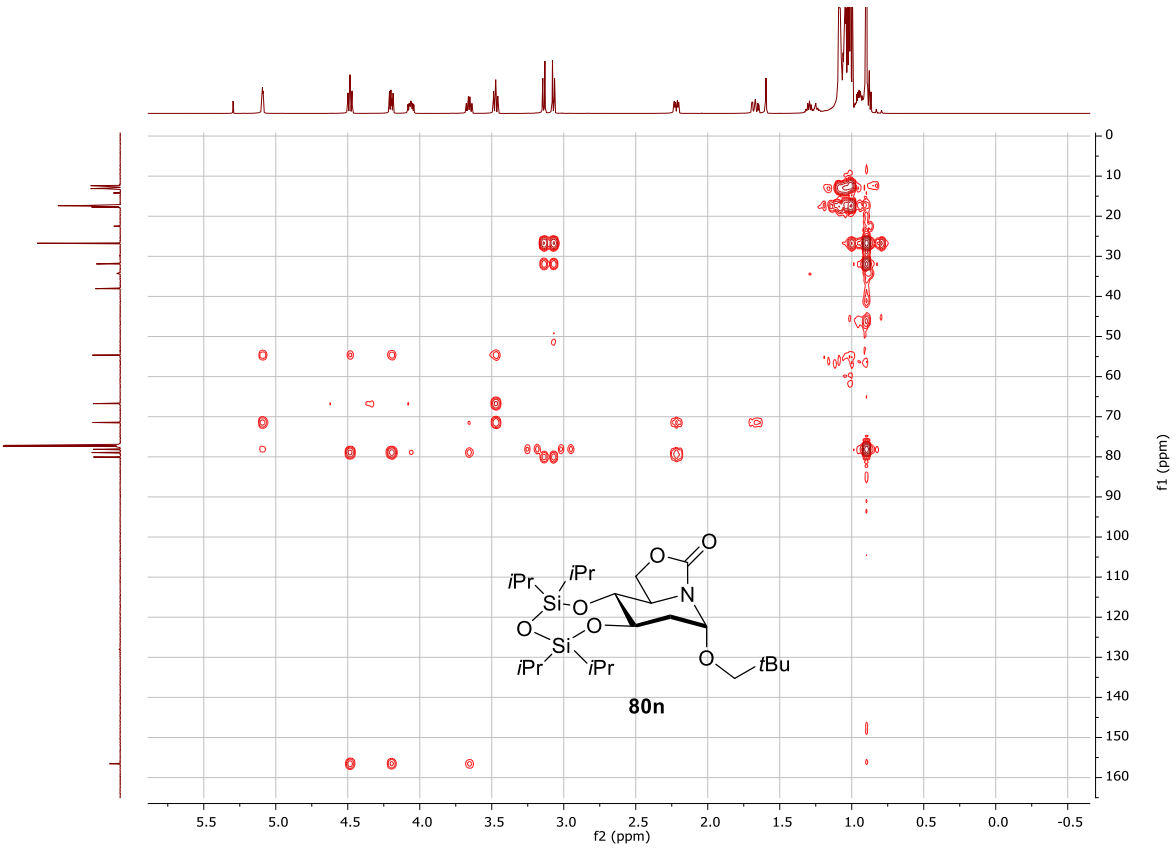

Figure 8.216. HMBC spectra for 80n

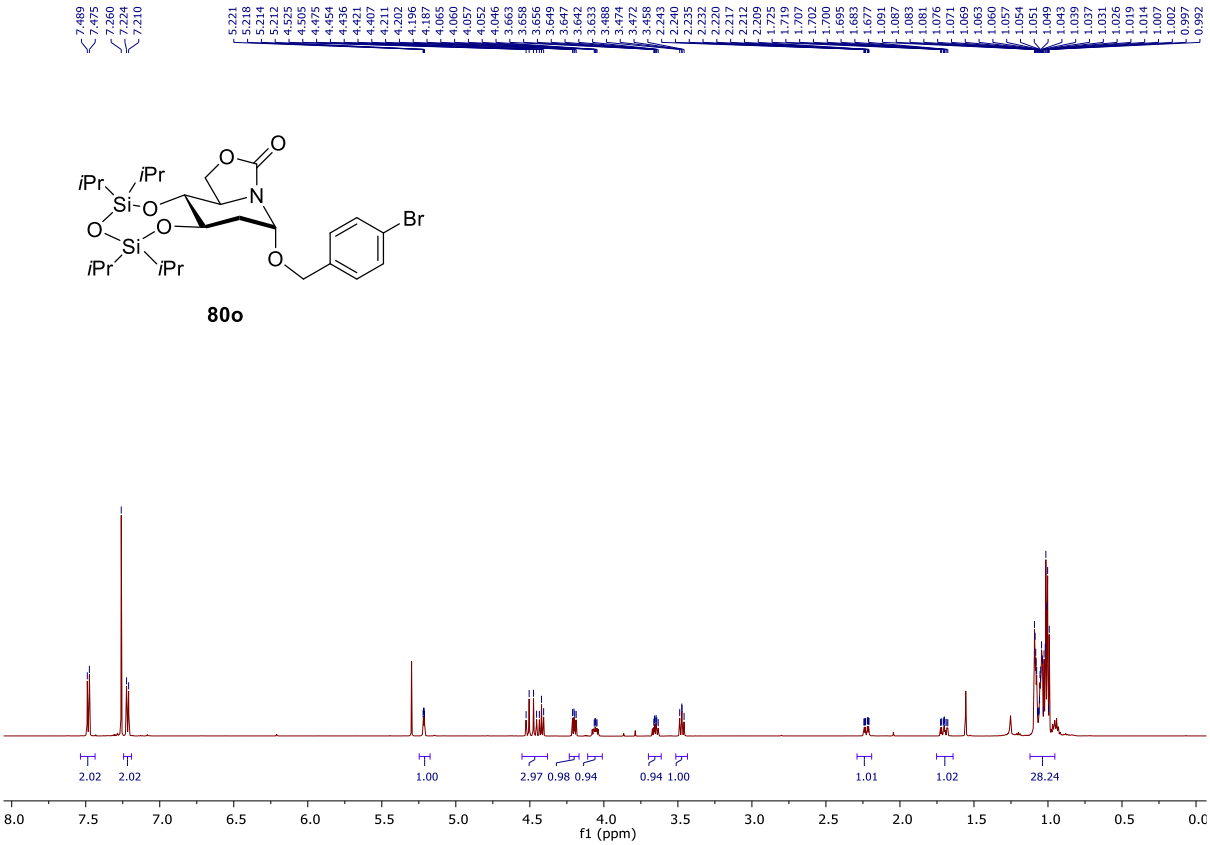

Figure 8.217. ^{1}H NMR spectra for 80o

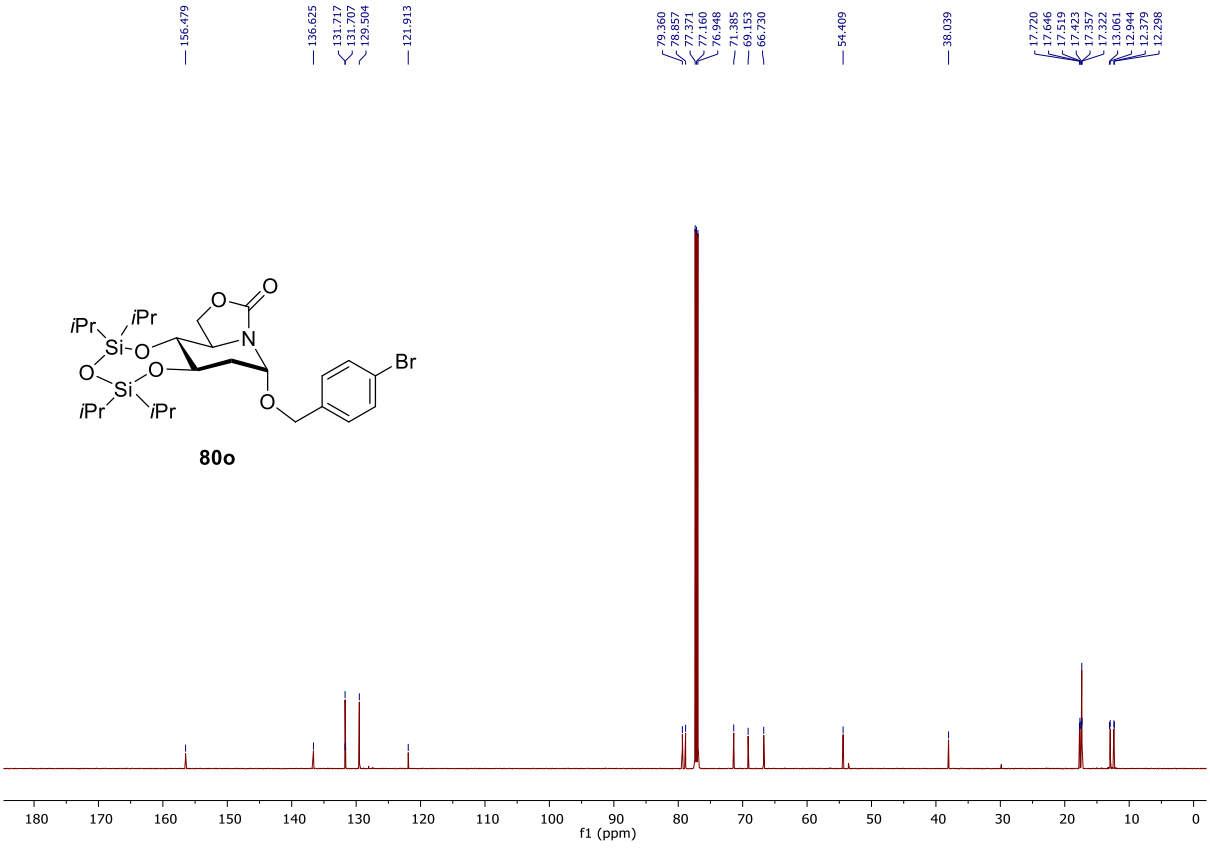

Figure 8.218. ^{13}C NMR spectra for 80o

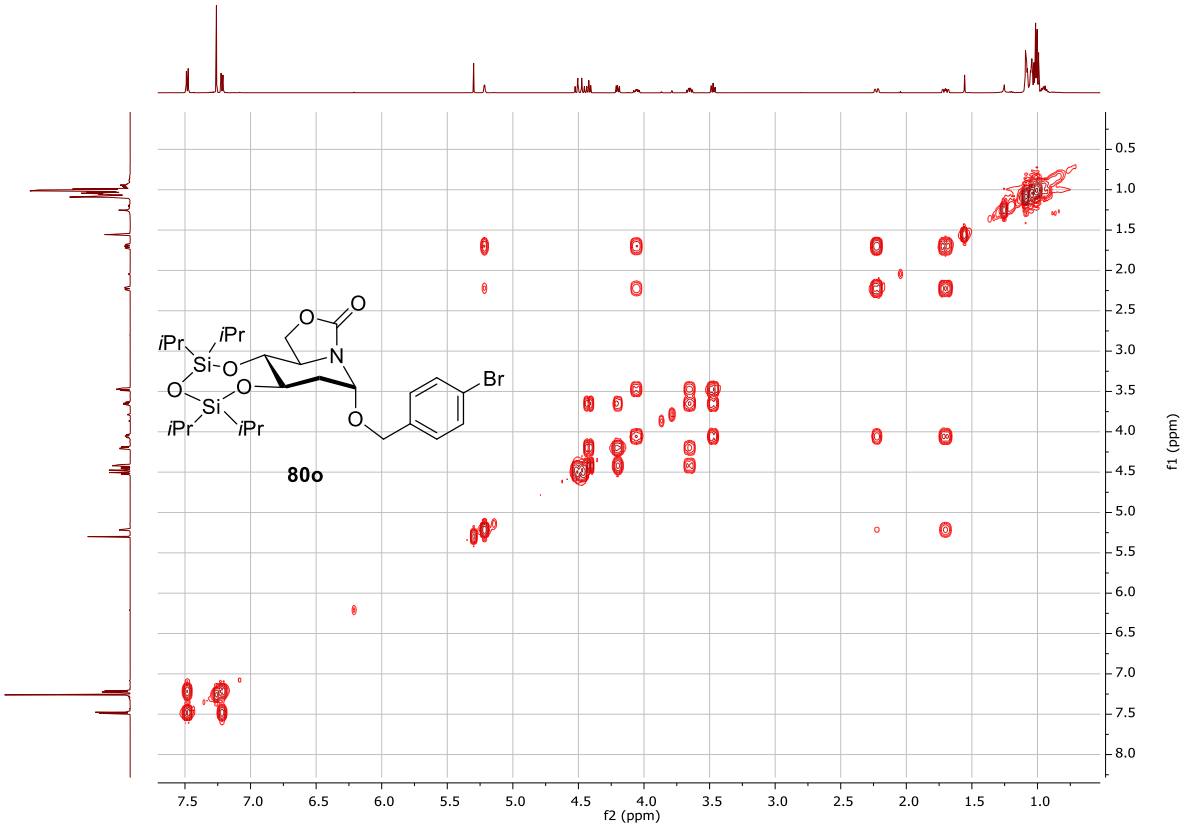

Figure 8.219. COSY spectra for 80o

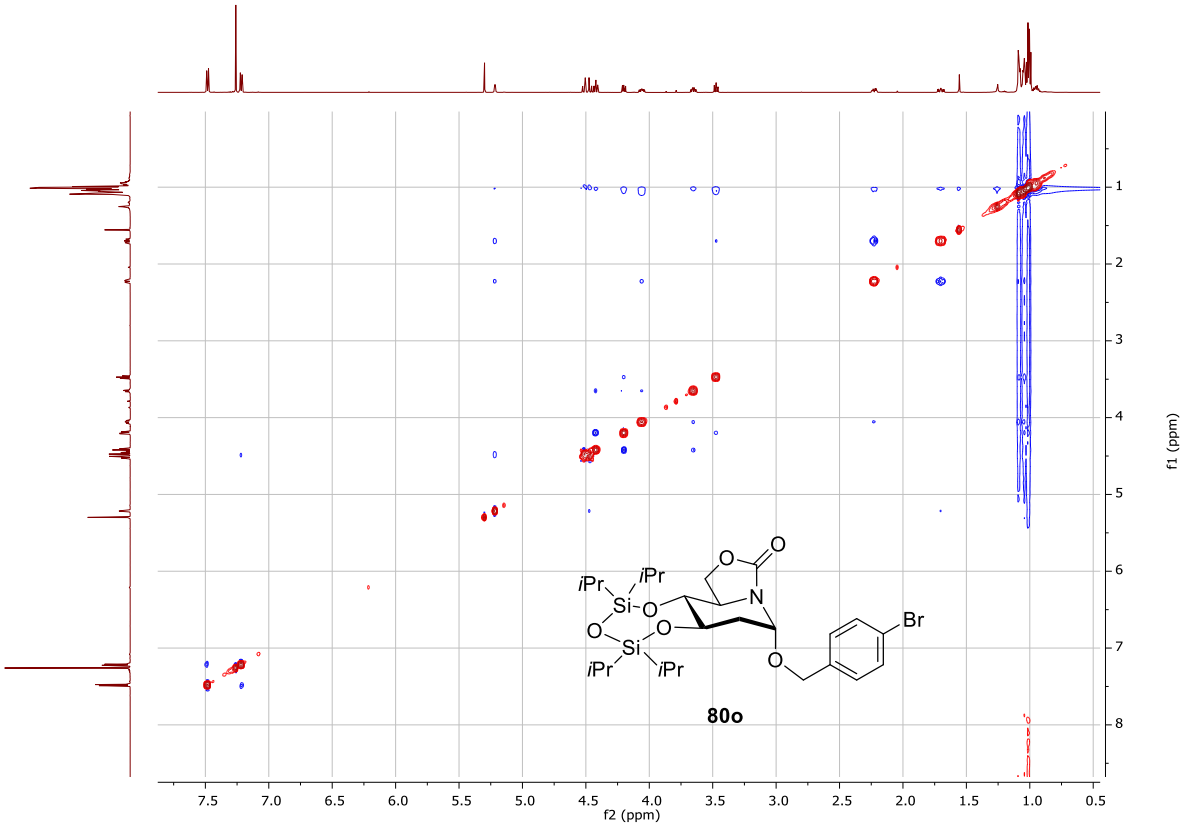

Figure 8.220. NOESY spectra for 80o

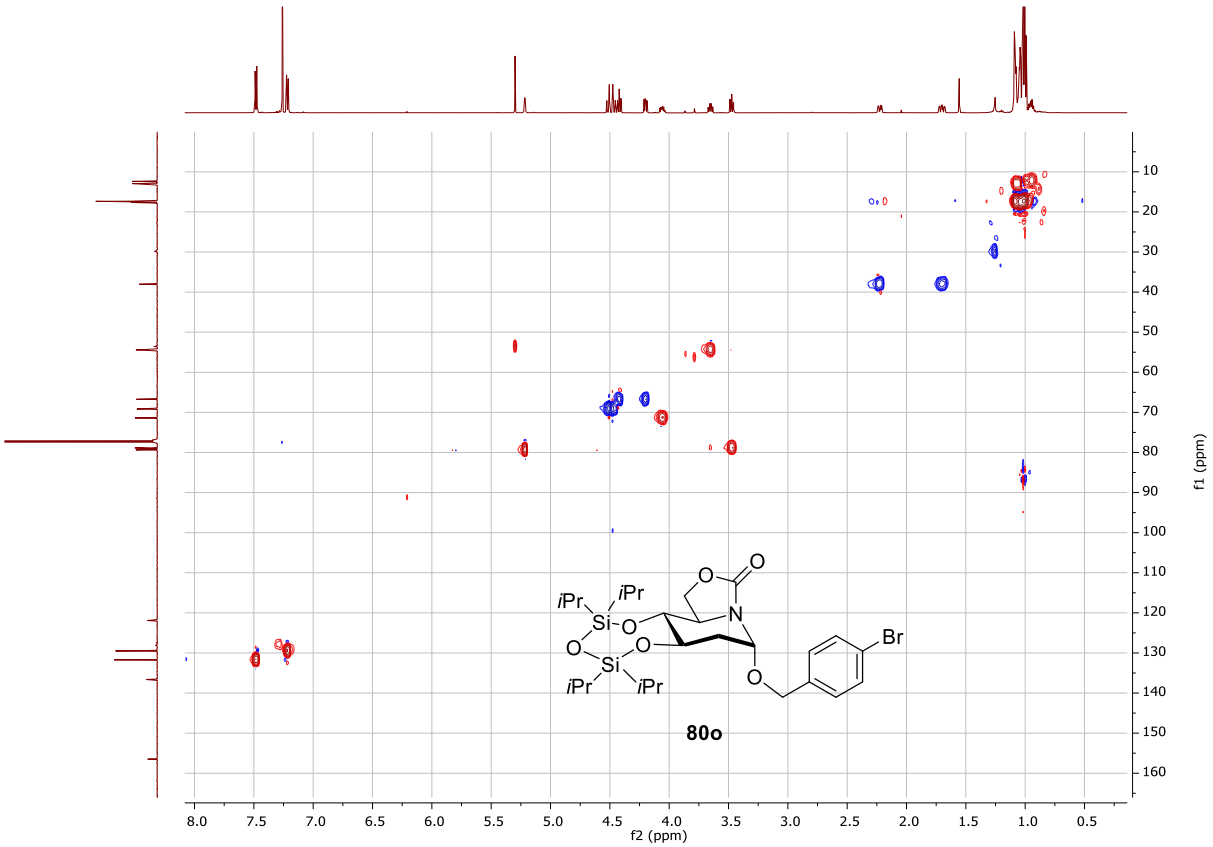

Figure 8.221. HSQC spectra for 80o

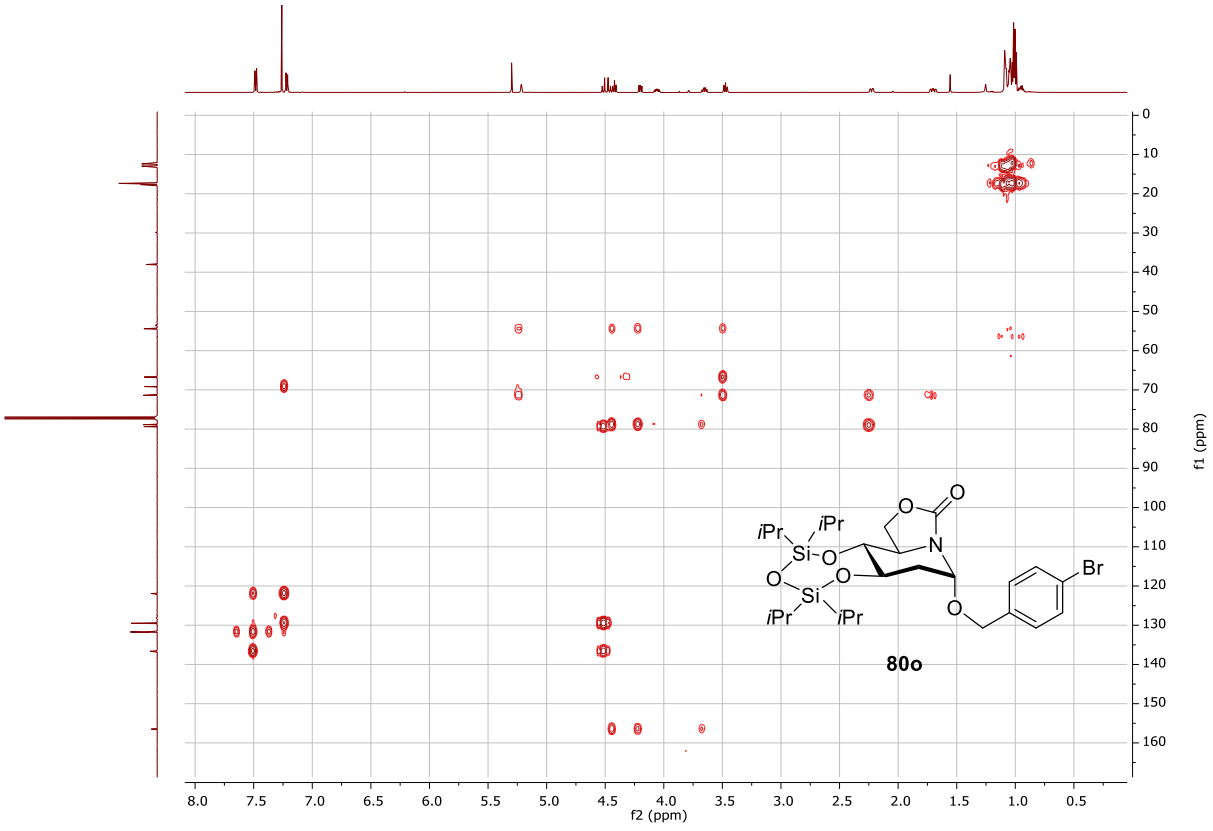

Figure 8.222. HMBC spectra for 80o

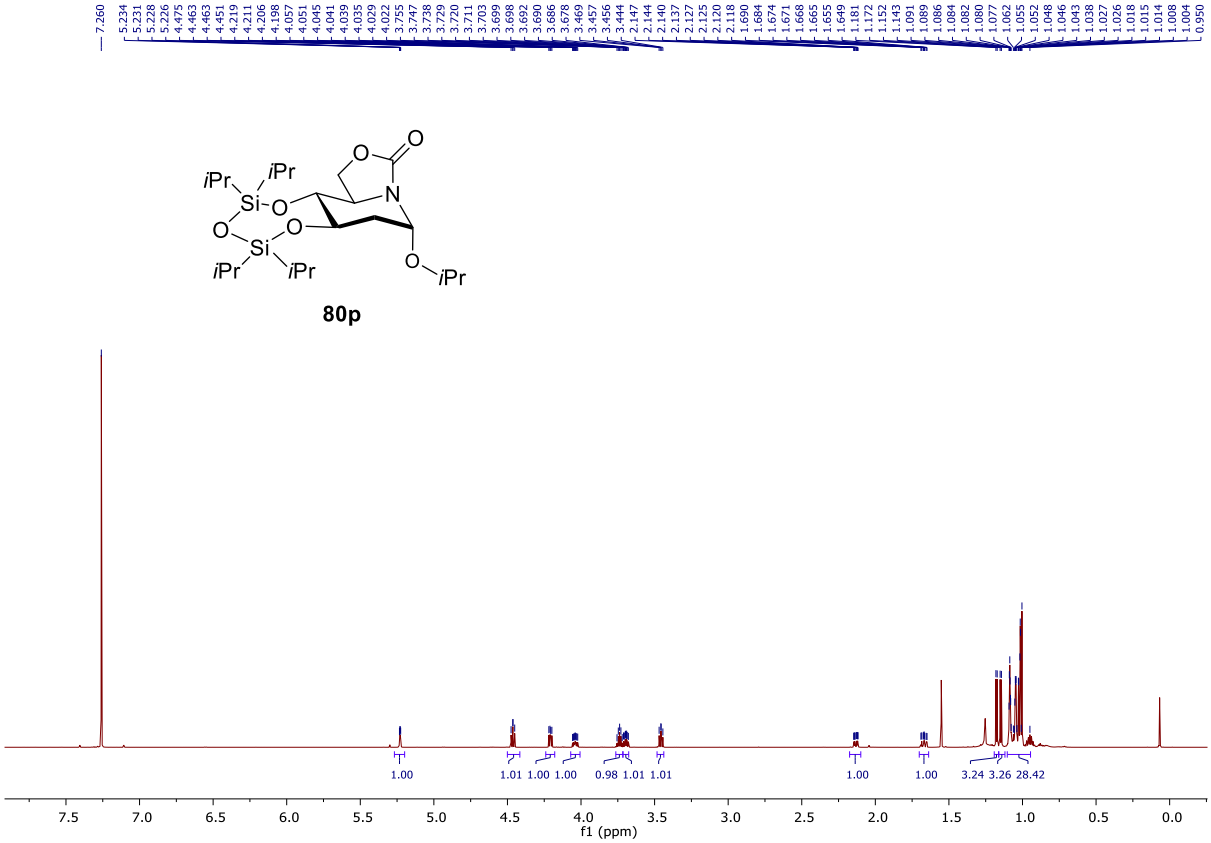

Figure 8.223. ^{1}H NMR spectra for 80p

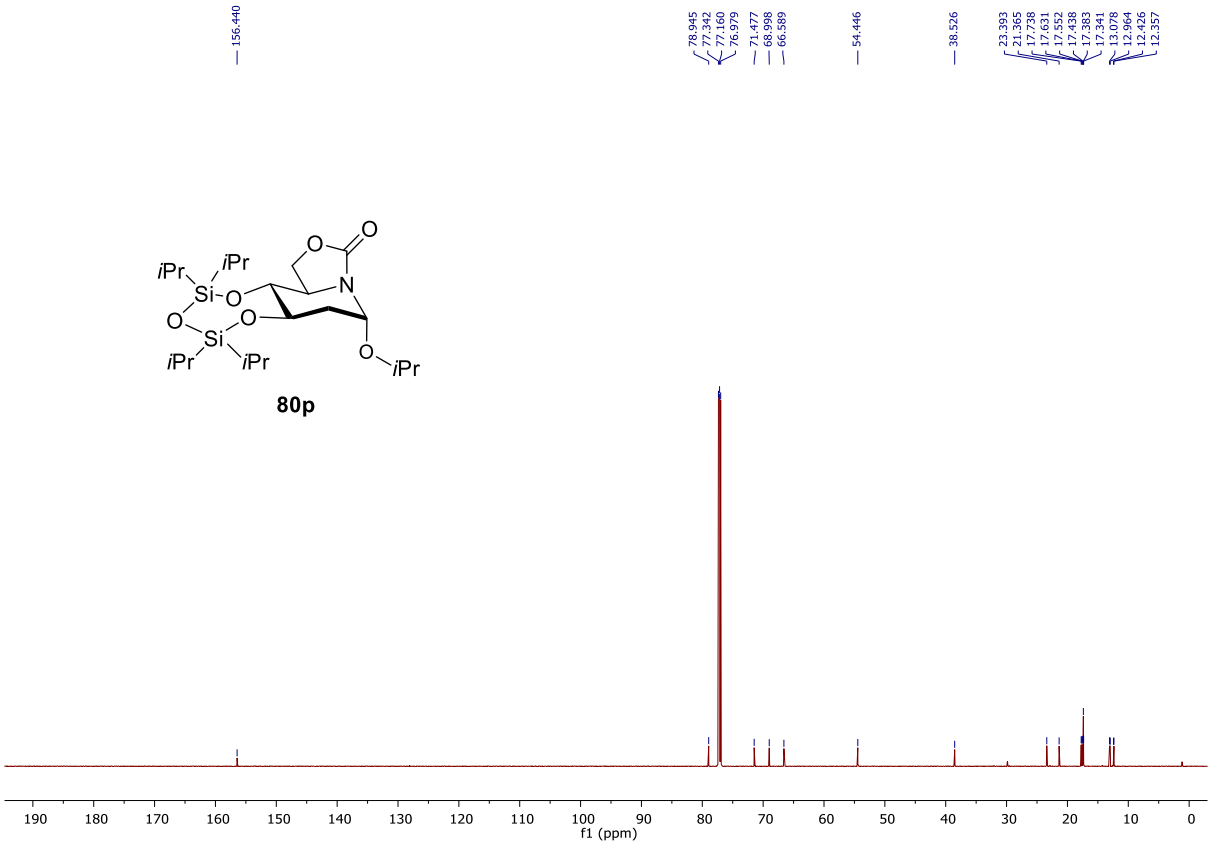

Figure 8.224. ^{13}C NMR spectra for 80p

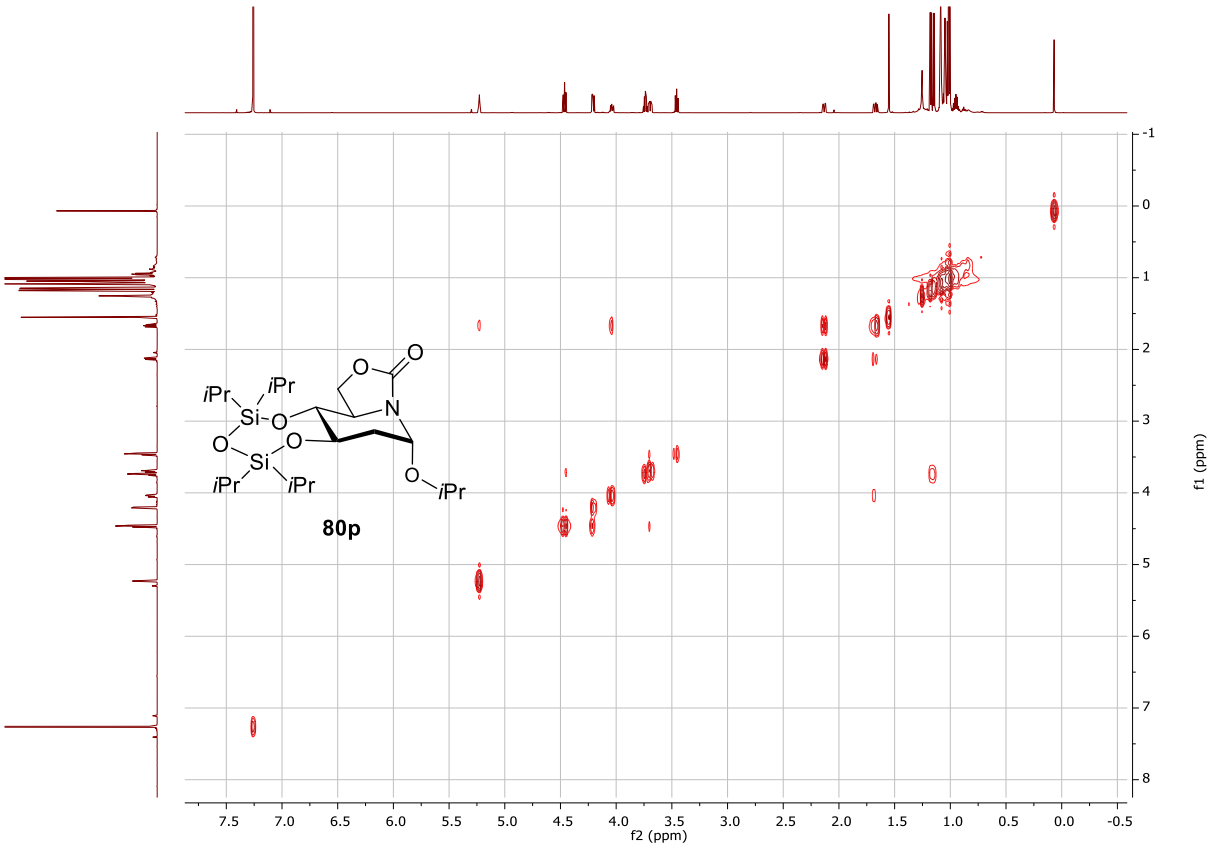

Figure 8.225. COSY spectra for 80p

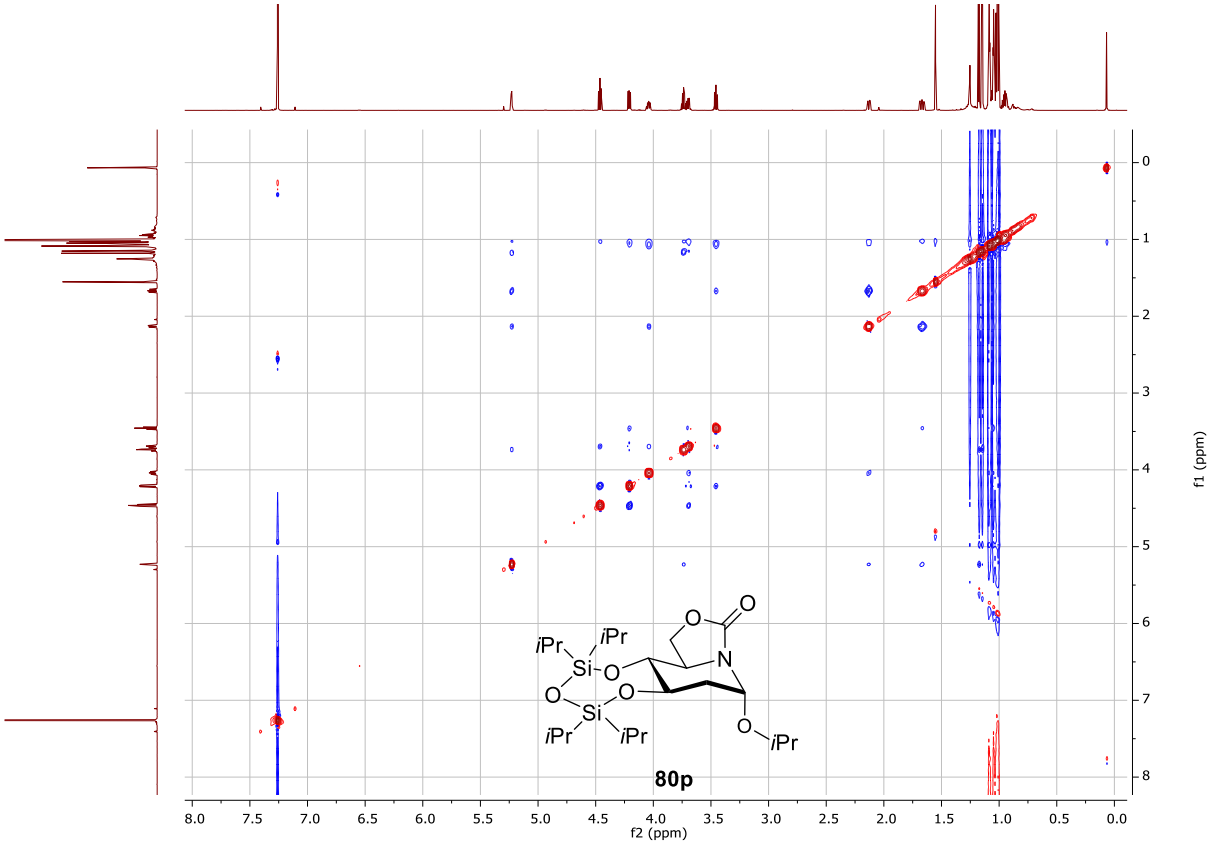

Figure 8.226. NOESY spectra for 80p

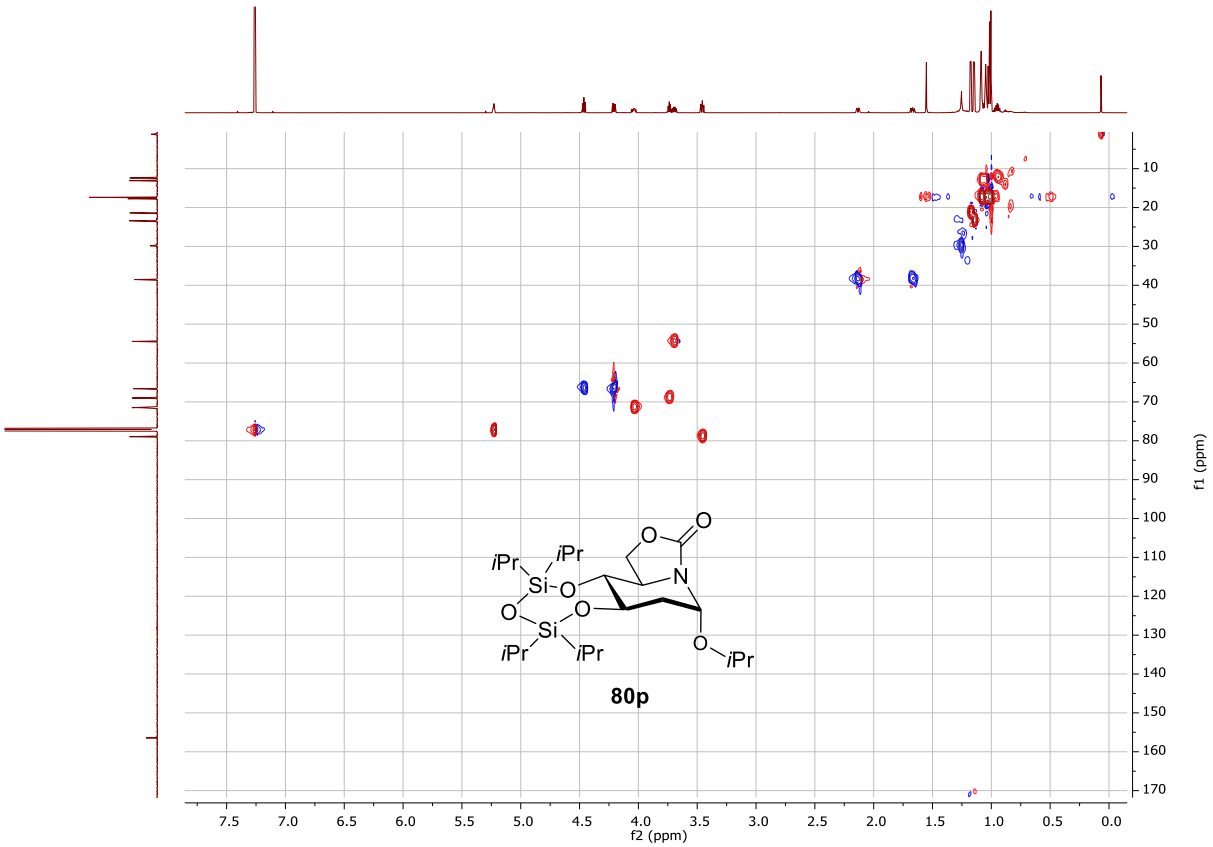

Figure 8.227. HSQC spectra for 80p

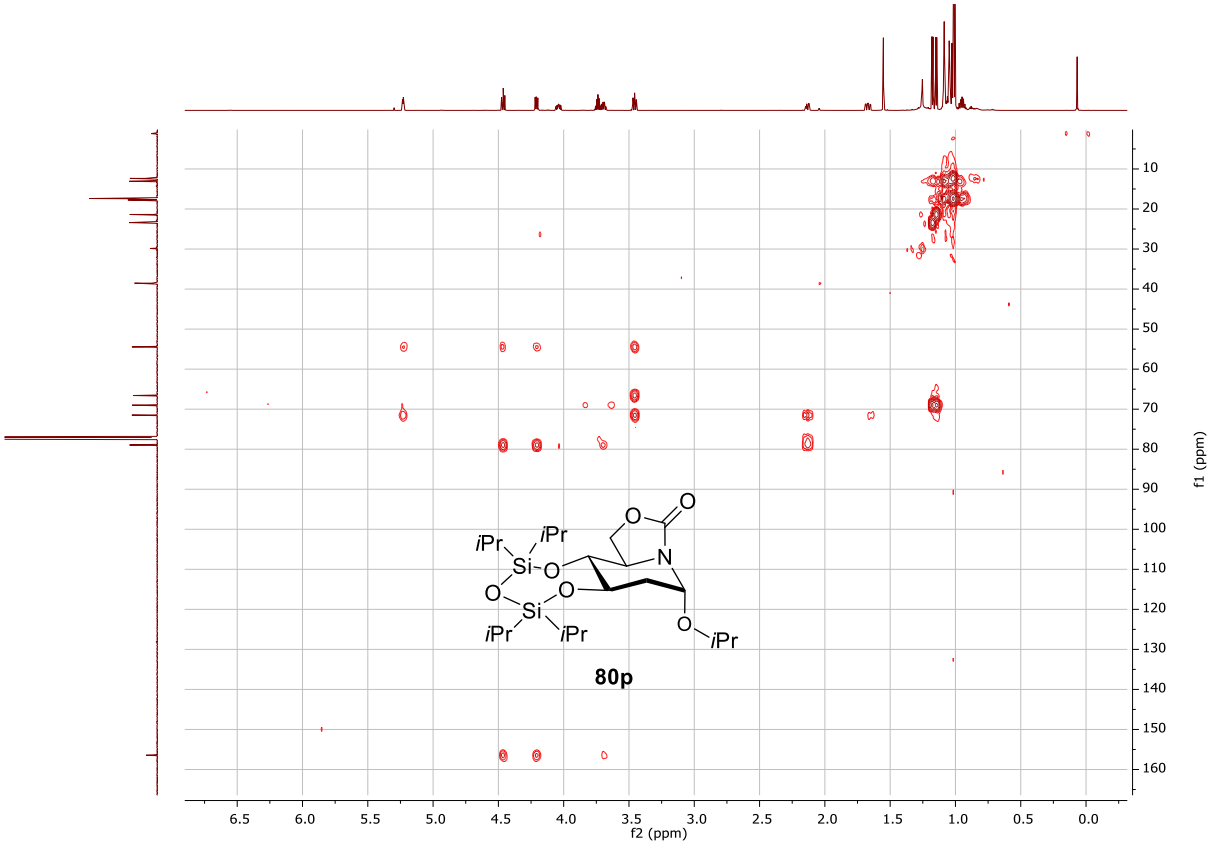

Figure 8.228. HMBC spectra for 80p

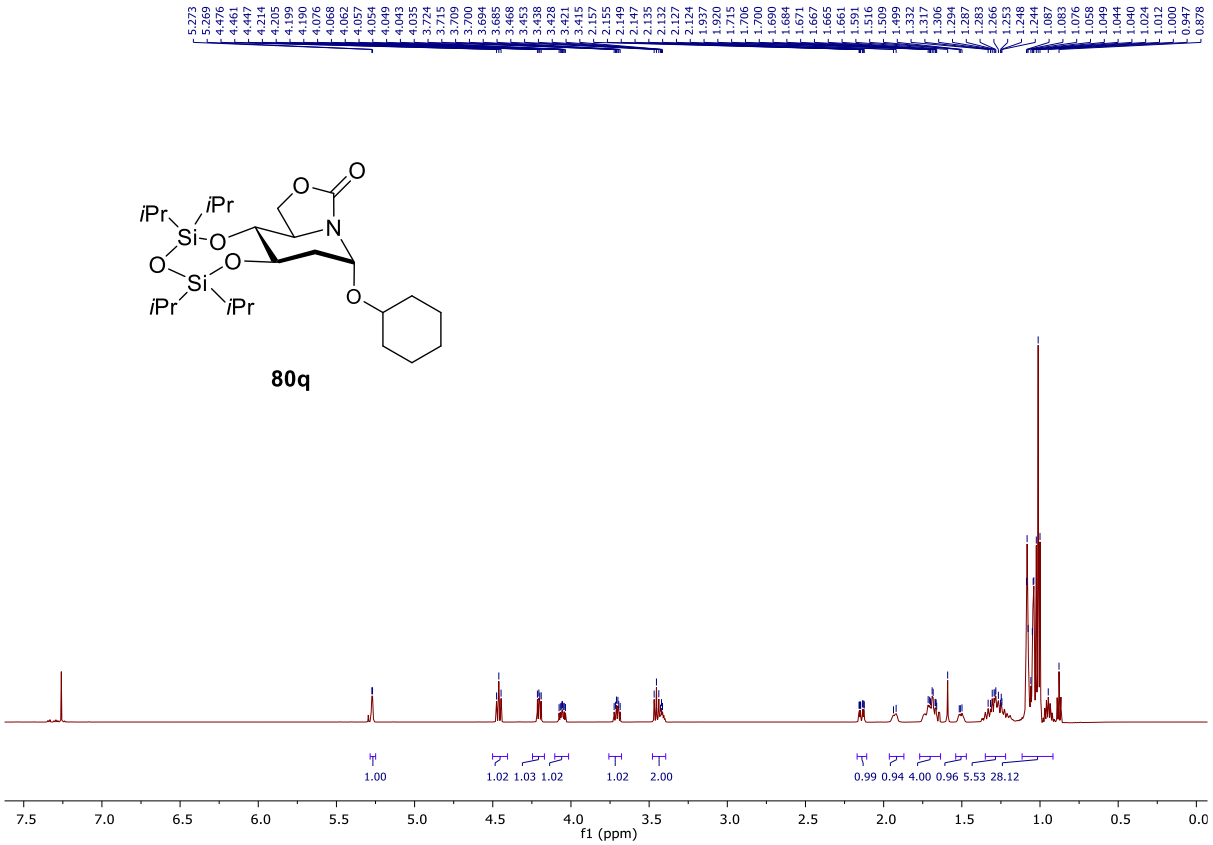

Figure 8.229. ^{1}H NMR spectra for 80q

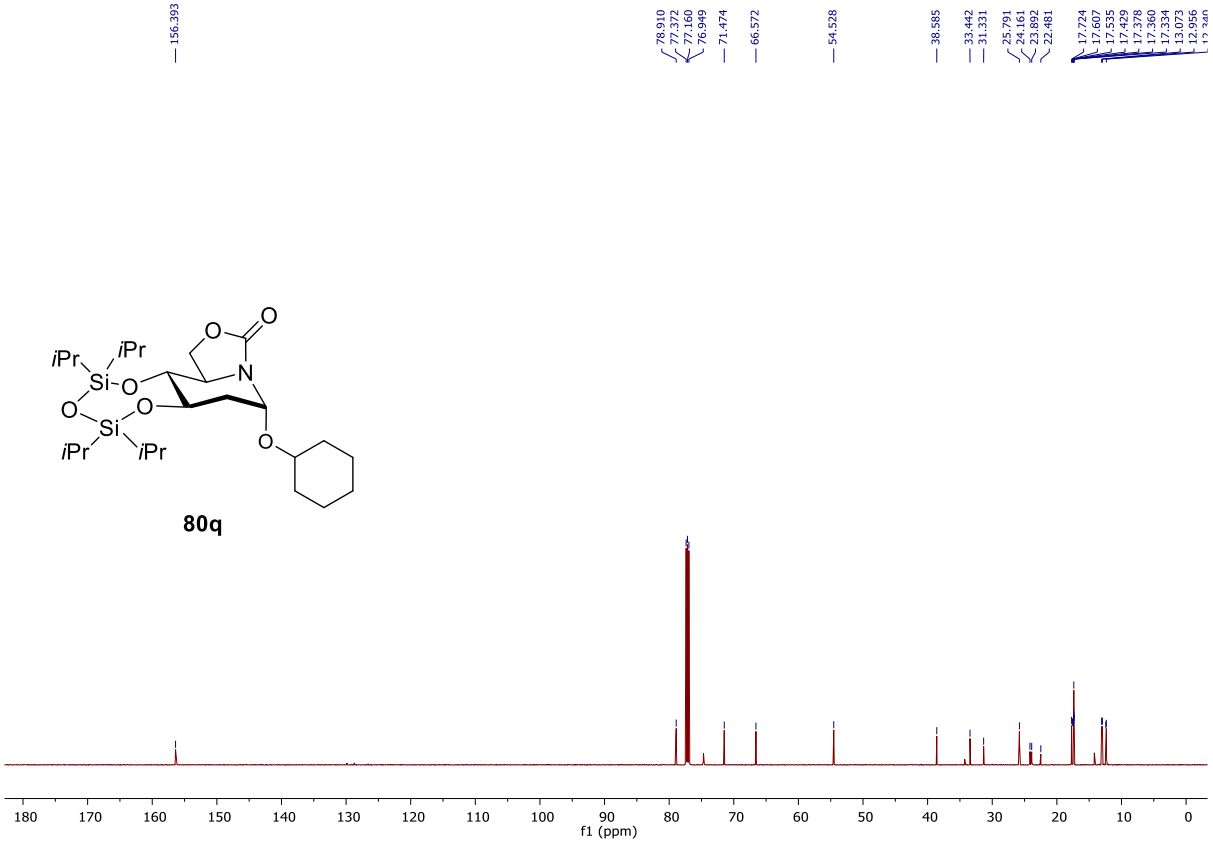

Figure 8.230. ^{13}C NMR spectra for 80q

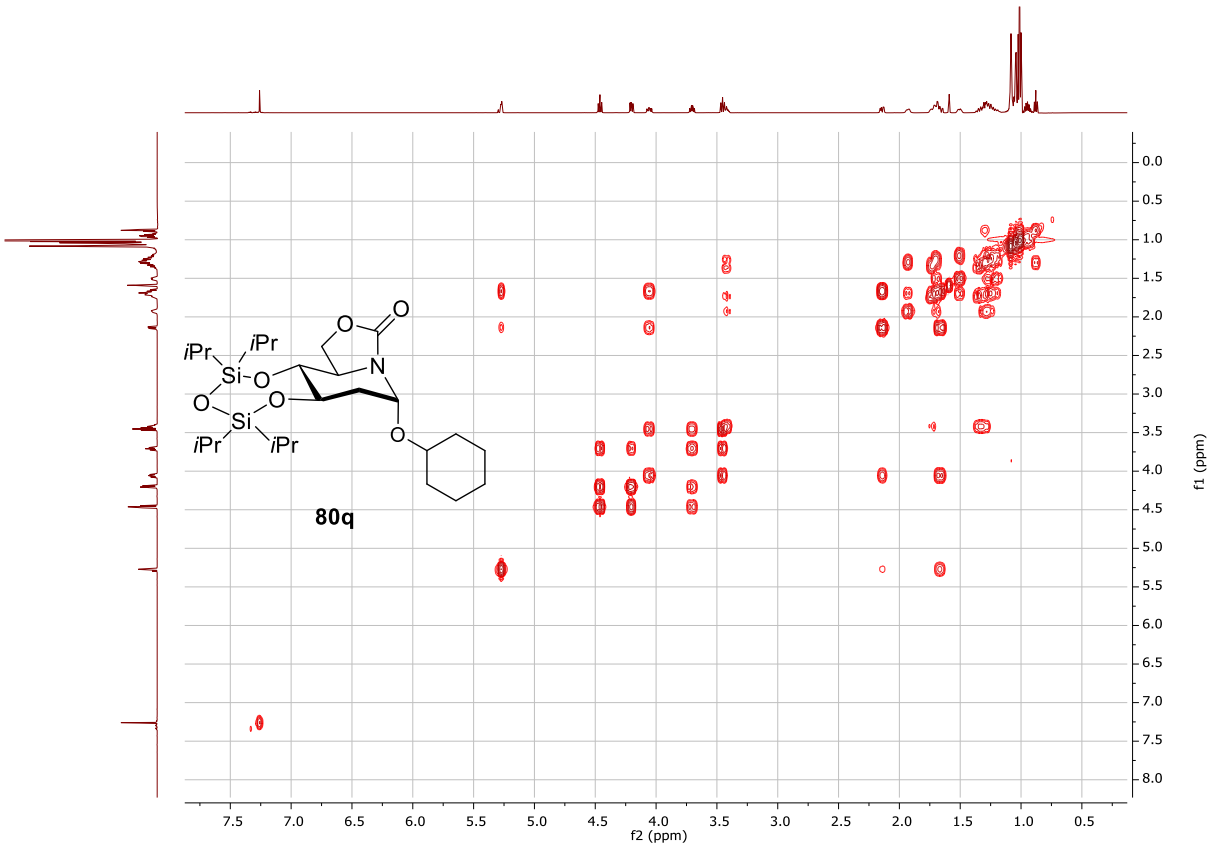

Figure 8.231. COSY spectra for 80q

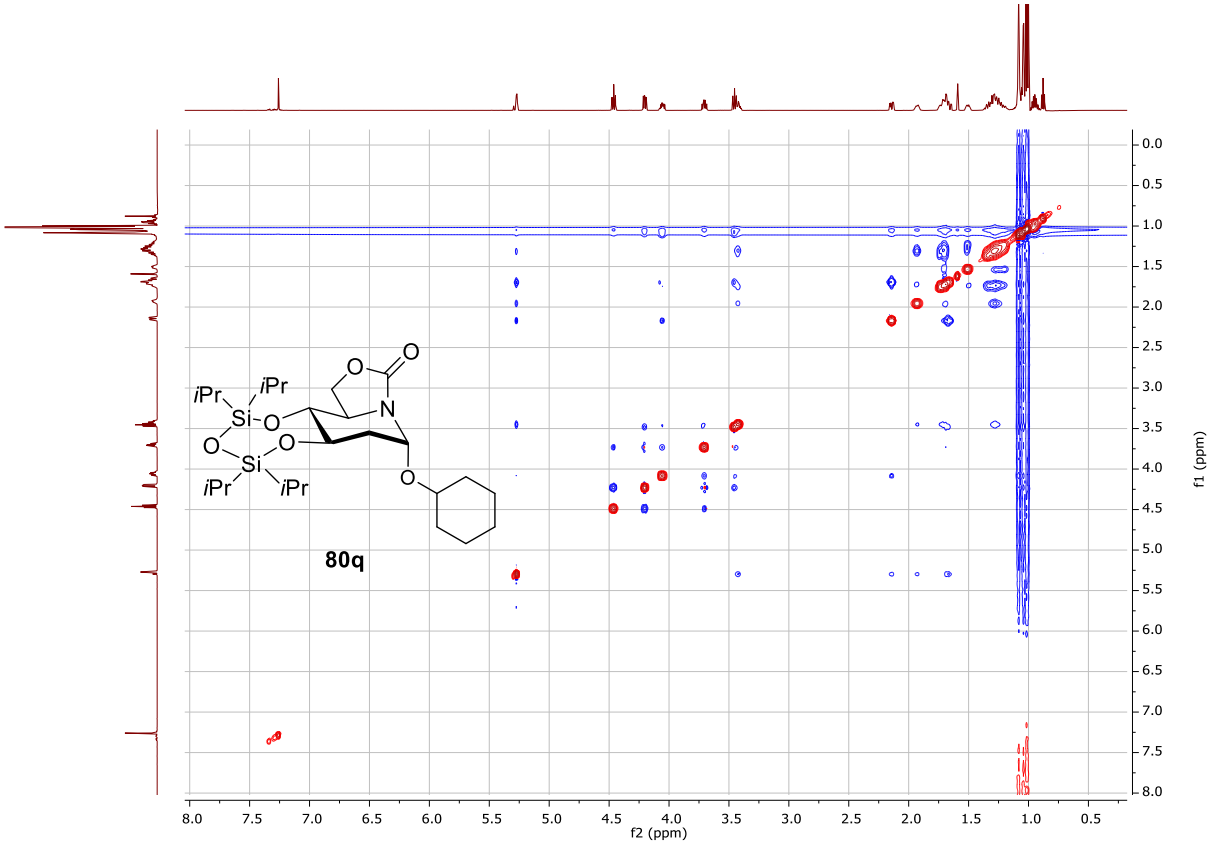

Figure 8.232. NOESY spectra for 80q

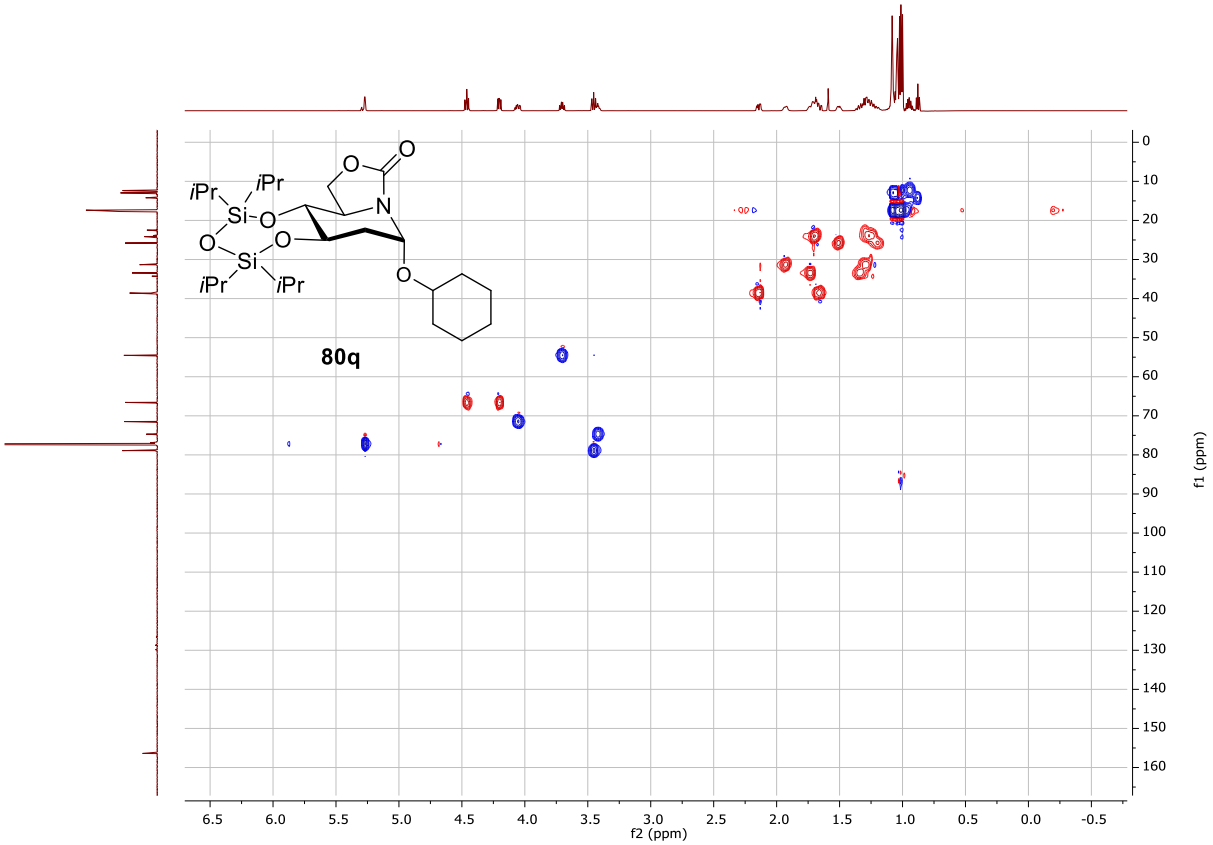

Figure 8.233. HSQC spectra for 80q

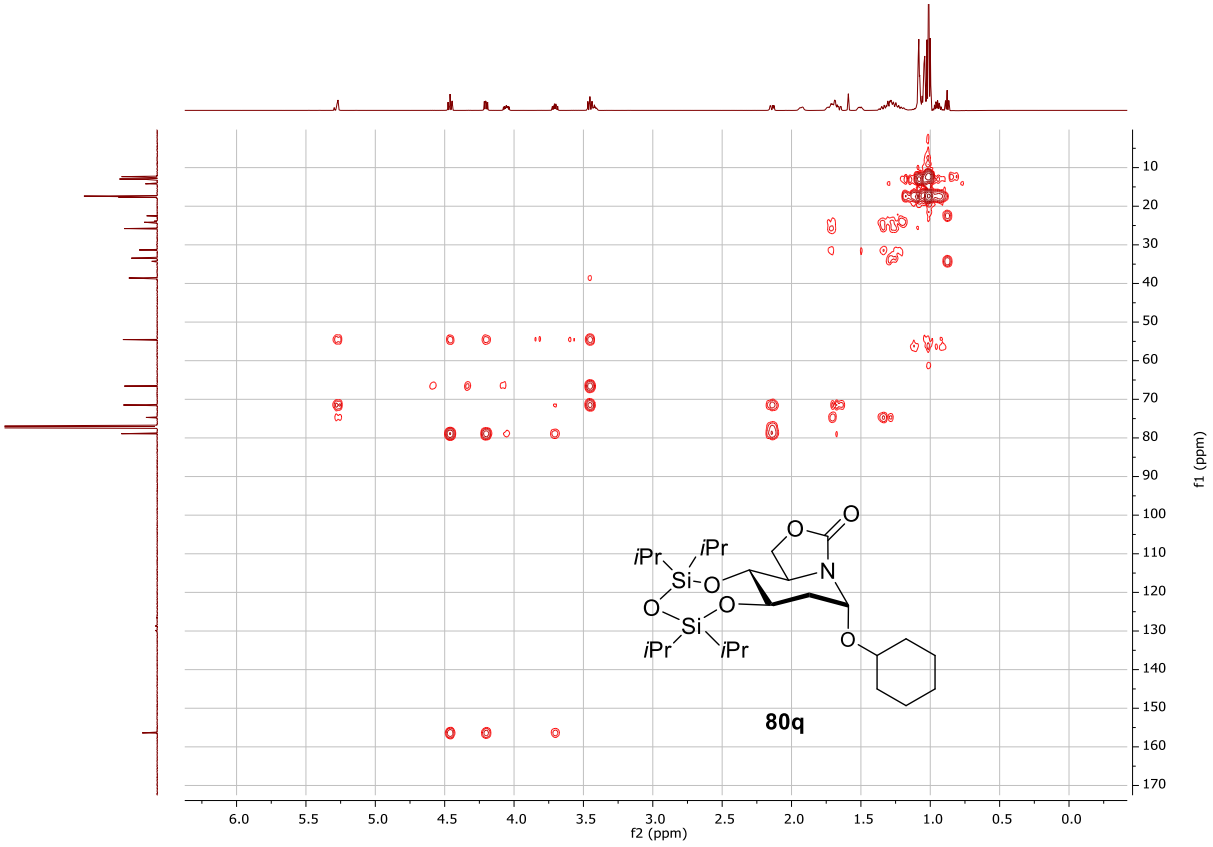

Figure 8.234. HMBC spectra for 80q

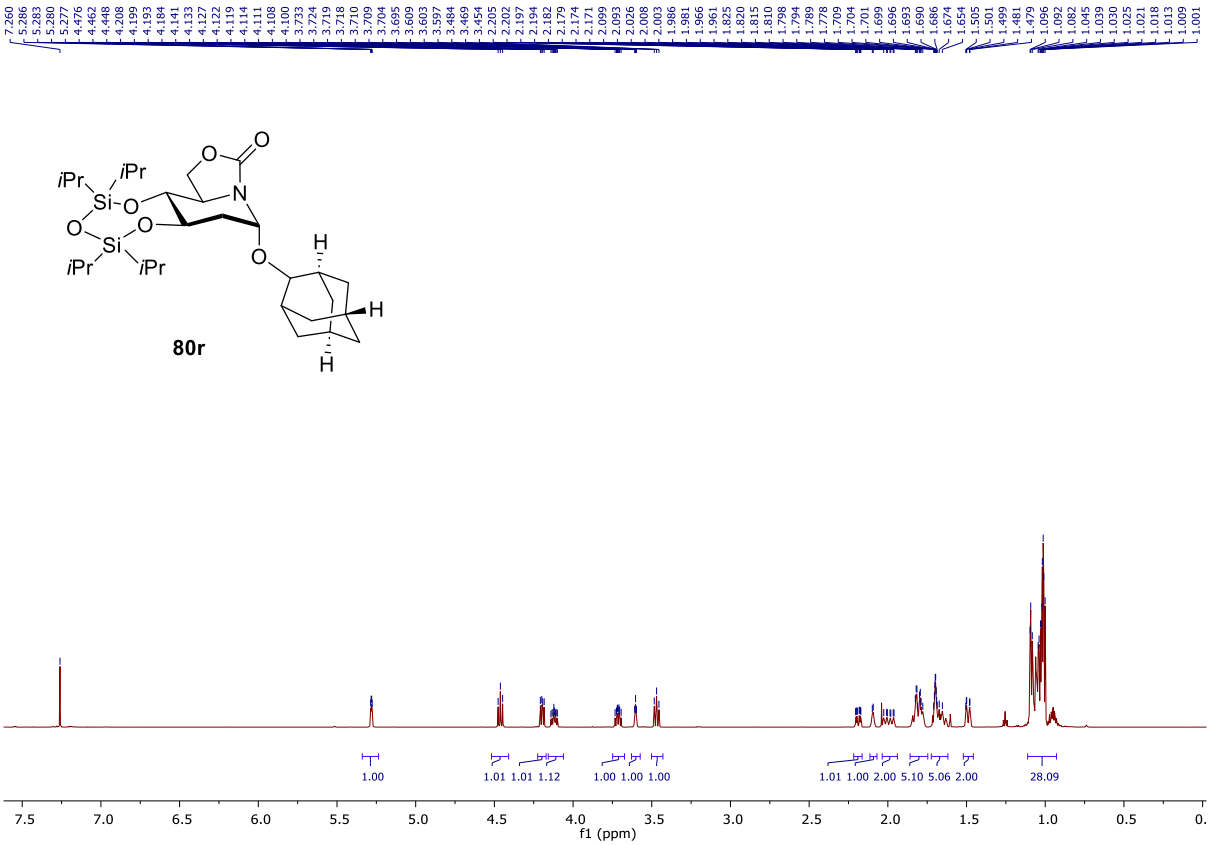

Figure 8.235. ^{1}H NMR spectra for 80r

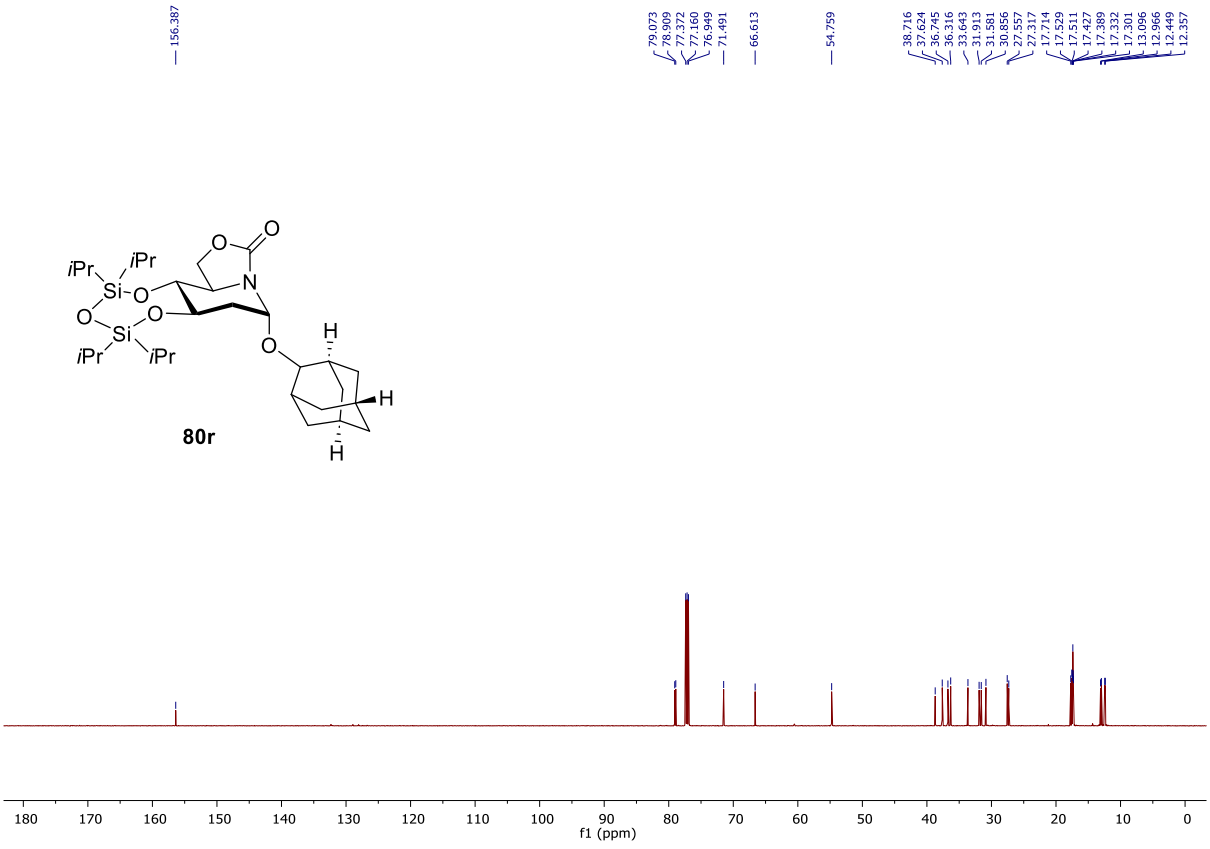

Figure 8.236. ^{13}C NMR spectra for 80r

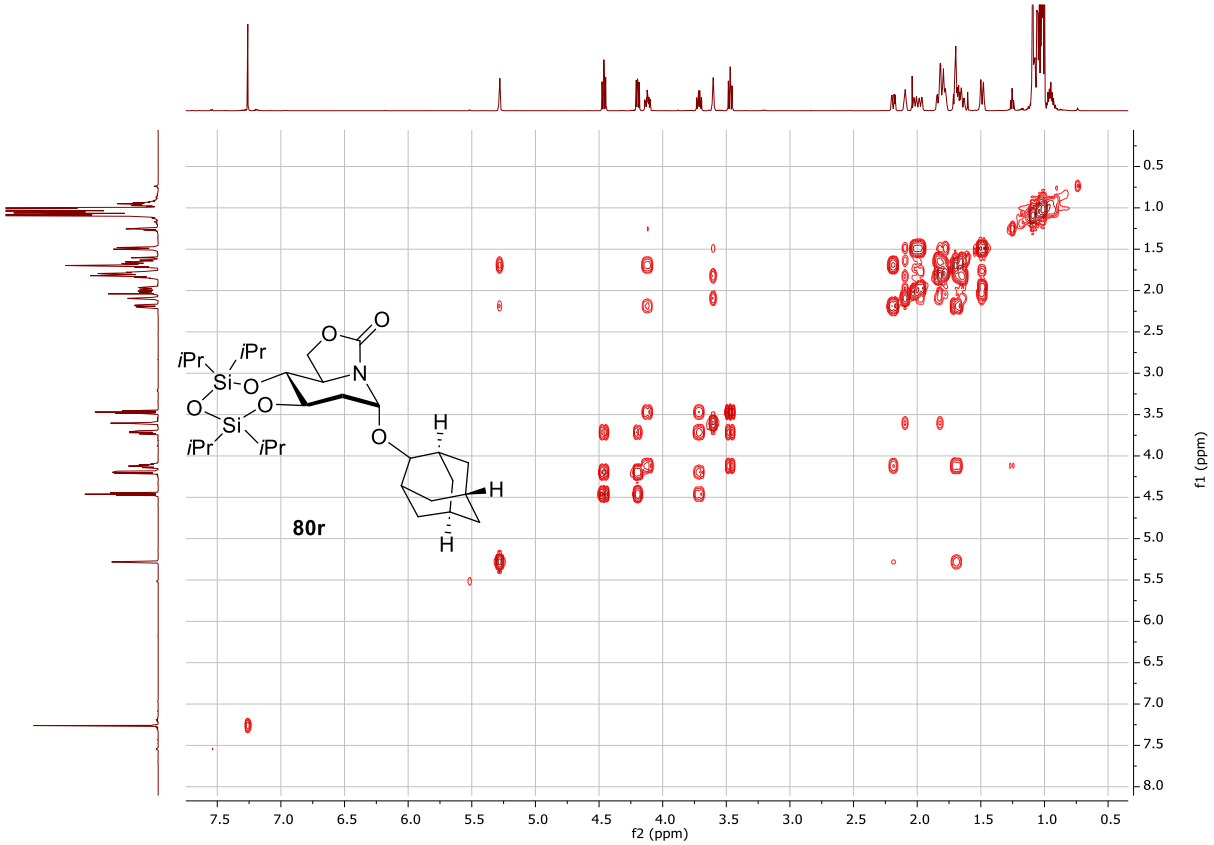

Figure 8.237. COSY spectra for 80r

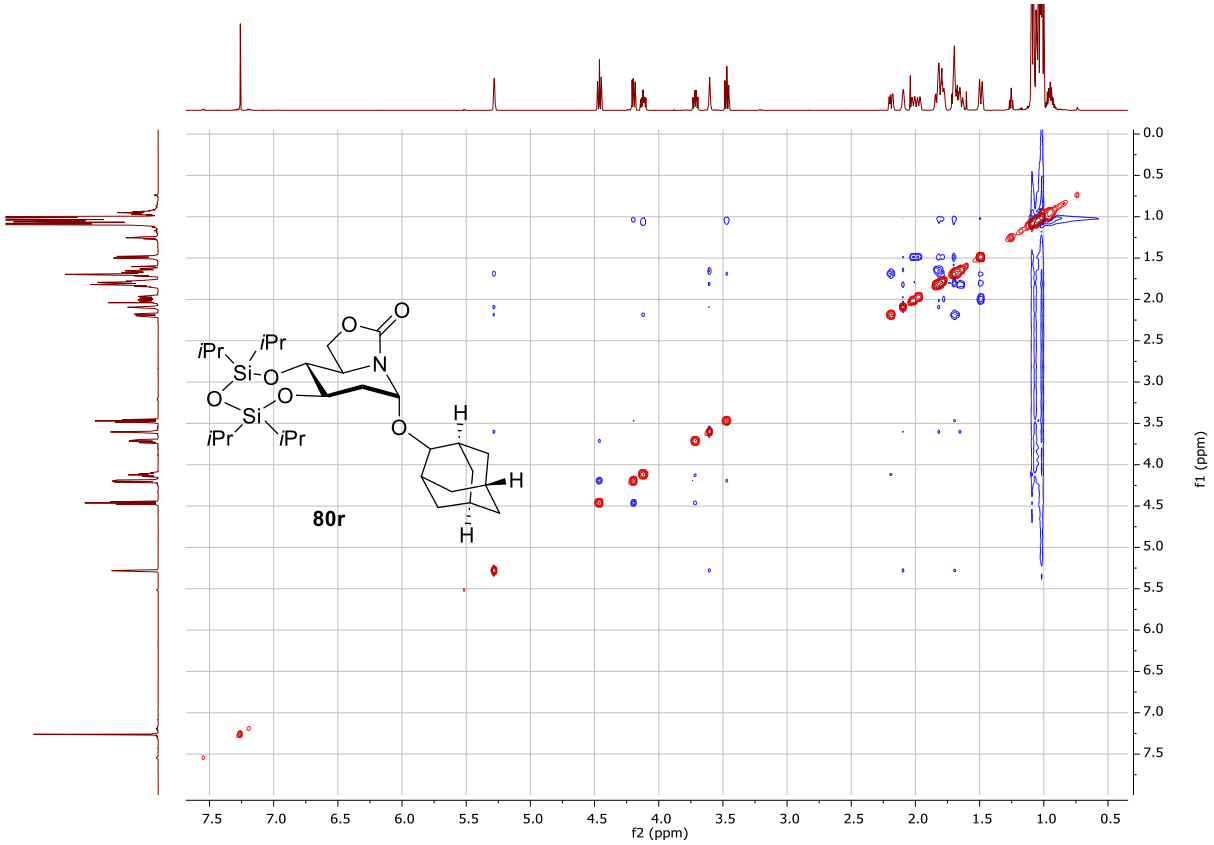

Figure 8.238. NOESY spectra for 80r

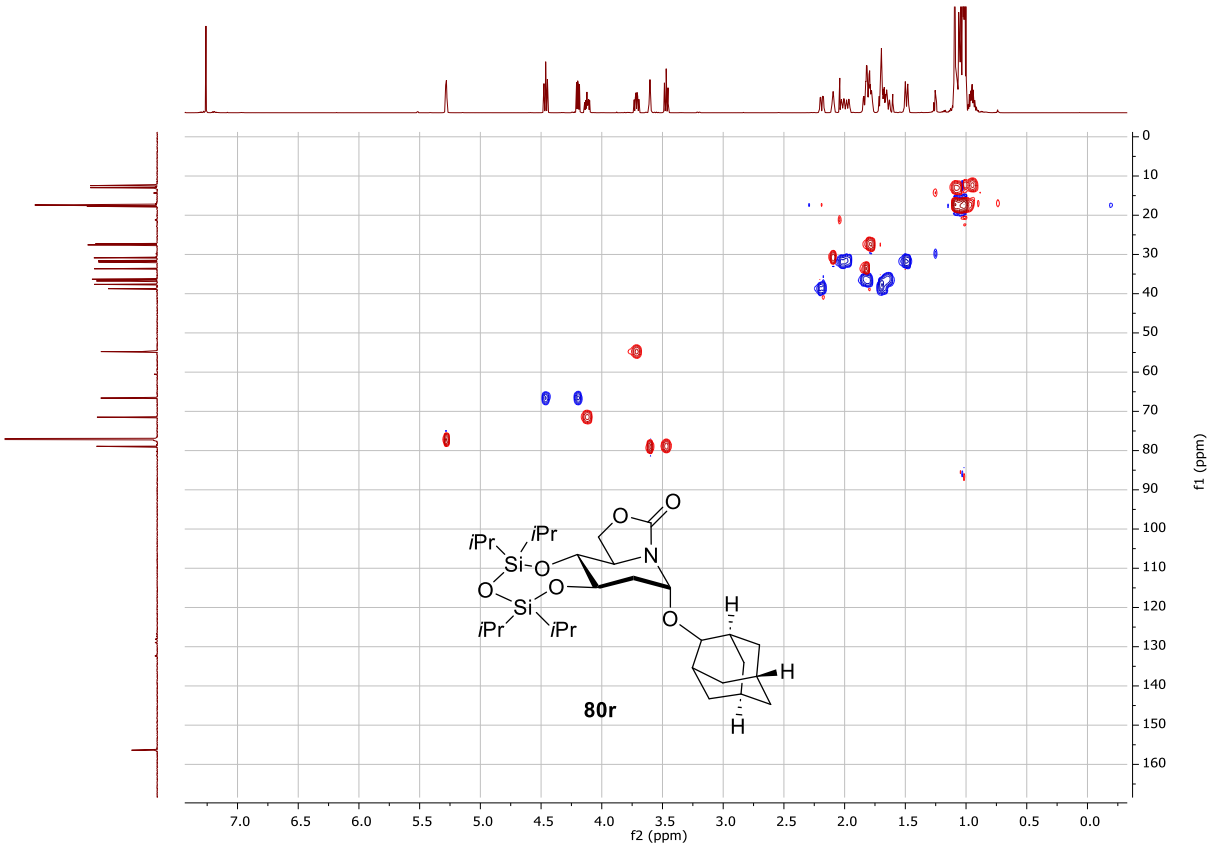

Figure 8.239. HSQC spectra for 80r

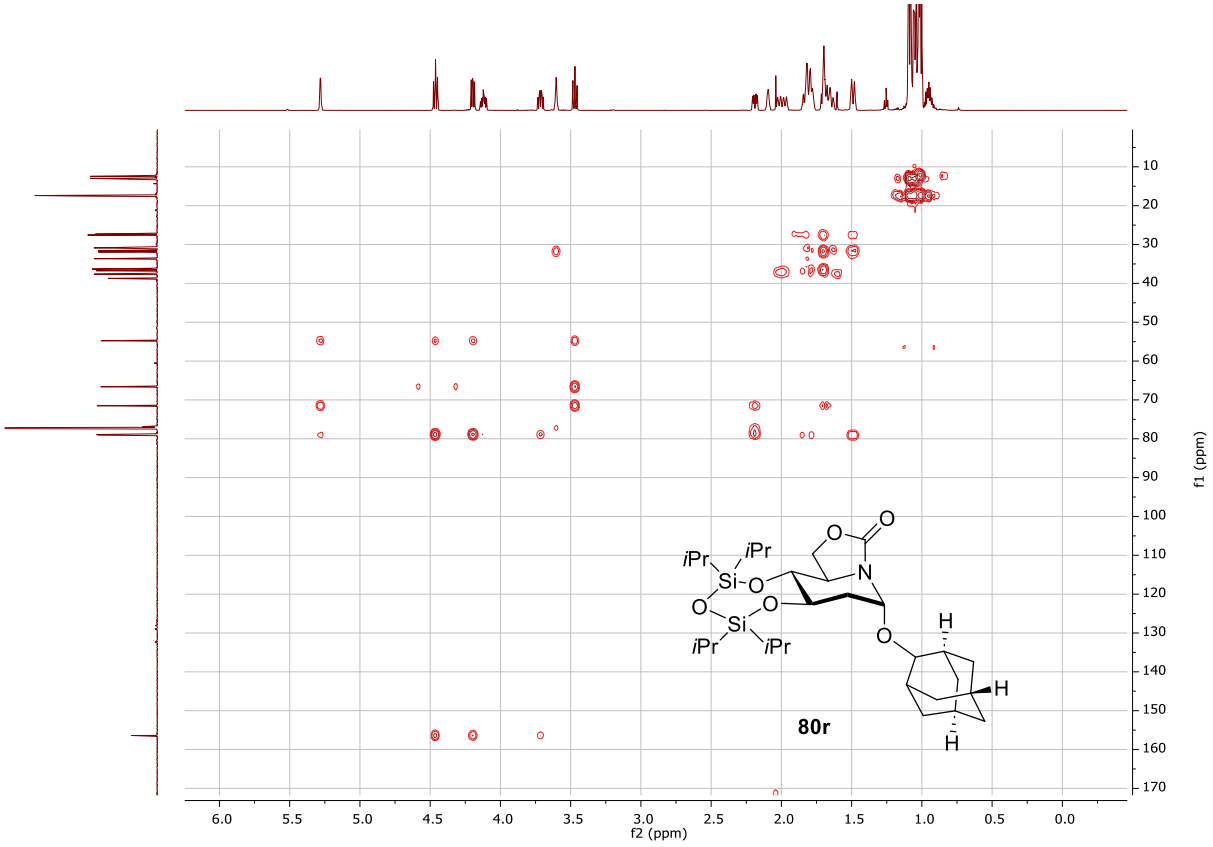

Figure 8.240. HMBC spectra for 80r

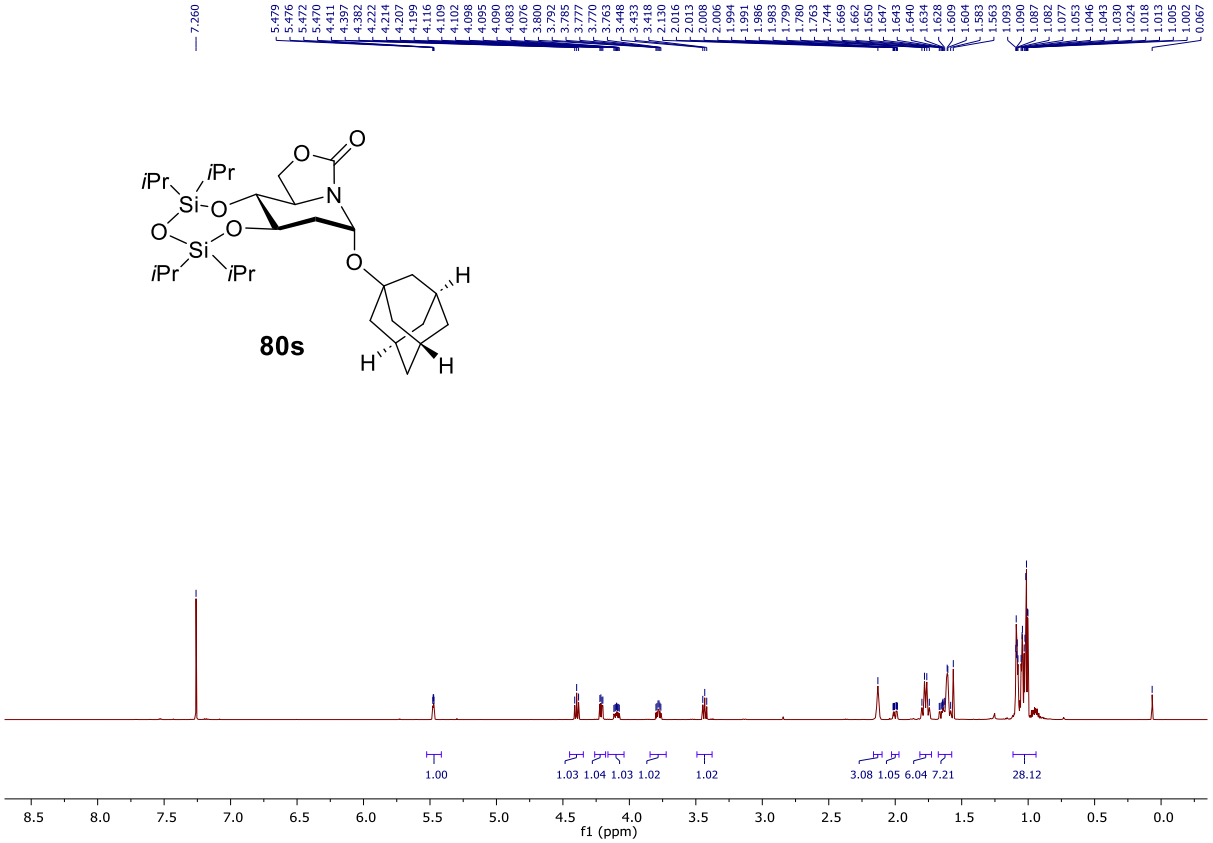

Figure 8.241. ^{1}H NMR spectra for 80s

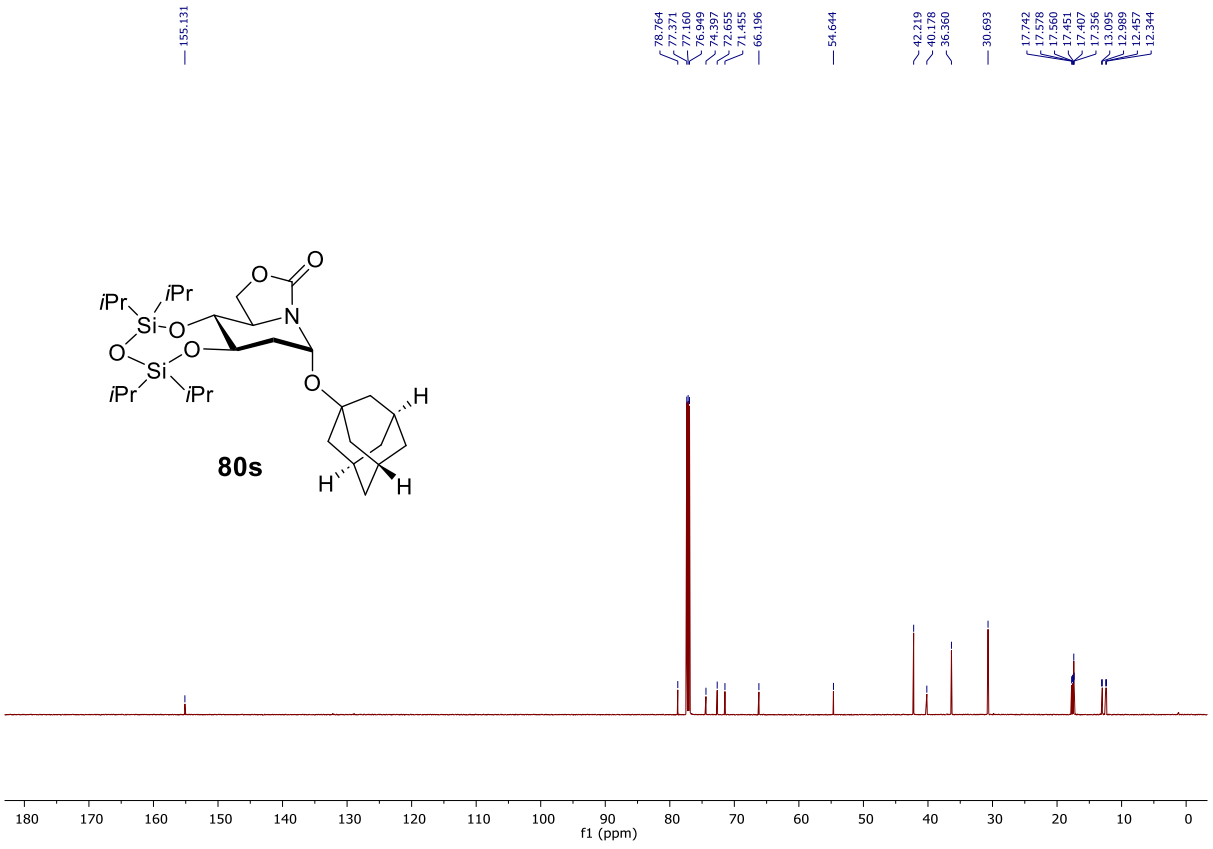

Figure 8.242. ^{13}C NMR spectra for 80s

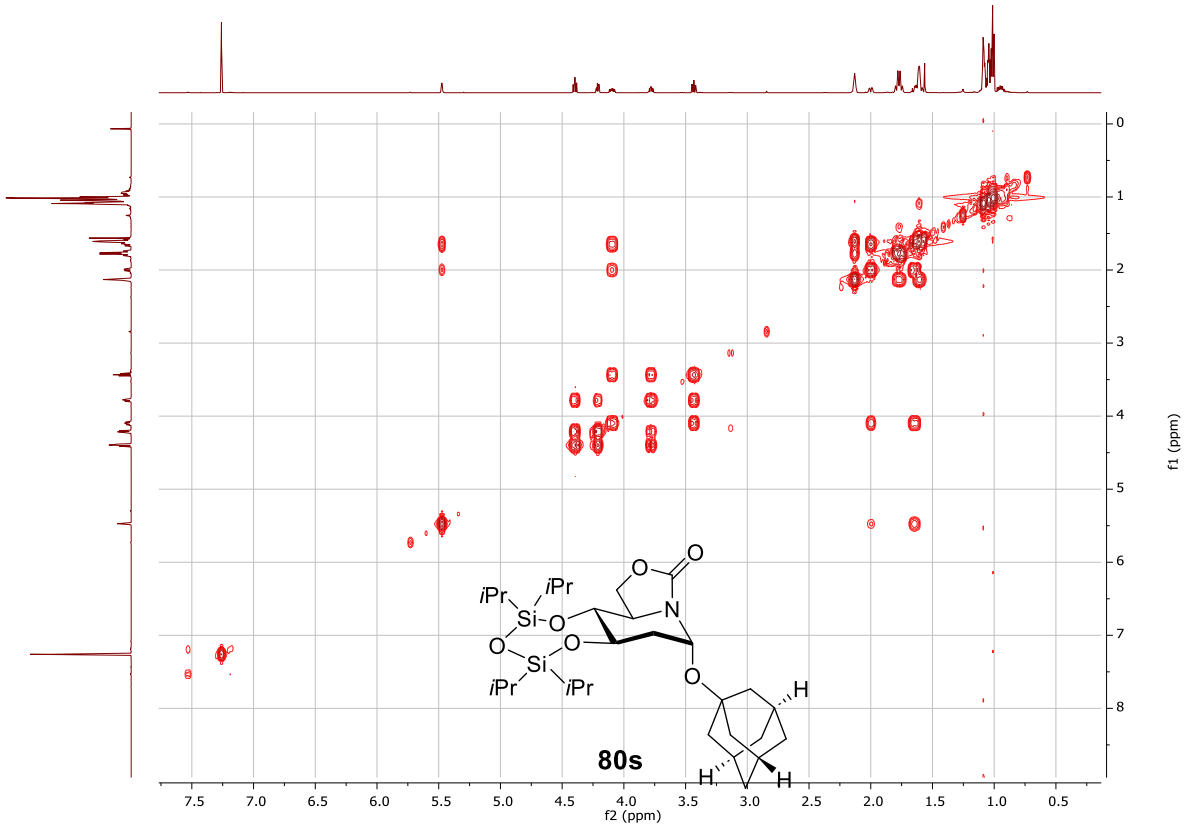

Figure 8.243. COSY spectra for 80s

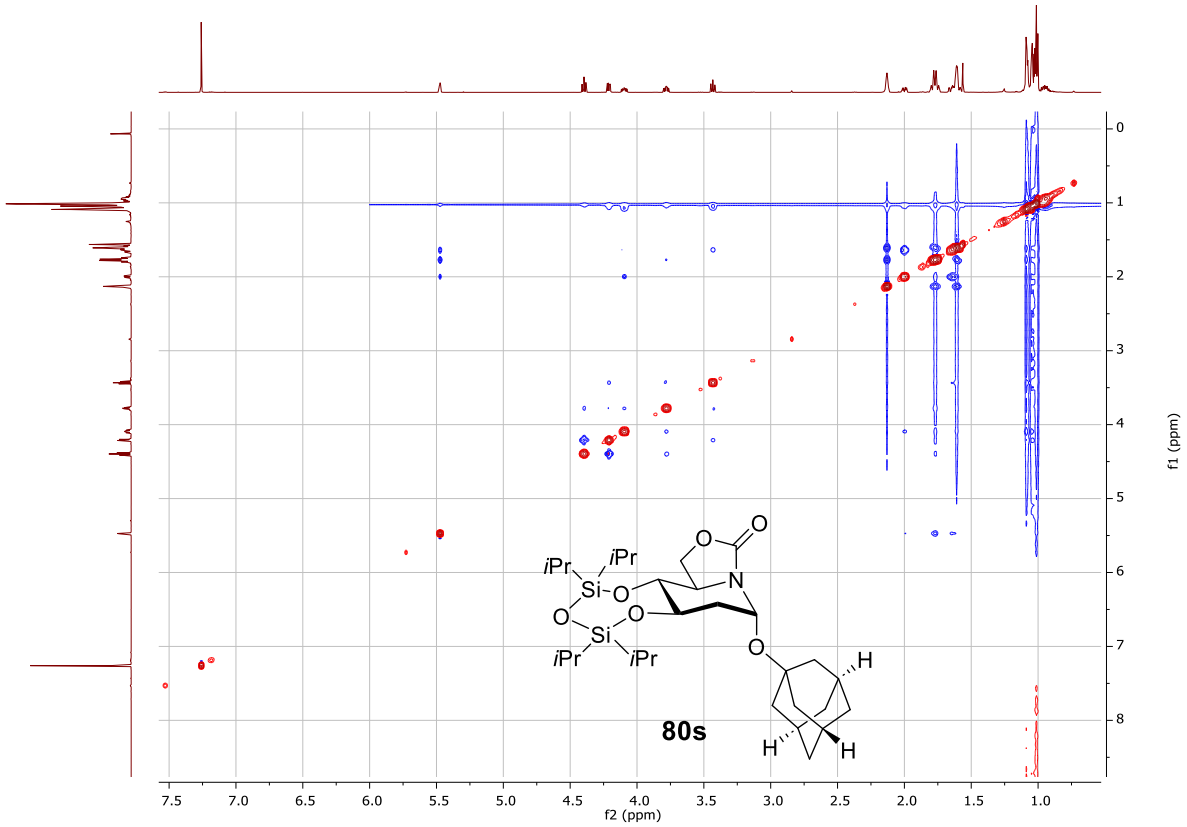

Figure 8.244. NOESY spectra for 80s

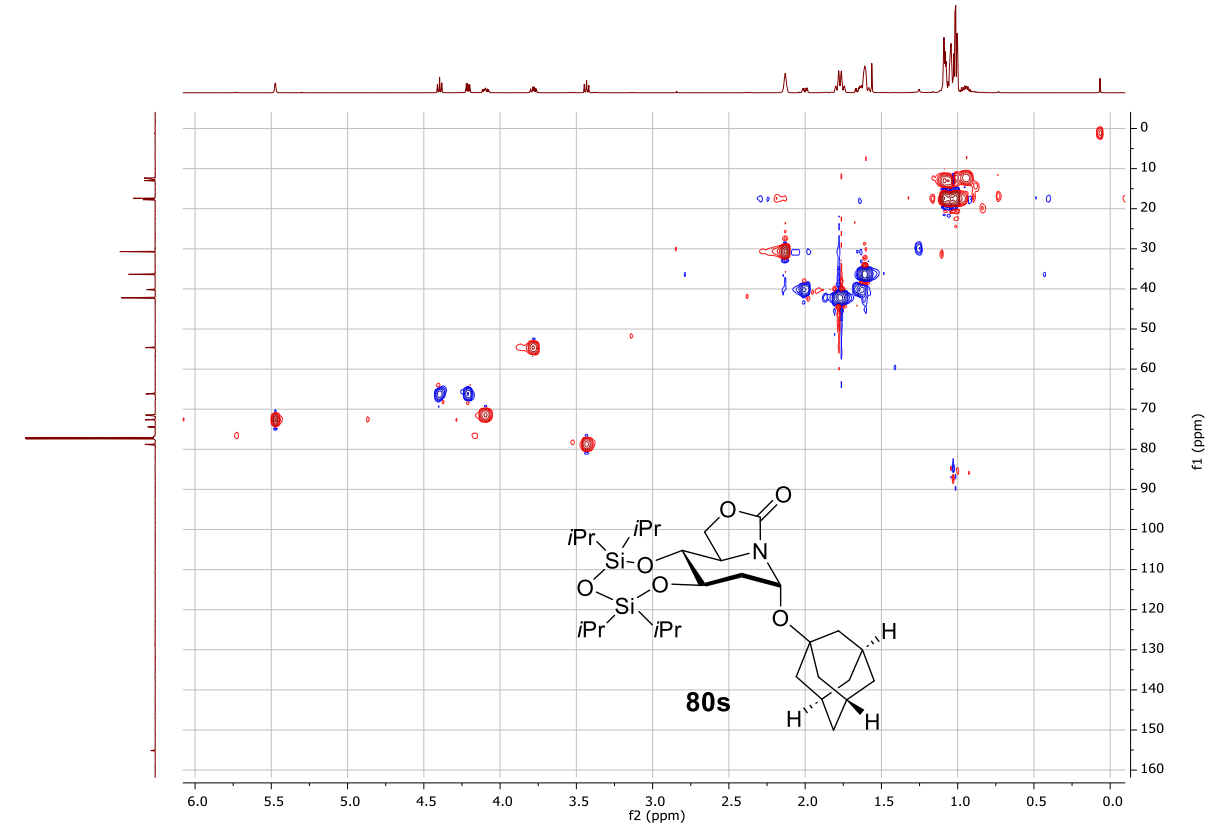

Figure 8.245. HSQC spectra for 80s

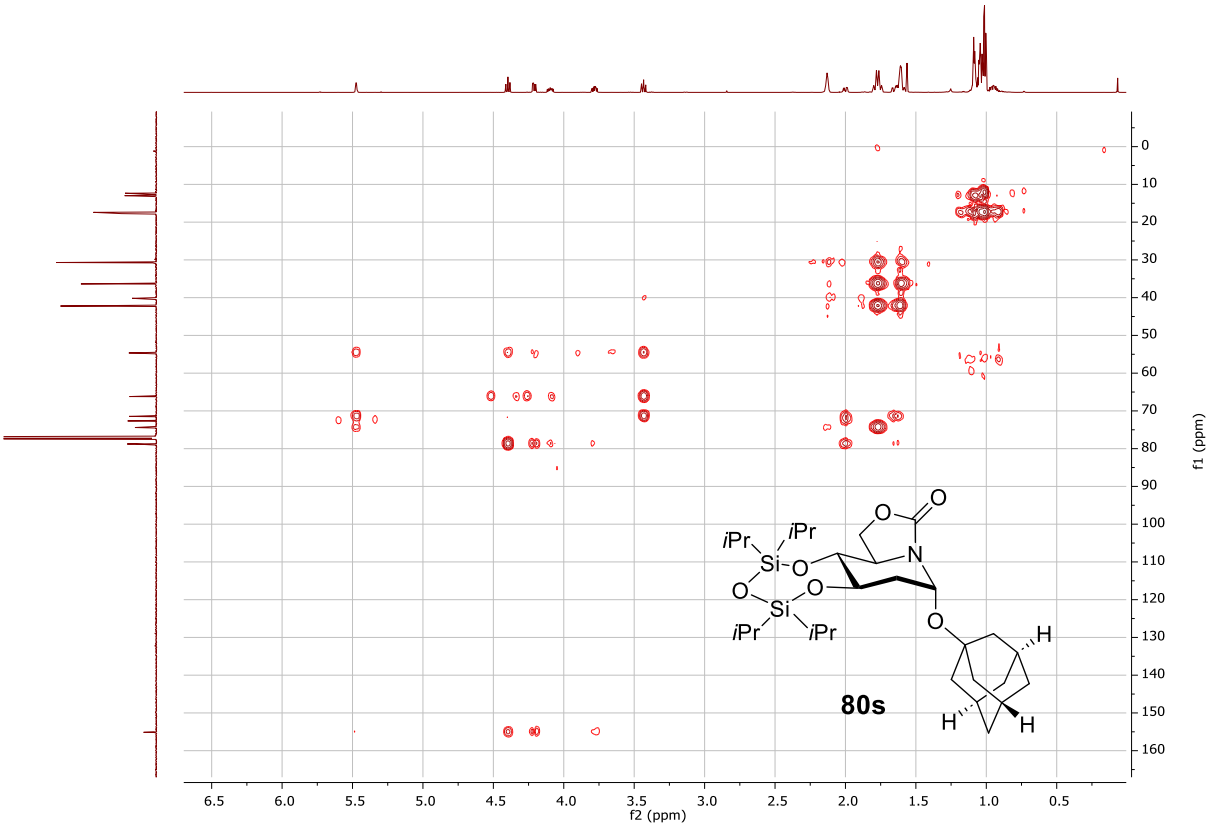

Figure 8.246. HMBC spectra for 80s

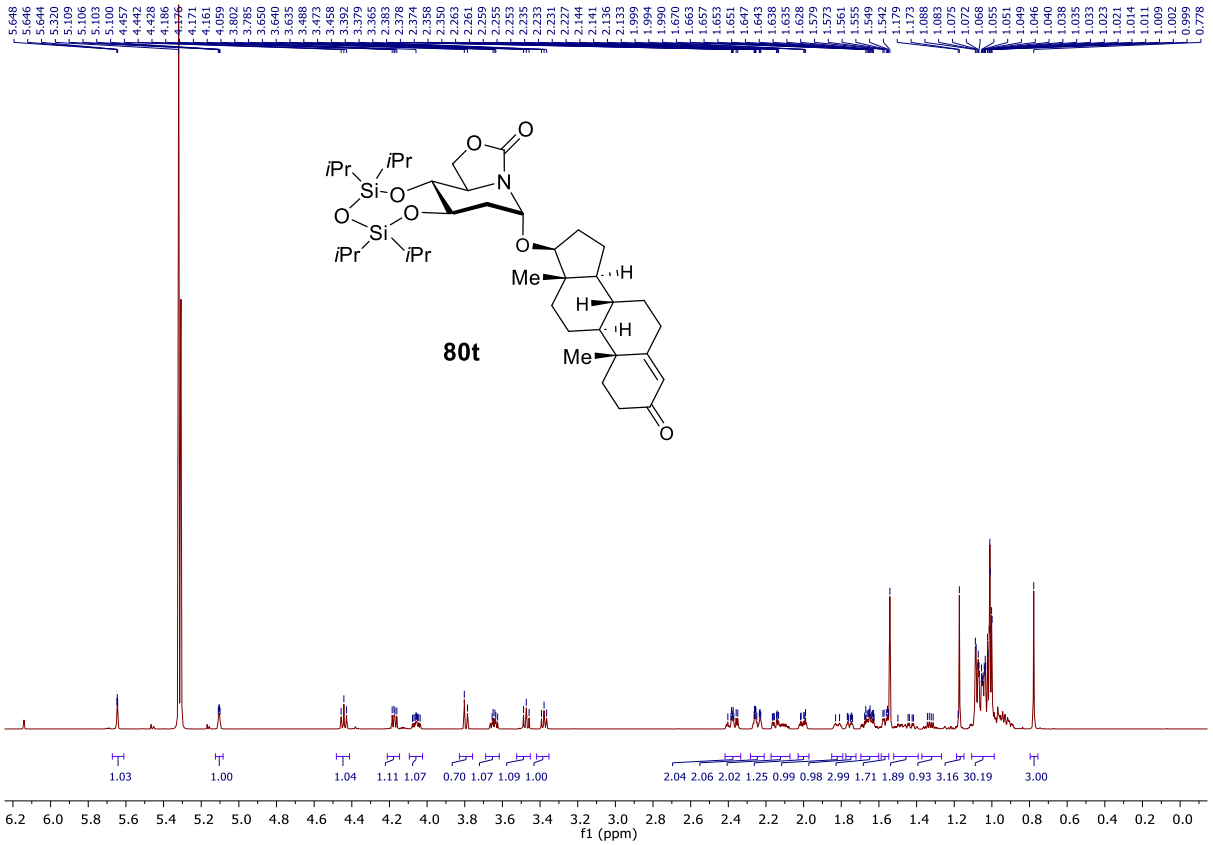

Figure 8.247. ^{1}H NMR spectra for 80t

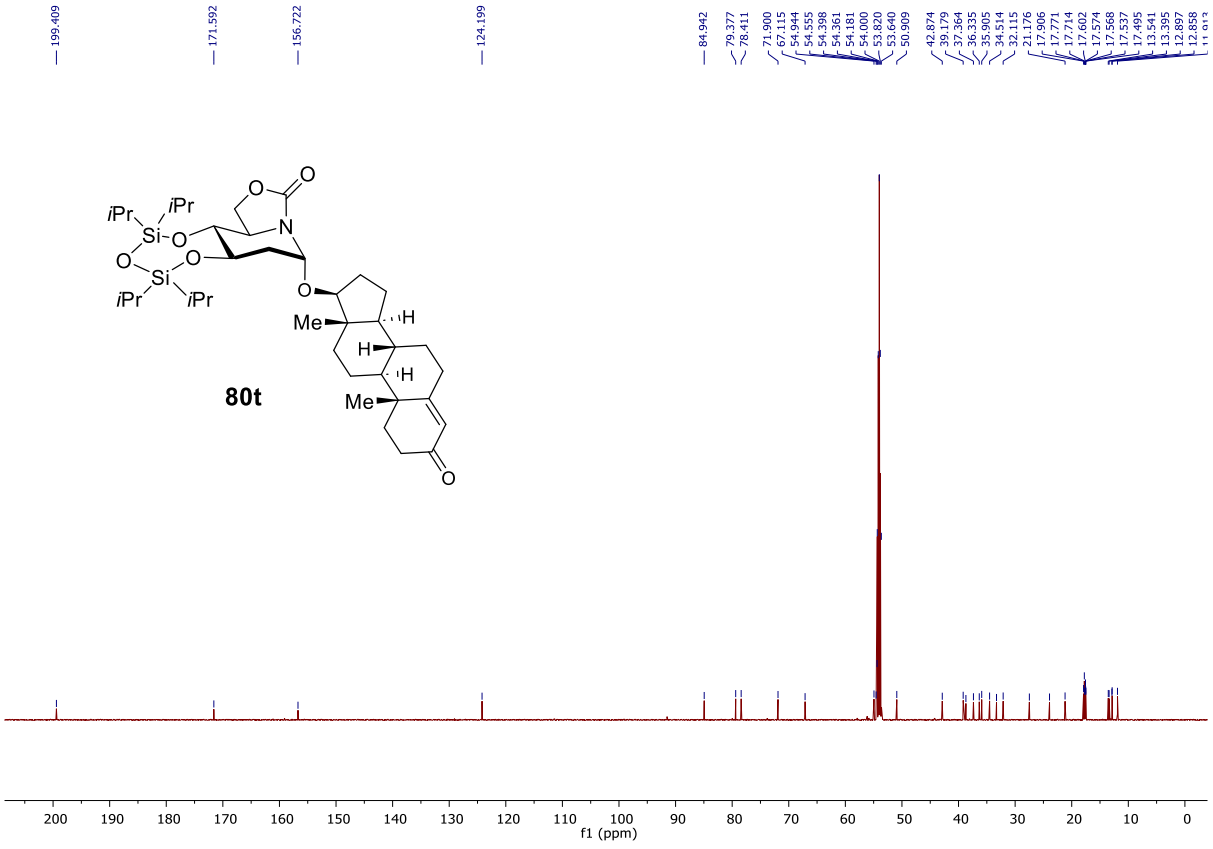

Figure 8.248. ^{13}C NMR spectra for 80t

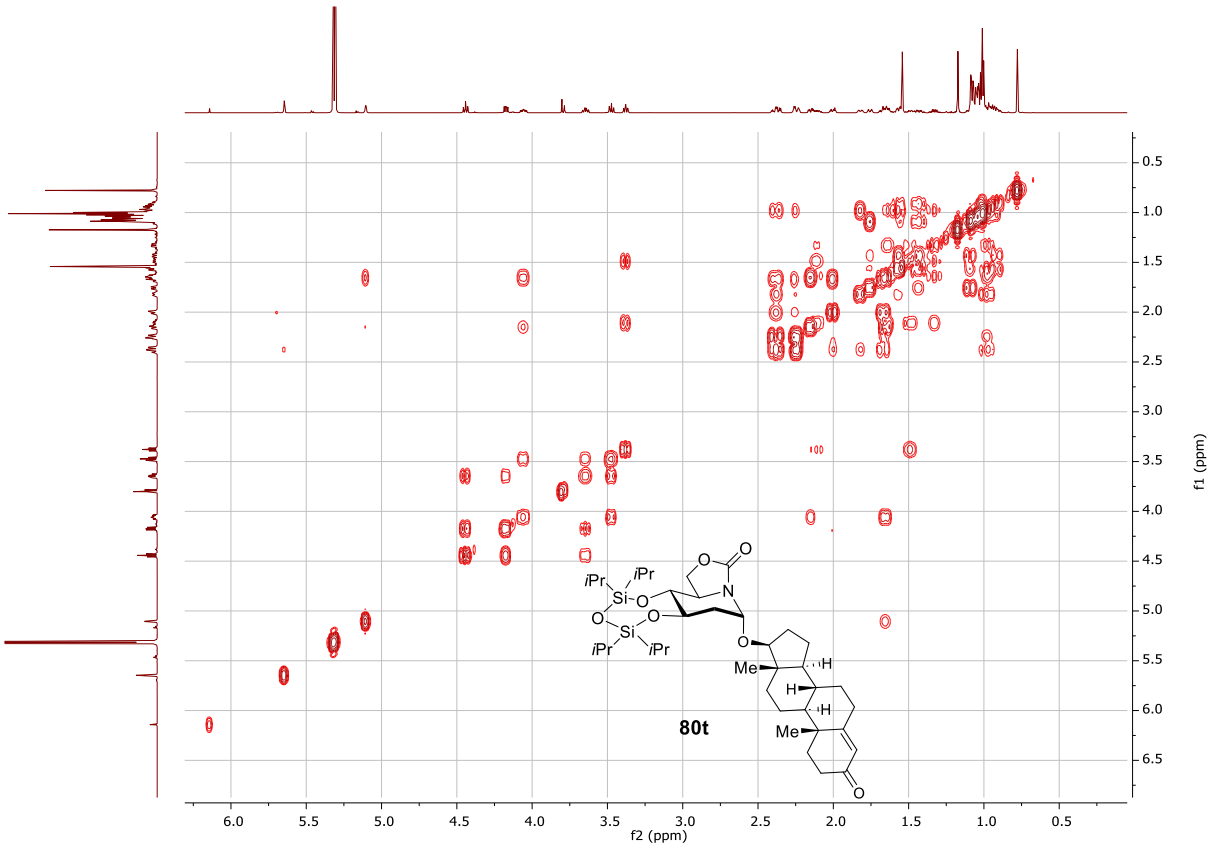

Figure 8.249. COSY spectra for 80t

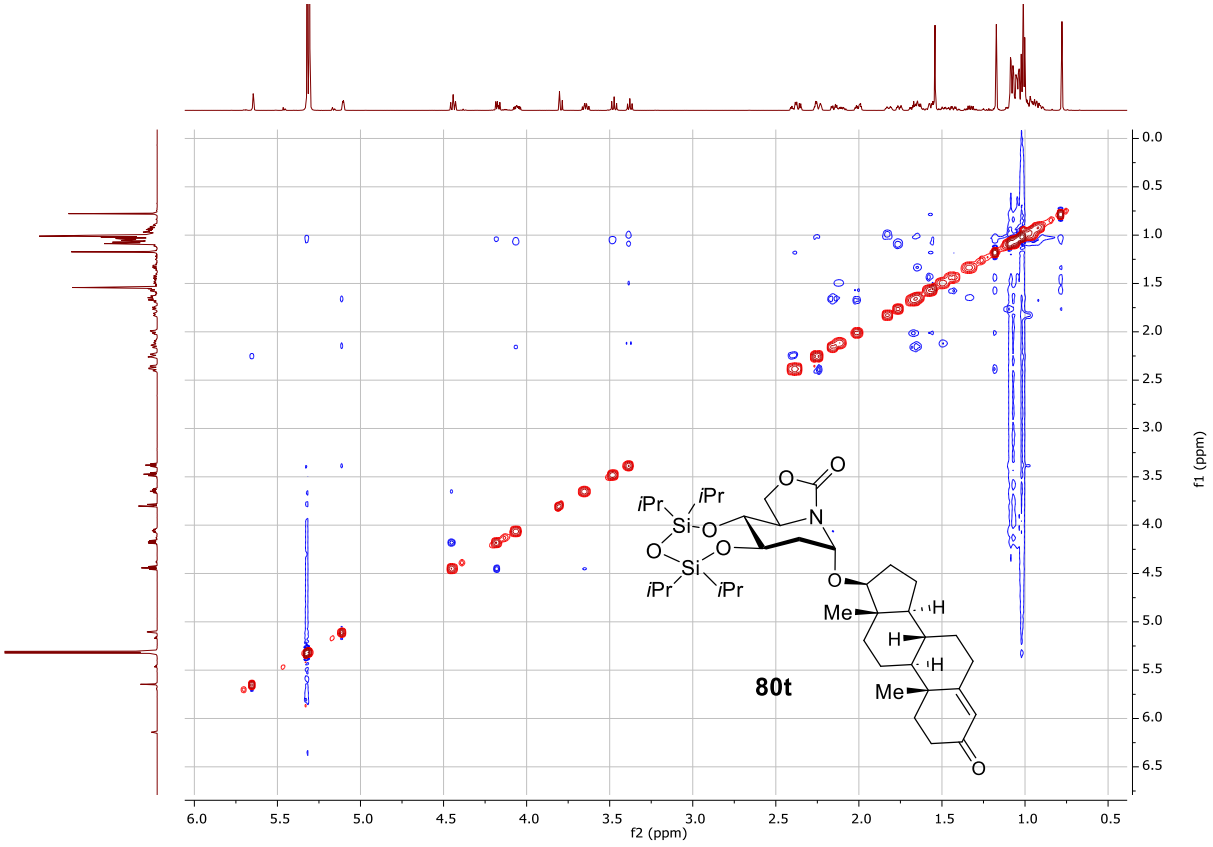

Figure 8.250. NOESY spectra for 80t

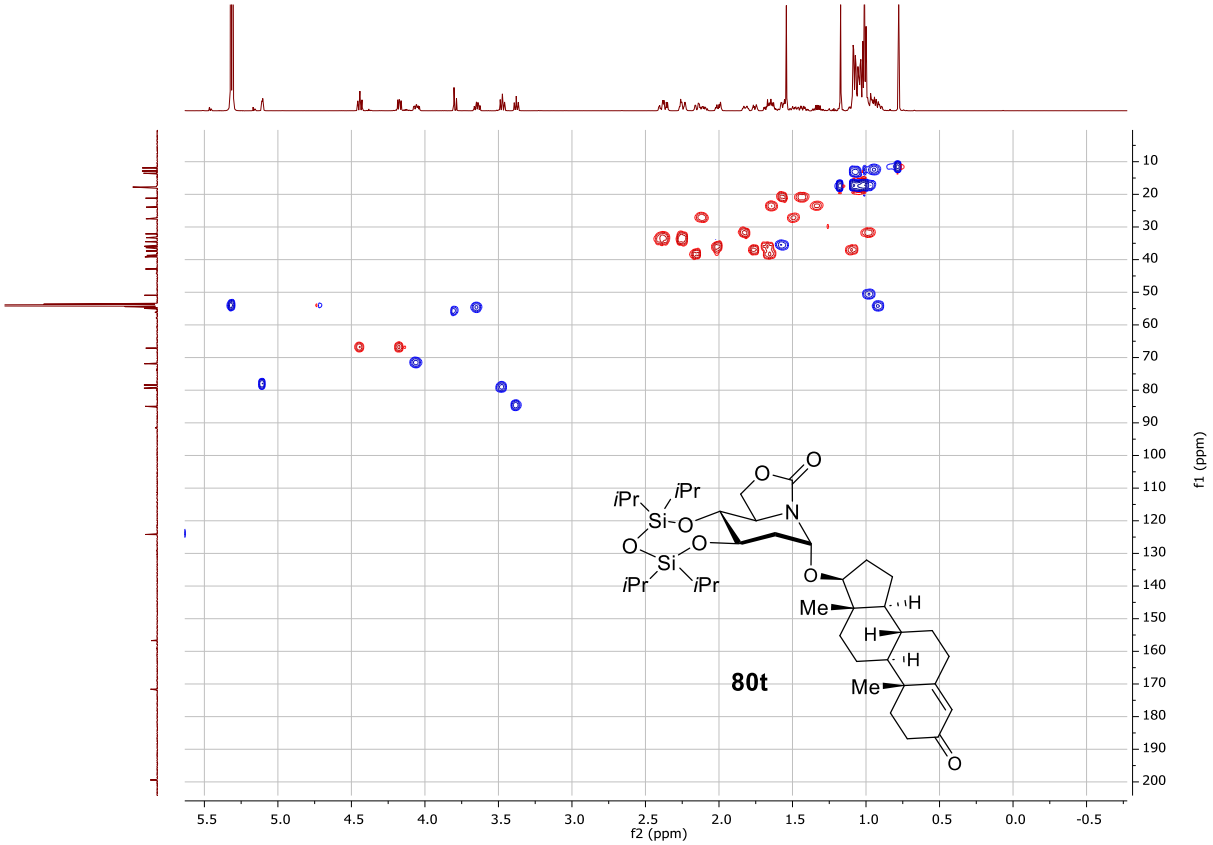

Figure 8.251. HSQC spectra for 80t

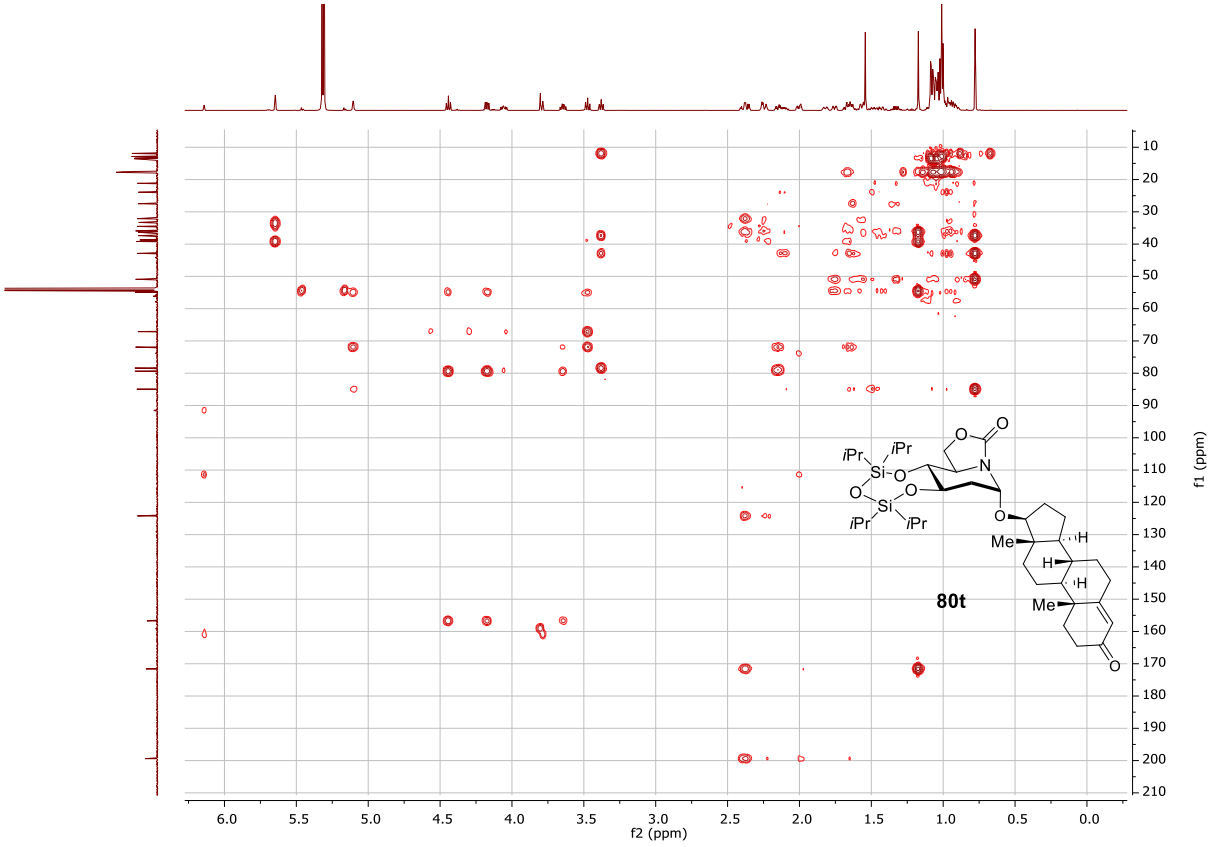

Figure 8.252. HMBC spectra for 80t

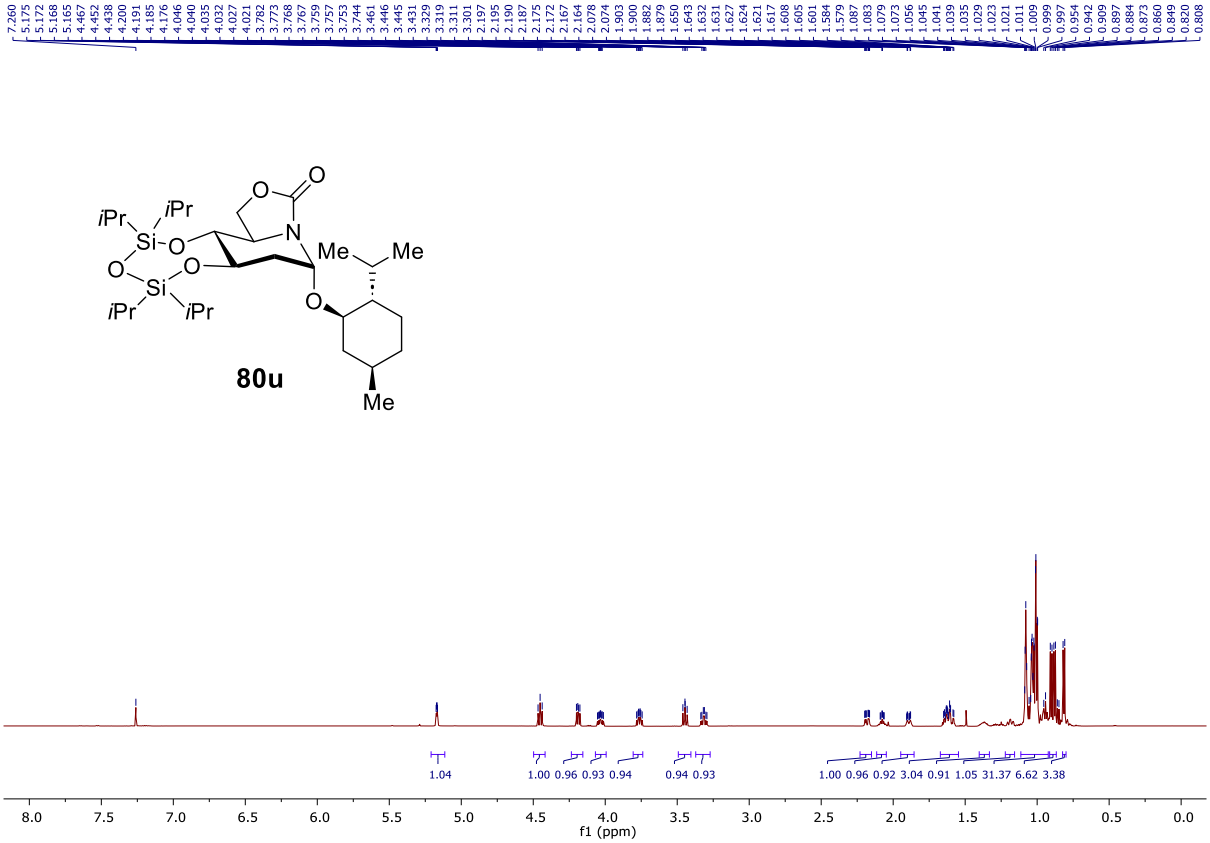

Figure 8.253. ^{1}H NMR spectra for 80u

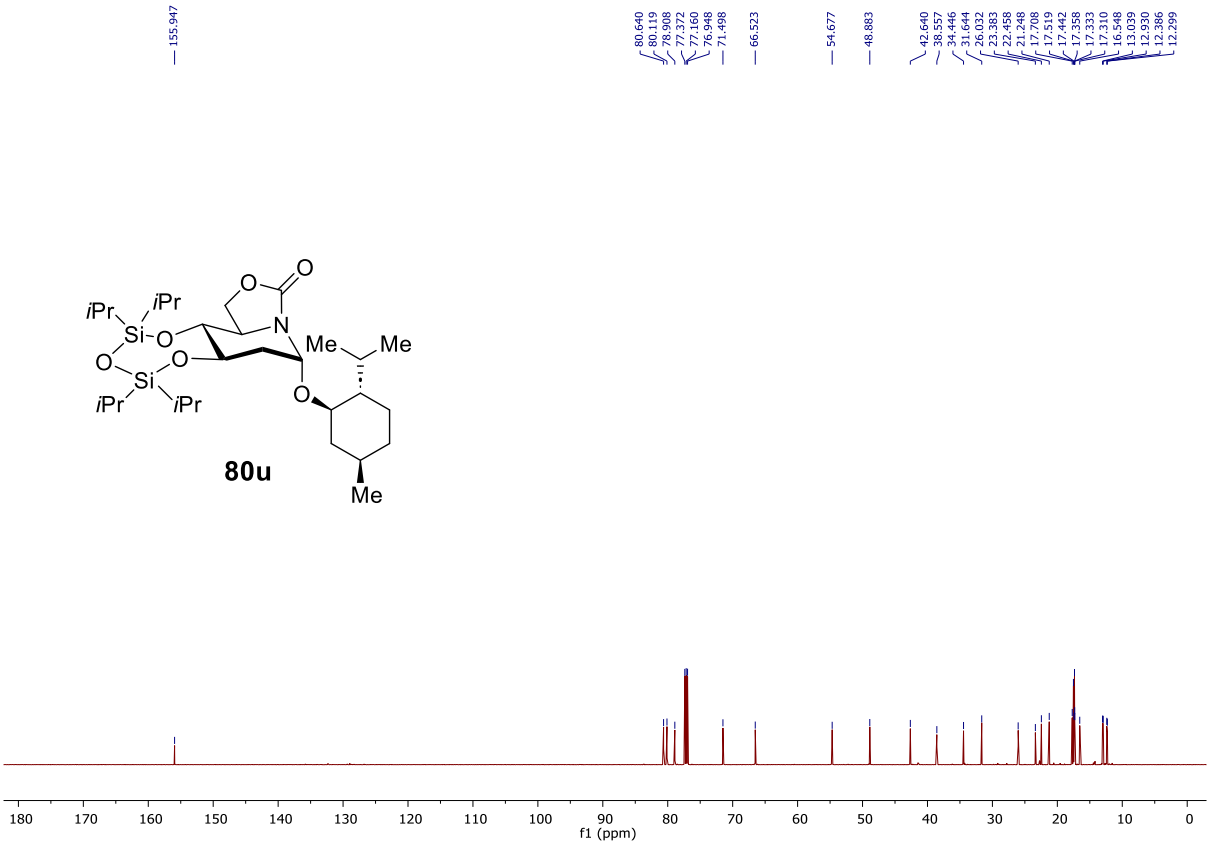

Figure 8.254. ^{13}C NMR spectra for 80u

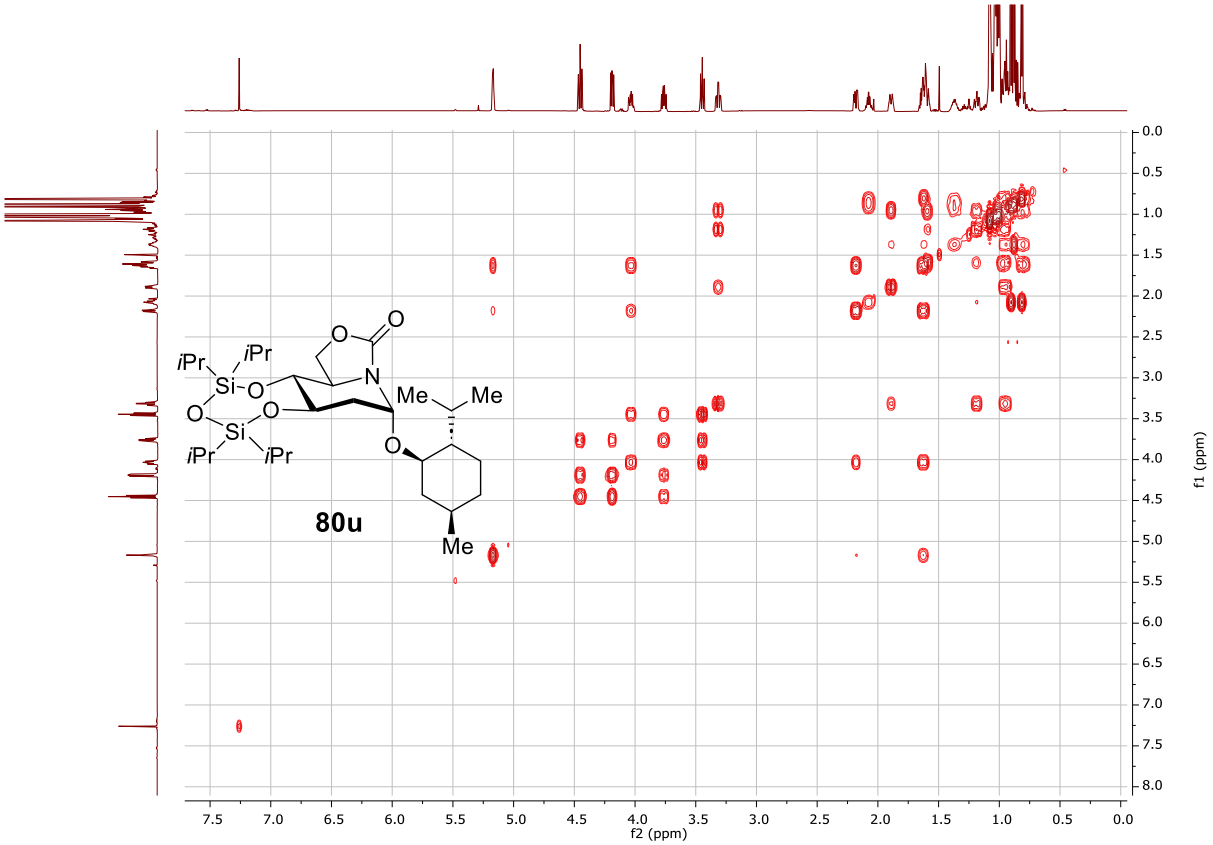

Figure 8.255. COSY spectra for 80u

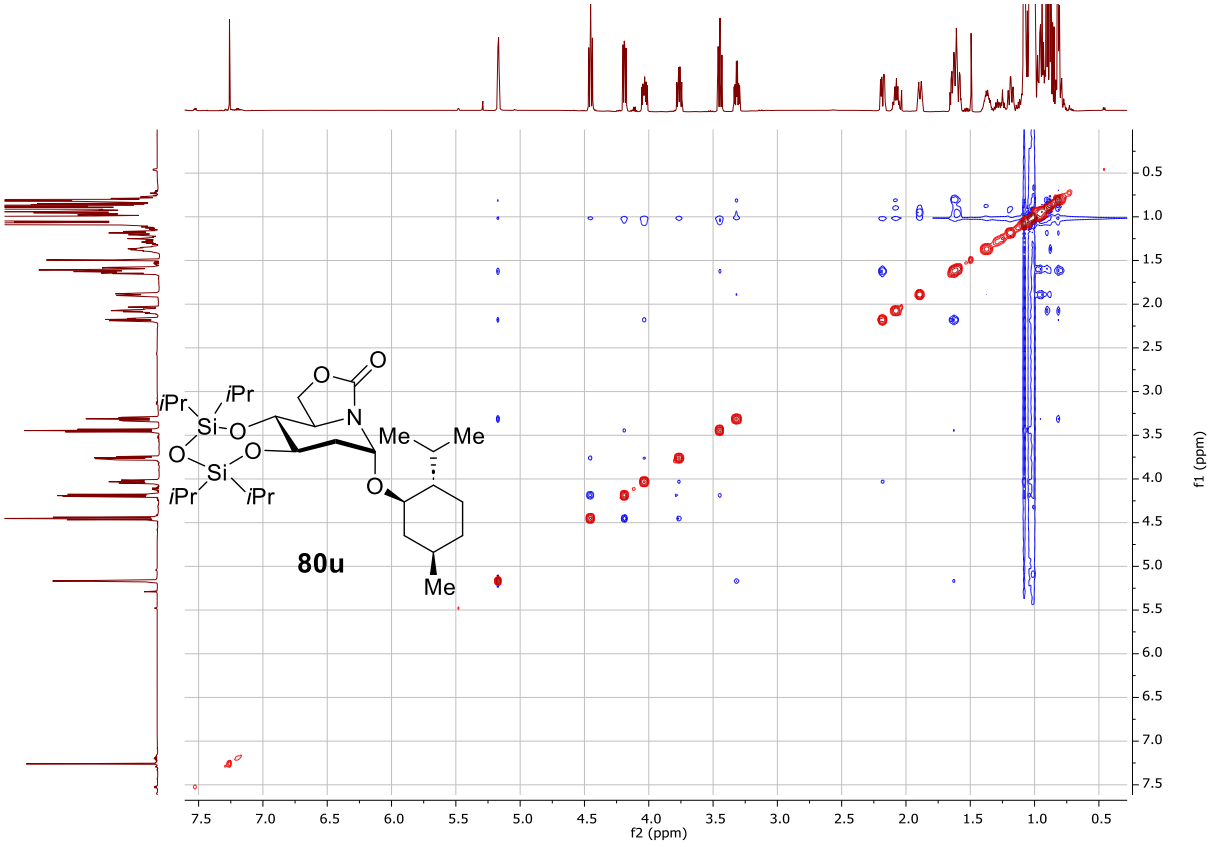

Figure 8.256. NOESY spectra for 80u

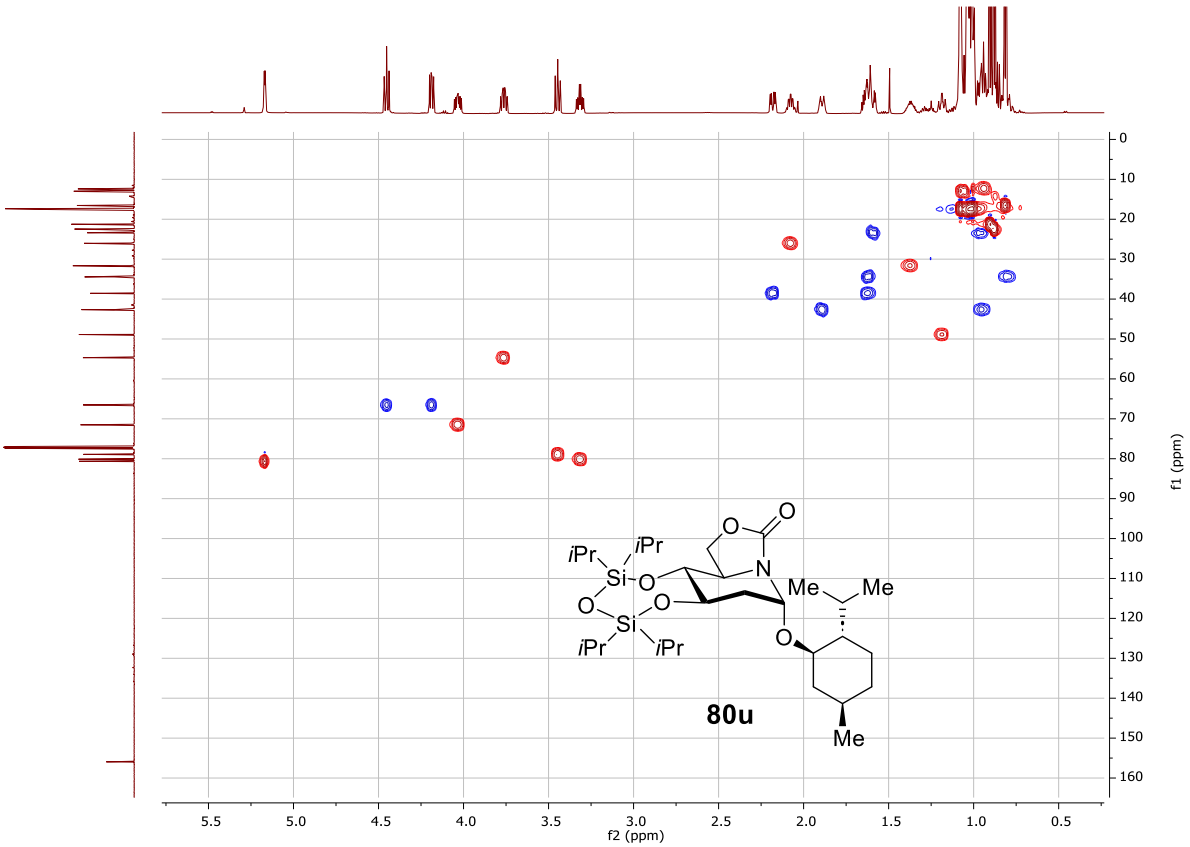

Figure 8.257. HSQC spectra for 80u

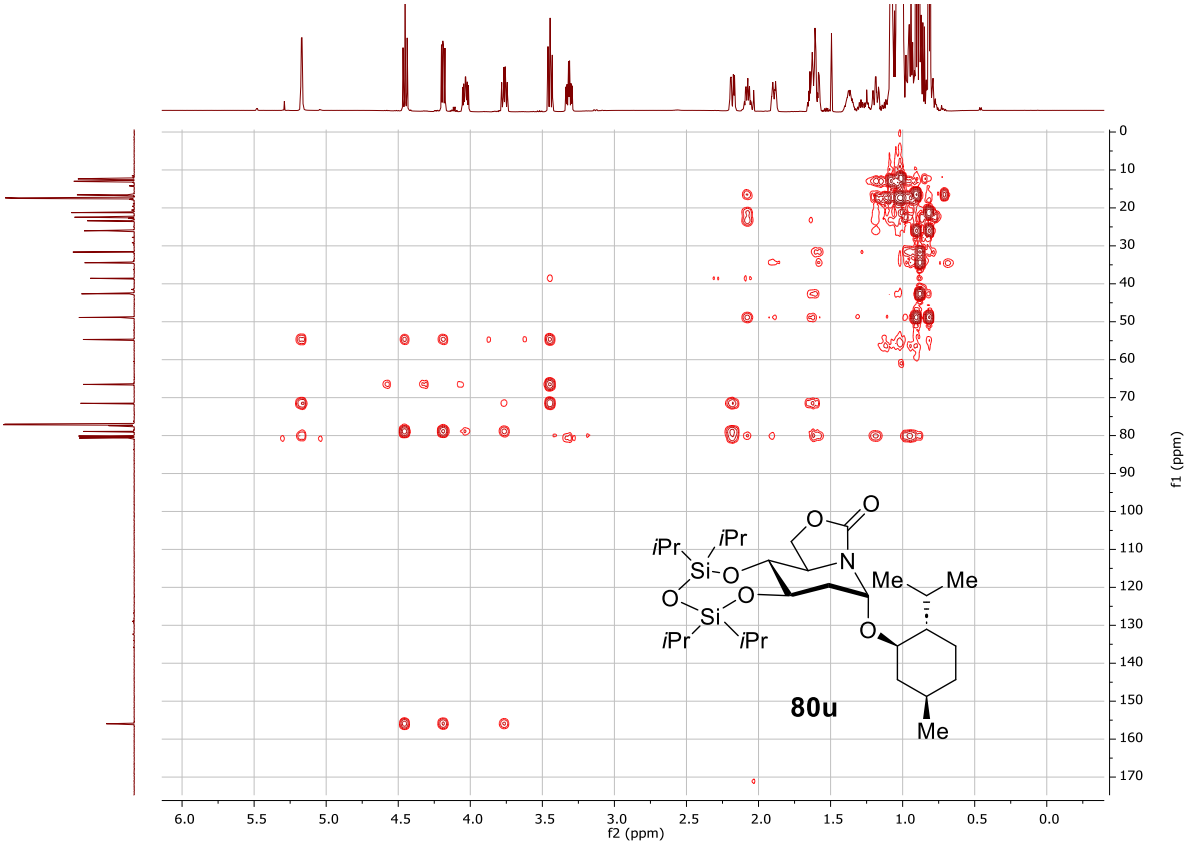

Figure 8.258. HMBC spectra for 80u

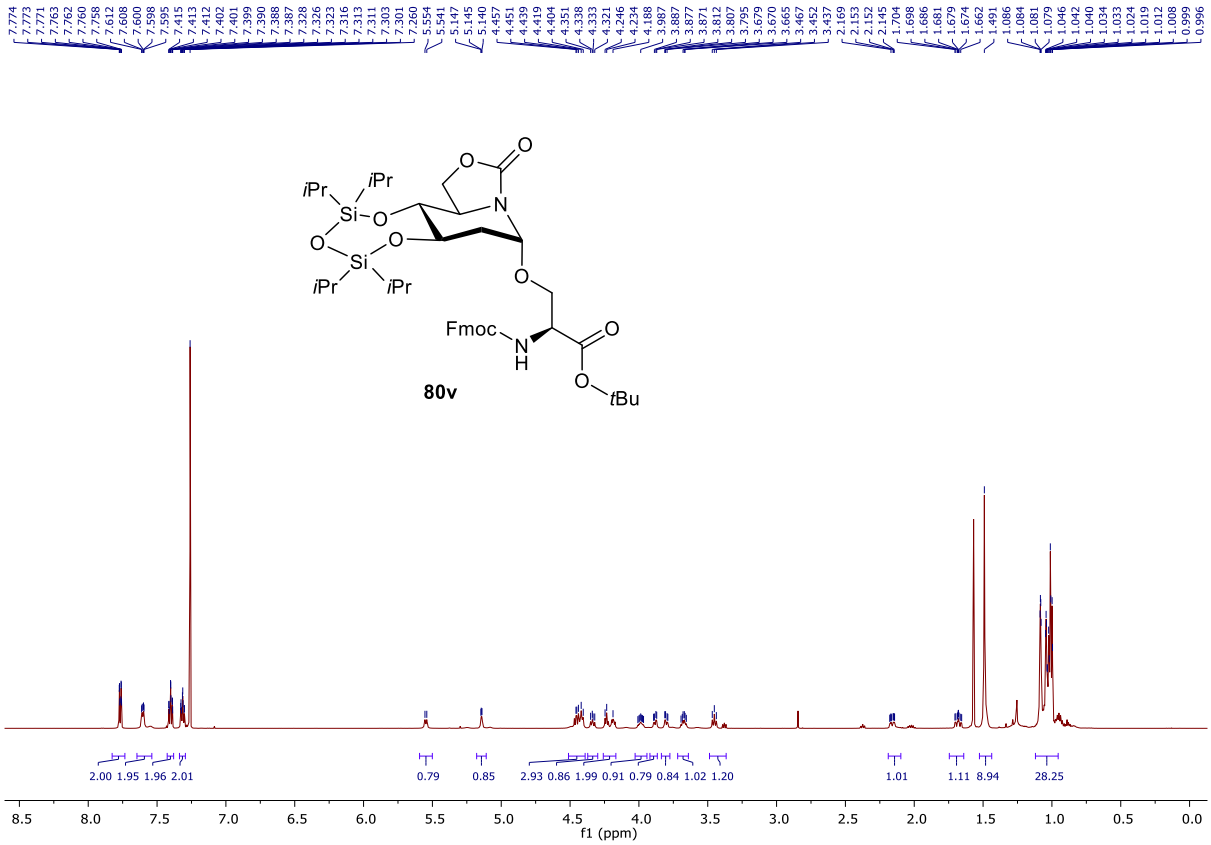

Figure 8.259. ^{1}H NMR spectra for 80v

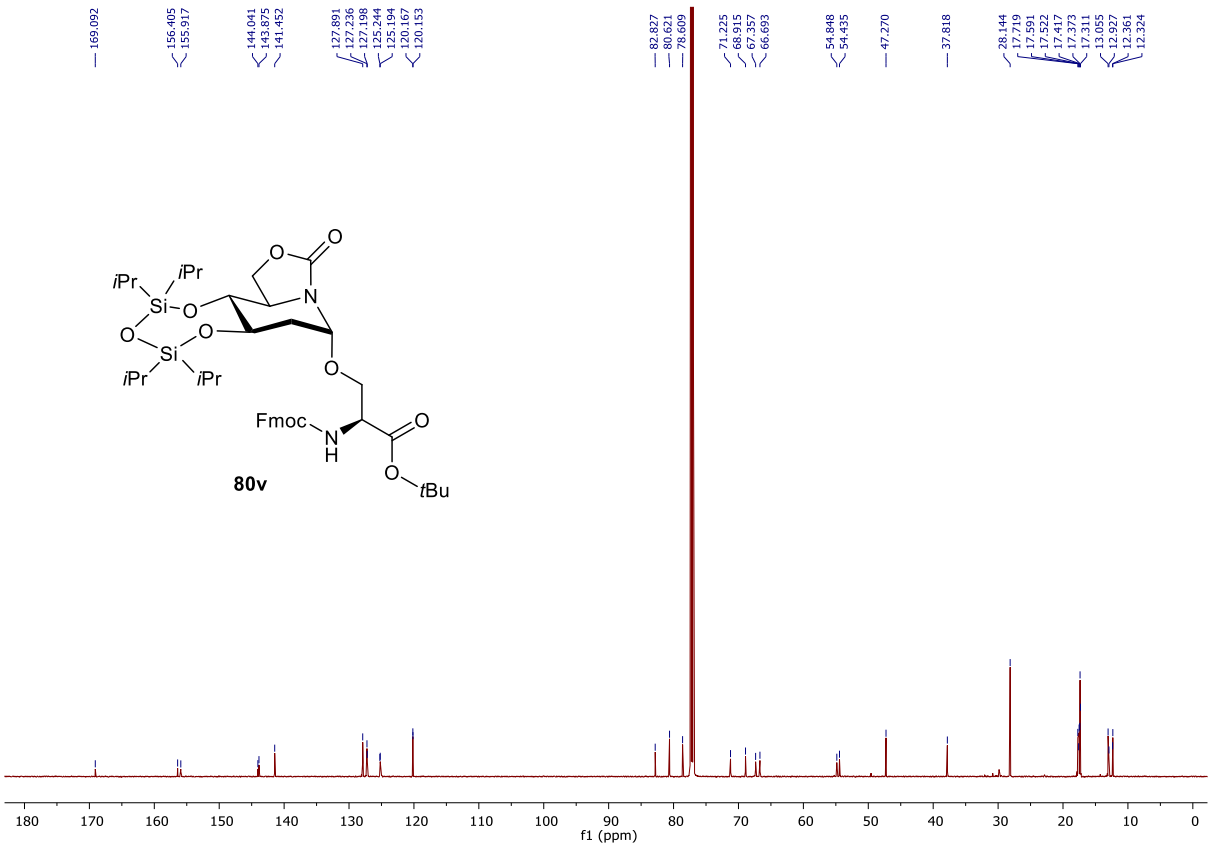

Figure 8.260. ^{13}C NMR spectra for 80v

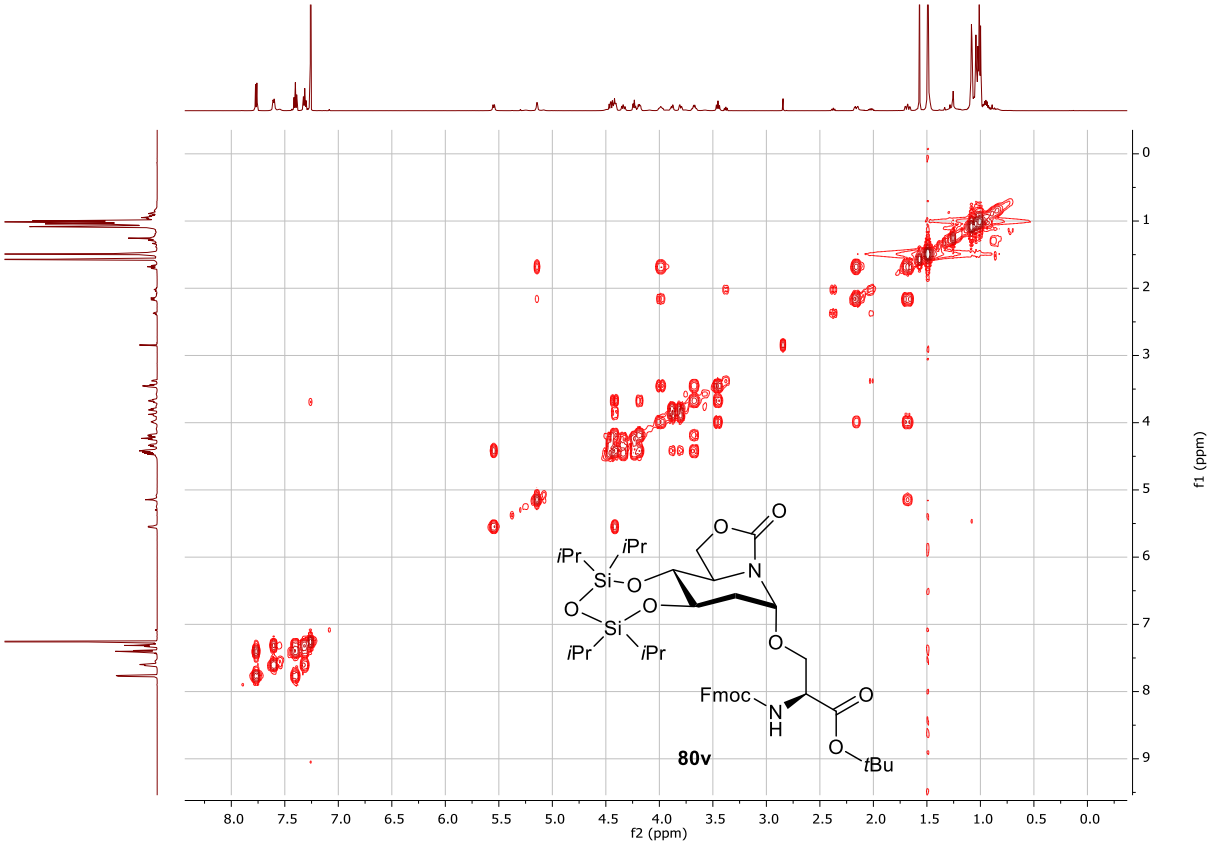

Figure 8.261. COSY spectra for 80v

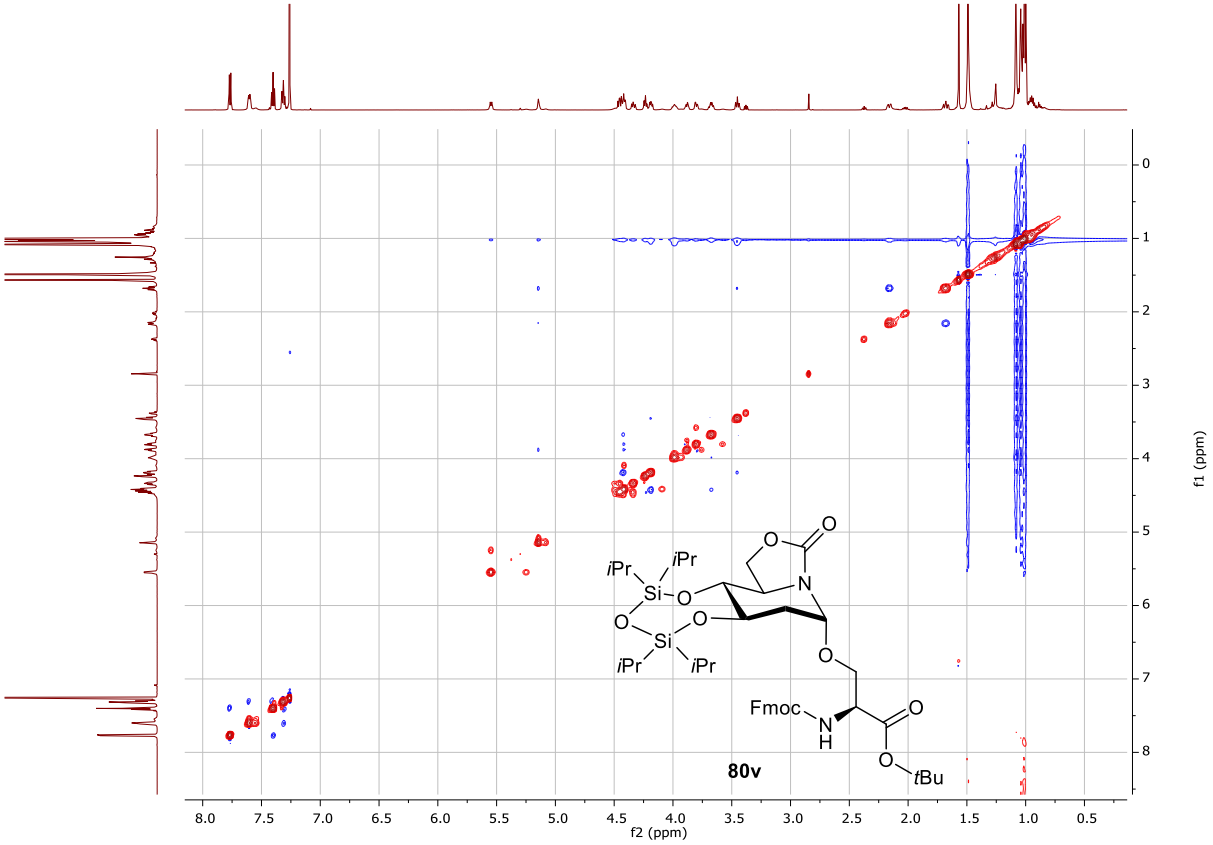

Figure 8.262. NOESY spectra for 80v

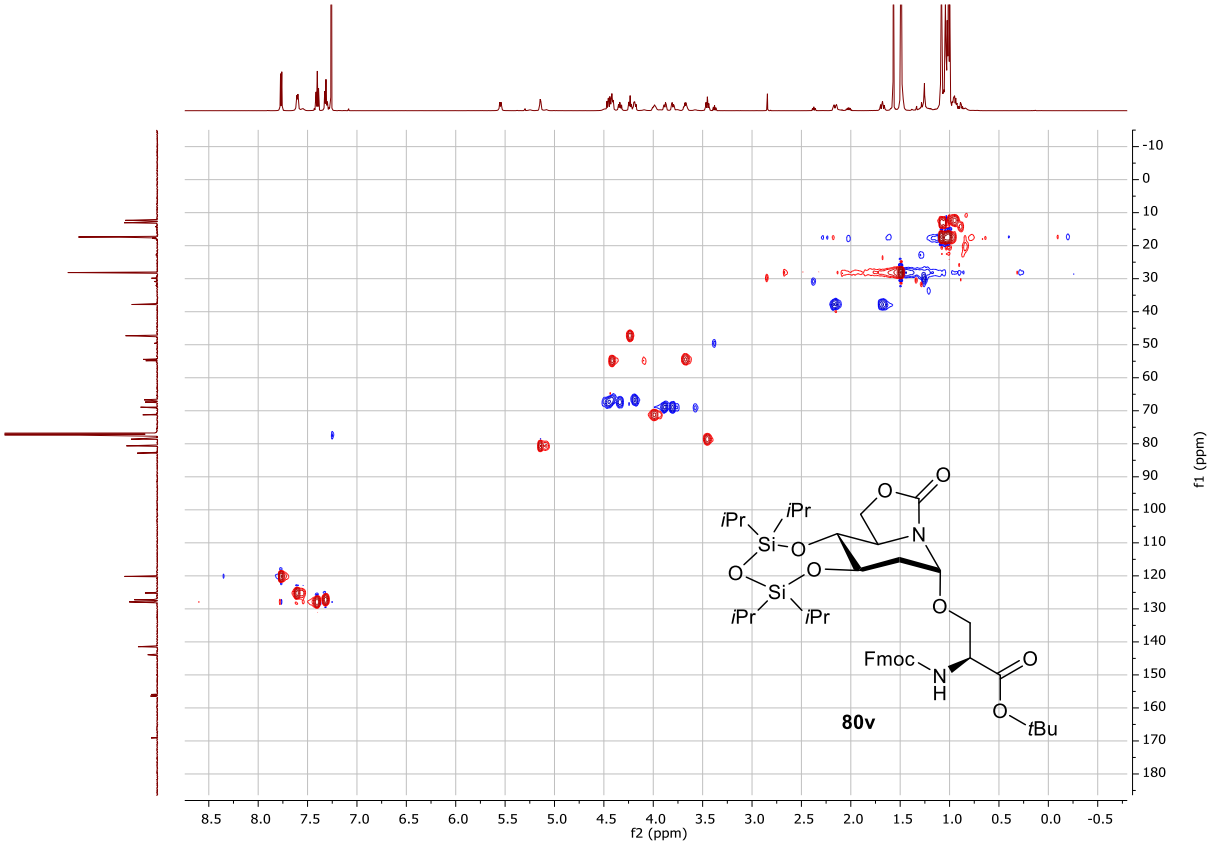

Figure 8.263. HSQC spectra for 80v

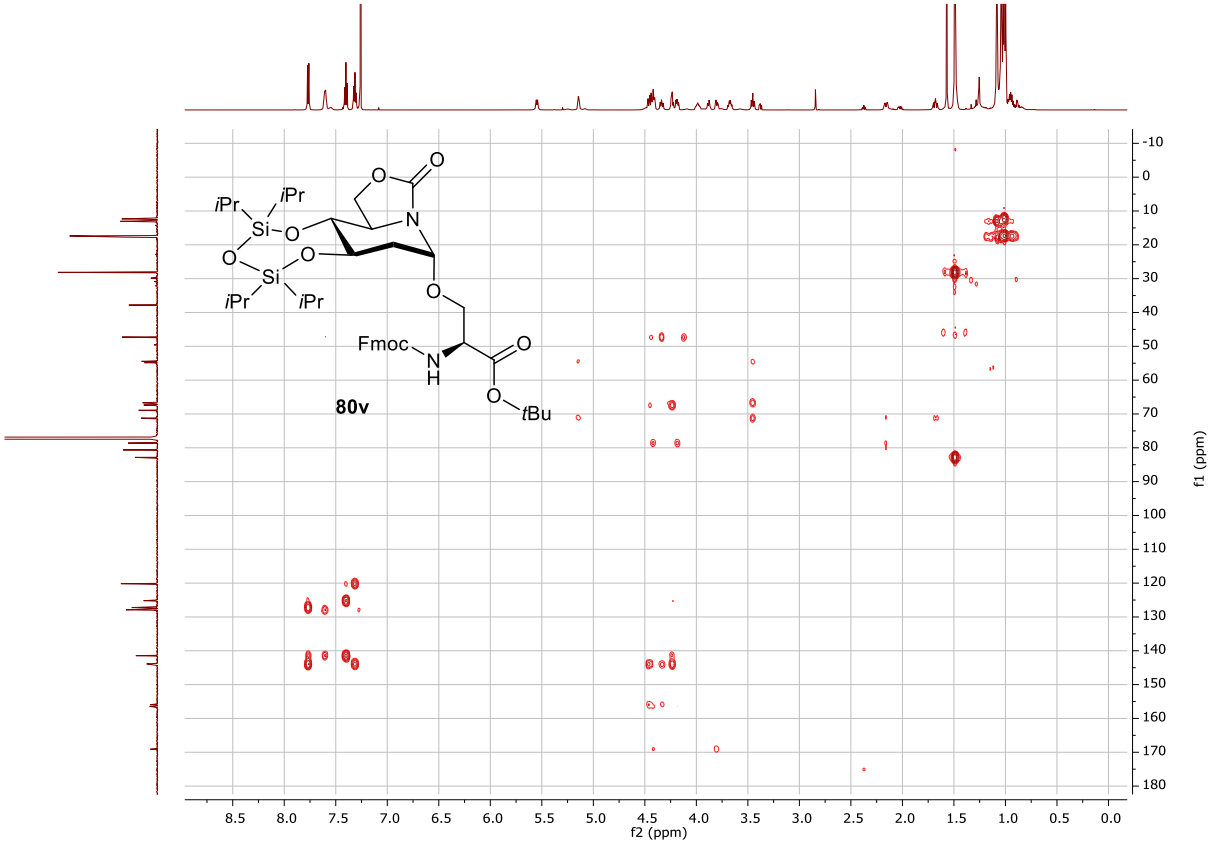

Figure 8.264. HMBC spectra for 80v

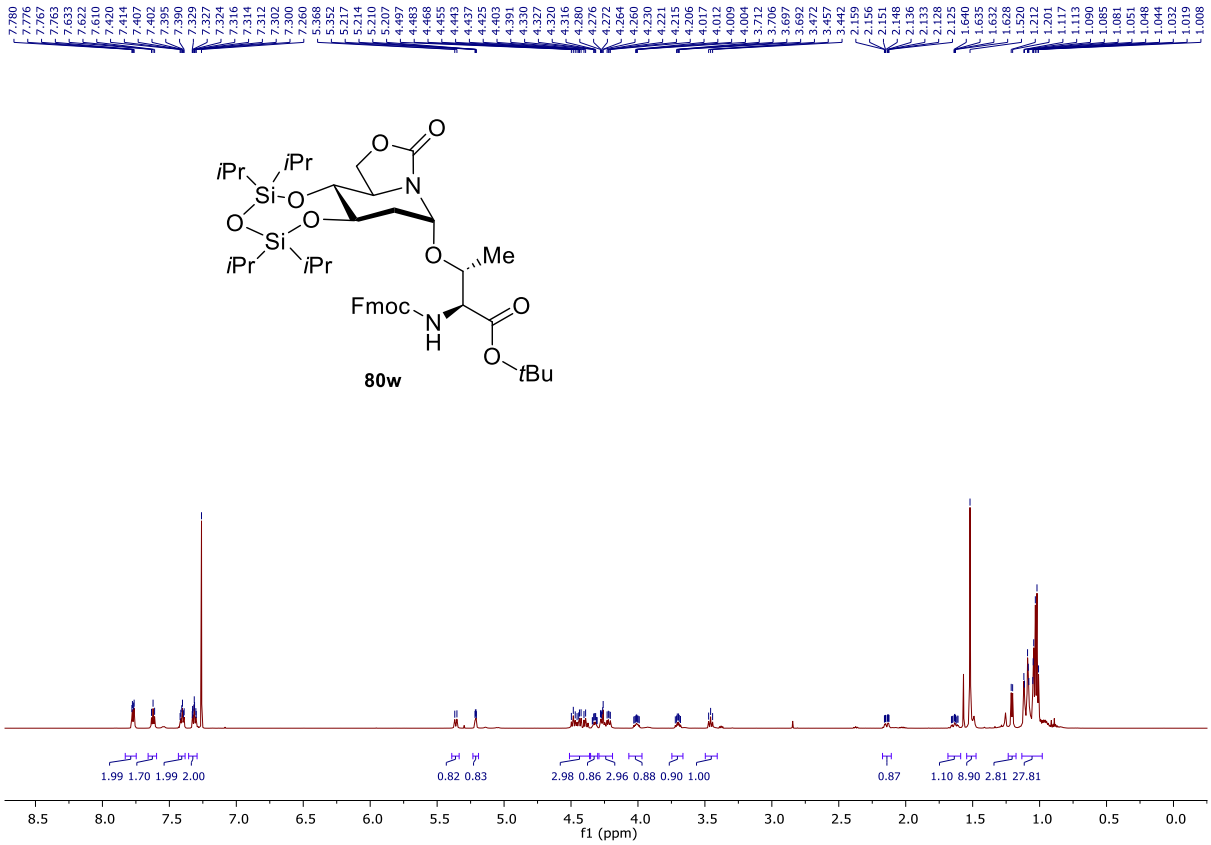

Figure 8.265. ^{1}H NMR spectra for 80w

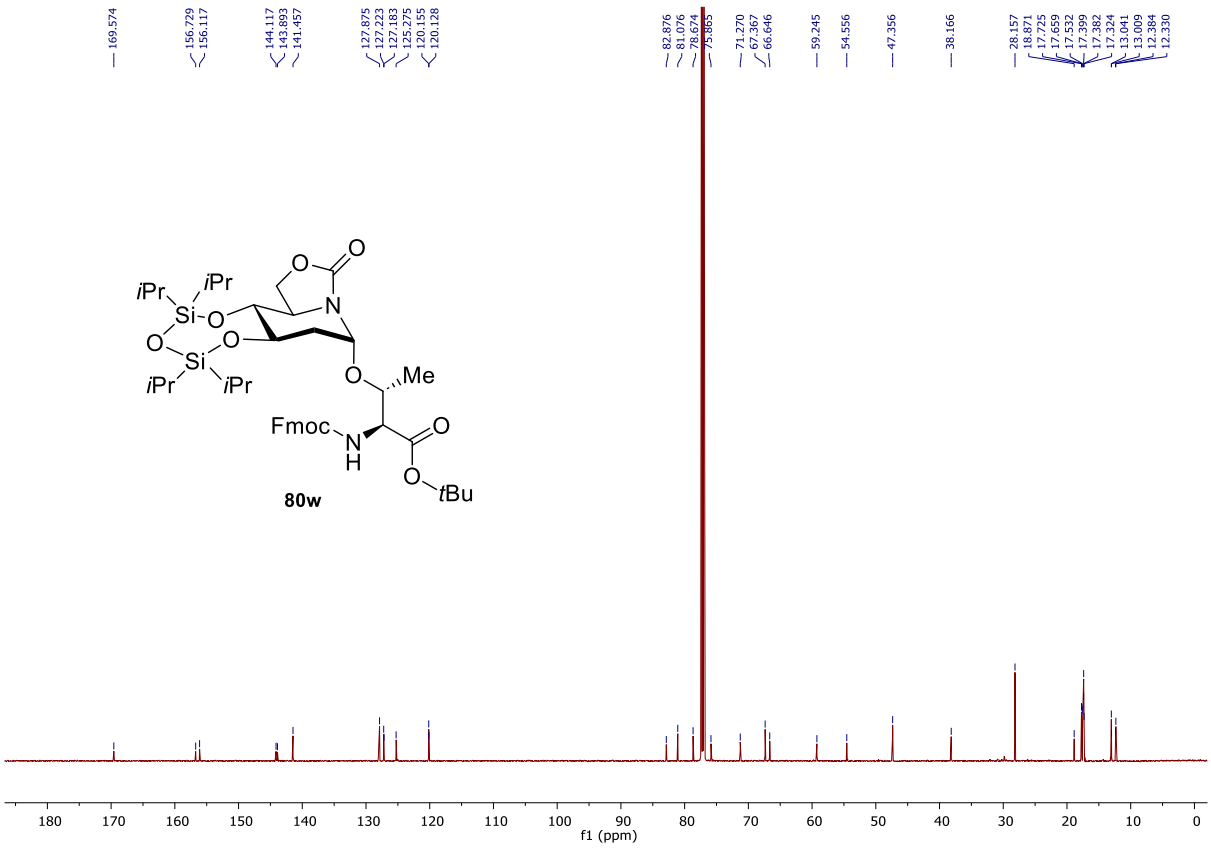

Figure 8.266. ^{13}C NMR spectra for 80w

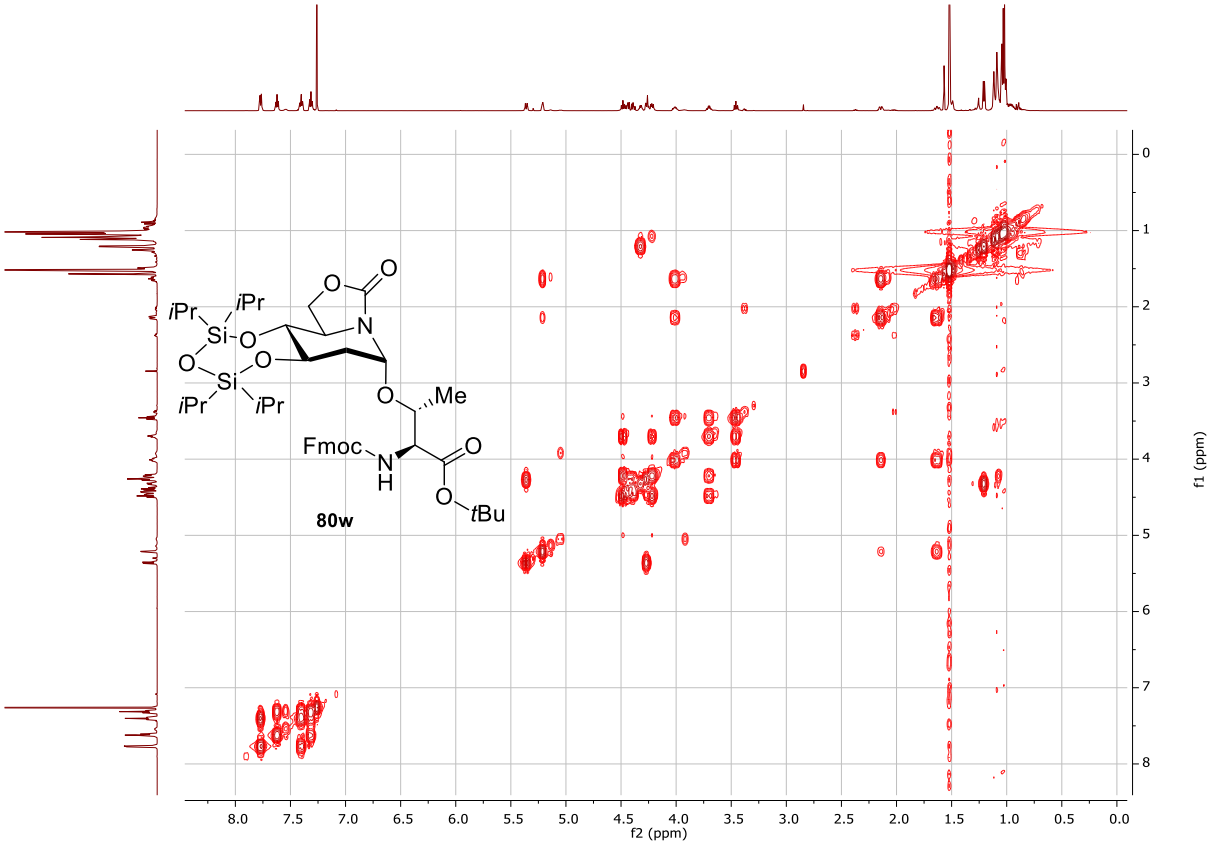

Figure 8.267. COSY spectra for 80w

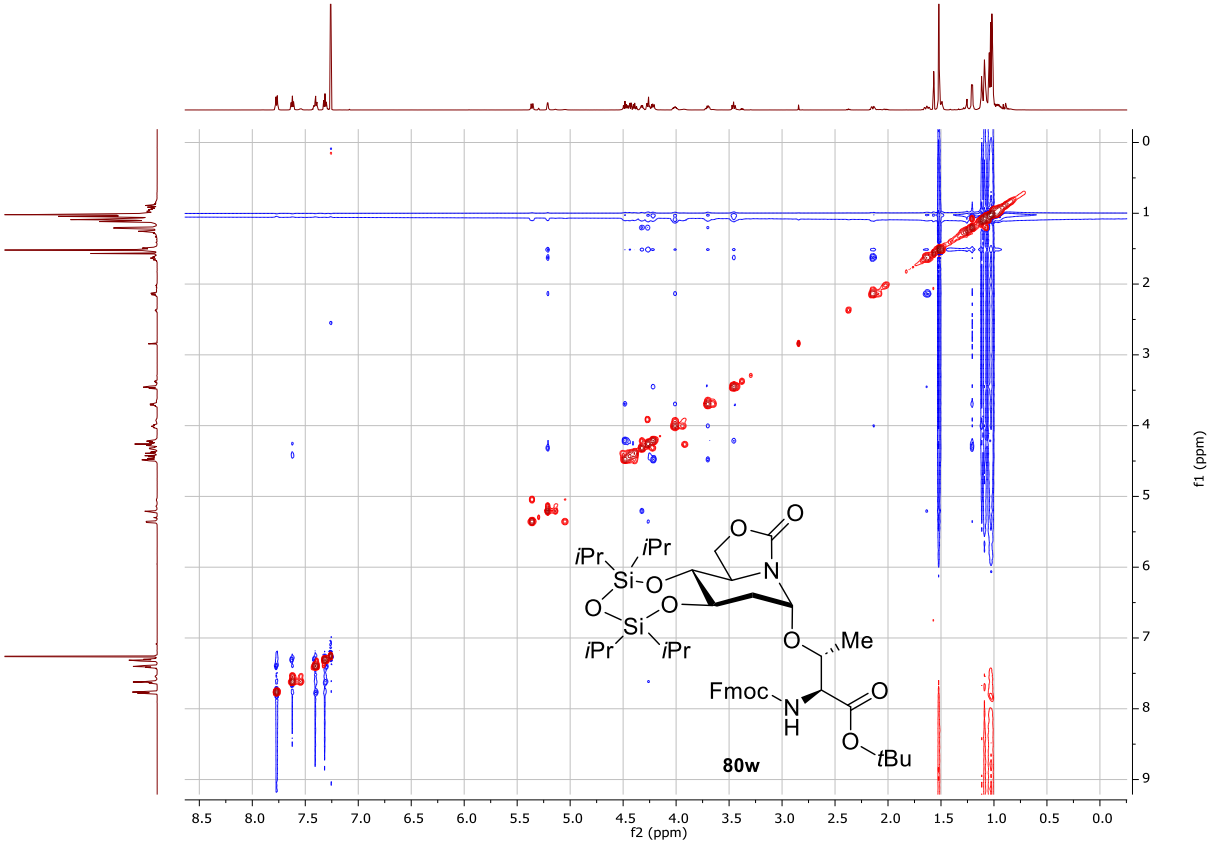

Figure 8.268. NOESY spectra for 80w

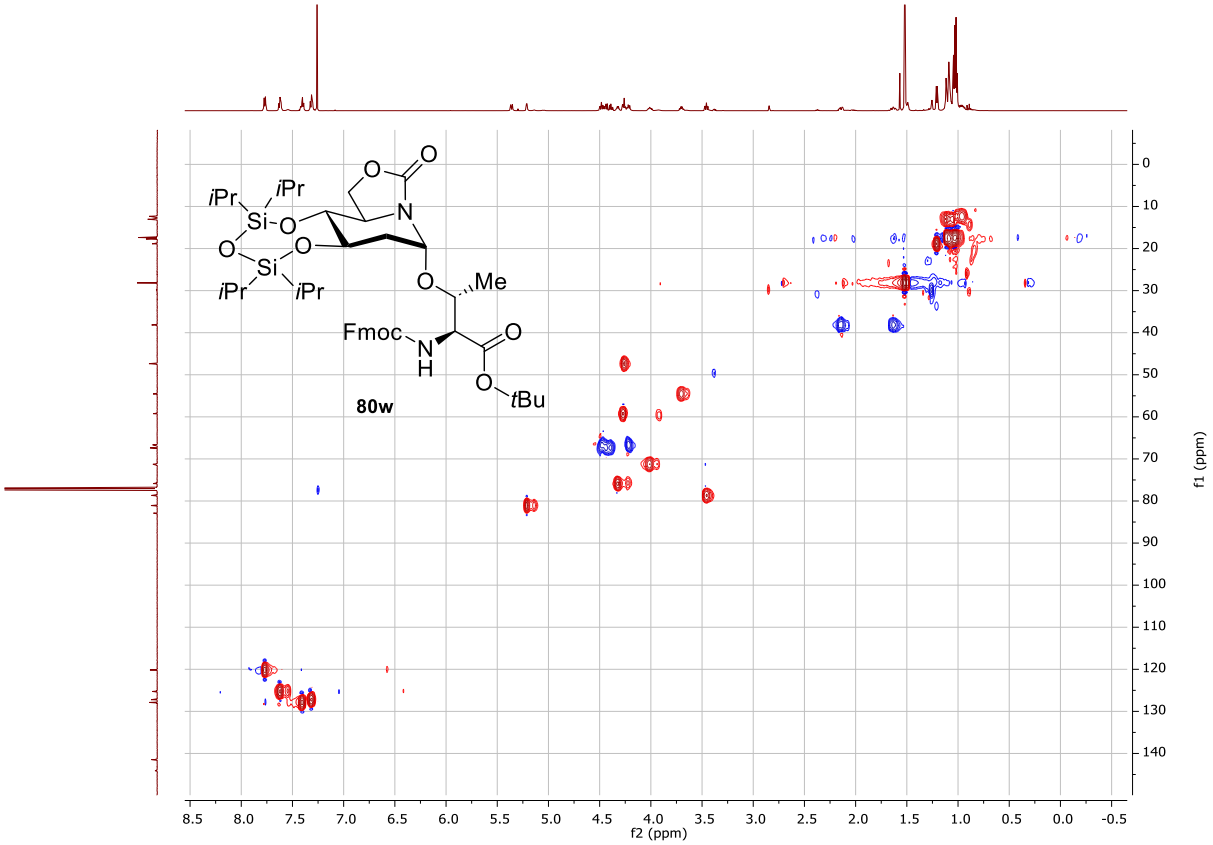

Figure 8.269. HSQC spectra for 80w

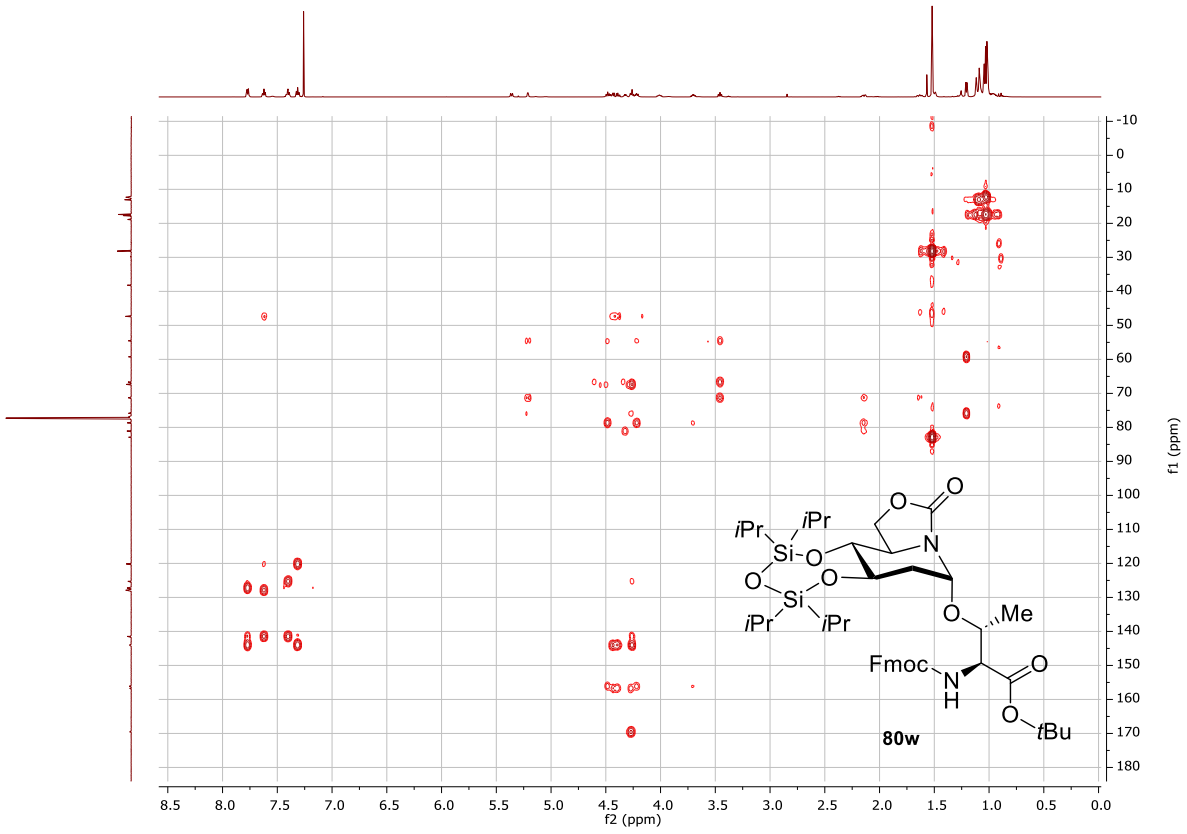

Figure 8.270. HMBC spectra for 80w

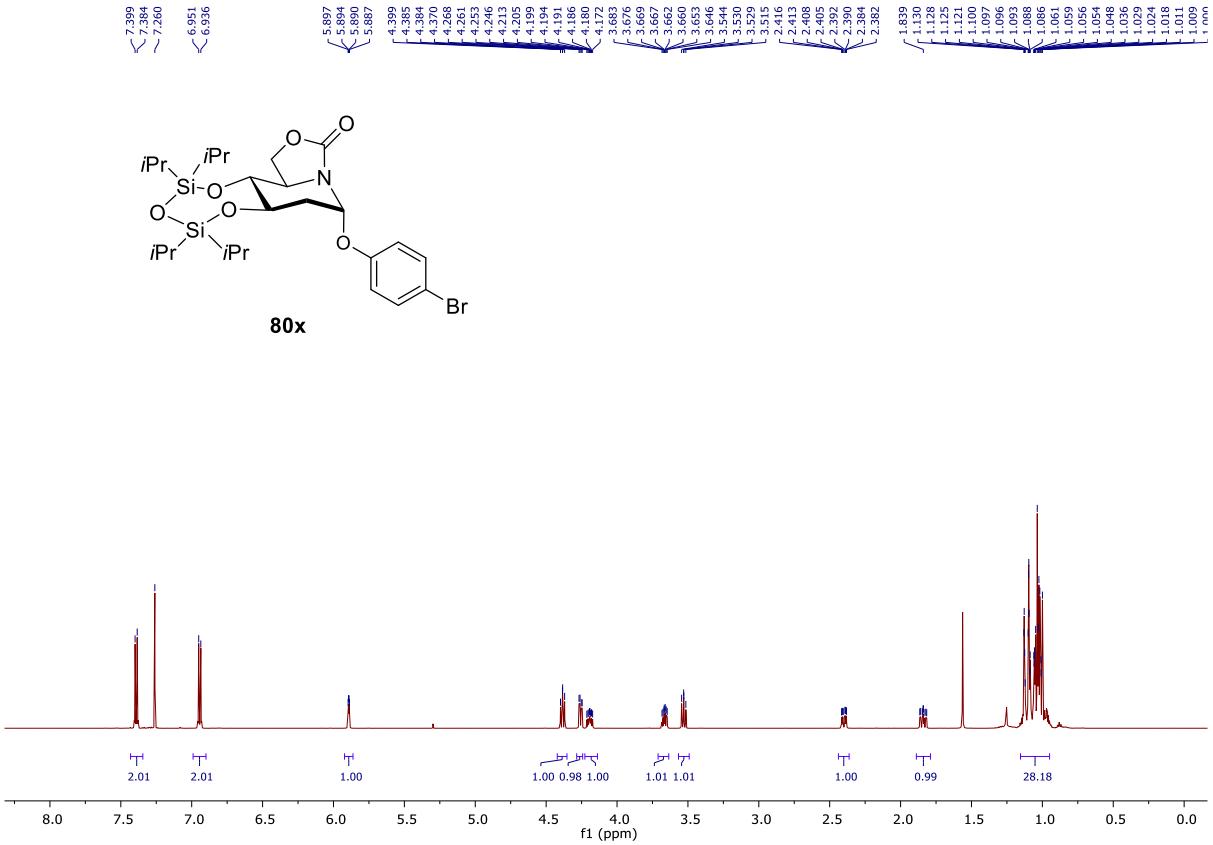

Figure 8.271. ^{1}H NMR spectra for 80x

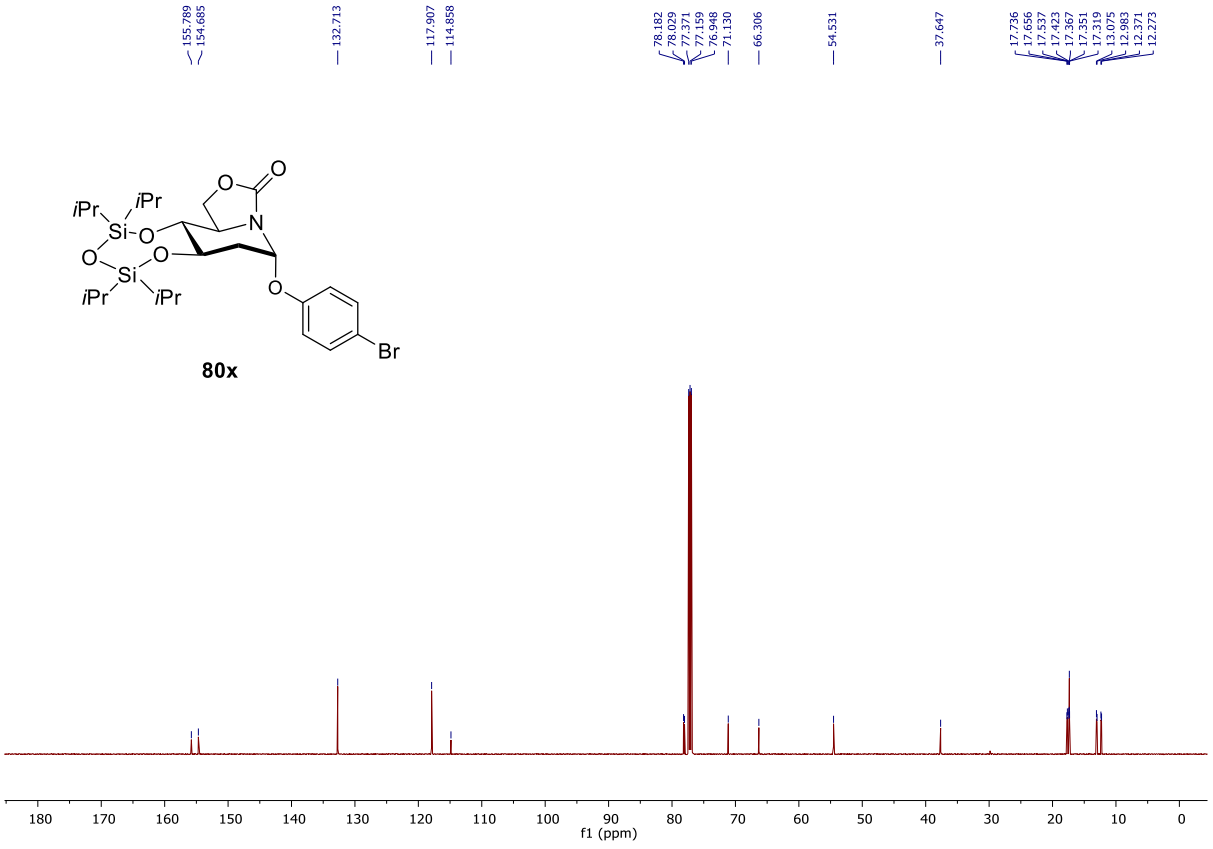

Figure 8.272. ^{13}C NMR spectra for 80x

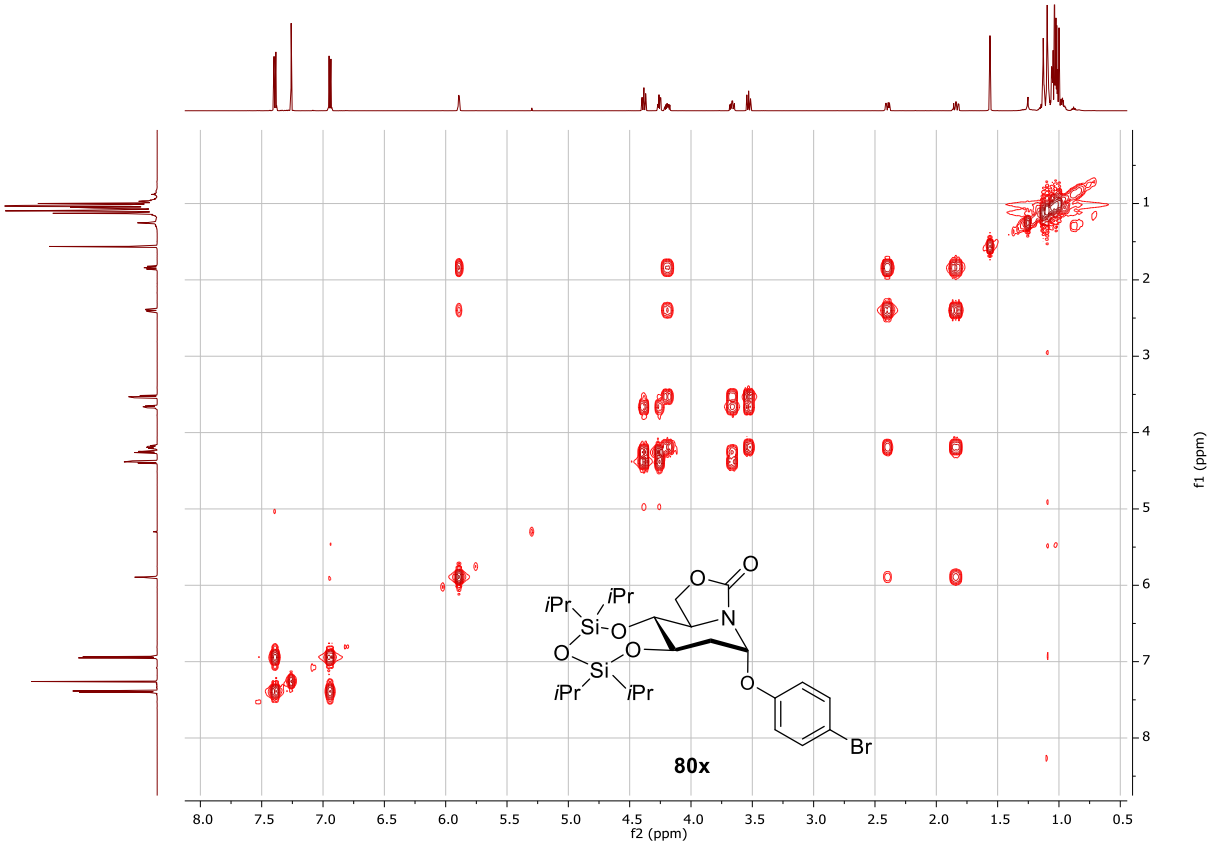

Figure 8.273. COSY spectra for 80x

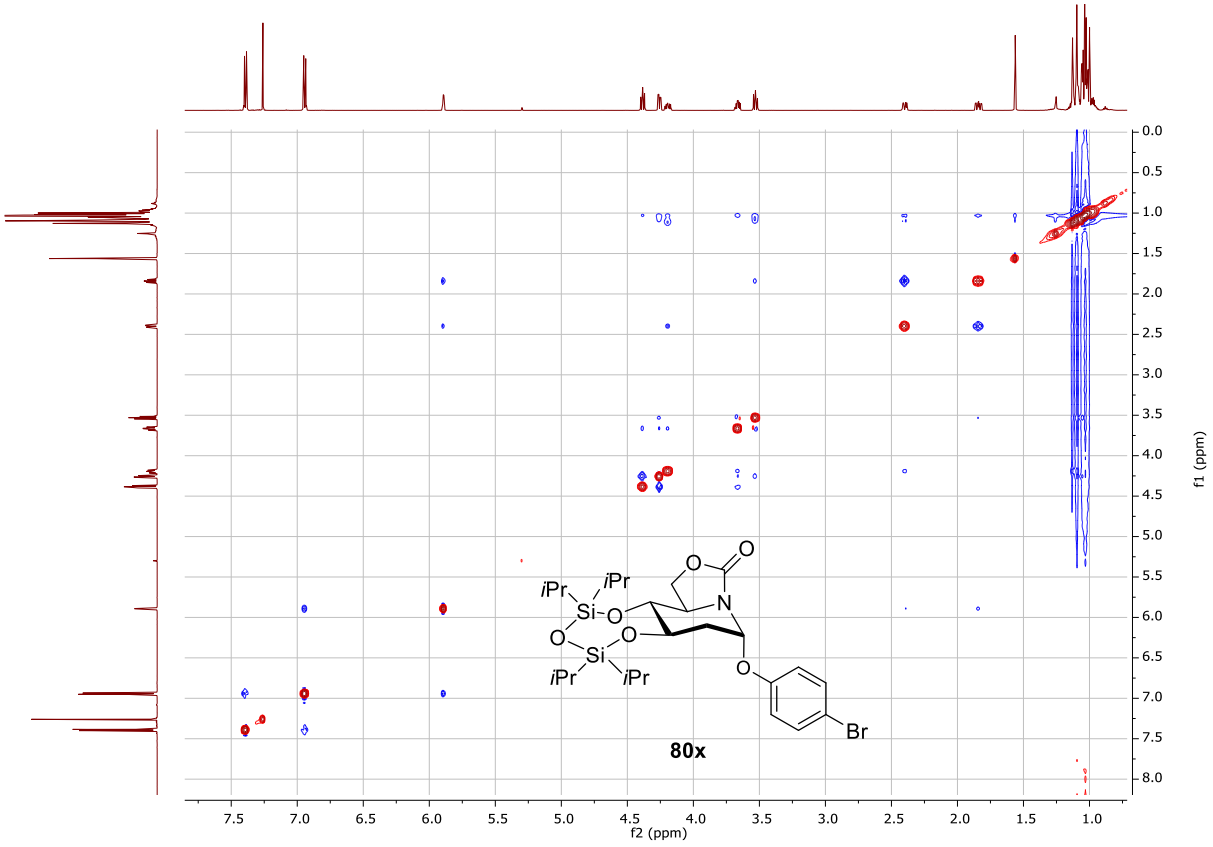

Figure 8.274. NOESY spectra for 80x

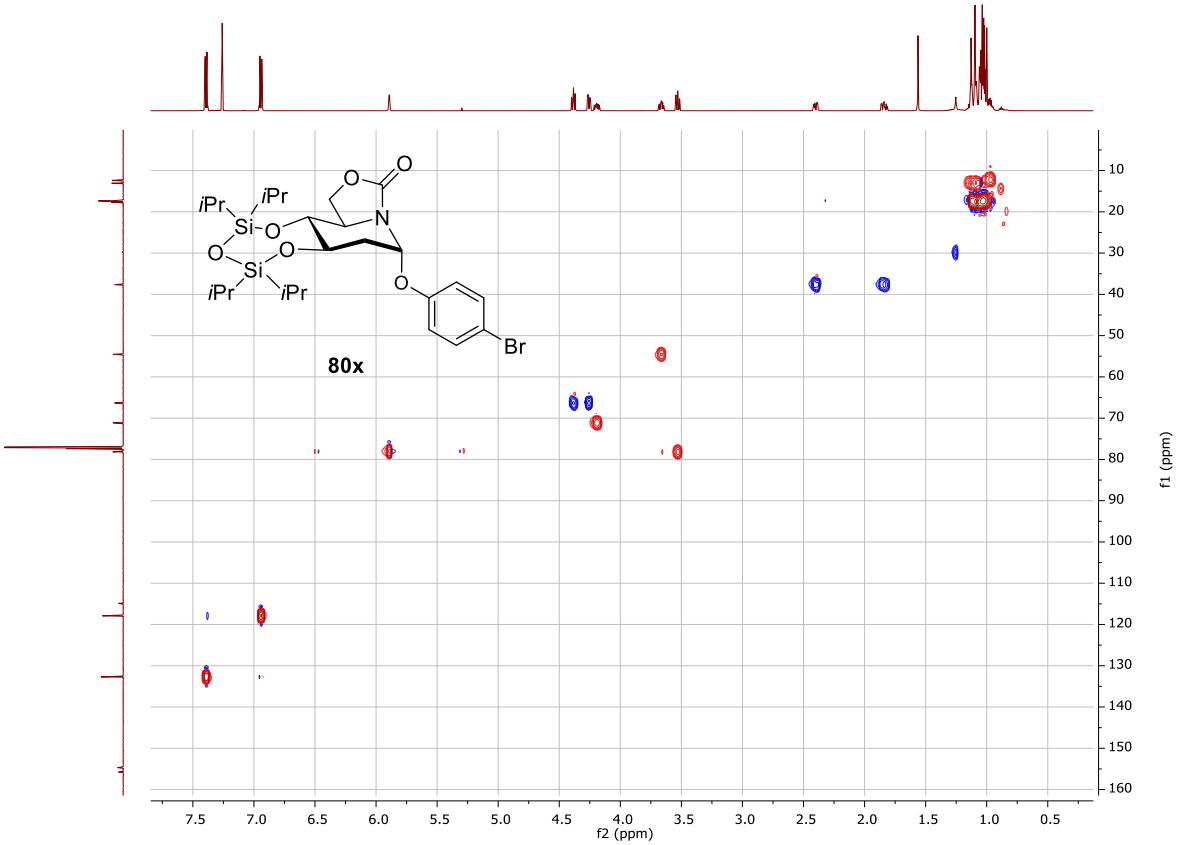

Figure 8.275. HSQC spectra for 80x

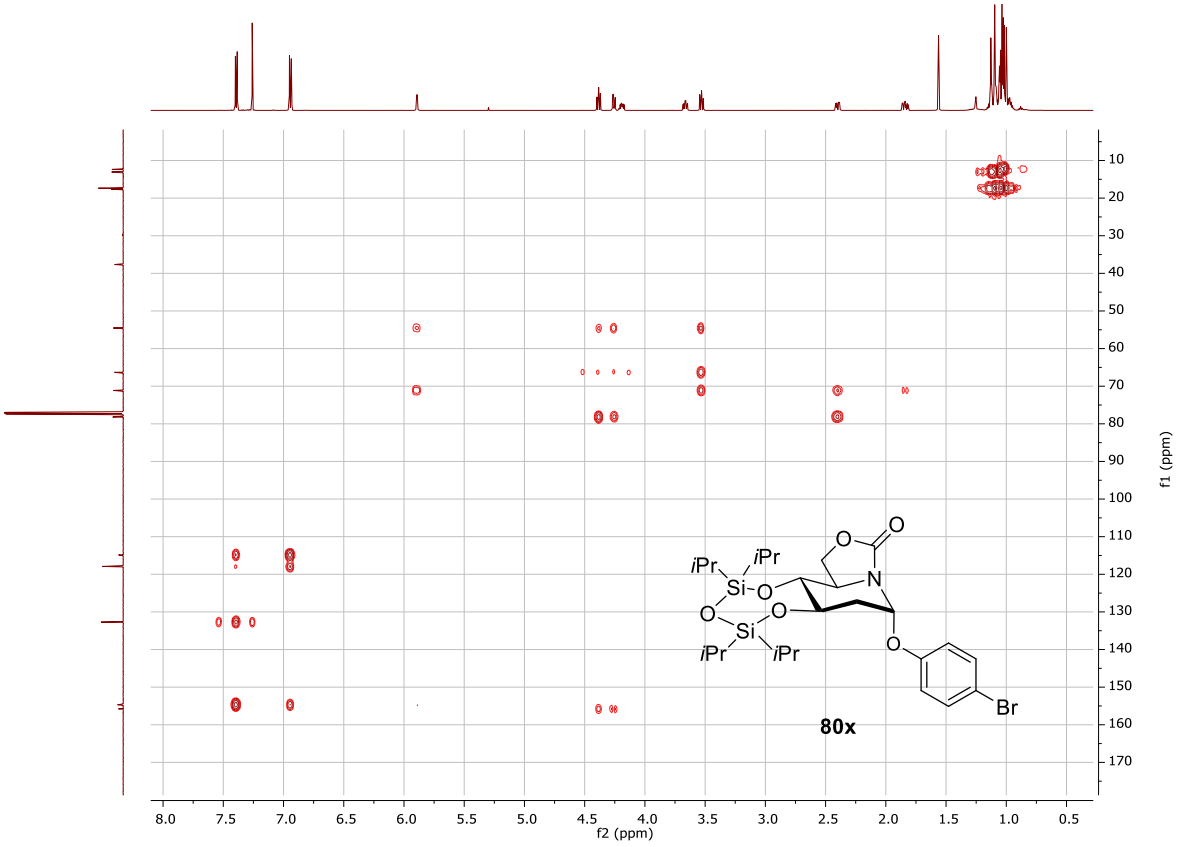

Figure 8.276. HMBC spectra for 80x

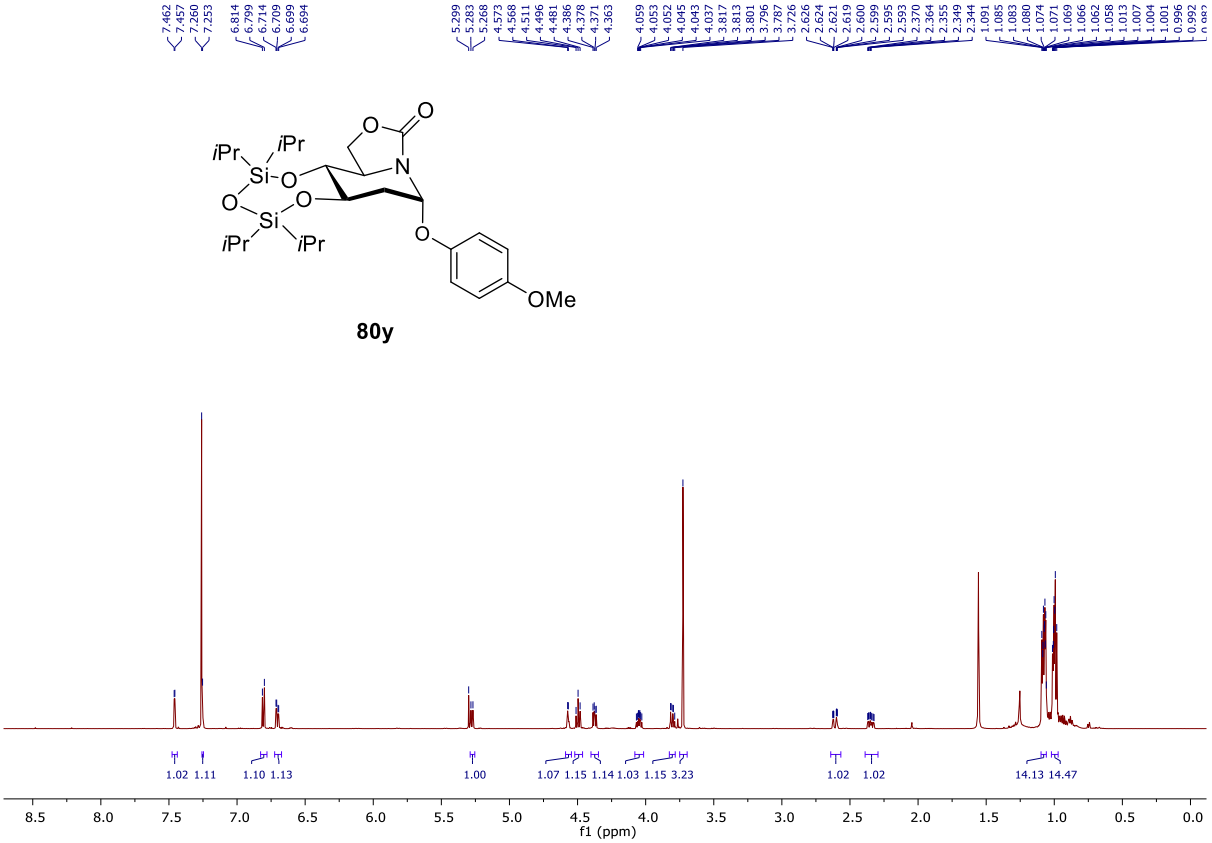

Figure 8.277. ^{1}H NMR spectra for 80y

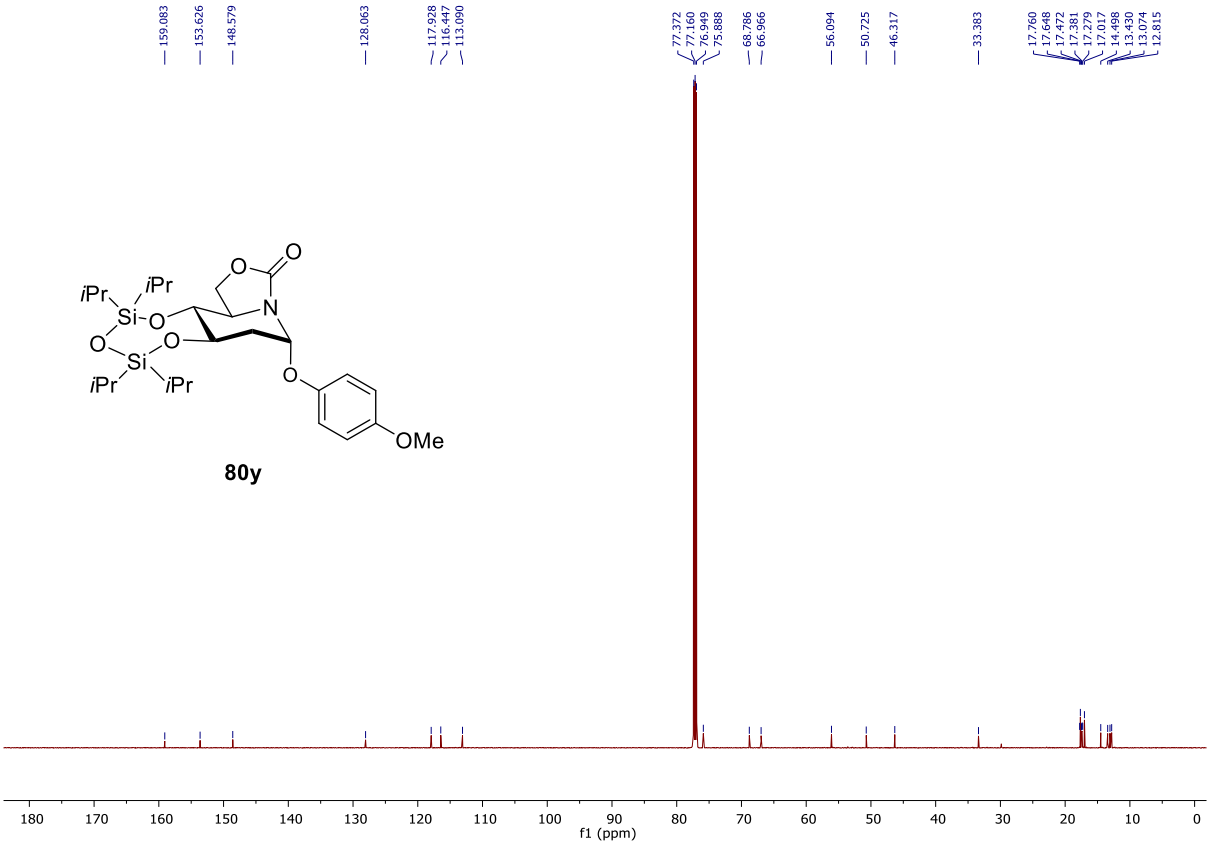

Figure 8.278. ^{13}C NMR spectra for 80y

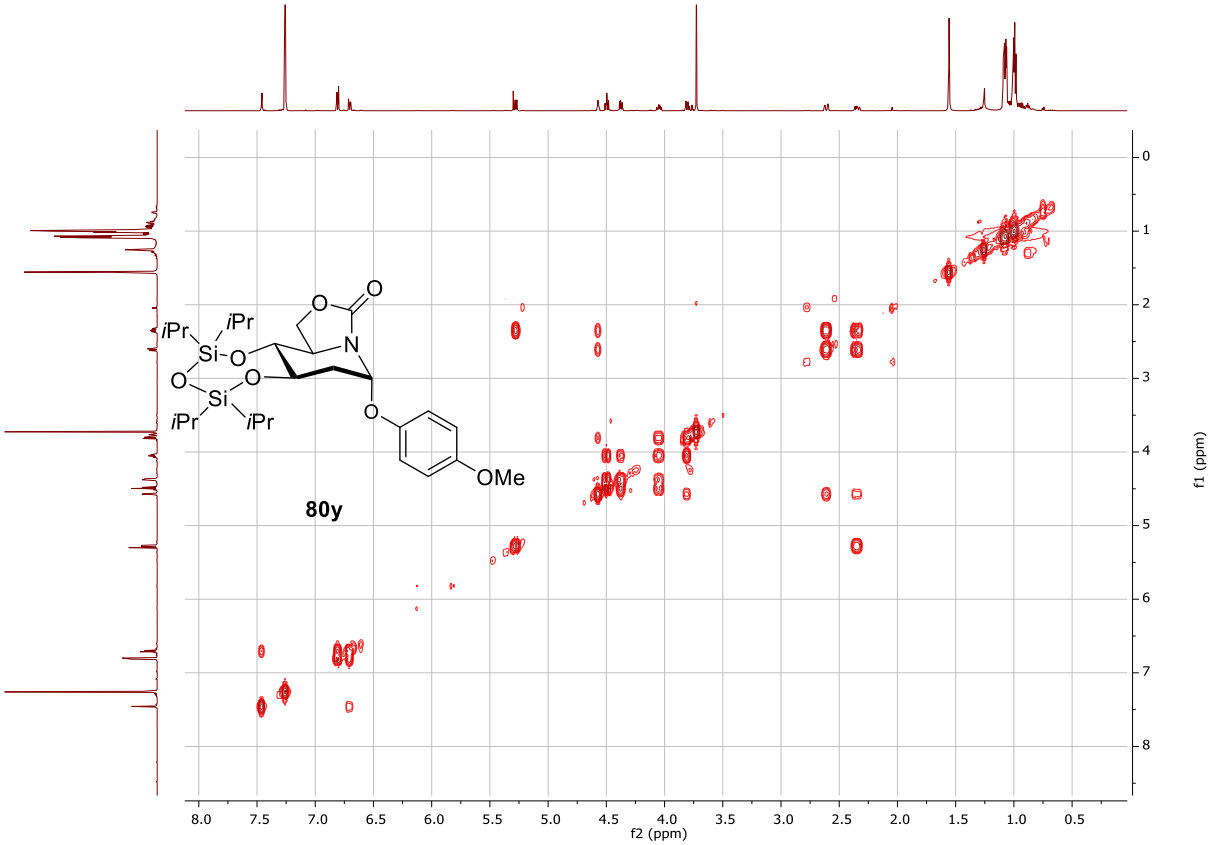

Figure 8.279. COSY spectra for 80y

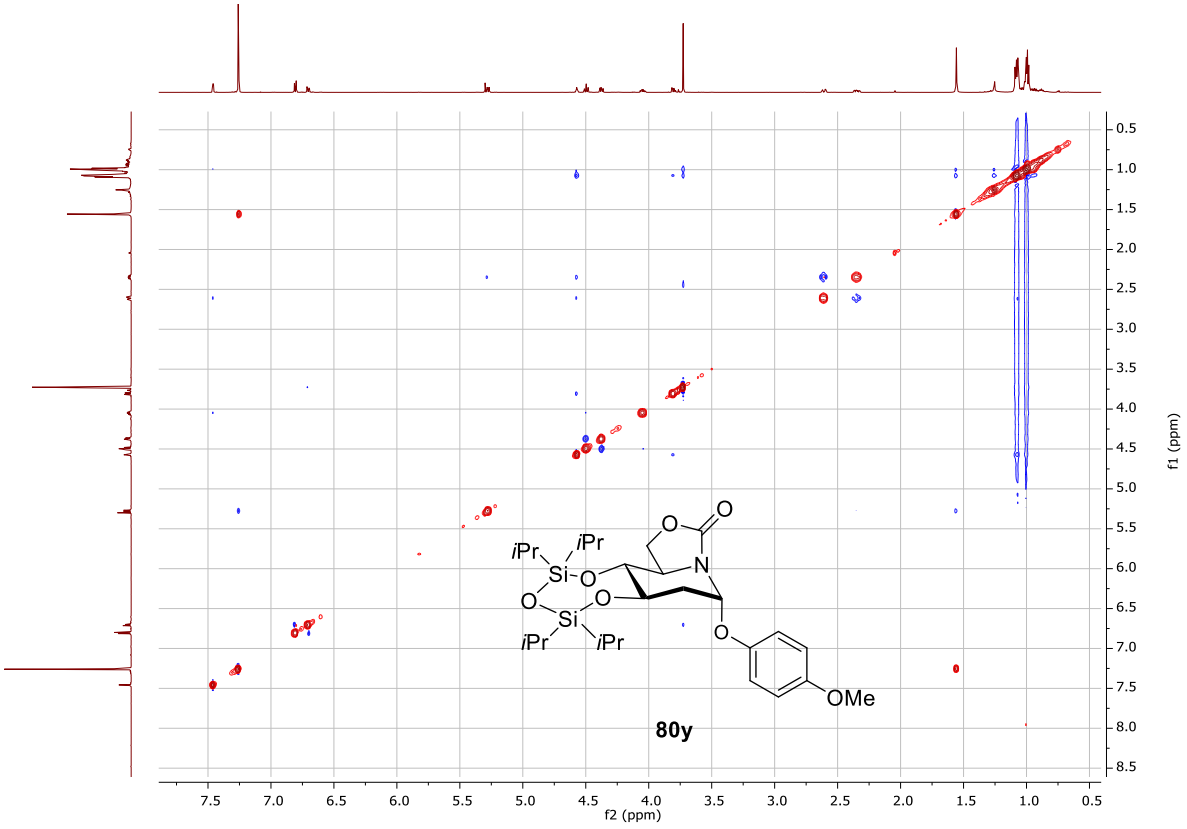

Figure 8.280. NOESY spectra for 80y

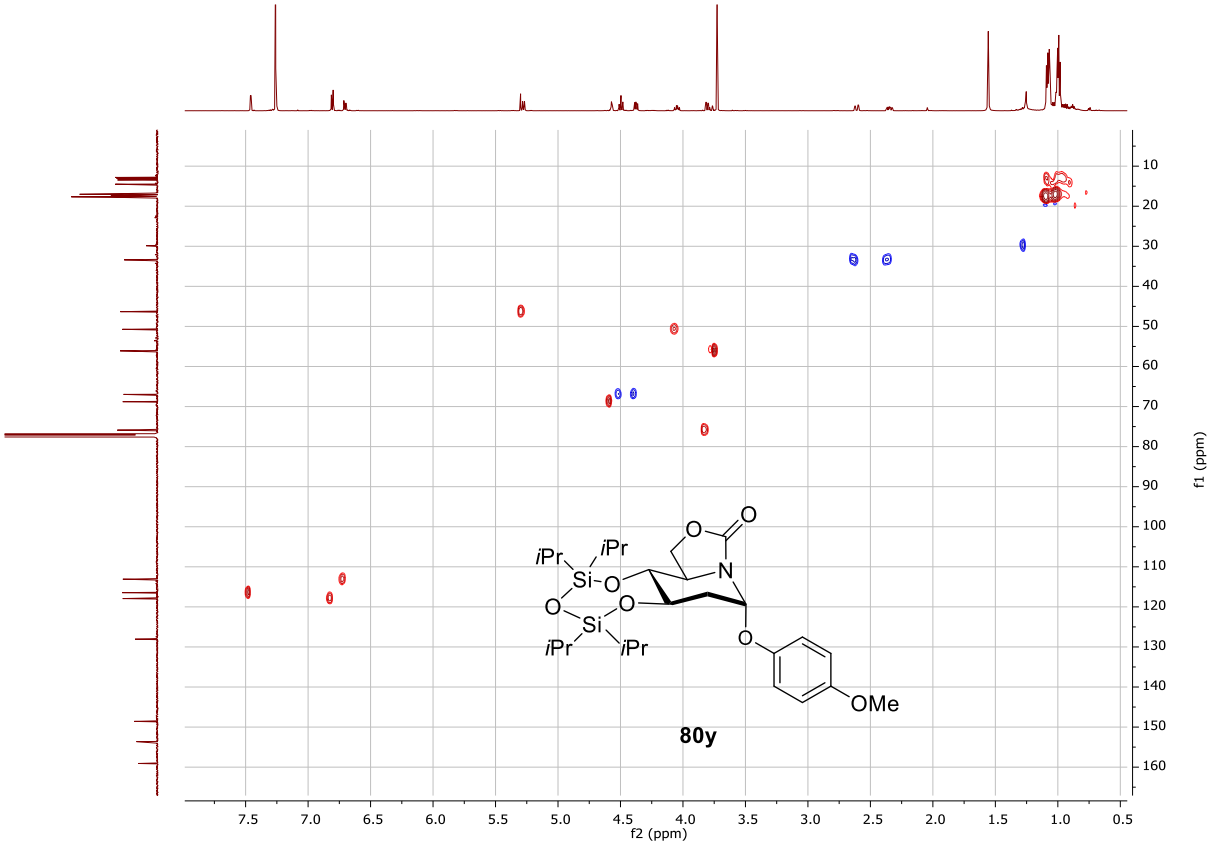

Figure 8.281. HSQC spectra for 80y

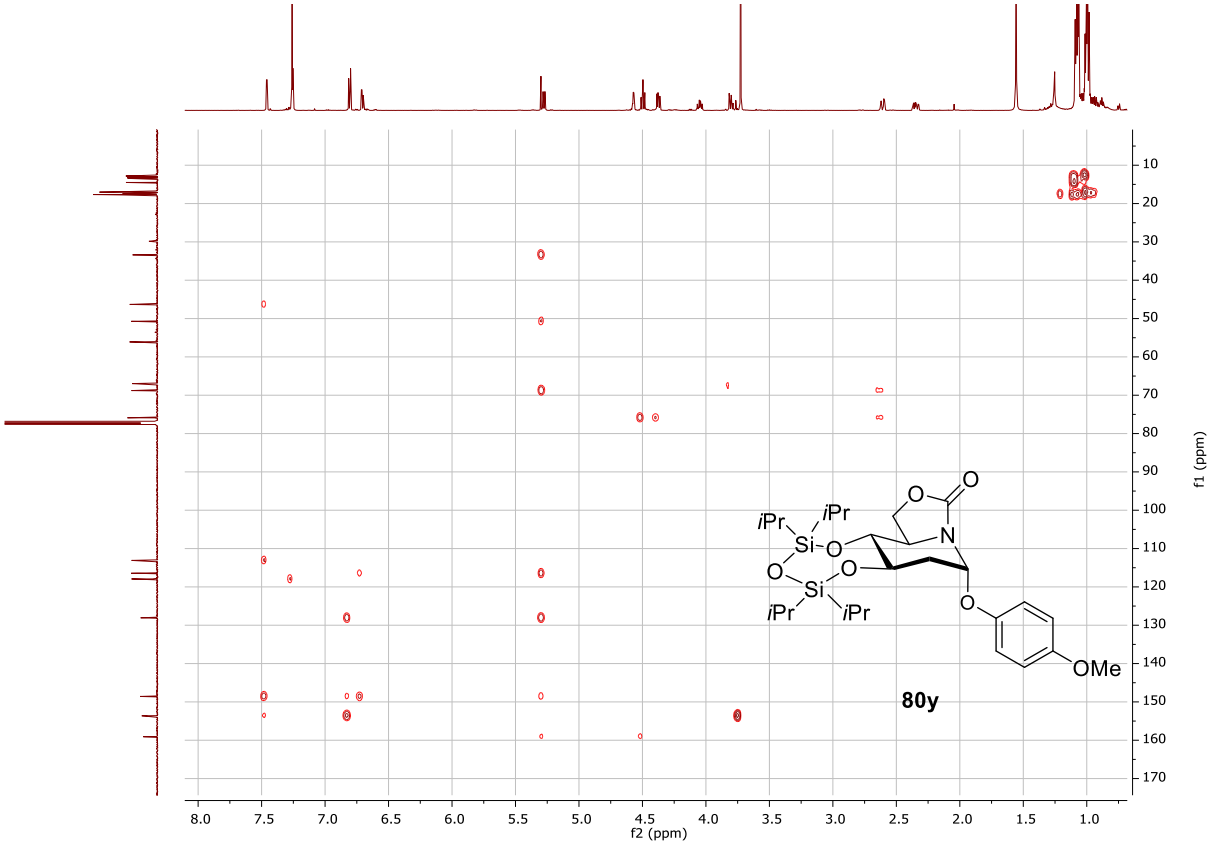

Figure 8.282. HMBC spectra for 80y

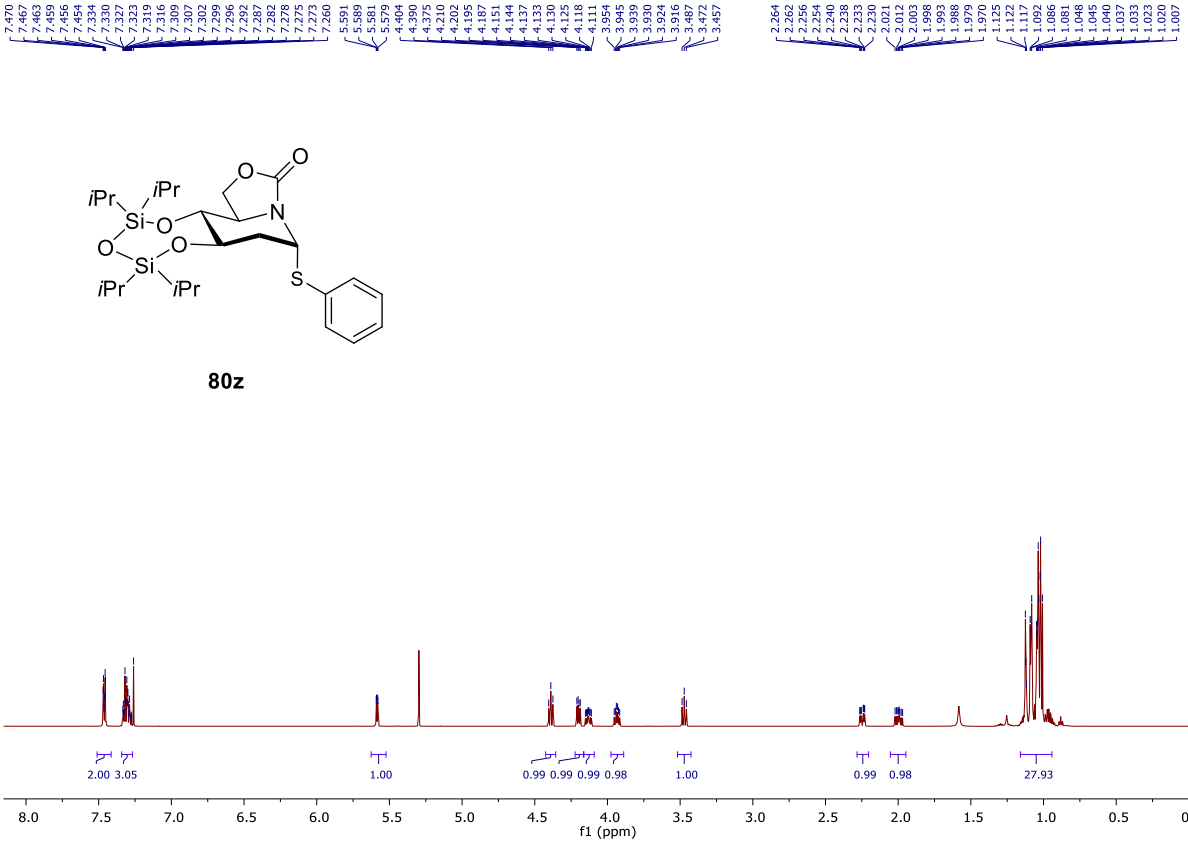

Figure 8.283. ^{1}H NMR spectra for 80z

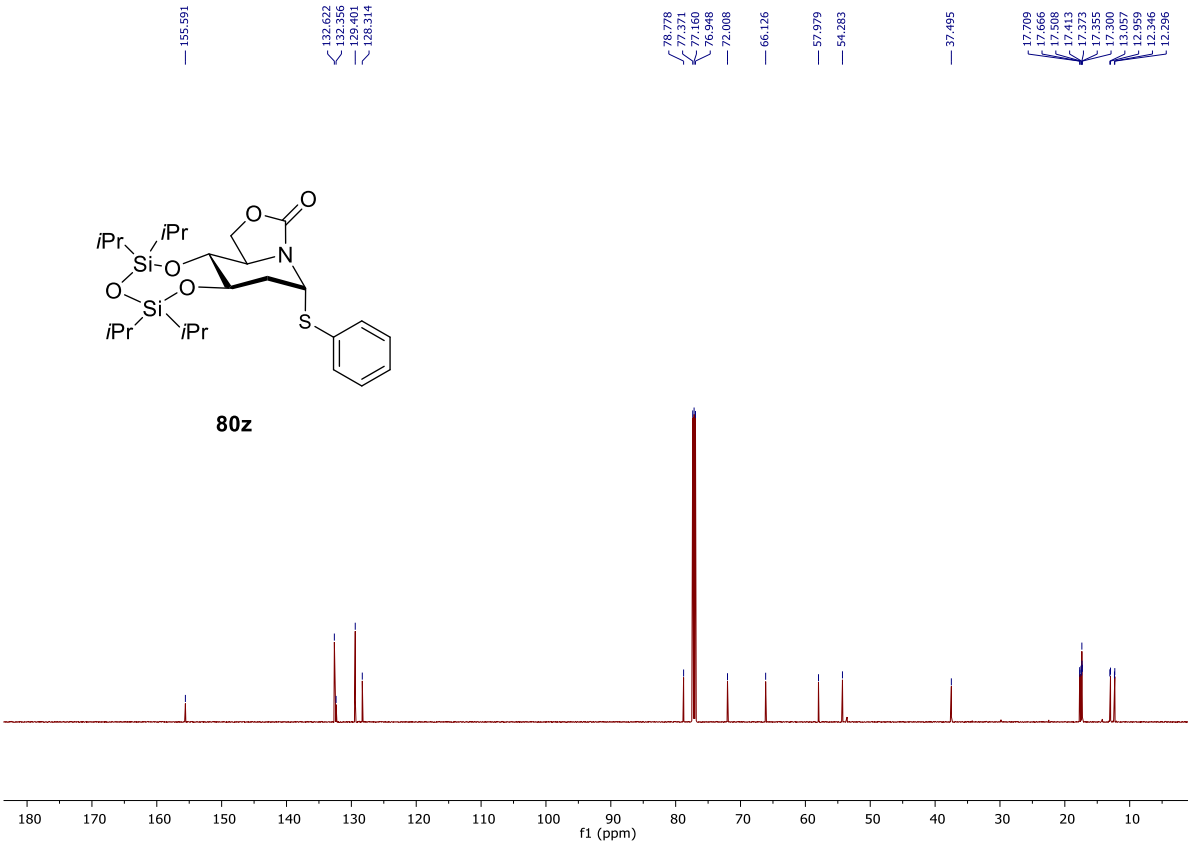

Figure 8.284. ^{13}C NMR spectra for 80z

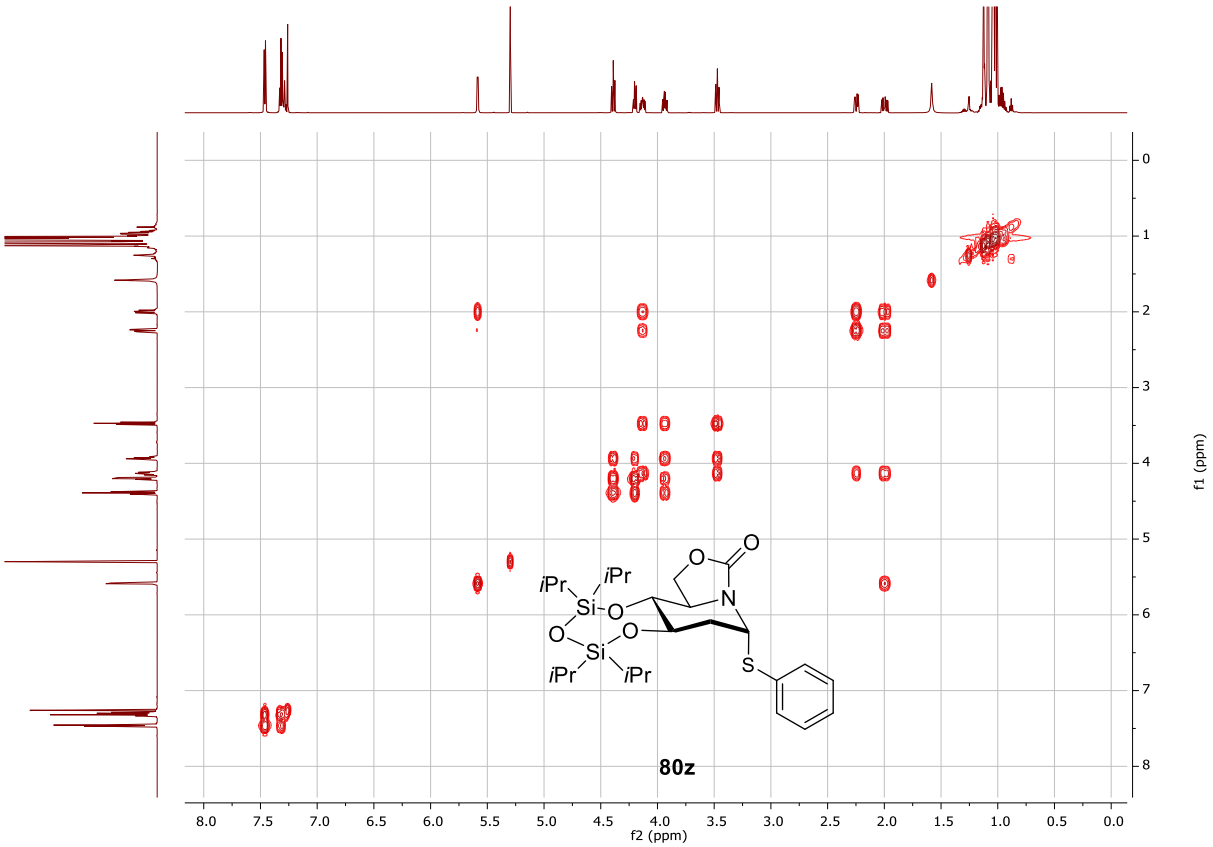

Figure 8.285. COSY spectra for 80z

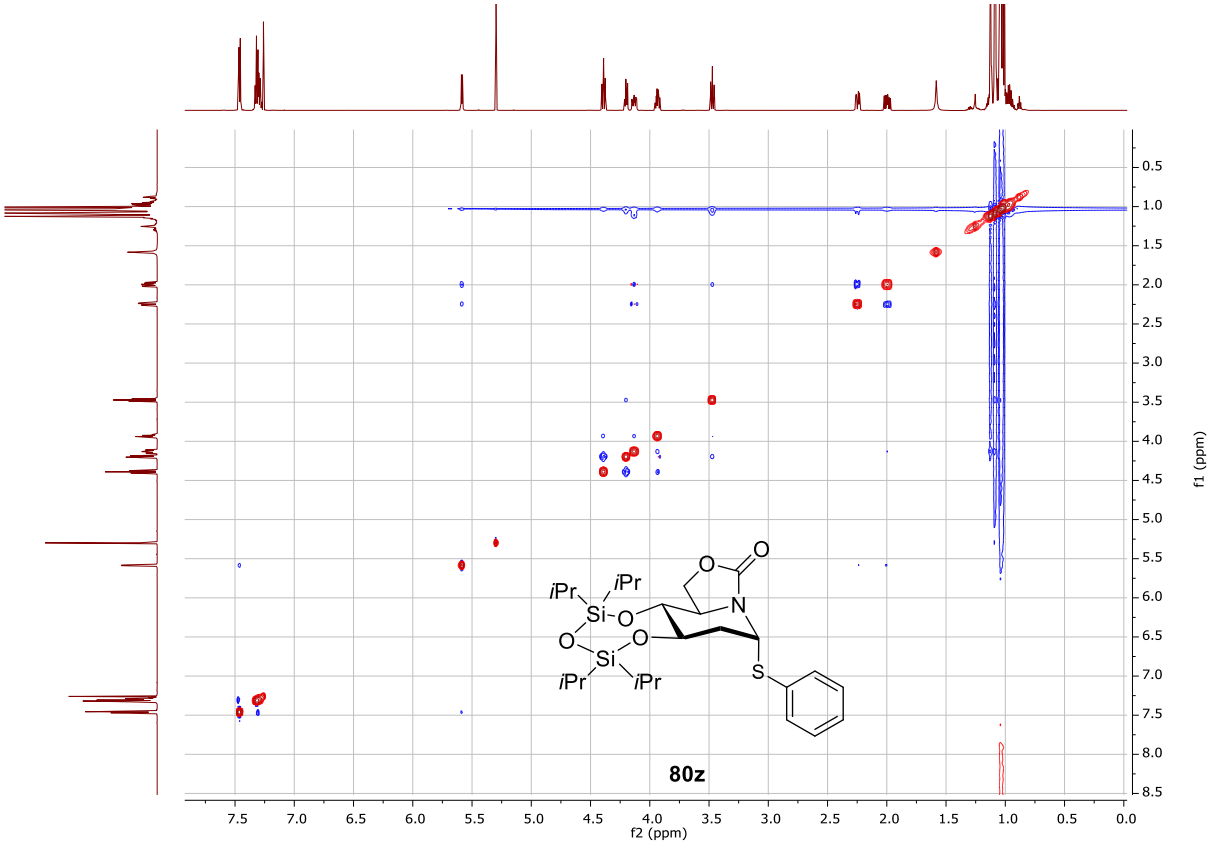

Figure 8.286. NOESY spectra for 80z

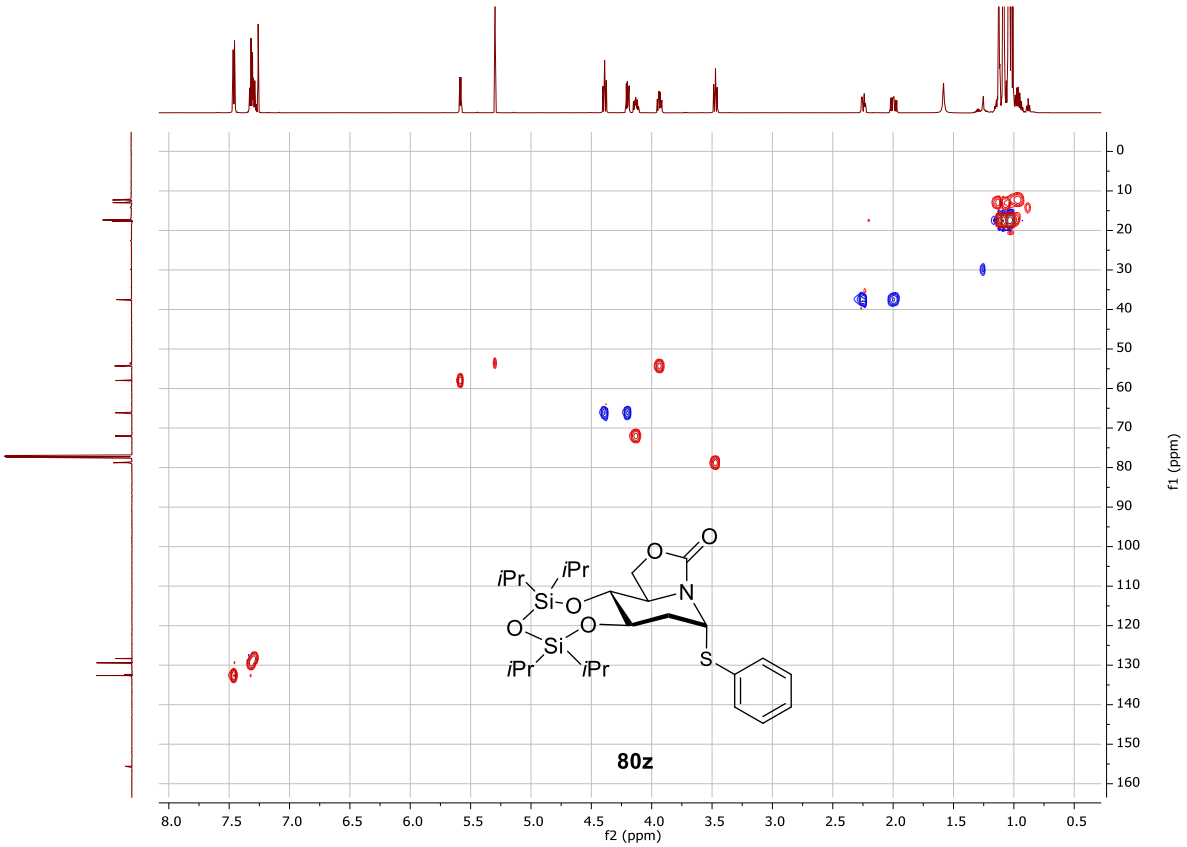

Figure 8.287. HSQC spectra for 80z

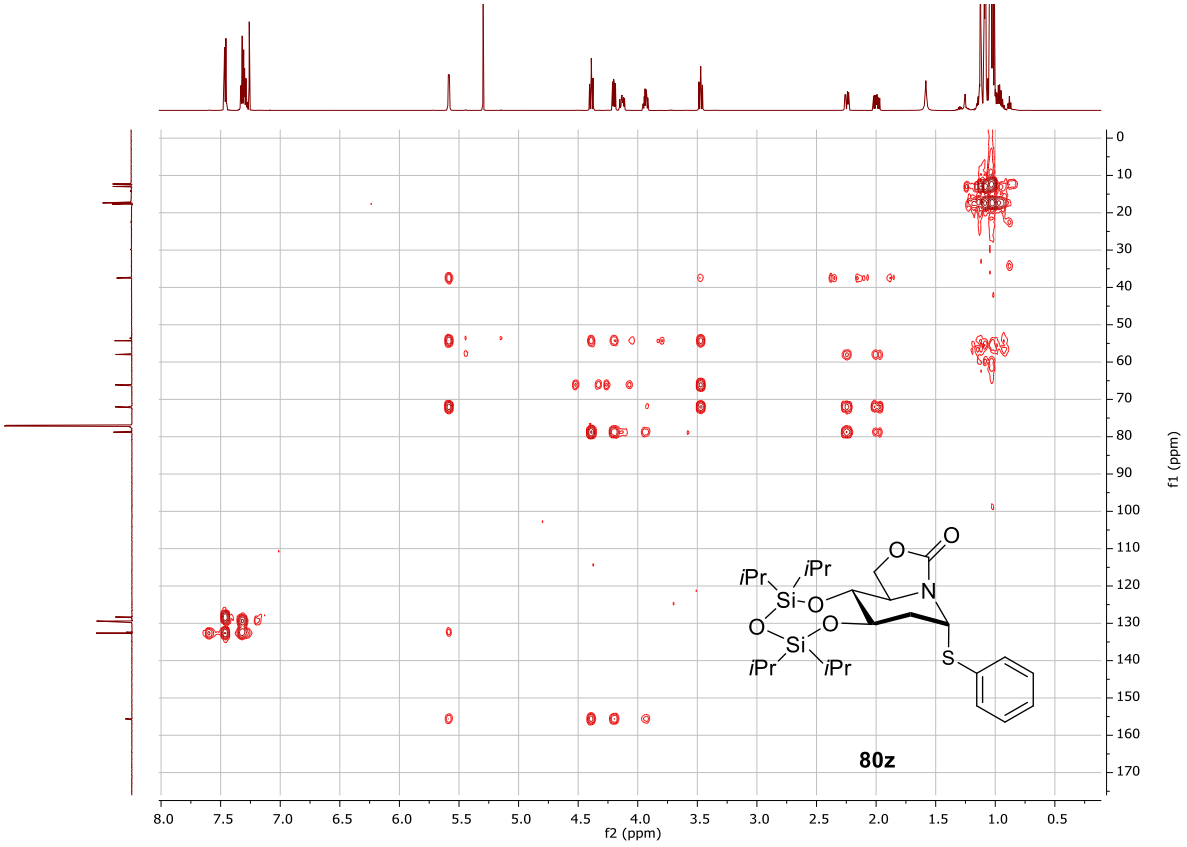

Figure 8.288. HMBC spectra for 80z

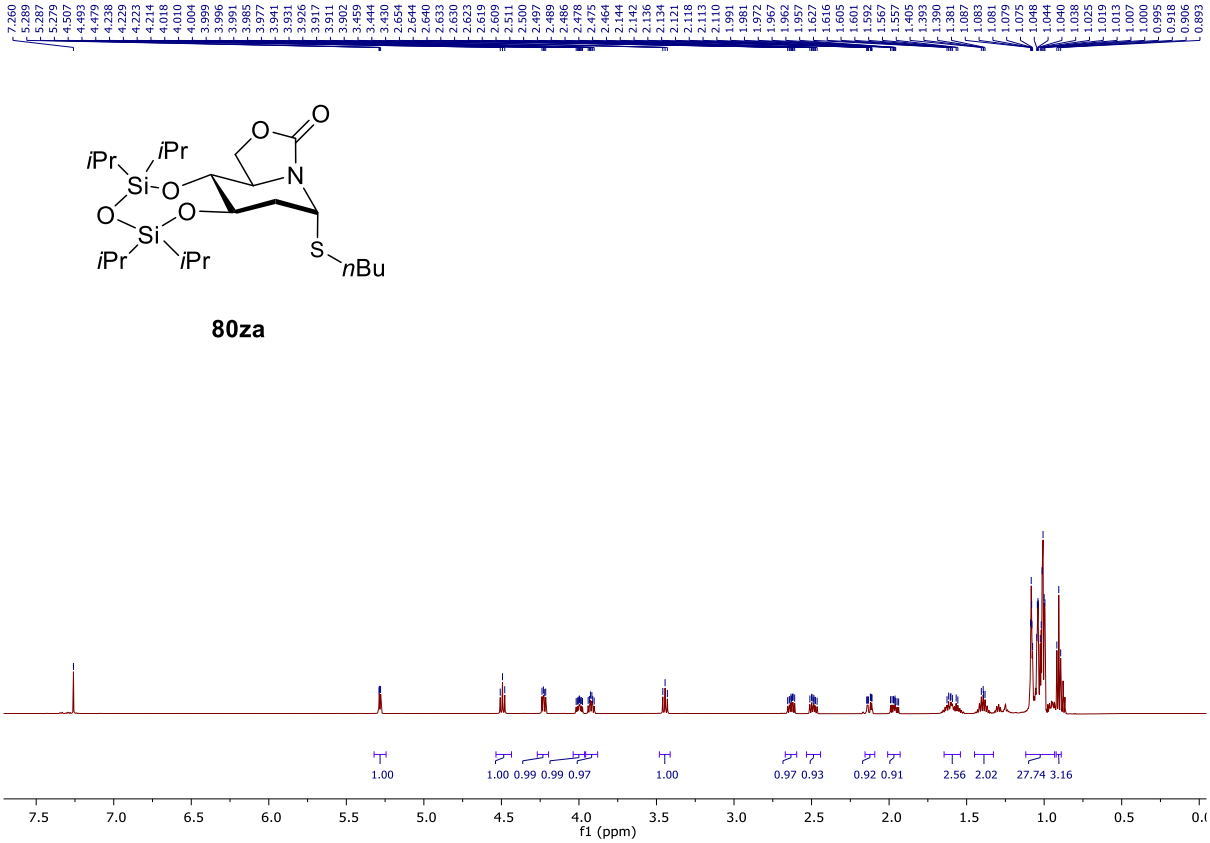

Figure 8.289. ^{1}H NMR spectra for 80za

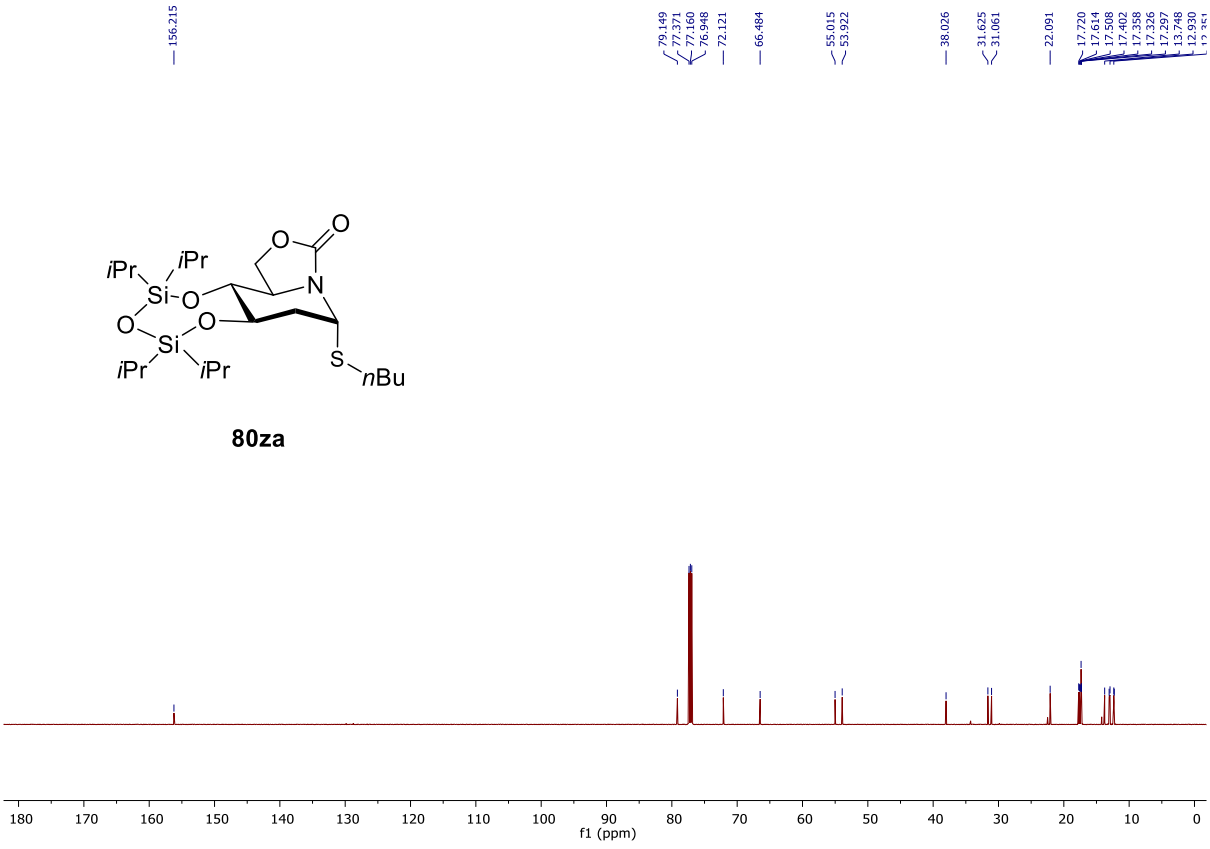

Figure8.290. ^{13}C NMR spectra for 80za

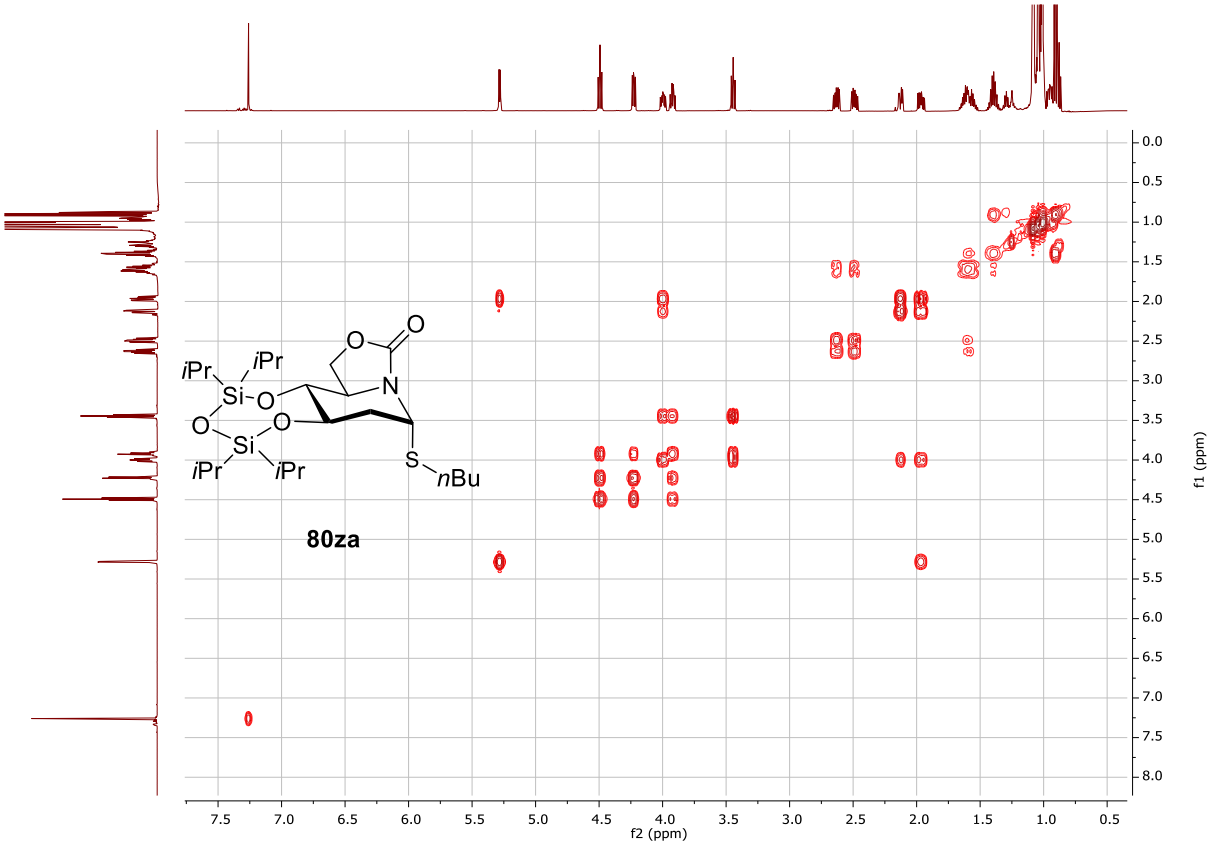

Figure 8.291. COSY spectra for 80za

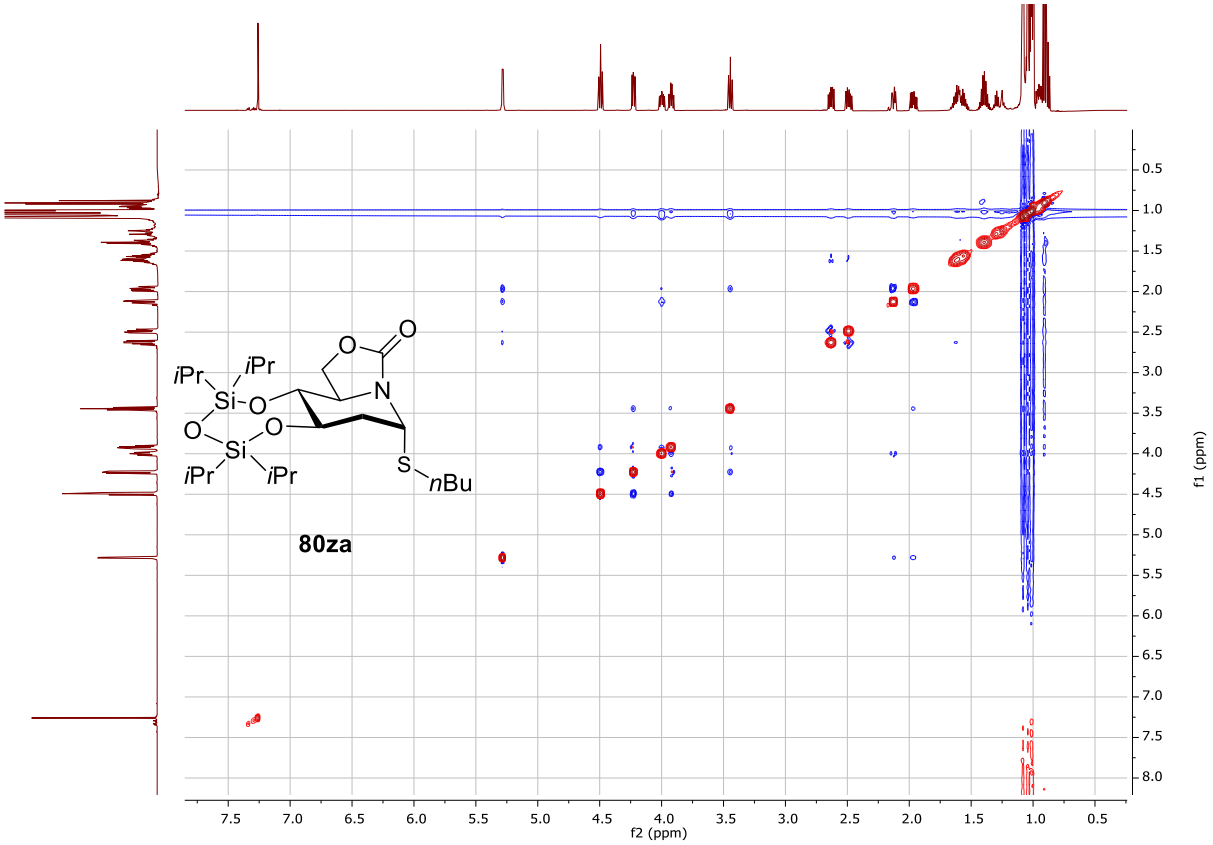

Figure 8.292. NOESY spectra for 80za

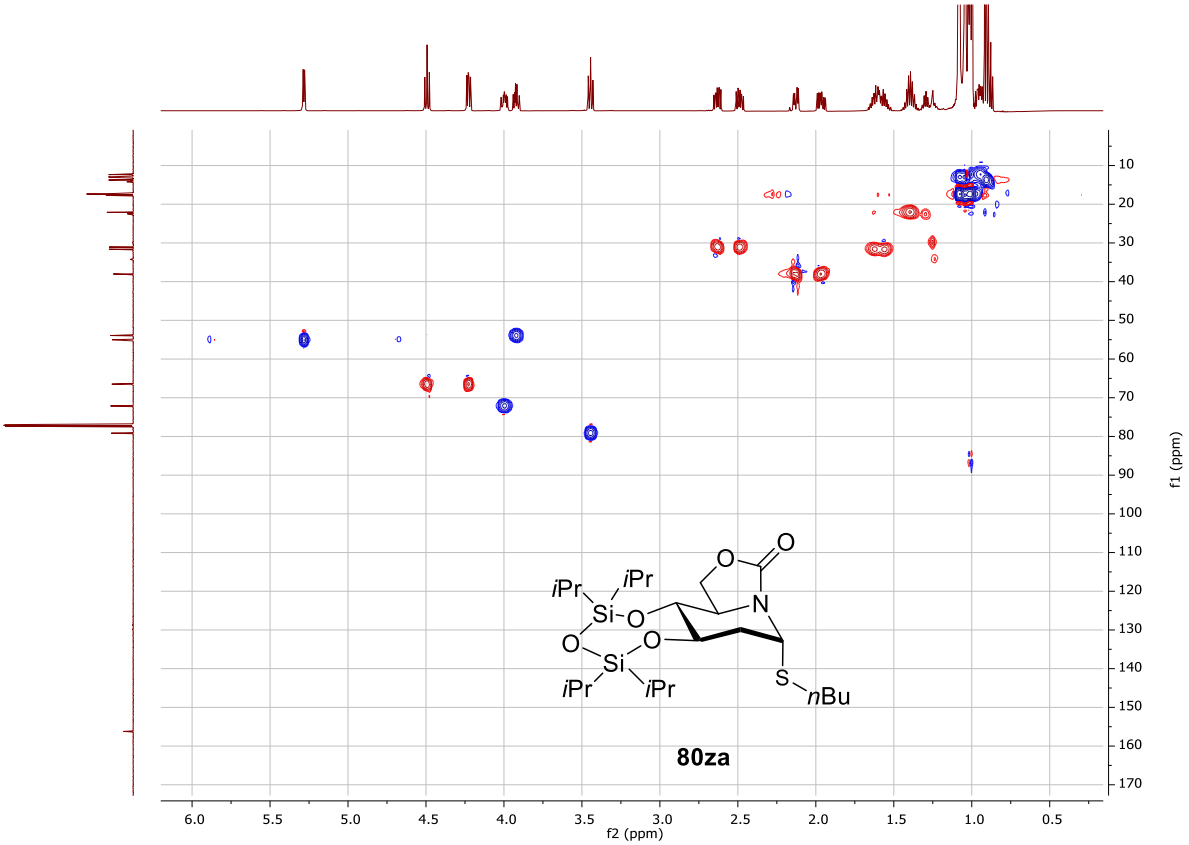

Figure 8.293. HSQC spectra for 80za

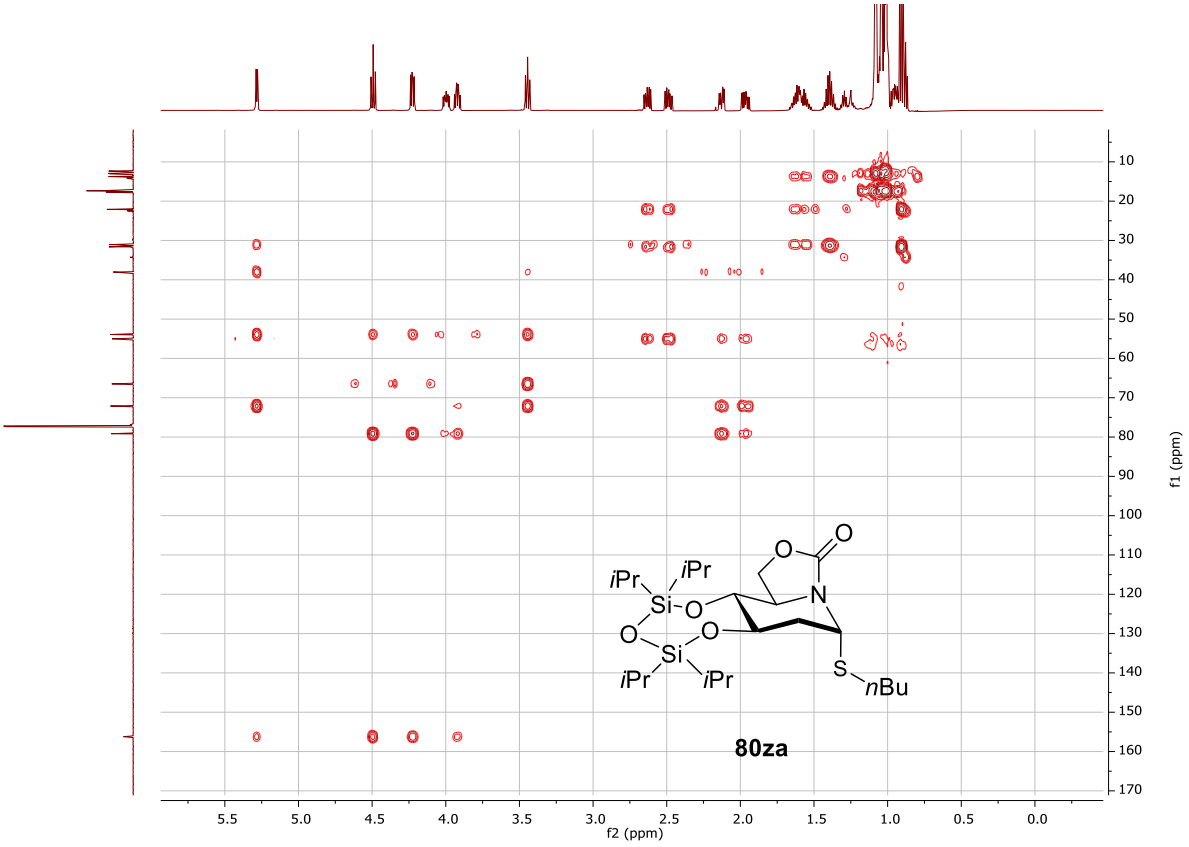

Figure 8.294. HMBC spectra for 80za

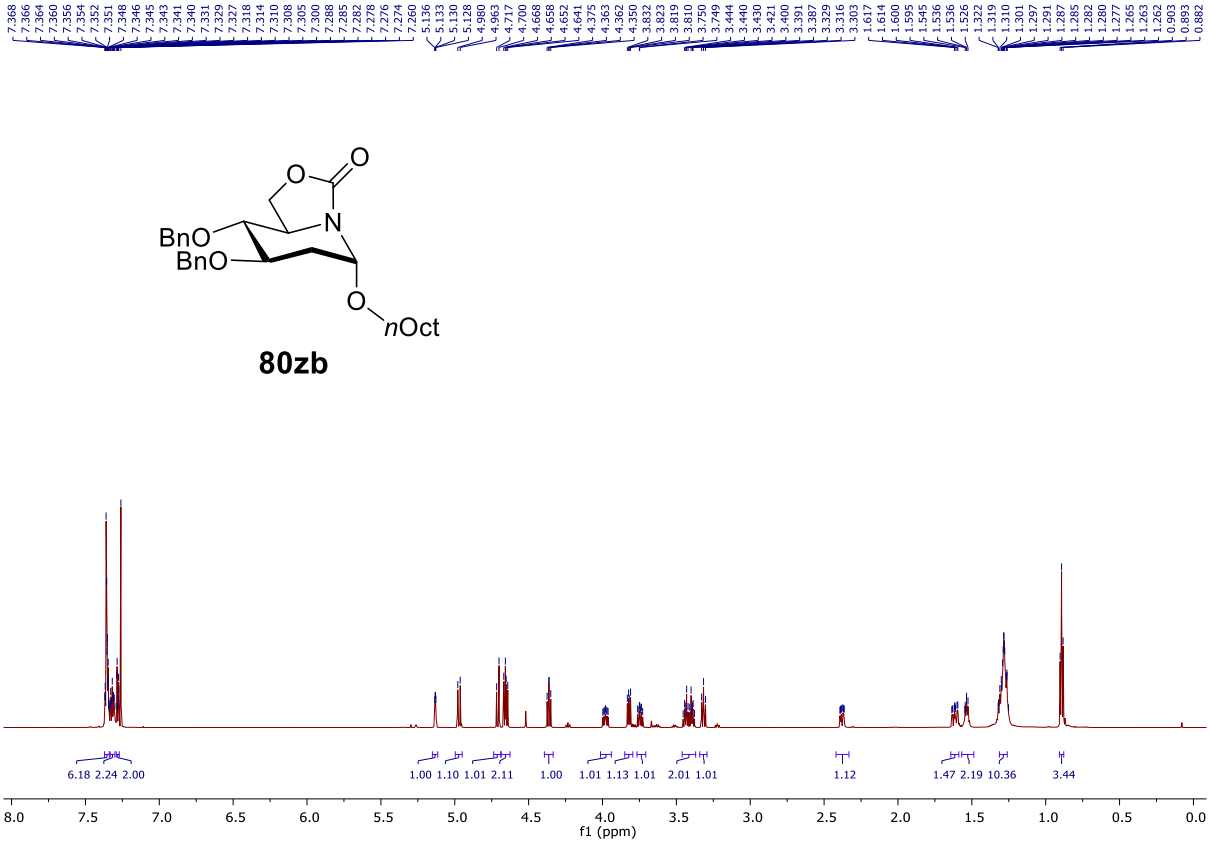

Figure 8.295. ^{1}H NMR spectra for 80zb

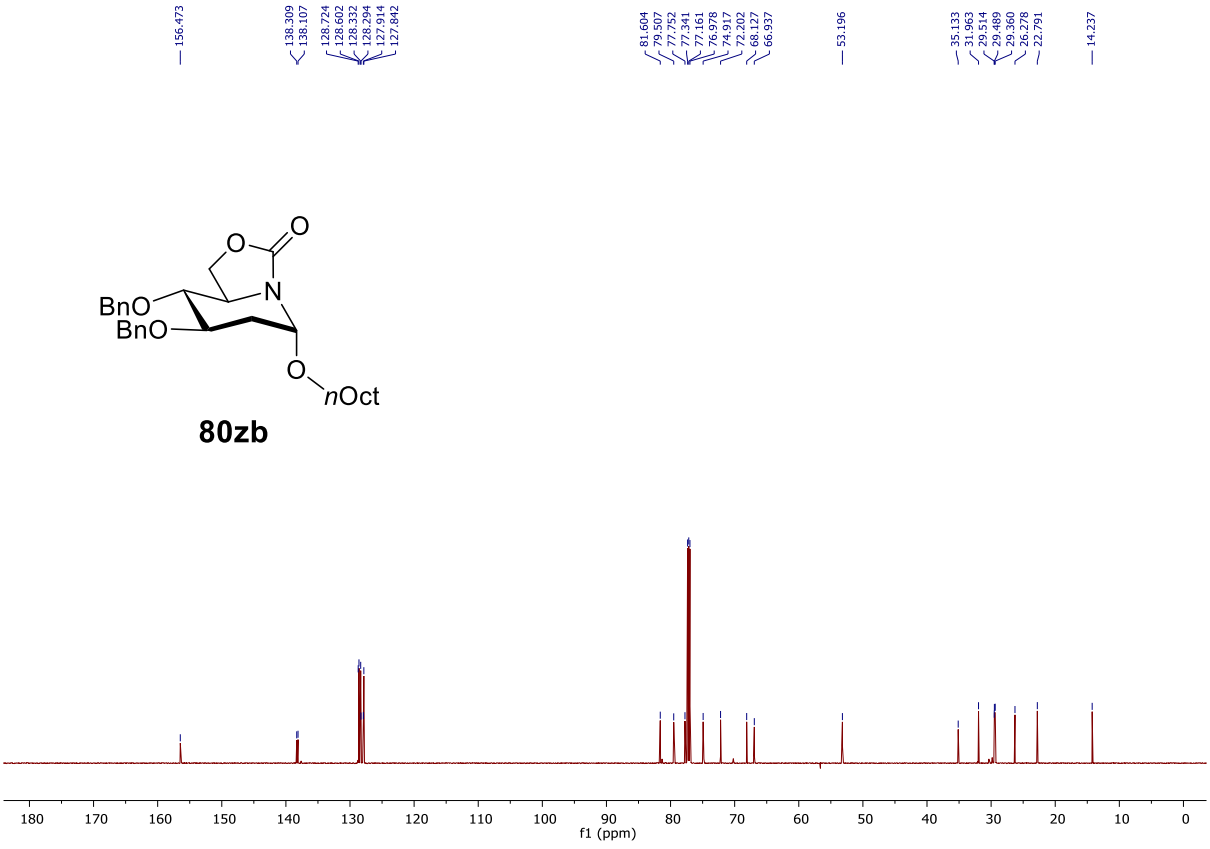

Figure 8.296. ^{13}C NMR spectra for 80zb

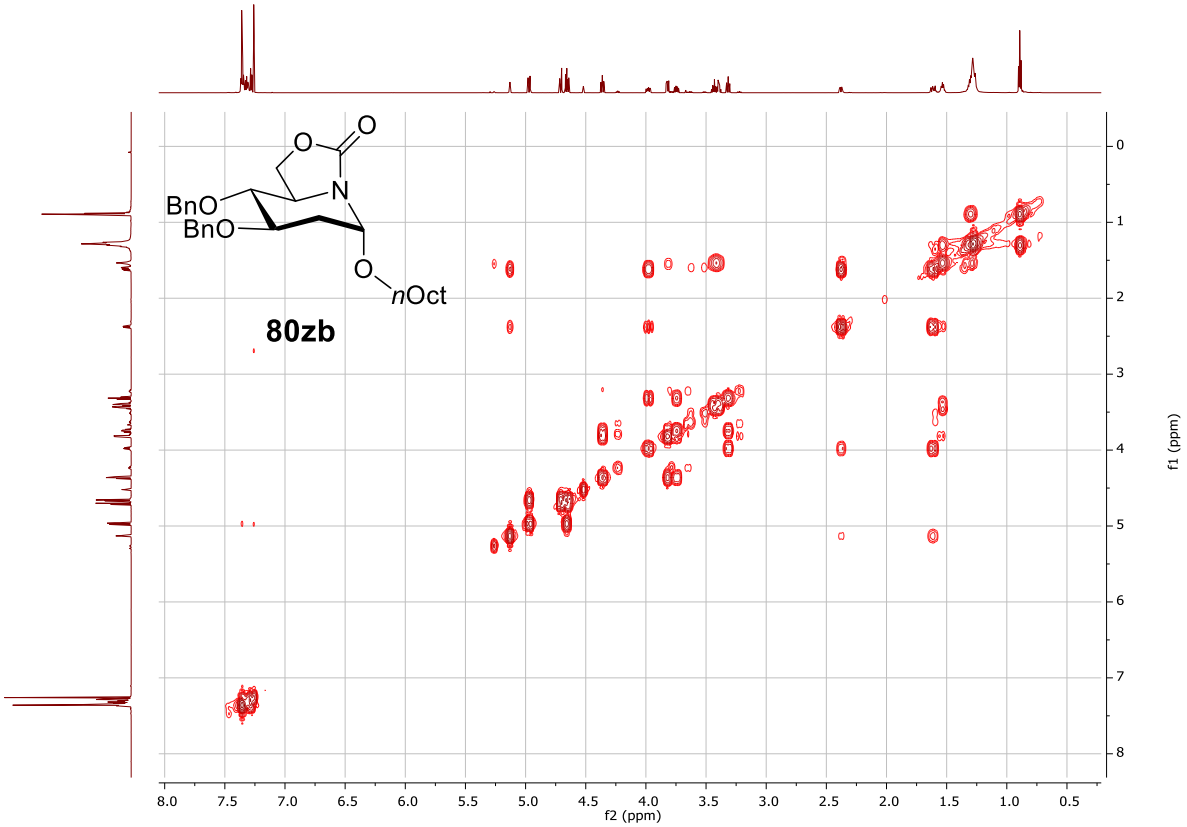

Figure 8.297. COSY spectra for 80zb

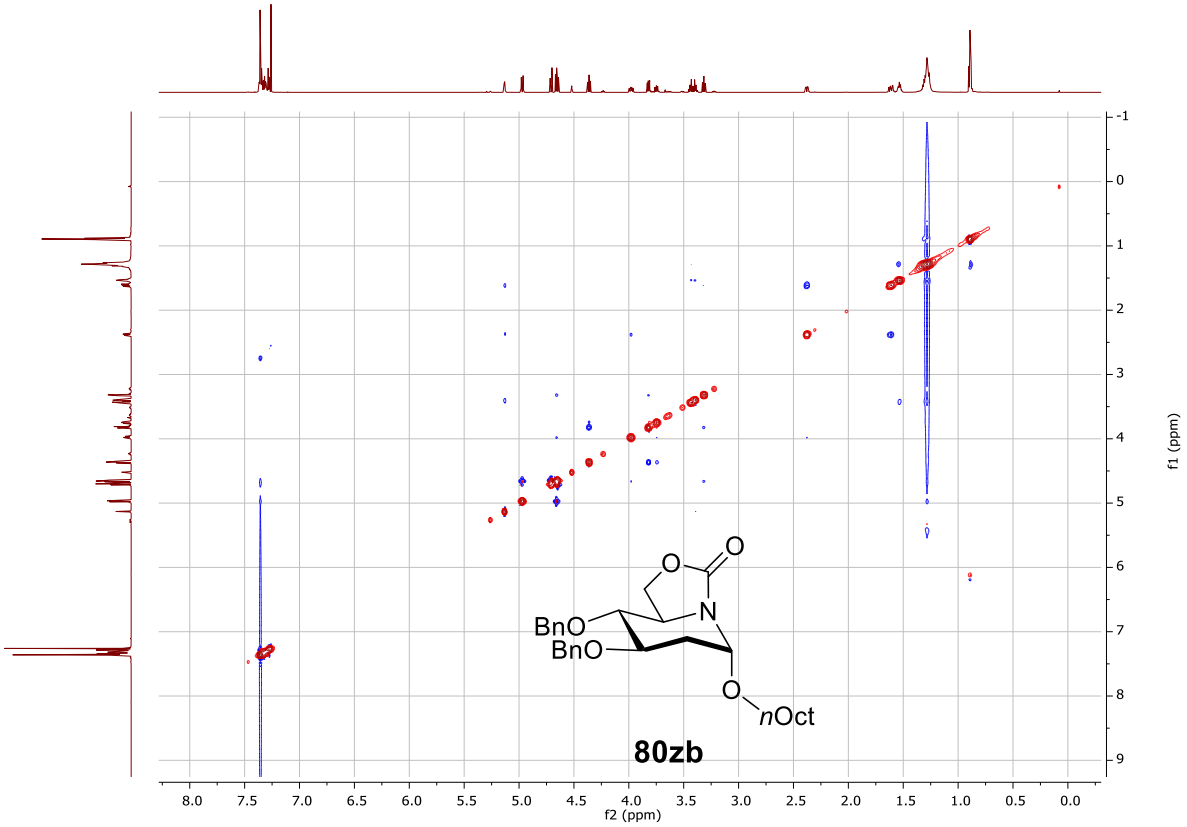

Figure 8.298. NOESY spectra for 80zb

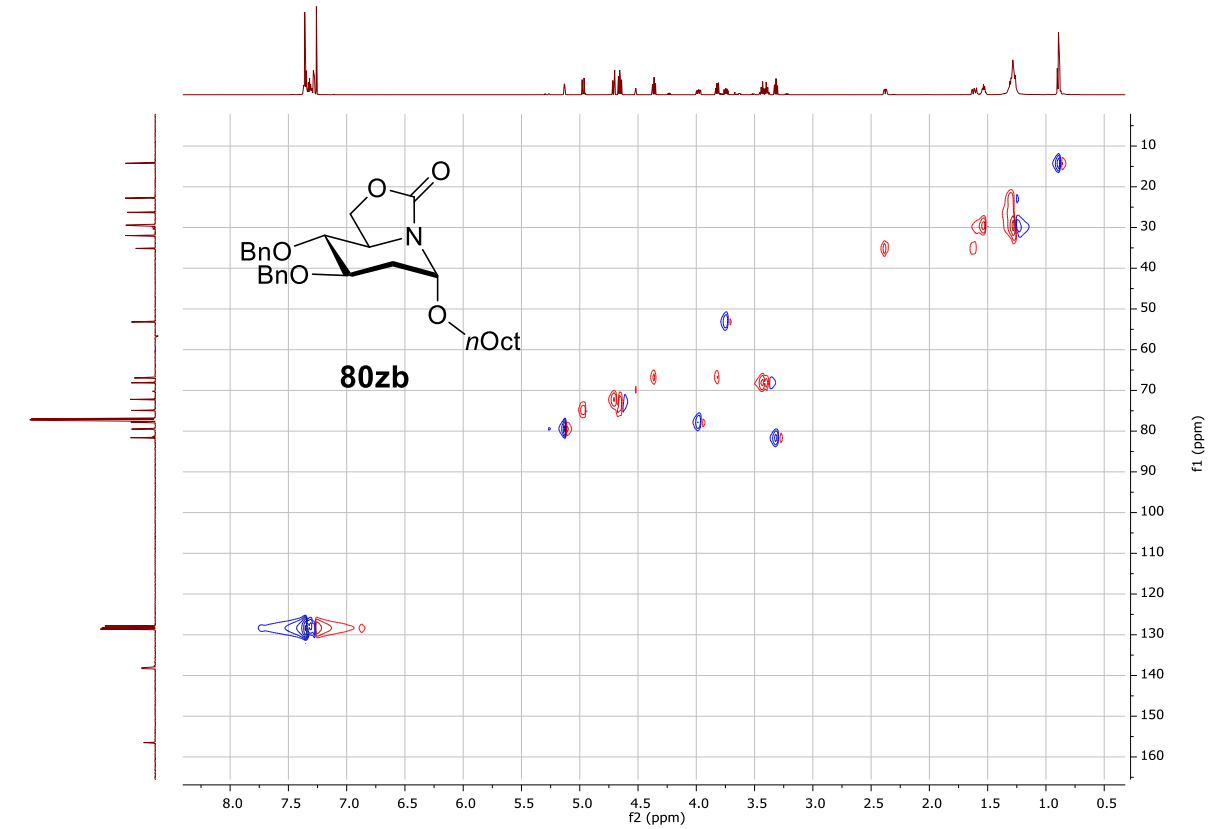

Figure 8.299. HSQC spectra for 80zb

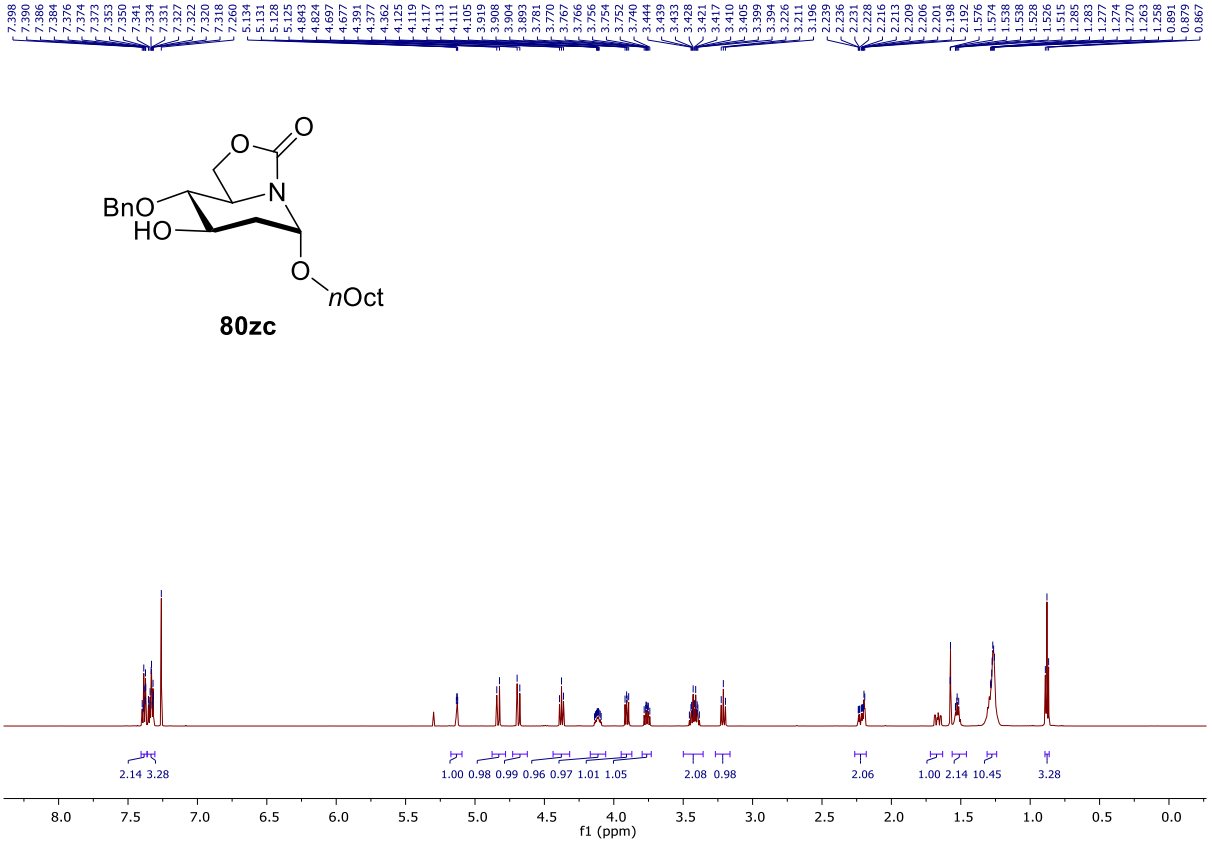

Figure 8.300. ^{1}H NMR spectra for 80zc

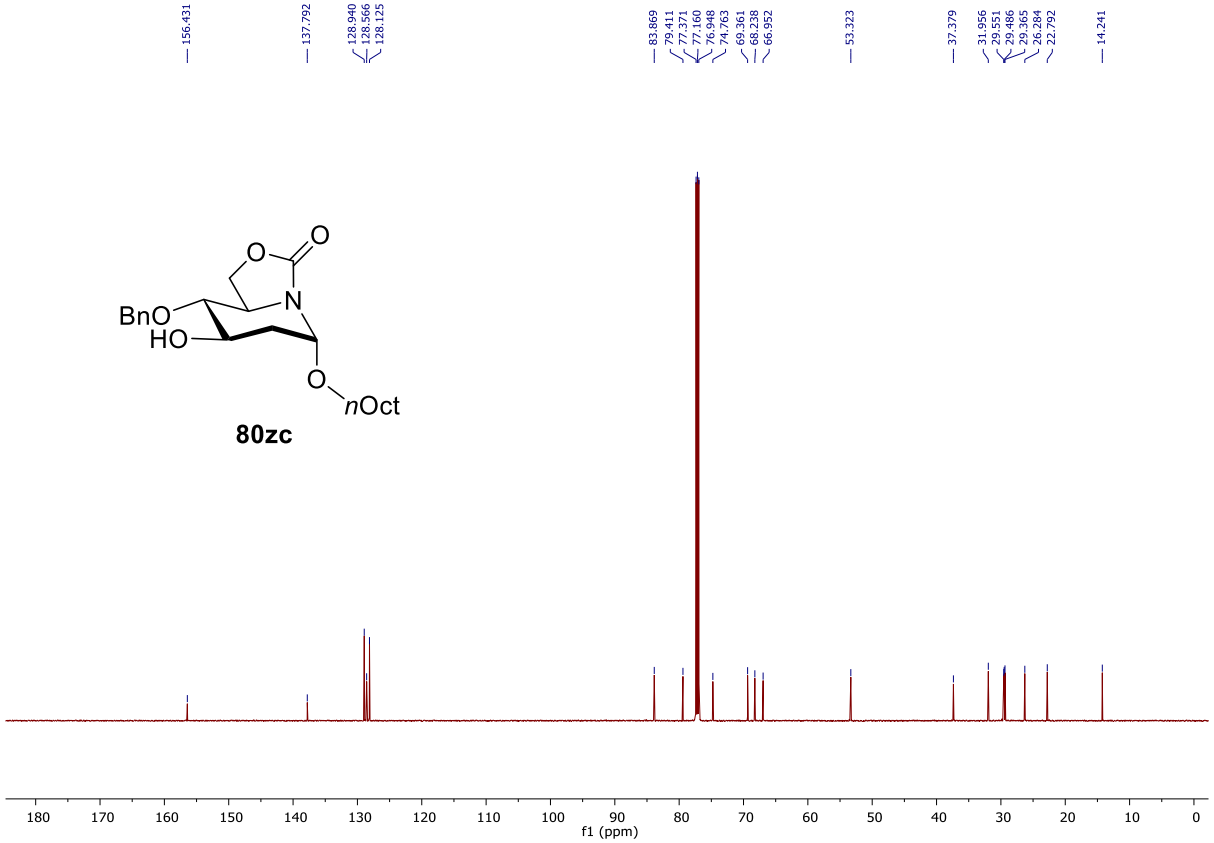

Figure 8.301. ^{13}C NMR spectra for 80zc

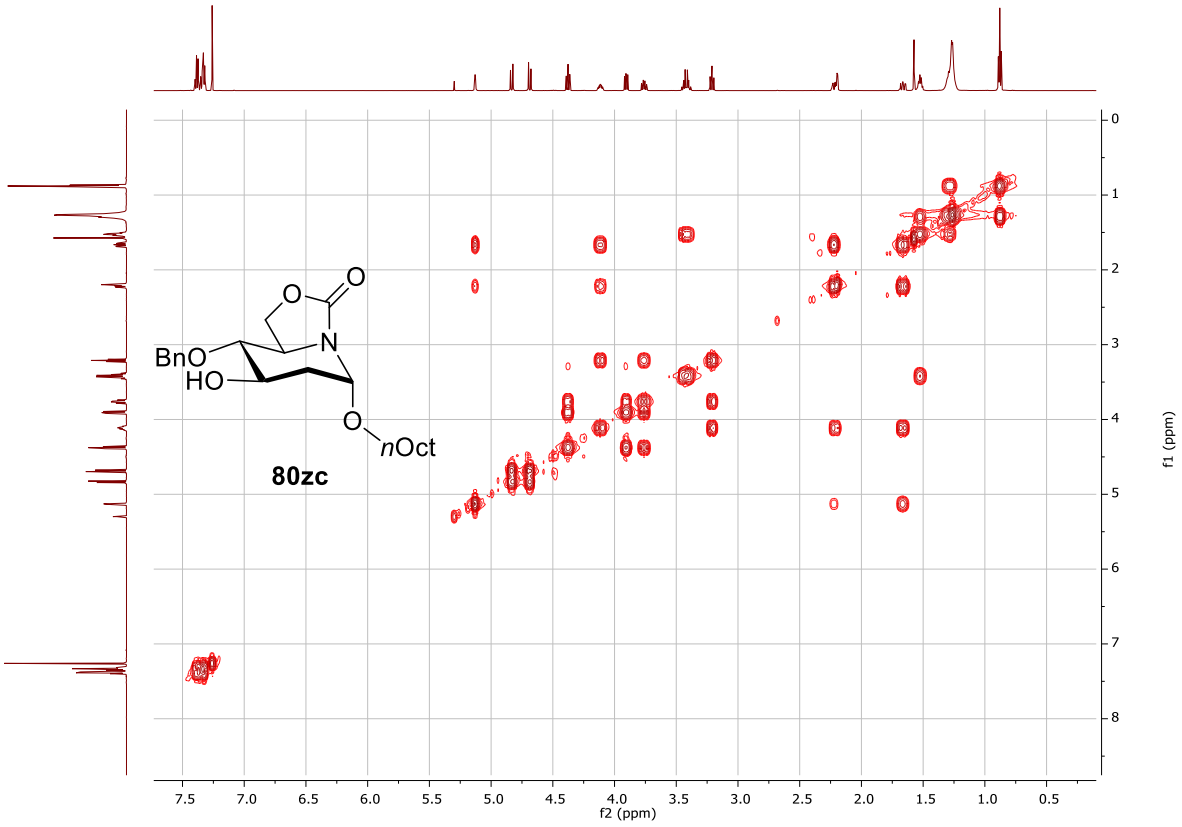

Figure 8.302. COSY spectra for 80zc

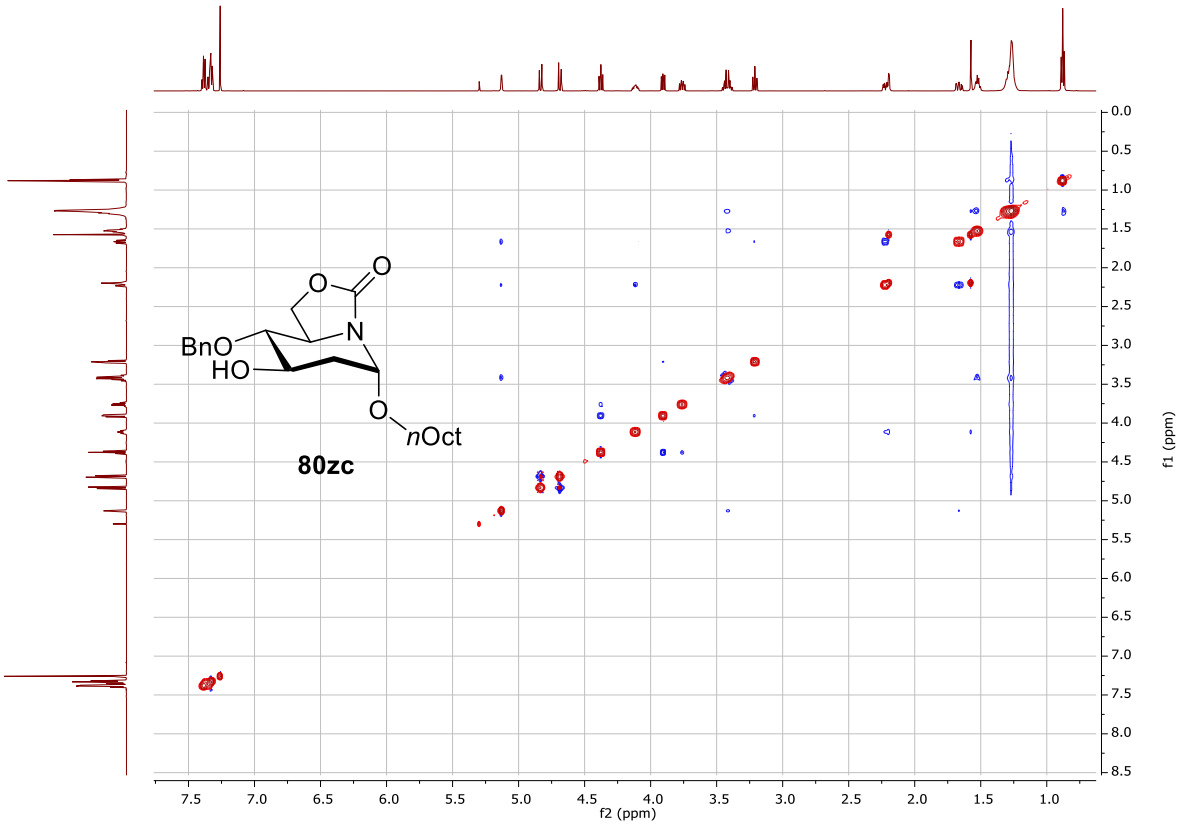

Figure 8.303. NOESY spectra for 80zc

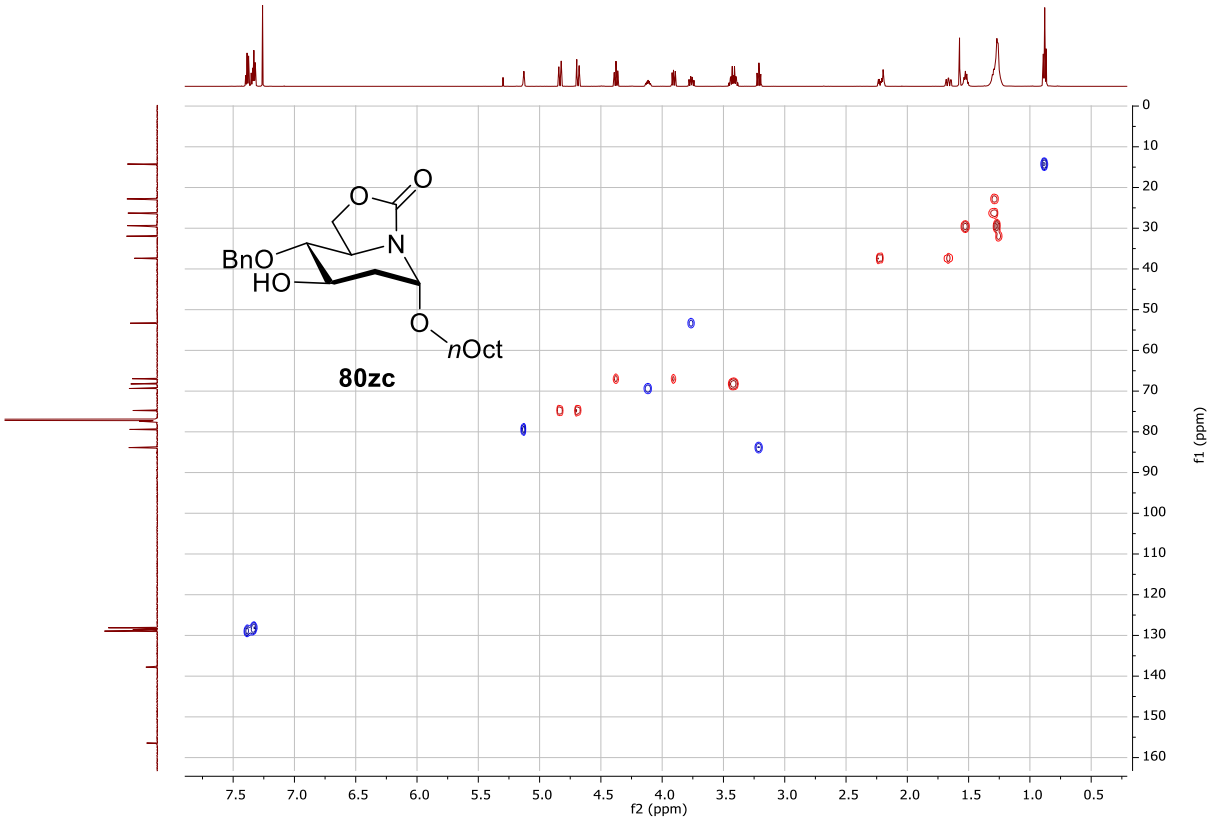

Figure 8.304. HSQC spectra for 80zc

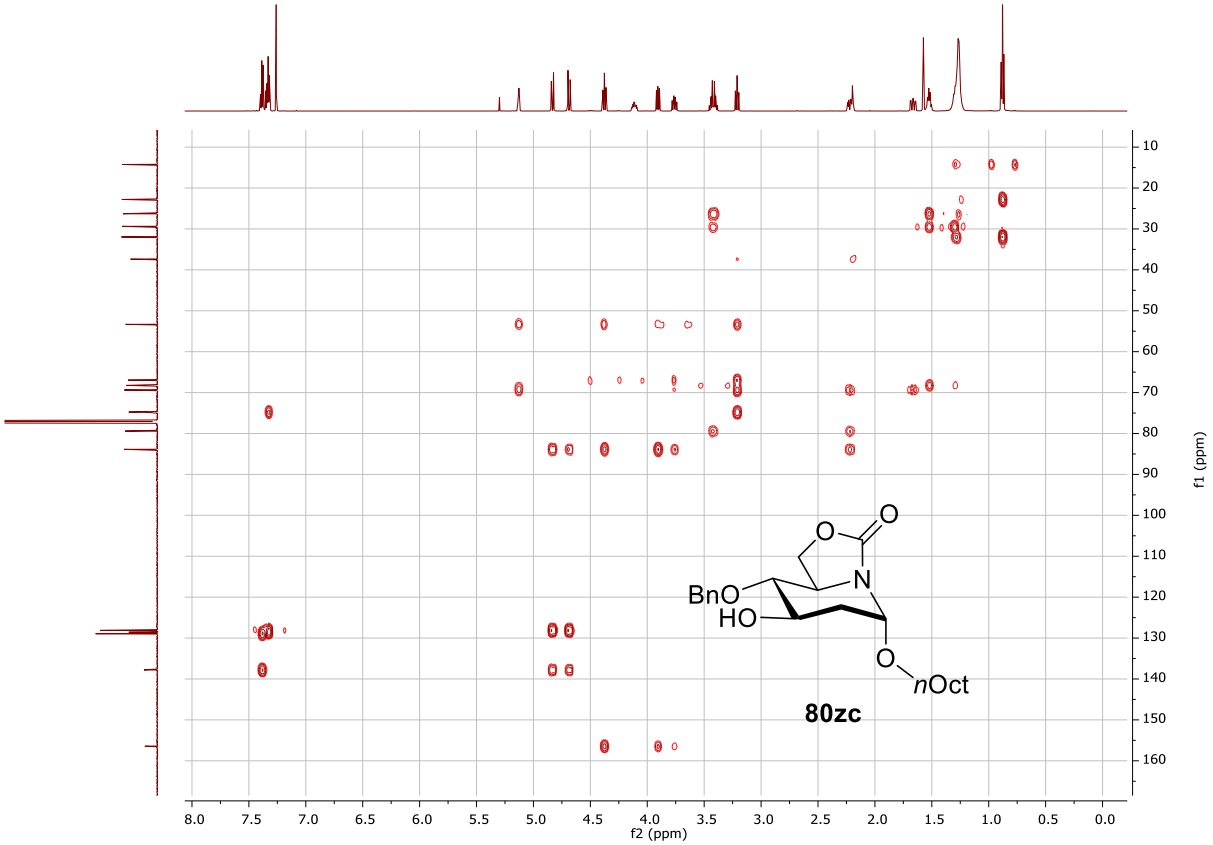

Figure 8.305. HMBC spectra for 80zc

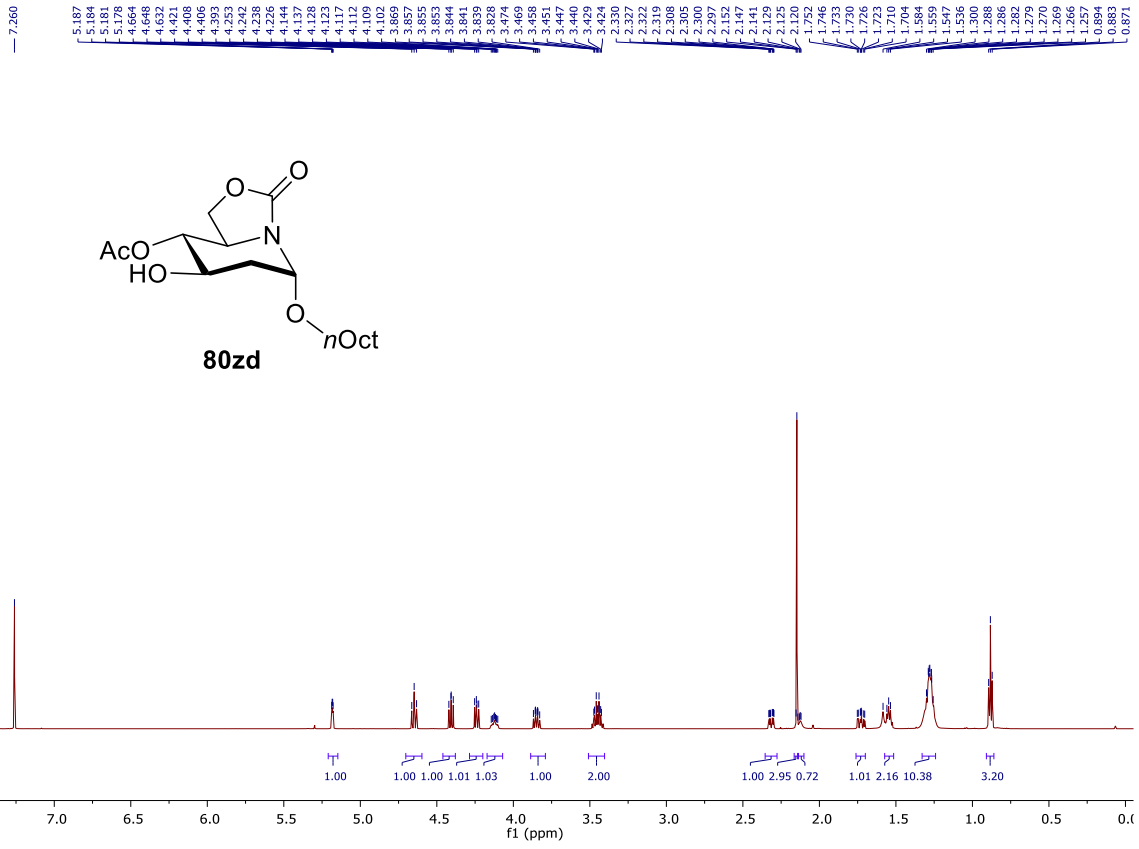

Figure 8.306. ^{1}H NMR spectra for 80zd

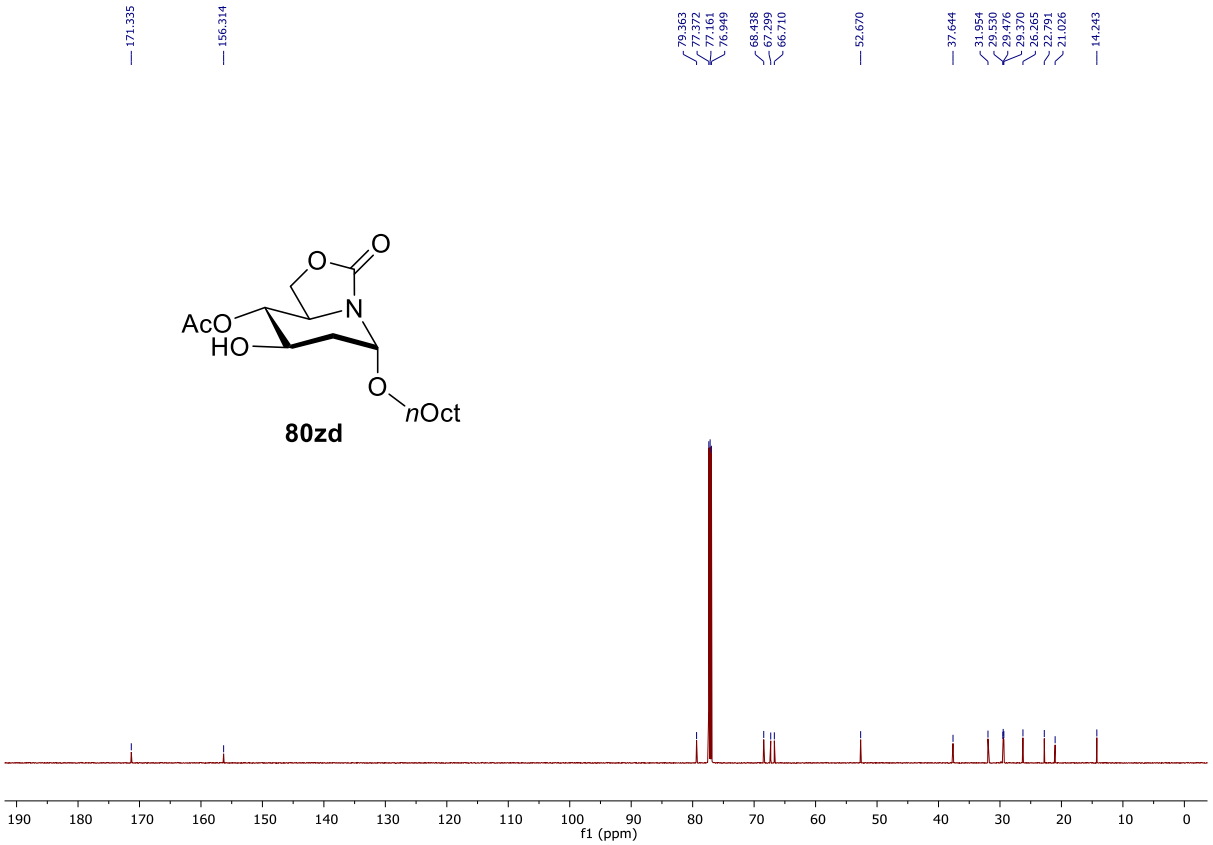

Figure 8.307. ^{13}C NMR spectra for 80zd

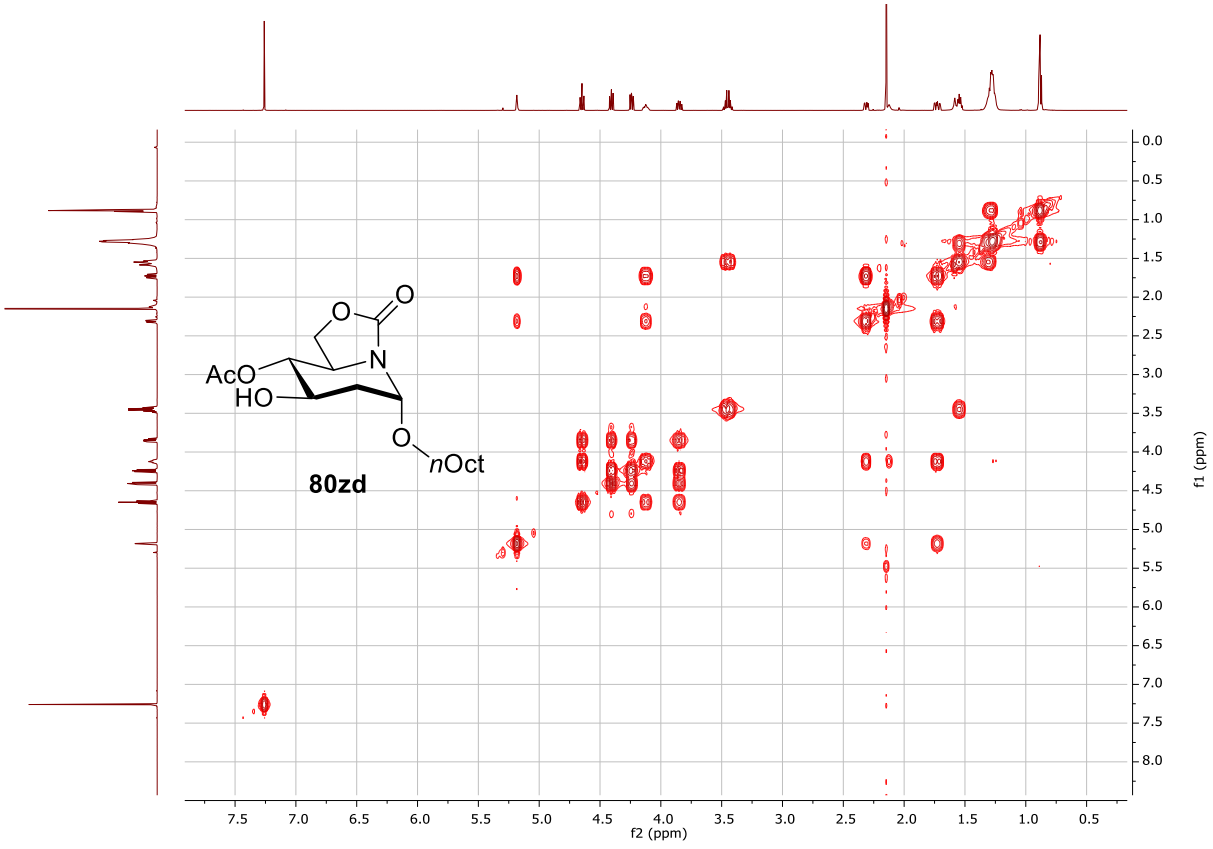

Figure 8.308. COSY spectra for 80zd

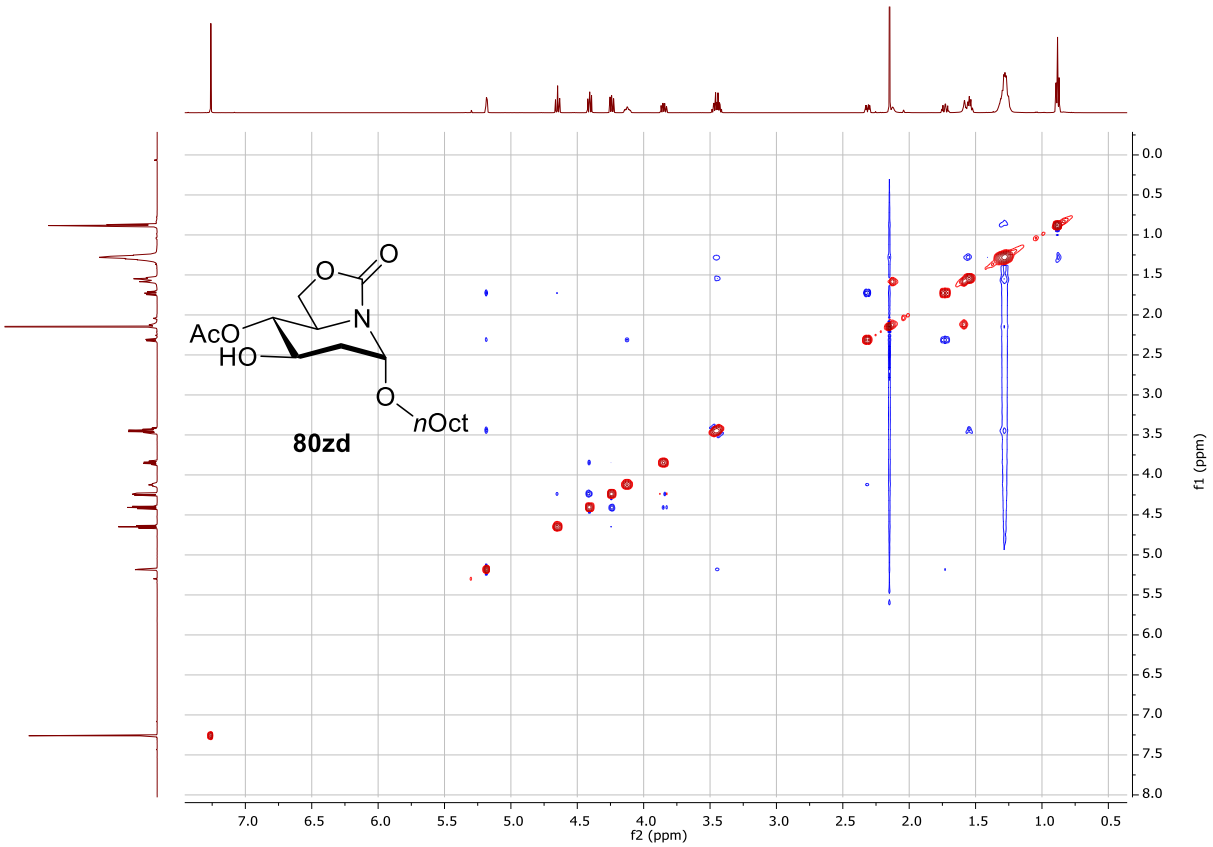

Figure 8.309. NOESY spectra for 80zd

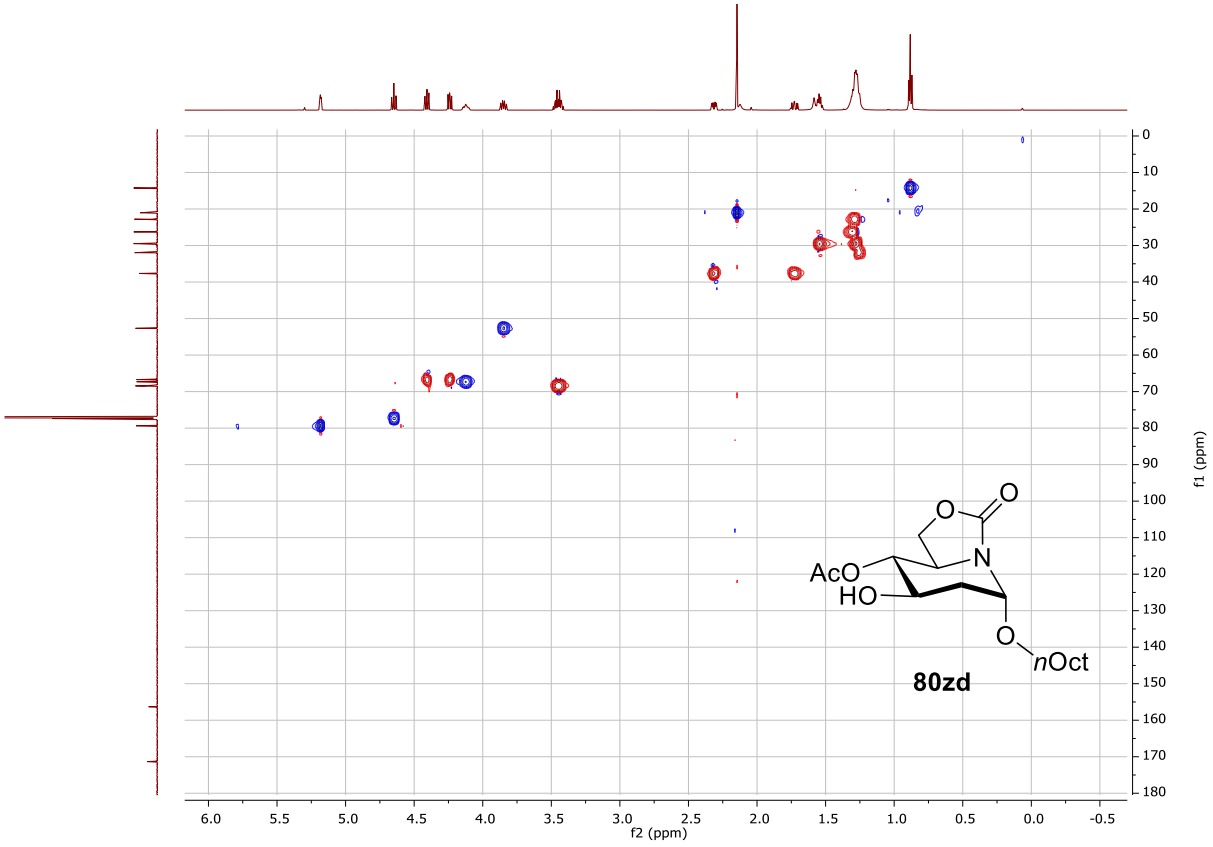

Figure 8.310. HSQC spectra for 80zd

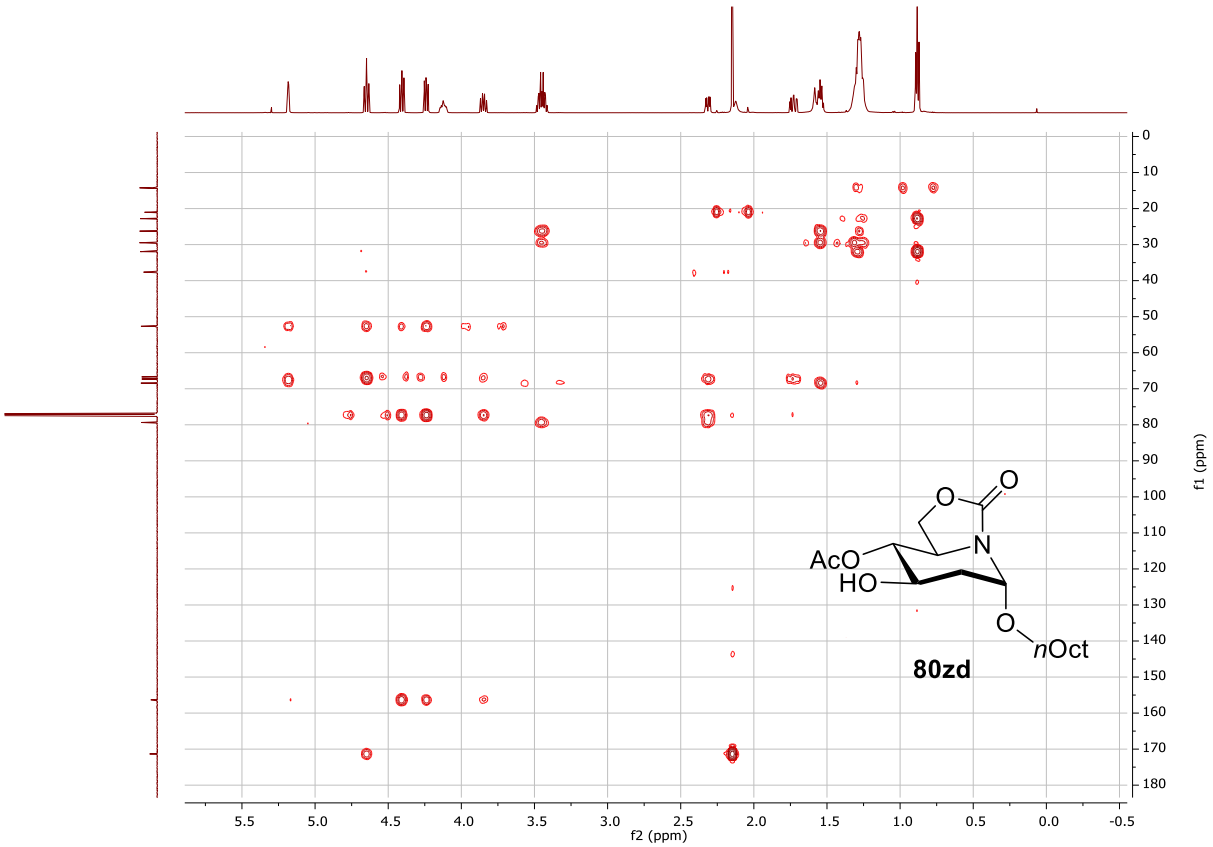

Figure 8.311. HMBC spectra for 80zd

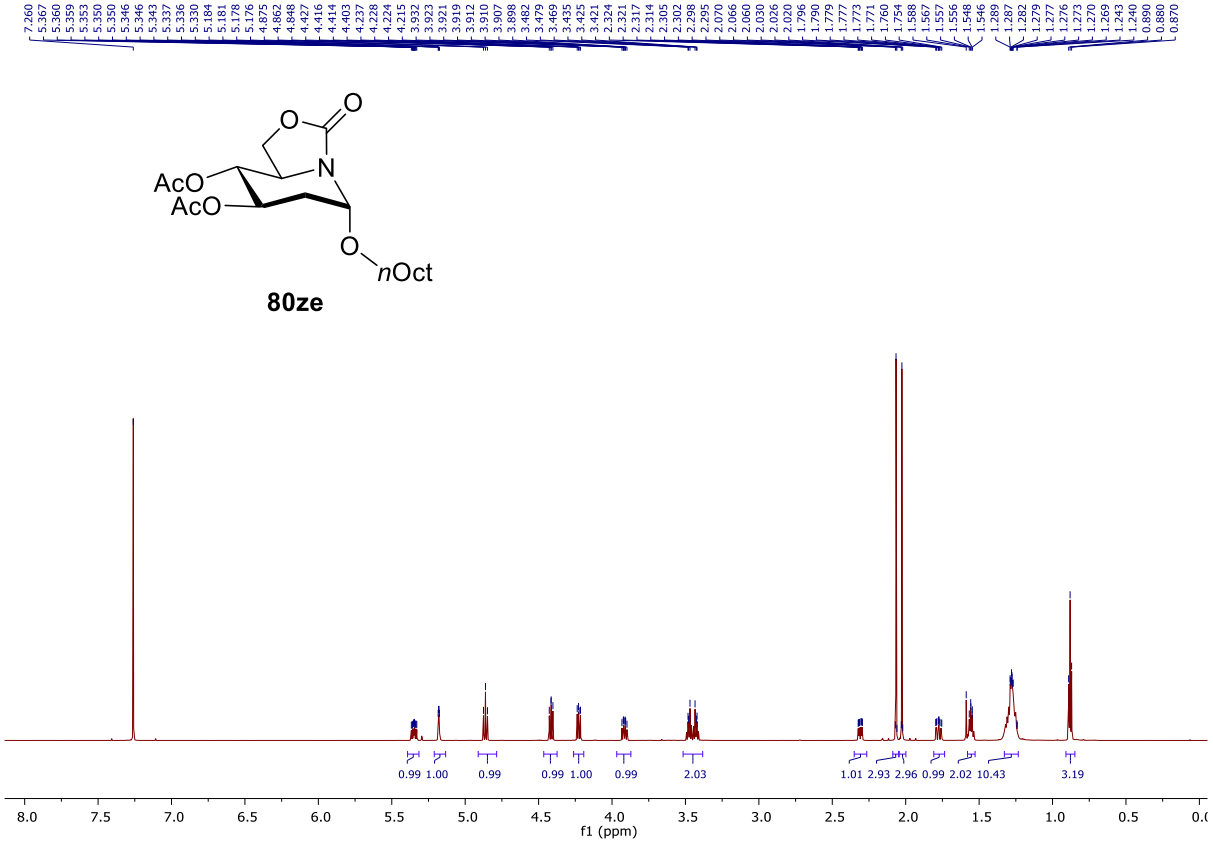

Figure 8.312. ^{1}H NMR spectra for 80ze

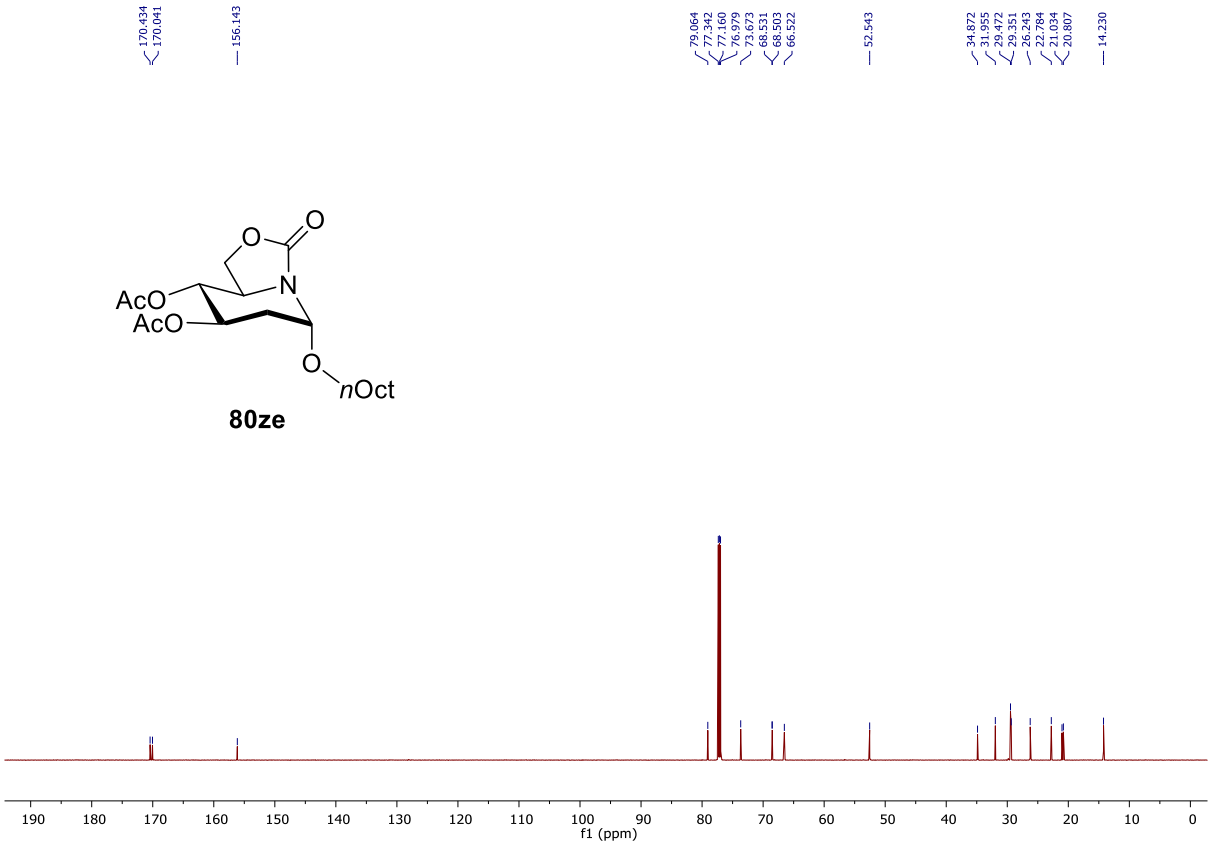

Figure 8.313. ^{13}C NMR spectra for 80ze

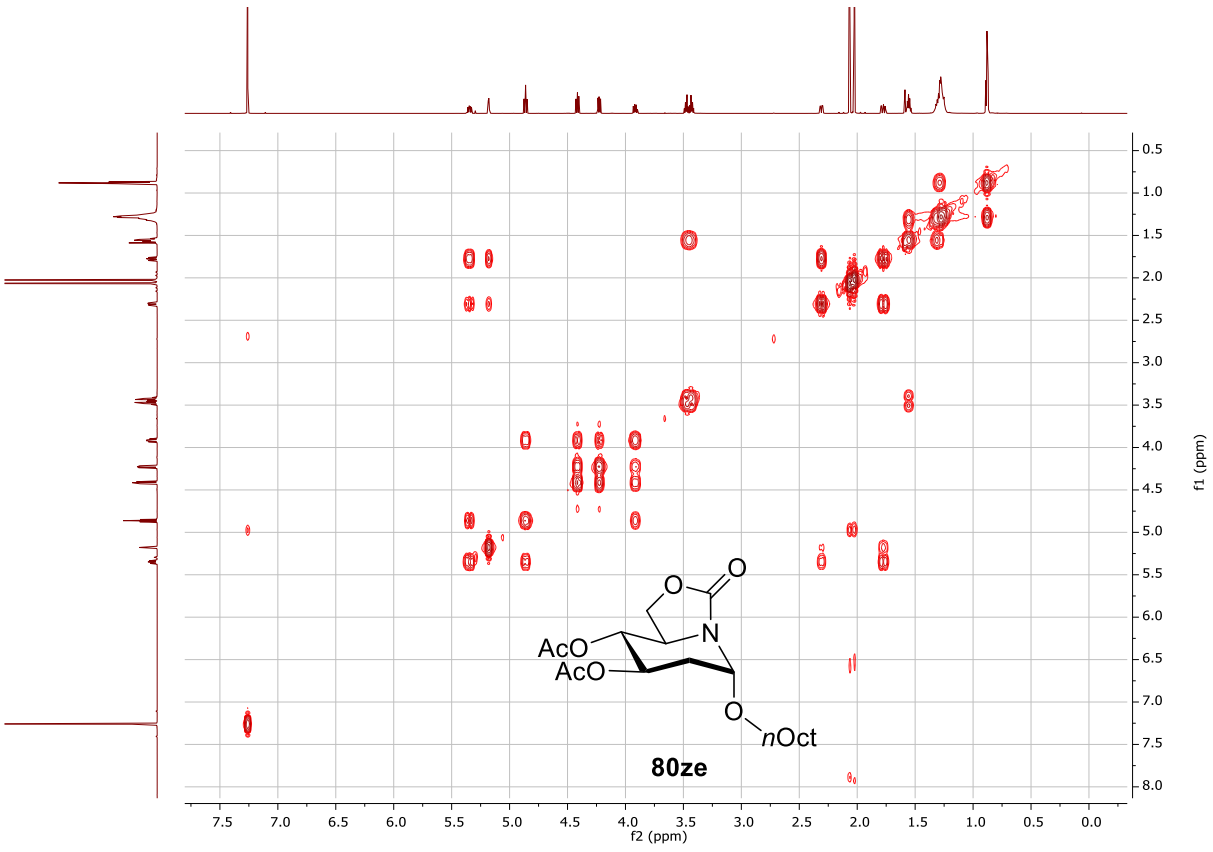

Figure 8.314. COSY spectra for 80ze

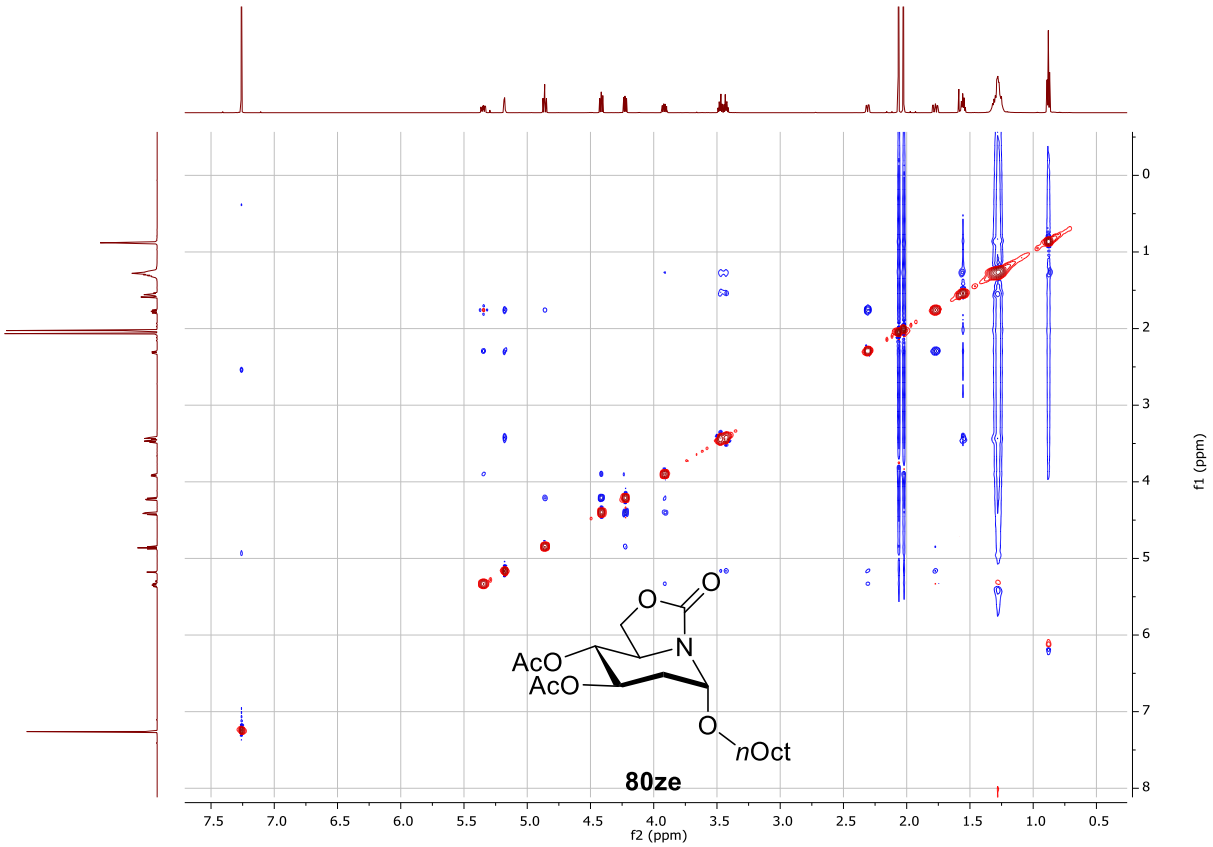

Figure 8.315. NOESY spectra for 80ze

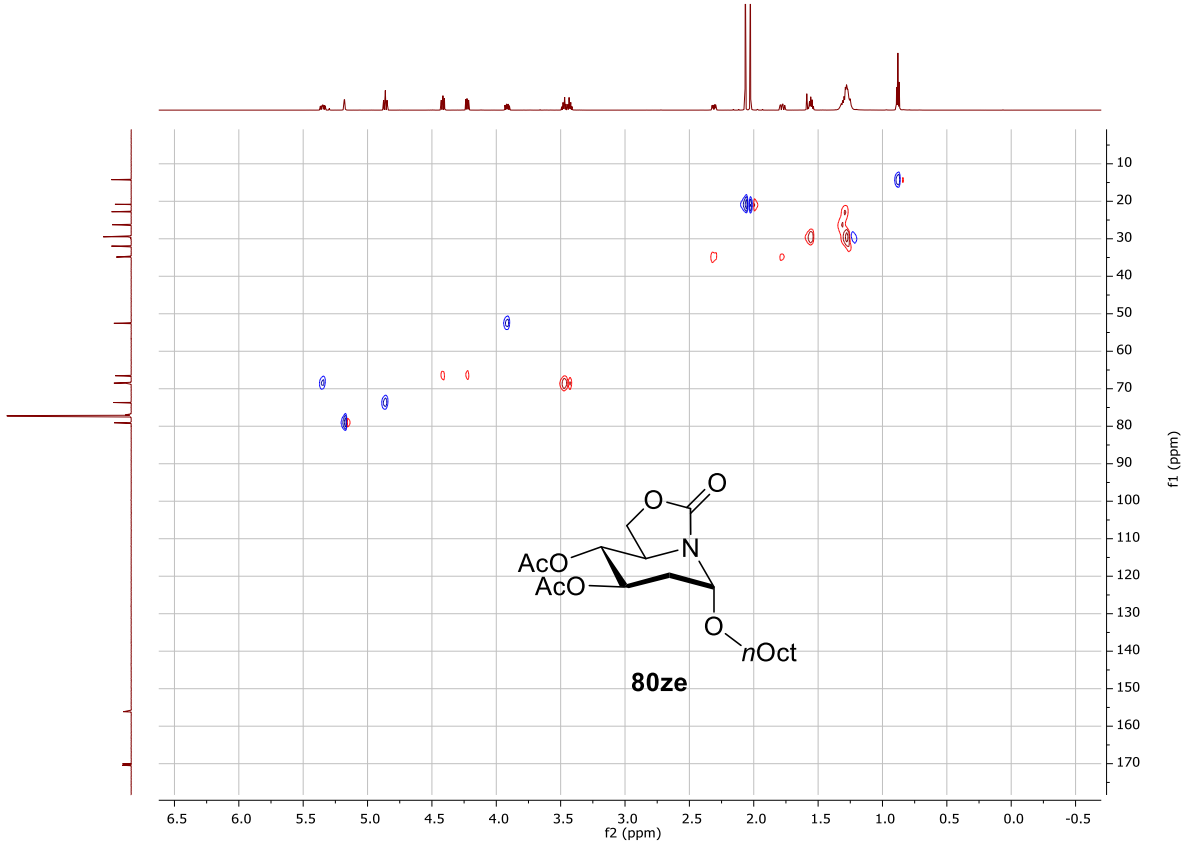

Figure 8.316. HSQC spectra for 80ze

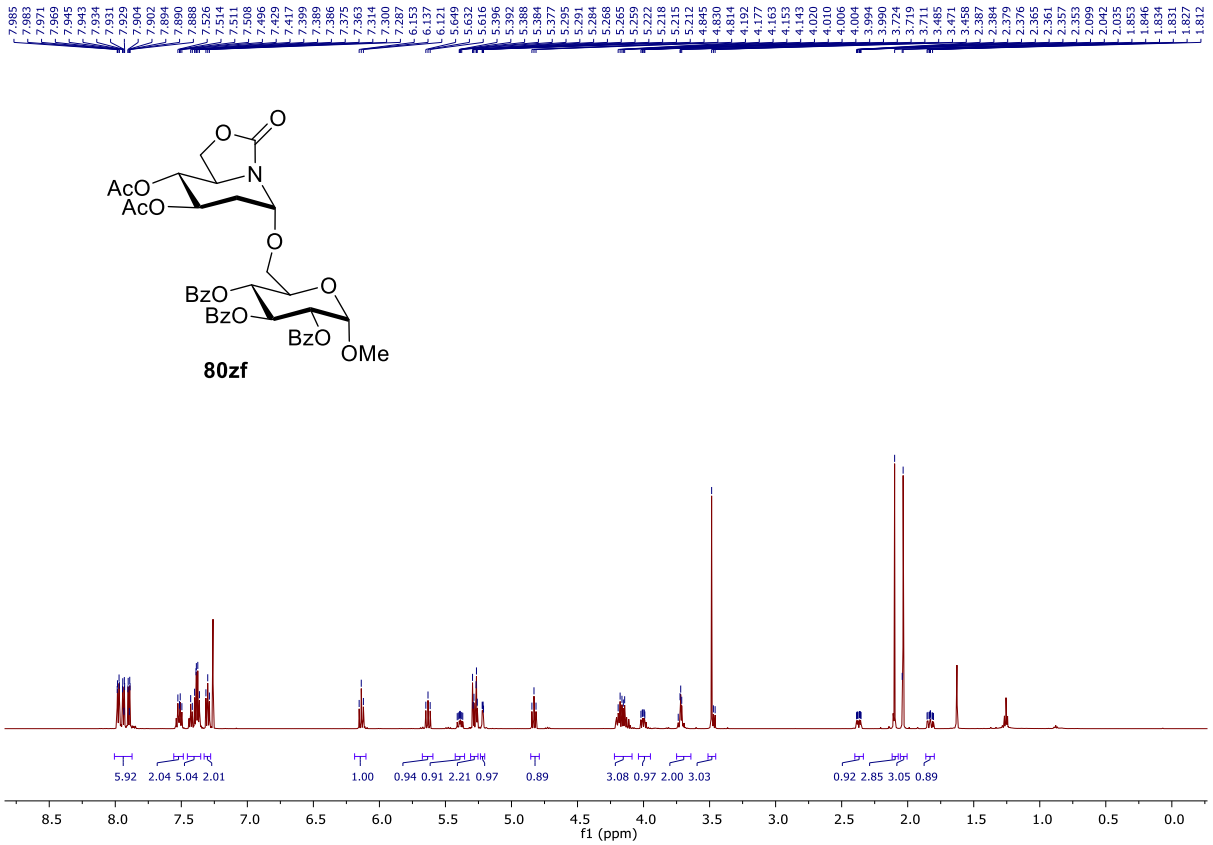

Figure 8.317. ^{1}H NMR spectra for 80zf

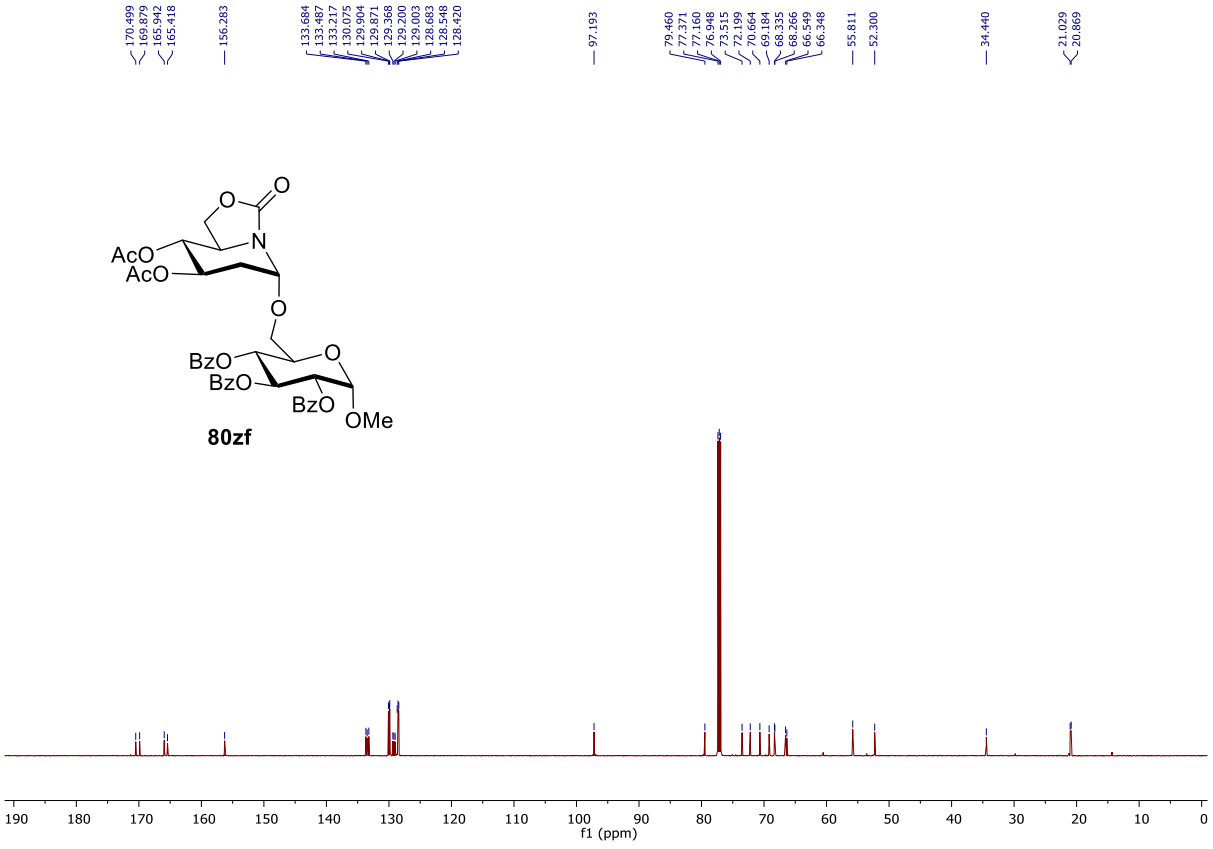

Figure 8.318. ^{13}C NMR spectra for 80zf

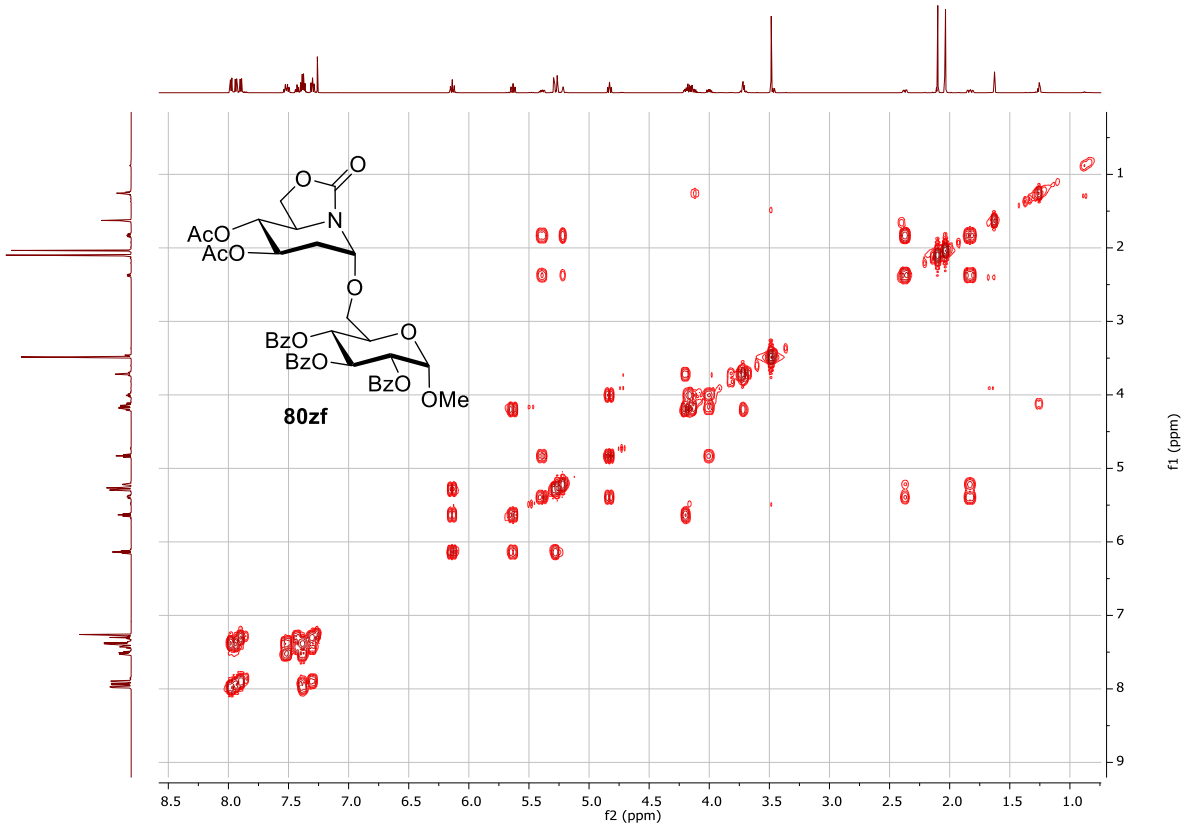

Figure 8.319. COSY spectra for 80zf

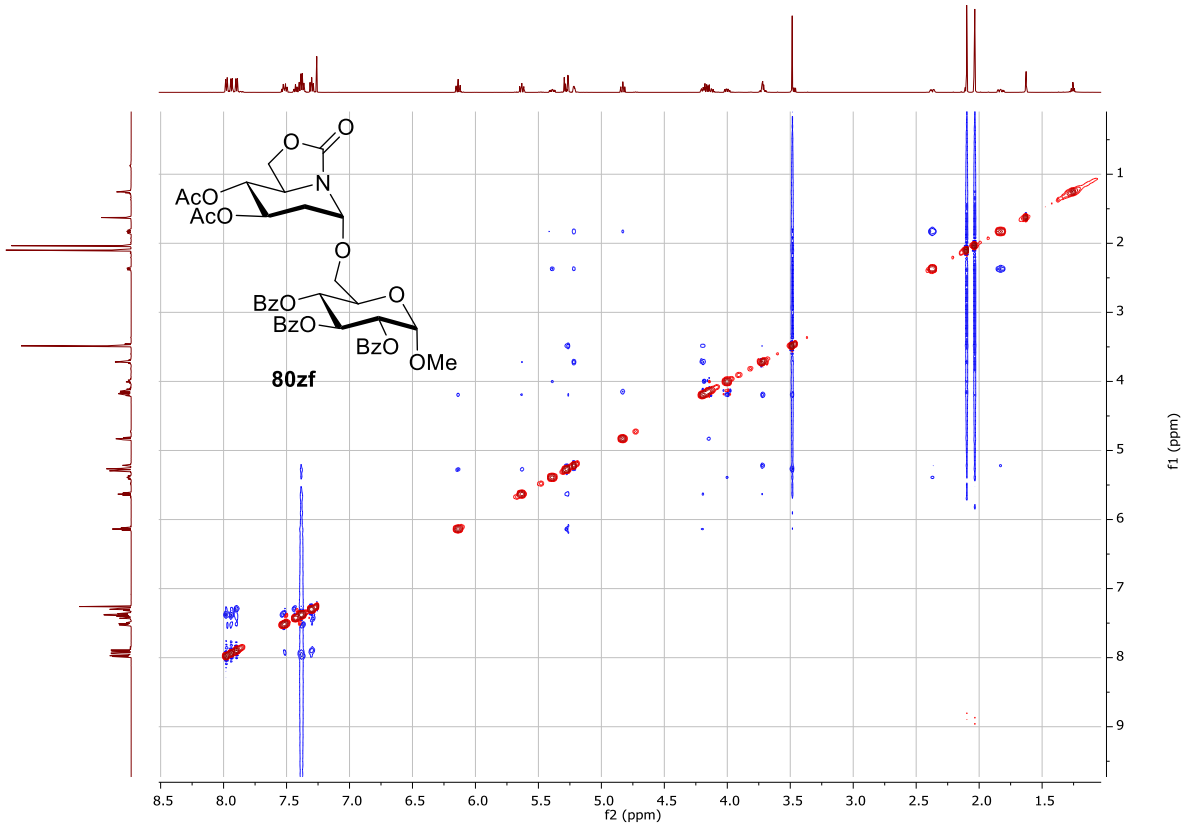

Figure 8.320. NOESY spectra for 80zf

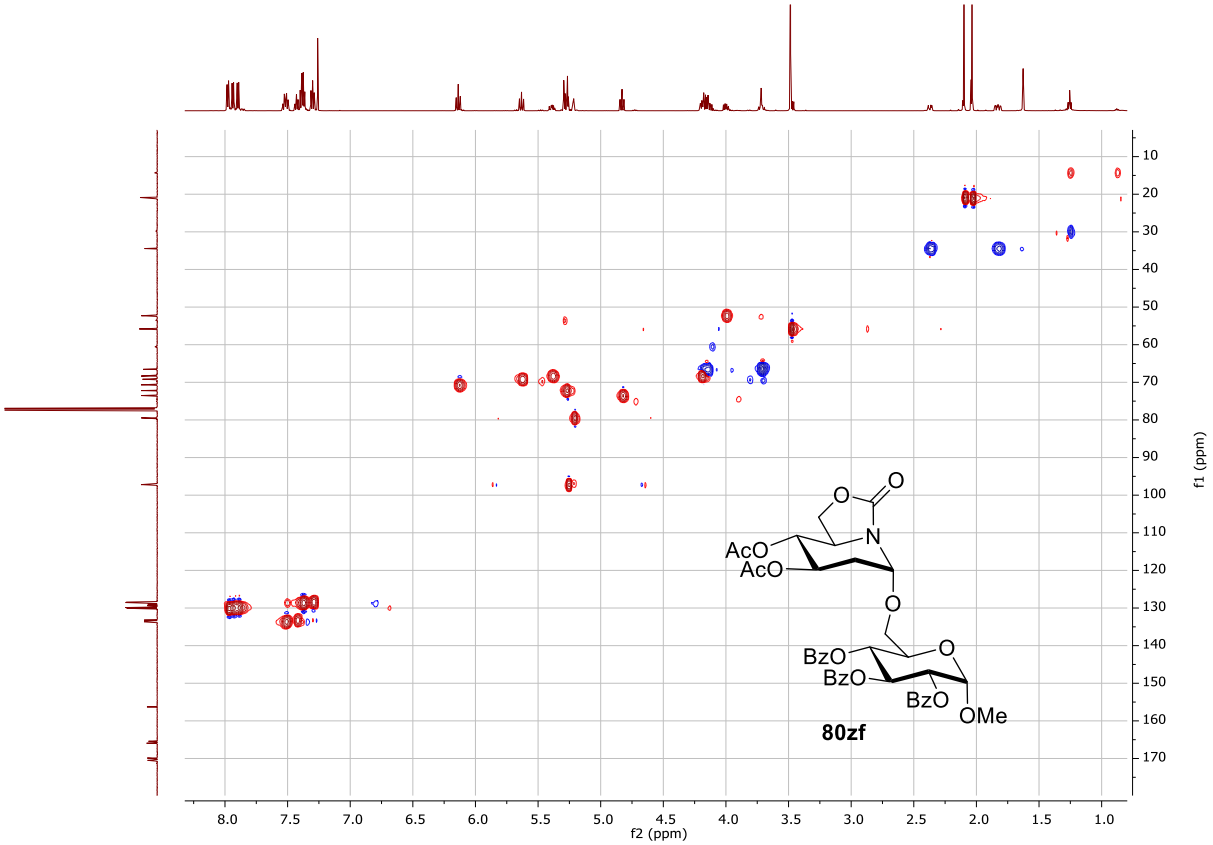

Figure 8.321. HSQC spectra for 80zf

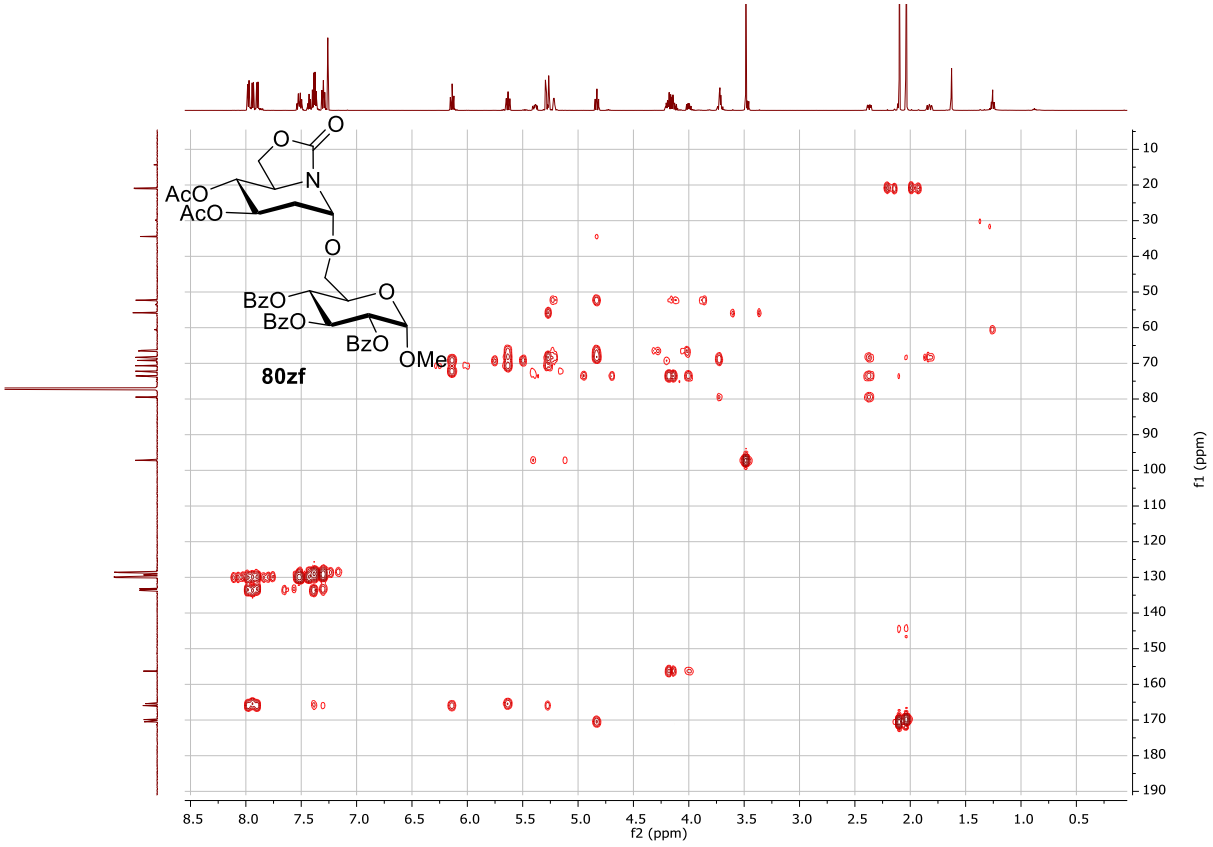

Figure 8.322. HMBC spectra for 80zf

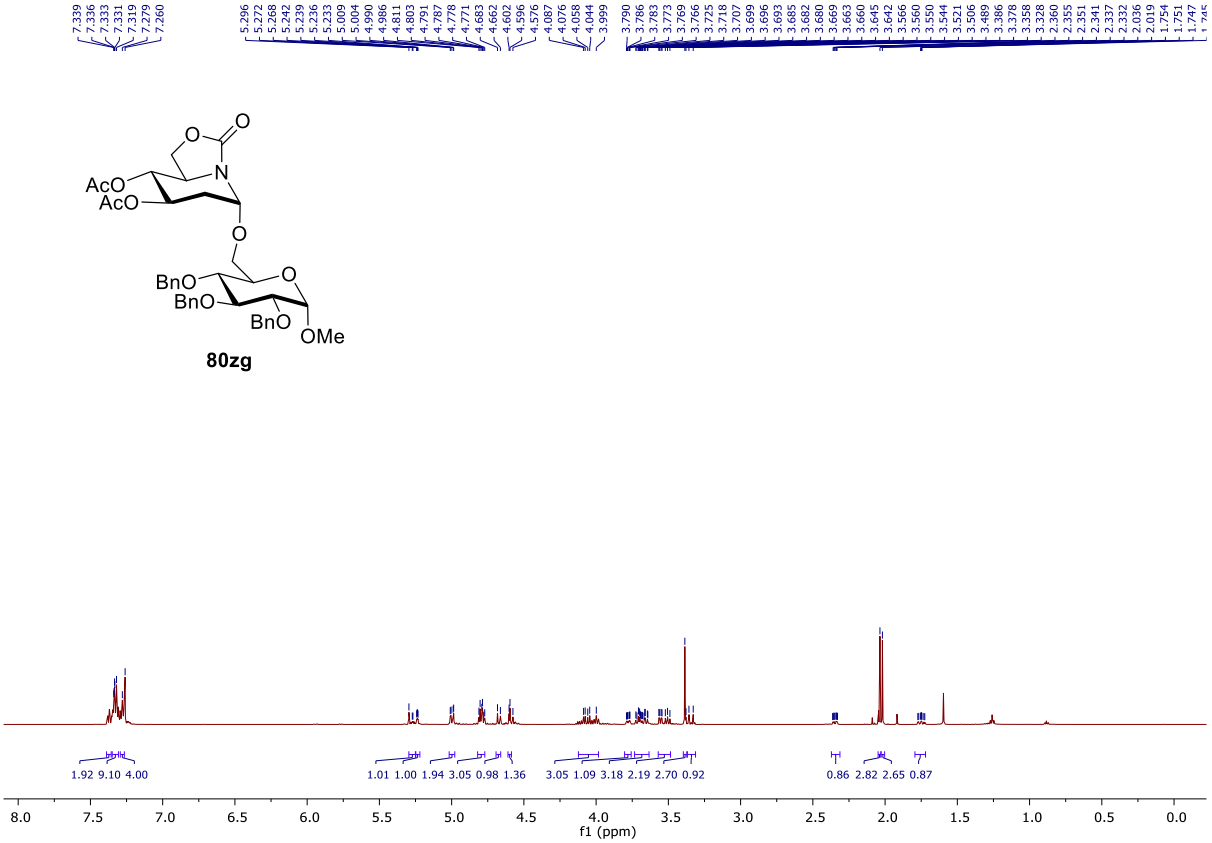

Figure 8.323. ^{1}H NMR spectra for 80zg

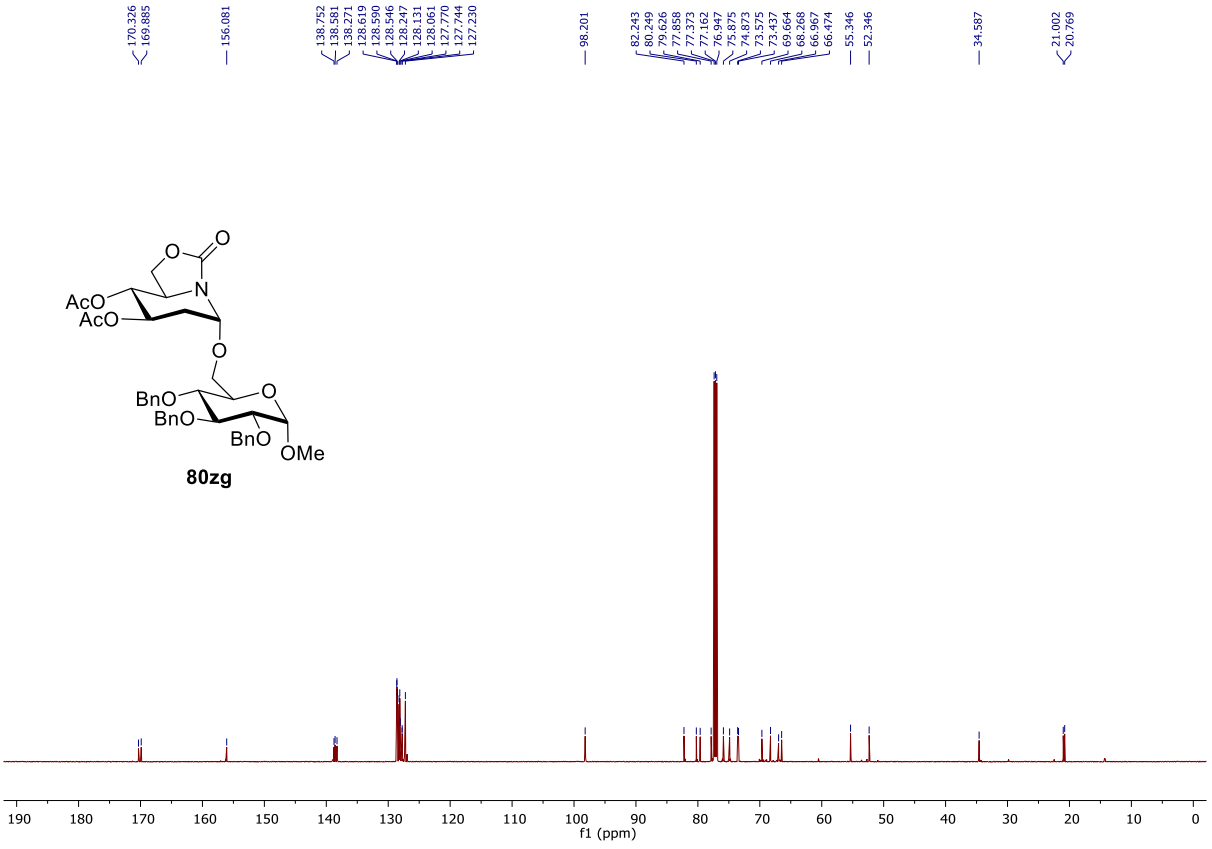

Figure 8.324. ^{13}C NMR spectra for 80zg

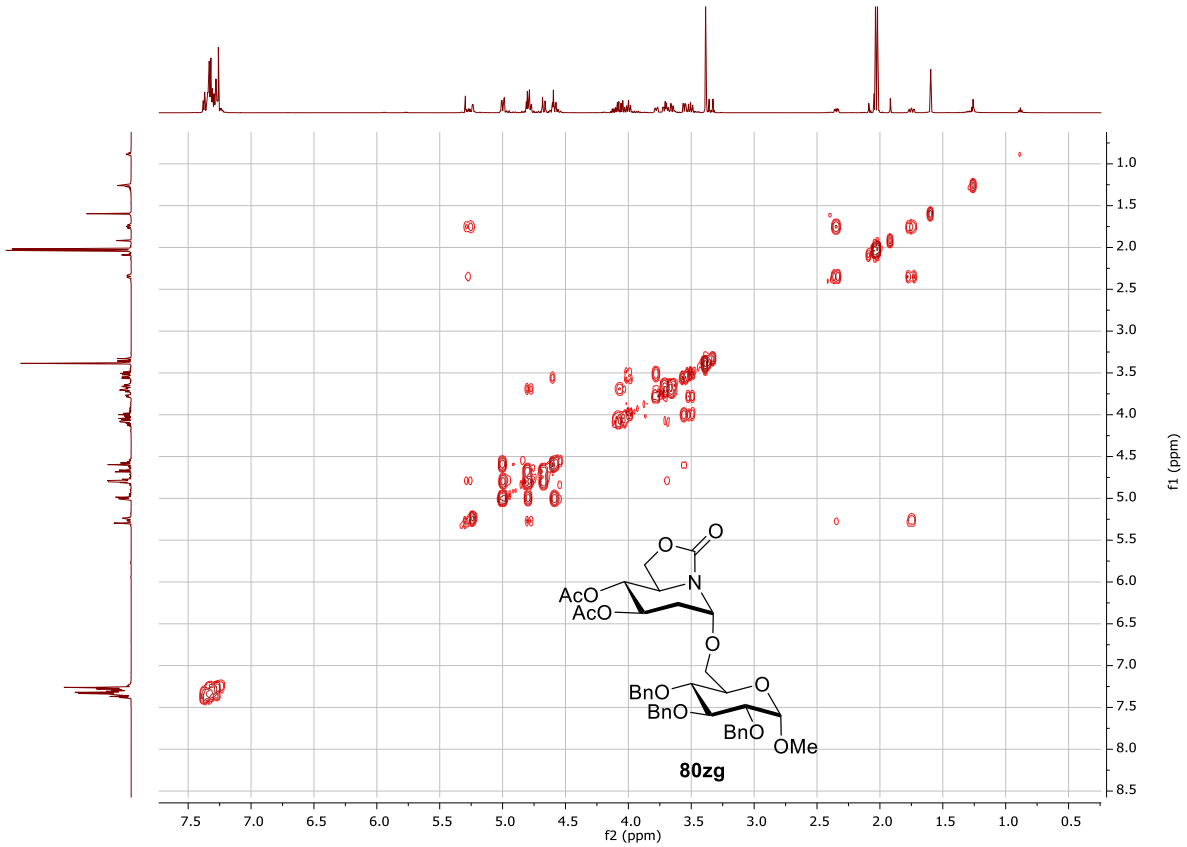

Figure 8.325. COSY spectra for 80zg

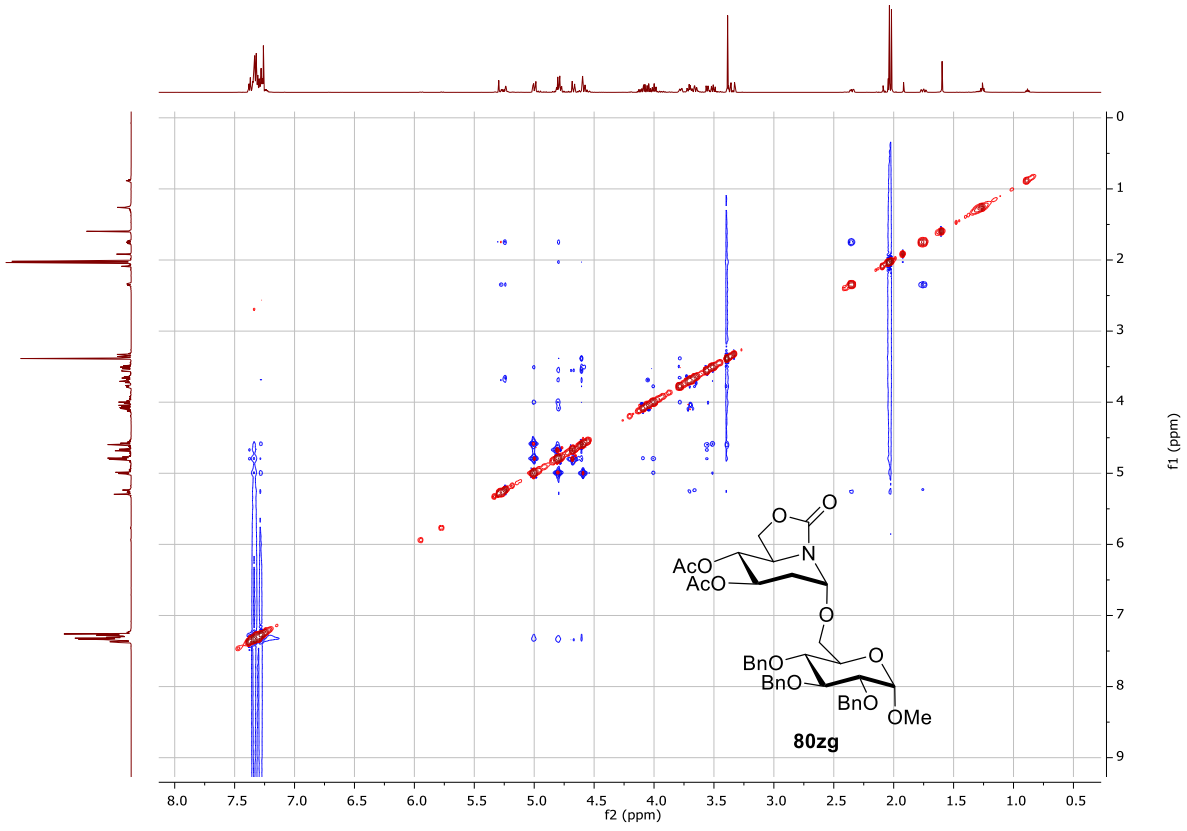

Figure 8.326. NOESY spectra for 80zg

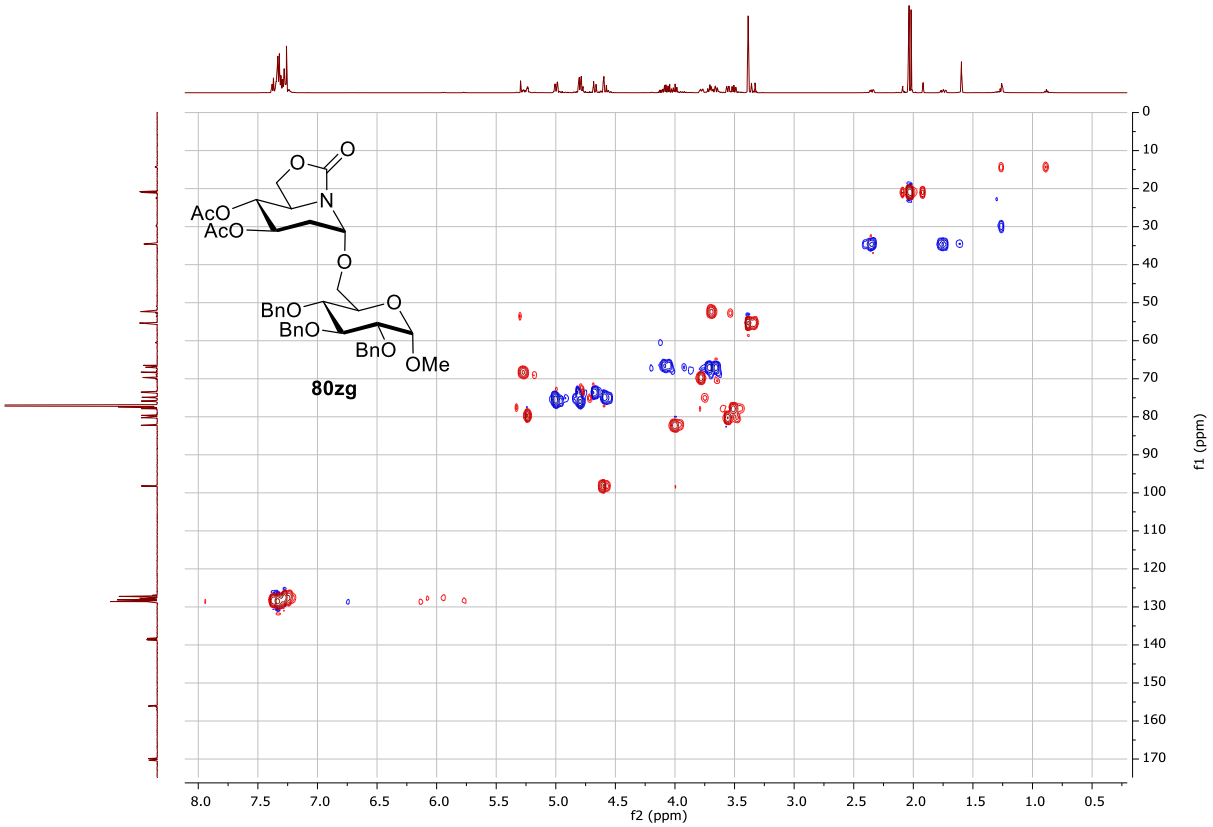

Figure 8.327. HSQC spectra for 80zg

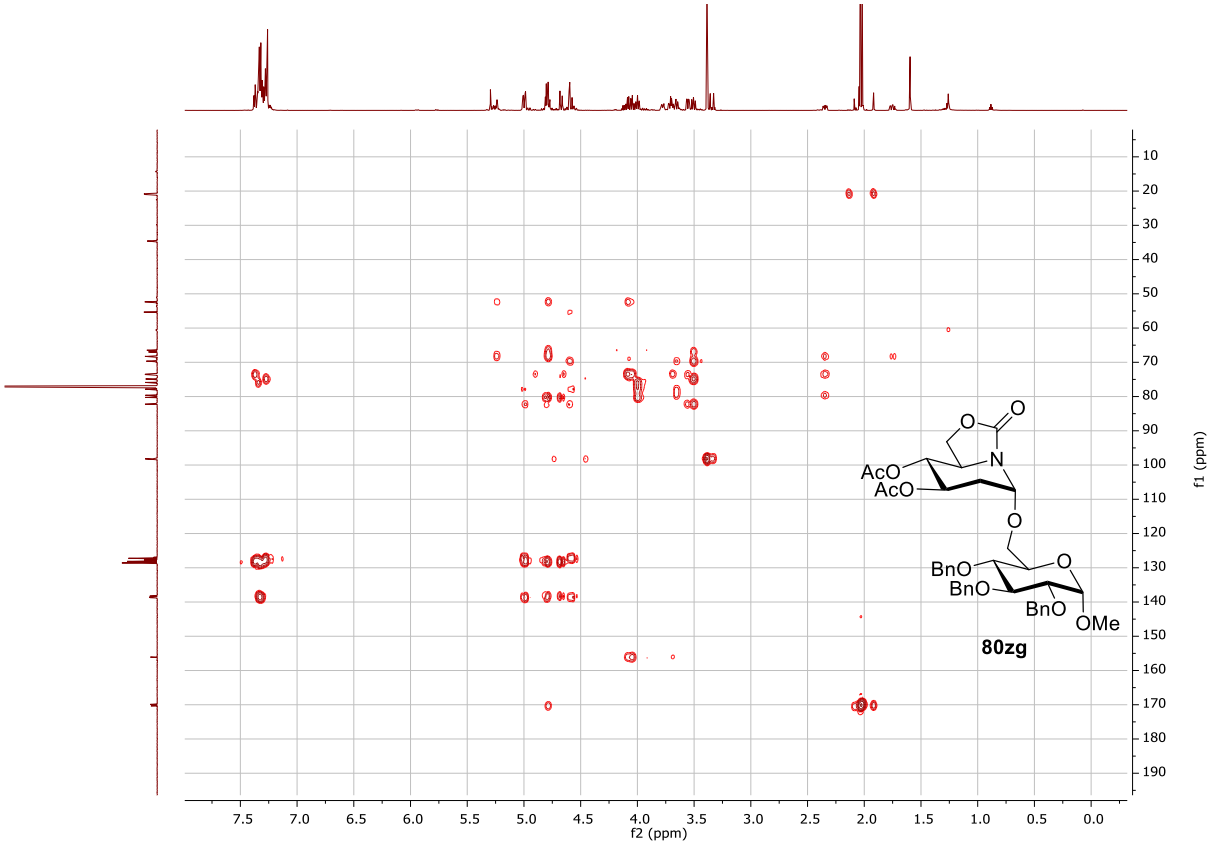

Figure 8.328. HMBC spectra for 80zg

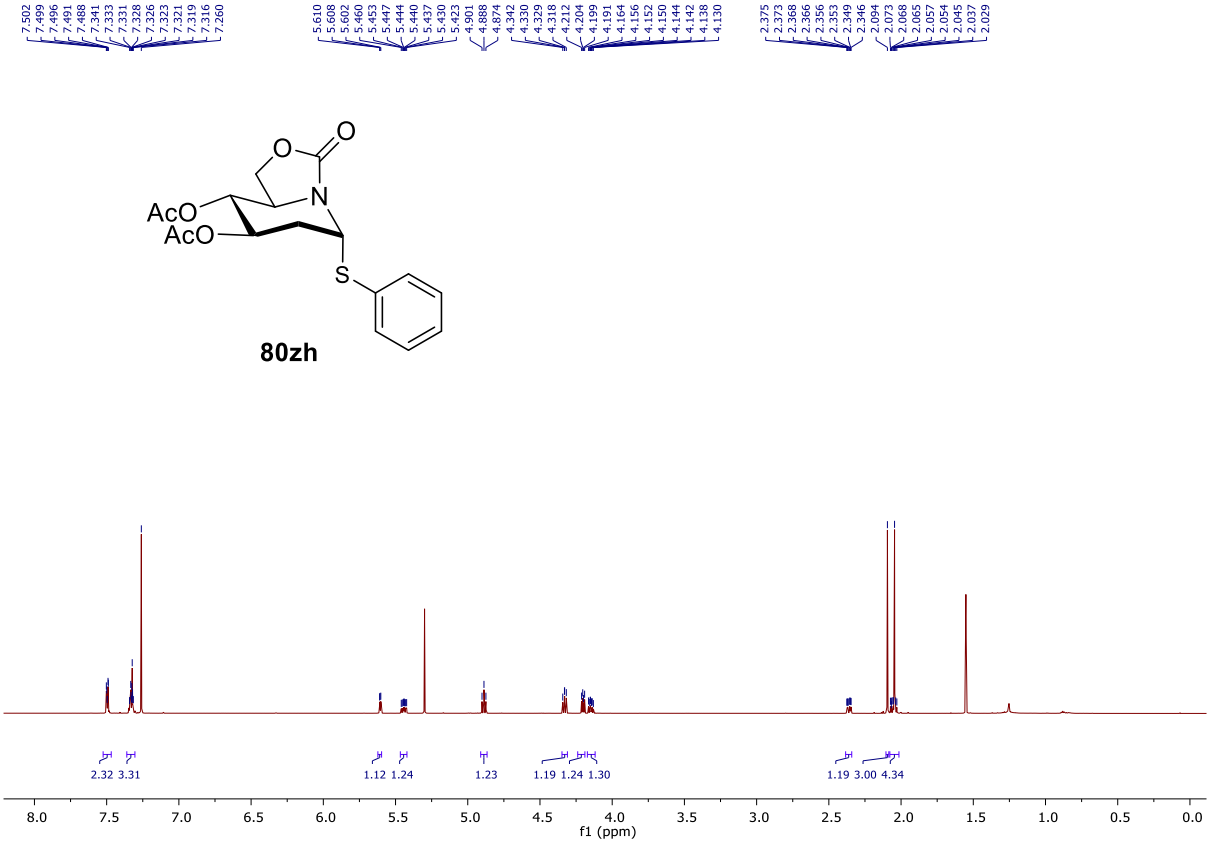

Figure 8.329. ^{1}H NMR spectra for 80zh

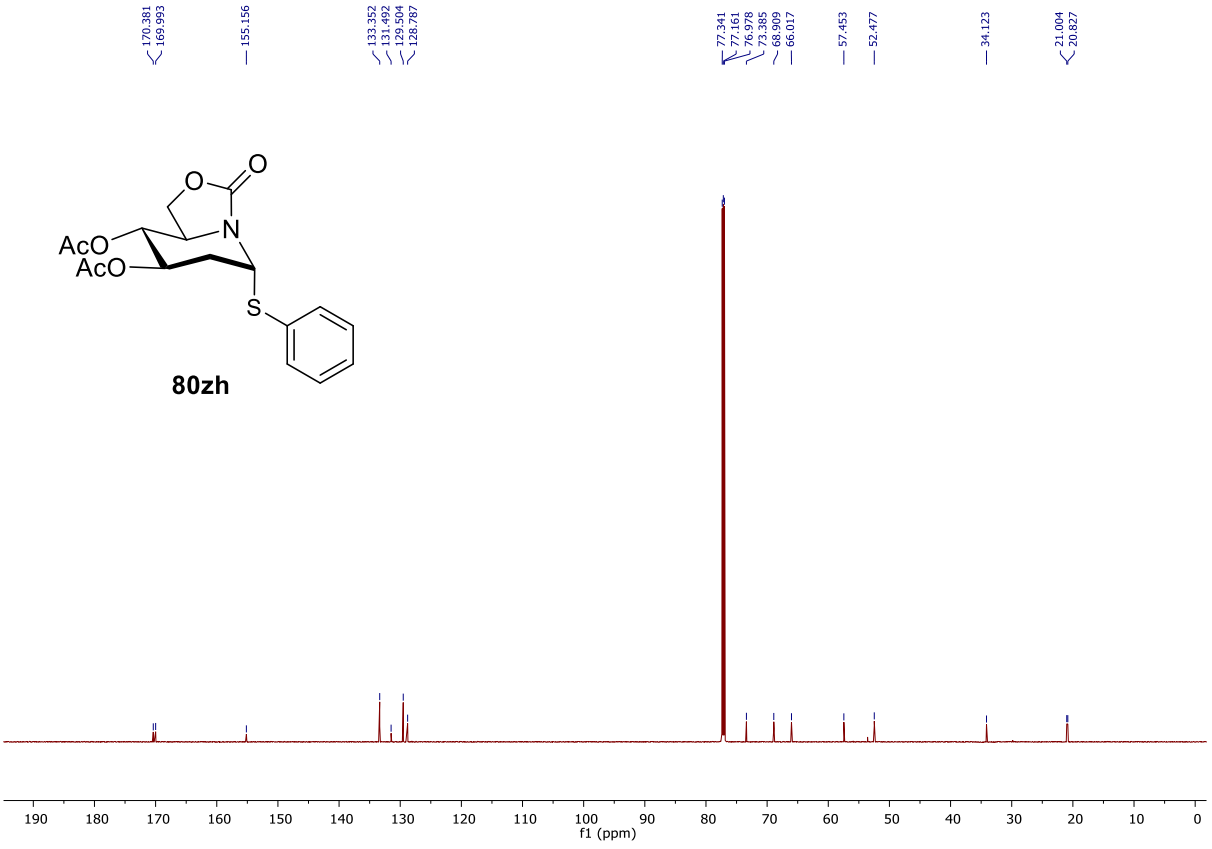

Figure 8.330. ^{13}C NMR spectra for 80zh

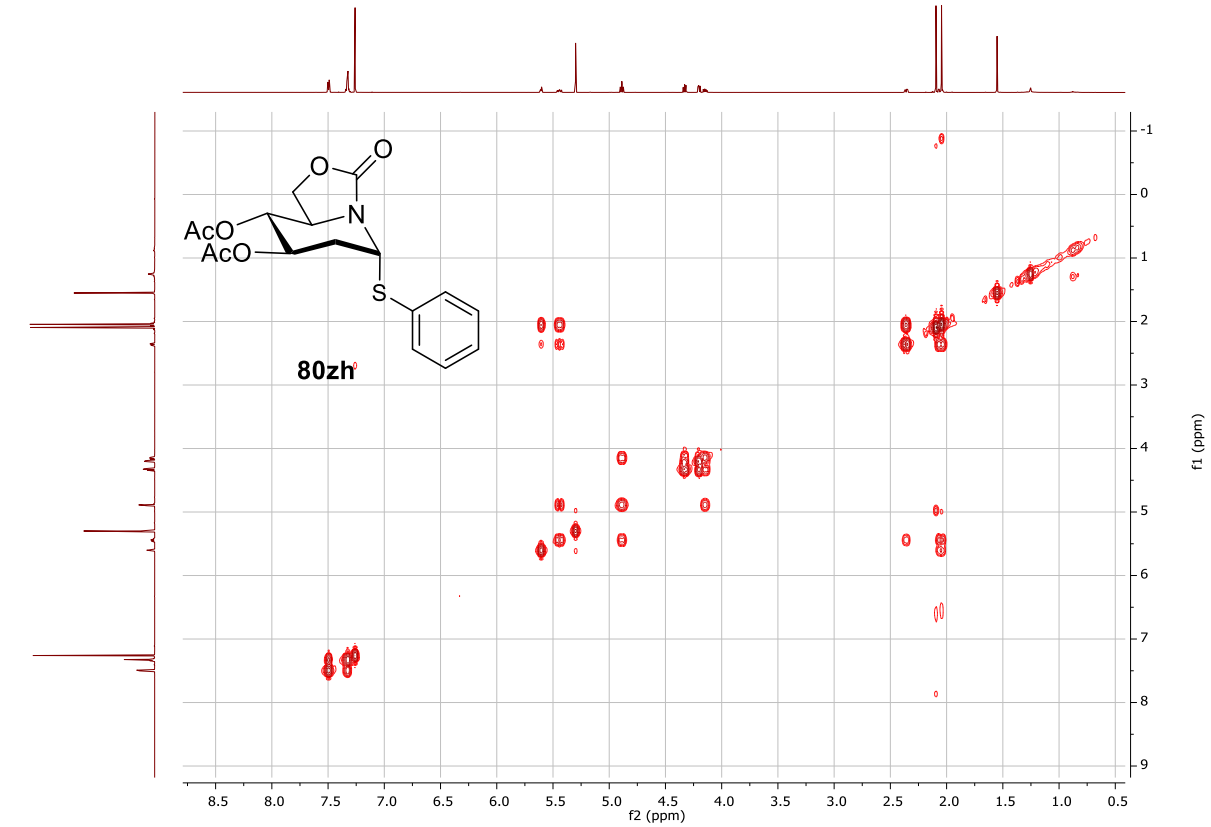

Figure 8.331. COSY spectra for 80zh

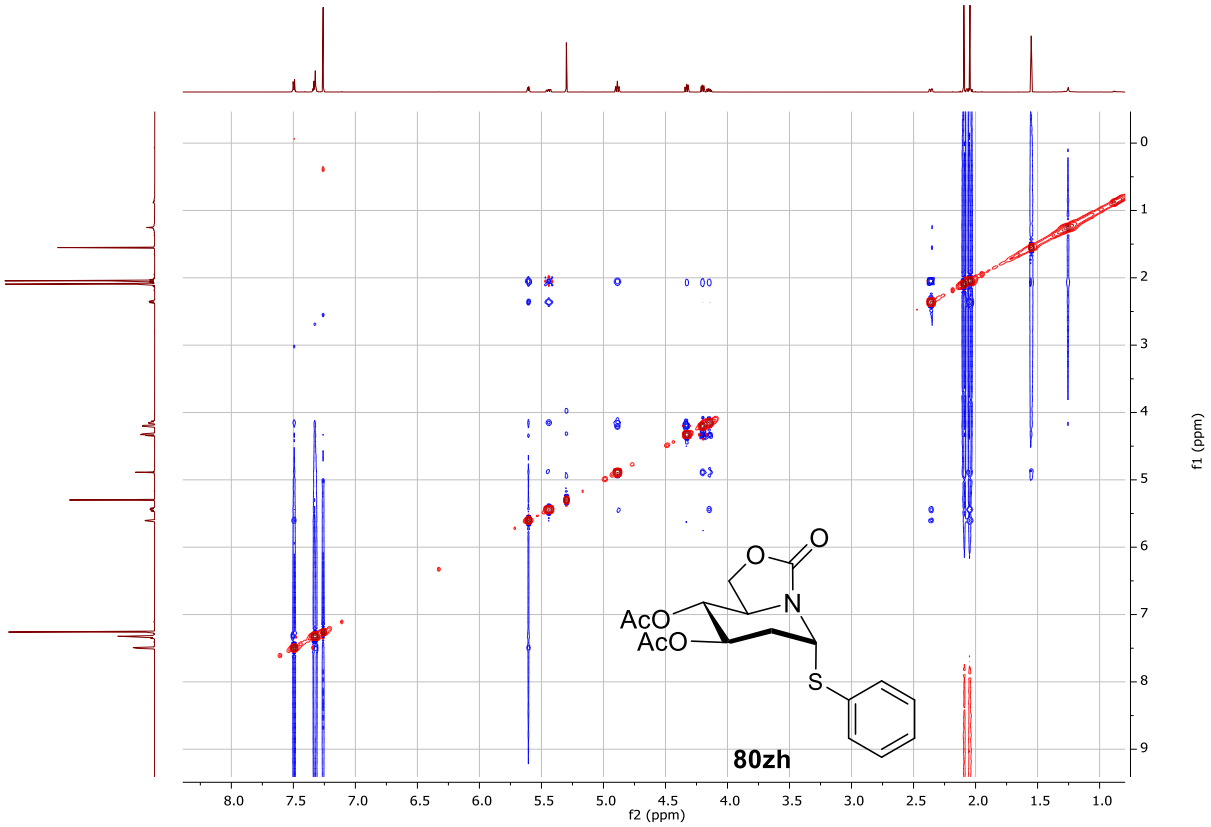

Figure 8.332. NOESY spectra for 80zh

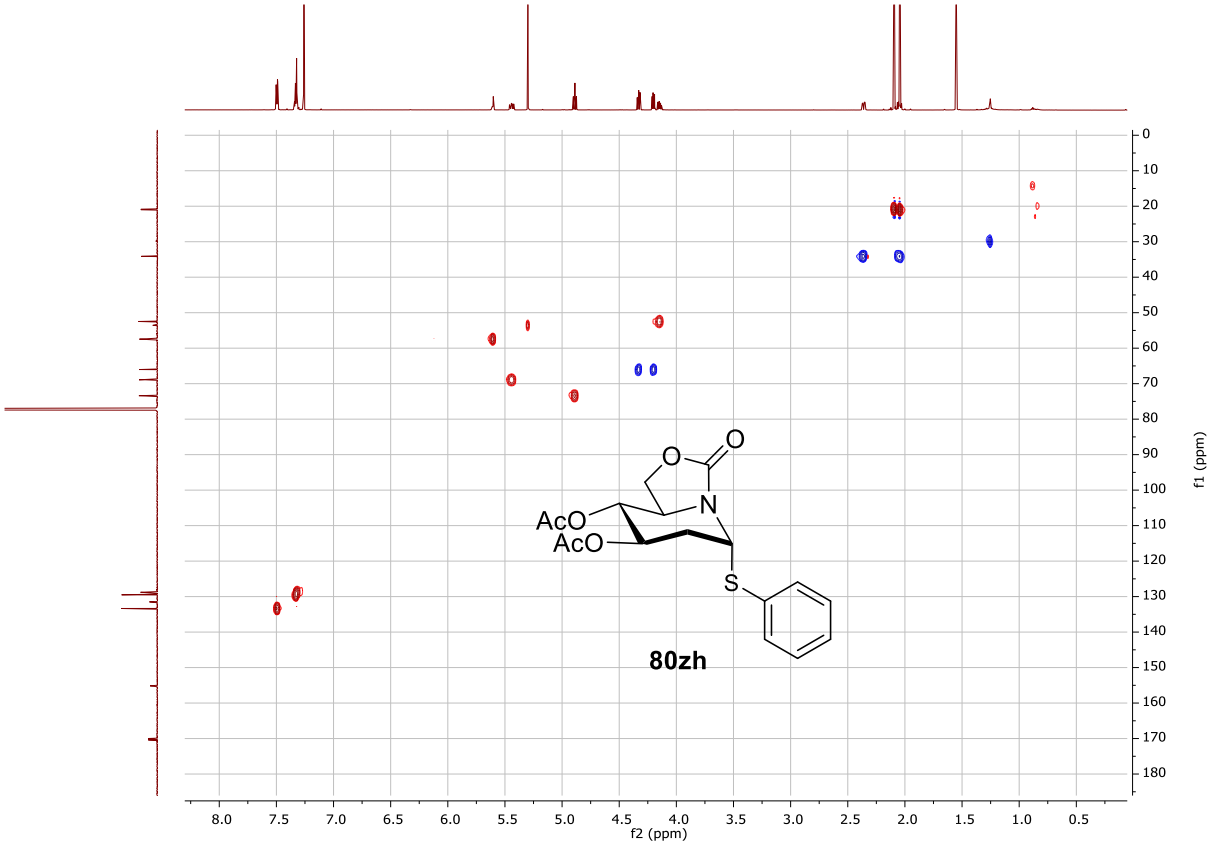

Figure 8.333. HSQC spectra for 80zh

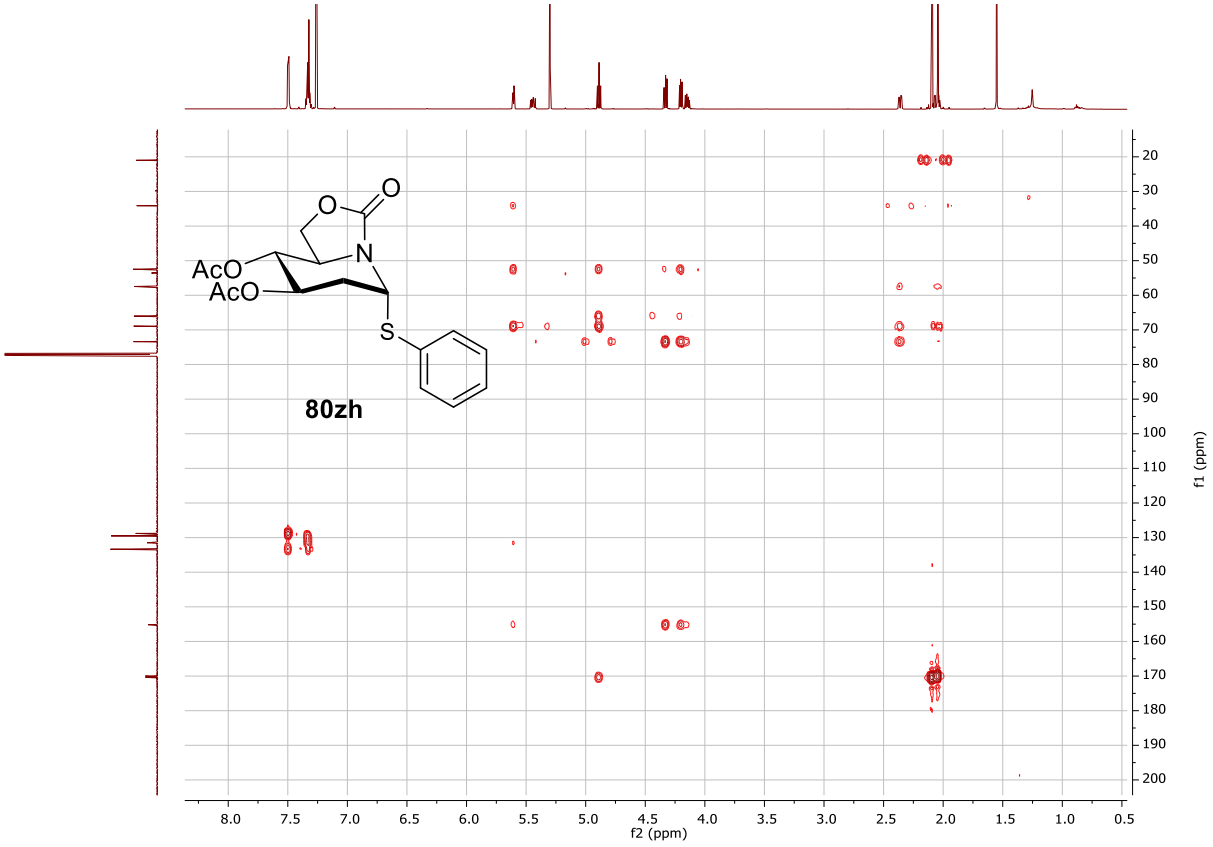

Figure 8.334. HMBC spectra for 80zh

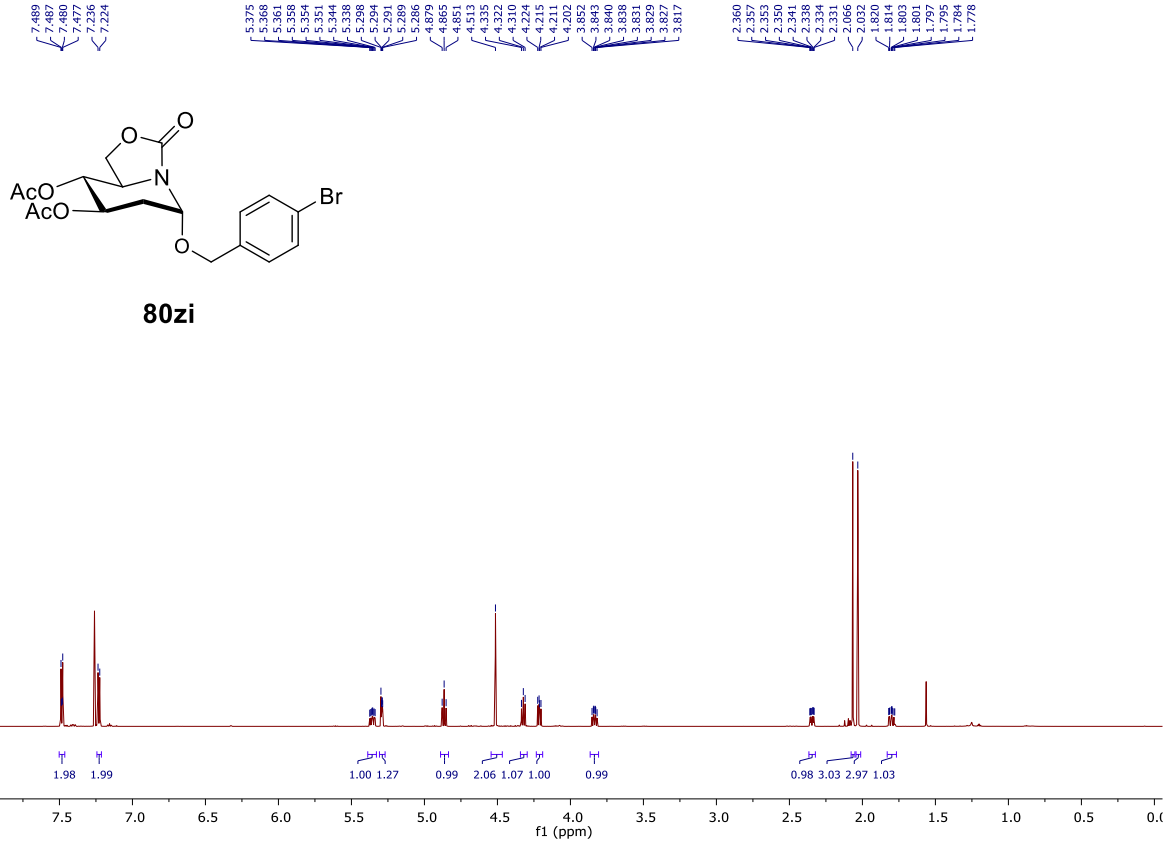

Figure 8.335. ^{1}H NMR spectra for 80zi

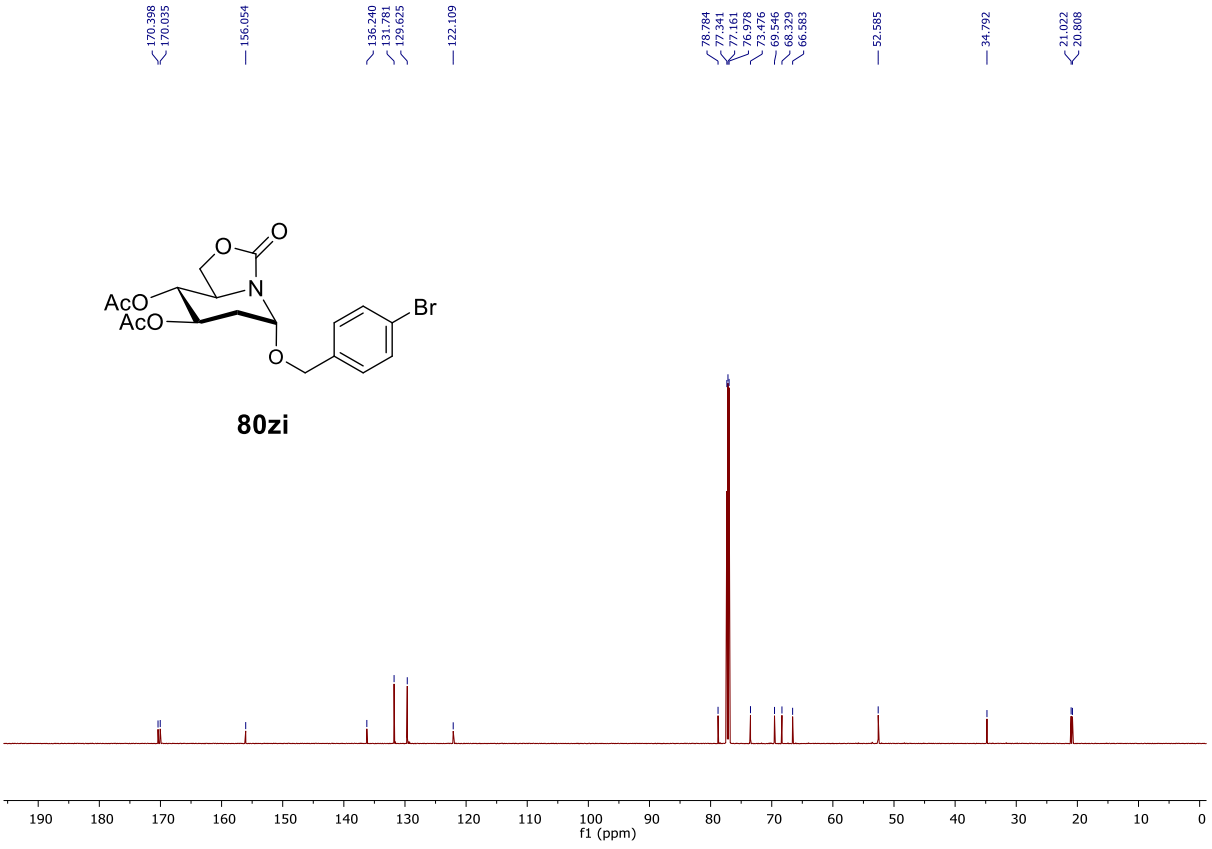

Figure 8.336. ^{13}C NMR spectra for 80zi

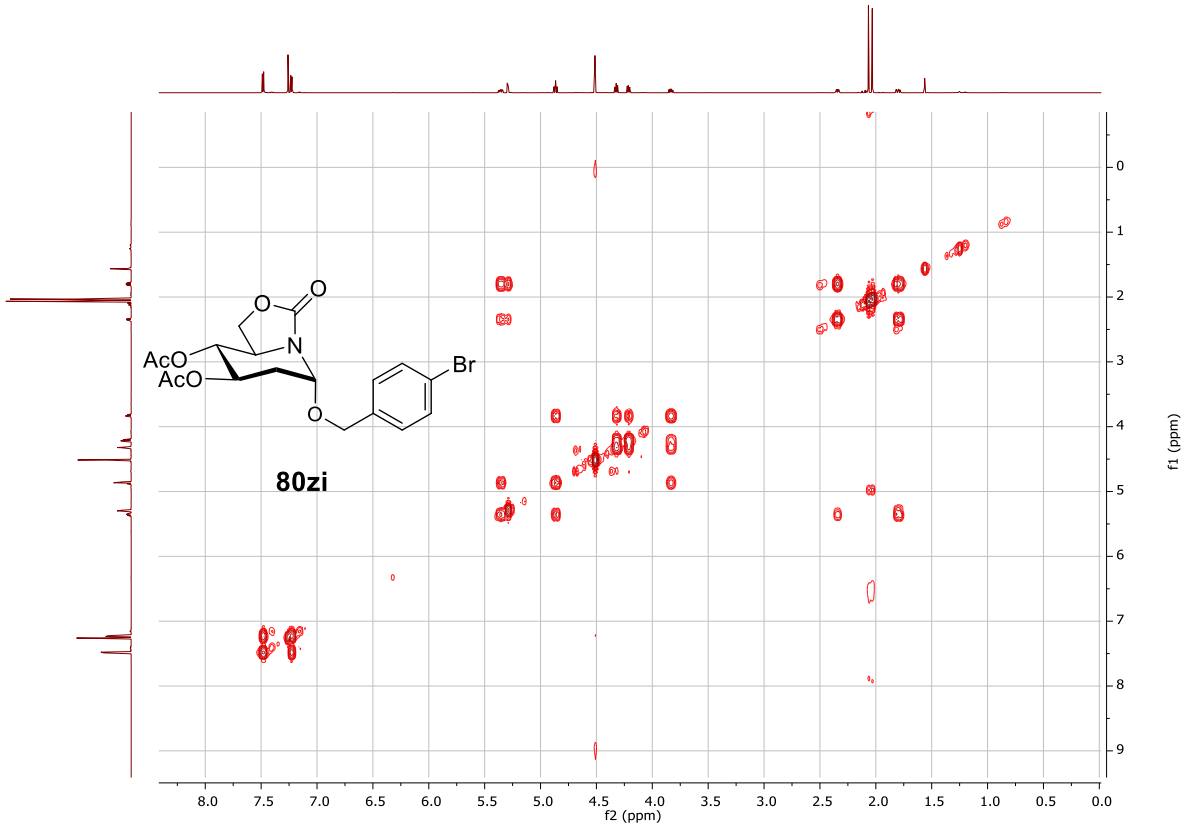

Figure 8.337. COSY spectra for 80zi

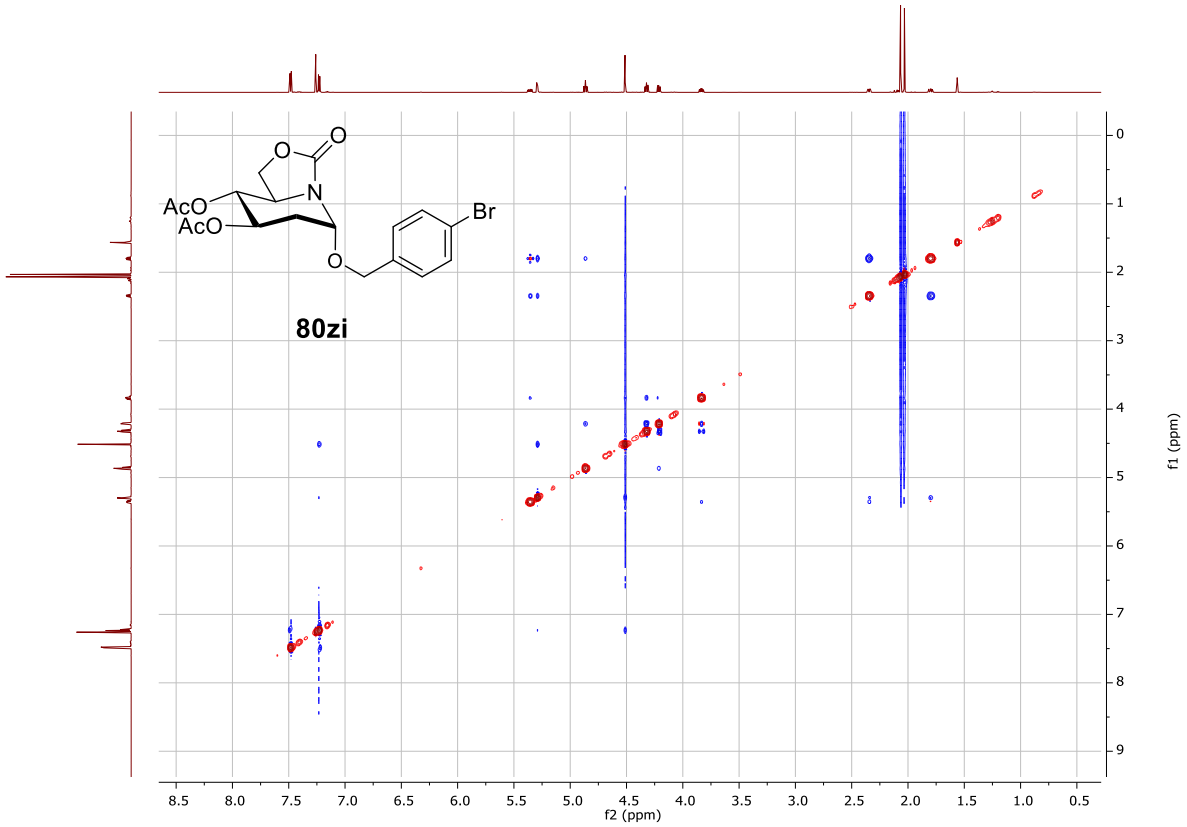

Figure 8.338. NOESY spectra for 80zi

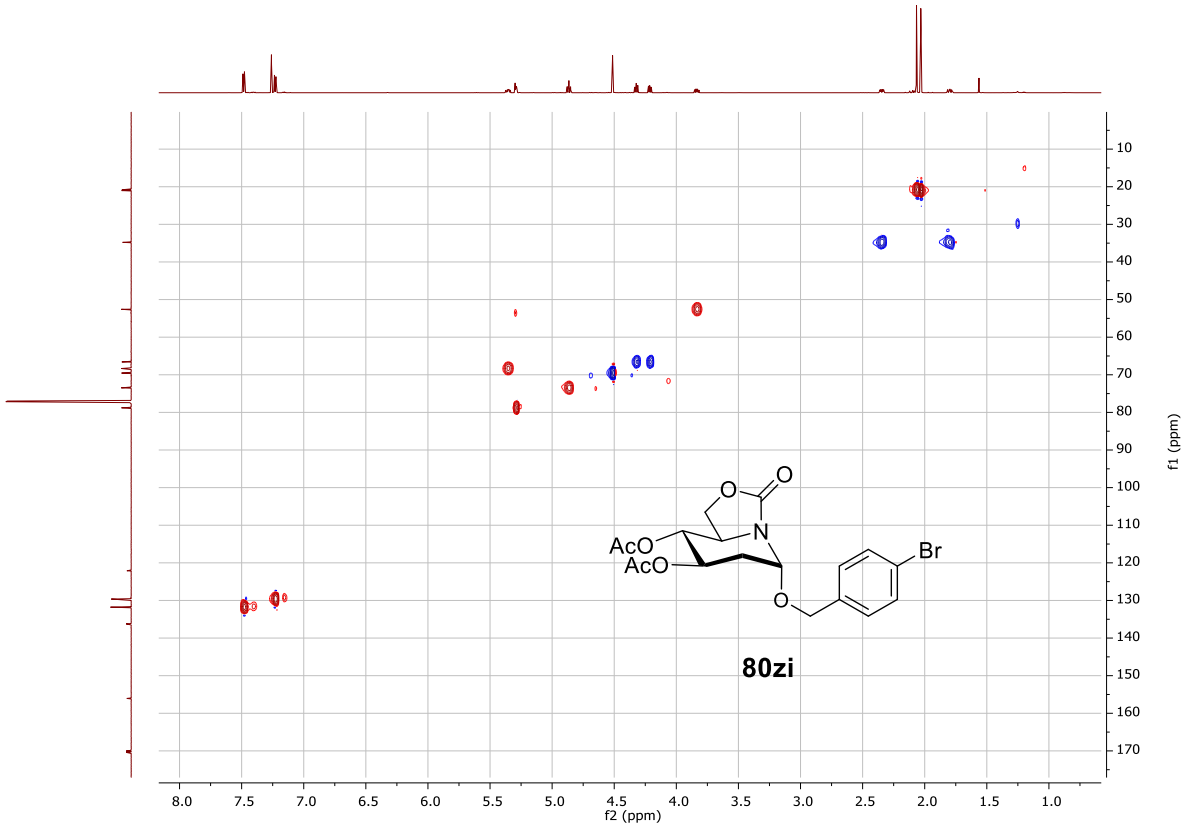

Figure 8.339. HSQC spectra for 80zi

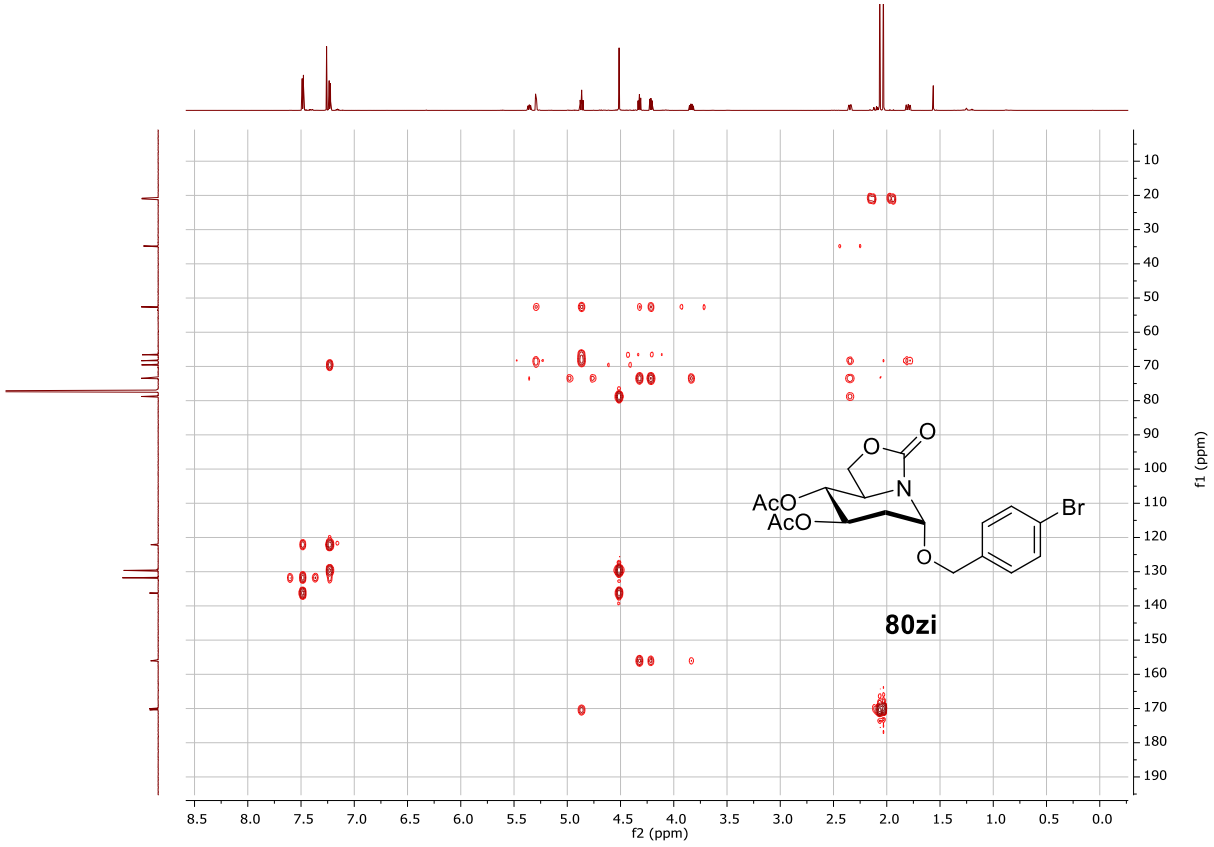

Figure 8.340. HMBC spectra for 80zi

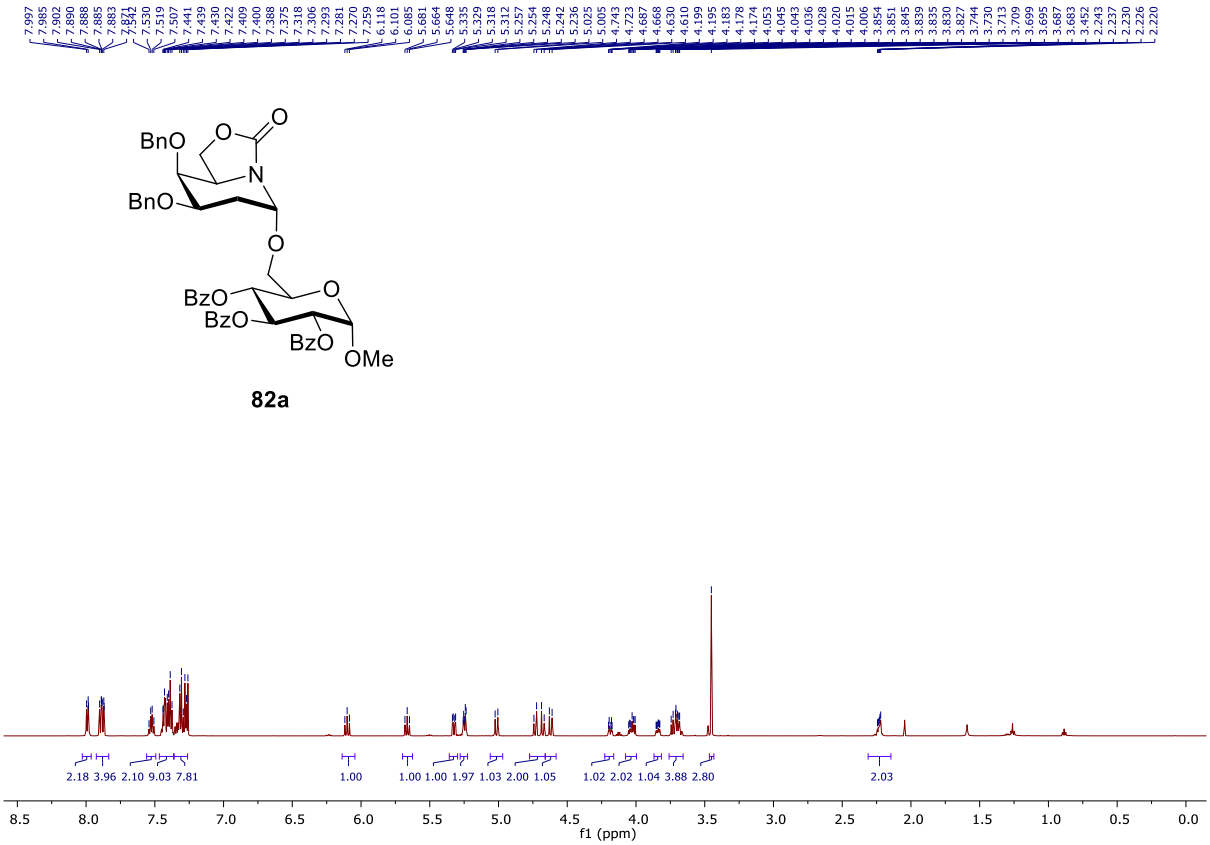

Figure 8.341. ^{1}H NMR spectra for 82a

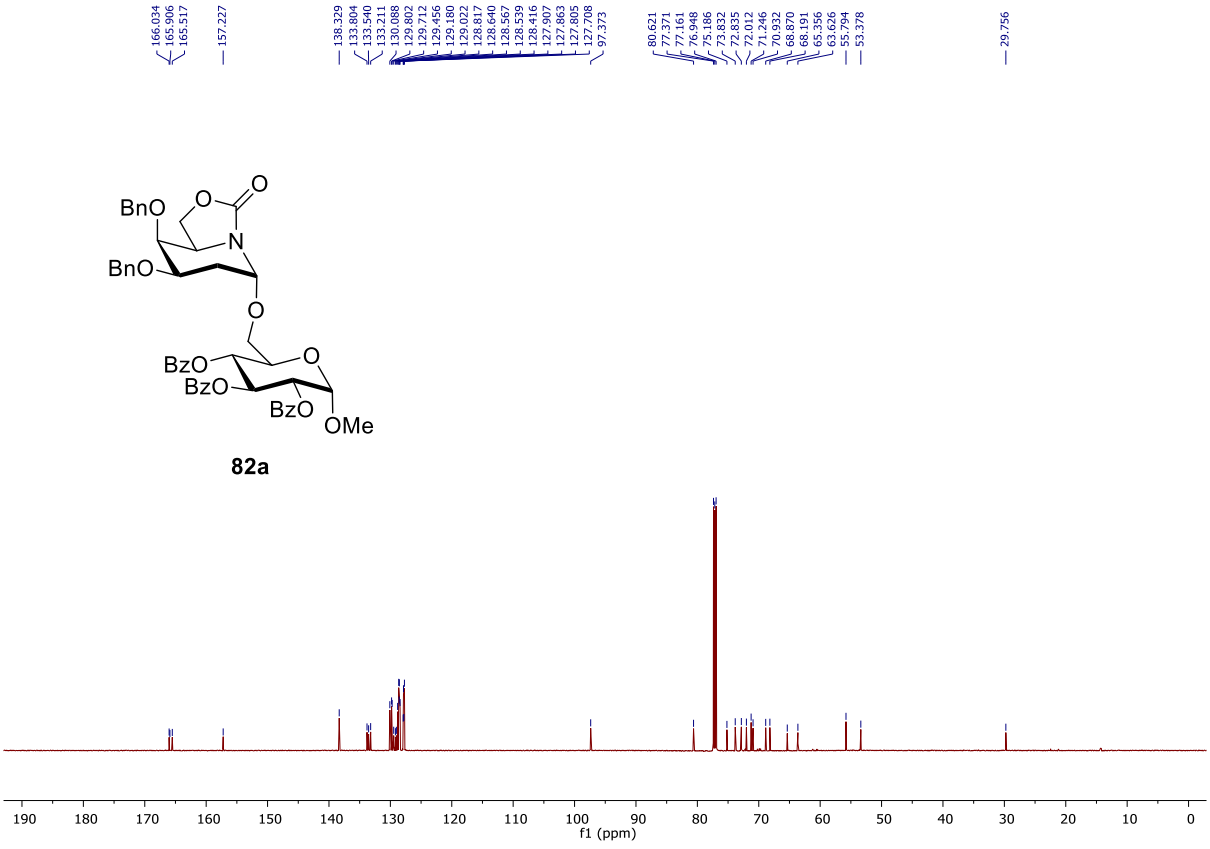

Figure 8.342. ^{13}C NMR spectra for 82a

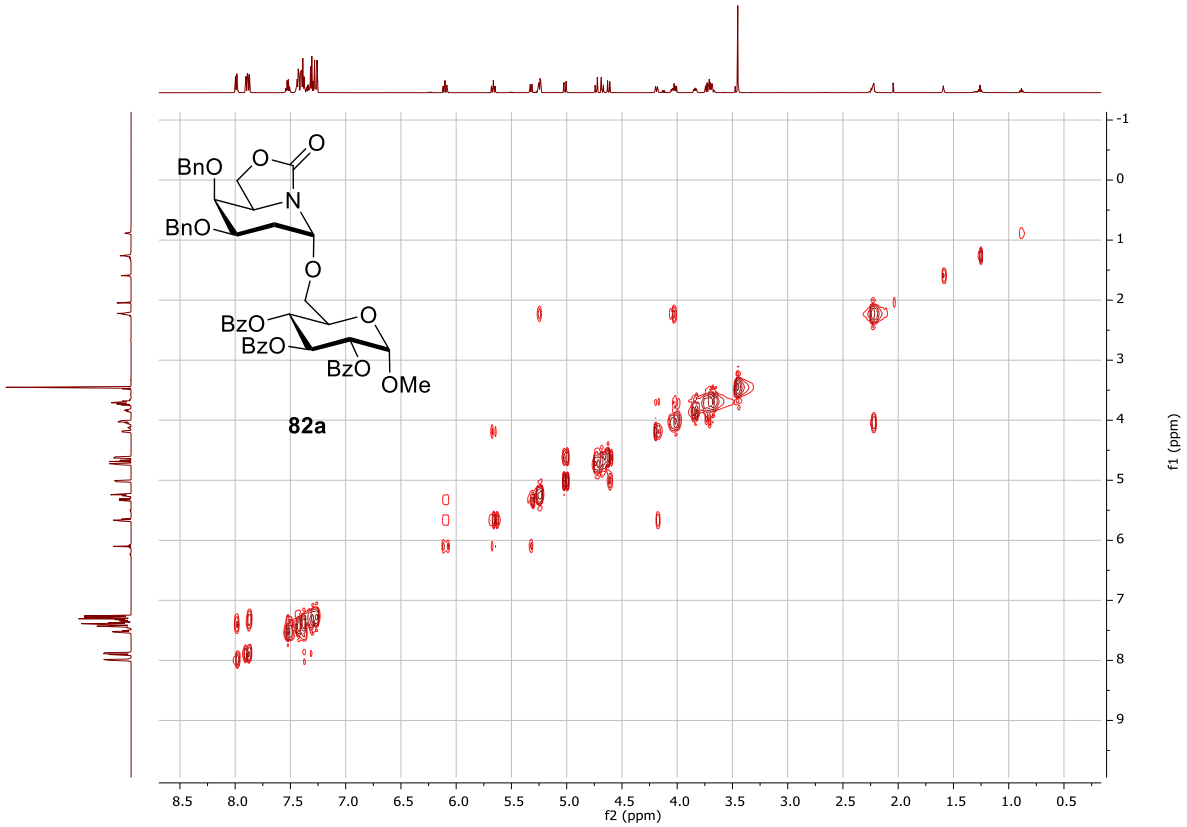

Figure 8.343. COSY spectra for 82a

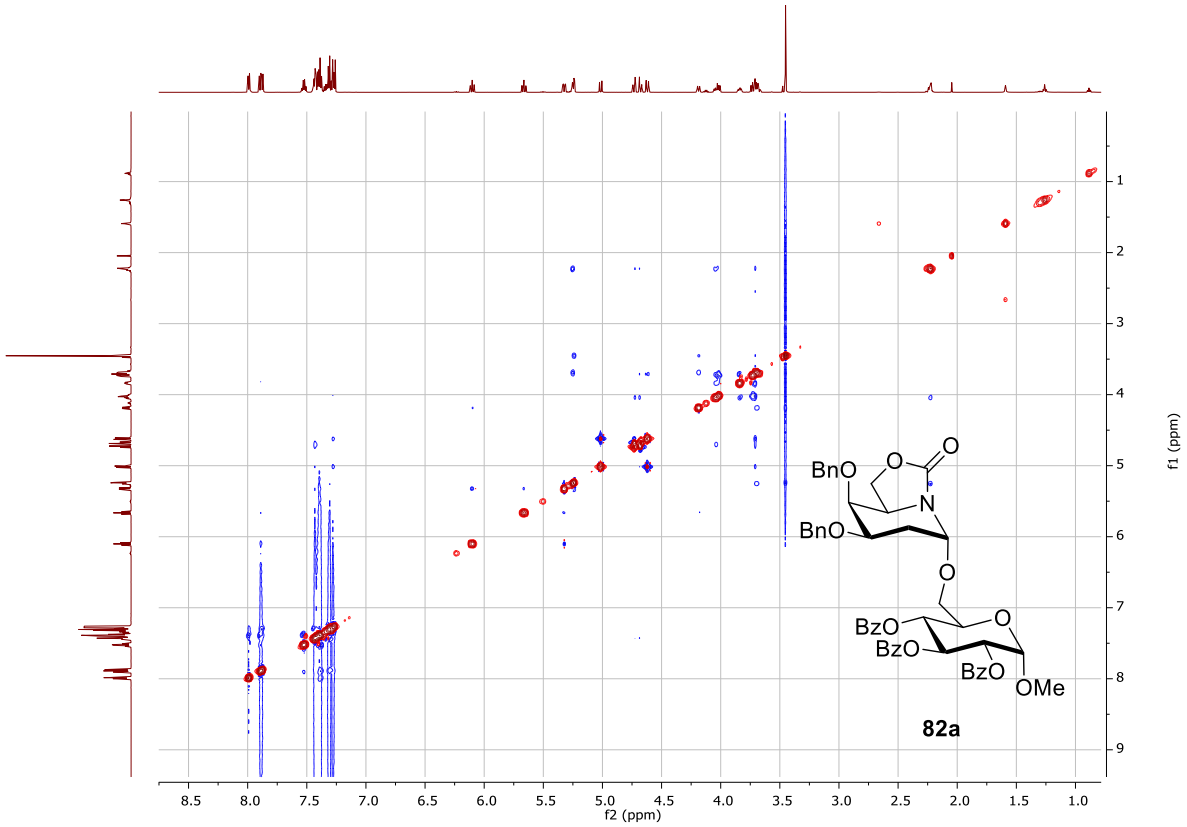

Figure 8.344. NOESY spectra for 82a

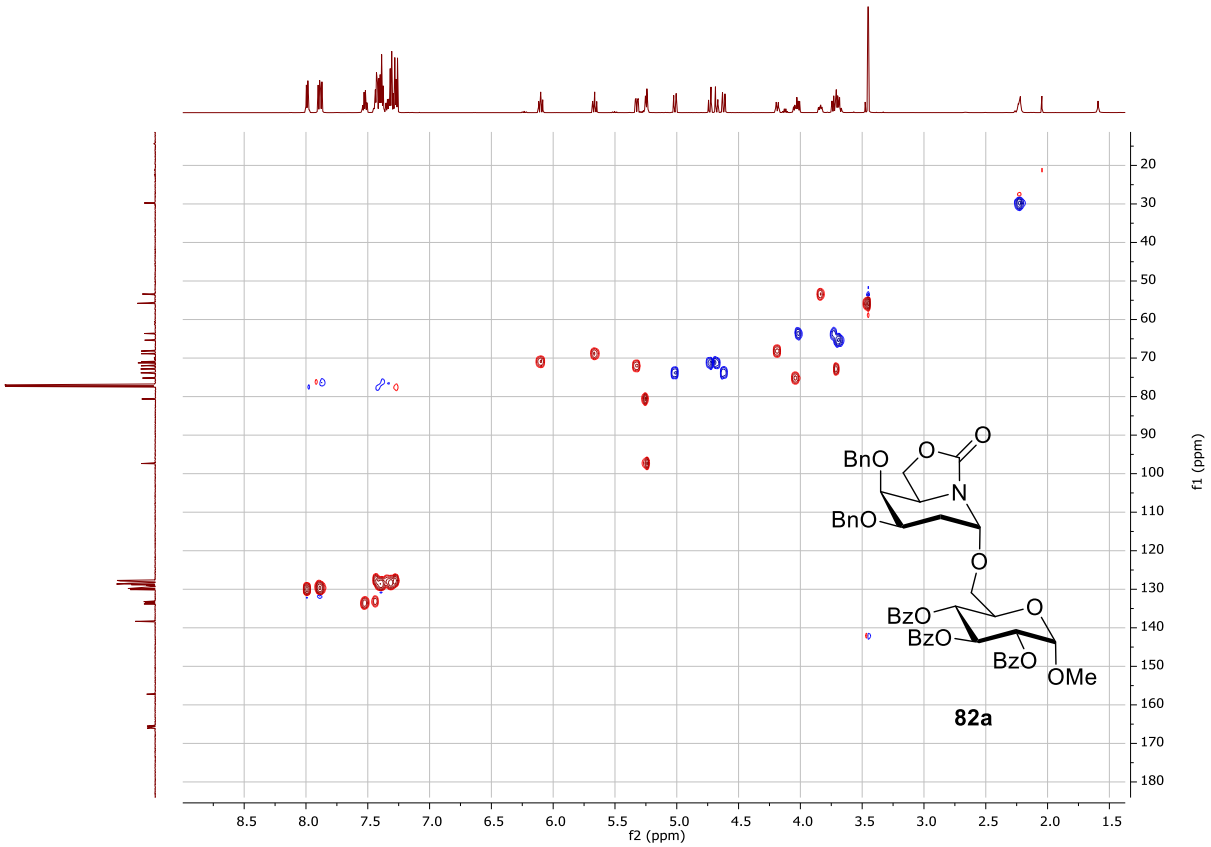

Figure 8.345. HSQC spectra for 82a

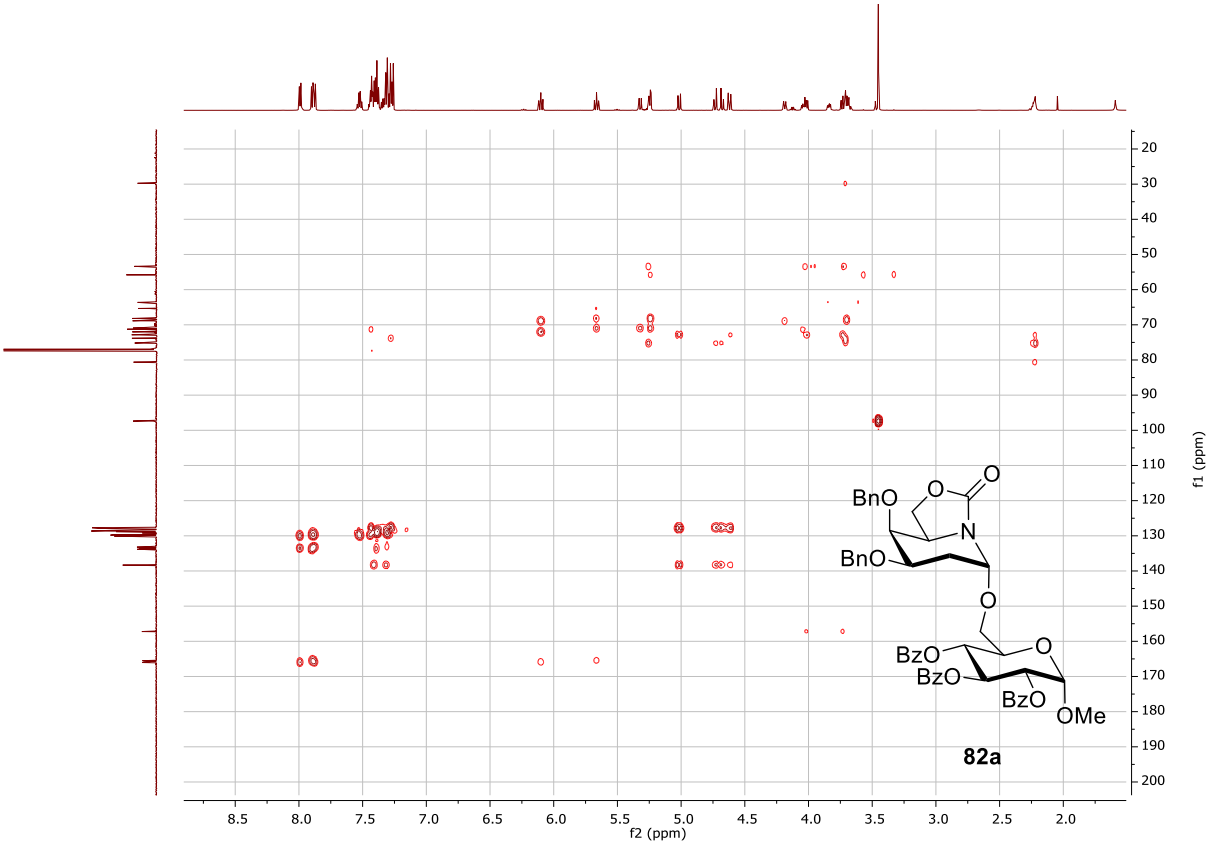

Figure 8.346. HMBC spectra for 82a

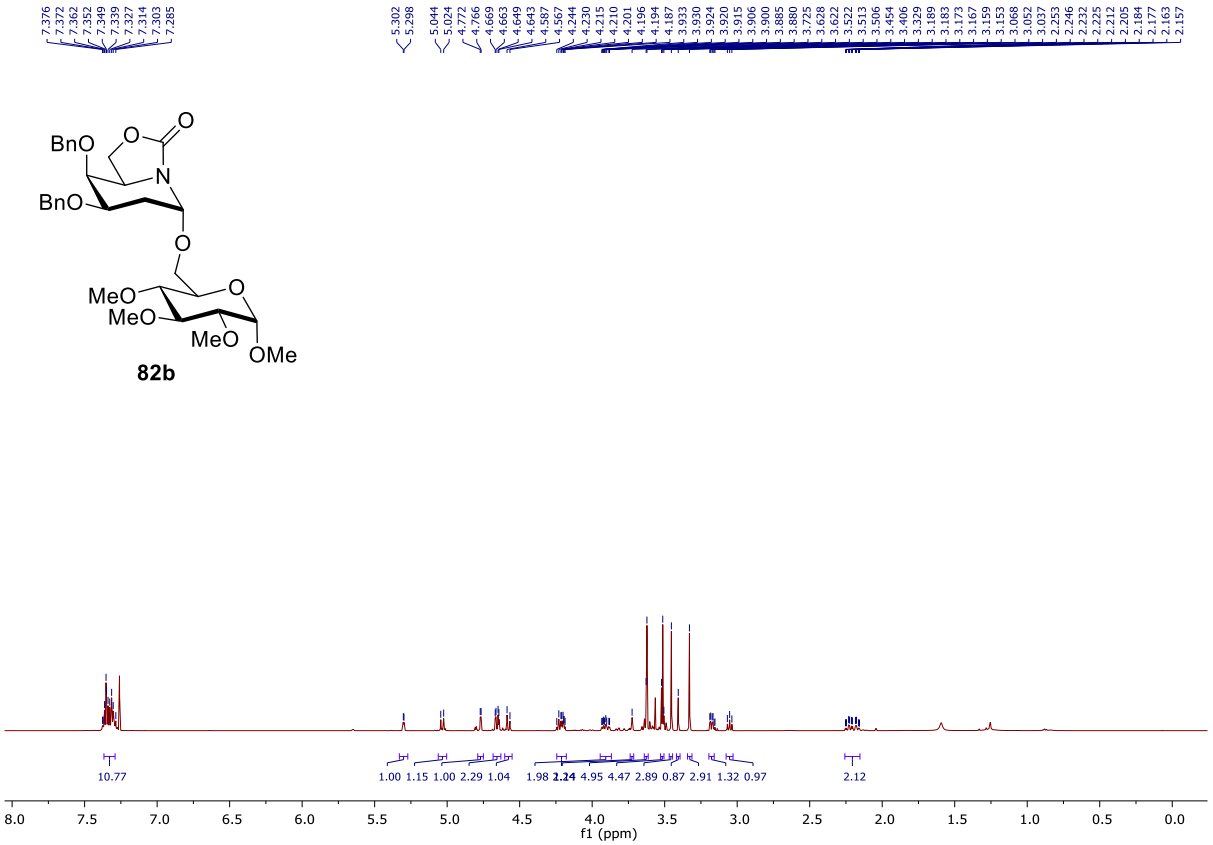

Figure 8.347. ^{1}H NMR spectra for 82b

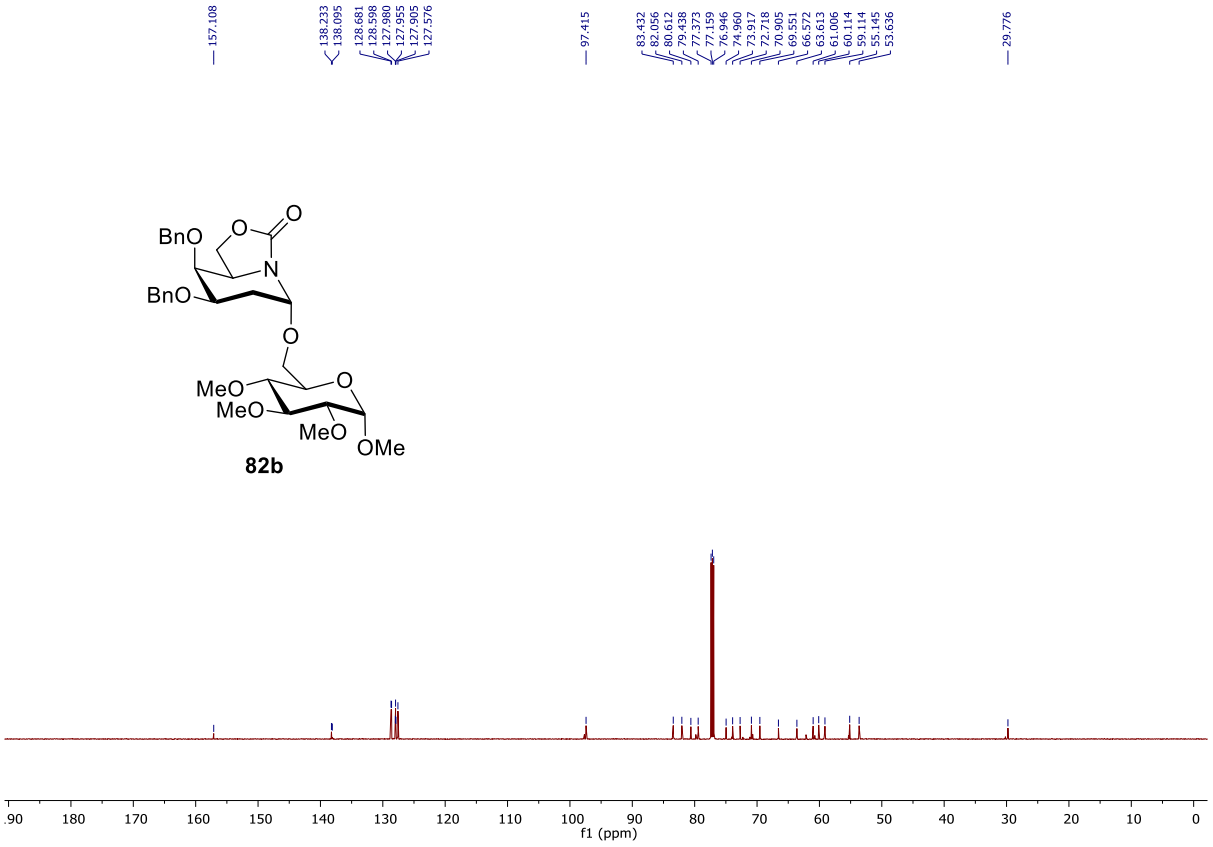

Figure 8.348. ^{13}C NMR spectra for 82b

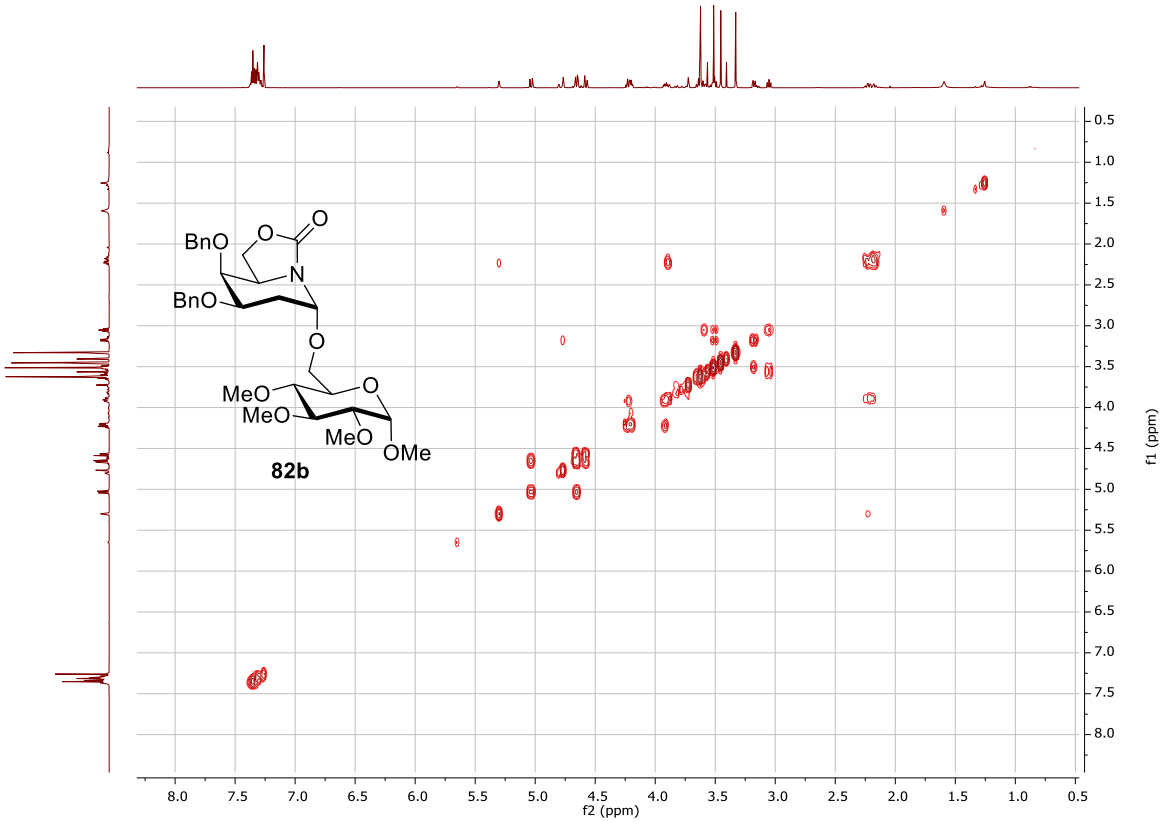

Figure 8.349. COSY spectra for 82b

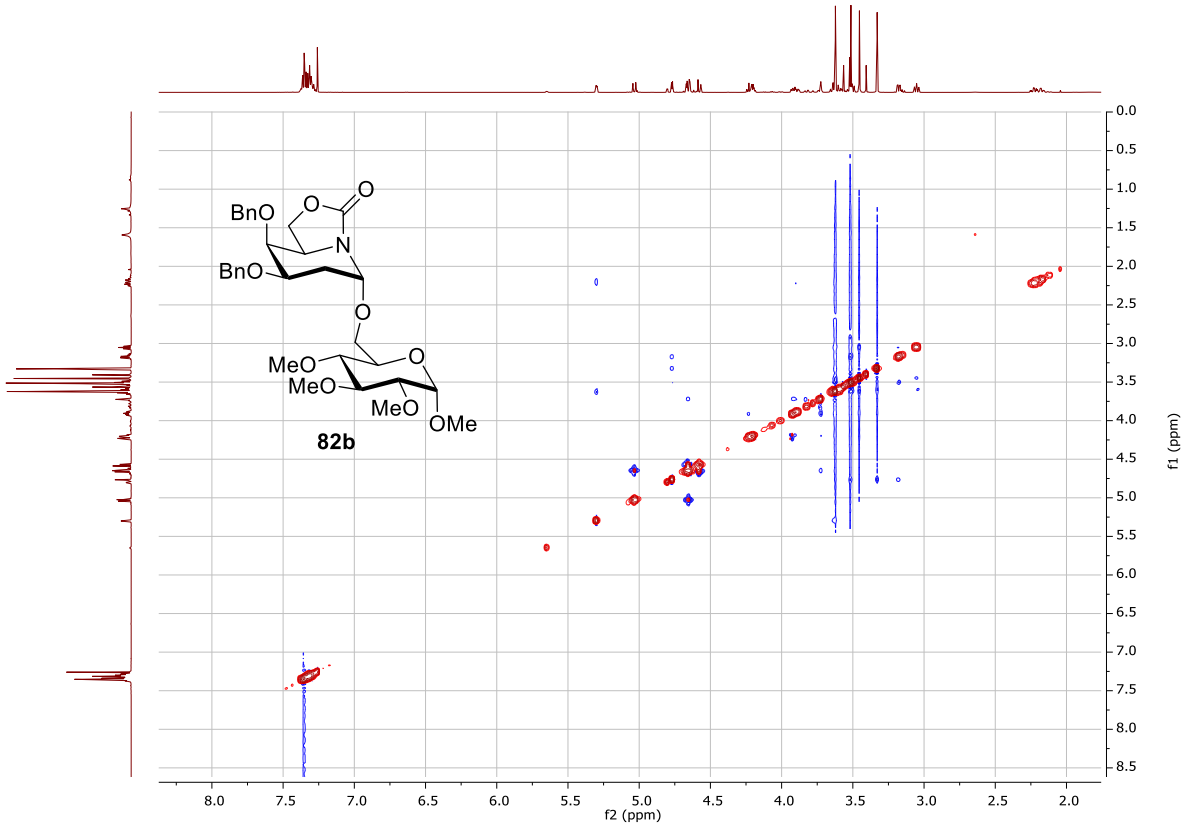

Figure 8.350. NOESY spectra for 82b

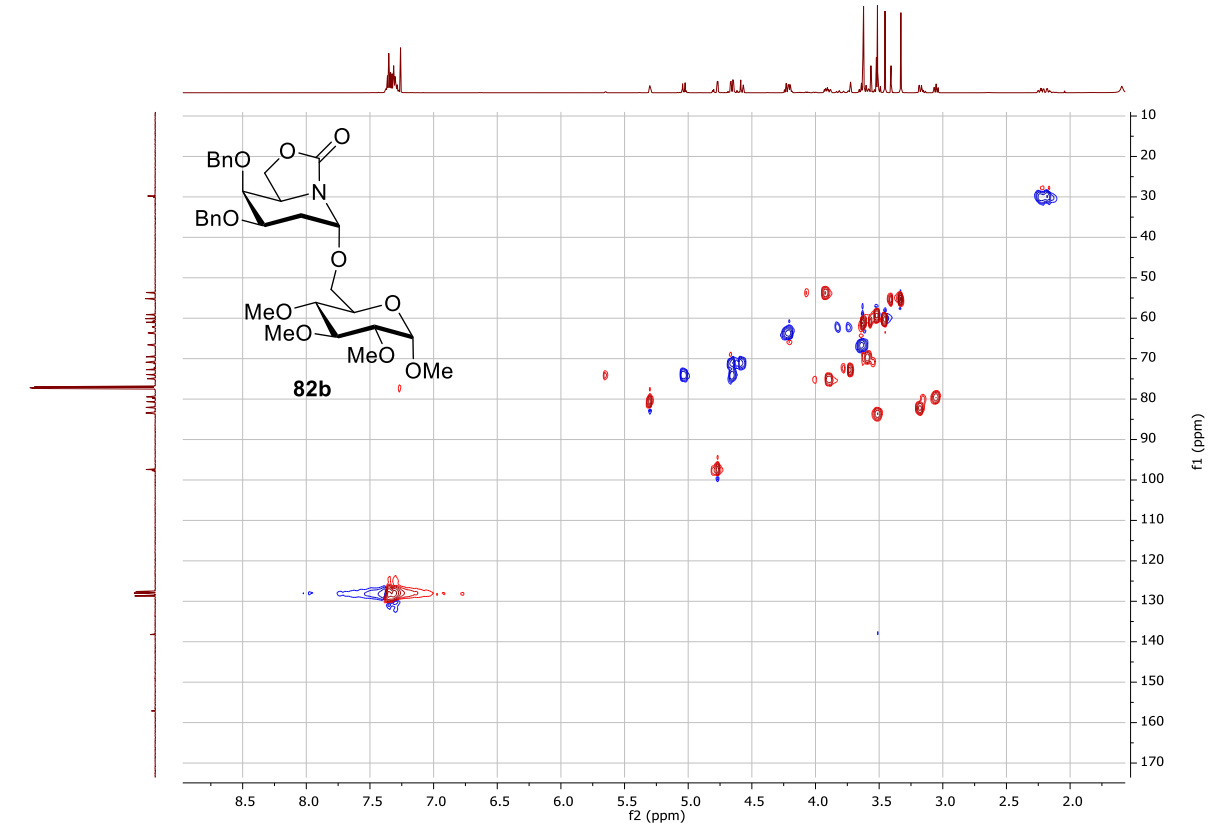

Figure 8.351. HSQC spectra for 82b

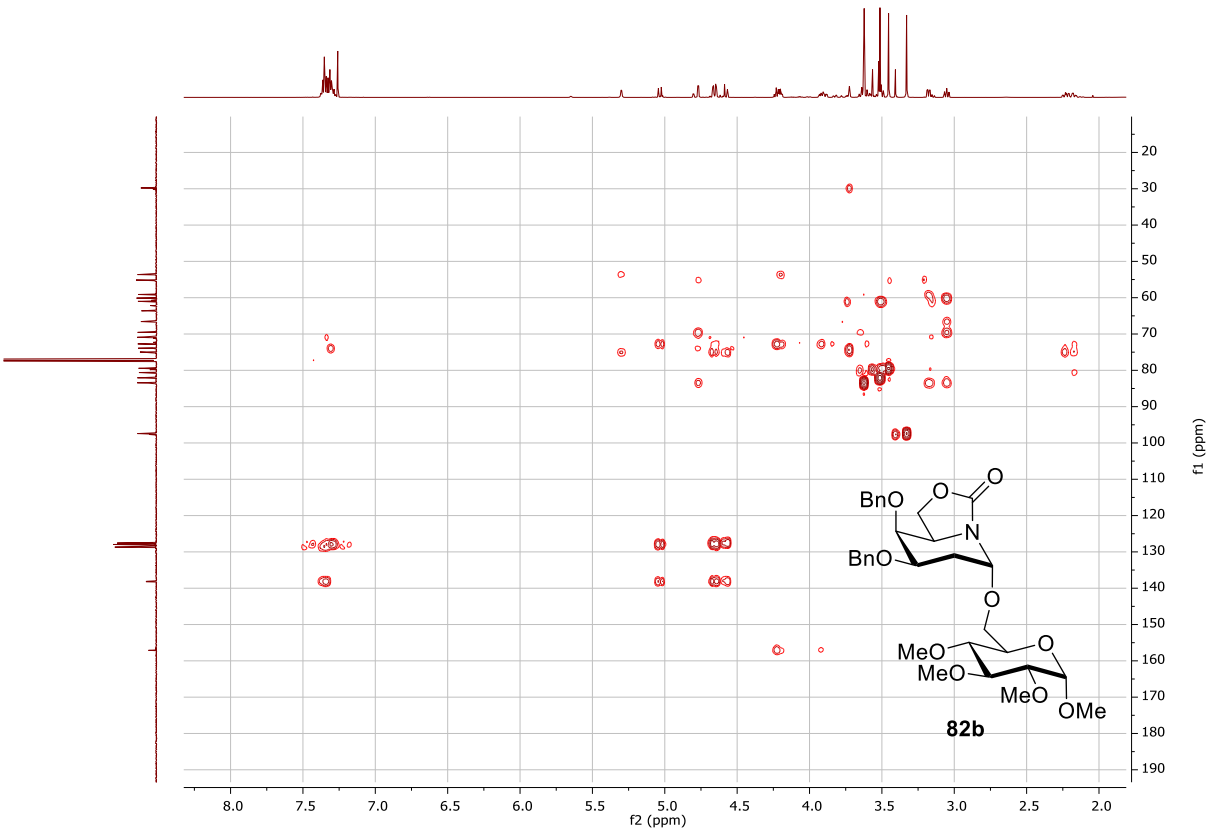

Figure 8.352. HMBC spectra for 82b

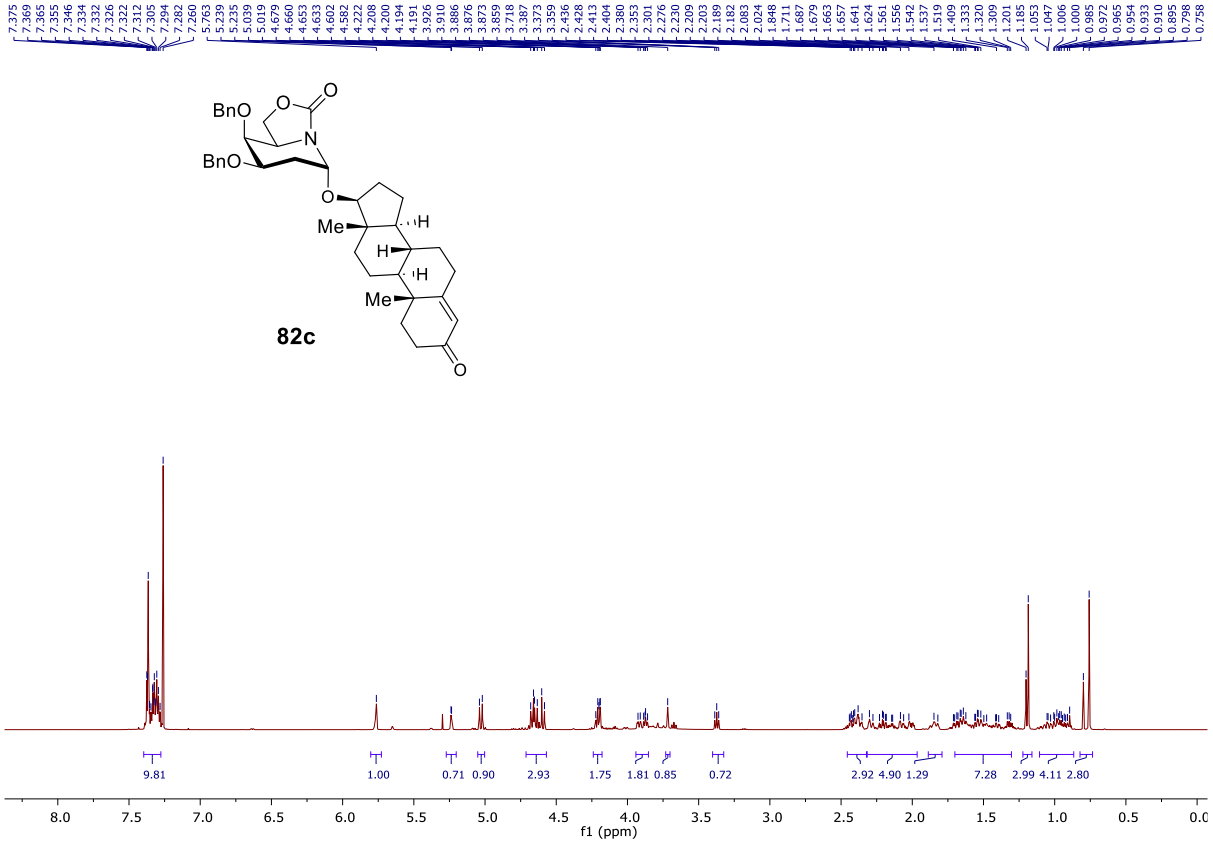

Figure 8.353. ^{1}H NMR spectra for 82c

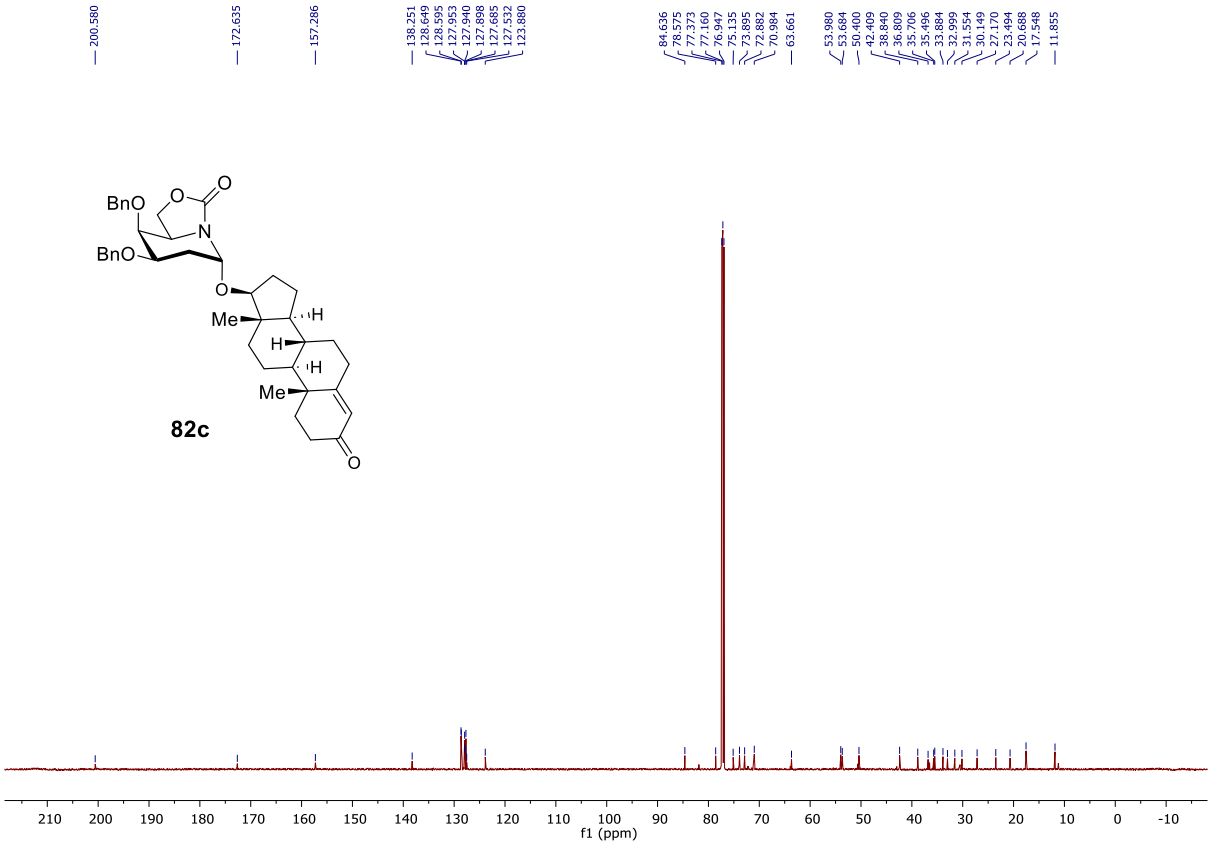

Figure 8.354. ^{13}C NMR spectra for 82c

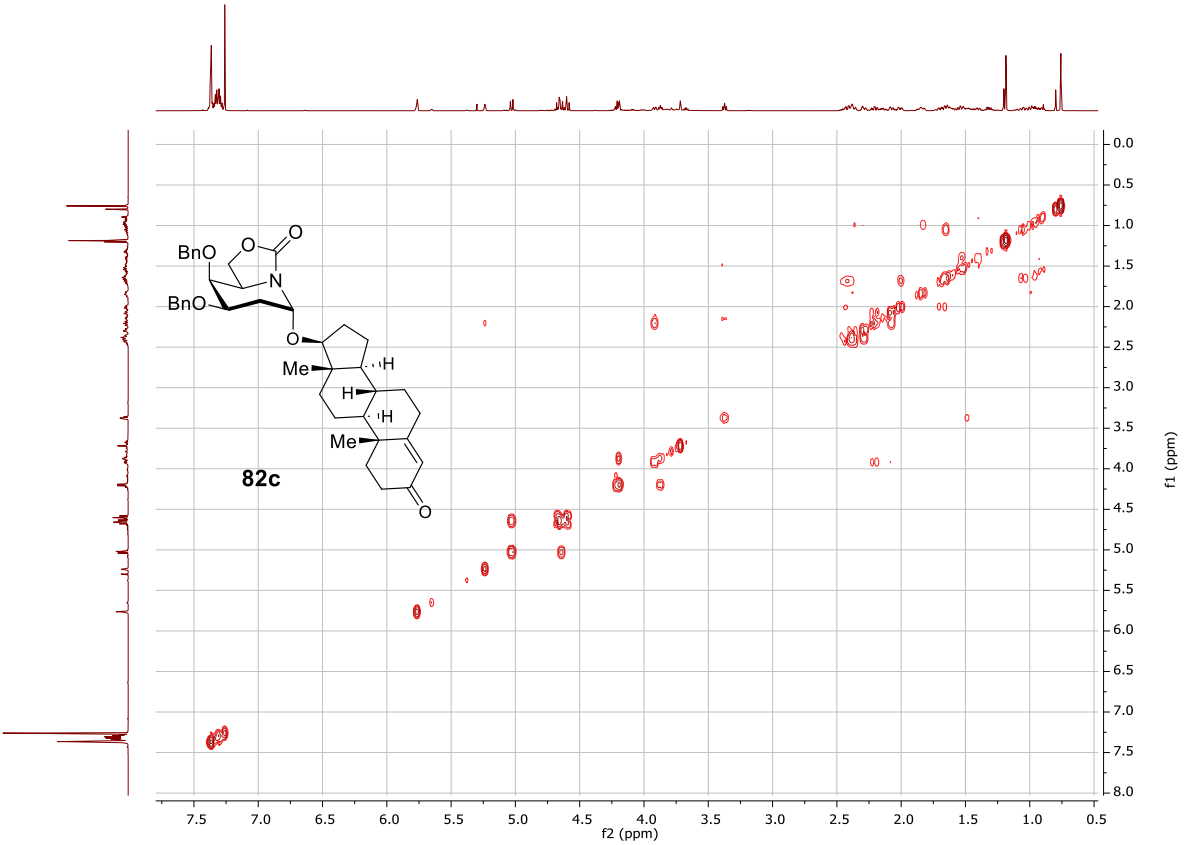

Figure 8.355. COSY spectra for 82c

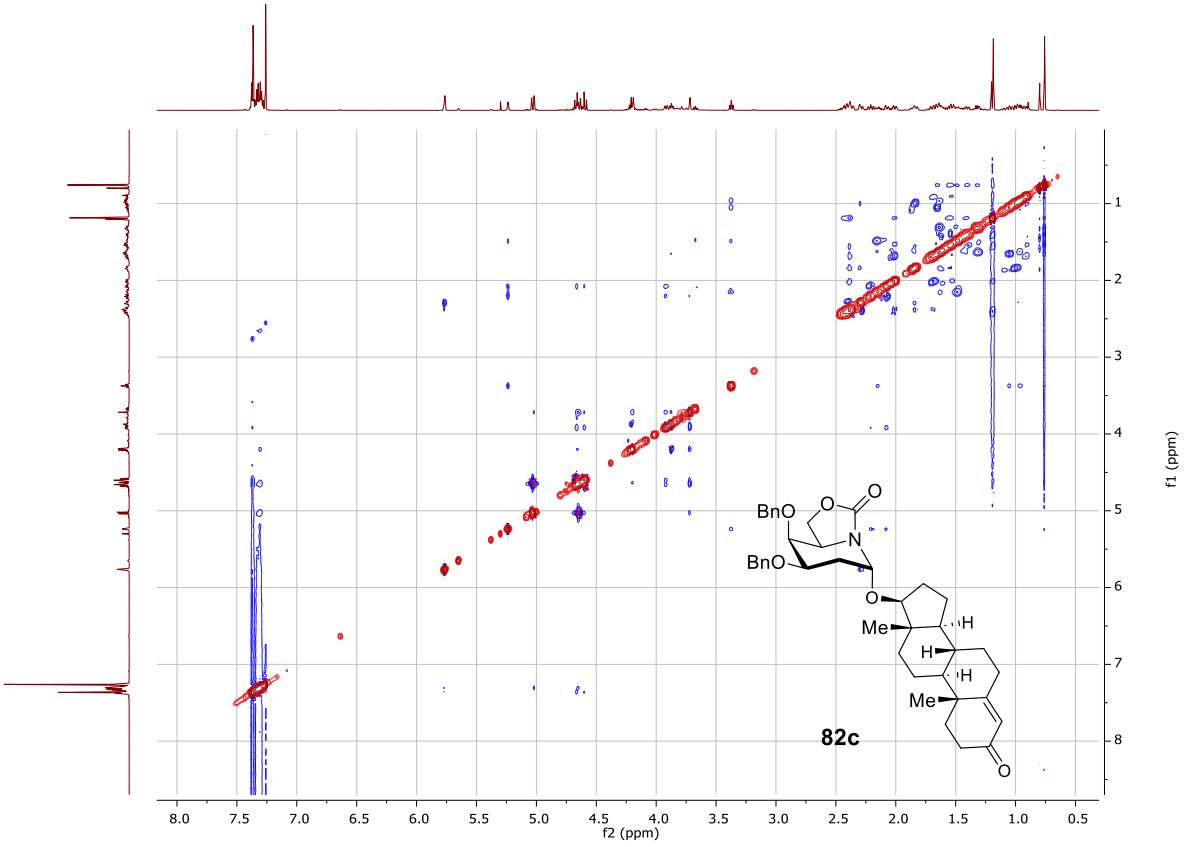

Figure 8.356. NOESY spectra for 82c

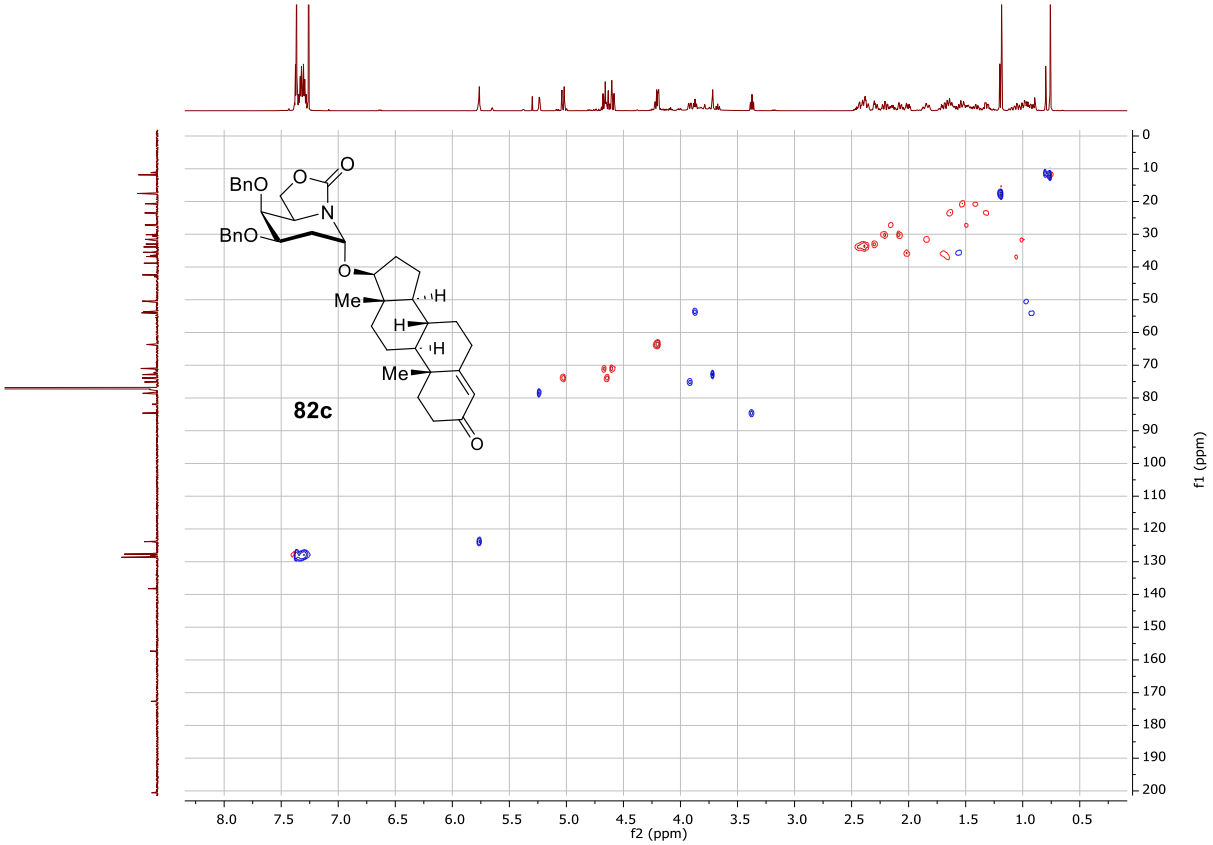

Figure 8.357. HSQC spectra for 82c

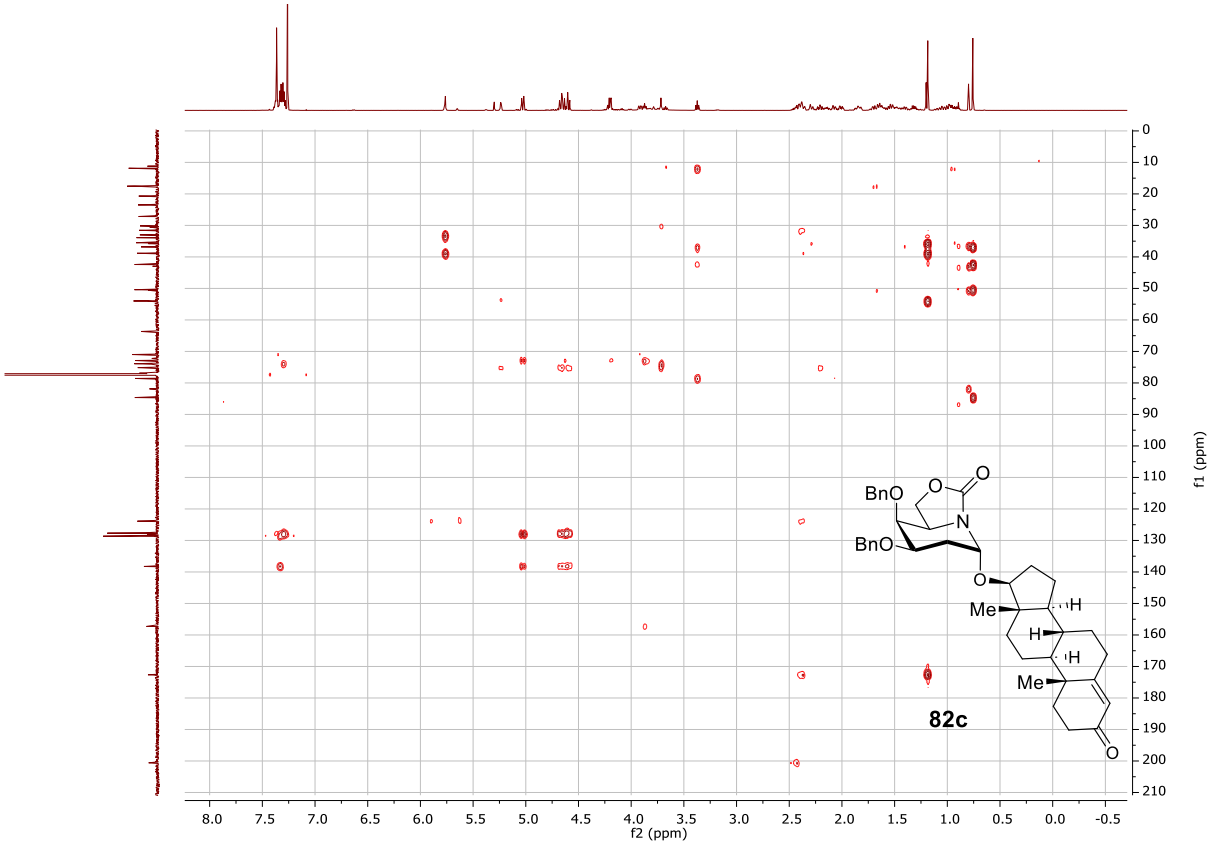

Figure 8.358. HMBC spectra for 82c

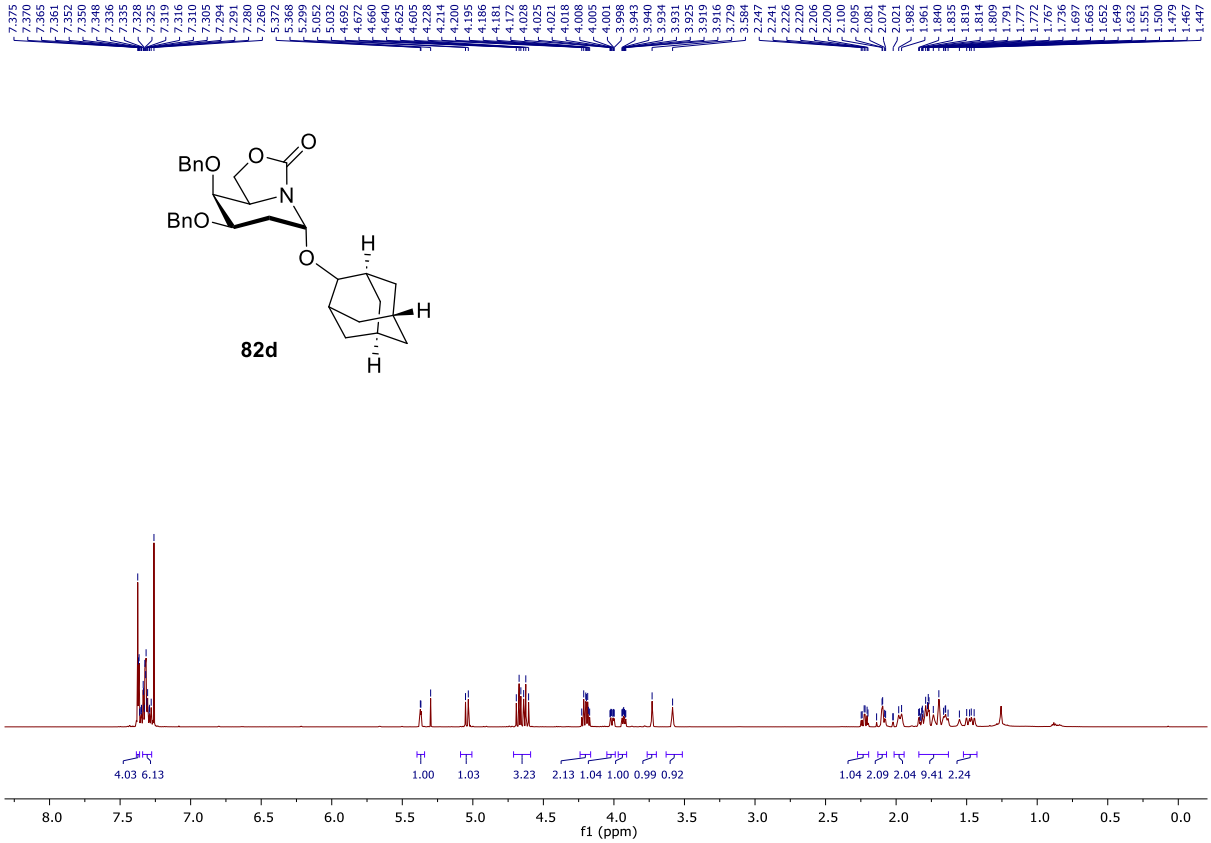

Figure 8.359. ^{1}H NMR spectra for 82d

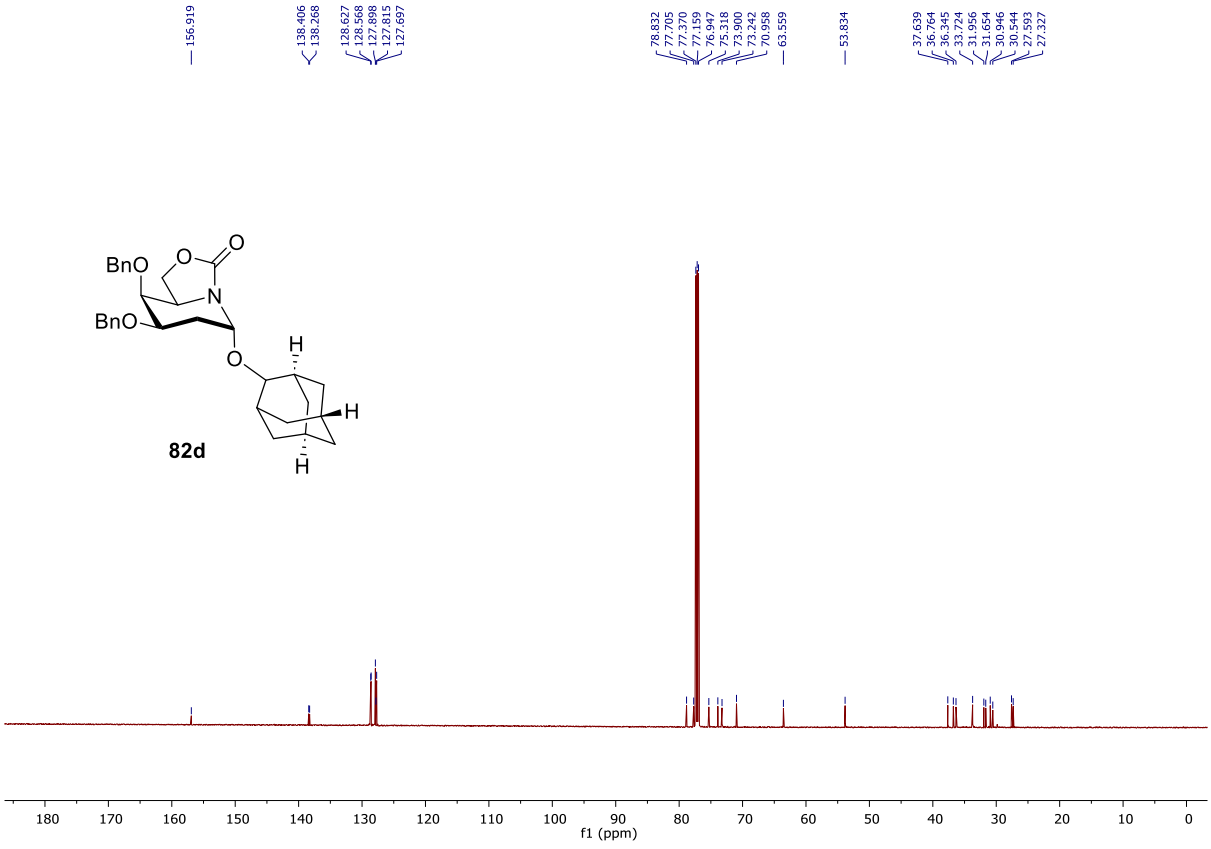

Figure 8.360. ^{13}C NMR spectra for 82d

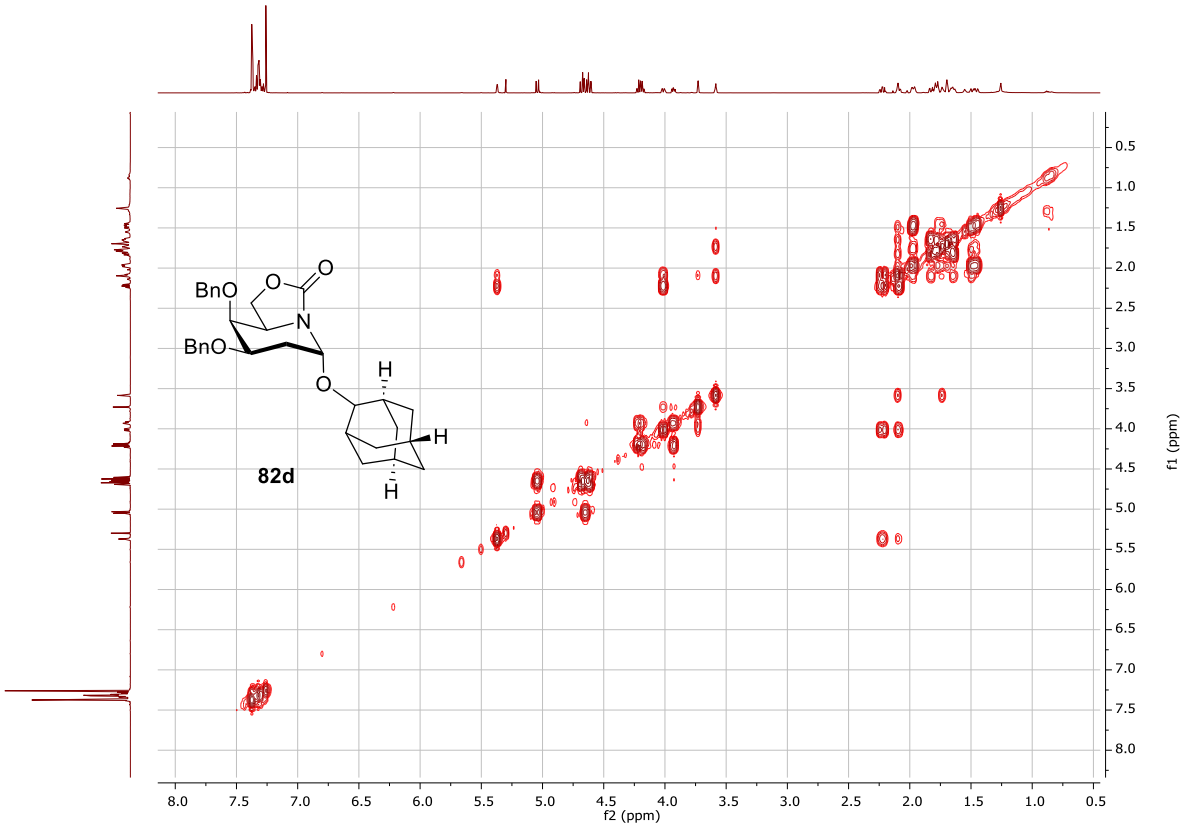

Figure 8.361. COSY spectra for 82d

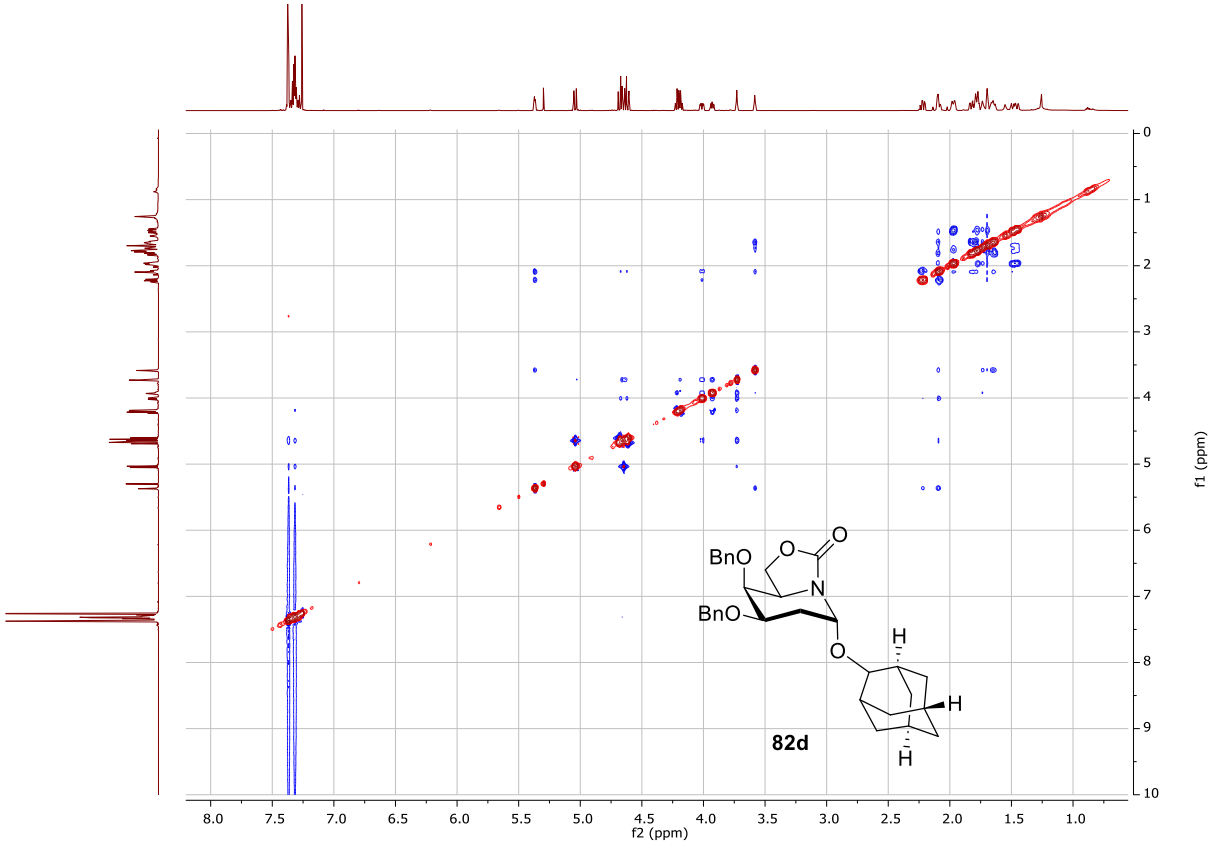

Figure 8.362. NOESY spectra for 82d

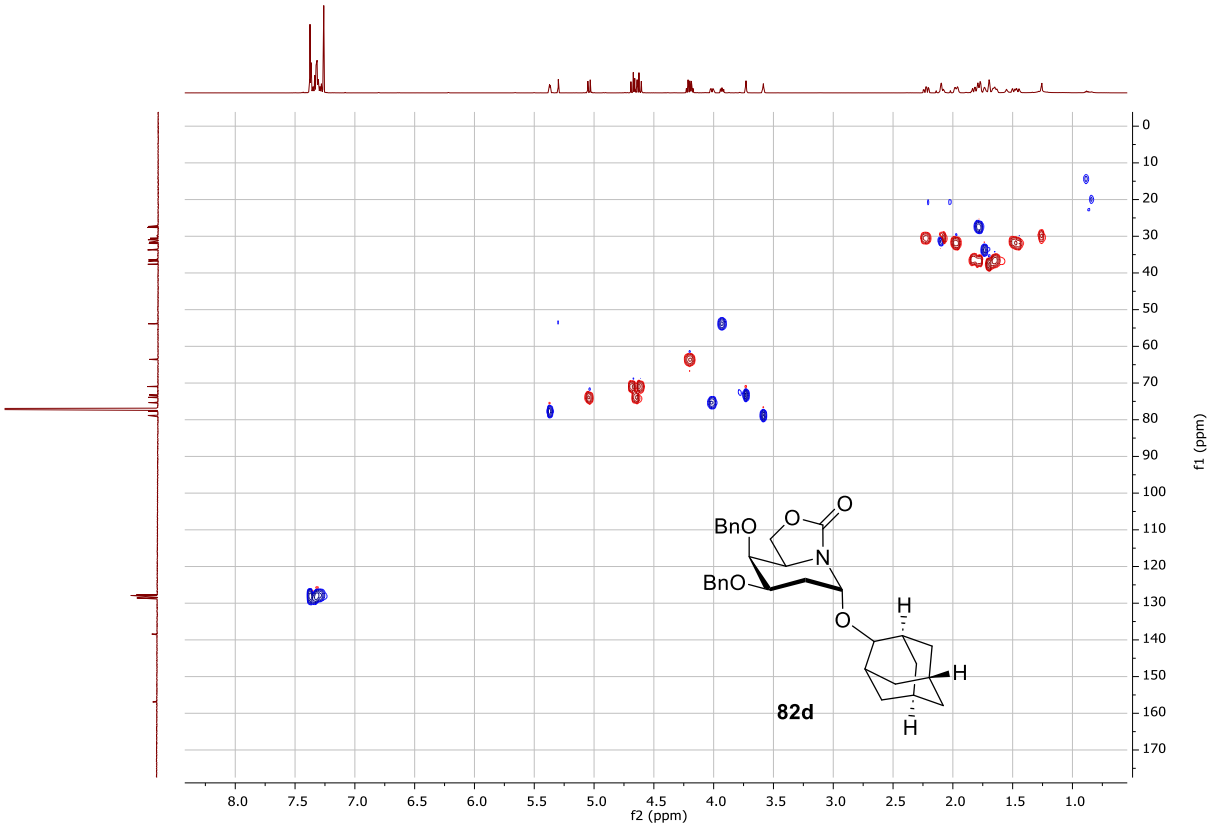

Figure 8.363. HSQC spectra for 82d

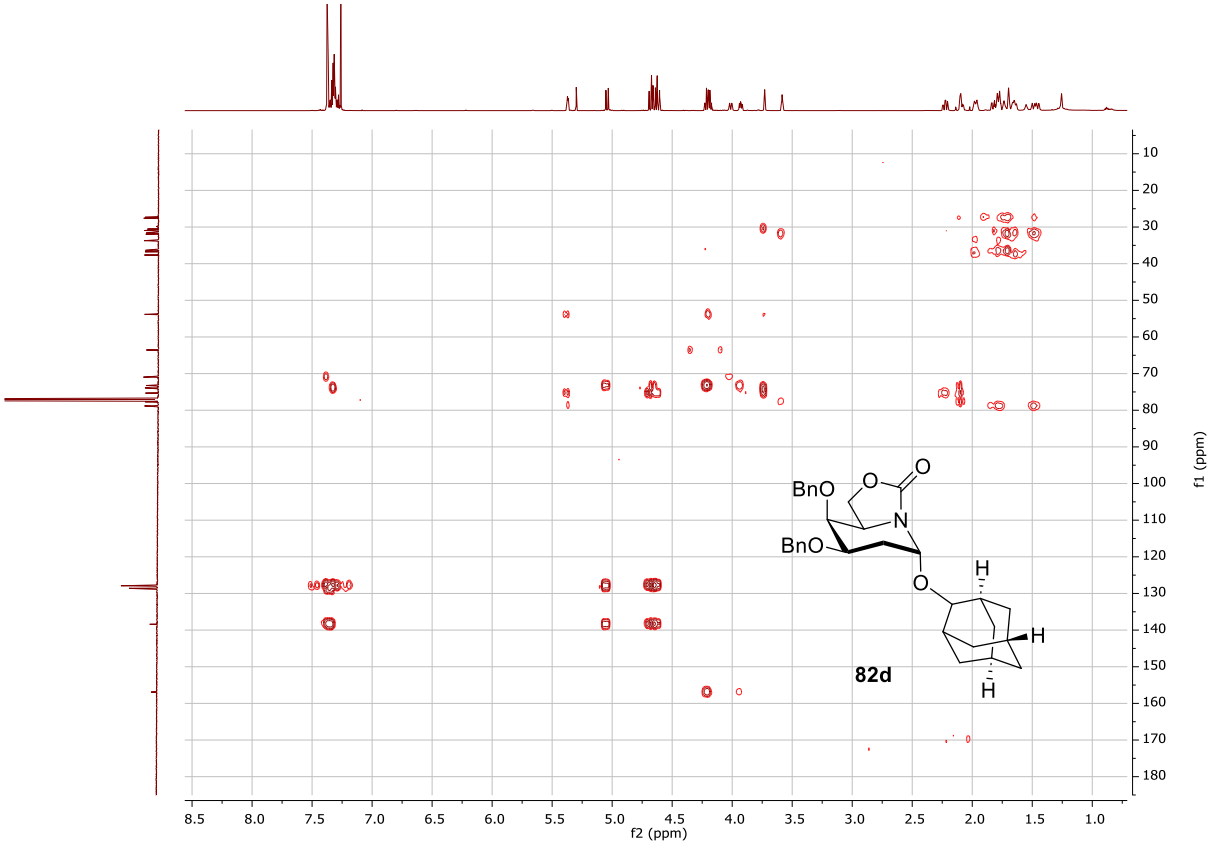

Figure 8.364. HMBC spectra for 82d

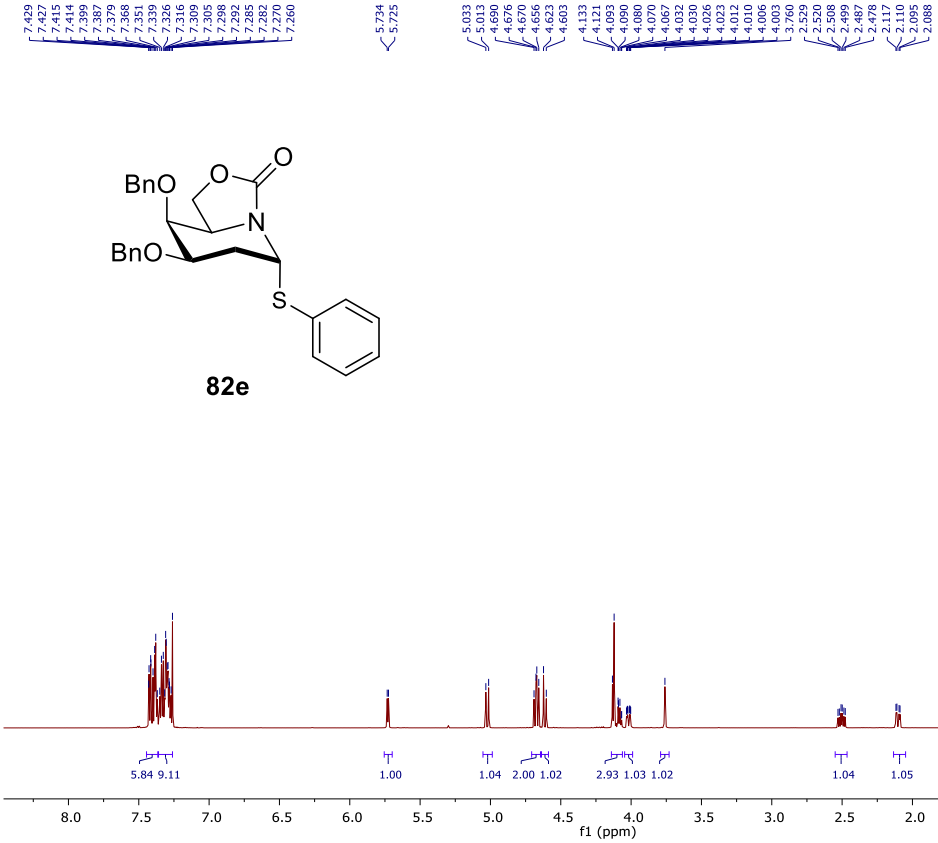

Figure 8.365. ^{1}H NMR spectra for 82e

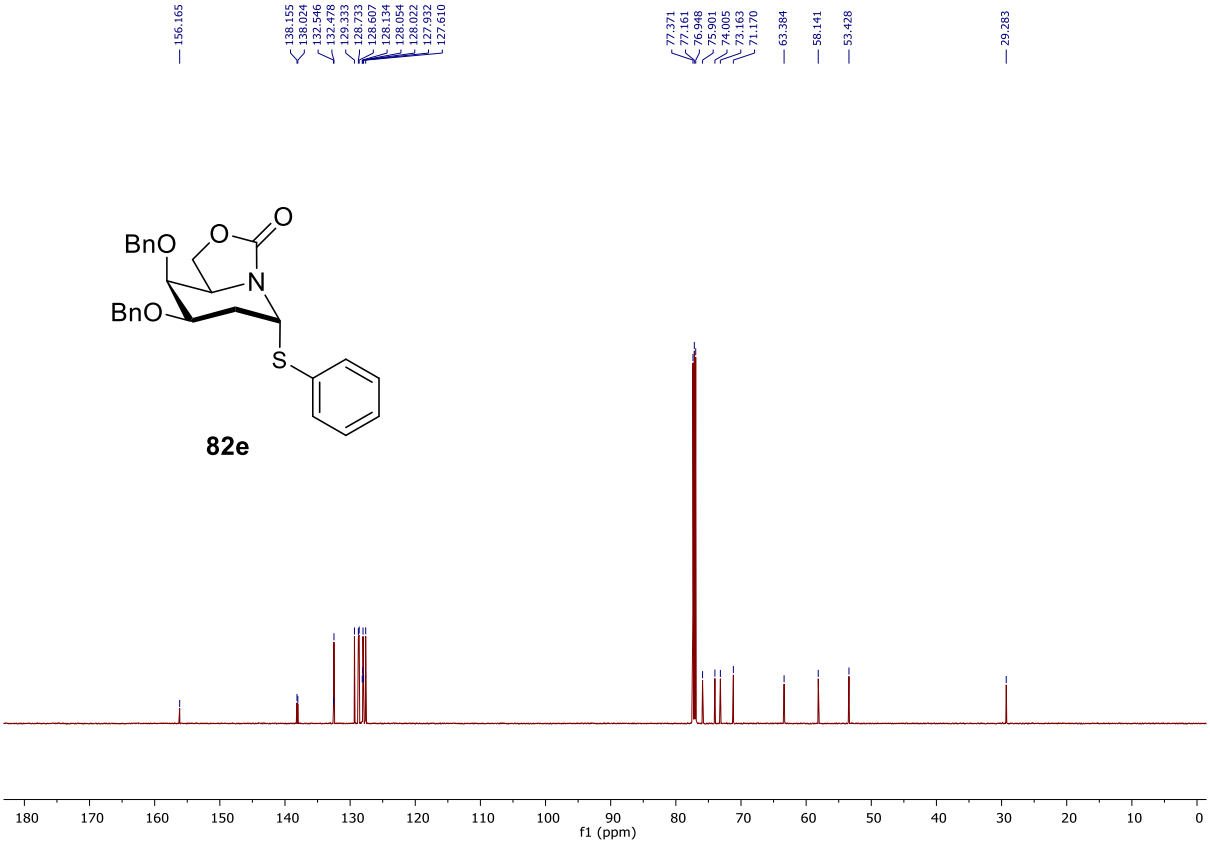

Figure 8.366. ^{13}C NMR spectra for 82e

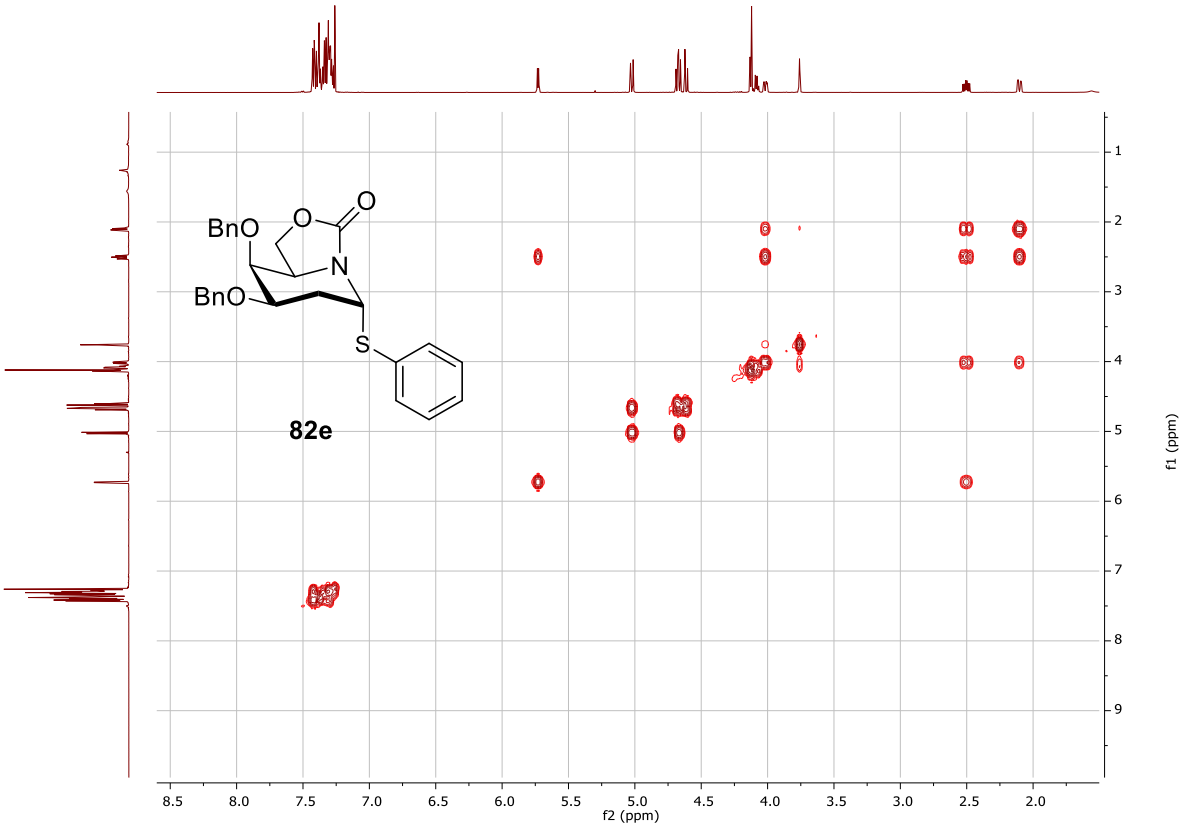

Figure 8.367. COSY spectra for 82e

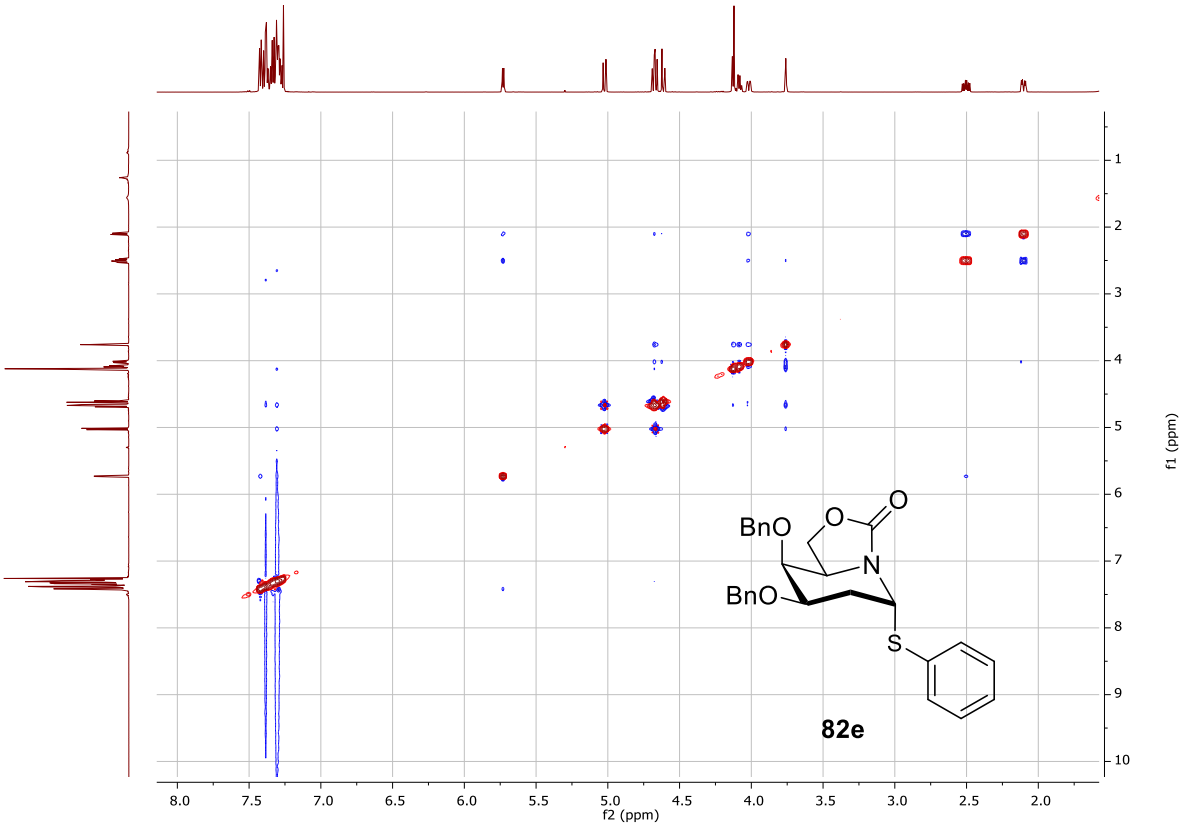

Figure 8.368. NOESY spectra for 82e

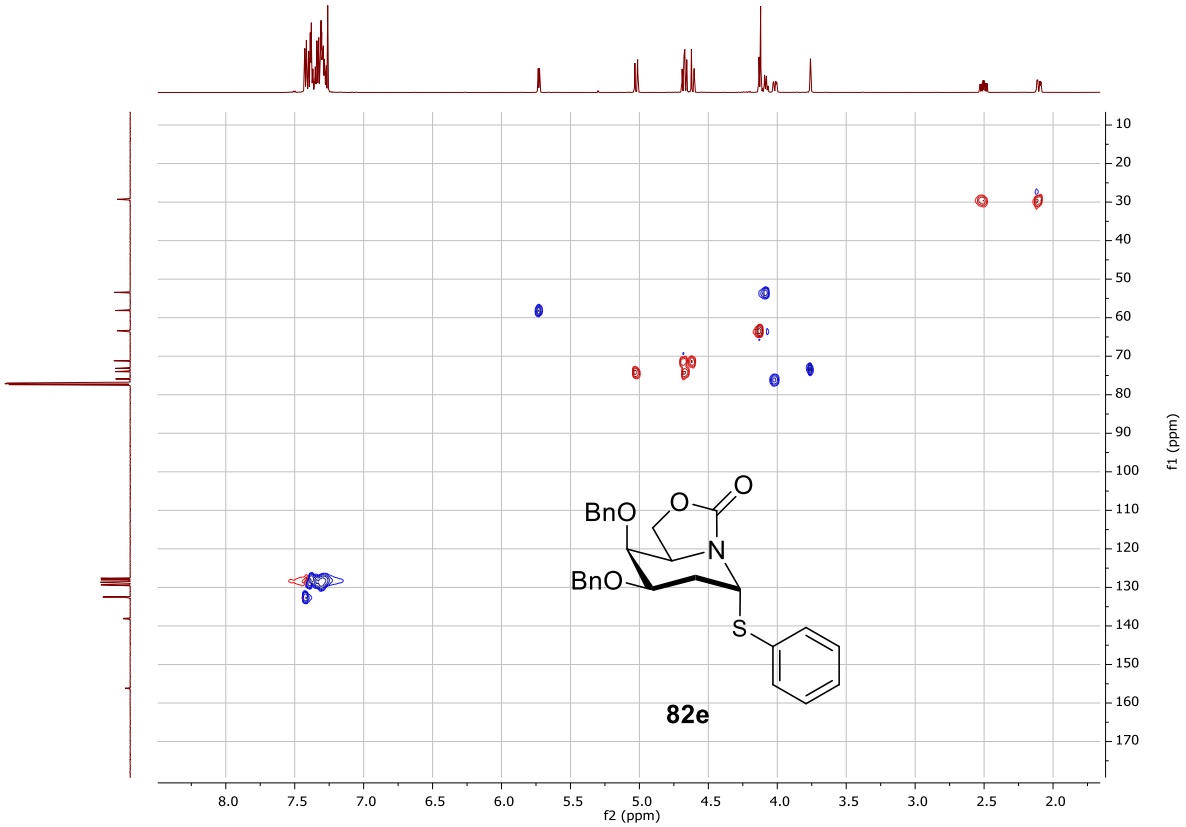

Figure 8.369. HSQC spectra for 82e

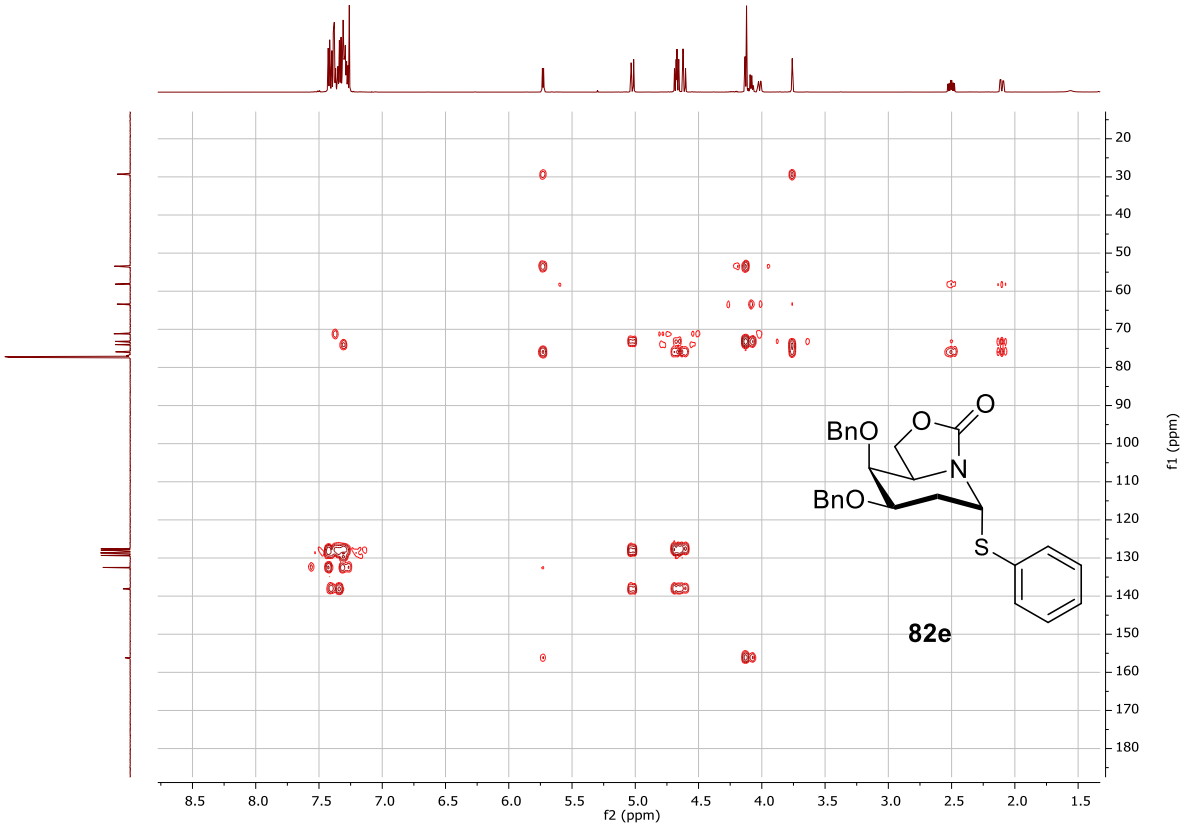

Figure 8.370. HMBC spectra for 82e

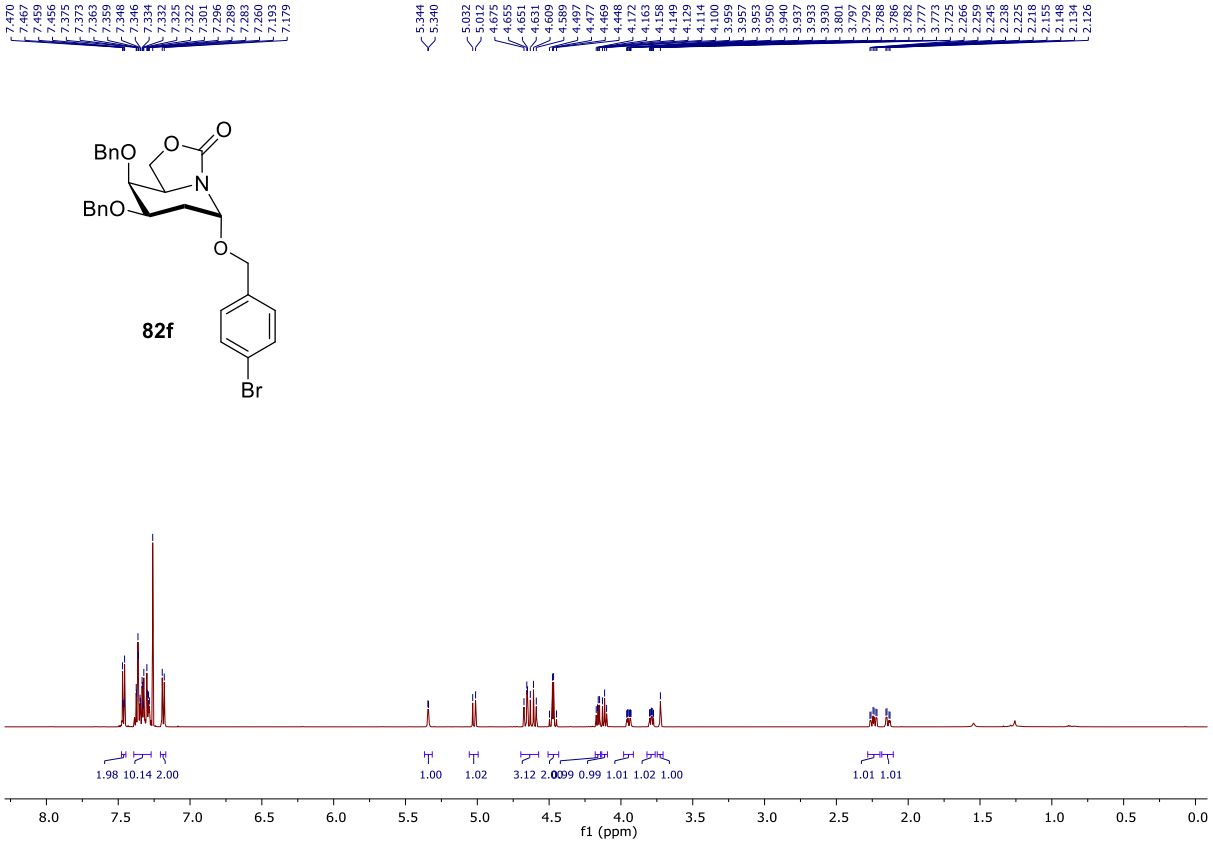

Figure 8.371. ^{1}H NMR spectra for 82f

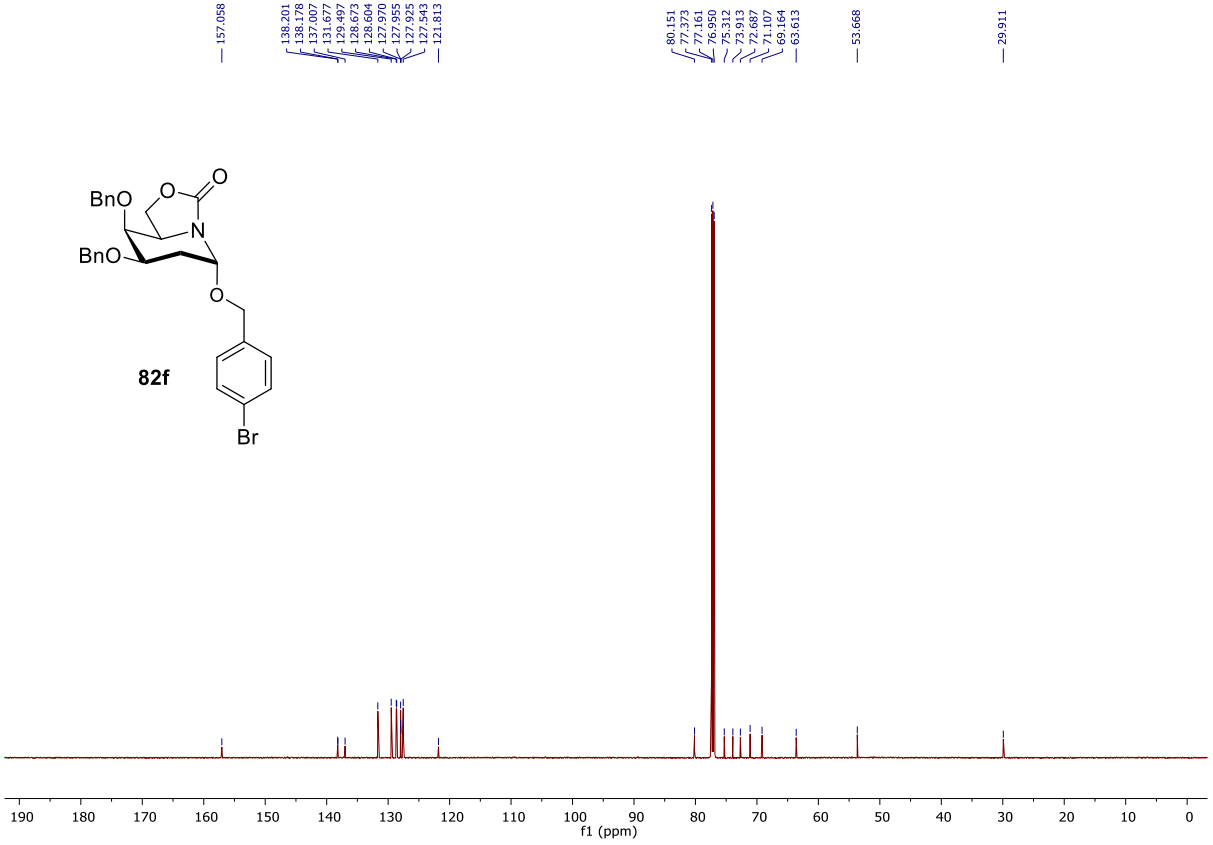

Figure 8.372. ^{13}C NMR spectra for 82f

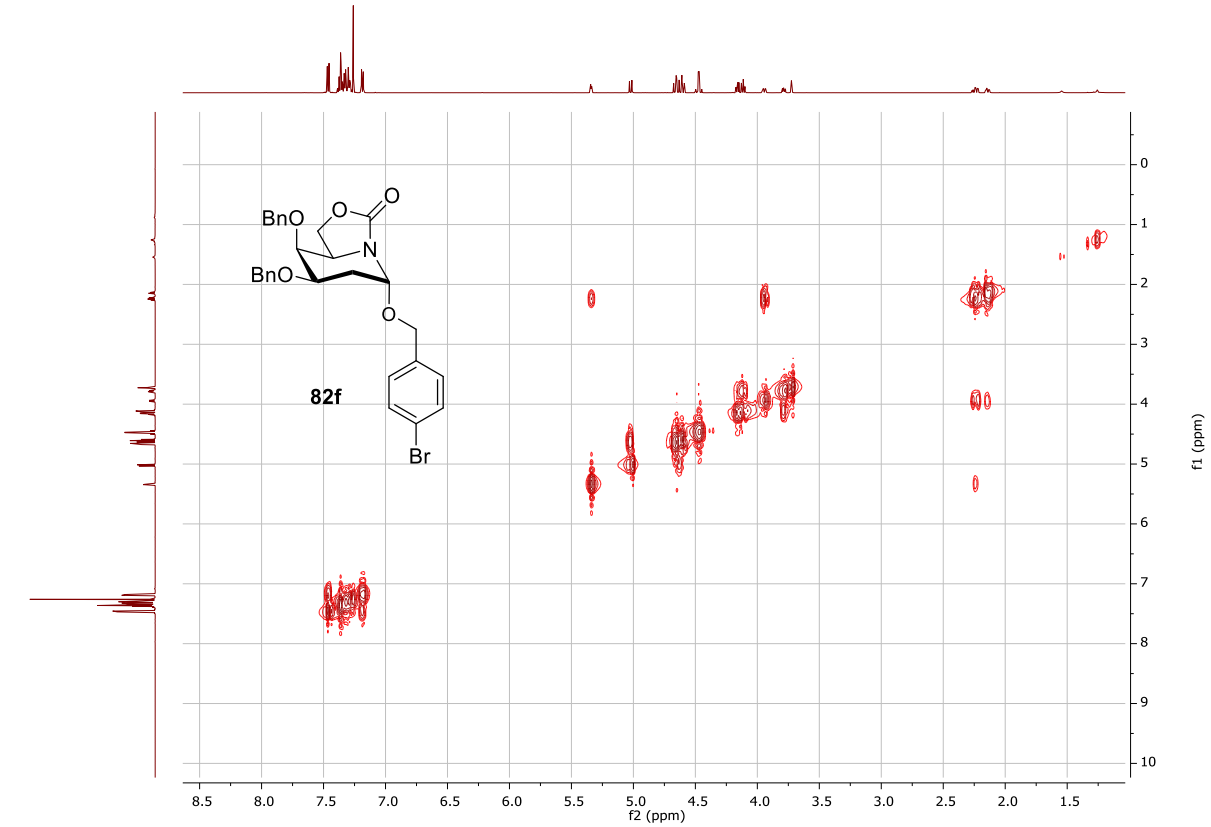

Figure 8.373. COSY spectra for 82f

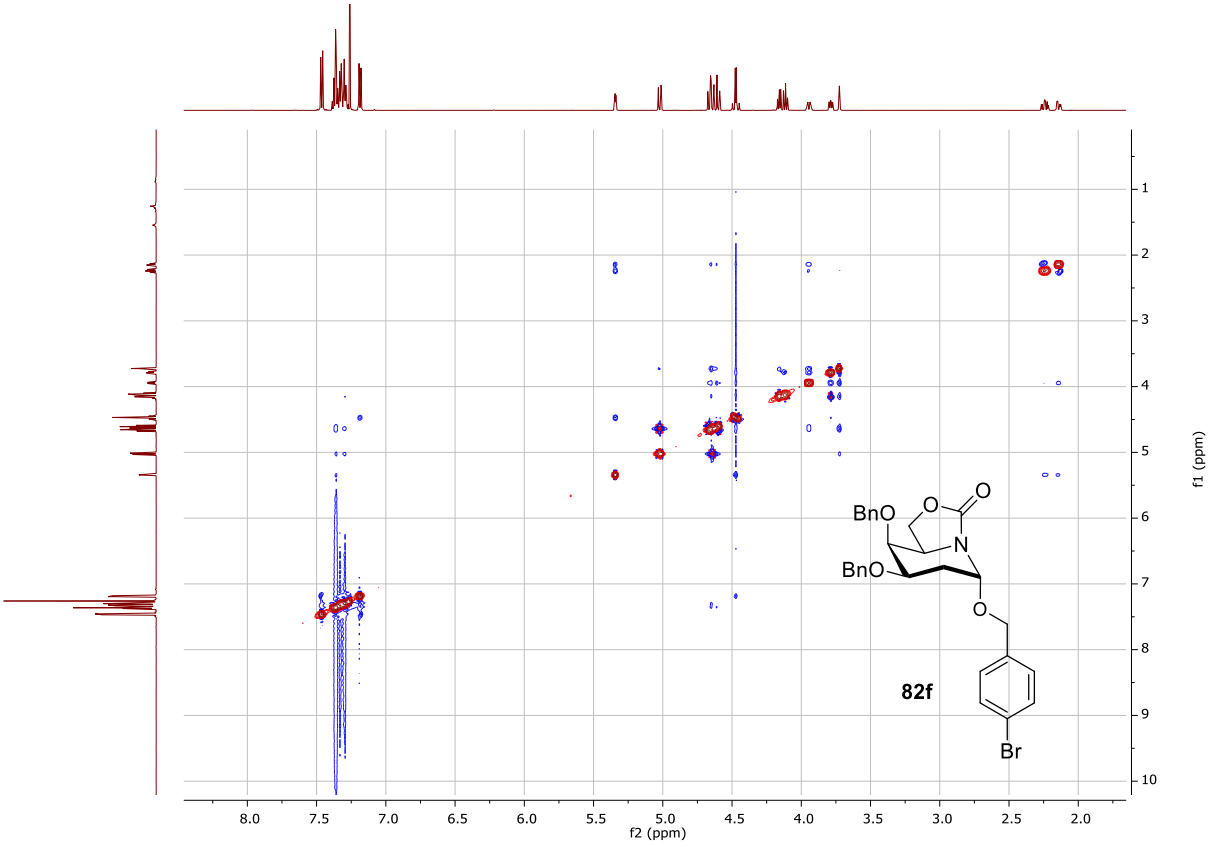

Figure 8.374. NOESY spectra for 82f

Figure 8.375. HSQC spectra for 82f

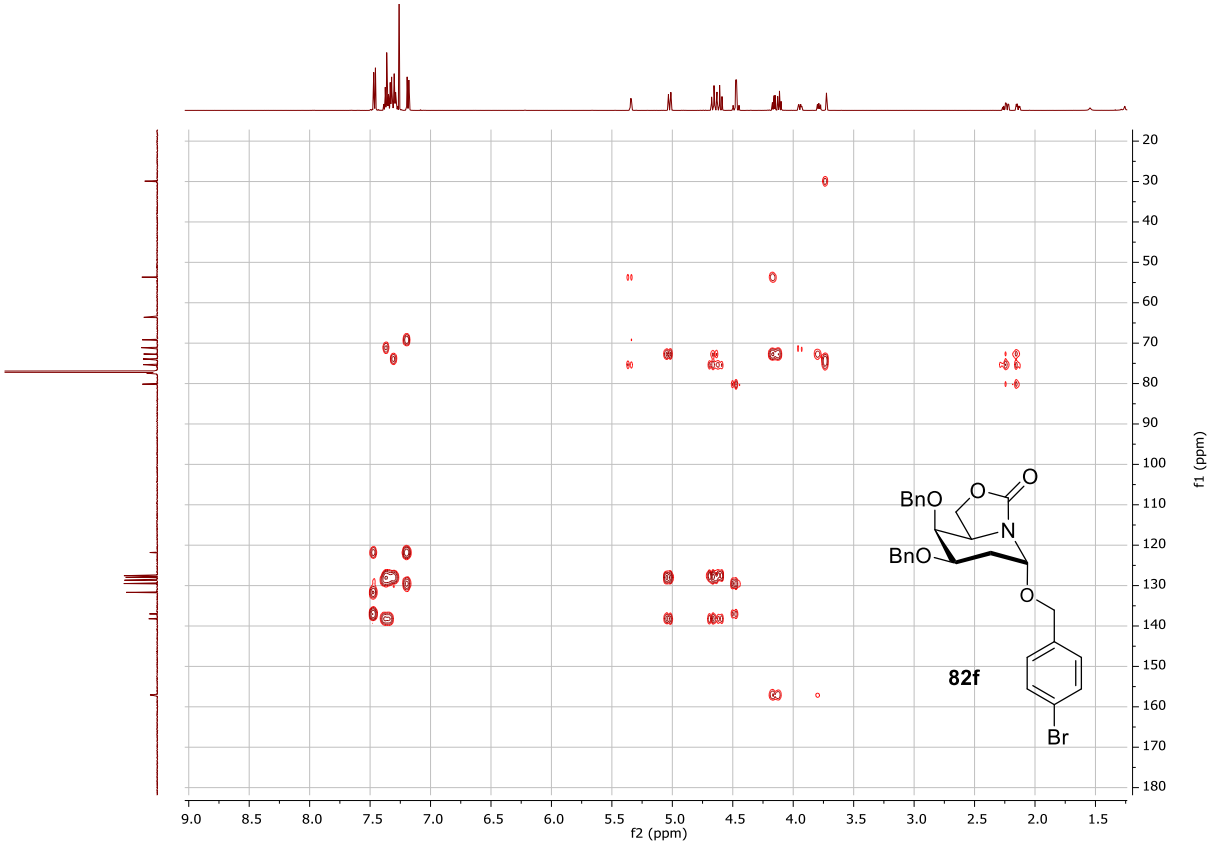

Figure 8.376. HMBC spectra for 82f

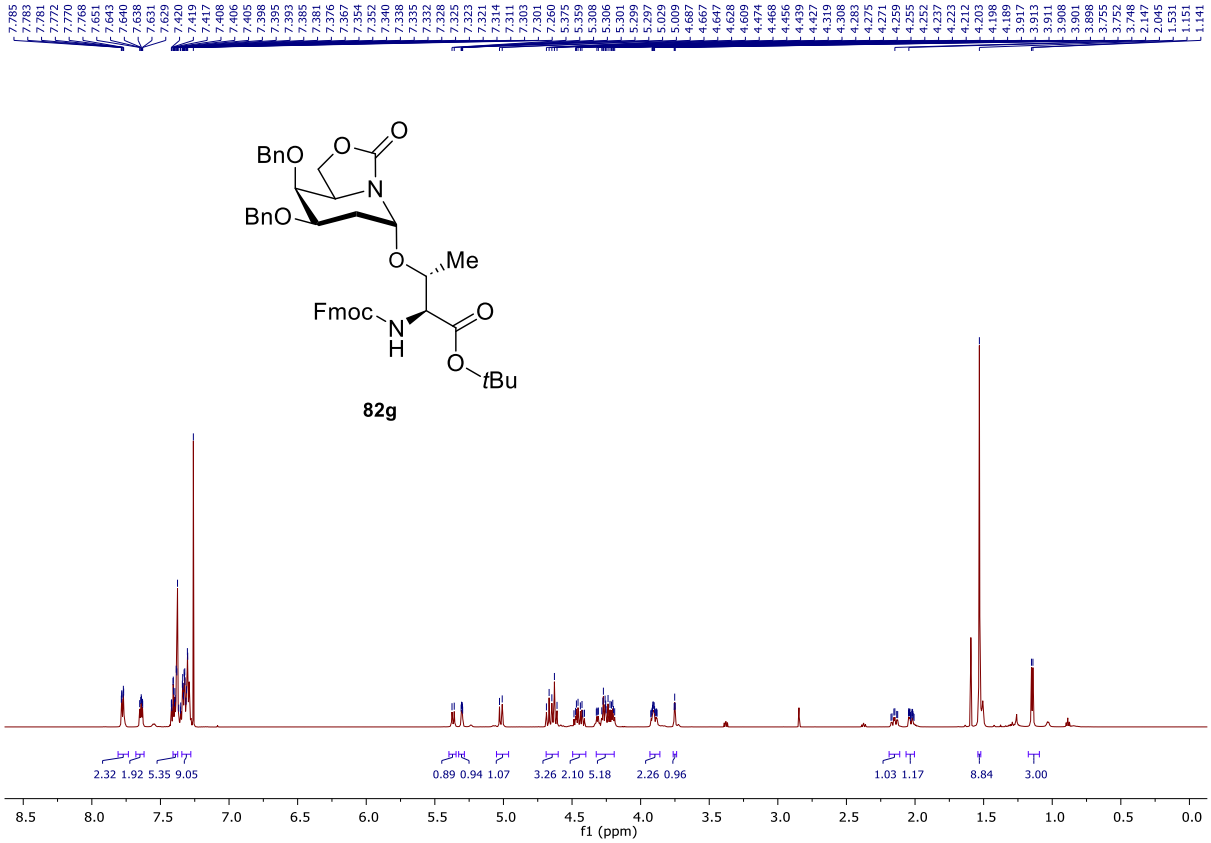

Figure 8.377. ^{1}H NMR spectra for 82g

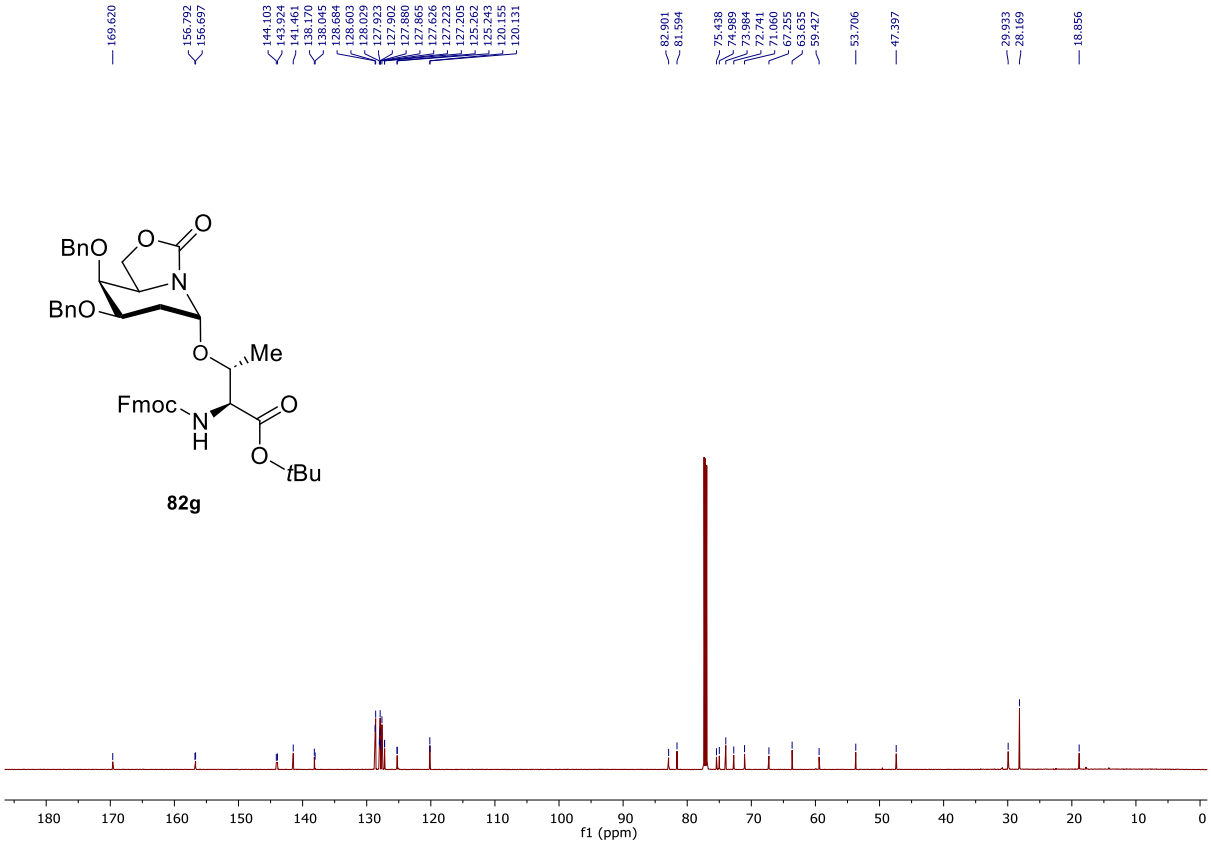

Figure 8.378. ^{13}C NMR spectra for 82g

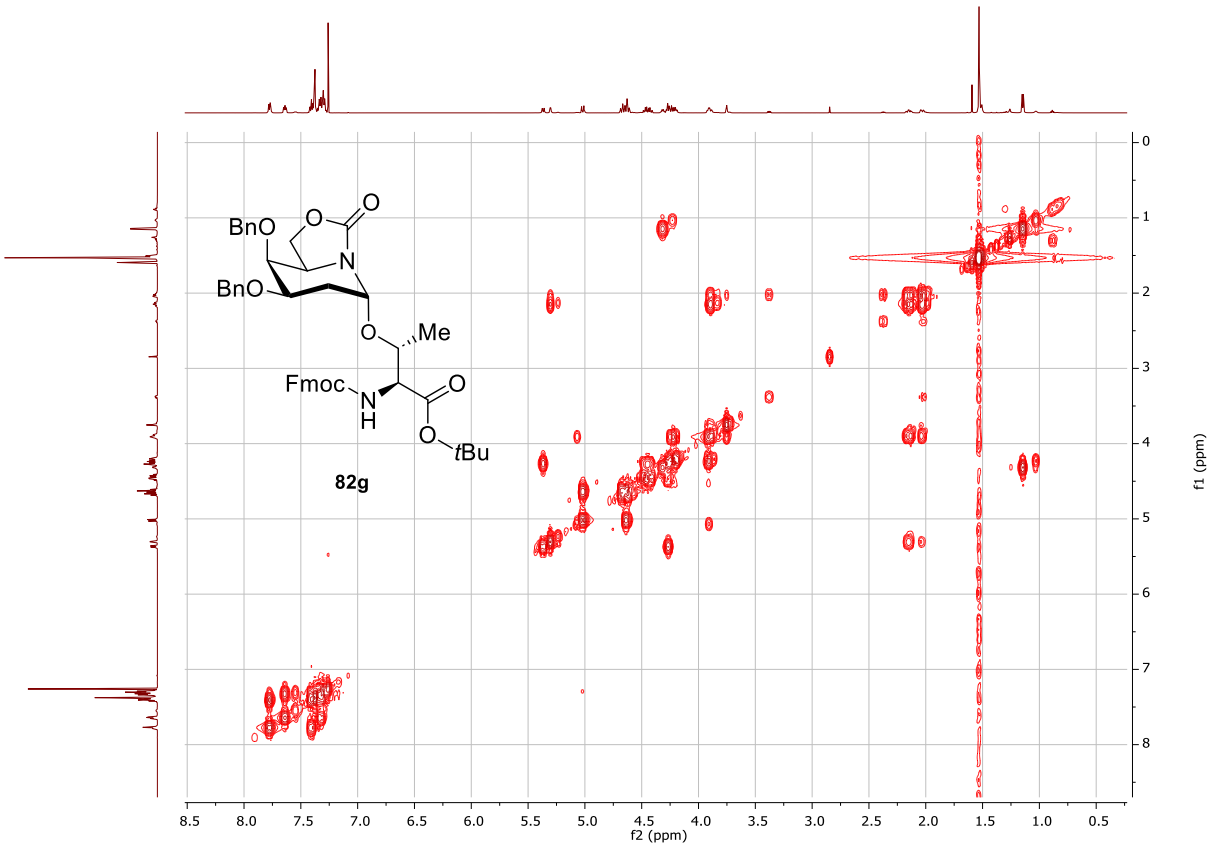

Figure 8.379. COSY spectra for 82g

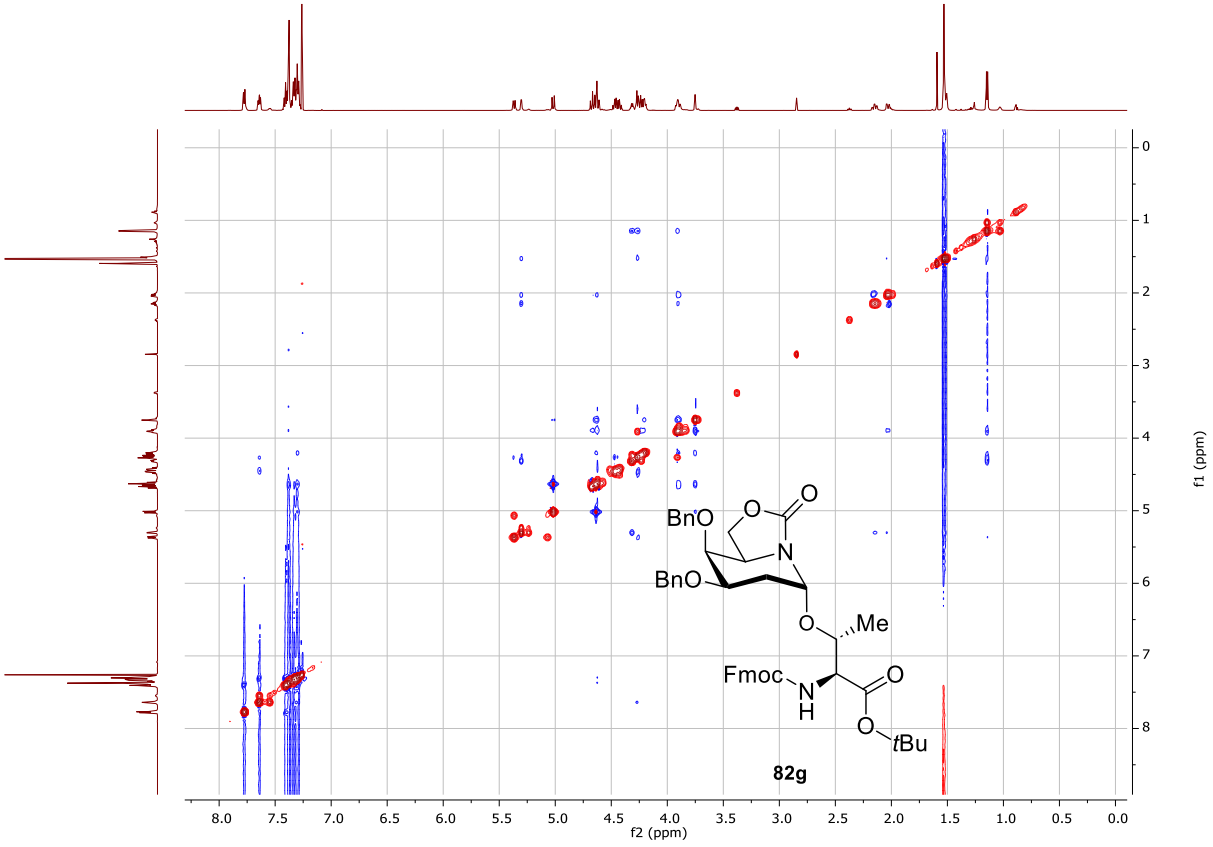

Figure 8.380. NOESY spectra for 82g

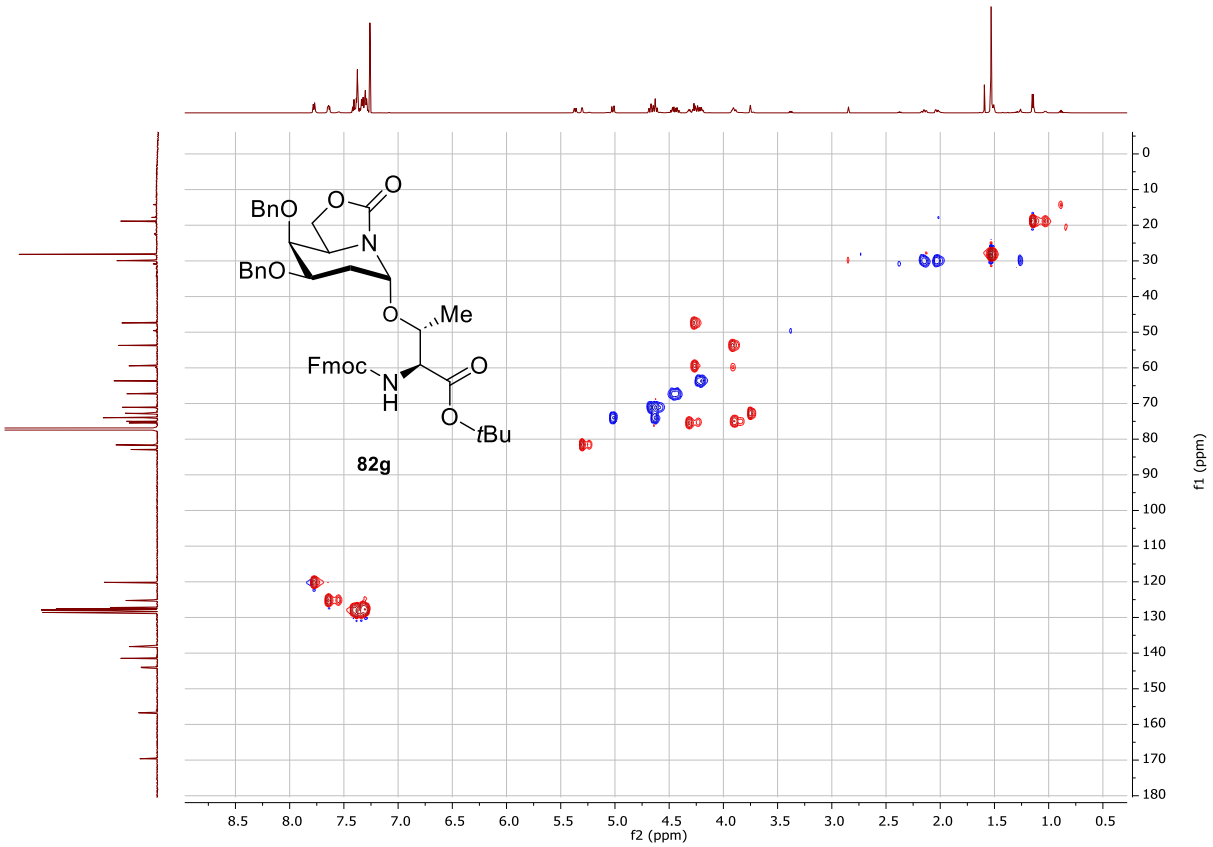

Figure 8.381. HSQC spectra for 82g

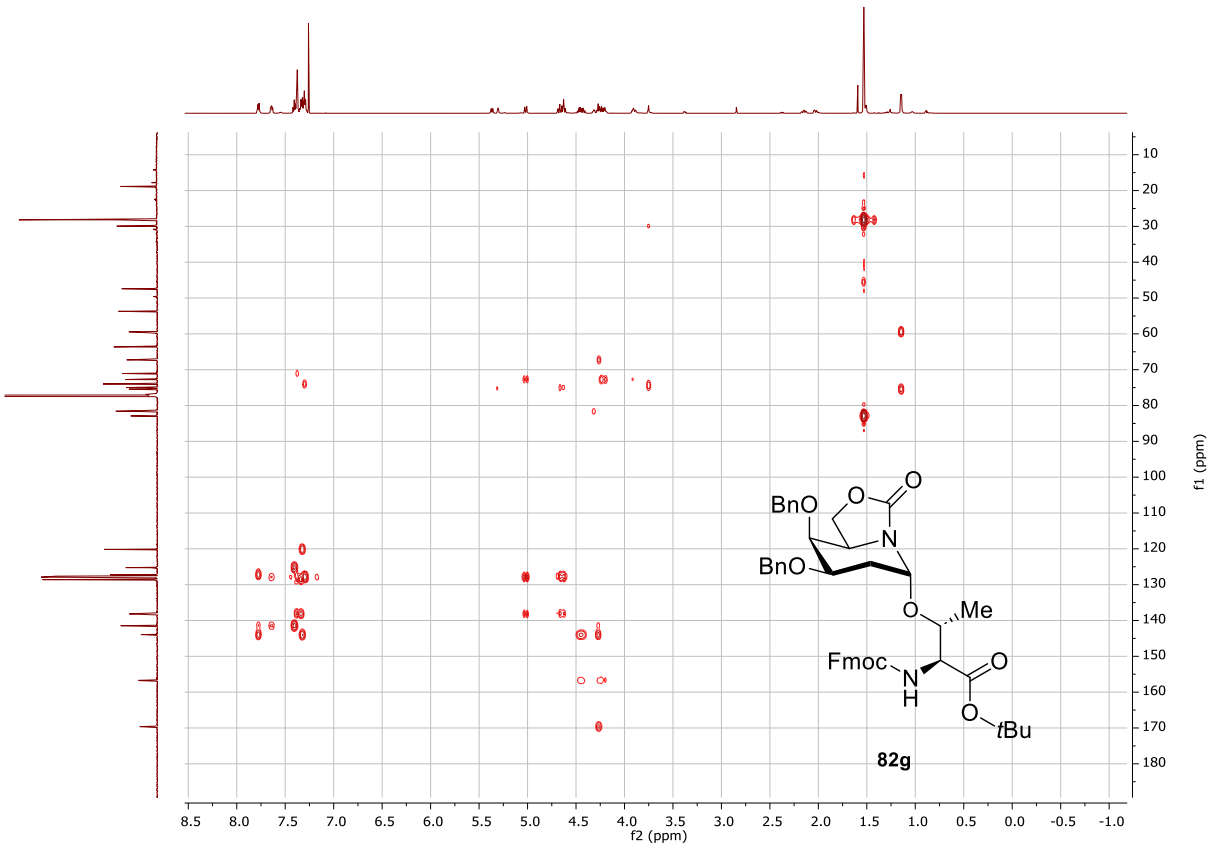

Figure 8.382. HMBC spectra for 82g

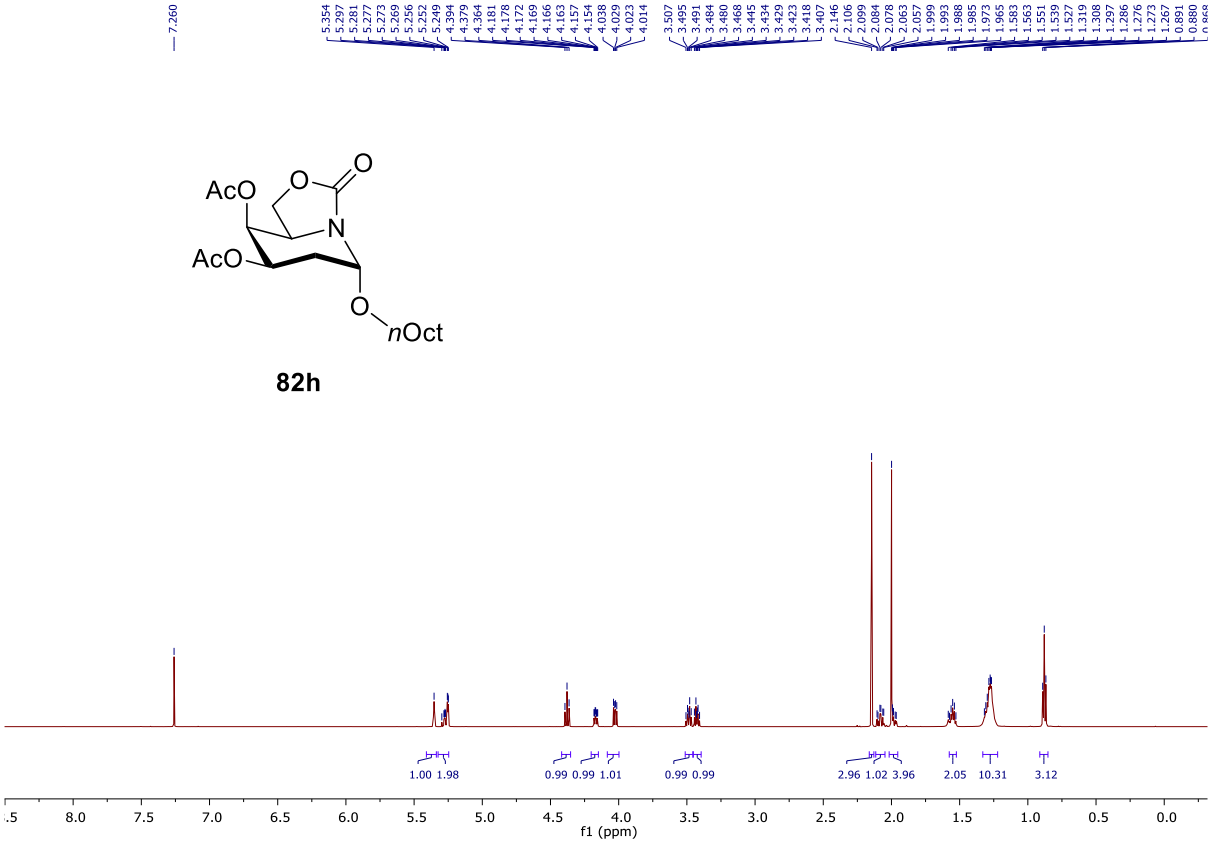

Figure 8.383. ^{1}H NMR spectra for 82h

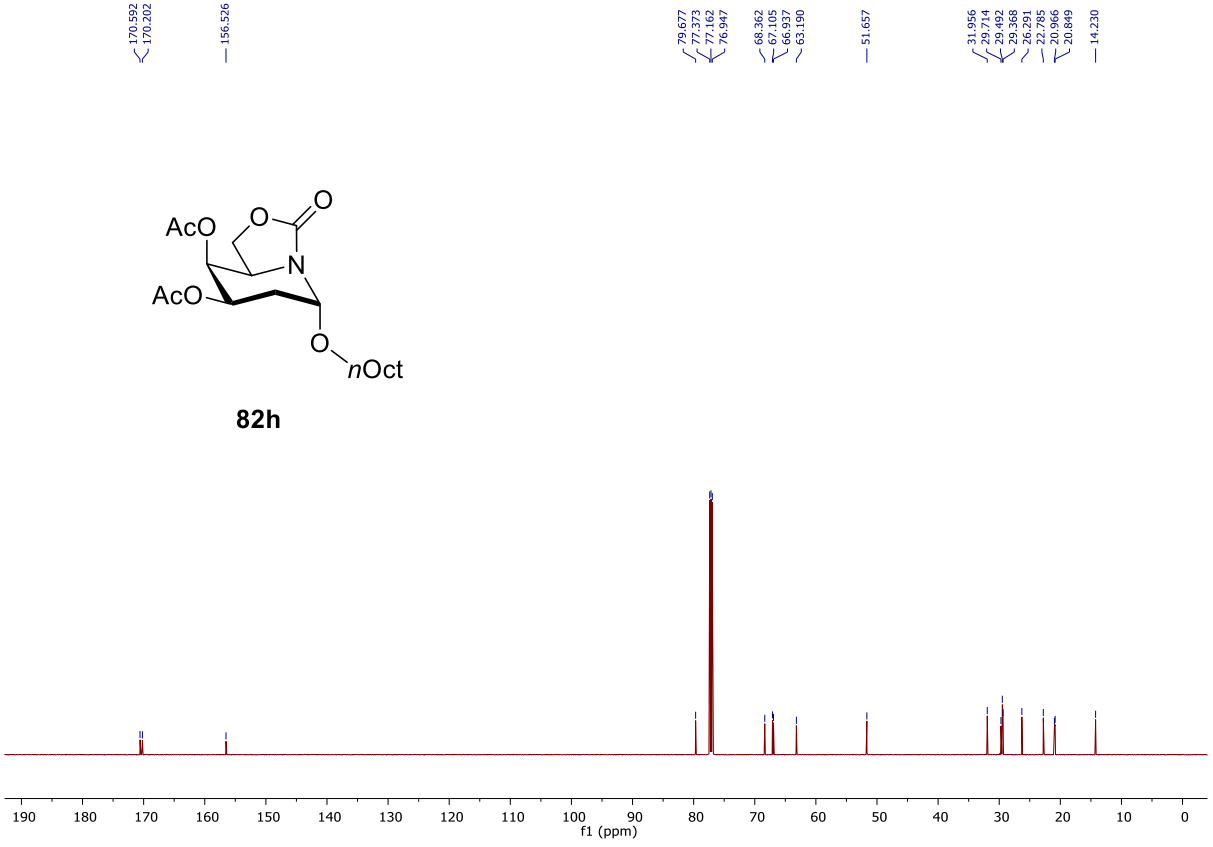

Figure 8.384. ^{13}C NMR spectra for 82h

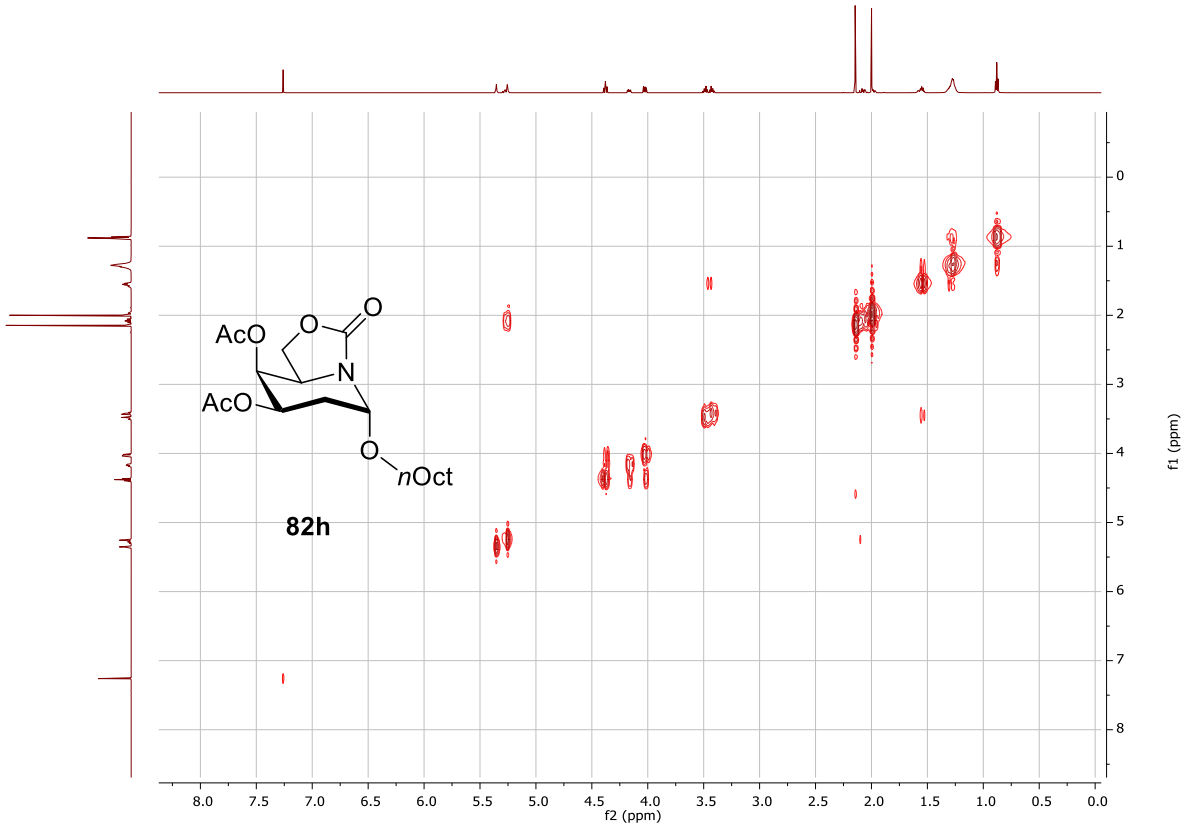

Figure 8.385. COSY spectra for 82h

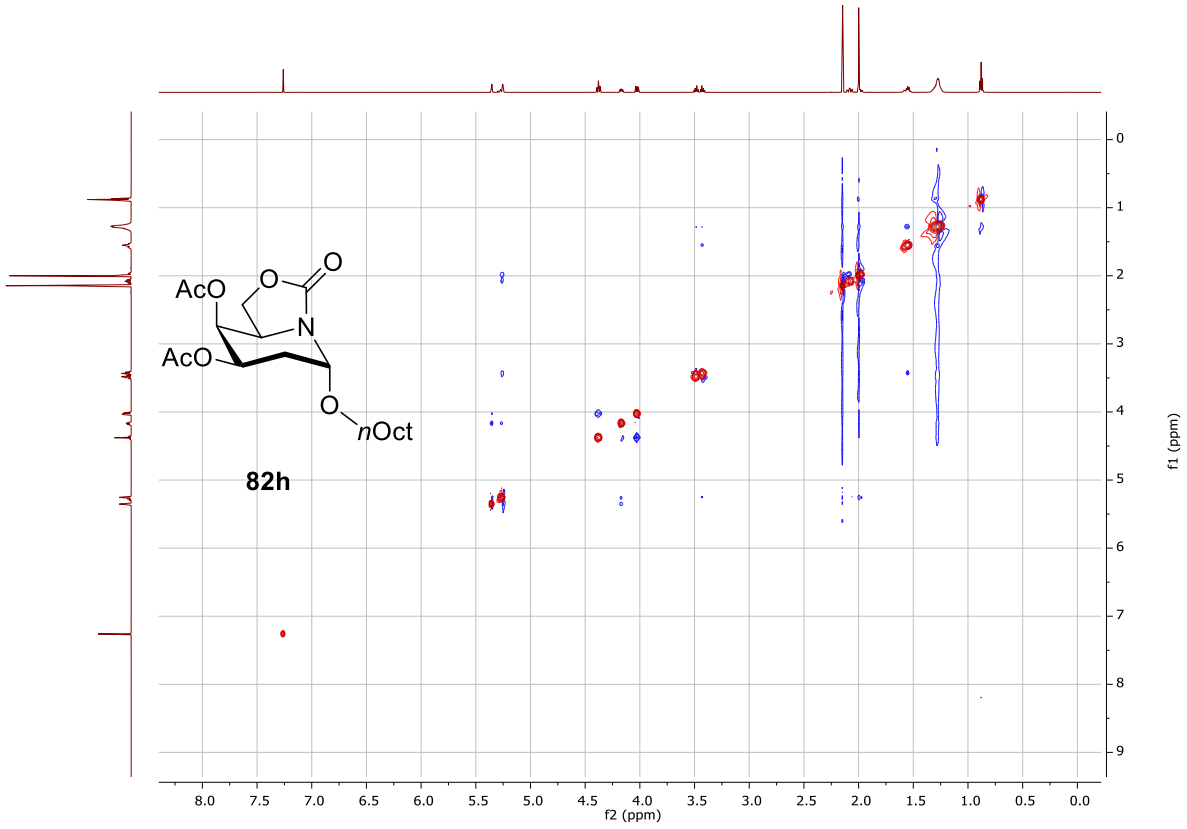

Figure 8.386. NOESY spectra for 82h

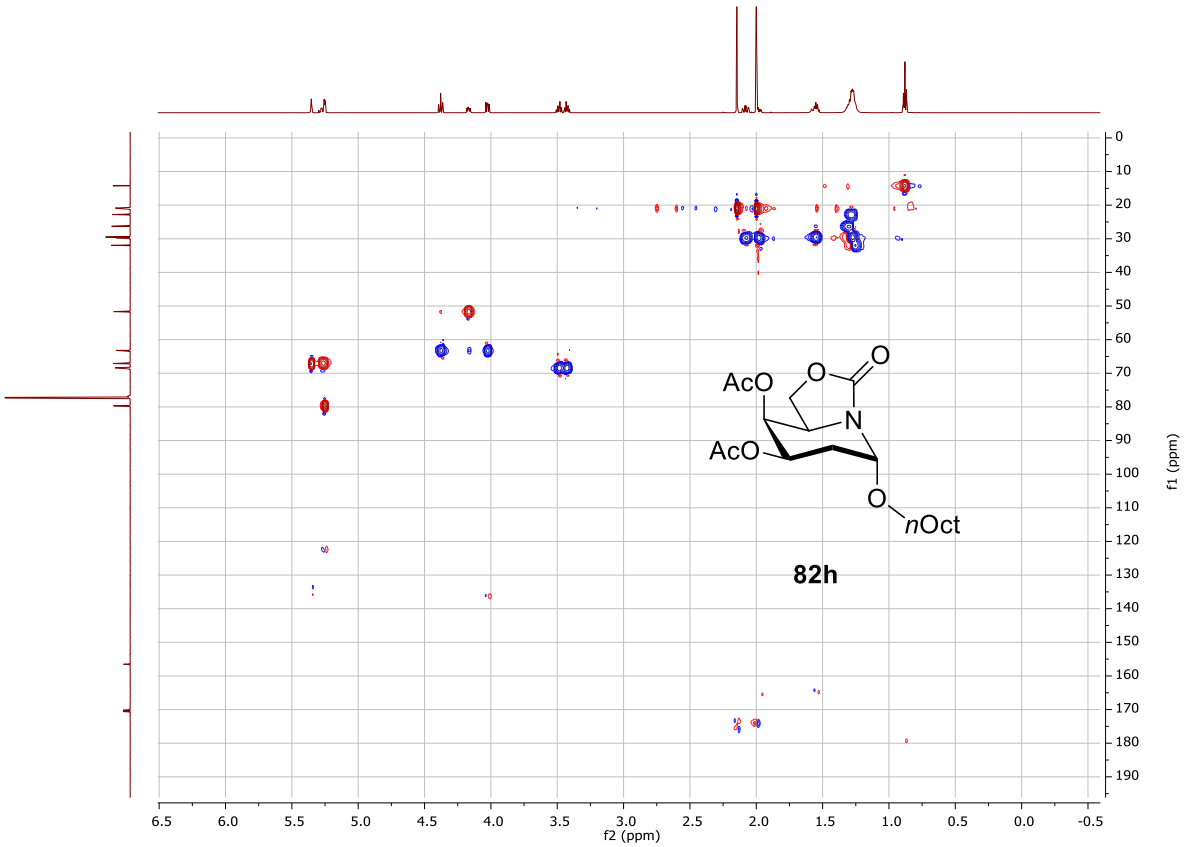

Figure 8.387. HSQC spectra for 82h

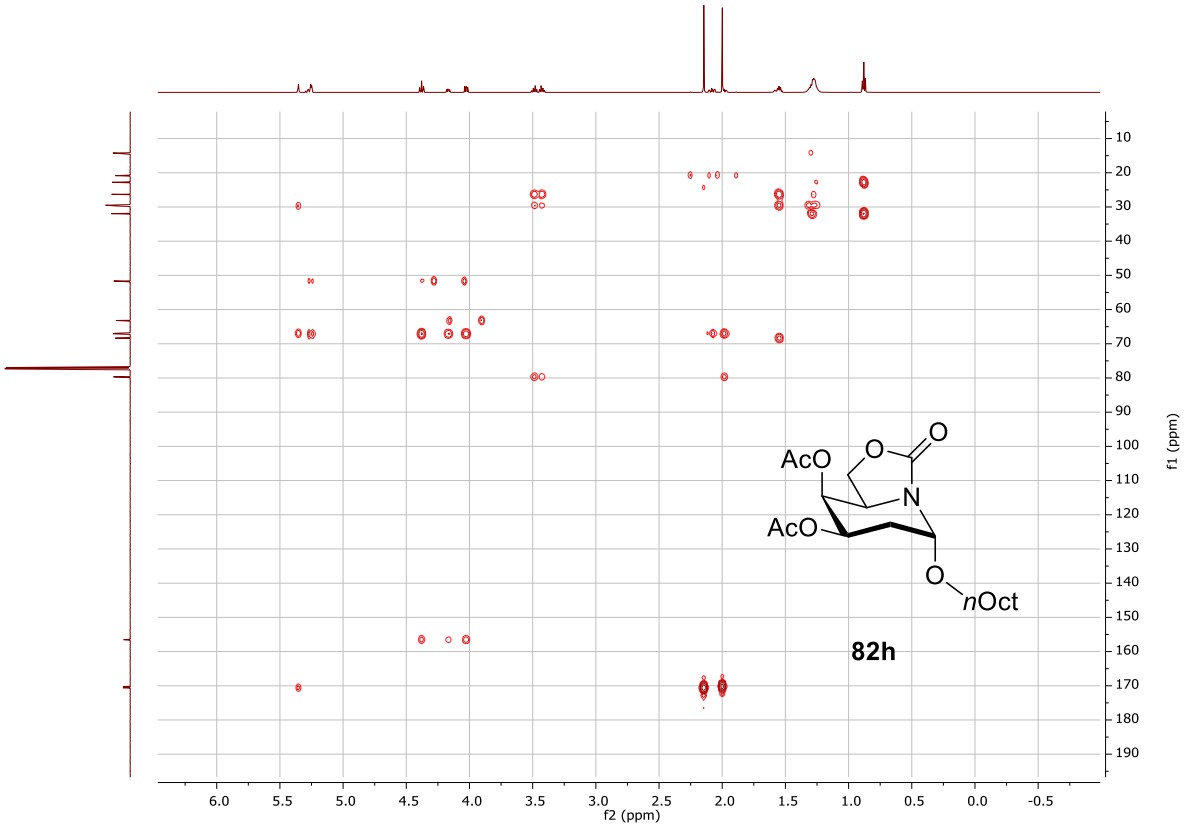

Figure 8.388. HMBC spectra for 82h

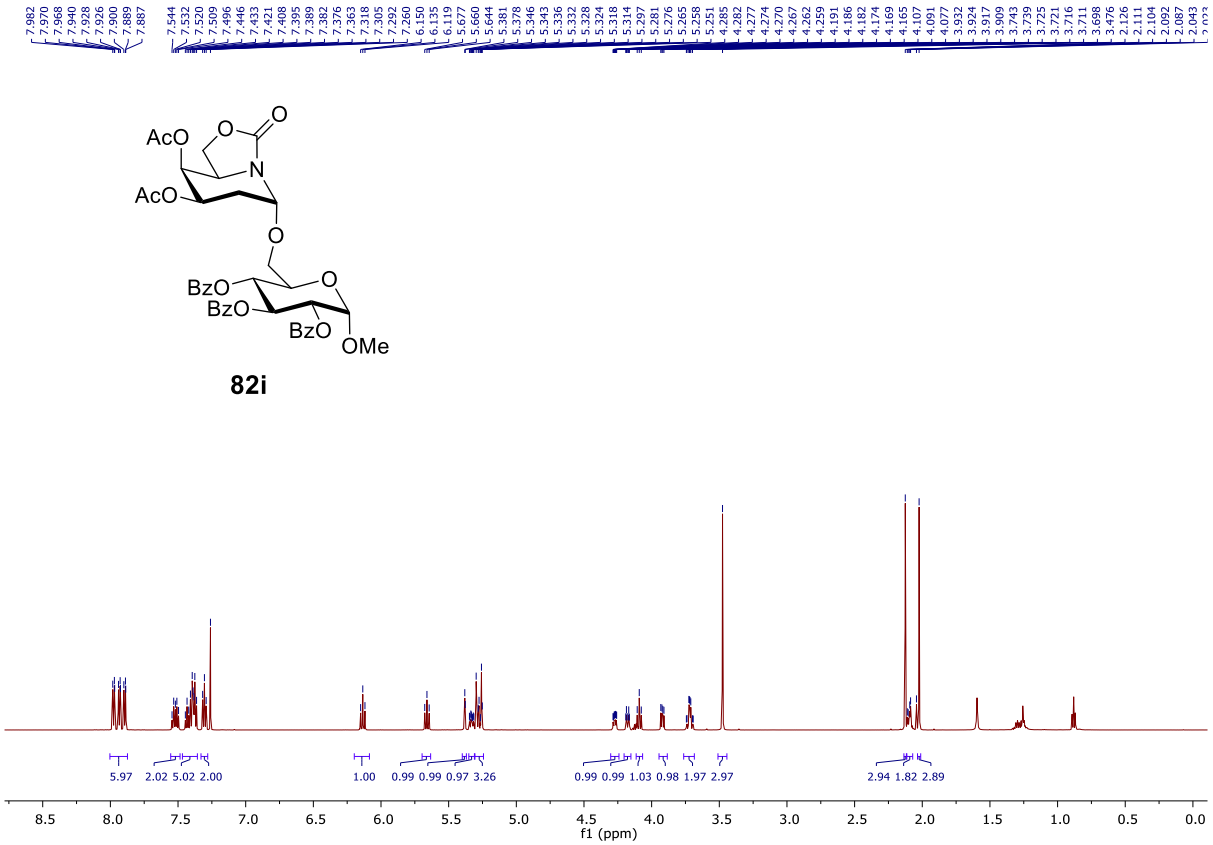

Figure 8.389. ^{1}H NMR spectra for 82i

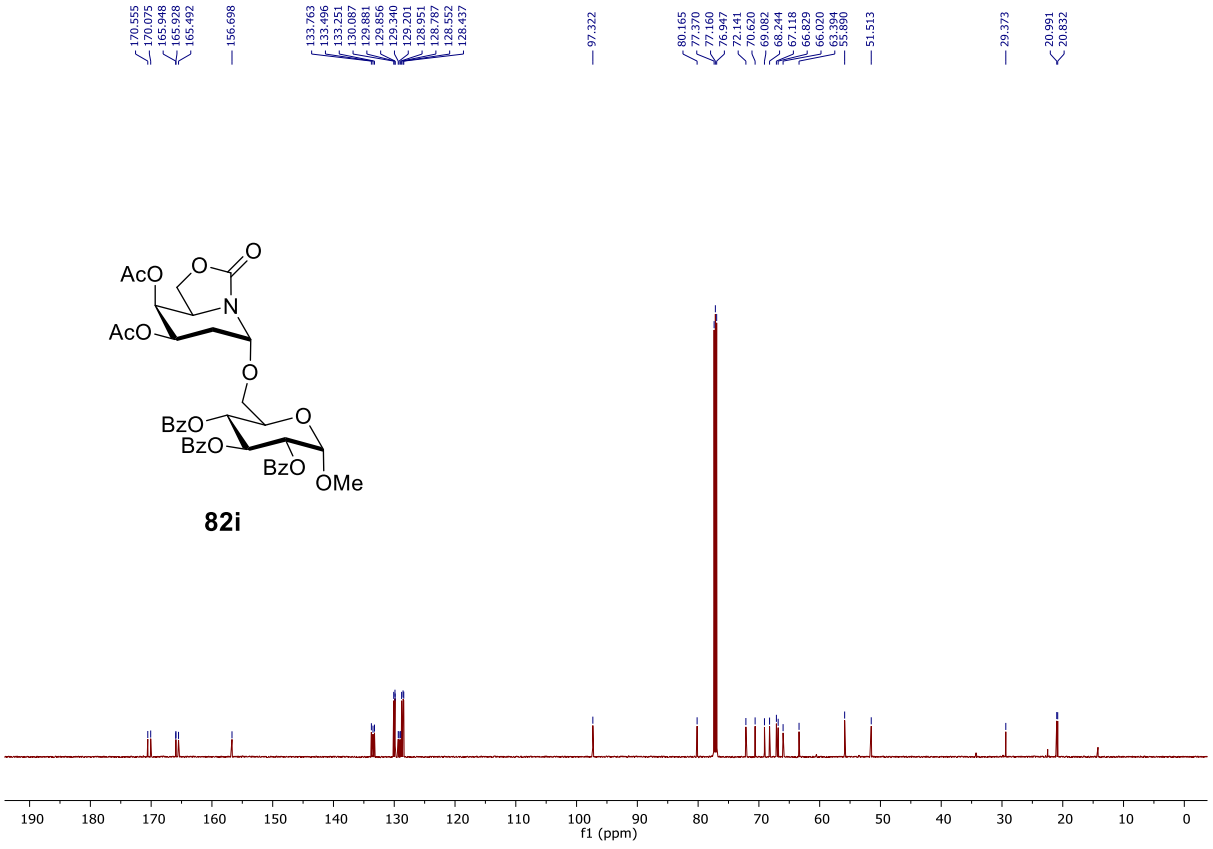

Figure 8.390. ^{13}C NMR spectra for 82i

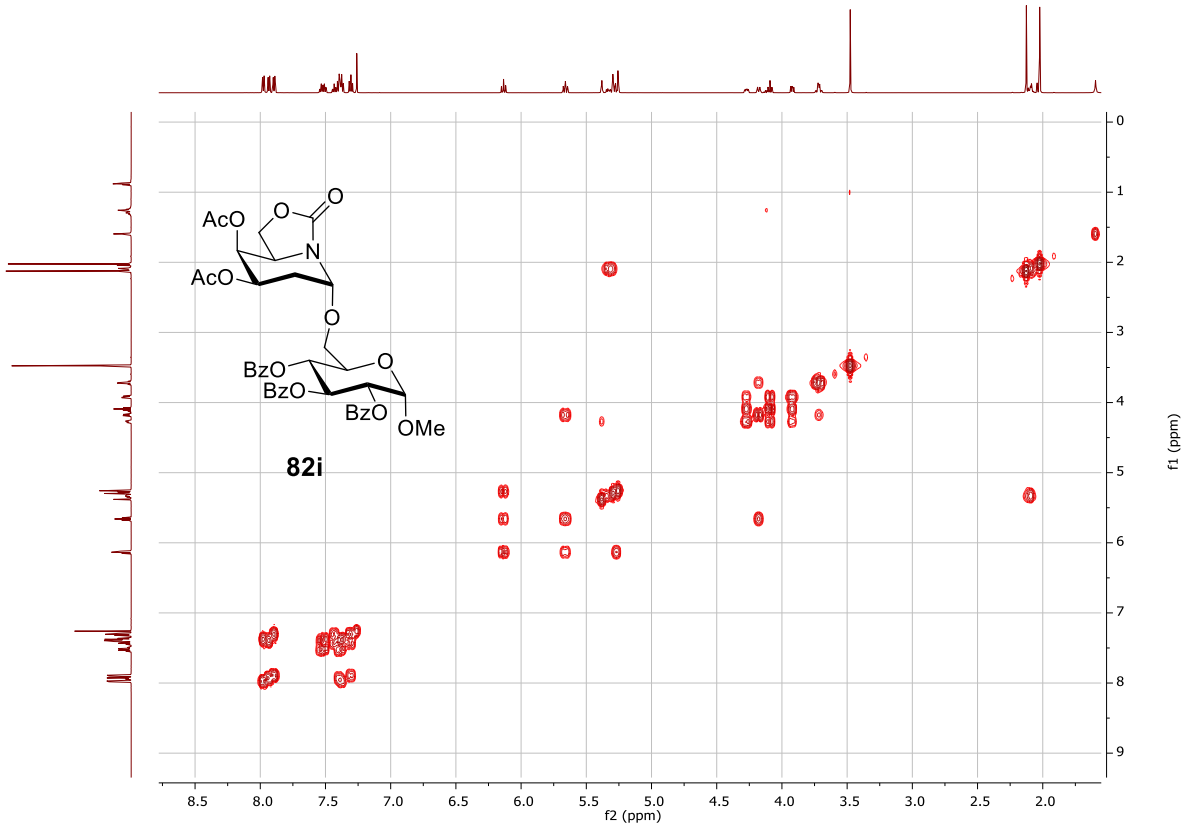

Figure 8.391. COSY spectra for 82i

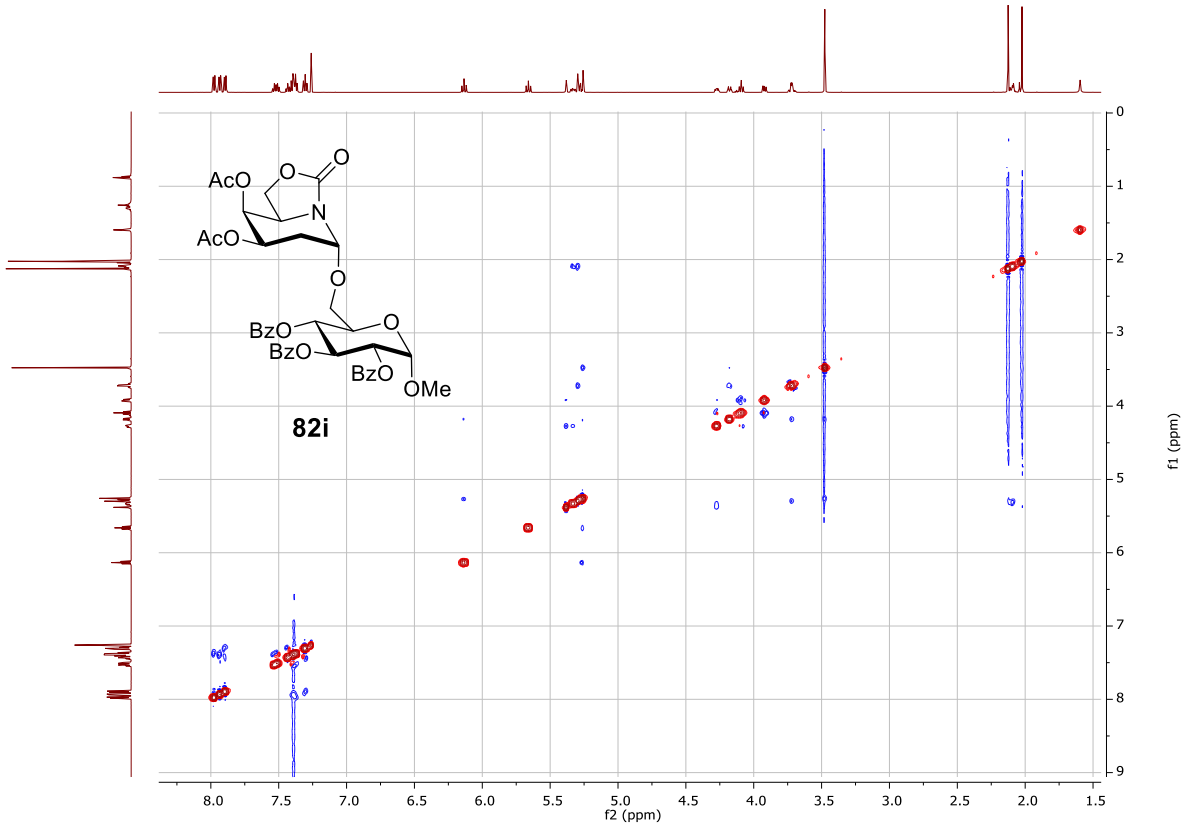

Figure 8.392. NOESY spectra for 82i

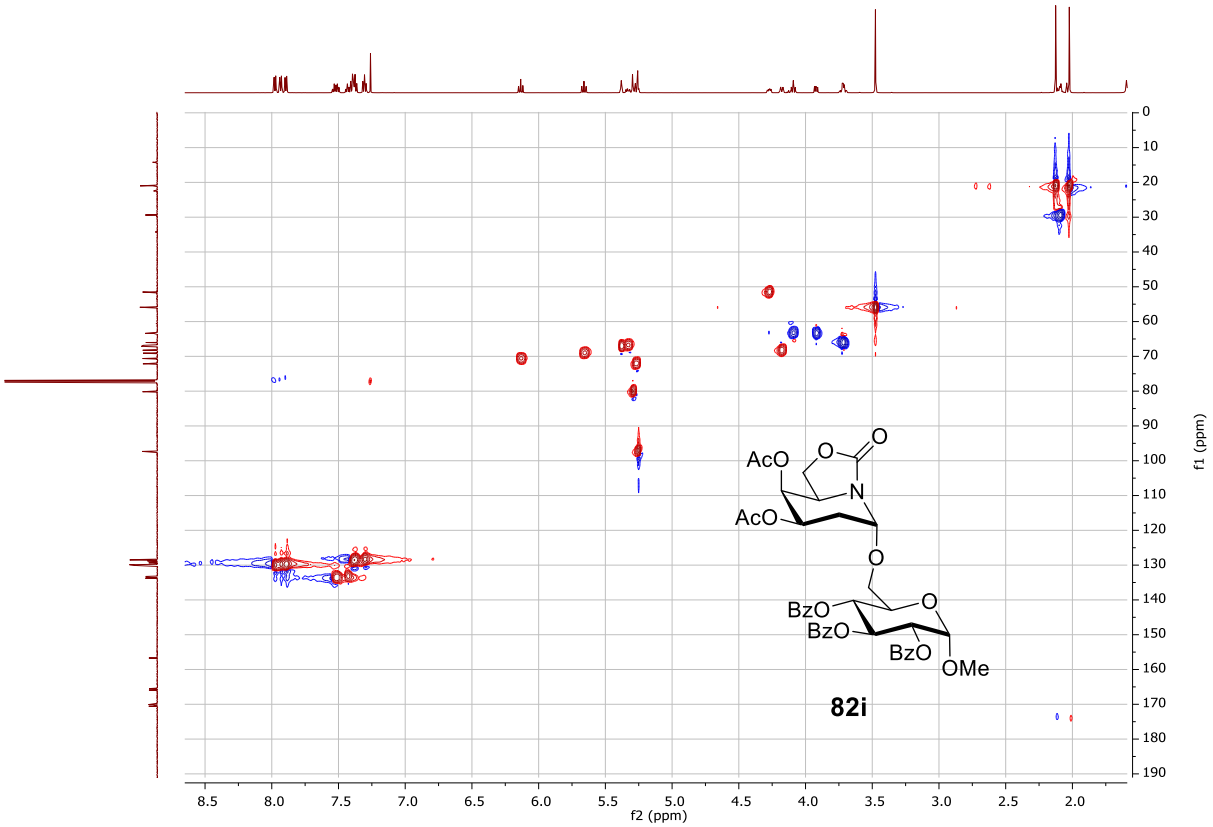

Figure 8.393. HSQC spectra for 82i

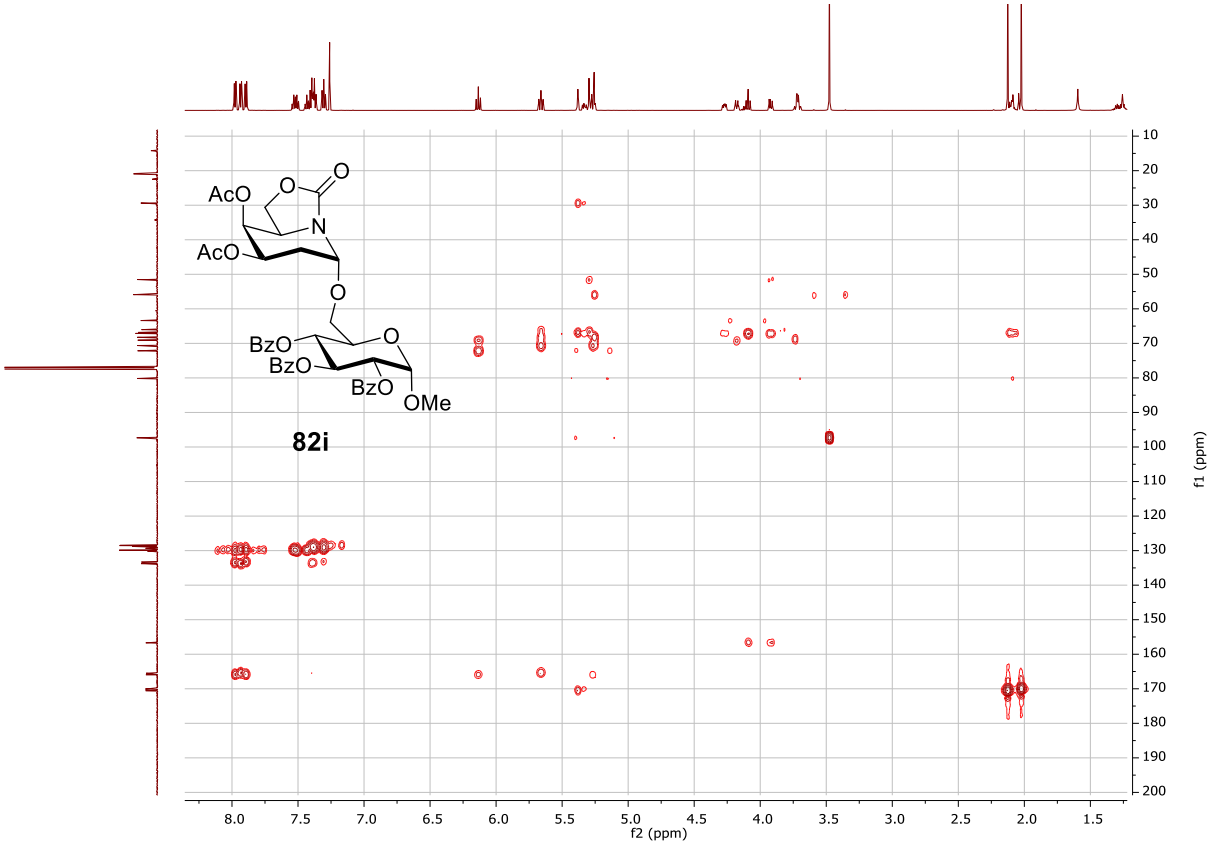

Figure 8.394. HMBC spectra for 82i

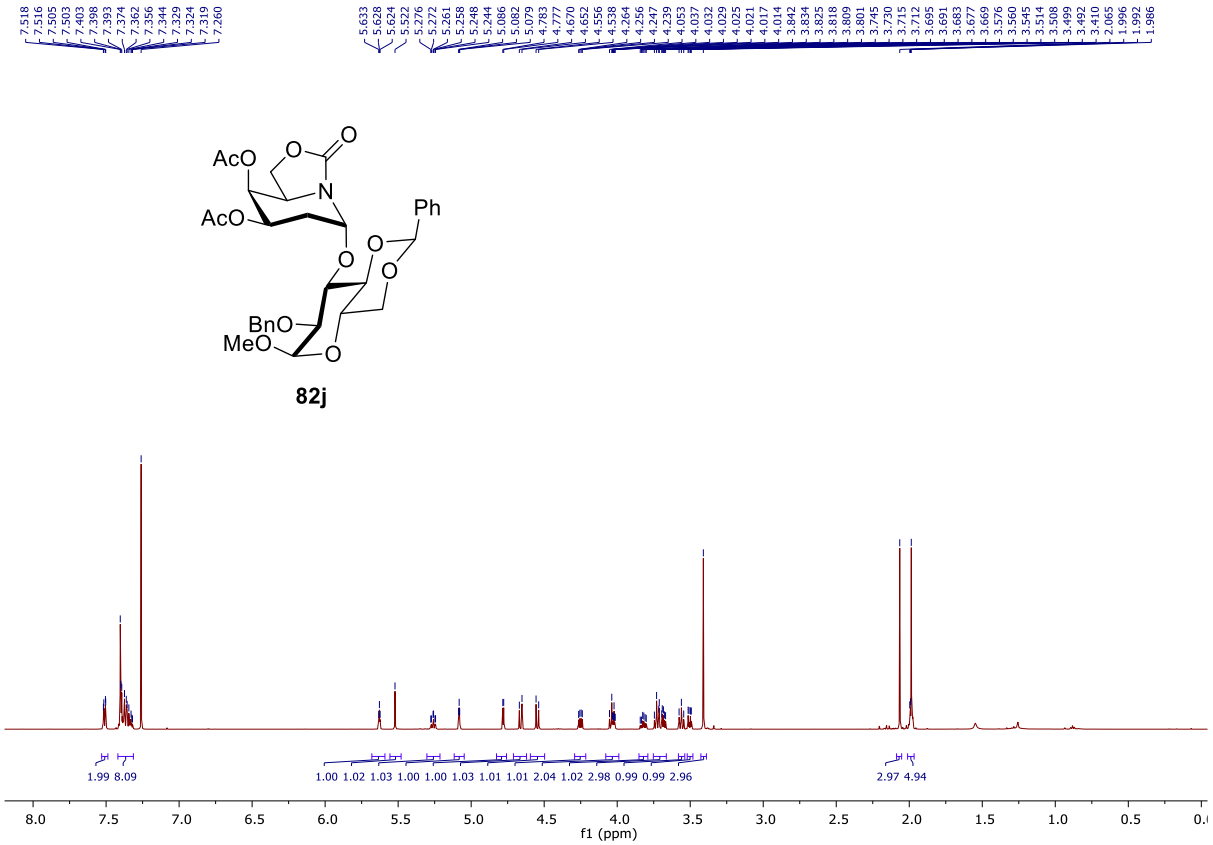

Figure 8.395. ^{1}H NMR spectra for 82j

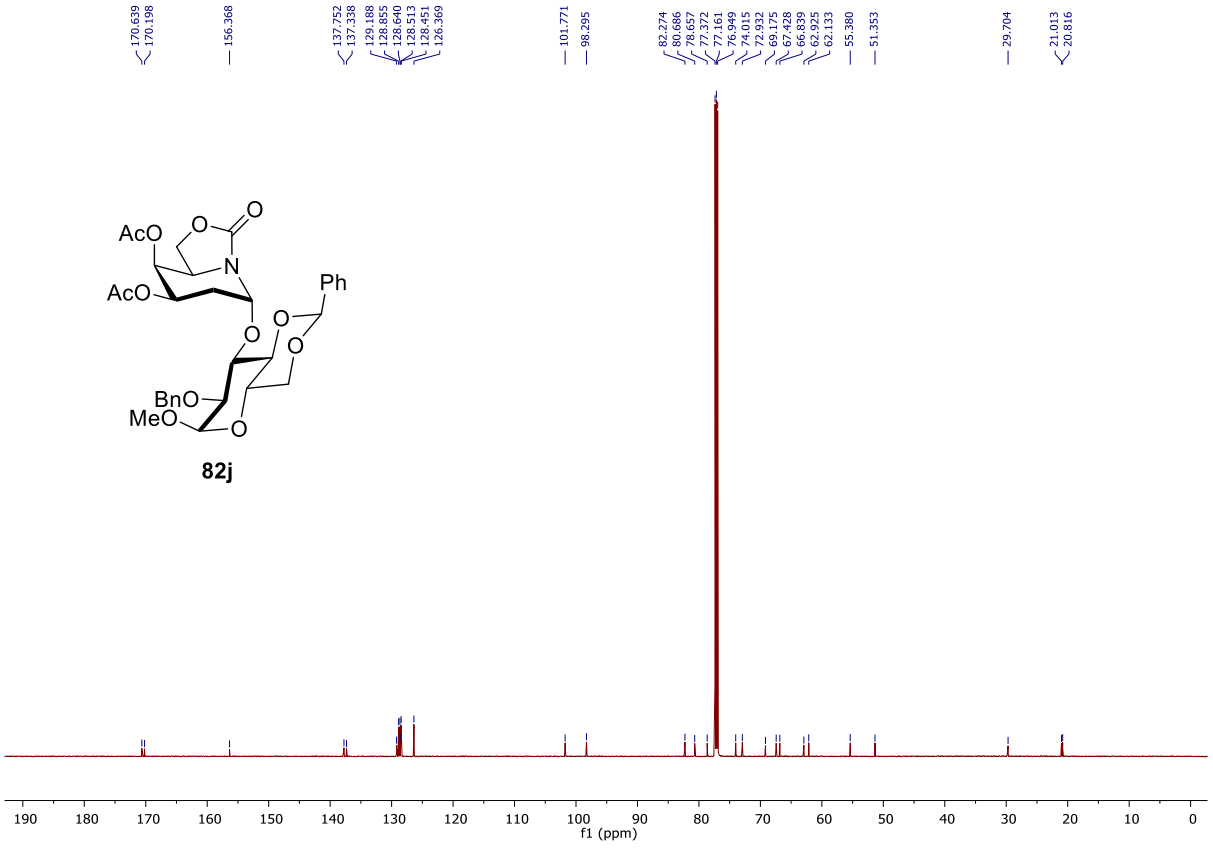

Figure 8.396. ^{13}C NMR spectra for 82j

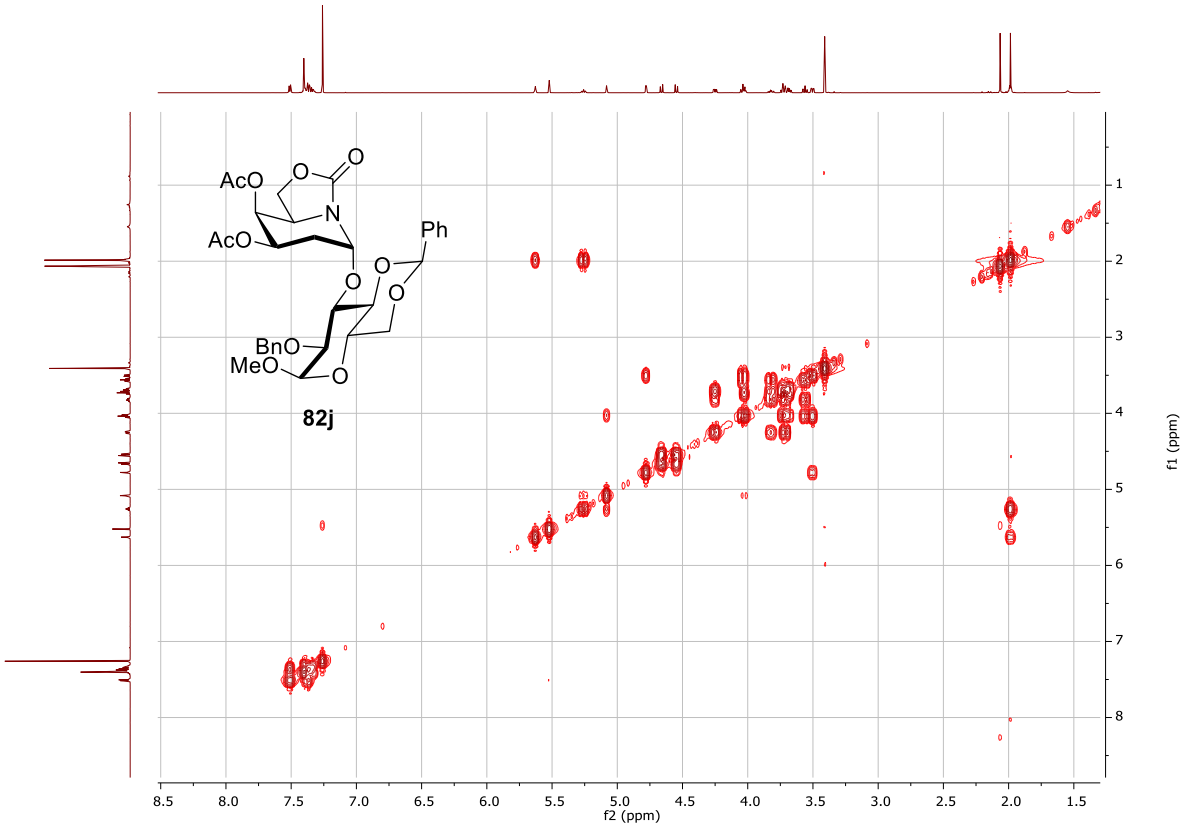

Figure 8.397. COSY spectra for 82j

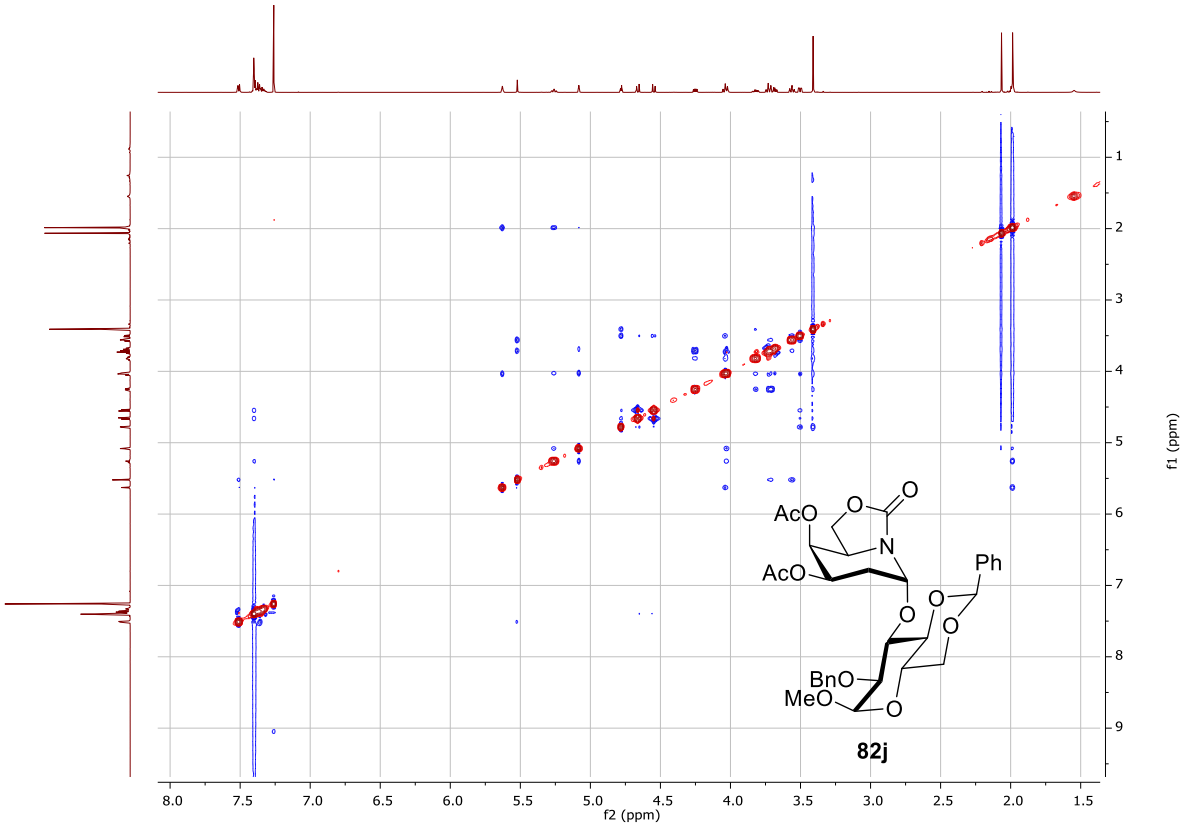

Figure 8.398. NOESY spectra for 82j

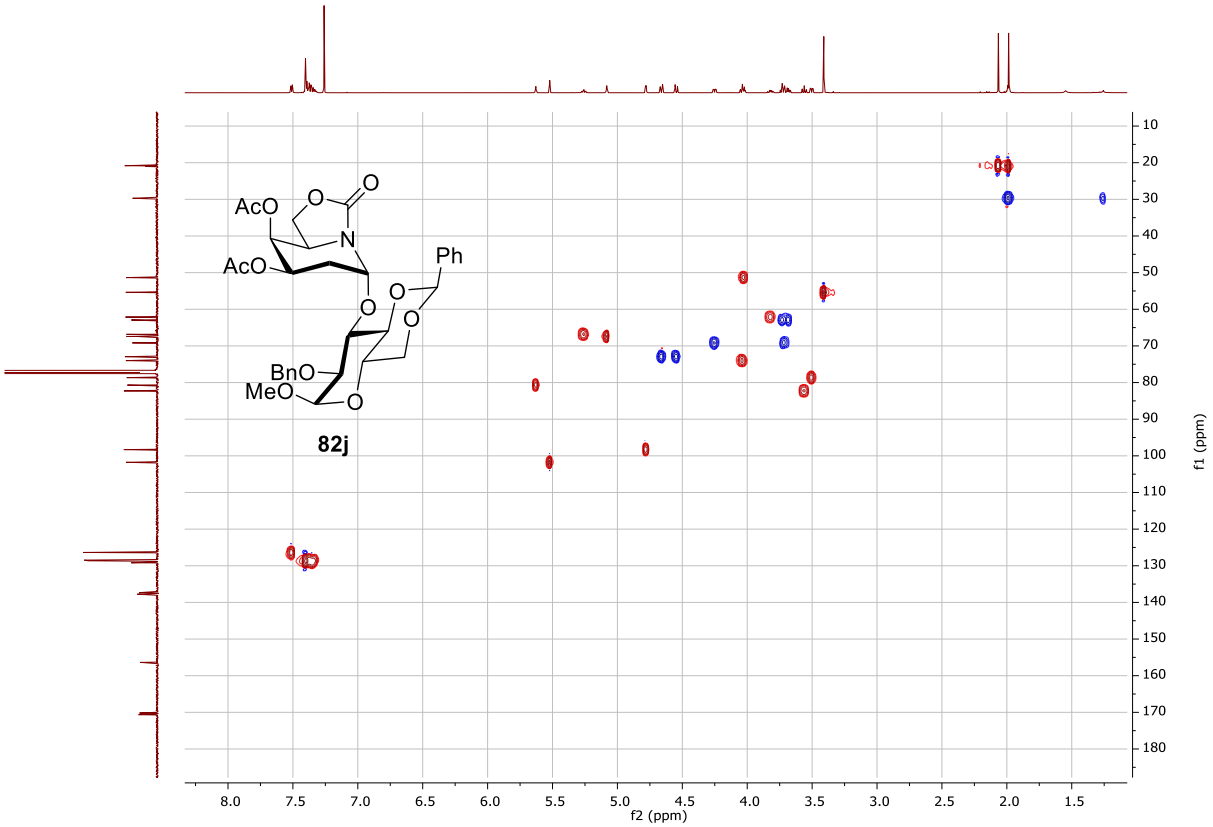

Figure 8.399. HSQC spectra for 82j

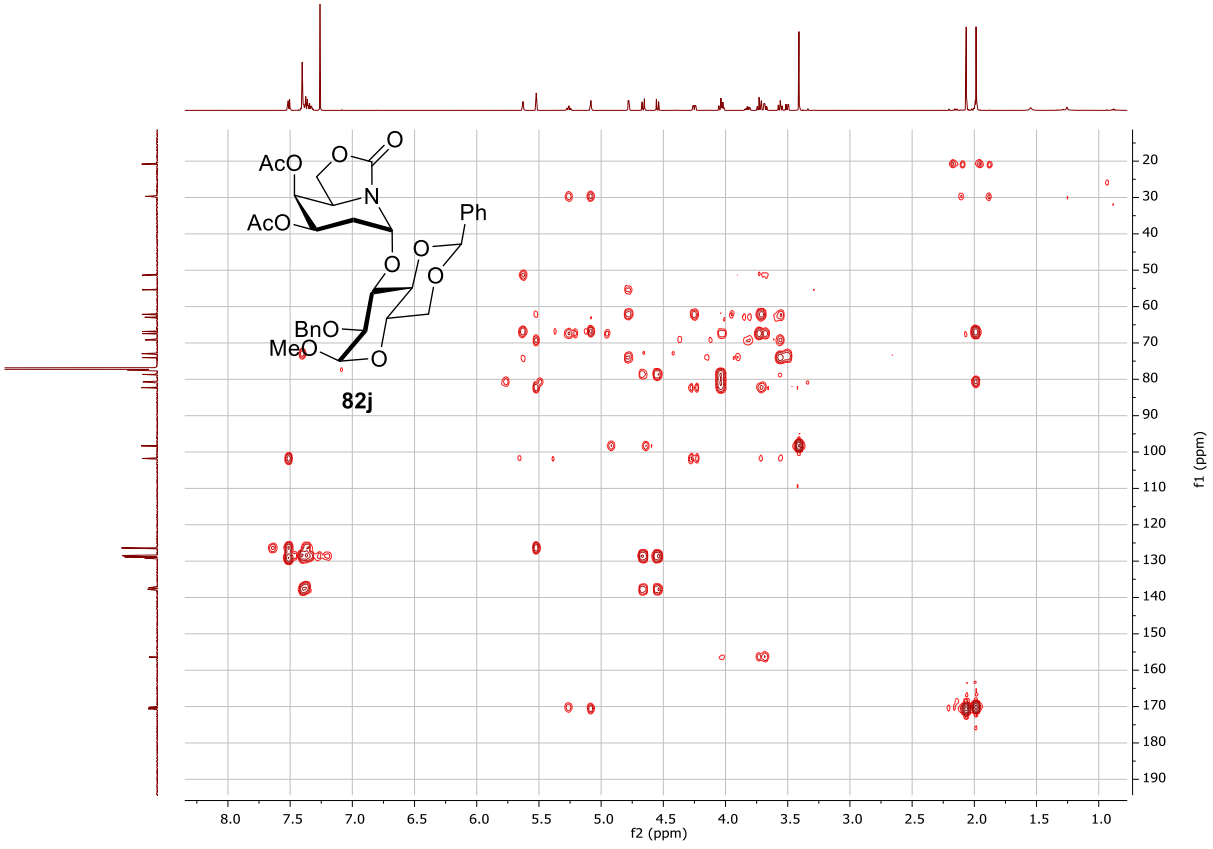

Figure 8.400. HMBC spectra for 82j

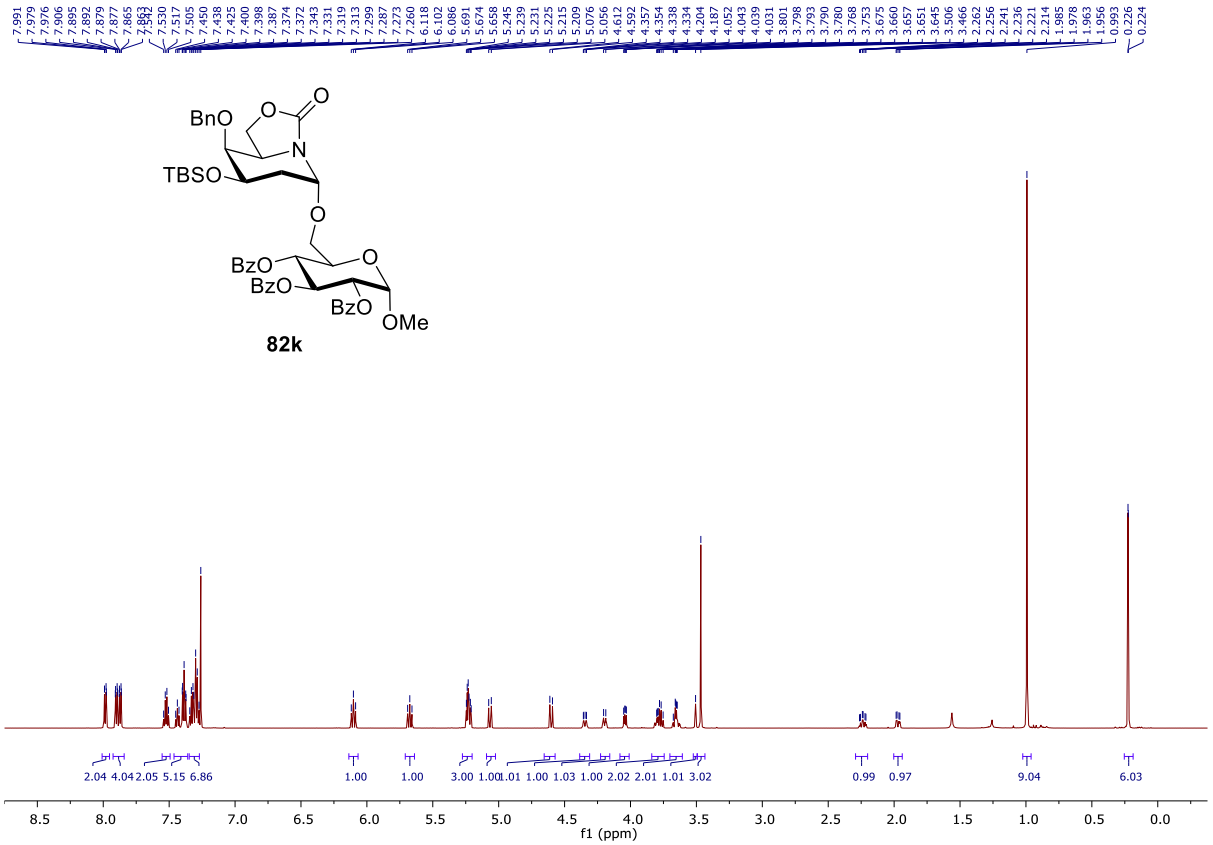

Figure 8.401. ^{1}H NMR spectra for 82k

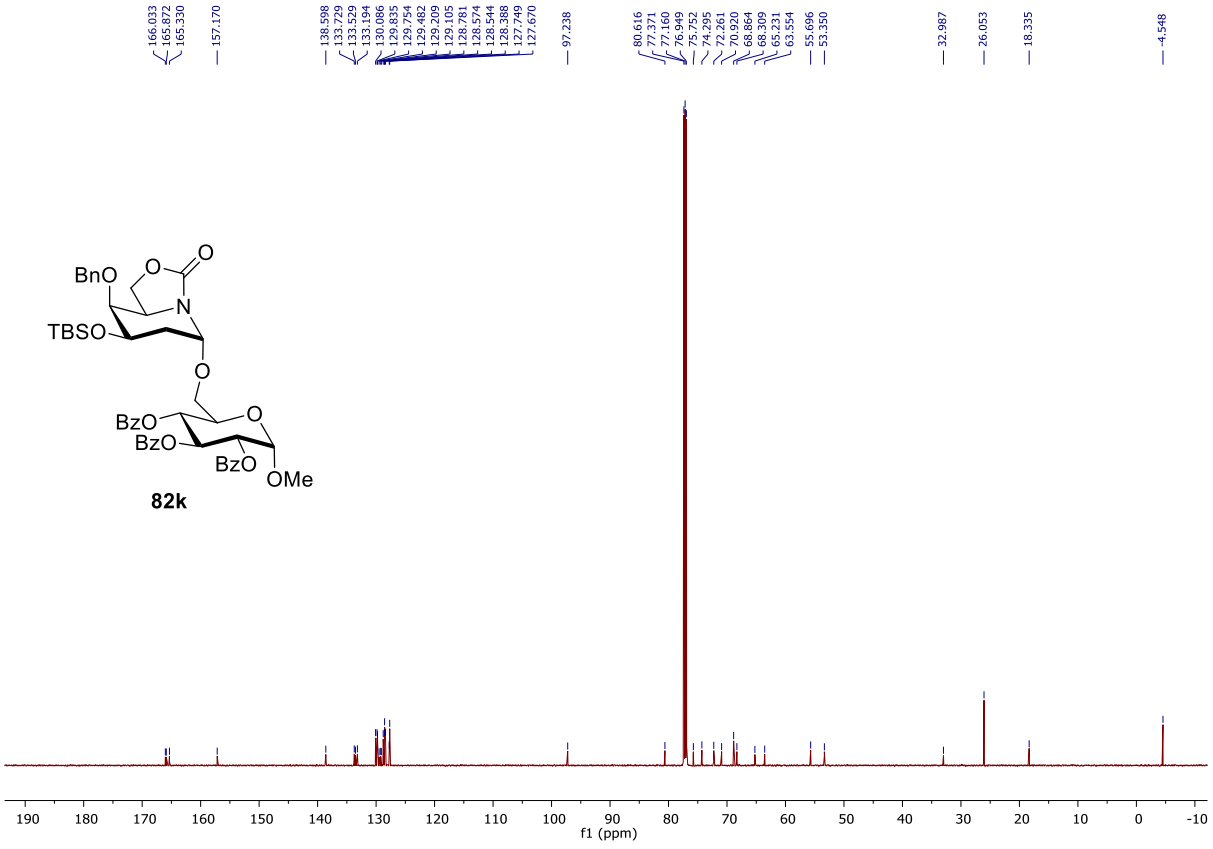

Figure 8.402. ^{13}C NMR spectra for 82k

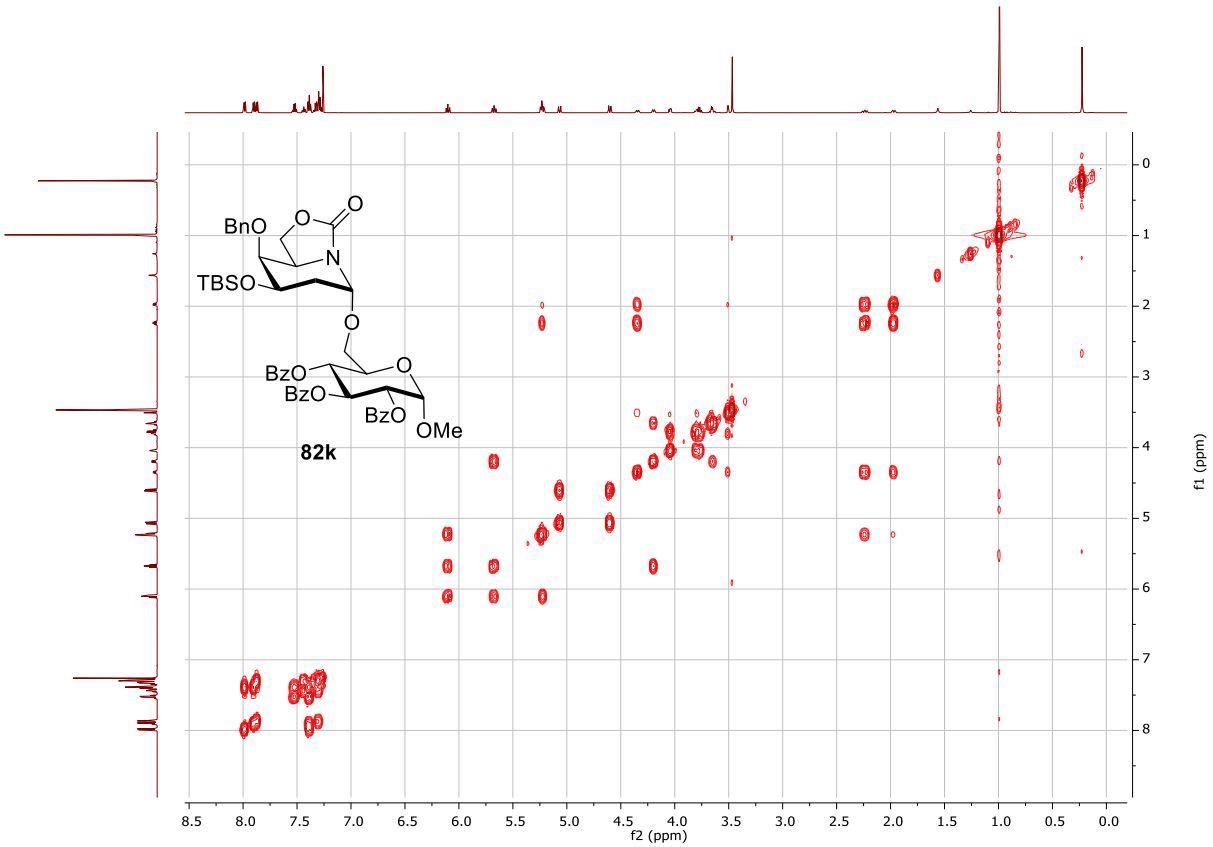

Figure 8.403. COSY spectra for 82k

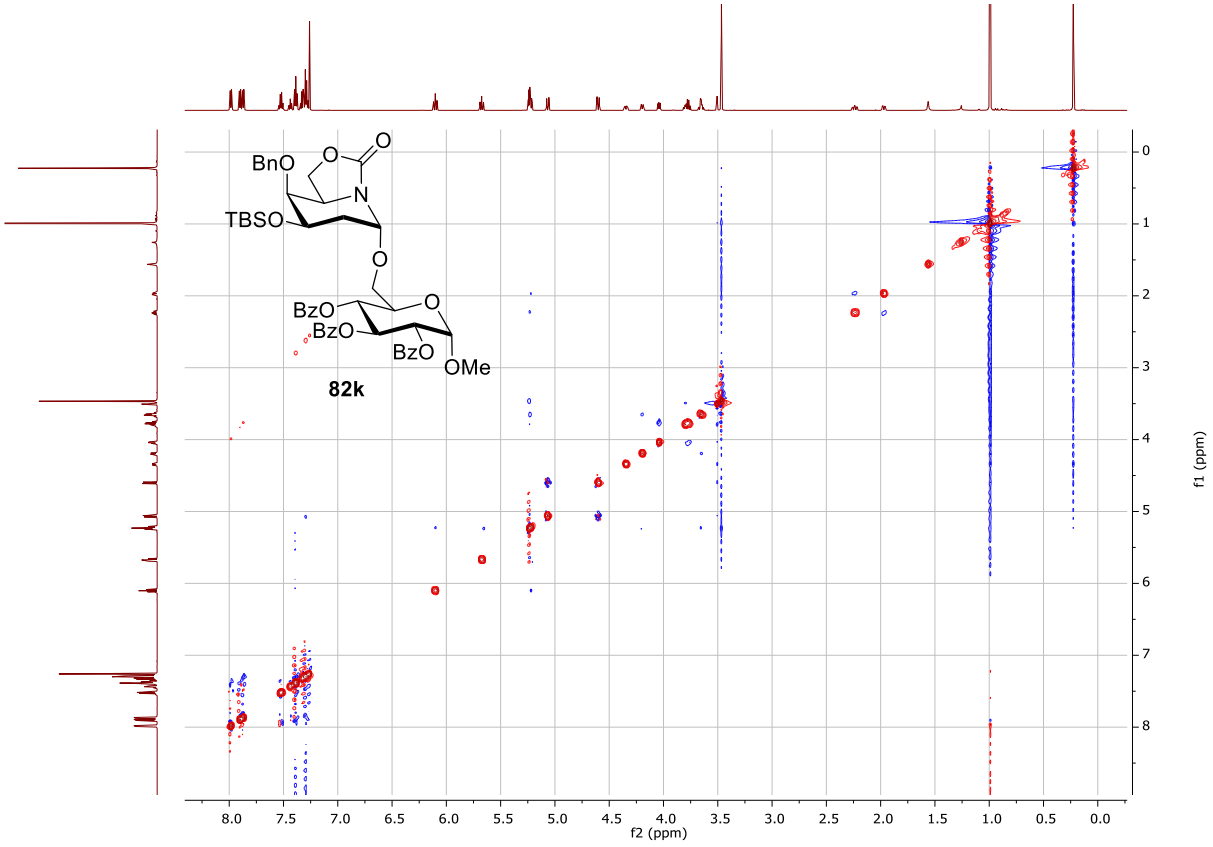

Figure 8.404. NOESY spectra for 82k

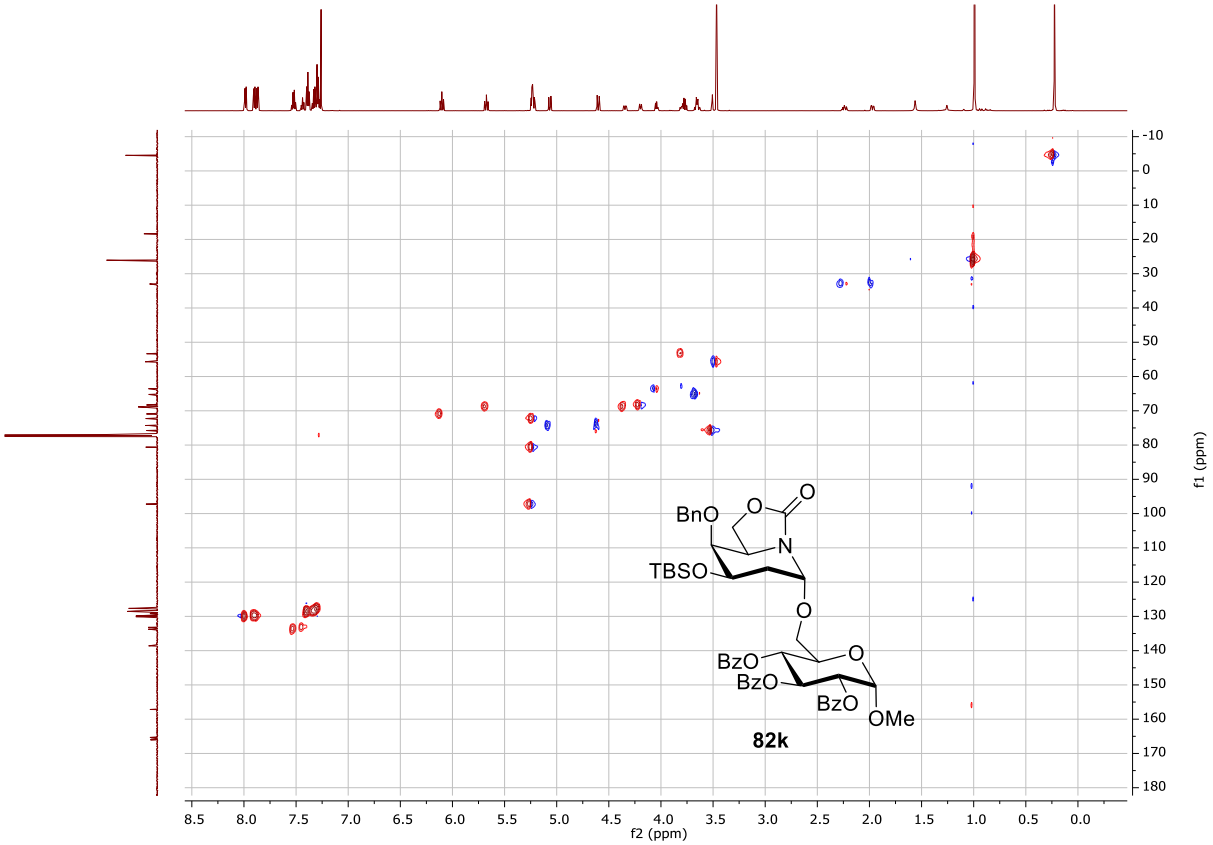

Figure 8.405. HSQC spectra for 82k

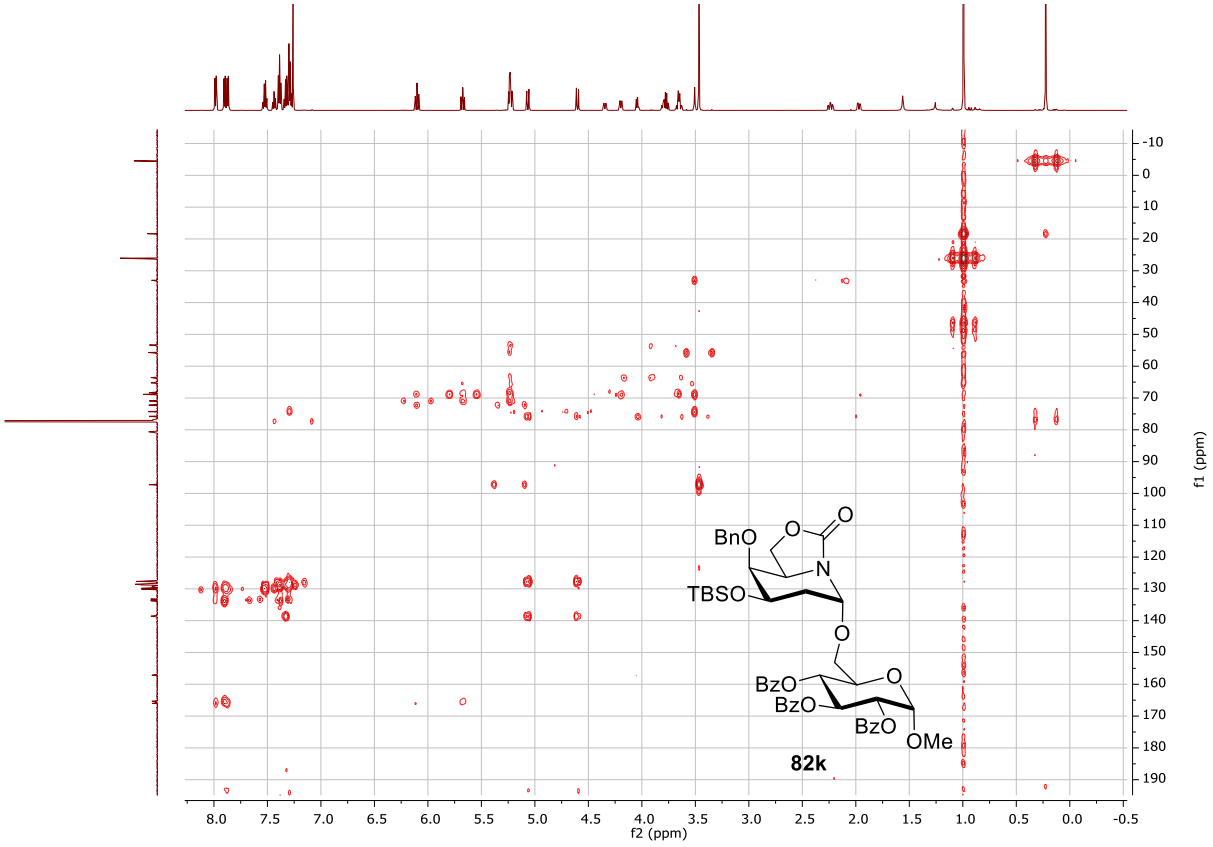

Figure 8.406. HMBC spectra for 82k

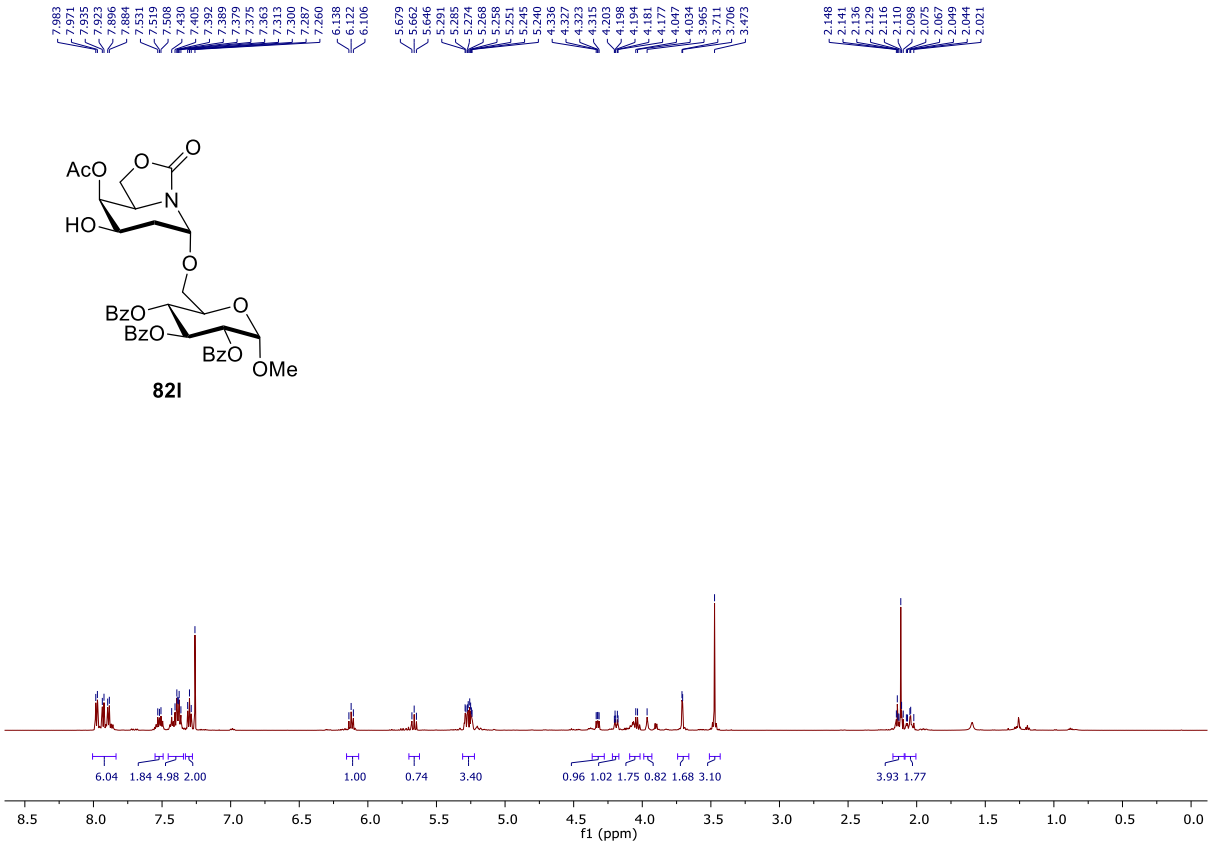

Figure 8.407. ^{1}H NMR spectra for 82l

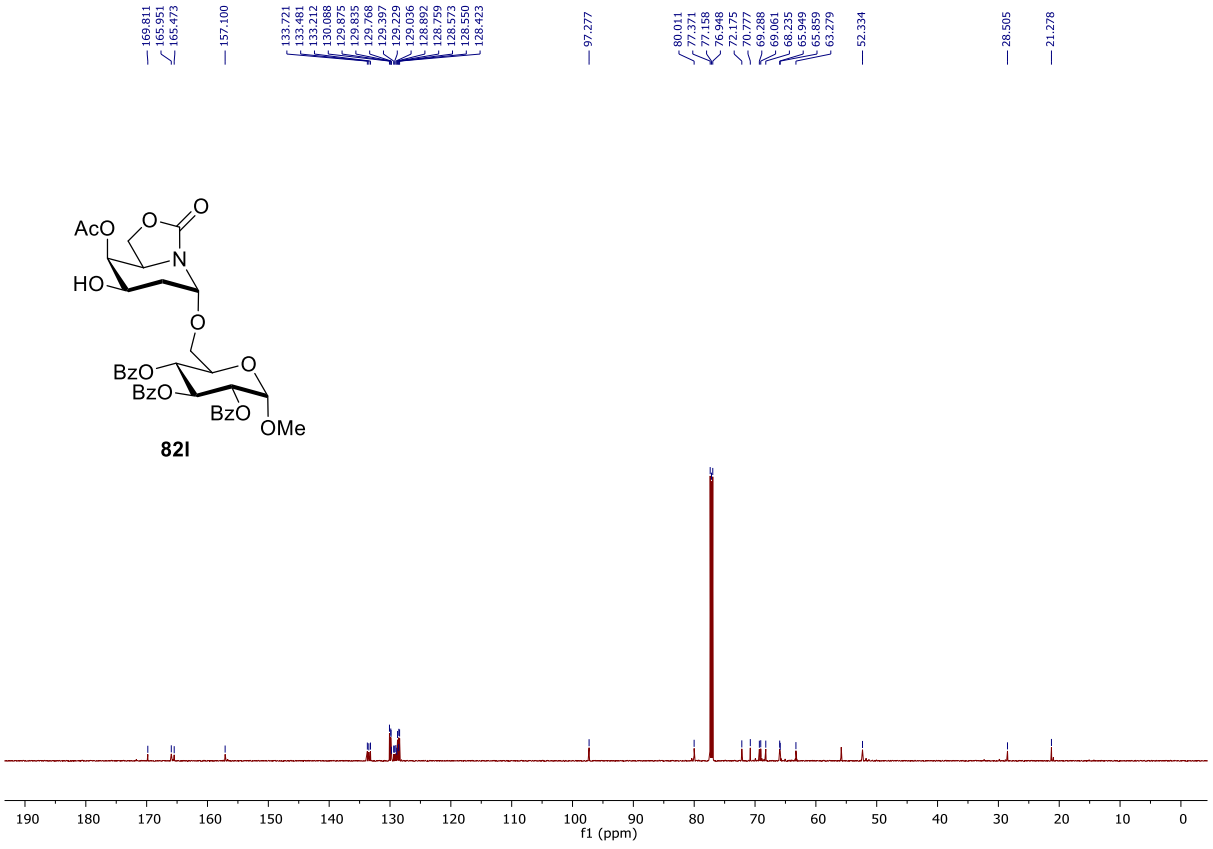

Figure 8.408. ^{13}C NMR spectra for 82l

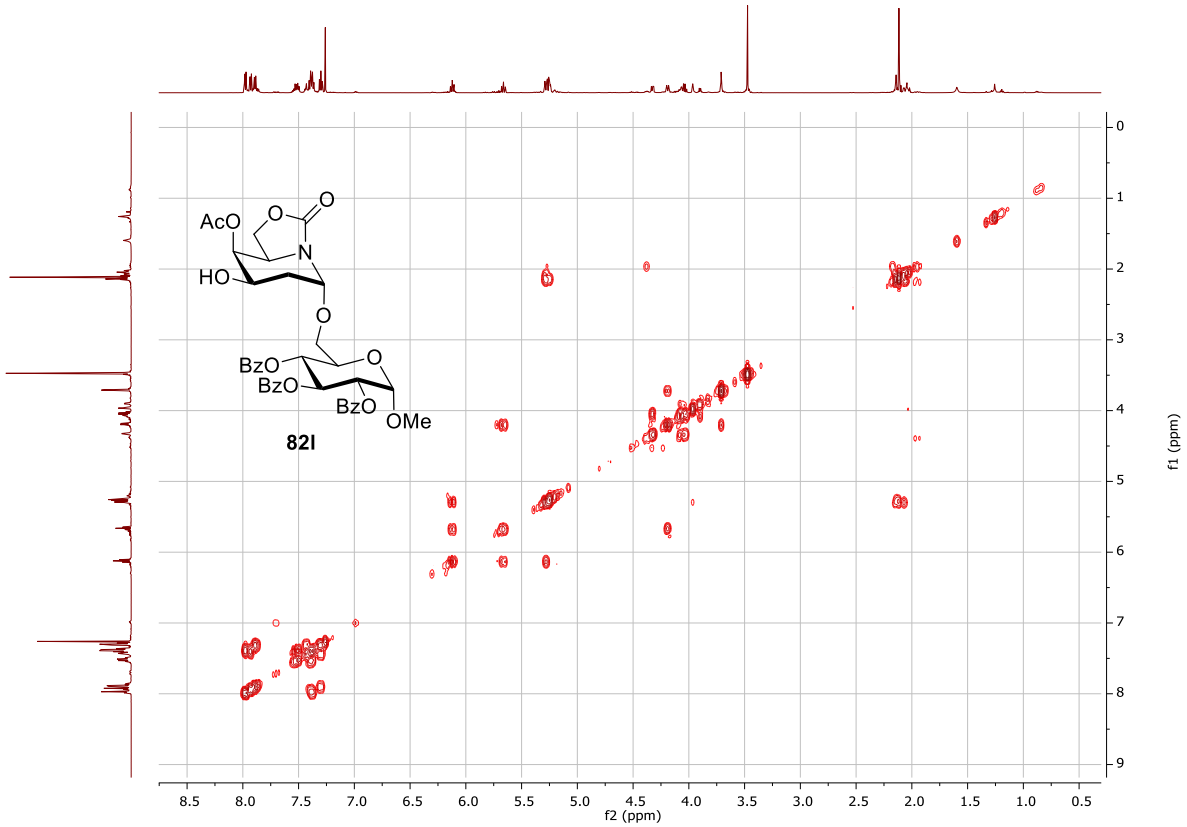

Figure 8.409. COSY spectra for 82l

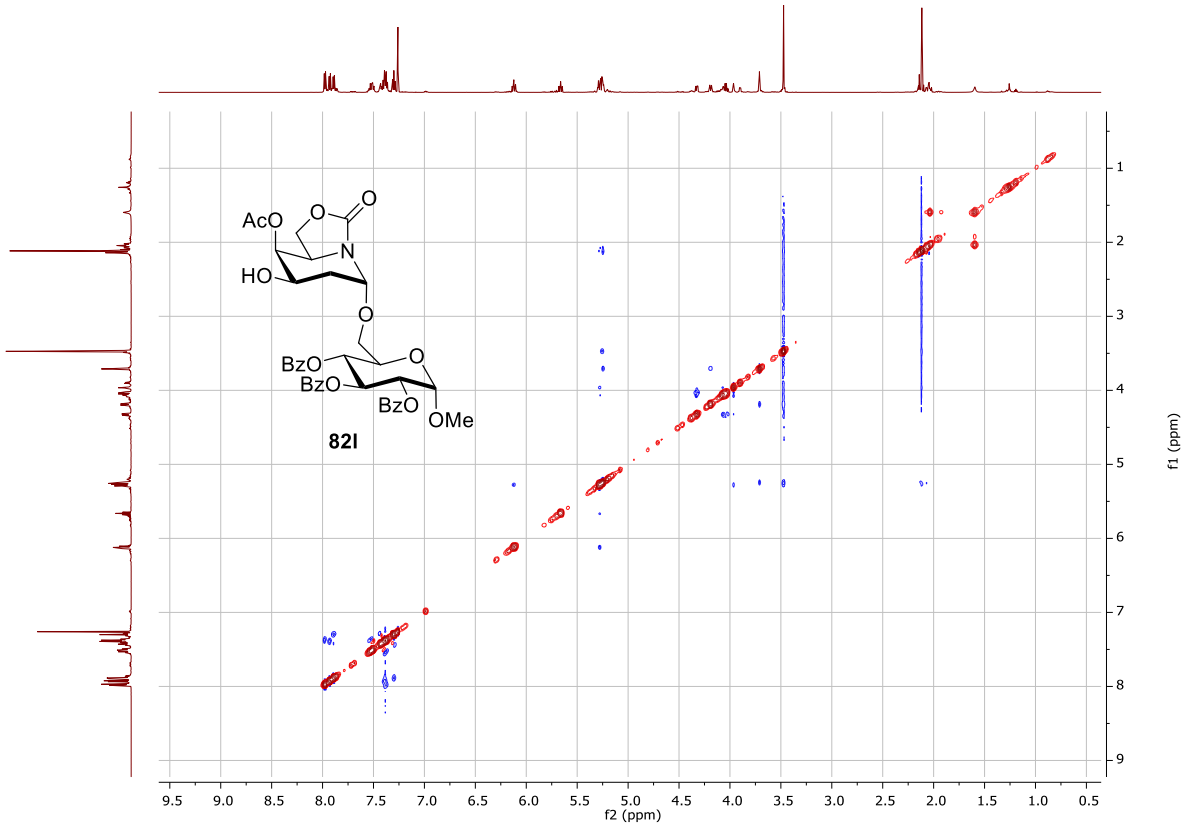

Figure 8.410. NOESY spectra for 82l

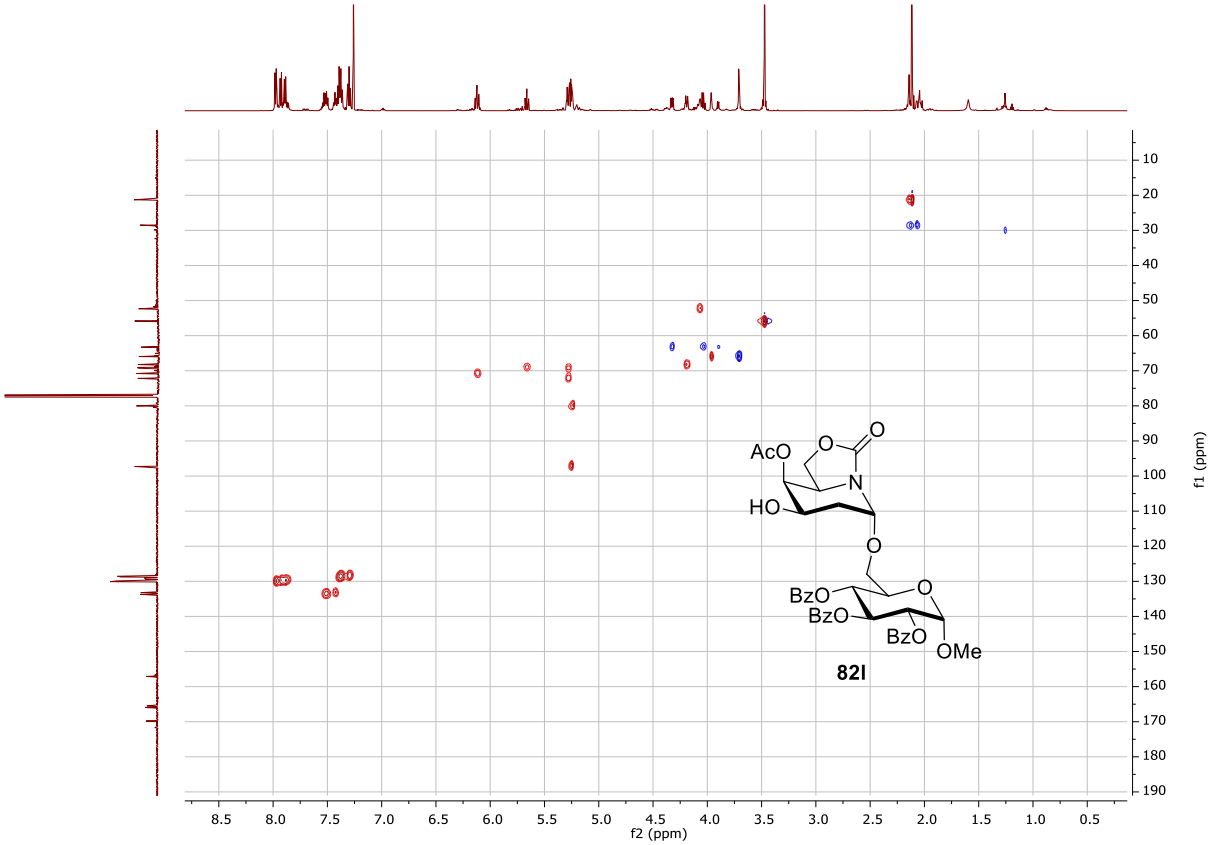

Figure 8.411. HSQC spectra for 82l

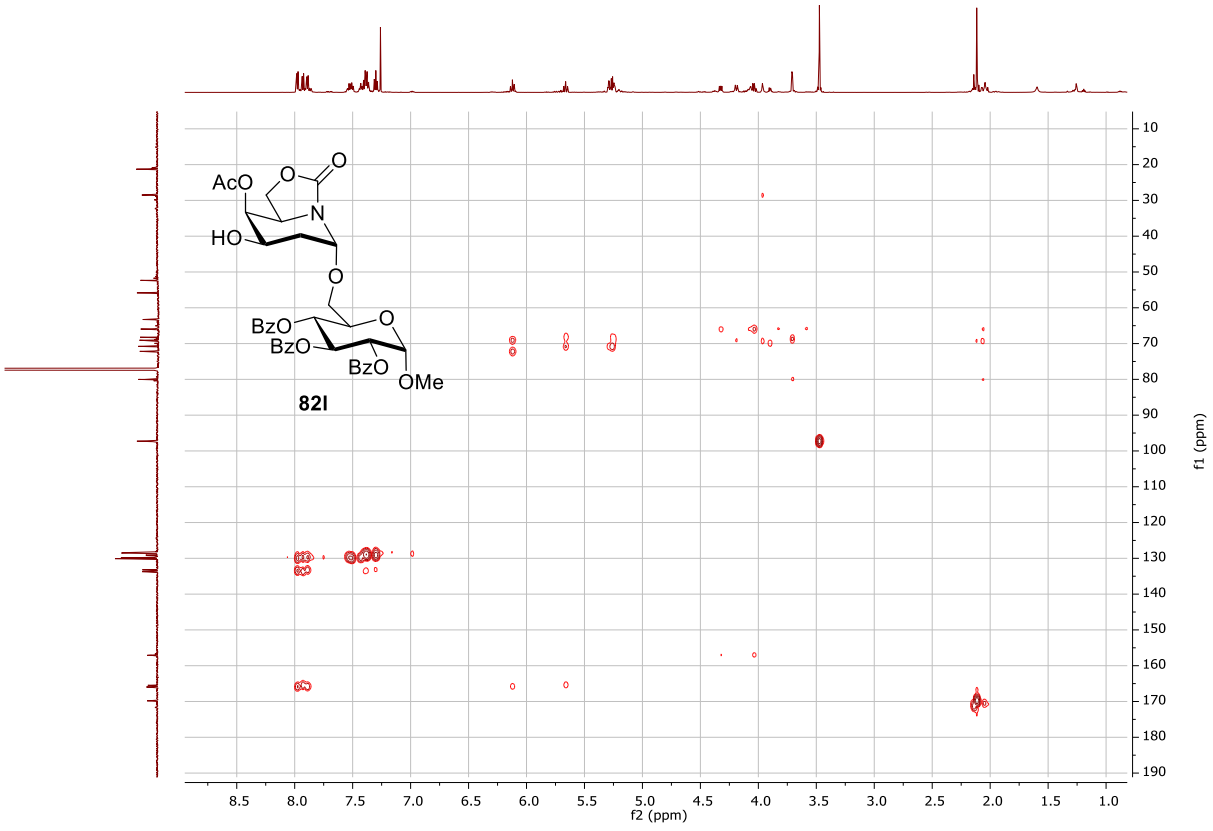

Figure 8.412. HMBC spectra for 82l

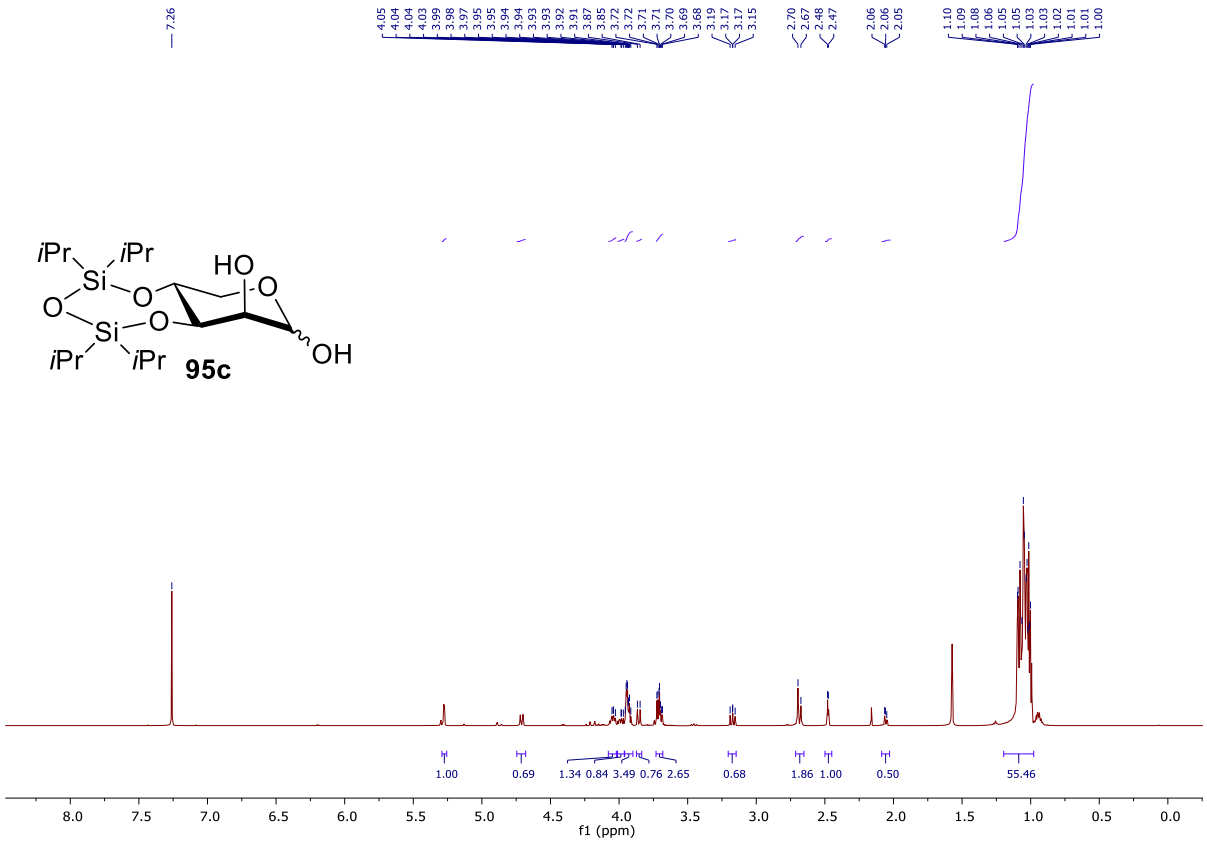

Figure 8.413. ^{1}H NMR spectra for 95c

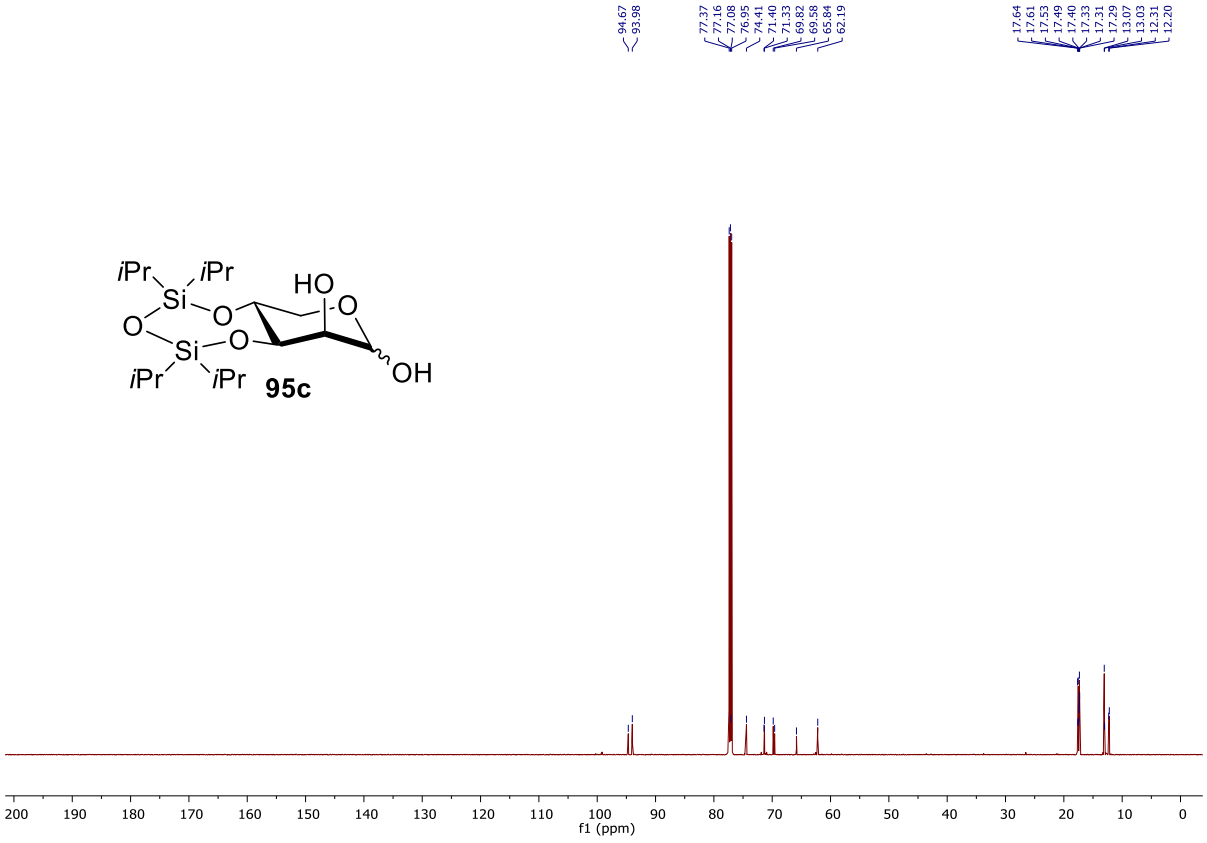

Figure 8.414. ^{13}C NMR spectra for 95c

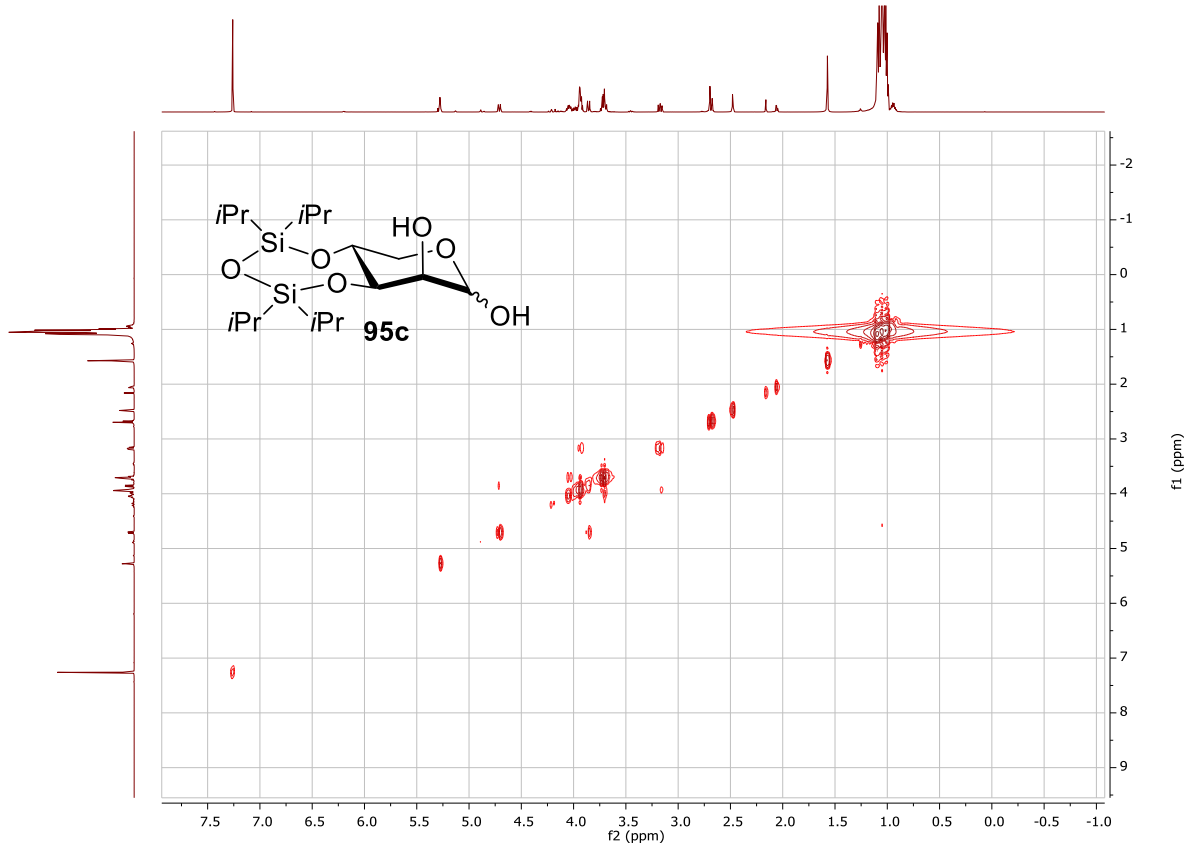

Figure 8.415. COSY spectra for 95c

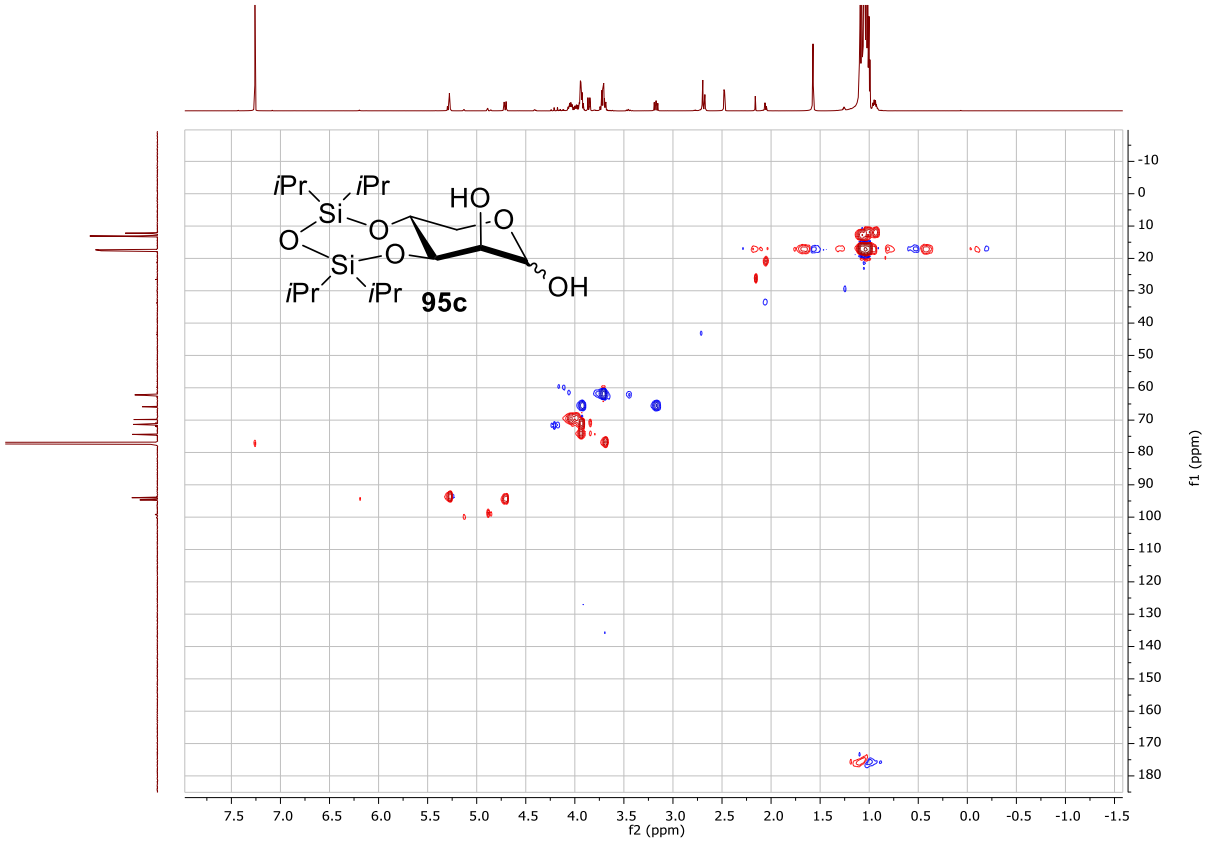

Figure 8.416. HSQC spectra for 95c

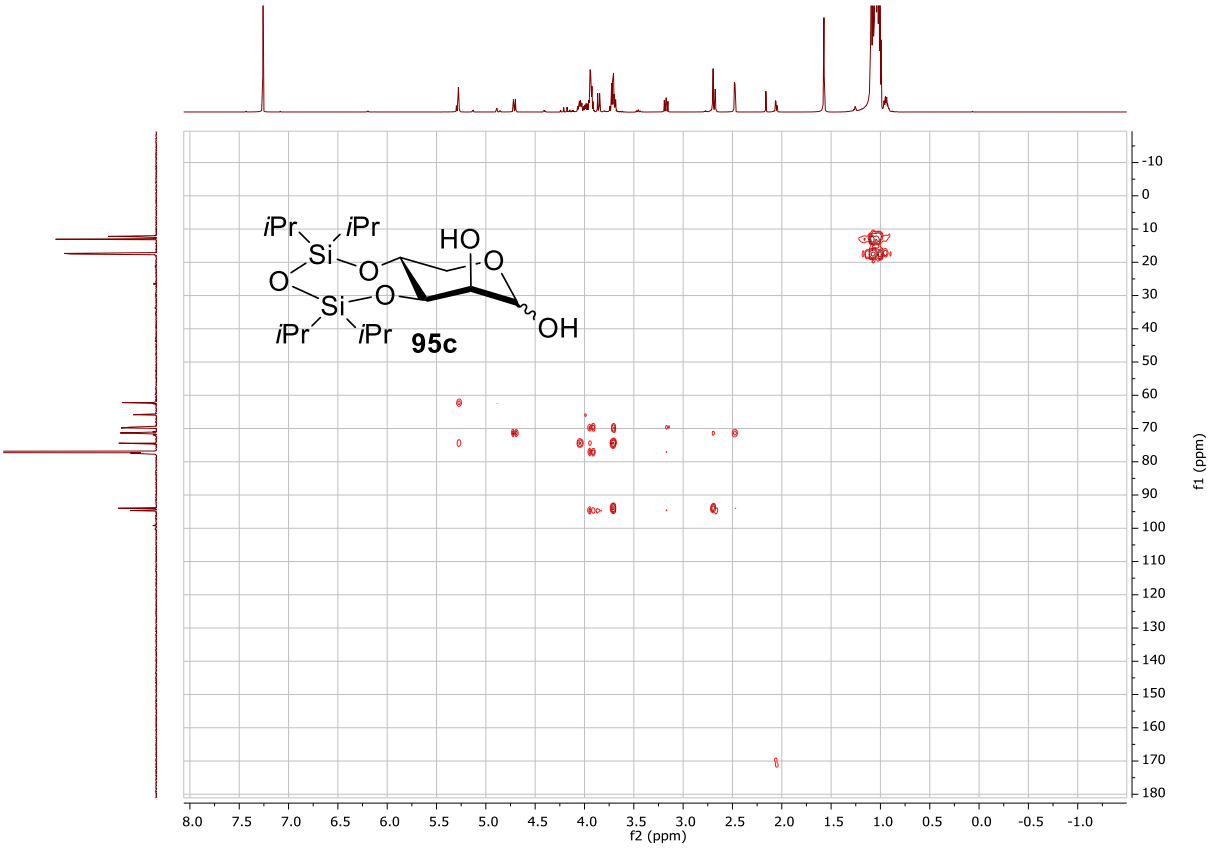

Figure 8.417. HMBC spectra for 95c

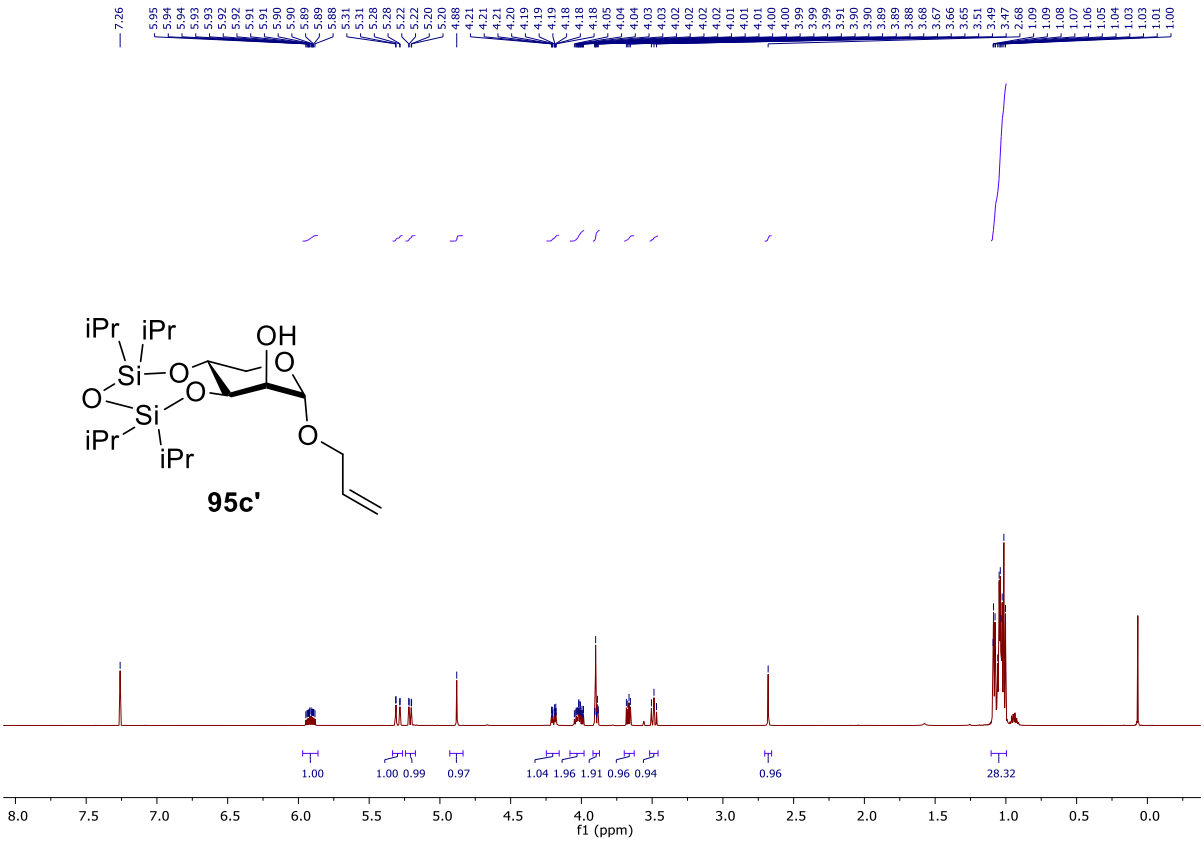

Figure 8.418. ^{1}H NMR spectra for 95c'

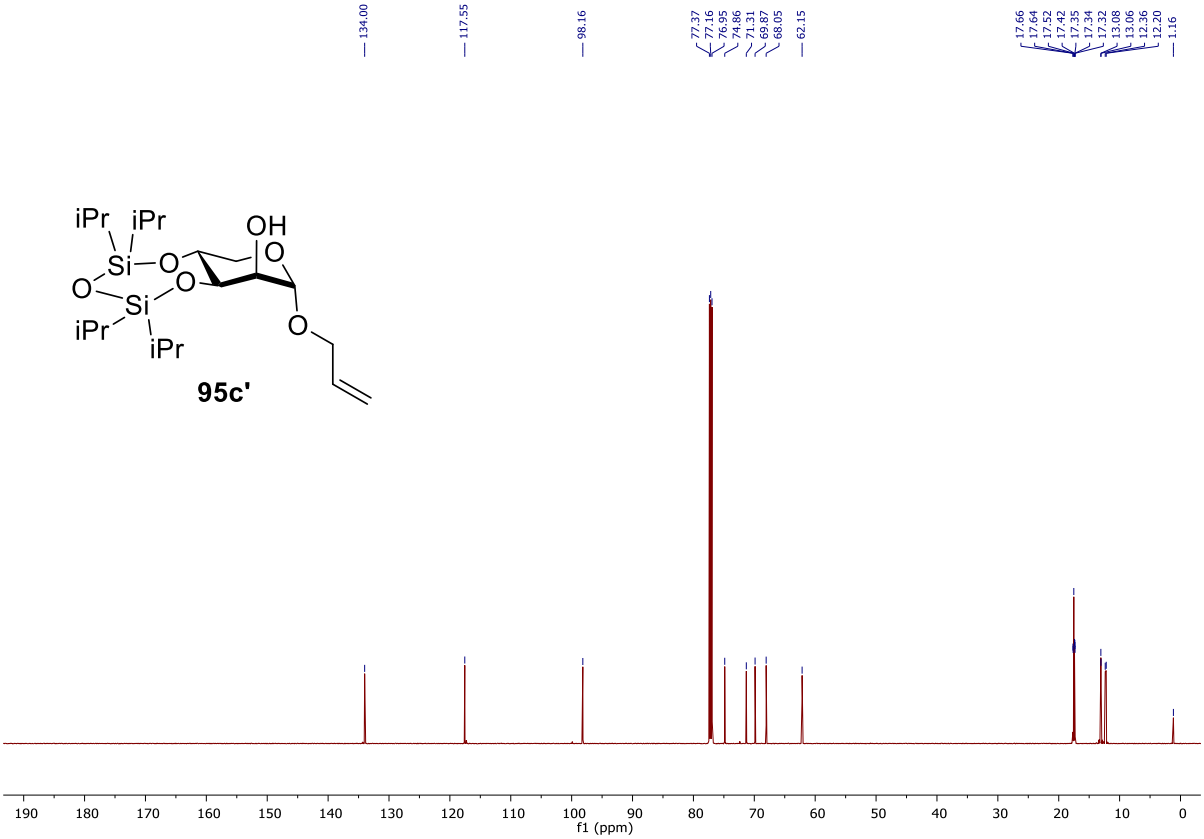

Figure 8.419. ^{13}C NMR spectra for 95c'

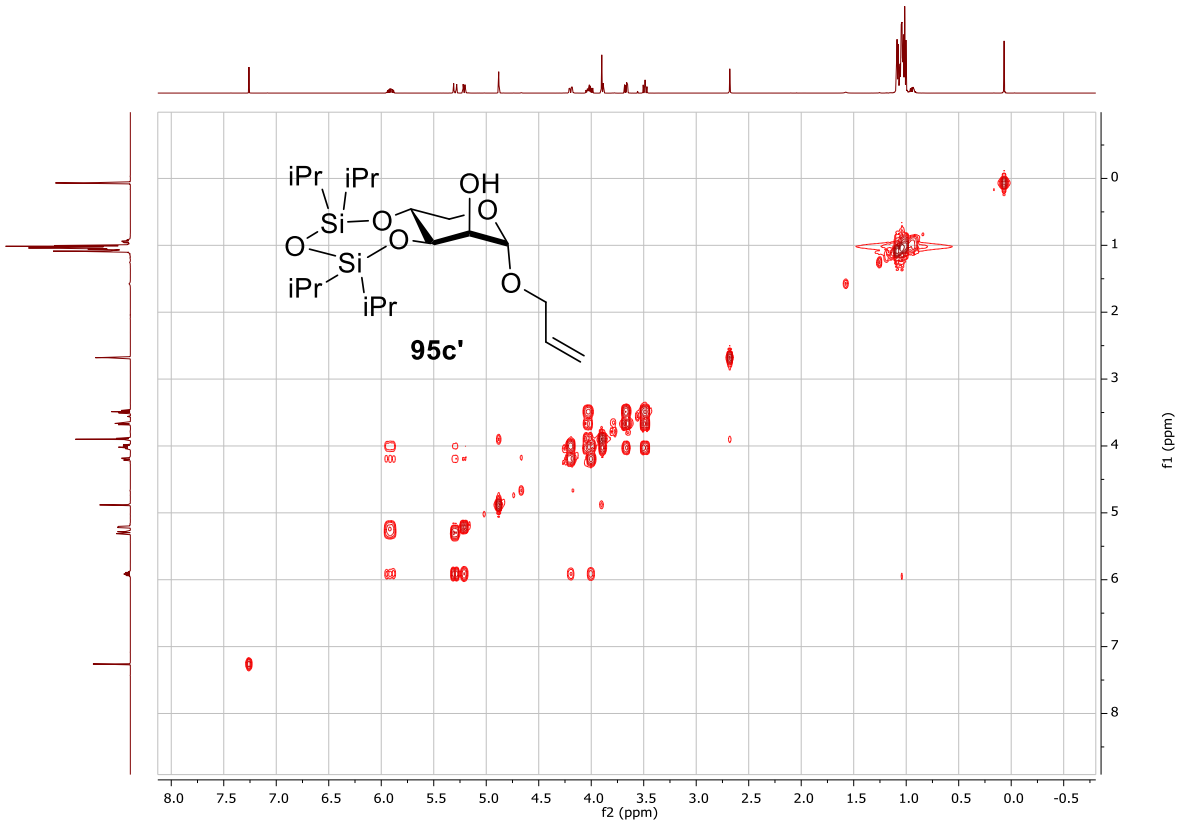

Figure 8.420. COSY spectra for 95c'

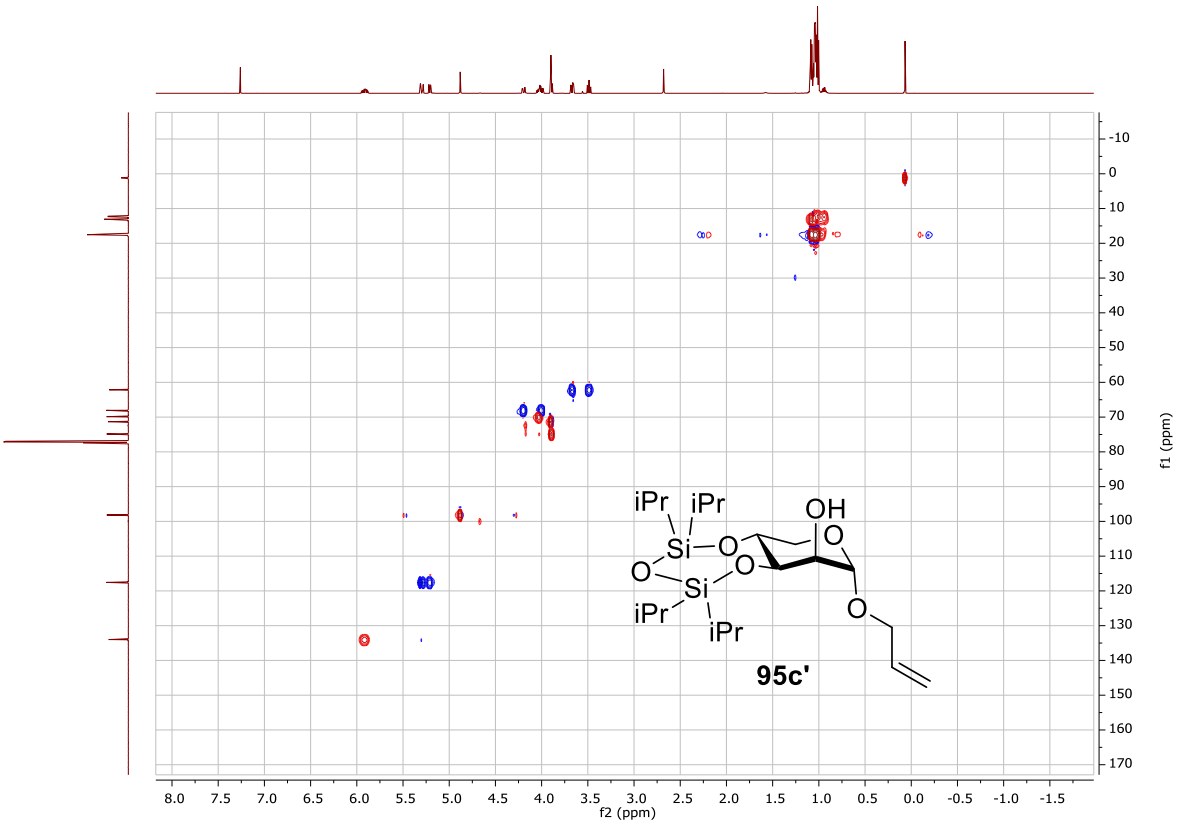

Figure 8.421. HSQC spectra for 95c'

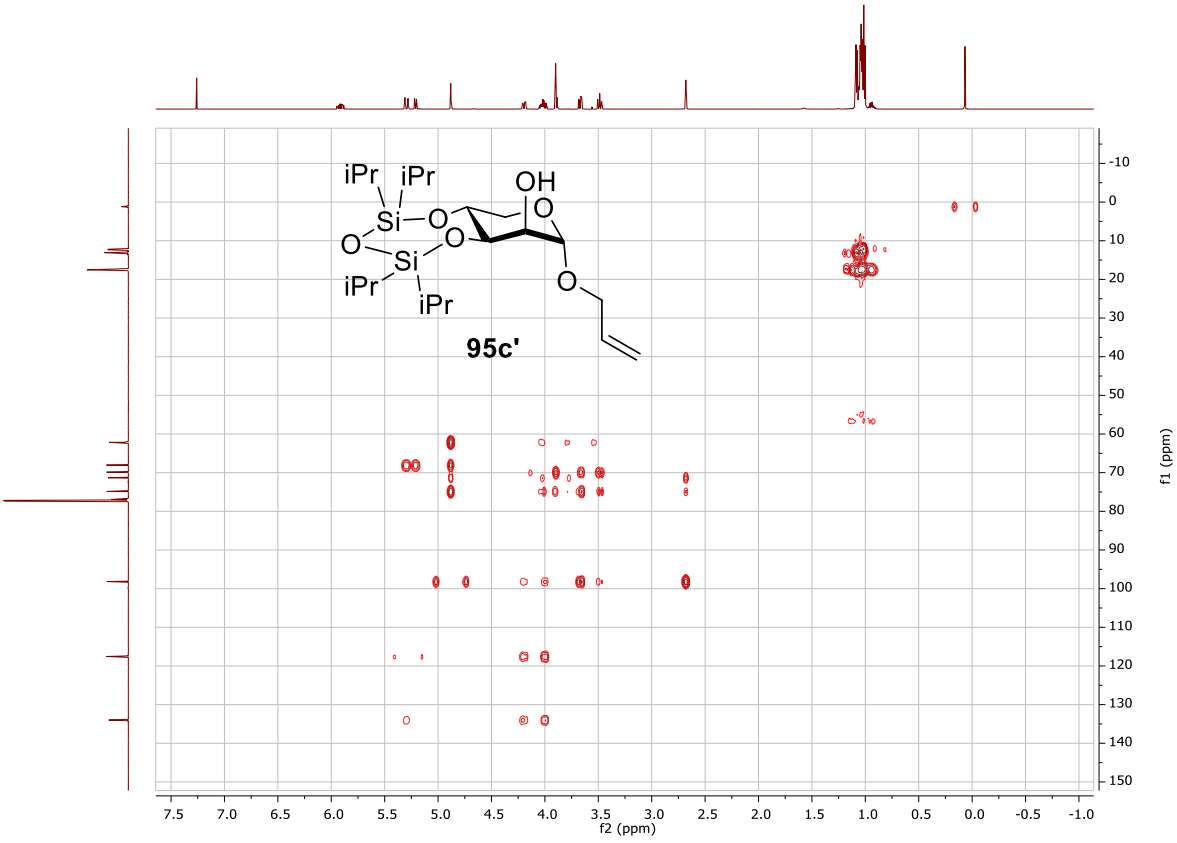

Figure 8.422. HMBC spectra for 95c'

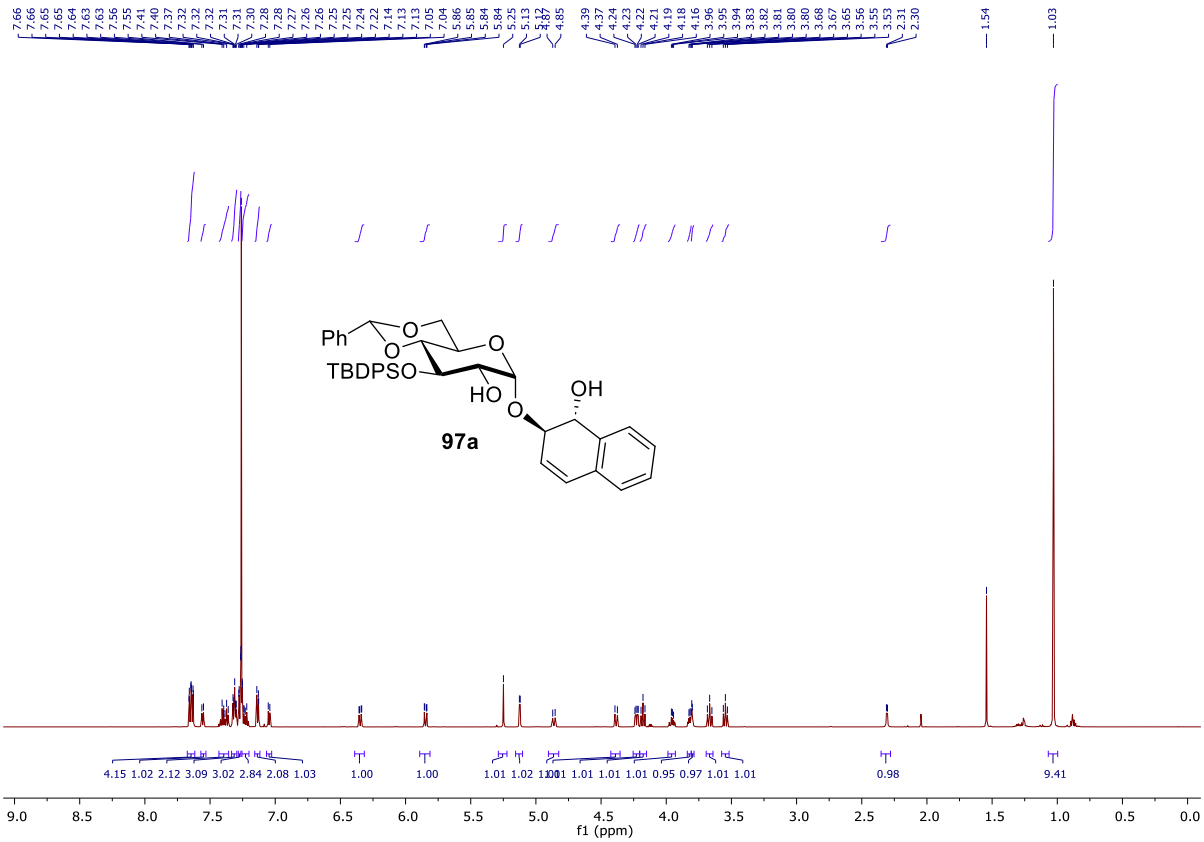

Figure 8.423. ^{1}H NMR spectra for 97a

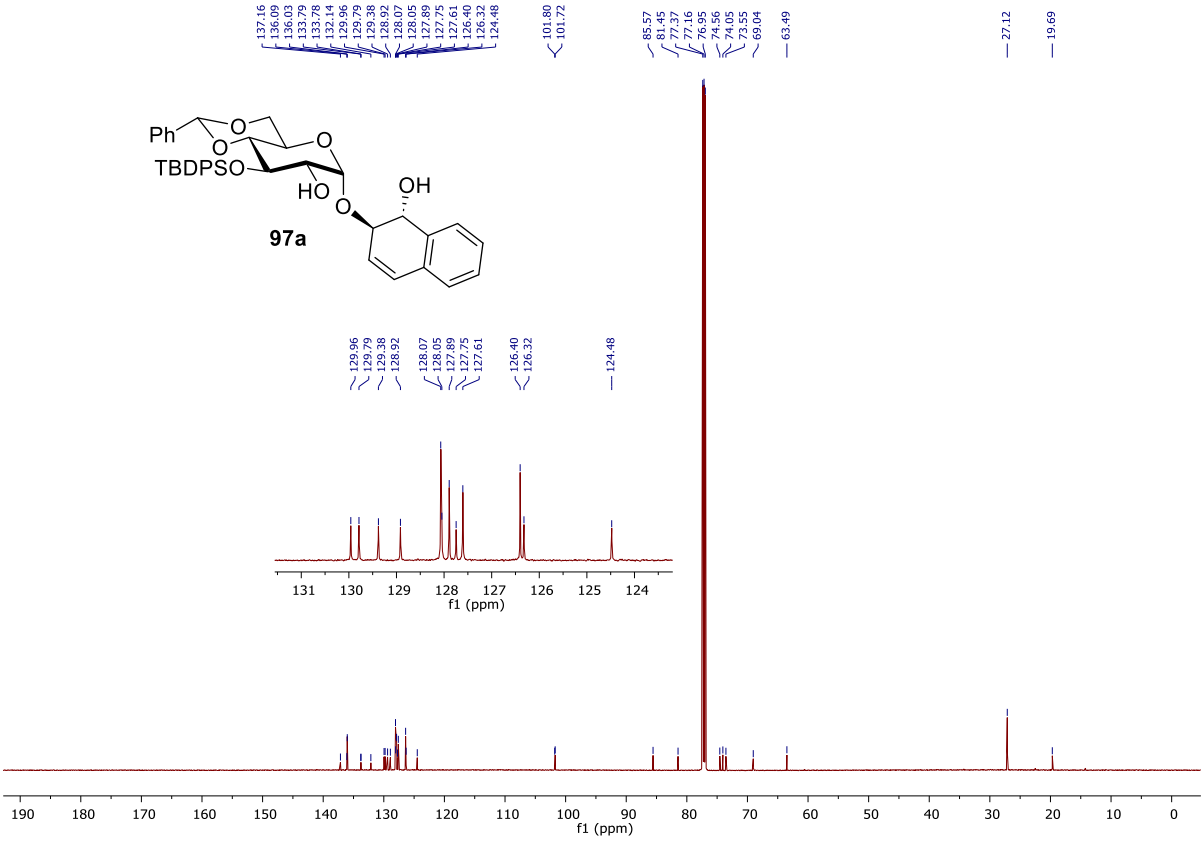

Figure 8.424. ^{13}C NMR spectra for 97a

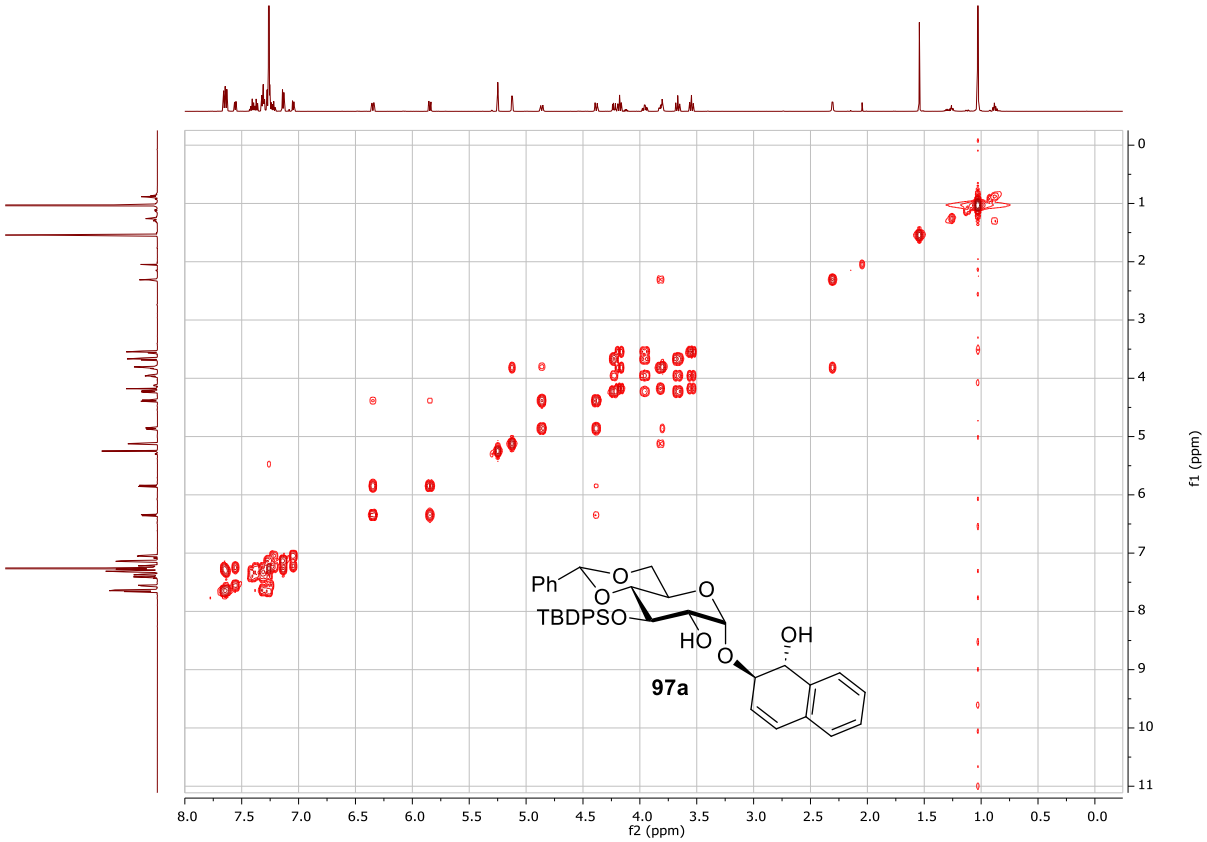

Figure 8.425. COSY spectra for 97a

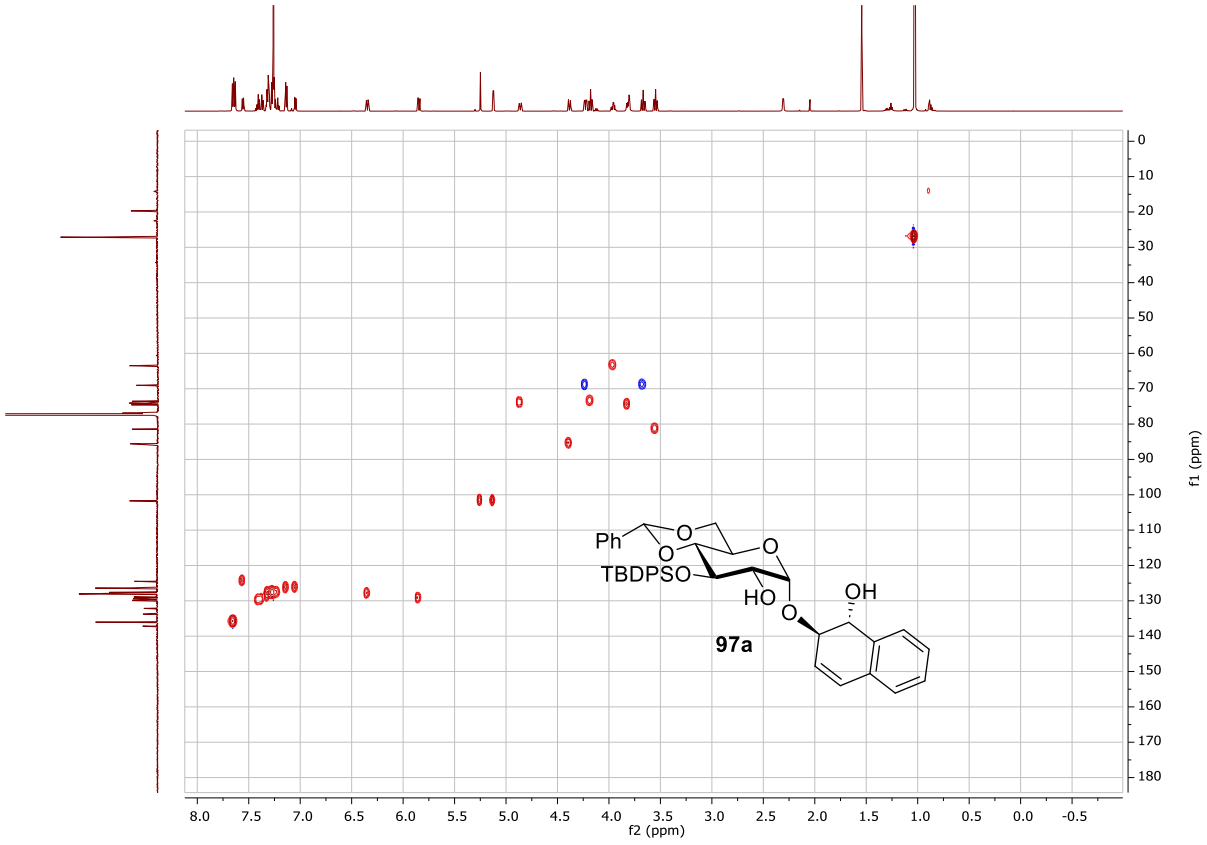

Figure 8.426. HSQC spectra for 97a

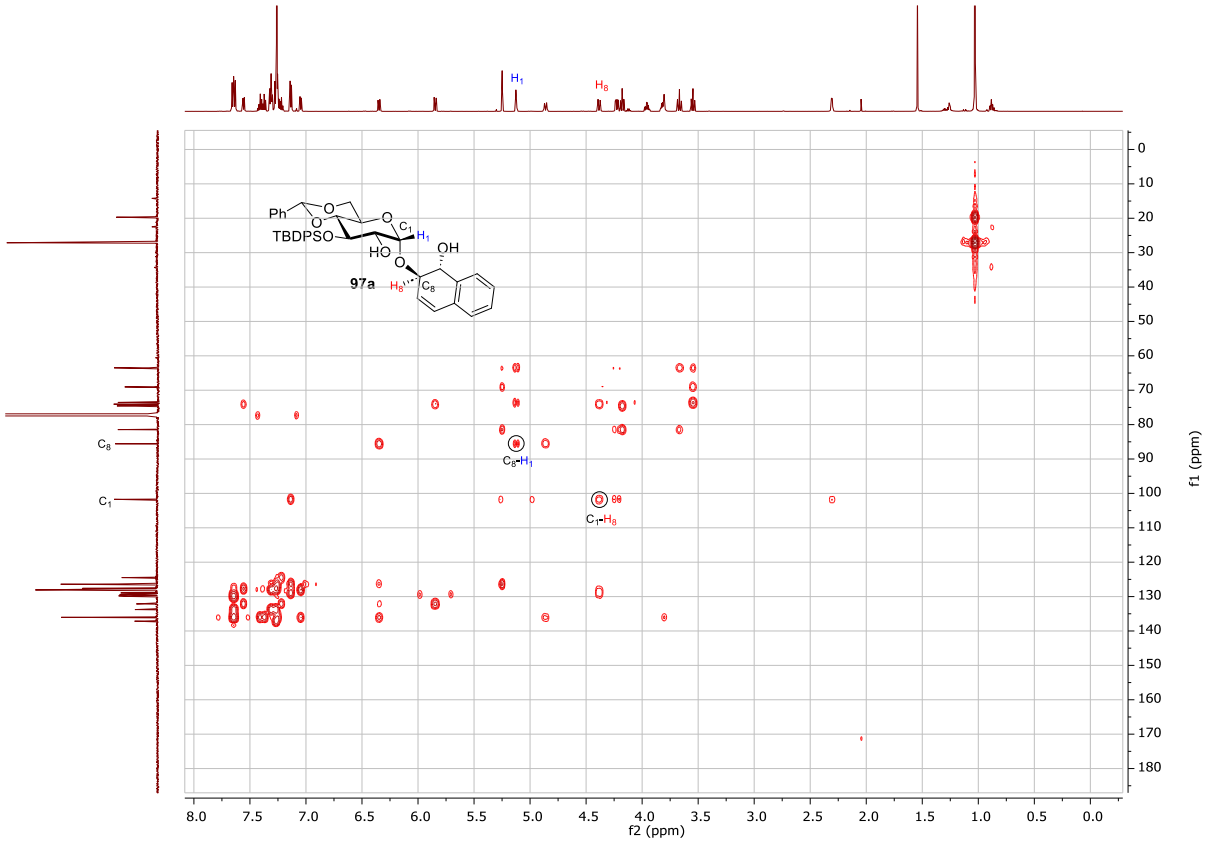

Figure 8.427. HMBC spectra for 97a

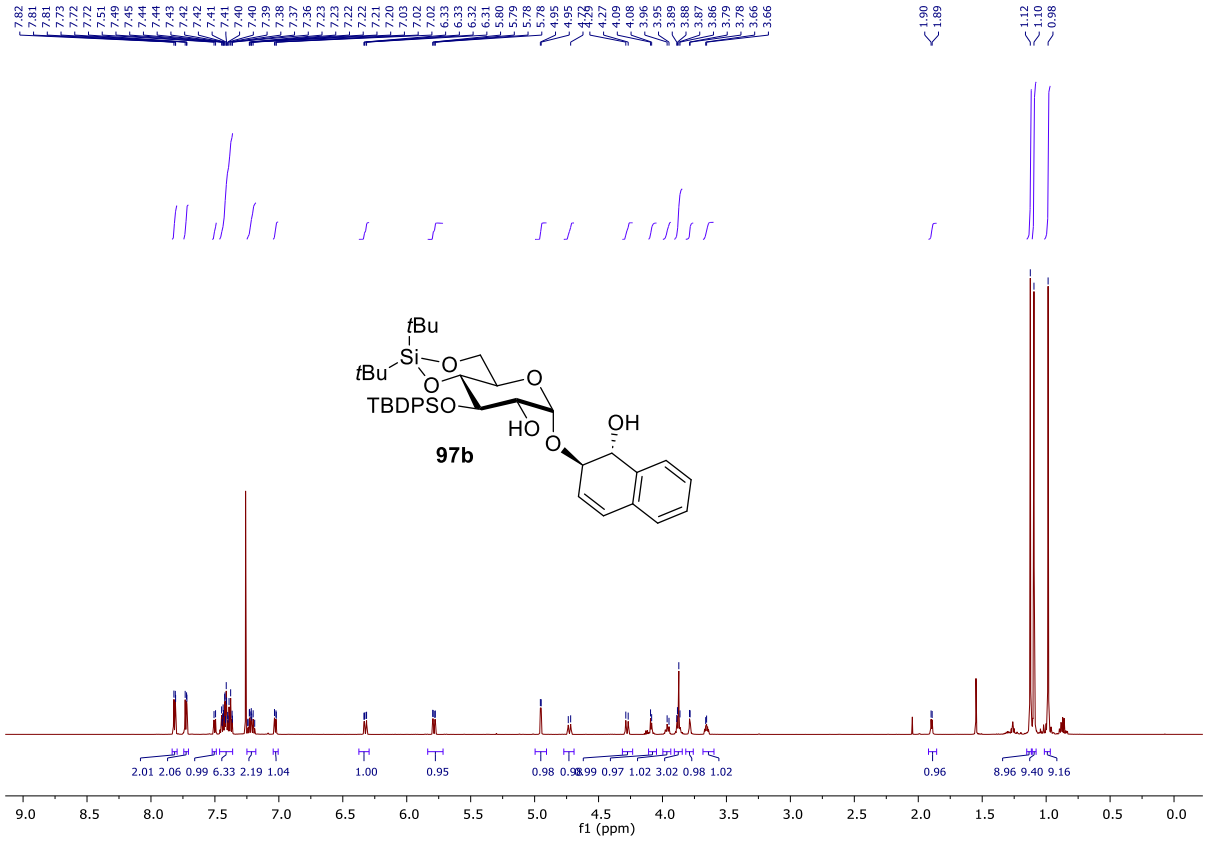

Figure 8.428. ^{1}H NMR spectra for 97b

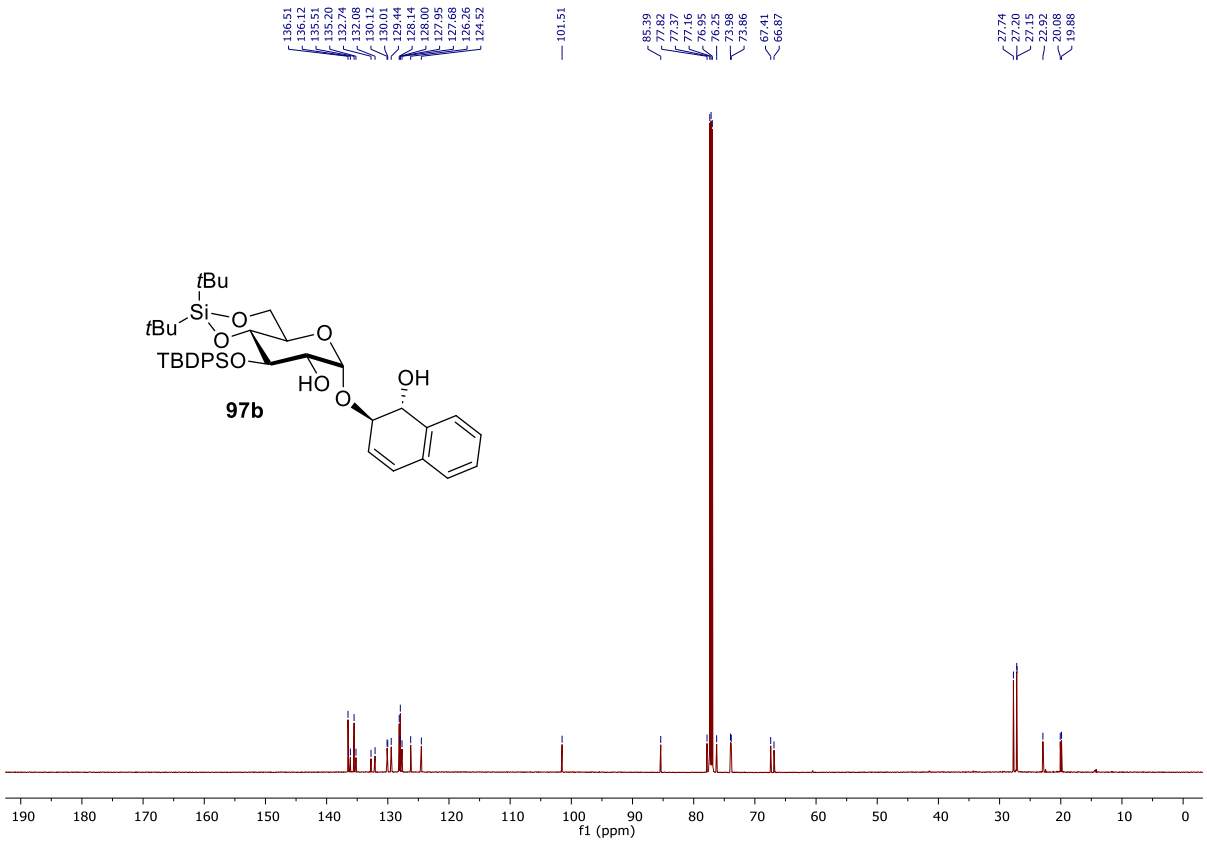

Figure 8.429. ^{13}C NMR spectra for 97b

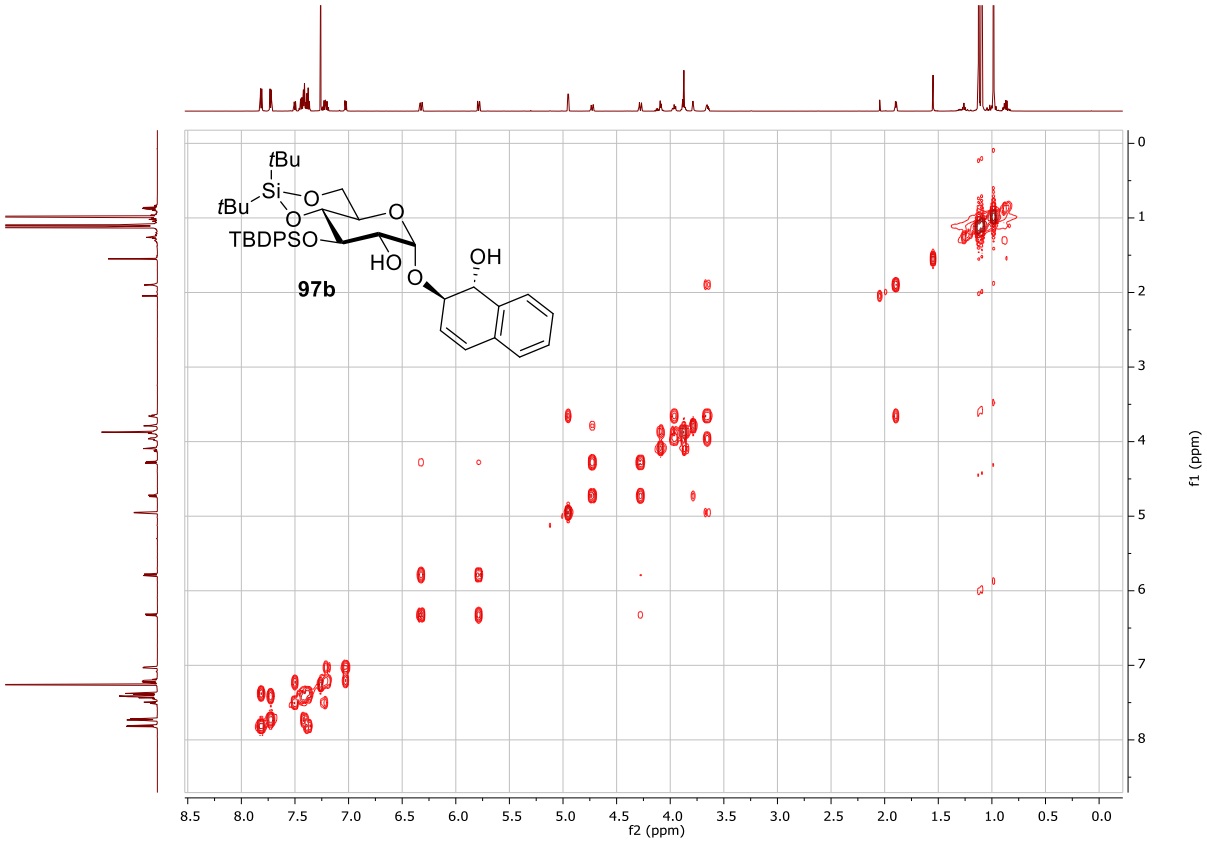

Figure 8.430. COSY spectra for 97b

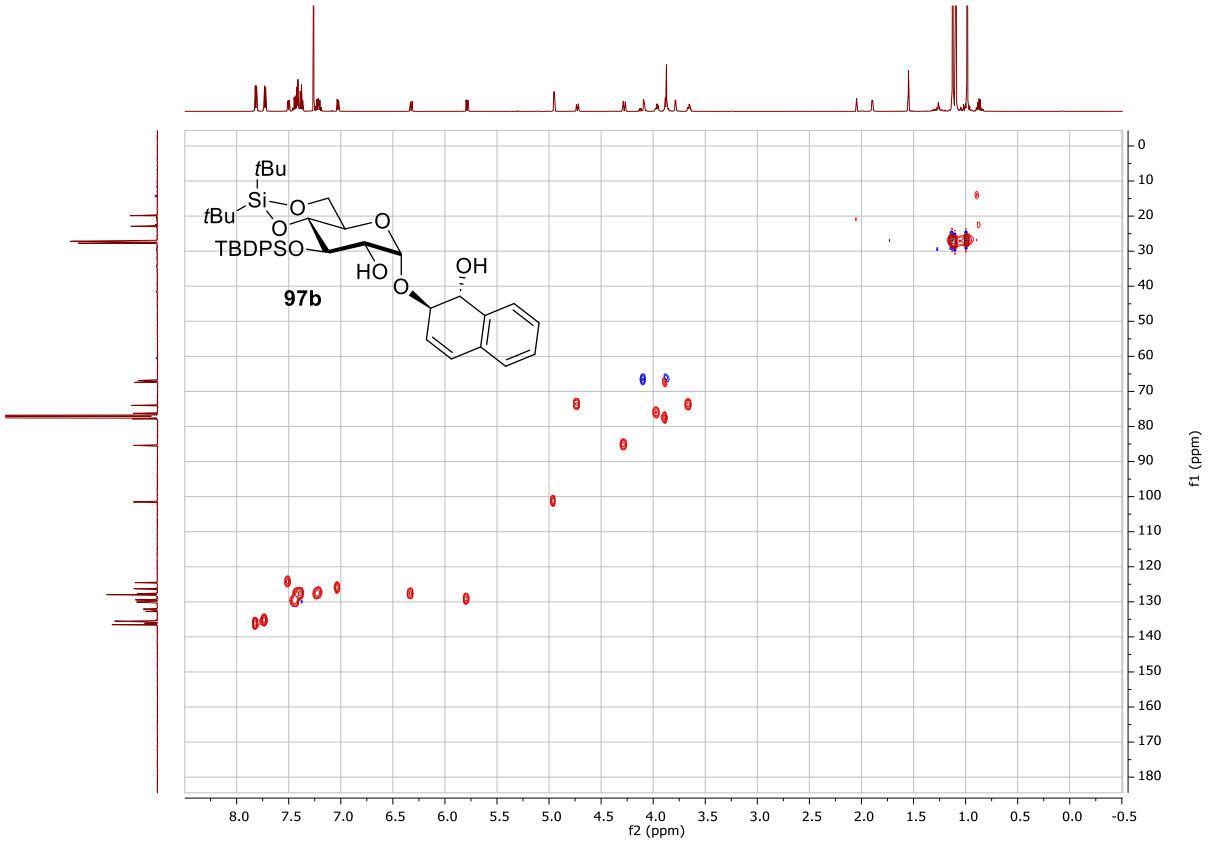

Figure 8.431. HSQC spectra for 97b

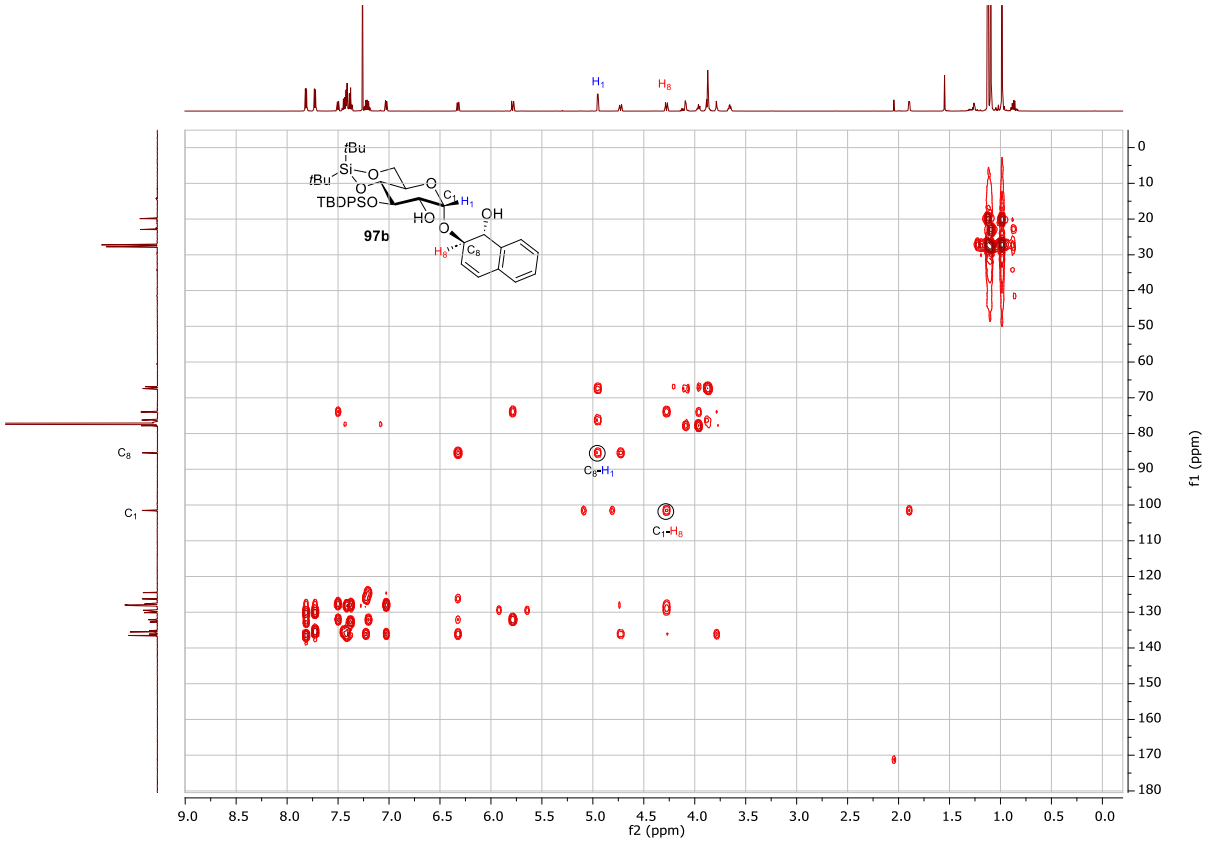

Figure 8.432. HMBC spectra for 97b

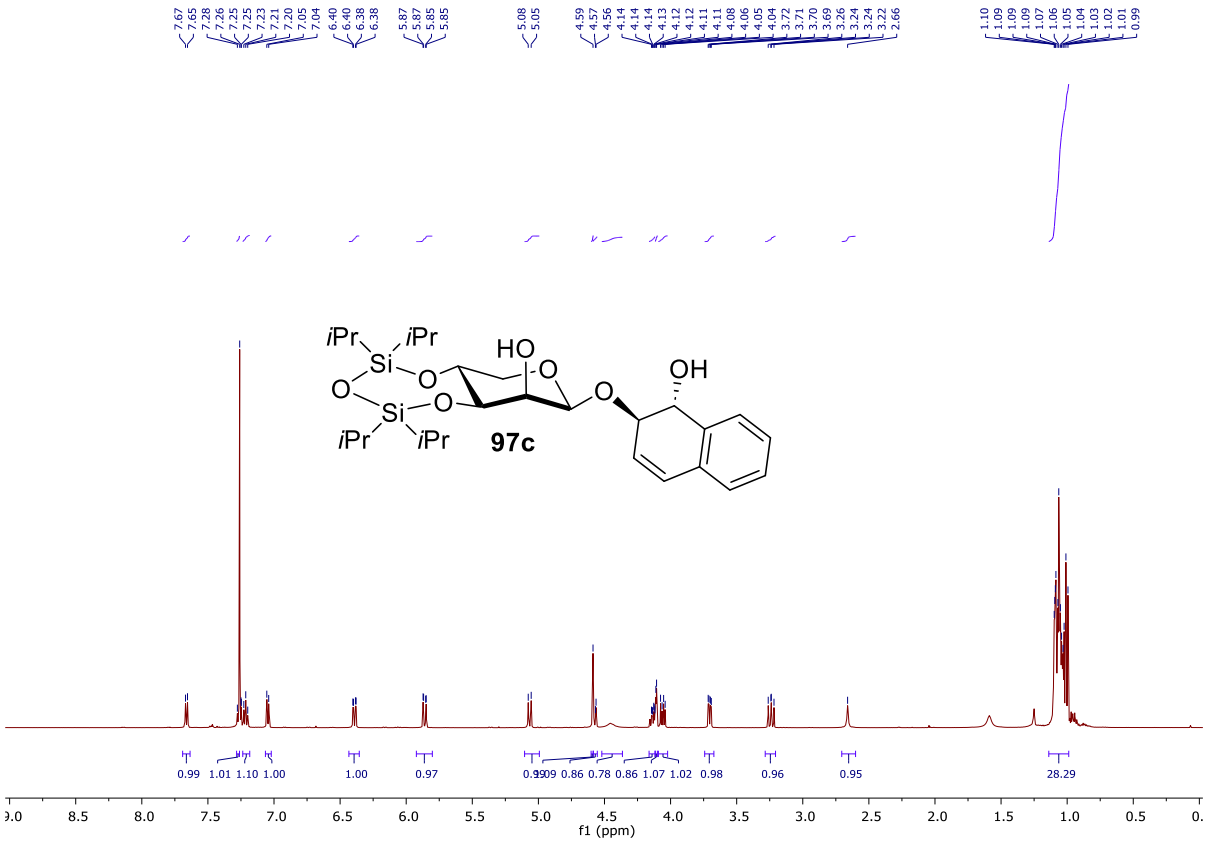

Figure 8.433. ^{1}H NMR spectra for 97c

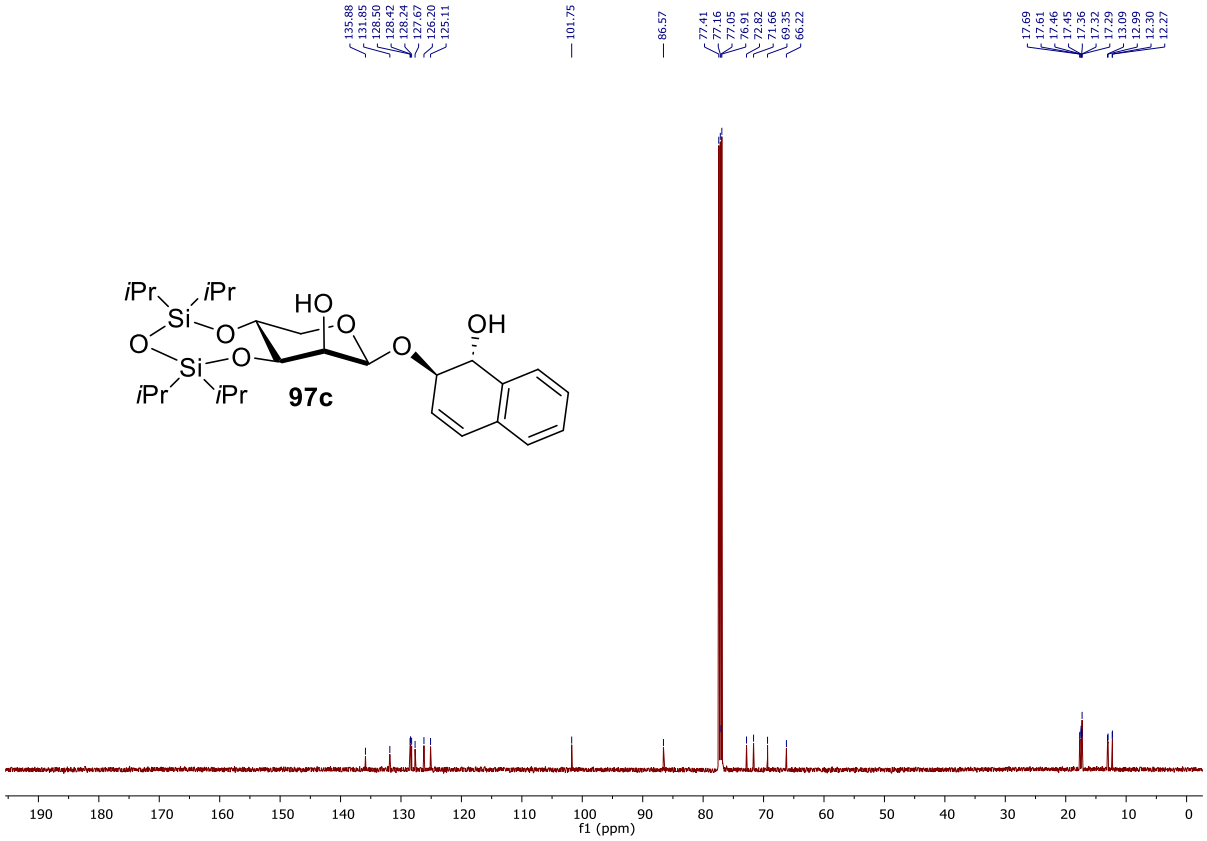

Figure 8.434. ^{13}C NMR spectra for 97c

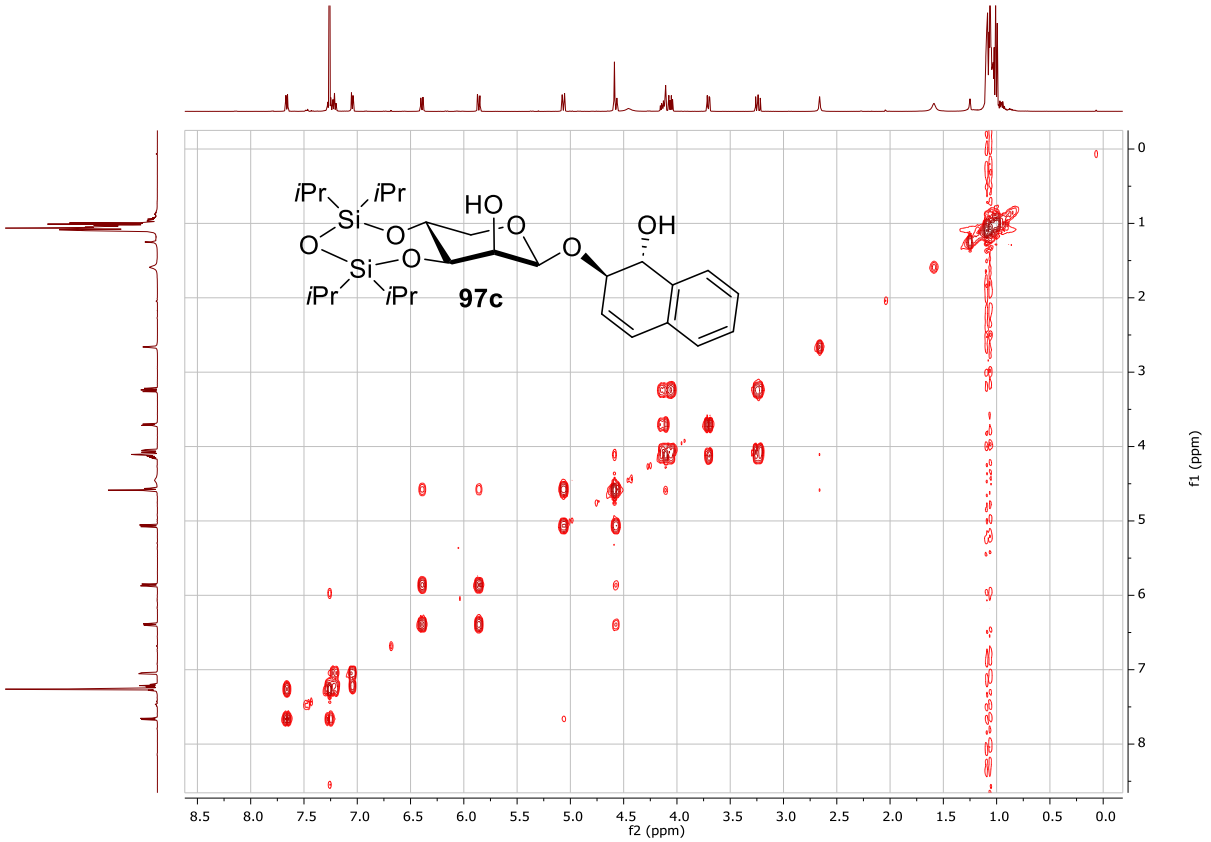

Figure 8.435. COSY spectra for 97c

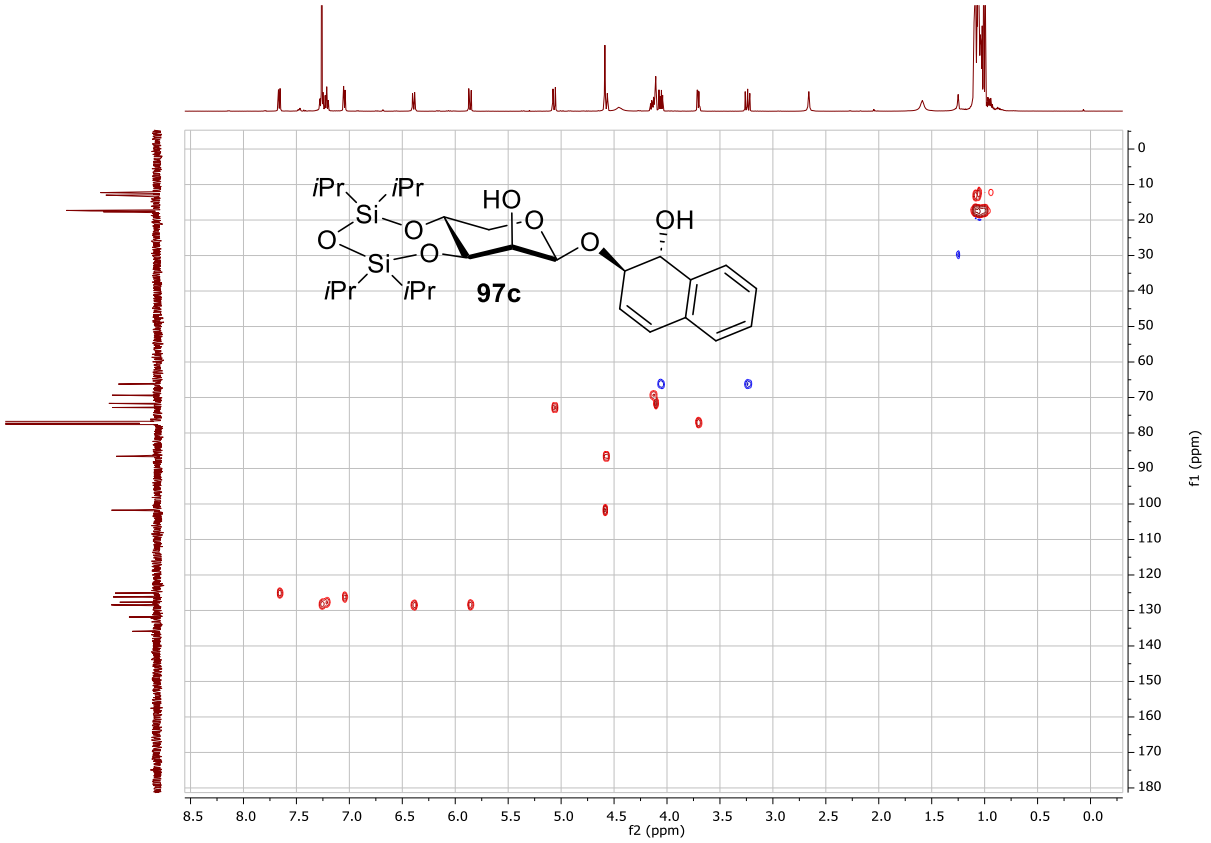

Figure 8.436. HSQC spectra for 97c

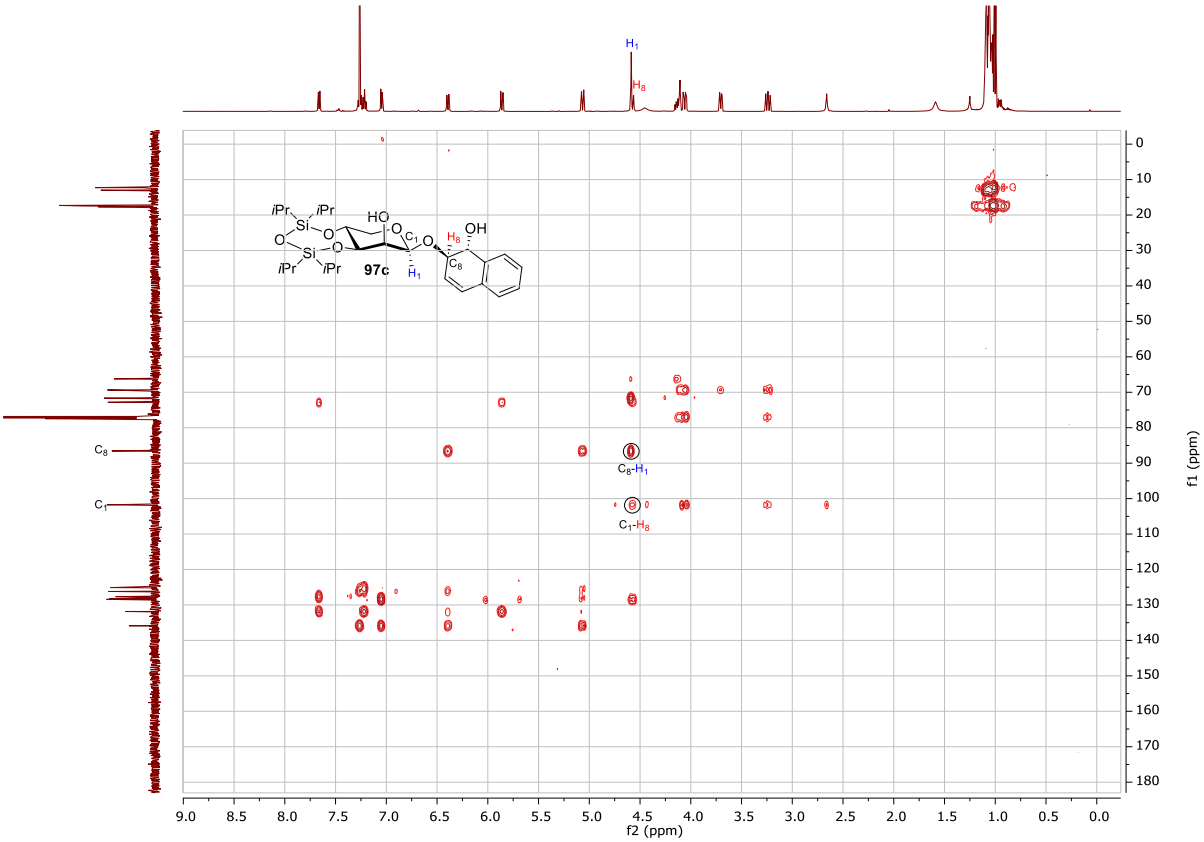

Figure 8.437. HMBC spectra for 97c

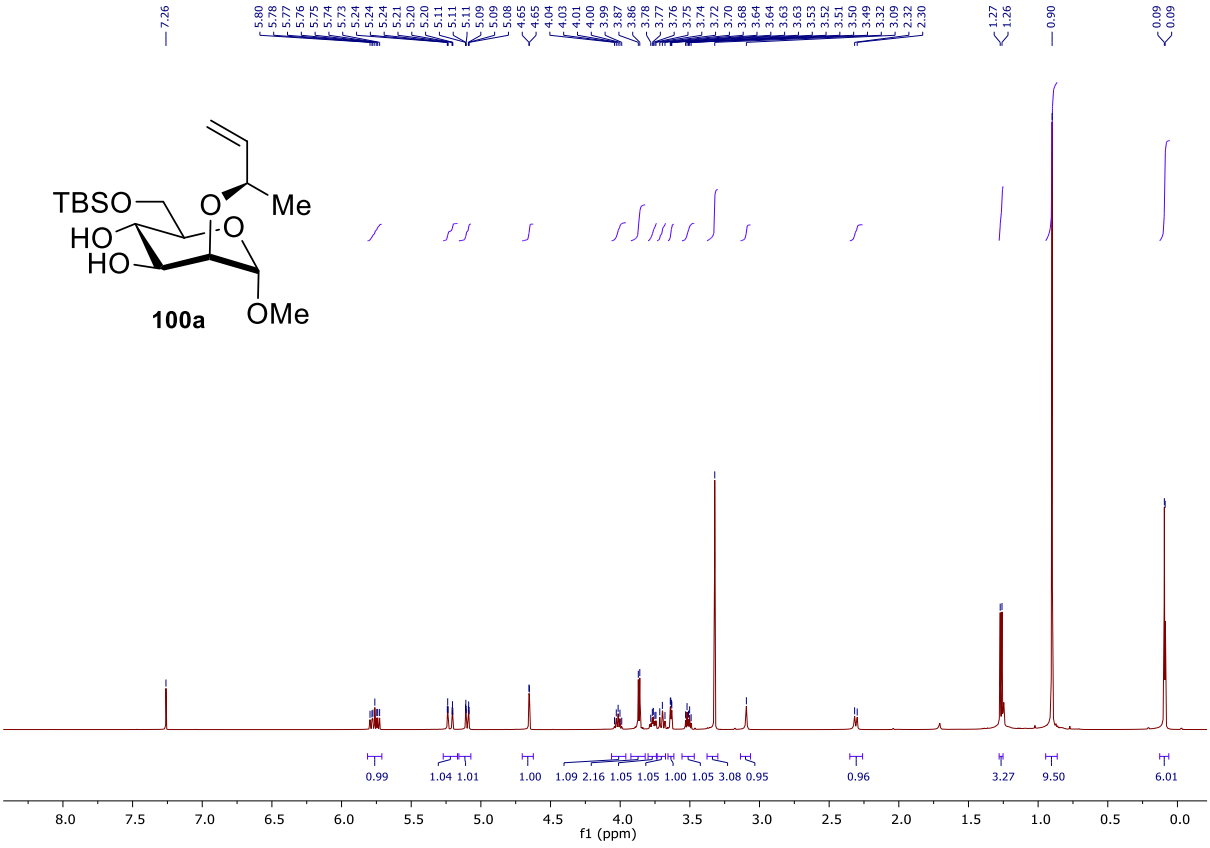

Figure 8.438. ^{1}H NMR spectra for 100a

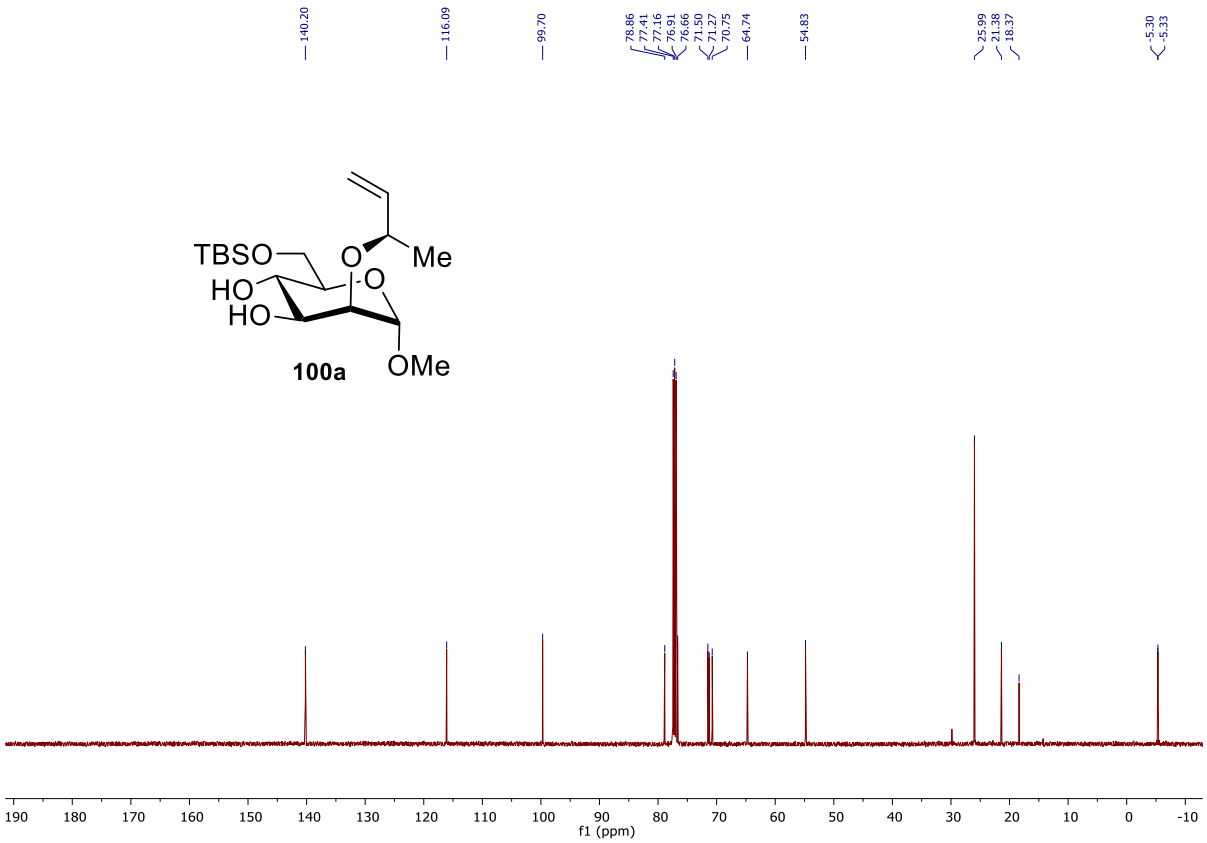

Figure 8.439. ^{13}C NMR spectra for 100a

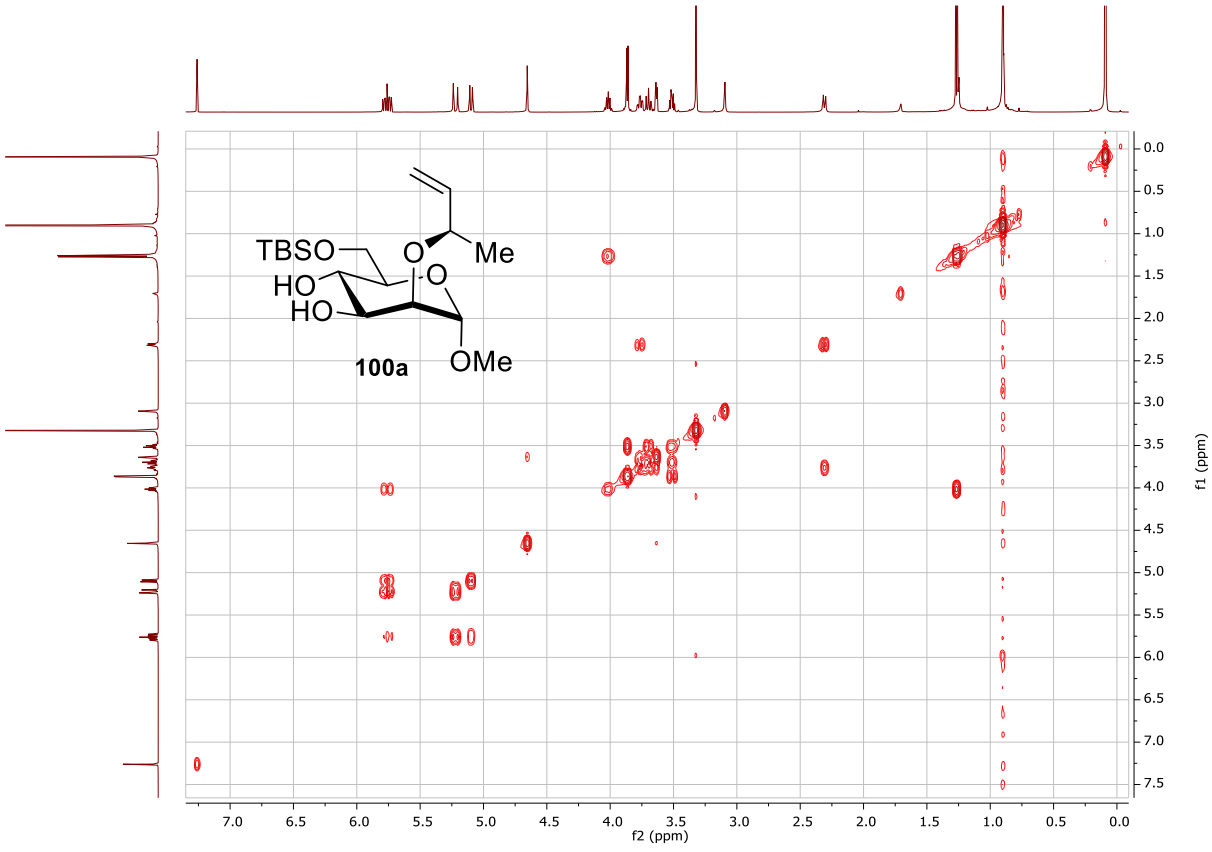

Figure 8.440. COSY spectra for 100a

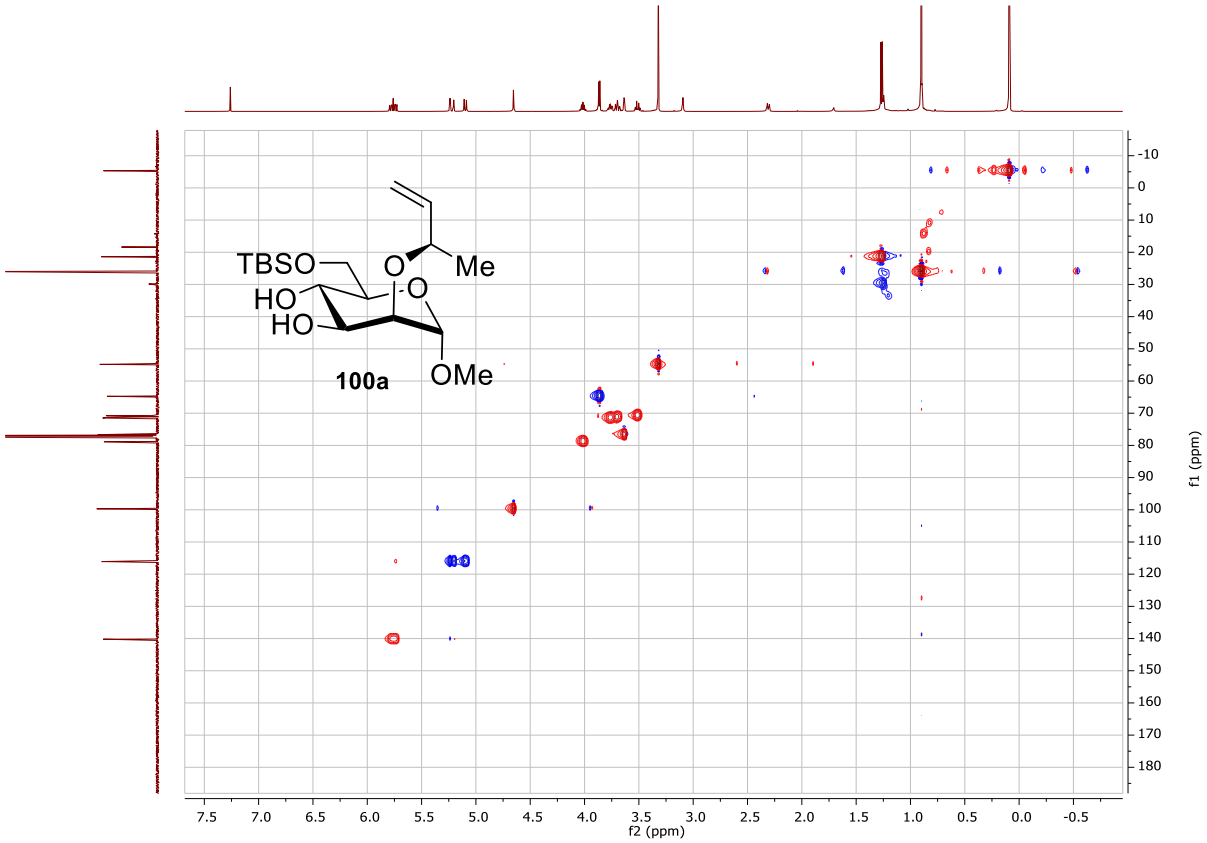

Figure 8.441. HSQC spectra for 100a

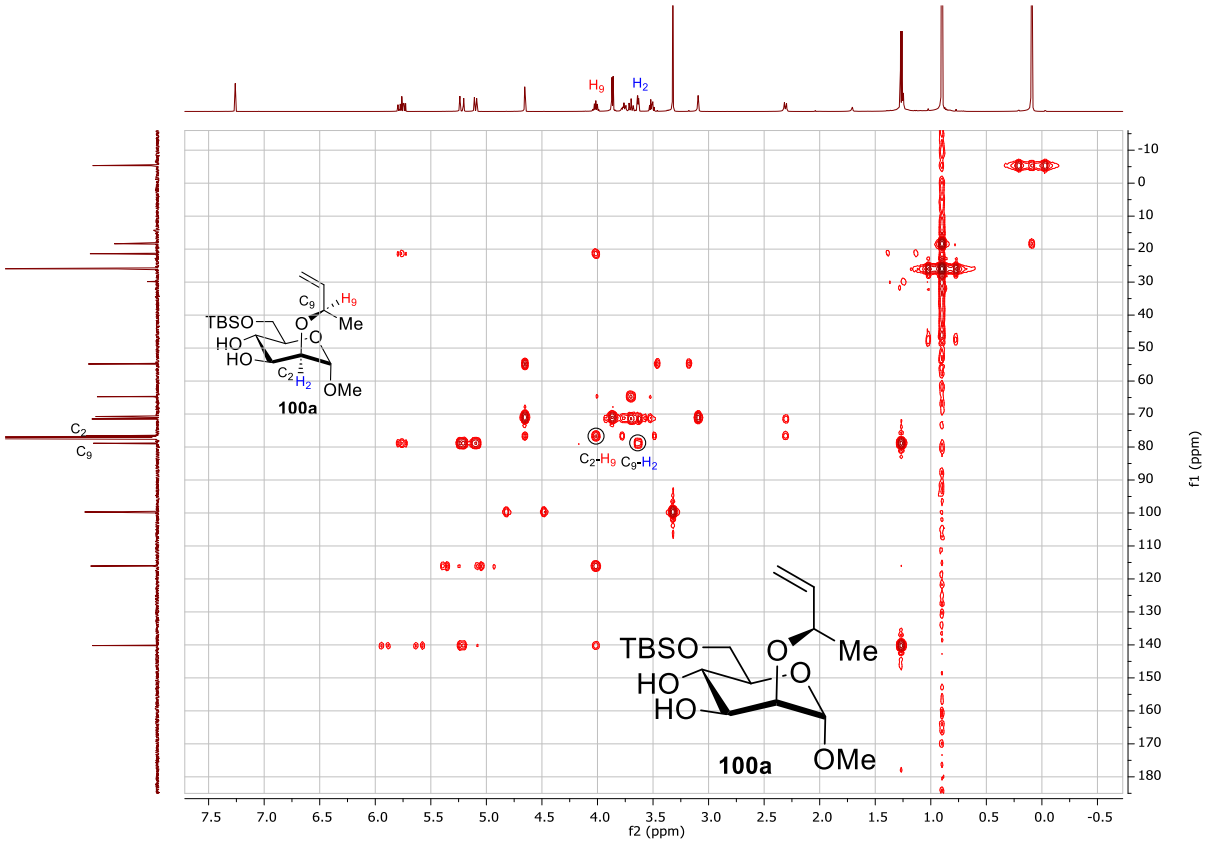

Figure 8.442. HMBC spectra for 100a

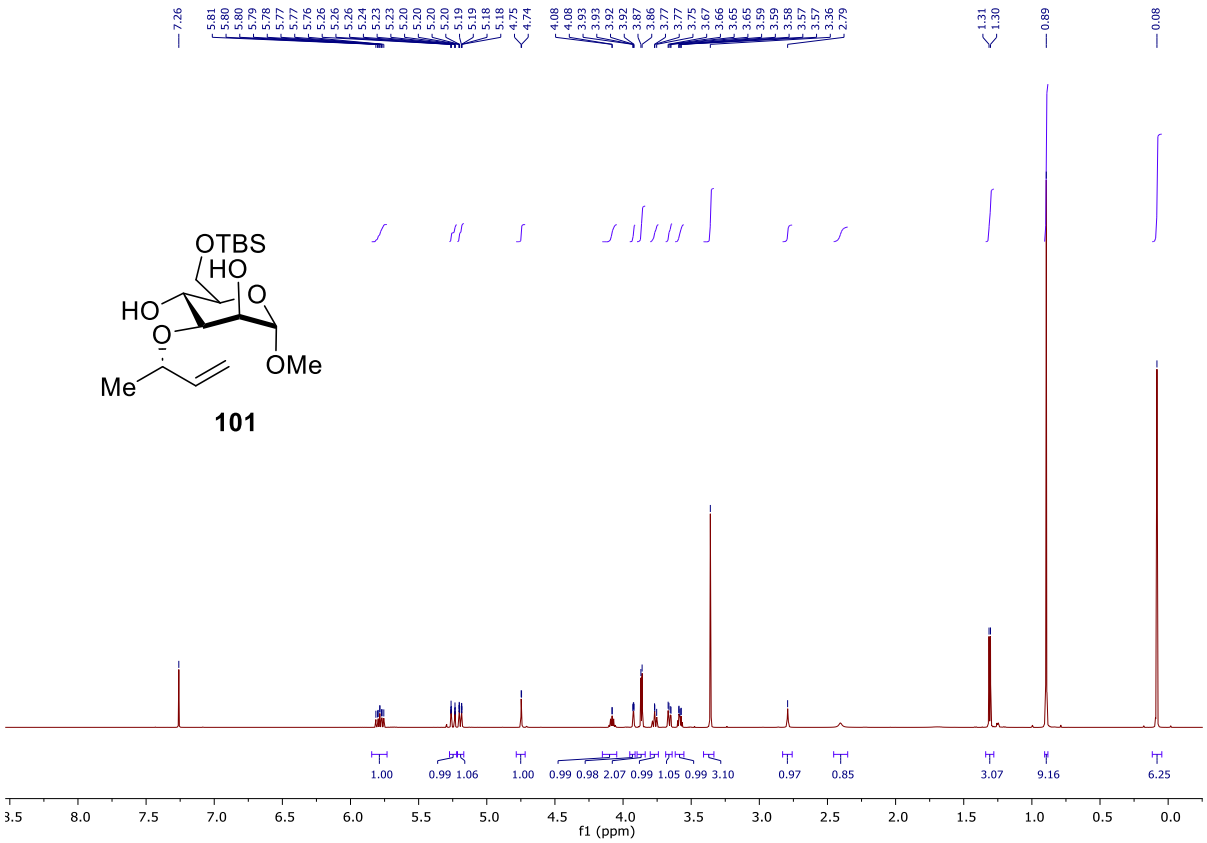

Figure 8.443. ^{1}H NMR spectra for 101

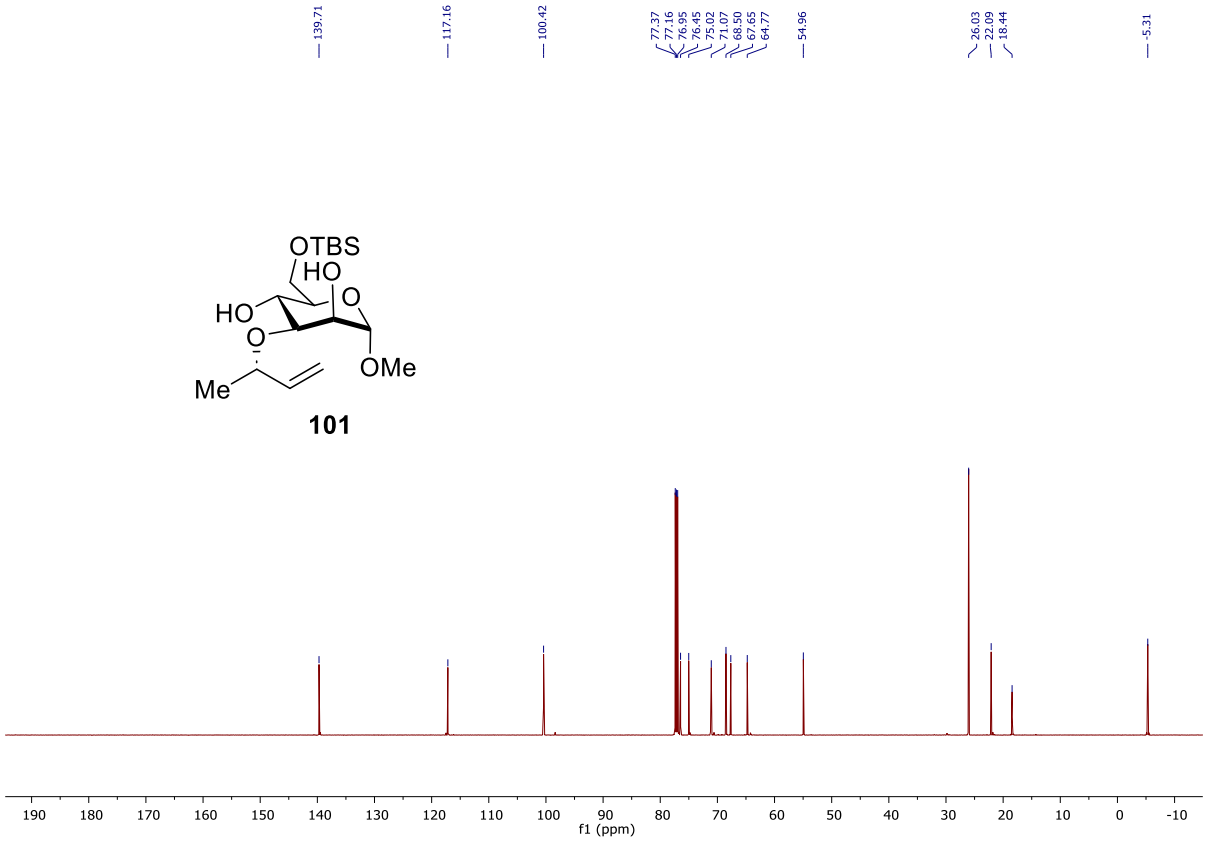

Figure 8.444. ^{13}C NMR spectra for 101

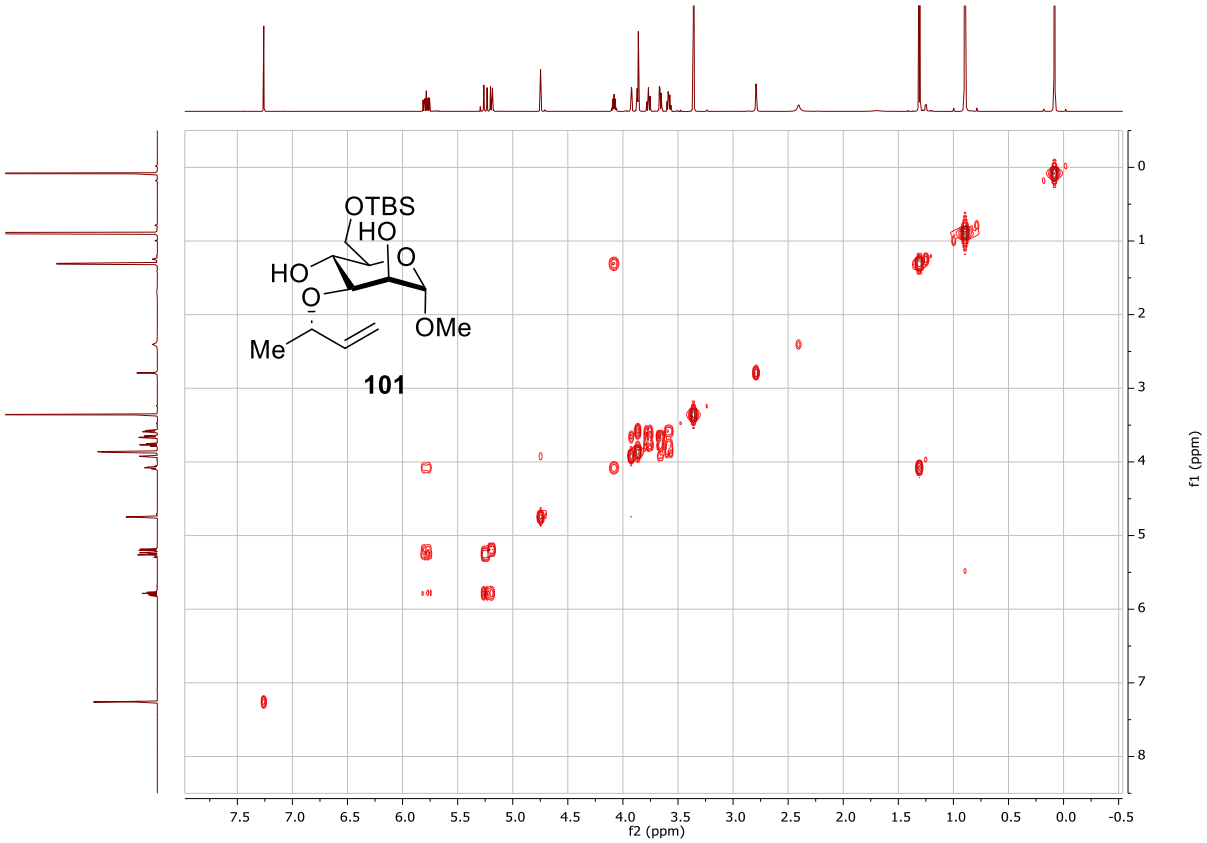

Figure 8.445. COSY spectra for 101

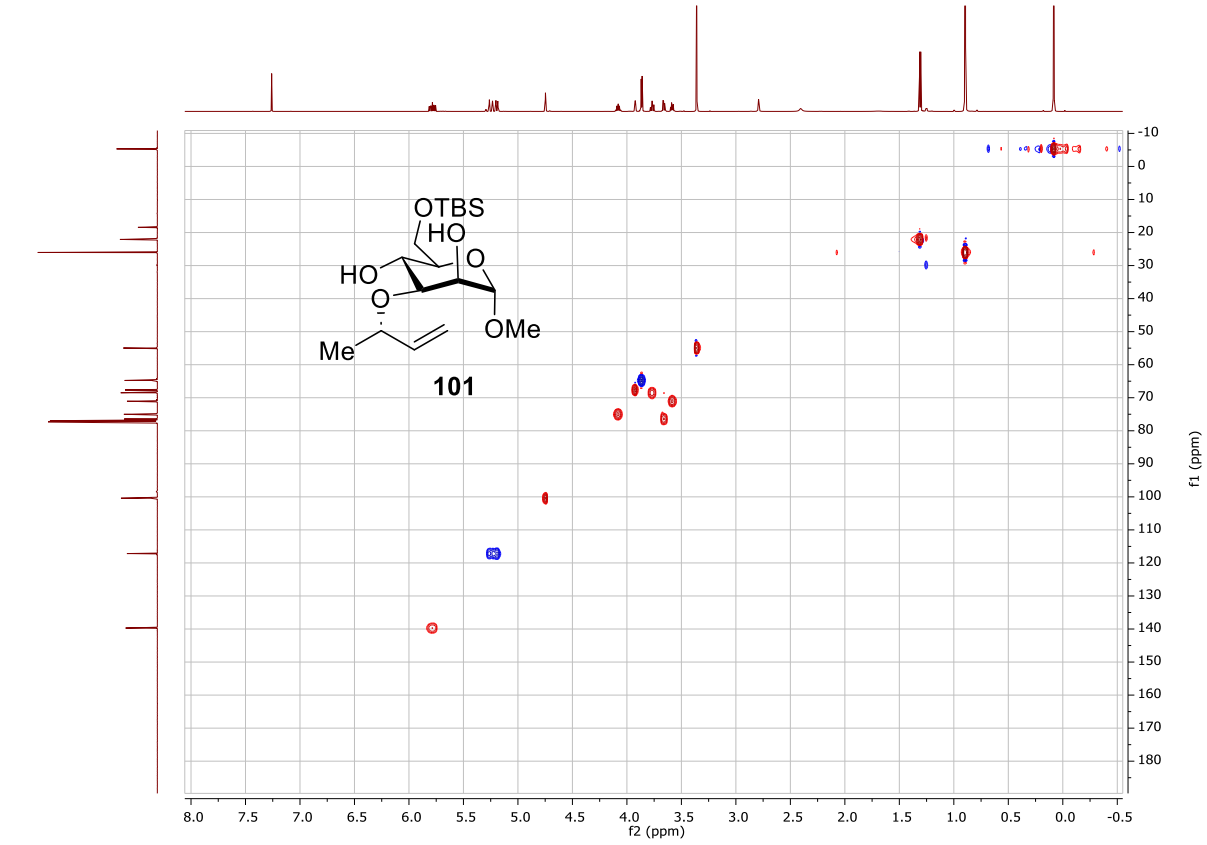

Figure 8.446. HSQC spectra for 101

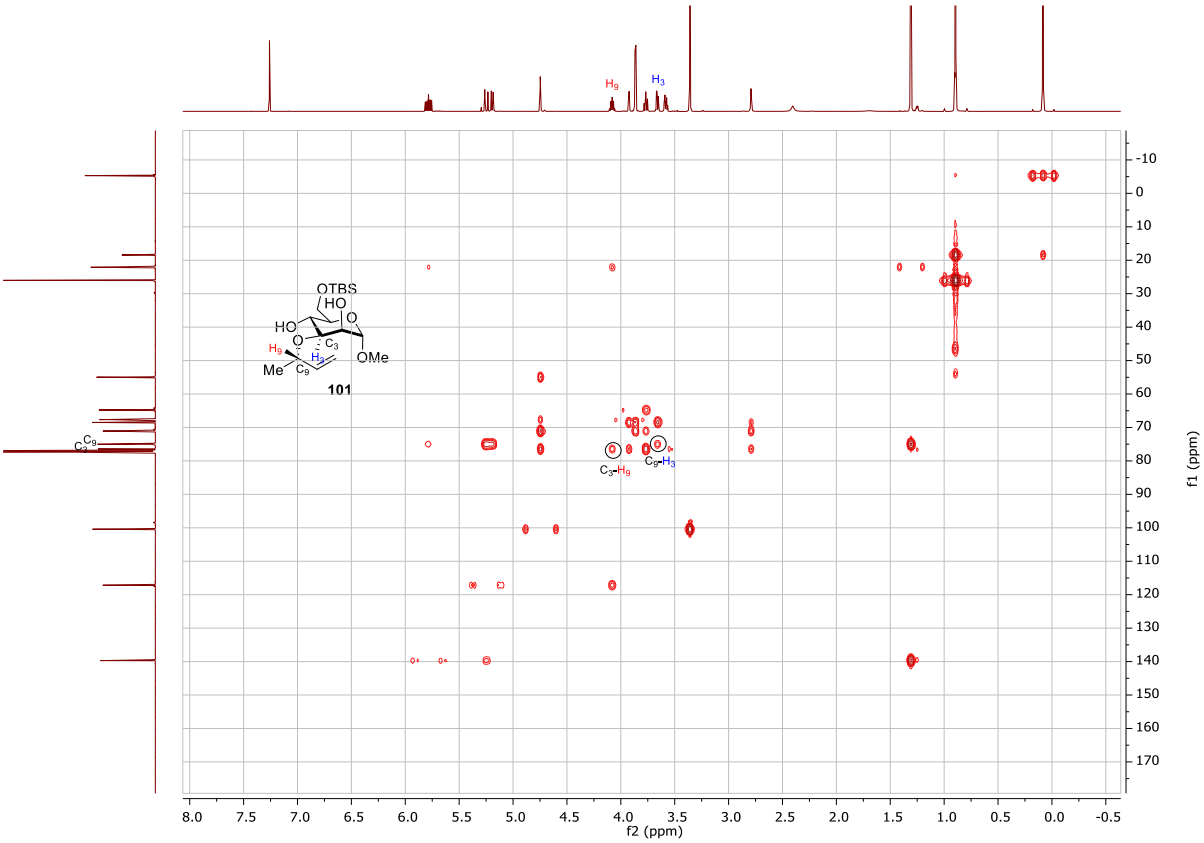

Figure 8.447. HMBC spectra for 101

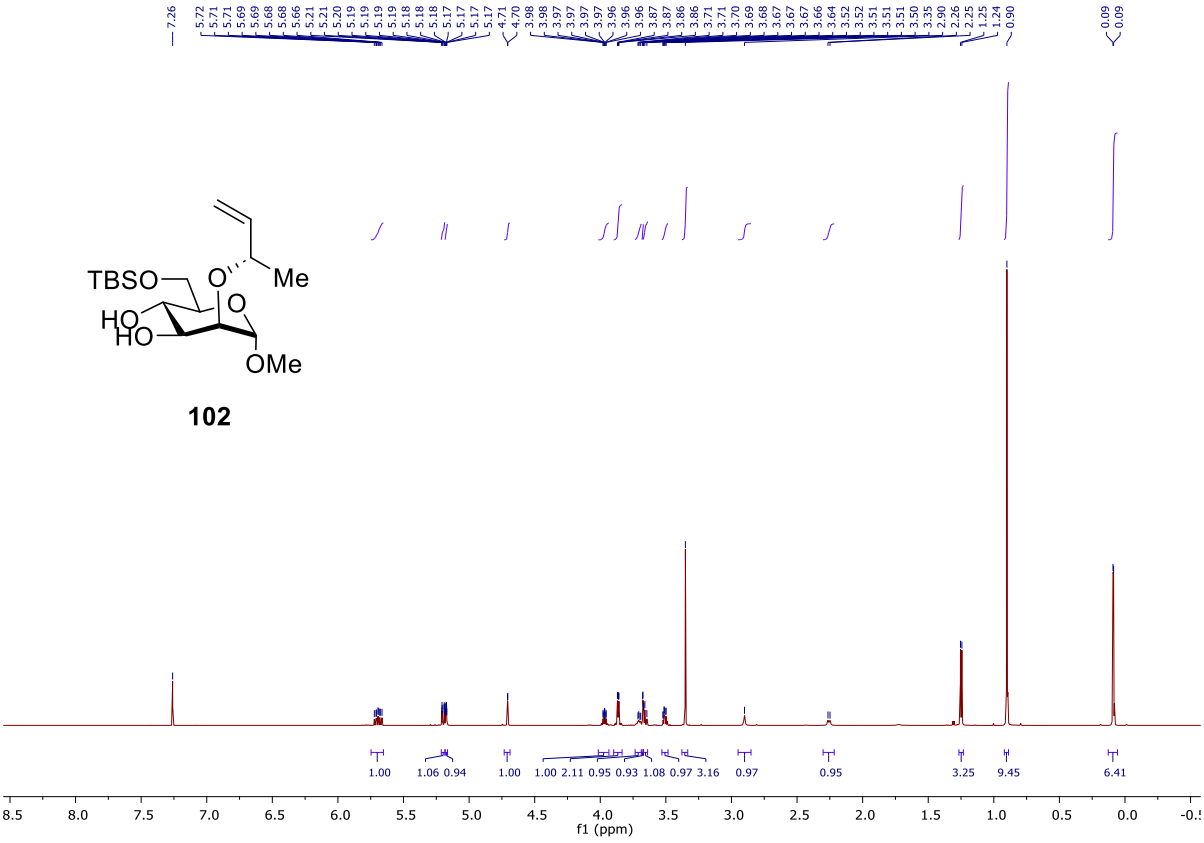

Figure 8.448. ^{1}H NMR spectra for 102

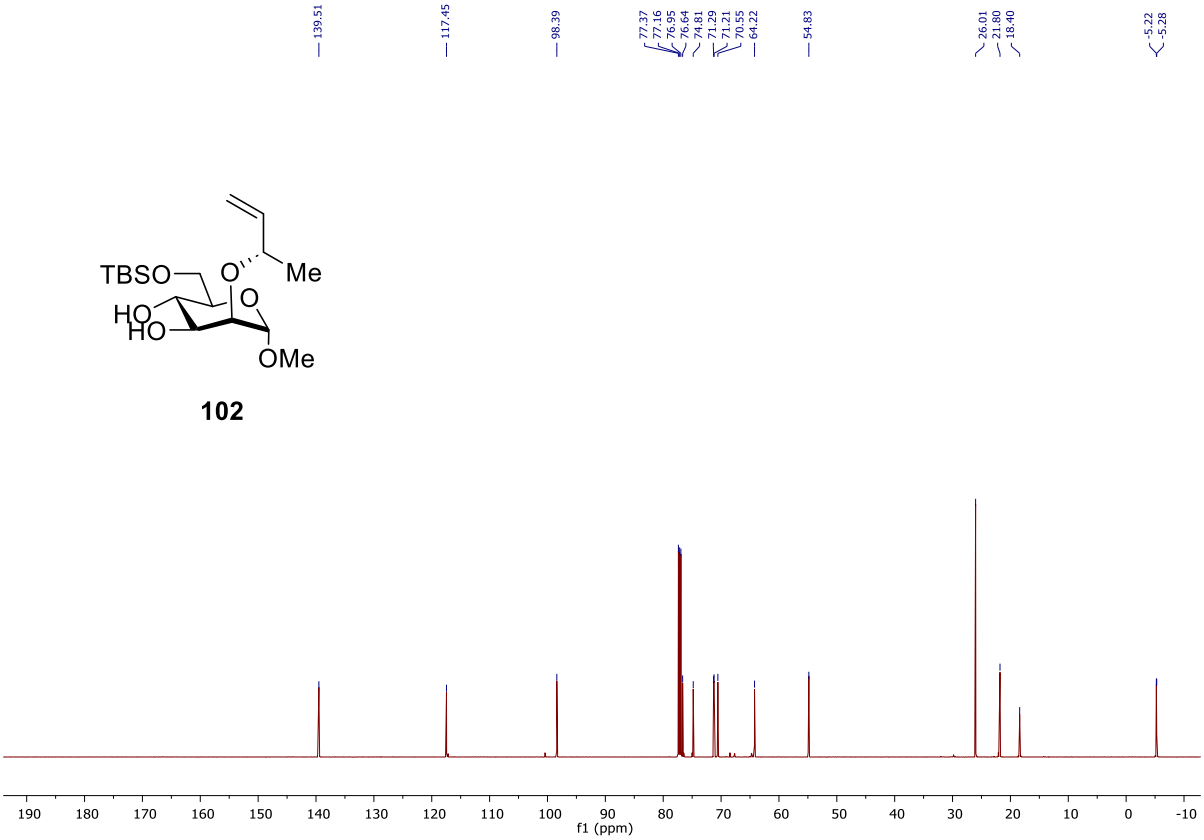

Figure 8.449. ^{13}C NMR spectra for 102

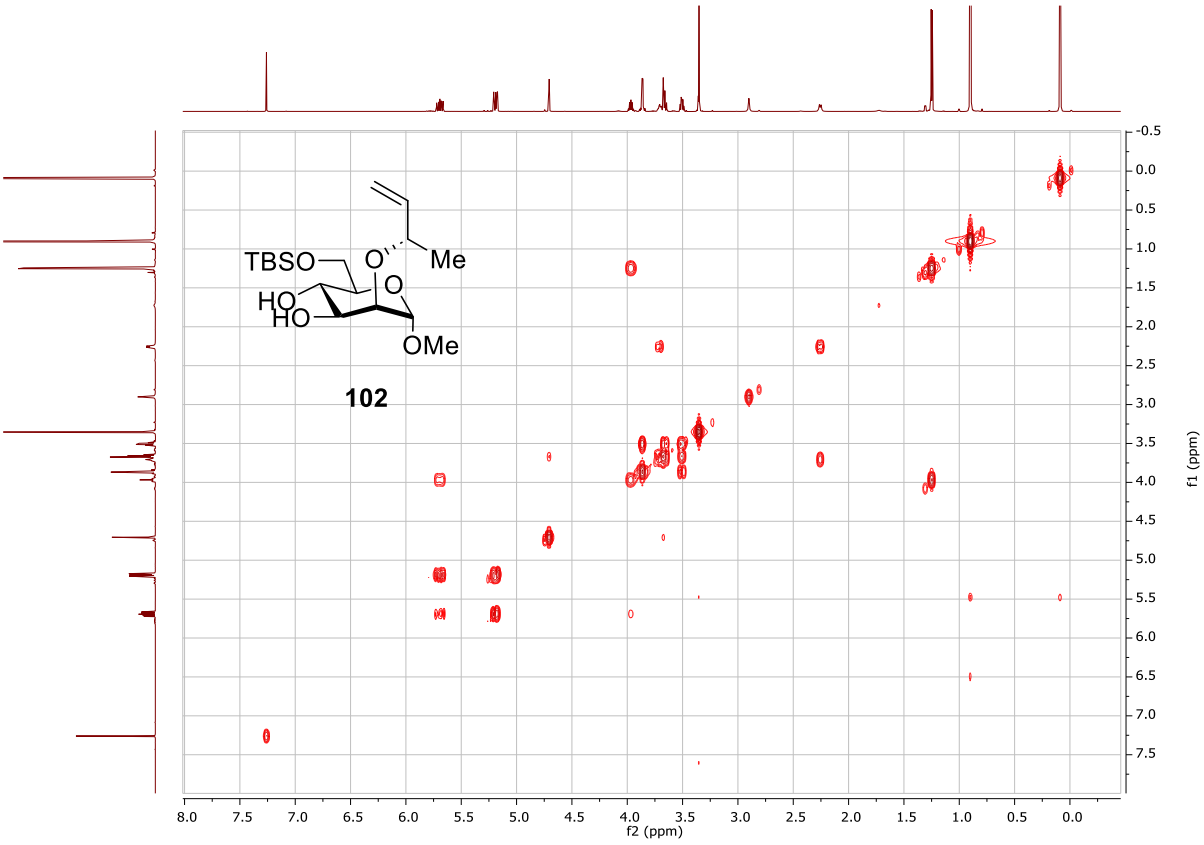

Figure 8.450. COSY spectra for 102

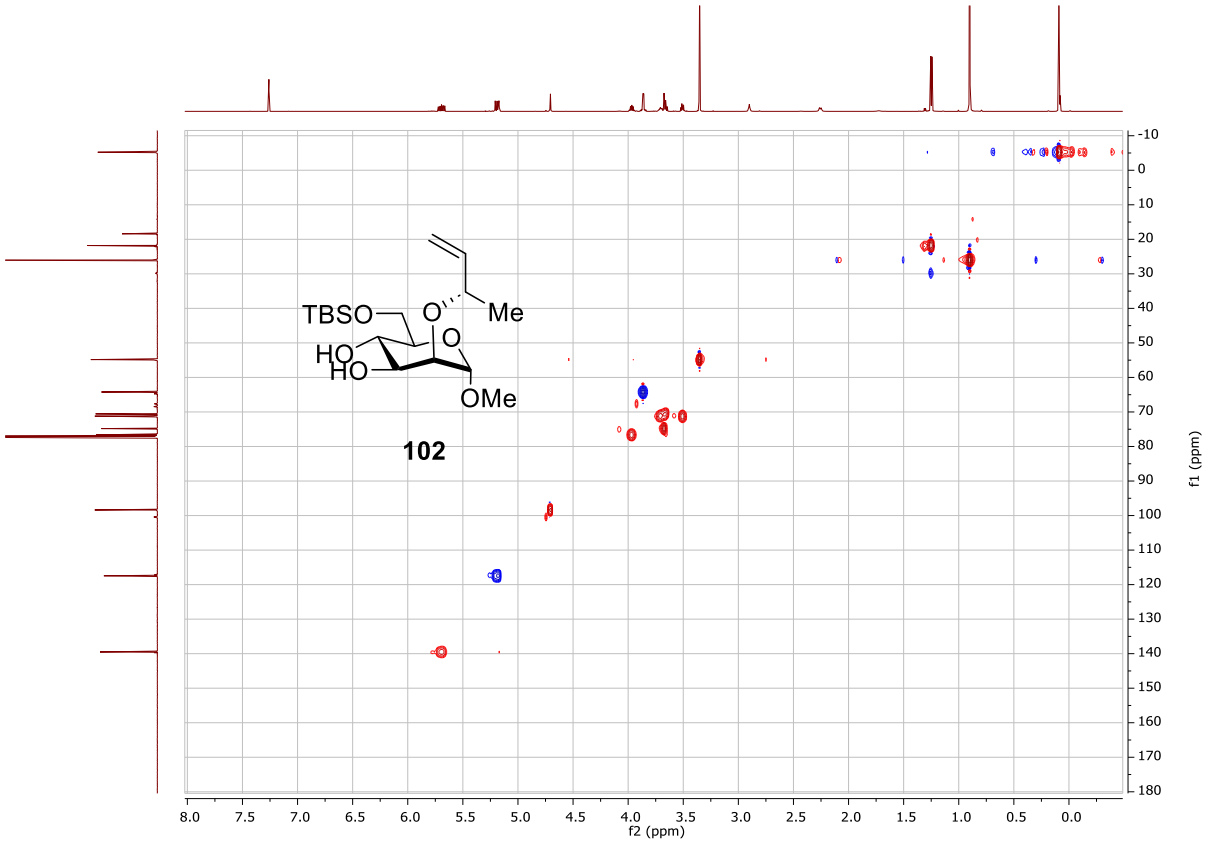

Figure 8.451. HSQC spectra for 102

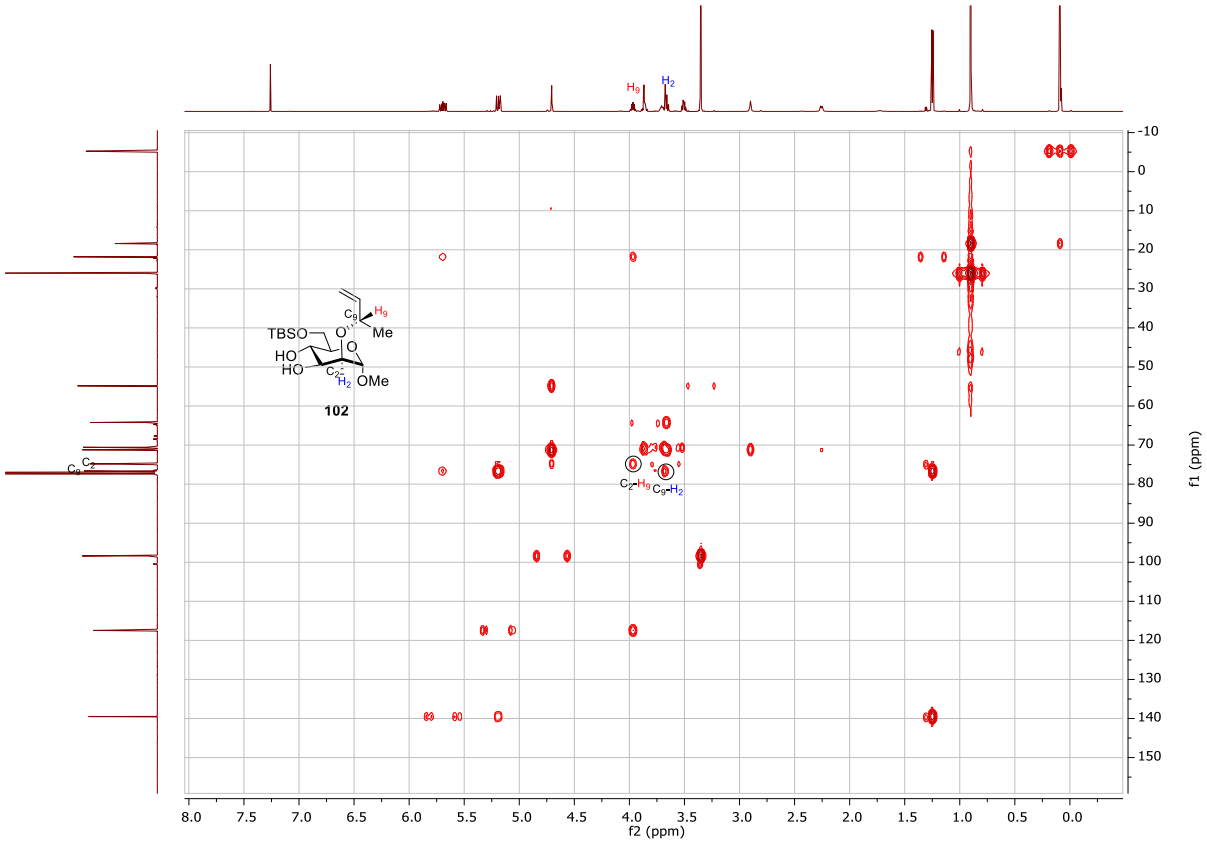

Figure 8.452. HMBC spectra for 102

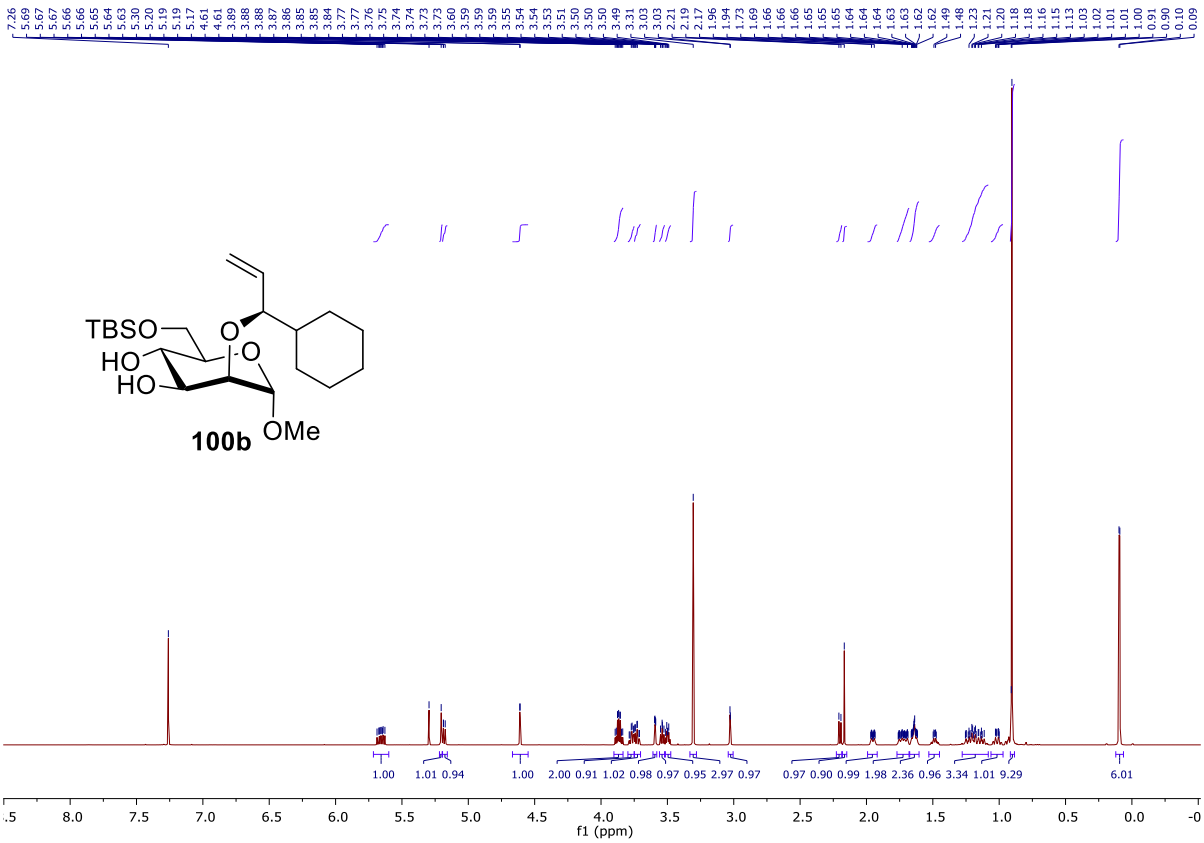

Figure 8.453. ^{1}H NMR spectra for 100b

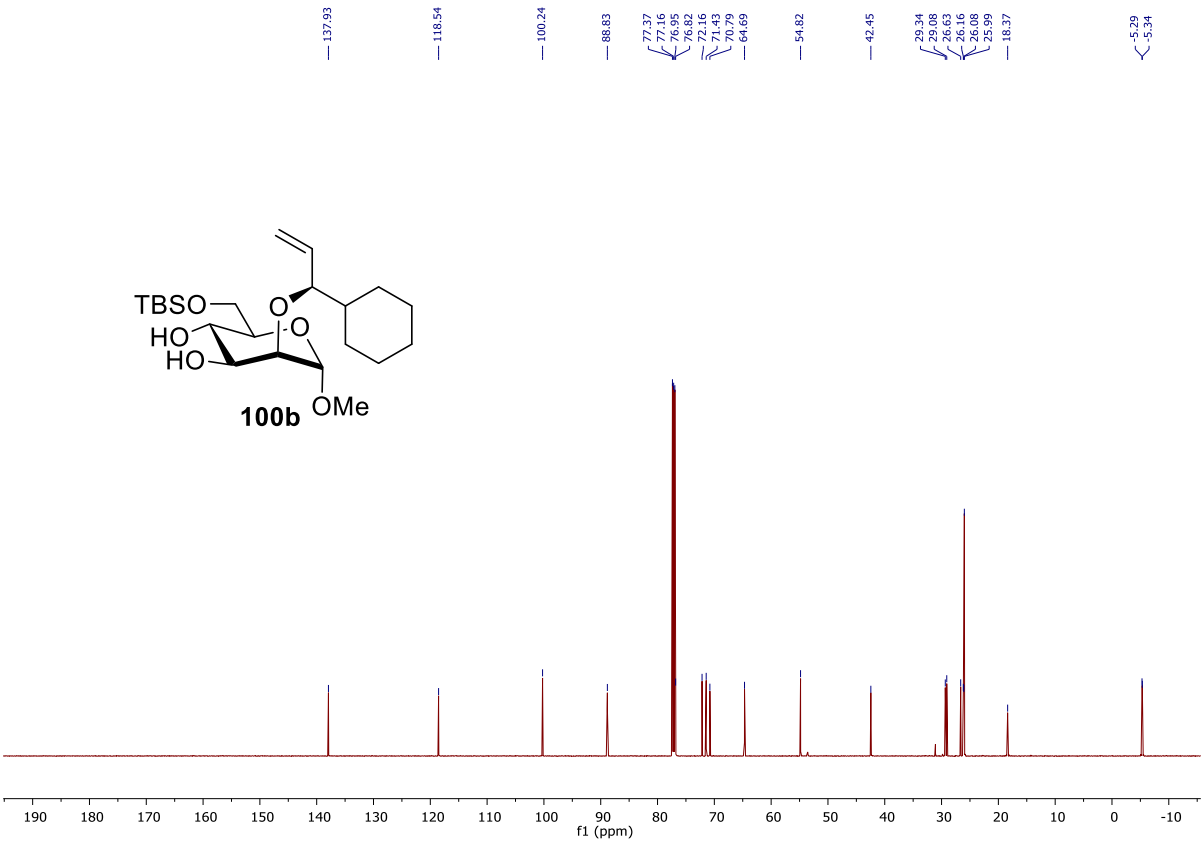

Figure 8.454. ^{13}C NMR spectra for 100b

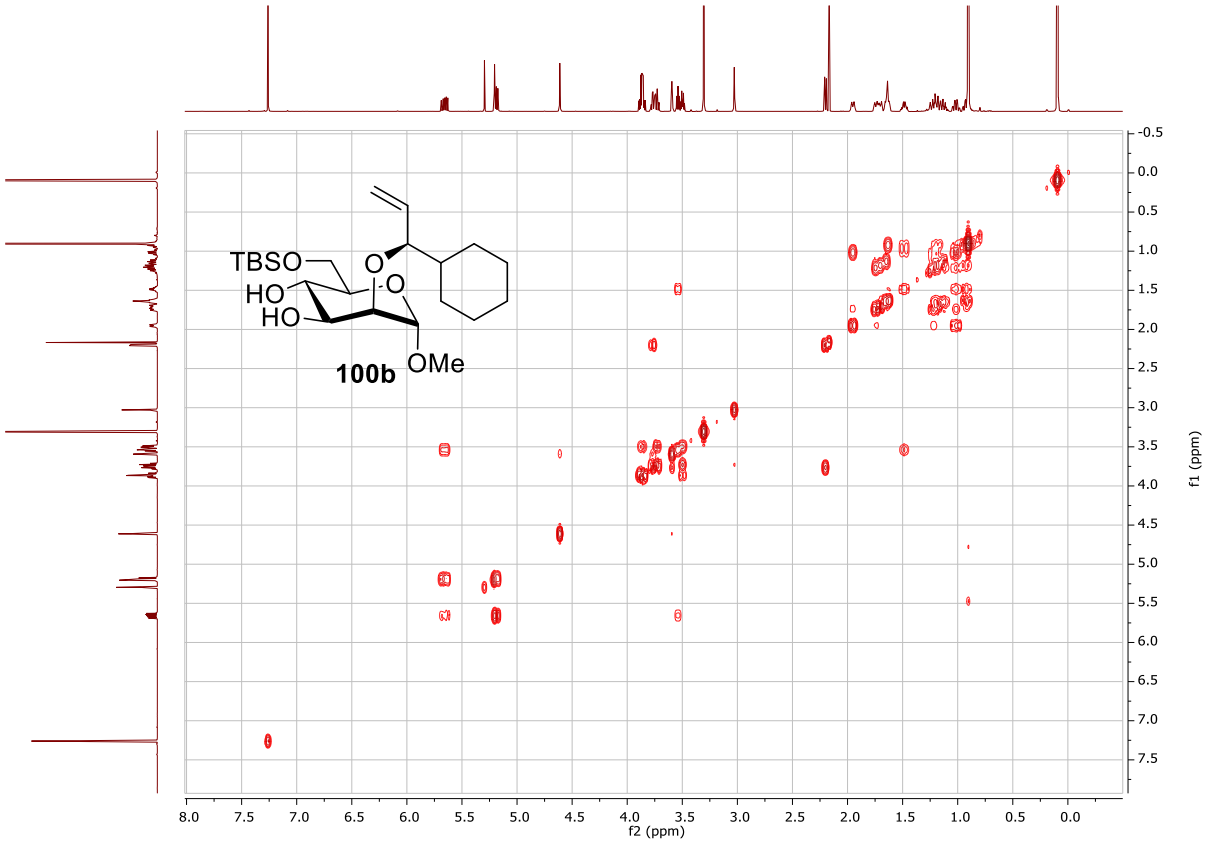

Figure 8.455. COSY spectra for 100b

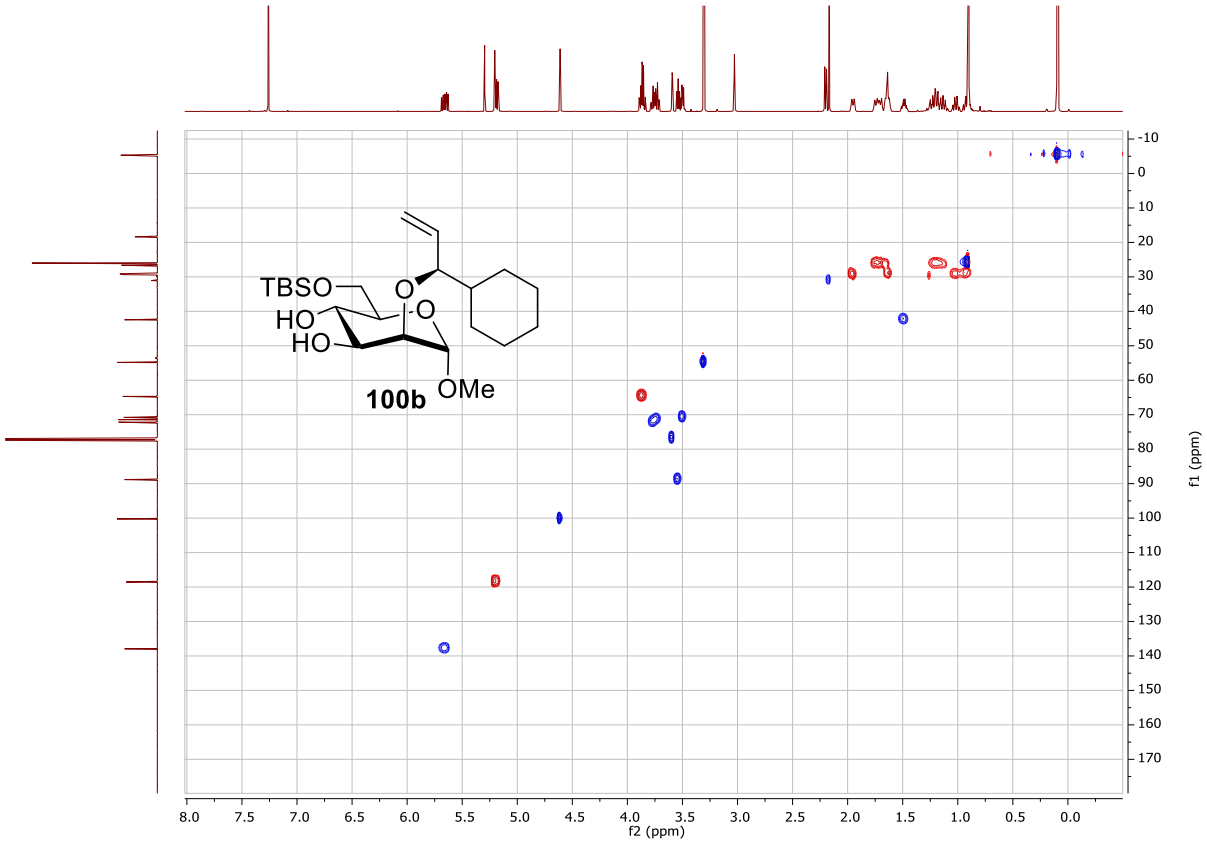

Figure 8.456. HSQC spectra for 100b

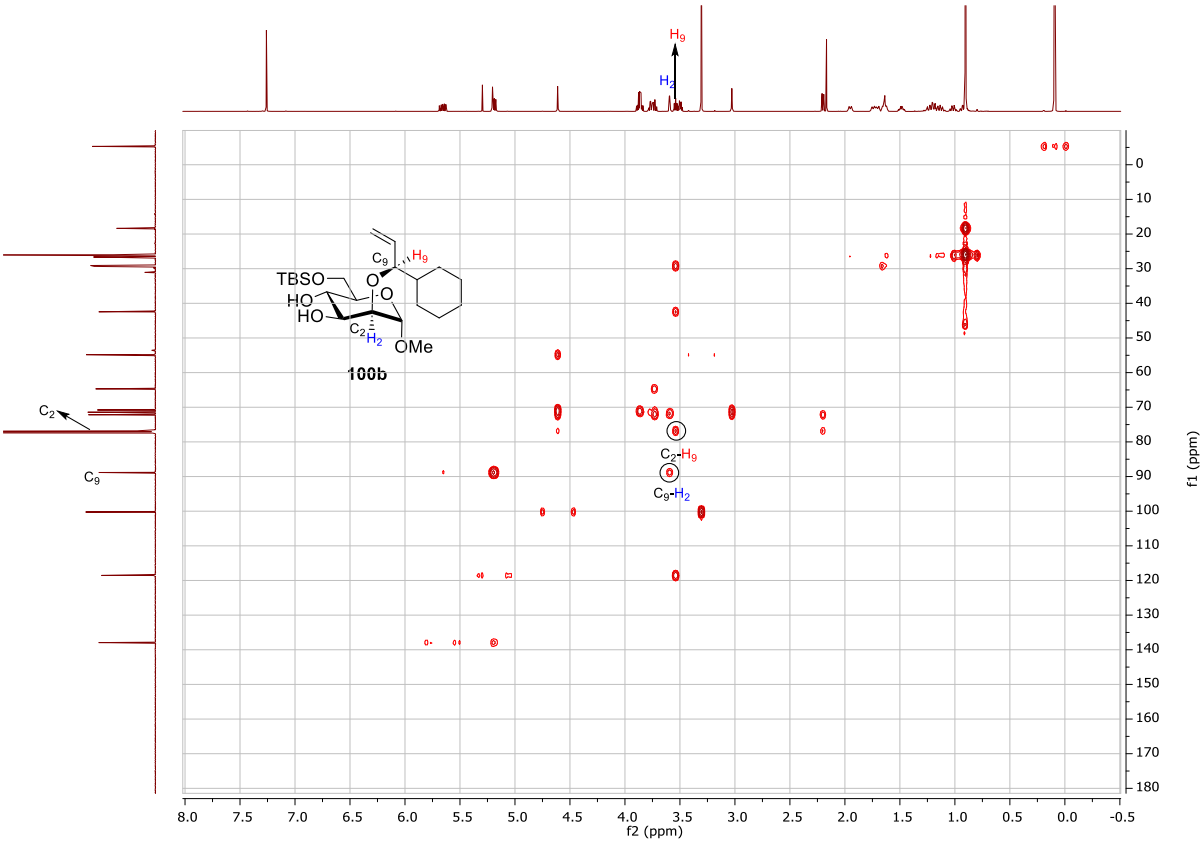

Figure 8.457. HMBC spectra for 100b

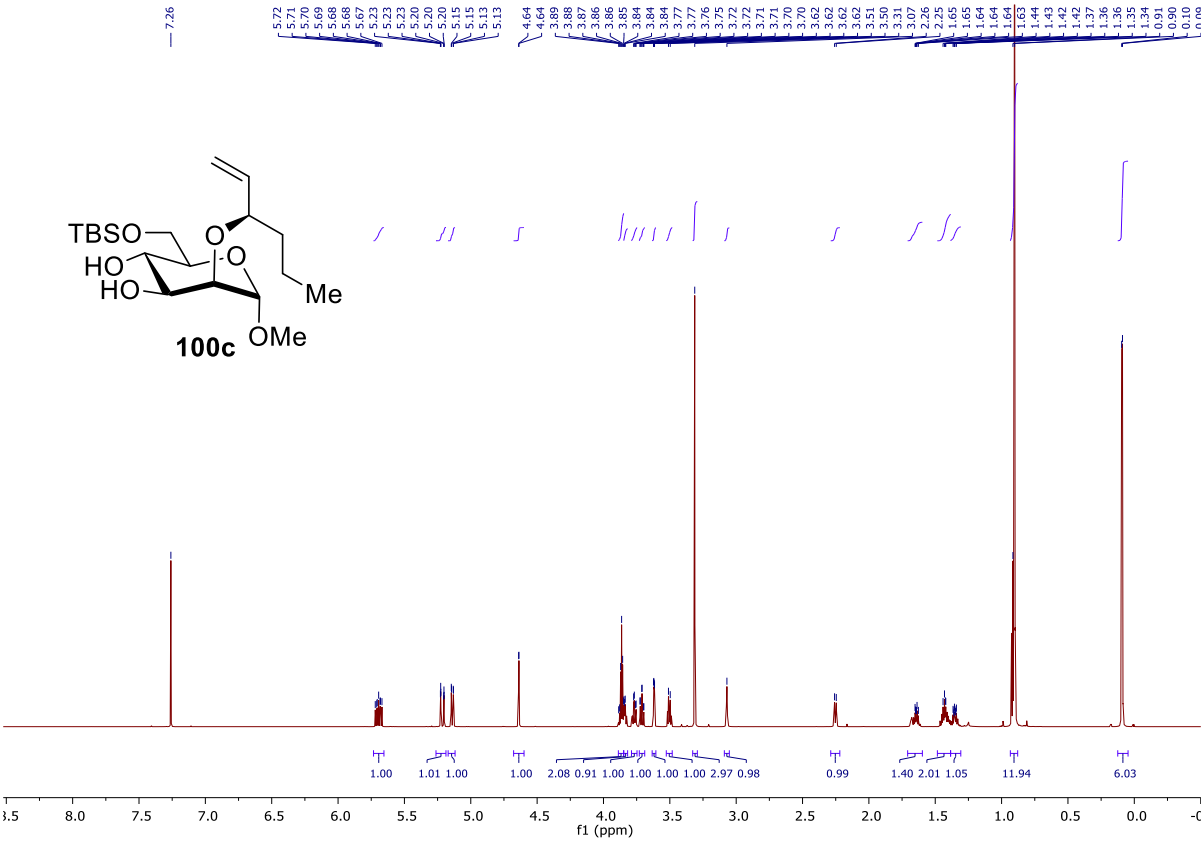

Figure 8.458. ^{1}H NMR spectra for 100c

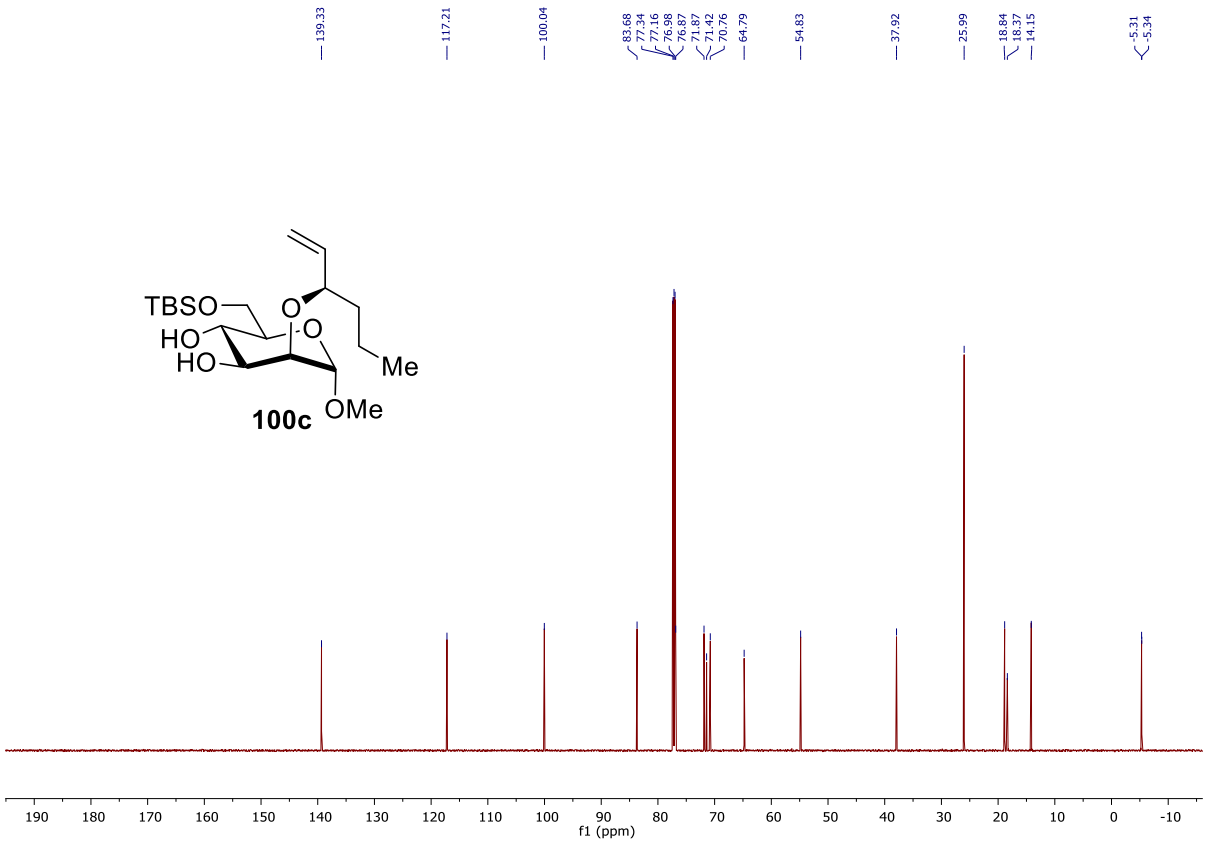

Figure 8.459. ^{13}C NMR spectra for 100c

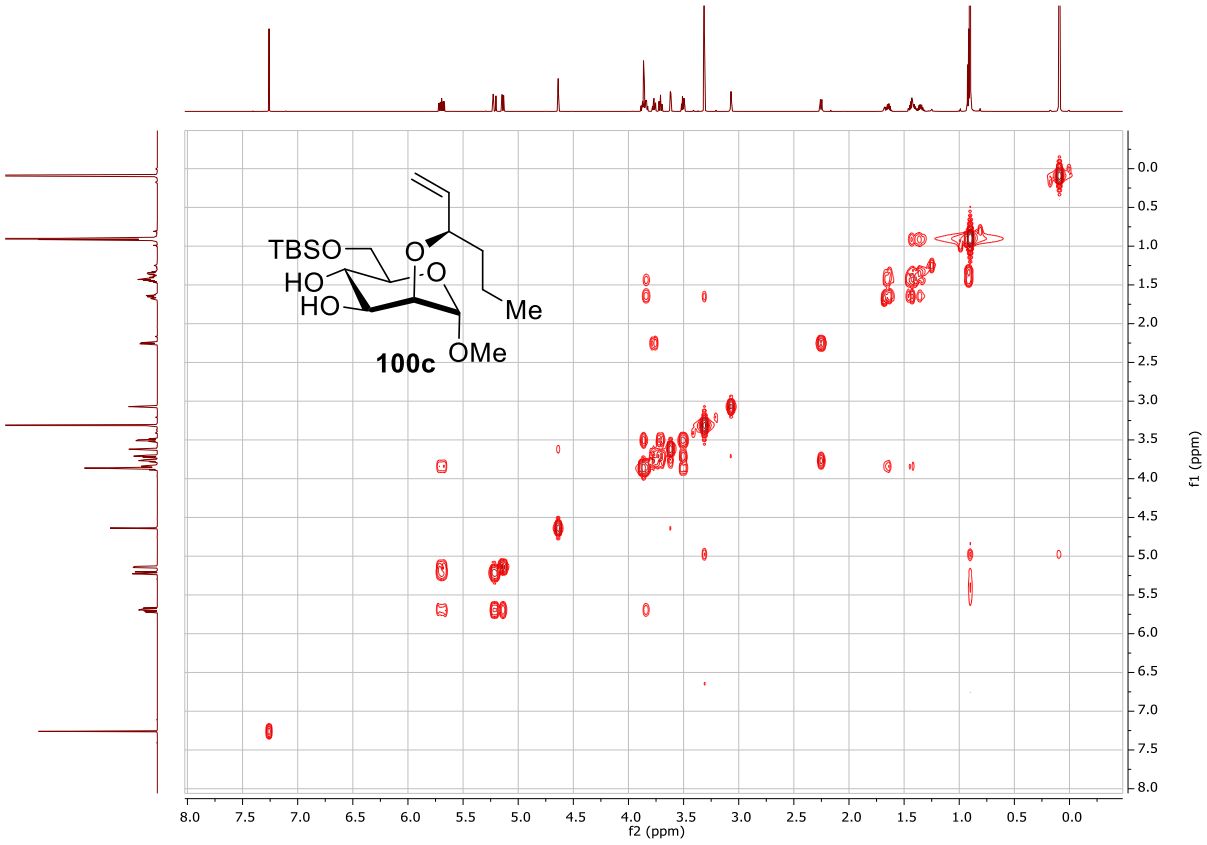

Figure 8.460. COSY spectra for 100c

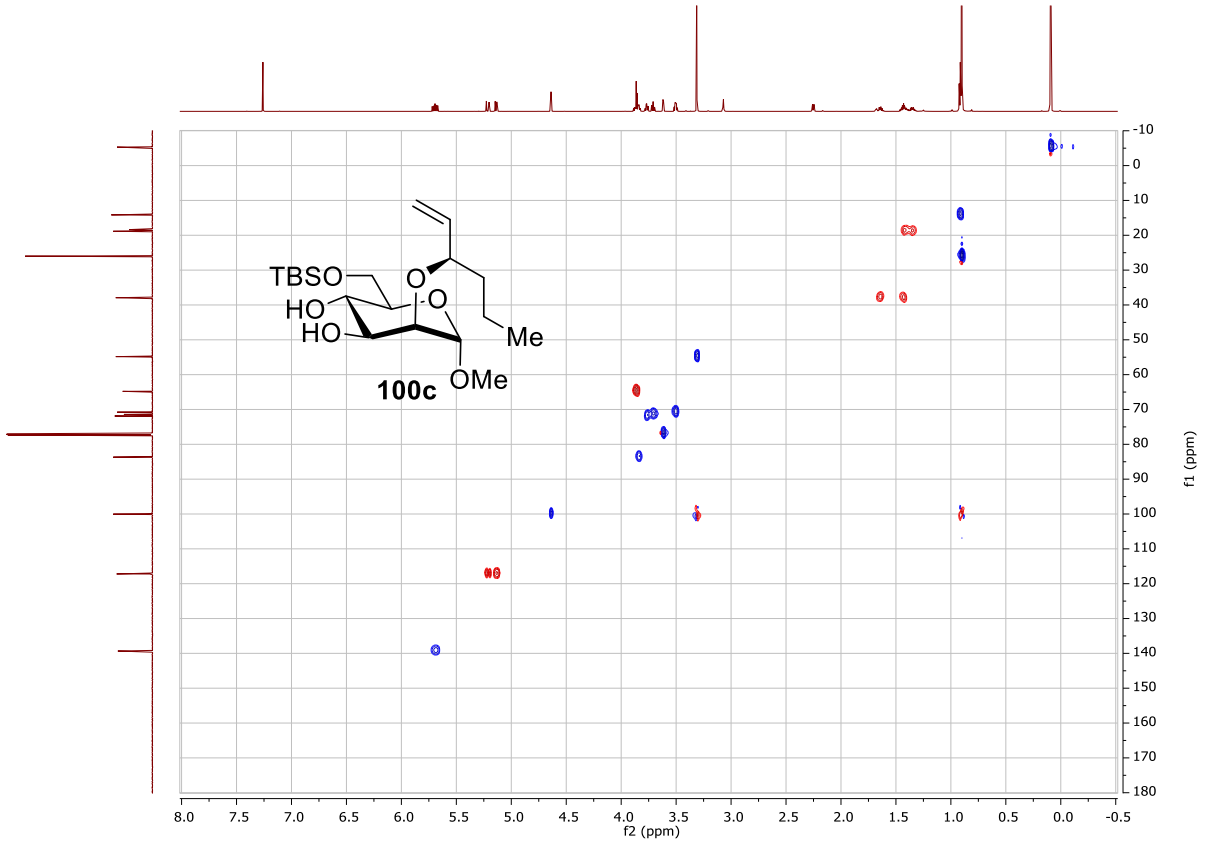

Figure 8.461. HSQC spectra for 100c

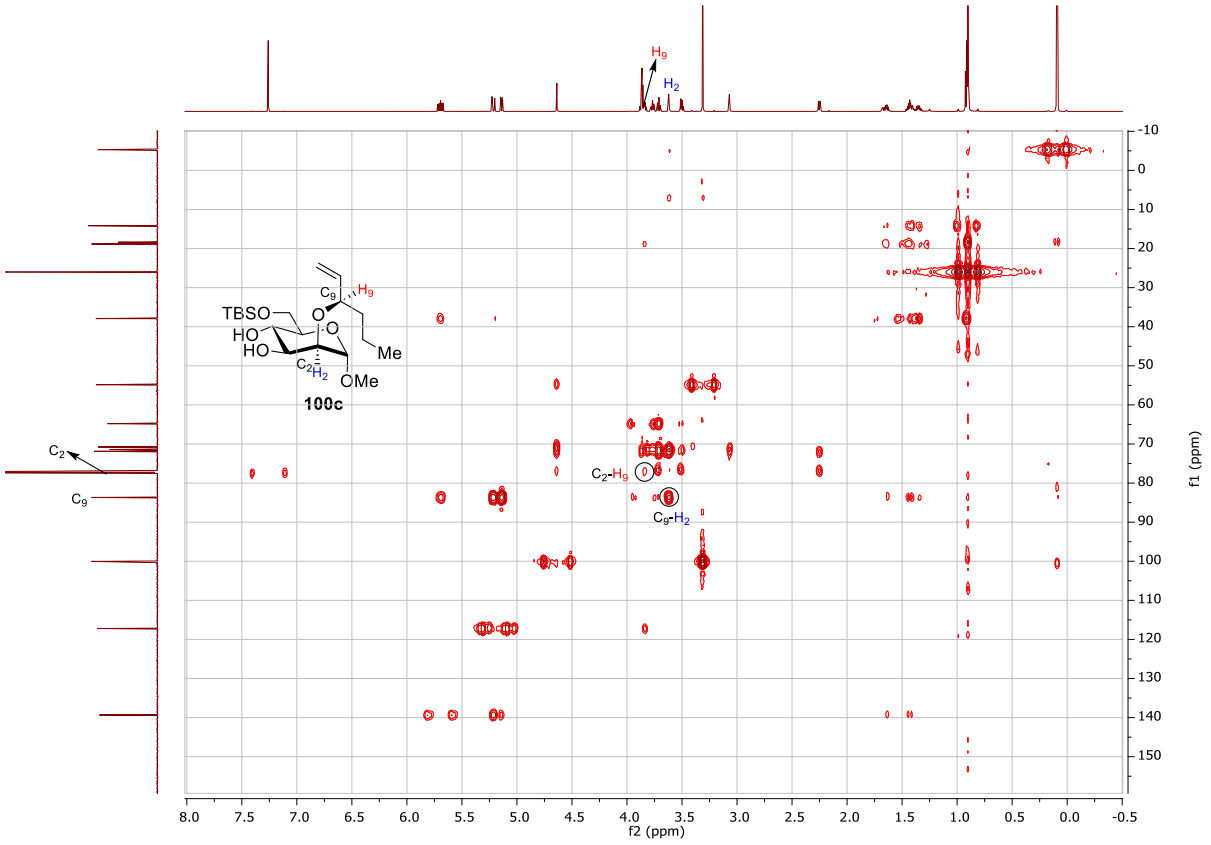

Figure 8.462. HMBC spectra for 100c

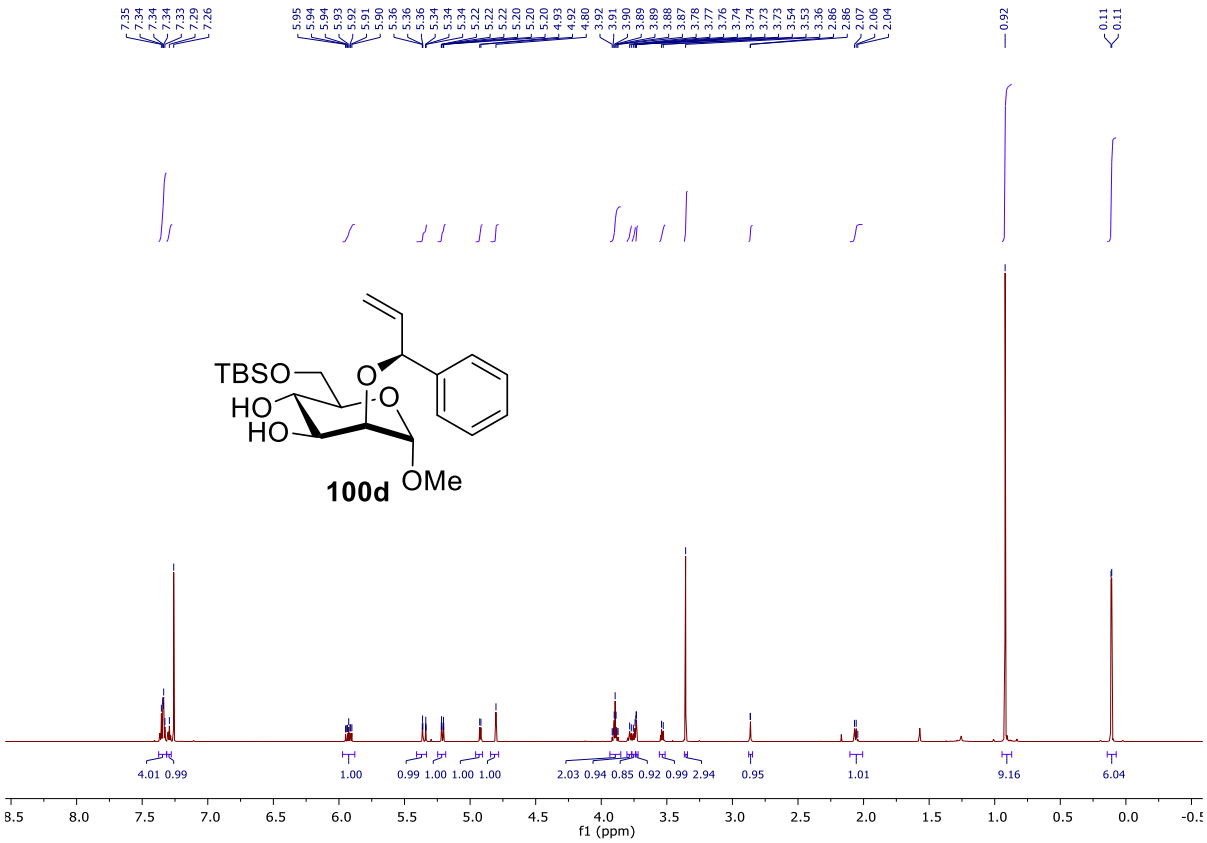

Figure 8.463. ^{1}H NMR spectra for 100d

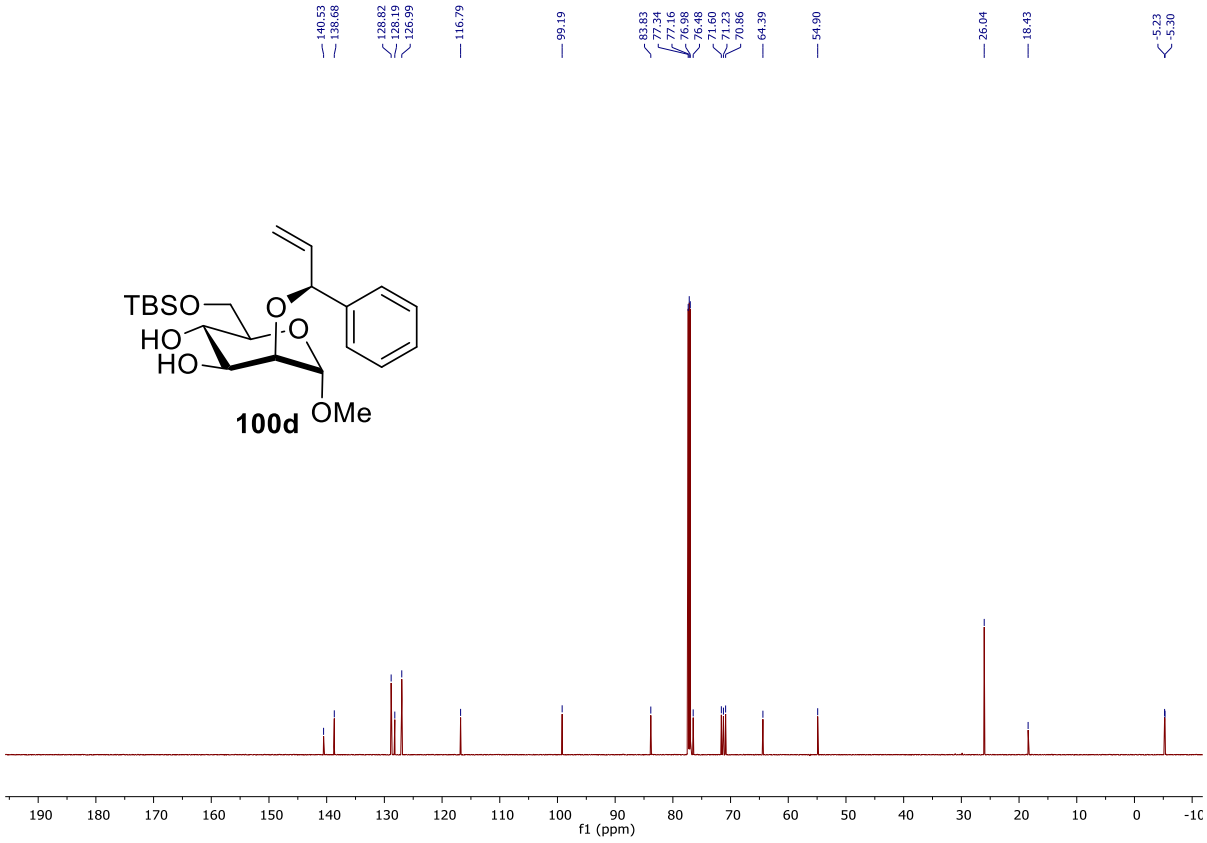

Figure 8.464. ^{13}C NMR spectra for 100d

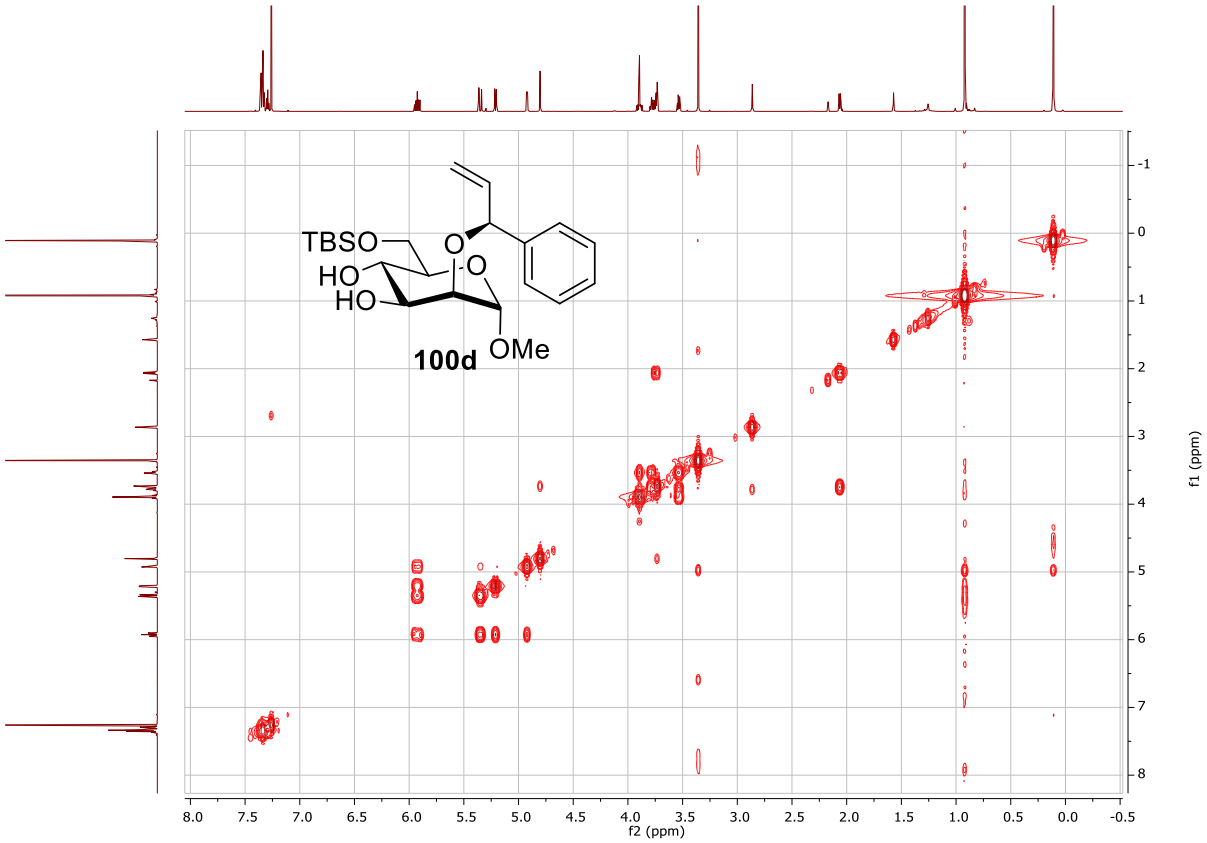

Figure 8.465. COSY spectra for 100d

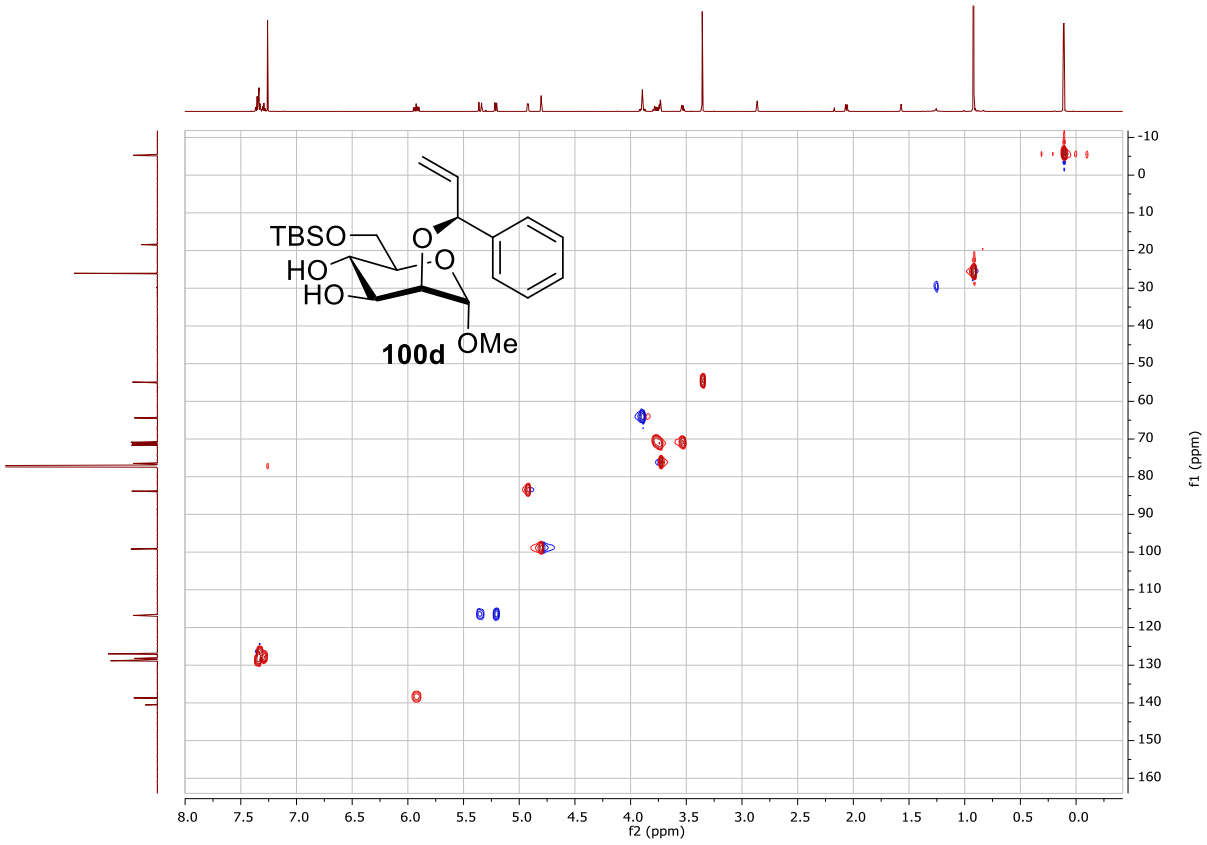

Figure 8.466. HSQC spectra for 100d

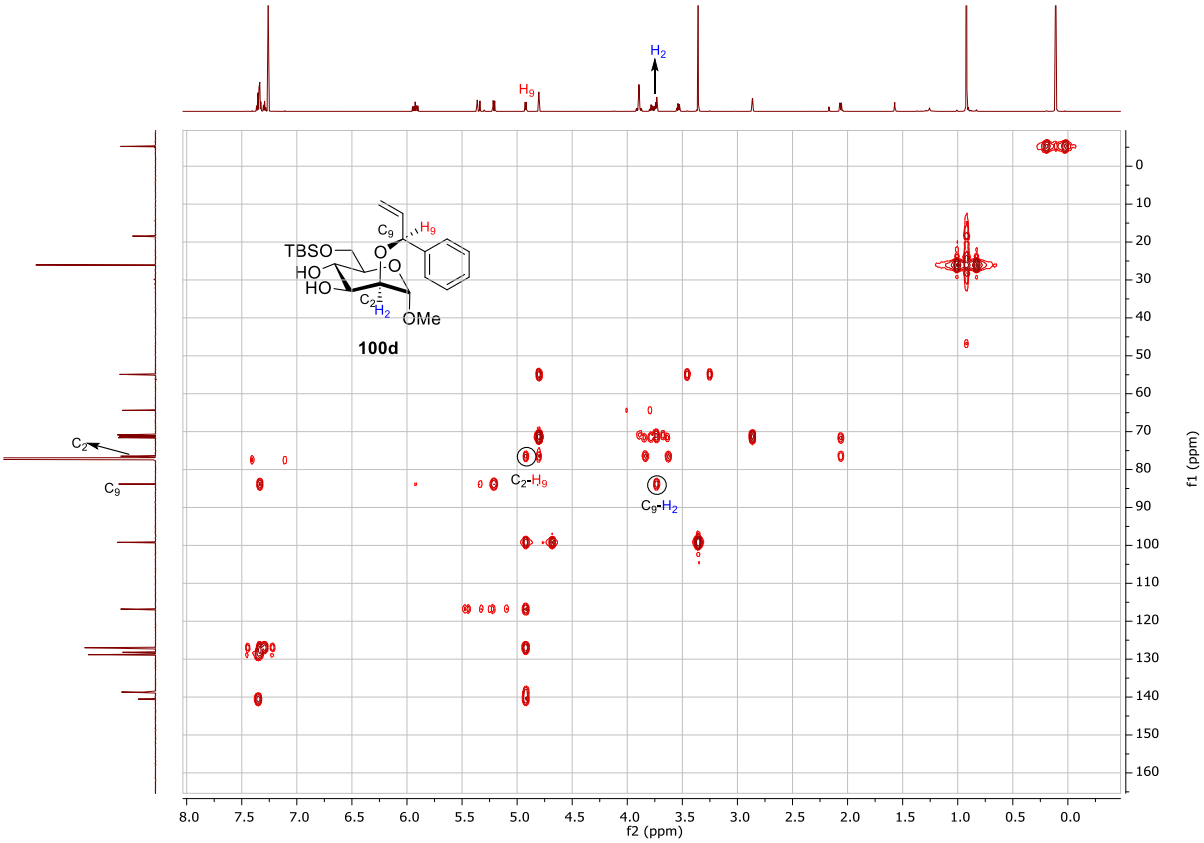

Figure 8.467. HMBC spectra for 100d

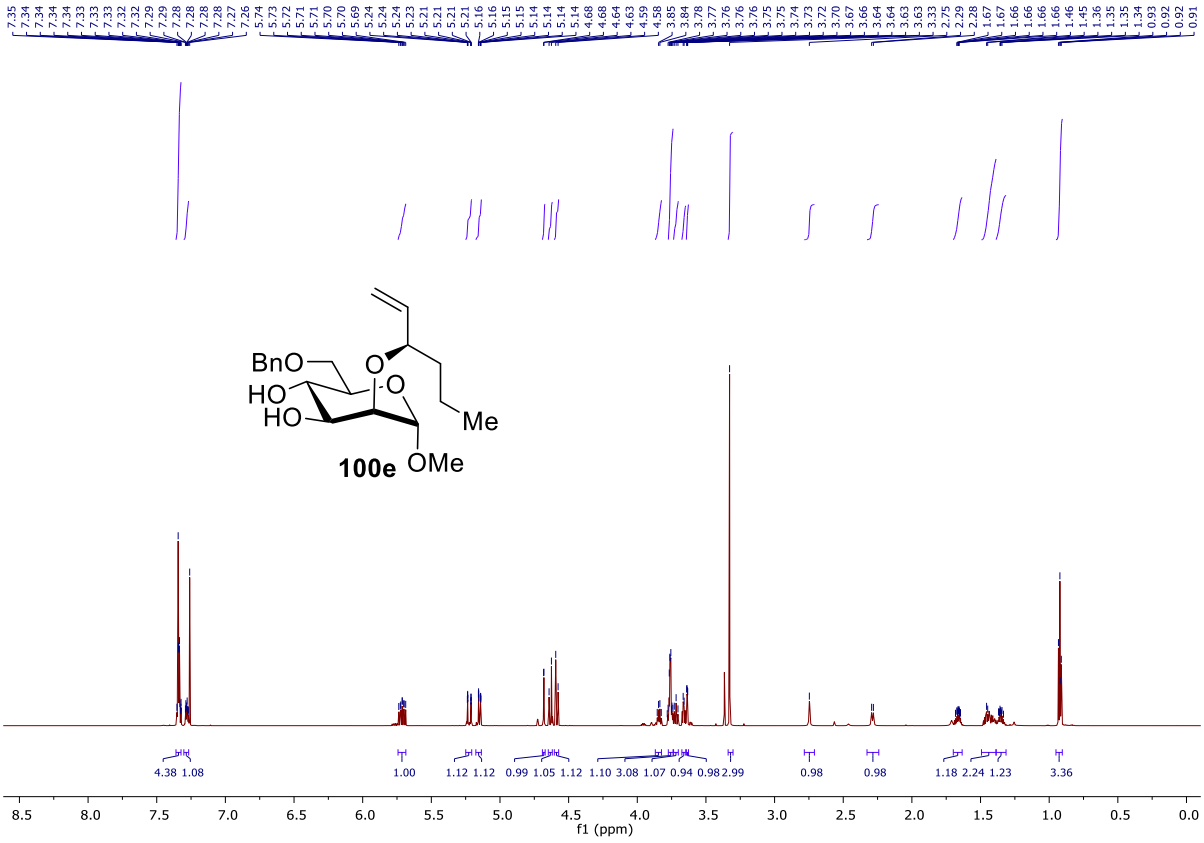

Figure 8.468. ^{1}H NMR spectra for 100e

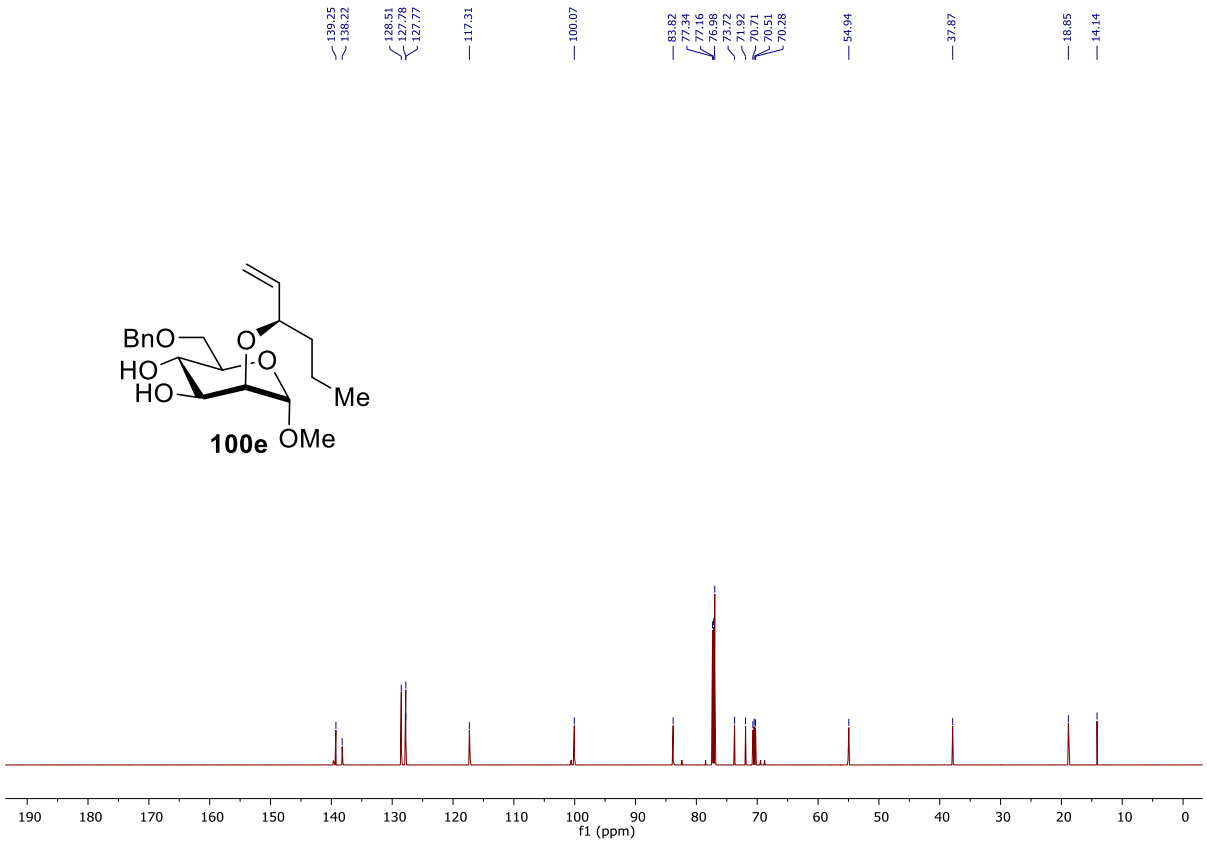

Figure 8.469. ^{13}C NMR spectra for 100e

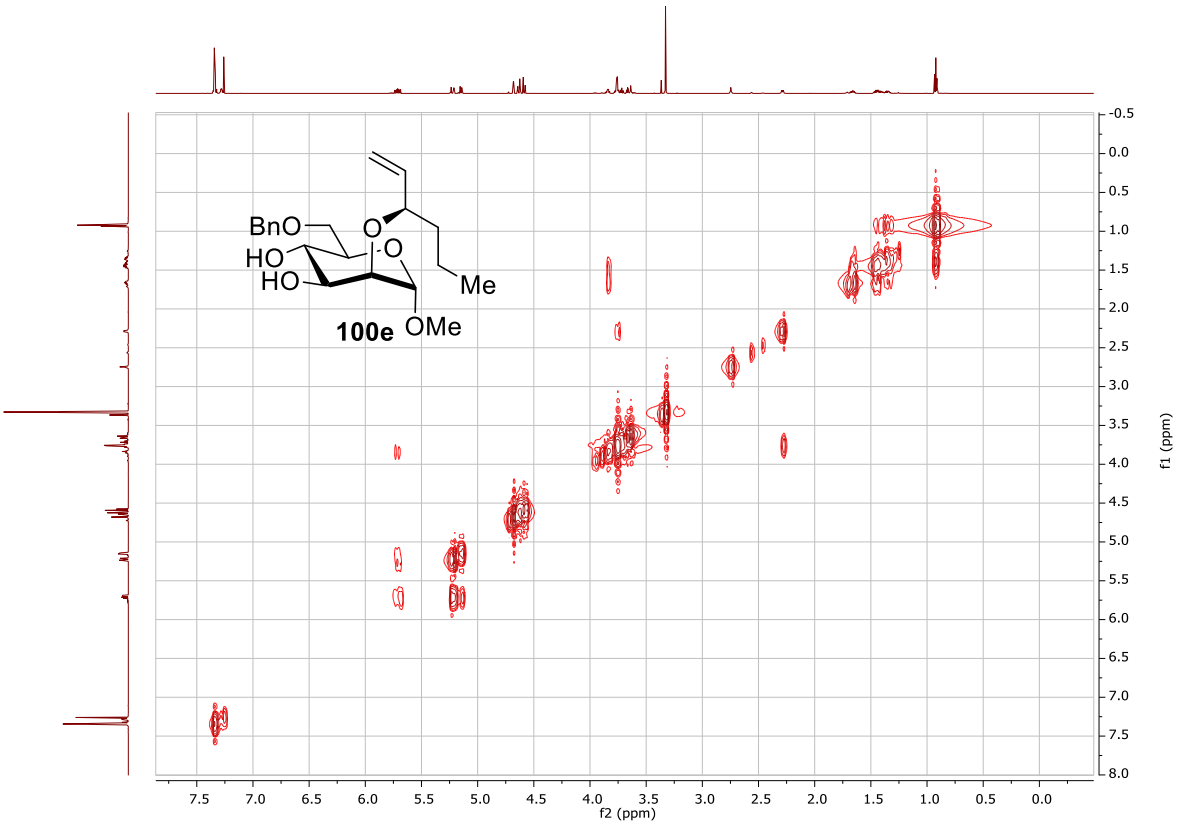

Figure 8.470. COSY spectra for 100e

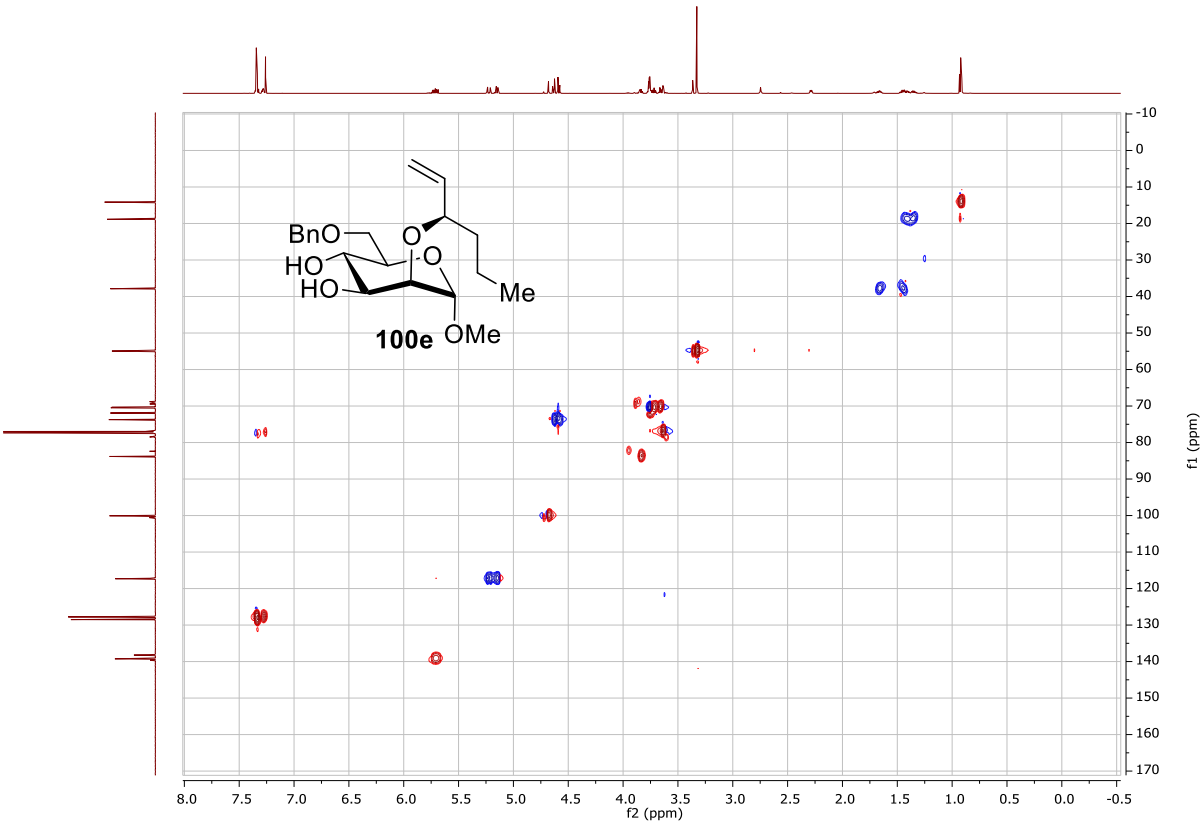

Figure 8.471. HSQC spectra for 100e

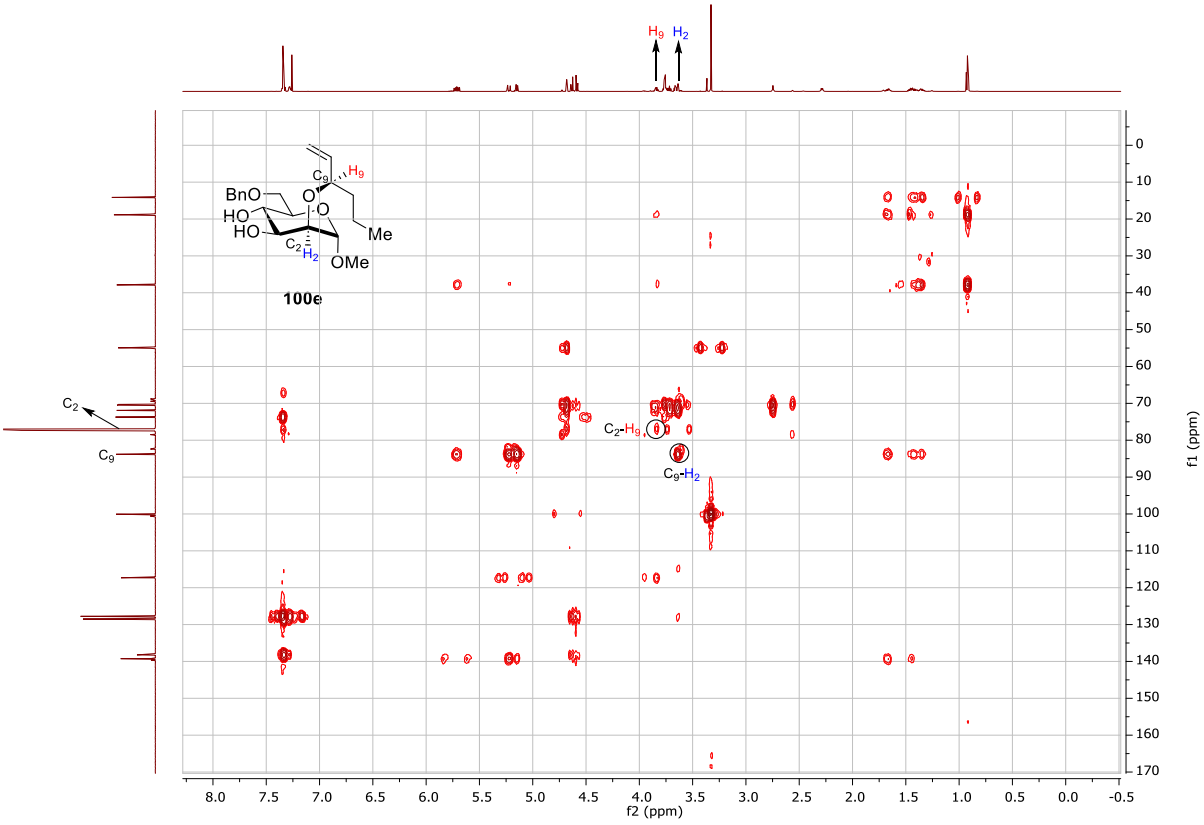

Figure 8.472. HMBC spectra for 100e

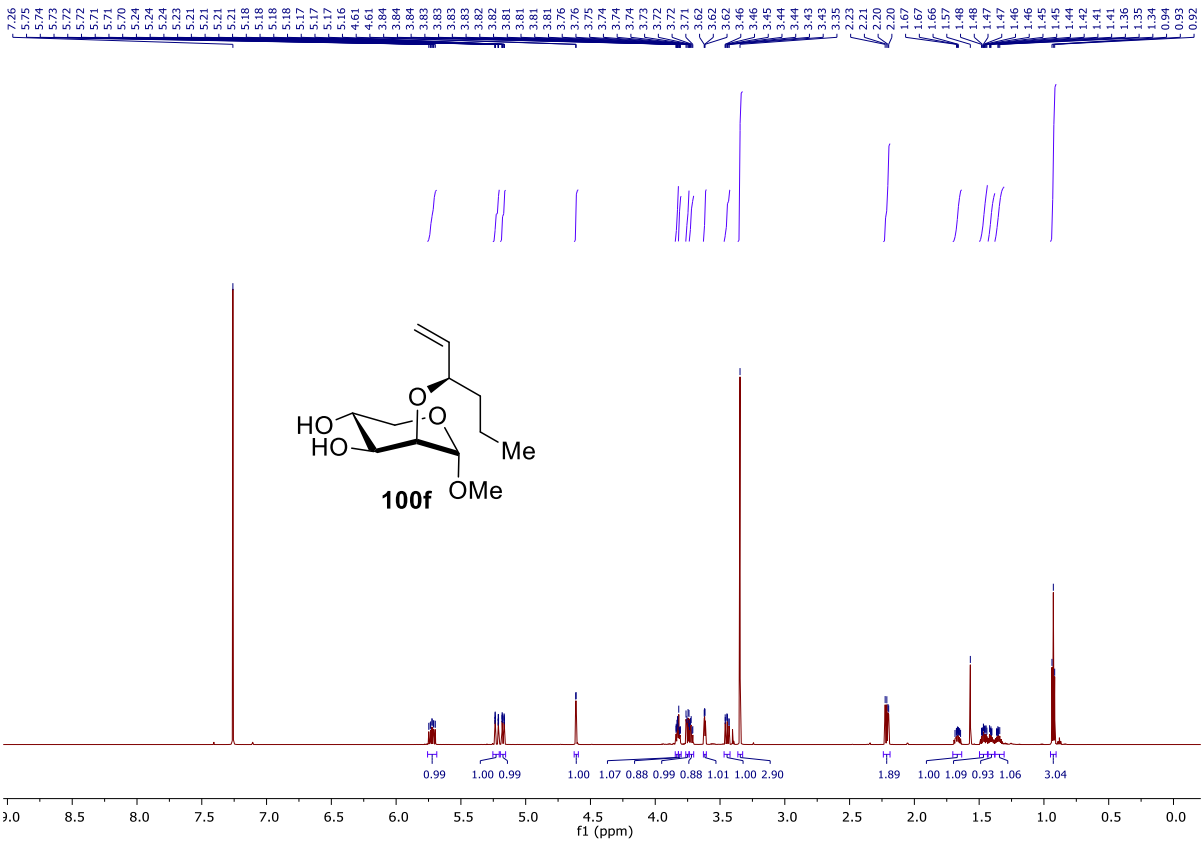

Figure 8.473. ^{1}H NMR spectra for 100f

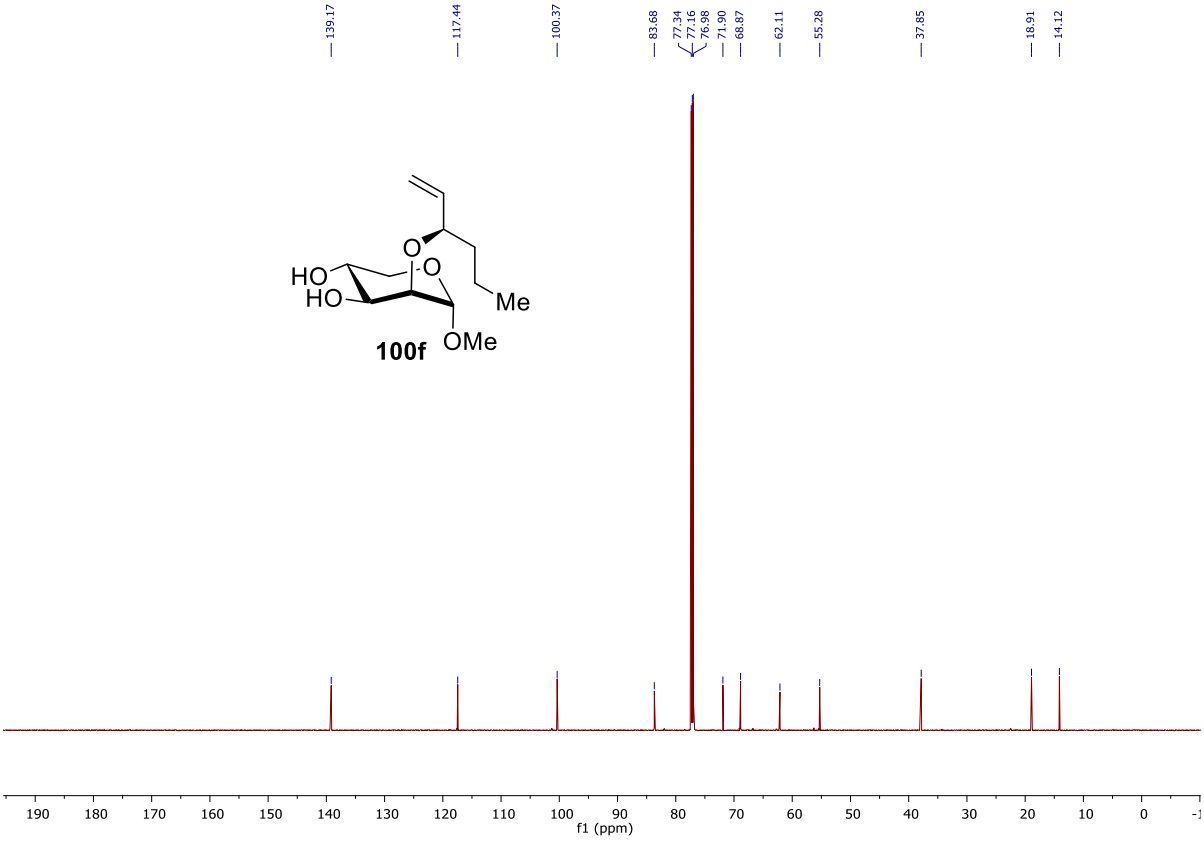

Figure 8.474. ^{13}C NMR spectra for 100f

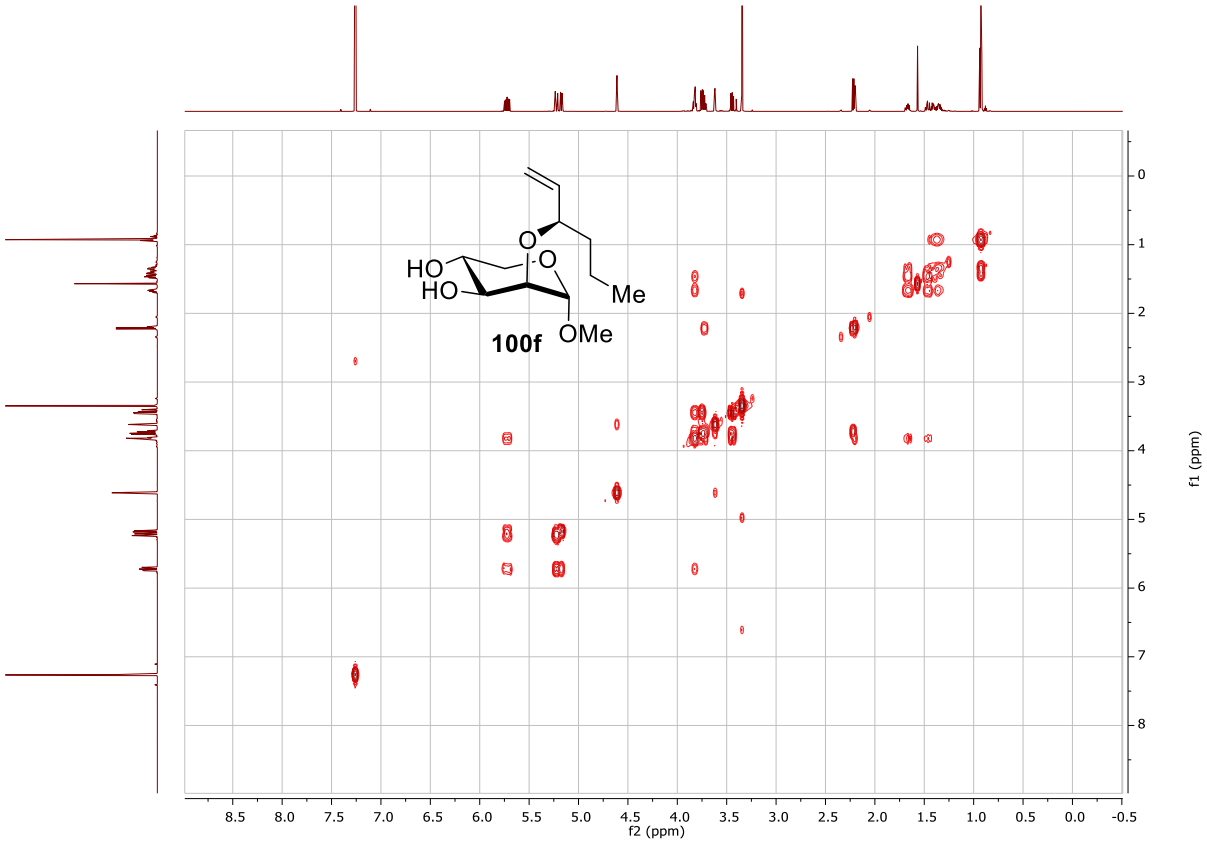

Figure 8.475. COSY spectra for 100f

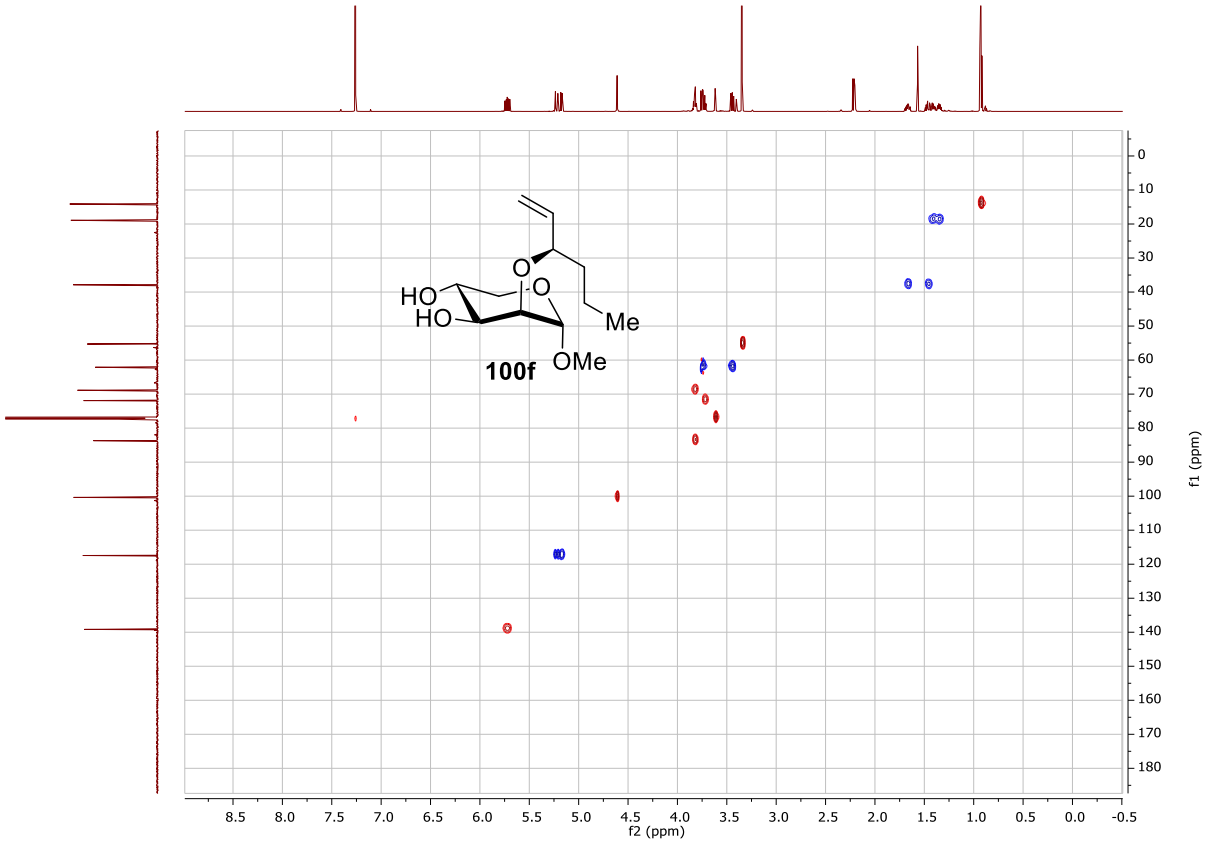

Figure 8.476. HSQC spectra for 100f

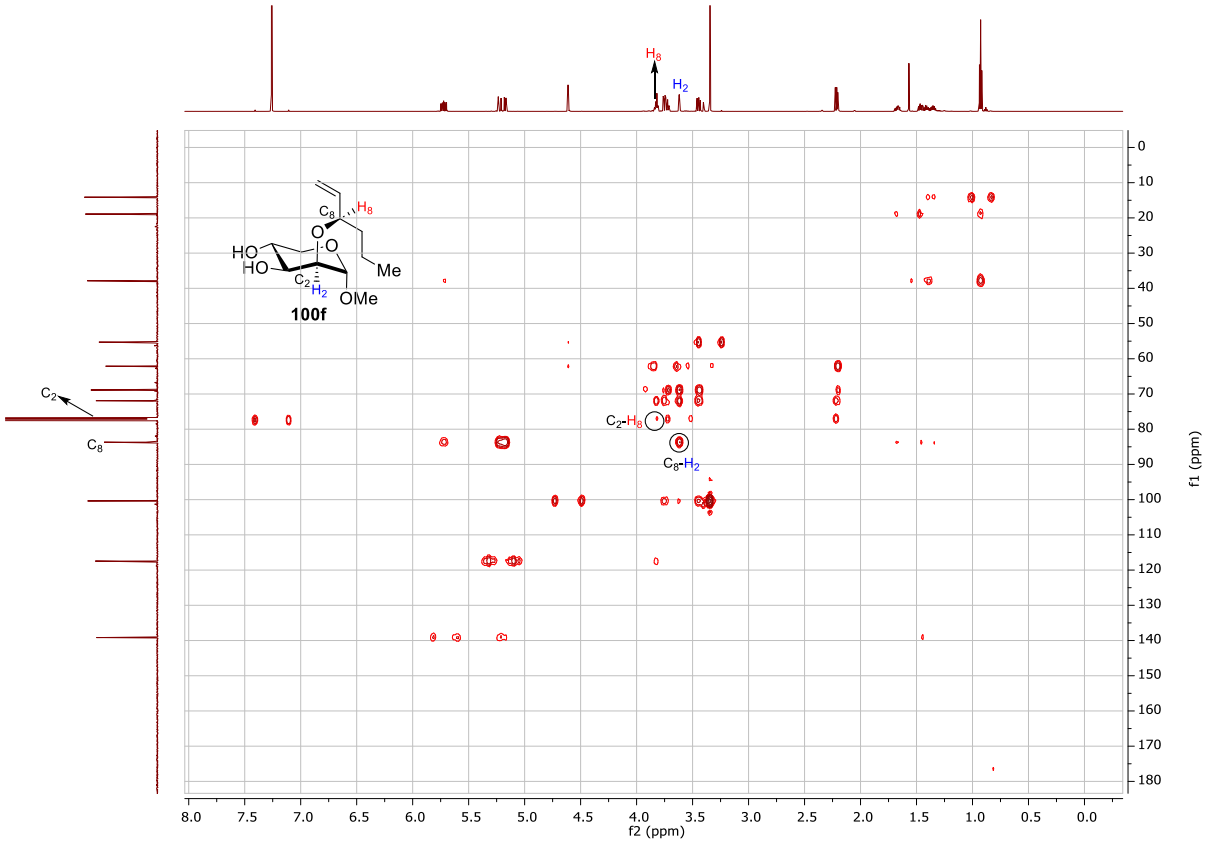

Figure 8.477. HMBC spectra for 100f